

University of Mississippi

eGrove

Electronic Theses and Dissertations

Graduate School

1-1-2015

Design, synthesis, and biological evaluation of sigma receptors (σ RS) ligands as potential pharmacotherapy for cancer and drug addiction

Walid Alsharif
University of Mississippi

Follow this and additional works at: <https://egrove.olemiss.edu/etd>



Part of the [Pharmacy and Pharmaceutical Sciences Commons](#)

Recommended Citation

Alsharif, Walid, "Design, synthesis, and biological evaluation of sigma receptors (σ RS) ligands as potential pharmacotherapy for cancer and drug addiction" (2015). *Electronic Theses and Dissertations*. 1454.
<https://egrove.olemiss.edu/etd/1454>

This Dissertation is brought to you for free and open access by the Graduate School at eGrove. It has been accepted for inclusion in Electronic Theses and Dissertations by an authorized administrator of eGrove. For more information, please contact egrove@olemiss.edu.

DESIGN, SYNTHESIS, AND BIOLOGICAL EVALUATION OF SIGMA RECEPTORS (σ RS)
LIGANDS AS POTENTIAL PHARMACOTHERAPY FOR CANCER AND DRUG
ADDICTION

A Dissertation
presented in partial fulfillment of requirements
for the degree of Doctor of Philosophy
in the Department of BioMolecular Sciences, Division of Medicinal Chemistry,
The University of Mississippi

by

WALID F. ALSHARIF

December 2, 2015

Copyright © 2015 by Walid F. Alsharif
ALL RIGHTS RESERVED

ABSTRACT

Sigma receptors are a well-defined unique class of receptors and are highly expressed in the central nervous system and also widely distributed in peripheral organs and tissues. There are two subtypes of sigma receptors: sigma-1 and sigma-2. These receptors are thought to be associated with functions and disorders such as inflammation, depression, anxiety, Alzheimer's disease, epilepsy and drug abuse. The sigma-1 receptor has been demonstrated to be involved in acute and chronic effects of cocaine and methamphetamine toxicities. However, the role of sigma-2 receptors is less clear due to the lack of availability of detailed protein structural information and truly selective sigma-2 ligands, which hindered the pharmacological characterization of the sigma-2 subtype. In fact, the sigma-2 receptor has not yet been cloned. Several reports indicated that the activation of sigma-2 receptor also induces growth arrest and cell death in various tumor cell lines. This gives sigma-2 ligands possible application as effective agents for the treatment of cancer. In this regard, searching for selective, high affinity sigma-2 ligands led to the design and synthesis a series of isothiocyanate compounds derived from a selective sigma-2 compounds developed in our laboratory as selective irreversible sigma-2 ligands. Also, in the search for an effective drug for the treatment of cocaine abuse and addiction, and based on our previous work on CM699 that showed its ability to attenuate the cocaine self-administration. We have found that stimulant self-administration (cocaine or methamphetamine) was blocked by dual inhibition of the DAT and sigma-receptors. However, CM699 had short half lives in Human and Rat liver microsomes assays (*in vitro*), and in rat *in*

vivo assay. Although CM699 had a half-life of 4.4 hr in rat, a compound with utility as a treatment for stimulant abuse will need a longer half-life, achieved either by structural change or by formulation. In this regard, we have made more analogs of CM699 in order to enhance blockade of cocaine self-administration and metabolic stability. Additionally, in an effort to continue to develop highly selective sigma ligands, we have synthesized a novel series of benzofuran-based ligands, and more analogs of the highly selective sigma-1, CM304.

DEDICATION

THIS DISSERTATION IS DEDICATED TO MY LOVING PARENTS

AND

MY WIFE

AND

MY PRECIOUS KIDS

SAJEDA, SOROOR, ALGHAIUQ, AND

ZAJER.

LIST OF ABBREVIATIONS AND SYMBOLS

| | |
|-------|---|
| °C | Degree Celsius |
| 5-HT | 5-hydroxytryptamine |
| i.p. | Intraperitoneal |
| KDa | Kilodalton |
| nM | Nanomolar |
| uM | Micromolar |
| κ | Kappa |
| μ mu | Micro mu |
| σRs | Sigma receptors |
| Akt | Protein kinase B |
| ADHD | Attention deficit hyperactive disorder |
| ADME | Absorption, distribution, metabolism, and excretion |
| BBB | Blood brain barrier |
| 9-BBN | 9-Borabicyclo[3.3.1]nonane |
| CB | Cerebellar |
| CDI | Carbonyldiimidazole |
| CN | Caudate nucleus |
| DAT | Dopamine transporter |
| DCM | Dichloromethane |

| | |
|-------|--|
| DMF | Dimethylformamide |
| DMSO | Dimethyl sulfoxide |
| DTG | Di-o-tolylguanidine |
| EGFR | Epidermal growth factor receptor |
| ER | Endoplasmic reticulum |
| ERK | Extracellular signal-regulated kinases |
| FC | Frontal cortex |
| HIV | Human immunodeficiency virus |
| IP3 | Inositol 1,4,5-triphosphate |
| MDMA | 3,4-methylenedioxyamphetamine |
| mg | Milligram |
| mg/kg | Milligram/kilogram |
| MMP9 | Matrix metalloproteinase-9 |
| NA | Nucleus accumbens |
| ND | Not determined |
| NET | Norepinephrine transporter |
| NGAL | Neutrophil gelatinase-associated lipocalin/lipocalin-2 |
| NMDA | N-methyl-D-aspartate |
| NMT | N, N-dimethyltryptamine |
| ON | Oligonucleotides |

| | |
|--------------------|--|
| PCP | Phencyclidine |
| PET | Positron emission tomography |
| PGRMC1 | Progesterone receptor membrane component 1 |
| PKA | Protein kinase A |
| 3-PPP | 3-hydroxyphenyl-N-propyl piperidine |
| PT | Putamen |
| psi | Pounds per square inch |
| SBDL-I and SBDL-II | Steroid binding domain-like regions |
| SERT | Serotonin transporter |
| SPECT | Single photon emission computed tomography |
| SSRI | Selective serotonin reuptake inhibitor |
| TCAs | Tricyclic antidepressants |
| TCDI | Thiocarbonyldiimidazole |
| TEA | Triethylamine |
| TFA | Trifluoroacetic acid |
| THF | Tetrahydrofuran |
| TLC | Thin-layer chromatography |
| TMDI and TMDII | Transmembrane domains |
| UDPGA | Uridine 5'-diphosphoglucuronic acid |
| VT | Ventral tagmental |

ACKNOWLEDGMENTS

It is a great privilege to express my deepest gratitude to my advisor Dr. Christopher R. McCurdy, for his support, encouragement, and guidance throughout my doctoral program. I am thankful to my advisor, Dr. Christopher R. McCurdy for the tremendous effort he invested in this dissertation and in my quest to become a researcher.

I am extremely grateful to my advisor; Dr. Christopher R. McCurdy for the numerous opportunities he provided me to not only grow as a medicinal chemist but also as an independent researcher. He guided me through tough times, and never doubted my abilities, not even when I doubted myself. He was with me at every phase of the learning process, patiently watching over my progress. He set a great example for me as a researcher, teacher and advisor.

I'd like to extend my appreciation to my committee members: Dr. Stephen J. Cutler, Dr. Bonnie A. Avery, and Dr. David A. Colby for their encouraging words, thoughtful criticism and for their time and attention.

I am extremely delighted to express my gratitude to Dr. Christopher R. McCurdy, Dr. Stephen J. Cutler, Dr. Mitchell Avery, Dr. Robert Doerksen, Dr. John Williamson, Dr. John Rimoldi, Dr. Bonnie A. Avery, and Dr. Daneel Ferreira for their lectures, which gave me tools that turned to be essential during my PhD research.

I'd like to acknowledge Dr. Christophe Mesangeau for his encouragement and practical advice.

I sincerely thank Dr. J. Francisco Leon, Dr. Mohammed Radwan, Dr. Mohamed Ali, and Dr. Amir Wahba for their cordial friendship timely support and help.

I thank my past lab-mates Dr. Rohit Bhat, Dr. David Watson, Dr. Marco Arribas for their valuable suggestions, generous help and warm company throughout the duration of my study.

I am thankful to the department staff members Ms. Candace G. Lowstuter, Ms. Sherrie Gussow, and Ms. Casey Stauber for assisting me with the administrative tasks necessary for completing my doctoral program.

I am grateful to Mohamed Jihan and Pankaj Pandey for their cordial friendship and moral support.

Finally, and most importantly, none of this would have been possible without the love and patience of my family; my parents, my wife, my brothers, and my sisters. Without their love, faith, inspiration, and encouragement over the years, I would not have reached my goal.

Walid Alsharif

TABLE OF CONTENTS

| | |
|--|-----------|
| Abstract..... | ii |
| Dedication..... | iv |
| List of abbreviations and symbols..... | v |
| Acknowledgments..... | viii |
| List of figures..... | xiii |
| List of tables..... | xxii |
| List of Schemes..... | xxiv |
| CHAPTER I: INTRODUCTION..... | 1 |
| 1. SIGMA RECEPTORS..... | 2 |
| 1.1 History..... | 2 |
| 1.2. Subtypes of sigma receptors..... | 3 |
| 1.2.1. Sigma-1 subtype..... | 4 |
| 1.2.2. Sigma-2 subtype..... | 6 |
| 1.3. Anatomical distribution of sigma receptors..... | 7 |
| 1.3.1 Nervous system..... | 7 |
| 1.3.2. Peripheral organs..... | 12 |
| 1.4. Subcellular distribution and functions of sigma receptors..... | 13 |
| 1.5. The role of sigma receptors in is deases..... | 16 |
| 1.5.1. Sigma receptors potential role in addiction and drug abuse..... | 16 |
| 1.5.2. Sigma receptors and analgesia..... | 24 |
| 1.5.3. Sigma receptors and depression..... | 26 |
| 1.5.4. Sigma receptors and Alzheimer’s disease..... | 28 |
| 1.5.5. Sigma receptors and schizophrenia..... | 30 |
| 1.5.6. Sigma Receptors and Cancer..... | 31 |
| 1.6. Endogenous and exogenous sigma receptors ligands..... | 33 |
| 1.6.1 Endogenous ligands..... | 33 |
| 1.6.2. Exogenous ligands..... | 34 |
| 1.7. Selective sigma ligands..... | 45 |
| 1.7.1 Selective sigma-1 ligands..... | 46 |
| 1.7.2 Selective sigma-2 ligands..... | 51 |
| 1.8. Dual probes for σ_1 receptors and the dopamine transporters..... | 59 |
| (Rimcazole analogs):..... | 59 |
| 1.9. Sigma receptor radioligands and PET imaging agents..... | 62 |
| 1.9.1. Sigma-1 receptor radioligand..... | 62 |
| 1.9.2. Sigma-2 receptor radioligands..... | 65 |
| CHAPTER II: SIGMA-2 RECEPTORS AND THEIR POTENTIAL ROLE IN ONCOLOGY..... | 68 |
| 2.1. Introduction..... | 69 |
| 2.2. Sigma-2 receptor and PGRMC1..... | 71 |
| 2.3. The most recent hypothetical sigma-2 receptor signaling pathways..... | 74 |

| | |
|---|------------|
| 2.4. Sigma-2 receptor as a biomarker..... | 76 |
| 2.5. Sigma-2 receptor ligands inducing apoptosis..... | 77 |
| 2.6. Sigma-2 receptor ligands as antitumor agents..... | 79 |
| 2.7. Sigma-2 receptor ligands as drug delivery vehicles..... | 80 |
| 2.8. Sigma-2 receptor ligands and low potential of toxicity to normal tissues..... | 81 |
| CHAPTER III: SIGMA RECEPTORS AND PSYCHOSTIMULANTS ABUSE | 83 |
| 3.1.1 Background..... | 84 |
| 3.1.2 Prevalence of psychostimulants abuse | 85 |
| 3.1.3 Psychostimulants mechanism of actions..... | 85 |
| 3.1.4 Examples of psychostimulants:..... | 87 |
| 3.2. Cocaine | 87 |
| 3.2.1 History..... | 88 |
| 3.2.2 Physiological and psychological effects of cocaine | 89 |
| 3.2.3. The dopamine reward system..... | 91 |
| 3.2.4. Approaches to potential treatment for cocaine abuse..... | 93 |
| 3.2.4.1. Dopamine receptor agonists and antagonists..... | 93 |
| 3.2.4.2. Dopamine reuptake inhibitors..... | 96 |
| 3.2.4.3. Opioid receptor system..... | 97 |
| 3.2.5. Sigma receptors and cocaine abuse..... | 100 |
| 3.2.5.1. Cocaine and behaviors | 101 |
| 3.2.5.2. Cocaine induced convulsions | 101 |
| 3.2.5.3. Cocaine induced lethality | 104 |
| 3.2.5.4. Cocaine induced locomotors stimulation..... | 105 |
| 3.2.5.5. Cocaine induced conditioned place preference..... | 106 |
| 3.2.5.6. Cocaine induced self-administration | 107 |
| 3.3. Methamphetamine | 112 |
| 3.3.1. Background..... | 113 |
| 3.3.2. Physiological and psychological effects of methamphetamine..... | 114 |
| 3.3.3. Approaches to potential treatment for methamphetamine abuse..... | 116 |
| 3.3.4. Sigma receptors and methamphetamine | 118 |
| 3.3.4.1. Sigma ligands as potential treatment for methamphetamine abuse | 120 |
| CHAPTER IV: IRREVERSIBLE SIGMA RECEPTORS LIGANDS AND PHOTOAFFINITY LABELING | 123 |
| 4. Irreversible sigma ligands..... | 124 |
| 4.1 Irreversible ligands derived from different structural classes of sigma ligands.... | 124 |
| 4.2 Photoaffinity labels | 130 |
| CHAPTER V: PHARMACOKINETICS AND METABOLIC STABILITY OPTIMIZATION..... | 138 |
| 5.1 Introduction..... | 139 |
| 5.2 Pharmacokinetic parameters and drug behavior..... | 140 |
| 5.2.1. C_{max} and t_{max} | 140 |

| | |
|--|------------|
| 5.2.2. Area under the curve (AUC) | 140 |
| 5.2.3. Clearance (CL) | 141 |
| 5.2.4. Bioavailability (F)..... | 141 |
| 5.2.5. Volume of distribution (V_D) | 142 |
| 5.2.6. Half-life ($t_{1/2}$)..... | 143 |
| 5.3. Metabolic stability enhancement | 143 |
| 5.4. Metabolic stability and Intrinsic metabolic clearance | 144 |
| 5.5. Advantages of enhancing metabolic stability..... | 146 |
| 5.6. Strategies to enhance metabolic stability..... | 146 |
| 5.6.1. Reducing lipophilicity..... | 148 |
| 5.6.2. Blocking metabolically labile groups..... | 151 |
| 5.6.3. Modification of metabolically labile groups | 156 |
| CHAPTER VI: RESEARCH DESIGN AND METHODS | 159 |
| 6.1 Rationale for design and synthesis selective sigma receptors ligands | 160 |
| 6.1.1 Benzofuran-based ligands..... | 162 |
| 6.1.2 Developing irreversible selective sigma-2 ligands..... | 169 |
| 6.1.3 Development of dual sigma receptors and DAT inhibitors and CM699 metabolic stability enhancement..... | 172 |
| 6.1.4 Development of new analogs of CM304 (Selective sigma-1 receptor ligand) | 178 |
| CHAPTER VII: BIOLOGICAL SCREENING, RESULTS AND DISCUSSION | 181 |
| 7.1 Biological screening methods | 182 |
| 7.1.1 Binding affinity assays | 182 |
| 7.1.2. Irreversible binding assays (Treatment of membranes with isothiocyanates). | 185 |
| 7.1.3. Metabolic stability study: (CM699 analogs) | 185 |
| 7.2 SAR study results and discussion | 186 |
| 7.2.1 Benzofuran series..... | 186 |
| 7.2.2 1,3-dihydro-2 <i>H</i> -benzo[<i>d</i>]imidazol-2-one and benzo[<i>d</i>]oxazol-2(3 <i>H</i>)-one derivatives | 190 |
| 7.3. Binding affinity and irreversible binding of isothiocyanate derivatives | 192 |
| 7.4 The novel CM699 analogs..... | 195 |
| 7.5 Novel CM304 analogs | 199 |
| CHAPTER VIII. CHEMICAL SYNTHESIS OF SIGMA RECEPTOR ANALOGUES..... | 200 |
| 8.1 Synthesis of a benzofuran-3-yl series | 201 |
| 8.2 Synthesis of isothiocyanate derivatives: | 203 |
| 8.2.1 Synthesis of 1,3-dihydro-2 <i>H</i> -benzo[<i>d</i>]imidazol-2-one | 203 |
| 8.2.2 Synthesis of 1,3-dihydro-2 <i>H</i> -benzo[<i>d</i>]imidazol-2-one derivatives (356-360) ... | 208 |
| 8.3 Synthesis of benzofuran derivative..... | 210 |
| 8.4 Synthesis of benzo[<i>d</i>]oxazol-2(3<i>H</i>)-one derivatives. | 210 |
| 8.5 Synthesis of benzo[<i>d</i>]thiazol-2(3<i>H</i>)-one derivatives | 212 |
| 8.6 Synthesis of CM699 derivatives..... | 213 |
| 8.6.1 Synthesis of 6-fluorobenzo[<i>d</i>]thiazol-2(3 <i>H</i>)-one (390) | 213 |
| 8.6.2 Synthesis of more analogs CM699 | 214 |
| 8.7 Synthesis of 3<i>H</i>-spiro[isobenzofuran-1,4'-piperidine]..... | 215 |

| | |
|--|------------|
| There are two routes have been followed to synthesize the 3H-spiro[isobenzofuran-1,4'-piperidine]..... | 215 |
| 8.7.1 The first synthetic route of 3H-spiro[isobenzofuran-1,4'-piperidine] | 215 |
| 8.7.2 The second synthetic route of 3H-spiro[isobenzofuran-1,4'-piperidine] | 216 |
| 8.8 Synthesis of 2'-methyl-3H-spiro[isobenzofuran-1,4'-piperidine] (489)..... | 217 |
| 8.9 Synthesis of spiro[isochromane-1,4'-piperidine]..... | 218 |
| 8.10 Synthesis of benzimidazolone derivatives of CM699 | 219 |
| 8.10.1 Synthesis of the de-methylated CM699 analog, 358 (WA294)..... | 219 |
| 8.10.2 Synthesis of 1-methyl-benzo[d]imidazol-2-one derivatives of CM699 | 219 |
| 8.11 Synthesis of spiro[isochromane-1,4'-piperidine] derivatives | 221 |
| 8.12 Synthesis of CM304 derivatives | 222 |
| 8.12.1 Synthesis of the first series of CM304 derivatives | 222 |
| 8.12.2 Synthesis of the second series of CM304 derivatives | 223 |
| 7.12.3 Synthesis of 494 (WA444a) and 461 (WA444b) | 225 |
| CHAPTER IX: EXPERIMENTAL SECTION..... | 227 |
| 9.2 Synthesis of a benzofuran-3-yl Series | 228 |
| 9.2.1 General procedure for the preparation of (253-266) and (267-272). | 235 |
| 9.2.2 General procedure for the preparation of (281-314)..... | 241 |
| 9.3 Synthesis of isothiocyanate derivatives: | 253 |
| 9.3.1 Synthesis of isothiocyanate derivatives of 1,3-dihydro-2H-benzo[d]imidazol-2-one | 253 |
| 9.4.3 Synthesis of the benzoimidazolone derivatives (356), (357), (358), (359), and (360). | 278 |
| 9.4.4 Synthesis of the isothiocyanate derivative of benzofuran..... | 286 |
| 9.4.5 Synthesis of benzoxazolone derivatives of isothiocyanate..... | 286 |
| 9.4.6. Synthesis of benzothiazolone derivatives of isothiocyanate..... | 293 |
| 9.5 Synthesis of CM699 derivatives..... | 300 |
| 9.5.1 Synthesis of benzo[d]thiazol-2(3H)-one and benzo[d]oxazol-2(3H)-one derivatives | 300 |
| 9.5.2 Synthesis of the de-methylated CM699 | 312 |
| 9.5.3 Synthesis of 1-methyl-benzo[d]imidazol-2-one derivatives of CM699 | 313 |
| 9.6 Synthesis of the heterocycle substituents..... | 328 |
| 9.6.1 Synthesis of 3H-spiro[isobenzofuran-1,4'-piperidine] | 328 |
| 9.6.2 Synthesis of 3H-spiro[isobenzofuran-1,4'-piperidine] (Second route)..... | 330 |
| 9.6.3 Synthesis of 2'-methyl-3H-spiro[isobenzofuran-1,4'-piperidine] (WA469)..... | 332 |
| 9.6.4 Synthesis of spiro[isochromane-1,4'-piperidine] (493) | 335 |
| 9.7 Synthesis of Spiro[isochromane-1,4'-piperidine] derivatives..... | 337 |
| 9.8 Synthesis of CM304 derivatives..... | 342 |
| CHAPTER X: CONCLUSION | 357 |
| BIBLIOGRAPHY | 361 |
| LIST OF APPENDICES..... | 430 |
| VITA..... | 885 |

LIST OF FIGURES

| | |
|--|----|
| Figure 1.1: Sigma-1 receptor structural representation of the transmembrane domains (TMDI and TMDII) and steroid binding domain-like regions (SBDL-I and SBDL-II). | 5 |
| Figure 1.2: The proposed endogenous sigma-1 ligand N,N-dimethyltryptamine. | 6 |
| Figure 1.3: Time-activity curves (TACs) from mouse positron emission tomography studies. | 8 |
| Figure 1.4: PET images and ex vivo autoradiography of sagittal brain sections (12 µm) obtained 60 minutes after administration of [¹⁸ F]CM304. | 9 |
| Figure 1.5: Rat brain PET/CT and ex vivo autoradiography. | 10 |
| Figure 1.6: Monkey brain PET/MR images from baseline dynamic imaging. | 11 |
| Figure 1.7: Structures of selective sigma ligands | 12 |
| Figure 1.8: Tritiated sigma receptor radioligands. | 13 |
| Figure 1.9: Structures of the selective sigma-2 ligand (WC-21) and PGRMC1 ligand (AG-205) | 15 |
| Figure 1.10: Chemical structure of cocaine | 18 |
| Figure 1.11: Structures of some selective sigma-1 antagonists | 19 |
| Figure 1.12: Structure of the selective sigma-1 antagonist, BD1047. | 20 |
| Figure 1.13: Chemical structure of methamphetamine | 21 |
| Figure 1.14: Structures of various sigma ligands | 22 |
| Figure 1.15: Structure of sigma-1 agonist, PRE084. | 23 |

| | |
|--|----|
| Figure 1.16: Sigma-1 receptor ligands and analgesia. | 25 |
| Figure 1.17: Sigma receptors ligands and depression. | 28 |
| Figure 1.18: Non-selective sigma ligands and Alzheimer's disease. | 30 |
| Figure 1.19: Sigma receptors ligands cited for their role in Schizophrenia. | 31 |
| Figure 1.20: MicroPET imaging study of [76Br] radiotracer in an EMT-6 tumor-bearing mouse. Structure and in vitro binding affinities (K _i values) of the 76Br-labeled benzamide analog. | 33 |
| Figure 1.21: Structures of neurosteroids that proposed to act as endogenous ligands for sigma receptors. | 33 |
| Figure 1.22: Diverse structural classes of sigma ligands and their affinities. | 35 |
| Figure 1.23: Variety of structural classes of sigma ligands. | 36 |
| Figure 1.24: Various sigma ligands with different structural entities. | 37 |
| Figure 1.25: The four regions proposed by Gilligan et al. for the binding of lead molecule | 38 |
| Figure 1.26: The Proposed Gilligan Model for sigma-1 receptor binding. | 39 |
| Figure 1.27: The non-rigid sigma benzomorphan substructures | 40 |
| Figure 1.28: Structures of phenylpentylamines | 40 |
| Figure 1.29: Structures of other phenylpentylamines and the effect of aromaticity on affinity | 40 |
| Figure 1.30: Structures of compounds 62 and 63 and importance of basic nitrogen. | 41 |

| | |
|--|----|
| Figure 1.31: Phenylpiperidines sigma receptor ligands | 41 |
| Figure 1.32: Importance of basic nitrogen. | 42 |
| Figure 1.33: Chemical structures of some piperidine and piperazine derivatives | 43 |
| Figure 1.34: Chemical structures of some other piperazine derivatives. | 43 |
| Figure 1.35: Cyclopentanoperhydrophenanthrene steroid nucleus | 44 |
| Figure 1.36: Glennon/Ablordeppey“Ar-X5-N” pharmacophore model for high binding affinity at sigma-1 receptor. | 45 |
| Figure 1.37: Tritiated sigma receptors ligands | 46 |
| Figure 1.38: Structures of haloperidol and its derivatives | 47 |
| Figure 1.39: Structure of the phenylacetamide derivative. | 44 |
| Figure 1.40: Structures of some propylamine compounds. | 48 |
| Figure 1.41: Selective sigma-1 of spirocyclic pyranopyrazoles. | 49 |
| Figure 1.42. Selective sigma-1 ligand with high affinity. | 50 |
| Figure 1.43: Selective sigma-1 of tetrahydronaphthalene derivatives. | 50 |
| Figure 1.44: Selective sigma-1 of benzo[d]thiazol-2(3H)one derivatives. | 51 |
| Figure 1.45: Structure of 12-methoxyibogamine or ibogaine and its binding affinity. | 53 |
| Figure 1.46: Structure and binding affinity of Siramesine | 53 |
| Figure 1.47: Piperazine derivatives with moderate sigma affinity. | 54 |
| Figure 1.48: Spiro-fusion with various alkyl substituents. | 55 |
| Figure 1.49: Spiro-fusion with high and low lipophilic substituents. | 55 |

| | |
|---|----|
| Figure 1.50: Spiropiperidines structure activity relationships | 56 |
| Figure 1.51: Simple Phenylalkylamines | 56 |
| Figure 1.52: Tropane analogs | 57 |
| Figure 1.53: General structure of flexible benzamides. | 57 |
| Figure 1.54: Two of the most selective σ_2 flexible benzamides. | 58 |
| Figure 1.55: RHM-1 analog. | 58 |
| Figure 1.56: SAR of the 6,7-dimethoxytetrahydroisoquinoline for sigma-2 binding | 59 |
| Figure 1.57: Rimcazole and its analogs. | 60 |
| Figure 1.58: The highly selective sigma-1 receptor radioligand. | 62 |
| Figure 1.59: The widely used selective sigma-1 [^{11}C labeled] radiotracer. | 63 |
| Figure 1.60: The widely used selective sigma-1 [^{18}F labeled] radiotracer. | 63 |
| Figure 1.61: Selective sigma-1 [^{18}F labeled] radiotracers. | 64 |
| Figure 1.62: In house developed selective sigma-1 radiotracers. | 65 |
| Figure 1.63: Generally accepted sigma-2 radioligand for binding assays. | 66 |
| Figure 1.64: Selective sigma-2 radiotracers used for tumors and binding assays. | 67 |
| Figure 2.1: Chemical structures of sigma-2 receptor ligands and PGRMC1 inhibitor, AG205. | 74 |
| Figure 2.2: Huang's hypothetical scheme of sigma-2 receptor/PGRMC1 signaling pathways in cancer cells | 76 |
| Figure 2.3: Chemical structures of some sigma-2 receptor ligands | 79 |

| | |
|--|-----|
| Figure 2.4: Chemical structures of the sigma-2 receptor ligand, CM572 | 82 |
| Figure 3.1: Chemical structure of cocaine. | 88 |
| Figure 3.2: Brain. Certain areas of brain are known to be involved in reward/reinforcement due to drugs. | 93 |
| Figure 3.3: Chemical structure of dopamine agonists | 95 |
| Figure 3.4: Chemical structure of dopamine antagonists | 96 |
| Figure 3.5: Structures of dopamine uptake inhibitors | 97 |
| Figure 3.6: Structures of opioid ligands | 99 |
| Figure 3.7: Chemical structure of selective sigma-2 ligand, CM398 that was developed in McCurdy's laboratory | 104 |
| Figure 3.8: Chemical structure of the highly selective sigma ligand, AC927. | 104 |
| Figure 3.9: Sigma receptor ligands that attenuate cocaine-induced locomotor sensitization. | 106 |
| Figure 3.10: Chemical structures of the sigma-1 antagonists, NE100, SA4503, and BD1047. | 107 |
| Figure 3.11: Chemical structures of rimcazole and its derivatives. | 109 |
| Figure 3.12: Effects of pre-treatment with rimcazole and its analogs on cocaine self-administration. | 109 |
| Figure 3.13: Chemical structures of selective DAT inhibitors | 110 |
| Figure 3.14: Effects of pre-treatment with DAT inhibitors on cocaine self- | 110 |

administration.

| | |
|---|-----|
| Figure 3.15: Effects of pre-treatment with sigma receptor antagonists on cocaine self-administration | 111 |
| Figure 3.16: Effects of pre-treatment with WIN 35,428 combined with sigma receptor antagonists on cocaine self-administration | 112 |
| Figure 3.17: Chemical structure of methamphetamine and amphetamine. | 113 |
| Figure 3.18: Several compounds cited for their potential treatment for methamphetamine abuse. | 117 |
| Figure 3.19: Chemical structure of sigma receptor ligands for methamphetamine abuse treatment | 119 |
| Figure 3.20: Chemical structure of sigma receptor ligands for methamphetamine abuse treatment | 120 |
| Figure 3.21: Chemical structures of sigma receptor ligands (SN79, CM156, and AZ66) that were developed in McCurdy's laboratory and pursued for potential methamphetamine abuse treatment. | 122 |
| Figure 4.1: Structure of phencyclidine and its derivative, metaphit. | 125 |
| Figure 4.2: Structures of phencyclidine based ligands. | 127 |
| Figure 4.3: Chemical structures of DTG and its isothiocyanate analog, DIGIT | 128 |
| Figure 4.4: Chemical structures of possible irreversible sigma ligands | 129 |
| Figure 4.5: Chemical structure of BNIT | 130 |

| | |
|---|-----|
| Figure 4.6: Structures of commonly used photo-reactive groups. | 131 |
| Figure 4.7: Aryl azide photoactivation. | 132 |
| Figure 4.8: Possible side reactions of aryl azides. | 132 |
| Figure 4.9: Diazirine derivatives photoactivation. | 133 |
| Figure 4.10: Benzophenone derivatives photoactivation | 134 |
| Figure 4.11: Chemical structure of [125I]Azidococaine | 135 |
| Figure 4.12: Chemical structure of [3H](+)-Azidophenazocine | 136 |
| Figure 4.13: Chemical structure of [3H]N3DTG. | 137 |
| Figure 5.1: Chemical structure of rhinovirus 3C protease lead inhibitors | 149 |
| Figure 5.2: Chemical structures of chemokine receptor (CCR5) antagonists. | 150 |
| Figure 5.3: Chemical structures of some piperidine-4-carboxamide CCR5 antagonists | 151 |
| Figure 5.4: Chemical structure of fluorinated compounds | 152 |
| Figure 5.5: Examples of blocking sites of potential oxidative metabolism | 152 |
| Figure 5.6: Chemical structure of compounds with fluorine atoms | 153 |
| Figure 5.7: Chemical modification of a series of adamantane inhibitors | 154 |
| Figure 5.8: Chemical structures and half-lives of compounds 266, 227. | 155 |
| Figure 5.9: Chemical structures and half-lives of BHAP reverse transcriptase inhibitors. | 155 |
| Figure 5.10: Chemical structures and half-lives of phospholipase A2 inhibitors. | 156 |
| Figure 5.11: An example of improving metabolic stability by cyclization. | 157 |
| Figure 5.12: Structure of zileuton showing the three groups used to define the structure– | 157 |

metabolism relationships of the N-hydroxyureas.

| | |
|--|-----|
| Figure 5.13: Chemical structures of 5-lipoxygenase inhibitors. | 158 |
| Figure 6.1: CM699 and CM304 structures. | 161 |
| Figure 6.2: Glennon/Ablordeppey“Ar-X5-N” pharmacophore model for high binding affinity at sigma-1 receptor. | 162 |
| Figure 6.3: Selective benzothiazolone, benzoimidazolone and indol-based sigma receptor ligands. | 163 |
| Figure 6.4: Bioisosteric heterocycle rings | 163 |
| Figure 6.5: The Proposed Benzofuran-based Sigma Ligands Pharmacophore. | 164 |
| Figure 6.6: Cocaine self-administration inhibition by CM699 | 173 |
| Figure 6.7: Plasma concentrations after administration of a single i.v. dose of 5 mg/kg produced a C _{max} of 1.84 µg/mL of CM699 at 5 min after injection. | 173 |
| Figure 6.8: CM699 metabolic degradation and possible protection strategy. | 175 |
| Figure 6.9: Sigma ligands developed in our laboratory and optimized for their metabolic stability. | 176 |
| Figure 6.10: The novel CM304 analogs | 179 |
| Figure 6.11: More novel CM304 derivatives. | 180 |
| Figure 7.1: Irreversible binding at sigma-1. | 194 |
| Figure 7.2: Irreversible binding at sigma-2. | 194 |
| Figure 7.3: Metabolic stability results of some CM699 analogs (362, 363, and 365) in | 198 |

human, rat, and mouse liver microsomes.

Figure 7.4: Metabolic stability results of CM699 in human, and rat liver microsomes. 198

LIST OF TABLES

| | |
|--|-----|
| Table 1.1: Selectivity of different enantiomers of SKF-10,047 to receptor sites | 2 |
| Table 1.2: Classification of sigma receptors | 3 |
| Table 1.3: Binding affinities of some sigma receptors endogenous ligands | 6 |
| Table 1.4: Affinities of (E)-8-benzylidene-5-(3-hydroxyphenyl)-2-methylmorphan-7-ones at sigma receptors | 52 |
| Table 1.5: Binding affinities at sigma-1 and DAT | 62 |
| Table 3.1: Affinity of cocaine for σ receptors in mouse (Brain & Heart) | 100 |
| Table 3.2: Structures of BD1008 analogs and their sigma receptors affinities | 102 |
| Table 3.3: Structures of BD1008 analogs (LR series) and their sigma receptors affinities | 103 |
| Table 3.4: Structures of BD1008 analogs (YZ series), and their sigma receptors affinities | 103 |
| Table 3.5: Binding affinities of various compounds to the DAT, σ_1 , or σ_2 receptors | 109 |
| Table 6.1: The newly synthesized benzofuran-based sigma receptor ligands | 164 |
| Table 6.2: Sigma-2 selective ligands previously synthesized in our laboratory | 170 |
| Table 6.3: The synthesized isothiocyanate derivatives and their precursors | 171 |
| Table 6.4: The newly synthesized CM699 analogs | 177 |
| Table 6.5: The newly synthesized CM304 derivatives | 179 |
| Table 7.1: Sigma receptors binding affinities | 186 |
| Table 7.2: Sigma receptors binding affinities for the piperazine derivatives | 188 |
| Table 7.3: Sigma receptors binding affinities for the piperazine derivatives | 189 |

| | |
|---|-----|
| Table 7.4: Sigma receptors binding affinity for the piperazine-2-one derivatives | 189 |
| Table 7.5: Sigma receptors binding affinities for the spiro-derivatives | 190 |
| Table 7.6: Sigma receptors binding affinities for 1,3-dihydro-2H-benzo[d]imidazole-2-one and benzo[d]oxazol-2(3H)-one derivatives | 191 |
| Table 7.7: Sigma receptor binding affinities and selectivity ratios | 193 |
| Table 7.8: The newly synthesized CM699 analogs | 196 |

LIST OF SCHEMES

| | |
|---|-----|
| 1. Scheme 1: Synthetic routes of the 3-ethylbenzofuran derivatives | 202 |
| 2. Scheme 2: Synthetic routes of the 3-butylbenzofuran derivatives | 203 |
| 3. Scheme 3a: Synthetic routes of isothiocyanate derivatives of benzoimidazolone heterocycle ring | 205 |
| 4. Scheme 3b: <i>N</i> -alkylation of 6-nitrobenzo[<i>d</i>]thiazol-2(3 <i>H</i>)-one. | 207 |
| 5. Scheme 4: Synthetic route of 1,3-dihydro-2 <i>H</i> - benzo[<i>d</i>]imidazol-2-one derivatives | 209 |
| 6. Scheme 5: The synthetic routes of the benzoimidazolone derivatives (356), (357), (358), (359), and (360) | 210 |
| 7. Scheme 6: Synthesis of benzo[<i>d</i>]oxazol-2(3 <i>H</i>)-one derivative | 211 |
| 8. Scheme 7: Synthetic routes of benzothiazolone derivatives of isothiocyanate. | 213 |
| 9. Scheme 8: Synthetic route of 6-fluorobenzo[<i>d</i>]thiazol-2(3 <i>H</i>)-one (390) | 214 |
| 10. Scheme 9: Synthetic routes of CM699 analogs | 215 |
| 11. Scheme 10: Synthesis of 3 <i>H</i> -spiro[isobenzofuran-1,4'-piperidine] | 216 |
| 12. Scheme 11: Synthesis of 3 <i>H</i> -spiro[isobenzofuran-1,4'-piperidine] [Different route] | 216 |
| 13. Scheme 12: synthesis of 2'-methyl-3 <i>H</i> -spiro[isobenzofuran-1,4'-piperidine], 489 (WA469) | 217 |
| 14. Scheme 13: Synthesis of spiro[isochromane-1,4'-piperidine]. (493) | 218 |
| 15. Scheme 14: Synthesis of the de-methylated CM699 analog | 219 |
| 16. Scheme 15: Synthesis of 1-methyl-benzo[<i>d</i>]imidazol-2-one derivatives of CM699 | 220 |

| | |
|---|-----|
| 17. Scheme 16: Synthetic routes of spiro[isochromane-1,4'-piperidine] derivatives | 221 |
| 18. Scheme 17: Synthetic route of CM304 derivatives | 222 |
| 19. Scheme 18: Synthetic route of the second series of CM304 derivatives | 224 |
| 20. Scheme 19: Synthetic route of 494 (WA444a) and 461 (WA444b) | 226 |

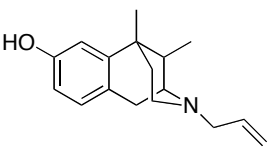
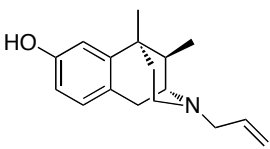
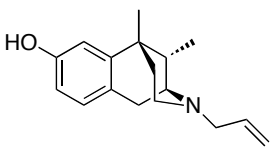
CHAPTER I: INTRODUCTION

1. Sigma receptors

1.1 History

Sigma receptors are a well-defined unique class of receptors, distinct from opioid receptors and phencyclidine binding sites. These receptors are thought to be associated with functions and disorders such as inflammation, depression, anxiety, Alzheimer's disease, epilepsy, drug abuse and cancer. In the beginning, Martin and colleagues¹ described sigma receptors as a subtype of opioid receptors. This classification was based on the psychotomimetic effects of various opioid agonists, including the prototype agonist, (\pm)-SKF 10,047 (N-allylnormetazocine) and related benzomorphans [Table 1.1]. However, in a later study, the (+)-isomer was found to produce actions that were insensitive to opiate antagonists,^{2, 3} while the observed pharmacology with the (-)-isomer was blocked by opiate antagonists such as naltrexone.^{4, 5} The name sigma was originated from the first letter 'S' of the SKF 10,047, which was later found to be a nonselective ligand that binds to multiple receptor proteins.¹

TABLE 1.1: SELECTIVITY OF DIFFERENT ENANTIOMERS OF SKF-10,047 TO RECEPTOR SITES.

| Characteristics | (\pm)-SKF-10,047 | (-)-SKF-10,047 | (+)-SKF-10,047 |
|-----------------|---|--|---|
| Structure |  |  |  |
| Affects | Opioid (μ , κ) receptor, NMDA receptor (PCP site), σ receptors | Opioid (μ , κ) receptor | NMDA receptor (PCP site), σ receptor |

Despite the early blurring history of sigma receptors, they have long been known to be involved in schizophrenia, seizures, anxiety, neuropsychiatric disorders and the psycho-stimulant

effects of drugs of abuse. Based on ligand selectivity in receptor-binding assays and tissue distribution of compound accumulation [Table 1.2], sigma receptors are hypothesized to exist in at least two subtypes, described as the sigma-1 and sigma-2 receptors.⁶⁻⁹

TABLE 1.2. CLASSIFICATION OF SIGMA RECEPTORS.

| Feature | SR1 receptor | SR2 receptor |
|---|---|--------------------------------------|
| Size | 25–29 kDa | 18–22 kDa |
| High tissue expression | Brain, heart, liver, spleen, gastrointestinal tract | Brain, liver, gastrointestinal tract |
| Relative affinity of (+) - benzomorphans | High to moderate | Low |

1.2. Subtypes of sigma receptors

The sigma-1 receptor was first cloned in 1996¹⁰ since then, it has been studied in greater detail because of the defined amino acid sequence and availability of selective sigma-1 ligands. The sigma-2 receptor has not yet been cloned due to the unavailability of detailed protein structural information and truly selective sigma-2 ligands.^{11,12} As a matter of fact, sigma-2 receptors are localized in the lipid rafts that hindered the detergent-extraction process without affecting the structural and functional integrity of this protein.¹³ Also, the amount of sigma-2 protein available in the prepared membranes from mammalian tissues is immensely low compared to the other proteins, which is about 0.1 µg/mg, as indicated by Ruoho et al. in the recent publication.¹⁴

Nevertheless, recently the sigma-2 receptor has been identified as a putative progesterone receptor membrane component 1 (PGRMC1) although there is still a debate in the field that this is the sigma-2 receptor.¹⁵

Most recently, Ruoho et al. published a work that refuting the idea of that sigma-2 receptor and progesterone receptor membrane component 1 (PGRMC1) are co-localized and have the same binding site.¹⁴ The results presented in their study, concluded that both sigma-2 and PGRMC1 proteins are derived from different genes as well as the PGRMC1 has no high affinity for DTG and haloperidol binding sites, indicating that both proteins are not identical.¹⁴

1.2.1. Sigma-1 Subtype

The sigma-1 subtype is well characterized and cloned from a number of different species including human, pig, rat, and mouse.^{10,16,17} It is comprised of 223 amino acids that share more than 90% identity across rodents and humans and less than 30% homology with other mammalian proteins. However, it is homologous in structure to fungal proteins involved in sterol biosynthesis, including yeast sterol isomerase. However, sigma-1 receptors do not possess sterol isomerase activity.¹⁰ They are hypothesized to be composed of two transmembrane (TM) - spanning regions with a C-terminal region enhanced alpha helices and beta sheets, which are believed to be essential for protein-protein interactions.^{16,17} The sigma-1 receptor ligand binding domain has also been identified with the help of protein purification¹⁸ and photoaffinity labeling studies.¹⁹⁻²³ Sigma-1 receptor (SR1) protein consists of three hydrophobic domains and two of these appear to be transmembrane domains. The steroid binding domain like I (SBDLI), steroid binding domain like II (SBDLII) and N-terminal region of transmembrane domain I (TM1) form a portion of the ligand binding site [Fig. 1.1].²⁴⁻²⁷

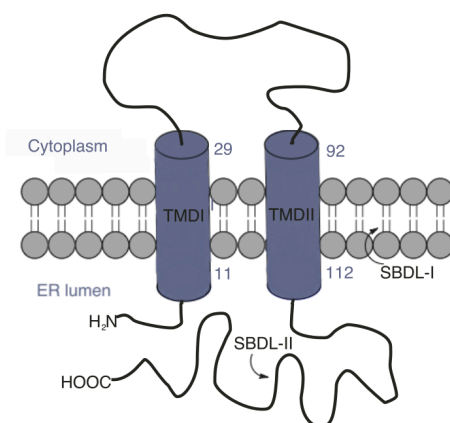


Figure 1.1. Sigma-1 receptor structural representation of the transmembrane domains (TMDI and TMDII) and steroid binding domain-like regions (SBDL-I and SBDL-II). [Adapted from ref. 27]

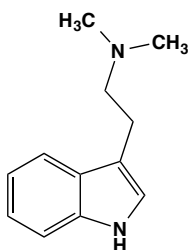
The sigma-1 receptor has been recognized as a chaperon protein located at the endoplasmic reticulum (ER) that modulates calcium signaling through inositol trisphosphate (IP3). A direct protein-protein interaction with another ER chaperone regulates the chaperone activity of sigma-1 receptor binding immunoglobulin protein/78 kDa glucose-regulated protein (BiP/GRP-78).²⁹ Sigma-1 receptors appear to translocate to the proximity of post-synaptic density and regulate various proteins through protein-protein interactions, for example; with GPCRs (e.g., μ opioid and dopamine D₁), and ion channels (e.g., potassium, sodium, and NMDA).²⁹ To date, no endogenous ligands for either subtype have been identified with certainty. Nevertheless, some neurosteroids, such as progesterone, pregnenolone, and testosterone displayed low affinities toward sigma-1 receptor, there has been no evidence to indicate that these neurosteroids play any physiological roles through interaction with this receptor.^{22,31,2} Recently, it was proposed that the *N,N*-dimethyltryptamine (DMT), (**1**) [Tab. 1.3][Fig. 1.2] acts as an endogenous ligand that binds to sigma-1 receptors and inhibits voltage-gated sodium ion [Na⁺] channels in both heterologous cells and native cardiac myocytes that express sigma-1

receptors. Moreover, it was found that DMT has affinity for the sigma-1 receptors falls in the μM range and it is comparable to the affinity of progesterone for the same sigma receptors subtype.³¹

TABLE 1.3. BINDING AFFINITIES OF SOME SR ENDOGENOUS LIGANDS.

| Endogenous Ligands | Affinity [Ki, nM] | |
|---------------------|-------------------|-------------------|
| | Sigma-1 receptors | Sigma-2 receptors |
| DMT | 14750 | 21710 |
| Progesterone | 130 | NA |

Several studies indicate that sigma-1 receptors have numerous implications in CNS functions and conditions including learning and memory (such as depression, anxiety, schizophrenia, psychosis, drug addiction, pain, Alzheimer's disease, Parkinson's disease, amyotrophic lateral sclerosis (ALS), retinal diseases, and stroke)³²⁻³⁴ in addition to their role in cancer,^{35,36} cardiovascular diseases,¹⁸ inflammatory and autoimmune diseases.¹⁹⁻²¹



1, DMT (*N,N*-dimethyltryptamine)

Figure 1.2: The proposed endogenous sigma-1 ligand *N,N*-dimethyltryptamine.

1.2.2. Sigma-2 Subtype

Not much is known about sigma-2 receptors structurally and pharmacologically due to the lack of availability of detailed protein structural information and a truly selective ligand for this subtype. Early photoaffinity-labeling studies have confirmed that the sigma-2 receptor (18–22 kDa) is smaller in size than the sigma-1 subtype (25–29 kDa).^{22,23} Although sigma-2 receptors have been found both in the CNS and in some periphery tissues, such as liver, GI tract, the exact

distribution of sigma-2 receptor is not very clear.⁶ A very recent study has suggested that sigma-2 receptors are a progesterone receptor membrane component 1 (PGRMC1) or localized within it; however, this protein (22 to 28 kDa) is larger than the 18-22 kDa protein mentioned above.¹⁵ Moreover, several studies indicated that sigma-2 receptors are enriched in lipid rafts where they are involved in cholesterol synthesis and calcium signaling through sphingolipid products.^{37,38} Sigma-2 receptors have been located in the various components of the cell such as plasma membrane, mitochondria, lysosomes, and ER, in addition to their association with cytochrome P450 proteins and their interactions, which are still unclear and under investigation. The sigma-2 receptor is highly expressed in various rapidly proliferating cancer cells and regarded as a cancer cell biomarker. Selective sigma-2 ligands have been demonstrated to particularly label the tumor locations, inhibit tumor growth, and induce cancer cells to promote apoptosis³⁹. In addition to the above mention facts, several reported studies have demonstrated that the sigma-2 receptors have many implications in CNS disorders such as depression and drug addiction as well as cancer, and inflammatory and autoimmune diseases.^{19,40,42} However, the lack of structural information of sigma-2 receptor has severely hindered the understanding of its signaling pathways, its physiological roles, and the development of truly selective sigma-2 ligands.

1.3. Anatomical distribution of sigma receptors

Sigma receptors are widely distributed throughout the body. They are highly expressed in the central nervous system and also widely distributed in peripheral organs and tissues.

1.3.1 Nervous system

Sigma receptors are highly concentrated in the central nervous system, where their actions have been extensively studied.⁴³ The highest concentrations of sigma receptors in the brain are found in brainstem motor regions, with significant densities also in limbic structures,

sensory areas, and areas associated with endocrine functions.⁴⁴⁻⁴⁶ Early functional studies was confirmed the role of sigma receptors in motor functions consistent with the enrichment of sigma-2 receptors in the substantia nigra.⁴⁸ Subsequent anatomical and functional studies have confirmed the involvement of both sigma-1 and sigma-2 subtypes in motor function.^{44,45,47} Sigma-1 receptors are predominantly distributed in the areas that are involved in memory, emotions, sensory and motor functions. They are concentrated in the hippocampus, hypothalamus, cerebral cortex, and various motor and cranial nuclei as well as dorsal horn in the spinal cord.⁴³⁻⁵²

In a collaborative work with McCurdy's lab, James and colleagues radiolabelled the highly selective sigma-1 ligand, CM304, with fluorine-18 to trace the radiotracer [¹⁸F]-CM304 in living subjects.⁵³ The *in vivo* kinetics of [¹⁸F]-CM304 were evaluated in mice using small animal PET. In which, brain PET scanning began 1 min prior to administration of [¹⁸F]-CM304 and stopped 60 min later. It was found that the [¹⁸F]-CM304 reached its maximum uptake in mouse brain within the first few minutes of imaging and gradually washed out to 65% of its maximum at 60 minutes after the administration as can be seen in the baseline time-activity curve illustrated in Figure 1.3.

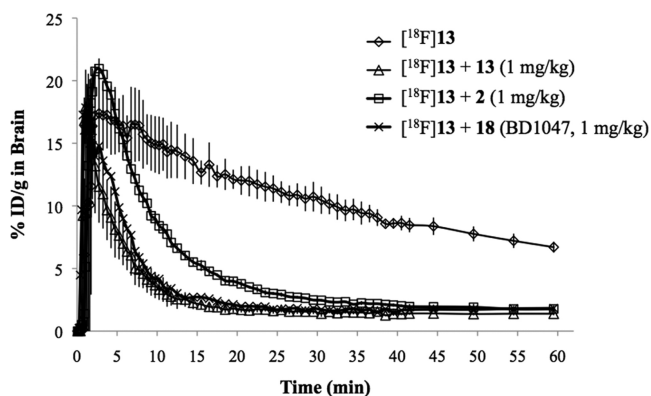


Figure 1.3: Time-activity curves (TACs) from mouse positron emission tomography studies. TACs represent accumulation of [¹⁸F]CM304 in whole mouse brain as a function of time for baseline, preblock with haloperidol, preblock with CM304, and preblock with [¹⁸F]CM304.⁵³

Subsequently, PET imaging in mice provided visual evidence that [^{18}F]CM304 was able to pass easily through blood brain barrier (BBB) and indicated to accumulate in the regions that well known for being rich of sigma-1 receptors. In order to get better and accurate interpretation of radioligand localization in particular brain regions, an ex vivo autoradiography was conducted, and the results from this study revealed that [^{18}F]CM304 accumulated in the midbrain, hippocampus, cortex, facial nucleus, and to a lesser extent in the cerebellum and thalamus as can be seen in Figure 1.4.⁵³

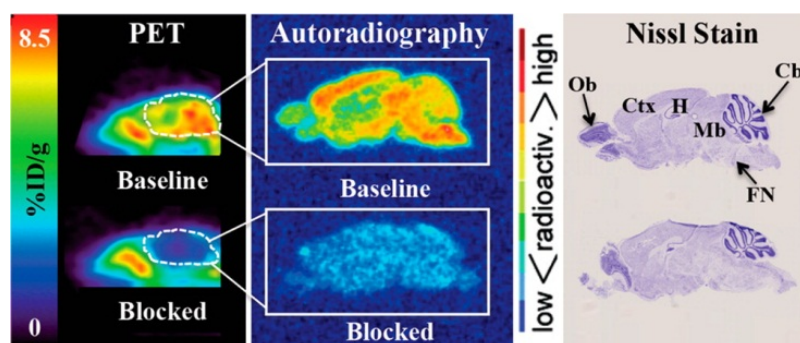


Figure 1.4: PET images and ex vivo autoradiography of sagittal brain sections (12 μm) obtained 60 minutes after administration of [^{18}F]CM304. Sections used for autoradiography were stained with Nissl for anatomical correlation. PET images were acquired just before perfusing mice and harvesting brain tissue for autoradiography. White dotted lines designate location of mouse brain in sagittal PET images: Cb = cerebellum, Ctx = cortex, FN = facial nucleus, H = hippocampus, Mb = midbrain, Ob = olfactory bulb.⁵³

Further studies by James and colleagues evaluated the distribution, kinetics and stability of [^{18}F]CM304, in rats and squirrel monkeys brains using PET.⁵⁴ In these studies, rats were administered [^{18}F]CM304 intravenously, and static PET scans were measured after 50 minutes. For blocking studies, rats were pretreated with SR1 selective ligand BD1047 10 min prior to tracer administration. A CT image was acquired after each PET scan to provide an anatomic reference frame for the respective PET data. After PET imaging, the rats were sacrificed and the brains were removed that allowed for autoradiography to be achieved. The baseline PET/CT

images shown in (Figure 1.5) again illustrated [¹⁸F]CM304's ability to cross the blood-brain barrier (BBB) and accumulate in brain tissue. Furthermore, the PET/CT images disclosed some accumulation of radioactivity in the rat skull. Also, accumulation of [¹⁸F]CM304 was located in the brain stem, cortex, cerebellum, hippocampus hypothalamus, thalamus, nucleus oculomotor, red nucleus, and caudate putamen. There was little uptake of [¹⁸F]CM304 in the corpus callosum and muscle. The ratio of brain-to-skull uptake at 60 min was found 3.1 ± 0.2 . Both blocking studies showed a reduction in the uptake of [¹⁸F]CM304.⁵⁴

Consequently, preliminary brain PET imaging of squirrel monkeys was conducted to assess the regional distribution and brain permeability of [¹⁸F]CM304 in a nonhuman primate.⁵⁴ A total of four brain PET images were attained. The monkeys were administered intravenously with [¹⁸F]CM304 in 500 microliters of sterile heparinized saline, followed by 500 microliters of sterile heparinized saline to flush the catheter. Seventy-five frames of dynamic PET data were yielded over a 120-minute period.

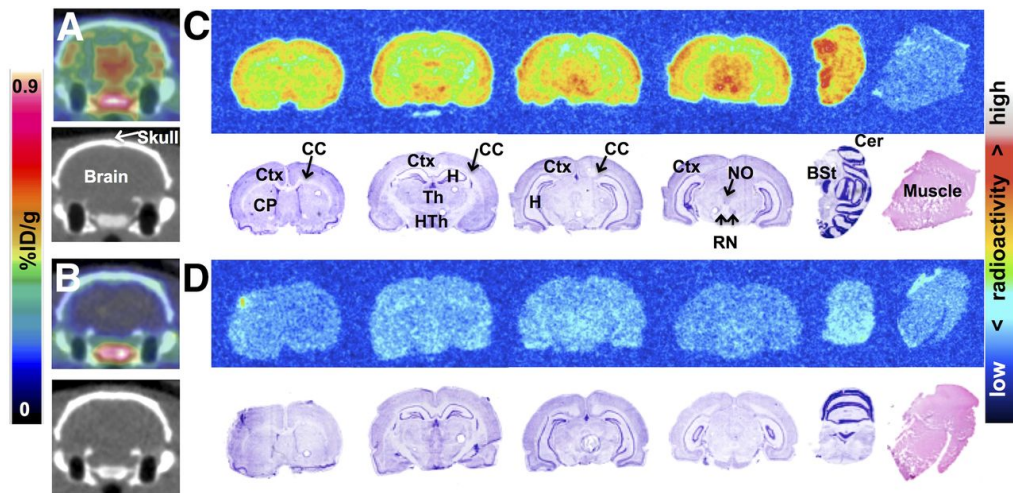


Figure 1.5: Rat brain PET/CT and ex vivo autoradiography. (A) Baseline coronal PET/CT images 50-60 minutes after intravenous administration of [¹⁸F]CM304. (B) PET/CT images from blocking study. (C) Autoradiography and nissl/H&E staining of coronal brain and muscle sections from baseline study. (D) Autoradiography and nissl/H&E staining of coronal brain and muscle sections from blocking studies. Bst = brain stem; CC = corpus callosum; Cer = cerebellum; CP = caudate-putamen; Ctx = cortex; H = hippocampus; HTh = hypothalamus; NO = nucleus oculomotor; RN = red nucleus; Th = thalamus.⁵⁴

Blocking studies involved pretreating monkeys with haloperidol 10 minutes prior to radioligand administration. Baseline brain PET/MR images in [Figure 1.6] indicate that [¹⁸F]-CM304 was able to penetrate the monkey blood brain barrier (BBB) and accumulate in the cingulate, frontal cortex, occipital cortex, parietal cortex, temporal cortex, vermis, hippocampus, striatum, and cerebellum. PET images also showed some accumulation of radioactivity in the monkey skull [Figure 1.6]. It was found also the brain-to-skull ratio at 60 min after injection was 1.2 ± 0.1 .⁵⁴

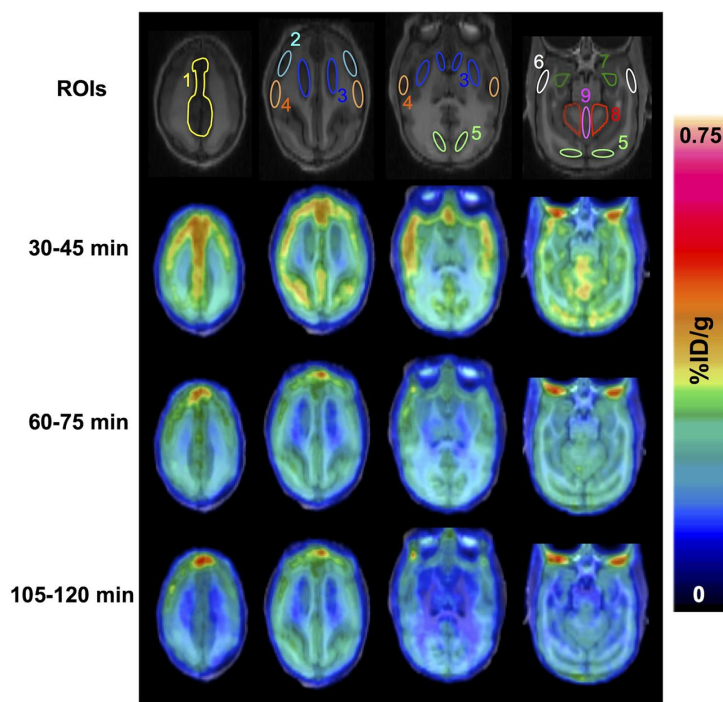


Figure 1.6: Monkey brain PET/MR images from baseline dynamic imaging. Summed axial images are shown for different time intervals after administration of [¹⁸F]CM304. Brain regions of interest are shown in MR images and are labeled as (1) cingulate cortex, (2) frontal cortex, (3) striatum, (4) parietal cortex, (5) occipital cortex, (6) temporal cortex, (7) hippocampus, (8) cerebellum, and (9) vermis.⁵⁴

In detailed study, Bouchard and Quirion were able to discriminate between the two subtypes of sigma receptors and showed that sigma-1 and sigma-2 receptors are differentially distributed in the brain.⁴⁴ They conducted autoradiographic studies using [³H]-DTG (2) (with the

presence of (+)-pentazocine, (**3**) [Fig. 1.7], and showed the sigma-2 distribution in the rat brain, where only few areas in the brain are specifically enriched with sigma-2 receptors such as the substantia nigra pars reticulata, central gray, oculomotor nucleus, nucleus accumbens, cerebellum, and motor cortex area.⁴⁴

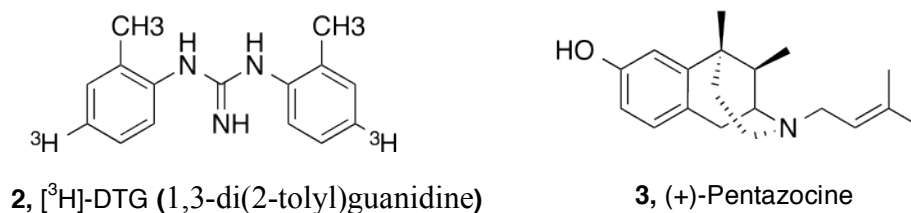


Figure 1.7: Structures of selective sigma ligands

1.3.2. Peripheral organs

In addition to the central nervous system, sigma receptors are also widely distributed in peripheral organs. A number of autoradiographic and binding assays studies showed that sigma receptors are enhanced in the mucosal and submucosal regions (GI tract), with less labeling in the muscular regions.⁵⁵ Furthermore, numerous studies showed sigma-1 receptors are also present in the liver^{23,29,56}, kidney²⁵, heart^{57,58}, spleen⁵⁹ and sexual organs.⁵⁷ Sigma-2 receptors are similar to sigma-1 receptors, have been found in various organs, including liver and kidney.²³ However, the actions of sigma-1 are believed to dominate over those of the sigma-2 subtype. It has been reported that the highest levels of both sigma receptor subtypes in the body are present in the liver.²³ Likewise, it was found the heart contains significant levels of sigma receptors, over 80% of these receptors are of the σ_1 subtype.⁶⁰ Similarly, the lung, the spleen and the eye are enriched in sigma-1 receptors,⁶¹ while gastrointestinal tract and kidney contain both sigma-1 and sigma-2 receptors.^{58,60,61}

1.4. Subcellular distribution and functions of sigma receptors

Early studies on subcellular distribution of sigma-1 receptors with radioligand binding experiments using sigma-1 radioligands [^3H](+)-pentazocine (**4**), [^3H](+)-SKF-10,047 (**5**), and [^3H](+)-3-PPP (**6**) [Fig. 1.8] confirmed the existence of sigma-1 receptors in mouse, rat and guinea pig brain membranes.^{10,62} It was found to be abundant in the microsomal membranes of the endoplasmic reticulum (ER) as well as in nuclear, mitochondrial and synaptic membranes.⁶³⁻

65

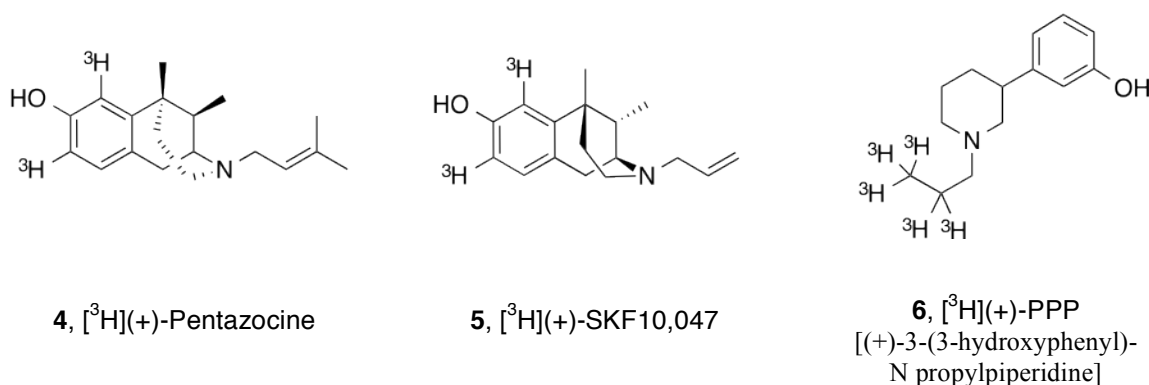


Figure 1.8. Tritiated sigma receptor radioligands.

Further immunohistochemical studies showed that sigma-1 receptors in the endoplasmic reticulum in neurons⁶⁶ besides several other cells such as oligodendrocytes⁶⁷ lymphocytes⁶⁸, retinal cells⁶⁹ and particular cancer cells.⁷⁰ Furthermore, electron microscopy studies in neurons from the rat hypothalamus and hippocampus, evidenced that sigma-1 receptors localize with the membrane of mitochondria, neuronal perikarya, some cisternae of the endoplasmic reticulum (ER) and dendrites.⁶² A recent study demonstrated that sigma-1 receptors are chaperon proteins clustered at the mitochondria-associated ER membrane (MAM).²⁸ The activity of this chaperon protein is regulated through a direct protein-protein interaction with another ER chaperone named binding immunoglobulin protein/78 kDa glucose-regulated protein (BiP/GRP-78).^{28,71}

Under normal conditions, sigma-1 receptors bind to BiP and upon sigma-1 receptor agonists binding or Ca^{2+} depletion in the ER, sigma-1 receptors dissociate from BiP, and shifting to the active state as a result of this dissociation. Alternatively, sigma-1 receptor antagonists enhance the binding of BiP with sigma-1 receptors and inhibit the agonists action as a result.^{28,33,71}

Under resting conditions, sigma-1 receptors regulate inositol triphosphate (IP_3) receptors via direct influx of calcium (Ca^{2+}) from MAM to mitochondria that activates the ATP generation through the tricarboxylic acid cycle (TCA) as well as production of the reactive oxygen species (ROS).²⁸ A study by Hayashi et al. showed that sigma-1 receptors mobilize at ER from MAM to more peripheral subcellular locations under cellular stress or ligand activation.⁷² Upon ligand activation, sigma-1 receptors translocate to the proximity of the cell membrane to participate in protein–protein interactions and modulate the activity of GPCRs such as μ opioid and dopamine D_1 , ion channels such as potassium, sodium, and NMDA, or signaling molecules such as calcium, protein kinases, and inositol phosphates.^{16,73-76} Similarly, numerous studies suggest that neuroactive steroids bind with moderate affinity to sigma-1 receptors that may modulate the activity of GABA and NMDA receptors in the CNS.^{77,78} These findings indicate the potential role of sigma-1 receptors in several neurological diseases, pain, amnesia, schizophrenia, depression, and neuroprotection.^{32,79,80}

Numerous pharmacological studies indicated that sigma-2 receptors might be lipid raft proteins that affect calcium signaling through sphingolipid products.^{37,38} Contrasting sigma-1 receptors, sigma-2 receptors do not seem to translocate and much less is known about sigma-2 receptor. For instance, the lack of structural information of sigma-2 receptor has severely hindered the understanding of its regulatory roles, its function, and its signaling pathways. Although, sigma receptors are widely distributed in the body and bind to a vast range of normal

tissues, both subtypes are highly expressed on tumor cell lines from human and rat tumor tissues. Nevertheless, there is evidence in the literature that sigma-2 receptors show a higher expression in malignant tumor cells than quiescent tumor cells.⁸¹⁻⁸³ Further studies showed increased expression of both sigma receptors in a variety of human and rodent cell lines can be used as a biomarker of tumor cell proliferation, which is making them a useful tool for imaging of cancers.⁸⁴ Recently, a photoaffinity binding study with a novel sigma-2 ligand (WC-21, (**7**)) compared with the PGRMC1 ligand (AG-205, (**8**))[Fig. 1.9], identified PGRMC1 as the putative sigma-2 receptor binding site.⁸⁵

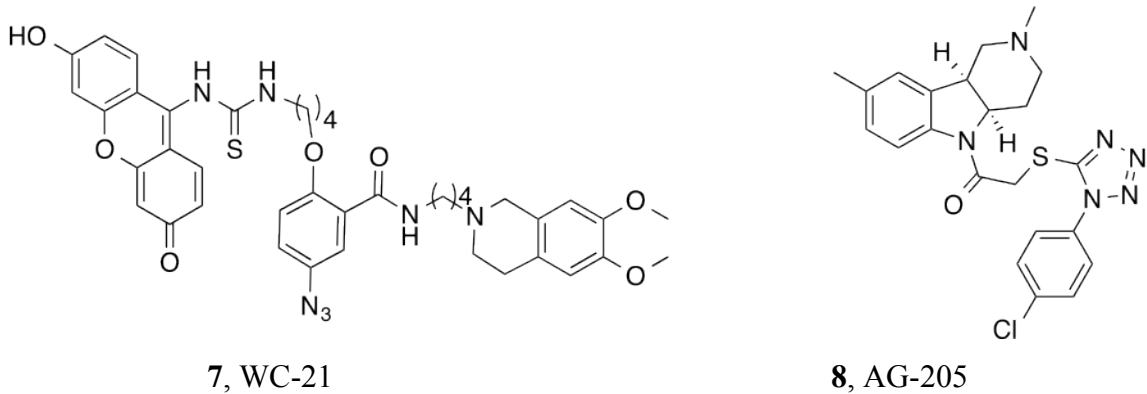


Figure 1.9: Structures of the selective sigma-2 ligand (WC-21) and PGRMC1 ligand (AG-205)

PGRMC1 protein has been shown previously to be implicated in regulation of steroid signaling, activation of cytochrome P450 (CYP450), anti-apoptosis, stimulation of tumor growth, pro-invasion, and metastasis.^{86,87} These findings suggest that PGRMC1 and sigma-2 receptors as a complex may couple with EGFR (epidermal growth factor receptor), mTOR (mammalian target of rapamycin), caspases, and ion channels.⁸⁸ Based on some recent published data, Huang et al. hypothesized that sigma-2 receptor stimulates EGFR signaling that may be the main carcinogenic pathway for this receptor. Furthermore, it may also activate CYP450 and promote sterol signaling, which may also be pro-oncogenic. Consequently, the inhibition of sigma-2

receptor by sigma-2 ligands may activate the caspase pathway and block the EGFR signaling pathway.⁸⁸

1.5. The Role of Sigma Receptors in Diseases

Since the discovery of the sigma receptors, multiple preclinical studies have implicated the receptor in several diseases. Through a variety of ways, sigma receptors strongly modulate the intracellular calcium concentration in both neuronal and non-neuronal cells.^{7,28,63,69,89,90} However, it is not clear whether this calcium regulation is mediated by sigma-1, or sigma-2, or both. By contrast, most of these effects seem to be mediated through indirect pathways.

Several studies have shown that sigma-1 receptors can translocate from the mitochondria associated membrane (MAM) at endoplasmic reticulum (ER) to other areas of the cell where they can interact with a variety of membrane proteins.^{72,89} These proteins include voltage-gated ion channels, glutamate and GABA ionotropic receptors, the dopamine D1 receptor (D1R), muscarinic and nicotinic acetylcholine receptors, neurotrophic tyrosine kinase receptor type 2 (TrkB), and intracellular targets, such as inositol triphosphate (IP3) receptors and kinases.^{89,91} Therefore, sigma-1 receptors have been implicated in many CNS disorders, including alcohol and cocaine addiction, Alzheimer's disease, amnesia, depression, age-related cognitive impairments, neuropathic pain, and stroke.

1.5.1. Sigma receptors potential role in addiction and drug abuse

Number of studies has demonstrated the crucial roles that sigma-1 receptors activation may play in addiction since it's well known for their involvement in serotonergic and dopaminergic systems. Cocaine and methamphetamine are the most common abused drugs that perform their psychostimulant actions by interacting with sigma receptors and mostly sigma-1 receptors.⁹²⁻⁹⁵

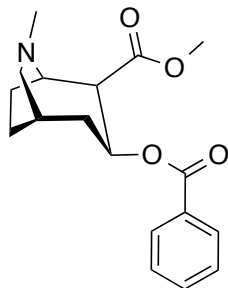
i) Cocaine

Cocaine (9)[Fig. 1.10] is one of the most highly consumed illicit drugs in the world, especially in United States. The use and abuse of cocaine is well known as a leading cause to many social and economic problems with an increased risk of HIV, hepatitis B, and C infections, and an increased incidence of crime, violence and psychosocial problems. Furthermore, there are no approved medications to treat cocaine abuse or addiction, which urges the need to develop novel and effective agents to battle this serious issue.⁹⁶

Nevertheless, opioid receptors have been investigated actively for their role in treatment of drug addiction. For instance, Kappa opioid receptors have been demonstrated to impact stress-induced drug and alcohol seeking behavior.^{97,98} It has been reported that stress is able to enhance drug and alcohol self-administration, and stimulation of the kappa receptor potentiates this effect. Conversely, blocking the kappa receptor with an antagonist inhibits stress-induced increases in cocaine self-administration and alcohol intake. It was also reported that kappa receptors and its endogenous ligand (dynorphin) are increased in the brains of cocaine abusers who died from cocaine toxicity.^{99,100} There has been great interest in developing a kappa antagonist for the treatment of addiction, however, clinical development of several kappa antagonists was halted as a result of vital side effects. For example, Pfizer has terminated the clinical studies with the developed kappa antagonist PF4455242 for toxicity reasons.¹⁰¹ Likewise, the National Institute on Drug Abuse ceased the translation of a kappa antagonist to human studies due to heart rhythms problems.^{101,102}

Cocaine is well known for its inhibition effect on dopamine transporters that results in a dopamine increase in the synapse, which plays a significant role in the behavioral effects of cocaine. Similarly, cocaine can bind to sigma receptors and activate them to produce their

stimulant effects. In actual fact, selective sigma receptor drugs modulate monoaminergic, and particularly dopaminergic and serotonergic, systems.^{87,88,90}



9. Cocaine

Figure 1.10: Chemical structure of cocaine

Several studies have demonstrated the ability of sigma receptor antagonists to attenuate a variety of behaviors that are elicited by acute administration of cocaine.^{6,92,93} Both sigma receptor subtypes appear to regulate the actions of cocaine; however, the role of sigma-2 receptors in these effects is less clear due to the lack of truly selective sigma-2 receptor ligands. Cocaine preferentially binds to sigma-1 receptors with a 10-fold higher affinity over sigma-2 receptors (K_i 2-7 mM and 29-31 mM, respectively). Cocaine is believed to activate sigma receptors and recent studies demonstrate that sigma-1 receptor activation plays an important role in reinforcement and addictive processes.^{6,92,93,95,103} Furthermore, several studies showed that co- or pre-administration of sigma-1 antagonists blocked the hyper-locomotion, sensitization, or the appetitive effect of cocaine using the conditioned place preference paradigm.¹⁰⁴ It is documented that sigma-1 receptor antagonism attenuates cocaine-induced stimulant effects and toxicities. For instance, many studies have reported that sigma-1 receptor antagonists such as haloperidol, rimcazole, BD1008 (**10**)[Fig. 1.11], BMY14802 (**11**)[Fig. 1.11] as well as anti-sense oligonucleotides mitigate the acute locomotor stimulatory effects, sensitization and convulsions induced by cocaine in rats.¹⁰⁴⁻¹⁰⁶ A recent behavioral studies performed in mice, intraperitoneal

or oral dosing with SN79 (**12**)[Fig. 1.11] before a convulsive or locomotor stimulant dose of cocaine resulted in a substantial mitigation of cocaine-induced convulsions and locomotor activity. In the same study, it has been also shown a significant attenuation in the development and expression of the sensitized response to repeated cocaine exposures.¹⁰⁷ Similarly, pretreatment of male mice with CM156 (**13**)[Fig. 1.11], prior to administering either a convulsive or locomotor stimulant dose of cocaine, resulted in a significant attenuation of these acute effects. CM156 also significantly reduced the expression of behavioral sensitization and place conditioning induced by sub-chronic exposure to cocaine.¹⁰⁸ In a separate study, CM156 a novel antagonist with high selectivity and affinity for sigma receptors was used to attenuate the expression of cocaine-induced conditioned place preference in mice. After microarray data analysis, four genes were found to be up-regulated and changes by cocaine when compared with controls.¹⁰⁹ This study suggests that the sigma receptor antagonist CM156 reverses alterations in gene expression that are associated with cocaine-induced reward, which provides another evidence for the potential use of sigma receptor antagonists in treatment of drug abuse.¹⁰⁹

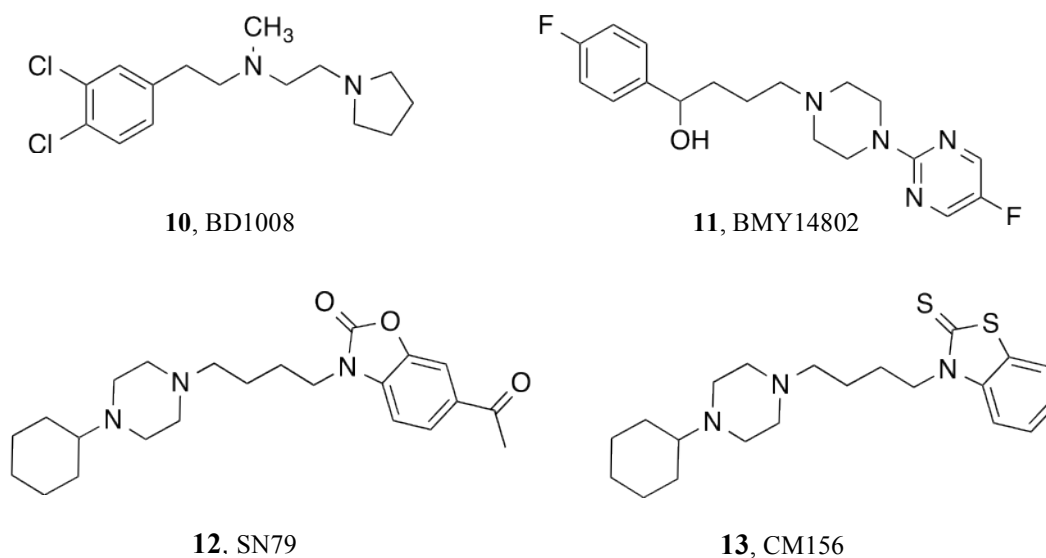
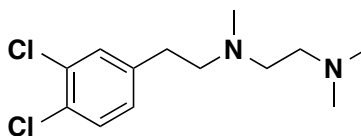


Figure 1.11: Structures of some selective sigma-1 antagonists

Alternatively, selective sigma-1 receptor agonists often mimic the actions of cocaine or shift the dose–response curve for cocaine to the left.^{92,106,110} Due to the fact that cocaine appears to act as an agonist at sigma receptors, several findings suggest that sigma receptor antagonists could alter the reinforcing effects of cocaine. A study by Martin-Fardon *et al.* (2007)¹¹¹ demonstrated the effect of sigma-1 receptor antagonist (BD1047 (**14**))[Fig. 1.12] on cocaine self-administration. In this study, BD1047 did not block the self-administration of cocaine, but did attenuate the cocaine reinstatement, demonstrating that sigma-1 receptors may play a role in the reinstatement induced by cocaine priming manipulations.¹¹¹ More recently, Hiranita *et al.*, provided a proof-of-concept showing that dual sigma receptor/DAT inhibitors effect cocaine self-administration in a dose-dependent manner to decrease cocaine self administration.¹¹²



14, BD1047

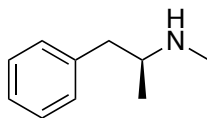
Figure 1.12: Structure of the selective sigma-1 antagonist, BD1047.

ii) Methamphetamine

Similar to cocaine, methamphetamine (**15**)[Fig. 1.13] is a psychostimulant, which is considered to be among the most abused substances worldwide. To date, there are no FDA approved medications to treat the harmful health consequences resulting from either cocaine or methamphetamine abuse.¹¹³ Like cocaine, methamphetamine binds to sigma receptors with a slight preference for sigma-1 receptors (2 μ M) over sigma-2 receptors (47 μ M).

The ability of BD1063 (**16**)[Fig. 1.14] and BD1047 (**14**)[Fig. 1.12] to significantly attenuate the locomotor stimulatory effects of methamphetamine suggested that antagonizing

sigma-1 receptors is enough to prevent the stimulant actions of methamphetamine.¹¹⁴



15, Methamphetamine

Figure 1.13: Chemical structure of methamphetamine

Additionally, a number of studies reported that sigma-1 receptor selective antagonists block the behavioral sensitization caused by methamphetamine in rats.¹¹⁵⁻¹¹⁷ Matsumoto *et al.* showed that AC927 (**17**)[Fig. 1.14], a highly selective sigma receptor ligand, attenuated a number of methamphetamine-induced effects, including hyperthermia, cytotoxicity in a neuronally-derived cell line, hyperlocomotion, and dopamine damage in the brain.¹¹⁷ Prior to this work, the selective sigma-1 ligand MS-377 (**18**)[Fig. 1.14] was reported to attenuate the development of behavioral sensitization induced by sub-chronic treatment with methamphetamine.¹¹⁶ In house work, the highly selective sigma receptors ligand CM156 (**13**)[Fig. 1.14] evaluated against methamphetamine-induced stimulant, hyperthermic, and neurotoxic effects. In this study, the highly selective sigma ligand CM156 was able to attenuate the effects of methamphetamine.¹¹⁸ Subsequently, the sigma receptor antagonist SN79 (**12**)[Fig. 1.14], that was developed in our laboratory was able to block methamphetamine-induced microglial activation and cytokine production, which has potential to mitigate the neurotoxic effects of methamphetamine.¹¹⁹ A more recent study conducted by Seminerio *et al.* showed AZ66 (**19**)[Fig. 1.14], a selective sigma receptors ligand, not only blocked the development of behavioral sensitization, but also significantly reversed the expression of methamphetamine-induced sensitization.¹²⁰ AZ66, a mixed SR1/SR2 antagonist derived from CM156 and improved

for metabolic stability, was found to significantly attenuate dopaminergic neurotoxicity and memory impairment produced by frequent exposure to methamphetamine.^{120,121}

Thus, sigma receptors are a valid and novel target for developing effective therapeutics for the treatment of methamphetamine and cocaine induced effects and could possibly be involved in the effects of other psychostimulant drugs.

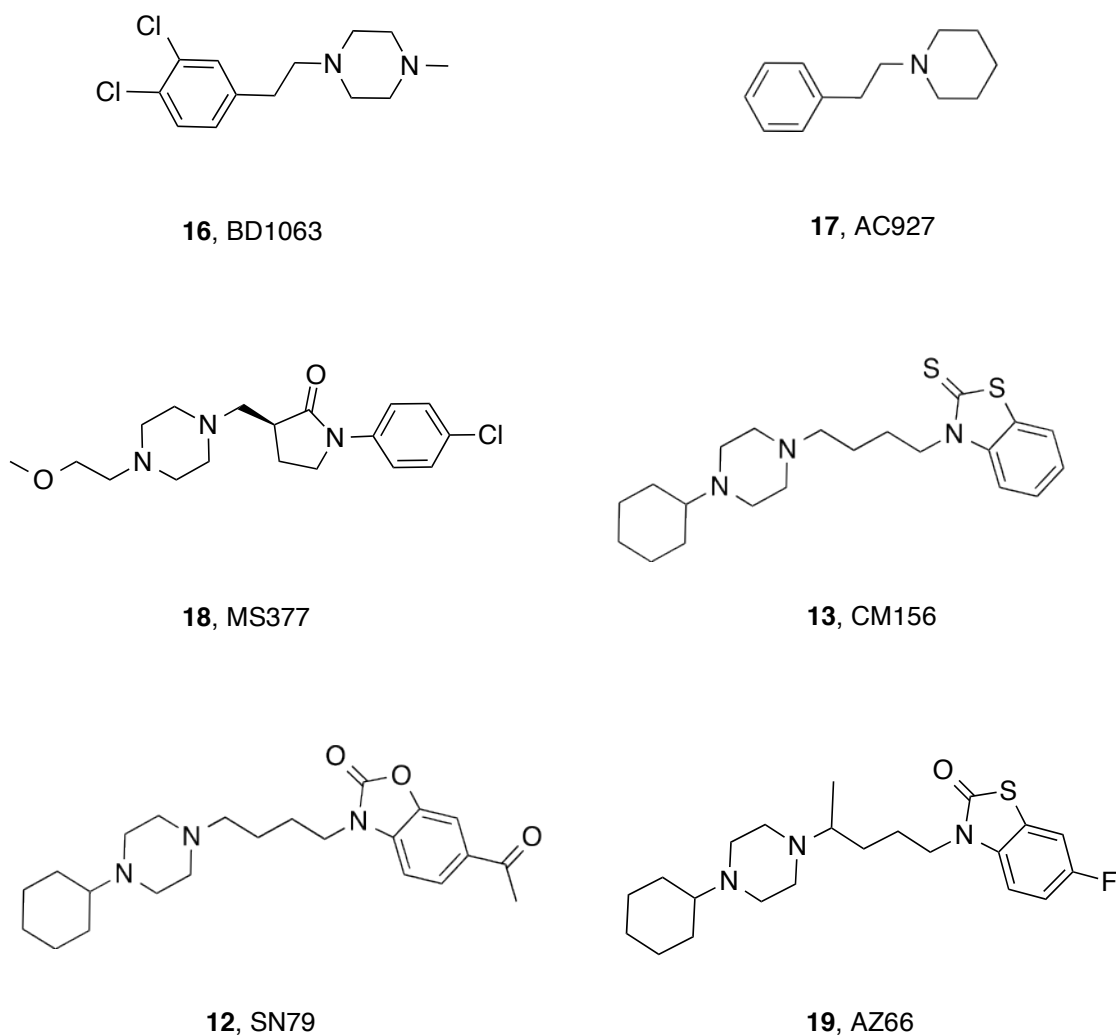
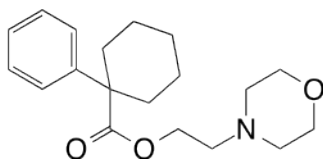


Figure 1,14: Structures of various sigma ligands

iii) Alcohol

According to SAMHSA's National Survey on Drug Use and Health (NSDUH), more

than half of all adults drink alcohol, with 6.6% meeting criteria for an alcohol use disorder [outlined in the Diagnostic and Statistical Manual of Mental Disorders (DSM)].¹²² Among Americans aged 12 or older, the use of illicit drugs has increased over the last decade from 8.3% of the population using illicit drugs in the past month in 2002 to 9.4% (24.6 million people) in 2013.¹²³ Accumulating data indicate that sigma receptor antagonism could mitigate the actions of alcohol even though alcohol does not have significant affinity for sigma receptors. Sigma receptor antagonists have been shown to attenuate ethanol-induced effects such as; locomotor activity, place conditioning, taste conditioning, and self-administration in excessive ethanol drinking models. Moreover, sigma receptor antagonists have been reported to attenuate these same behaviors in NMDA independent, long-term potentiation in early adolescent exposed animals.^{124,125} The effect of ethanol on sigma-1 receptors was first, studied by Maurice et al., 2003 in the conditioned place preference test.¹²⁴ In this study, the sigma-1 receptor agonist, PRE-084 (**20**)[Fig. 1.15], increased the ethanol-induced conditioned place preference in a dose-dependent manner whereas the sigma-1 receptor antagonist, BD1047, dose dependently attenuated ethanol-induced locomotion and blocked ethanol-induced place and taste conditioning.¹²⁴ In another study, the sigma-1 receptor antagonist, BD1063, was found to decrease ethanol self-administration and reinforcing effects of ethanol in two different models of excessive ethanol intake.¹²⁵



20, PRE084

Figure 1.15: Structure of sigma-1 agonist, PRE084.

A gene expression study, Miyatake *et al.*, linked sigma-1 receptor polymorphisms to

alcoholism. Analysis of 307 alcoholic and 302 control subjects, found polymorphisms in the 5'-upstream region: T-485A and TT-241-240.¹²⁶ Additionally, it was realized that the transcriptional activities of the A-485 and TT-241-240 alleles were significantly reduced, indicating a higher expression of sigma receptors. The gathered data in this study, suggested that a lower expression of sigma-1 receptors, supposedly seen in control subjects as implicated by the gene reporter assay, protect those people from alcoholism.¹²⁶ Ethanol does not seem to interact with sigma receptors; however, based on the above studies it has been hypothesized that sigma-1 receptor might be involved in neuroadaptive mechanisms that lead to chronic ethanol abuse. Thus, sigma-1 receptors are correlated to the drug abuse behaviors in a similar way to those seen with methamphetamine and cocaine.

1.5.2. Sigma receptors and analgesia

Sigma receptors are highly distributed in areas of great importance in pain control in the central nervous system. These areas include the superficial layers of the spinal cord dorsal horn, the locus ceruleus, the periaqueductal gray matter, and rostral ventral medulla.^{127,128} The involvement of sigma receptors in opioid analgesia was first reported in the 1990s.¹²⁹ Shortly thereafter, a study by Mei & Pasternak, showed that sigma-1 receptors were involved in the analgesia mediated by mu-, delta-, and kappa (1&3) opioid receptors.¹³⁰ In earlier studies they found that the sigma receptor antagonist, haloperidol (**21**)[Fig. 1.16], potentiates opioid-induced analgesia while the sigma receptor agonist (+)-pentazocine attenuates opioid analgesia.^{131,132} Consequently, another study by Cendan et al., showed that pain resulting from formalin-induction was decreased in sigma-1 receptor knockout mice.¹³³ Furthermore, intrathecal (i.t.) administration of the sigma-1 receptor antagonist BD1047, in mice reduced formalin-induced pain and attenuated the phosphorylation of N-methyl-D-aspartate (NMDA) receptor subunit 1

induced by formalin.¹³⁴ The neurosteroid sigma-1 receptor agonist, DHEA (**22**)[Fig. 1.16], induced a rapid pronociceptive action in sciatic-neuropathic rats. Furthermore, the sigma-1 receptor antagonist, BD1047, blocked the transient pronociceptive effect provoked by DHEA.¹³⁵

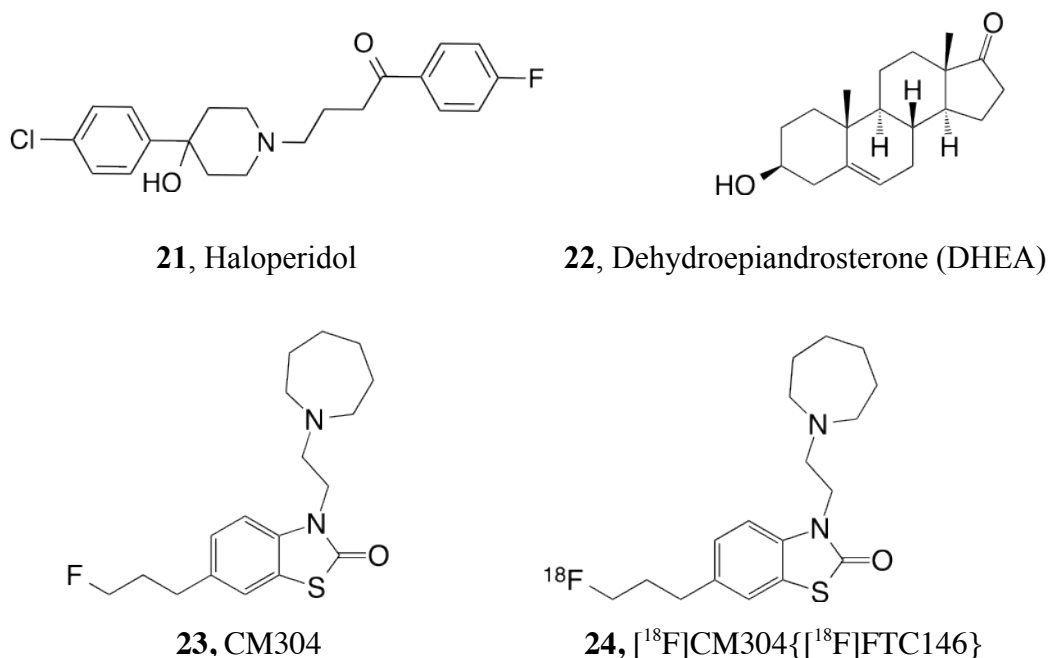


Figure 1.16. Sigma-1 receptor ligands and analgesia.

It has been demonstrated that the sigma-1 receptor facilitates (+)-morphine induced anti-analgesia via actions at supra-spinal and spinal sites.¹³⁵⁻¹³⁷ Also, some other reports showed that opioid ligand-induced antinociception is mitigated by sigma-1 agonists and potentiated by sigma-1 antagonists.¹³⁸⁻¹⁴¹ Although results from the above mentioned studies have demonstrated strong evidence that sigma-1 receptors affect opioid analgesia, the exact molecular mechanism needs to be definitively established and certainly warrants further investigation.

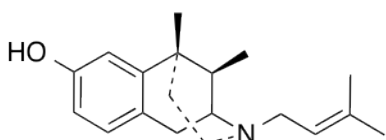
In different studies, it was indicated that sigma-1 antagonists were able to attenuate painful behavior in inflammatory pain and neuropathic models efficiently.¹⁴²⁻¹⁴⁵ There is an

accumulated evidence in literature demonstrated that peripheral pain injury initiates multiple structural and functional changes in peripheral, spinal cord, and supraspinal sites that contribute to the development of neuropathic pain. Moreover, it was found that injured sensory neurons have reduced voltage-gated Ca^{2+} influx and decreased intracellular Ca^{2+} stores, which can be related to a potential role of sigma-1 receptor in neuropathic pain since store depletion triggers sigma-1 receptor, and consequently, stimulation of sigma-1 receptors decreases intracellular Ca^{2+} .¹⁴⁶⁻¹⁴⁹ Recently, the highly selective sigma-1 radioligand, ^{18}F -CM304 (^{18}F -FTC146)(**23,24**)[Fig. 1.16] was studied by PET/MRI a neuropathic pain in animal model that showed a high accumulation of the radioligand at the site of the nerve injury. This finding provides a strong evidence for involvement of sigma-1 receptor in peripheral neuropathic pain, which can be very useful in diagnosis and treatment of nerve injury-induced neuropathic pain. Also, it's noteworthy to mention that the ^{18}F -CM304 (^{18}F -FTC146) has been approved by the FDA in May 2015 to initiate first human studies on peripheral neuropathic pain.

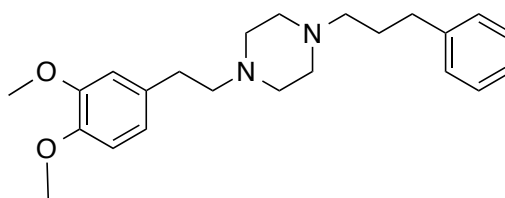
1.5.3. Sigma receptors and depression

Some neurotransmitter systems such as serotonergic and glutamatergic systems are involved in the pathophysiology of depression. Likewise, sigma-1 receptor ligands play a modulatory role in several neurotransmitter systems. A number of behavioral studies have demonstrated the effect of sigma-1 ligands on the antidepressant activity of the existing antidepressant drugs. Several available antidepressant drugs, such as tricyclic antidepressants, monoamine oxidase inhibitors, selective serotonin reuptake inhibitors (SSRIs), and latest generations of antidepressant drugs, bind to sigma receptors.¹⁵⁰ Numerous sigma-1 agonists decreased immobility in the forced swimming test, which was blocked by several sigma-1 antagonists. These sigma-1 agonists include the following; (+)-pentazocine (**3**), SA4503 (**25**),

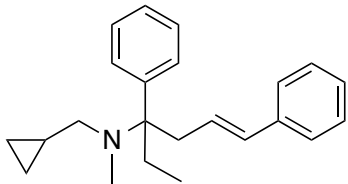
JO-1784 (**26**), DHEAS (**27**), donepezil (**28**), pregnenolone sulfate (**29**), UMB23 (**30**), and others [Fig. 1.17].^{91,151-155} Moreover, the selective sigma-1 agonists (+)-pentazocine and SA4503 reduced immobility time in the tail suspension test, and this effect was antagonized by NE-100 (**31**)[Fig. 1.17] a sigma-1 antagonist.¹⁵⁶ The sigma-1 receptor agonist igmesine (JO-1784) has shown antidepressant activity in the olfactory bulbectomy (OBX) depression model.¹⁵⁶ On the other hand, the selective sigma-2 receptor ligand siramesine (**32**)[Fig. 1.17] demonstrates antidepressant activity in the chronic mild stress model of depression.¹⁵⁷



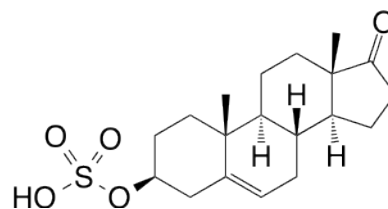
3, (+)-Pentazocine



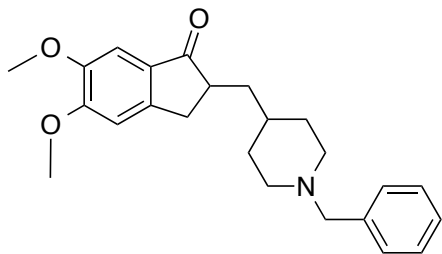
25, SA4503



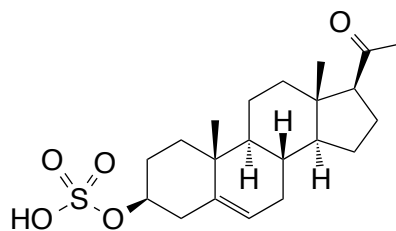
26, Igmesine (JO-1784)



27, Dehydroepiandrosterone Sulfate (DHEAS)



28, Donepezil



29, Pregnenolone Sulfate

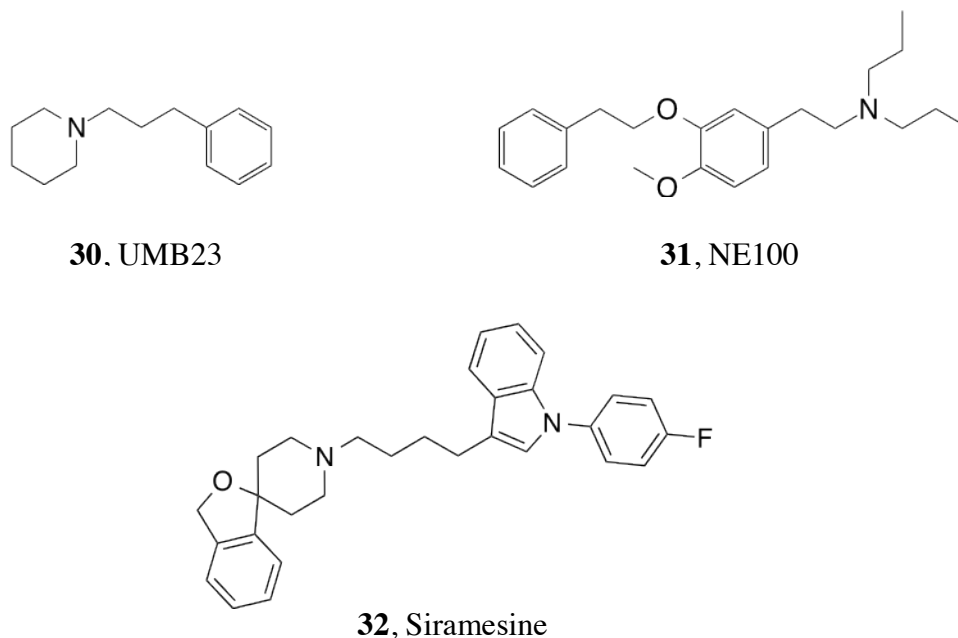


Figure 1.17: Sigma receptors ligands and depression.

Based on the above-mentioned studies, there are three lines of evidence confirmed that sigma-1 receptor agonists can employ an effective antidepressant activity:

- Sigma-1 agonists can potentiate NMDA or cholinergic neurotransmission as they improved cognitive activity in various amnesia models.¹⁵⁸
- Sigma-1 agonists can behave as antidepressants as demonstrated in a study utilizing low doses of the antidepressant sertraline, a selective serotonin reuptake inhibitor (SSRI). Also clorgyline, a monoamine oxidase inhibitor, selectively potentiated the effect of N-Methyl-D-aspartate receptor (NMDAR).¹⁵⁹
- Selective serotonin reuptake inhibitors (SSRIs) and tricyclic antidepressants (TCAs) showed discrepancy in binding affinity to sigma-1 receptors. For instance, fluvoxamine and sertraline have a K_i values lower than 100 nM at sigma-1 receptors.¹⁶⁰

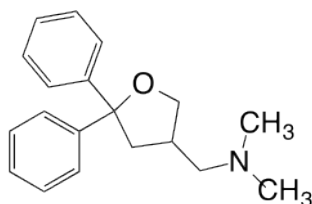
1.5.4. Sigma receptors and Alzheimer's disease

A number of accumulated reports have indicated that sigma receptors play a part in complex biological processes of the central nervous system, which can be implicated in neurodegenerative disorders such as Alzheimer's disease.^{161,162} Alzheimer's disease is an irreversible progressive neurodegenerative disorder damaging the brain structure and characterized by:

- 1) Presence of extracellular senile plaques composed of insoluble extracellular aggregates of amyloid- β (A β) proteins derived by proteolytic cleavage of the amyloid precursor protein, and/or
- 2) Presence of neurofibrillary tangles composed of intracellular deposits of paired helical filaments of hyperphosphorylated Tau proteins.^{163,164}

Some selective sigma-1 ligands, such as (+)-pentazocine, PRE-084, or SA4503 attenuated, in a dose dependent and bell-shaped manner, the memory deficits observed in mice seven days after β 25–35 peptide injection.¹⁶⁵ Similarly, when the selective sigma-1 ligand, PRE084, or the non-selective ligands which act also as sigma-1 agonists, like donepezil (cholinesterase inhibitor) and ANAVEX1-41 (**33**)[Fig. 1.18] (muscarinic receptor ligand), were injected together with β 25–35 peptide into mice, blocked the β 25–35 peptide-induced toxicity in the hippocampus and also attenuated the learning and memory deficits in mice.^{164,165} Nevertheless, an *in vitro* study by Marrazzo et al., in 2005 showed the first evidence that sigma-1 receptor ligands could display some neuroprotective activity against amyloid toxicity, and interestingly enough the neuroprotective effects of these compounds were blocked by the sigma-1 receptor antagonist, NE-100.¹⁶⁶ In a recent study, Li *et al.* group¹⁶⁷, 2010 demonstrated that the neurosteroid dehydroepiandrosterone (DHEA) dose-dependently attenuated the A β 25–35-induced neuronal loss by activating sigma-1 receptor. They also indicated that the DHEA effect

could be produced by the sigma-1 receptor agonist, PRE-084 and that the DHEA effect was blocked by the sigma-1 receptor antagonist NE-100.¹⁶⁷ The above observations indicate that the sigma receptor ligands might have therapeutic potential in Alzheimer's disease and potentially, other neurodegenerative disorders.



33, ANAVEX1-41

Figure 1.18: Non-selective sigma ligands and Alzheimer's disease.

1.5.5. Sigma receptors and schizophrenia

The dopamine hypothesis remains the dominant hypothesis for the pathophysiology of schizophrenia, which involves enhanced mesolimbic dopamine and glutamate functions as well as the intricate relationship between dopamine, glutamate, and sigma receptors in this disorder.¹⁶⁸ As a matter of fact, the blockade of NMDA receptors by phencyclidine (PCP) induces schizophrenia-like psychosis in humans. Schizophrenia is characterized by positive symptoms such as delusions and hallucinations, negative symptoms such as “flat affect”, and cognitive impairments.^{169,170} However, antipsychotic drug development in schizophrenia has focused mainly on agents that reduce the positive symptoms of schizophrenia.¹⁷¹ Although several antipsychotics possess high affinities for sigma receptors (e.g. haloperidol), the involvement of sigma receptors in schizophrenia has not been clearly demonstrated.²⁰ The nonselective sigma-1 receptor antagonist BMY14802 (**11**), panamesine, E5842 (**34**) [Fig. 1.19] and MS377 (**18**) [Fig. 1.14] inhibit apomorphine-induced climbing.¹⁷²⁻¹⁷⁵ Furthermore, DTG (**35**) [Fig. 1.19], SR31742A (**36**) [Fig. 1.19], panamesine (**37**) [Fig. 1.19], rimcazole and E5842

inhibit amphetamine-induced locomotor activity.^{172,173,176,177} However, rimcazole (**38**) [Fig. 1.19] and BD1047 had little effect on apomorphine-induced climbing, furthermore this latter compound had little effect on acute amphetamine-induced hyperlocomotion. Although rimcazole has a substantial affinity for sigma receptor and was proposed as a treatment for schizophrenia, research was halted due to initiation of seizures.^{178,179} Moreover, a number of post-mortem studies have exhibited abnormalities in glutamate concentrations and glutamate receptor densities in schizophrenic brains, in addition to some biochemical and behavioral studies have suggested that antipsychotic drugs may alter NMDA receptor functions.

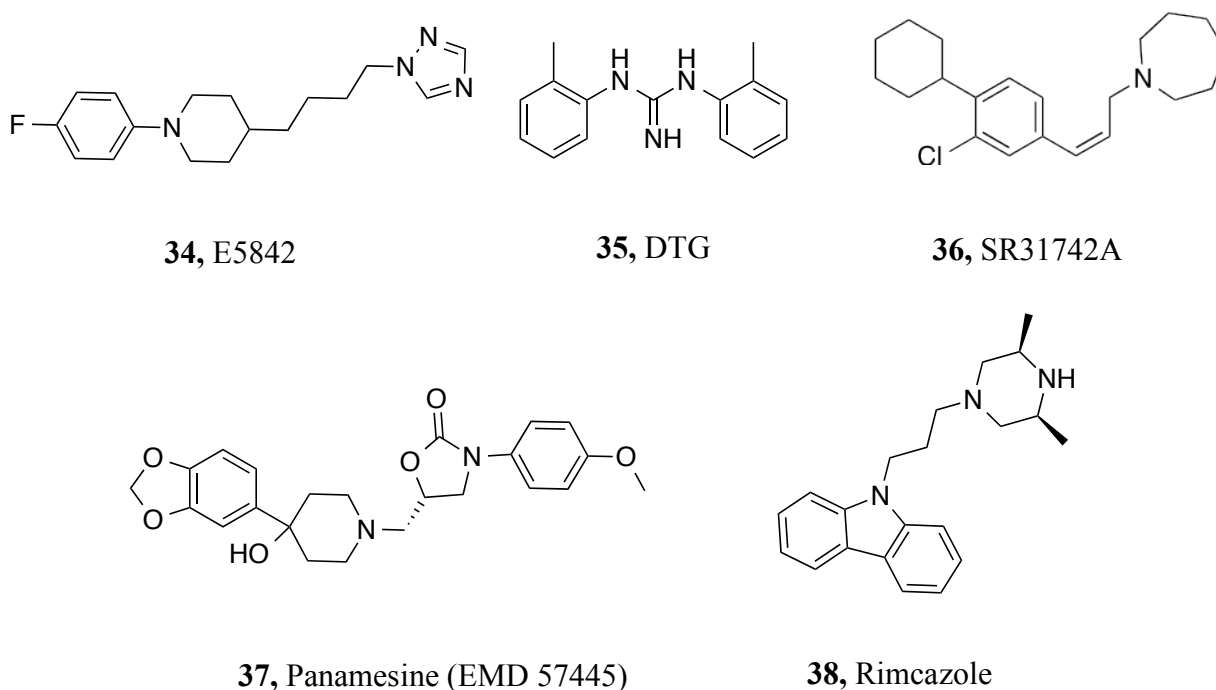


Figure 1.19: Sigma receptors ligands cited for their role in Schizophrenia.

1.5.6. Sigma receptors and cancer

The role of sigma receptors in cancer has received much attention from researchers since the discovery of the presence of these receptors in several human and rodent cancer cell lines.^{180,181} In 2004, Spruce *et al.*, showed that sigma receptor ligands including: rimcazole,

haloperidol, BD1047, and BD1063, caused a dose and time dependent decline in cell viability in tumor cell lines.¹⁸¹ Subsequently, Wang *et al.* in the same year (2004) found that sigma-1 receptors were expressed in those cells and that the sigma-1 receptor antagonists, haloperidol, and progesterone produced a dose-dependent inhibition of the growth of those cells at high concentrations.¹⁸² Subsequently, a study conducted by Aydar *et al.* , in 2006 found that human breast cancer cell lines expressed much higher levels of sigma-1 receptors, which significantly reduced the cancer cell line's proliferation by siRNA compared to that of control cells.¹⁸³ Likewise, sigma-2 receptors and their role in cancer are much more important and active area of the cancer research than sigma-1 receptors. A number of studies have identified the sigma-2 receptor as a biomarker for proliferating tumor cells.^{83,184} Furthermore, several studies by Bowen and coworkers found that sigma-2 agonists are able to mediate a novel caspase-independent apoptotic pathway containing ceramide in numerous breast tumor cell lines.^{38,185,186} Subsequent studies by Vilner *et al.* have shown that there was a high density of sigma-2 and sigma-1 receptors in a wide variety of human and murine tumor cells.¹⁸⁰ Similarly, a study by Ostenfeld *et al.*,¹⁸⁷ (2005) found that the selective sigma-2 ligand, siramesine, was able to cause tumor cell death through a caspase-independent mechanism. Further work identified this activity could be related to or involve autophagosomes and lysosomes.^{188,189} More recently, Haller *et al.*, (2012)¹⁹⁰ reported that sigma-2 receptors have a 10-fold higher density in proliferating tumor cells than in quiescent tumor cells and because of this observation, sigma-2 receptor agonists are able to kill tumor cells via apoptotic and non-apoptotic mechanisms. Subsequently, Mach *et al.* reported a MicroPET imaging study of the benzamide ⁷⁶Br- labeled radiotracer analog (**39**)[1.20] in an EMT-6 tumor-bearing mouse showed high uptake of the radiotracer in the tumors and low uptake in the surrounding normal tissues [Fig. 1.20].^{189,190}

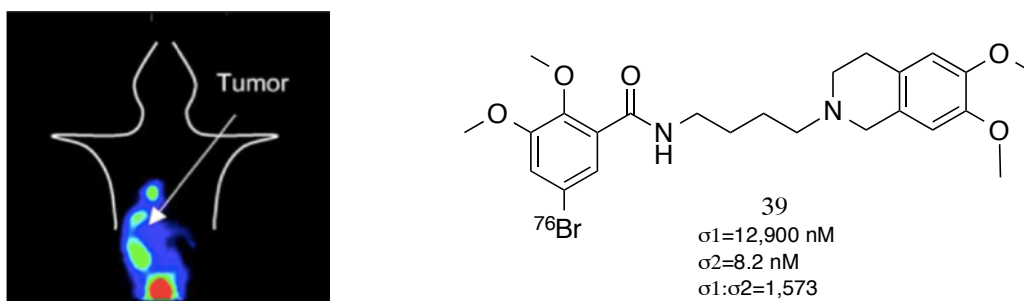


Figure 1.20. MicroPET imaging study of [^{76}Br] radiotracer in an EMT-6 tumor-bearing mouse. Structure and in vitro binding affinities (K_i values) of the ^{76}Br -labeled benzamide analog.¹⁹⁰

1.6. Endogenous and exogenous sigma receptors ligands

1.6.1 Endogenous ligands

To date, no endogenous ligands have been identified for either sigma receptor subtype. However, certain neurosteroids, such as progesterone (40) [Fig. 1.21], testosterone (41) [Fig. 1.21], and pregnenolone (42) [Fig. 1.21], displayed low affinities for sigma-1 receptor. There is no evidence to indicate that these neurosteroids play any physiological roles through interaction with this receptor.²⁰ Therefore, it has been hypothesized that sigma receptors are remotely linked to enzymes of steroid biosynthesis.¹⁹¹ In recent study N, N-Dimethyltryptamine (DMT) (1) has been identified as a potential endogenous ligand for sigma-1 receptors while the physiological concentration in the brain tissues is very low and thus its role as a sigma-1 modulator needs to be confirmed.¹⁹² Furthermore, neuropeptide Y and peptide YY have been proposed as endogenous ligands for sigma receptors.¹⁹³ Due to the lack of availability of detailed protein structural information and truly selective sigma-2 ligands, much less is known about sigma-2 receptor, its function, and its regulatory roles.

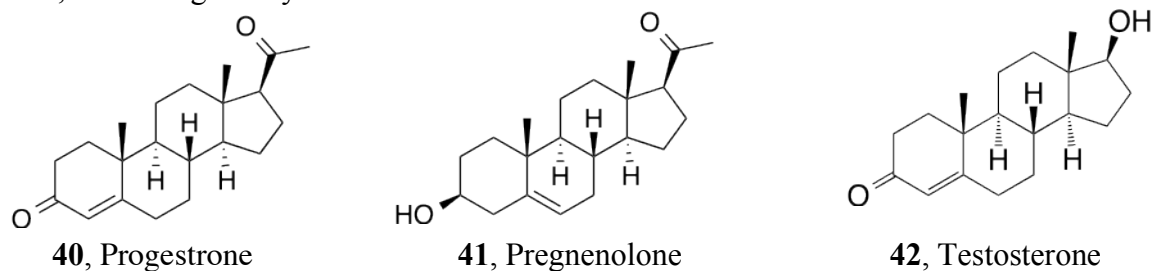
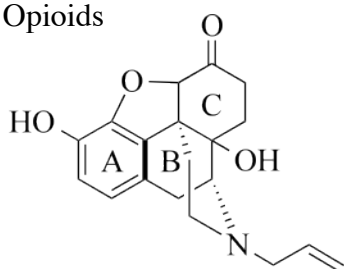


Figure 1.21: Structures of neurosteroids that proposed to act as endogenous ligands for sigma receptors.

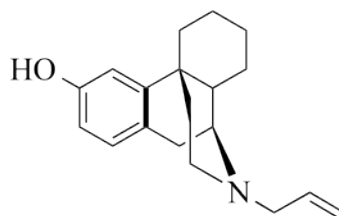
1.6.2. Exogenous ligands

Due to the fact that sigma receptors bind to compounds with diverse structures, initial studies with early sigma ligands were limited. It was assumed that sigma receptors might have good flexibility at the active site, or these diverse agents might be sharing some common features. Apparently, the lack of selective compounds that do not interact with other biological systems, urges the need for developing such selective compounds to explore the unknown biological functions displayed by sigma receptors. It was noticed that the importance of basic nitrogen for a compound to have sigma receptors affinity.¹⁹⁵ The initial efforts started by evaluation of structural determinants from various drug classes.¹⁹⁶ The early observation was that three drug classes, opioids, morphinans and benzomorphan with more bulky compounds had lower affinity [Fig. 1.22]. Hence, the smaller benzomorphan, which lack the C ring, had better affinity than the other two classes. It appears that lipophilic substituents are preferred for high affinity agents. The fourth early-identified class is phenylpiperidine that includes fentanyl and meperidine. Also, these compounds showed higher affinity for sigma receptors than bulky opioids and morphinans as can be seen in [Figure 1.22].

i) Opioids

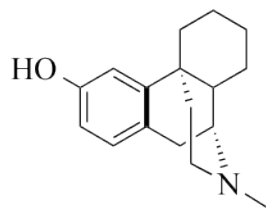


43, Naloxone
 $IC_{50} > 100,000$ nM

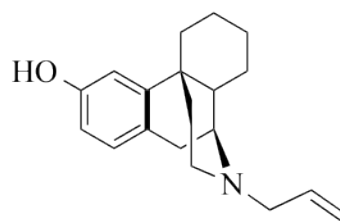


44, Levallorphan
 $IC_{50} = 1890 \pm 140$ nM

ii) Morphinans

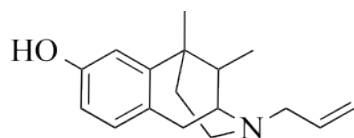


45, Levorphanol
 $IC_{50} > 10,000$ nM

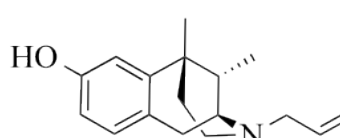


46, Levallorphan
 $IC_{50} = 1890 \pm 140$ nM

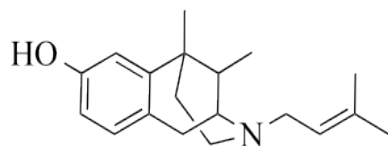
iii) **Benzomorphans**



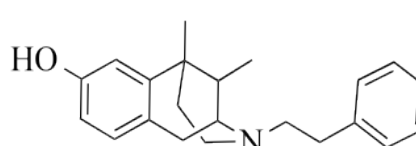
47, (±) SKF10,047
 $IC_{50} = 395 \pm 14$ nM



48, (+)-SKF10,047
 $IC_{50} = 365 \pm 14$ nM

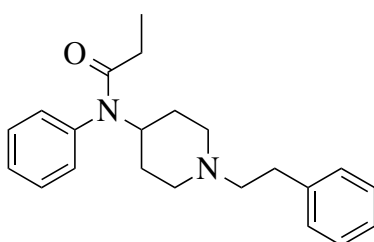


49, (±) Pentazocine
 $IC_{50} = 25 \pm 2$ nM

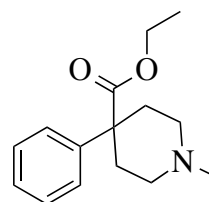


50, (±) Phenazocine
 $IC_{50} = 46 \pm 10$ nM

iv) **Phenylpiperidines**



51, Fentanyl
 $IC_{50} = 354 \pm 52$ nM



52, Meperidine
 $IC_{50} = 2290 \pm 430$ nM

Figure 1.22: Diverse structural classes of sigma ligands and their affinities.

Sigma receptors are an interesting group of receptors because of their broad accommodation of diverse structural groups.¹⁹⁷⁻¹⁹⁹ Therefore, they have been presented to bind a variety of drug classes including, for example, anxiolytics, antipsychotic agents (eg. butyrophenones, phenothiazines, thioxanthenes), tricyclic antidepressants (TCAs), monoamine oxidase inhibitors (MAOIs), antineoplastic agents, anticholinergics, inhibitors of cytochrome oxidase, steroids such as progesterone (**40**) [Fig. 1.23], DHEA (**22**) [Fig. 1.23] and pregnenolone (**41**) [Fig. 1.23], drugs of abuse such as cocaine (**9**) [Fig. 1.23], methamphetamine (**13**) [Fig. 1.23], methylenedioxymethamphetamine (MDMA)(**53**) [Fig. 1.23], and phencyclidine.^{197,199}

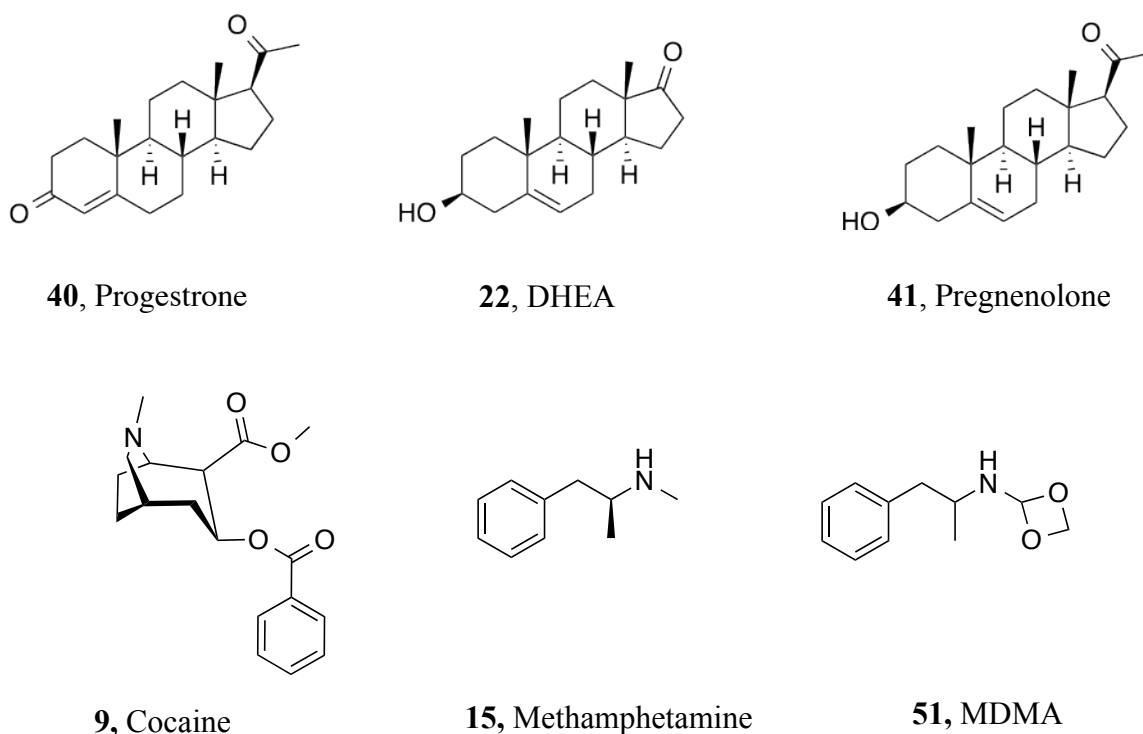
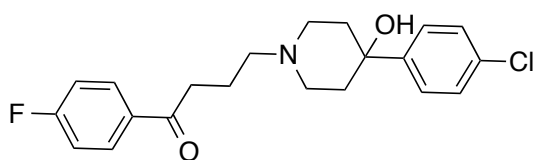


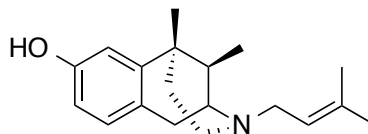
Figure 1.23: Variety of structural classes of sigma ligands.

Consequently, a variety of compounds with different structural and pharmacological entities showed considerable affinity for sigma receptors, for example, haloperidol⁷² (**21**),

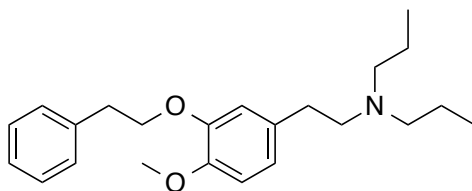
benzomorphans like (+)-pentazocine (**3**), alkylamines like NE100 (**31**),²⁰⁰ phenylalkylpiperidine²⁰¹ (**54**), phenylalkylpiperazine²⁰¹ (**55**), and octahydro[*f*] benzoquinolone (**56**), [Fig. 1.24].²⁰²



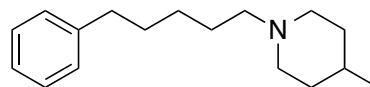
21, Haloperidol
 $K_i, \sigma_1 = 0.65$ nM



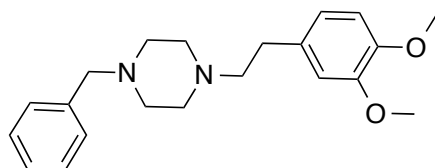
3, (+) Pentazocine
 $K_i, \sigma_1 = 1.03$ nM



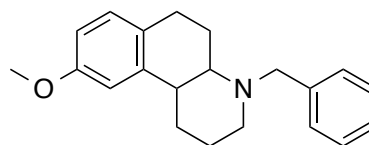
31, NE-100
 $K_i, \sigma_1 = 1.03$ nM



54, Phenylalkylpiperidine
 $K_i, \sigma_1 = 0.07$ nM



55, Phenylalkylpiperazine
 $K_i, \sigma_1 = 1.75$ nM



56, Octahydrobenzo[*f*]quinolone
 $K_i, \sigma_1 = 5.0$ nM

Figure 1.24: Various sigma ligands with different structural entities.

Prior to the identification of sigma receptors, there were two main issues hindered the development of pharmacophore models for sigma receptors:

- 1) Till 1992 sigma receptor ligands were assumed to bind to a lone homogenous receptor.
- 2) Structural diversity of compounds were found to bind sigma receptors with high affinity.

Thus, over the last four decades, tremendous efforts were put forth to find a universal pharmacophore model to explain the diversity of binding ligands. Gilligan *et al.*,²⁰² in 1992 identified a lead compound with selectivity for sigma receptors ($K_i = 6$ nM). In this model they divided the lead molecule to four regions consistent with four pharmacophore elements as follow[Fig. 1.25].²⁰²

- a) A distal aromatic ring (Region A)
- b) A nitrogen heterocycle (Region C)
- c) A space between the heterocycle and the distal aromatic ring (Region B)
- d) A substituent on the nitrogen heterocycle (Region D).

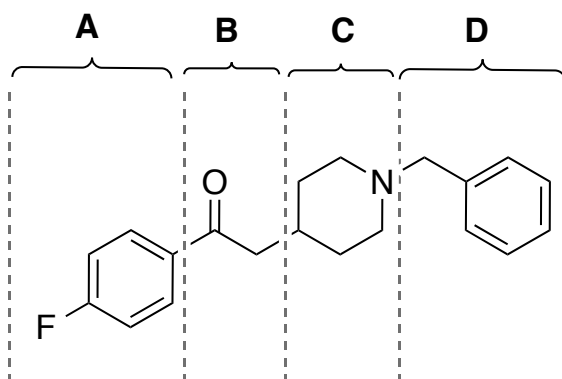


Figure 1.25: The four regions proposed by Gilligan *et al.* for the binding of lead molecule.²⁰²

After testing a variety of structural compounds, they came up with the conclusion that four specific pharmacophore elements important to optimal sigma binding and oral activity in antimescaline or anti-aggression tests. For sigma-1 receptor binding, the ligand should have: a) a basic nitrogen atom, b) two hydrophobic groups with different distances from the basic N atom, and c) a H-bonding center midway between the basic N and the distal hydrophobic site [Fig. 1.26].

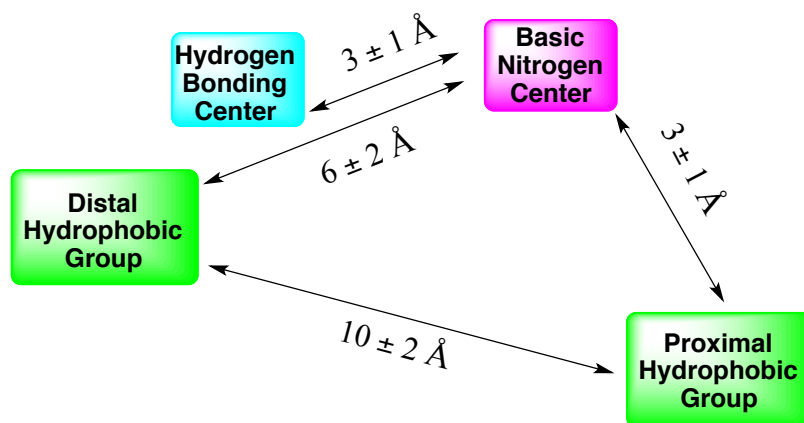


Figure 1.26: The Proposed Gilligan Model for sigma-1 receptor binding.[Adapted from ref. 202]

In this model, Gilligan *et al.* illustrated the preference of the aromatic rings at the distal hydrophobic site for optimal *in vivo* activity. Moreover, they found that the chemical nature of the N-substituent and the distance and orientation between the basic nitrogen and the proximal hydrophobic moiety play a significant role in selectivity between sigma receptors binding and dopamine D₁ and serotonin 5HT₂ receptors binding.²⁰²

Later, Glennon and Ablordeppy identified a pharmacophore model for binding of benzomorphan analogs at sigma receptors as a result of continued studies that begun in late 1980s. It was found that the non-rigid substructure phenylethylamine (**58**) [Fig. 1.27] of benzomorphan (**57**) [Fig. 1.27], still has affinity for sigma receptors and that affinity varied, depending upon stereochemistry and the nature of R and X.²⁰³ Compound **58** was one of the highest affinity with 165-fold higher affinity than N-allylnormetazocine derivative (if R= -CH₂-C₃H₅). Subsequently, it was obvious that the rigid benzomorphan structure was not critical for high-affinity binding. Further study of SAR discovered that a phenylpentylamine moiety, not phenylethylamine moiety, in compound (**59**) [Fig. 1.27]. was significant for high affinity.^{203,204}

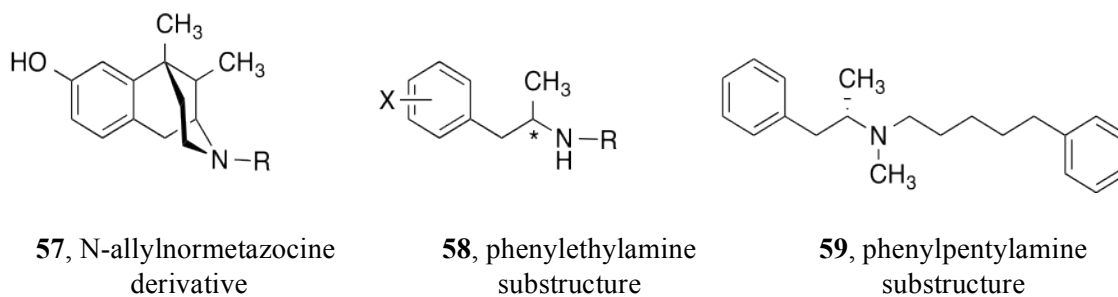


Figure 1.27: The non-rigid sigma benzomorphan substrates

Also, it was found both secondary and tertiary amines able to bind; however, with tertiary amines, one of the amine substituents could not be much larger than a methyl group [Fig. 1.28].

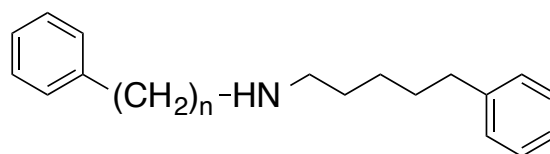


Figure 1.28 Structures of phenylpentylamines

Furthermore, when phenyl rings are replaced with cyclohexyl rings, the affinity was retained indicating that the interaction with sigma receptors involves a hydrophobic interaction rather than aromatic interaction; thus, phenyl rings had no significance for affinity with sigma receptors and they could be removed without loss in affinity, for example compound **60** ($K_i = 2.6$ nM) and compound **61** ($K_i = 2.4$ nM) [Fig. 1.29]. This finding, denoting the existence of a hydrophobic pocket in the sigma receptors.^{205,206}

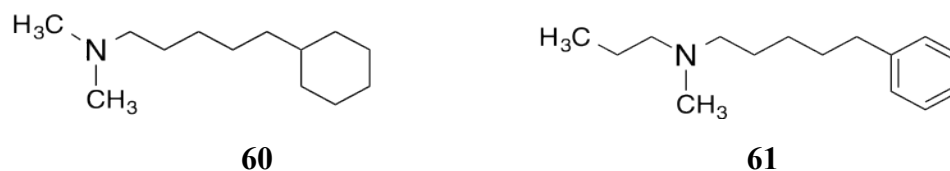


Figure 1.29: Structures of other phenylpentylamines and the effect of aromaticity on affinity

Consequently, the authors examined the role of the basic nitrogen, and they found that the

removal of the piperidine nitrogen of compound (**62**)[Fig. 1.30] reduced the affinity toward sigma receptors ($K_i, \sigma_1 > 36,000$ nM) compared to compound (**63**)[Fig. 1.30] ($K_i, \sigma_1 = 38$ nM), demonstrating the importance of the basic nitrogen for sigma-1 receptor binding.

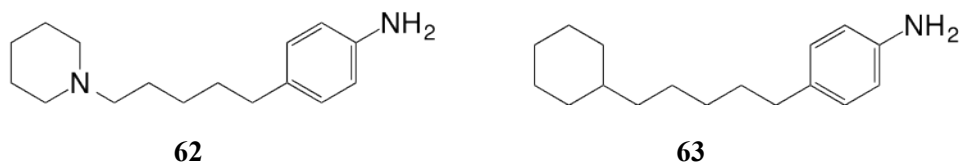


Figure 1.30: Structures of compounds 62 and 63 and importance of basic nitrogen.

Next, researchers examined the phenylpiperidine and phenylpiperazine derivatives since they possess the approximate dimensions of phenylethylamine.²⁰⁶ For instance, in haloperidol, which is a piperidine-containing butyrophenone, if the phenylpentylamine moiety is an important pharmacophoric contributor, it should be possible to extend the butyrophenone chain of haloperidol to a valerophenone (**64**)[Fig. 1.31] ($\sigma K_i = 2.3$ nM), which were found to bind with several-fold higher affinity than haloperidol (**21**) ($\sigma K_i = 10$ nM). Moreover, it was found removal of polar substituents, to give phenylpentylamine (**65**)[Fig. 1.31], resulted in improvement of affinity, which was one of the highest affinities to sigma receptors at that time. Also, replacement of the phenyl-A ring, piperidinyl phenyl ring of (**65**) by hydrogen retained the affinity (**66**; $\sigma K_i = 1.9$ nM)[Fig. 1.31].²⁰⁷

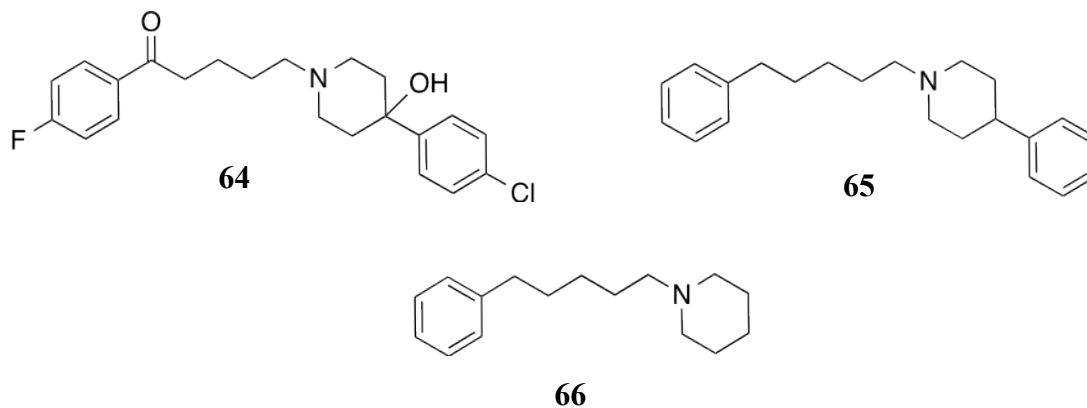


Figure 1.31: Phenylpiperidines sigma receptor ligands

Further examination investigated the importance of the basic nitrogen of compound (**67**) [Fig. 1.32] with quaternary nitrogen, which showed decreased affinity ($K_i, \sigma^{-1} = 242$ nM) compared to the non-quaternized compound (**68**) [Fig. 1.32] ($K_i, \sigma^{-1} = 5.1$ nM).²⁰⁹ Likewise, quaternization of haloperidol to **69** [Fig. 1.32] ($K_i, \sigma_1 = 274$ nM, $\sigma_2 = 23$ nM) resulted in a >50-fold reduction in sigma-1 affinity, but in little change in sigma-2 affinity.²⁰⁹ Therefore, it's clear that the quaternization of the basic nitrogen can effect selectivity as well as affinity.

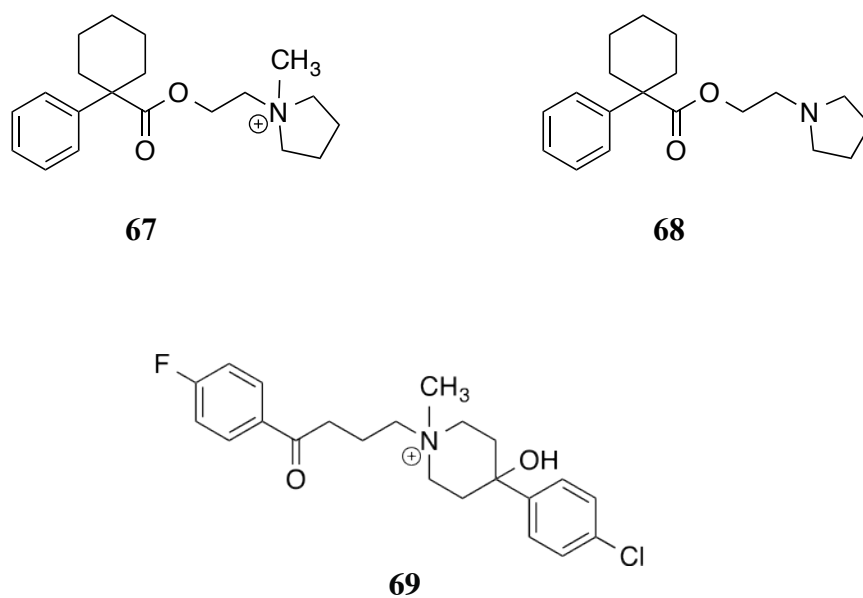


Figure 1.32: Importance of basic nitrogen.

In another study which examined the importance of both nitrogen atoms of piperazine, it was observed that basic nitrogen attached to the alkyl chain was substantial for sigma receptor binding. In comparison between the affinities of piperazine (**70**) with piperidines (**71**) and (**72**) showed that compounds (**70**) and (**71**) have nearly the same affinity ($K_i, \sigma_1 = 1.4$ nM and 1.3 nM respectively), but piperidine (**72**) ($K_i, \sigma_1 = 0.07$ nM), binds with 20-fold higher affinity implying that (**70**), (**71**) and (**72**) are binding in a different manner [Fig. 29].⁶

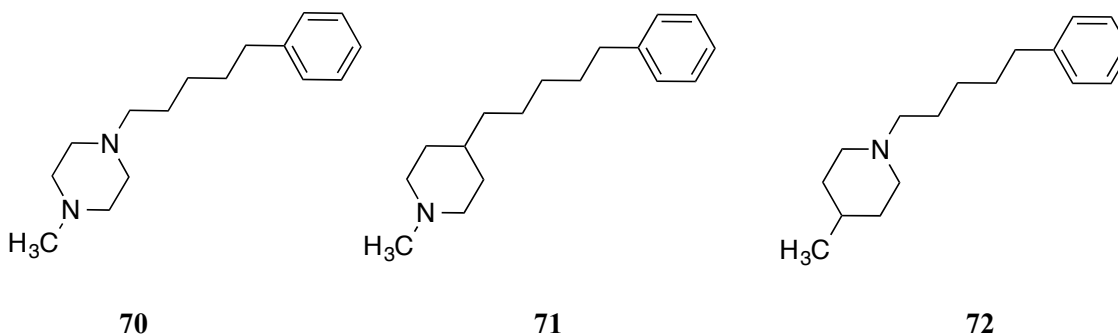


Figure 1.33 Chemical structures of some piperidine and piperazine derivatives

Consequently, it was found the disubstitution of the piperazine ring is crucial for activity. For example, compounds (73) and (75) did not show any affinity for σ receptors; however, upon the introduction of phenylbutyl moiety in compounds (74) and (76), the affinity was increased by >50,000-fold. Surprisingly, compound (74) ($K_i = 0.2$ nM) had a higher affinity than compound (76) ($K_i = 125$ nM). One explanation is that the presence of the carbonyl group in compound (76) decreased the basicity of the benzylic nitrogen atom of (74) which is thought to be required for high-affinity binding. On the other hand, the carbonyl group of (76) may just not be tolerated by the receptor [Fig. 1.34].²¹⁰

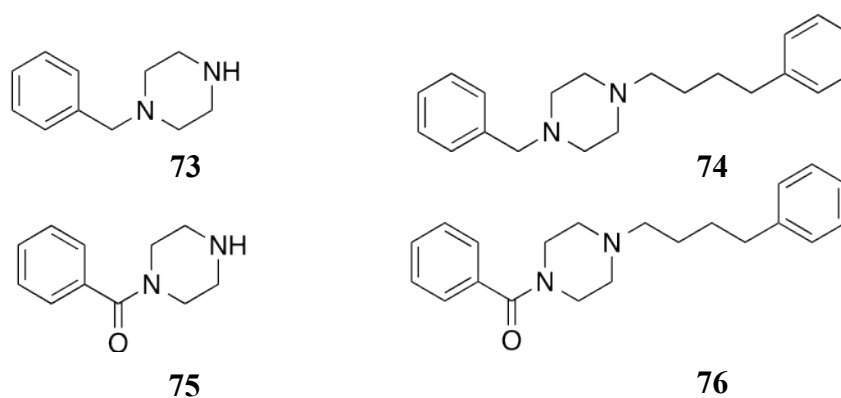


Figure 1.34: Chemical structures of some other piperazine derivatives.

Attractively, several steroids were found to bind to sigma receptors with noticeable affinity, such as progesterone and pregnenolone, displaying affinity of 300 nM and 3 μ M,

respectively despite of lacking the basic nitrogen.²⁰ Further investigation of the steroids revealed that they possess embedded within their structure a hydrophobic or aryl ring and a carbon chain of at least five atoms.

The cyclopentanoperhydrophenanthrene (77) [Fig. 1.35] steroid nucleus was found to embed an aryl ring and a carbon chain of five atoms in the rigid structure. Also, the introduction of basic nitrogen in the form of a piperidine ring led to compound 1.67 with high affinity for both the subtypes (K_i , σ -1 = 66 nM, K_i , σ -2 = 24 nM).⁶

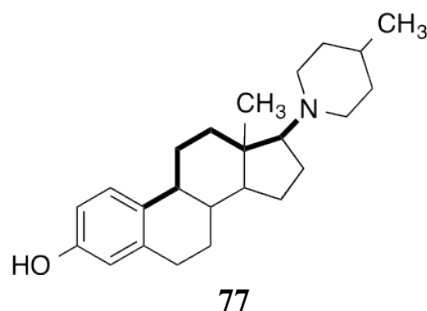


Figure 1.35. Cyclopentanoperhydrophenanthrene steroid nucleus

Consequently, it was evidenced that the Ar-X₅-N moiety, where Ar is either a hydrophobic group such as cyclohexyl or an aromatic moiety, is a common pharmacophoric feature of many high-affinity sigma-1 ligands. Several agents that bind at sigma receptors share the Ar-X₅-N pharmacophore: an aryl or some other hydrophobic group separated from an amine by a five-membered chain. The spacer group “X” can be linear or branched including unsaturation and cyclic structures, and can contain functionalities such as a ketone, amino, or ester group. Also, it was found that the highest affinity is usually correlated with an alkyl chain, and the chain length contributes to sigma-1 affinity and the optimum affinity was obtained with a five atoms length. In regard to the terminal amine “N”, it can be secondary, tertiary, or quaternary but might be only limited bulk tolerated with tertiary and quaternary amines. For a typical binding affinity, at least one hydrophobic substituent is required to be attached to the

amine, and bulk tolerance might also allow the “X” group to be slightly longer or shorter than five atoms. Also, these findings emphasized that “Ar” is not required to be an aromatic ring and that its interaction with sigma receptor is more likely to be a hydrophobic interaction.⁶ Accordingly, Glennon and Ablordeppy summarized the above-mentioned findings by proposing the Ar-C5-N pharmacophore model for high affinity sigma-1 binding as follow [Fig. 1.36]:⁶

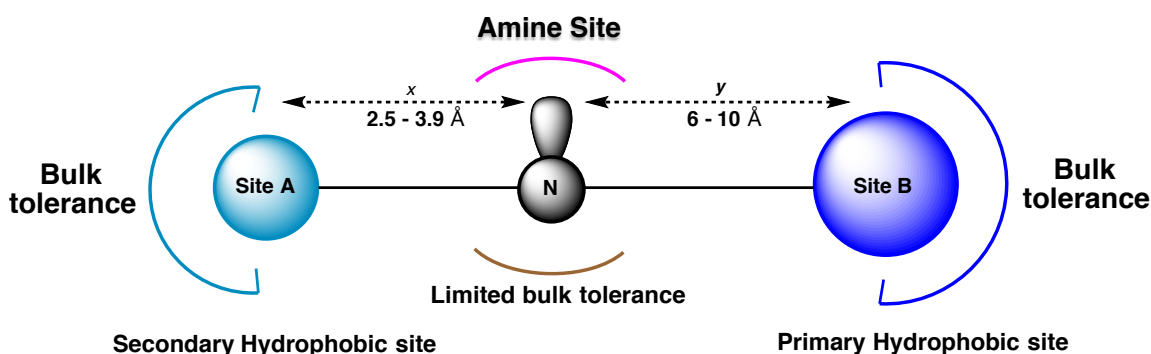


Figure 1.36. Glennon/Ablordeppy “Ar-X5-N” pharmacophore model for high binding affinity at sigma-1 receptor. [Adapted from ref. 6]

It is noteworthy to mention that some other pharmacophore models have been proposed for both sigma receptors; however, they cannot be used for database mining since they only explain the binding characteristic of one class of compounds.^{211,212}

1.7. Selective sigma ligands

The initial interest that followed sigma receptors discovery was renewed in the early 1990s when two subtypes, sigma-1 and sigma-2 were identified. This discovery urged intense efforts into the search for compounds with selectivity for each sigma receptor subtype. (+)-Pentazocine exhibited selectivity for sigma receptors that showed 500-fold selectivity over sigma-2 receptors, and undeniably the tritiated (+)-pentazocine (**4**) [Fig. 1.37] is used in sigma-1 receptor binding assays.^{212,213} On the other hand, the non-selective ligand, [³H]DTG (**2**) [Fig. 1.37] has been accepted as a radioligand to label sigma-2 receptors in presence of the unlabeled

(+)-pentazocine to mask sigma-1 site. Subsequently, researchers have been made huge efforts to find selective sigma ligands for both subtypes.^{212,213}

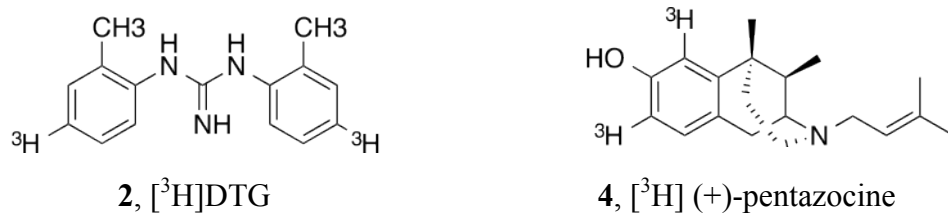
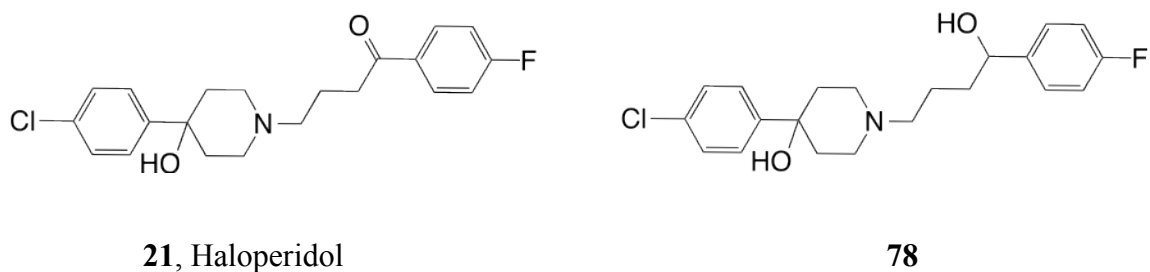


Figure 1.37: Tritiated sigma receptors ligands

1.7.1 Selective sigma-1 ligands

i) Haloperidol derivatives

Haloperidol (**21**) [Fig. 1.38] and its related compounds have been displayed to possess high affinity for sigma-receptors, with a slight preference for sigma-1 over sigma-2.²¹⁴ Further studies showed the reduction of the ketone in haloperidol resulted in decreasing the dopamine D₂ affinity that gives this compound (**78**) [Fig. 1.38] relative selectivity for sigma receptors over the other off targets. A haloperidol derivative, E-5842 (**34**) [Fig. 1.38], showed an affinity of 4 nM for sigma-1 receptors and 55 fold selectivity over sigma-2 receptors. It has also showed moderate affinity for α_1 A adrenergic (K_i = 119 nM), α_1 B adrenergic (K_i = 116 nM), and α_2 B adrenergic (K_i = 89 nM), receptors and displayed low affinity for dopamine D₂ (K_i >1000 nM), D₃ (K_i = 418 nM) receptors and 5-HT_{1A} (K_i = 460 nM) and 5-HT₂ (K_i = 817 nM) receptors. Interestingly, E-5842 has been shown to hold potential as an antipsychotic agent.^{172,215,216}



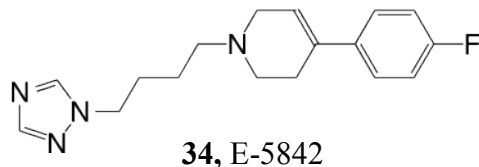


Figure 1.38. Structures of haloperidol and its derivatives

ii) Phenylacetamides

A similar compound to E-5842, N-(1-benzylpiperidin-4-yl)phenylacetamide (**79**) [Fig. 1.39] showed a selectivity of 187 fold over sigma-2 receptors with no affinity for dopamine D₂ (K_i >1000 nM), D₃ (K_i >1000 nM) receptors.²¹⁷ Subsequent studies, showed that the introduction of a halogen on both aromatic rings led to an increase in selectivity for sigma-1 over sigma-2 receptor.²¹⁸

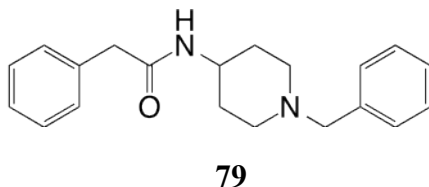


Figure 1.39. Structure of the phenylacetamide derivative.

iii) Dipropylamines

NE-100 (**31**) [Fig. 1.40], is a dipropylamine class of compound that showed high affinity for sigma-1 receptors with an IC₅₀ of 1.54 nM, and moderate selectivity of 55 fold over sigma-2 receptors.²¹⁹ In a subsequent study, it was found that both propyl groups are not necessary for affinity at sigma receptors, and that the mono-propyl analog **80** possesses a significant affinity. It was also found that the introduction of alkyl groups alpha to such a secondary amine in compound (**81**) [Fig. 1.40] actually led to increases in affinity and selectivity for sigma-1 receptors.²⁰⁰

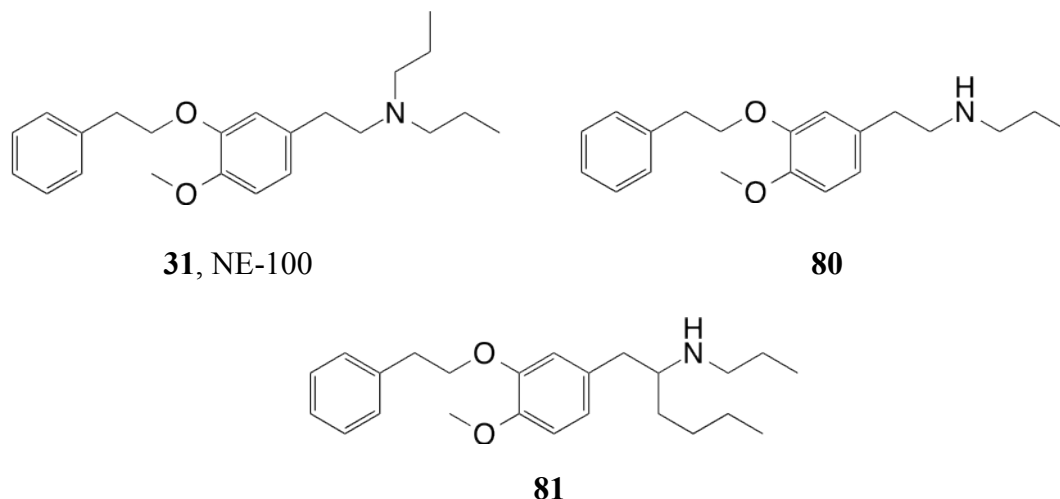


Figure 1.40. Structures of some propylamine compounds.

iv) Spirocyclic pyranopyrazoles

A series of spirocyclic pyranopyrazoles was synthesized by Schläger and colleagues resulting in the potent and selective sigma-1 receptor ligand (**82**) [Fig. 1.41] ($K_i = 0.94$ nM, 730-fold selectivity for sigma-1 over sigma-2 receptors).²²¹ Subsequent modification and introduction of a methyl group as can be seen in compound (**83**) [Fig. 1.41] displayed low affinity and selectivity for sigma-1 receptors ($K_i = 18.9$ nM, > 56-fold selectivity for sigma-1 over sigma-2 receptors). However, introducing a phenyl group at the pyrazole heterocycle (**84**) [Fig. 1.41] restored the affinity with $K_i = 0.97$ nM, and 326-fold selectivity for sigma-1 over sigma-2 receptors. Similarly, replacement of the pyrazole heterocycle of the spirocyclic derivatives with a thiophene ring gave high affinity selective sigma-1 ligands. Furthermore, benzene (**85**) [Fig. 1.41] substitution at the piperidine ring showed higher affinity and selectivity for sigma-1 receptors than cyclohexylmethyl (**86**) [Fig. 1.41] substitutions with $K_i, \sigma_1 = 1.1$ nM, and 900-fold selectivity for sigma-1 receptors. Conversely, the introduction of basic or polar groups reduced the affinity as can be seen in compound (**87**) and (**88**) [Fig. 1.41]²²² Additionally, 1'-benzyl-3,4-

dihydrospiro[2H-1-benzothiopyran-2, 4'-piperidine] (Spipethane) (**89**) [Fig. 1.41] has been shown to possess 832 fold selectivity for sigma-1 receptors with low affinities for other receptors such as dopamine D2 ($K_i = 10,400$ nM), α 1A adrenergic ($K_i >10,000$ nM), α 1B adrenergic ($K_i >10,000$ nM), 5-HT2 ($K_i = 7,600$ nM), M2 ($K_i = 10,800$ nM), M3 ($K_i >10,000$ nM), opioid ($K_i >10,000$ nM) and PCP ($K_i >10,000$ nM) receptors.^{223,224}

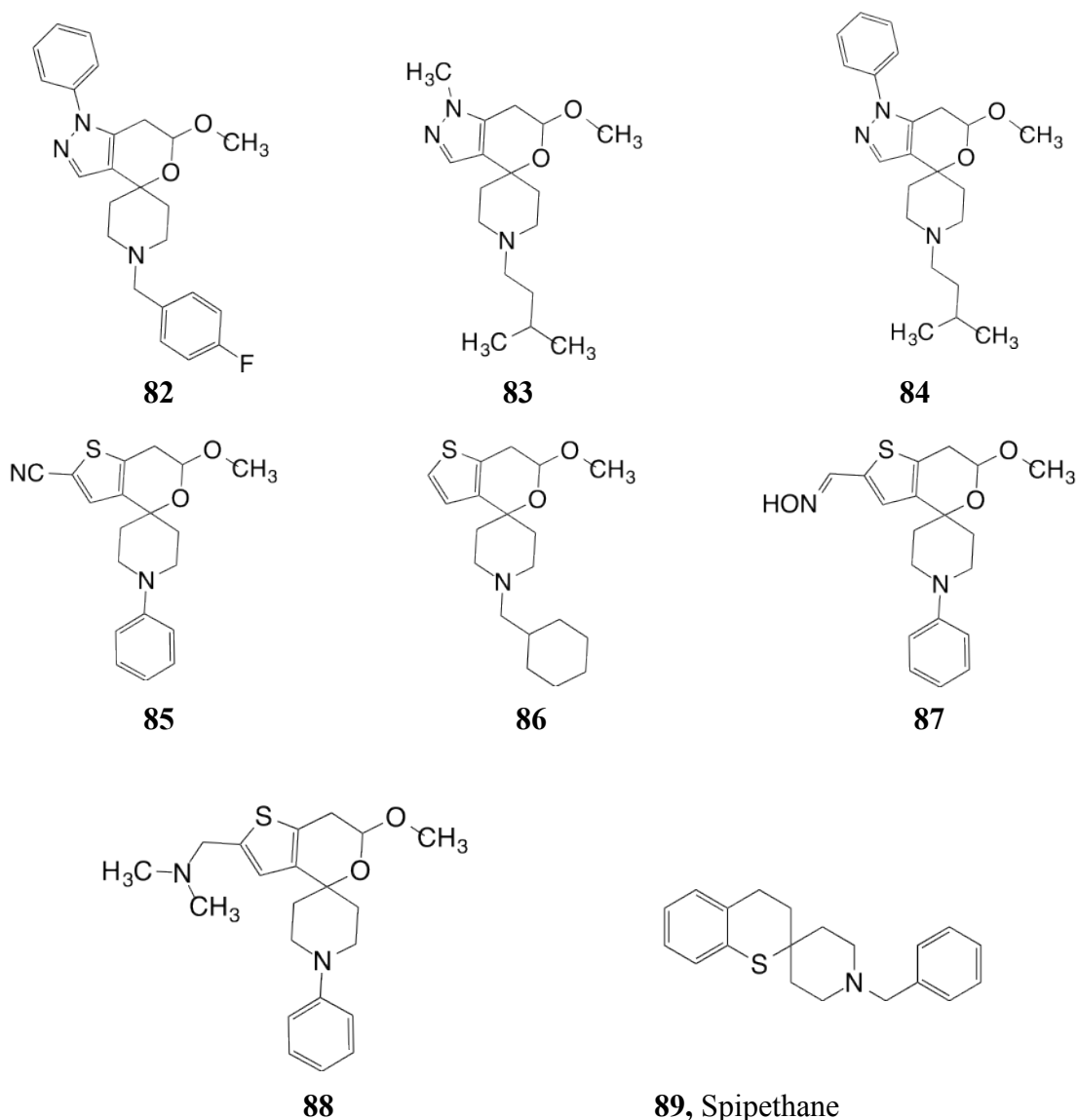
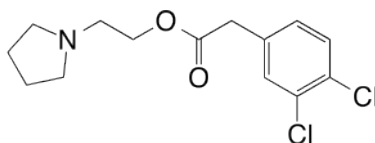


Figure 1.41: Selective sigma-1 of spirocyclic pyranopyrazoles.

v) **Various Selective sigma-1 ligands**

A simple achiral monoamine, AC915 (**90**) [Fig. 1.42], showed high affinity for sigma-1 receptors ($K_i = 4.89$ nM) and excellent selectivity of > 2040 fold over sigma-2 receptors.²²²



90. AC915

Figure 1.42. Selective sigma-1 ligand with high affinity.

Furthermore, numerous tetrahydronaphthalene derivatives have been synthesized and evaluated for their affinity toward sigma receptors. These derivatives showed high affinity for sigma receptors, as exemplified in compounds (**91**) and (**92**) [Fig. 1.43] ($IC_{50} = 0.016$ nM and 0.008 nM respectively) and both compounds showed high selectivity by more than 100,000 fold for sigma-1 over sigma-2.²²⁴ Subsequent structure activity relationship study revealed that upon replacement of the cyclohexyl ring with aromatic ring in compound (**93**) [Fig. 1.43] resulted in decreasing the sigma-1 selectivity to 680 fold.²²⁵ Further replacement of piperidine with cyclohexylpiperazine in compound (**94**) [Fig. 1.43], sigma-1 selectivity was 406 fold over sigma-2.²²⁶

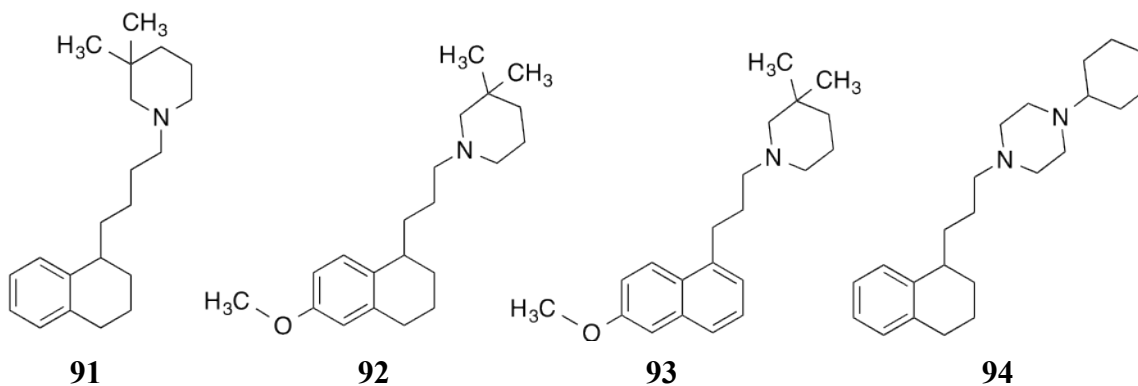


Figure 1.43: Selective sigma-1 of tetrahydronaphthalene derivatives.

The benzo[*d*]thiazol-2(3*H*)-one derivative, SN56, (**95**) [Fig. 1.44] has shown high affinity ($K_i = 0.56$ nM) and over 1000 fold selectivity for sigma-1 receptor. This compound was also tested against a panel of receptors including dopamine (D_1 and D_2), 5-HT, α_1 , α_2 , β_1 , β_2 , H1, H2 and was found to have only moderate affinity for α_2 ($K_i = 205$ nM) and H1 ($K_i = 311$ nM) receptors.²²⁷ Further structural features investigation of benzo[*d*]thiazol-2(3*H*)one derivatives that was performed in our laboratory identified compound (**96**) [Fig. 1.44] as a high affinity ligand for sigma-1 receptors, with sigma-1 $K_i = 4.5$ nM, and a 484-fold selectivity over sigma-2 receptors.²²⁸

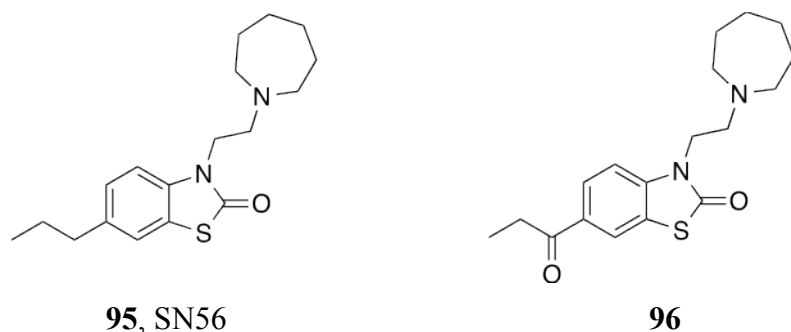


Figure 1.44: Selective sigma-1 of benzo[*d*]thiazol-2(3*H*)one derivatives.

1.7.2 Selective sigma-2 ligands

i) Morphans

Compound CB-64D (**99**) and compound CB-184 (**101**) [Tab. 1.4] were the first reported highly selective sigma-2 receptor ligands that belonging to the (E)-8-benzylidene-5-phenylmorphan-7-ones class.²²⁹ These compounds developed in 1990s from 2-methyl-5-(3-hydroxyphenyl) morphan **97** [Tab. 1.4], were also found to have high affinity for μ opioid receptors. Subsequent introduction of the benzylidene moiety at the C-8 position (**98-101**) [Tab. 1.4] led to decrease of μ receptors affinity whereas the affinity at the sigma-2 subtype

improved.²³⁰ Interestingly, both sigma subtypes demonstrated opposite enantioselectivity with sigma-1 binding the (-)-isomers with a 300-fold higher affinity than the (+)-isomers, and the sigma-2 binding the (+)-isomers with 3- to 10-fold higher affinity than the (-)-isomers. Hence, (+)-isomers of CB64D and CB184 exhibited the highest sigma-2 over sigma-1 receptor selectivity with 185-fold and 554-fold, respectively [Table 3]. In addition, these (+)-morphans showed very low affinities for the muscarinic receptors, PCP binding sites and the other opioid receptors such as κ and δ .^{230, 231}

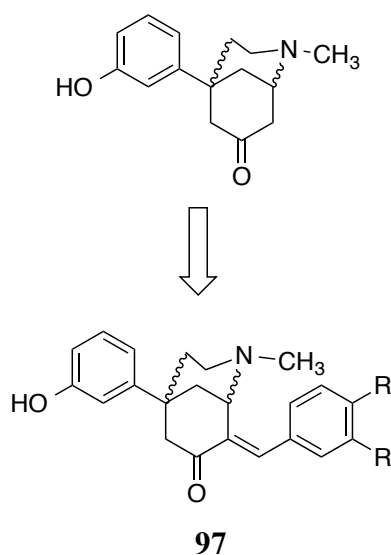


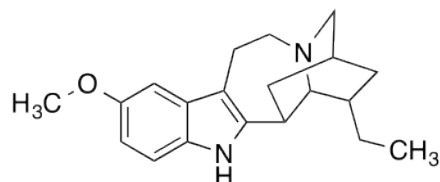
Table 1.4: Affinities of (E)-8-benzylidene-5-(3-hydroxyphenyl)-2-methylmorphan-7-ones at sigma receptors. [Adapted from ref. 231]

| Compound | Configuration | R | K _i (nM) | | Ratio selectivity |
|---------------------|---------------|----|---------------------|------------|---------------------|
| | | | σ_1 | σ_2 | σ_1/σ_2 |
| 98 , CB-64L | (-)-1S,5S | H | 10.5±1.6 | 153±3 | 0.07 |
| 99 , CB-64D | (+)-1R,5R | H | 3063 ±78 | 16.5±2.7 | 185 |
| 100 , CB-182 | (-)-1S,5S | Cl | 27.3±2.8 | 35.5±8.8 | 0.77 |
| 101 , CB-184 | (+)-1R,5R | Cl | 7436±308 | 13.4±2.0 | 554 |

ii) Ibogaine

Ibogaine or 12-methoxyibogamine (**102**) [Fig. 1.45] is a hallucinogen indole alkaloid derived from the root of the African shrub *Tabernanthe iboga*, which displayed a moderate

sigma-2 ($K_i = 201$ nM) over sigma-1 selectivity with 40-fold.²³¹ However, it has a downside that it interacts with a range of biological systems including sigma-2 receptors and thus it is not suitable to use to explore the actions of sigma-2 receptors in vivo assays.^{231,232,233}

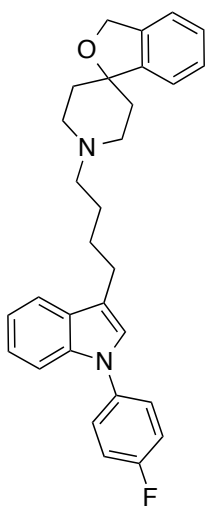


102, Ibogaine
 $K_i, \sigma-1 = 9310$ nM
 $\sigma-2 = 90.4$ nM
 $\sigma-1/\sigma-2 = 103$

Figure 1.45: Structure of 12-methoxyibogamine or ibogaine and its binding affinity.

iii) Spirocyclic ligands

Siramesine (**31**)[Fig. 1.46] is another recently reported selective sigma-2 ligand discovered shortly after CB184 and CB64D were published. It was developed from studies on low efficacy 5-HT_{1A} agonists.²³⁴



32, Siramesine
(Lu-28-179)

IC_{50}
 $\sigma-1 = 17$ nM
 $\sigma-2 = 0.12$ nM
 $\sigma-1/\sigma-2 = 140$

Figure 1.46: Structure and binding affinity of Siramesine

Besides siramesine, several other piperazine derivatives displayed high affinity for 5-HT_{1A} and moderate affinity at sigma receptors, in particular, the 1-(2-methoxyphenyl) piperazine derivative (**103**)[Fig. 1.47].²³⁵

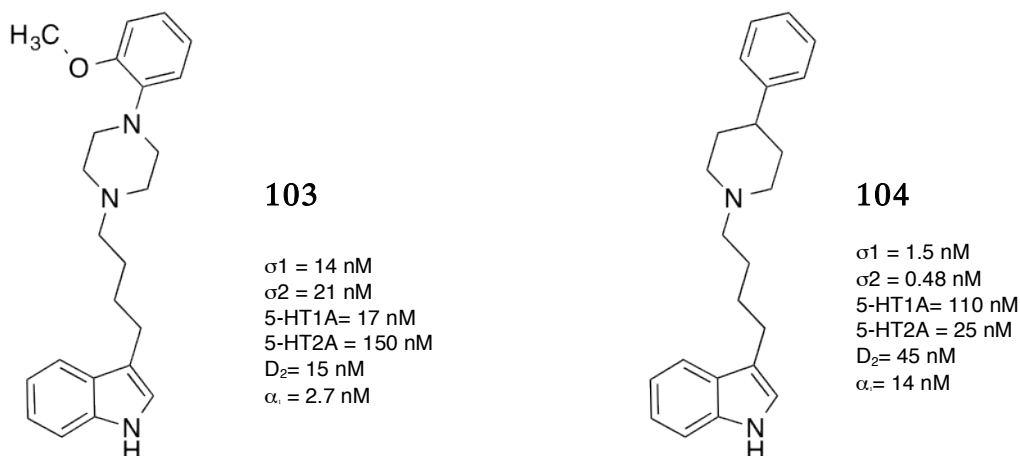


Figure 1.47: Piperazine derivatives with moderate sigma affinity.

It was clear that replacement of the piperazine by a piperidine ring enhanced affinity at both sigma subtypes to the same extent as when a 4-fluorobenzene was used in spite of the 2-methoxybenzene. However, the highest sigma-2 receptor affinity was obtained from the unsubstituted, 4-phenylpiperidine derivative (**104**) [Fig. 1.47]. It was also found that introduction of 4-fluorophenyl at the indole N-atom removed the affinity for 5-HT_{1A} receptors and reduced the affinity at 5-HT_{2A}, sigma-1 and D₂ sites. Both 4-phenylpiperidine and 4-(4 fluorophenyl) piperidine derivatives within this series of compounds exhibited subnanomolar affinities at sigma-2 receptor, with valuable selectivity versus the sigma-1 subtype (up to 100-fold for the 4-phenylpiperidine). Alternatively, the N-(4-fluorophenyl) piperazine derivatives exhibited a 10-fold lower affinity at both sigma subtypes as compared to their piperidine analogs. Therefore, the piperidine derivatives were investigated further and the phenyl ring connected to the piperidine ring via spiro fusion as can be seen in siramesine and its analogs.^{231, 234}

Based on the above mention studies, there are structural requirements for siramesine and related molecules to have unique sigma-2 selectivity:

1) Substituents at the piperidine N-atom (**105**)[Fig. 1.48] are important for sigma-2 affinity and selectivity. For instance, small alkyl substituents such as methyl or ethyl resulted in loss of affinity at both sigma sites, whereas an increase of chain length led to an increase of sigma affinity with a consistent change towards sigma-2 selectivity.^{231,234}

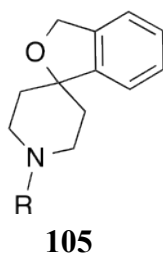
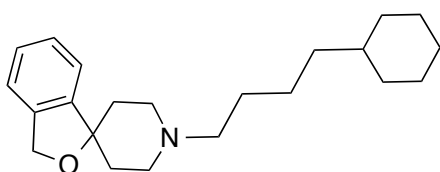
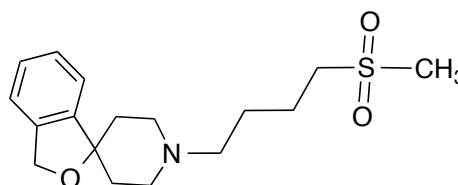


Figure 1.48: Spiro-fusion with various alkyl substituents.

Compound (**106**) [Fig. 1.49]. (high lipophilic) and (**107**) [Fig. 1.49]. (less lipophilic) showed a direct correlation between the affinity at sigma-2 receptors and the lipophilicity of the structures as can be seen in [Fig. 1.49].



106, IC₅₀
 $\sigma_1 = 1.5$ nM
 $\sigma_2 = 0.07$ nM



107, IC₅₀
 $\sigma_1 = 6.3$ nM
 $\sigma_2 = 430$ nM

Figure 1.49. Spiro-fusion with high and low lipophilic substituents.

2) Introducing groups such as a fluorine atom or a CF₃ group on the benzene ring of the spiro-piperidine benzene moiety resulted in decrease of affinity or loss of selectivity [Fig. 46].

3) Modification of the O- atom position by inserting a methylene ring to enlarge the ring size resulted in a decrease of affinity and selectivity towards sigma-2 receptors. Also, replacement of oxygen with sulfur displayed high affinity and selectivity toward sigma-2 receptors with a 250-fold sigma-2 versus sigma-1 selectivity [Fig. 1.50].^{231,234}

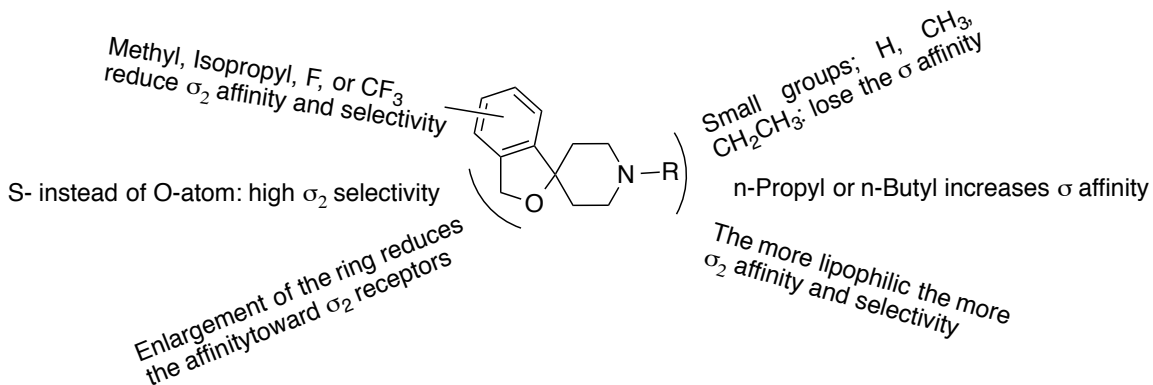


Figure 1.50: Spiropiperidines structure activity relationships.²³¹

iv) Arylpropylamines

It has been observed that ibogaine and CB-184 contain arylpropyl amines and show sigma-2 selectivity, while the selective sigma-1 compound, NE-100 possesses a phenylethylamine moiety. This finding opened the way to investigate a variety of phenethyl and phenylpropyl amines. The phenylpropylpiperidine (**108**) [Fig.1.51] demonstrated a four-fold preference toward sigma-2 receptors, which could be improved with other substituents as can be seen in compound (**109**) [Fig.1.51].^{6,200}



Figure 1.51: Simple Phenylalkylamines.

v) Tropane analogs

A novel tropane-based ligand (**110**)[Fig. 1.52] has been reported by Mach *et al.* was found to display high affinity for sigma-2 receptors ($K_i = 5 \text{ nM}$) with 500 fold greater selectivity over sigma-1 receptors.²³⁶ The para-amine substitution improved the selectivity, compared to the unsubstituted phenyl analog that demonstrated much lower selectivity for sigma-2 receptors. On the other hand, the related tropane-containing ligand (+)-SM-21 (**111**)[Fig. 1.52] has been reported to have substantial affinity for sigma-2 receptors, and is currently used as a sigma-2 antagonist in behavioral assays.^{237,238}

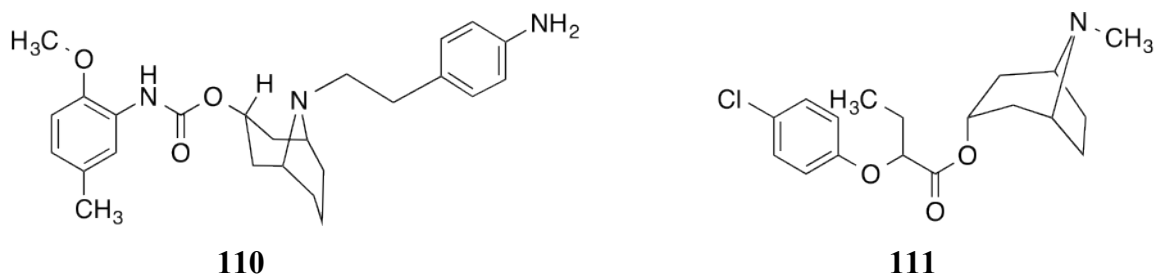


Figure 1.52: Tropane analogs

vi) Benzamides

Benzamides are another class of compounds that were developed from dopamine D_3 receptor ligands, which also displayed high affinity for sigma receptors. Further modification led to substituted benzamides connected to the N-atom of 6,7 dimethoxytetrahydroisoquinoline motif by a 4-methylene chain, characterized by high sigma-2 selectivity (**112**) [Fig 1.53].²³⁹

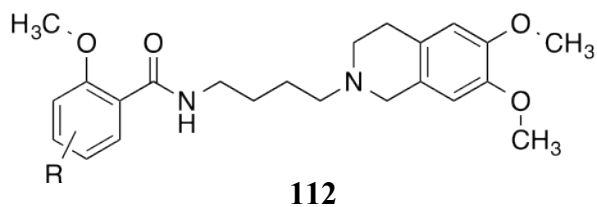


Figure 1.53: General structure of flexible benzamides.

Compounds such as 5-methyl-2-methoxy-N-[4-(6,7-dimethoxy-3,4-dihydro-1H-isoquinolin-2-yl)butyl]benzamide (RHM-1;**113**) [Fig. 1.54] and N-[4-(6,7-dimethoxy-3,4-dihydro-1H-isoquinolin-2-yl)butyl]-2-(2-fluoroethoxy)-5-iodo-3-methoxybenzamide (ISO-1; **114**) [Fig. 1.54] are highly sigma-2 selective flexible benzamides.²³⁹

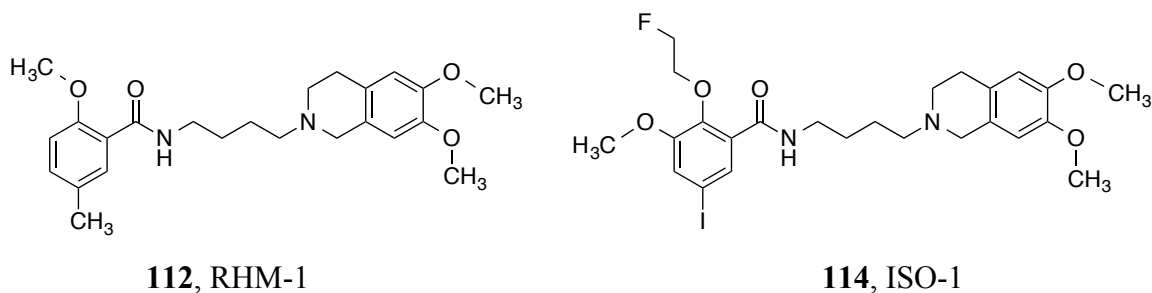


Figure 1.54: Two of the most selective σ flexible benzamides.

Subsequent modification on RHM-1 led to the development of high affinity sigma-2 ligands, the N-[4-(6,7-dimethoxy-3,4-dihydro-1H-isoquinolin-2-yl)butyl]-5-bromo-2,3-dimethoxybenzamide (**115**) (sigma-1, $K_i = 12.900$ nM; sigma-2, $K_i = 8.2$ nM)[Fig. 1.55].^{240,241}

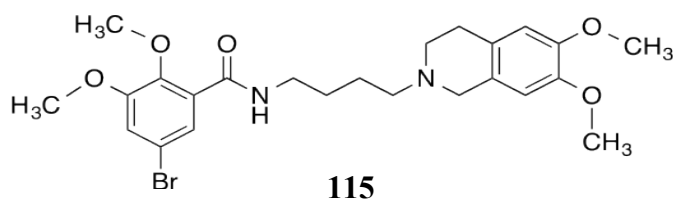


Figure 1.55: RHM-1 analog.

Further studies confirmed that the 6,7-dimethoxy substitutions were significant for achieving high sigma-2 affinity, whereas substitution with methylene-dioxy, ethylene-dioxy and propylene-dioxy proved to decrease sigma-2 receptor affinity. Once the N-atom containing ring was opened, a dramatic decline in sigma affinity was observed. The effect of the conformational freedom of the 6,7-dimethoxytetrahydroisoquinoline on sigma receptor interactions was

investigated where the five-membered and seven-membered rings containing the N-atom fused to the benzene ring to mimic the 6,7 dimethoxytetrahydroisoquinoline structure. The five-membered fused ring provided a 10-fold higher sigma-2 affinity than the tetrahydroisoquinoline lead compound while the seven-membered ring reduced sigma-2 affinity by a 40-fold suggesting that a higher conformational freedom of the basic nucleus has a negative effect on sigma-2 binding. Moreover, varied changes to the position of the N-atom within the ring were explored and the optimum results obtained with the tetrahydroisoquinoline position and that was explained to the basic character alteration of the N-atom [Fig. 1.56].^{231,241}

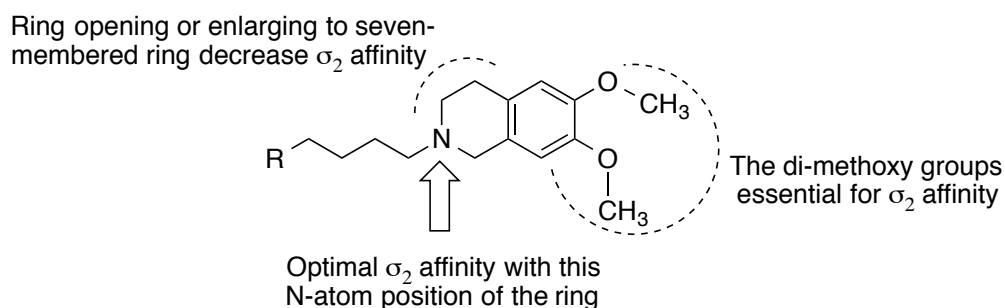


Figure 1.56: SAR of the 6,7-dimethoxytetrahydroisoquinoline for sigma-2 binding. [Adapted from ref. 231]

1.8. Dual probes for sigma-1 receptors and the dopamine transporters

(Rimcazole analogs):

A number of studies provided evidence that sigma receptors and cocaine are associated. For instance, it was reported that cocaine binds with a moderate affinity to sigma receptors in concentrations similar to those were achieved by cocaine in the brain (*in vivo*).¹⁰³ Consequently, a number of sigma ligands such as BMY 14802 (**11**) and rimcazole (**33**) [Fig. 1.57] have been displayed to attenuate locomotor and rewarding effects of cocaine.^{242,243} Moreover, the sigma-1 receptor antagonists CM156, NE-100 and BD1047 displayed significant attenuation of cocaine-induced place preference.^{108,109,243} Additionally, several other studies showed that sigma-1

receptor antagonists block the development of sensitization to cocaine in rats.^{242,243} Although, there is no similarity in the homology between sigma receptors and dopamine transporters proteins, intriguingly, it seems that there is a linkage to the cocaine binding site on the dopamine transporter (DAT) and the sigma-1 antagonist binding site. For example, the potent DAT inhibitor GBR 12909 (**119**) [Fig. 1.57] was described to effectively displace [³H](+)-3-(3-hydroxyphenyl)-N-(1-propyl)piperidine ([³H] 3-PPP) from sigma receptors in rat brain (IC₅₀ = 48 nM)²⁴⁴, and isothiocyanate analog of the sigma antagonist rimcazole has been exhibited to bind irreversibly to the DAT, in rat caudate-putamen.^{245,246}

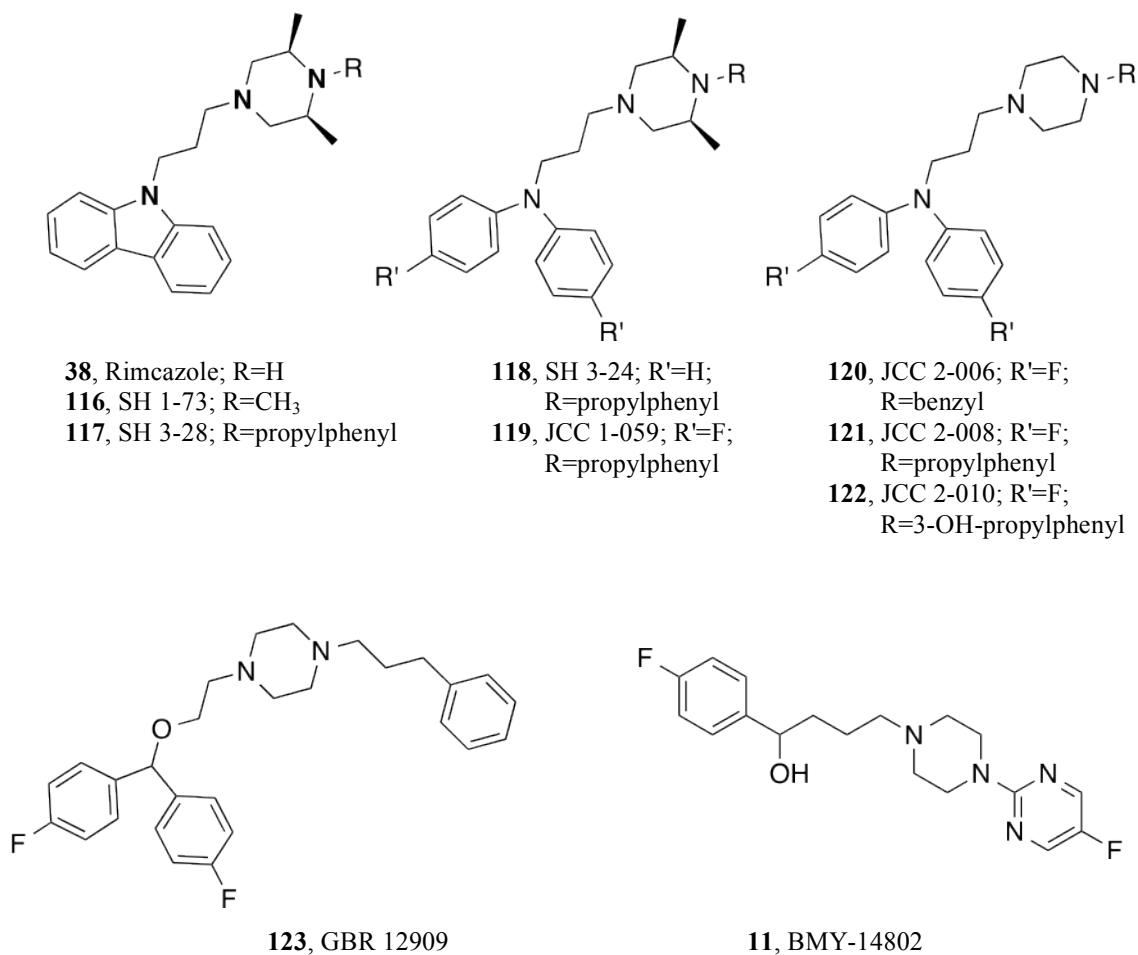


Figure 1.57: Rimcazole and its analogs.

Based on these findings, a series of rimcazole analogs was synthesized as potential dopamine uptake inhibitors, and their structure-activity relationships at dopamine transporter DAT, serotonin transporter (SERT), norepinephrine transporter (NET), and sigma-1 receptors were extensively studied. In this study, it was found substitutions on the carbazole ring of rimcazole led to decrease binding affinities at both sigma-1 receptors and the DAT.^{247,248} Furthermore, N-methylation of the terminal piperazine nitrogen (SH 1-73, **(116)**) resulted in a small increase in binding affinity at sigma-1 receptors ($K_i = 552$ nM) but in a slightly less active DAT compound ($K_i = 436$ nM).²⁴⁸ Conversely, introducing a propylphenyl group, on the terminal piperazine nitrogen (SH 3-28, **(117)**), as seen with GBR 12909 (**(123)**), led to increase and retention in sigma receptor and DAT binding affinities, respectively. Similarly, replacement of carbazole ring with a diphenylamine connected with the N-propylphenyl substituent resulted in a potent rimcazole analog SH 3-24 (**(118)**) [Fig. 1.57] ($K_i = 97$ nM at sigma-1 and 61 nM at DAT).²⁴⁸ Also, placing a fluorine atom at *para*-position of the diphenylamine moiety (JJC 1-059)(**(119)**) [Fig. 1.57] led to appreciably increase in both sigma-1 receptor and DAT binding ($K_i = 11.1$ nM and 22.8 nM, respectively).^{247,248} Reducing the lipophilicity by removing the methyl groups from the piperazine ring (JJC 2-008)(**(121)**) [Fig. 1.57] also reduced sigma-1 receptor binding affinity ($K_i = 66.2$ nM) while retaining high affinity for DAT ($K_i = 18$ nM). Remarkably, the N-benzyl analog (JJC 2-006)(**(120)**) [Fig. 1.57] displayed the highest affinity for sigma-1 receptors in the demethylated analogs ($K_i = 13.1$ nM). [Data is shown in Table. 4].^{247,248} These findings, suggested that compounds with the dual actions at both sigma-1 receptors and the dopamine transporter DAT may prove to be a novel strategy for the development of a cocaine-abuse medication and is being investigated toward this goal.

Table 1.5: Binding affinities at sigma-1 and DAT

| Compound | [³ H](+)-Pentazocine(σ ₁) K _i (nM) ^a | [³ H]WIN 35,428 (DAT) K _i (nM) | σ ₁ /DAT |
|-----------|--|---|---------------------|
| Cocaine | 8830 ± 860 ^b | 187 ± 19 ^a | 47 |
| GBR 12909 | 318 ± 18 ^a | 11.9 ± 1.9 ^a | 27 |
| Rimcazole | 908 ± 99 ^a | 224 ± 16 ^a | 4.1 |
| SH 3-24 | 97.2 ± 14.0 ^a | 61.0 ± 6.1 ^a | 1.6 |
| SH 1-73 | 552 ± 110 ^a | 436 ± 44 ^a | 1.3 |
| SH 3-28 | 104 ± 0.4 ^a | 263 ± 34 ^a | 0.4 |
| JJC 1-059 | 11.1 ± 0.8 ^b | 22.8 ± 2.0 ^b | 0.5 |
| JJC 2-008 | 66.2 ± 3.6 ^b | 18.1 ± 2.7 ^b | 3.7 |
| JJC 2-006 | 13.1 ± 1.2 ^b | 27.6 ± 3.9 ^b | 0.5 |
| JJC 2-010 | 372 ± 21 ^b | 8.5 ± 0.8 ^b | 44 |

a: [246]; b:[248] These experiments evaluated nine structurally diverse sigma ligands for displacement of [³H]WIN 35,428 binding at DAT in rat caudate-putamen and displacement of [³H](+)-pentazocine binding at sigma-1 receptors.

1.9. Sigma receptor radioligands and PET imaging agents

These radioligands are tools derived from ligands with a high affinity and selectivity and they are mostly useful for characterizing the functions of receptor systems as well as mapping their distributions.

1.9.1. Sigma-1 receptor radioligand

The highly selective sigma-1 receptor ligand, (+)-pentazocine (**3**)[Fig. 1.58], (K_i, σ₁ = 3.1 nM; σ₂ = 1542 nM; σ₂/σ₁ = 500), was developed by De Costa *et al.* into an optically pure radioligand, which currently used in sigma-1 binding assays. However, [³H](+)-pentazocine (**4**) [Fig. 1.58], has significant limitations; it is difficult to synthesize, has limited chemical stability, and can be problematic to obtain.²⁴⁹

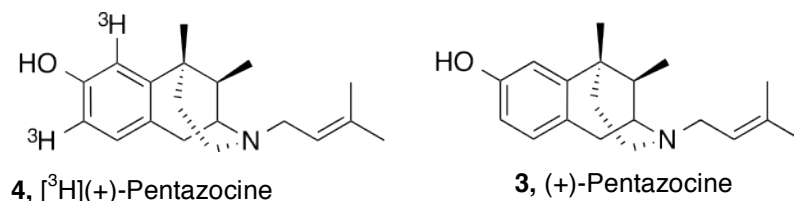


Figure 1.58: The highly selective sigma-1 receptor radioligand.

The implication of sigma receptors in several CNS disorders, as well as cancer, has inspired the development of many carbon-11 labelled and fluorine-18-labelled ligands for non-invasively imaging these sites using positron emission tomography (PET). However, fluorine-18 ($t_{1/2} = 109.8$ min) has a longer half-life compared to carbon-11 ($t_{1/2} = 20.4$ min), which allows multi-step synthetic sequences that can be extended over hours.²⁵⁰ Positron imaging tomography (PET) is a noninvasive technique that is widely used to study sigma-1 receptor expression in mammalian brain as well as to enumerate receptor occupancy and physiological response. As of the higher densities of sigma-1 receptors in the CNS, radiotracers targeting this subtype are important for PET imaging of the brain. SA4503 (**124**) [Fig. 1.59] is a relatively selective sigma-1 receptor agonist ($K_i = 4.4$ nM, $\sigma_1/\sigma_2 = 55$), which is the most widely used ^{11}C labeled radiotracer.⁶¹ It has been used in the PET imaging of sigma-1 receptors in monkey^{251,252} and human brain.²⁵³

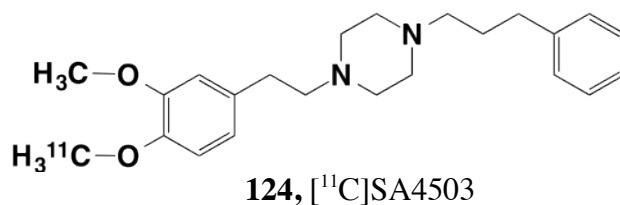


Figure 1.59: The widely used selective sigma-1 [^{11}C labeled] radiotracer.

On the other hand, a sigma-1 receptor selective fluorine-18-labeled SA4503 (**125**) [Fig. 1.60] analog was synthesized by *Ishiwata et al.* to perform the biodistribution, kinetic and metabolism studies of this radioligand in rodents and rhesus monkeys.²⁵⁴

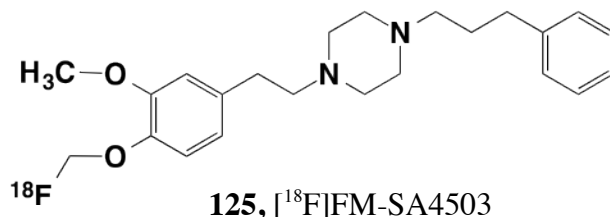


Figure 1.60: The widely used selective sigma-1 [^{18}F labeled] radiotracer.

Moreover, the ^{18}F -1-(3-Fluoropropyl)-4-(4-cyanophenoxymethyl)piperidine, [^{18}F]FPS (**126**) [Fig. 1.61] has shown subnanomolar affinity and moderate selectivity for sigma-1 receptors. This radioligand has been evaluated in rat brain and tumor bearing animal models.¹⁹⁰ Spirocyclic sigma-1 receptors ligand WMS-1813 (**127**) [Fig. 1.61] with high affinity ($K_i = 1.4$ nM) and exceptional selectivity was labelled with ^{18}F and evaluated in experimental animals, which showed high uptake in the brain.²⁵⁵

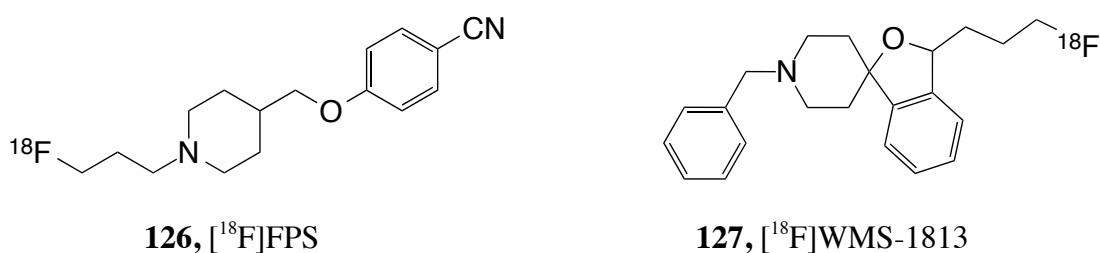


Figure 1.61: Selective sigma-1 [^{18}F labeled] radiotracers.

In our laboratory, several 2(3*H*)-benzoxazolones and 2(3*H*)-benzothiazolones have been synthesized and evaluated for their binding affinity toward sigma receptors.^{228,256} Some of these have demonstrated high selectivity toward sigma-1 receptors, such as SN56 (**95**) [Fig. 1.62], with more than 1000 ratio selectivity for sigma-1 over sigma-2 ($\sigma_1 K_i = 0.56$ nM, $\sigma_1/\sigma_2 > 1000$), and CM304 (**23**) [Fig. 1.62] with more than 145,000 ratio selectivity for sigma-1 over sigma-2 ($\sigma_1 K_i = 0.0025$ nM, $\sigma_1/\sigma_2 > 45,000$).²²⁸ CM304 was obtained from SN56 by terminal fluorine-for-hydrogen substitution of the propyl chain. [^{18}F]FTC-146 (**24**) [Fig. 1.62] is a radiolabeled analog of CM304 that showed good correlation between [^{18}F]FTC-146 accumulation and sigma-1 receptor expression.²⁵⁶

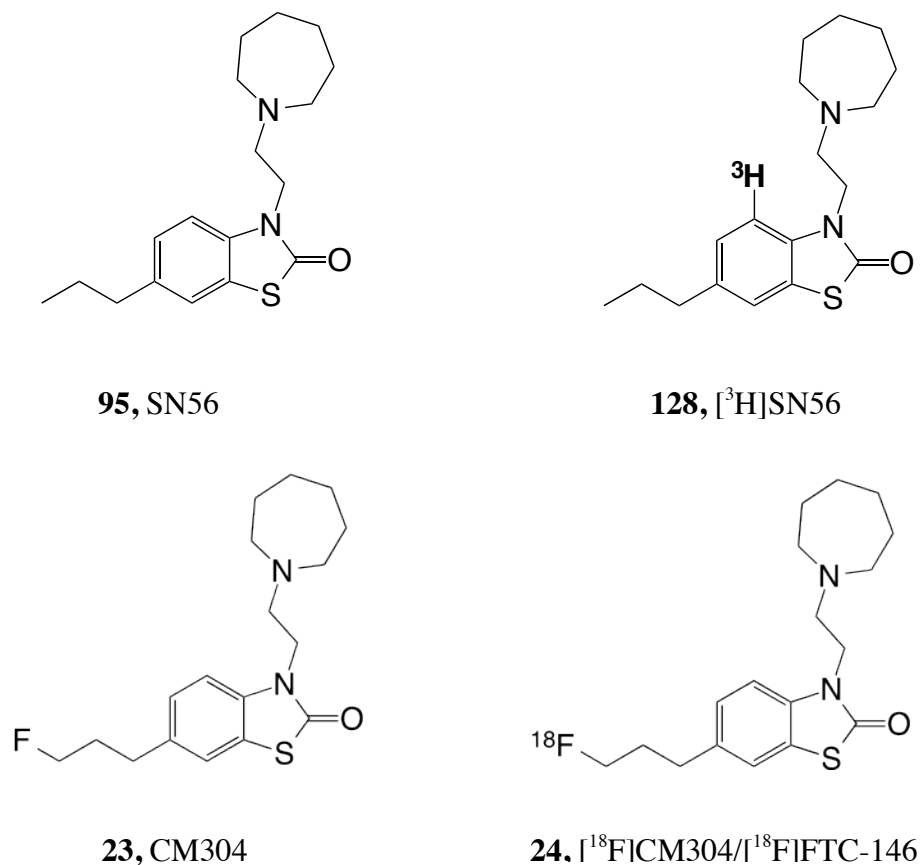


Figure 1.62: In house developed selective sigma-1 radiotracers.

Based on the studies of [¹⁸F]CM304/ [¹⁸F]FTC-146 in mice, rats, and squirrel monkeys, the radioligand accumulated in regions known to include high levels of sigma-1 receptors, which suggests that the PET signal specifically binds to sigma-1 receptors *in vivo*.^{53,54} Further study in our laboratory indicated that the [³H]-SN56 (**128**) [Fig. 1.62] possesses high affinity and selectivity for the σ_1 receptor, and appears to be a feasible alternative for [³H](+)-pentazocine in radioligand binding assays since the [³H]-SN56 has more than 70 fold higher affinity for the sigma-1 receptor than [³H](+)-pentazocine.²⁵⁸

1.9.2. Sigma-2 receptor radioligands

[³H]-DTG (1,3-di(2-tolyl)guanidine) (**2**) [Fig. 1.63] is a non selective ligand which has mixed affinity for both sigma-1 and sigma-2 receptors (K_i , σ_1 = 41 nM; σ_2 = 49 nM); however,

it is being accepted as a radioligand in the presence of (+)-pentazocine to mask sigma-1 sites.²⁵⁷

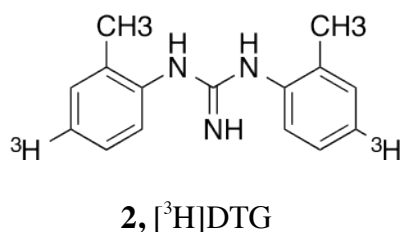


Figure 1.63: Generally accepted sigma-2 radioligand for binding assays.

Several studies have reported that sigma-2 receptors are over expressed on malignant tissues therefore sigma-2 selective radiotracers may be clinically useful in tumor imaging. For instance, the selective sigma-2 radioligand, 5-⁷⁶Br-bromo-N-(4-(3,4-dihydro-6,7-dimethoxy-isoquinolin-2(*1H*))yl)butyl)-2,3-dimethoxy-benzamide (**32**) [Fig. 1.64] (K_i , σ -1 = 12,900 nM; σ -2 = 8.2 nM; σ -1/ σ -2 = 1573), has been studied in the mice EMT-6 tumor models, and showed high uptake of the radiotracer in the tumors and low uptake in the surrounding normal tissues.^{190,258}

RHM-1 (**112**) is one of the first flexible benzamides with a 300-fold higher affinity for sigma-2 versus sigma-1 receptors (K_i , σ -1 = 3078 nM; σ -2 = 10.3 nM) that was developed by Mach and coworkers.²⁵⁹ It has been radiolabeled with tritium (**129**) [Fig. 1.64], and it is routinely used for sigma-2 binding assays.²²⁴ Similarly, ISO-1 (**130**) [Fig. 1.64], a benzamide selective sigma-2 ligand, has been examined in EMT-6 tumor mouse models as potential PET probe as ¹⁸F radiolabeled compound (K_i , σ -1 = 2150 nM; σ -2 = 0.26 nM; σ -1/ σ -2 = 8190), which is also radiolabeled with ¹²⁵I of the same molecule provides a sigma-2 radioligand that has been recently used for binding assays, ISO-2 (**131**) [Fig. 1.64] (K_i , σ -1 = 2150 nM; σ -2 = 0.26 nM; σ -1/ σ -2 = 8190).^{260,261} However, none of these ligands have replaced the standard of using DTG in binding assays.

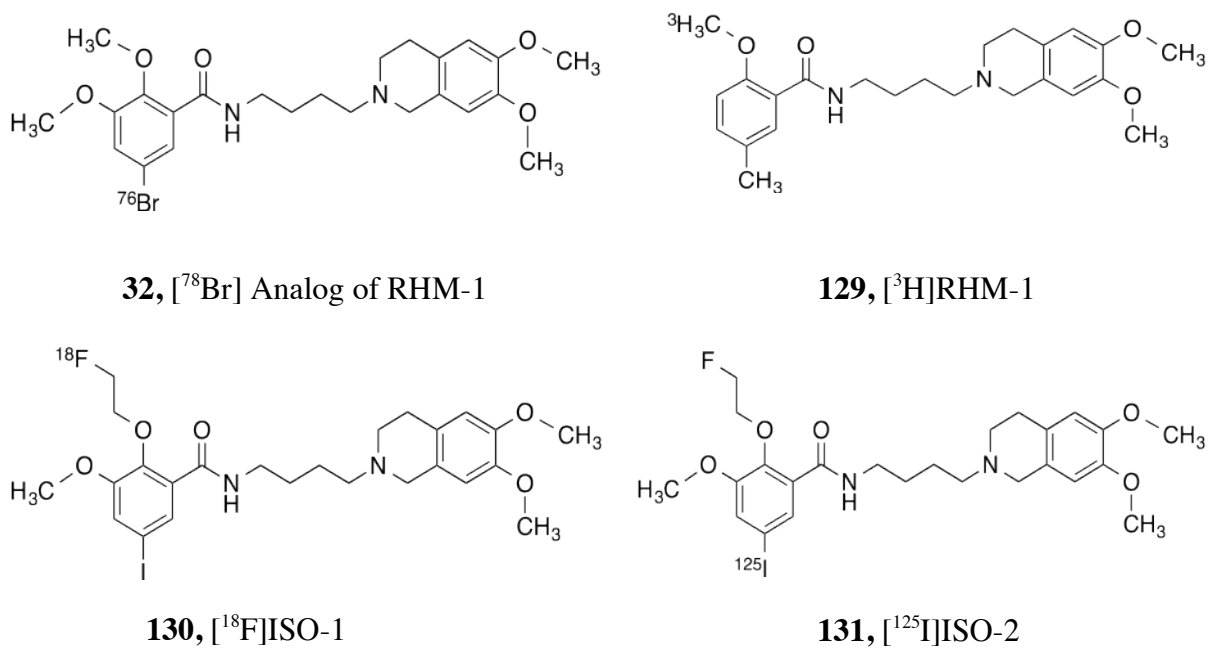


Figure 1.64. Selective sigma-2 radiotracers used for tumors and binding assays.

**CHAPTER II: SIGMA-2 RECEPTORS AND THEIR POTENTIAL ROLE IN
ONCOLOGY**

2.1. Introduction

Cancer is a state of cellular growth, which occurs when some normal cells become abnormal and continue to grow and subdivide abnormally and out of control. According to the World Health Organization (WHO), in 2012 there were 14.1 million new cancer cases, 8.2 million cancer deaths and 32.6 million people living with cancer (within 5 years of diagnosis) worldwide.²⁶²

Conventional chemotherapeutic agents are cytotoxic, which act by killing cells that divide rapidly under both cancerous conditions and normal conditions, including cells in the bone marrow, digestive tract, and hair follicles.²⁶³ Consequently, these agents results in the well-known and serious side effects of chemotherapy, for example, decreased production of blood cells (Myelosuppression),^{263,264} inflammation of the lining of the digestive tract (Mucositis)²⁶⁴⁻²⁶⁶ and hair loss (Alopecia)²⁶⁶.

In the search for novel and selective cancer therapies that can be used alone or in combination with existing chemotherapies to achieve maximum efficacy and safety to the surrounding normal tissues and reduce the *toxic* side effects that associated with the nonselective classical chemotherapies, a tremendous amount of effort invested in research, and this can be evidenced from the amount of recent publications highlighting the overexpression of sigma-2 receptor in numerous cancer tissues.^{263,265} These results strongly support the potential implications of sigma-2 ligands in cancer diagnosis and therapy. Therefore, this chapter focuses on the involvement of sigma-2 receptor in cancer biology and the potential therapeutic contributions of the sigma-2 receptor ligands in oncology.

As previously mentioned, sigma receptors represent a unique class of proteins,

and it has been accepted that there are two subtypes of sigma receptors, denoted sigma-1 and sigma-2 based on pharmacological and molecular studies. Sigma-1 receptor has been cloned and characterized as a 24 kDa single polypeptide having no homology with any other known mammalian proteins whereas the sigma-2 subtype is a 18-21 kDa protein that has not yet been cloned. Consequently, much less is known about the sigma-2 than the sigma-1 due to the absence of detailed structural information of the protein and the lack of truly selective sigma-2 ligands hampered the isolation and characterization of this protein. However, recent studies led to identify sigma-2 receptor protein as the progesterone receptor membrane component 1 (PGRMC1).⁸⁵

Since the discovery of sigma receptors by Martin and colleagues¹ in 1976, extensive studies have been conducted on sigma receptors and their functions in the central nervous, motor, endocrine, immune systems, addiction, and cancer.¹⁻⁴ These studies demonstrated that sigma receptors are involved in several pathologies of the central nervous system, including depression, anxiety, schizophrenia, and Alzheimer's disease, and they are now considered as therapeutic targets for the treatment of these diseases.²⁶⁷⁻²⁶⁹ Furthermore, sigma receptors have been shown to be overexpressed in many cancer tissues from both neural and non-neural origins.³⁵ However, malignant tumor cells display a higher expression of sigma-2 receptors than quiescent tumor cells. It was reported that sigma-2 receptor is expressed about 10-fold more in proliferating tumor cells compared with quiescent tumor cells and because ligand binding to this receptor can result in tumor cell death both via apoptotic and non-apoptotic mechanisms.³⁶ Furthermore, activation of sigma-2 receptors with sigma-2 ligands induces antiproliferative and cytotoxic effects in tumor cells *in vitro* as well as in *in vivo*

preclinical models.²³¹ Therefore, sigma-2 receptors are promising targets for tumor diagnosis and treatment.

2.2. Sigma-2 receptor and PGRMC1

It has been known for years now that sigma-2 ligands inhibit progesterone binding to a microsomal fraction of porcine liver, proposing that the high-affinity toward progesterone binding sites are part of a sigma receptors complex.²⁷⁰ However, a significant study by Xu et al., in 2011 provided the proof of concept that sigma-2 receptor and PGRMC1 are correlated and co-located.⁸⁵

PGRMC1 (progesterone receptor membrane component 1) is a protein that has been reported recently as a valid biomarker of cancer^{37,87,271,272} due to its upregulation in numerous types of cancers, such as ovary, breast, thyroid, lung, and colon,⁸⁶ as well as its necessity for cancer formation, growth, proliferation, and metastasis.⁸⁷ Therefore, PGRMC1 represents a vital biomarker for cancer progression and a potential target for anticancer drug discovery and development.^{86,273,274} More recently, proteomic studies also showed that PGRMC1 is expressed in high levels in the proliferative cells of human endometrium.²⁷⁵ PGRMC1 regulates cell growth and proliferation through interactions between its Cytochrome b5 binding domain and other potential binding partners, which include Insig-1, PAIR-BP1, and P450 proteins.^{273, 275-280} It's also stimulating P450 and its activity that promote cholesterol synthesis.⁸⁶ In addition, it was found that cancer cell proliferation and invasion was inhibited by the PGRMC1 inhibitor, AG205 (**8**) [Fig. 2.1], and this is mostly by inhibition of ERK1/2 phosphorylation.⁸⁵⁻⁸⁷

On the other hand, several other studies have shown that the sigma-2 receptor density in proliferative breast cancer cells is about 10-fold higher than in quiescent breast

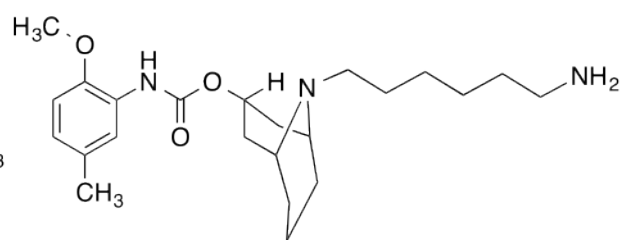
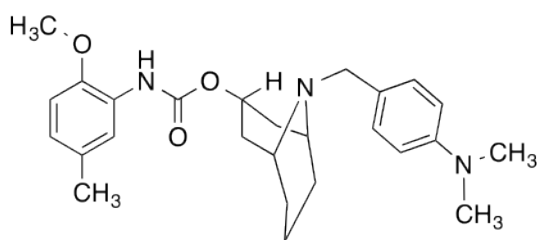
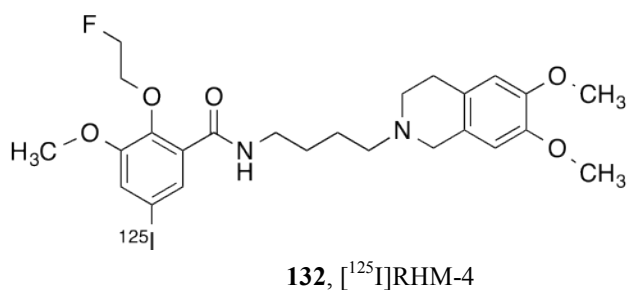
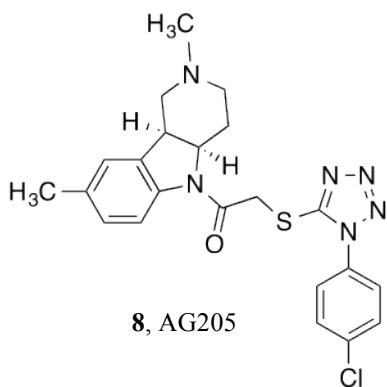
cancer cells.⁸³ Consequently, sigma-2 receptor has been validated as a biomarker for tumor cell proliferation both *in vitro* and *in vivo*, and as a target for chemotherapy⁸³ Sigma-2 receptor expression is upregulated during the transition from quiescence to proliferation and down-regulated during the transition from proliferation to quiescence.²⁴⁷

Based on the above mentioned findings, PGRMC1 protein and sigma-2 receptor share some common features, and due to this similarity, Mach and colleagues conducted a series of experiments and have concluded that sigma-2 receptor is likely to be the PGRMC1 protein or located within PGRMC1 protein complex based on the following facts:⁸⁵

- a) The selective sigma-2 ligand binding, [¹²⁵I]RHM-4 (**132**) [Fig. 2.1], was blocked not only by other sigma-2 ligands, such as DTG, siramesine, WC26 (**133**) [Fig. 61], SV119 (**134**)[Fig. 2.1], but also by the PGRMC1 protein inhibitor, AG-205.^{82,83}
- b) The selective fluorescent sigma-2 ligand, WC-21 (**7**) [Fig. 2.1], cross-linked a protein that shares similar sequence as that of PGRMC1 protein.
- c) Both the anti-PGRMC1 antibody and the fluorescent sigma-2 ligand, SW120 (**135**)[Fig. 2.1], labeled the same intracellular sites under confocal microscopy.
- d) Cells with a decreased PGRMC1 protein (PGRMC1 knockdown) level also exhibited reduced sigma-2 receptor binding, likewise cells with a higher PGRMC1 protein expression (PGRMC1 transfection) showed higher sigma-2 receptor binding.⁸⁸

However, these findings need to be confirmed since numerous questions have been raised and urged the search for answers; for example, the molecular mass of sigma-

2 receptor is about 21.5 kDa while the PGRMC1 protein is from 22 to 28 kDa range.^{6,185,273,281-283} Also, the tumor cell proliferation, growth, and metastasis were inhibited by PGRMC1 protein inhibitors, whereas sigma-2 antagonists stimulate tumor cell proliferation and sigma-2 agonists induce apoptosis according to many published reports. Further, PGRMC1 is reported to bind to P450 resulting in the stimulation of its activity and increased cholesterol synthesis,⁸⁶ which has not been reported for the sigma-2 receptor. Moreover, none of the sigma-2 ligands have been reported to bind to PGRMC1 protein or even PGRMC1 protein ligands to bind to sigma-2 receptors.^{36,284} Therefore, a controversy still exists as to the validity of PGRMC1 as the actual sigma-2 receptor protein. Most recently, Rouho and coworkers showed evidence for a smaller molecular weight protein as the sigma-2 receptor in stark contrast to the results shown for the PGRMC1 protein.



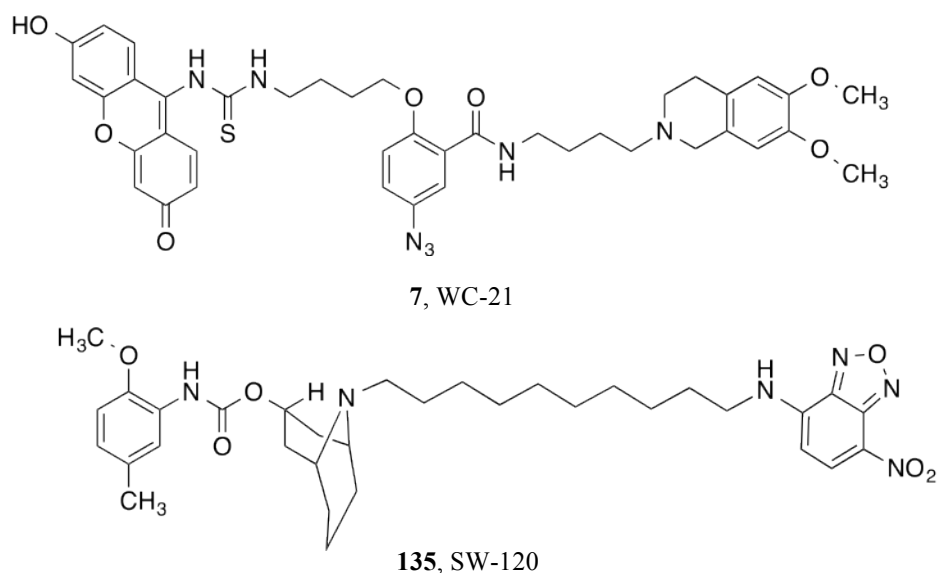


Figure 2.1. Chemical structures of sigma-2 receptor ligands and PGRMC1 inhibitor, AG205.

2.3. The most recent hypothetical sigma-2 receptor signaling pathways

A number of studies have shown that sigma-2 receptor over-expressed in proliferative cells, which is in agreement with the well-known PGRMC1 protein. In addition, the recent finding that sigma-2 receptors and PGRMC1 proteins are co-located and competed for the same PGRMC1 ligands or sigma-2 ligands.⁸⁵ From one hand, several studies have demonstrated that the PGRMC1 protein interacts with epidermal growth factor receptor (EGFR),²⁷¹ plasminogen activator inhibitor RNA-binding protein 1 (PAIR-BP1),²⁷³ insulin-induced gene/SREBP cleavage activating protein/sterol regulatory element binding protein (Insig-1/Scap/SREBP) complex,³⁷ and neutrophil gelatinase-associated lipocalin (NGAL).²⁷² Further, it has been reported that PGRMC1 protein involved in activation of P450, antiapoptosis, cell invasion, metastasis, stimulation of tumor growth, and regulation of steroid signaling.^{86,87}

On the other hand, sigma-2 receptor ligands have been reported in some studies for their ability to reduce the expression of downstream effectors of mTOR pathway

signaling (p70S6K and 4EBP1), trigger caspase-3, activate PARP-1 (poly [ADP-ribose] polymerase 1) cleavage and DNA fragmentation, and suppress the expression of cyclin D1.²⁸⁵ Consequently, it was found that sigma-2 receptor ligands mobilize intracellular calcium ion,²⁸⁶⁻²⁸⁸ facilitate potassium channel,²⁸⁹ and induce oxidative stress.²⁹⁰

Based on the published hypothetic models on sigma-2/ PGRMC1 proteins functions such as S2R^{Pgrmc1} to NGAL signaling,²⁷² and S2R^{Pgrmc1} to diverse effectors' paths.³⁴ In addition to the above-mentioned studies, Huang and co-workers⁸⁸ proposed four signaling pathways for sigma-2/ PGRMC1 proteins to employ their regulatory roles in cancer as follow:

- 1) Stimulation of EGFR signaling promotes cell proliferation, and inhibition of EGFR signaling promotes apoptosis.
- 2) Sigma-2/PGRMC1 proteins interact with PAIR-BP1 and Insig-1/Scap/SREBP and regulate sterol synthesis and progesterone signaling.
- 3) Sigma-2/PGRMC1 proteins activate P450 and regulate lipid metabolism.
- 4) Sigma-2/PGRMC1 proteins inhibit ER stress, which instigates calcium ions release, subsequent caspases activation, and promote cancer cell death.

When sigma-2 receptor over-expressed (in cancerous situations), it stimulates the signaling pathways of EGFR such as RAS/RAF/ERK pathway, PLC/PKC/NF- κ B pathway, and PI3K/Akt/mTOR pathway that promote cell proliferation and invasion. Additionally, sigma-2 receptor can stimulate P450 metabolism pathway, initiating the Insig-1/Scap/SREBP pathway, and blocking the caspase pathway. Upon sigma-2 receptor /ligand binding, the interaction between sigma-2 receptors and their effectors will be interrupted/inhibited, developing a reversion in its proliferative action and induction of

apoptosis as a result.⁸⁸

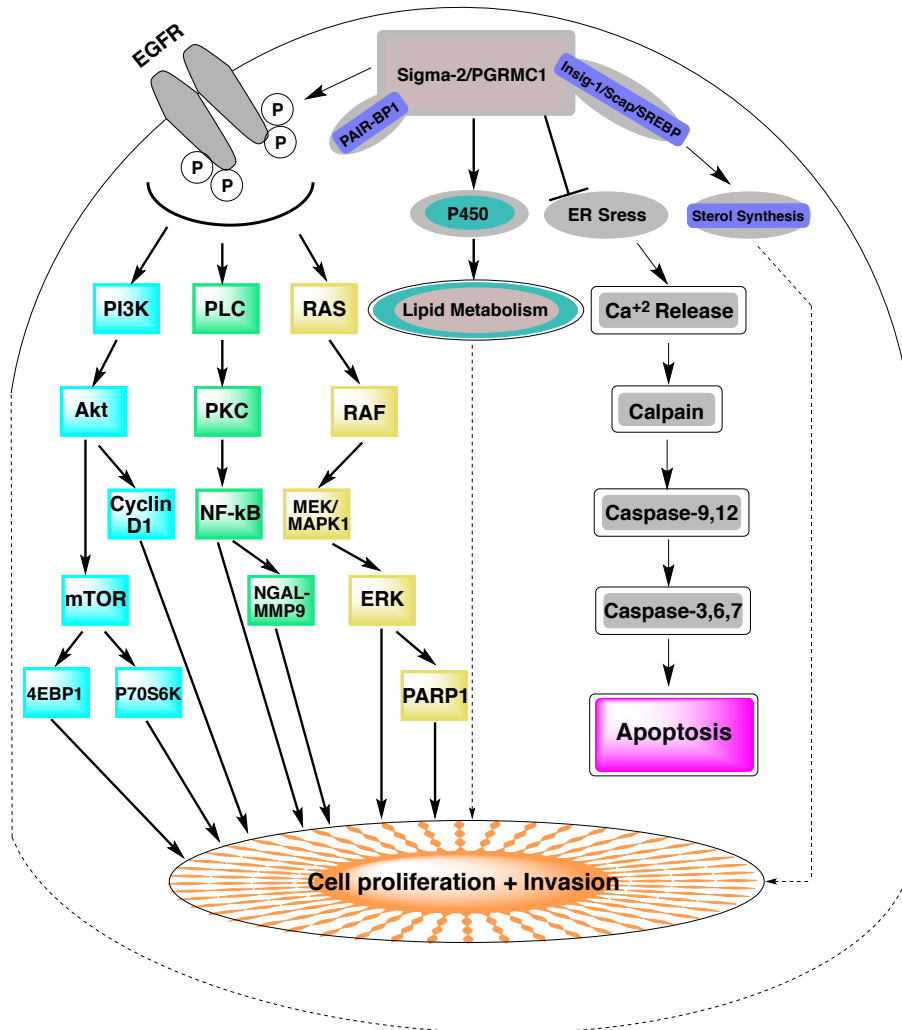


Figure 2.2: Huang’s hypothetical scheme of sigma-2 receptor/PGRMC1 signaling pathways in cancer cells [Adapted from ref. 88]

2.4. Sigma-2 receptor as a biomarker

Potential Use as an Imaging Target for Cancer Diagnosis:

The importance of sigma-2 receptors in oncology is well reported in literature since it has proven to be over-expressed in a higher density in human cancer cells as compared to most normal tissues.²⁹⁰ Hellewell and Bowen were the first to identify sigma-2 receptor through receptor binding studies in rat PC12 adrenal pheochromocytoma cells.²² There are two types of cell populations in each solid tumor;

proliferative cells and quiescent cells. The tumor cell proliferation is generally measured by the ratio of the proliferative cells to the quiescent cells. Similarly, the growth fraction is measured by the ratio of the number of proliferative cells in a solid tumor to the total number of proliferative cells and quiescent cells.²⁹² It has been reported the usefulness of sigma-2 receptor as a biomarker in determining the proliferative cells and quiescent cells of solid tumors using positron emission tomography (PET), and single photon emission computed tomography (SPECT).³⁶ For instance, Mach and co-workers showed that the density of sigma-2 receptors in proliferating cells was 10-fold greater than the density observed in quiescent cells.^{83,281} Moreover, using PET technology, Mach and co-workers used a [¹¹C] labeled sigma-2 ligand to image EMT-6 breast tumor location in female BALB/C mice.²⁹³ Also, Hawkins and co-workers used a radiolabeled sigma-2 ligand, [¹⁸F]-RHM-4, to visualize the tumor site using Micro-PET imaging technique.²⁹⁴

Furthermore, it was observed that the up-regulation and down-regulation of sigma-2 receptors in the transition state between the proliferative and quiescent states in mammary mouse cells.¹⁸⁵ Consequently, these results suggested that the sigma-2 receptor is a biomarker of cell proliferation in breast tumors, and likewise, this can be used to study the other tumors that have high density of sigma-2 receptors.¹⁸¹

2.5. Sigma-2 receptor ligands inducing apoptosis

It has been suggested that both Ca⁺² release from the endoplasmic reticulum (ER) and the resulting capacitive Ca⁺² influx are apoptogenic.^{269,295} Sigma-2 receptor agonists have been believed to inhibit tumor cell proliferation, and induce apoptosis while sigma-2 receptor antagonists promote tumor cell survival.³⁶ Some studies have shown that the selective sigma-2 receptor agonist, CB-64D (**99**) [Fig. 2.3] or selective sigma-1 antagonist ligands cause a rapid transient release of Ca⁺² from the ER to the cytosol in

various cancer cells, including neuroblastoma, breast adenocarcinoma, and colon carcinoma.^{286,296} In the same studies they have suggested that this intracellular Ca^{+2} affects protein kinase C activity and induces cancer cell apoptosis.^{286,296} An additional study examined the effect of the sigma ligands (+)-SKF10,047, (-)-SKF10,047, (+)-pentazocine, (-)-pentazocine, DTG (**35**) [Fig. 2.3], haloperidol (**21**) [Fig. 2.3], rimcazole, and RHAL (**78**) [Fig. 2.3] on proliferation of human mammary adenocarcinoma (MCF-7, MDA), melanoma (Chinnery), and cells colon carcinoma (LIM1215, WIDr).²⁶³ Dose-dependent rounding, detachment and cell death were observed in all cell lines, and the most potent inhibitors of cellular proliferation were obtained from Rimcazole and RHAL.²⁹⁷ It was found that the inositol 1,4,5-triphosphate (IP3) receptor is involved in the sigma-2-agonist induced intracellular calcium release.²⁸⁸ The escalation of cytosolic Ca^{2+} is associated with a prompt drop of metabolic activity and cellular ATP concentrations that results in cell death.²⁸⁸ In a different study by Kashiwagi and co-workers, was found that sigma-2 receptor ligands stimulate caspase-3 activity and exhibit concentration and time-dependent induction of tumor cell apoptosis, whereas a sigma-1 receptor ligand, pentazocine, does not have such effect.²⁹⁴ Further, the most selective sigma-2 ligands, siramesine, showed potent anticancer activity against several tumor cell lines deriving from lung, breast, cervix, and prostate. Consequently, in a recent study, siramesine was found to induce caspase-3 dependent apoptosis in lens epithelial cells suggesting its potential use to treat posterior capsular opacification.^{188,284,294,298} Stimulation of sigma-2 receptors induces anti-proliferative and cytotoxic effects in tumor cells *in vitro* as well as in *in vivo* preclinical models.²⁹² Thus, sigma-2 receptors are valid targets for tumor diagnosis and treatment.

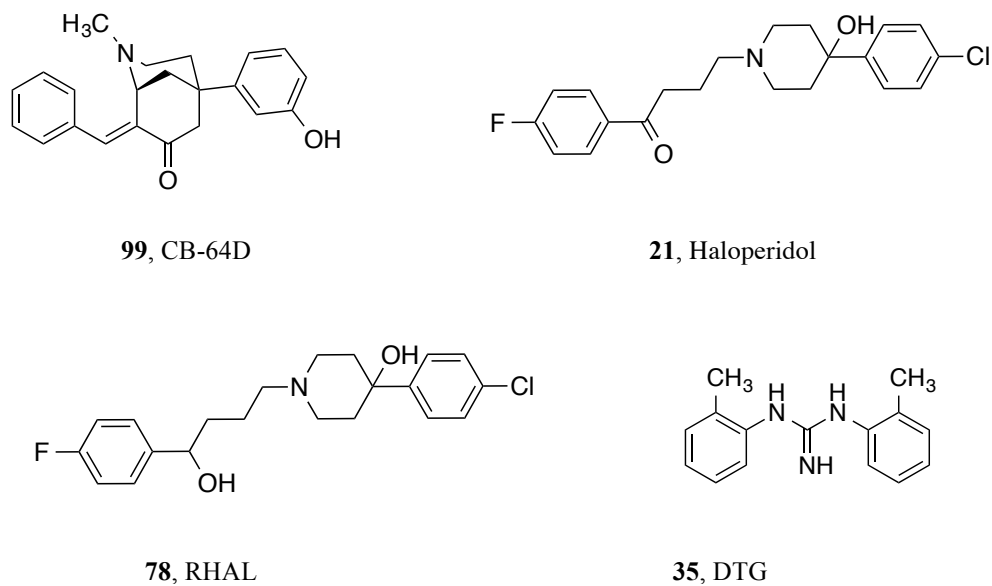


Figure 2.3: Chemical structures of some sigma-2 receptor ligands

2.6. Sigma-2 receptor ligands as antitumor agents

The idea of targeting sigma-2 receptors is supported by increasing the number of publications that demonstrated the importance of sigma-2 receptor in curing several cancer cell types.^{36, 299, 300} Numerous sigma-2 ligands have been shown to induce *in vitro* and *in vivo*, cancer cell death by activation of multiple pathways to exert such effect, including caspases activation, reactive oxygen species, lysosomal leakage, autophagy and modulation of Ca^{2+} release by intracellular stores. However, activation of the pathways depends on tumor cell type and on the structure of the sigma-2 ligands.^{188, 285, 301} Sigma-2 receptors significantly enhance the pharmacological effects of other anticancer drugs such as paclitaxel, gemcitabine synergistically in a combination treatment by increasing caspase-3 activity, and inducing apoptosis. For instance, a study conducted by Mach and colleagues in mice with pancreatic adenocarcinoma showed that the sigma-2 selective ligand, SV119, gemcitabine, and paclitaxel alone caused approximately 3%, 6%, 5%

escalation in caspase-3 activity, respectively while SV119 combined with gemcitabine, or SV119 combined with paclitaxel caused around 20% and 30% escalation in caspase-3 activity, respectively. The synergistic effects of sigma-2 receptor ligands and anticancer agents were observed in both *in vitro* and *in vivo* animal studies.^{186,302,303} Recent *in vivo* studies combining the anticancer agent, doxorubicin, with sigma-2 ligands in several *in vitro* cancer cell lines display an additive effect in the inhibiting of tumor growth.³⁰⁴⁻²⁰⁷ Therefore, combination of traditional anticancer agents with sigma-2 ligands appears to have a favorable synergistic effect in inhibiting the tumor growth, and hence a very promising area of research.

2.7. Sigma-2 receptor ligands as drug delivery vehicles

The major limitation of traditional cancer chemotherapies is the severe toxicity to normal tissues developing from a lack of selectivity of these agents. Accordingly, new selective targeting for cancer cells has been suggested as an urging need to develop new treatments.³⁰⁸

There are two approaches have been reported for targeting sigma ligands as drug delivery agents. One approach was nanoparticle technique in which the sigma ligands were conjugated with various nanoparticles, such as polyethylene glycol or through direct linking at the end of an alkyl chain of the sigma-2 receptor ligand covalently. Prior to injecting the newly formed ligands into experimental animals, the nanoparticles were filled with appropriate cytostatic or cytotoxic agents. The second technique is to use antitumor peptides or antisense oligonucleotides to conjugate with sigma-2 receptor ligands also by direct covalent linking that can be administered systemically.³⁰⁹ Mach and colleagues proposed and synthesized five SV119-anticancer drug conjugates, and they

indicated that these SV119 conjugates provided high affinities for sigma-2 receptor and high activities of inhibiting Akt and enhanced induction of caspase-3 activity.³⁰⁶ In a different study, Zhang and colleagues used the same sigma-2 ligand, SV119, to design SV119-liposomes conjugates and accordingly to evaluate the uptake of these conjugates by tumor cells compared to normal cells and they found the high uptake of SV119-liposomes by tumor cells but not by normal cells.³¹⁰ Therefore, sigma-2 receptors are a promising anticancer target and the selective sigma-2 ligands are a valid target for developing new anticancer drug delivery vehicles.

2.8. Sigma-2 receptor ligands and low potential of toxicity to normal tissues

Multiple sigma-2 ligands seem to cause the inhibition of tumor growth and cell death after their administration by affecting various signaling pathways. Consequently, several other studies have proven that sigma-2 receptor ligands are potent anti-proliferative and pro-apoptotic against many cancer cells; however, they did not develop any kind of toxicities and appear to be safe in normal cells.³⁶ A study by Kashiwagi and colleagues conducted on the sigma-2 selective ligand, WC26, it was found that this sigma-2 ligand was mainly toxic for tumor cells with no or very minimal toxicity in normal cells.³⁰³ In another study by Hornick and colleagues found that the selective sigma-2 ligands SW43, SV119, and siramesine displaying exceptional proapoptotic activities, potentiation of gemcitabine anticancer activity without noticeable toxicities in normal tissues.³⁰² Recently, Spitzer and his colleagues discovered that the sigma-2 ligand, SV119-Bim, had very minimal and transient toxicities as determined by slightly increased levels of amylase, caspase-3, and lipase activities in pancreas, which vanished after 2 weeks of treatment without any noticeable organ damages.³⁰⁶ More recently, in a

Micro-PET imaging study of a radiolabeled sigma-2 ligand in an EMT-6 tumor-bearing mouse by Mach and his colleagues, it was noticed the high uptake of radiotracer in the EMT-6 tumors and low uptake in the surrounding normal tissues indicating the low potential of toxicity in normal tissues.¹⁹¹ Since selective sigma-2 ligands can kill tumor cells by both apoptotic and non-apoptotic pathways with no or minimal toxicities in normal tissues, it suggests that this receptor is a new target for the development of safer chemotherapeutic agents. Recently, Hilary *et al.* investigated the effect of CM572 (**136**)[Fig. 2.5], a potent and selective partial agonist at sigma-2 receptors, on breast and pancreatic tumor cell lines in addition to the neuroblastoma line. In this study, CM572 was able to induce dose-dependent cell death these cell lines.³¹¹

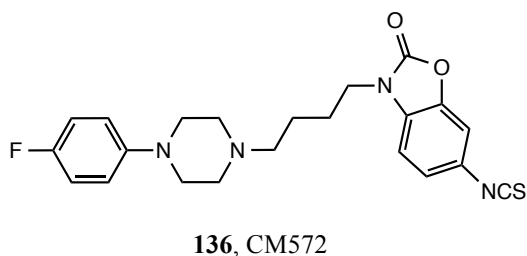


Figure 2.4: Chemical structures of the sigma-2 receptor ligand, CM572

CHAPTER III: SIGMA RECEPTORS AND PSYCHOSTIMULANTS ABUSE

3.1 Introduction

3.1.1 Background

Psychostimulants or central nervous system (CNS) stimulants are psychoactive substances that produce transitory enhancements in either mental or physical functions or both. As the name suggests a CNS stimulant is any agent that activates, enhances, or increases stimulatory neuronal activity. The resultant effects may include increases in attention, alertness, locomotion and energy as well as elevation of blood pressure, heart rate, and respiration. Stimulants are also sometimes referred to as "uppers" due to their "up" feeling effect in opposite to depressants which usually called "downers" owing to their "down" effect and decreases in mental and/or physical function.^{312,313} As stimulants are capable of improving mood and mitigating anxiety, depression, lethargy, fatigue, and some can even induce feelings of euphoria, they are extensively used throughout the world as prescription medicines and licit or illicit substances of entertaining use or abuse. For long time, stimulants were used to lessen asthma and other respiratory problems, neurological conditions, obesity and a variety of other disorders. However, as their liability of abuse and addiction became evident, the medical use of stimulants started to diminish. Stimulants are now being prescribed to treat only limited health problems, including attention deficit hyperactivity disorder (ADHD), narcolepsy, and depression in certain cases that non-responded to other medications. Most stimulants exert their effects by facilitating the activity of certain neurotransmitters in central and synaptic nervous system such as dopamine and norepinephrine.³¹²⁻³¹⁴ Improper use of stimulants (other than when used as prescribed by a doctor) can lead to hostility, paranoia, and even psychotic symptoms. Improper stimulant use (abuse) can also result in harmfully elevated body temperature, irregular heartbeat, heart failure, and seizures.^{96,123,313,314}

3.1.2 Prevalence of Psychostimulants Abuse

According to the 2012 World Drug Report issued from the United Nations Office on Drugs and Crimes,³¹⁵ about 230 million people, or 5 percent of the world's adult population, are estimated to have used an illicit drug at least once in 2010. Problem drug users number about 27 million, which is 0.6 percent of the world adult population. According to the same report, cocaine and other drugs are directly linked to the deaths of around 0.2 million people each year, destroying families and bringing despair to many people in their community. Illicit drugs undermine economic and social development and contribute to crime, instability, insecurity and the spread of serious diseases such as HIV, hepatitis B, and hepatitis C.³¹⁵ Additionally, in 2013, the National Survey on Drug Use and Health (NSDUH),⁹⁶ reported that an estimated 24.6 million Americans (9.4 percent of the population) aged 12 or older were current illicit drug users. There were 1.5 million current cocaine users aged 12 or older, or 0.6 percent of the population, and the number and percentage of past month methamphetamine users in 2013 (595,000 or 0.2 percent). Illicit drugs include marijuana, cocaine, heroin, hallucinogens, inhalants, or prescription-type psychotherapeutics (pain relievers, tranquilizers, stimulants, and sedatives) used non-medically.^{96,123} These numbers indicate the serious negative health consequences on drug abusers besides the heavy financial burden on society to treat such outcomes.

3.1.3 Psychostimulants mechanism of actions

For stimulants to exert their actions they must first get to the brain. This can through one of the four most usual routes of administering psychoactive substances:

- 1) Oral consumption.
- 2) Inhalation of smokes into lungs.

- 3) Intranasal consumption through snorting.
- 4) Intravenously by using a syringe.

In oral consumption, the swallowed substance goes to stomach and gastrointestinal tract (GIT) where some of these substances are absorbed through the digestive tract into the bloodstream while the rest are broken down by metabolism. Substance inhaled by snorting will be absorbed by nasal mucosa and entered directly the bloodstream. Similarly, smoked substances will be absorbed by the large surface area of the lung as in a gaseous stage and entered easily into the bloodstream. Once the psychoactive substance gets into the bloodstream, it will be distributed through out the body. However, before entering the brain, the substance has to pass the blood brain barrier (BBB), which is a layer of cells that surround blood vessels with tight cell wall junctions that prevent the large or charged molecules from passing the blood brain barrier (BBB) into the brain. In the same time, it does let the small (such as cocaine and methamphetamine) and neutral molecules to enter the brain.^{96,314,316}

Generally, stimulants are a variety of compounds that excite the central nervous system or make a change in body's metabolic activities. There are two ways for a stimulant to function, one-way is to enhance or mimic the effects of neurotransmitters that prepare our bodies to “fight or flight” during threatening situations in which increase heart rate, blood pressure, and respiration. Catecholamines that include epinephrine, norepinephrine, and dopamine are the best examples of such neurotransmitters. The second way for a stimulant to exert its effect is by blocking transmission of the signals from one nerve to another and inhibiting the propagation system of that signal as a result. Neurotransmitters are molecules released in the gap between the two nerves called a “synapse”, where these neurochemicals are responsible for transmitting the signals from one neuronal cell to another. After each signal, the synapse needs to be cleaned to

prepare for the next signal through degradation or re-uptake. Stimulants such as cocaine block the reuptake mechanism and increase the dopamine/epinephrine availability in the synapse and intensify the signal that may result in euphoria or hallucinations.^{316,317}

3.1.4 Examples of psychostimulants:

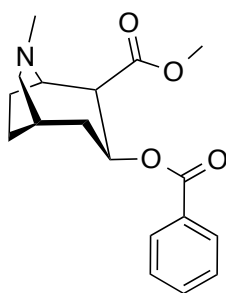
1. Cocaine
2. Amphetamines (dextroamphetamine and methamphetamine)
3. Amphetamine derivatives used to treat ADHD (methylphenidate; Pemoline; Cylert)
4. Variety of drugs formerly used to treat obesity (fenfluramine; Pondimin, phentermine; under trade names as lonamin, Obe-Nix, Adipex-P, Oby-Trim, and Fastin, and phenmetrazine; Preludin)
5. Caffeine and theophylline (psychoactive drug in coffee and other caffeinated beverages) and nicotine (ingredient in tobacco).

This chapter will focus on cocaine and methamphetamine since they are the most common abused drugs that perform their psychostimulant actions by interacting with sigma receptors and mostly sigma-1 receptors.

3.2. Cocaine

Cocaine (3)[Fig. 3.1] is one of the most highly consumed illicit drugs in the world and especially in United States. The use and abuse of cocaine is well known to be a leading cause of many social and economic problems including an increased risk of HIV, hepatitis B, and C infections, and an increased incidence of crime, violence and psychosocial problems. Furthermore, there are no approved medications to treat cocaine abuse or addiction, which urges

the need to develop novel and effective agents to battle this serious issue.^{96,123}



9. Cocaine

Figure 3.1: Chemical structure of cocaine.

3.2.1 History

Cocaine is one of the oldest known psychoactive substances. The historical use and abuse of cocaine has started at the end of 6th century. Coca leaves, have been the source of chewed and ingested cocaine for thousands of years and the purified cocaine has been an abused substance for more than 100 years.^{318,319}

It's generally agreed upon, the chewing of the coca plant leaves, *Erythroxylum coca*, began the sixth century A.D. As a matter of fact, learning the full story of coca's uses by the Incas is hindered by their lack of a written language. However, archeological evidence of this habit was found in Indian mummies, which were discovered to be buried with supplies of coca leaves as well as in a variety of pottery portraying the characteristic cheek bulge of the coca chewer. Although coca use predated the Incan civilization, it is most commonly associated with this empire, which became the dominant influence in what is now Bolivia, Peru, Ecuador and Columbia during the 11th century. Later under the rule of Topa Inca, coca plantations had become a state control and coca use was quite restricted by the end of the 15th century.³¹⁸⁻³²⁰

In 16th and 17th centuries, the Spanish colonists noticed how the Indians of what now Chile, Bolivia, Peru and Columbia were able to ease fatigue, stomach disorders, skin ulcerations, venereal diseases, headache and muscular pains by chewing the leaves of the coca shrub *Erythroxylum coca*. Spanish physicians also began promoting its therapeutic use for skin disorders, colds, laryngitis, asthma, rheumatism, and toothaches. Antonio Julian, a former Jesuit, in the 18th century urged the use of coca by the laboring classes of Spain, believing that it would improve both their health and productivity.³¹⁸⁻³²⁰

In 1860, Albert Niemann, a German chemist, extracted pure cocaine from the leaves of *Erythroxylum coca*, and he was the first to synthesize cocaine in pure form. Later, cocaine was used as a mild stimulant much like caffeine in tea and was added to several proprietary beverages such as Coca-cola for the next 25 years.³¹⁹ In 1914, United States regulated the distribution of non-medical use of cocaine through the Harrison Narcotic Act.^{318,320,321} In 1970, when the use and abuse of cocaine increased again, the Controlled Substances Act, consequently made cocaine illegal in the United States.³²² The cheap freebase form of cocaine, known as “crack”, became available and caused a higher incidence of cocaine abuse in the society. Consequently, due to its extensive abuse and popularity during 1980s and 1990s, it was labeled “the drug of the 1980s and 1990s”. Cocaine was classified as a Schedule II drug, considered to have strong potential for abuse or addiction but also to have legitimate medical use.³¹⁷ Even today it is a Schedule II drug, meaning it is associated with a significant abuse liability and can only be prescribed by physicians for sensible medical uses like local anesthesia.³²²

3.2.2 Physiological and psychological effects of cocaine

Cocaine can be obtained from the coca leaves using a relatively simple method by extracting it with an organic solvent resulting in a coca paste containing nearly 80% cocaine. It is

generally sold on the street as a fine, white, crystalline powder (HCl salt) and is also known as “coke”, “C”, “flake” and “blow” or as a free base which known as “crack”.³¹⁸⁻³²⁰ Cocaine, chemically, is the methyl ester of benzoylecgonine or [1R, 2R, 3S, 5S]-3-(benzoyloxy)-8-methyl-8- azabicyclo-[3.2.1]octane-2-carboxylic acid methyl ester. The cocaine displays effects that vary with its plasma concentrations in accordance to the routes of administration. Patterns of its effects and plasma concentrations vary with different routes of administration. The primary routes of administration are oral, intranasal, intravenous and inhalation. In a single dose, both smoking and intravenous injections produce extremely high rate of absorption (500-1000µg/ml) compared with snorting (100-500µg/ml).^{323,324}

Cocaine has been shown to exclusively interrupt the dopamine neurotransmitter system by overstimulating the receptors on the postsynaptic neuron, either by increasing the amount of dopamine in the synapse through excessive presynaptic release or by inhibiting dopamine's pattern of reuptake or chemical breakdown.³²⁵ Cocaine use increases the amount of dopamine (DA) in the CNS, which elevates the mood and the motor activity. Consequently, when the level of cocaine subside in the brain, the dopamine (DA) amount decreases to normal and the euphoric feeling diminish as well.

There are numerous psychological as well as physiological effects correlated with cocaine abuse. Cocaine has two main pharmacological applications. Cocaine is the only drug known to have local anesthetic and central nervous system (CNS) stimulant properties. Cocaine exerts its local anesthetic actions by blocking the transmission of sensory impulses within nerve cells by preventing the influx of Na⁺ into the cell. This effect is most noticeable when cocaine is applied to the skin or to mucous membranes. Moreover, cocaine hydrochloride has been approved for use as a local anesthetic in surgery of the larynx, throat, and nose.³²⁶

The psychological manifestations range from euphoria to anxiety, depression and severe drug dependence.³²⁷ Prolonged use of cocaine affects the cardiovascular system (CVS), the respiratory system as well as the central nervous system (CNS). It puts an individual at the risk of angina pectoris, hypertension, myocardial infarctions and hemorrhages.³²⁸ Cocaine abuse can disrupt the normal neuronal circuitry and may even lead to severe seizures in case of overdose.³²⁹ Comparably, chronic use can lead to respiratory failure and death. Cocaine's effects on the central nervous system include cerebral infarction, cerebral blood loss, and stroke. Cocaine can also produce seizures or convulsions. Eventually, heavy consumption and overdose of cocaine can actually result in death for some cases.³³⁰

Accumulating reports, based on animal studies and brain imaging studies in humans, have shown that chronic use of cocaine can affect the dopaminergic neurons in the reward system of the brain. These areas of the limbic system include the nucleus accumbens and ventral tagmental area (VTA), which could account for the possible mechanistic reasons behind addiction to cocaine.³³¹ Numerous animal studies have demonstrated that high doses of stimulants can lead to neurotoxicity by damaging nerve endings. As a matter of fact, more studies need to be conducted to expand our knowledge of the stimulants effects on the human brain as brain imaging techniques are developing rapidly.³³²

3.2.3. The dopamine reward system

Also called the brain reward system or the limbic reward system, which is the brain circuit that necessary for the neurological reinforcement system. This circuit has been traced between the nucleus accumbens and the ventral tegmental area (VTA)[Fig. 3.2].³³³ Psychoactive substances affect the limbic reward system as well as the nucleus accumbens by increasing the release of the dopamine that controls the feeling of pleasure such as euphoria and satisfaction in

addition to having roles in motivation, cognition, and movement.³³³⁻³³⁵ Consuming high doses of stimulants will lead to release higher levels of dopamine in the brain that boost mood and motor activity; however, too much cocaine can produce irritability, nervousness, aggressiveness, and paranoia that approaches schizophrenia, as well as hallucinations and weird thoughts. Alternatively, too little dopamine in the brain results in the tremors and paralysis of Parkinson's disease.³³⁴⁻³³⁶ There is an increasing amount of evidence suggesting that the nucleus accumbens is the critical site for dopamine elevation among drug abusers, and dopamine has been linked to all substances abuse and addiction and even labeled as the master molecule of addiction.³³⁷

Normally, nucleus accumbens neurons function in predictable manner as follow:

- 1- An electrical signal reaches the target point at the pre-synapse
- 2- The presynaptic neuron triggers the dopamine release into the synapse
- 3- The dopamine transmits through the synapse toward the postsynaptic neuron target and exerts its excitatory effect to generate internal electrical signal in the neuron.
- 4- The extra dopamine in the synapse will be enzymatically deactivated or reabsorbed by dopamine reuptake transporters (DAT).³³⁸

Cocaine interacts with the dopamine and the limbic reward systems to exert its major effects including the reinforcing effects. Similarly, cocaine has the ability to block the reuptake of dopamine by synapse via dopamine reuptake transporters (DAT) blockade that will increase the availability of dopamine in the synapse and prolong the postsynaptic neurons firing.³³⁹

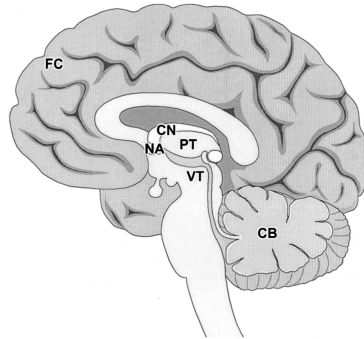


Figure 3.2: Brain. Certain areas of brain are known to be involved in reward/reinforcement due to drugs. These include the nucleus accumbens (NA), ventral tegmental (VT), and frontal cortex (FC). Other abbreviations are cerebellar (CB), putamen (PT), and caudate nucleus (CN).³³³

3.2.4. Approaches to potential treatment for cocaine abuse

A significant increase in the dopamine concentration in the brain has been observed in a microdialysis study on the brain after cocaine administration.³⁴⁰ Likewise, considerable evidence has accumulated, from animal studies over the recent years, suggesting that the dopamine transporter is a vital target for reinforcing effects of cocaine.^{341,342} For years the dopamine hypothesis received much attention from researchers as one of the most valid strategies to target cocaine abuse and addiction. The hypothesis proposes that cocaine acts as an indirect dopamine agonist by inhibiting the reuptake of dopamine from the synapse via the dopamine reuptake transporters (DAT).³⁴³⁻³⁴⁵ Consequently, several analogues were designed and analyzed that would block the access of cocaine to DAT, but the majority of them suffered from the limitation of having abuse liabilities similar to or greater than cocaine.³⁴⁶ Correspondingly, a number of medications have disclosed promising results in preclinical and early clinical trials, but no medication with proven efficacy is available for the treatment of cocaine addiction.³⁴⁷⁻³⁵⁰

3.2.4.1. Dopamine receptor agonists and antagonists

Since dopamine exerts its function through direct binding to and activating dopamine receptors, they are a logical target for cocaine abuse. Also, it has been suggested that a partial dopamine receptor agonist should suppress the cocaine effect, acting as a functional antagonist.³⁵¹ There are five subtypes of dopamine receptors that have been identified (D₁, D₂, D₃, D₄, and D₅), and all of these belong to the G protein-coupled receptor superfamily. However, only three subtypes (D₁, D₂, and D₃) are thought to be involved in the cocaine reinforcing effects.³⁵²

Numerous animal studies have indicated that dopamine receptor agonists such as bromocriptine (**137**)[Fig. 3.3] and apomorphine (**138**)[Fig. 3.3] retain self-administration in monkeys,^{353,354} and in rodents^{355,356} respectively. The full-efficacy D₁ agonist, SKF82958 (**142**)[Fig. 3.3], was able to maintain self-administration in monkeys; nevertheless, the D₁-selective partial agonist, SKF38393 (**141**)[Fig. 3.3], failed to maintain self-administration.^{354,357,358} The D₃ agonist, BP897 (**143**)[Fig. 3.3], has shown to attenuate the physical dependence behavior of cocaine without inducing any reinforcement by itself.³⁵⁸ A powerful decrease in cocaine self-administration has been observed when rats pretreated with dopamine agonists selective for the D₃ receptor 7-OH DPAT (**140**)[Fig. 3.3] and quinpirole(**139**)[Fig. 3.3] at doses that were not reinforcing by themselves. These results suggest that D₃ receptor may be involved in the reinforcing effects of cocaine and may be a useful target for developing a pharmacotherapy for cocaine abuse.³⁵⁹ It is interesting to note that no sigma receptor affinities have been reported for the D₃ receptor ligands. Furthermore, numerous studies on the behavioral effects of cocaine was found that some dopamine uptake inhibitors and dopamine agonists substitute for cocaine.³⁶⁰⁻³⁶²

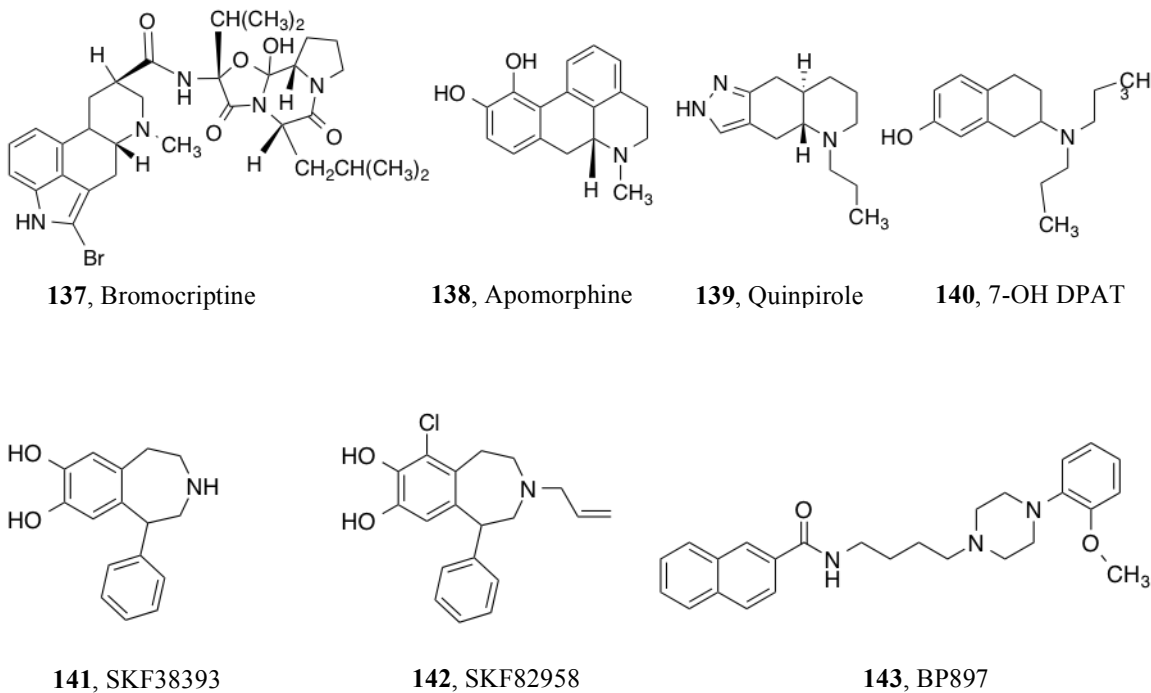
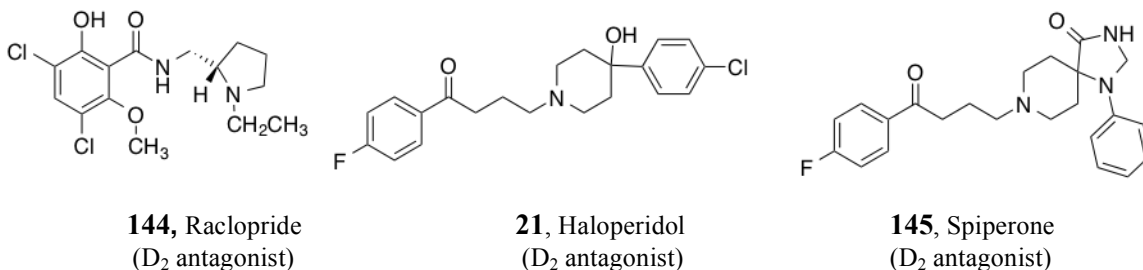
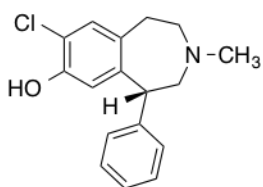


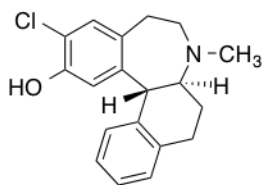
Figure 3.3: Chemical structure of dopamine agonists

As cocaine results in elevated dopamine levels in the synapse and results in excessive stimulation of dopamine receptors, inhibitors of the dopamine receptors have also been considered for antagonist medications. Conversely, dopamine D₂ antagonists such as raclopride (**144**)[Fig. 3.4], haloperidol (**21**)[Fig. 3.4] and spiperone(**145**)[Fig. 3.4] decreased the behavioral effects of cocaine.³⁶³⁻³⁶⁷ Similarly, the D₁ antagonists SCH 23390 (**146**)[Fig. 3.4] and SCH 39166 (**147**)[Fig. 3.4], and D₂ antagonists such as YM 09151-2 (**148**)[Fig. 3.4] attenuated reinforcing effects of cocaine.^{359,368}

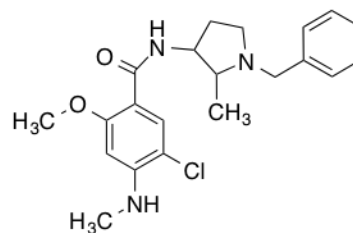




146, SCH23390
(D₁ antagonist)



148, YM09151-2
(D₂ antagonist)

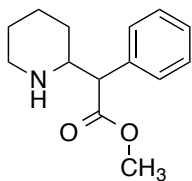


147, SCH39166
(D₁ antagonist)

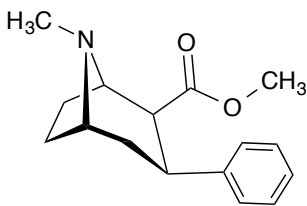
Figure 3.4: Chemical structure of dopamine antagonists

3.2.4.2. Dopamine reuptake inhibitors

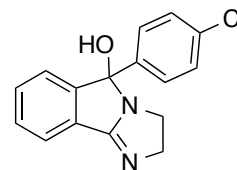
A growing number of studies have revealed that the primary target for cocaine in human body is dopamine transporter (DAT), and it has been proposed that the rewarding and reinforcing effects of cocaine are facilitated predominantly by its inhibition of DAT.^{341,364,369,370} Therefore, rigorous studies and research focused on the development of cocaine analogs and other dopamine transporter inhibitors including analogs of methylphenidate (**149**)[Fig. 3.5], WIN 35,065-2 (**150**)[Fig. 3.5], mazindol (**151**)[Fig. 3.5], GBR12909 (**152**)[Fig. 3.5], benztropine (**153**)[Fig. 3.5], and nomifensine (**154**)[Fig. 3.5], in order to find an effective treatment for cocaine abuse. These compounds have known to be potent and selective for the dopamine transporter and have been considered as viable substitute medications.³⁵¹⁻³⁸² However, preclinical studies of these agents in nonhuman primates have shown the potential for abuse in humans, which may be a problem with all substitute medications.³⁸³⁻³⁸⁴



149, Methylphenidate



150, WIN 35,065-2



151, Mazindol

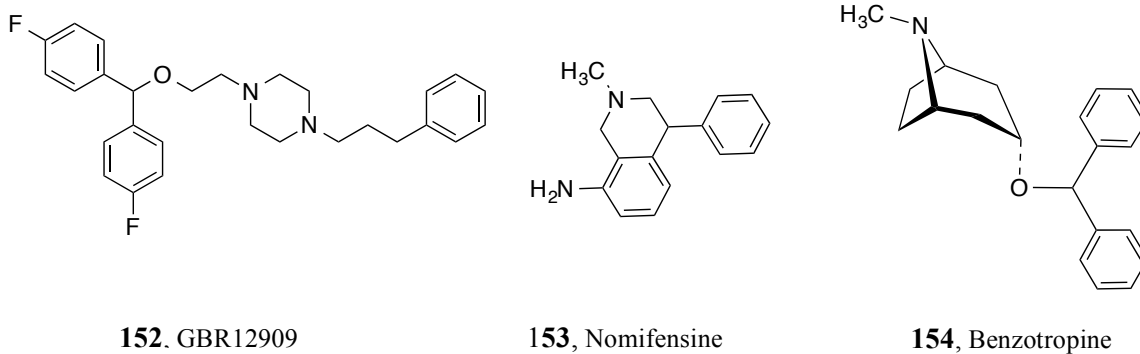


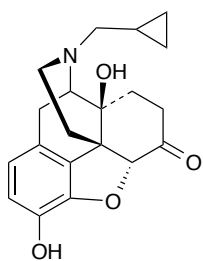
Figure 3.5: Structures of dopamine uptake inhibitors

3.2.4.3. Opioid receptor system

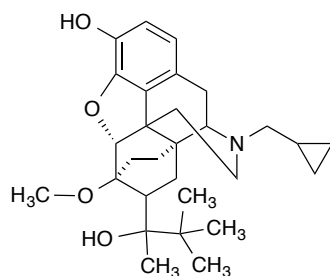
Since cocaine acts as an indirect dopamine receptor agonist, by inhibiting the dopamine transporter and enhancing extracellular dopamine, opioids indirectly modulate extracellular dopamine level in the mesolimbic and dopaminergic system.^{385,386} Opioid receptors are classified into four subtypes, mu (MOR), delta (DOR), kappa (KOR), and the opioid like receptor-1 or nociception receptor (ORL-1/NOR). Among of these receptors, MOR and DOR increase dopamine release in the mesolimbic areas upon activation while activation of KOR suppresses dopamine release.³⁸⁷

Over the last several years, multiple studies have been conducted to explore the effect of opioid ligands on cocaine self-administration in animals; however, the results have not been consistent. For example, the opioid antagonist, naltrexone (**155**)[Fig. 3.6], has shown confusing results on cocaine self-administration in rats where was either no change, decrease or increase in its effect on cocaine self-administration.³⁸⁸ Similarly, mixed opioid agonist-antagonists are reported to antagonize the reinforcing effect of cocaine during self-administration. For instance, buprenorphine, non-selective opioid agonist, decreases the cocaine self-administration in humans, Rhesus monkeys and rats.³⁸⁹⁻³⁹¹ Moreover, the kappa-selective agonists U50,488

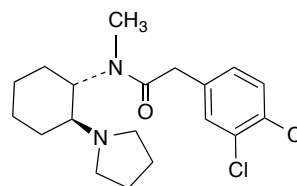
(**156**)[Fig. 3.6] and spiradoline (**157**)[Fig. 3.6] attenuated cocaine self-administration in rats while the kappa opioid receptor antagonist norbinaltorphimine (nor-BNI) (**158**)[Fig. 3.6] failed to produce any effect on cocaine self-administration but fully antagonized the effect of U50,488 (**159**)[Fig. 3.6].⁸² Therefore, opioid receptors suggested to have a modulatory role in cocaine self-administration system.⁸³ As a matter of fact, several κ opioid (KOP) receptors agonists such as U50,488H (**160**)[Fig. 3.6], U69,593 (**161**)[Fig. 3.6] and the novel neoclerodane diterpene salvinorin A (**162**)[Fig. 3.6] have been demonstrated to have anti-addiction effects in preclinical models of addiction; however, side effects such as depression, sedation, dysphoria, and aversion rendered them from further clinical studies.³⁹² Salvinorin A (**163**)[Fig. 3.6], a novel kappa-opioid receptor agonist that obtained from a plant named “*Salvia divinorum*”, has been pursued as a potential treatment for drug abuse and addiction for years.³⁹² However, the rapid metabolism of Salvinorin A halted it from further clinical development. Several other attempts have been performed to make more derivatives of Salvinorine A in order to overcome the metabolic and side effect issues, and the results were very promising in developing anti-addictive therapy with longer duration of action.³⁹² For instance, β tetrahydropyran (Salvinorin B) (**162**)[Fig. 3.6], Salvinorine A analog, was revealed to have anti-addiction effects in preclinical studies similar to those reported for Salvinorin A with a better pharmacokinetic profile and different side effect.³⁹³



155. Naltrexone



156. Buprenorphine



157. U50.488

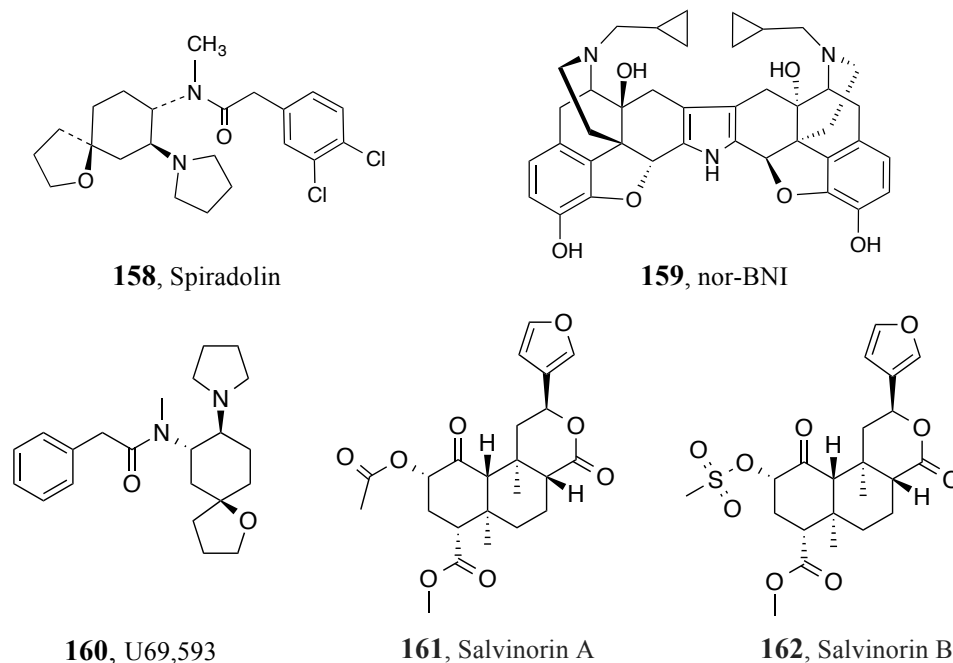


Figure 3.6: Structures of opioid ligands

Alternatively, anti-drug vaccine is another promising approach to treat drug overdose or addiction by dropping the drug level in the brain through anti-drug antibodies binding before passing to the brain.³⁹⁴ As drugs of abuse are small molecules and readily cross the blood brain barrier, their binding to anti-drug antibodies will prevent them from crossing blood brain barrier and thus minimizing the drug level in the brain.³⁹⁴ Numerous reports in literature of anti-drug antibodies/vaccines tested for opioids, phencyclidine, nicotine, methamphetamine, and cocaine addiction. Some of these anti-drug antibodies/vaccines have been assessed in clinical trials and have displayed favorable effects.^{395,396} Currently, clinical studies are being performed for vaccines against cocaine and nicotine in addition to anti-methamphetamine monoclonal antibody.³⁹⁶ So far, these approaches seem to be very exciting and promising as potential therapies for drug overdose and addiction.

3.2.5. Sigma receptors and cocaine abuse

As mentioned above, sigma receptors bind a variety of drugs that are abused, and can modulate the behavioral effects of these drugs. The involvement of sigma receptors in cocaine and methamphetamine has been extensively studied and reported.

Cocaine is well known for its inhibition effect on dopamine transporters. This inhibition results in an increase in dopaminergic neurotransmission that plays a significant role in the behavioral effects of cocaine. In actual fact, selective sigma receptor ligands modulate monoaminergic, and particularly dopaminergic, and serotonergic systems. Additionally, a number of recent studies demonstrated that sigma-1 receptor activation plays an important role in reinforcement and addictive processes.^{92,93,95} Several studies have demonstrated the ability of sigma receptor antagonists to attenuate a variety of behaviors that are stimulated by the acute administration of cocaine. Similarly, cocaine can bind to sigma receptors and activate them to produce its stimulant effects. The interaction between cocaine and sigma receptors was first reported in 1988.¹⁰³ Cocaine preferentially binds to sigma-1 receptors with an affinity of about 2 μM , and thus activates the sigma-1 receptor to induce its effect [Table 1].¹⁰³ Cocaine has about a 10 fold higher affinity toward sigma-1 receptors over sigma-2 receptors in mouse brain.^{106,397}

Table 3.1: Affinity of cocaine for σ receptors in mouse (Brain & Heart)

| Tissue | Sigma-1 | Sigma-2 |
|--------|-------------|-------------------|
| Brain | 2 \pm 0.2 | 31 \pm 4 |
| Heart | 5 \pm 1 | n.d. ¹ |

¹= The affinities of the cocaine for σ_2 receptors in the heart were not determined because this subtype comprises less than 20% of σ receptors in cardiac tissue, making it difficult to reliably detect specific binding across a wide range of competing ligand concentrations.⁸⁸

Furthermore, Several studies showed that co- or pre-administration of sigma-1 antagonists blocked the hyperlocomotion, sensitization, or the appetitive effect of cocaine using the conditioned place preference paradigm.¹⁰⁴⁻¹⁰⁶ It is also documented that sigma-1 receptor antagonism attenuates cocaine-induced toxicities and stimulant effects, however the role of

sigma-2 receptors in these effects is less clear.^{92,110}

3.2.5.1. Cocaine and behaviors

For years, cocaine has been known to interact with sigma receptors at concentrations that are achievable *in vivo*.¹⁰³ However, pharmacological and molecular biological tools to selectively manipulate these targets have demonstrated that selective antagonists and antisense oligodeoxynucleotides against sigma receptors attenuate the convulsive, lethal, locomotor stimulatory, and rewarding effects of cocaine.^{106,110} Both sigma receptor subtypes appear to play a significant role on mitigating many behavioral effects of cocaine.³⁹⁷ These effects are assumed to involve modulation of typical neurotransmitter systems such as dopamine and glutamate and modifications in drug-induced neuroadaptations including changes in gene and protein expression. Hence providing another feasible target for the development of anti-cocaine agents.^{92,93,95,103-106}

3.2.5.2. Cocaine induced convulsions

Convulsions are a measure of behavioral toxicity with clinical significance of cocaine intoxication, which are not responsive to common antiepileptic medications and can be difficult to treat in overdose situations.³⁹⁸ A number of studies that have been conducted to date demonstrating that antagonism of sigma receptors using either pharmacological antagonists or molecular knockdown of the sigma-1 subtype sufficient to attenuate cocaine-induced convulsions.^{106,110} Several momentous sigma receptor antagonists, such as BMY-14802 and haloperidol, have been reported to significantly attenuate cocaine-induced convulsions in mice.^{399,400} The later developed sigma receptor antagonists, such as BD1008 and its analogs (BD1018, BD1047, BD1060, BD1063, BD1067, LR132, LR172, LR176, YZ-011, YZ-027, and YZ-032) have significantly attenuated the convulsive effects of cocaine.⁹³ [Tab. 3.2 & 3.3]

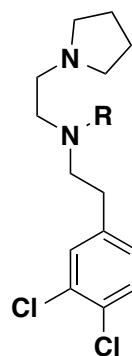
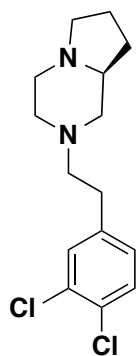
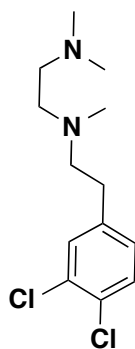


Table.3.2: Structures of BD1008 analogs and their sigma receptors affinities

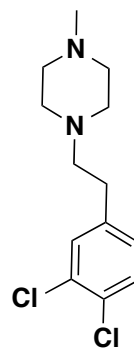
| Compound | R | σ_1 | σ_2 |
|--------------|------------|------------|------------|
| BD1008,(10) | -CH3 | 2±1 | 8±2 |
| BD1060,(163) | H | 3±0.1 | 156±45 |
| BD1067,(164) | -CH2CH3 | 2±0.5 | 39±1 |
| BD1052,(165) | -CH2CH=CH2 | 2±0.5 | 60±3 |



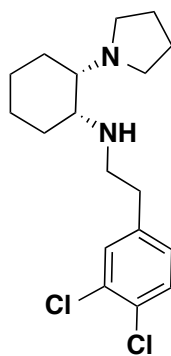
BD1018
166



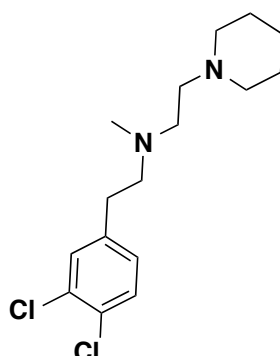
BD1047
14



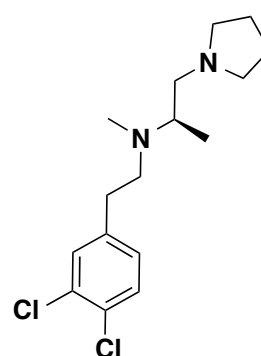
BD1063
167



LR132
168



LR172
169



LR176
170

Table 3.3: Structures of BD1008 analogs (LR series) and their sigma receptors affinities⁹³

| Compound | σ_1 | σ_2 |
|----------------------|------------|------------|
| BD1047 (14) | 0.9±0.1 | 47±0.6 |
| BD1063(167) | 9±1 | 449±11 |
| LR132(168) | 2±0.1 | 701±375 |

[Rae Matsumoto, 2003]

Consequently, recent studies suggest that selective antagonism of the sigma-2 subtype, using newly developed subtype selective ligands, similarly decreases the convulsive effects of cocaine.⁴⁰¹ Alternatively, sigma receptor agonists induced the convulsive effects of cocaine with a shift to the left in the cocaine dose–response curve.^{106,110,402} [Tab. 3.4]

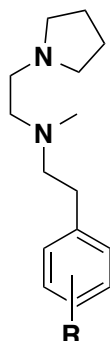
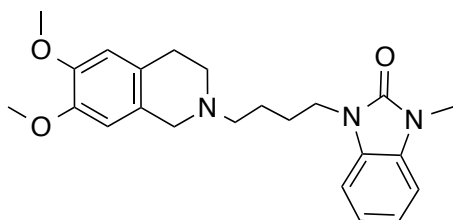


Table 3.4: Structures of BD1008 analogs (YZ series), and their sigma receptors affinities.⁸⁸

| Compound | R | σ_1 | σ_2 |
|----------------------|-----------|------------|------------|
| YZ-011(169) | m-methoxy | 24±2 | 209±22 |
| YZ-027(170) | m-nitro | 6±2 | 95±0.7 |
| YZ-032(171) | o-amine | 291±38 | 640±25 |

However, the sigma-1 -preferring agonist (+)-pentazocine and the sigma-2-preferring agonist CM398 (**172**)[Fig. 3.7] do not significantly shift the cocaine dose–response curve for convulsions indicating the dual influence at the two subtypes is required to induce optimal

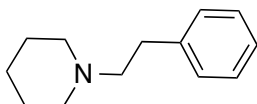
behavioral effects.⁴⁰³



172, CM398

Figure 3.7. Chemical structure of selective sigma-2 ligand, CM398 that was developed in McCurdy's laboratory

AC927, one of the ethylamine class derivatives, was evaluated for their sigma receptor affinity and anticocaine activity. The results revealed that AC927 has high affinity for sigma receptors (K_i , $\sigma_1 = 30$ nM; $\sigma_2 = 138$ nM) and selectivity over a set of other receptors. At the same time, it was found that this compound attenuated cocaine-induced convulsions, locomotor activity, lethality and conditioned place preference in mice.^{397,404}



17. AC927

Figure 3.8. Chemical structure of the highly selective sigma ligand, AC927.

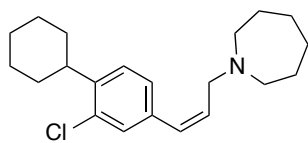
3.2.5.3. Cocaine induced lethality

It is noteworthy that sigma receptor antagonists can reduce the lethal effects of cocaine overdose, since death is the ultimate toxic endpoint of overdose situations. Respiratory depression and cardiovascular collapse are the primary causes of deaths from cocaine overdose, due to the existence of sigma receptors in heart and lung as well as the brain that makes them visible targets for pharmacotherapeutic intervention.^{106,405,407} Numerous studies indicated that pre-treatment of mice with the sigma receptor antagonists (BD1008, BD1018, BD1047, BD1060,

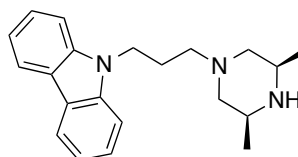
BD1063, BD1067, BMY-14802, haloperidol, LR132, LR172, LR176, reduced haloperidol, YZ-011, YZ-027, YZ-032) have been reported to attenuate cocaine-induced lethality.^{106,403,407} Also, post-treatment of mice with the sigma receptor antagonists (LR132, YZ-011) significantly attenuates cocaine-induced lethality.^{106,402}

3.2.5.4. Cocaine induced locomotor stimulation

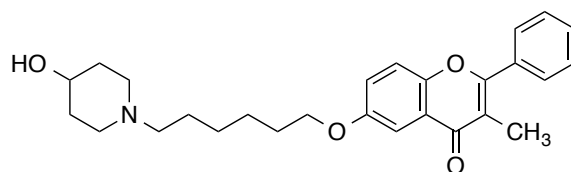
Cocaine, beside its toxic effects that are operational in overdose situations, also possesses psychomotor stimulant effects that contribute to its addiction potential. Several sigma receptor antagonists are capable of attenuating the acute locomotor stimulant effects of cocaine. Thus, locomotor activity is a convenient experimental measure of the stimulant actions of cocaine.^{106,401,406,108} A number of sigma receptor compounds have been reported to attenuate the locomotor stimulatory effects of cocaine in rodents such as BD1008, BD1018, BD1047, BD1063, LR132, LR172, YZ-011, YZ-027, and YZ-032.^{242,402,407} The involvement of sigma receptors was confirmed by antisense oligos that knock down the levels of brain sigma-1 receptor in mice, which produces a similar effect.¹⁰⁵ Alternately, it has been reported that the sigma receptor agonist DTG enhances the locomotor stimulatory effects of cocaine in rats.⁴⁰⁸ Behavioral sensitization or reverse tolerance can result from repeated administration of cocaine to animals over time. In this regard, several sigma receptor compounds remarkably reduce the development of cocaine-induced locomotor sensitization such as SR 31742A, NPC 16377, rimcazole, and BMY-14802.^{243,409}



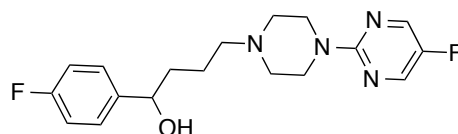
36, SR31742A



38, Rimcazole



173, NBC16377



11, BMY-14802

Figure 3.9: Sigma receptor ligands that attenuate cocaine-induced locomotor sensitization.

3.2.5.5. Cocaine induced conditioned place preference

The conditioned place preference is an experimental method to measure the rewarding properties of drugs. It is a model of drug seeking based on the fact that when given a choice, animals will return to and spend more time in an environment in which they previously experienced a drug that was rewarding or avoid an environment in which they previously experienced an aversive drug. Numerous sigma receptor antagonists have been shown to block place conditioning produced by stimulant drugs, mainly cocaine. Cocaine produces strong place conditioning, and introducing sigma receptor antagonists drastically attenuates the cocaine induced place conditioning.^{104,105,406} It was first reported by Romieu *et al.* in 2000,¹⁰⁴ in this study, the sigma receptor antagonists, NE-100 (**31**)[Fig. 3.10] and BD 1047 (**14**)[Fig. 3.10], dose-dependently blocked the place conditioning produced by cocaine in mice. Moreover, progesterone, a neurosteroid that acts as a sigma-1 receptor antagonist under a variety of conditions, produces similar effects as other sigma receptor antagonists and antisense knockdown.⁴¹⁰ Recently it has been reported that the sigma-1 receptor agonist (+)-pentazocine has no substantial effects on the development of cocaine-induced place conditioning, while

SA4503 (**25**)[Fig. 3.10] attenuates it.⁴¹¹ The sigma receptor antagonists were effective in blocking both locomotor stimulation and place conditioning produced by stimulant drugs. On the other hand, sigma receptor agonists by themselves were inactive in inducing the effect that their antagonists were effective in blocking. Hence, sigma receptor antagonists appear capable of preventing the response to frequent administration of cocaine.

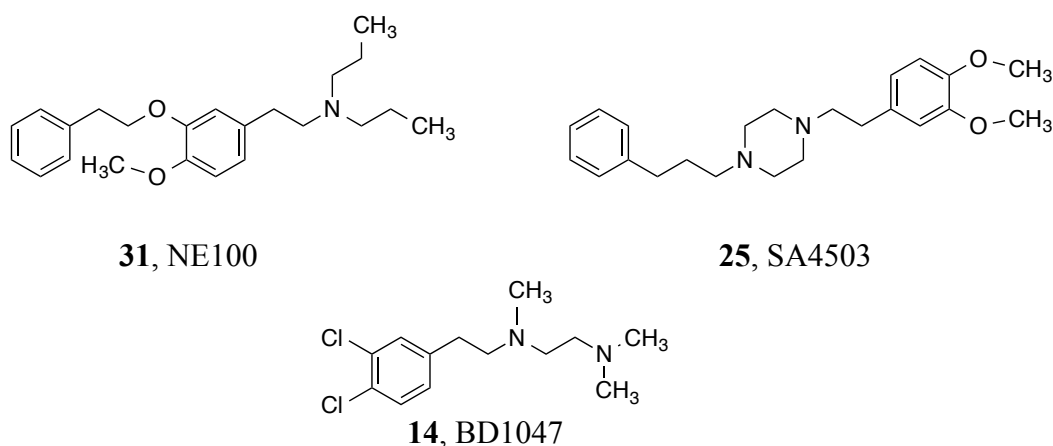


Figure 3.10: Chemical structures of the sigma-1 antagonists, NE100, SA4503, and BD1047.

3.2.5.6. Cocaine induced self-administration

Drug self-administration paradigm is an important experimental procedure in drug abuse research. Also, it's well known that laboratory animals are capable of self-administer of cocaine similar to humans. An early study by Slifer and Balster⁴¹² compared the reinforcing effects of the stereoisomers of the 6,7-benzomorphan, SKF 10,047 and cyclazocine, to those of PCP in rhesus monkeys trained to self administer cocaine. None of the racemic forms, (-) enantiomers of SKF 10,047, or cyclazocine were self-administered while both (+)-SKF 10,047 and (+)-cyclazocine were self-administered. Since the cocaine appears to act as an agonist at sigma receptors, it was suggested that sigma receptor antagonists could alter the reinforcing effect of cocaine.⁴¹²

Recently Martin-Fardon et al.¹¹¹ examined the effect of BD 1047 on cocaine self-administration in rats. In that study, BD 1047 pretreatment did not affect cocaine self-

administration. In the same study, they found that pretreatment of rats with sigma receptor antagonists had no effect on cocaine self-administration. However, pretreatment with sigma receptor agonists produced a leftward shift in the cocaine dose-effect curve.¹¹¹ A later study that examined a wide range of doses of BD 1047 and its analogs (BD 1008 and BD 1063) similarly found a lack of effects on self-administration of a broad range of cocaine doses.⁴¹³

A study by Matsumoto *et al.* in 2001, suggested that the interaction between cocaine and sigma receptor ligands is a competitive antagonism of effects of cocaine mediated by sigma receptors.¹¹⁰ However, in a subsequent study by Izenwasser *et al.*, 1993,⁴¹⁴ found that numerous sigma receptor ligands, including rimcazole, blocked dopamine uptake and had micromolar affinity for the DAT. Therefore, some sigma receptor ligands may alter the effects of cocaine through an action at the DAT.⁴¹⁴ In this regard, a recent finding⁴¹⁵ revealed that rimcazole analogs bind to the DAT in a way favoring a DAT conformation that renders it less accessible to the extracellular space. In contrast, cocaine analogs bind to the DAT in a way that favors an outwardfacing conformation.^{415,416}

Consequently, the interaction of rimcazole and its analogs with cocaine may diverge from that of other sigma receptor antagonists because of their dual actions, and this may more effectively block cocaine self-administration. Based on these findings, Hiranita *et al.*,¹¹² in 2011 conducted a series of experiments to assess whether dual actions at these sites contribute to the blockade of cocaine self-administration through combinations of compounds selective for these sites [Table 3.5]. Rimcazole (**38**) [Fig. 3.11] and its analogs [Fig. 3.12] [Tab. 3.5] have exhibited dose dependent decrease of cocaine self-administration with no effect on food reinforcement.¹¹²

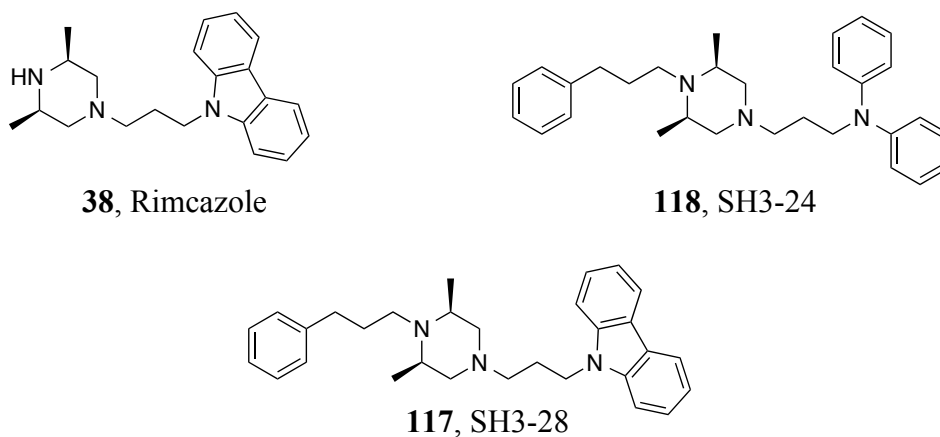


Figure 3.11: Chemical structures of rimcazole and its derivatives.

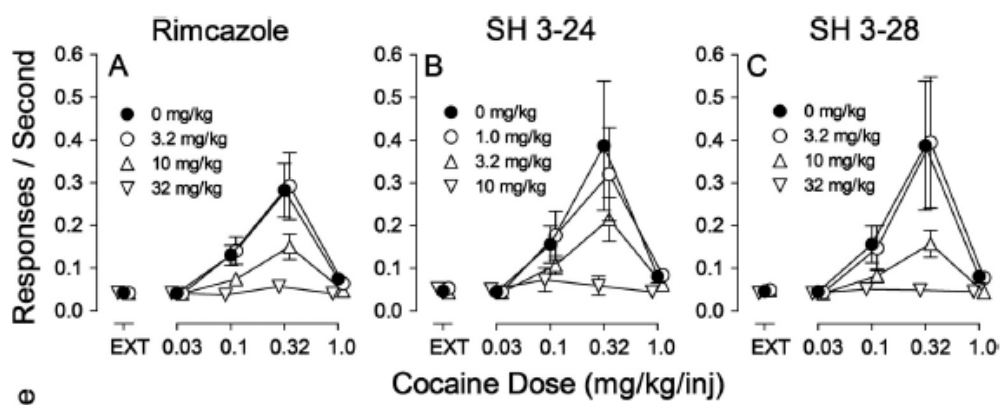


Figure 3.12: Effects of pre-treatment with rimcazole and its analogs on cocaine self-administration. [Adapted from ref. 112]

Table 3.5: Binding affinities of various compounds to the DAT, σ_1 , or σ_2 receptors

| Compound | Ki Value (mM) | | |
|-----------------|-------------------------------|--------------------|------------------------|
| | DAT | σ_1 | σ_2 |
| WIN 35,428 | 5.24 (4.92–5.57) ^a | 5700 (4060–8020) | 4160 (3120–5550) |
| SH 3-24 | 12.2 (10.8–13.8) | 22.9 (18.5–28.2) | 20.0 (15.7–25.6) |
| Nomifensine | 21.0 (18.9–23.3) | 8240 (5360–12,700) | 65,200 (54,300–78,300) |
| Methylphenidate | 65.8 (61.2–70.8) | 6780 (4520–10,200) | 37,400 (21,200–66,100) |
| Cocaine | 76.6 (72.6–80.5) | 5190 (3800–7060) | 19,300 (16,000–23,300) |
| Rimcazole | 96.6 (77.3–121) | 883 (661–1180) | 238 (171–329) |
| SH 3-28 | 188 (166–213) | 19.0 (15.3–23.6) | 47.2 (40.4–55.2) |
| AC927 | 1,930 (1610–2320) | 53.1 (45.6–61.8) | 78.9 (48.2–129) |
| BD 1008 | 2,510 (2250–2790) | 2.13 (1.77–2.56) | 16.6 (13.0–21.1) |
| BD 1047 | 3,220 (2820–3670) | 3.13 (2.68–3.65) | 47.5 (36.7–61.4) |
| NE-100 | 3,590 (3,210–4,000) | 2.48 (2.13–2.88) | 121 (91.9–159) |
| BD 1063 | 8,020 (7100–9060) | 8.81 (7.15–10.9) | 625 (447–877) |

The values listed are Ki values \pm S.E.M. (95% confidence limits), with the exception of the value for WIN 35,428 at the DAT, which is a Kd value obtained from a homologous competition study. See Materials and Methods for details of the assay procedures and derivation of Ki values.

A series of other sigma antagonists (lacking DAT affinity) do not seem to show this effect across the range that did not alter rates of food reinforcement.¹¹² DAT inhibitors like WIN 35,428 (**174**)[Fig.3.13], methylphenidate(**149**)[Fig.3.13], and nomifensine(**153**)[Fig.3.13], themselves show self-administration by shifting the cocaine dose response curve leftward.^{112,413}

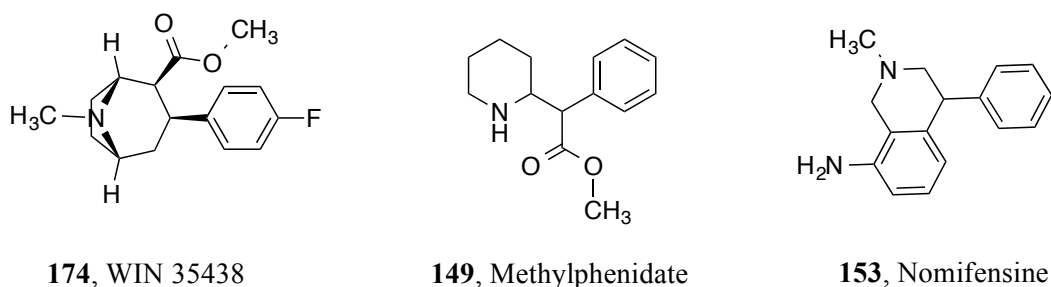


Figure 3.13: Chemical structures of selective DAT inhibitors.

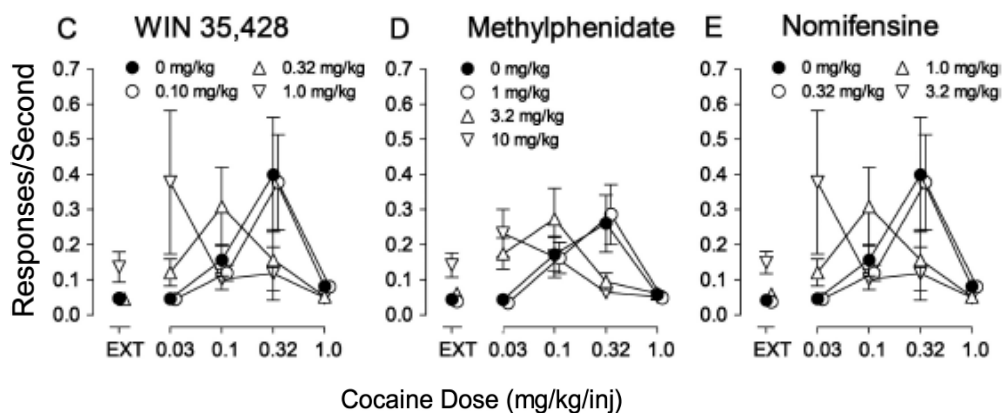


Figure 3.14: Effects of pre-treatment with DAT inhibitors on cocaine self-administration. [Adapted from ref. 112]

When studied alone, selective DAT inhibitors and sigma receptor antagonists do not possess rimcazole like blockade of self-administration. In contrast to the effects of rimcazole and its analogs, the selective sigma receptor antagonists, AC927 (**17**) and NE-100(**31**) (Table 3.5), generally had no significant effects on the self-administration of cocaine [Fig. 3.15].¹¹²

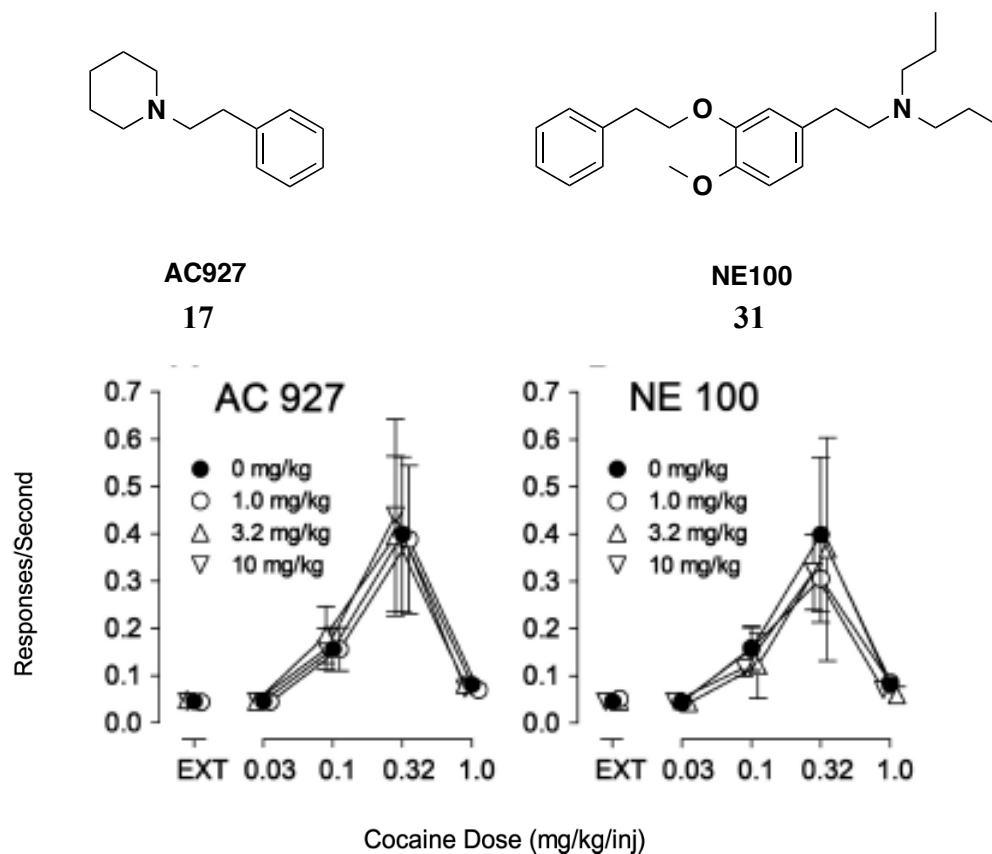
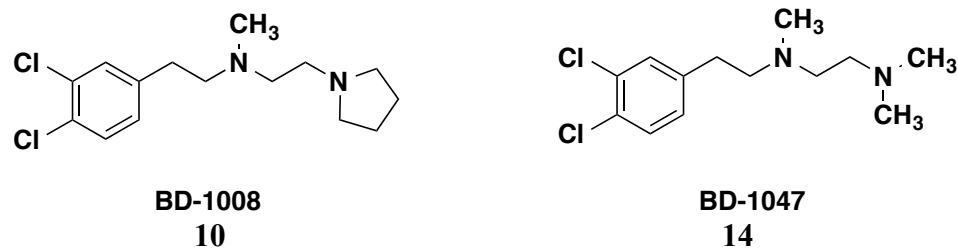


Figure 3.15. Effects of pre-treatment with sigma receptor antagonists on cocaine self-administration [Adapted from ref. 112]

On the other hand, combinations of WIN 35,428 (174) [Fig. 3.13] and other sigma antagonists BD 1008 (10) [Fig. 3.16] and BD 1047 (14) [Fig. 3.16] decreased self-administration without effects on food maintained responding.¹¹²

Thus, the dual effect on both DAT and sigma receptors will decrease the cocaine self-administration and this can serve as potential treatment for stimulant abuse with low liability of abuse as suggested in the above-mentioned studies. [Fig. 3.16]



0.1 mg/kg WIN 35,428

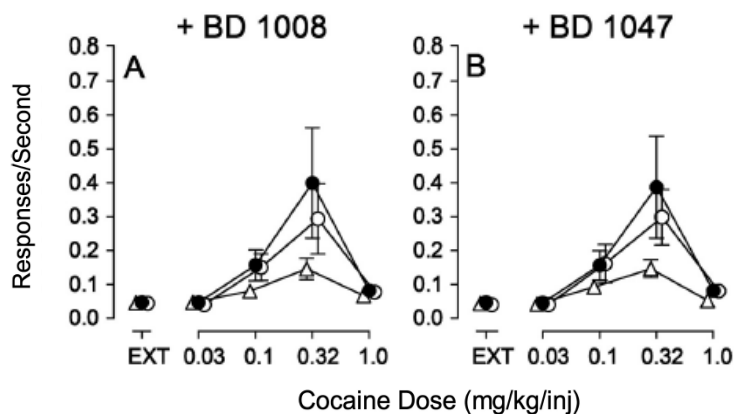


Figure 3.16. Effects of pre-treatment with WIN 35,428 combined with sigma receptor antagonists on cocaine self-administration.[Adapted from ref. 112]

Although, rimcazole showed dose dependent inhibition of cocaine self-administration, it is not an ideal candidate for development a treatment for cocaine addiction since clinical trials with rimcazole as a potential antipsychotic agent showed a lack of efficacy and an incidence of seizures that terminated its further development.⁴¹⁸

3.3. Methamphetamine

Methamphetamine (METH) (**15**)[Fig. 3.17] is a substance that stimulates the central nervous system, and it can be injected, snorted, smoked, or ingested orally. The term ‘amphetamines’ is often used to refer to a group of amphetamine-related drugs, including amphetamine (AMP) (**175**)[Fig. 3.17] and METH.⁴¹⁹ [Fig. 3.17]

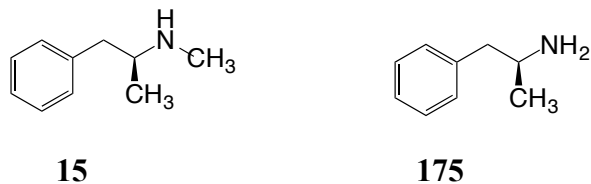


Figure 3.17: Chemical structure of methamphetamine and amphetamine.

3.3.1. Background

Methamphetamine is one of the most abused substances worldwide, and in United States in particular. Commonly known on the street as speed, crank, crystal, ice, glass, or meth. Similar to cocaine, pharmaceutically manufactured methamphetamine is classified as a Schedule II drug reflecting its high abuse potential and limited medical usefulness.^{320,326,419} A Japanese pharmacologist, Nagayoshi Nagai, first synthesized methamphetamine in 1893 from its parent drug, amphetamine. In 1919, Akira Ogata synthesized crystallized methamphetamine through reduction of ephedrine using red phosphorus and iodine. Near 1932 pharmaceutically manufactured amphetamine was being used medically in nasal spray for the treatment of asthma and in 1937 it was available for the treatment of narcolepsy by prescription.^{320,420,421}

Afterwards, more potent forms of the drug were developed including dextroamphetamine and methamphetamine, which were extensively used in the military during the World War II. In the same time, amphetamines were widely used by American and Japanese military pilots to keep them awake on long exploration and bombing operations. After World War II, a large supply of amphetamine stored by the Japanese military became available in Japan under the street name *shabu*. Consequently, the Japanese Ministry of Health banned it in 1951. In the United States, Abbott Laboratories took the approval from FDA in 1944 for the treatment of narcolepsy, chronic alcoholism, mild depression, Parkinsonism, hay fever, and cerebral arteriosclerosis.^{420,421}

Intravenous and oral use of methamphetamine became widespread as an emerging drug subculture of the late 1950s and throughout the 1960s. However, oral amphetamines became exclusively popular as diet pills to suppress appetite and enhance weight loss. As it became increasingly obvious that the dangers of amphetamine use overshadowed the therapeutic benefits, many pharmaceutical amphetamines were taken off the market. Later, in 1970, the legal production of stimulant drugs was severely restricted by the 1970 Controlled Substance Act in the United States. However, this resulted in increased illicit production, mainly of methamphetamine, during the 1980s. In the 1990's, use of methamphetamine, mainly concentrated on the west coast of the U.S. and in Hawaii, spread to the Midwest, South, and later the problem spread across the country.^{320,420-422}

3.3.2. Physiological and psychological effects of methamphetamine

Similar to cocaine, methamphetamine accumulates the neurotransmitter dopamine in certain brain areas leading to intense stimulation and feelings of euphoria. However, in contrast to cocaine, which is rapidly removed and metabolized in the body, methamphetamine is metabolized more slowly and a larger proportion of the drug remains unchanged in the body hence extending its pharmacologic effects. While 50 percent of cocaine is metabolically removed from the body within 1 to 2 hour, 50 percent of methamphetamine is removed within 8 to 12 hours. This also allows more time for methamphetamine to exert its neurotoxicological effects.^{320,326}

The physiological effects of methamphetamine, generally similar to those of cocaine, include increased heart rate, elevated blood pressure, elevated body temperature, increased respiratory rate, and pupillary dilation. In addition to other acute effects such as rapid heart rate, irregular heart rate, and irreversible, stroke-producing damage to small blood vessels in the brain.^{326,419}

The psychological effects of methamphetamine, like those of cocaine, include feelings of euphoria, increased alertness, increased vigor, decreased food intake, and decreased sleep time. High doses of methamphetamine may produce irritability, aggressive behavior, excitement, auditory hallucinations, and paranoia (delusions and psychosis). Similarly, methamphetamine overdose severely elevated body temperature and caused convulsions, which can result in death if it's not treated immediately. Continued use of methamphetamine can develop tolerance to the behavioral effects, and repeated exposure may produce sensitization. Methamphetamine users mood changes are common among methamphetamine users, and they easily tend to engage in violent behavior.^{320,326,419}

Addiction to methamphetamine is believed to be as same as that of cocaine since the neurological effects of methamphetamine are similar to the effects produced by cocaine, which increased levels of dopamine in the limbic reward system. The withdrawal syndrome of methamphetamine is more intense and prolonged than that of cocaine due to the longer effects of methamphetamine. There are three major differences between cocaine and methamphetamine:

- 1) Methamphetamine enhances CNS neurotransmission by increasing the presynaptic release of dopamine within the limbic reward system.
- 2) In contrast to cocaine, methamphetamine does cross-neuronal cell membranes and enters into the vesicles where neurons store dopamine, which can cause neurotoxicity indirectly by mobilizing dopamine out of the safe storage vesicles within the neuron and into the neuron's cytoplasm where it is converted to toxic and reactive chemicals.⁴²³
- 3) Methamphetamine is metabolized at a much slower rate than that of cocaine, which results in a longer duration of action, and allows more time to exert its neurotoxicological

effects.^{326,423,424}

3.3.3. Approaches to potential treatment for methamphetamine abuse

Methamphetamine addiction is a serious public health problem and concern worldwide for which there are no approved pharmacological treatments and its growing use has generated an urgent need to address this concern. Several potential therapeutic targets for the treatment of methamphetamine addiction have been identified, and they are currently being studied for treatment of methamphetamine dependence.

A number of studies have shown that serotonergic medications may attenuate the reinforcing effects of amphetamine.^{425,426} Similarly, blockade of serotonergic and noradrenergic reuptake may lessen the depressive methamphetamine withdrawal symptoms.⁴²⁷ Therefore, antidepressants, including selective serotonin reuptake inhibitors (SSRIs) and tricyclic antidepressants (TCAs), have been studied as potential treatments for methamphetamine dependence. Imipramine (**176**)[Fig. 3.18], a selective serotonin reuptake inhibitor (SSRI), has been shown to improve treatment retention but not urine drug screen results, depression scores, or craving in an outpatient setting.⁴²⁸ Recently, a study by Elkashef and colleagues showed that bupropion (**177**)[Fig. 3.18], a dopamine and norepinephrine reuptake inhibitor maybe effective as a treatment for methamphetamine dependence.⁴²⁹ Furthermore, amineptine (**178**)[Fig. 3.18], a dopamine reuptake inhibitor with mild stimulant properties and mirtazapine (**179**)[Fig. 3.18], a serotonin 5HT₂ inhibitor, have presented promise as treatments for methamphetamine withdrawal symptoms.⁴³⁰⁻⁴³³ However, paroxetine (**180**)[Fig. 3.18], fluoxetine (**181**)[Fig. 3.18], and sertraline (**182**)[Fig. 3.18] failed to attenuate methamphetamine withdrawal symptoms.⁴³⁴⁻⁴³⁶ Moreover, because of the effects of dopamine and 5HT on amphetamines, antipsychotics have also been considered as well for methamphetamine dependence treatment. For instance,

treatment with risperidone (**184**)[Fig. 3.18], a D₂ and 5HT_{2A} antagonist, has resulted in substantial decrease in methamphetamine withdrawal symptoms.⁴³⁷ Modafinil (**183**)[Fig. 3.18] is a mild stimulant with effects similar to those of amphetamines, was approved as a medication for narcolepsy. Several studies have confirmed that its use does not cause elation or euphoria like amphetamine and methamphetamine, indicating its low potential of abuse.⁴³⁸ Treatment with modafinil (**183**)[Fig. 3.18] resulted in decreased withdrawal symptoms such as hypersomnia, nighttime awakenings, poor concentration and low mood.⁴³⁸

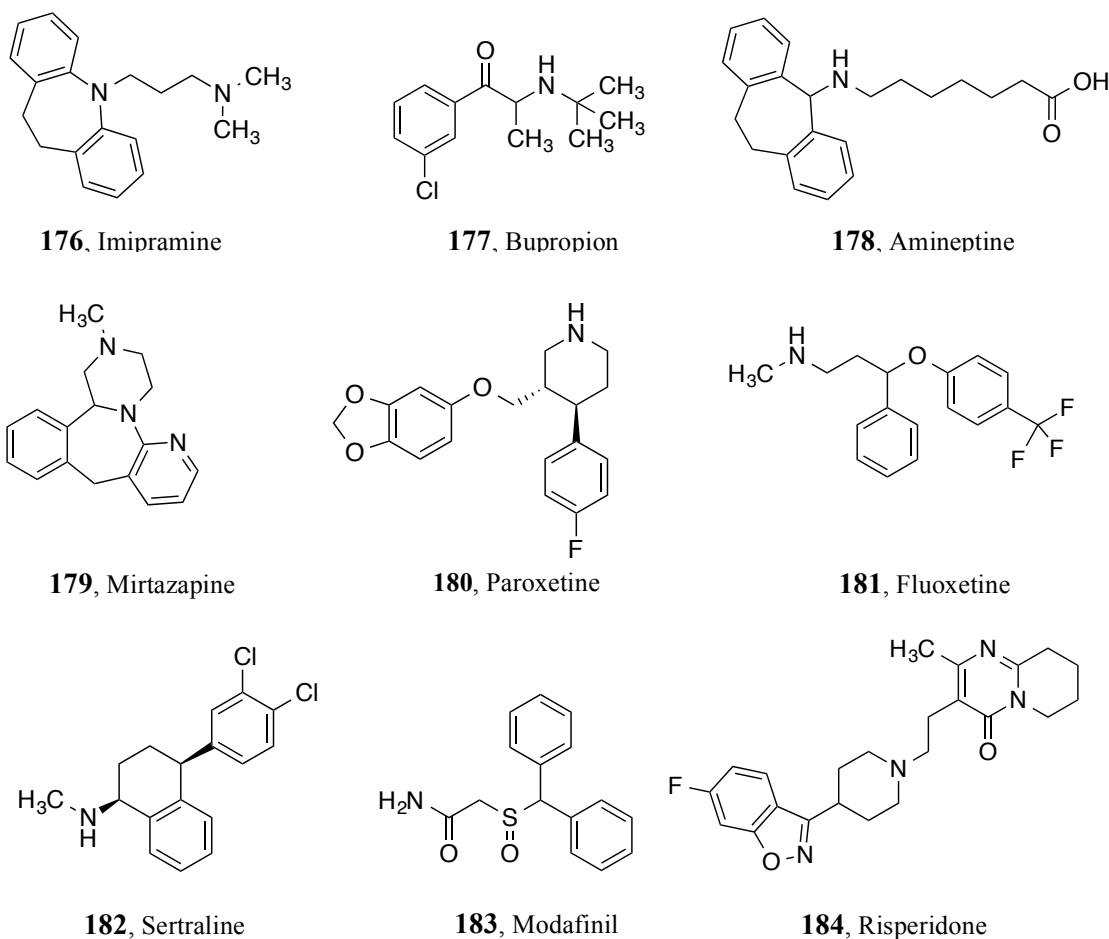


Figure 3.18: Several compounds cited for their potential treatment for methamphetamine abuse.

Additionally, there is some evidence that dexamphetamine, which is commonly used for

the treatment of attention deficit hyperactive disorder (ADHD) in children as well as narcolepsy and epilepsy, has been used to treat methamphetamine addiction aiming to substitute the methamphetamine use with a safer medication, which avoids withdrawal, reduces cravings, and regulates dose and mode of administration.⁴³⁹

3.3.4. Sigma receptors and methamphetamine

It is not unpredicted that sigma-1 ligands regulate some effects of methamphetamine since this psychostimulant interacts with sigma-1 receptors in a micromolar range affinity, and with a 20-fold higher affinity over sigma-2 receptors.¹¹⁴ Earlier studies have showed that methamphetamine interacts with sigma receptors and the antagonism of these receptors can attenuate methamphetamine induced locomotor stimulation and neurotoxicity.¹¹⁴ In these studies found that the sigma-1 antagonists, BMY10802 (**11**)[Fig. 3.19], NE100 (**31**)[Fig. 3.19], and MS-377 (**18**)[Fig. 3.19] weakly modulated the acute motor effects of methamphetamine.^{115,440,441} Later it was found that the selective sigma-1 antagonists BD 1063 (**167**)[Fig. 3.19] and BD 1047 (**14**)[Fig. 3.19], as well as sigma-1 antisense oligodeoxynucleotide, blocked methamphetamine-induced locomotor activity.¹¹⁴ Furthermore, BMY 14802 and MS-377 sigma-1 antagonists, inhibited the behavioral sensitization induced by the repeated administration of methamphetamine.^{115,441,442} Subsequent studies have confirmed that sigma receptor antagonists mitigate the neurotoxic effects of methamphetamine. Interestingly, some selective sigma receptor antagonists prevented methamphetamine induced depletions in striatal dopamine and serotonin levels, striatal dopamine transporter expression and hyperthermia.¹¹⁷ However, the exact role of the sigma-2 receptors in methamphetamine-induced effects is still undetermined.

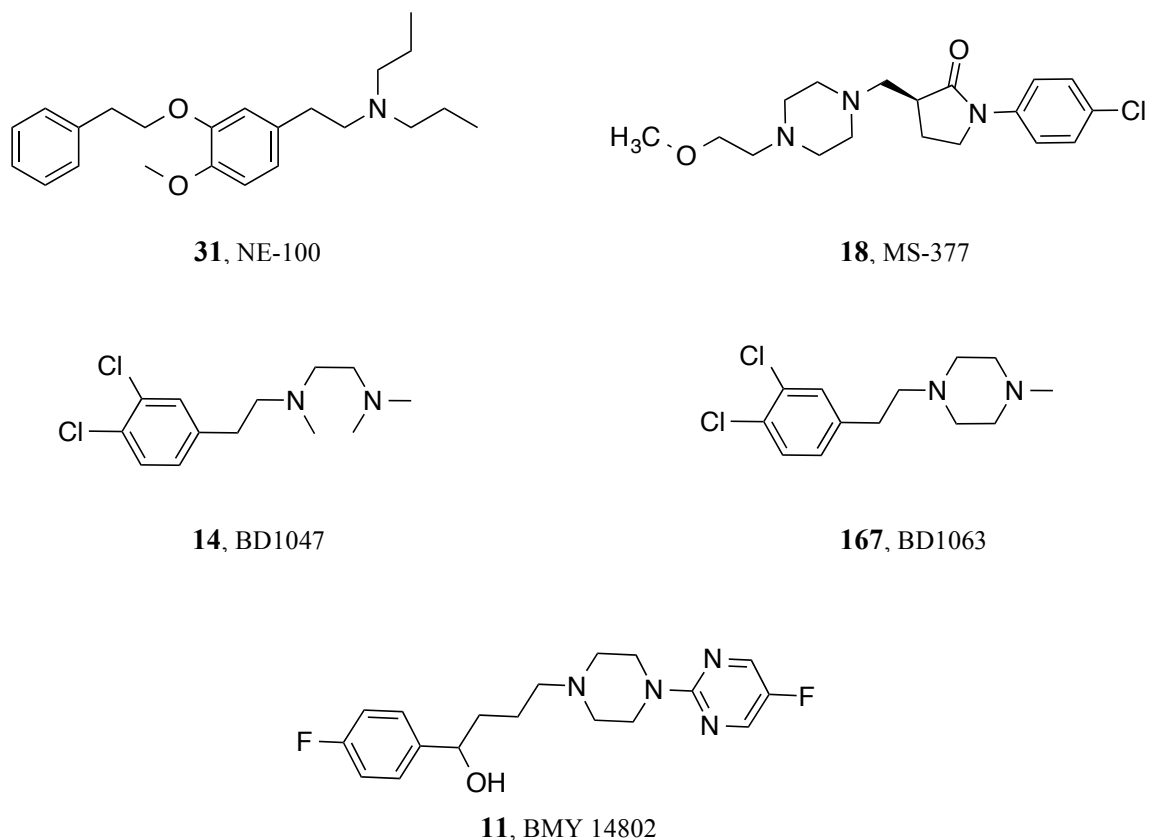


Figure 3.19: Chemical structure of sigma receptor ligands for methamphetamine abuse treatment.

Similar to cocaine, laboratory animals self-administer methamphetamine, which can lead to addiction related behaviors. Consequently, some studies have shown the ability of methamphetamine self-administration to alter sigma-1 systems.⁴⁴³ There is evidence that sigma-1 receptors are up-regulated in several brain regions in rodents that self-administer methamphetamine, and these changes are specific to self-administering animals, as compared to yoked controls who passively receive the same amount of methamphetamine.^{443,444} In another previous study, it was found a down regulation of DA D₂ autoreceptors with methamphetamine self administration, would increase adenylate cyclase, and thus protein kinase A (PKA) activity. Therefore, the results suggest that sigma-1 up-regulation, induced by methamphetamine self-administration is mediated by increased PKA activity due to DA D₂ autoreceptor down-

regulation.⁴⁴⁵ Furthermore, several other studies have indicated that the alterations in sigma-1 receptor expression are linked to frequent psychostimulant exposure under different conditions and that these changes may explain a functional module that needs to be fully understood.⁴⁴⁶⁻⁴⁴⁸

3.3.4.1. Sigma ligands as potential treatment for methamphetamine abuse

The first selective sigma ligand that was used to investigate its effect on methamphetamine abuse is (\pm)-BMY14802 (**11**)[Fig. 3.20].⁴⁴⁹ This compound was able to attenuate methamphetamine induced dopaminergic neuropathology and prevented the decrease in D₁ and D₂ dopamine receptor number in mice pretreated with (\pm)-BMY14802. Similarly, its ketone metabolite, BMY14786 (**185**)[Fig. 3.20]., attenuated the methamphetamine-induced effects. Moreover, in a different study, the well-known selective sigma-1 receptor ligand, MS-377 attenuated the behavioral sensitization induced by methamphetamine treatment in rats.⁴⁴¹ Also, it has been reported that the highly selective sigma receptor ligand, AC927 (**17**)[Fig. 3.20]., decreased some of the methamphetamine-induced effects. Due to the high selectivity of AC927 toward sigma receptors compared to other 29 targets, suggested that its action mainly was conducted through sigma receptors effect.¹¹⁷

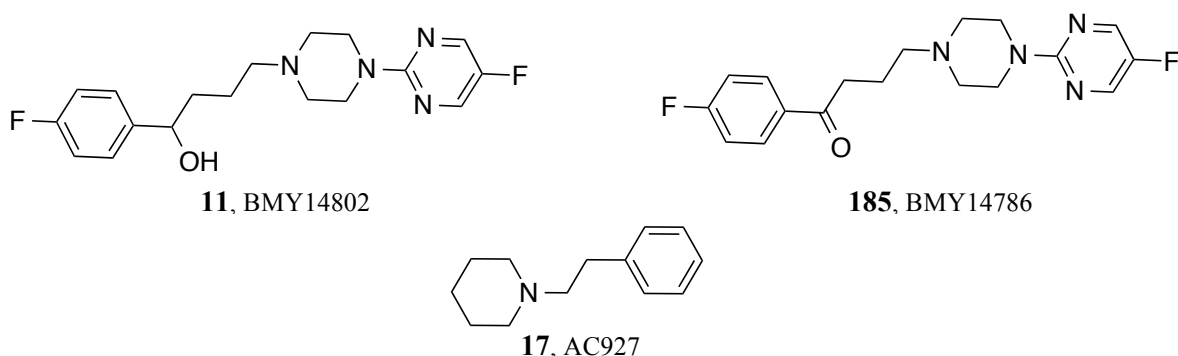
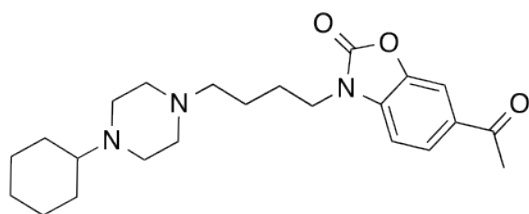
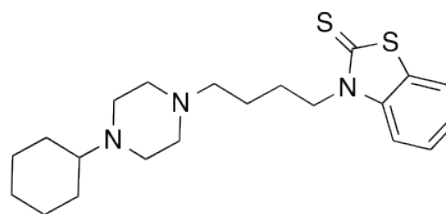


Figure 3.20: Chemical structure of sigma receptor ligands for methamphetamine abuse treatment

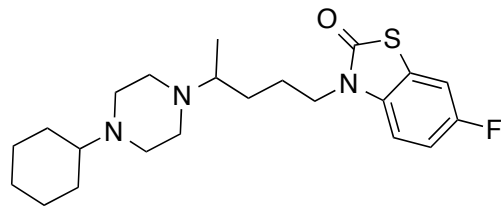
Furthermore, the two sigma-1 antagonists, BD1047 and BD1063 [Fig. 3.19] attenuated the locomotor stimulatory effects of methamphetamine. Consequently, the antisense oligodeoxynucleotide was also able to attenuate the response to methamphetamine through down-regulation of the brain sigma-1 receptors.¹⁴¹ More recently, a study by *Kushal et al.*,³⁴ 2013 on the SN79 (**12**) [Fig. 3.20], a putative sigma receptor antagonist with nanomolar affinity and selectivity for sigma receptors over 57 other binding sites, and its effect on the hyperthermia and neurotoxicity induced by methamphetamine at high doses. In this study, they found pretreatment with SN79 provided protection against methamphetamine-induced hyperthermia and striatal dopaminergic and serotonergic neurotoxicity in male, Swiss Webster mice. Conversely, the di-o-tolylguanidine (DTG) (**35**), a sigma receptor agonist, enhanced the lethal effects of methamphetamine, while it did not aggravate methamphetamine-induced hyperthermia. Interestingly, these results were very consistent with the effects of other sigma receptor antagonists, including AC927 (**17**) [Fig. 3.20] and CM156 (**13**) [Fig. 3.20], and these results concluded that the SN79 (**12**) [Fig. 3.20] is a potentially promising drug candidate to mitigate many effects of methamphetamine [Fig. 3.21].^{34,117,118} Moreover, in a recent study conducted by Seminerio et al. indicated that AZ66 (**19**) [Fig. 3.20], a selective sigma receptors ligand, not only blocked the development of behavioral sensitization, but also significantly reversed the expression of methamphetamine-induced sensitization.¹²⁰ AZ66, was found to remarkably attenuate dopaminergic neurotoxicity and memory impairment produced by frequent exposure to methamphetamine.^{120,121}



12, SN79



13, CM156



19, AZ66

Figure 3.21: Chemical structures of sigma receptor ligands (SN79, CM156, and AZ66) that were developed in McCurdy's laboratory and pursued for potential methamphetamine abuse treatment

**CHAPTER IV: IRREVERSIBLE SIGMA RECEPTORS LIGANDS AND
PHOTOAFFINITY LABELING**

4. Irreversible sigma ligands

Irreversible ligands are tools that are mostly useful for isolating a specific protein and characterizing the functions associated with that protein. These ligands should be made from compounds that possess high affinity and selectivity to the targeted protein. Most importantly, the modified molecules should not obstruct binding with the same receptor site and allow an additional covalent bond to be formed with the same protein. Similarly, these compounds also have to possess reactive groups on their structures to form an electrophilic center that can bind to the targeted receptor irreversibly with a covalent bond such as the nitrogen mustards, haloacetamides, aldol esters, Michael acceptors, or the isothiocyanates.⁴⁵⁰ The well-designed irreversible ligand first needs to bind to the receptor site as a first recognition step, and then irreversibly by forming a strong covalent bond as a second recognition step. It is important to re-evaluate the selectivity/specificity for the binding of the irreversible ligand to avoid probability of a non-specific covalent bond or the cross reaction with other physiological enzymes.⁴⁵¹

4.1 Irreversible ligands derived from different structural classes of sigma ligands

The use of selective irreversible probes has showed to be extremely useful in the isolation, purification, and characterization of many receptor systems. Selectivity and high affinity of a ligand are important attributes for designing successful irreversible probes as well as an understanding of structure activity relationships to incorporate the electrophilic moiety on the molecule where it will not affect these.⁴⁵¹

4.1.1 Analogues of phencyclidine

In an effort to gain a better understanding of phencyclidine (PCP) receptors, the irreversible ligand, meta-isothiocyanate derivative of 1-[1-(3-isothiocyanatophenyl) cyclohexyl]

piperidine (Metaphit) (**187**)[Fig. 4.1], was synthesized and used to study such important receptors. It was found the metaphit able to alter the binding sites that already labeled with [³H]PCP in rat brain, and antagonize several effects produced by phencyclidine.⁴⁵²⁻⁴⁵⁶ Also, metaphit binds reversibly at high concentrations to μ opioid receptors labeled with [³H]dihydromorphine and to muscarinic receptors labeled with [³H]QNB (quinuclidinyl benzilate); however, it does not exhibit affinity toward benzodiazepine receptors labeled with [³H]diazepam.⁴⁵² Moreover, it was found that metaphit antagonizes the motor stimulation induced by cocaine, and reduces the capacity of 5-HT₂ receptors labeled with [³H]ketanserin.^{457,458}



Figure 4.1: Structure of phencyclidine and its derivative, metaphit.

Studies on phencyclidine and some sigma receptor ligands with a similar structure to benzomorphan showed a clear connection between them since they display psychotomimetic actions.⁴⁵⁹⁻⁴⁶¹ Furthermore, (+)-N-Allyl-normetazocine [(+)-SKF-10,047] and cyclazocine appear to share several pharmacologic properties of phencyclidine.^{462,463} Interestingly, (-)-SKF-10,047, displays an affinity for μ opioid receptors ($K_i = 3.6 \pm 0.05$ nM), whereas the (+)-isomer shows an affinity for both sigma and phencyclidine receptors. However, sigma receptors demonstrate preference for the (+)-cis-isomer of the N-substituted N-normetazocines, particularly when they bear bulky nitrogen substituents compared to the other derivatives of phencyclidine.⁴⁶⁴⁻⁴⁶⁶

Accordingly, Bluth *et al.* examined the cross reactivity between sigma receptors and PCP recognition sites and whether the metaphit is able to acylate sigma sites.⁴⁶⁷ It was found that metaphit displaces both [³H]DTG and [³H]3-PPP from sites in guinea pig brain membranes in a competitive and irreversible manner. It is important to note that metaphit produces an irreversible inhibition of the sigma receptor sites, which depends on the ligand that was used in the experiment. The order of sensitivity is [³H]DTG > [³H](+)-3PPP >> [³H](+)-SKF-10,047, the values of IC₅₀ correspond respectively to 2, 10, and 50 mM, which reflects the different manner of interactions of benzomorphan and non-benzomorphan structure with the sigma sites.⁴⁶⁷ These results were explained by a theory of Bowen *et al.* that proposed a multi-site model for the sigma receptors, allosteric model or multiple sigma receptor types.⁴⁶⁸ Based on this theory, metaphit interacts in a different manner with these different sites and therefore have a different ability in inhibiting the binding of these ligands.

Therefore, the acylating metaphit binds irreversibly to an adjacent nucleophilic site and not targeted directly the binding site of sigma receptors. This may give a chance to the competing ligands to replace metaphit from the ligand-binding site while it still binds covalently to the receptor, which appears as a competitive inhibition. Another explanation suggested that metaphit acts as a competitive inhibitor of [³H]DTG and [³H](+)-3-PPP, whereas the high concentrations of competing ligands as is the case for PCP receptors should not overcome the acylation of sigma sites by metaphit. A subsequent study by Reid *et al.* in 1990,⁴⁶⁹ showed that metaphit and several other phencyclidine-based ligands bind to both sigma and PCP sites and produce a wash-resistant inhibition.⁴⁶⁹ In the same study, they found the most potent sigma receptor inhibitor was cinnamoyl-PCP (**188**)[Fig. 4.2], and next to it, was the isothiocyanate derivative of phencyclidine, ETOX-NCS (**189**)[Fig. 4.2]. These two compounds were able to

inhibit [³H]DTG binding at low concentration (1 μM) whereas the other compounds inhibited the binding at a higher concentration (10 μM), and a better inhibition was obtained at 100 μM; however, (±)-MK-801-NCS (**190**)[Fig. 4.2] showed an equivalent effect at all concentrations.⁴⁷⁰

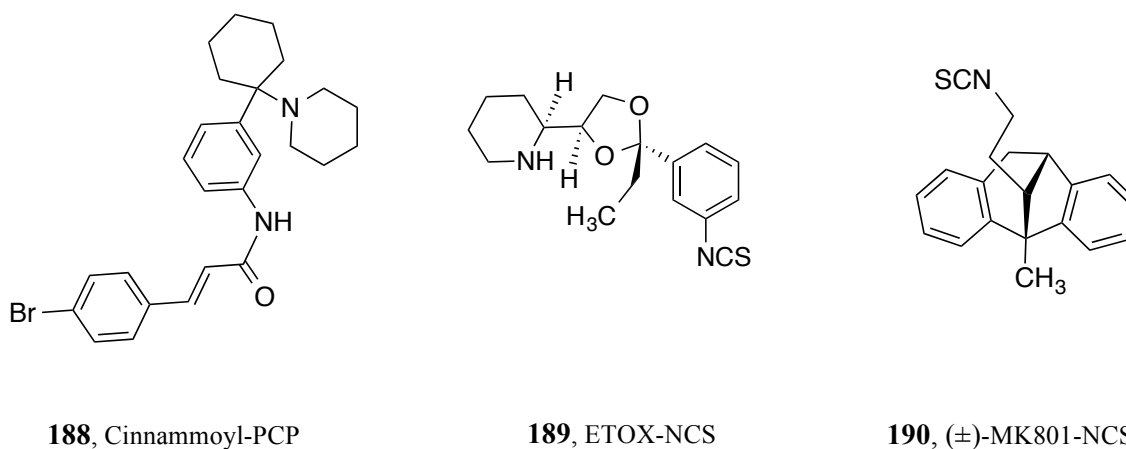


Figure 4.2: Structures of phencyclidine based ligands.

A recent study by Zhang and coworkers showed that metaphit inhibited the DTG-induced inhibition of calcium channels by more than 95% indicating the irreversible sigma receptor antagonist activity of metaphit.⁴⁷⁰

4.1.2 Analogs of guanidine

DTG, di-o-tolyl-guanidine, is one of the most selective sigma ligands with a guanidine structure that was first demonstrated as a sigma ligand by Weber and coworkers.⁴⁷¹ It has no substantial affinity toward the other receptor systems even though it cannot differentiate between both sigma receptor subtypes, (K_i , $\sigma_1 = 12$ nM and $\sigma_2 = 38$ nM).^{471,472} The structure of DTG (**35**)[Fig. 4.3], was modified to the isothiocyanate derivative, 1-(2-methyl-4-isothiocyanatophenyl)-3-(2-methylphenyl)guanidine (DIGIT) (**191**)[Fig. 4.3], without affecting the sigma receptors affinity, and has the ability to inhibit sigma sites labeled with

[³H]DTG.⁴⁷³ In contrast to metaphit, DIGIT does not show substantial affinity for PCP receptors labeled with [³H]TCP. Furthermore, it does not have an effect on the binding of dopaminergic receptors labeled with [³H]spiperone, opioid receptors labeled with [³H]dihydromorphine or benzodiazepine receptors labeled with [³H]flunitrazepa. However, it does inhibit the binding of [³H](+)-3-PPP. To study the irreversible binding of DIGIT, membranes were pretreated with 50 nM DIGIT resulted in 50% binding inhibition of [³H]DTG, and the binding of [³H]DTG to the membranes pretreated with DIGIT did not take place even after several wash out procedures indicating the irreversible binding of DIGIT. However, the DTG ligand that has no isothiocyanate group was easily washed out, indicating that the wash-resistant binding is mainly due to the covalent bond that was made by the isothiocyanate group.⁴⁷³

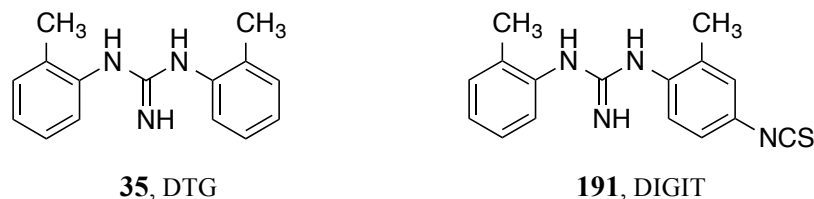


Figure 4.3: Chemical structures of DTG and its isothiocyanate analog, DIGIT.

4.1.3 Analogs of 3-phenylpiperidine

Among of the two isomers of the 3-hydroxyphenyl-N-propyl piperidine (3-PPP), the R-(+)-3-PPP isomer shows a preference for sigma-1 receptor (σ_1 K_i = 5 nM; σ_2 K_i = 442 nM). These results guided the synthesis of irreversible sigma ligand derivatives from the 3-hydroxyphenyl-N-propyl piperidine (3-PPP), for example R-(+)-3-(4-isothiocyanato-3-methoxyphenyl)-1-propyl piperidine (**192**) [Fig. 4.4] and R-(+)-1-(2-isothiocyanatoethyl)-3-(3-methoxyphenyl)piperidine (**193**) (Fig. 4.4).⁴⁷⁴ It was found that the newly synthesized ligands are able to inhibit the binding of [³H](+)-3-PPP in a variable manners with an IC_{50} = 40 nM, and 12,000 nM, respectively. Also, the radioligand binding is not recoverable even after several

washout procedures demonstrating the irreversible binding of the isothiocyanate through a covalent bond.⁴⁷⁴

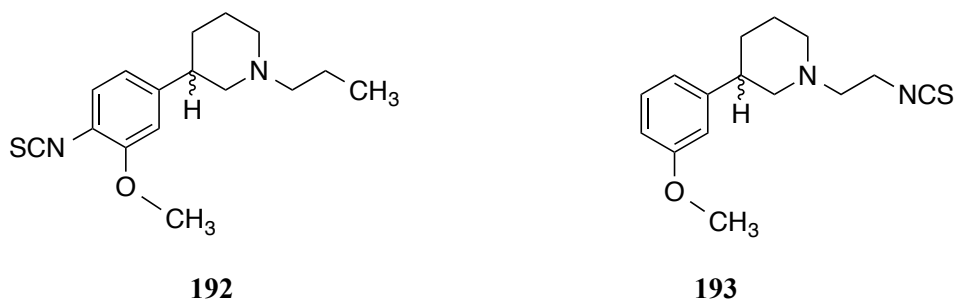


Figure 4.4: Chemical structures of possible irreversible sigma ligands

4.1.4 Analogs of benzomorphan

(+)-Pentazocine and (+)-SKF-10,047 are benzomorphan derivatives with a high selectivity for sigma-1 sites that have been used in a tritiated form as selective sigma-1 receptor probes. In the early 1990s, Carroll *et al.* synthesized a series of *N*-substituted derivatives of (+)- and (-)-*cis*-*N*-normetazocine to evaluate their affinity against three different receptor systems, sigma-1, phencyclidine, and μ opioid receptors.⁴⁶⁶ Among the synthesized compounds, (+)-*cis*-*N*-benzyl-*N*-normetazocine, a compound with a high affinity for sigma-1 receptor with $K_i = 0.67$ nM and a low affinity for sigma-2 receptor with $K_i = 1710$ nM. Some modifications have been made on this compound resulted in making the irreversible ligand, (+)-*cis*-*N*-(4-isothiocyanatobenzyl)-*N*-normetazocine (BNIT) (**194**) [Fig. 4.5] for sigma-1 receptors.^{475,476} Membranes pretreated with BNIT at a concentration of 0.1 μ M resulted in a decrease in the B_{max} of [³H](+)-pentazocine binding by about 40% with respect to the control, and greater effect was obtained with 1 μ M concentration. Also, the binding of [³H](+)-pentazocine is not recoverable, even after several washout procedures of the pretreated membranes with BNIT.⁴⁷⁶ Similarly, and in the same study,

several saturation experiments conducted with [³H]DTG in the presence of (+)-pentazocine to block sigma-1 receptors, have indicated how the values of B_{max} are the same as those obtained when the membranes were pretreated with BNIT at 1 and 5 μM concentrations, as were the K_d values.⁴⁷⁶ Interestingly, BNIT does not cause a loss of sigma-2 sites labeled by [³H]DTG; on the other hand, the binding of [³H](+)-pentazocine is not recoverable, even after several washout procedures of the membranes pretreated with BNIT. Therefore, it is clear that BNIT is only able to block sigma-1 sites selectively and irreversibly.⁴⁷⁶

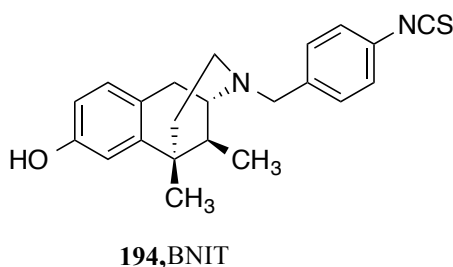


Figure 4.5: Chemical structure of BNIT

4.2 Photoaffinity labels

Photoaffinity labels are also irreversible ligands but unlike the affinity labels, they are bearing a reactive group in a dormant form that becomes an electrophile only when it is irradiated. These reactive groups can be, an epoxide, a Michael acceptor, or a reactive alkyl halide in the photoaffinity probe structures. Westheimer was the first who introduced the photoaffinity compounds in the early 1960, as a concept of photoaffinity labeling.⁴⁷⁷ Later, it was proven that the photoaffinity technique to be an efficient approach to identify various target proteins that can be useful in the fields of chemical biology and medicinal chemistry.⁴⁷⁸

Photoaffinity probes can be utilized in various biological and medicinal applications, for example:⁴⁷⁹

- 1) Characterization of the structure and function of biological molecules.

- 2) Identification of the targets of biological active compounds.
- 3) Determination of the selectivity and affinity of ligand-target complexes.
- 4) Isolation and characterization of the unidentified enzymes or receptors.
- 5) Exploration of ligand-receptor interactions.
- 6) Identification of amino acid residues at protein-protein, and proteins-lipid interfaces.

However, there are also some limitations:

- 1) Photolabeling is a low efficiency process.
- 2) Photolabeling has some stability issues.
- 3) It has a selectivity issue due to its ability to react with any types of bond or residue without any preference.
- 4) UV-irradiation damages the targeted proteins.
- 5) In general, *in vivo* work is difficult to be performed.

There are three major types of photoreactive groups that are commonly used in photoaffinity labeling; arylazides (**195**), diazirines (**196**), and benzophenones (**197**). [Fig. 4.6]

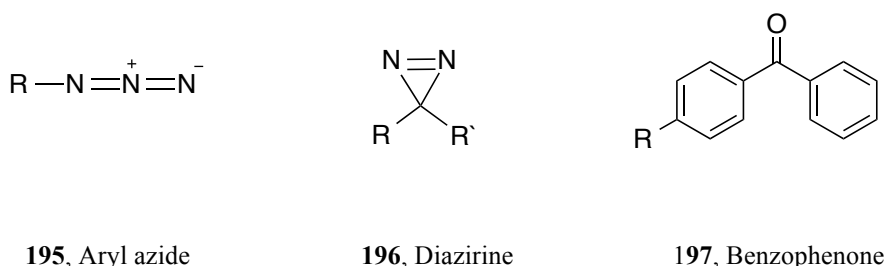


Figure 4.6: Structures of commonly used photo-reactive groups.

Amongst all the photoreactive groups, aryl azides [Fig. 4.7] are the most used group that forms an extremely reactive nitrogen molecule upon UV activation. The photoactivation of an aryl azide creates the wanted singlet nitrene, which can produce a triplet nitrene through

intersystem crossing. [Fig. 4.7]

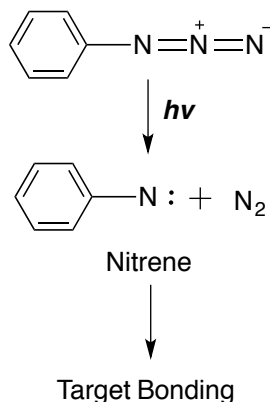


Figure 4.7: Aryl azide photoactivation.

However, the 1,2-azacycloheptatetraene can be generated as a result of singlet nitrene rearrangement and a bicyclic benzazirine formation at particular temperature. The formed 1,2-azacycloheptatetraene can interact with the other distance nucleophilic groups and reduce the photolabeling specificity.[Fig. 4.8] ^{477,480-483}

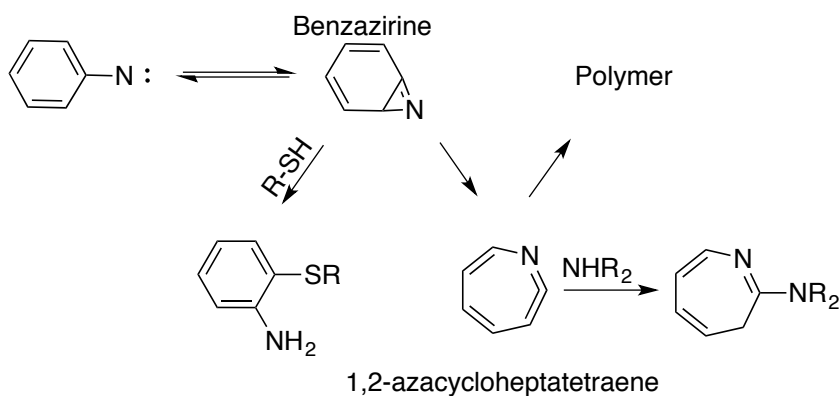


Figure 4.8: Possible side reactions of aryl azides.

Diazirine group is highly reactive upon photoactivation and relatively inactive towards nucleophilic attack, alkaline and acidic conditions. It generates a reactive carbene that binds covalently with the closest target molecule through C–C, C–H, O–H, or X–H incorporation.[Fig.

4.9] However, the diazine derivatives synthesis involves long and complicated synthetic procedures.⁴⁸¹

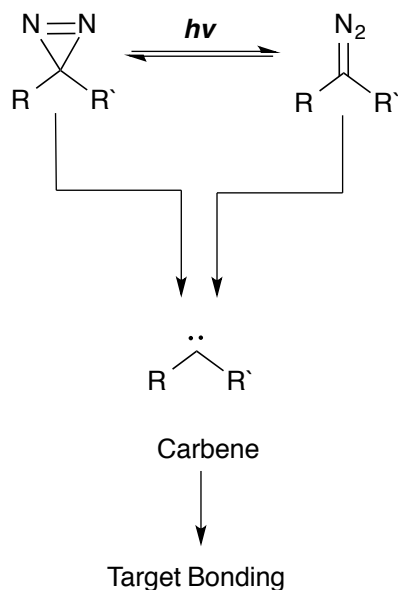


Figure 4.9: Diazirine derivatives photoactivation.

Several building blocks constructed on benzophenone are commercially available. Therefore, the benzophenone photoaffinity probes can easily be synthesized by linking commercially available benzophenone derivatives to the probe.⁴⁸⁴ Benzophenones are stable in most organic solvents and compatible with several synthetic routes. Upon photoactivation, benzophenone generates reactive triplet carbonyl states that can react with inactive C-H bonds.[Fig. 4.10] However, benzophenone has a major drawbacks are that their requirement for long irradiation times that can lead to low specificity, and their bulkiness that can obstruct the binding with the target proteins.^{477,485,486}

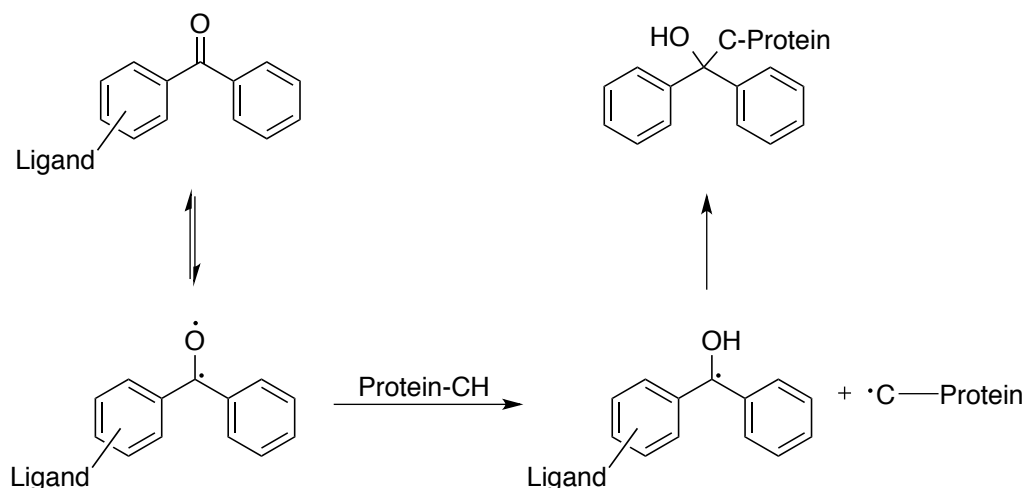
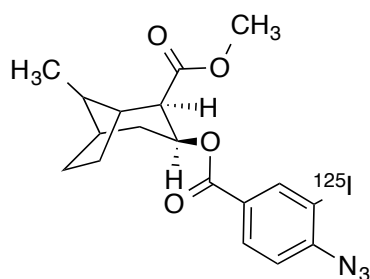


Figure 4.10: Benzophenone derivatives photoactivation.

4.2.1 Photoaffinity labels built on variety of sigma ligands

4.2.1.1 Iodo-azidococaine

Based on the moderate affinity of (-)-cocaine toward sigma receptors ($K_i = 6.7 \pm 0.3 \mu\text{M}$), several subsequent studies have been conducted in attempts to develop better sigma ligands and led to the synthesis of (-)-3-iodo-4-azidococaine (**198**) [Fig. 4.11].¹⁰³ This compound shows a substantial increase in the affinity for sigma receptors regardless to the added substitutions to the original molecule, (-)-cocaine.⁴⁸⁷ In order to obtain the photoaffinity label [¹²⁵I]N₃-cocaine, (-)-3-iodo-4-azidococaine was radiolabeled with ¹²⁵I. This photoaffinity probe was able to label a Mr 26,000 protein in various tissues including rat liver, and brain in addition to human placenta that was blocked by numerous sigma ligands, such as haloperidol, DTG, (+)- and (-)-3-PPP, carbetapentane, and dextromethorphan.⁴⁸⁷

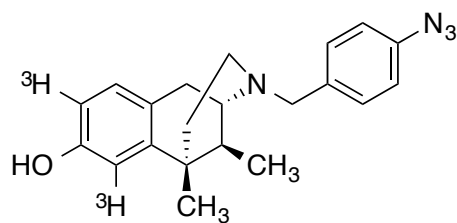


198, [¹²⁵I]Azidococaine

Figure 4.11 Chemical structure of [¹²⁵I]Azidococaine

4.2.1.2 Azido-phenazocine

Many studies have been conducted in effort to develop selective sigma-1 ligands, and some of these studies demonstrated the enantiospecificity of the (±)-benzomorphans in which they found the specificity of (+)-benzomorphans for sigma-1 receptors, while the (-)-enantiomers show some preference for sigma-2 receptors with less discrimination between both subtypes.⁴⁵⁰ Also, some of the earlier efforts led to synthesize [³H](+)-azidophenazocine (**199**) [Fig. 4.12], the photoactive benzomorphan derivative, which was able to label sigma-1 receptors with a high affinity similar to that of its related compound (+)-pentazocine ($\sigma_1 K_i = 1.34 \pm 0.21$ nM) when incubated in the dark with guinea pig brain membranes.⁴⁸⁸ Furthermore, the (+)-azidophenazocine was able to compete with other sigma ligands and blocked the binding to lymphocyte binding sites when incubated under reversible conditions.⁴⁸⁹ Upon photoactivation, (+)-azidophenazocine labeled four proteins in lymphocyte membranes: Mr 57,000, Mr 33,000, Mr 27,000, and Mr 22,000. However, further studies showed that only Mr 57,000 protein is blocked by sigma ligands, indicating that Mr 57,000 is a sigma receptor protein.^{489,466}

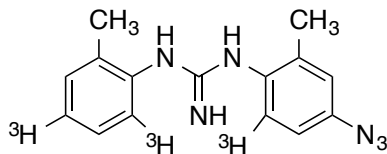


199, [³H](+)-Azidophenazocine

Figure 4.12. Chemical structure of [³H](+)-Azidophenazocine

4.2.1.3 Azido-DTG

Several reports have been published showing the tremendous amount of effort put into identification and characterization of the molecular properties of sigma receptors, and some of this work demonstrated the use of radiolabeled photoaffinity ligands bearing an azide group. Consequently, the synthesis of [³H]N₃DTG, 1-(4-azido-2-methyl[6-³H]phenyl)-3-(2-methyl[4,6-³H]phenyl)guanidine (**200**) [Fig. 4.13], was first reported by Kavanaugh *et al.* in 1988,⁴⁹⁰ and the binding studies of this ligand showed that it has high affinity for sigma receptors as same as [³H]DTG.⁴⁹⁰ A protein with a molecular mass of 29 kDa was irreversibly labeled after guinea pig brain membranes were photoactivated in the presence of [³H]N₃DTG, and labeling of this protein was completely blocked by many putative sigma ligands.⁴⁹⁰ In a subsequent study by Hellewell and Bowen,⁸ a polypeptide of Mr 25,000 in guinea pig brain membranes was photolabeled by [³H]N₃DTG.^{8,451} However, the differences between the two polypeptides in this study and that of Kavanaugh *et al.*⁴⁹⁰ was reasoned to the difference in the experimental conditions that were used. In contrast to guinea pig brain, two polypeptides of Mr 18,000 and Mr 21,000 were photolabeled in PC12 cells, and based on these findings, Bowen and colleagues proposed the two subtypes of sigma receptors with different molecular size; sigma-1 and sigma-2.⁸



200, [³H]N₃DTG

Figure 4.13: Chemical structure of [³H]N₃DTG.

From the above mentioned studies, proteins photolabeled by [¹²⁵I]N₃-cocaine, [³H](+)-azidophenazocine, and [³H]N₃DTG with a molecular size 25–29 kDa range are described as the sigma receptor, and the photolabeled proteins of 18–21.5 kDa range are described as sigma-2 receptor. However, sigma-2 receptor has not yet been cloned. Thus, Photoaffinity probes will play an important role in further molecular and pharmacological studies of sigma receptors.

**CHAPTER V: PHARMACOKINETICS AND METABOLIC STABILITY
OPTIMIZATION**

5.1 Introduction

For more than three decades, studying metabolism and other pharmacokinetic properties of a drug candidate have tremendously helped in improving bioavailability and metabolic stability of new drugs and increased the overall success rate. For the most part, progress in automated molecular biology, high-throughput pharmacological screens and combinatorial synthesis has led to an accelerated process of drug discovery and development, especially in the pharmaceutical industry. Also, a number of studies have indicated that metabolism of a new drug candidate by the host organism is one of the most significant elements of the pharmacokinetic properties of a drug.

Today, more than ever, bringing new molecules to market that will have not only the required activity, but also reasonable potency and duration of action, is the major concern of medicinal chemists. Accordingly, both bioavailability and half-life are essential contributors to the concept of metabolic stability. A drug candidate with a poor pharmacological activity, low bioavailability and high toxicity most likely will have a low success rate. In addition, the high expense, long time of development, and high risk of failure have also influenced the drug discovery process and bringing new drugs to market. Absorption, distribution, metabolism and excretion (ADME) are the four major determinants of pharmacokinetics. Therefore, an ideal drug candidate should possess both good pharmacological activities as well as good pharmacokinetic properties. The importance of early *in vitro* and *in vivo* pharmacokinetic studies has become well recognized in the drug discovery process, and are usually employed in an attempt to optimize both the pharmacokinetic properties and potency of a drug candidate at the same time. High clearance rates and high metabolic liabilities of candidates usually leads to poor bioavailability and/or the formation of active or toxic metabolites. Therefore, understanding the metabolism and

other pharmacokinetic parameters of a new drug candidate is needed in the early stage of drug discovery process. In most cases, metabolism can generate active, inactive, and reactive/toxic metabolites of drugs. Knowing such information can be very helpful as a basis for judging whether or not a drug candidate is worth further development.⁴⁹¹⁻⁴⁹³

In drug discovery process, preliminary pharmacokinetic studies are generally performed in rodents or the other species used for the evaluation of *in vivo* efficacy. Subsequently, experiments are conducted in a large animal species such as dog or monkey for better description and to generate useful data in predicting human pharmacokinetic parameters.⁴⁹¹⁻⁴⁹³

5.2 Pharmacokinetic parameters and drug behavior

5.2.1. C_{\max} and t_{\max}

C_{\max} is the maximum observed concentration in the concentration-time profile (C_{\max}) and the time to reach that concentration (t_{\max} , which equals 0 for i.v. bolus dosing), after intravenous (i.v.) or extravascular drug administration.⁴⁹²

5.2.2. Area under the curve (AUC)

The AUC is the initial measure of overall exposure following i.v or extravascular administration of a drug, once blood, plasma or serum drug concentrations are plotted versus time. However, the linear trapezoidal method is the most commonly used method to determine AUC.

The area of each trapezoid is calculated as:

$$\text{AUC } t_1 \rightarrow t_2 = \frac{(C_2 + C_1)}{2} \times (t_2 - t_1).$$

The extrapolated area from t_{last} is estimated as;

$$\text{AUC } t_{\text{last}} \rightarrow \infty = C_{\text{last}} / \lambda_z \quad (\lambda_z = \text{terminal rate constant})$$

Total AUC or AUC $0 \rightarrow \infty$ equal the sum of these areas:

$$\text{AUC } 0 \rightarrow \infty = \text{AUC}_{0-t_{\text{last}}} + \text{AUC}_{t_{\text{last}} \rightarrow \infty}.$$

AUC is expressed in units of concentration X time (e.g. ng X h/mL)

AUC is the most important initial pharmacokinetic parameter used to calculate clearance and bioavailability. However, $t_{1/2}$ or AUC have received more attention in practical work.⁴⁹²

5.2.3. Clearance (CL)

Clearance (CL) is a proportionality factor that relates the rate of drug elimination (in mass/time) to blood or plasma concentrations.

$$\text{Rate of elimination} = \text{CL} \times C.$$

Clearance is expressed in units of volume/time and can be described as the volume of blood or plasma that must be cleared of drug per unit time to produce the observed rate of elimination.⁴⁹²

5.2.4. Bioavailability (F)

Bioavailability is one of the principal pharmacokinetic properties of drugs, and can be defined as the fraction of an administered dose of unchanged drug that reaches the systemic circulation.

Absolute bioavailability is the amount of drug from a formulation that reaches the systemic circulation relative to an intravenous (IV) dose.

Bioavailability is calculated as the ratio of area under the curve (AUC) for the test and reference formulation/route of administration, and absolute bioavailability calculated as:

$$F = \frac{AUC_{oral}}{AUC_{iv}}$$

Whereas, *relative bioavailability* is the amount of drug from a formulation that reaches the systemic circulation relative to a different formulation (non-IV) such as oral solution, and calculated as:

$$F_{rel} = \frac{AUC_{formulation1}}{AUC_{formulation2}}$$

5.2.5. Volume of distribution (V_D)

The volume of distribution (V) is a proportionality factor that relates the amount of drug in the body to the concentration of drug measured in a biological fluid.

$$\text{Amount of drug in body} = V \times C.$$

V at t = 0 is known as V_c

Volume of distribution is a function of plasma protein and tissue binding,

$$V = V_p + V_t \times \frac{f_u}{f_{uT}}$$

Where,

V_D = the apparent volume of distribution.

f_u = the fraction unbound in plasma.

V_p = the volume of plasma.

f_{uT} = the fraction unbound in tissue.

V_t = the apparent volume of tissue.

5.2.6. Half-life ($t_{1/2}$)

The half-life of a drug is the time it takes for its concentration in blood or plasma to decrease by half. By examining the ln drug concentration versus time profile, one can determine how many half-lives best describe drug loss. There is a single elimination rate constant k_{elim} when only one phase is observed, and half-life is calculated as:

$$t_{1/2} = \frac{0.693}{k_{elim}} = \frac{V}{CL} \times 0.693.$$

Half-life is a secondary pharmacokinetic parameter, which is a function of clearance and distribution of the drug, and that reasoned to as CL increases, $t_{1/2}$ decreases, and as V_D increases, $t_{1/2}$ increases.⁴⁹²

5.3. Metabolic stability enhancement

In the past, several approaches have been applied to optimize metabolic stability of drug candidates. For many years, optimizing the pharmacokinetic properties of new chemical entities in drug discovery has been by trial and error. Numerous drugs have been optimized by using traditional methods, such as empirical methods and experience for structural modification in drug discovery and development. On the other hand, a lot of effort has been applied recently to improve metabolic stability using knowledge-based systems, rapid chemical synthetic methods, pharmacophore models, and X-ray crystallography.⁴⁹¹⁻⁴⁹³

Converting a lipophilic drug molecule to a water-soluble form *in vivo*, which can be readily excreted, usually known as metabolism or biotransformation. Enzymes in the liver and other body tissues catalyze the chemical process of drug metabolism in organism system. There

are two categories of drug metabolism reactions: Phase I and Phase II reactions. Phase I metabolism involves introduction of polar functional groups (OH, COOH, NH₂, SH etc.) into the drug molecule, which results in a small increase in their hydrophilicity. Cytochrome P450, flavin-containing monooxygenases, esterases, and amidases are the most significant enzymes involved in Phase I metabolism. Phase II biotransformation reactions include glucoronidation, acetylation, methylation, conjugation with glutathione, glycine or glutamic acid. Phase II biotransformation leads to significant increase in the hydrophilicity of drug molecule enhancing rapid excretion in urine.⁴⁹¹⁻⁴⁹³

In successful drug design and development, it is important to determine, and then improve the exposure–activity-toxicity relationship, which is also known as “the rule of three”, for drug candidates, and hence their suitability for improvement and development. There are two approaches that evaluate the metabolism of a compound *in vitro* and *in vivo* investigation. But, since *in vitro* studies generally allow for higher throughput at less cost than *in vivo* studies, they have now become an essential part of modern drug discovery. Numerous *in vitro* methods are available to evaluate metabolic stability; however, liver microsomes are the most common and widely used method. Generally, *in vitro* studies can be used along with *in vivo* experiments to select the animal model with a metabolism that is most similar to human.⁴⁹¹

5.4. Metabolic stability and intrinsic metabolic clearance

Rane *et al.* was reported the first practical attempt to relate *in vivo* pharmacokinetics to *in vitro* drug metabolism.⁴⁹⁴ In the same study, using the concept of intrinsic metabolic clearance (CL_{int}), they demonstrate the *in vitro* metabolism rates correlated well with hepatic extraction ratios determined from isolated perfused rat livers. Later, the concept of *in vitro-in vivo* correlations has been steadily reviewed.⁴⁹⁵⁻⁴⁹⁹

Intrinsic clearance (Cl_{int}) as defined by Houston, is the proportionality factor between drug concentration at the enzyme site (C_e) and rate of metabolism.^{495,496}

$$Cl_{int} = \text{Rate of metabolism}/C_e$$

From the Michaelis-Menten relationship for enzyme catalyzed reactions, rate of metabolism is related to concentration at the catalytic site, maximum velocity of reaction (V_{max}) and a constant known as the Michaelis constant (K_m) which in practical terms is defined as the substrate concentration at half maximal velocity.^{499,500}

$$CL_{int} = \frac{V_{max}}{K_m}$$

K_m and V_{max} can easily be measured *in vitro*.

Subsequent work by Obach *et al.* in which they reviewed the above principals and made prediction of human clearance from CL_{int} data determined from *in vitro* metabolism experiments. They use *in vitro* half-life method to determine CL_{int} , which is shown in the equation below.⁵⁰¹

$$CL_{int} = \frac{0.693}{in\ vitro\ t_{1/2} \times \text{amount liver incubation} \times F_u}$$

Where,

$t_{1/2}$ = half-life of the *in vitro* incubation

f_u = fraction unbound to microsomal protein.

Incubating a given drug with liver subcellular preparations for an appropriate period and measuring the disappearance of parent drug determined the *in vitro* half-life. Plotting ln % remaining vs time, then measuring the slope of this plot determined half-life:

$$t_{1/2} = 0.693 / \text{slope}$$

5.5. Advantages of enhancing metabolic stability

Enhancement of metabolic stability generally allows for better control of pharmacokinetics as well as reduces reactive intermediates formation such as electrophilic, alkylating metabolites. Below there are some other advantages of optimizing metabolic stability of drug candidates.⁵⁰²

1. Enhanced resemblance between dose and plasma concentration, which in turn reduce or even eliminate the need for expensive therapeutic monitoring.
2. Improved bioavailability and half-life that allow lower and less frequent dosing, which in turn leads to improve in patient compliance.
3. Decreased clearance that will result in a lower overall dose.
4. Decrease in metabolic turnover rates from different species that allows a better extrapolation of animal data to humans.
5. Irregularity in drug levels from patient-to-patient and intra-patient can be reduced, since it is mainly based on differences in drug metabolic capacity.
6. Decrease in metabolism reduces the risk of drug-drug interactions.
7. Decrease in metabolism reduces the risk of food-drug interaction due to the reduced dose.
8. Reducing the number and significance of active metabolites and hence cutting the need for further studies on drug metabolites in animals and humans.

5.6. Strategies to enhance metabolic stability

Optimization of microsomal stability of a chemical entity can be performed by *in vitro* metabolism studies to confirm formation of metabolites, as well as to provide quantitative analysis of major metabolites. Similarly, understanding the route through which a compound is metabolized and the pharmacokinetics of its metabolites is essential for the successful

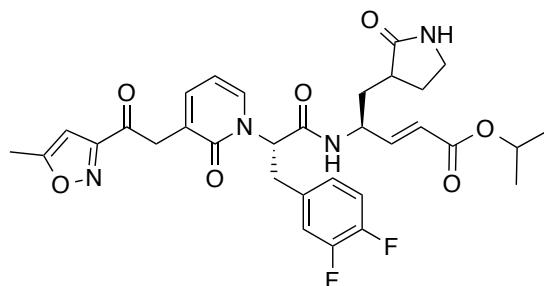
optimization of a drug candidate. Decades of study in drug metabolism have generated a plenty of qualitative observations on how to design metabolic stability into molecules. Recently, the advance in synthetic, analytical, and computational chemistry tools has accelerated the drug discovery and development process with high success rate. Therefore, numerous modifications can be used to improve metabolic stability, after recognizing moieties that contribute to activity and other functional groups necessary for activity. In general, metabolism can be reduced by incorporation of stable functional groups as blocking groups at metabolically susceptible sites or by decreasing the lipophilicity of the compound. Accordingly, numerous strategies have been applied to modify the molecular structure of a candidate compound to improve its metabolic stability:^{503,504}

- Deactivation of aromatic rings to facilitate oxidation through substitution with strongly electron-withdrawing groups (e.g. F, CF₃, SO₂NH₂, SO₃⁻).
- Incorporation of a steric bulk N-t-butyl group to prevent N-dealkylation.
- Substitution of a susceptible ester linkage with an amide group.
- Constraining the molecule in a conformation that is unfavorable to the metabolic pathway, more typically, protecting the labile moiety by steric shielding.
- Avoidance of phenolic function, which have consistently been shown to be rapidly glucuronidated.
- Avoidance of other conjugation reactions as primary clearance pathways would also be advised in the design stage in any drug that is to be administered orally.
- The optimum strategy is to anticipate the probable route of metabolism and prepare the expected metabolite if it has adequate intrinsic activity. For example, N-oxides are frequently as active as the parent amine but do not undergo further N-oxidation.

5.6.1. Reducing lipophilicity

Reducing the overall lipophilicity of a drug candidate is one of the most successful strategies for optimizing the metabolic stability of that candidate. However, lipophilic groups are usually involved in the binding to the biological target and they are vital for membrane permeability, which limits the application of this strategy. It has been reported that the binding site of metabolizing enzymes is mostly lipophilic in nature and thus these enzymes more readily accept lipophilic molecules.⁵⁰⁴ There are two approaches have been used successfully to reduce the lipophilicity of compounds, one is to remove lipophilic groups or moieties from the structure without compromising activity, and the other approach is accomplished through introduction of polar isosteres into molecules. For better understanding, literature based examples will be presented below to help in explanation of metabolic stability optimization approaches.

In a study by Dragovich *et al.* on the human rhinovirus 3C protease inhibitor (**201**) [Fig. 5.1] that displayed poor oral bioavailability *in vivo* in monkey, they found replacement of the benzyl group with substituents that possess low lipophilicity to obtain the propargyl analog (**202**) [Fig. 5.1] and the ethyl analog (**203**) [Fig. 5.1], led to reduction in calculated logP values in both analogs, improved oral bioavailability and retained the same activity when compared to the parent molecule.⁵⁰⁴



201

EC₅₀ = 0.078 μM
clogP = 2.070
C 7 h = 0.012 μM

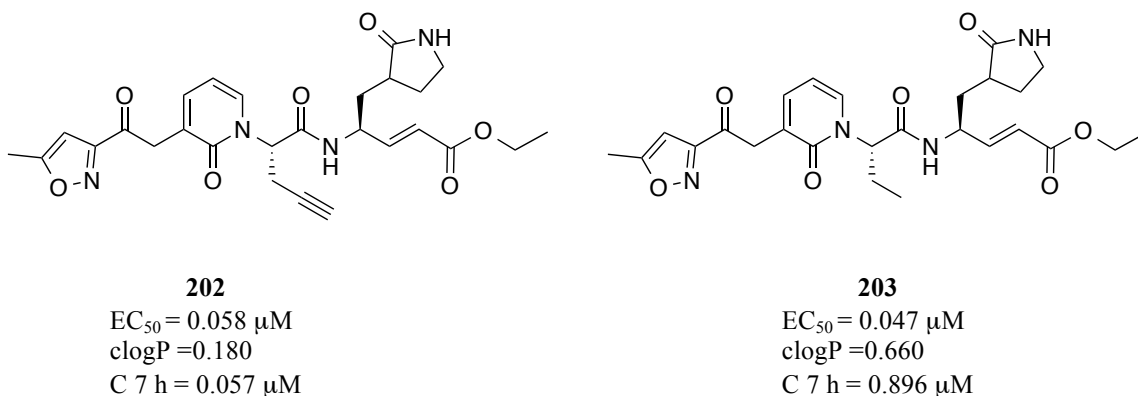
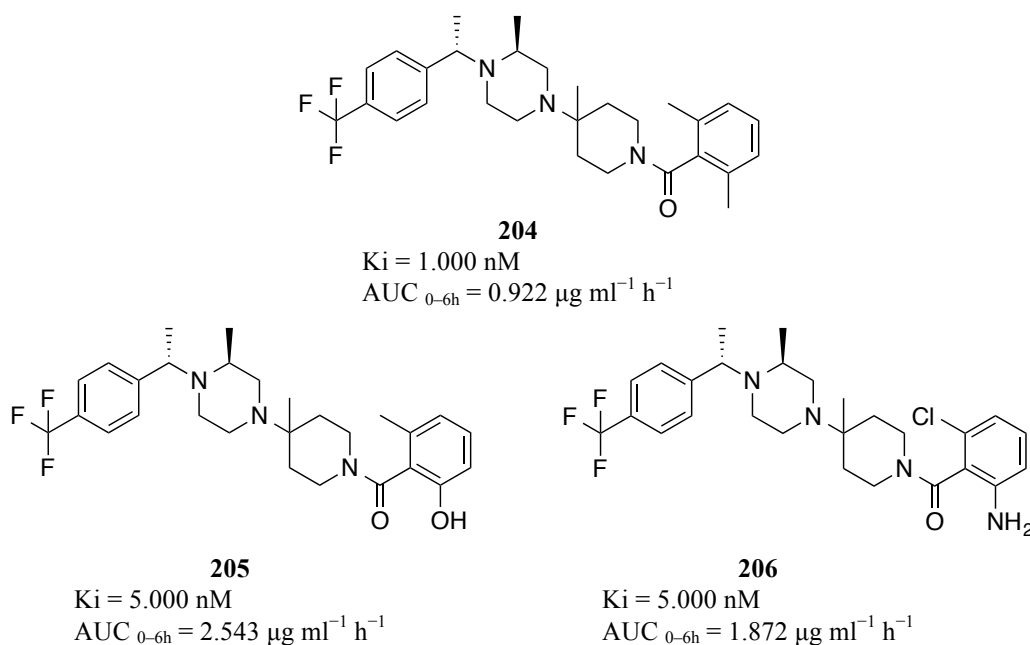


Figure 5.1: Chemical structure of rhinovirus 3C protease lead inhibitors

Alternatively, reduction of the lipophilicity by introducing isosteric atoms or polar functional groups into the molecule to increase the overall polarity is another approach that has been applied to enhance the pharmacokinetic profile of a chemokine receptor antagonist lead as HIV-1 inhibitor (**204**) [Fig. 5.2]. It was found that introduction of polar moieties such as the salicylamide (**205**) [Fig. 5.2], the anthranilamide (**206**) [Fig. 5.2], and the nicotinamide (**207**) [Fig. 5.2] afforded significant improvement in oral blood levels and area under curve of these ligands. In addition, the pyridine N-oxide (**208**) [Fig. 5.2] gave the optimum results in terms of potency and oral bioavailability in rat, dog and monkey.⁵⁰⁵



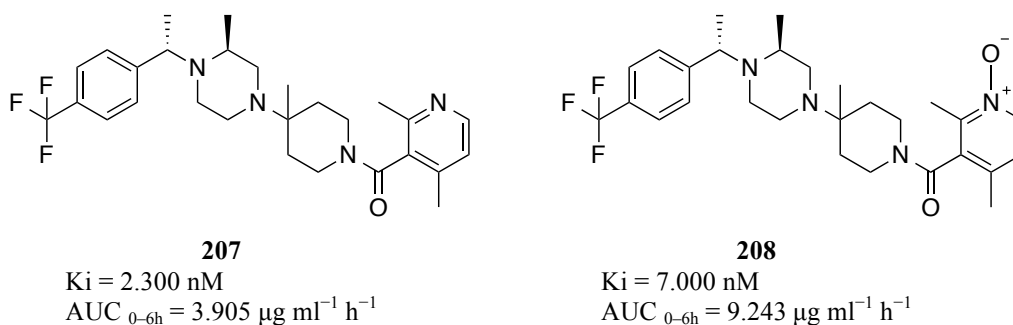
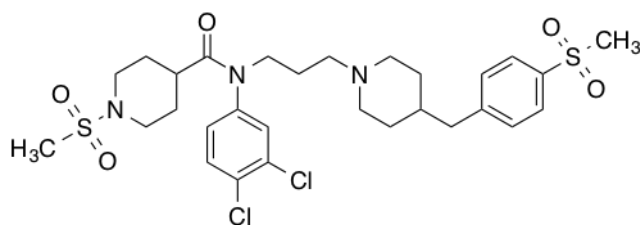
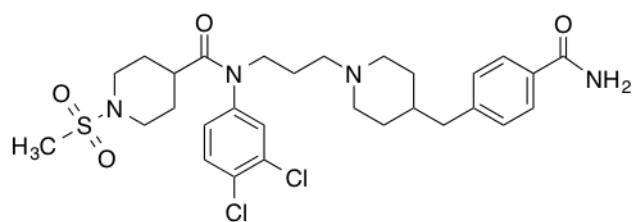


Figure 5.2: Chemical structures of chemokine receptor (CCR5) antagonists.

Another work by Imamura *et al.*⁵⁰⁶ presents another example to confirm the strategy of reducing lipophilicity to optimize metabolic stability of drug candidates. They incorporated various polar groups into a previously described piperidine-4-carboxamide CCR5 antagonist (**209**) [Fig. 5.3], which suffered from rapid oxidative metabolism in human hepatic microsomes and the human metabolic liability hampered further development.⁵⁰⁶ Insertion a carboxamide group into the phenyl ring of the 4- benzylpiperidine moiety gave the less lipophilic compound (**210**) [Fig. 5.3], which had both high metabolic stability and good inhibitory activity of HIV-1. Moreover, replacing the methylsulfonyl group with an acetyl group and one chloro atom with a methyl group to afford compound (**211**) [Fig. 5.3] that displayed a 5-fold increase in potency in the membrane fusion assay and also was found to be metabolically stable in human hepatic microsomes.⁵⁰⁶



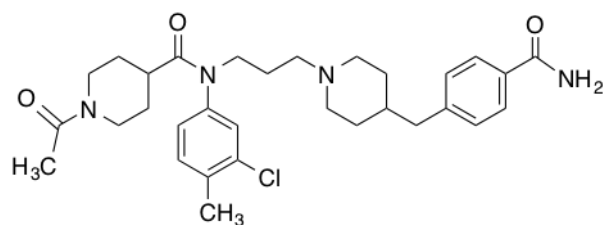
209
 $IC_{50} = 0.80 \text{ (nM)}$
 $ClogP = 3.9$



210

IC₅₀ = 5.80 (nM)

ClogP = 4



211

IC₅₀ = 0.42 (nM)

ClogP = 3.3

Figure 5.3.: Chemical structures of some piperidine-4-carboxamide CCR5 antagonists

5.6.2. Blocking metabolically labile groups

Blocking vulnerable sites through incorporation of stable groups or by removing the possibly labile groups from the molecule can enhance the metabolic stability of a drug candidate. Sites that are susceptible to oxidation can be blocked by introducing a halogen atom such as fluorine or by replacing the benzylic CH₂ with an isostere such as oxygen.

Stratford and co-workers reported an example of blocking the potential metabolic sites by introducing fluorine atom on an aromatic ring in order to block the aromatic oxidation. They found introduction of fluorine atom on the aromatic ring of compound 153186 (**212**) [Fig. 5.4] resulted in 18-fold enhancement in metabolic stability of the di-fluoro analog 368227 (**213**) [Fig. 5.4], and more than 2-fold of the di-fluoro analog 366094 (**214**) [Fig. 5.4] compared with the unsubstituted phenyl ring of parent molecule.⁵⁰⁷

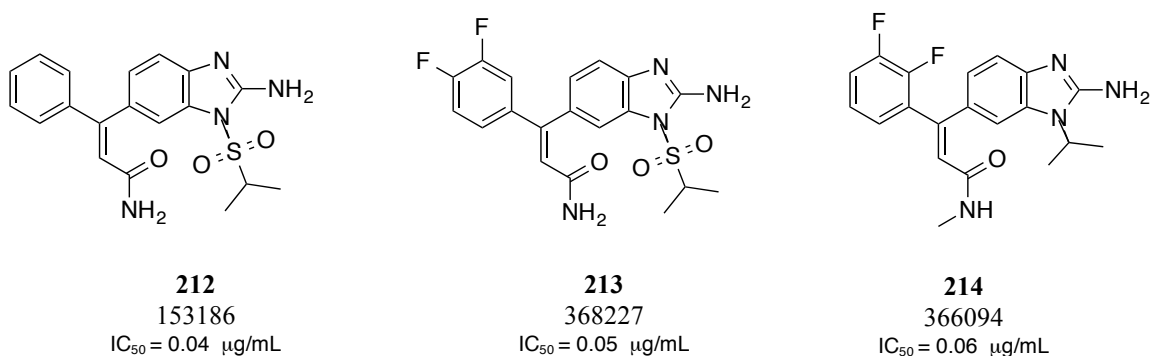


Figure 5.4: Chemical structure of fluorinated compounds

Another work by Victor and co-workers provides an example of blocking sites of potential oxidative metabolism to optimize metabolic stability.⁵⁰⁸ The replacement of a methyl group susceptible to allylic oxidation (**215**) [Fig. 5.5] with a hydrogen resulted in analog (**216**) [Fig. 5.5] with five-fold improvement. An additional improvement of about two-fold was obtained in analog (**218**) [Fig. 5.5] by the introduction of an acetylenyl moiety and a 4-fluoro substitution on the phenyl ring of (**217**) [Fig. 5.5] to block a potential oxidation on the aromatic ring.⁵⁰⁸

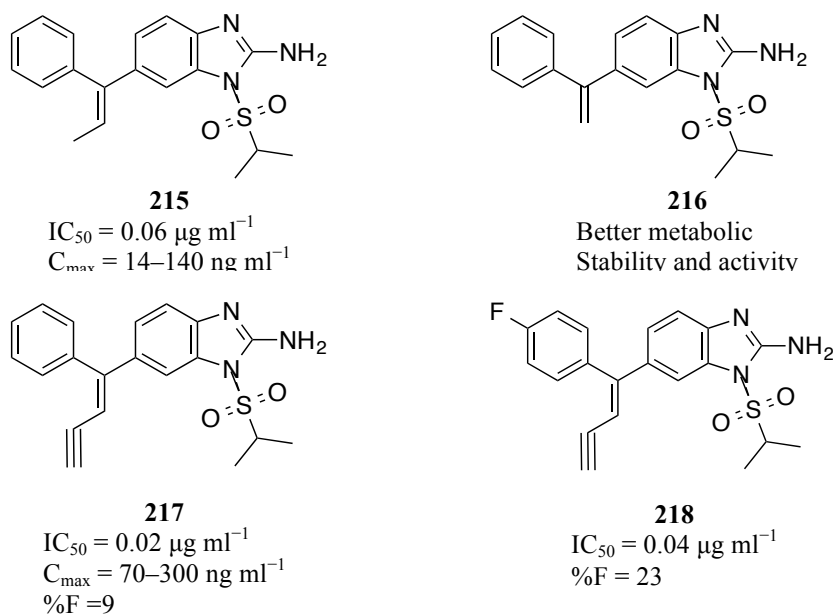


Figure 5.5: Examples of blocking sites of potential oxidative metabolism

Another example of blocking the metabolic sites was provided by Childers *et al.*⁵⁰⁹ to improve the metabolic stability of quinolyl-piperazinyl piperidine analog (**219**) [Fig. 5.6], which exhibited potent and selective 5-HT_{1A} antagonism; however, suffered from poor metabolic stability as a result of aromatic oxidation. Introducing a fluorine atom on position 5 of quinoline ring afforded compound (**220**) [Fig. 5.6] with retained activity and marginal improve in metabolic stability in human microsomal assay. Subsequent substitutions in both the 2- and 4-positions of the quinoline ring gave compound (**221**) [Fig. 5.6] with enhanced metabolic stability in rat and human microsomal assays, and with loss of its potency.⁵⁰⁹

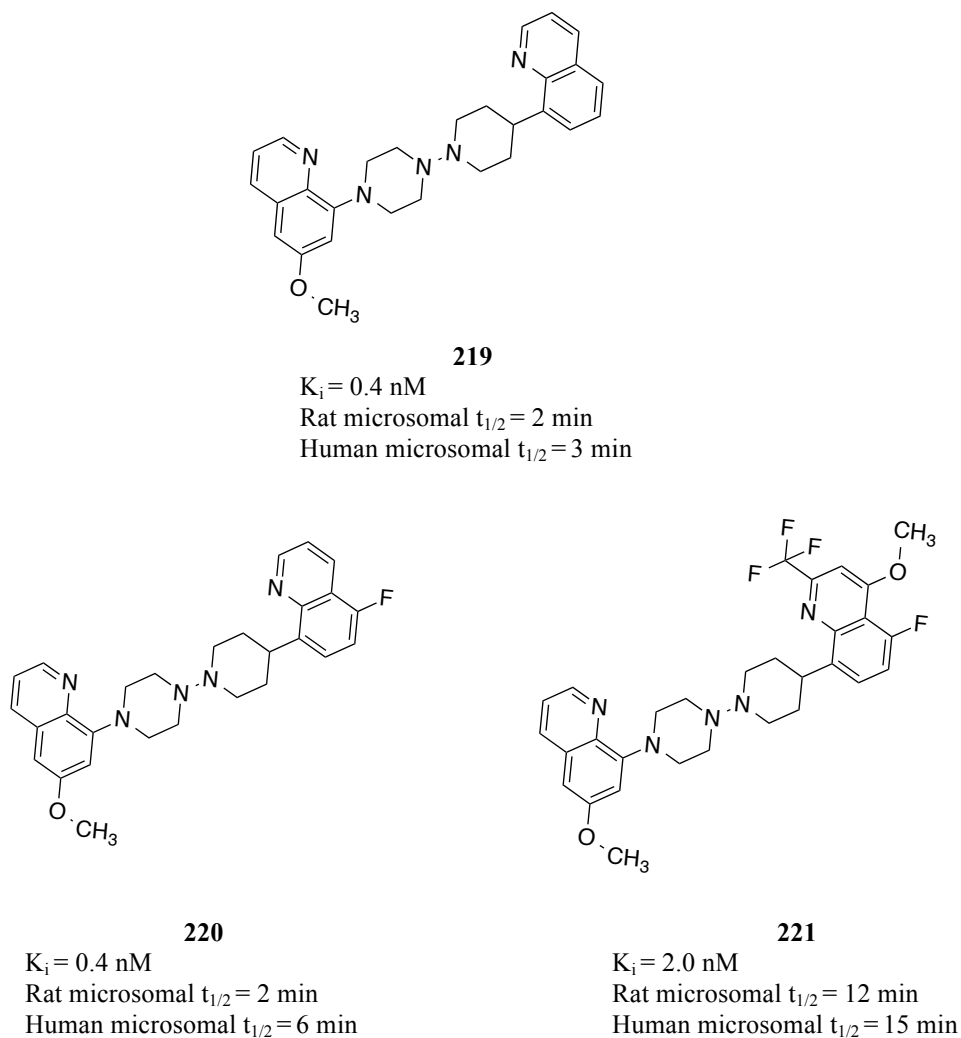


Figure 5.6: Chemical structure of compounds with fluorine atoms

Rohde and co-workers synthesized a series of E-5-hydroxy-2-adamantane inhibitors beginning from a rapidly metabolized adamantane 11 β -hydroxysteroid dehydrogenase type 1 inhibitor (11 β -HSDI) (**222**) [Fig. 5.7] in attempt to improve potency and metabolic stability.⁵¹⁰ Metabolic profile study of adamantanes showed that there are three potential metabolic labile sites, aryl ring oxidation, adamantane oxidation and N-piperazine dealkylation. Introducing a hydroxyl group on the adamantane ring afforded compound (**223**) [Fig. 5.7] with improved metabolic stability. Also, to block the aryl oxidation on the pyridine ring, trifluoromethyl was introduced to obtain compound (**224**) [Fig. 5.7] that showed greater metabolic stability than (**223**) [Fig. 5.7]. Additionally, to block N-dealkylation, a bulk steric group (methyl group) was incorporated onto the methylene ring adjacent to the nitrogen heteroatom of the piperazine ring resulted in even better metabolic stability (**225**) [Fig. 5.7].⁵¹⁰ Interestingly, it was found that the mono-methyl substitution compound has better potency with improved metabolic stability profile in both mouse and human experiments than the di-substituted analog.

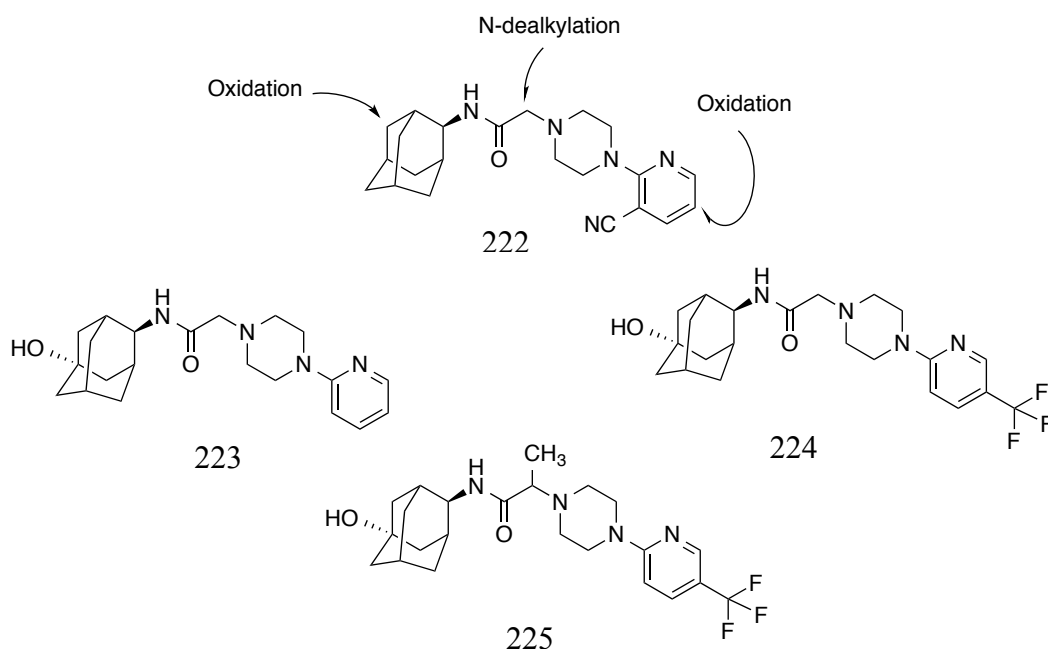


Figure 5.7: Chemical modification of a series of adamantane inhibitors

Another example was reported by Lin, N. H. *et al.* showing the removal of a metabolically soft spot to enhance the metabolic stability and bioavailability.⁴⁹⁶ A 50-fold increase in potency at nicotinic receptors was observed when the N-demethyl analog (**227**) [Fig. 5.8] was used instead of the N-methyl analog (**226**) [Fig. 5.8]. This can be explained as that the N-methyl is more liable to metabolism by N-demethylation.⁵¹¹



Figure 5.8: Chemical structures and half-lives of compounds 266, 227.

The work by Genin and co-workers on developing BHAP reverse transcriptase inhibitors with an effort to improve the metabolic stability, they achieved an approximate 4-fold enhancement in metabolic stability when they replaced a metabolically vulnerable 3-isopropylamino moiety on the parent molecule (**228**) [Fig. 5.9] with an ethoxy group to obtain compound (**229**) [Fig. 5.9], which proved to be more stable when compared with the stability of the lead compound.⁵²⁰

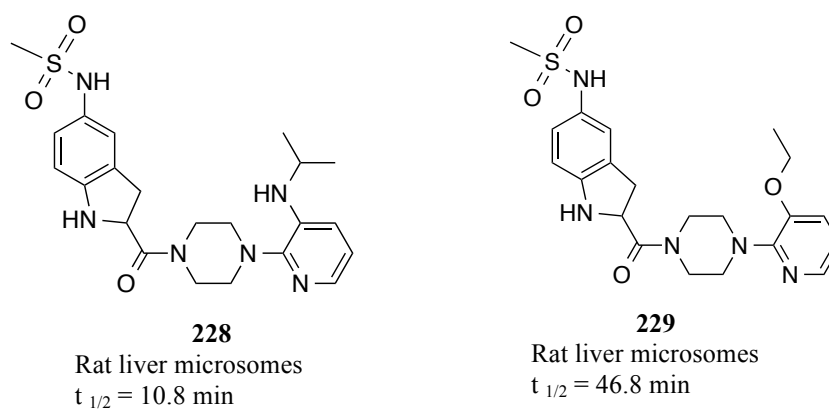


Figure 5.9: Chemical structures and half-lives of BHAP reverse transcriptase inhibitors.

5.6.3. Modification of metabolically labile groups

In addition to oxidation, it's well documented that amidases and esterases in the liver can hydrolyze amides and esters, respectively. Also, as a part of Phase II reactions, introduction of polar groups such as glucuronides and sulfates to the drug molecule makes them more water-soluble, and easily excreted; therefore, it can be targeted as a suitable strategy to improve the overall metabolic stability.

A work conducted by Blanchard *et al.* illustrates the above-mentioned approach with an effort to improve the bioavailability of phospholipase A₂ inhibitors. They observed a 22-fold improvement in bioavailability for an amide (**231**) [Fig. 5.10] as well as increase in the metabolic stability when compared with the corresponding ester (**230**) [Fig. 5.10].⁵¹³

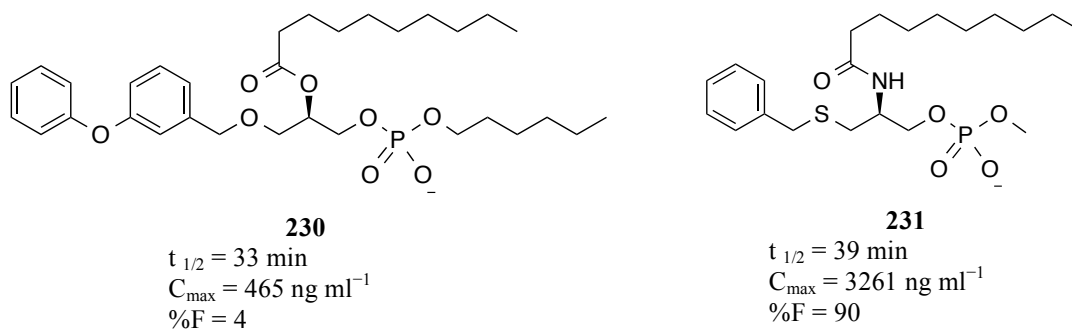


Figure 5.10: Chemical structures and half-lives of phospholipase A₂ inhibitors.

Another work by Zhuang, Z.P. *et al.*⁴¹⁴ demonstrates the development and optimization of a series of new arylpiperazine benzamido derivatives as potential ligands for 5-hydroxytryptamine-1A (5-HT_{1A}) receptors; however, the low brain uptake observed in the human subject was attributed to rapid metabolism via amide hydrolysis. In the same study, they reported that the cyclized amide derivative afforded compound (**233**) [Fig. 5.11] with more than 2-fold improvement in amide stability compared with the open-chain lead compound(**232**) [Fig.

5.11].⁴¹⁴

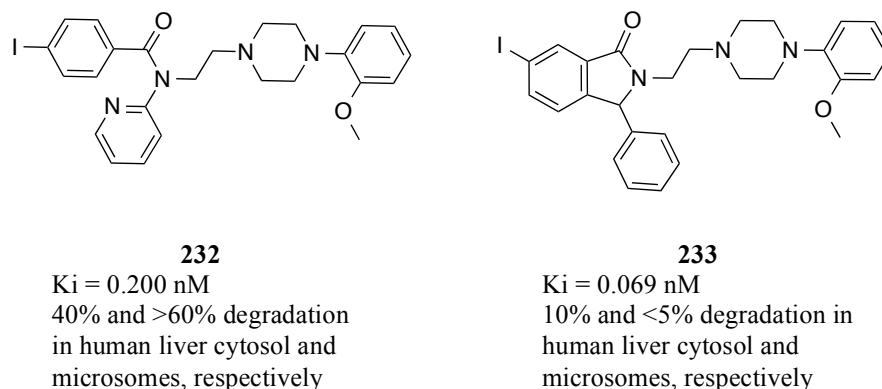


Figure 5.11: An example of improving metabolic stability by cyclization.

An extensive SAR study on *N*-hydroxyurea inhibitors of 5-lipoxygenase revealed that glucuronidation of the *N*-hydroxyl moiety was an activity-limiting step and thus became a vital key to improve metabolic stability of such compounds.⁵¹⁵

The *N*-hydroxyurea compounds related to zileuton were divided into three areas for structural modification; the template, the linking group and the pharmacophore.

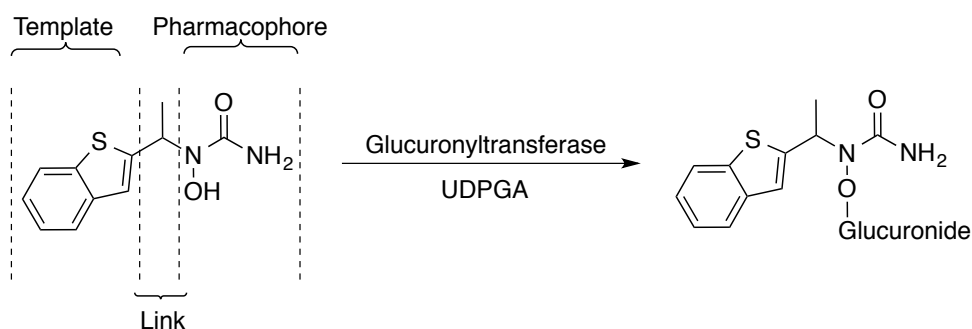


Figure 5.12: Structure of zileuton showing the three groups used to define the structure–metabolism relationships of the *N*-hydroxyureas.

The *N*-hydroxyurea moiety was recognized as an optimal pharmacophore for potency and selectivity; therefore, it was not touched for metabolic stability studies. However, the template and link modules attracted most of the attention to optimize zileuton derivatives *in vivo*, in

monkey.

Alternatively, the linker group links the template with the *N*-hydroxyurea pharmacophore was modified, and then the process was repeated with the benzthiophene template. Every compound was evaluated for its stability to glucuronidation of *N*-hydroxyurea. Among the tested molecules, compounds with acetylene linker groups were mostly found to have lower uridine 5'-diphosphoglucuronic acid (UDPGA) rates than any of the other tested links. This lower UDPGA rate results in the longest *in vivo* duration in monkey. Obviously, the rigid conformation structure of the acetylene group interrupts binding in the active site of uridine 5'-diphosphate-glucuronosyltransferase and hence reduces conjugation as can be seen in Figure 5.13.⁵¹⁵

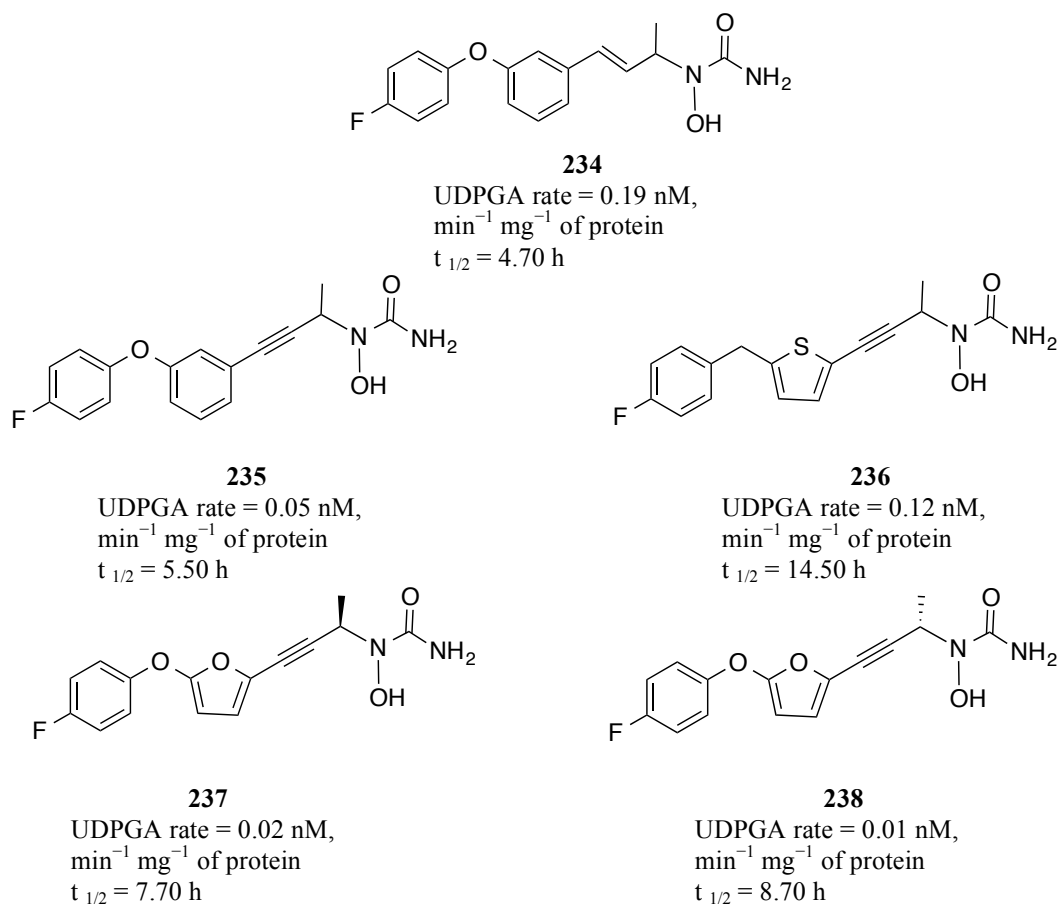


Figure 5.13: Chemical structures of 5-lipoxygenase inhibitors.

CHAPTER VI: RESEARCH DESIGN AND METHODS

6.1 Rationale for design and synthesis selective sigma receptors ligands

Several lines of evidence support the idea of targeting sigma receptors for development of therapeutics that could treat numerous diseases and their manifestation as well as for designing imaging agents to understand the pathophysiology associated with sigma receptors. An increase number of reports confirmed the validity of sigma receptors in treatment of cancer and drug addiction as reviewed in the previous chapters.

Consequently, the main focus of our laboratory is to design novel selective ligands for both sigma subtypes to get better structural and pharmacological understanding, which can contribute to developing treatments for cancer and drug abuse. Several reports over the years have indicated the involvement of sigma receptors in modulating the physiological actions of drugs of abuse such as cocaine and methamphetamine besides their role in apoptosis and cell death. Also, a number of the recent publications have confirmed the over-expression of sigma receptors in tumor cells to up 10 folds compared to the normal cells, which makes sigma receptors a valid target for cancer treatment.

Our research involves the design and synthesis of novel sigma receptor ligands as potential medications for cancer and drug addiction. Also, our research is contributing to the effort of identification of structural features necessary to develop ligands with high affinity and selectivity for both sigma receptor subtypes.

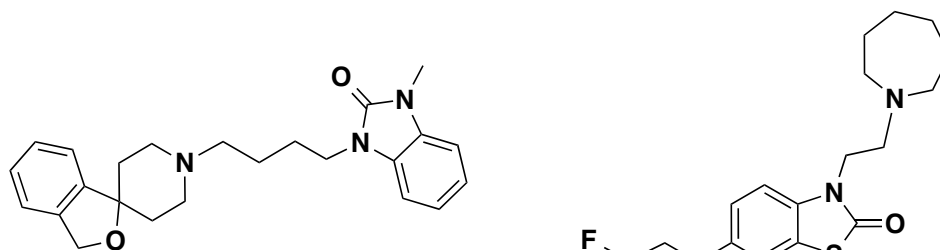
The specific aims of my dissertation are:

- 1) Design and synthesis of original benzofuran-based ligands for both sigma-1 and sigma-2 receptors;
- 2) Design and synthesis of irreversible selective sigma-2 ligands that may serve as

pharmacological tools to isolate and characterize sigma-2 receptor;

3) Development and synthesis of novel agents with a dual inhibition effect on DAT and sigma receptors, also with an attempt to improve the metabolic stability of the less stable CM699 ligand (**240**) [Fig. 6.1] as potential stimulant abuse (cocaine & methamphetamine) pharmacotherapy;

4) Synthesis and development of new analogs of the highly selective sigma-1 receptor ligand CM304 (**23**) [Fig. 6.1].



240, CM699
Ki

$\sigma_1 = 17$ nM
 $\sigma_2 = 0.014$ nM

CM699 and CM304 structures.

23, CM304
Ki

$\sigma_1 = 0.0025$ nM
 $\sigma_2 = 364.16$ nM

Figure 6.1:

Before

proceeding further, it is

important to

understand the nature of sigma receptors as shallow proteins that can accept a variety of ligands. It is assumed that there is some flexibility at the active sites of sigma receptors, since sigma receptors are able to interact with variety of ligands. Consequently, these diverse ligands might share some common features allowing them to interact with the same target. Subsequent studies and structural determinations of various sigma ligand classes proved the importance of the basic nitrogen for a compound to have sigma receptor affinity as well as the two hydrophobic groups (distal & proximal) with different distances from the basic nitrogen [Fig. 6.2].¹⁹⁴

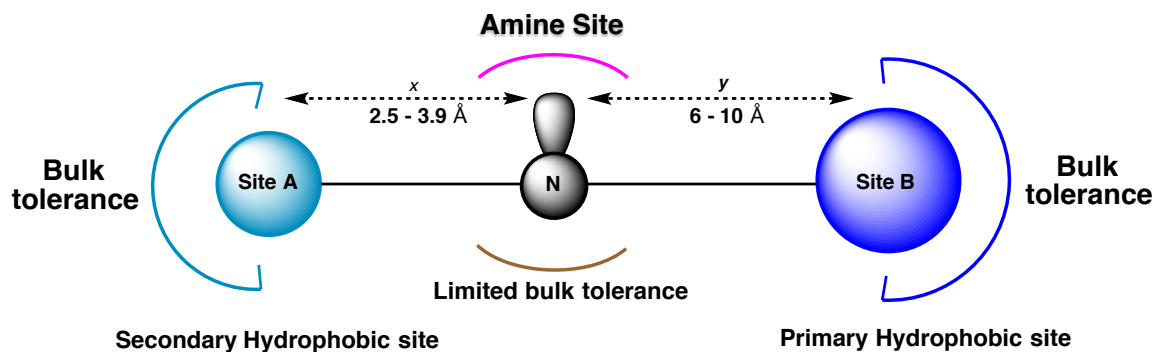
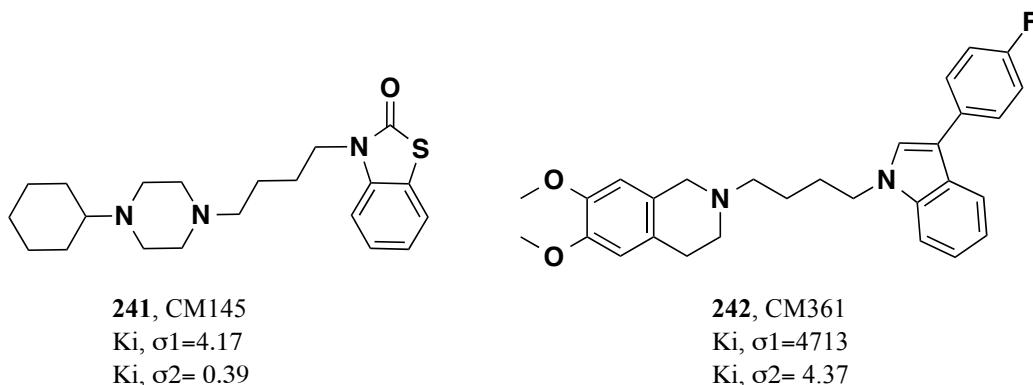
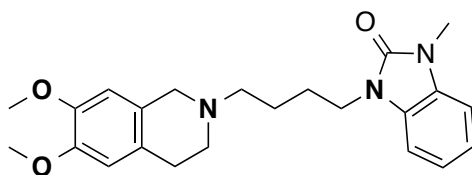


Figure 6.2: Glennon/Ablordeppey "Ar-X5-N" pharmacophore model for high binding affinity at sigma-1 receptor. [Adapted from ref. 6]

6.1.1 Benzofuran-based ligands

Previous work in our laboratory, reported a series of indoles, benzoxazolinones, benzothiazolinones, and benzoimidazolones with high mixed selectivity for both sigma receptor subtypes. Among the synthesized compounds, the 3-(4-(4-cyclohexylpiperazin-1-yl)butyl)benzo[d]thiazol-2(3H)-one (**241**) [Fig. 6.4], was found to have subnanomolar preference toward sigma-2 over sigma-1 receptors.⁵¹⁶ A subsequent study carried out in our laboratory, identified the 2-(4-(3-(4-fluorophenyl)indol-1-yl)butyl)-6,7-dimethoxy-1,2,3,4-tetrahydroisoquinoline, as a selective sigma-2 receptor ligand with a favorable selectivity ratio ($\sigma_1/\sigma_2 = 395$) (**242**) [Fig. 6.4].⁵¹⁷ Consequently, 1-(4-(6,7-dimethoxy-3,4-dihydroisoquinolin-2(1H)-yl)butyl)-3-methyl-1,3-dihydro-2H-benzo[d]imidazol-2-one was found to have preference for sigma-2 receptor over sigma-1 receptor with selectivity ratio ($\sigma_1/\sigma_2 = 1302$) (**242**) [Fig. 6.3].

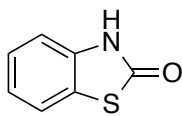




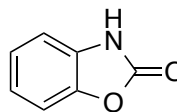
243, CM398
 Ki, σ_1 =560
 Ki, σ_2 = 0.47

Figure 6.3: Selective benzothiazolone, benzoimidazolone and indol-based sigma receptor ligands.

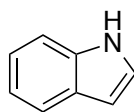
Therefore, it is noteworthy to synthesize and examine a new series of benzofuran-based compounds since the benzofuran is a typical isostere for indole, benzoxazole and benzothiazole rings (**244-246**) [Fig. 6.4].



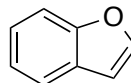
244
 benzo[d]thiazol-2(3H)-one



245
 benzo[d]oxazol-2(3H)-one



246
 1H-indole



247
 benzofuran

Figure 6.4: Bioisosteric heterocycle rings

Furthermore, it was observed in our laboratory that the optimal number of methylenes for the link between the amine and heterocyclic ring was found to be two for better sigma-1 receptors affinity, and four for substantial affinity toward sigma-2 receptors.

Thus, in a search for novel selective sigma receptor ligands and based on our previous findings, we designed a series of novel benzofuran derivatives in which we explored the two

carbon linker and four carbon linker between the heterocyclic ring and the basic nitrogen to determine the $\sigma_{1/2}$ receptors selectivity as well as exploring different substituents on a basic nitrogen of the heterocycle ring (secondary hydrophobic site) in attempt to build our structure affinity relationship (SAffiR) as can be seen in Figure 6.5.

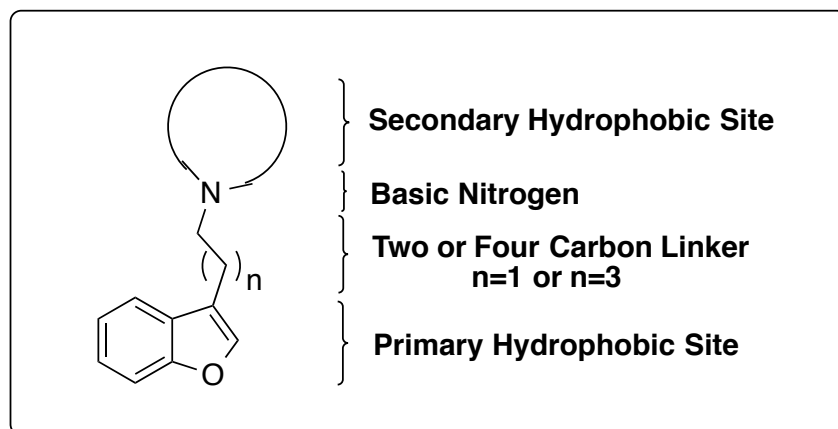


Figure 6.5: The Proposed Benzofuran-based Sigma Ligands Pharmacophore.

The newly synthesized compounds are summarized in the following table: [Tab. 6.1]

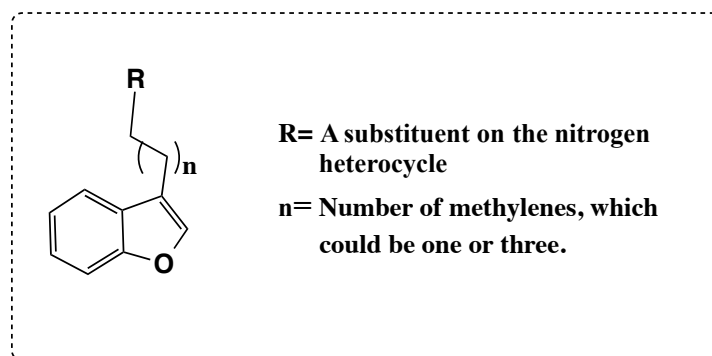
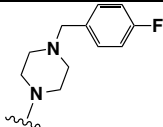
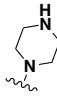
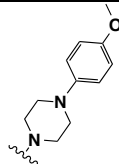
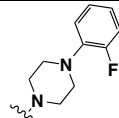
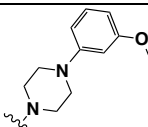
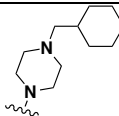
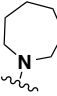
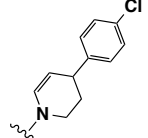
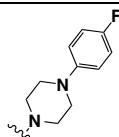
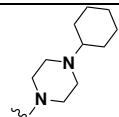
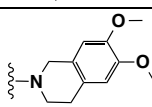
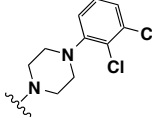
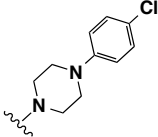
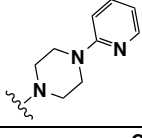
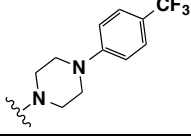
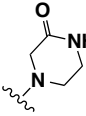
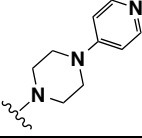
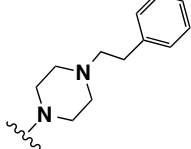
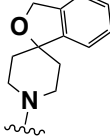
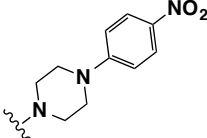
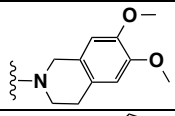
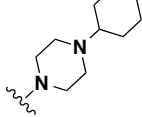
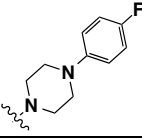
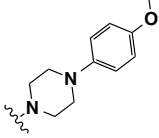
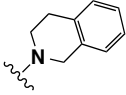
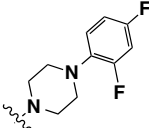
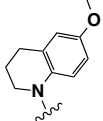
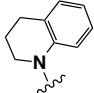
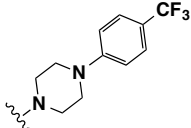
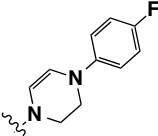
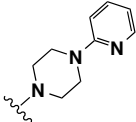
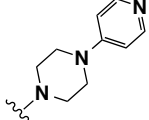
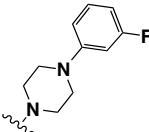
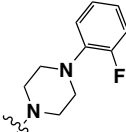
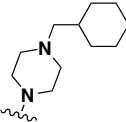
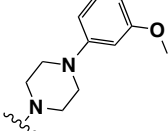


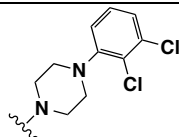
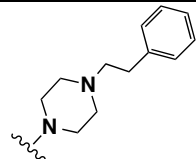
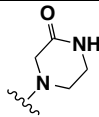
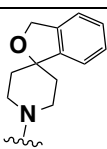
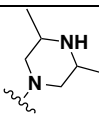
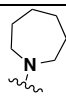
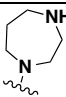
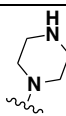
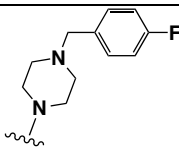
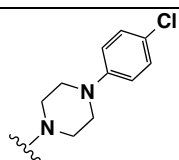
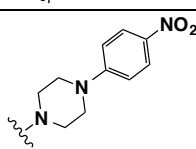
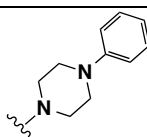
Table 6.1: The newly synthesized benzofuran-based sigma receptor ligands.

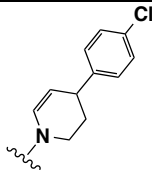
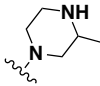
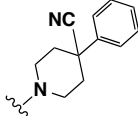
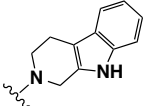
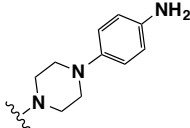
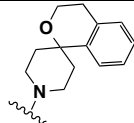
| Compound No | Notebook Entry | n "Number of methylenes" | R "Different substituents on basic nitrogen" |
|--------------------|-----------------------|------------------------------------|--|
| | | | |

| | | | |
|-----|-----------|---|---|
| 253 | WA101 | 1 |  |
| 254 | WA102 | 1 |  |
| 255 | WA104 | 1 |  |
| 256 | WA106 | 1 |  |
| 257 | WA107/182 | 1 |  |
| 258 | WA111 | 1 |  |
| 259 | WA123 | 1 |  |
| 260 | WA124 | 1 |  |
| 261 | WA134 | 1 |  |
| 262 | WA144 | 1 |  |
| 263 | WA181 | 1 |  |
| 264 | WA183 | 1 |  |

| | | | |
|-----|-------|---|---|
| 265 | WA184 | 1 |  |
| 266 | WA193 | 1 |  |
| 267 | WA196 | 1 |  |
| 268 | WA199 | 1 |  |
| 269 | WA204 | 1 |  |
| 270 | WA205 | 1 |  |
| 271 | WA207 | 1 |  |
| 272 | WA210 | 1 |  |
| 281 | WA169 | 3 |  |
| 282 | WA170 | 3 |  |
| 283 | WA171 | 3 |  |
| 284 | WA172 | 3 |  |

| | | | |
|-----|-------|---|---|
| 285 | WA173 | 3 |  |
| 286 | WA174 | 3 |  |
| 287 | WA175 | 3 |  |
| 288 | WA176 | 3 |  |
| 289 | WA177 | 3 |  |
| 290 | WA178 | 3 |  |
| 291 | WA179 | 3 |  |
| 292 | WA211 | 3 |  |
| 293 | WA212 | 3 |  |
| 294 | WA213 | 3 |  |
| 295 | WA214 | 3 |  |
| 296 | WA215 | 3 |  |

| | | | |
|-----|-------|---|---|
| 297 | WA216 | 3 |  |
| 298 | WA217 | 3 |  |
| 299 | WA218 | 3 |  |
| 300 | WA220 | 3 |  |
| 301 | WA221 | 3 |  |
| 302 | WA222 | 3 |  |
| 303 | WA223 | 3 |  |
| 304 | WA224 | 3 |  |
| 305 | WA225 | 3 |  |
| 306 | WA226 | 3 |  |
| 307 | WA227 | 3 |  |
| 308 | WA228 | 3 |  |

| | | | |
|-----|-------|---|---|
| 309 | WA230 | 3 |  |
| 310 | WA231 | 3 |  |
| 311 | WA232 | 3 |  |
| 312 | WA240 | 3 |  |
| 313 | WA254 | 3 |  |
| 314 | WA496 | 3 |  |

6.1.2 Developing irreversible selective sigma-2 ligands

Selective-irreversible binding of ligands to a protein is one of the most useful techniques to characterize and understand functions associated to that protein. Irreversible ligands are usually agents derived from ligands with high affinity and selectivity to the same-targeted protein. Slight chemical modification on these ligands can allow for a covalent bond to be formed with the same receptor. These modifications are generally conducted by introducing a reactive group such as the isothiocyanate, azide, nitrogen mustards, Michael acceptors, haloacetamides, and aldol esters that can bind irreversibly to the protein. The resulting ligands contain an electrophilic center that can bind covalently to a nucleophilic site in the receptor, which in turn will block the receptor if the compound is an antagonist or act as a functional antagonist if the compound is an agonist.^{450,518}

To accomplish this goal, high affinity sigma-2 ligands developed in our laboratory were utilized in the design and synthesis a novel series of isothiocyanate compounds [Table 6.2].

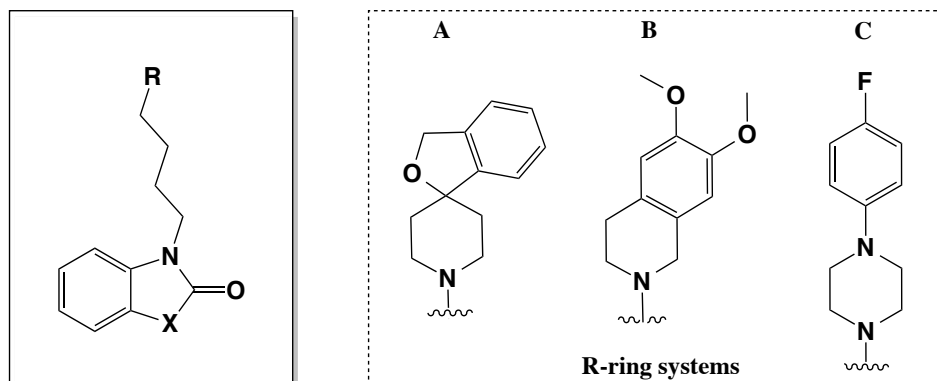


Table 6.2: Sigma-2 selective ligands previously synthesized in our laboratory.

| Comp. No: | Compound | R | X | Affinity (K _i , nM) | | σ_1/σ_2 ratio selectivity |
|-----------|----------|---|--|--------------------------------|--------------|---------------------------------------|
| | | | | σ_1 | σ_2 | |
| 243 | CM398 | B | NCH ₃ | 560.4± 8.7 | 0.43± 0.02 | 1303 |
| 240 | CM699 | A | NCH ₃ | 16.6± 1.1 | 0.014±0.0003 | 1143 |
| 315 | CM777 | C | N(CH ₂) ₂ CH ₃ | 752.4±51.4 | 0.66± 0.01 | 1140 |
| 316 | CM775 | C | N(CH ₃) ₄ CH ₃ | 2274± 187 | 4.27± 0.29 | 533 |
| 317 | CM778 | C | NPh | 543±8.8 | 6.69±0.51 | 81 |
| 318 | CM322 | C | NPh-4-F | 118.46±48.37 | 1.67±0.16 | 71 |

In this regard, we have incorporated an isothiocyanate moiety on our previous selective sigma-2 compounds and their analogs [Table 6.3].

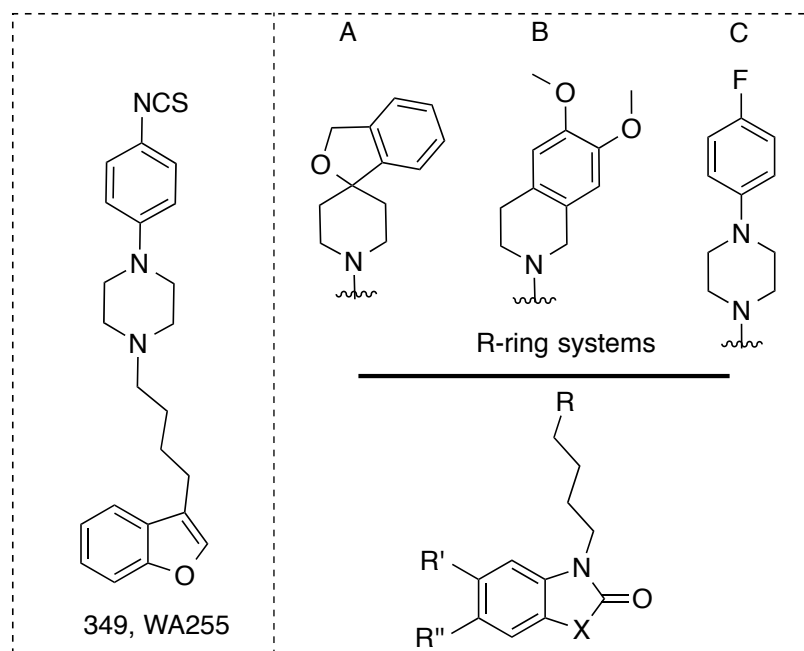


Table 6.3: The synthesized isothiocyanate derivatives and their precursors.

| Compound No | NB Entry | R ₁ | R ₂ | X | R ₃ |
|-------------|----------|-----------------|-----------------|--|----------------|
| 319 | WA248 | NO ₂ | H | NCH ₃ | B |
| 320 | WA256 | NO ₂ | H | NCH ₃ | A |
| 321 | WA262 | NO ₂ | H | N(CH ₂) ₂ CH ₃ | C |
| 322 | WA266 | NO ₂ | H | N(CH ₂) ₄ CH ₃ | B |
| 323 | WA267 | NO ₂ | H | N(CH ₂) ₄ CH ₃ | A |
| 324 | WA303 | NO ₂ | H | N(CH ₂) ₂ CH ₃ | A |
| 325 | WA334 | NO ₂ | H | N(CH ₂) ₂ CH ₃ | B |
| 326 | WA336 | NO ₂ | H | N(CH ₂) ₄ CH ₃ | C |
| 327(472b) | WA402 | H | NO ₂ | NCH ₃ | C |
| 328(472b) | WA420 | H | NO ₂ | N(CH ₂) ₄ CH ₃ | C |
| 329 | WA249 | NH ₂ | H | NCH ₃ | B |
| 330 | WA257 | NH ₂ | H | NCH ₃ | A |
| 331 | WA263 | NH ₂ | H | N(CH ₂) ₂ CH ₃ | C |
| 332 | WA268 | NH ₂ | H | N(CH ₂) ₄ CH ₃ | A |
| 333 | WA300 | NH ₂ | H | N(CH ₂) ₄ CH ₃ | B |
| 334 | WA304 | NH ₂ | H | N(CH ₂) ₂ CH ₃ | A |
| 335 | WA337 | NH ₂ | H | N(CH ₂) ₂ CH ₃ | B |
| 336 | WA338 | NH ₂ | H | N(CH ₂) ₂ CH ₃ | C |
| 337(473a) | WA403 | H | NH ₂ | NCH ₃ | C |
| 338(473b) | WA421 | H | NH ₂ | N(CH ₂) ₄ CH ₃ | C |
| 339 | WA250 | NCS | H | NCH ₃ | B |
| 340 | WA258 | NCS | H | NCH ₃ | A |
| 341 | WA264 | NCS | H | N(CH ₂) ₂ CH ₃ | C |
| 342 | WA269 | NCS | H | N(CH ₂) ₄ CH ₃ | B |
| 343 | WA306 | NCS | H | N(CH ₂) ₂ CH ₃ | B |
| 344 | WA349 | NCS | H | N(CH ₂) ₄ CH ₃ | C |
| 345 | WA350 | NCS | H | N(CH ₂) ₄ CH ₃ | B |
| 346 | WA352 | NCS | H | N(CH ₂) ₂ CH ₃ | B |
| 347(474a) | WA404 | H | NCS | NCH ₃ | C |

| | | | | | |
|-----------|-------|-----------------|-----------------|--|----|
| 348(474b) | WA422 | H | NCS | N(CH ₂) ₄ CH ₃ | C |
| 349 | WA255 | --- | --- | --- | -- |
| 356 | WA365 | H | H | NH | C |
| 357 | WA367 | H | H | NPh-NO ₂ | C |
| 359 | WA371 | H | H | NPh-NH ₂ | C |
| 360 | WA372 | H | H | NPh-NCS | C |
| 364 | WA394 | NO ₂ | H | O | C |
| 365 | WA409 | NO ₂ | H | O | A |
| 366 | WA410 | NO ₂ | H | O | B |
| 367 | WA396 | NH ₂ | H | O | C |
| 368 | WA411 | NH ₂ | H | O | B |
| 369 | WA412 | NH ₂ | H | O | A |
| 370 | WA397 | NCS | H | O | C |
| 371 | WA433 | NCS | H | O | B |
| 372 | WA434 | NCS | H | O | A |
| 376 | WA413 | H | NO ₂ | S | C |
| 377 | WA414 | H | NO ₂ | S | B |
| 378 | WA415 | H | NO ₂ | S | A |
| 379 | WA416 | H | NH ₂ | S | C |
| 380 | WA417 | H | NH ₂ | S | B |
| 381 | WA418 | H | NH ₂ | S | A |
| 382 | WA423 | H | NCS | S | B |
| 383 | WA435 | H | NCS | S | C |
| 384 | WA436 | H | NCS | S | A |

6.1.3 Development of dual sigma receptors and DAT inhibitors and CM699 metabolic stability enhancement

There are no approved medications to treat stimulant (cocaine & methamphetamine) abuse or addiction, which urges the need to develop novel and effective agents to battle this serious issue. Recently, a dual targeting approach of inhibiting sigma-1 receptors and dopamine transporters demonstrated blockade of cocaine self-administration in rats.¹¹² Having years of experience in the synthesis of high affinity sigma receptor ligands, we have retrospectively analyzed our library of compounds and discovered a ligand with these properties (CM699). Indeed, this lead compound was able to inhibit cocaine self-administration in rats without substituting for cocaine [Fig. 6.6].

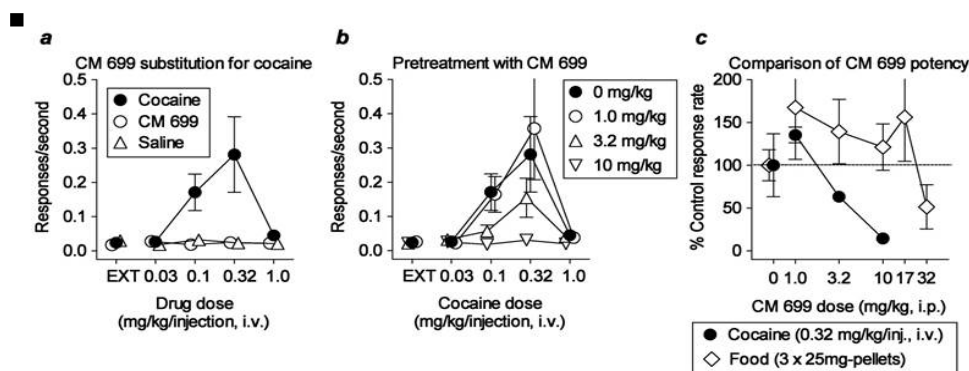


Figure 6.6: **a)** When substituted for cocaine, CM699 failed to maintain self-administration. Rates of responding obtained with CM699 substitution for cocaine were no different from those obtained with saline substituted for cocaine (compare open circles to triangles). **b)** When administered before opportunities to self-administer cocaine, CM699 produced a dose-dependent insurmountable antagonism of cocaine self-administration. **c)** CM699 exhibited specificity in producing decreases in cocaine self-administration, producing those decreases at doses that had no effects of responding maintained by non-drug food reinforcement.¹¹²

However, CM699 has a short half-life in human and rat liver microsome stability assays (*in vitro*), 12.7 and 4.4 min respectively. In the whole rat (*in vivo*), CM699 has a 4.4 hr half-life indicating a less than desirable profile to move forward into pre-clinical development [Fig. 6.7]. Although CM699 had a half-life of 4.4 hr in rat, it had a less than 1% oral bioavailability and was determined to be a lead for optimization studies. In this regard, we have decided to make analogs of CM699 in order to maintain or enhance blockade of cocaine self-administration and importantly, improve the pharmacokinetic profile.

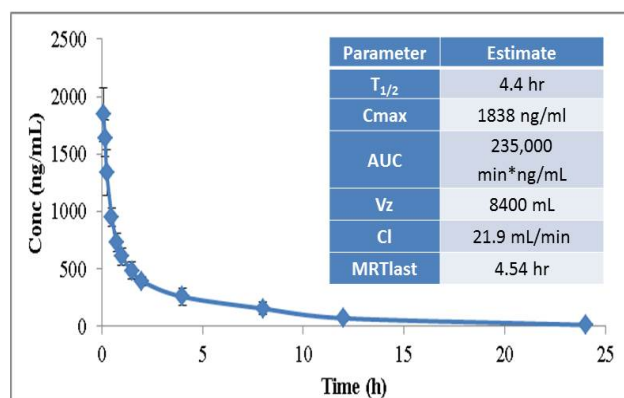


Figure 6.7: Plasma concentrations after administration of a single i.v. dose of 5 mg/kg produced a C_{max} of 1.84 $\mu\text{g/mL}$ of CM699 at 5 min after injection. Concentrations declined exponentially with an overall $T_{1/2}$ of 4.4 hr (Fig. 6.7) indicating a rapid distribution of the novel σR ligand in to the tissues. The distribution of CM699 was found to be extensive, which may be a desirable property for a compound acting on central nervous system. The elimination of CM699 from the systemic circulation was rapid as evidenced by its high clearance.

Our approach towards improving metabolic stability is to block the vulnerable sites of metabolism. As a first step of the research, we are targeting the two vulnerable sites, C6/C5 on the aromatic ring of the benzimidazolone ring and the carbon adjacent to the piperidine moiety, which are potentially labile towards metabolic oxidation and N-dealkylation, respectively by the microsomal enzymes.

To do so, first, we thought that blocking these sites by more stable functional groups, would be able to enhance the metabolic stability and protect the ligand from quick degradation, as seen in [Figure 6.7].

The second object was the selection of functional groups to block these sites. These groups should have minor effects on the physicochemical and conformational properties of the compound and in turn should not alter the affinity and selectivity. Fluorine atom is one of the most popular and widely used groups to block aromatic oxidation for several reasons:

- 1) It has the high electronegativity and therefore it is possible that the electron withdrawing character deactivates the aromatic ring towards metabolic oxidation.
- 2) The fluorine can exert a minor steric demand at receptor sites as its van der Waal radius is between hydrogen and oxygen atom.
- 3) The C-F bond is highly non-polarized and can participate in hydrogen bonding and electrostatic interaction suggesting the enhanced binding affinity for the protein active site.
- 4) Furthermore, fluorine increases lipophilicity and this can improve the bioavailability of the fluorinated compounds.

On the other hand, to prevent the N-dealkylation, our approach was to incorporate a methyl group on one of the carbons adjacent to the basic nitrogen in the piperidine core to

increase steric hindrance around the tertiary amine whereby the microsomal enzymes cannot perform their function. The selection of a methyl group for protecting molecules from metabolism is well documented and frequently used in the design and discovery of drug candidates. Based on the aforementioned concepts, we have synthesized new analogs of CM699 and incorporated the fluorine on the aromatic ring and methyl group on the carbon adjacent to the piperidine ring or both functionalities as well as making more derivatives using appropriate heterocyclic substituents that showed good preference for sigma receptors in previous work in our laboratory. Our approach towards improving metabolic stability is to block the vulnerable sites of metabolism as can be seen in Figure 6.8.

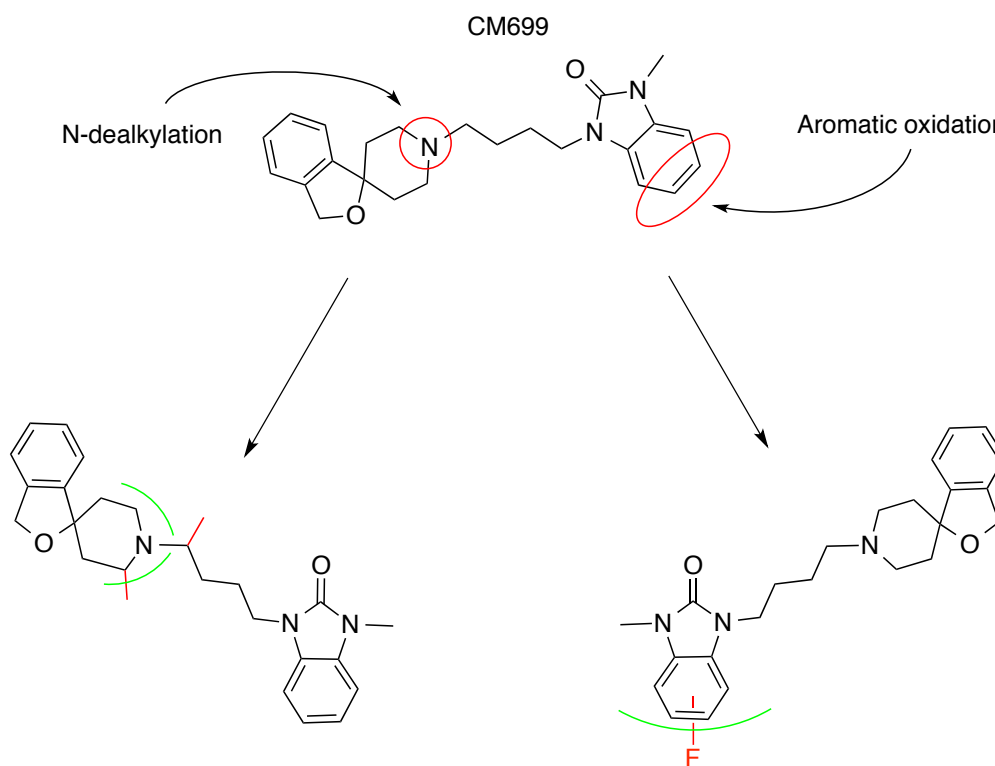


Figure 6.8: CM699 metabolic degradation and possible protection strategy.

Previous work in our laboratory led to develop a remarkable ligand, CM156 (3-(4-(4-cyclohexyl piperazin-1-yl)butyl)benzo[d]thiazole-2(3H)-thione), and this ligand was evaluated

for its affinity for sigma receptors and its anticocaine potency. The results disclosed that it has a high affinity and selectivity for both σ_1 and σ_2 receptors (K_i , $\sigma_1 = 1.28$ nM, $\sigma_2 = 0.64$ nM) over a set of none-sigma binding sites. In addition, it significantly attenuated the cocaine-induced convulsions; however, this compound showed a very short half-life profile. Subsequent work in our laboratory, two approaches was followed to improve the metabolic stability, by blocking the two vulnerable sites, C-6 on the aromatic ring (aromatic oxidation) and the carbon adjacent to the nitrogen of piperazine heterocyclic ring (N-dealkylation)[Fig. 6.9].

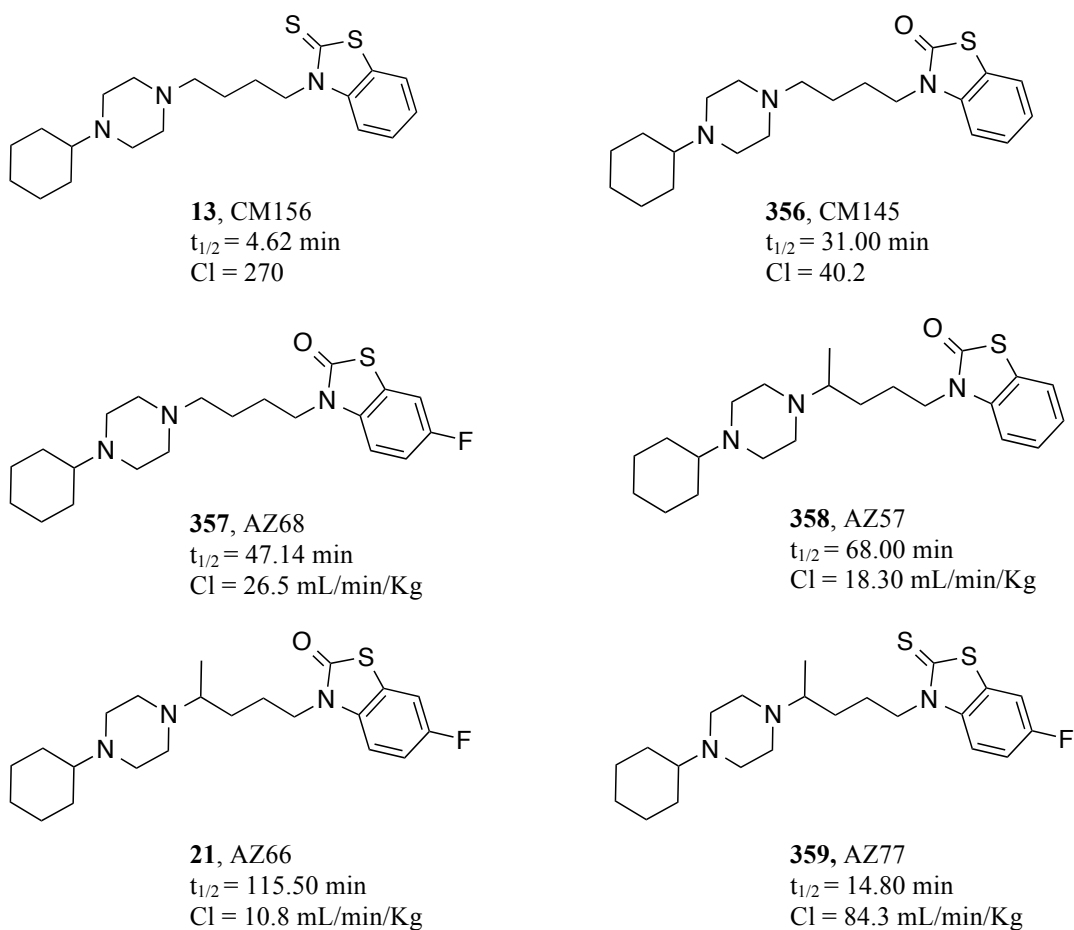


Figure 6.9: Sigma ligands developed in our laboratory and optimized for their metabolic stability.

With that in mind, and in addition to the literature based information that reviewed in the

metabolic stability chapter (Chapter IV), I have synthesized a novel series of CM699 analogs in which I tried to explore different heterocyclic rings in addition to blocking the possible metabolic sites using fluorine and methyl groups to prevent both the aromatic oxidation on the proximal heterocyclic ring and *N*-dealkylation on the carbon adjacent to the basic nitrogen of piperidine ring, respectively. The newly synthesized molecules are summarized in Table 6.6.

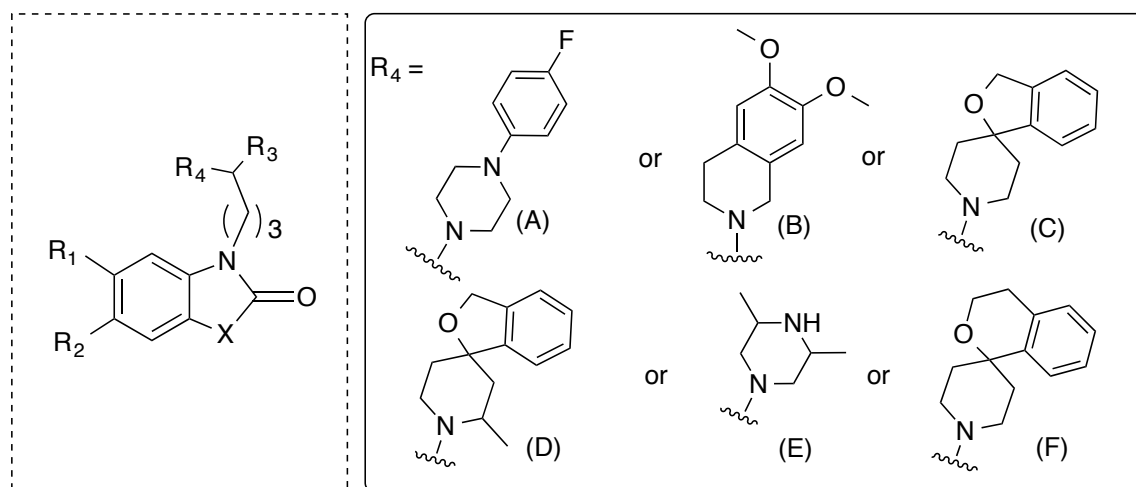


Table 6.4: The newly synthesized CM699 analogs.

| Compd No | NB Entry | R ₁ | R ₂ | R ₃ | R ₄ | X |
|----------|----------|----------------|----------------|-----------------|----------------|------------------|
| 240 | CM699 | H | H | H | C | NCH ₃ |
| 394 | WA153 | H | F | H | E | S |
| 395 | WA157 | H | F | CH ₃ | E | S |
| 396 | WA241 | H | F | H | C | S |
| 397 | WA242 | H | F | CH ₃ | C | S |
| 398 | WA478 | H | F | H | D | S |
| 399 | WA483 | H | H | H | D | O |
| 400 | WA484 | H | H | H | D | S |
| 401 | WA497 | H | F | H | F | S |
| 403 | WA294 | H | H | H | C | NH |
| 423 | WA378 | H | F | H | C | NCH ₃ |
| 424 | WA379 | H | F | H | A | NCH ₃ |
| 425 | WA380 | H | F | H | B | NCH ₃ |
| 426 | WA428 | F | H | H | A | NCH ₃ |
| 427 | WA429 | F | H | H | C | NCH ₃ |
| 428 | WA430 | F | H | H | B | NCH ₃ |
| 429 | WA475 | H | H | H | D | NCH ₃ |
| 430 | WA476 | H | F | H | D | NCH ₃ |
| 431 | WA481 | H | H | CH ₃ | C | NCH ₃ |
| 432 | WA486 | F | H | H | D | NCH ₃ |
| 433 | WA490 | H | F | CH ₃ | C | NCH ₃ |
| 434 | WA491 | F | H | CH ₃ | C | NCH ₃ |

| | | | | | | |
|-----|-------|---|---|-----------------|---|------------------|
| 435 | WA514 | H | H | H | F | NCH ₃ |
| 436 | WA515 | H | H | H | F | O |
| 437 | WA516 | H | F | H | F | NCH ₃ |
| 438 | WA517 | F | H | H | F | NCH ₃ |
| 439 | WA518 | H | H | CH ₃ | F | NCH ₃ |
| 440 | WA519 | F | H | CH ₃ | F | NCH ₃ |
| 441 | WA520 | H | H | H | F | S |
| 442 | WA522 | H | F | CH ₃ | F | NCH ₃ |

6.1.4 Development of new analogs of CM304 (Selective sigma-1 receptor ligand)

CM304, a highly selective sigma-1 receptor ligand, was developed in our laboratory, and was found to have high affinity (0.0025 nM) for sigma-1 receptors and high selectivity (> 145,000 fold) over sigma-2 receptors. Furthermore, the compound was tested by NovaScreen profile, and the results confirmed the great selectivity of CM304 for sigma-1 receptors over the other off-target receptors.⁵³ Such incredible selectivity has the potential to serve as a novel diagnostic tool and could be useful in finding effective treatment as sigma-1 receptors have been correlated with several human cancers, psychiatric conditions, and neurodegenerative diseases. However, preliminary studies have shown that the CM304 has low bioavailability (<1%) and a short half-life (4.2 min in mouse liver microsomes assay and 12.6 minutes in rat liver microsomes assay). This urges the need to develop more analogs by introducing little modifications on the original compound with maintaining the important features for such selectivity. Previous work by Saïd *et al.*²²⁷ with a subsequent extensive SAR studies in our laboratory showed four significant features to maintain the favorable selectivity:

- 1) Azepane ring.
- 2) A two carbon chain linker between benzo[*d*]thiazol-2(3*H*)-one and azepane ring.
- 3) A benzo[*d*]thiazol-2(3*H*)-one heterocycle.
- 4) Alkyl chain at the sixth position of benzo[*d*]thiazol-2(3*H*)-one ring, and the optimum results were obtained from propyl derivatives.

Therefore, based on the aforementioned information and analysis, we synthesized novel derivatives by introducing proton acceptor or donor groups on propyl or ethyl side chain that may enhance the selectivity and overcome the pharmacokinetic issues [Fig. 6.8; 6.9][Tab. 6.7].

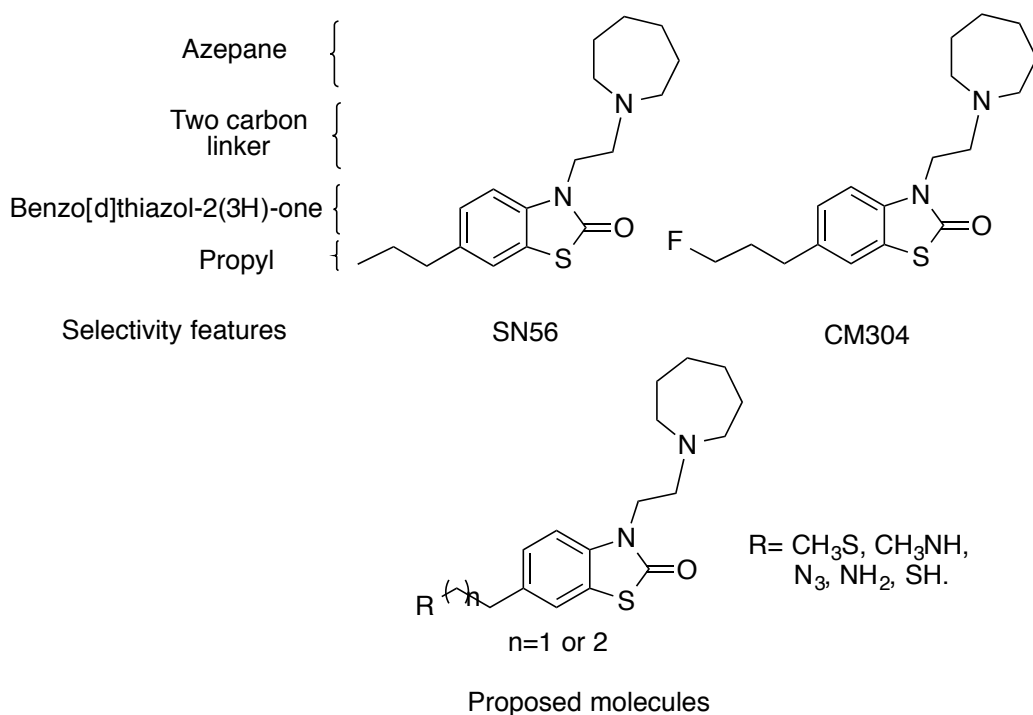


Figure 6.10: The novel CM304

Table 6.5: The newly synthesized CM304 derivatives.

| Compd No | Notebook Entry | n | R |
|----------|----------------|---|------------------|
| 449 | WA325 | 2 | SCH ₃ |
| 450 | WA357 | 1 | SCH ₃ |
| 453 | WA329 | 1 | N ₃ |
| 455 | WA343 | 1 | NH ₂ |
| 454 | WA345 | 2 | N ₃ |
| 456 | WA346 | 2 | NH ₂ |
| 451 | WA353 | 2 | SH |
| 452 | WA354 | 1 | SH |

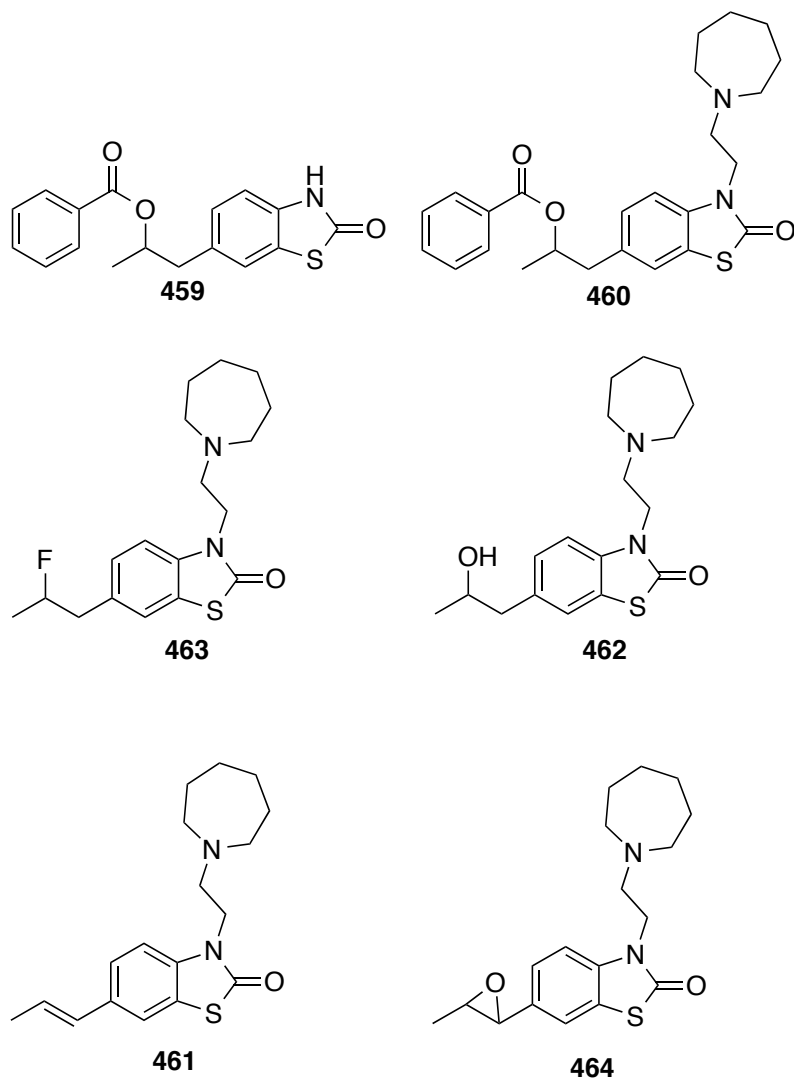


Figure 6.11: More novel CM304 derivatives.

CHAPTER VII: BIOLOGICAL SCREENING, RESULTS AND DISCUSSION

7.1 Biological screening methods

7.1.1 Binding affinity assays

7.1.1.1 Sigma 1 receptor binding (benzofuran series and CM699 analogs)

Frozen whole guinea pig brains (minus cerebellum) were thawed on ice, weighed and homogenized (with a glass and teflon apparatus) in 10 mM Tris-HCl with 0.32 M sucrose pH 7.4 (10 ml/gm tissue). The homogenate was centrifuged at 800 x g for 10 min at 4° C. The supernatant was collected into a clean centrifuge tube the remaining pellet was re-suspended by vortex in 10 ml buffer (tissue) and re-spun at 12,500 x g for 10 min at 4° C. The supernatants were pooled and spun at 28,000 x g for 15 min at 4° C. The supernatant was discarded and the remaining pellet was resuspended at 3ml/gram (original wet weight; O.W.W.) in 10 mM Tris-HCl with 0.32 M sucrose, pH 7.4 and mixed by vortexing. The tissue suspension was incubated at 25° C (water bath) for 15 minutes. The tissue was then re-spun at 28,000 x g for 15 minutes. The supernatant was poured off and the pellet was gently re-suspended in experimental buffer to 80 mg/ml (O.W.W).

Ligand binding experiments were conducted in polypropylene assay tubes containing 0.5 ml of 50 mM Tris-HCl buffer, pH 8.0 for 120 minutes at room temperature. Each tube contained 3 nM [³H] Pentazocine (specific activity 28 Ci/mmol, Perkin Elmer Life Science) and 8.0 mg tissue (O.W.W.). Nonspecific binding was determined using 10 μM haloperidol. Incubations were terminated by rapid filtration through Whatman GF/B filters, presoaked in 0.3% PEI (polyethylenimine), using a Brandel R48 filtering manifold (Brandel Instruments Gaithersburg, Maryland). The filters were washed twice with 5ml cold buffer (10 mM Tris-HCl, pH 8.0) and transferred to scintillation vials. Cytoscint (MP Biomedicals, OH) (3.0ml) was added and the

vials were counted the next day using a Tri Carb 2910 liquid scintillation counter (Perkin Elmer Life Sciences, MA) . Data were analyzed by using GraphPad Prism software (San Diego, CA).

7.1.1.2 Sigma 2 receptor binding (Benzofuran series and CM699 analogs)

Frozen whole guinea pig brains (minus cerebellum) were thawed on ice weighed and homogenized (with a glass and teflon apparatus) in 10 mM Tris-HCl with 0.32 M sucrose pH 7.4 (10 ml/gm tissue). The homogenate was centrifuged at 800 x g for 10 min at 4° C. The supernatant was collected into a clean centrifuge tube the remaining pellet was re-suspended by vortex in 10 ml buffer (tissue) and re-spun at 12,500 x g for 10 min at 4° C. The supernatants were pooled and spun at 28,000 x g for 15 min at 4° C. The supernatant was discarded and the remaining pellet was resuspended at 3ml/gram (original wet weight; O.W.W.) in 10 mM Tris-HCl with 0.32 M sucrose, pH 7.4 and mixed by vortexing. The tissue suspension was incubated at 25° C (water bath) for 15 minutes. The tissue was then re-spun at 28,000 x g for 15 minutes. The supernatant was poured off and the pellet was gently re-suspended in experimental buffer to 80 mg/ml (O.W.W).

Ligand binding experiments were conducted in polypropylene assay tubes containing 0.5 ml of 50 mM Tris-HCl buffer, pH 8.0 for 120 minutes at room temperature. Each tube contained 3 nM [³H] DTG (specific activity 48 Ci/mmol, Perkin Elmer Life Science, MA), 200 nM (+)-pentazocine (Sigma Aldrich, MO) and 8.0 mg tissue (O.W.W.). Nonspecific binding was determined using 100 μM haloperidol. Incubations were terminated by rapid filtration through Whatman GF/B filters, presoaked in 0.3% PEI (polyethylenimine), using a Brandel R48 filtering manifold (Brandel Instruments Gaithersburg, Maryland). The filters were washed twice with 5ml cold buffer (10 mM Tris-HCl, pH 8.0) and transferred to scintillation vials. Cytoscint (MP Biomedicals, OH) (3.0ml) was added and the vials were counted the next day using a Tri

Carb 2910 liquid scintillation counter (Perkin Elmer Life Sciences, MA). Data were analyzed by using GraphPad Prism software (San Diego, CA).

7.1.1.3 Dopamine transporter binding (CM699 analogs)

Brains from male Sprague-Dawley rats weighing 200-225 g (Bioreclamation) were removed, striatum dissected and quickly frozen. Membranes were prepared by homogenizing tissues in 20 volumes (w/v) of ice cold modified sucrose phosphate buffer (0.32M sucrose, 7.74 mM Na₂HPO₄, 2.26 mM NaH₂PO₄, pH adjusted to 7.4) using a Brinkman Polytron (setting 6 for 20 sec.) and centrifuged at 50,000 x g for 10 min at 4°C. The resulting pellet was resuspended in buffer, recentrifuged and resuspended in buffer to a concentration of 10 mg/ml.

Ligand binding experiments were conducted in assay tubes containing 0.5 ml sucrose phosphate buffer for 120 min on ice. Each tube contained 0.5nM [³H] WIN-35428 (specific activity 76 Ci/mmol, PerkinElmer Life Sciences, MA) and 1.0 mg striatal tissue (original wet weight). Nonspecific binding was determined using 0.1 mM cocaine HCl (Sigma). Incubations were terminated by rapid filtration through Whatman GF/B filters, presoaked in 0.05% PEI (polyethyleneimine), using a Brandel R48 filtering manifold (Brandel Instruments Gaithersburg, Maryland). The filters were washed twice with 5ml cold buffer and transferred to scintillation vials. Cytoscint (MP Biomedicals, OH) (3.0ml) was added and the vials were counted the next day using a Perkin Elmer Tri-Carb 2910 liquid scintillation counter (Perkin Elmer Life Sciences, MA). Data were analyzed by using GraphPad Prism software (San Diego, CA).

7.1.1.4 Radioligand binding assays. (For isothiocyanate derivatives)

The assays were performed using rat liver homogenates using previously published procedures.²³ Sigma-1 receptors were labeled with 5 nM [³H](+)-pentazocine. Sigma-2 receptors were labeled with 3 nM [³H]DTG in the presence of 100 nM (+)-pentazocine to block sigma-1

receptors. Nonspecific binding was determined in the presence of 10 μ M Haloperidol. K_i values were determined using GraphPad Prism software (San Diego, CA).

7.1.2. Irreversible binding assays (Treatment of membranes with isothiocyanates)

Membranes were incubated with the various isothiocyanates at concentrations of 100nM or 1 μ M for 60 min at R.T. in 20 mM Hepes, pH 7.4 at a protein concentration of 0.30 mg/ml. The preparation was then diluted to a protein concentration of 0.018 mg/ml with buffer and centrifuged at 37,000 \times g for 10 min. The pellet was resuspended to the original volume with buffer and centrifuged again. Following resuspension to the original volume with 20 mM Hepes pH 7.4 the preparation was allowed to incubate for 60 min at R.T. to allow for dissociation of noncovalently bound isothiocyanate. The protein preparation was then subjected to centrifugation at 37,000 \times g for 10 min and resuspended to a protein concentration of 0.6 mg/ml and used directly in the radioligand assay described above. The control membranes were treated in the identical manner without exposure to the isothiocyanate. This washout method was shown to effect complete dissociation of 500 nM SN-79 from sigma receptors.

7.1.3. Metabolic stability study (CM699 analogs)

Metabolic stability of the synthesized molecules (5 μ M) was performed in Tris buffer (50 mM, pH 7.4) with Human, Rat and Mouse liver microsomes at 37 $^{\circ}$ C in 1 mL of incubation mixture. The incubation mixture composed of Tris buffer (50 mM, pH 7.4), liver microsomes (1 mg/mL) and regenerating system. The reactions were started by the addition of regenerating system and were terminated at predetermined time points by the addition of equal volume of acetonitrile. Zero time incubations served as a 100% value. The samples were then centrifuged and the supernatant was injected on to UPLC.

7.2 SAR Study results and discussion

7.2.1 Benzofuran series

The binding affinities of benzofuran analogs towards sigma receptors are illustrated in Tab. 7.1. Interestingly, most of the compounds have displayed good affinity for both sigma subtypes.

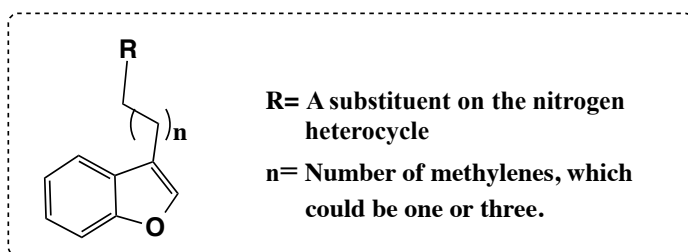
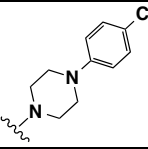
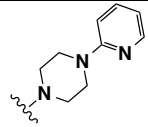
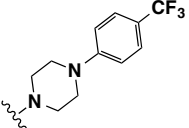
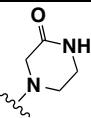
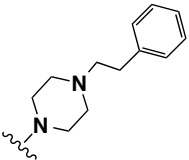
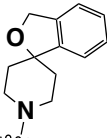
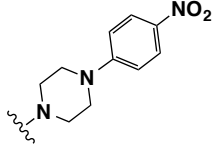
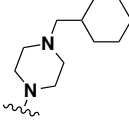
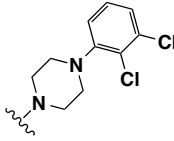
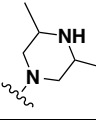
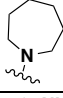
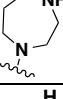

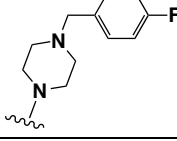
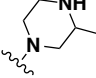
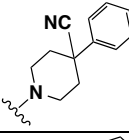
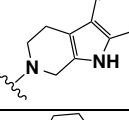
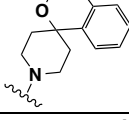
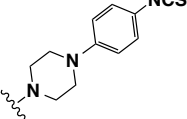


Table 7.1. Sigma receptors binding affinities.

| Compd. No | Notebook Entry | n "Number of methylenes" | R "Different substituents on basic nitrogen" | $\sigma 1$ Ki \pm SEM (nM) | $\sigma 2$ Ki \pm SEM (nM) |
|-----------|----------------|-----------------------------|---|---------------------------------|---------------------------------|
| 256 | WA184 | 1 |  | 28.7 (25.5-32.3) | 121 (90.2-163) |
| 257 | WA193 | 1 |  | 167 (147-190) | 1070 (790-1,450) |
| 269 | WA196 | 1 |  | 87.6 (77.1-99.5) | 593 (452-779) |
| 270 | WA199 | 1 |  | 17,000 (12,600-22,900) | 34,400 (20,700-57,200) |
| 272 | WA205 | 1 |  | 0.739 (0.645-0.846) | 6.95 (4.33-11.1) |
| 273 | WA207 | 1 |  | 5.47 (4.86-6.16) | 8.11 (4.11-16.0) |

| | | | | | |
|-----|-------|---|---|------------------------|------------------------|
| 274 | WA210 | 1 |  | 2,990 (2,510-3,550) | 2,456 (1,870-3,230) |
| 278 | WA214 | 3 |  | 2.15 (1.85-2.49) | 6.71 (4.32-10.4) |
| 280 | WA216 | 3 |  | 48.5 (41.8-56.1) | 514 (412-640) |
| 284 | WA221 | 3 |  | 58.9 (52.9-65.6) | 872 (732-1,040) |
| 285 | WA222 | 3 |  | 0.485 (0.426-0.554) | 8.22 (5.17-13.1) |
| 286 | WA223 | 3 |  | 25.1 (22.8-27.5) | 398 (323-491) |
| 287 | WA224 | 3 |  | 49.1 (43.2-55.8) | 3,590 (2,560-5,040) |
| 288 | WA225 | 3 |  | 3.90 (3.39-4.50) | 32.9 (23.9-45.2) |
| 293 | WA231 | 3 |  | 17.1 (15.1-19.3) | 494 (327-745) |
| 294 | WA232 | 3 |  | 1.71 (1.42-2.07) | 14.3 (11.1-18.3) |
| 295 | WA240 | 3 |  | 192 (176-210) | 193 (148-251) |
| 297 | WA496 | 3 |  | 3.40 (3.07-3.78) | 6.25 (5.07-7.71) |
| 349 | WA255 | 3 |  | 125 ± 51 | 176 ± 22 |

[Inhibition of the binding of radioligands labeling sigma-1 and sigma-2 receptors]. Sigma receptors affinities (K_i in nM) were determined in guinea pig brain homogenates. Sigma-1 receptors were labeled with [^3H](+)-pentazocine.

Sigma-2 receptors were labeled with [³H]DTG in the presence of (+)-pentazocine to block sigma-1 receptors. Nonspecific binding was determined in the presence of haloperidol.

The un-substituted piperazine ring in 1-(4-(benzofuran-3-yl)butyl)piperazine (**287**), showed the best affinity and selectivity towards sigma-1 receptor, among the other tested piperazine derivatives illustrated in [Tab. 7.2], with 73 σ -2/ σ -1 selectivity ratio. The 3,5-dimethyl piperazine derivative (**284**) showed the least selectivity with 15 σ -2/ σ -1 selectivity ratio as can be seen in [Tab. 7.2].

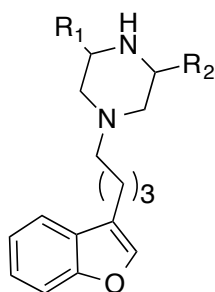


Table 7.2: Sigma receptors binding affinities for the piperazine derivatives

| Compound | R ₁ | R ₂ | σ_1 | σ_2 | σ_2/σ_1 ratio selectivity |
|----------|-----------------|-----------------|------------------|---------------------|---|
| A 284 | CH ₃ | CH ₃ | 58.9 (52.9-65.6) | 872 (732-1,040) | 14.8 |
| 287 | H | H | 49.1 (43.2-55.8) | 3,590 (2,560-5,040) | 73 |
| 293 | H | CH ₃ | 17.1 (15.1-19.3) | 494 (327-745) | 29 |

Also, the ring size expansion in the homopiperazine derivative (**286**) showed preference for sigma-1 over sigma-2; however, increasing the size of the ring has reduced the selectivity from 73 to 16 σ -2/ σ -1 selectivity ratio compared to the piperazine motif in compound (**287**). Replacing the homopiperazine in compound (**286**) with azepane ring (**285**) gave better affinity with the same σ -2/ σ -1 selectivity ratio, 17 [Tab. 7.3].

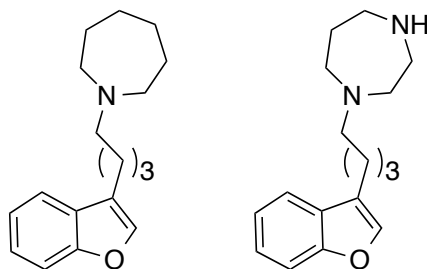


Table 7.3. Sigma receptors binding affinities for the piperazine derivatives

| Compound | σ_1 | σ_2 | σ_2/σ_1 ratio selectivity |
|----------|------------------------|---------------------|---|
| 285 | 0.485 (0.426-0.554) | 8.22 (5.17-13.1) | 17 |
| 286 | 25.1 (22.8-27.5) | 398 (323-491) | 16 |

Surprisingly, introducing a ketone group on position 3 or 5 of the piperazine ring in derivative (**270**) with two-carbon space linker significantly reduced the affinity for both sigma receptors subtypes. [Tab. 7.4]

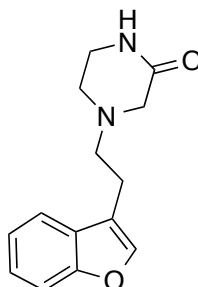


Table 7.4. Sigma receptors binding affinity for the piperazine-2-one derivatives

| Compound | σ_1 | σ_2 |
|----------|---------------------------|---------------------------|
| 270 | 17,000 (12,600-22,900) | 34,400 (20,700-57,200) |

The spiro-substituted compounds (**273**) and (**297**) showed good affinity towards both sigma subtypes, and the carbon space linker between the two heterocycle rings seems to have no effect on the selectivity [Tab. 7.5].

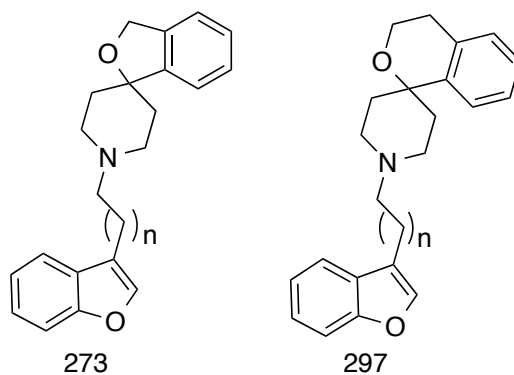


Table 7.5. Sigma receptors binding affinities for the spiro-derivatives

| Compound | n | σ_1 | σ_2 |
|----------|---|---------------------|---------------------|
| 273 | 1 | 5.47 (4.86-6.16) | 8.11 (4.11-16.0) |
| 297 | 3 | 3.40 (3.07-3.78) | 6.25 (5.07-7.71) |

The phenylpiperazine derivatives showed good affinity with some preference for sigma-1 over sigma-2. So far, most of the tested ligands have exhibited good affinity for both sigma receptors. Unfortunately, the binding affinities for the rest of the series toward sigma receptor subtypes have not been completed. Therefore, to build a clear structure affinity relationship (SAfiR), we have to get all the designed molecules tested for their affinity against sigma receptors.

7.2.2 1,3-dihydro-2H-benzo[d]imidazol-2-one and benzo[d]oxazol-2(3H)-one derivatives

This series of compounds was derived from the previously developed sigma-2 compounds that showed preference for sigma-2 over sigma-1. Surprisingly, all of the synthesized molecules retained comparable affinity and preference/selectivity toward sigma-2 receptors. The best results were obtained from compounds (**335**), and (**322**) that exhibited good affinity and selectivity towards sigma-2 with σ_1/σ_2 selectivity ratio of 734 and 472, respectively as described in [Tab. 7.6].

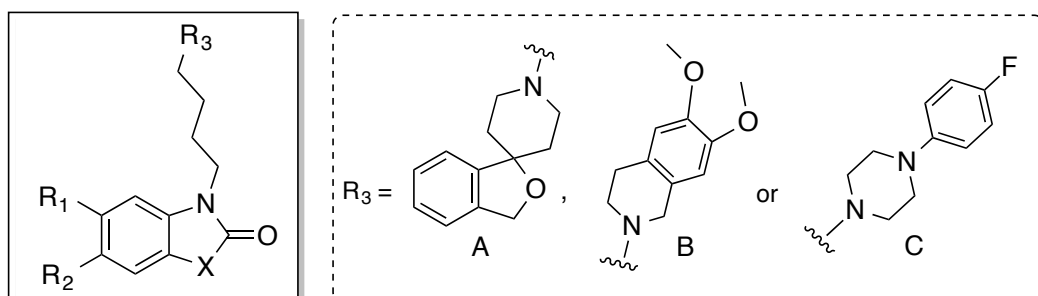


Table 7.6: Sigma receptors binding affinities for 1,3-dihydro-2*H*-benzo[*d*]imidazol-2-one and benzo[*d*]oxazol-2(3*H*)-one derivatives.

| Compd. No | Notebook Entry | R ₁ | R ₂ | X | R ₃ | σ ₁ Ki(nM) | σ ₂ Ki(nM) | σ ₁ /σ ₂ ratio selectivity |
|-----------|----------------|-----------------|----------------|--|----------------|---------------------------|-----------------------|--|
| 319 | WA248 | NO ₂ | H | NCH ₃ | B | 149 (135-164) | 5.32 (3.86-7.34) | 28 |
| 321 | WA262 | NO ₂ | H | N(CH ₂) ₂ CH ₃ | C | 18.3 (16.5-20.3) | 4.22 (3.21-5.56) | 4.33 |
| 322 | WA266 | NO ₂ | H | N(CH ₂) ₄ CH ₃ | B | 1,410 (1,250-1,600) | 2.99 (2.08-4.24) | 471.6 |
| 323 | WA267 | NO ₂ | H | N(CH ₂) ₄ CH ₃ | A | 24.7 (21.4-28.5) | 5.67 (4.32-7.45) | 4.4 |
| 324 | WA303 | NO ₂ | H | N(CH ₂) ₂ CH ₃ | A | 13.3 (12.2-14.6) | 3.81 (2.95-4.92) | 3.5 |
| 325 | WA334 | NO ₂ | H | N(CH ₂) ₂ CH ₃ | B | 85.1 (76.8-94.4) | 3.40 (2.43-4.78) | 25 |
| 326 | WA336 | NO ₂ | H | N(CH ₂) ₄ CH ₃ | C | 447 (402-497) | 4.16 (2.98-5.80) | 107.5 |
| 329 | WA249 | NH ₂ | H | NCH ₃ | B | 9,360 (6,960-12,600) | 61.9 (42.6-90.0) | 151.2 |
| 330 | WA257 | NH ₂ | H | NCH ₃ | A | 257 (229-288) | 15.0 (12.0-18.9) | 17 |
| 331 | WA263 | NH ₂ | H | N(CH ₂) ₂ CH ₃ | C | 147 (130-165) | 81.3 (63.6-104) | 2 |
| 332 | WA268 | NH ₂ | H | N(CH ₂) ₄ CH ₃ | A | 280 (241-325) | 11.5 (9.28-14.3) | 24.4 |
| 333 | WA300 | NH ₂ | H | N(CH ₂) ₄ CH ₃ | B | 2,710 (2,170-3,390) | 15.3 (12.1-19.4) | 177 |
| 334 | WA304 | NH ₂ | H | N(CH ₂) ₂ CH ₃ | A | 252 (223-284) | 11.8 (9.66-14.3) | 21.3 |
| 335 | WA337 | NH ₂ | H | N(CH ₂) ₂ CH ₃ | B | 21,200 (10,500-42,600) | 28.9 (23.1-36.0) | 733.6 |
| 336 | WA338 | NH ₂ | H | N(CH ₂) ₂ CH ₃ | C | 1,880 (1,560-2,250) | 34.2 (28.1-41.6) | 55 |
| 356 | WA365 | H | H | NH | C | 65.8 (59.3-73.0) | 22.7 (17.3-29.7) | 3 |
| 357 | WA367 | H | H | NPh ₄ -NO ₂ | C | 246 (205-295) | 5.67 (4.32-7.45) | 43.4 |
| 359 | WA371 | H | H | NPh ₄ -NH ₂ | C | 4,010 (3,410-4,710) | 38.4 (30.6-48.3) | 104.5 |
| 364 | WA394 | NO ₂ | H | O | C | 44.0 (38.3-50.5) | 11.9 (9.78-14.5) | 3.7 |

Sigma receptors binding affinities. [Inhibition of the binding of radioligands labeling sigma-1 and sigma-2 receptors]. Sigma receptors affinities (K_i in nM) were determined in guinea pig brain homogenates. Sigma-1 receptors were labeled with [^3H](+)-pentazocine. Sigma-2 receptors were labeled with [^3H]DTG in the presence of (+)-pentazocine to block sigma-1 receptors. Nonspecific binding was determined in the presence of haloperidol.

From the above illustrated results, it is important to notice that compounds with the 6,7-dimethoxy-1,2,3,4-tetrahydroisoquinoline motif have the best affinity toward sigma-2 receptors, and compounds with the 1-(4-fluorophenyl)piperazine motif come next to the isoquinoline derivatives in their preference towards sigma-2 receptors. Alternatively, compounds that bearing the 3*H*-spiro[isobenzofuran-1,4'-piperidine] motif displayed an excellent affinity towards both subtypes.

Additionally, the length of the substitutions (propyl, pentyl, or para-substituted phenyl) on the nitrogen number one of benzoimidazolone moiety, appears to play a part of sigma-2 receptor preference.

7.3. Binding affinity and irreversible binding of isothiocyanate derivatives

Irreversible binding is one of the most useful approaches that has been developed for receptor antagonists that may bind covalently to a receptor. We have found incorporation of isothiocyanate moiety to our previous selective sigma-2 compounds resulted in producing electrophilic center that can bind covalently to the sigma-2 receptor's nucleophilic site, which in turn will block the receptor if the compound is an antagonist or act as functional antagonism if the compound is an agonist. To accomplish this goal, high affinity sigma-2 ligands developed in our laboratory were utilized in the design and synthesis a novel series of isothiocyanate compounds [table 7.7]

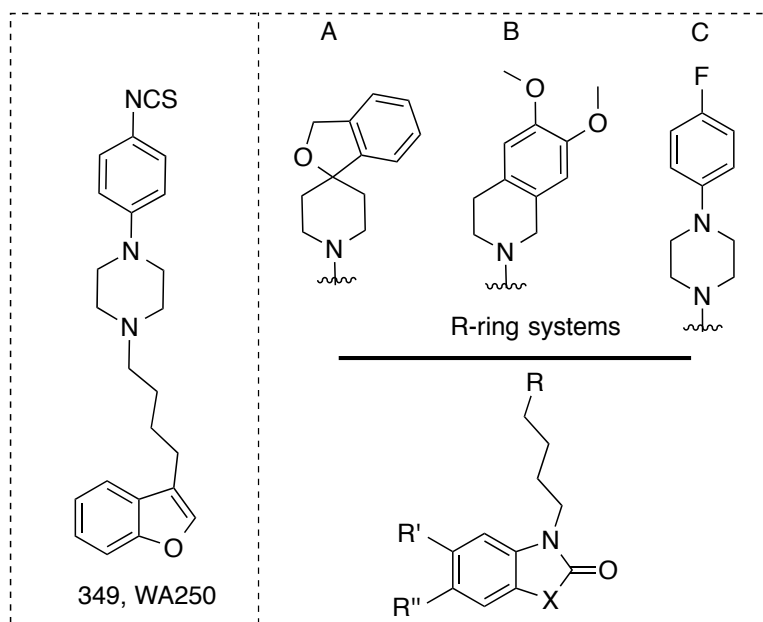


Table 7.7: Sigma receptor binding affinities and selectivity ratios.

| Compd. No | Notebook Entry | R' | R'' | X | R | σ_1 Ki(nM) | σ_2 Ki(nM) | σ_1/σ_2 ratio selectivity |
|-----------|----------------|-------|-----|--|-----|-------------------|-------------------|---------------------------------------|
| 339 | WA250 | NCS | H | NCH ₃ | B | 1225±145 | 322± 6 | 3.8 |
| 340 | WA258 | NCS | H | NCH ₃ | A | 1502±86 | 1548±60 | 0.97 |
| 341 | WA264 | NCS | H | N(CH ₂) ₂ CH ₃ | C | 373±37 | 320± 34 | 1.2 |
| 342 | WA269 | NCS | H | N(CH ₂) ₄ CH ₃ | B | 794±44 | 90± 4 | 8.8 |
| 343 | WA306 | NCS | H | N(CH ₂) ₂ CH ₃ | B | 542±18 | 377 ±41 | 1.4 |
| 344 | WA349 | NCS | H | N(CH ₂) ₄ CH ₃ | C | 795643±4843 | 314.2±7.8 | 2533 |
| 345 | WA350 | NCS | H | N(CH ₂) ₄ CH ₃ | B | 2231±202 | 111± 9 | 20.1 |
| 346 | WA352 | NCS | H | N(CH ₂) ₂ CH ₃ | B | 1170±116 | 216± 12 | 5.4 |
| 349 | WA255 | ----- | --- | ----- | --- | 125± 51 | 176 ± 22 | 0.7 |
| 360 | WA372 | H | H | NPh4-NCS | C | 434±119 | 349 ± 2 | 1.2 |

Affinities (Ki in nM) were determined in rat liver homogenates. Sigma-1 receptors were labeled with [³H](+)-pentazocine. Sigma-2 receptors were labeled with [³H]DTG in the presence of (+)-pentazocine to block sigma-1 receptors. Nonspecific binding was determined in the presence of haloperidol. The values in this table represent the mean ± SEM from replicate assays.

In order to perform the irreversible binding assays, the isothiocyanate derivatives have been evaluated first for their binding affinity against both sigma subtypes, as illustrated in [Tab. 7.7]. Some of these compounds showed good preference for sigma-2 receptors and mainly (**342**), (**344**), (**345**), and (**346**). For a ligand to have a good irreversible binding it must demonstrate good binding affinity so it must have the opportunity to bind covalently at the targeted protein, which is sigma-2 receptor in this case. However, we have conducted the irreversible binding assays for

all the isothiocyanate molecules listed in [Tab. 7.7]. The results of the irreversible binding assays described in the following figures. Fig. 7.1 shows the irreversible binding at sigma-1 receptors, and Fig. 7.2 demonstrates the irreversible binding at sigma-2 receptors.

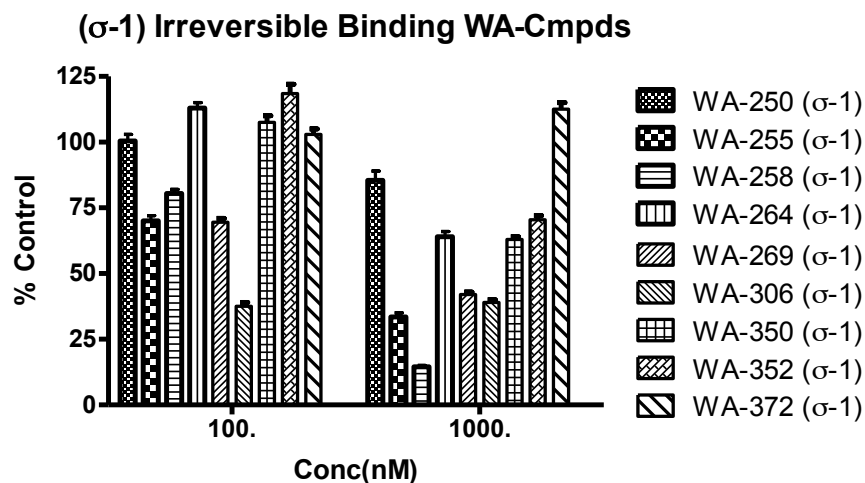


Figure 7.1: Irreversible binding at sigma-1. σ -1 binding remaining after pretreatment of membranes with isothiocyanates at 100 nM and 1 μ M and subsequent washout procedure. Binding is compared to control membranes with no exposure to isothiocyanate but subjected to same washout procedure. Values are expressed as the percent binding remaining relative to control not treated with irreversible ligand but subjected to identical conditions. Control binding for [3 H](+)-pentazocine was $1,633 \pm 127$ dpm.

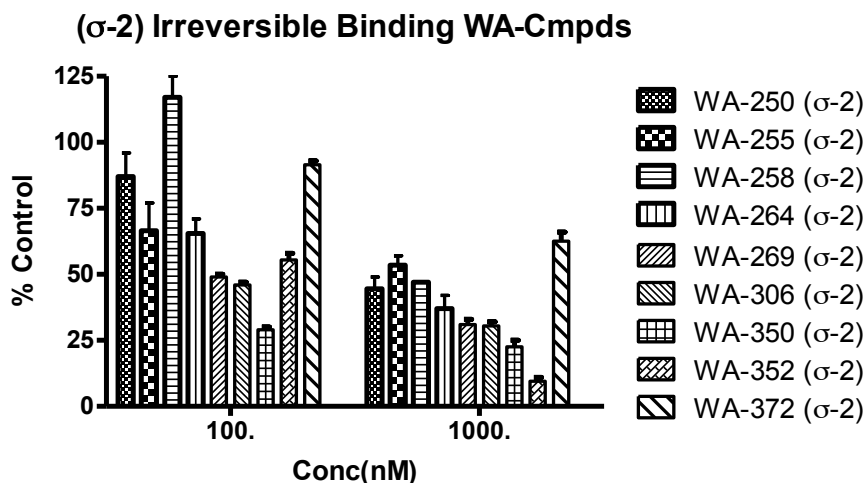


Figure 7.2: Irreversible binding at sigma-2. σ -2 binding remaining after pretreatment of membranes with isothiocyanates at 100 nM and 1 μ M and subsequent washout procedure. Binding is compared to control membrane with no exposure to isothiocyanate but subjected to same washout procedure. Values are expressed as the percent binding remaining relative to control not treated with irreversible ligand but subjected to identical conditions. Control binding for [3 H]DTG was $7,138 \pm 301$ dpm. WA-350 & WA-352 bind irreversibly to σ -2 receptor while the others do not show statistically significant results.

It is obvious from the above figures that the isothiocyanate compounds have little effect on sigma-1 receptors compared to their binding at sigma-2 receptors; however, here we were interested in those compounds that have the most selectivity ones towards sigma-2 receptors. Among the tested compounds, **345 (WA350)**, and **346 (WA352)** showed a significant binding (covalently) at sigma-2 receptors with no or a little binding (Covalently) at sigma-1 receptors. Interestingly, compound **345 (WA350)**, showed higher affinity and selectivity for sigma-2 over sigma-1(covalently).

Compound **344 (WA349)** showed excellent binding affinity towards sigma-2 over sigma-1 with 2533 σ -1/ σ -2 selectivity ratio. We are currently awaiting the completion of this series of compounds in irreversible binding assays, a long with the others, and will include them in a future publication.

7.4 The novel CM699 analogs

The CM699 derivatives were synthesized and their affinities toward sigma receptors and dopamine transporters were measured using radioligand binding assays as previously described in Tab. 7.8. Several compounds retained comparable affinity towards sigma receptors and dopamine transporters (DAT). These compounds screened include: **362 (WA241)**, **365 (WA378)**, **369 (WA429)**, **371 (WA475)**, **372 (WA476)**, **373 (WA478)**, **376 (WA484)**, and **377 (WA486)**. Among these compounds, **365 (WA378)** had affinities of 5.70, 0.967, and 203 nM at sigma-1 receptors, sigma-2 receptors, and DAT, respectively, and **373 (WA478)** had affinities of 7.96, 10.4, and 328 nM at sigma-1 receptors, sigma-2 receptors, and DAT, respectively while CM699 had affinities of 14.0, 2.30 and 318 nM at the same respective sites.

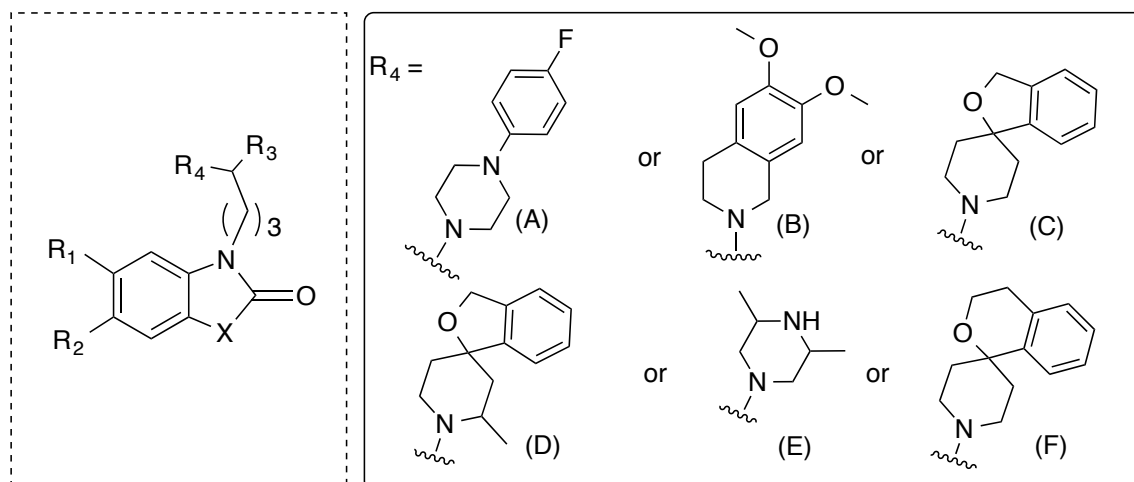


Table 7.8: The newly synthesized CM699 analogs.

| Comp No | NB Entry | R ₁ | R ₂ | R ₃ | R ₄ | X | DAT K _i ± SEM (nM) | Sigma-1 K _i ± SEM (nM) | Sigma-2 K _i ± SEM (nM) |
|---------|----------|----------------|----------------|-----------------|----------------|------------------|----------------------------------|--------------------------------------|--------------------------------------|
| 240 | CM699 | H | H | H | C | NCH ₃ | 318 (290-350) | 14.0 (11.1-17.7) | 2.30 (1.37-3.88) |
| 360 | WA153 | H | F | H | E | S | NA | NA | NA |
| 361 | WA157 | H | F | CH ₃ | E | S | NA | NA | NA |
| 362 | WA241 | H | F | H | C | S | 301 (242-375) | 2.18 (1.58-3.01) | 0.667 (0.415-1.07) |
| 363 | WA242 | H | F | CH ₃ | C | S | 1,250 (1030-1520) | 3.92 (3.16-4.85) | 2.58 (1.16-5.76) |
| 364 | WA294 | H | H | H | C | NH | 1570 (1,390-1,770) | 18.0 (16.4-19.8) | 10.9 (7.66-15.5) |
| 365 | WA378 | H | F | H | C | NCH ₃ | 203 (187-221) | 5.70 (4.98-6.52) | 0.967 (0.7491-2.5) |
| 366 | WA379 | H | F | H | A | NCH ₃ | 38.7 (33.9-44.2) | 2.33 (1.83-2.95) | 5,770 (4,780-6,960) |
| 367 | WA380 | H | F | H | B | NCH ₃ | 10,500 (8,550-12,900) | 339 (307-375) | 1.69 (1.35-2.11) |
| 368 | WA428 | F | H | H | A | NCH ₃ | 3,940 (2980-5210) | 46.1 (31.8-66.8) | 2.90 (1.78-4.72) |
| 369 | WA429 | F | H | H | C | NCH ₃ | 336(266-424) | 7.28 (5.97-8.87) | 1.48 (0.759-2.84) |
| 370 | WA430 | F | H | H | B | NCH ₃ | 4,810 (3490-6630) | 243 (216-273) | 5.44 (3.56-8.32) |
| 371 | WA475 | H | H | H | D | NCH ₃ | 342 ± 42.8 | 51.0 ± 0.738 | 8.01 (5.56-11.5) |
| 372 | WA476 | H | F | H | D | NCH ₃ | 414 (370-464) | 24.3 (22.8-26.9) | 4.93 (3.41-7.12) |
| 373 | WA478 | H | F | H | D | S | 328 ± 24.9 | 7.96 ± 1.18 | 10.4 (8.01-13.6) |
| 374 | WA481 | H | H | CH ₃ | C | NCH ₃ | 2,610 ± 90.5 | 17.9 ± 1.48 | 2.02 (1.42-2.88) |
| 375 | WA483 | H | H | H | D | O | 1,210 ± 144 | 7.88 ± 0.532 | 9.19 (4.17-20.3) |
| 376 | WA484 | H | H | H | D | S | 390 ± 52.6 | 10.0 ± 0.792 | 5.26 (3.86-7.17) |
| 377 | WA486 | F | H | H | D | NCH ₃ | 475 ± 37.3 | 22.8 ± 0.831 | 6.26 (4.31-9.08) |
| 378 | WA490 | H | F | CH ₃ | C | NCH ₃ | 1,460 ± 177 | 12.1 ± 1.62 | 1.83 (1.35-2.48) |
| 379 | WA491 | F | H | CH ₃ | C | NCH ₃ | 1,590 (1,390-1,810) | 8.31 (7.55-9.15) | 0.781 (0.500-1.22) |
| 297 | WA496 | --- | --- | --- | F | --- | 873 (749-1020) | 3.4 (3.07-3.78) | 6.25 (5.07-7.71) |
| 380 | WA497 | H | F | H | F | S | NA | NA | NA |

Table 7.8: Sigma receptors and dopamine transporter binding affinities. [Inhibition of the binding of radioligands labeling dopamine transporter, sigma-1 and sigma-2 receptors].

Sigma receptors affinities (K_i in nM) were determined in guinea pig brain homogenates. Sigma-1 receptors were labeled with [³H](+)-pentazocine. Sigma-2 receptors were labeled with [³H]DTG in the presence of (+)-pentazocine to block sigma-1 receptors. Nonspecific binding was determined in the presence of haloperidol. DAT affinities (K_i in nM) were determined in rat brain homogenates. DAT were labeled with [³H] WIN 35428. Nonspecific binding was determined in the presence of cocaine HCl. [Values in parentheses are 95% confidence limits].

From the obtained results, we can conclude that:

1. Introducing the methyl group adjacent to the piperidine ring on the carbon of butyl linker significantly decreased the DAT affinity.
2. However; introduction of the methyl group on the carbon of the piperidine ring and adjacent to basic nitrogen has retained the affinity toward sigma receptors and DAT.
3. Also, insertion of the fluorine atom at position 6 of the heterocyclic ring showed some preference towards sigma receptors and DAT, while insertion it at position 5 decreased the affinity towards DAT, and with a little effect on sigma receptors.
4. Both benzothiazolone and benzoimidazolone rings have shown good affinity towards sigma receptors and DAT.

The next step was to screen the compounds that retained the affinity towards sigma receptors and DAT, for their stability in liver microsome assays. So far, we have tested three of these compounds in human, rat, and mouse liver microsomes. All of the three analogs showed superior metabolic stability to CM699 as described in Fig. 7.3, and Fig. 7.4.

***In vitro* half-life and CL_{int}:** The percent of the parent compound remaining was plotted *versus* time. The slope of the line gave the rate constant *k* for the disappearance of parent compound, from which an *in vitro* *t*_{1/2} can be calculated. CL_{int} can be calculated using the following formula:

$$CL_{int} = k \text{ (min}^{-1}\text{)} \times [V]/[P] = (\text{L/mg} \times \text{min})$$

[V] is the incubation volume in μl and [P] is the amount of microsomal protein in mg in the incubation.

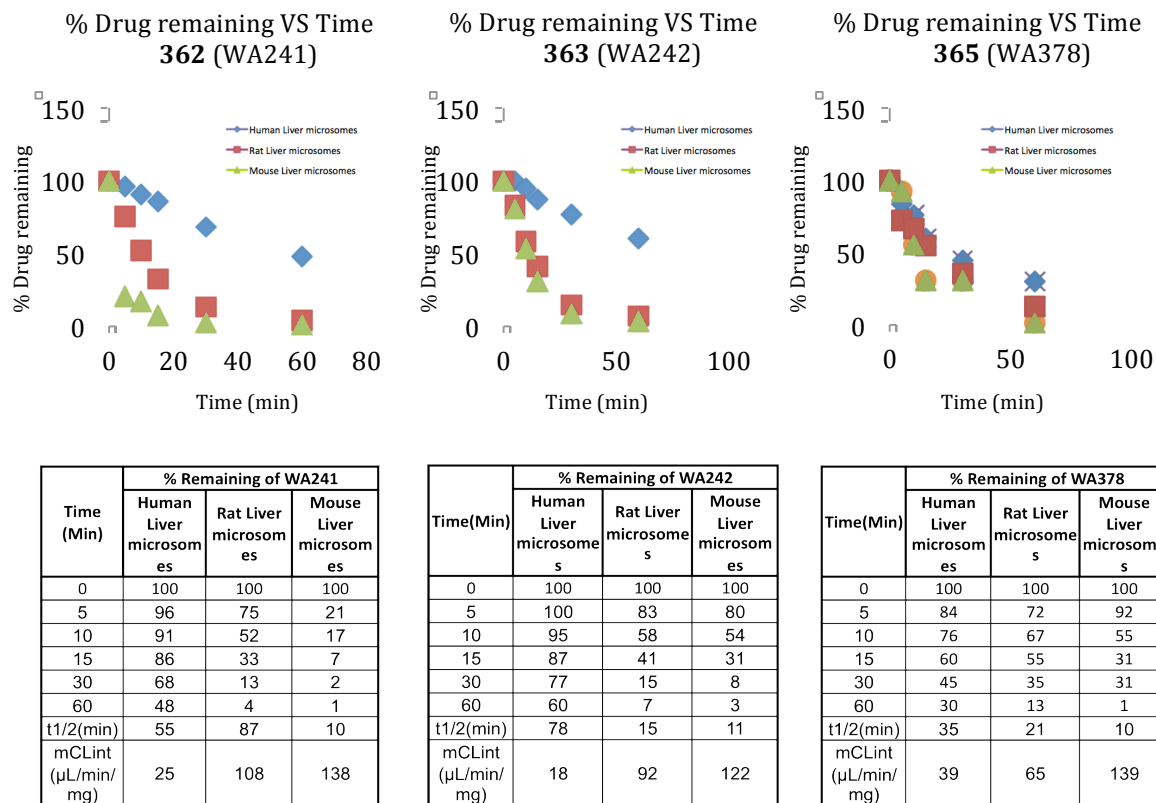


Figure 7.3: Metabolic stability results of some CM699 analogs (362, 363, and 365) in human, rat, and mouse liver microsomes

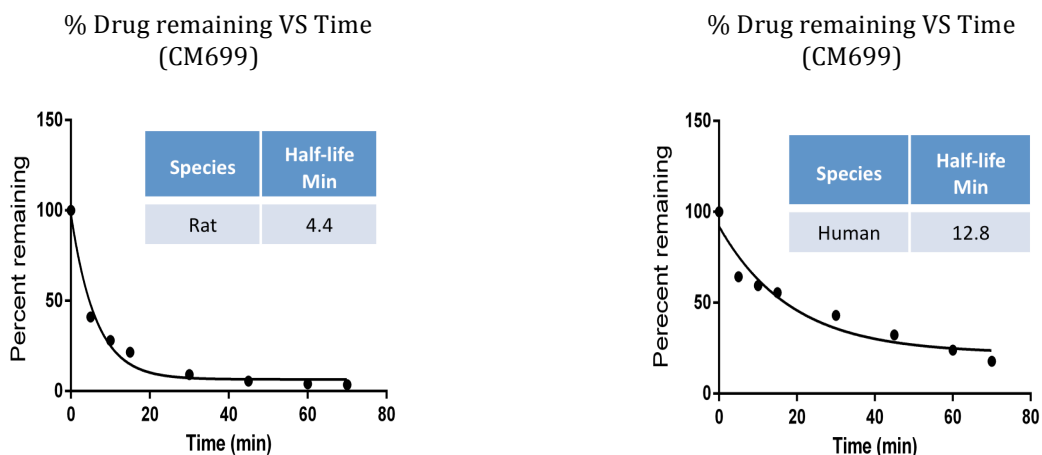


Figure 7.4: Metabolic stability results of CM699 in human, and rat liver microsomes

Interestingly, compound **363** (WA242) that was protected from aromatic oxidation on the

benzothiazolone ring and also from the N-dealkylation at the carbon adjacent to the piperidine ring, showed the longest half-life among the tested analogs, which was 78 minutes in human liver microsomes.

These results validate our approach towards improving the metabolic stability by blocking the vulnerable sites on CM699. Subsequently, the revealed results suggest that the developed compounds may be useful as a pharmacological tool in developing new treatments for stimulant abuse (cocaine or methamphetamine), and this approach could be a turning point in the development of medications to treat drug addiction.

7.5 Novel CM304 analogs

A series of CM304 analogs have been synthesized and characterized and their affinities toward sigma receptor subtypes have not been completed. However, the overall design was to reduce the lipophilicity of CM304 in order to enhance its pharmacokinetic profile.

CHAPTER VIII. CHEMICAL SYNTHESIS OF SIGMA RECEPTOR ANALOGUES

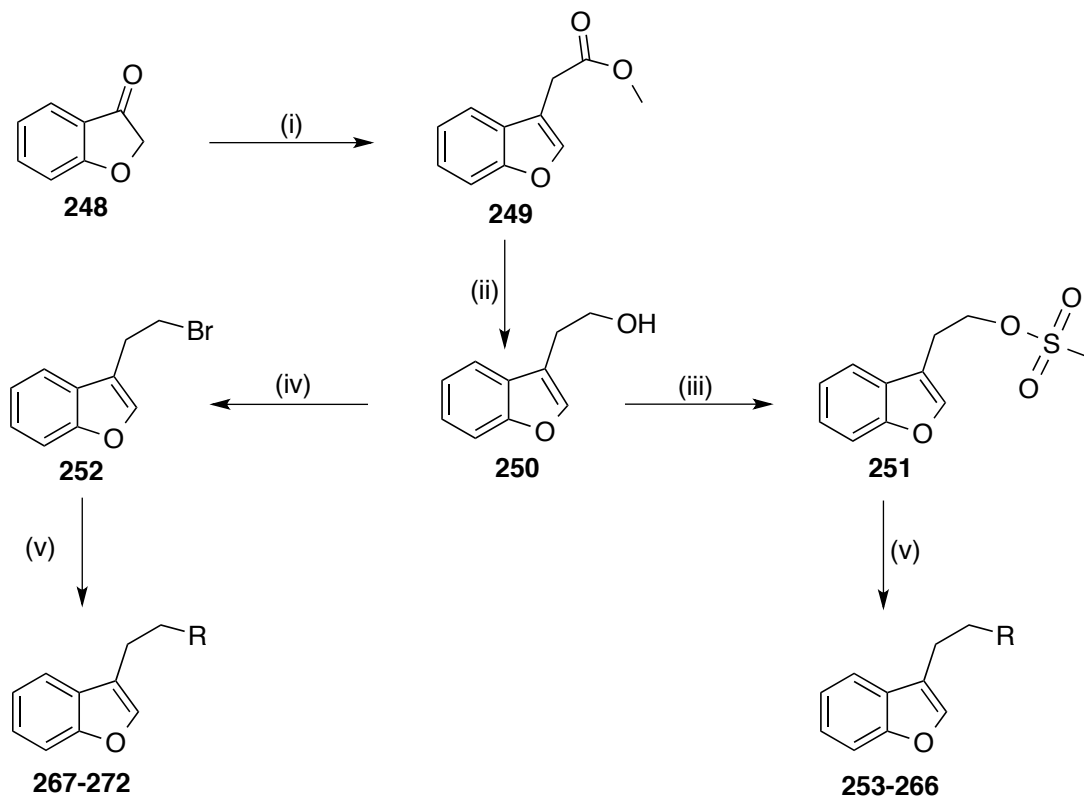
8.1 Synthesis of a Benzofuran-3-yl Series

The approach that I followed in the synthesis of these compounds includes two groups of compounds. One group has two-space linker, and the other one has four-space linker between the benzofuran heterocyclic ring and other appropriate heterocyclic moieties. The space linker length was chosen based on previous work in our laboratory that indicated the preference of two carbon linkers for sigma-1 receptors, and the four-carbon linkers for sigma-2 receptors.

The commercially available 3-coumaranone (**248**) was subjected to a Horner–Wadsworth–Emmons reaction, using sodium hydride and trimethylphosphoacetate in THF at 0 °C to afford the methyl acetate (**249**), which in turn reduced to the primary alcohol (**250**) using lithium aluminium hydride in THF at 0 °C. Compound (**250**) was either treated with methanesulfonyl chloride to obtain the mesylate (**251**) or subjected to Appel reaction to give compound (**252**) 3-(2-bromoethyl)benzofuran. Both compounds (**251**) & (**252**) were reacted with various heterocyclic molecules in presence of anhydrous potassium carbonate in DMF to give the two carbon linker derivatives (**253-266**) and (**267-272**) respectively [Scheme 1].

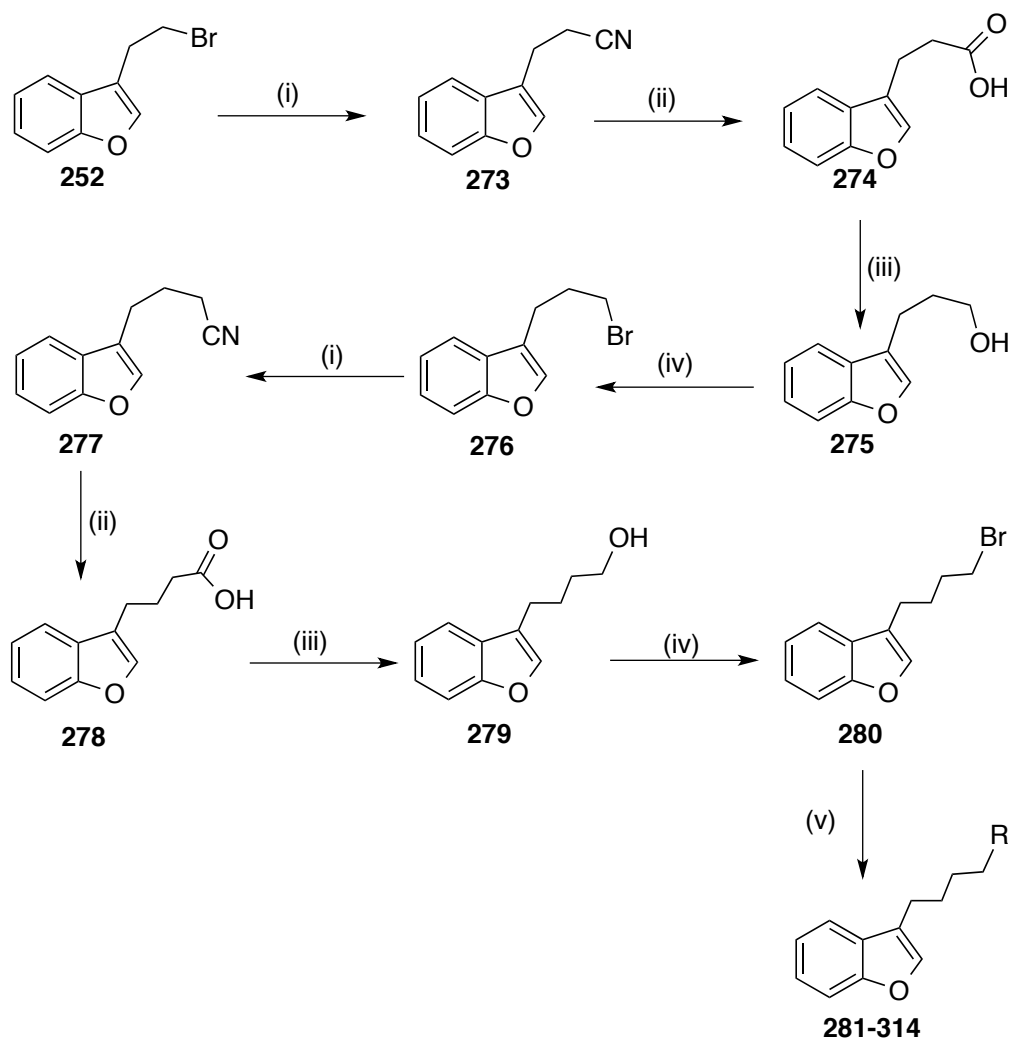
Compound (**252**) was subjected to alkyl elongation process to get the four carbon linker, first was treated with sodium cyanide to obtain the nitrile intermediate (**273**) that was subjected to hydrolysis with aqueous sodium hydroxide afforded the acid derivative (**274**) [Scheme 2]. A subsequent reduction to compound (**274**) using LiAlH_4 in THF afforded alcoholic compound (**275**) with three carbon linker that was subjected to the same previous reactions to obtain the four carbon linker compound (**280**) as shown in Scheme 2. Finally, compound (**280**) was reacted with various and appropriate heterocyclic derivatives to obtain (**281-314**) compounds as can be seen in Scheme 2.

Scheme 1: Synthetic routes of the 3-ethylbenzofuran derivatives synthetic routes



Reagents and conditions:(i) NaH, THF, trimethylphosphoacetate, 0 °C, 30min, r.t., 2 h; (ii) LiAlH₄, THF, 0 °C , 30min, r.t. , 1h; (iii) CH₃SO₂Cl, DCM, Et₃N, 0 °C-r.t. 4h; (iv) CBr₄, CH₂Cl₂, triphenylphosphine, 0 °C - r.t., overnight; (v) Corresponding cyclic amine, K₂CO₃, DMF, 65 °C, 1-3h.

Scheme 2: Synthetic routes of the 3-butylbenzofuran derivatives



Reagents and conditions: (i) NaCN, DMF, overnight, H₂O; (ii) KOH, H₂O, EtOH, reflux, 1h; (iii) LiAlH₄, THF, 0 °C-r.t., overnight, 0 °C, H₂O, 1N HCl (pH 4); (iv) 1-(4-nitrophenyl)piperazine or corresponding cyclic amine, K₂CO₃, DMF, 60 °C, 1-3h.

8.2 Synthesis of isothiocyanate derivatives:

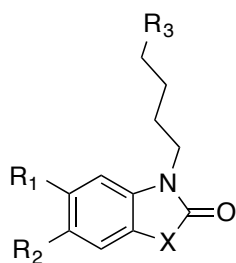
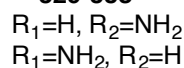
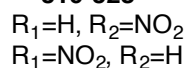
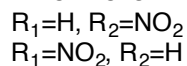
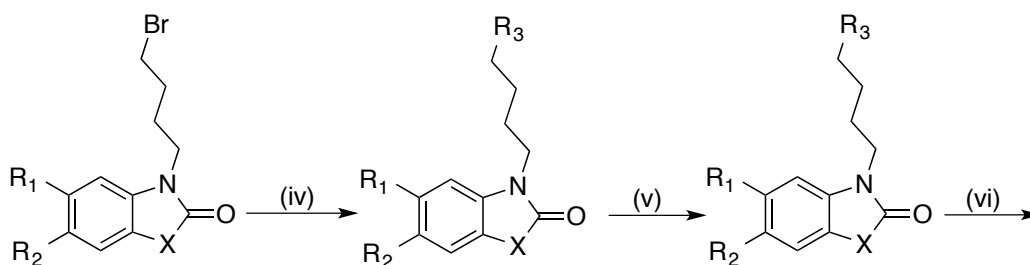
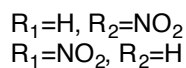
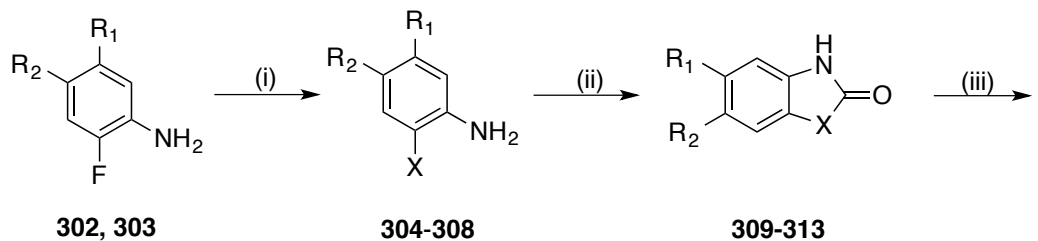
8.2.1 Synthesis of 1,3-dihydro-2*H*-benzo[*d*]imidazol-2-one

The 1,3-dihydro-2*H*-benzo[*d*]imidazol-2-one derivatives (319-328, 329-3238, 339-338,

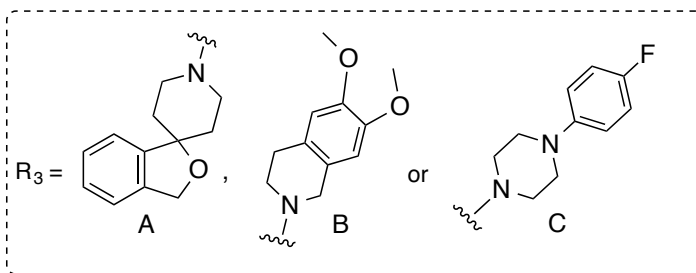
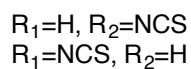
and **348-350**) were prepared as described in scheme 3, from the commercially available 2-fluoro-4 or 5-nitroaniline, which were reacted with the appropriate alkylamine derivatives, to give the alkylamine intermediates (**304-308**) followed by ring closure using carbonyldiimidazole (CDI) in THF to obtain 5 or 6-nitrobenzimidazolone derivatives (**309-313**). *N*-alkylation of the heterocyclic nitrogen atom with 1,4-dibromobutane in presence of anhydrous K₂CO₃ in DMF, followed by coupling with different heterocyclic substituents as simple *N*-alkylation reactions to afford the nitro derivatives (**319-328**) that were then subjected to hydrogenation (30 psi) in presence of 10% palladium activated charcoal and methanol as a solvent to form the aniline precursors (**329-338**). Finally the isothiocyanate compounds (**339-348**) were obtained from the aniline precursors using thiophosgene or thiocarbonyldiimidazole in presence of triethylamine in DCM or DMF.

Alternatively, compounds **474a** (WA404) and **474b** (WA422) were obtained as can be seen in [Scheme 3b] by subjecting the synthesized, 5-nitro-1,3-dihydro-2*H*-benzo[*d*]imidazol-2-one **466** (WA313) to *N*-alkylation reactions using methyl iodide in acetone and pentyl iodide in DMF to get mixtures of 1-alkyl-6-nitro-1,3-dihydro-2*H*-benzo[*d*]imidazol-2-one **468** & **470** (minor products) and 1-alkyl-5-nitro-1,3-dihydro-2*H*-benzo[*d*]imidazol-2-one **467** & **469** (major products). These compounds were separated by column chromatography and compared with the synthesized ones on the thin layer chromatography to distinguish between the two isomers. Also, the ¹⁵N-NMR and ¹⁵N-HMBC-NMR were conducted for (**469**) and (**470**) to see the N-H correlations and to confirm which is which.

Scheme 3a: Synthetic routes of isothiocyanate derivatives of benzoimidazolone heterocycle ring



339-348



| Compd No: | R ₁ | R ₂ | X | Compd No: | R ₁ | R ₂ | X |
|-----------|-----------------|-----------------|--|-----------|-----------------|-----------------|--|
| 304 | H | NO ₂ | NCH ₃ | 309 | H | NO ₂ | NCH ₃ |
| 305 | NO ₂ | H | NCH ₃ | 310 | NO ₂ | H | NCH ₃ |
| 306 | NO ₂ | H | N(CH ₂) ₂ CH ₃ | 311 | NO ₂ | H | N(CH ₂) ₂ CH ₃ |
| 307 | H | NO ₂ | N(CH ₂) ₄ CH ₃ | 312 | H | NO ₂ | N(CH ₂) ₄ CH ₃ |
| 308 | NO ₂ | H | N(CH ₂) ₄ CH ₃ | 313 | NO ₂ | H | N(CH ₂) ₄ CH ₃ |

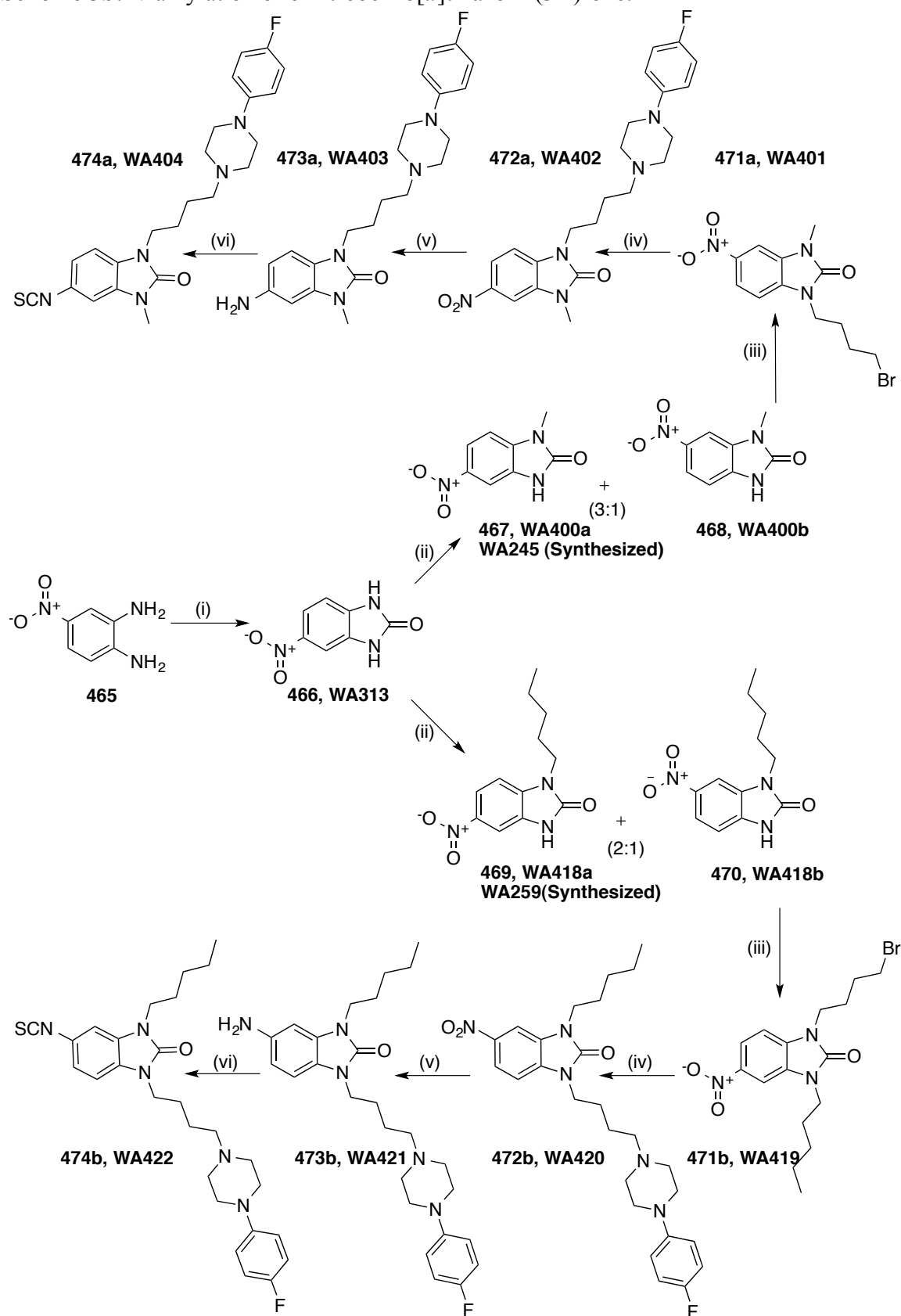
| Compd No: | R ₁ | R ₂ | X |
|-----------|-----------------|-----------------|--|
| 314 | H | NO ₂ | NCH ₃ |
| 315 | NO ₂ | H | NCH ₃ |
| 316 | NO ₂ | H | N(CH ₂) ₂ CH ₃ |
| 317 | H | NO ₂ | N(CH ₂) ₄ CH ₃ |
| 318 | NO ₂ | H | N(CH ₂) ₄ CH ₃ |

| Compd. No | Notebook Entry | R ₁ | R ₂ | X | R ₃ |
|-----------|----------------|-----------------|-----------------|--|----------------|
| 319 | WA248 | NO ₂ | H | NCH ₃ | B |
| 320 | WA256 | NO ₂ | H | NCH ₃ | A |
| 321 | WA262 | NO ₂ | H | N(CH ₂) ₂ CH ₃ | C |
| 322 | WA266 | NO ₂ | H | N(CH ₂) ₄ CH ₃ | B |
| 323 | WA267 | NO ₂ | H | N(CH ₂) ₄ CH ₃ | A |
| 324 | WA303 | NO ₂ | H | N(CH ₂) ₂ CH ₃ | A |
| 325 | WA334 | NO ₂ | H | N(CH ₂) ₂ CH ₃ | B |
| 326 | WA336 | NO ₂ | H | N(CH ₂) ₄ CH ₃ | C |
| 327(472b) | WA402 | H | NO ₂ | NCH ₃ | C |
| 328(472b) | WA420 | H | NO ₂ | N(CH ₂) ₄ CH ₃ | C |
| 329 | WA249 | NH ₂ | H | NCH ₃ | B |
| 330 | WA257 | NH ₂ | H | NCH ₃ | A |
| 331 | WA263 | NH ₂ | H | N(CH ₂) ₂ CH ₃ | C |
| 332 | WA268 | NH ₂ | H | N(CH ₂) ₄ CH ₃ | A |
| 333 | WA300 | NH ₂ | H | N(CH ₂) ₄ CH ₃ | B |
| 334 | WA304 | NH ₂ | H | N(CH ₂) ₂ CH ₃ | A |
| 335 | WA337 | NH ₂ | H | N(CH ₂) ₂ CH ₃ | B |
| 336 | WA338 | NH ₂ | H | N(CH ₂) ₂ CH ₃ | C |
| 337(473a) | WA403 | H | NH ₂ | NCH ₃ | C |
| 338(473b) | WA421 | H | NH ₂ | N(CH ₂) ₄ CH ₃ | C |
| 339 | WA250 | NCS | H | NCH ₃ | B |
| 340 | WA258 | NCS | H | NCH ₃ | A |
| 341 | WA264 | NCS | H | N(CH ₂) ₂ CH ₃ | C |
| 342 | WA269 | NCS | H | N(CH ₂) ₄ CH ₃ | B |
| 343 | WA306 | NCS | H | N(CH ₂) ₂ CH ₃ | B |
| 344 | WA349 | NCS | H | N(CH ₂) ₄ CH ₃ | C |
| 345 | WA350 | NCS | H | N(CH ₂) ₄ CH ₃ | B |
| 346 | WA352 | NCS | H | N(CH ₂) ₂ CH ₃ | B |
| 347(474a) | WA404 | H | NCS | NCH ₃ | C |
| 348(474b) | WA422 | H | NCS | N(CH ₂) ₄ CH ₃ | C |

Reagents and conditions: (i) H₂N-R, K₂CO₃, DMF, r.t or 80 °C, 18hr; H₂N-CH₃, H₂O, overnight, 95 °C; (ii) CDI, THF, 65 °C, 18hr.; (iii) 1,4-dibromobutane, K₂CO₃, DMF, 45-60 °C, 2-4hr.; (iv) 6,7-dimethoxy-1,2,3,4-tetrahydroisoquinolin-1-(4-fluorophenyl)piperazine, 3*H*-spiro[isobenzofuran-1,4'-piperidine] (56%, 65%, and 58%), K₂CO₃, DMF, 60 °C, 3-6hr; (v) 10%Pd/C,H₂ (20psi), MeOH, 2hr; (vi) Thiophosgene, TEA, DCM, 0 °C - r.t., 2 hr or thiocarbonyldiimidazole, TEA, DMF, r.t, 30 min.

Subsequent *N*-alkylation to **468** & **470** with 1,4-dibromobutane in presence of anhydrous potassium carbonate in anhydrous DMF afforded the 4-bromobutyl intermediates **471a** & **471b**. Followed by coupling reaction with 1-(4-fluorophenyl) piperazine in a simple *N*-alkylation reaction to afford compounds (**472a**) and (**472b**) in a good yield.

Scheme 3b: *N*-allylation of 6-nitrobenzo[*a*]thiazol-2(3*H*)-one.



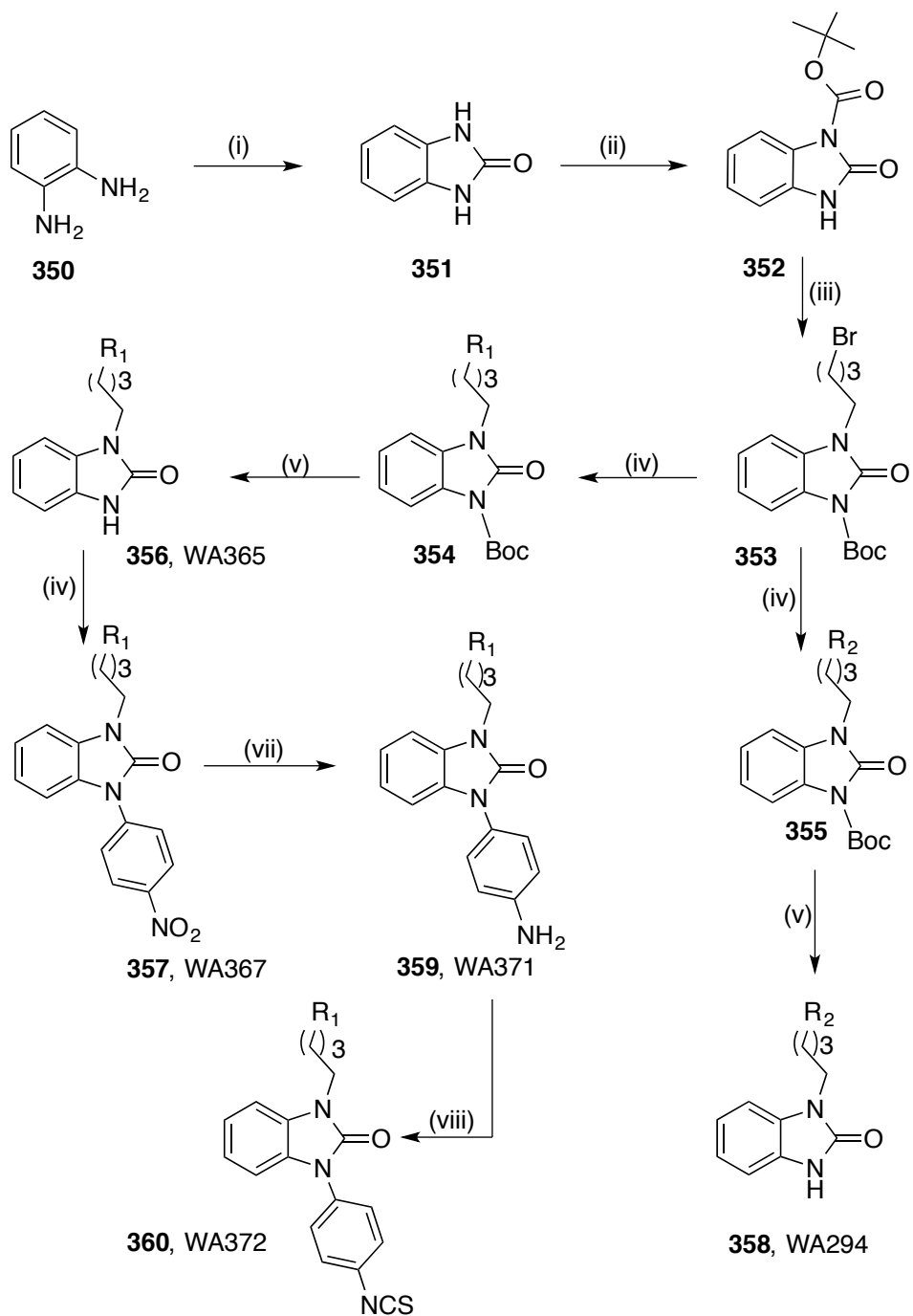
Reagents and conditions: (i) CDI, THF, 65 °C, 2hr; (ii) CH₃I, KOH (powdered), Acetone, r.t., 24hr; or CH₃(CH₂)₃CH₂I, K₂CO₃, DMF, r.t., overnight; (iii) 1,4-dibromobutane, K₂CO₃, DMF, 60 °C, 2hr; (iv) 1-(4-fluorophenyl)piperazine, K₂CO₃, DMF, 60 °C, 3 hr; (v) 10% Pd/C, H₂ (20 psi), MeOH, 2hr; (vi) 2 hr or thiocarbonyldiimidazole, TEA, DMF, r.t, 30 min.

The later compounds, **(472a)** and **(472b)** were treated with palladium (10%) over activated charcoal in methanol and under hydrogen pressure (20 psi) in Parr apparatus to obtain the aniline precursors **(473a)** and **(473b)**. The final isothiocyanate compounds **(474a, 474b)** were obtained from isothianation reactions using thiocarbonyldiimidazole (TCDI) in presence of TEA in DMF at room temperature.[Scheme 3b]

8.2.2 Synthesis of 1,3-dihydro-2*H*-benzo[*d*]imidazol-2-one derivatives (356-360)

The 1,3-dihydro-2*H*-benzo[*d*]imidazol-2-one derivatives **(356-360)**[Scheme 5] were synthesized starting from the commercially available molecule, 1,2-phenylenediamine **(350)**, which was subjected to ring closure using CDI in freshly distilled THF at 65 °C for 18 h to obtain 1,3-dihydro-2*H*-benzo[*d*]imidazol-2-one **(351)** as a white precipitate. A subsequent protection using di-*tert*-butyl dicarbonate for one of the heterocyclic nitrogen atoms **(352)** to allow the *N*-alkylation on the other side with 1,4-dibromobutane in presence of anhydrous K₂CO₃ in dry DMF to give compound **(353)**. *N*-alkylation with the appropriate heterocyclic motifs to afford compounds **(354)** and **(355)**, followed by Boc deprotection to afford **(356)**, and **(358)**. Compound **(356)** was reacted with 1-fluoro-4-nitrobenzene in presence of anhydrous K₂CO₃ in dry dimethyl sulfoxide (DMSO) to give compound **(357)** in a good yield. Subsequently, compound **(357)** was subjected to hydrogenation (30 psi) in presence of 10% palladium activated charcoal to give the aniline derivative **(359)**. Treatment of compound **(330)** with thiophosgene and triethylamine in DCM led to the isothiocyanate **(360)** [Scheme 4].

Scheme 4: Synthetic route of 1,3-dihydro-2*H*- benzo[*d*]imidazol-2-one derivatives

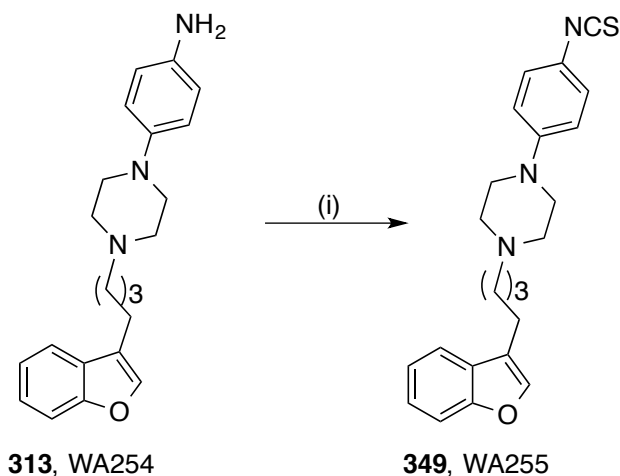


Reagents and conditions: (i) CDI, THF, 65 °C, 18h; (ii) Di-tert-butyl dicarbonate, NaH, DMF, 0°C-r.t., 3hr; (iii) 1,4-dibromobutane, K₂CO₃, DMF, 45-60 °C, 2hr; (iv) 1-(4-fluorophenyl)piperazine, K₂CO₃, DMF, 60 °C, 3hr; (v) Trifluoroacetic acid (TFA), CH₂Cl₂, r.t., 3hr; (vi) 1-fluoro-4-nitrobenzene, K₂CO₃, DMSO, 100 °C, overnight; (vii) 10% Pd/C, H₂ (20 psi), MeOH, 2hr; (viii) Thiophosgene, TEA, DCM, 0 °C - r.t., 2hr or thiocarbonyldiimidazole, TEA, DMF, r.t., 30 min.

8.3 Synthesis of benzofuran derivative

The compound **349** (WA255) was obtained as described in [Scheme 4], in which the **296** (WA254), was treated with thiophosgene and TEA in methylene chloride (DCM) as a solvent at 0 °C. Then the reaction mixture was stirred at room temperature for 2 hours to afford the final isothiocyanate compound **349** (WA255). [Scheme 5]

Scheme 5: Synthetic route of the isothiocyanate derivative of benzofuran. **349** (WA255)



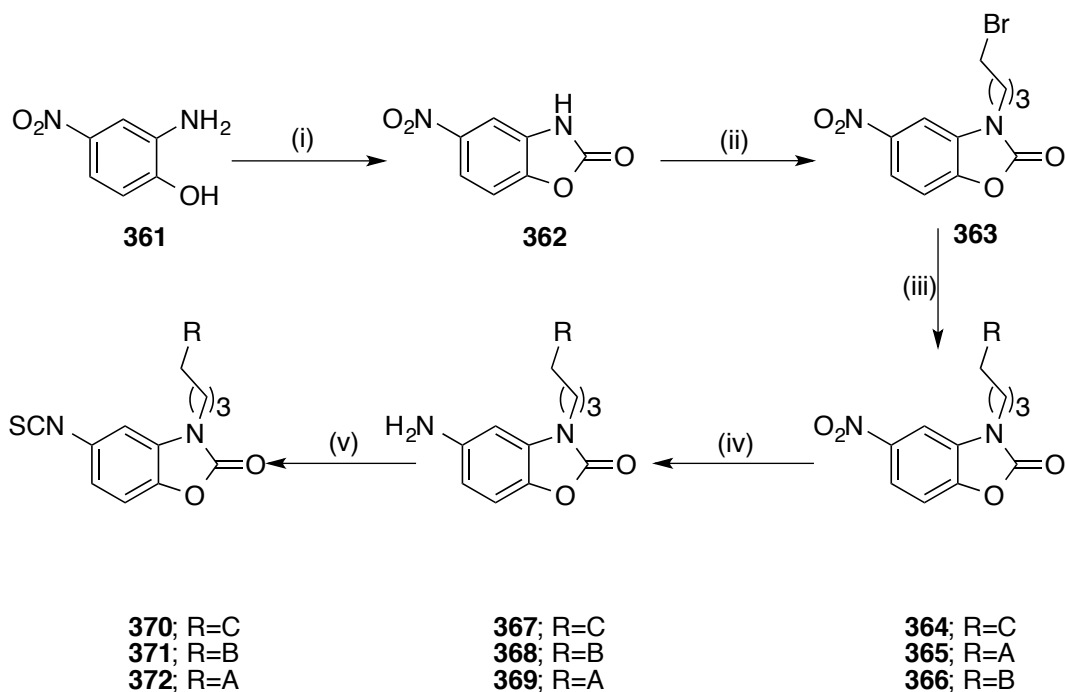
Reagents and conditions: (i) Thiophosgene, TEA, DCM, 0 °C - r.t., 2h.

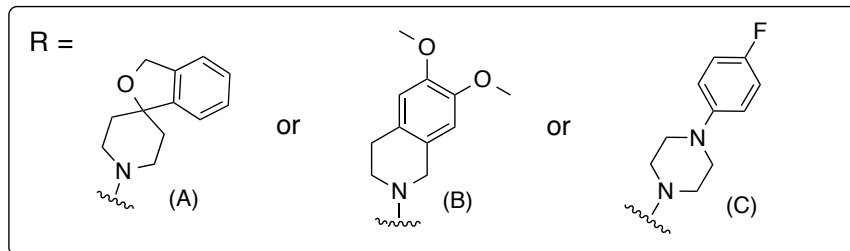
8.4 Synthesis of benzo[d]oxazol-2(3H)-one derivatives.

The isothiocyanate derivatives of benzo[d]oxazol-2(3H)-one were synthesized from the commercially available building block 2-amino-4-nitrophenol (**361**) that was subjected to ring closure by carbonyldiimidazole (CDI) treatment in freshly distilled tetrahydrofuran (THF) and stirred at 65 °C to obtain 5-nitrobenzo[d]oxazol-2(3H)-one (**362**) [Scheme 6]. Compound (**362**)

was treated with 2,4-dibromobutane in anhydrous dimethylformamide (DMF) as a simple *N*-alkylation reaction to afford compound (**363**), 3-(4-bromobutyl)-5-nitrobenzo[*d*]oxazol-2(3*H*)-one, in a good yield. This compound was coupled with the appropriate heterocycle motifs (A, B, and C)[Scheme 6] in presence of anhydrous potassium carbonate in anhydrous dimethylformamide (DMF) and heated at 65°C to get the three nitro compounds (**364**), (**365**), and (**366**)[Scheme 6]. The later compounds were treated with 10% palladium activated charcoal under 20 psi hydrogen pressure in Parr apparatus for two hours to afford the aniline precursors (**367**), (**368**), and (**369**) [Scheme 6]. Finally, the isothiocyanate derivatives were obtained in a reasonable yield from subjecting the anilines precursors (**370**), (**371**), and (**372**) to thiocarbonyldiimidazole (TCDI) and triethylamine (TEA) in anhydrous dimethylformamide (DMF) at room temperature for 30 minutes. [Scheme 6]

Scheme 6: Synthesis of benzo[*d*]oxazol-2(3*H*)-one derivatives



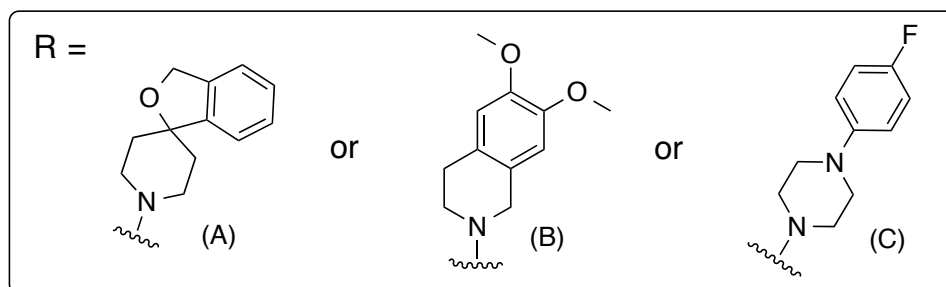
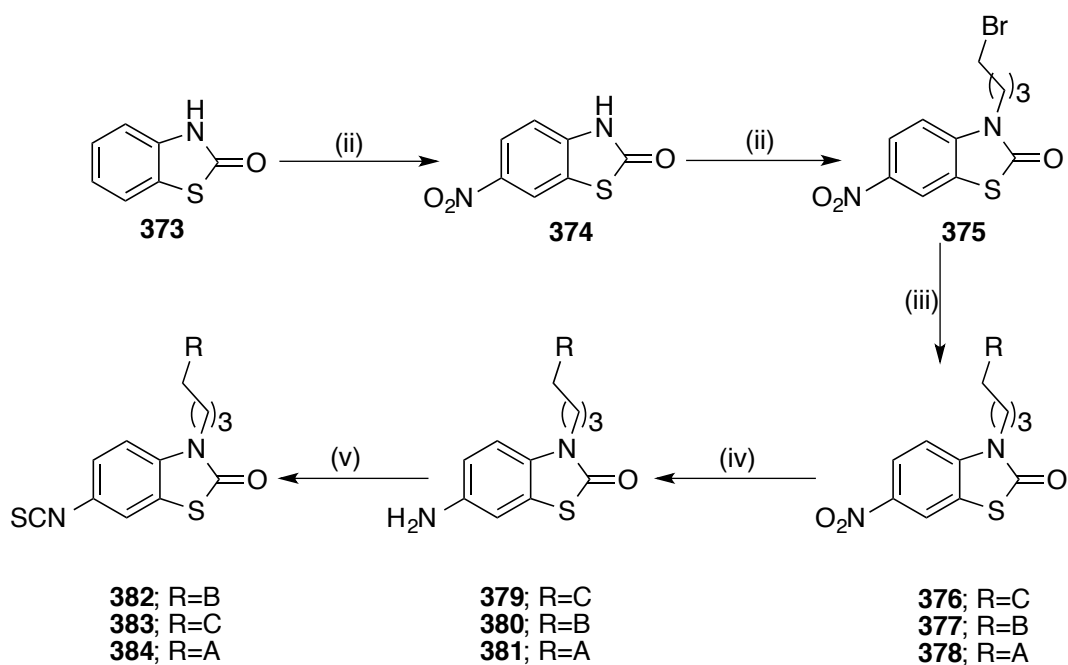


Reagents and conditions: (i) CDI, THF, 65 °C, 18h; (ii) 1,4-dibromobutane, K₂CO₃, DMF, 60 °C, 2h; (iii) 3*H*-spiro[isobenzofuran-1,4'-piperidine], 1-(4-fluorophenyl)piperazine, or 6,7-dimethoxy-1,2,3,4-tetrahydroisoquinoline, K₂CO₃, DMF, 60 °C, 3-6 h; (iv) 10%Pd/C, H₂ (20 psi), MeOH, 2h; (v) Thiocarbonyldiimidazole, TEA, DMF, rt.

8.5 Synthesis of benzo[*d*]thiazol-2(3*H*)-one derivatives

Similarly, the isothiocyanate derivatives of benzo[*d*]thiazol-2(3*H*)-one were synthesized starting from the commercially available benzo[*d*]thiazol-2-ol (**373**) [Scheme 7] that was treated with nitric acid (68%) for half an hour at room temperature to obtain 6-nitrobenzo[*d*]thiazol-2(3*H*)-one (**374**) [Scheme 7], which was subjected to *N*-alkylation reaction with 1,4-dibromobutane in presence of anhydrous potassium carbonate in anhydrous dimethylformamide (DMF) to afford compound (**375**) [Scheme 7]. Compound (**375**) was subjected to coupling reactions with the appropriate heterocyclic substituents to give the nitro precursors (**376**), (**377**), and (**378**) [Scheme 7], which were treated with 10% palladium activated charcoal under 20 psi hydrogen pressure in Parr apparatus for two hours to afford the aniline precursors (**379**), (**380**), and (**381**) [Scheme 7]. The final isothiocyanate compounds (**382**), (**383**), and (**384**) [Scheme 7] were synthesized by treating the aniline precursors with thiocarbonyldiimidazole (TCDI) in presence of triethylamine TEA in anhydrous DMF at room temperature. [Scheme 7]

Scheme 7: Synthetic routes of benzo[*d*]thiazol-2(3*H*)-one



Reagents and conditions: (i) HNO₃ (68%), 50 °C, 0.5h- rt, 2h; (ii) 1,4-dibromobutane, K₂CO₃, DMF, 60 °C, 2h; (iii) 3*H*-spiro[isobenzofuran-1,4'-piperidine], 1-(4-fluorophenyl)piperazine, or 6,7-dimethoxy-1,2,3,4-tetrahydroisoquinoline, K₂CO₃, DMF, 60 °C, 3-6 h; (iv) 10%Pd/C, H₂ (20psi), MeOH, 2h; (v) Thiocarbonyldiimidazole, TEA, DMF, rt.

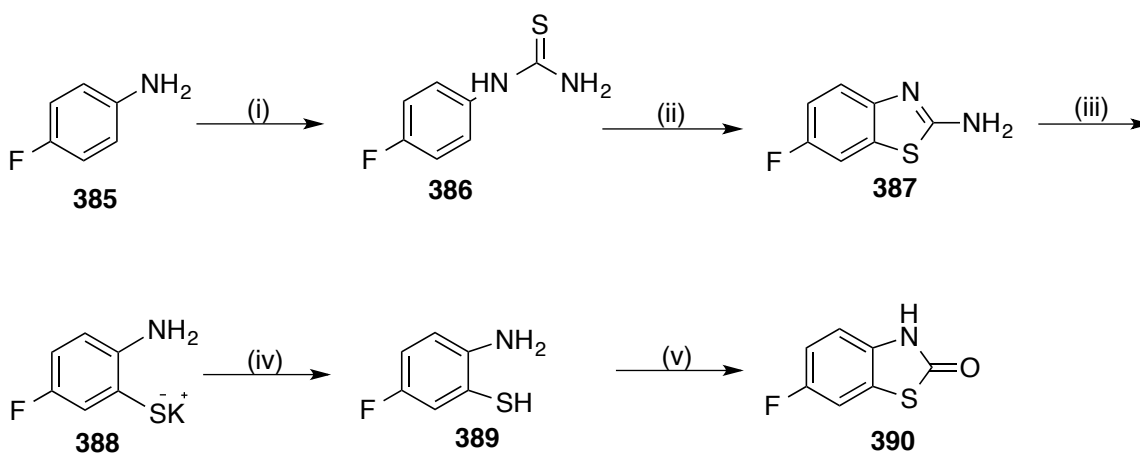
8.6 Synthesis of CM699 Derivatives

8.6.1 Synthesis of 6-fluorobenzo[*d*]thiazol-2(3*H*)-one (390)

Compound (390) was synthesized from the commercially available 4-fluoroaniline upon reaction

with ammonium thiocyanate in water afforded 4-fluorophenylthiourea (**386**), which in turn was cyclized through bromination reaction resulting in 6-fluoro-2-aminobenzothiazole (**387**). 2-Amino-5-fluoro-benzenethiol (**389**) was obtained by hydrolytic cleavage using potassium hydroxide then neutralization using acetic acid to afford the free base (**389**). The thiol (**389**) was recycled by treating it with carbonyldiimidazole (CDI) to afford the final compound (**390**).

Scheme 8: Synthetic route of 6-fluorobenzo[*d*]thiazol-2(3*H*)-one (**390**)



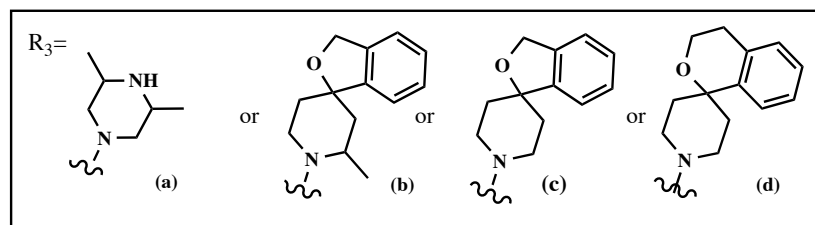
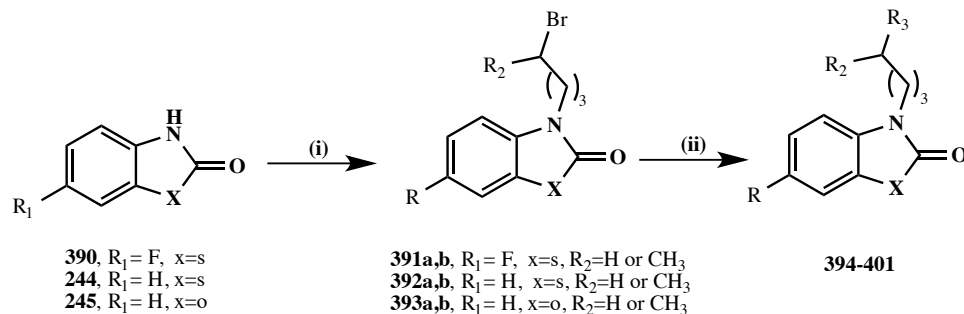
Reagents and conditions: (i) NH_4SCN , H_2O , reflux, 3 h; (ii) Br_2 , CHCl_3 , 50 min at 0°C , reflux, 2 h; (iii) KOH ; (iv) Glacial acetic acid (v) CDI, THF, reflux, 2 h.

8.6.2 Synthesis of more analogs CM699

Subjecting the corresponding heterocycle ring to N-alkylation reaction with 1, 4-dibromobutane or 1,4-dibromopentane afforded the 4-bromoalkyl intermediates (**391a**, **391b**), (**392a**, **392b**), and (**393a**, **393b**), followed by coupling with the appropriate heterocycle substituents (A, B, C, and D) to afford the targeted compounds (**394-401**) in good yields.

[Scheme 9]

Scheme 9: Synthetic routes of CM699 analogs



394; x=s, R₁=F, R₂=H, R₃=a
395; x=s, R₁=F, R₂=CH₃, R₃=a
396; x=s, R₁=F, R₂=H, R₃=c
397; x=s, R₁=F, R₂=CH₃, R₃=c

398; x=s, R₁=F, R₂=H, R₃=b
399; x=o, R₁=H, R₂=H, R₃=b
400; x=s, R₁=H, R₂=H, R₃=b
401; x=s, R₁=F, R₂=H, R₃=d

Reagents and conditions: (i) NH₄SCN, H₂O, reflux, 3 h; (ii) Br₂, CHCl₃, 50 min at 0 °C, reflux, 2 h; (iii) KOH; (iv) Glacial acetic acid (v) CDI, THF, reflux, 2 h; (vi) Dibromoalkane, K₂CO₃, DMF at 60 °C, 2 h; (vii) 3H-spiro[isobenzofuran-1,4'-piperidine], K₂CO₃, DMF, 3 h at 60 °C.

8.7 Synthesis of 3H-spiro[isobenzofuran-1,4'-piperidine]

There are two routes have been followed to synthesize the 3H-spiro[isobenzofuran-1,4'-piperidine].

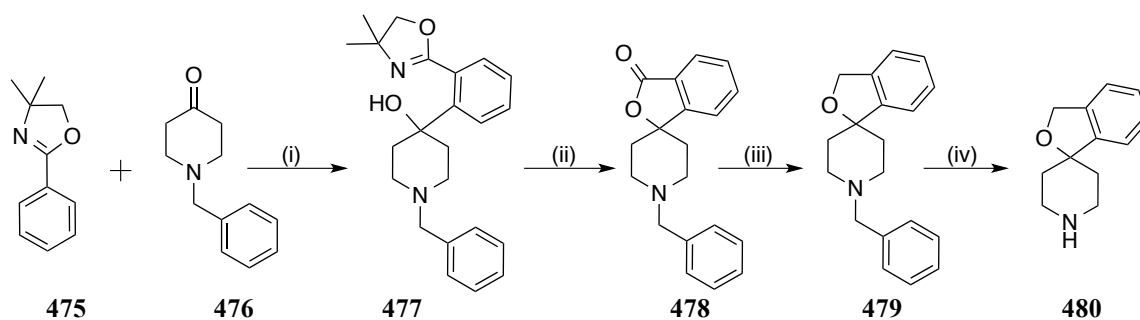
8.7.1 The first synthetic route of 3H-spiro[isobenzofuran-1,4'-piperidine]

The first route was started with the commercially available 4,4-dimethyl-2-phenyl-4,5-dihydrooxazole as can be seen in [Scheme 10].

The commercially available 4,4-dimethyl-2-phenyl-4,5-dihydrooxazole (**475**) in freshly distilled THF was cooled down to -70 °C under argon and added dropwise n-butyllithium. Then was treated with *N*-benzyl-4-piperidone (**476**) to afford the intermediate, compound (**477**), which in turn was acidified with 3 *N* HCl and refluxed for 5 hours to afford 1'-benzyl-3H-

spiro[isobenzofuran-1,4'-piperidin]-3-one (**478**). Subsequent reduction of the ketone group in compound (**478**) by 1M Borane-THF gave compound (**479**), 1'-benzyl-3*H*-spiro [isobenzofuran-1,4'-piperidine], followed by the de-benzylation (deprotection) by subjecting to hydrogenation over Parr apparatus (45 psi) in presence of palladium 10% over activated charcoal for 5 hr to give compound (**480**). [Scheme 10]

Scheme 10: Synthesis of 3*H*-spiro[isobenzofuran-1,4'-piperidine]

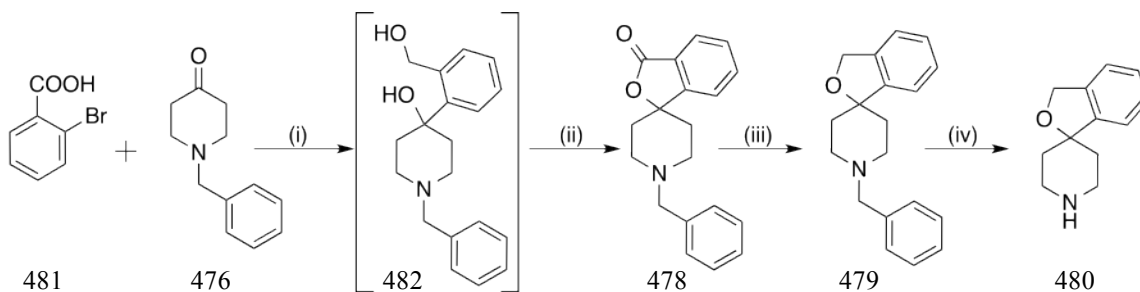


Reagents and conditions: (i) n-BuLi 2.5M, THF, -78°C; N-benzyl-piperidine-4-one, 30 min, -78°C to rt; overnight. (ii) H₂O, 3N HCl, reflux, 5 h, pH 2.5 (iii) 1.8 M Borane-THF, 0 °C to reflux overnight, 0 °C, 6 N HCl, pH 10 (iv) H₂ (45 psi), 10 % Pd/C, HCl; H₂O: Acetic acid (2mL, 60mL, 40mL), 5 h.

8.7.2 The second synthetic route of 3*H*-spiro[isobenzofuran-1,4'-piperidine]

Unfortunately, the yield from the previous [Scheme 10] was not good. So, it was interesting for us to follow different synthetic route to get better yield of the targeted compound. 2-Bromo-benzoic acid with *N*-benzyl piperidone when used as starting material gave the final product (**480**) with 83 % yield. The second synthetic route is outlined in [Scheme 11].

Scheme 11: Synthesis of 3*H*-spiro[isobenzofuran-1,4'-piperidine] [Different route]

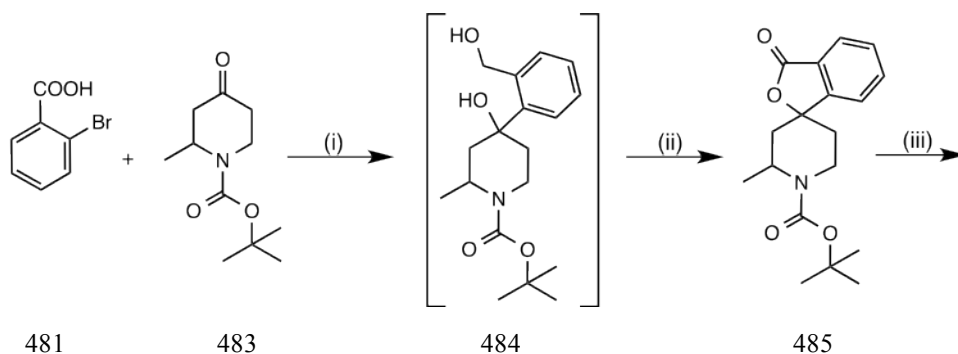


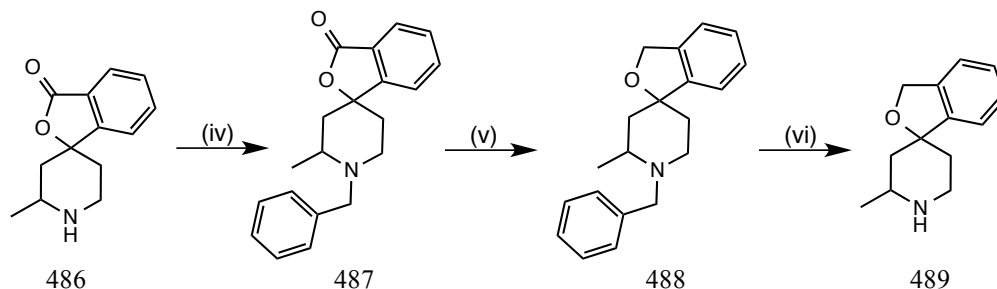
Reagents and conditions: (i) n-BuLi 2.5M, THF, -78°C; N-benzyl-piperidine-4-one, 30 min, -78°C to rt; overnight. (ii) H₂O, reflux, 1h, pH 2.5 (iii) (CH₃)₂S * BH₃, THF, 0 °C to reflux (iv) 1-chloroethyl chloroformate, r.t, 5h, CH₃OH; reflux, 30 min.

8.8 Synthesis of 2'-methyl-3*H*-spiro[isobenzofuran-1,4'-piperidine] (489, WA469)

The synthetic route that used to synthesize the 2'-methyl-3*H*-spiro[isobenzofuran-1,4'-piperidine] (**489**) is similar to the one outlined in the previous scheme; however, in this scheme the starting material was *tert*-butyl 2-methyl-4-oxopiperidine-1-carboxylate instead of 1-benzyl-2-methylpiperidin-4-one, which is too expensive. It was much cheaper to start with the Boc protected 2-methylpiperidin-4-one. The 2-bromobenzoic acid was treated with *tert*-butyl 2-methyl-4-oxopiperidine-1-carboxylate (**483**) to get the intermediate (**484**) followed by pH adjustment to 2.5 with 3N HCl and then was refluxed for an hour to obtain compound (**485**). The de-protection of Boc (**486**) and re-protection with benzyl (**486**) were performed in order to obtain better and clean reaction in the next step. The reduction of the ketone group in compound (**487**) using borane-methylsulfide in THF helped make the ketone more susceptible to nucleophilic attack by the H⁻ from another molecule of borane, which led to formation of compound (**488**). The later compound (**488**) treated with the reducing agent, 1-chloroethyl chloroformate, to afford the targeted compound (**489**). [Scheme 12]

Scheme 12: synthesis of 2'-methyl-3*H*-spiro[isobenzofuran-1,4'-piperidine], **489** (WA469)



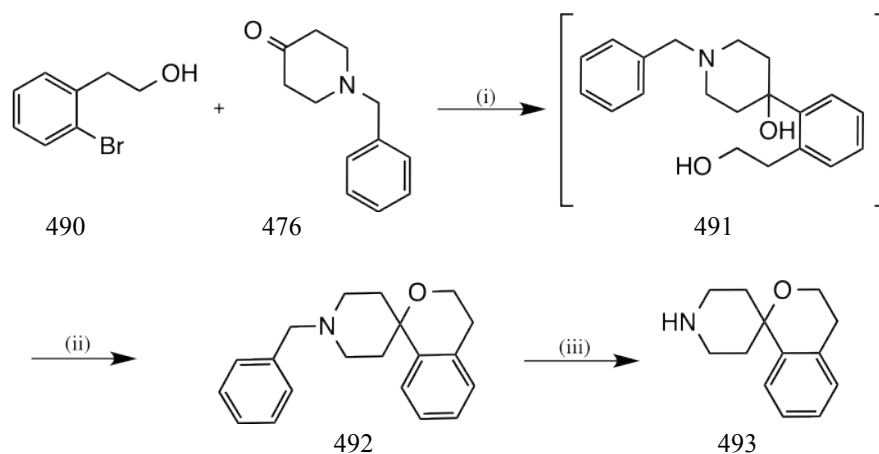


Reagents and conditions: (i) BuMgCl, n-BuLi 2.5M, THF, -78°C , 30 min; (ii) Acetic acid, H_2O , reflux, 1h, pH 2.5 (iii) TFA, DCM, 2h, r.t.; (iv) Benzylbromide, K_2CO_3 , DMF; (v) $(\text{CH}_3)_2\text{S} \cdot \text{BH}_3$, THF, 0°C to reflux (vi) 1-chloroethyl chloroformate, r.t, 5h, CH_3OH ; reflux, 30 min.

8.9 Synthesis of spiro[isochromane-1,4'-piperidine]

Compound (**491**) was obtained from treating 2-bromophenyl ethyl alcohol with 1-benzyl-4-piperidone in dry THF at -60°C in presence of n-butyl lithium, followed by ring closure using methanesulfonyl chloride. Then the reaction mixture was refluxed for 5 hr and basified to obtain the cyclic compound (**492**). Subsequent hydrogenation in the Parr apparatus (45 psi) in the presence of 10% palladium on charcoal afforded the targeted molecule (**493**) in a good yield.

Scheme 13: Synthesis of spiro[isochromane-1,4'-piperidine]. (**493**)



Reagents and conditions: (i) n-BuLi, hexane 2.5M, THF, -78°C , N-benzyl-piperidine-4-one, 30 min, -60°C to rt, 72h, NH_4Cl , Na_2CO_3 2M aq. solution to pH 11; (ii) Et_3N , THF, MeSO_2Cl , 4h, reflux, Quenching with H_2O , 1M aq.

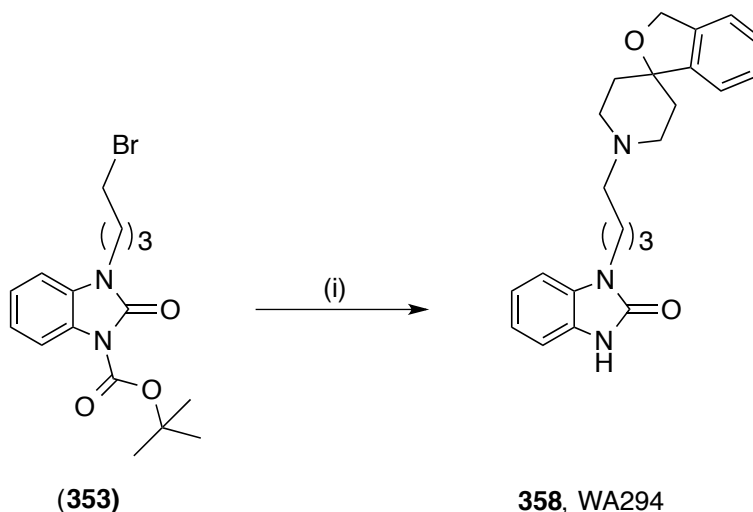
NaOH; (iii) H₂, 10% Pd/C, EtOH, 18h.

8.10 Synthesis of benzimidazolone derivatives of CM699

8.10.1 Synthesis of the de-methylated CM699 analog, 358 (WA294)

The demethylated analog of CM699, **358** (WA294) was obtained by subjecting compound (**355**) to coupling with 3*H*-spiro[isobenzofuran-1,4'-piperidine]-HCl in presence of anhydrous potassium carbonate in anhydrous DMF and heated at 160 °C in microwave reactor for 30 minutes to obtain the de-protected analog of CM699, **358** (WA294) [Scheme 14].

Scheme 14: Synthesis of the de-methylated CM699 analog



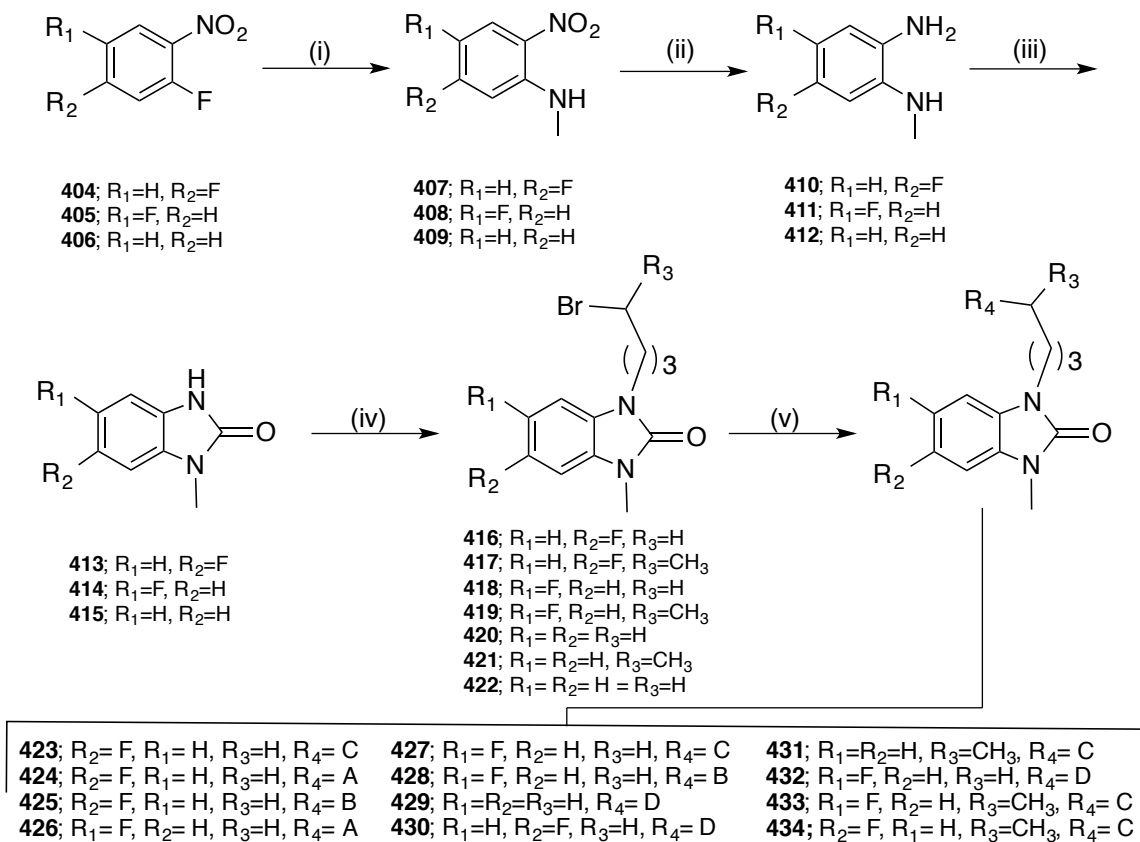
Reagents and conditions: (i) 3*H*-spiro[isobenzofuran-1,4'-piperidine], K₂CO₃, DMF, 160 °C 30 min. in

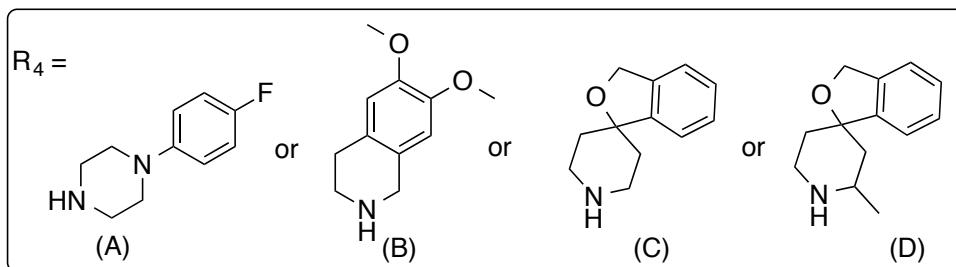
8.10.2 Synthesis of 1-methyl-benzo[*d*]imidazol-2-one derivatives of CM699

The 1-methyl-benzo[*d*]imidazol-2-one derivatives of CM699 were synthesized as described in [Scheme 15] from the commercially available difluoronitrobenzene or 2-

fluoronitrobenzene building blocks (**404-406**), which were reacted with methylamine in 40% water solution to afford (**407,408, and 409**). The methylamine derivatives (**407,408, and 409**) were subjected to hydrogenation at 30 psi of hydrogen pressure on a Parr apparatus to afford compound (**410, 411, and 412**) followed by ring closure using CDI in freshly distilled THF gave the desired (**413, 414, and 415**) derivatives. The bromoalkyl precursors (**416-422**) obtained from the *N*-alkylation on the heterocyclic nitrogen with 1,4-dibromobutane or 1,4-dibromopentane in presence of anhydrous potassium carbonate in anhydrous DMF. A subsequent coupling with the appropriate heterocyclic motifs [A, B, C, or D] in presence of anhydrous K₂CO₃ in dry DMF gave the targeted compounds (**423-434**) [Scheme 15].

Scheme 15: Synthesis of 1-methyl-benzo[*d*]imidazol-2-one derivatives of CM699



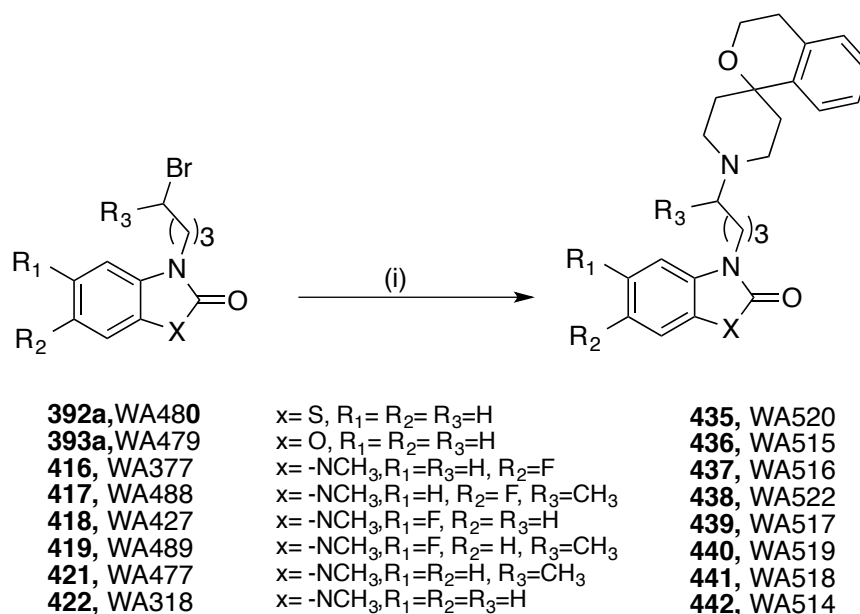


Reagents and conditions: (a) H₂N-CH₃, H₂O, overnight, 95 °C; (b) 10%Pd/C, H₂ (20 psi), MeOH, 2hr; (c) CDI, THF, 65 °C, 18hr; (d) 1,4-dibromopentane/1,4-dibromobutane, K₂CO₃, DMF, 60 °C, 2hr; (e) 3*H*-spiro[isobenzofuran-1,4'-piperidine], 1-(4-fluorophenyl)piperazine, and 6,7-dimethoxy-1,2,3,4-tetrahydroisoquinoline, K₂CO₃, DMF, 60 °C, 3-6 hr.

8.11 Synthesis of spiro[isochromane-1,4'-piperidine] derivatives

The spiro[isochromane-1,4'-piperidine] compounds were obtained from the previous prepared bromoalkyls of corresponding heterocycle rings (**392a**, **393a**, and **416-422**), which were subjected to coupling with spiro[isochromane-1,4'-piperidine] in a simple *N*-alkylation reactions in presence of anhydrous potassium carbonate in anhydrous DMF to afford the final desired molecules (**435-442**)[Scheme 16].

Scheme 16: Synthetic routes of spiro[isochromane-1,4'-piperidine] derivatives



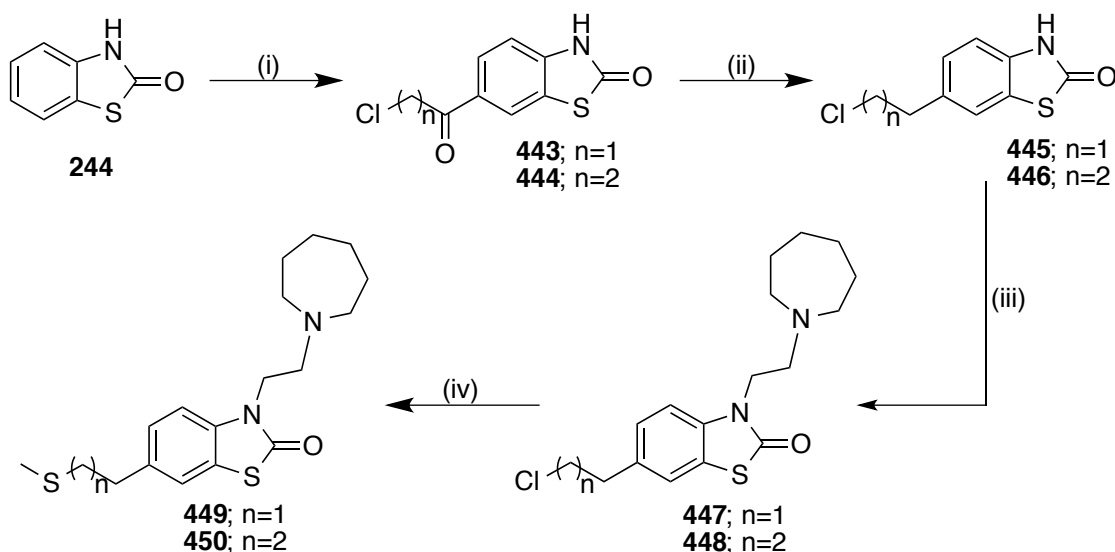
Reagents and conditions: (i) Spiro[isochromane-1,4'-piperidine], K₂CO₃, DMF, 60 °C, 3-6 h.

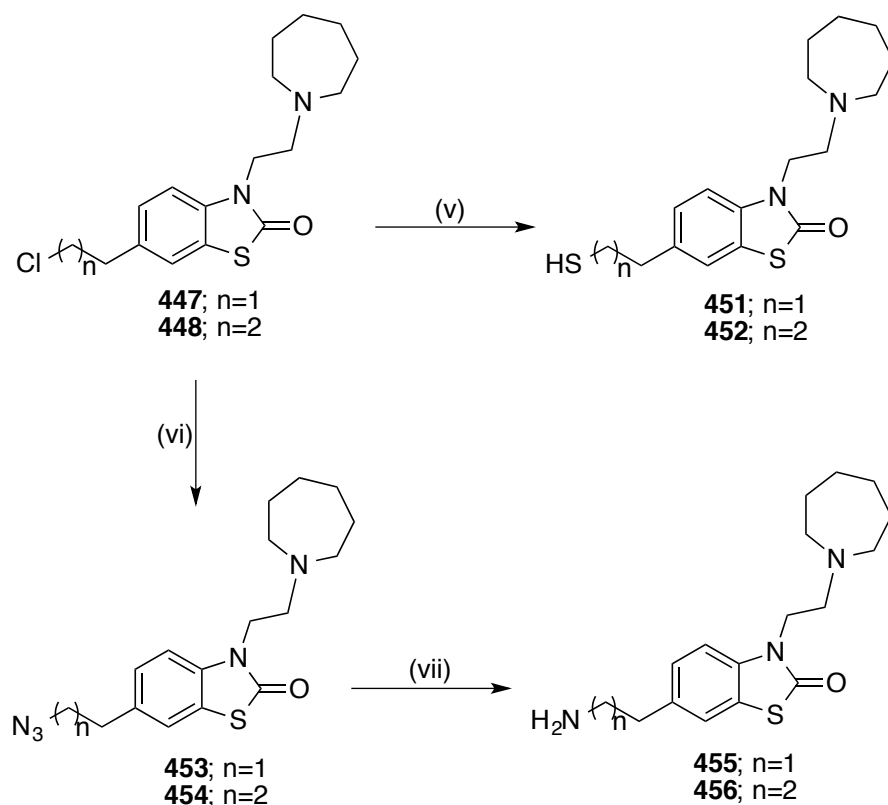
8.12 Synthesis of CM304 derivatives

8.12.1 Synthesis of the first series of CM304 derivatives

The CM304 analogs were prepared according to [Scheme 17]. The first step in the synthesis was a Friedel-Crafts acylation in which the commercially available 2-hydroxybenzothiazole (**244**) was reacted with the acyl halides, 2-chloroacetyl chloride or 3-chloropropionyl chloride in presence of AlCl_3 , a Lewis acid catalyst to afford (**443**), and (**444**) compounds. Subsequent selective reduction of the ketone group using triethylsilane and trifluoroacetic acid to get the both compounds (**445**), and (**446**). The resulting compounds were reacted with 2-(hexamethyleneimino)ethyl chloride hydrochloride to add an azepane functional group to the existing nitrogen, as a simple N-alkylation reaction to give both (**447**), and (**448**) compounds. The later compounds were subjected to several subsequent reactions to obtain the final eight targeted molecules (**449-456**) as illustrated in [Scheme 17].

Scheme 17: Synthetic route of CM304 derivatives





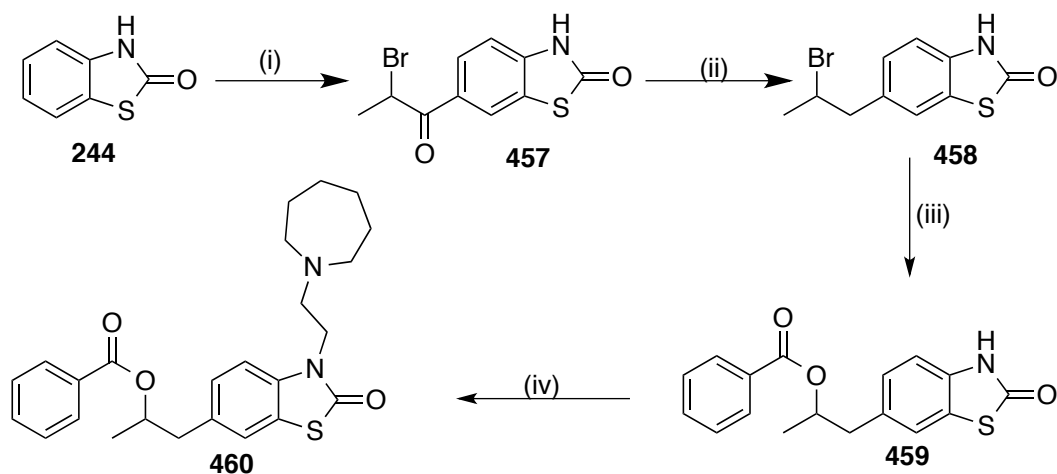
Reagents and Conditions: (i) 3-Chloropropionyl chloride or 2-chloroacetyl chloride, AlCl_3 -DMF, 45°C to 80°C , 4h; (ii) TES, TFA, rt, 4h; (iii) 2-(Hexamethyleneimino)ethyl chloride-HCl, KHCO_3 , DMF, 95°C , 30min; (iv) CH_3SNa , EtOH, r.t., overnight; (v) Thiourea, H_2O , reflux, 48 hr, aq. NaOH 40%, 2hr; (vi) NaN_3 , acetonitrile, KI, 70°C , overnight; (vii) 10% Pd/C, H_2 (30 psi), MeOH, r.t., overnight.

8.12.2 Synthesis of the second series of CM304 derivatives

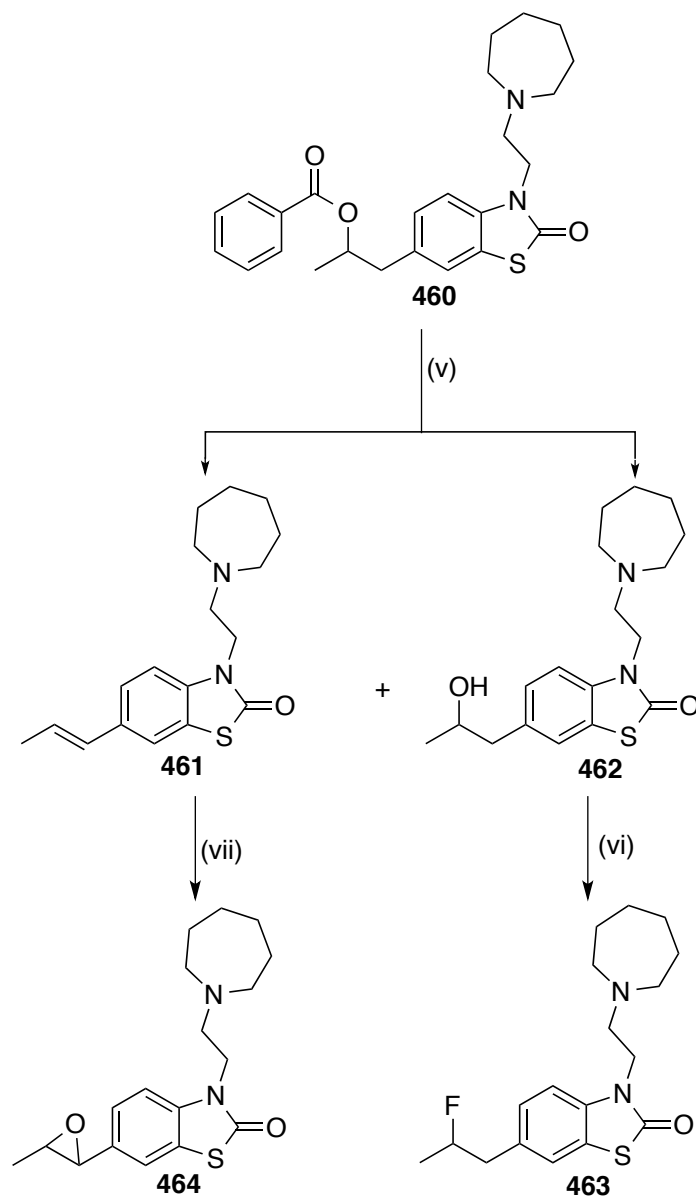
The other derivatives of CM304 were prepared according to [Scheme 18] by subjecting the commercially available building block 2-hydroxybenzothiazole (**244**) to Friedel-Crafts acylation to afford (**457**), followed by a selective reduction to the ketone group using triethylsilane in TFA to obtain (**458**). The resulting compound (**458**) was subjected to esterification reaction with benzoic acid to form the benzoate ester (**459**) followed by coupling with 1-(2-chloroethyl)azepane using anhydrous potassium carbonate in dry DMF to afford compound (**460**). After the hydrolysis of (**460**) using sodium hydroxide and water, two compounds were obtained due to the elimination process that resulted in alkene formation (**461**)

in addition to the targeted alcoholic compound (**462**). Compound (**462**) was subjected to fluorination reaction using the fluorinating reagent, DeoxoFluor in DCM, to obtain the desired fluorinated molecule (**463**). Since compound (**461**) was formed in enough amount as a byproduct of the hydrolysis reaction, I decided to convert the alkene (**461**) to alcohol (**462**) through the hydroboration oxidation (regioselective addition on alkene) in two subsequent steps to end up by the net addition of water across the double bond using 9-BBN as a hydroboration reagent. However, the oxidative cleavage step in the reaction didn't take place and ended up with epoxide formation, compound (**464**) as illustrated in [Scheme 18].

Scheme 18: Synthetic routes of the second series of CM304 derivatives



Reagents and Conditions: (i) 2-Bromopropionyl chloride, AlCl_3 -DMF, 45°C to 80°C , 2h; (ii) TES, TFA, rt, 4h; (iii) Benzoic acid, DMF, K_2CO_3 , 72°C , 6h; (iv) 2-(Hexamethyleneimino)ethyl chloride-HCl, K_2CO_3 , DMF, 65°C , 2h

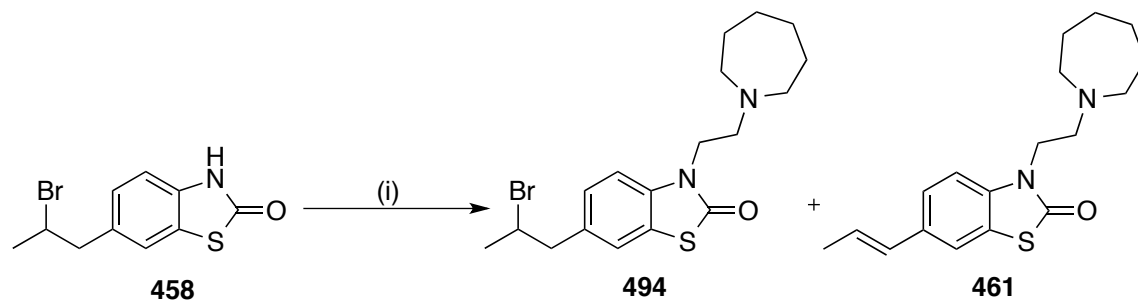


Reagents and Conditions: (v) NaOH, MeOH/H₂O, reflux, 6h; (vi) Deoxofluor, DCM, -78^oC to rt, 2h; (vii) 9-BBN-THF, 3 N aq. NaOH, 50% H₂O₂ solution in water, 1hr.

7.12.3 Synthesis of 494 (WA444a) and 461 (WA444b)

Compound (**494**) was obtained from treating the previously synthesized compound (**458**) with excess amount (6-8 eq.) of 2-(hexamethylethylamino)ethyl chloride hydrochloride to afford a mixture of compounds (**494**) and (**461**)[Scheme 19]. Compound (**461**) was formed as a result of bromine elimination, which very expected in such kind of reactions.

Scheme 19: Synthetic route of **494** (WA444a) and **461** (WA444b)



Reagents and Conditions: (i) 2-(Hexamethyleneimino)ethyl chloride-HCl (6 eq.), sodium bicarbonate, DMF, 50⁰C -120⁰C, 30 min.

CHAPTER IX: EXPERIMENTAL SECTION

9.1 General consideration: Reagents and starting materials were obtained from commercial suppliers and were used without purification. Precoated silica gel 60 F₂₅₄ aluminium backed plates from EMD were used for thin-layer chromatography (TLC). Column chromatography was performed on silica gel 60 (Sorbent Technologies). ¹H and ¹³C NMR spectra were obtained on a Bruker APX400 at 400 and 100 MHz, respectively. The mass spectra (MS) were recorded on a Waters Aquity Ultra Performance LC with ZQ detector in ESI mode. Analytical HPLC was performed on an automated Waters Alliance system equipped with a XBridge[®] C₁₈ 2.5mm (4.6 x 75 mm i.d., 2.5 μm), column or XBridge[®] C₁₈ 5mm (4.6 x 75 mm i.d., 5μm), with a flow rate of 1 ml/min.; λ_{max} = 254 nm; mobile phase A: CH₃CN and mobile phase B: H₂O (0.2% triethylamine) linear gradient in 12 min. Chemical names were generated using ChemDraw Ultra (CambridgeSoft, version 13.0 or 14.0). The overall yields, ¹H and ¹³C NMR data for final compounds are reported in its free base form.

9.2 Synthesis of a benzofuran-3-yl Series

Methyl 2-(benzofuran-3-yl) acetate. 249 (WA94) To a stirred suspension of NaH (60% wt in *mineral oil*, 1.25 g, 52 mmol, 1.4 equiv.) in anhydrous *THF* (20 mL) at 0 °C under argon was added dropwise a solution of trimethyl phosphonoacetate (7 mL, 48.3 mmol, 1.3 equiv.) in anhydrous *THF* (20 mL). The reaction mixture was stirred 30 min. at 0 °C, then was added slowly a solution of 3-coumaranone (5 g, 37.27 mmol, 1 equiv.) in anhydrous *THF* (100 mL), and the mixture was stirred for 2h at room temperature. After reaction completion, the mixture was poured into ammonium chloride solution, extracted with ethyl acetate, and the organic layer was washed with brine, dried over anhydrous magnesium sulphate, filtered and concentrated. After evaporation, the residue was purified by chromatography on a silica gel column using ethyl

acetate/hexanes (5:5) as the eluent to give 4.3 g (60.5%) of methyl 2-(benzofuran-3-yl) acetate as colorless oil. MS (ESI) m/z 191 $[M+1]^+$. ^1H NMR (400 MHz, Chloroform- d) δ 7.65 (d, J = 1.3 Hz, 1H), 7.59 (dd, J = 7.3, 1.5 Hz, 1H), 7.53 – 7.48 (m, 1H), 7.36 – 7.25 (m, 2H), 3.74 (d, J = 7.5 Hz, 5H). ^{13}C NMR (101 MHz, CDCl_3) δ 171.11, 155.21, 142.89, 127.60, 124.48, 122.66, 119.65, 113.06, 111.53, 52.14, 29.51.

2-(benzofuran-3-yl)ethan-1-ol. 250 (WA95) To a stirred suspension of LiAlH_4 (1.717 g, 45 mmol, 2 equiv.) in anhydrous *THF* (100 mL) at 0 °C under argon was added dropwise a solution of methyl 2-(benzofuran-3-yl) acetate (4.3 g, 22.6 mmol, 1 equiv.) in anhydrous THF (20 mL). The reaction mixture was stirred 30 min. at 0 °C, and for 5 h at room temperature. The mixture was then cooled with an ice bath and 1.8 mL of water was added, followed by 1.8 mL of 15% NaOH aqueous solution and 3.6 mL of water. The solid was filtered and the filtrate was evaporated. The residue was purified by chromatography on a silica gel column using a gradient of ethyl ether/methanol (100:0 to 95:5) as the eluent to give 3 g (81.7%) of 2-(benzofuran-3-yl)ethan-1-ol as yellow oil. MS (ESI) m/z 201.35 $[M+39]^+$. ^1H NMR (400 MHz, Chloroform- d) δ 7.75 – 6.99 (m, 5H), 3.90 (t, J = 6.5 Hz, 2H), 2.93 (t, J = 6.4 Hz, 2H), 2.03 (s, 1H). ^{13}C NMR (101 MHz, CDCl_3) δ 155.38, 142.16, 127.99, 124.37, 122.46, 119.55, 116.80, 111.56, 61.71, 27.06.

2-(benzofuran-3-yl)ethyl methanesulfonate. 251 (WA96/WA103) To a solution of 2-(1-benzofuran-3-yl)ethanol (1 g, 6.16 mmol) in anhydrous methylene chloride (30 ml), under argon at 0 °C, was added triethylamine (1.5 mL, 11.11 mmol), and followed by methanesulfonyl chloride (0.98g, 8.6 mmol) under argon at 0 °C for 40 min. Then, the reaction mixture warmed

up to room temperature and left for 4 h. After reaction completion, the reaction mixture washed with 5% NaHCO₃ (25 mL), and brine solution. The organic layer was dried over anhydrous magnesium sulfate, filtered, and concentrated. The residue was purified by chromatography on a silica gel column using ethyl acetate/hexane (5:5) as eluent to afford 1 g (67.5%) of 2-(benzofuran-3-yl)ethyl methanesulfonate, as a yellow solid. MS (ESI) *m/z* 241.43 [M+1]⁺. ¹H NMR (400 MHz, Chloroform-*d*) δ 7.66 – 7.42 (m, 3H), 7.40 – 7.18 (m, 2H), 4.49 (t, *J* = 6.7 Hz, 2H), 3.16 (t, *J* = 7.1 Hz, 2H), 2.92 (s, 3H). ¹³C NMR (101 MHz, CDCl₃) δ 194.66, 155.26, 142.41, 127.47, 124.61, 122.71, 119.28, 115.14, 111.67, 68.50, 37.44, 24.00.

3-(2-bromoethyl)benzofuran. 252 (WA136/141/189) To a solution of 2-(1-benzofuran-3-yl)ethanol (8.50 g, 52.5 mmol) in anhydrous methylene chloride (100 ml), under argon at 0 °C, was added carbon tetrabromide (43 g, 129 mmol). To the reaction mixture was then added triphenylphosphine (41.24 g, 157 mmol) dropwise over a 30 min. period. The reaction mixture was warmed up to room temperature and left overnight. After evaporation, the residue was purified by chromatography on a silica gel column using ethyl acetate/hexane (3:7) as eluent to afford 9.5 g (80.5%) of 3-(2-bromoethyl)-1-benzofuran as colorless oil. MS (ESI) *m/z* 225.48 [M+1]⁺. ¹H NMR (400 MHz, Chloroform-*d*) δ 7.59 – 7.54 (m, 2H), 7.54 – 7.49 (m, 1H), 7.37 – 7.25 (m, 2H), 3.67 (t, *J* = 7.4 Hz, 2H), 3.29 (td, *J* = 7.3, 1.0 Hz, 2H). ¹³C NMR (101 MHz, CDCl₃) δ 155.28, 142.08, 127.42, 124.49, 122.58, 119.19, 117.52, 111.68, 77.36, 77.04, 76.72, 31.20, 27.58.

3-(benzofuran-3-yl)propanenitrile. 273 (WA147/160/191) To a solution of 3-(2-bromoethyl)-1-benzofuran (1.52 g, 6.75 mmol) in anhydrous dimethylformamide (DMF) (5 mL), under argon at room temperature, was added sodium cyanide (0.66 g, 13.5 mmol). The reaction mixture stirred

at room temperature, and left overnight. The reaction mixture was then poured into water (20 mL) and extracted with ethyl acetate (3x). The organic layer was washed with brine, dried over anhydrous magnesium sulfate, filtered and concentrated. The residue was purified by chromatography on a silica gel column using ethyl acetate/hexane (3:7) as eluent to afford 0.93 g (80 %) of 3-(benzofuran-3-yl)propanenitrile, as colorless oil. MS (ESI) m/z 194.41 $[M+23]^+$. ^1H NMR (400 MHz, Chloroform-*d*) δ 7.58 (s, 1H), 7.53 (dd, $J = 9.5, 7.8$ Hz, 2H), 7.37 – 7.29 (m, 2H), 3.07 (t, $J = 7.3$ Hz, 2H), 2.72 (t, $J = 7.3$ Hz, 2H). ^{13}C NMR (101 MHz, CDCl_3) δ 155.40, 141.95, 126.98, 124.77, 122.76, 119.06, 119.00, 116.96, 111.81, 20.18, 17.71.

3-(benzofuran-3-yl)propanoic acid. 274 (WA148/161/191) To a solution of ethanol (20 ml) and H_2O (35 ml) cooled to 0°C and treated with KOH, 85% (14 g, 0.3 mol) was added 3-(1-benzofuran-3-yl)propanenitrile (0.93 g, 5.4 mmol) and the reaction mixture refluxed for 18 h. The reaction mixture was cooled down to room temperature and poured over ice water. It was then neutralized with concentrated HCl, and extracted with ethyl acetate (3x). The combined organic layer was treated with brine, dried over anhydrous magnesium sulfate, filtered and concentrated. The residue was purified by chromatography on a silica gel column using dichloromethane/methanol (9.5:0.5) as eluent to afford 0.87 g (84.5%) of 3-(1-benzofuran-3-yl)propanoic acid as a white solid. MS (ESI) m/z 213.42 $[M+23]^+$. ^1H NMR (400 MHz, Chloroform-*d*) δ 10.74 (d, $J = 329.3$ Hz, 1H), 7.64 – 7.43 (m, 3H), 7.39 – 7.21 (m, 2H), 3.05 (t, $J = 7.5$ Hz, 2H), 2.80 (t, $J = 7.5$ Hz, 2H). ^{13}C NMR (101 MHz, CDCl_3) δ 179.09, 155.34, 141.41, 127.67, 124.39, 122.46, 119.30, 118.63, 111.56, 33.56, 18.76.

3-(benzofuran-3-yl)propan-1-ol. WA275 (WA149/162/192) To a suspension of LiAlH₄ (0.2 g, 5.2 mmol) in anhydrous THF (25 mL) at 0 °C under argon was added dropwise a solution of 3-(1-benzofuran-3-yl)propanoic acid (0.87 g, 4.6 mmol) in anhydrous THF (5 mL). The reaction mixture was stirred 30 min. at 0 °C, and left overnight at room temperature. The mixture was then cooled with an ice bath and quenched with 2 mL, followed by acidification to 4 pH with 1N HCl. The THF was evaporated, and the residue was extracted with ethyl acetate (3x), treated with brine, dried over anhydrous magnesium sulfate, filtered, and concentrated. The remaining residue was purified by chromatography on a silica gel column using a gradient of dichloromethane/methanol (9.5:0.5) as eluent to give 3 g (70%) of 3-(1-benzofuran-3-yl)propan-1-ol as colorless oil. MS (ESI) *m/z* 176.32 [M]⁺. ¹H NMR (400 MHz, Chloroform-*d*) δ 7.39 (dd, *J* = 11.3, 7.9 Hz, 2H), 7.30 (s, 1H), 7.21 (t, *J* = 7.4 Hz, 1H), 7.11 (t, *J* = 7.4 Hz, 1H), 6.88 (s, 1H), 3.47 (s, 2H), 2.87 (t, *J* = 7.7 Hz, 2H), 2.61 (t, *J* = 7.9 Hz, 2H). ¹³C NMR (101 MHz, CDCl₃) δ 155.21, 141.13, 127.70, 124.24, 122.30, 119.23, 119.04, 111.40, 50.68, 34.68, 19.16.

3-(3-bromopropyl)benzofuran. 276 (WA154/164/197) To a solution of 3-(1-benzofuran-3-yl)propan-1-ol (0.55 g, 3.12 mmol) in anhydrous methylene chloride (15 ml), under argon at 0 °C, was added carbon tetrabromide (1.55 g, 4.7 mmol). To the reaction mixture was then added triphenylphosphine (0.9 g, 3.43 mmol) dropwise over a 30 min. period. The reaction mixture was warmed up to room temperature and left overnight. After evaporation, the residue was purified by chromatography on a silica gel column using ethyl acetate/hexane (3:7) as eluent to afford 0.46 g (61.6%) of 3-(3-bromopropyl)benzofuran, as yellow oil. MS (ESI) *m/z* 240 [M+1]⁺. ¹H NMR (400 MHz, Chloroform-*d*) δ 7.63 – 7.58 (m, 1H), 7.55 – 7.48 (m, 2H), 7.40 – 7.26 (m, 2H), 3.48

(td, $J = 6.4, 1.2$ Hz, 2H), 2.98 – 2.85 (m, 2H), 2.38 – 2.22 (m, 2H). ^{13}C NMR (101 MHz, CDCl_3) δ 155.45, 141.59, 127.93, 124.34, 122.42, 119.51, 118.60, 111.58, 33.18, 31.81, 21.85.

4-(benzofuran-3-yl)butanenitrile. 277 (WA156/165/200) To a solution of 3-(3-bromopropyl)benzofuran (0.46 g, 1.9 mmol) in anhydrous dimethylformamide (DMF) (2 mL), under argon at room temperature, was added sodium cyanide (0.19 g, 3.9 mmol). The reaction mixture stirred at room temperature, and left overnight. The reaction mixture was then poured into water (20 mL) and extracted with ethyl acetate (3x). The organic layer was washed with brine, dried over anhydrous magnesium sulfate, filtered and concentrated. The residue was purified by chromatography on a silica gel column using ethyl acetate/hexane (2:8) as eluent to afford 0.316 g (89 %) of 4-(benzofuran-3-yl)butanenitrile, as colorless oil that was used in the next step without further characterization.

4-(benzofuran-3-yl)butanoic acid. 278 (WA166/158/202) To a solution of ethanol (5 ml) and H_2O (10 ml) cooled to 0°C and treated with KOH, 85% (4.36 g, 92.7 mmol) was added 4-(benzofuran-3-yl)butanenitrile (0.316 g, 1.7 mmol) and the reaction mixture refluxed for 18 h. The reaction mixture was cooled down to room temperature and poured over ice water. It was then neutralized with concentrated HCl, and extracted with ethyl acetate (3x). The combined organic layer was treated with brine, dried over anhydrous magnesium sulfate, filtered and concentrated. The residue was purified by chromatography on a silica gel column using dichloromethane/methanol (9.5:0.5) as eluent to afford 0.316 g (91.8%) of 4-(benzofuran-3-yl)butanoic acid as a yellow solid. MS (ESI) m/z 227.42 $[\text{M}+23]^+$. ^1H NMR (400 MHz, Chloroform- d) δ 10.08 (s, 1H), 7.58 (dd, $J = 7.4, 1.5$ Hz, 1H), 7.52 – 7.42 (m, 2H), 7.35 – 7.22

(m, 2H), 2.78 (t, $J = 7.5$ Hz, 2H), 2.48 (t, $J = 7.3$ Hz, 2H), 2.13 – 2.04 (m, 2H). ^{13}C NMR (101 MHz, CDCl_3) δ 179.91, 155.41, 141.37, 127.96, 124.25, 122.35, 119.55, 119.30, 111.51, 33.47, 23.97, 22.83.

4-(benzofuran-3-yl) butan-1-ol. 279 (WA159/167) To a suspension of LiAlH_4 (0.1 g, 2.63 mmol) in anhydrous THF (25 mL) at 0 °C under argon was added dropwise a solution of 4-(benzofuran-3-yl)butanoic acid (0.5 g, 2.45 mmol) in anhydrous THF (5 mL). The reaction mixture was stirred 30 min. at 0 °C, and left overnight at room temperature. The mixture was then cooled with an ice bath and quenched with 2 mL, followed by acidification to 4 pH with 1N HCl. The THF was evaporated; the residue was extracted with ethyl acetate (3x), treated with brine, dried over anhydrous magnesium sulfate, filtered, and concentrated. The remaining residue was purified by chromatography on a silica gel column using a gradient of dichloromethane/methanol (9.5:0.5) as eluent to give 0.417 g (90%) of 4-(benzofuran-3-yl) butan-1-ol as colorless oil. MS (ESI) m/z 189.36 $[\text{M}-1]^+$. ^1H NMR (400 MHz, Chloroform- d) δ 7.57 (dd, $J = 7.6, 1.4$ Hz, 1H), 7.48 (d, $J = 8.0$ Hz, 1H), 7.43 (d, $J = 4.1$ Hz, 1H), 7.32 – 7.22 (m, 2H), 3.69 (t, $J = 6.4$ Hz, 2H), 2.77 – 2.69 (m, 2H), 1.85 – 1.77 (m, 3H), 1.72 – 1.64 (m, 2H). ^{13}C NMR (101 MHz, CDCl_3) δ 155.36, 141.09, 128.21, 124.09, 122.19, 120.25, 119.58, 111.42, 77.36, 77.04, 76.73, 62.64, 32.44, 25.24, 23.33.

3-(4-bromobutyl)benzofuran. 280 (WA163/168/208) To a solution of 4-(benzofuran-3-yl) butan-1-ol (0.41 g, 2.27 mmol) in anhydrous methylene chloride (15 ml), under argon at 0 °C, was added carbon tetrabromide (3.7 g, 11 mmol). To the reaction mixture was then added triphenylphosphine (1.78 g, 6.8 mmol) dropwise over a 30 min. period. The reaction mixture was

warmed up to room temperature and left overnight. After evaporation, the residue was purified by chromatography on a silica gel column using ethyl acetate/hexane (3:7) as eluent to afford 0.55 g (83%) of 3-(4-bromobutyl)benzofuran, as yellow oil. ^1H NMR (400 MHz, Chloroform-*d*) δ 7.57 (dd, $J = 7.5, 1.4$ Hz, 1H), 7.51 – 7.43 (m, 2H), 7.29 (dtd, $J = 20.9, 7.4, 1.2$ Hz, 2H), 3.47 (t, $J = 6.5$ Hz, 2H), 2.74 (t, $J = 7.0$ Hz, 2H), 2.01 – 1.88 (m, 4H). ^{13}C NMR (101 MHz, CDCl_3) δ 155.39, 141.15, 128.08, 124.20, 122.29, 119.81, 119.54, 111.49, 77.36, 77.05, 76.73, 33.50, 32.34, 27.52, 22.75.

9.2.1 General Procedure for the preparation of (253-266) and (267-272).

2-(benzofuran-3-yl)ethyl methanesulfonate or 3-(2-bromoethyl)-1-benzofuran (1 equiv.) and K_2CO_3 (3 equiv.) was added to 5-10 ml of anhydrous DMF. The mixture was heated at 60°C and an appropriate heterocyclic amine (1.3 equiv.) was added. The mixture was stirred and heated at 60°C for 2-6 h. After completion, the reaction mixture was cooled to room temperature and poured into water, and extracted (3x) with ethyl acetate. The organic layer was washed with brine, dried over sodium sulfate, and concentrated under reduced pressure. The product was purified by column chromatography over silica gel using ethyl acetate/hexanes as an eluent (20:80 to 50:50) to obtain the final compounds in good yields.

1-(2-(benzofuran-3-yl)ethyl)-4-(4-fluorobenzyl)piperazine. (253, WA101) (64%) ^1H NMR (400 MHz, Chloroform-*d*) δ 7.57 (d, $J = 7.3$ Hz, 1H), 7.52 – 7.42 (m, 2H), 7.38 – 7.19 (m, 4H), 7.02 (t, $J = 8.7$ Hz, 2H), 3.49 (d, $J = 13.4$ Hz, 2H), 2.96 – 2.85 (m, 2H), 2.77 – 2.70 (m, 2H), 2.57 (d, $J = 27.7$ Hz, 8H). ^{13}C NMR (101 MHz, CDCl_3) δ 163.22, 160.79, 155.21, 141.42, 133.78, 130.67, 128.17, 124.16, 122.27, 119.51, 118.39, 115.11, 114.90, 111.45, 62.21, 57.89, 53.13, 21.41. MS (ESI) m/z 339.71 $[\text{M}+1]^+$.

1-(2-(benzofuran-3-yl)ethyl)piperazine. 254 (WA102) (73%) ¹H NMR (400 MHz, Chloroform-*d*) δ 7.56 (d, *J* = 7.3 Hz, 1H), 7.51 – 7.42 (m, 2H), 7.33 – 7.20 (m, 2H), 2.95 (t, *J* = 4.8 Hz, 3H), 2.92 – 2.83 (m, 2H), 2.69 (dd, *J* = 9.1, 6.7 Hz, 2H), 2.54 (s, 4H), 2.21 (s, 2H). ¹³C NMR (101 MHz, CDCl₃) δ 155.19, 141.41, 128.15, 124.15, 122.26, 119.49, 118.38, 111.44, 77.37, 77.05, 76.73, 58.47, 54.32, 45.97, 21.17. MS (ESI) *m/z* 231.57 [M+1]⁺.

1-(2-(benzofuran-3-yl)ethyl)-4-(4-methoxyphenyl)piperazine. 255 (WA104)(76%) ¹H NMR (400 MHz, DMSO-*d*₆) δ 8.07 – 8.00 (m, 2H), 7.93 (d, *J* = 3.4 Hz, 1H), 7.80 (d, *J* = 7.8 Hz, 1H), 7.59 (d, *J* = 8.0 Hz, 1H), 7.38 – 7.27 (m, 2H), 7.22 – 7.14 (m, 2H), 4.77 (t, *J* = 12.1 Hz, 2H), 4.59 (t, *J* = 12.1 Hz, 2H), 4.41 (d, *J* = 13.2 Hz, 2H), 4.27 (t, *J* = 12.5 Hz, 4H), 3.85 (s, 3H), 3.46 – 3.27 (m, 2H). ¹³C NMR (101 MHz, DMSO) δ 155.12, 143.60, 141.04, 127.47, 125.23, 123.10, 122.66, 120.38, 115.19, 115.00, 111.92, 66.60, 60.27, 57.67, 56.32, 16.41. MS (ESI) *m/z* 337.61 [M+1]⁺.

1-(2-(benzofuran-3-yl)ethyl)-4-(2-fluorophenyl)piperazine. 256 (WA106) (67%) ¹H NMR (400 MHz, Methanol-*d*₄) δ 7.61 (td, *J* = 5.0, 4.3, 2.7 Hz, 2H), 7.48 – 7.40 (m, 1H), 7.25 (dtd, *J* = 18.3, 7.3, 1.3 Hz, 2H), 7.11 – 6.99 (m, 2H), 6.96 (tdd, *J* = 9.5, 6.0, 2.9 Hz, 2H), 4.38 (t, *J* = 6.6 Hz, 2H), 3.60 – 3.46 (m, 4H), 3.09 – 3.00 (m, 2H), 2.93 (s, 2H), 2.87 (s, 2H). ¹³C NMR (101 MHz, MeOD) δ 156.96, 155.47, 155.34, 154.53, 142.12, 139.76, 139.68, 127.95, 124.36, 124.32, 123.99, 122.91, 122.83, 122.15, 119.22, 119.19, 116.62, 115.67, 115.47, 110.88, 64.63, 50.20, 50.17, 43.60, 22.98. MS (ESI) *m/z* 325.61 [M+1]⁺.

1-(2-(benzofuran-3-yl)ethyl)-4-(3-methoxyphenyl)piperazine. 257 (WA107)(54%) ¹H NMR (400 MHz, DMSO-d₆) δ 8.03 (d, *J* = 9.2 Hz, 2H), 7.92 (s, 1H), 7.80 (d, *J* = 7.6 Hz, 1H), 7.59 (d, *J* = 8.0 Hz, 1H), 7.46 – 7.05 (m, 4H), 4.76 (t, *J* = 9.7 Hz, 2H), 4.59 (t, *J* = 12.7 Hz, 2H), 4.41 (d, *J* = 13.2 Hz, 2H), 4.27 (t, *J* = 12.5 Hz, 3H), 3.85 (s, 3H), 3.58 – 3.18 (m, 2H), 2.49 (s, 1H). ¹³C NMR (101 MHz, DMSO) δ 171.82, 161.20, 155.12, 143.59, 141.04, 136.37, 127.47, 125.22, 123.09, 122.66, 120.38, 115.19, 111.92, 66.60, 60.27, 57.67, 56.32, 16.41. MS (ESI) *m/z* 337.61 [M+1]⁺.

1-(2-(benzofuran-3-yl)ethyl)-4-(cyclohexylmethyl)piperazine. 258 (WA111)(65%) ¹H NMR (400 MHz, Chloroform-*d*) δ 7.56 (d, *J* = 7.5 Hz, 1H), 7.51 – 7.43 (m, 2H), 7.31 – 7.21 (m, 2H), 2.93 – 2.84 (m, 2H), 2.71 (dd, *J* = 9.4, 6.5 Hz, 2H), 2.60 (s, 2H), 2.49 (s, 2H), 2.16 (d, *J* = 7.1 Hz, 2H), 1.83 – 1.63 (m, 6H), 1.50 (ddp, *J* = 11.1, 7.3, 3.8 Hz, 1H), 1.24 – 1.11 (m, 4H), 0.89 (tt, *J* = 12.3, 6.2 Hz, 4H). ¹³C NMR (101 MHz, CDCl₃) δ 155.20, 141.40, 128.18, 124.12, 122.24, 119.52, 118.42, 111.42, 65.67, 57.96, 53.62, 53.19, 35.02, 31.95, 26.81, 26.17, 21.39. MS (ESI) *m/z* 327.55 [M+1]⁺.

1-(2-(benzofuran-3-yl)ethyl)azepane-HCl. 259 (WA123) (89%) ¹H NMR (400 MHz, Chloroform-*d*) δ 7.58 (d, *J* = 7.4 Hz, 1H), 7.54 – 7.41 (m, 2H), 7.26 (dq, *J* = 14.8, 7.1 Hz, 2H), 6.31 (s, 1H), 2.90 (s, 4H), 2.87 – 2.70 (m, 4H), 1.68 (d, *J* = 33.4 Hz, 8H). ¹³C NMR (101 MHz, CDCl₃) δ 155.19, 141.46, 128.18, 124.12, 122.25, 119.53, 118.36, 111.42, 57.52, 55.35, 27.60, 27.00, 21.68. MS (ESI) *m/z* 244.61 [M+1]⁺.

1-(2-(benzofuran-3-yl)ethyl)-4-(4-chlorophenyl)-1,2,3,4-tetrahydropyridine. 260 (WA124) (71%) ¹H NMR (400 MHz, Chloroform-*d*) δ 7.60 (d, *J* = 7.0 Hz, 1H), 7.55 – 7.45 (m, 2H), 7.41

– 7.22 (m, 6H), 6.10 (s, 1H), 3.50 – 3.20 (m, 2H), 3.20 – 2.77 (m, 6H). ¹³C NMR (101 MHz, CDCl₃) δ 155.25, 141.42, 139.16, 136.38, 134.13, 132.75, 128.42, 128.13, 126.20, 124.21, 122.31, 119.49, 118.30, 111.49, 57.66, 53.11, 50.30, 28.03, 21.82. . MS (ESI) *m/z* 338.64 [M+1]⁺.

1-(2-(benzofuran-3-yl)ethyl)-4-(4-fluorophenyl)piperazine. 261 (WA137) (65%) ¹H NMR (400 MHz, Chloroform-d) δ 7.60 (d, *J* = 7.2 Hz, 1H), 7.58 – 7.43 (m, 2H), 7.43 – 7.17 (m, 2H), 7.15 – 6.73 (m, 4H), 3.43 – 2.47 (m, 11H), 2.02 (d, *J* = 29.8 Hz, 1H). ¹³C NMR (101 MHz, CDCl₃) δ 155.22, 141.50, 128.13, 124.21, 122.31, 119.49, 117.83, 115.63, 115.41, 111.49, 57.85, 53.19, 50.16, 21.40. MS (ESI) *m/z* 325.74 [M+1]⁺.

1-(2-(benzofuran-3-yl)ethyl)-4-cyclohexylpiperazine. 262 (WA144) (58%) ¹H NMR (400 MHz, Chloroform-d) δ 7.80 – 7.09 (m, 5H), 3.12 – 2.63 (m, 10H), 2.31 – 1.58 (m, 6H), 1.56 – 1.01 (m, 8H). ¹³C NMR (101 MHz, CDCl₃) δ 155.19, 141.42, 128.04, 124.21, 122.31, 119.44, 118.10, 111.46, 64.26, 57.47, 52.10, 48.65, 28.17, 25.59, 21.33. MS (ESI) *m/z* 313.74 [M+1]⁺.

2-(2-(benzofuran-3-yl)ethyl)-6,7-dimethoxy-1,2,3,4-tetrahydroisoquinoline. 263 (WA181) (55%) ¹H NMR (400 MHz, Methanol-*d*₄) δ 7.67 – 7.59 (m, 2H), 7.51 – 7.39 (m, 1H), 7.33 – 7.19 (m, 2H), 6.69 (d, *J* = 14.0 Hz, 2H), 3.79 (d, *J* = 1.6 Hz, 6H), 3.69 (s, 2H), 3.10 – 2.96 (m, 2H), 2.94 – 2.80 (m, 6H). ¹³C NMR (101 MHz, MeOD) δ 155.41, 147.89, 147.51, 141.55, 127.87, 125.92, 125.86, 123.93, 122.05, 119.13, 117.96, 111.57, 110.83, 109.81, 57.28, 55.10, 55.04, 50.63, 27.73, 20.67. MS (ESI) *m/z* 338.70 [M+1]⁺.

1-(2-(benzofuran-3-yl)ethyl)-4-(2,3-dichlorophenyl)piperazine. 264 (WA183) (72%) ^1H NMR (400 MHz, Methanol- d_4) δ 7.68 – 7.58 (m, 2H), 7.48 – 7.41 (m, 1H), 7.29 – 7.19 (m, 4H), 7.14 – 7.04 (m, 1H), 3.11 (d, $J = 5.2$ Hz, 4H), 3.02 – 2.92 (m, 2H), 2.89 – 2.70 (m, 6H). ^{13}C NMR (101 MHz, MeOD) δ 155.39, 151.04, 141.63, 133.50, 127.85, 127.64, 126.99, 124.48, 123.94, 122.07, 119.11, 118.77, 117.81, 110.84, 57.47, 52.83, 50.56, 20.34. MS (ESI) m/z 413.68 $[\text{M}+39]^+$.

1-(2-(benzofuran-3-yl)ethyl)-4-(4-chlorophenyl)piperazine. 165 (WA184) (66%) ^1H NMR (400 MHz, Chloroform- d) δ 7.72 – 7.57 (m, 1H), 7.58 – 7.45 (m, 2H), 7.37 – 7.20 (m, 4H), 6.87 (d, $J = 8.9$ Hz, 2H), 3.23 (dd, $J = 6.2, 3.7$ Hz, 4H), 3.02 – 2.88 (m, 2H), 2.88 – 2.61 (m, 6H). ^1H NMR (400 MHz, Chloroform- d) δ 7.64 – 7.56 (m, 1H), 7.56 – 7.46 (m, 2H), 7.35 – 7.21 (m, 4H), 6.87 (d, $J = 8.9$ Hz, 2H), 3.23 (dd, $J = 6.2, 3.7$ Hz, 4H), 2.99 – 2.90 (m, 2H), 2.85 – 2.66 (m, 6H). MS (ESI) m/z 341.64 $[\text{M}+1]^+$.

1-(2-(benzofuran-3-yl)ethyl)-4-(pyridin-2-yl)piperazine. 266 (WA193) (69%) ^1H NMR (400 MHz, Chloroform- d) δ 8.20 (d, $J = 5.0$ Hz, 1H), 7.60 – 7.41 (m, 4H), 7.31 – 7.19 (m, 2H), 6.61 (dt, $J = 15.7, 8.9$ Hz, 2H), 3.59 (t, $J = 5.2$ Hz, 4H), 2.93 – 2.87 (m, 2H), 2.76 – 2.69 (m, 2H), 2.65 (t, $J = 5.1$ Hz, 4H). ^{13}C NMR (101 MHz, CDCl_3) δ 159.50, 155.20, 147.94, 141.48, 137.44, 128.16, 124.19, 122.31, 119.53, 118.33, 113.33, 111.46, 107.08, 57.93, 52.98, 45.22, 21.40. MS (ESI) m/z 308.62 $[\text{M}+1]^+$.

1-(2-(benzofuran-3-yl)ethyl)-4-(4-(trifluoromethyl)phenyl)piperazine. 267 (WA196) (55%) ^1H NMR (400 MHz, Chloroform- d) δ 7.75 – 7.43 (m, 5H), 7.30 (dt, $J = 19.8, 7.1$ Hz, 2H), 6.94

(p, $J = 10.3, 9.0$ Hz, 2H), 3.93 – 3.54 (m, 2H), 3.39 – 3.34 (m, 2H), 3.14 – 2.89 (m, 2H), 2.85 – 2.73 (m, 3H), 1.28 (s, 2H). ^{13}C NMR (101 MHz, CDCl_3) δ 155.25, 153.17, 141.51, 128.04, 126.38, 124.28, 122.37, 119.47, 118.05, 115.08, 114.59, 111.52, 57.66, 52.69, 47.77, 21.15. MS (ESI) m/z 375.61 $[\text{M}+1]^+$.

4-(2-(benzofuran-3-yl)ethyl)piperazin-2-one. 268 (WA199) (88%) ^1H NMR (400 MHz, $\text{DMSO-}d_6$) δ 7.80 (s, 1H), 7.65 (dd, $J = 7.5, 1.4$ Hz, 1H), 7.52 (d, $J = 8.0$ Hz, 1H), 7.26 (dtd, $J = 20.4, 7.3, 1.3$ Hz, 2H), 3.15 (dd, $J = 6.3, 4.5$ Hz, 2H), 3.01 (s, 2H), 2.88 – 2.79 (m, 2H), 2.72 – 2.60 (m, 4H), 1.98 (s, 1H). ^{13}C NMR (101 MHz, DMSO) δ 168.12, 154.96, 142.65, 128.35, 124.64, 122.83, 120.30, 118.59, 111.68, 57.15, 56.54, 49.12, 40.71, 21.03. MS (ESI) m/z 245.52 $[\text{M}+1]^+$.

1-(2-(benzofuran-3-yl)ethyl)-4-(pyridin-4-yl)piperazine. 269 (WA204) (73%) ^1H NMR (400 MHz, $\text{Methanol-}d_4$) δ 8.14 (s, 1H), 7.68 – 7.57 (m, 2H), 7.44 (d, $J = 8.1$ Hz, 1H), 7.32 – 7.19 (m, 2H), 6.91 – 6.81 (m, 2H), 3.50 – 3.39 (m, 4H), 2.98 – 2.88 (m, 2H), 2.80 – 2.71 (m, 2H), 2.67 (dd, $J = 6.6, 3.3$ Hz, 4H). ^{13}C NMR (101 MHz, MeOD) δ 155.55, 155.36, 148.03, 141.63, 127.92, 123.93, 122.06, 119.13, 117.99, 110.84, 57.43, 52.22, 45.20, 20.55. MS (ESI) m/z 308.61 $[\text{M}+1]^+$.

1-(2-(benzofuran-3-yl)ethyl)-4-phenethylpiperazine. 270 (WA205) (74%) ^1H NMR (400 MHz, $\text{Chloroform-}d$) δ 7.58 (d, $J = 7.5$ Hz, 1H), 7.55 – 7.44 (m, 2H), 7.34 – 7.20 (m, 7H), 2.98 – 2.88 (m, 2H), 2.88 – 2.82 (m, 2H), 2.81 – 2.47 (m, 12H). ^{13}C NMR (101 MHz, CDCl_3) δ 155.22, 141.44, 140.29, 128.70, 128.40, 128.18, 126.06, 124.16, 122.28, 119.52, 118.40, 111.46, 60.53,

57.92, 53.21, 53.17, 33.62, 21.42. MS (ESI) m/z 335.67 [M+1]⁺.

1'-(2-(benzofuran-3-yl)ethyl)-3*H*-spiro[isobenzofuran-1,4'-piperidine]. 271(WA207) (77%)

¹H NMR (400 MHz, Chloroform-*d*) δ 7.67 – 7.56 (m, 1H), 7.56 – 7.44 (m, 2H), 7.36 – 7.15 (m, 6H), 5.10 (s, 2H), 3.07 – 2.92 (m, 4H), 2.89 – 2.79 (m, 2H), 2.58 (td, J = 12.1, 11.5, 2.6 Hz, 2H), 2.09 (td, J = 13.3, 4.5 Hz, 2H), 1.89 – 1.81 (m, 2H). ¹³C NMR (101 MHz, CDCl₃) δ 155.26, 145.50, 141.42, 138.90, 128.17, 127.65, 127.41, 124.19, 122.31, 121.08, 120.83, 119.55, 118.39, 111.47, 84.57, 70.79, 58.22, 50.17, 36.58, 21.47. MS (ESI) m/z 334.65 [M+1]⁺.

1-(2-(benzofuran-3-yl)ethyl)-4-(4-nitrophenyl)piperazine. 272 (WA210) (83%)

¹H NMR (400 MHz, DMSO-*d*₆) δ 8.11 – 8.00 (m, 2H), 7.84 (s, 1H), 7.72 – 7.62 (m, 1H), 7.54 (d, J = 7.9 Hz, 1H), 7.34 – 7.22 (m, 2H), 6.98 (dd, J = 10.0, 3.4 Hz, 2H), 4.31 (t, J = 6.6 Hz, 2H), 3.45 (d, J = 12.5 Hz, 8H), 3.00 (t, J = 6.6 Hz, 2H). ¹³C NMR (101 MHz, DMSO) δ 154.98, 154.83, 143.14, 137.47, 128.22, 126.15, 124.79, 122.96, 120.20, 117.00, 113.08, 111.75, 64.55, 46.26, 43.04, 23.41. MS (ESI) m/z 353.72;355.77 [M+2, M+4]⁺.

9.2.2 General Procedure for the preparation of (281-314).

3-(4-bromobutyl)-1-benzofuran (**280**) (1 equiv.) and anhydrous potassium carbonate (3 equiv.) was added to 5-10 ml of anhydrous DMF. The mixture was heated at 60⁰C and an appropriate heterocyclic amine (1.3 equiv.) was added. The mixture was stirred and heated at 60⁰C for 2-6 h. After completion, the reaction mixture was cooled to room temperature and poured into water, and extracted (3x) with ethyl acetate. The organic layer was washed with brine, dried over sodium sulfate, and concentrated under reduced pressure. The product was purified by column chromatography over silica gel using ethyl acetate/hexanes as the eluent (20:80 to 50:50) to

obtain the final compounds in good yields.

2-(4-(benzofuran-3-yl)butyl)-6,7-dimethoxy-1,2,3,4-tetrahydroisoquinoline. (281, WA169)

(66%) ^1H NMR (400 MHz, Chloroform-*d*) δ 7.56 (d, $J = 7.4$ Hz, 1H), 7.52 – 7.40 (m, 2H), 7.35 – 7.17 (m, 2H), 6.63 – 6.50 (m, 2H), 3.86 (s, 6H), 3.55 (s, 2H), 2.86 – 2.80 (m, 2H), 2.72 (dt, $J = 11.4, 6.5$ Hz, 4H), 2.56 (d, $J = 7.0$ Hz, 2H), 1.76 (dt, $J = 32.2, 6.9$ Hz, 4H). ^{13}C NMR (101 MHz, CDCl_3) δ 155.36, 147.48, 147.17, 141.08, 136.38, 128.26, 126.62, 126.20, 124.04, 122.15, 120.31, 119.62, 111.39, 109.49, 58.07, 55.92, 55.81, 51.09, 28.67, 27.04, 26.92, 23.50. MS (ESI) m/z 366.72 $[\text{M}+1]^+$.

1-(4-(benzofuran-3-yl)butyl)-4-cyclohexylpiperazine. 282 (WA170) (66%)

^1H NMR (400 MHz, Chloroform-*d*) δ 7.55 (d, $J = 7.6$ Hz, 1H), 7.46 (d, $J = 8.0$ Hz, 1H), 7.40 (s, 1H), 7.32 – 7.18 (m, 2H), 2.80 – 2.26 (m, 12H), 2.02 – 1.55 (m, 9H), 1.39 – 1.21 (m, 4H), 1.22 – 1.02 (m, 2H). ^{13}C NMR (101 MHz, CDCl_3) δ 155.35, 141.05, 136.38, 124.04, 122.14, 120.24, 119.58, 111.40, 63.76, 58.25, 53.11, 48.71, 28.66, 26.93, 26.56, 26.13, 25.77, 23.45. MS (ESI) m/z 341.76 $[\text{M}+1]^+$.

1-(4-(benzofuran-3-yl)butyl)-4-(4-fluorophenyl)piperazine. 283 (WA171) (68%)

^1H NMR (400 MHz, Chloroform-*d*) δ 7.57 (d, $J = 7.5$ Hz, 1H), 7.53 – 7.40 (m, 2H), 7.40 – 7.20 (m, 2H), 7.15 – 6.74 (m, 4H), 3.34 – 3.03 (m, 4H), 2.73 (t, $J = 7.4$ Hz, 2H), 2.72 – 2.54 (m, 4H), 2.57 – 2.34 (m, 2H), 1.78 (dt, $J = 15.1, 7.4$ Hz, 2H), 1.74 – 1.59 (m, 2H). ^{13}C NMR (101 MHz, CDCl_3) δ 158.31, 155.37, 148.01, 141.06, 128.23, 124.07, 122.16, 120.28, 119.59, 117.78, 117.71, 115.58, 115.36, 111.43, 58.32, 53.28, 50.15, 26.92, 26.66, 23.48. MS (ESI) m/z 353.62 $[\text{M}+1]^+$.

1-(4-(benzofuran-3-yl)butyl)-4-(4-methoxyphenyl)piperazine. 284 (WA172) (64%) ¹H NMR (400 MHz, DMSO-*d*₆) δ 7.82 (s, 1H), 7.65 (d, *J* = 7.4 Hz, 1H), 7.53 (d, *J* = 8.0 Hz, 1H), 7.27 (dt, *J* = 21.6, 7.3 Hz, 2H), 7.10 (d, *J* = 8.5 Hz, 2H), 6.90 (d, *J* = 8.6 Hz, 2H), 3.70 (s, 3H), 3.61 (dd, *J* = 28.4, 12.2 Hz, 4H), 3.43 – 3.27 (m, 2H), 3.27 – 3.02 (m, 4H), 2.70 (t, *J* = 7.4 Hz, 2H), 1.83 (dd, *J* = 10.2, 5.8 Hz, 2H), 1.72 (q, *J* = 7.4 Hz, 2H). ¹³C NMR (101 MHz, DMSO) δ 155.12, 142.49, 128.21, 124.70, 122.86, 120.24, 119.90, 119.37, 115.03, 111.75, 55.77, 55.42, 50.60, 47.87, 26.10, 23.17, 22.73. MS (ESI) *m/z* 365.66 [M+1]⁺.

2-(4-(benzofuran-3-yl)butyl)-1,2,3,4-tetrahydroisoquinoline. 285 (WA173) (69%) ¹H NMR (400 MHz, Chloroform-*d*) δ 7.59 (d, *J* = 7.5 Hz, 1H), 7.53 – 7.41 (m, 2H), 7.28 (dt, *J* = 24.0, 7.2 Hz, 2H), 7.18 – 7.08 (m, 3H), 7.06 – 6.99 (m, 1H), 3.65 (s, 2H), 2.93 (t, *J* = 5.5 Hz, 2H), 2.74 (s, 4H), 2.61 – 2.51 (m, 2H), 1.87 – 1.68 (m, 4H). ¹³C NMR (101 MHz, CDCl₃) δ 155.39, 141.09, 134.86, 134.35, 128.64, 128.28, 126.59, 126.07, 125.56, 124.06, 122.17, 120.36, 119.64, 111.42, 58.18, 56.26, 51.03, 29.14, 27.04, 26.96, 23.52. MS (ESI) *m/z* 306.61 [M+1]⁺.

1-(4-(benzofuran-3-yl)butyl)-4-(2,4-difluorophenyl)piperazine. 286 (WA174) (45%) ¹H NMR (400 MHz, Chloroform-*d*) δ 7.57 (d, *J* = 7.3 Hz, 1H), 7.54 – 7.38 (m, 2H), 7.38 – 7.17 (m, 2H), 7.09 – 6.72 (m, 3H), 3.20 – 2.96 (m, 4H), 2.73 (t, *J* = 7.4 Hz, 2H), 2.63 (s, 4H), 2.55 – 2.38 (m, 2H), 1.78 (dt, *J* = 15.2, 7.5 Hz, 2H), 1.65 (q, *J* = 14.6, 11.2 Hz, 2H). ¹³C NMR (101 MHz, CDCl₃) δ 159.11, 156.70, 155.38, 154.31, 141.07, 136.71, 128.24, 124.07, 122.17, 120.29, 119.60, 119.34, 110.76, 110.55, 110.52, 104.90, 104.64, 104.39, 58.34, 53.30, 50.93, 50.90, 26.92, 26.66, 23.48. MS (ESI) *m/z* 371.59 [M+1]⁺.

1-(4-(benzofuran-3-yl)butyl)-6-methoxy-1,2,3,4-tetrahydroquinoline. 287 (WA175) (57%)

^1H NMR (400 MHz, Chloroform-*d*) δ 7.59 (dd, $J = 7.3, 1.6$ Hz, 1H), 7.55 – 7.47 (m, 1H), 7.44 (t, $J = 1.3$ Hz, 1H), 7.37 – 7.21 (m, 2H), 6.68 (dd, $J = 8.9, 3.1$ Hz, 1H), 6.62 (d, $J = 3.0$ Hz, 1H), 6.55 (d, $J = 8.9$ Hz, 1H), 3.77 (s, 3H), 3.44 – 3.10 (m, 4H), 2.76 (q, $J = 7.5, 7.0$ Hz, 4H), 2.04 – 1.90 (m, 2H), 1.88 – 1.62 (m, 4H). ^{13}C NMR (101 MHz, CDCl_3) δ 155.40, 150.61, 141.10, 140.03, 128.24, 124.10, 123.89, 122.21, 120.32, 119.61, 115.35, 112.47, 111.89, 111.46, 55.84, 51.90, 49.46, 28.39, 26.81, 26.11, 23.56, 22.49. MS (ESI) m/z 336.68 $[\text{M}+1]^+$.

1-(4-(benzofuran-3-yl)butyl)-1,2,3,4-tetrahydroquinoline-HCl. 288 (WA176) (68%)

^1H NMR (400 MHz, Chloroform-*d*) δ 14.22 (s, 1H), 7.67 (d, $J = 8.0$ Hz, 1H), 7.49 (d, $J = 7.7$ Hz, 1H), 7.44 (d, $J = 8.1$ Hz, 1H), 7.40 (s, 1H), 7.34 – 7.25 (m, 3H), 7.25 – 7.16 (m, 2H), 3.64 – 3.45 (m, 2H), 3.45 – 3.20 (m, 2H), 2.91 (t, $J = 6.6$ Hz, 2H), 2.73 (t, $J = 7.4$ Hz, 2H), 2.27 – 2.10 (m, 2H), 2.11 – 1.88 (m, 2H), 1.86 – 1.68 (m, 2H). ^{13}C NMR (101 MHz, CDCl_3) δ 155.33, 141.29, 136.00, 130.59, 130.38, 129.31, 127.80, 124.28, 124.06, 122.36, 119.41, 119.28, 111.51, 58.29, 48.07, 26.27, 24.65, 24.18, 23.03, 16.23. MS (ESI) m/z 306.54 $[\text{M}+1]^+$.

1-(4-(benzofuran-3-yl)butyl)-4-(4-(trifluoromethyl)phenyl)piperazine. 289 (WA177) (51%)

^1H NMR (400 MHz, Chloroform-*d*) δ 7.54 – 7.40 (m, 5H), 7.34 – 7.20 (m, 2H), 6.90 (d, $J = 8.4$ Hz, 2H), 3.69 (s, 4H), 3.51 – 3.33 (m, 2H), 3.06 (s, 2H), 2.89 (s, 2H), 2.73 (t, $J = 6.7$ Hz, 2H), 1.88 (s, 2H), 1.29 (d, $J = 11.4$ Hz, 2H). ^{13}C NMR (101 MHz, CDCl_3) δ 155.38, 151.60, 141.32, 127.77, 126.73, 126.69, 124.37, 122.43, 119.39, 119.14, 115.81, 111.56, 56.86, 51.26, 45.80, 25.94, 23.25, 22.93. MS (ESI) m/z 403.56 $[\text{M}+1]^+$.

1-(4-(benzofuran-3-yl)butyl)-4-(4-fluorophenyl)-1,2,3,4-tetrahydropyrazine. 290 (WA178)

(79%) ^1H NMR (400 MHz, Chloroform-*d*) δ 7.56 (t, $J = 12.1$ Hz, 1H), 7.45 (q, $J = 15.2, 11.6$ Hz, 2H), 7.39 – 7.21 (m, 4H), 7.01 (t, $J = 8.5$ Hz, 2H), 6.00 (d, $J = 3.8$ Hz, 1H), 3.15 (q, $J = 3.1$ Hz, 1H), 2.90 – 2.59 (m, 4H), 2.60 – 2.40 (m, 4H), 1.78 (dq, $J = 19.3, 11.8, 9.6$ Hz, 2H), 1.67 (dt, $J = 18.2, 9.4$ Hz, 2H). ^{13}C NMR (101 MHz, CDCl_3) δ 155.37, 141.08, 136.37, 134.11, 128.26, 126.47, 126.39, 124.06, 122.16, 121.75, 120.31, 119.61, 115.13, 114.92, 111.41, 58.14, 53.27, 50.37, 28.26, 27.00, 23.51. MS (ESI) m/z 350.68; 350.55 [M, M+1] $^+$.

1-(4-(benzofuran-3-yl)butyl)-4-(pyridin-2-yl)piperazine. 291 (WA179) (61%)

^1H NMR (400 MHz, Chloroform-*d*) δ 8.21 (d, $J = 4.9$ Hz, 1H), 7.56 (d, $J = 7.5$ Hz, 1H), 7.52 – 7.39 (m, 3H), 7.32 – 7.20 (m, 2H), 6.63 (t, $J = 8.1$ Hz, 2H), 3.57 (t, $J = 4.9$ Hz, 4H), 2.72 (t, $J = 7.4$ Hz, 2H), 2.58 (t, $J = 5.0$ Hz, 4H), 2.46 (t, $J = 7.6$ Hz, 2H), 1.77 (p, $J = 7.4$ Hz, 2H), 1.66 (q, $J = 8.0$ Hz, 2H). ^{13}C NMR (101 MHz, CDCl_3) δ 159.51, 155.38, 147.91, 141.08, 137.48, 128.23, 124.09, 122.20, 120.26, 119.61, 113.34, 111.43, 107.12, 58.53, 58.38, 53.03, 46.13, 45.14, 26.92, 26.52, 24.70, 23.47, 1.06. MS (ESI) m/z 336.57 [M+1] $^+$.

1-(4-(benzofuran-3-yl)butyl)-4-(pyridin-4-yl)piperazine. 292 (WA211) (76%)

^1H NMR (400 MHz, Methanol-*d*₄) δ 8.12 (d, $J = 6.7$ Hz, 2H), 7.63 – 7.49 (m, 2H), 7.42 (d, $J = 7.8$ Hz, 1H), 7.32 – 7.16 (m, 2H), 7.00 (d, $J = 6.7$ Hz, 2H), 3.64 – 3.48 (m, 4H), 2.71 (t, $J = 7.4$ Hz, 2H), 2.66 – 2.51 (m, 4H), 2.46 (dd, $J = 8.7, 6.4$ Hz, 2H), 1.75 (p, $J = 7.4$ Hz, 2H), 1.68 – 1.56 (m, 2H). ^{13}C NMR (101 MHz, MeOD) δ 156.43, 155.44, 142.76, 141.28, 128.07, 123.85, 121.99, 120.10, 119.31, 110.84, 107.64, 57.50, 52.04, 45.30, 26.52, 25.69, 22.77. MS (ESI) m/z 336.63 [M+1] $^+$.

1-(4-(benzofuran-3-yl)butyl)-4-(3-fluorophenyl)piperazine. 293 (WA212) (76%) ^1H NMR (400 MHz, Methanol- d_4) δ 7.56 (dd, $J = 7.2, 1.6$ Hz, 1H), 7.51 (s, 1H), 7.42 (d, $J = 8.0$ Hz, 1H), 7.30 – 7.11 (m, 3H), 6.73 – 6.57 (m, 2H), 6.50 (td, $J = 8.3, 2.5$ Hz, 1H), 3.12 (dd, $J = 6.4, 3.8$ Hz, 4H), 2.70 (t, $J = 7.4$ Hz, 2H), 2.60 – 2.46 (m, 4H), 2.44 – 2.31 (m, 2H), 1.72 (p, $J = 7.3$ Hz, 2H), 1.59 (tt, $J = 10.1, 5.8$ Hz, 2H). ^{13}C NMR (101 MHz, MeOD) δ 165.02, 162.62, 155.47, 153.04, 152.94, 141.20, 129.92, 129.82, 128.08, 123.81, 121.95, 120.10, 119.28, 110.98, 110.96, 110.83, 105.34, 105.12, 102.23, 101.98, 57.95, 52.64, 47.90, 26.70, 25.78, 22.83. MS (ESI) m/z 353.72 $[\text{M}+1]^+$.

1-(4-(benzofuran-3-yl)butyl)-4-(2-fluorophenyl)piperazine-2HCl. 294 (WA213) (68%) ^1H NMR (400 MHz, DMSO- d_6) δ 11.32 (s, 1H), 7.83 (s, 1H), 7.68 – 7.61 (m, 1H), 7.53 (d, $J = 8.0$ Hz, 1H), 7.34 – 7.20 (m, 2H), 7.20 – 7.10 (m, 2H), 7.05 (ddt, $J = 15.3, 7.6, 6.0$ Hz, 2H), 5.38 (s, 1H), 3.52 (d, $J = 11.6$ Hz, 2H), 3.45 (d, $J = 12.2$ Hz, 2H), 3.24 (t, $J = 12.2$ Hz, 2H), 3.15 (td, $J = 13.9, 11.9, 7.6$ Hz, 4H), 2.70 (t, $J = 7.3$ Hz, 2H), 1.90 – 1.77 (m, 2H), 1.72 (q, $J = 7.3$ Hz, 2H). ^{13}C NMR (101 MHz, DMSO) δ 156.49, 155.12, 154.06, 142.51, 138.80, 138.71, 128.21, 125.44, 125.41, 124.70, 123.86, 123.78, 122.86, 120.23, 119.99, 119.97, 119.87, 116.69, 116.49, 111.75, 55.58, 51.20, 47.33, 47.30, 26.12, 23.12, 22.73. MS (ESI) m/z 353.69 $[\text{M}+1]^+$.

1-(4-(benzofuran-3-yl)butyl)-4-(cyclohexylmethyl)piperazine. 295 (WA214) (82%) ^1H NMR (400 MHz, Methanol- d_4) δ 7.60 – 7.52 (m, 2H), 7.43 (d, $J = 7.9$ Hz, 1H), 7.29 – 7.19 (m, 2H), 2.73 (t, $J = 7.3$ Hz, 2H), 2.58 (s, 3H), 2.50 – 2.41 (m, 4H), 2.18 (d, $J = 6.9$ Hz, 2H), 1.86 – 1.45 (m, 12H), 1.38 – 1.13 (m, 4H), 0.91 (td, $J = 11.8, 3.0$ Hz, 2H). ^{13}C NMR (101 MHz, MeOD) δ

155.48, 141.23, 128.02, 123.78, 121.91, 119.99, 119.22, 110.77, 65.14, 57.80, 52.52, 52.23, 34.60, 31.56, 26.64, 26.32, 25.74, 25.49, 22.75. MS (ESI) m/z 355.77 [M+1]⁺.

1-(4-(benzofuran-3-yl)butyl)-4-(3-methoxyphenyl)piperazine. 296 (WA215) (63%) ¹H NMR (400 MHz, Methanol-*d*₄) δ 7.60 – 7.49 (m, 2H), 7.47 – 7.39 (m, 1H), 7.23 (dtd, $J = 19.2, 7.3, 1.3$ Hz, 2H), 7.11 (t, $J = 8.1$ Hz, 1H), 6.53 – 6.40 (m, 3H), 3.73 (d, $J = 4.1$ Hz, 3H), 3.15 – 3.09 (m, 4H), 2.76 – 2.67 (m, 2H), 2.62 – 2.51 (m, 4H), 2.44 – 2.35 (m, 2H), 1.79 – 1.67 (m, 2H), 1.65 – 1.54 (m, 2H). ¹³C NMR (101 MHz, MeOD) δ 160.64, 155.47, 152.53, 141.22, 129.36, 128.07, 123.81, 121.95, 120.09, 119.28, 110.81, 108.64, 104.61, 102.28, 57.98, 54.18, 52.78, 48.52, 26.72, 25.75, 22.82. MS (ESI) m/z 365.62 [M+1]⁺.

1-(4-(benzofuran-3-yl)butyl)-4-(2,3-dichlorophenyl)piperazine. 297 (WA216) (68%) ¹H NMR (400 MHz, Methanol-*d*₄) δ 7.62 – 7.51 (m, 2H), 7.46 – 7.40 (m, 1H), 7.28 – 7.18 (m, 4H), 7.05 (td, $J = 6.3, 3.1$ Hz, 1H), 3.08 – 2.99 (m, 4H), 2.76 – 2.71 (m, 2H), 2.69 – 2.54 (m, 4H), 2.49 – 2.41 (m, 2H), 1.76 (p, $J = 7.3$ Hz, 2H), 1.69 – 1.58 (m, 2H). ¹³C NMR (101 MHz, MeOD) δ 155.48, 151.11, 141.21, 133.47, 128.06, 127.60, 124.38, 123.77, 121.91, 120.08, 119.24, 118.71, 110.78, 58.03, 52.93, 50.57, 26.75, 25.79, 22.82. MS (ESI) m/z 403.57 [M+1]⁺.

1-(4-(benzofuran-3-yl)butyl)-4-phenethylpiperazine. 298 (WA217) (78%) ¹H NMR (400 MHz, Methanol-*d*₄) δ 7.64 – 7.50 (m, 2H), 7.42 (d, $J = 8.2$ Hz, 1H), 7.30 – 7.17 (m, 7H), 2.85 – 2.78 (m, 2H), 2.72 (t, $J = 7.3$ Hz, 2H), 2.58 (ddq, $J = 24.6, 11.1, 6.1$ Hz, 8H), 2.52 – 2.38 (m, 4H), 1.74 (p, $J = 7.4$ Hz, 2H), 1.68 – 1.54 (m, 2H). ¹³C NMR (101 MHz, MeOD) δ 155.47, 141.23, 139.69, 128.27, 128.10, 125.81, 123.79, 121.93, 120.04, 119.24, 110.79, 59.95, 57.85,

52.27, 52.15, 32.58, 26.68, 25.65, 22.77. MS (ESI) m/z 363.66 $[M+1]^+$.

4-(4-(benzofuran-3-yl)butyl)piperazin-2-one. 299 (WA218) (70%) ^1H NMR (400 MHz, $\text{DMSO-}d_6$) δ 7.76 (s, 1H), 7.70 (s, 1H), 7.62 (dd, $J = 7.5, 1.4$ Hz, 1H), 7.52 (d, $J = 8.1$ Hz, 1H), 7.33 – 7.19 (m, 2H), 3.11 (t, $J = 5.3$ Hz, 2H), 2.87 (s, 2H), 2.65 (t, $J = 7.5$ Hz, 2H), 2.48 (s, 2H), 2.36 (t, $J = 7.2$ Hz, 2H), 1.66 (p, $J = 7.5$ Hz, 2H), 1.50 (p, $J = 7.4$ Hz, 2H). ^{13}C NMR (101 MHz, DMSO) δ 168.21, 155.11, 142.24, 128.35, 124.61, 122.79, 120.46, 120.23, 111.70, 57.36, 56.85, 49.19, 40.80, 26.70, 26.24, 23.04. MS (ESI) m/z 373.59 $[M+1]^+$.

1'-(4-(benzofuran-3-yl)butyl)-3*H*-spiro[isobenzofuran-1,4'-piperidine]. 300 (WA220) (91%) ^1H NMR (400 MHz, $\text{Methanol-}d_4$) δ 7.64 – 7.55 (m, 2H), 7.44 (dd, $J = 7.8, 1.3$ Hz, 1H), 7.32 – 7.18 (m, 6H), 4.87 (s, 2H), 3.21 – 3.10 (m, 2H), 2.88 – 2.72 (m, 6H), 2.10 (td, $J = 13.7, 4.6$ Hz, 2H), 1.85 – 1.71 (m, 6H). ^{13}C NMR (101 MHz, MeOD) δ 155.50, 144.15, 141.35, 138.69, 127.97, 127.76, 127.23, 123.84, 121.97, 120.90, 120.30, 119.79, 119.22, 110.80, 83.15, 70.45, 57.48, 49.56, 34.67, 26.41, 24.94, 22.64. MS (ESI) m/z 362.88 $[M+1]^+$.

1-(4-(benzofuran-3-yl)butyl)-3,5-dimethylpiperazine. 301 (WA221) (84%) ^1H NMR (400 MHz, $\text{Methanol-}d_4$) δ 7.64 – 7.51 (m, 2H), 7.43 (d, $J = 8.0$ Hz, 1H), 7.33 – 7.18 (m, 2H), 3.16 – 2.99 (m, 2H), 2.98 – 2.85 (m, 2H), 2.73 (dt, $J = 14.4, 7.4$ Hz, 2H), 2.55 – 2.38 (m, 2H), 1.97 – 1.49 (m, 7H), 1.16 (t, $J = 5.7$ Hz, 6H). ^1H NMR (400 MHz, $\text{DMSO-}d_6$) δ 9.69 (s, 1H), 7.90 (d, $J = 5.7$ Hz, 1H), 7.78 (d, $J = 7.5$ Hz, 1H), 7.56 (d, $J = 8.0$ Hz, 1H), 7.30 (dt, $J = 20.8, 7.4$ Hz, 2H), 3.78 (s, 2H), 3.76 – 3.53 (m, 6H), 3.43 (dd, $J = 18.3, 10.3$ Hz, 4H), 3.32 – 3.16 (m, 4H), 2.37 – 2.08 (m, 2H). ^{13}C NMR (101 MHz, MeOD) δ 155.48, 141.28, 128.05, 123.81, 121.95, 120.06,

119.29, 110.81, 57.59, 57.38, 50.72, 48.27, 48.06, 47.85, 47.63, 47.42, 47.21, 46.99, 26.39, 25.50, 22.75, 16.55. MS (ESI) m/z 287.63 $[M+1]^+$.

1-(4-(benzofuran-3-yl)butyl)azepane. 302 (WA222) (65%) ^1H NMR (400 MHz, Methanol- d_4) δ 7.63 – 7.53 (m, 2H), 7.43 (dd, $J = 7.8, 1.2$ Hz, 1H), 7.25 (dtd, $J = 20.5, 7.3, 1.3$ Hz, 2H), 3.04 – 2.96 (m, 4H), 2.87 (dd, $J = 9.0, 6.3$ Hz, 2H), 2.76 (t, $J = 6.6$ Hz, 2H), 1.85 – 1.71 (m, 8H), 1.67 (p, $J = 2.8$ Hz, 4H). ^{13}C NMR (101 MHz, MeOD) δ 155.51, 141.33, 127.95, 123.84, 121.95, 119.74, 119.18, 110.78, 57.35, 54.79, 26.26, 26.23, 24.88, 24.76, 22.57. MS (ESI) m/z 272.64 $[M+1]^+$.

1-(4-(benzofuran-3-yl)butyl)-1,4-diazepane. 303 (WA223) (87%) ^1H NMR (400 MHz, Methanol- d_4) δ 7.63 – 7.50 (m, 2H), 7.48 – 7.39 (m, 1H), 7.24 (dtd, $J = 20.4, 7.3, 1.3$ Hz, 2H), 4.91 (s, 1H), 3.00 – 2.89 (m, 4H), 2.81 – 2.64 (m, 6H), 2.58 – 2.48 (m, 2H), 1.87 – 1.78 (m, 2H), 1.78 – 1.66 (m, 2H), 1.64 – 1.52 (m, 2H). ^{13}C NMR (101 MHz, MeOD) δ 155.47, 141.20, 128.06, 123.77, 121.90, 120.12, 119.23, 110.77, 57.61, 55.41, 54.16, 46.37, 45.72, 27.51, 26.64, 26.39, 22.80. MS (ESI) m/z 273.66 $[M+1]^+$.

1-(4-(benzofuran-3-yl)butyl)piperazine. 304 (WA224) (78%) ^1H NMR (400 MHz, Methanol- d_4) δ 7.62 – 7.51 (m, 2H), 7.43 (d, $J = 8.0$ Hz, 1H), 7.30 – 7.18 (m, 2H), 2.84 (t, $J = 5.0$ Hz, 4H), 2.71 (t, $J = 7.4$ Hz, 2H), 2.53 – 2.32 (m, 6H), 1.74 (q, $J = 7.5$ Hz, 2H), 1.60 (td, $J = 8.5, 4.2$ Hz, 2H). ^{13}C NMR (101 MHz, MeOD) δ 155.47, 141.20, 128.05, 123.76, 121.89, 120.07, 119.22, 110.76, 58.53, 53.18, 48.02, 44.52, 26.71, 25.50, 22.78. MS (ESI) m/z 259.67 $[M+1]^+$.

1-(4-(benzofuran-3-yl)butyl)-4-(4-fluorobenzyl)piperazine. 305 (WA225) (90%) ^1H NMR (400 MHz, Methanol- d_4) δ 7.62 – 7.52 (m, 2H), 7.42 (d, $J = 7.9$ Hz, 1H), 7.34 (ddd, $J = 8.5, 5.5, 2.7$ Hz, 2H), 7.27 – 7.17 (m, 2H), 7.10 – 7.02 (m, 2H), 3.56 (s, 2H), 2.99 – 2.54 (m, 10H), 1.83 – 1.61 (m, 4H). ^{13}C NMR (101 MHz, MeOD) δ 155.46, 141.38, 132.56, 130.96, 130.88, 127.94, 123.88, 122.01, 119.73, 119.26, 114.81, 114.59, 110.83, 60.82, 57.02, 51.98, 50.52, 26.16, 24.47, 22.57. MS (ESI) m/z 367.61 $[\text{M}+1]^+$.

1-(4-(benzofuran-3-yl)butyl)-4-(4-chlorophenyl)piperazine. 306 (WA226) (75%) ^1H NMR (400 MHz, Methanol- d_4) δ 7.62 – 7.52 (m, 2H), 7.43 (d, $J = 8.0$ Hz, 1H), 7.29 – 7.16 (m, 4H), 6.90 (td, $J = 6.9, 2.9$ Hz, 2H), 3.14 (q, $J = 5.8, 5.0$ Hz, 4H), 2.73 (t, $J = 7.4$ Hz, 2H), 2.63 – 2.53 (m, 4H), 2.49 – 2.38 (m, 2H), 1.76 (p, $J = 7.3$ Hz, 2H), 1.62 (ddd, $J = 15.4, 9.2, 5.9$ Hz, 2H). ^{13}C NMR (101 MHz, MeOD) δ 155.49, 149.94, 141.22, 128.43, 123.77, 121.91, 120.08, 119.23, 117.07, 110.77, 57.99, 52.72, 48.39, 48.24, 48.03, 47.81, 47.60, 47.39, 47.18, 46.96, 26.73, 25.76, 22.79. MS (ESI) m/z 369.56 $[\text{M}+1]^+$.

1-(4-(benzofuran-3-yl)butyl)-4-(4-nitrophenyl)piperazine. 307 (WA227) (80%) ^1H NMR (400 MHz, Methanol- d_4) δ 8.93 – 8.81 (m, 2H), 8.58 (d, $J = 7.2$ Hz, 1H), 8.44 (d, $J = 7.6$ Hz, 1H), 8.33 (d, $J = 8.0$ Hz, 1H), 8.07 (dt, $J = 22.3, 7.4$ Hz, 2H), 7.81 (dd, $J = 10.3, 3.1$ Hz, 2H), 4.31 – 4.14 (m, 4H), 3.50 (dt, $J = 14.8, 7.2$ Hz, 2H), 3.25 (t, $J = 5.1$ Hz, 4H), 3.16 (t, $J = 7.3$ Hz, 2H), 2.50 (p, $J = 7.5$ Hz, 2H), 2.34 (p, $J = 7.4$ Hz, 2H). ^{13}C NMR (101 MHz, MeOD) δ 155.93, 143.05, 138.07, 136.38, 129.17, 126.95, 125.42, 123.60, 121.28, 121.05, 113.80, 112.52, 58.52, 53.56, 47.58, 41.42, 41.21, 41.01, 40.80, 40.59, 40.38, 40.17, 27.62, 27.16, 23.92. MS (ESI) m/z 380.58 $[\text{M}+1]^+$.

1-(4-(benzofuran-3-yl)butyl)-4-phenylpiperazine. 308 (WA228) (73%) ^1H NMR (400 MHz, Methanol- d_4) δ 7.55 (dd, $J = 7.4, 1.5$ Hz, 1H), 7.49 (s, 1H), 7.45 – 7.38 (m, 1H), 7.21 (dddd, $J = 11.1, 9.3, 5.9, 1.9$ Hz, 4H), 6.89 (d, $J = 8.1$ Hz, 2H), 6.81 (t, $J = 7.3$ Hz, 1H), 3.21 – 3.05 (m, 4H), 2.67 (t, $J = 7.4$ Hz, 2H), 2.51 (dd, $J = 6.3, 3.9$ Hz, 4H), 2.45 – 2.31 (m, 2H), 1.70 (p, $J = 7.4$ Hz, 2H), 1.57 (ddt, $J = 15.1, 10.2, 5.8$ Hz, 2H). ^{13}C NMR (101 MHz, MeOD) δ 155.50, 151.21, 141.21, 128.69, 128.12, 123.84, 121.98, 120.16, 119.66, 119.30, 115.98, 110.87, 57.98, 52.80, 48.66, 26.73, 25.79, 22.86. MS (ESI) m/z 335.31 $[\text{M}+1]^+$.

1-(4-(benzofuran-3-yl)butyl)-4-(4-chlorophenyl)-1,2,3,4-tetrahydropyridine. 309 (WA230) (69%) ^1H NMR (400 MHz, Chloroform- d) δ 7.61 – 7.54 (m, 1H), 7.49 – 7.42 (m, 2H), 7.32 (d, $J = 8.8$ Hz, 2H), 7.29 – 7.21 (m, 3H), 6.06 (tt, $J = 3.5, 1.6$ Hz, 1H), 3.15 (q, $J = 3.0$ Hz, 2H), 2.78 – 2.66 (m, 4H), 2.53 (tt, $J = 9.0, 7.2, 5.1$ Hz, 4H), 1.82 – 1.61 (m, 4H). ^{13}C NMR (101 MHz, CDCl_3) δ 155.37, 141.08, 139.30, 133.99, 132.62, 128.37, 128.26, 126.17, 124.06, 122.48, 122.16, 120.31, 119.61, 111.41, 58.15, 53.31, 50.32, 28.06, 26.99, 23.51. MS (ESI) m/z 366.66 $[\text{M}+1]^+$.

1-(4-(benzofuran-3-yl)butyl)-3-methylpiperazine. 310 (WA231) (84%) ^1H NMR (400 MHz, Methanol- d_4) δ 7.61 – 7.51 (m, 2H), 7.43 (d, $J = 8.0$ Hz, 1H), 7.30 – 7.18 (m, 2H), 2.97 – 2.70 (m, 8H), 2.43 – 2.35 (m, 2H), 2.00 (td, $J = 11.5, 11.0, 3.3$ Hz, 1H), 1.79 – 1.56 (m, 5H), 1.04 (d, $J = 6.4$ Hz, 3H). ^{13}C NMR (101 MHz, MeOD) δ 155.48, 141.21, 128.04, 123.75, 121.88, 120.06, 119.22, 110.75, 59.92, 58.22, 52.24, 49.86, 46.95, 26.67, 25.51, 22.76, 17.88. MS (ESI) m/z 273.76 $[\text{M}+1]^+$.

1-(4-(benzofuran-3-yl)butyl)-4-phenylpiperidine-4-carbonitrile. 311 (WA232) (71%) ^1H NMR (400 MHz, Methanol- d_4) δ 7.63 – 7.17 (m, 10H), 3.05 (dt, $J = 12.5, 3.6$ Hz, 2H), 2.74 (q, $J = 6.0, 4.6$ Hz, 2H), 2.54 – 2.36 (m, 4H), 2.08 (dt, $J = 12.6, 6.2$ Hz, 4H), 1.77 (p, $J = 7.3$ Hz, 2H), 1.64 (ddt, $J = 15.2, 10.7, 5.8$ Hz, 2H). ^{13}C NMR (101 MHz, MeOD) δ 155.49, 141.23, 140.12, 128.73, 128.06, 127.85, 125.24, 123.78, 121.91, 121.70, 120.08, 119.25, 110.78, 57.86, 50.45, 42.28, 35.68, 26.67, 25.96, 22.79. MS (ESI) m/z 359.67 $[\text{M}+1]^+$.

2-(4-(benzofuran-3-yl)butyl)-2,3,4,9-tetrahydro-1H-pyrido[3,4-*b*]indole. 312 (WA240) (72%) ^1H NMR (400 MHz, DMSO- d_6) δ 10.65 (s, 1H), 7.76 (s, 1H), 7.63 (d, $J = 7.7$ Hz, 1H), 7.52 (d, $J = 8.1$ Hz, 1H), 7.26 (tt, $J = 19.3, 7.5$ Hz, 4H), 6.95 (dt, $J = 27.5, 7.3$ Hz, 2H), 3.57 (s, 2H), 3.16 (d, $J = 3.0$ Hz, 2H), 2.74 – 2.64 (m, 5H), 2.57 (t, $J = 7.1$ Hz, 2H), 1.78 – 1.57 (m, 4H). ^{13}C NMR (101 MHz, DMSO) δ 155.12, 142.22, 136.31, 133.39, 128.39, 127.13, 124.60, 122.78, 120.66, 120.54, 120.25, 118.63, 117.72, 111.69, 111.28, 106.92, 57.35, 51.28, 50.58, 49.05, 40.63, 40.42, 40.21, 40.00, 39.79, 39.58, 39.37, 26.89, 23.14, 21.71. MS (ESI) m/z 345.58 $[\text{M}+1]^+$.

4-(4-(4-(benzofuran-3-yl)butyl)piperazin-1-yl)aniline. 313 (WA254) (65%) ^1H NMR (400 MHz, Methanol- d_4) δ 7.61 – 7.53 (m, 2H), 7.46 – 7.41 (m, 1H), 7.24 (dtd, $J = 19.8, 7.3, 1.3$ Hz, 2H), 6.85 – 6.80 (m, 2H), 6.74 – 6.67 (m, 2H), 3.36 (s, 2H), 3.05 – 2.99 (m, 4H), 2.77 – 2.71 (m, 2H), 2.63 – 2.56 (m, 4H), 2.48 – 2.40 (m, 2H), 1.76 (p, $J = 7.4$ Hz, 2H), 1.63 (ddt, $J = 15.2, 10.5, 5.9$ Hz, 2H). ^{13}C NMR (101 MHz, MeOD) δ 155.48, 143.89, 141.24, 141.17, 128.05, 123.78, 121.92, 120.07, 119.25, 118.51, 116.40, 110.77, 58.01, 52.87, 50.56, 26.74, 25.75, 22.80. MS

(ESI) m/z 350.64 $[M+1]^+$.

1'-(4-(benzofuran-3-yl)butyl)spiro[isochromane-1,4'-piperidine]. 314 (WA496) To a solution of 3-(4-bromobutyl)benzofuran (WA208) (0.05g, 0.1382 mmol) in 3 mL DMF were added (0.06g, 0.4347 mmol) of potassium carbonate and (0.034g, 0.1674 mmol) of spiro[isochromane-1,4'-piperidine]-HCl, and the reaction mixture heated at 65 °C for 3 h, then the mixture extracted with ethyl acetate and water, treated with brine, dried over magnesium sulfate and the solvent evaporated using *vacuu* then purified by column chromatography (EtOAc: Hexane) to afford 0.034g of 1'-(4-(benzofuran-3-yl)butyl)spiro[isochromane-1,4'-piperidine] as yellow oil in 67% yield. MS (ESI) m/z 376.65 $[M^++1]$. ^1H NMR (400 MHz, Methanol- d_4) δ 7.62 – 7.57 (m, 1H), 7.55 (s, 1H), 7.46 – 7.41 (m, 1H), 7.31 – 7.19 (m, 2H), 7.19 – 7.05 (m, 4H), 3.87 (t, $J = 5.5$ Hz, 2H), 2.77 (dt, $J = 13.9, 6.4$ Hz, 6H), 2.51 – 2.39 (m, 4H), 2.03 (td, $J = 13.5, 4.4$ Hz, 2H), 1.86 (dd, $J = 14.4, 2.6$ Hz, 2H), 1.80 – 1.61 (m, 4H). ^{13}C NMR (101 MHz, MeOD) δ 155.50, 141.41, 141.23, 133.56, 128.44, 128.05, 125.87, 124.88, 123.75, 121.89, 120.05, 119.22, 110.75, 72.68, 58.43, 58.30, 48.90, 35.88, 29.18, 26.90, 25.96, 22.82.

9.3 Synthesis of isothiocyanate derivatives:

9.3.1 Synthesis of isothiocyanate derivatives of 1,3-dihydro-2H-benzo[d]imidazol-2-one

N -methyl-4-nitrobenzene-1,2-diamine. 305 (WA244) 2g (12.81 mmol) of 2-fluoro-5-nitroaniline, and 5 mL (40% in water) of methylamine stirred and heated at 95 °C overnight. The reaction was evaporated and the residue was purified by silica gel (0 to 90 % ethyl acetate in hexanes) to give (2-amino-4-nitrophenyl)methylamine as a redish-orange solid. MS (ESI) m/z 168.2 $[M+1]^+$. ^1H NMR (400 MHz, DMSO- d_6) δ 7.54 (dd, $J = 8.9, 2.7$ Hz, 1H), 7.40 (d, $J = 2.7$

Hz, 1H), 6.41 (d, $J = 8.9$ Hz, 1H), 6.27 (d, $J = 5.1$ Hz, 1H), 5.15 (s, 2H), 2.84 (d, $J = 4.6$ Hz, 3H).
 ^{13}C NMR (101 MHz, DMSO) δ 144.09, 136.95, 134.94, 116.42, 107.30, 106.85, 30.06.

1-methyl-5-nitro-1,3-dihydro-2H-benzo[d]imidazol-2-one. 310 (WA245) A solution of (2-amino-4-nitrophenyl)methylamine (2 g, 11.96 mmol) and 1,1'-carbonyldiimidazole (CDI) (1.98 g, 12.22 mmol) in tetrahydrofuran (50 mL) was stirred at 65°C for 20 hours. The reaction mixture was then cooled to 0°C. The resulting precipitate was filtered and dried to give (2 g, 10.3541 mmol, 86.5 % yield) of 1-methyl-5-nitro-3-hydrobenzimidazol-2-one as beige solid. MS (ESI) m/z 194.5 $[\text{M}+1]^+$. ^1H NMR (400 MHz, DMSO- d_6) δ 11.41 (s, 1H), 7.96 (dd, $J = 8.7, 2.2$ Hz, 1H), 7.70 (d, $J = 2.2$ Hz, 1H), 7.24 (d, $J = 8.7$ Hz, 1H), 3.33 (s, 3H). ^{13}C NMR (101 MHz, DMSO) δ 155.10, 141.81, 136.89, 128.60, 118.07, 107.61, 104.13, 27.32.

3-(4-bromobutyl)-1-methyl-5-nitro-1,3-dihydro-2H-benzo[d]imidazol-2-one. 315 (WA247)
To a solution of 1-methyl-5-nitro-1,3-dihydro-2H-benzo[d]imidazol-2-one (WA245) (1.5g, 7.76 mmol) in 5 mL DMF were added (3.2g, 23.2 mmol) of potassium carbonate and (8.38g, 38.8 mmol) of 1,4-dibromobutane, and the reaction mixture heated at 60 °C for 3 hr, then the mixture extracted with CH_2Cl_2 and water, dried over sodium sulfate and the solvent evaporated using *vacuo* then purified by column chromatography (EtOAc: Hexane) to get 2.2g of compound 4 as yellow oil in 86.4% yield. MS (ESI) m/z 350.45 $[\text{M}+23]^+$. ^1H NMR (400 MHz, DMSO- d_6) δ 8.13 (d, $J = 2.2$ Hz, 1H), 8.04 (dd, $J = 8.7, 2.2$ Hz, 1H), 7.34 (d, $J = 8.7$ Hz, 1H), 3.96 (t, $J = 6.6$ Hz, 2H), 3.56 (t, $J = 6.3$ Hz, 2H), 3.41 (d, $J = 5.2$ Hz, 3H), 1.81 (dddd, $J = 21.7, 15.0, 8.1, 3.7$ Hz, 4H). ^{13}C NMR (101 MHz, DMSO) δ 154.50, 142.18, 135.66, 129.36, 118.37, 107.93, 103.80, 40.33, 35.00, 29.77, 27.87, 27.03.

3-(4-(6,7-dimethoxy-3,4-dihydroisoquinolin-2(1H)-yl)butyl)-1-methyl-5-nitro-1,3-dihydro-2H-benzo[d]imidazol-2-one. 319 (WA248) To a solution of compound 4 (0.4g, 1.22 mmol) in 5 mL DMF were added (0.5g, 3.62 mmol) of potassium carbonate and (0.336g, 1.46 mmol) of 6,7-dimethoxy-1,2,3,4-tetrahydroisoquinoline, and the reaction mixture heated at 60 °C for 5 hr, then the mixture extracted with CH₂Cl₂ and water, dried over sodium sulfate and the solvent evaporated using *vacuu* then purified by column chromatography (EtOAc: Hexane) to get 0.301g of compound 5 as brown residue in 56% yield. MS (ESI) m/z 439 [M-1]⁺. ¹H NMR (400 MHz, DMSO-*d*₆) δ 8.12 – 8.00 (m, 2H), 7.33 (d, *J* = 8.8 Hz, 1H), 6.58 (d, *J* = 20.0 Hz, 2H), 3.96 (t, *J* = 7.2 Hz, 3H), 3.67 (s, 6H), 3.33 (s, 4H), 2.60 (dt, *J* = 41.6, 6.0 Hz, 4H), 2.42 (t, *J* = 7.1 Hz, 2H), 1.71 (t, *J* = 7.5 Hz, 2H), 1.54 (q, *J* = 7.7, 7.3 Hz, 2H). ¹³C NMR (101 MHz, DMSO) δ 154.50, 147.53, 147.28, 142.13, 135.65, 129.43, 127.02, 126.32, 118.31, 112.16, 110.34, 107.90, 103.77, 57.45, 55.89, 55.53, 51.12, 41.12, 28.73, 27.86, 26.13, 24.00.

3-(4-(3H-spiro[isobenzofuran-1,4'-piperidin]-1'-yl)butyl)-1-methyl-5-nitro-1,3-dihydro-2H-benzo[d]imidazol-2-one. 320 (WA256) To a solution of compound 4 (0.3g, 0.91 mmol) in 3 mL DMF were added (0.4g, 2.9 mmol) of potassium carbonate and (0.25g, 11.1 mmol) of 6,7-dimethoxy-1,2,3,4-tetrahydroisoquinoline-HCl, and the reaction mixture heated at 60 °C for 6 hr, then the mixture extracted with ethylacetate and water, washed with brine and dried over sodium sulfate and the solvent evaporated using *vacuu* then purified by column chromatography (EtOAc: Hexane) to get 0.2235g of compound 6 as yellow solid in 56% yield. MS (ESI) m/z 437 [M+1]⁺. ¹H NMR (400 MHz, Methanol-*d*₄) δ 8.13 – 8.05 (m, 2H), 7.30 – 7.15 (m, 5H), 5.02 (s, 2H), 4.03 (t, *J* = 7.0 Hz, 2H), 3.48 (s, 3H), 3.01 – 2.93 (m, 2H), 2.58 (dt, *J* = 12.2, 9.2 Hz, 4H), 2.05 – 1.96 (m, 2H), 1.87 – 1.64 (m, 6H). ¹³C NMR (101 MHz, MeOD) δ 154.98, 144.71, 142.62, 138.68,

134.99, 129.03, 127.55, 127.14, 120.80, 120.32, 117.91, 107.11, 103.34, 83.77, 70.27, 57.44, 49.63, 40.69, 35.27, 26.46, 25.79, 22.93.

4-nitro-N¹-propylbenzene-1,2-diamine. 306 (WA246) 3g (19.23 mmol) of 2-fluoro-5-nitroaniline, and 1.7g (28.76 mmol) of propylamine dissolved in 15 mL DMF, stirred, and heated at 60°C overnight. The reaction mixture extracted with ethyl acetate and water three times, washed with brine, dried over sodium sulfate, the solvent evaporated using *vacuu* and the residue was purified by silica gel (0 to 75 % ethyl acetate in hexanes) to give 2.2g of compound 2b as dark-red crystals in 58.6 % yield. MS (ESI) *m/z* 218.66 [M+1]⁺. ¹H NMR (400 MHz, DMSO-*d*₆) δ 7.51 (dd, *J* = 8.9, 2.7 Hz, 1H), 7.40 (d, *J* = 2.7 Hz, 1H), 6.45 (d, *J* = 8.9 Hz, 1H), 5.85 (d, *J* = 5.0 Hz, 1H), 5.10 (d, *J* = 10.6 Hz, 1H), 3.26 (d, *J* = 9.2 Hz, 1H), 3.20 – 3.10 (m, 2H), 1.62 (h, *J* = 7.3 Hz, 2H), 0.95 (t, *J* = 7.4 Hz, 3H). ¹³C NMR (101 MHz, DMSO) δ 143.12, 136.94, 134.77, 116.34, 107.73, 107.26, 45.13, 22.02, 11.98.

4-nitro-N¹-pentylbenzene-1,2-diamine: 308 (WA252) 3g (19.23 mmol) of 2-fluoro-5-nitroaniline, and 2.5g (28.68 mmol) of pentylamine dissolved in 15 mL DMF, stirred, and heated at 60 °C overnight. The reaction mixture extracted with ethyl acetate and water three times, washed with brine, dried over sodium sulfate, the solvent evaporated using *vacuu* and the residue was purified by silica gel (0 to 80 % ethyl acetate in hexanes) to give 3.3g of compound 2b as dark-red crystals in 77 % yield. MS (ESI) *m/z* 222.69 [M-1]⁺/ 246.74 [M+23]⁺. ¹H NMR (400 MHz, Methanol-*d*₄) δ 7.71 – 7.63 (m, 1H), 7.62 – 7.52 (m, 1H), 6.50 (t, *J* = 7.0 Hz, 1H), 4.90 (s, 1H), 3.41 – 3.09 (m, 3H), 1.70 (dp, *J* = 14.6, 7.2 Hz, 2H), 1.49 – 1.28 (m, 4H), 0.95 (dt, *J* = 14.2,

7.1 Hz, 4H). ^{13}C NMR (101 MHz, MeOD) δ 143.83, 137.07, 133.25, 117.31, 109.43, 106.86, 43.08, 29.04, 28.31, 22.17, 12.99.

5-nitro-1-propyl-1,3-dihydro-2H-benzo[d]imidazol-2-one: 309 (WA251) A solution of 4-nitro- N^1 -propylbenzene-1,2-diamine (1.5 g, 7.7 mmol) and 1,1'-carbonyldiimidazole (CDI) (1.24 g, 7.65 mmol) in tetrahydrofuran (40 mL) was stirred at 65°C for 18 hours. The reaction mixture was then cooled to 0°C. The resulting precipitate was filtered and dried to give (0.88g, 4mmol, 51.6% yield) of 5-nitro-1-propyl-1,3-dihydro-2H-benzo[d]imidazol-2-one as brown solid. MS (ESI) m/z 220.61 $[\text{M}-1]^+$. ^1H NMR (400 MHz, DMSO- d_6) δ 11.39 (s, 1H), 8.01 – 7.93 (m, 1H), 7.75 – 7.70 (m, 1H), 7.33 (d, $J = 8.7$ Hz, 1H), 3.80 (t, $J = 7.1$ Hz, 2H), 1.65 (h, $J = 7.2$ Hz, 2H), 0.85 (t, $J = 7.4$ Hz, 3H). ^{13}C NMR (101 MHz, DMSO) δ 154.97, 141.78, 136.37, 128.64, 118.08, 107.81, 104.27, 42.32, 21.60, 11.40.

3-(4-bromobutyl)-5-nitro-1-propyl-1,3-dihydro-2H-benzo[d]imidazol-2-one. 316 (WA333)
To a solution of 5-nitro-1-propyl-1,3-dihydro-2H-benzo[d]imidazol-2-one (WA251/WA332) (0.85g, 3,84 mmol) in 3 mL DMF were added (1.6g, 11.6 mmol) of potassium carbonate and (4.15g, 19.2 mmol) of 1,4-dibromobutane, and the reaction mixture heated at 60 °C for 3 hr, then the mixture extracted with CH_2Cl_2 and water, dried over sodium sulfate and the solvent evaporated using *vacuu* then purified by column chromatography (EtOAc: Hexane) to get 1.22g of 3-(4-bromobutyl)-5-nitro-1-propyl-1,3-dihydro-2H-benzo[d]imidazol-2-one as yellow oil in 87% yield. MS (ESI) m/z 378.46 $[\text{M}+23]^+$. ^1H NMR (500 MHz, Methanol- d_4) δ 8.07 (s, 2H), 7.32 (d, $J = 8.5$ Hz, 1H), 4.04 (t, $J = 6.4$ Hz, 2H), 3.95 (t, $J = 7.0$ Hz, 2H), 3.54 – 3.45 (m, 2H), 1.98 – 1.89 (m, 4H), 1.81 (h, $J = 7.3$ Hz, 2H), 1.01 – 0.94 (m, 3H). ^{13}C NMR (126 MHz, MeOD)

δ 154.88, 142.55, 134.45, 128.98, 117.89, 107.36, 103.41, 42.68, 40.06, 32.20, 29.48, 26.48, 21.29, 10.04.

5-nitro-1-pentyl-1,3-dihydro-2H-benzo[d]imidazol-2-one. 313 (WA259) A solution of 4-nitro- N^1 -pentylbenzene-1,2-diamine (1.5 g, 6.7 mmol) and 1,1'-carbonyldiimidazole (CDI) (1.088 g, 6.716 mmol) in tetrahydrofuran (40 mL) was stirred at 65°C for 18 hours. The reaction mixture was then cooled to 0°C. The resulting precipitate was filtered and dried to give (1.4 g, 5.62 mmol, 83.7 % yield) of 5-nitro-1-pentyl-1,3-dihydro-2H-benzo[d]imidazol-2-one as beige solid. MS (ESI) m/z 248.69 $[M-1]^+$ / 272.73 $[M+23]^+$. 1H NMR (400 MHz, Methanol- d_4) δ 8.06 (tt, $J = 6.5, 2.4$ Hz, 1H), 7.89 (s, 1H), 7.25 (dd, $J = 9.1, 5.1$ Hz, 1H), 3.93 (dd, $J = 9.2, 5.2$ Hz, 2H), 3.35 (d, $J = 6.5$ Hz, 1H), 1.76 (p, $J = 7.4$ Hz, 2H), 1.36 (hd, $J = 8.9, 8.2, 2.9$ Hz, 4H), 0.94 – 0.85 (m, 3H). 1H NMR (400 MHz, Methanol- d_4) δ 8.06 (tt, $J = 6.5, 2.4$ Hz, 1H), 7.89 (s, 1H), 7.25 (dd, $J = 9.1, 5.1$ Hz, 1H), 3.93 (dd, $J = 9.2, 5.2$ Hz, 2H), 3.35 (d, $J = 6.5$ Hz, 1H), 1.76 (p, $J = 7.4$ Hz, 2H), 1.36 (hd, $J = 8.9, 8.2, 2.9$ Hz, 4H), 0.94 – 0.85 (m, 3H).

3-(4-bromobutyl)-5-nitro-1-pentyl-1,3-dihydro-2H-benzo[d]imidazol-2-one. 318 (WA261/WA307) To a solution of compound 3c (2g, 8.0321 mmol) in 5 mL DMF were added (3.33g, 24.1 mmol) of potassium carbonate and (8,67g, 40.14 mmol) of 1,4-dibromobutane, and the reaction mixture heated at 60 °C for 3 hr, then the mixture extracted with CH_2Cl_2 and water, dried over sodium sulfate and the solvent evaporated using *vacuu* then purified by column chromatography (EtOAc: Hexane) to get 3g of compound 4c as yellow oil in 97.5% yield. MS (ESI) m/z 406.48 $[M+23]^+$. 1H NMR (400 MHz, Chloroform- d) δ 8.10 (dd, $J = 8.6, 2.3$ Hz, 1H), 7.90 (d, $J = 2.2$ Hz, 1H), 7.04 (dd, $J = 8.7, 4.0$ Hz, 1H), 3.96 (dt, $J = 26.6, 6.9$ Hz, 4H), 3.47 (t, J

= 5.9 Hz, 2H), 2.02 – 1.92 (m, 4H), 1.83 – 1.71 (m, 2H), 1.36 (tq, $J = 8.3, 4.3$ Hz, 4H), 0.92 (dt, $J = 13.8, 6.9$ Hz, 3H). ^{13}C NMR (101 MHz, CDCl_3) δ 154.39, 142.37, 136.38, 134.64, 129.10, 118.33, 106.79, 103.28, 41.65, 40.50, 32.67, 29.52, 28.83, 27.98, 26.81, 22.24, 13.89.

3-(4-(6,7-dimethoxy-3,4-dihydroisoquinolin-2(1H)-yl)butyl)-5-nitro-1-propyl-1,3-dihydro-2H-benzo[d]imidazol-2-one. 325 (WA334) To a solution of 3-(4-bromobutyl)-5-nitro-1-propyl-1,3-dihydro-2H-benzo[d]imidazol-2-one (WA260) (0.4g, 1.22 mmol) in 5 mL DMF were added (0.5g, 3.62 mmol) of potassium carbonate and (0.336g, 1.46 mmol) of 6,7-dimethoxy-1,2,3,4-tetrahydroisoquinoline, and the reaction mixture heated at 60 °C for 5 hr, then the mixture extracted with CH_2Cl_2 and water, dried over sodium sulfate and the solvent evaporated using *vacuu* then purified by column chromatography (EtOAc: Hexane) to get 0.301g of 3-(4-(6,7-dimethoxy-3,4-dihydroisoquinolin-2(1H)-yl)butyl)-5-nitro-1-propyl-1,3-dihydro-2H-benzo[d]imidazol-2-one as brown residue in 56% yield. MS (ESI) m/z 469.64 $[\text{M}+1]^+$. ^1H NMR (400 MHz, $\text{DMSO}-d_6$) δ 8.09 (d, $J = 2.3$ Hz, 1H), 8.02 (dd, $J = 8.6, 2.2$ Hz, 1H), 7.40 (d, $J = 8.6$ Hz, 1H), 6.61 (s, 1H), 6.55 (s, 1H), 3.97 (t, $J = 7.1$ Hz, 2H), 3.87 (t, $J = 7.1$ Hz, 2H), 3.37 (s, 2H), 3.28 (s, 5H), 2.64 (d, $J = 5.8$ Hz, 2H), 2.54 (t, $J = 5.8$ Hz, 2H), 2.42 (t, $J = 7.0$ Hz, 2H), 1.70 (dh, $J = 14.6, 7.4$ Hz, 4H), 1.52 (p, $J = 7.5$ Hz, 2H), 1.19 (s, 1H), 0.85 (t, $J = 7.4$ Hz, 3H). ^{13}C NMR (101 MHz, MeOD) δ 154.85, 147.77, 147.39, 142.49, 134.43, 129.05, 125.98, 125.86, 117.82, 111.50, 109.69, 107.30, 103.46, 57.23, 55.08, 55.06, 55.01, 50.64, 42.64, 40.78, 27.69, 25.88, 23.38, 21.31, 10.08.

3-(4-(4-(4-fluorophenyl)piperazin-1-yl)butyl)-5-nitro-1-propyl-1,3-dihydro-2H-benzo[d]imidazol-2-one. 321 (WA262) To a solution of 3-(4-bromobutyl)-5-nitro-1-propyl-1,3-

dihydro-2*H*-benzo[*d*]imidazol-2-one (WA260) (0.35g, 0.84 mmol) in 3 mL DMF were added (0.35g, 2.53 mmol) of potassium carbonate and (0.182g, 1.01 mmol) of 1-(4-fluorophenyl)piperazine, and the reaction mixture heated at 60 °C for 5 hr, then the mixture extracted with CH₂Cl₂ and water, dried over sodium sulfate and the solvent evaporated using *vacuu* then purified by column chromatography (EtOAc: Hexane) to get 0.325g of 3-(4-(4-(4-fluorophenyl)piperazin-1-yl)butyl)-5-nitro-1-propyl-1,3-dihydro-2*H*-benzo[*d*]imidazol-2-one as yellow residue in 84.7% yield. MS (ESI) *m/z* 456.97 [M+1]⁺. ¹H NMR (400 MHz, Methanol-*d*₄) δ 8.13 – 8.04 (m, 2H), 7.35 – 7.27 (m, 1H), 6.94 (ddd, *J* = 7.1, 5.7, 3.3 Hz, 4H), 4.03 (t, *J* = 7.1 Hz, 2H), 3.94 (t, *J* = 7.1 Hz, 2H), 3.35 (s, 2H), 3.11 – 3.07 (m, 3H), 2.63 (dd, *J* = 6.3, 3.8 Hz, 3H), 2.53 – 2.46 (m, 2H), 1.81 (ddt, *J* = 14.5, 11.5, 7.2 Hz, 4H), 1.63 (td, *J* = 10.4, 9.2, 6.6 Hz, 2H), 0.96 (t, *J* = 7.4 Hz, 3H). ¹³C NMR (101 MHz, MeOD) δ 154.85, 147.87, 142.53, 134.45, 129.06, 117.86, 117.76, 114.99, 114.78, 107.35, 103.46, 57.35, 52.76, 49.44, 42.66, 40.71, 25.73, 23.00, 21.31, 10.07.

3-(4-(3*H*-spiro[isobenzofuran-1,4'-piperidin]-1'-yl)butyl)-5-nitro-1-propyl-1,3-dihydro-2*H*-benzo[*d*]imidazol-2-one. 324 (WA303) To a solution of 3-(4-bromobutyl)-5-nitro-1-propyl-1,3-dihydro-2*H*-benzo[*d*]imidazol-2-one (WA260) (0.5g, 1.4 mmol) in 5 mL DMF were added (0.58g, 4.20 mmol) of potassium carbonate and (0.318g, 1.41 mmol) of 3*H*-spiro[isobenzofuran-1,4'-piperidine] HCl,, and the reaction mixture heated at 60 °C for 5 hr, then the mixture extracted with CH₂Cl₂ and water, dried over sodium sulfate and the solvent evaporated using *vacuu* then purified by column chromatography (EtOAc: Hexane) to get 0.42g of 3-(4-(3*H*-spiro[isobenzofuran-1,4'-piperidin]-1'-yl)butyl)-5-nitro-1-propyl-1,3-dihydro-2*H*-benzo[*d*]imidazol-2-one as yellow oil in 65% yield. MS (ESI) *m/z* 465.71 [M+1]⁺. ¹H NMR (400

MHz, Chloroform-*d*) δ 8.09 (dt, $J = 8.7, 2.2$ Hz, 1H), 7.97 – 7.88 (m, 1H), 7.28 (q, $J = 2.9, 2.3$ Hz, 2H), 7.19 (dq, $J = 8.9, 5.4, 4.7$ Hz, 2H), 7.04 (dd, $J = 8.8, 2.9$ Hz, 1H), 5.06 (d, $J = 3.6$ Hz, 2H), 3.98 (t, $J = 6.9$ Hz, 2H), 3.89 (t, $J = 7.3$ Hz, 2H), 3.46 (s, 2H), 3.23 – 3.14 (m, 2H), 2.84 – 2.68 (m, 4H), 2.24 (td, $J = 13.6, 4.4$ Hz, 2H), 2.03 (s, 2H), 2.00 (s, 2H), 1.81 – 1.78 (m, 2H), 0.97 (t, $J = 7.3$ Hz, 3H). ^{13}C NMR (101 MHz, CDCl_3) δ 154.50, 144.33, 142.42, 138.53, 134.66, 129.10, 127.90, 127.58, 121.03, 120.97, 118.31, 106.79, 103.38, 83.50, 70.96, 56.89, 50.59, 49.32, 43.20, 40.92, 34.85, 25.98, 21.68, 11.24.

3-(4-(6,7-dimethoxy-3,4-dihydroisoquinolin-2(1H)-yl)butyl)-5-nitro-1-pentyl-1,3-dihydro-2H-benzo[d]imidazol-2-one. 322 (WA266/299/308) To a solution of 3-(4-bromobutyl)-5-nitro-1-pentyl-1,3-dihydro-2H-benzo[d]imidazol-2-one (WA261) (0.6g, 1.56 mmol) in 5 mL DMF were added (0.65g, 4.7 mmol) of potassium carbonate and (0.43g, 1.87 mmol) of 6,7-dimethoxy-1,2,3,4-tetrahydroisoquinoline, and the reaction mixture heated at 60 °C for 3 hr, then the mixture extracted with CH_2Cl_2 and water, dried over sodium sulfate and the solvent evaporated using *vacuu* then purified by column chromatography (EtOAc: Hexane) to get 0.7g of 3-(4-(6,7-dimethoxy-3,4-dihydroisoquinolin-2(1H)-yl)butyl)-5-nitro-1-pentyl-1,3-dihydro-2H-benzo[d]imidazol-2-one as yellow oil in 90% yield. MS (ESI) m/z 497.91 $[\text{M}+1]^+$. ^1H NMR (400 MHz, Methanol-*d*₄) δ 8.12 – 8.04 (m, 2H), 7.33 – 7.26 (m, 1H), 6.65 (s, 1H), 6.58 (s, 1H), 4.09 – 4.02 (m, 2H), 3.97 (t, $J = 7.2$ Hz, 2H), 3.80 – 3.75 (m, 6H), 3.00 (s, 1H), 2.87 (s, 1H), 2.79 (t, $J = 5.9$ Hz, 2H), 2.69 (t, $J = 5.9$ Hz, 2H), 2.56 (t, $J = 7.7$ Hz, 2H), 1.90 – 1.63 (m, 6H), 1.36 (dq, $J = 7.8, 4.5, 3.6$ Hz, 3H), 0.94 – 0.88 (m, 3H). ^{13}C NMR (101 MHz, MeOD) δ 154.81, 147.79, 147.41, 142.51, 134.37, 129.08, 125.98, 125.87, 117.84, 111.53, 109.72, 107.28, 103.49, 57.23, 55.08, 50.63, 41.09, 40.79, 35.54, 30.25, 28.53, 27.70, 25.88, 23.36, 21.93, 12.91.

3-(4-(4-(4-fluorophenyl)piperazin-1-yl)butyl)-5-nitro-1-pentyl-1,3-dihydro-2H-

benzo[d]imidazol-2-one. 326 (WA336/265) To a solution of 3-(4-bromobutyl)-5-nitro-1-pentyl-1,3-dihydro-2H-benzo[d]imidazol-2-one (WA261) (0.6g, 1.6 mmol) in 5 mL DMF were added (0.662g, 4.8 mmol) of potassium carbonate and (0.35g, 1.94 mmol) of 1-(4-fluorophenyl)piperazine, and the reaction mixture heated at 60 °C for 6 hr, then the mixture extracted with CH₂Cl₂ and water, dried over sodium sulfate and the solvent evaporated using *vacuu* then purified by column chromatography (EtOAc: Hexane) to get 0.62g of 3-(4-(4-(4-fluorophenyl)piperazin-1-yl)butyl)-5-nitro-1-pentyl-1,3-dihydro-2H-benzo[d]imidazol-2-one as brown residue in 80% yield. MS (ESI) *m/z* 484.98 [M+1]⁺. ¹H NMR (400 MHz, Methanol-*d*₄) δ 8.08 (d, *J* = 7.4 Hz, 2H), 7.34 – 7.26 (m, 1H), 7.01 (td, *J* = 8.5, 4.5 Hz, 4H), 4.13 – 4.04 (m, 2H), 3.97 (t, *J* = 7.2 Hz, 2H), 3.56 (q, *J* = 9.6, 8.2 Hz, 2H), 3.45 (d, *J* = 7.5 Hz, 5H), 3.32 (d, *J* = 13.0 Hz, 2H), 2.08 – 1.83 (m, 5H), 1.76 (s, 1H), 1.46 – 1.22 (m, 5H), 1.00 – 0.85 (m, 4H). ¹³C NMR (101 MHz, MeOD) δ 158.76, 156.39, 154.82, 146.79, 142.54, 134.47, 129.00, 118.22, 118.15, 118.00, 115.24, 115.02, 107.37, 103.46, 69.38, 63.17, 44.50, 41.18, 40.51, 28.55, 27.67, 25.23, 21.95, 18.86, 12.95.

3-(4-(3H-spiro[isobenzofuran-1,4'-piperidin]-1'-yl)butyl)-5-nitro-1-pentyl-1,3-dihydro-2H-

benzo[d]imidazol-2-one. 323 (WA267) To a solution of compound 3-(4-bromobutyl)-5-nitro-1-pentyl-1,3-dihydro-2H-benzo[d]imidazol-2-one (WA261) (0.2g, 0.52 mmol) in 3 mL DMF were added (0.216g, 1.565 mmol) of potassium carbonate and (0.118g, 0.522 mmol) of 3H-spiro[isobenzofuran-1,4'-piperidine] HCl, and the reaction mixture heated at 60 °C for 5 hr, then the mixture extracted with CH₂Cl₂ and water, dried over sodium sulfate and the solvent

evaporated using *vacuo* then purified by column chromatography (EtOAc: Hexane) to get 0.15g of 3-(4-(3H-spiro[isobenzofuran-1,4'-piperidin]-1'-yl)butyl)-5-nitro-1-pentyl-1,3-dihydro-2H-benzo[d]imidazol-2-one as brown residue in 58% yield. MS (ESI) m/z 493.94 $[M+1]^+$. ^1H NMR (500 MHz, Methanol- d_4) δ 8.16 – 8.09 (m, 2H), 7.37 – 7.25 (m, 5H), 4.86 (s, 3H), 4.08 (q, $J = 8.7, 7.9$ Hz, 2H), 4.00 (t, $J = 7.3$ Hz, 2H), 3.17 (d, $J = 12.2$ Hz, 2H), 2.85 (s, 2H), 2.12 (td, $J = 13.6, 4.5$ Hz, 2H), 1.90 – 1.73 (m, 8H), 1.40 – 1.32 (m, 4H), 0.94 – 0.87 (m, 4H). ^{13}C NMR (126 MHz, MeOD) δ 154.90, 144.12, 142.61, 138.70, 134.43, 129.05, 127.76, 127.24, 120.90, 120.32, 117.94, 107.40, 103.50, 83.11, 70.45, 56.89, 49.52, 41.14, 40.47, 34.62, 28.54, 27.65, 25.54, 22.28, 21.93, 12.89.

5-amino-3-(4-(6,7-dimethoxy-3,4-dihydroisoquinolin-2(1H)-yl)butyl)-1-methyl-1,3-dihydro-2H-benzo[d]imidazol-2-one. 329 (WA249) To a solution of 3-(4-(6,7-dimethoxy-3,4-dihydroisoquinolin-2(1H)-yl)butyl)-1-methyl-5-nitro-1,3-dihydro-2H-benzo[d]imidazol-2-one (0.3g, 0.68 mmol) in methanol (50 mL) was added to 10% Palladium on carbon catalyst (0.033g) and stirred under a hydrogen atmosphere (20psi) for 2h. The mixture was filtered through celite and evaporated in *vacuo* to give 0.235g of

5-amino-3-(4-(6,7-dimethoxy-3,4-dihydroisoquinolin-2(1H)-yl)butyl)-1-methyl-1,3-dihydro-2H-benzo[d]imidazol-2-one as grey residue in 84% yield. MS (ESI) m/z 411 $[M+1]^+$. ^1H NMR (400 MHz, Methanol- d_4) δ 6.88 (dd, $J = 13.6, 8.3$ Hz, 1H), 6.64 (d, $J = 19.9$ Hz, 3H), 6.55 (d, $J = 8.2$ Hz, 1H), 3.87 (q, $J = 7.0, 6.2$ Hz, 2H), 3.77 (s, 6H), 3.53 (s, 2H), 3.34 (d, $J = 9.2$ Hz, 5H), 2.80 (t, $J = 6.0$ Hz, 2H), 2.70 (t, $J = 6.0$ Hz, 2H), 2.53 (t, $J = 7.6$ Hz, 2H), 1.78 (p, $J = 7.1$ Hz, 2H), 1.64 (p, $J = 7.7$ Hz, 2H). ^{13}C NMR (101 MHz, MeOD) δ 154.69, 147.83, 147.45, 142.71, 129.74,

125.89, 125.83, 122.44, 111.53, 109.76, 109.19, 108.15, 96.19, 57.26, 55.10, 55.03, 50.53, 40.29, 27.61, 25.95, 23.36.

3-(4-(3H-spiro[isobenzofuran-1,4'-piperidin]-1'-yl)butyl)-5-amino-1-methyl-1,3-dihydro-2H-benzo[d]imidazol-2-one. 330 (WA257) To a solution of 3-(4-(3H-spiro[isobenzofuran-1,4'-piperidin]-1'-yl)butyl)-1-methyl-5-nitro-1,3-dihydro-2H-benzo [d]imidazol-2-one (0.223g, 0.512 mmol) in methanol (75ml) was added to 10% Palladium on carbon catalyst (0.033g) and stirred under a hydrogen pressure (20 psi) for 2h. The mixture was filtered through celite and evaporated in *vacuo* to give 0.16g of 3-(4-(3H-spiro[isobenzofuran-1,4'-piperidin]-1'-yl)butyl)-5-amino-1-methyl-1,3-dihydro-2H-benzo[d]imidazol-2-one as brown residue in 76% yield. MS (ESI) m/z 407.90 [M+1]⁺. ¹H NMR (400 MHz, DMSO-*d*₆) δ 7.25 (s, 4H), 6.79 (d, J = 8.2 Hz, 1H), 6.43 (s, 1H), 6.33 (d, J = 8.2 Hz, 1H), 4.95 (s, 2H), 4.78 (s, 2H), 3.73 (t, J = 6.9 Hz, 2H), 3.23 (s, 3H), 2.70 (d, J = 10.8 Hz, 2H), 2.32 (t, J = 7.0 Hz, 2H), 2.23 (t, J = 11.6 Hz, 2H), 1.84 (td, J = 12.9, 4.6 Hz, 2H), 1.65 (t, J = 7.6 Hz, 2H), 1.57 (d, J = 13.2 Hz, 2H), 1.44 (t, J = 7.6 Hz, 2H). ¹³C NMR (101 MHz, MeOD) δ 154.69, 145.17, 142.77, 138.69, 129.79, 127.40, 127.07, 122.42, 120.73, 120.35, 109.15, 108.14, 96.14, 84.25, 70.14, 57.96, 49.65, 40.38, 35.68, 26.08, 25.97, 23.50.

5-amino-3-(4-(4-(4-fluorophenyl)piperazin-1-yl)butyl)-1-propyl-1,3-dihydro-2H-benzo[d]imidazol-2-one. 331 (WA263) To a solution of 3-(4-(4-(4-fluorophenyl)piperazin-1-yl)butyl)-5-nitro-1-propyl-1,3-dihydro-2H-benzo[d]imidazol-2-one (0.3g, 0.6585 mmol) in methanol (75ml) was added to 10% Palladium on carbon catalyst (0.035g) and stirred under a hydrogen pressure (20psi) for 2h. The mixture was filtered through celite and evaporated in

vacuo to give 0.2g of 5-amino-3-(4-(4-(4-fluorophenyl)piperazin-1-yl)butyl)-1-propyl-1,3-dihydro-2H-benzo[d]imidazol-2-one as brown residue in 71% yield. MS (ESI) m/z 426.71 $[M+1]^+$. ^1H NMR (400 MHz, DMSO- d_6) δ 7.05 – 6.97 (m, 2H), 6.89 (dd, $J = 9.2, 4.6$ Hz, 2H), 6.81 (d, $J = 8.2$ Hz, 1H), 6.42 (d, $J = 2.0$ Hz, 1H), 6.31 (dd, $J = 8.2, 2.0$ Hz, 1H), 4.77 (s, 2H), 3.70 (dt, $J = 21.7, 7.0$ Hz, 4H), 3.00 (t, $J = 4.8$ Hz, 4H), 2.42 (t, $J = 4.9$ Hz, 4H), 2.30 (t, $J = 7.2$ Hz, 2H), 1.70 – 1.53 (m, 4H), 1.42 (p, $J = 7.4$ Hz, 2H), 0.82 (t, $J = 7.3$ Hz, 3H). ^{13}C NMR (101 MHz, DMSO) δ 157.54, 155.20, 154.03, 148.39, 148.37, 144.06, 130.21, 120.58, 117.46, 117.38, 115.74, 115.52, 108.70, 107.37, 95.09, 57.61, 53.08, 49.40, 42.18, 40.44, 26.08, 23.87, 21.74, 11.50.

5-amino-3-(4-(4-(4-fluorophenyl)piperazin-1-yl)butyl)-1-pentyl-1,3-dihydro-2H-

benzo[d]imidazol-2-one. (336, WA338) To a solution of 3-(4-(4-(4-fluorophenyl)piperazin-1-yl)butyl)-5-nitro-1-pentyl-1,3-dihydro-2H-benzo[d]imidazol-2-one (WA336) (1.5g, 3.1018 mmol) in methanol (100ml) was added to 10% Palladium on carbon catalyst (0.2g) and stirred under a hydrogen pressure (20psi) for 2h. The mixture was filtered through celite and evaporated in *vacuo* to give 1.2g of 5-amino-3-(4-(4-(4-fluorophenyl)piperazin-1-yl)butyl)-1-pentyl-1,3-dihydro-2H-benzo[d]imidazol-2-one as brown residue in 85% yield. MS (ESI) m/z 454.79 $[M+1]^+$. ^1H NMR (400 MHz, DMSO- d_6) δ 7.00 (t, $J = 8.8$ Hz, 2H), 6.92 – 6.84 (m, 2H), 6.79 (dd, $J = 8.3, 4.8$ Hz, 1H), 6.42 (d, $J = 2.0$ Hz, 1H), 6.31 (dd, $J = 8.2, 2.0$ Hz, 1H), 4.76 (s, 2H), 3.77 – 3.65 (m, 4H), 2.99 (t, $J = 4.9$ Hz, 4H), 2.41 (t, $J = 5.0$ Hz, 4H), 2.28 (t, $J = 7.3$ Hz, 2H), 1.68 – 1.51 (m, 4H), 1.41 (t, $J = 7.5$ Hz, 2H), 1.21 (dq, $J = 18.5, 10.5, 9.5, 4.5$ Hz, 4H), 0.80 (t, $J = 7.1$ Hz, 3H). ^{13}C NMR (101 MHz, DMSO) δ 157.54, 153.99, 148.38, 144.05, 130.21, 120.51, 117.45, 117.37, 115.73, 115.51, 108.65, 107.40, 95.12, 57.63, 53.08, 49.41, 28.76, 28.03, 26.06, 23.86, 22.20, 14.30.

5-amino-3-(4-(6,7-dimethoxy-3,4-dihydroisoquinolin-2(1H)-yl)butyl)-1-propyl-1,3-dihydro-2H-benzo[d]imidazol-2-one. 335 (WA337) To a solution of 3-(4-(6,7-dimethoxy-3,4-dihydroisoquinolin-2(1H)-yl)butyl)-5-nitro-1-propyl-1,3-dihydro-2H-benzo[d]imidazol-2-one (1.2g, 2.561 mmol) in methanol (100ml) was added to 10% Palladium on carbon catalyst (0.2g) and stirred under a hydrogen pressure (20psi) for 2h. The mixture was filtered through celite and evaporated in *vacuo* to give 0.8g of 5-amino-3-(4-(6,7-dimethoxy-3,4-dihydroisoquinolin-2(1H)-yl)butyl)-1-propyl-1,3-dihydro-2H-benzo[d]imidazol-2-one as brown residue in 80% yield. MS (ESI) m/z 439 [M+1]⁺. ¹H NMR (400 MHz, Methanol-*d*₄) δ 7.02 – 6.51 (m, 7H), 3.90 (t, J = 6.9 Hz, 2H), 3.83 – 3.78 (m, 4H), 3.78 (d, J = 1.5 Hz, 4H), 3.54 (s, 2H), 3.35 (s, 4H), 2.81 (t, J = 5.8 Hz, 2H), 2.72 (t, J = 5.9 Hz, 2H), 2.59 – 2.53 (m, 2H), 1.77 (dt, J = 19.7, 7.3 Hz, 4H), 1.68 – 1.62 (m, 2H), 0.93 (t, J = 7.4 Hz, 3H). ¹³C NMR (101 MHz, MeOD) δ 154.60, 147.85, 147.47, 142.53, 129.77, 125.84, 125.82, 121.77, 111.54, 109.75, 109.21, 108.50, 96.28, 57.25, 55.09, 55.03, 50.55, 42.12, 40.20, 27.58, 25.86, 23.32, 21.42, 10.10.

5-amino-3-(4-(6,7-dimethoxy-3,4-dihydroisoquinolin-2(1H)-yl)butyl)-1-pentyl-1,3-dihydro-2H-benzo[d]imidazol-2-one. (333, WA295/300/312) To a solution of 3-(4-(6,7-dimethoxy-3,4-dihydroisoquinolin-2(1H)-yl)butyl)-5-nitro-1-pentyl-1,3-dihydro-2H-benzo[d]imidazol-2-one (0.35g, 0.7047 mmol) in methanol (100 ml) was added to 10% Palladium on carbon catalyst (0.028g) and stirred under a hydrogen pressure (20 psi) for 2h. The mixture was filtered through celite and evaporated in *vacuo* to give 0.265g of 5-amino-3-(4-(6,7-dimethoxy-3,4-dihydroisoquinolin-2(1H)-yl)butyl)-1-pentyl-1,3-dihydro-2H-benzo[d]imidazol-2-one as brown residue in 80% yield. MS (ESI) m/z 467.69 [M+1]⁺. 2HCl salt: ¹H NMR (400 MHz, DMSO-*d*₆) δ 10.55 (s, 2H), 7.35 – 7.24 (m, 2H), 7.10 (dd, J = 8.2, 1.9 Hz, 1H), 6.80 (d, J = 13.1 Hz, 2H), 4.38

(d, $J = 15.1$ Hz, 1H), 4.13 (d, $J = 15.0$ Hz, 1H), 3.86 (dt, $J = 20.6, 6.8$ Hz, 4H), 3.72 (d, $J = 3.8$ Hz, 6H), 3.56 (d, $J = 9.4$ Hz, 2H), 3.20 (s, 4H), 2.87 (d, $J = 16.4$ Hz, 1H), 1.81 (s, 2H), 1.72 (s, 2H), 1.64 (q, $J = 7.2$ Hz, 2H), 1.36 – 1.20 (m, 4H), 0.91 – 0.78 (m, 4H). ^{13}C NMR (101 MHz, MeOD) δ 154.50, 147.76, 147.39, 142.53, 129.78, 126.03, 121.70, 111.48, 109.71, 109.19, 108.47, 96.29, 57.32, 55.06, 55.00, 50.55, 48.24, 48.02, 47.81, 47.73, 47.60, 47.39, 47.31, 47.17, 46.96, 40.52, 40.23, 28.60, 27.70, 25.89, 23.37, 21.98, 12.95.

3-(4-(3H-spiro[isobenzofuran-1,4'-piperidin]-1'-yl)butyl)-5-amino-1-propyl-1,3-dihydro-2H-benzo[d]imidazol-2-one. (334, WA304) To a solution of 3-(4-(3H-spiro[isobenzofuran-1,4'-piperidin]-1'-yl)butyl)-5-nitro-1-propyl-1,3-dihydro-2H-benzo [d]imidazol-2-one (0.375g, 0.8072 mmol) in methanol (50ml) was added to 10% Palladium on carbon catalyst (0.033g) and stirred under a hydrogen pressure (20psi) for 2h. The mixture was filtered through celite and evaporated in *vacuo* to give 0.23g of 3-(4-(3H-spiro[isobenzofuran-1,4'-piperidin]-1'-yl)butyl)-5-amino-1-propyl-1,3-dihydro-2H-benzo[d]imidazol-2-one as brown residue in 65.5% yield. MS (ESI) m/z 435.72 $[\text{M}+1]^+$. ^1H NMR (400 MHz, DMSO- d_6) δ 7.23 (d, $J = 2.1$ Hz, 4H), 6.81 (d, $J = 8.2$ Hz, 1H), 6.42 (d, $J = 2.0$ Hz, 1H), 6.30 (dd, $J = 8.3, 2.0$ Hz, 1H), 4.93 (s, 2H), 4.76 (s, 2H), 3.70 (dt, $J = 22.2, 7.0$ Hz, 4H), 2.72 – 2.64 (m, 2H), 2.31 (t, $J = 7.2$ Hz, 2H), 2.26 – 2.15 (m, 2H), 1.82 (td, $J = 12.9, 4.5$ Hz, 2H), 1.71 – 1.51 (m, 6H), 1.42 (p, $J = 7.5$ Hz, 2H), 0.82 (t, $J = 7.4$ Hz, 3H). ^{13}C NMR (101 MHz, DMSO) δ 154.04, 146.13, 144.06, 139.23, 130.23, 127.82, 127.63, 121.56, 121.27, 120.57, 108.70, 107.35, 95.11, 84.47, 70.25, 58.00, 50.09, 42.18, 40.50, 36.54, 26.13, 24.19, 21.73, 11.50.

3-(4-(3H-spiro[isobenzofuran-1,4'-piperidin]-1'-yl)butyl)-5-amino-1-pentyl-1,3-dihydro-2H-benzo[d]imidazol-2-one. 332 (WA268) To a solution of 3-(4-(3H-spiro[isobenzofuran-1,4'-

piperidin]-1'-yl)butyl)-5-nitro-1-pentyl-1,3-dihydro-2H-benzo[d]imidazol-2-one (0.225g, 0.4567 mmol) in methanol (75ml) was added to 10% Palladium on carbon catalyst (0.03g) and stirred under a hydrogen pressure (20psi) for 2h. The mixture was filtered through celite and evaporated in *vacuo* to give 0.16g of 3-(4-(3H-spiro[isobenzofuran-1,4'-piperidin]-1'-yl)butyl)-5-amino-1-pentyl-1,3-dihydro-2H-benzo[d]imidazol-2-one as brown residue in 76% yield. MS (ESI) *m/z* 463.92 [M+1]⁺. ¹H NMR (400 MHz, DMSO-*d*₆) δ 7.23 (q, *J* = 4.5, 3.8 Hz, 4H), 6.79 (dd, *J* = 8.2, 5.3 Hz, 1H), 6.42 (d, *J* = 2.0 Hz, 1H), 6.30 (dt, *J* = 8.2, 1.9 Hz, 1H), 4.93 (s, 2H), 4.76 (s, 2H), 3.71 (dt, *J* = 11.3, 6.9 Hz, 3H), 2.67 (d, *J* = 11.0 Hz, 2H), 2.30 (t, *J* = 7.2 Hz, 2H), 2.21 (td, *J* = 11.9, 11.3, 2.5 Hz, 2H), 1.82 (td, *J* = 12.8, 4.4 Hz, 2H), 1.71 – 1.50 (m, 6H), 1.43 (q, *J* = 7.4 Hz, 2H), 1.36 – 1.12 (m, 4H), 0.88 – 0.76 (m, 4H). ¹³C NMR (101 MHz, DMSO) δ 153.99, 146.13, 144.05, 139.23, 130.24, 127.83, 127.63, 121.56, 121.25, 120.50, 108.66, 107.36, 95.13, 84.46, 70.25, 58.00, 50.08, 40.52, 40.46, 36.54, 28.76, 28.02, 26.09, 24.16, 22.20, 14.31.

3-(4-(6,7-dimethoxy-3,4-dihydroisoquinolin-2(1H)-yl)butyl)-5-isothiocyanato-1-methyl-1,3-dihydro-2H-benzo[d]imidazol-2-one. 339 (WA250) A solution of 5-amino-3-(4-(6,7-dimethoxy-3,4-dihydroisoquinolin-2(1H)-yl)butyl)-1-methyl-1,3-dihydro-2H-benzo[d]imidazol-2-one (WA249) (0.13g, 0.3166 mmol) in dry DCM is added (0.088g, 0.87mmol) of TEA, then cooled down to 0 °C and treated with thiophosgene (0.0365g, 0.3173mmol). The orange solution was stirred at r.t. under an argon atmosphere for 2hr. Solvents were removed in *vacuo*, and the residue was purified by column chromatography using DCM/MeOH (95/5) eluent to afford 0.1g of 3-(4-(6,7-dimethoxy-3,4-dihydroisoquinolin-2(1H)-yl)butyl)-5-isothiocyanato-1-methyl-1,3-dihydro-2H-benzo [d]imidazol-2-one as brown residue in 70% yield. MS (ESI) *m/z* 453.69 [M+1]⁺. ¹H NMR (400 MHz, Chloroform-*d*) δ 6.99 (dd, *J* = 8.3, 1.8 Hz, 1H), 6.89 (dd, *J*

= 5.1, 3.2 Hz, 2H), 6.60 (s, 1H), 6.52 (s, 1H), 3.95 – 3.81 (m, 8H), 3.58 (s, 2H), 3.41 (s, 3H), 2.84 (t, $J = 5.9$ Hz, 2H), 2.74 (t, $J = 5.8$ Hz, 2H), 2.59 (t, $J = 7.3$ Hz, 2H), 1.83 (p, $J = 7.2$ Hz, 2H), 1.72 – 1.62 (m, 2H). ^{13}C NMR (101 MHz, MeOD) δ 154.67, 147.80, 147.40, 134.12, 129.52, 128.96, 125.64, 125.52, 124.53, 119.04, 111.42, 109.63, 108.20, 105.46, 57.12, 55.10, 55.02, 54.93, 50.57, 40.64, 27.53, 26.24, 25.84, 23.23.

3-(4-(3H-spiro[isobenzofuran-1,4'-piperidin]-1'-yl)butyl)-5-isothiocyanato-1-methyl-1,3-dihydro-2H-benzo[d]imidazol-2-one. 340 (WA258) A solution of 3-(4-(3H-spiro[isobenzofuran-1,4'-piperidin]-1'-yl)butyl)-5-amino-1-methyl-1,3-dihydro-2H-benzo[d]imidazol-2-one (WA257) (0.07g, 0.1721 mmol) in dry DCM is added (0.048g, 0.4752mmol) of TEA, then cooled down to 0 °C and treated with thiophosgene (0.02g, 0.1739mmol). The orange solution was stirred at r.t. under an argon atmosphere for 2hr. Solvents were removed in vacuo, and the residue was purified by column chromatography using DCM/MeOH (95/5) eluent to afford 0.055g of 3-(4-(3H-spiro[isobenzofuran-1,4'-piperidin]-1'-yl)butyl)-5-isothiocyanato-1-methyl-1,3-dihydro-2H-benzo[d]imidazol-2-one as brown residue in 71% yield. MS (ESI) m/z 449 $[\text{M}+1]^+$. ^1H NMR (400 MHz, Methanol- d_4) δ 7.32 – 7.19 (m, 5H), 7.13 – 6.97 (m, 2H), 4.88 (s, 2H), 3.94 (t, $J = 6.1$ Hz, 2H), 3.40 (q, $J = 8.0, 6.1$ Hz, 6H), 3.20 – 3.08 (m, 3H), 2.26 (td, $J = 13.6, 4.5$ Hz, 2H), 1.84 (t, $J = 8.8$ Hz, 6H). ^{13}C NMR (101 MHz, MeOD) δ 154.73, 143.50, 138.70, 134.15, 129.44, 129.05, 128.01, 127.39, 124.59, 121.07, 120.41, 119.20, 108.34, 105.47, 82.34, 70.71, 56.41, 49.51, 40.21, 33.89, 26.41, 25.37, 21.58.

3-(4-(4-(4-fluorophenyl)piperazin-1-yl)butyl)-5-isothiocyanato-1-propyl-1,3-dihydro-2H-benzo[d]imidazol-2-one. 341 (WA264) A solution of 5-amino-3-(4-(4-(4-fluorophenyl)piperazin-1-yl)butyl)-1-propyl-1,3-dihydro-2H-benzo[d]imidazol-2-one (WA263)

(0.14g, 0.329 mmol) in dry DCM is added (0.091g, 0.9mmol) of TEA, then cooled down to 0 °C and treated with thiophosgene (0.038g, 0.33mmol). The orange solution was stirred at r.t. under an argon atmosphere for 2hr. Solvents were removed in *vacuo*, and the residue was purified by column chromatography using DCM/MeOH (95/5) eluent to afford 0.065g of 3-(4-(4-(4-fluorophenyl)piperazin-1-yl)butyl)-5-isothiocyanato-1-propyl-1,3-dihydro-2H-benzo[d]imidazol-2-one as brown residue in 42% yield. MS (ESI) m/z 468.75 [M+1]⁺. ¹H NMR (400 MHz, Methanol-*d*₄) δ 7.23 – 7.12 (m, 2H), 7.04 (dd, J = 8.3, 2.0 Hz, 1H), 6.94 (td, J = 4.8, 2.9 Hz, 4H), 3.94 (t, J = 7.0 Hz, 2H), 3.87 (t, J = 7.2 Hz, 2H), 3.16 – 3.06 (m, 4H), 2.61 (q, J = 7.0, 4.8 Hz, 4H), 2.45 (s, 2H), 1.79 (dt, J = 14.4, 6.9 Hz, 4H), 1.59 (td, J = 8.8, 8.4, 3.9 Hz, 2H), 0.95 (q, J = 7.8, 7.2 Hz, 3H). ¹³C NMR (101 MHz, MeOD) δ 158.45, 156.09, 154.64, 147.91, 134.40, 134.40, 129.64, 128.40, 124.61, 119.02, 117.83, 117.75, 115.01, 114.79, 108.56, 105.57, 57.41, 52.79, 49.54, 42.40, 40.56, 25.71, 23.09, 21.34, 10.11.

3-(4-(4-(4-fluorophenyl)piperazin-1-yl)butyl)-5-isothiocyanato-1-pentyl-1,3-dihydro-2H-benzo[d]imidazol-2-one. 344, (WA349) To a solution of 1,1'-thiocarbonyldiimidazole (0.0183g, 0.1026mmol) dissolved in 2mL DMF at 50 °C was added dropwise a preprepared solution of 5-amino-3-(4-(4-(4-fluorophenyl)piperazin-1-yl)butyl)-1-pentyl-1,3-dihydro-2H-benzo[d]imidazol-2-one (0.1g, 0.2142 mmol) and (0.026g, 0.2574 mmol) TEA in dry DMF 1mL for 5 min. Then the mixture was stirred for 25 min at r.t, the mixture was diluted with water and extracted with DCM. The organic layer washed with brine, dried over sodium sulfate, and filtered. The filtrate concentrated in *vacuo*, and purified by column chromatography on silica gel with ethyl acetate/hexanes to give 0.08g of 3-(4-(4-(4-fluorophenyl)piperazin-1-yl)butyl)-5-isothiocyanato-1-pentyl-1,3-dihydro-2H-benzo[d]imidazol-2-one as brown residue in 73% yield. MS (ESI) m/z 496.63 [M+1]⁺. ¹H NMR (400 MHz, Methanol-*d*₄) δ 7.23 – 7.12 (m, 2H), 7.05 (d,

$J = 8.4$ Hz, 1H), 6.95 (d, $J = 7.1$ Hz, 4H), 3.92 (dt, $J = 16.3, 7.2$ Hz, 4H), 3.10 (t, $J = 5.0$ Hz, 4H), 2.63 (t, $J = 4.9$ Hz, 4H), 2.47 (t, $J = 7.8$ Hz, 2H), 1.76 (dp, $J = 22.6, 7.4$ Hz, 4H), 1.58 (q, $J = 7.7$ Hz, 2H), 1.35 (dd, $J = 15.5, 8.3$ Hz, 4H), 0.89 (d, $J = 7.1$ Hz, 3H). ^{13}C NMR (101 MHz, MeOD) δ 158.49, 156.12, 154.59, 147.86, 134.39, 129.65, 128.34, 124.63, 119.02, 117.86, 117.79, 115.01, 114.78, 108.53, 105.57, 57.36, 52.76, 49.50, 40.81, 40.52, 28.55, 27.69, 25.67, 23.00, 21.95, 12.93.

3-(4-(6,7-dimethoxy-3,4-dihydroisoquinolin-2(1H)-yl)butyl)-5-isothiocyanato-1-propyl-1,3-dihydro-2H-benzo[d]imidazol-2-one. 346 (WA352) To a solution of 1,1'-thiocarbonyldiimidazole (0.0682g, 0.3826mmol) dissolved in 2mL DMF at 50 °C was added dropwise a pre-prepared solution of 5-amino-3-(4-(6,7-dimethoxy-3,4-dihydroisoquinolin-2(1H)-yl)butyl)-1-propyl-1,3-dihydro-2H-benzo[d]imidazol-2-one (0.14g, 0.3192 mmol) and TEA (0.038g, 0.383 mmol) in dry DMF 1mL for 5 min. Then the mixture was stirred for 25 min at r.t, the mixture was diluted with water and extracted with DCM. The organic layer washed with brine, dried over sodium sulfate, and filtered. The filtrate concentrated in vacuo, and purified by column chromatography on silica gel with ethyl acetate/hexanes to give 0.1g of 3-(4-(6,7-dimethoxy-3,4-dihydroisoquinolin-2(1H)-yl)butyl)-5-isothiocyanato-1-propyl-1,3-dihydro-2H-benzo[d]imidazol-2-one as brown residue in 65% yield. MS (ESI) m/z 481.77 $[\text{M}+1]^+$. ^1H NMR (400 MHz, Methanol- d_4) δ 7.18 (d, $J = 2.0$ Hz, 1H), 7.13 (d, $J = 8.4$ Hz, 1H), 7.01 (dd, $J = 8.3, 1.9$ Hz, 1H), 6.65 (s, 1H), 6.58 (s, 1H), 3.92 (t, $J = 7.0$ Hz, 2H), 3.85 (t, $J = 7.2$ Hz, 2H), 3.76 (d, $J = 2.4$ Hz, 6H), 3.51 (s, 2H), 2.79 (t, $J = 6.0$ Hz, 2H), 2.68 (t, $J = 6.0$ Hz, 2H), 2.56 – 2.48 (m, 2H), 1.75 (dq, $J = 9.8, 7.5$ Hz, 4H), 1.63 (td, $J = 8.9, 7.5, 4.3$ Hz, 2H), 0.93 (t, $J = 7.4$ Hz, 3H). ^{13}C NMR (101 MHz, MeOD) δ 154.61, 147.79, 147.41, 134.19, 129.59, 128.39, 125.79, 125.77,

124.50, 119.02, 111.48, 109.66, 108.52, 105.59, 57.20, 55.09, 55.03, 50.62, 42.39, 40.58, 27.67, 25.82, 23.31, 21.36, 10.15.

3-(4-(6,7-dimethoxy-3,4-dihydroisoquinolin-2(1H)-yl)butyl)-5-isothiocyanato-1-pentyl-1,3-dihydro-2H-benzo[d]imidazol-2-one. **345 (WA350)** To a solution of 1,1'-thiocarbonyldiimidazole (0.0682g, 0.3826mmol) dissolved in 2 mL DMF at 50 °C was added dropwise a pre-prepared solution of 5-amino-3-(4-(6,7-dimethoxy-3,4-dihydroisoquinolin-2(1H)-yl)butyl)-1-propyl-1,3-dihydro-2H-benzo[d]imidazol-2-one (0.1g, 0.2142 mmol) and TEA (0.026g, 0.257 mmol) in dry DMF 1mL for 5 min. Then the mixture was stirred for 25 min at r.t, the mixture was diluted with water and extracted with DCM. The organic layer washed with brine, dried over sodium sulfate, and filtered. The filtrate concentrated in *vacuo*, and purified by column chromatography on silica gel with ethyl acetate/hexanes to give 0.08g of 3-(4-(6,7-dimethoxy-3,4-dihydroisoquinolin-2(1H)-yl)butyl)-5-isothiocyanato-1-pentyl-1,3-dihydro-2H-benzo[d]imidazol-2-one as brown residue in 73% yield. MS (ESI) m/z 409.76 $[M+1]^+$. ^1H NMR (400 MHz, Methanol- d_4) δ 7.17 (d, $J = 1.9$ Hz, 1H), 7.12 (d, $J = 8.4$ Hz, 1H), 7.01 (dd, $J = 8.3$, 2.0 Hz, 1H), 6.64 (s, 1H), 6.57 (s, 1H), 3.89 (dt, $J = 19.7$, 7.1 Hz, 4H), 3.76 (d, $J = 2.7$ Hz, 6H), 3.49 (s, 2H), 2.78 (t, $J = 5.9$ Hz, 2H), 2.66 (t, $J = 5.9$ Hz, 2H), 2.51 (dd, $J = 8.6$, 6.7 Hz, 2H), 1.84 – 1.56 (m, 6H), 1.42 – 1.23 (m, 4H), 0.88 (t, $J = 6.9$ Hz, 3H). ^{13}C NMR (101 MHz, MeOD) δ 154.53, 147.77, 147.39, 129.62, 128.34, 125.95, 125.84, 124.49, 119.01, 111.48, 109.67, 108.46, 105.59, 57.26, 55.09, 55.02, 50.63, 40.81, 40.60, 28.57, 27.77, 27.72, 25.85, 23.36, 21.97, 13.00.

3-(4-(3H-spiro[isobenzofuran-1,4'-piperidin]-1'-yl)butyl)-5-isothiocyanato-1-propyl-1,3-

dihydro-2H-benzo[d]imidazol-2-one. 343 (WA306) A solution of 3-(4-(3H-spiro[isobenzofuran-1,4'-piperidin]-1'-yl)butyl)-5-amino-1-propyl-1,3-dihydro-2H-benzo[d]imidazol-2-one (0.16g, 0.368 mmol) in dry DCM is added (0.093g, 0.92mmol) of TEA, then cooled down to 0 °C and treated with thiophosgene (0.042g, 0.3652 mmol). The orange solution was stirred at r.t. under an argon atmosphere for 2hr. Solvents were removed in *vacuo*, and the residue was purified by column chromatography using DCM/MeOH (90/10) eluent to afford 0.12g of 7a as brown residue in 68% yield. MS (ESI) m/z 477.64 [M+1]⁺. ¹H NMR (400 MHz, Methanol-*d*₄) δ 7.30 – 7.18 (m, 4H), 7.18 – 7.12 (m, 2H), 7.04 (dd, J = 8.4, 2.0 Hz, 1H), 4.86 (s, 2H), 3.94 (t, J = 6.9 Hz, 2H), 3.86 (t, J = 7.1 Hz, 2H), 2.93 – 2.85 (m, 2H), 2.57 – 2.44 (m, 4H), 1.97 (td, J = 13.5, 4.5 Hz, 2H), 1.83 – 1.67 (m, 6H), 1.62 (h, J = 7.7, 6.6 Hz, 2H), 0.93 (t, J = 7.4 Hz, 3H). ¹³C NMR (101 MHz, MeOD) δ 154.65, 144.87, 138.68, 134.39, 129.63, 128.41, 127.50, 127.14, 124.62, 120.79, 120.34, 119.06, 108.57, 105.57, 83.94, 70.25, 57.60, 49.64, 42.41, 40.56, 35.45, 25.81, 23.10, 21.35, 10.13.

5-nitro-1,3-dihydro-2H-benzo[d]imidazol-2-one. 466 (WA313) To a solution of 4-nitrobenzene-1,2-diamine (10g, 65.3 mmol) in 200 mL of freshly distilled THF was added (14g, 86.34 mmol) of carbonyldiimidazole, and the reaction mixture refluxed for 2 hr to afford 9 g of 5-nitro-1,3-dihydro-2H-benzo[d]imidazol-2-one as yellow precipitate in 77% yield. MS (ESI) m/z 178.33 [M-1]⁺. ¹H NMR (400 MHz, DMSO-*d*₆) δ 11.24 (s, 2H), 7.87 (d, J = 8.6 Hz, 1H), 7.66 (s, 1H), 7.04 (d, J = 8.7 Hz, 1H). ¹³C NMR (101 MHz, DMSO) δ 155.90, 141.64, 136.06, 130.09, 118.12, 108.42, 104.05.

1-methyl-6-nitro-1,3-dihydro-2H-benzo[d]imidazol-2-one. 467 (WA400) To a solution of 5-nitro-1,3-dihydro-2H-benzo[d]imidazol-2-one (WA313) (5g, 27.85 mmol) in 100 mL acetone

was added portionwise powdered KOH (1.6g, 28.51 mmol). Then a solution of methyl iodide in 50 mL acetone was added dropwise over 15 min and left for 24 hr at room temperature. The yellow precipitate was purified by column chromatography using MeOH:DCM as an eluent to obtain, 1-methyl-6-nitro-1,3-dihydro-2*H*-benzo[*d*]imidazol-2-one (**467**, **WA400a**) and 1-methyl-5-nitro-1,3-dihydro-2*H*-benzo[*d*]imidazol-2-one (**468**, **WA400b**) in 1:3 ratio, (0.6g:1.8g) as yellow solid. MS (ESI) *m/z* 192.59 [M-1]⁺. WA400a: ¹H NMR (400 MHz, DMSO-*d*₆) δ 11.40 (s, 1H), 8.01 – 7.95 (m, 2H), 7.27 (d, *J* = 8.4 Hz, 1H), 3.37 (s, 3H). ¹³C NMR (101 MHz, DMSO) δ 154.61, 142.00, 135.50, 130.04, 118.24, 107.59, 103.58, 27.73. WA400b: MS (ESI) *m/z* 192.59 [M-1]⁺. ¹H NMR (400 MHz, DMSO-*d*₆) δ 11.42 – 11.36 (m, 1H), 7.96 (dd, *J* = 8.7, 2.3 Hz, 1H), 7.68 (d, *J* = 2.2 Hz, 1H), 7.23 (d, *J* = 8.7 Hz, 1H), 3.32 (s, 3H). ¹³C NMR (101 MHz, DMSO) δ 155.10, 141.81, 136.88, 128.58, 118.06, 107.59, 104.10, 27.31, 27.21.

1-(4-bromobutyl)-3-methyl-5-nitro-1,3-dihydro-2*H*-benzo[*d*]imidazol-2-one. 317

(WA401/WA406) To a solution of 1-methyl-6-nitro-1,3-dihydro-2*H*-benzo[*d*]imidazol-2-one (WA400B) (0.6g, 3.1062 mmol) in 10 mL DMF were added (1.28g, 9.27 mmol) of potassium carbonate and (2.68g, 12.4 mmol) of 1,4-dibromobutane, and the reaction mixture heated at 65 °C for 2 hr, then the mixture extracted with ethyl acetate and water, dried over sodium sulfate and the solvent evaporated using *vacuu* then purified by column chromatography (EtOAc: Hexane) to afford 0.775g of 1-(4-bromobutyl)-3-methyl-5-nitro-1,3-dihydro-2*H*-benzo[*d*]imidazol-2-one as yellow oil in 76% yield. MS (ESI) *m/z* 350.71 [M+23]⁺. ¹H NMR (400 MHz, DMSO-*d*₆) δ 8.12 (q, *J* = 2.7 Hz, 1H), 8.04 – 8.00 (m, 1H), 7.33 (dd, *J* = 8.7, 2.5 Hz, 1H), 3.95 (ddt, *J* = 7.2, 4.8, 2.3 Hz, 2H), 3.56 (td, *J* = 6.2, 2.3 Hz, 2H), 3.41 – 3.37 (m, 3H), 1.86 – 1.74 (m, 4H). ¹³C NMR (101 MHz, DMSO) δ 154.46, 142.14, 135.63, 129.32, 118.34, 107.89, 103.77, 40.31, 35.01, 29.76, 27.87, 27.04.

1-(4-(4-(4-fluorophenyl)piperazin-1-yl)butyl)-3-methyl-5-nitro-1,3-dihydro-2H-

benzo[d]imidazol-2-one. 327 (WA402) To a solution of 1-(4-bromobutyl)-3-methyl-5-nitro-1,3-dihydro-2H-benzo[d]imidazol-2-one (WA401) (0.744g, 2.26 mmol) in 8 mL DMF were added (0.938g, 6.79 mmol) of potassium carbonate and (0.5g, 2.31 mmol) of 1-(4-fluorophenyl)piperazine, and the reaction mixture heated at 65 °C for 2 hr, then the mixture extracted with ethyl acetate and water, dried over sodium sulfate and the solvent evaporated using *vacuo* then purified by column chromatography (EtOAc: Hexane) to afford 0.73g of 1-(4-(4-(4-fluorophenyl)piperazin-1-yl)butyl)-3-methyl-5-nitro-1,3-dihydro-2H-benzo[d]imidazol-2-one as a yellow oil in 75% yield. MS (ESI) m/z 428.72 $[M+1]^+$. ^1H NMR (400 MHz, Chloroform-*d*) δ 8.10 (ddd, $J = 8.6, 5.0, 2.2$ Hz, 1H), 7.90 (dd, $J = 7.0, 2.2$ Hz, 1H), 7.04 (dd, $J = 12.7, 8.6$ Hz, 1H), 6.98 – 6.91 (m, 2H), 6.90 – 6.83 (m, 2H), 3.98 (td, $J = 7.3, 4.2$ Hz, 2H), 3.49 (d, $J = 3.6$ Hz, 3H), 3.11 (dd, $J = 6.3, 3.7$ Hz, 4H), 2.59 (q, $J = 5.4$ Hz, 4H), 2.44 (q, $J = 6.6, 6.0$ Hz, 2H), 1.84 (h, $J = 7.3$ Hz, 2H), 1.61 (p, $J = 7.4$ Hz, 2H). ^{13}C NMR (101 MHz, CDCl_3) δ 158.30, 155.93, 154.57, 147.93, 142.56, 135.09, 129.99, 129.23, 118.31, 117.80, 117.73, 115.55, 115.33, 106.53, 103.29, 57.74, 53.24, 50.13, 41.41, 27.56, 26.18, 23.91.

5-amino-1-(4-(4-(4-fluorophenyl)piperazin-1-yl)butyl)-3-methyl-1,3-dihydro-2H-

benzo[d]imidazol-2-one. 337 (WA403) To a solution of 1-(4-(4-(4-fluorophenyl)piperazin-1-yl)butyl)-3-methyl-5-nitro-1,3-dihydro-2H-benzo[d]imidazol-2-one (WA402) (0.6g, 1.4 mmol) in methanol (200ml) was added to 10% Palladium on carbon catalyst (0.1g) and stirred under a hydrogen pressure (40psi) for 2h. The mixture was filtered through celite and evaporated in *vacuo* and the residue was purified by column chromatography using MeOH/DCM as an eluent to give 0.45g of 5-amino-3-(4-(4-(4-fluorophenyl)piperazin-1-yl)butyl)benzo[d]oxazol-2(3H)-

one as brown solid in 80% yield. MS (ESI) m/z 398.97 $[M+1]^+$. ^1H NMR (400 MHz, DMSO- d_6) δ 7.01 (td, $J = 8.8, 1.9$ Hz, 2H), 6.89 (ddt, $J = 6.7, 4.6, 1.9$ Hz, 2H), 6.78 (dd, $J = 8.2, 1.7$ Hz, 1H), 6.41 (d, $J = 2.1$ Hz, 1H), 6.31 (dt, $J = 8.2, 1.9$ Hz, 1H), 4.76 (s, 2H), 3.76 – 3.67 (m, 2H), 3.21 (d, $J = 1.7$ Hz, 3H), 3.00 (dd, $J = 6.7, 3.3$ Hz, 4H), 2.43 (t, $J = 4.9$ Hz, 4H), 2.29 (s, 2H), 1.62 (td, $J = 17.2, 15.8, 8.3$ Hz, 2H), 1.44 (q, $J = 7.2$ Hz, 2H). ^{13}C NMR (101 MHz, DMSO) δ 154.14, 148.40, 144.22, 130.20, 121.28, 117.46, 117.39, 115.75, 115.53, 108.50, 107.36, 95.04, 57.67, 53.12, 49.41, 40.55, 27.20, 26.18, 23.92.

1-(4-(4-(4-fluorophenyl)piperazin-1-yl)butyl)-5-isothiocyanato-3-methyl-1,3-dihydro-2H-benzo[d]imidazol-2-one. 347 (WA404) To a solution of thiocarbonyldiimidazole (0.1614 g, 0.9056 mmol) dissolved in DMF (2 mL) at 50 °C was added dropwise a pre-prepared solution of 5-amino-3-(4-(4-(4-fluorophenyl)piperazin-1-yl)butyl)benzo[d]oxazol-2(3H)-one (WA403) (0.3 g, 0.7547 mmol) and triethylamine (0.0914 g, 0.905 mmol) in DMF (3 mL) for 5 min. After the mixture was stirred for 30 min at room temperature, the reaction mixture was diluted with water and extracted with ethylacetate. The combined organic layers were washed with water, brine, dried over sodium sulfate, and filtered. The filtrate was concentrated in *vacuo*, and the residue was purified by column chromatography using Ethylacetate/Hexane (20/80) eluent to afford 0.2 g of 1-(4-(4-(4-fluorophenyl)piperazin-1-yl)butyl)-5-isothiocyanato-3-methyl-1,3-dihydro-2H-benzo[d]imidazol-2-one as brown residue in 60% yield. MS (ESI) m/z 440.87 $[M+1]^+$. ^1H NMR (400 MHz, Methanol- d_4) δ 7.01 (tdt, $J = 14.2, 9.6, 5.2$ Hz, 2H), 6.90 (ddt, $J = 16.2, 8.2, 4.9$ Hz, 5H), 3.93 – 3.82 (m, 2H), 3.40 – 3.33 (m, 3H), 3.10 – 2.95 (m, 4H), 2.59 – 2.47 (m, 4H), 2.39 (dt, $J = 16.8, 8.0$ Hz, 2H), 1.78 (q, $J = 8.2, 7.8$ Hz, 2H), 1.58 (dd, $J = 16.4, 8.9$ Hz, 2H). ^{13}C NMR (101 MHz, DMSO) δ 157.50, 155.17, 154.26, 148.41, 128.72, 117.47, 117.40, 117.38,

116.77, 115.73, 115.70, 115.51, 115.48, 107.08, 103.82, 57.66, 53.15, 49.43, 28.14, 27.30, 26.34, 23.90.

3-(4-bromobutyl)-1-methyl-5-nitro-1,3-dihydro-2H-benzo[d]imidazol-2-one. 314 (WA407)

To a solution of 1-methyl-5-nitro-1,3-dihydro-2H-benzo[d]imidazol-2-one (WA400A) (1.5 g, 7.7655 mmol) in 15 mL DMF were added (3.2g, 23.18 mmol) of potassium carbonate and 6.7 g, 31.018 mmol) of 1,4-dibromobutane, and the reaction mixture heated at 65 °C for 2 hr, then the mixture extracted with ethyl acetate and water, dried over sodium sulfate and the solvent evaporated using *vacu* then purified by column chromatography (EtOAc: Hexane) to afford 2 g of 3-(4-bromobutyl)-1-methyl-5-nitro-1,3-dihydro-2H-benzo[d]imidazol-2-one as yellow oil in 80% yield. MS (ESI) *m/z* 328.59 [M+1]⁺. ¹H NMR (400 MHz, Methanol-*d*₄) δ 8.92 (d, *J* = 2.2 Hz, 1H), 8.84 – 8.81 (m, 1H), 8.13 (d, *J* = 8.7 Hz, 1H), 4.74 (dd, *J* = 11.5, 6.1 Hz, 2H), 4.37 (t, *J* = 6.0 Hz, 2H), 4.21 (d, *J* = 7.4 Hz, 3H), 2.61 (h, *J* = 8.4, 5.7 Hz, 4H). ¹³C NMR (101 MHz, MeOD) δ 155.28, 142.96, 136.44, 130.13, 119.14, 108.68, 104.56, 41.13, 35.78, 30.58, 28.66, 27.84.

3-(4-(6,7-dimethoxy-3,4-dihydroisoquinolin-2(1H)-yl)butyl)-5-isothiocyanato-1-pentyl-1,3-dihydro-2H-benzo[d]imidazol-2-one. 342 (WA269)

A solution of 5-amino-3-(4-(6,7-dimethoxy-3,4-dihydroisoquinolin-2(1H)-yl)butyl)-1-pentyl-1,3-dihydro-2H-benzo[d]imidazol-2-one (0.107g, 0.2316 mmol) in dry DCM is added (0.064g, 0.6336mmol) of TEA, then cooled down to 0 °C and treated with thiophosgene (0.026g, 0.2313 mmol). The orange solution was stirred at r.t. under an argon atmosphere for 2hr. Solvents were removed in *vacuo*, and the residue was purified by column chromatography using DCM/MeOH (90/10) eluent to afford 0.09g of 7a as brown residue in 77% yield. MS (ESI) *m/z* 409.76 [M+1]⁺. ¹H NMR (400 MHz, Methanol-*d*₄) δ 7.17 (d, *J* = 1.9 Hz, 1H), 7.12 (d, *J* = 8.4 Hz, 1H), 7.01 (dd, *J* = 8.3, 2.0 Hz, 1H),

6.64 (s, 1H), 6.57 (s, 1H), 3.89 (dt, $J = 19.7, 7.1$ Hz, 4H), 3.76 (d, $J = 2.7$ Hz, 6H), 3.49 (s, 2H), 2.78 (t, $J = 5.9$ Hz, 2H), 2.66 (t, $J = 5.9$ Hz, 2H), 2.51 (dd, $J = 8.6, 6.7$ Hz, 2H), 1.84 – 1.56 (m, 6H), 1.42 – 1.23 (m, 4H), 0.88 (t, $J = 6.9$ Hz, 3H). ^{13}C NMR (101 MHz, MeOD) δ 154.53, 147.77, 147.39, 129.62, 128.34, 125.95, 125.84, 124.49, 119.01, 111.48, 109.67, 108.46, 105.59, 57.26, 55.09, 55.02, 50.63, 40.81, 40.60, 28.57, 27.77, 27.72, 25.85, 23.36, 21.97, 13.00.

9.4.3 Synthesis of the benzoimidazolone derivatives (356), (357), (358), (359), and (360).

Synthesis of 1,3-dihydro-2H-benzo[*d*]imidazol-2-one. 351 (WA277) A solution of benzene-1,2-diamine (**350**) (5 g, 46.19 mmol) and 1,1'-carbonyldiimidazole (CDI) (7.5g, 46.25mmol) in freshly prepared tetrahydrofuran (50 mL) was stirred at 85°C for 18 hours. The reaction mixture was then cooled to 0°C. The resulting precipitate was filtered and dried to give (4 g, 68.5 % yield) of 1,3-dihydro-2H-benzo[*d*]imidazol-2-one as beige crystals. MS (EI) m/z 135 ($\text{M}^+ + 1$), 133 ($\text{M}^+ - 1$). ^1H NMR (400 MHz, DMSO- d_6) δ 10.59 (s, 2H), 6.91 (s, 4H). ^{13}C NMR (101 MHz, DMSO) δ 155.77, 130.10, 120.87, 108.96.

***tert*-butyl 2-oxo-2,3-dihydro-1H-benzo[*d*]imidazole-1-carboxylate. 352 (WA278)** To a solution of 1,3-dihydro-2H-benzo[*d*]imidazol-2-one (1.3g, 9.7 mmol) in anhydrous DMF (15 mL) was added 2.6 g of NaH (60% wt in mineral oil) portionwise under argon and stirring. After 45 min. di-*tert*-butyl dicarbonate (2.1g, 9.62 mmol) in 10 mL DMF was added dropwise then stirred at room temperature overnight. The reaction mixture was then poured into ice-cold NH_4Cl saturated solution, and filtered to afford 1.4g (61.6%) of *tert*-butyl 2-oxo-2,3-dihydro-1H-benzo[*d*]imidazole-1-carboxylate as a white solid. MS (EI) m/z 257 ($\text{M}^+ + 23$), 233.55 ($\text{M}^+ - 1$). ^1H NMR (400 MHz, DMSO- d_6) δ 10.57 (s, 1H), 7.62 (d, $J = 7.9$ Hz, 1H), 7.11 (t, $J = 7.6$ Hz, 1H),

7.06 – 6.94 (m, 2H), 1.57 (s, 9H). ¹³C NMR (101 MHz, DMSO) δ 151.21, 148.85, 129.02, 127.15, 124.18, 121.63, 114.16, 109.50, 84.02, 28.09.

***tert*-butyl 3-(4-bromobutyl)-2-oxo-2,3-dihydro-1*H*-benzo[*d*]imidazole-1-carboxylate. 353**

(WA279) To a solution of *tert*-butyl 2-oxo-2,3-dihydro-1*H*-benzo[*d*]imidazole-1-carboxylate (1.4g, 6 mmol) in 50 mL water were added (1.6g, 11.6 mmol) of potassium carbonate and (5g, 23.14 mmol) of 1,4-dibromobutane, and the reaction mixture heated at 100 °C for 10 h, then the mixture extracted with CH₂Cl₂ and water, dried over NaSO₄ and the solvent evaporated using *vaccu* then purified by column chromatography (EtOAc: Hexane) to get 0.87g of *tert*-butyl 3-(4-bromobutyl)-2-oxo-2,3-dihydro-1*H*-benzo[*d*]imidazole-1-carboxylate as a white solid in 40% yield. MS (EI) *m/z* 367.68 (M⁺-1). ¹H NMR (400 MHz, DMSO-*d*₆) δ 7.70 (dd, *J* = 8.0, 1.1 Hz, 1H), 7.27 – 7.18 (m, 2H), 7.11 (td, *J* = 7.7, 1.5 Hz, 1H), 3.84 (t, *J* = 6.7 Hz, 2H), 3.56 (t, *J* = 6.4 Hz, 2H), 1.87 – 1.71 (m, 4H), 1.58 (s, 9H). ¹³C NMR (101 MHz, DMSO) δ 150.38, 148.63, 129.68, 125.99, 124.33, 122.18, 114.21, 108.69, 84.42, 39.96, 35.02, 29.88, 28.11, 26.54.

1-(4-(4-(4-fluorophenyl)piperazin-1-yl)butyl)-1,3-dihydro-2*H*-benzo[*d*]imidazol-2-one. 356

(WA365) To a solution of *tert*-butyl 3-(4-bromobutyl)-2-oxo-2,3-dihydro-1*H*-benzo[*d*]imidazole-1-carboxylate (1g, 2.7 mmol) in 10 mL DMF were added (1.12g, 8.11 mmol) of potassium carbonate and (0.583g, 3.23 mmol) of 1-(4-fluorophenyl)piperazine-HCl, and the reaction mixture heated at 65 °C for 6 h, then the mixture extracted with ethylacetate and water, washed with brine and dried over magnesium sulfate and the solvent evaporated using *vaccu* then purified by column chromatography (EtOAc: Hexane) to get 0.8g of 1-(4-(4-(4-fluorophenyl)piperazin-1-yl)butyl)-1,3-dihydro-2*H*-benzo[*d*]imidazol-2-one as brown oil in 66% yield. MS (EI) *m/z* 369.87 (M⁺+1). ¹H NMR (400 MHz, DMSO-*d*₆) δ 10.84 (s, 1H), 7.12 – 7.08 (m, 1H), 7.03 – 6.94 (m, 5H), 6.89 (dd, *J* = 9.2, 4.6 Hz, 2H), 3.79 (t, *J* = 7.0 Hz, 2H), 3.00 (dd, *J*

= 6.2, 3.7 Hz, 4H), 2.43 (t, $J = 4.9$ Hz, 4H), 2.31 (t, $J = 7.2$ Hz, 2H), 1.66 (dd, $J = 8.8, 6.0$ Hz, 2H), 1.45 (p, $J = 7.4$ Hz, 2H). ^{13}C NMR (101 MHz, DMSO) δ 155.19, 154.67, 148.38, 130.64, 128.73, 121.08, 120.84, 117.46, 117.38, 115.75, 115.53, 109.17, 108.15, 57.53, 53.09, 49.42, 40.06, 26.09, 23.81.

1-(4-(4-(4-fluorophenyl)piperazin-1-yl)butyl)-3-(4-nitrophenyl)-1,3-dihydro-2H-

benzo[*d*]imidazol-2-one. 357 (WA367) To a solution of 1-(4-(4-(4-fluorophenyl)piperazin-1-yl)butyl)-1,3-dihydro-2H-benzo[*d*]imidazol-2-one (1.4g, 3.8 mmol) in 10 mL DMSO were added (1.6g, 11.59 mmol) of potassium carbonate and (1 g, 7.08 mmol) of 1-fluoro-4-nitrobenzene, and the reaction mixture heated at 100 °C for 3 hr, then the mixture extracted with ethylacetate and water, washed with brine and dried over MgSO_4 and the solvent evaporated using *vacuu* then purified by column chromatography (EtOAc: Hexane) to get 0.9g of 1-(4-(4-(4-fluorophenyl)piperazin-1-yl)butyl)-3-(4-nitrophenyl)-1,3-dihydro-2H-benzo[*d*]imidazol-2-one as a yellow solid in 50% yield. MS (EI) m/z 490.80 ($\text{M}^+ + 1$). ^1H NMR (400 MHz, $\text{DMSO-}d_6$) δ 8.43 – 8.37 (m, 2H), 7.93 – 7.88 (m, 2H), 7.36 (d, $J = 7.8$ Hz, 1H), 7.27 (d, $J = 7.9$ Hz, 1H), 7.20 (t, $J = 7.6$ Hz, 1H), 7.11 (t, $J = 7.7$ Hz, 1H), 7.01 (t, $J = 8.8$ Hz, 2H), 6.90 (dd, $J = 9.2, 4.6$ Hz, 2H), 3.94 (t, $J = 7.1$ Hz, 2H), 3.02 (t, $J = 4.9$ Hz, 4H), 2.45 (t, $J = 5.0$ Hz, 4H), 2.34 (t, $J = 7.1$ Hz, 2H), 1.75 (p, $J = 7.2$ Hz, 2H), 1.52 (p, $J = 7.3$ Hz, 2H). ^{13}C NMR (101 MHz, DMSO) δ 157.54, 155.20, 152.41, 148.39, 145.78, 140.97, 129.92, 127.93, 126.28, 125.29, 123.19, 121.96, 117.46, 117.39, 115.75, 115.53, 109.32, 109.27, 57.50, 53.12, 49.43, 41.01, 25.93, 23.80.

1-(4-aminophenyl)-3-(4-(4-(4-fluorophenyl)piperazin-1-yl)butyl)-1,3-dihydro-2H-

benzo[*d*]imidazol-2-one. 359 (WA371) To a solution of 1-(4-(6,7-dimethoxy-3,4-dihydroisoquinolin-2(1*H*)-yl)butyl)-3-(4-nitrophenyl)-1,3-dihydro-2H-benzo[*d*]imidazol-2-one

(0.65g, 1.32 mmol) in methanol (150 mL) was hydrogenated in the Parr apparatus (45 psi) in the presence of 10% palladium on charcoal (0.53 g) for 3 h. Filtration of the catalyst, concentrated and dried to afford 0.4 g (61%) of 1-(4-aminophenyl)-3-(4-(4-(4-fluorophenyl)piperazin-1-yl)butyl)-1,3-dihydro-2*H*-benzo[*d*]imidazol-2-one as brown oil. MS (EI) m/z 460.83 ($M^+ + 1$). ^1H NMR (400 MHz, Methanol- d_4) δ 7.24 (d, $J = 7.7$ Hz, 1H), 7.19 – 7.10 (m, 3H), 7.06 (td, $J = 7.6$, 1.2 Hz, 1H), 6.94 (pd, $J = 8.1$, 6.7, 3.7 Hz, 5H), 6.88 – 6.80 (m, 2H), 4.01 (t, $J = 6.9$ Hz, 2H), 3.09 (t, $J = 5.1$ Hz, 2H), 2.66 (s, 4H), 2.61 (t, $J = 5.1$ Hz, 4H), 2.51 – 2.40 (m, 2H), 1.85 (p, $J = 7.1$ Hz, 2H), 1.71 – 1.51 (m, 2H). ^{13}C NMR (101 MHz, MeOD) δ 158.48, 156.12, 154.11, 148.15, 130.19, 128.92, 127.29, 123.56, 121.70, 121.41, 117.85, 117.77, 115.15, 115.00, 114.78, 108.46, 108.05, 57.53, 52.76, 49.48, 39.03, 25.87, 23.22.

1-(4-(4-(4-fluorophenyl)piperazin-1-yl)butyl)-3-(4-isothiocyanatophenyl)-1,3-dihydro-2*H*-benzo[*d*]imidazol-2-one. 360 (WA372) A solution of 1-(4-aminophenyl)-3-(4-(4-(4-fluorophenyl)piperazin-1-yl)butyl)-1,3-dihydro-2*H*-benzo[*d*]imidazol-2-one (0.3g, 0.6528 mmol) in dry DMF (5 mL) is added (0.080g, 0.79 mmol) of TEA, then cooled down to 0 °C and treated with 1,1'-thiocarbonyldiimidazole (0.14g, 0.78 mmol). The mixture was stirred at r.t. under argon atmosphere for 2hr. Solvents were removed in vacuo, and the residue was purified by column chromatography using DCM/MeOH (90/10) eluent to afford 0.2g of 1-(4-(4-(4-fluorophenyl)piperazin-1-yl)butyl)-3-(4-isothiocyanatophenyl)-1,3-dihydro-2*H*-benzo[*d*]imidazol-2-one as brown residue in 61% yield. MS (EI) m/z 502.81 ($M^+ + 1$). ^1H NMR (400 MHz, Chloroform- d) δ 7.61 – 7.54 (m, 2H), 7.42 – 7.33 (m, 2H), 7.19 – 7.08 (m, 4H), 6.98 – 6.84 (m, 4H), 4.00 (t, $J = 7.0$ Hz, 2H), 3.11 (t, $J = 4.8$ Hz, 4H), 2.60 (t, $J = 4.9$ Hz, 4H), 2.46 (t, $J = 7.4$ Hz, 2H), 1.88 (p, $J = 7.3$ Hz, 2H), 1.66 (t, $J = 7.8$ Hz, 2H). ^{13}C NMR (101 MHz, CDCl_3) δ 158.29, 155.92, 152.99, 147.97, 147.95, 136.49, 133.65, 130.13, 129.52, 128.73, 126.75,

122.38, 121.53, 117.77, 117.70, 115.58, 115.36, 108.68, 108.15, 77.42, 77.10, 76.78, 57.83, 53.21, 50.13, 41.14, 26.15, 24.10.

1-(4-(3*H*-spiro[isobenzofuran-1,4'-piperidin]-1'-yl)butyl)-1,3-dihydro-2*H*-benzo[*d*]

imidazol-2-one. 358 (WA294) To a solution of *tert*-butyl 3-(4-bromobutyl)-2-oxo-2,3-dihydro-1*H*-benzo[*d*]imidazole-1-carboxylate (**353**) (0.3 g, 0.817 mmol) in 10 mL DMF were added (0.22 g, 1.6 mmol) of potassium carbonate and (0.2 g, 0.88 mmol) of 3*H*-spiro[isobenzofuran-1,4'-piperidine] -HCl, and the reaction mixture heated at 60 °C for 6 hr, then the mixture extracted with ethylacetate and water, washed with brine and dried over anhydrous magnesium sulfate and the solvent evaporated using *vacuu* to get the protected compound (**355**) that was treated with trifluoroacetic acid (TFA) in methylene chloride (DCM) and stirred at room temperature for 3hr. The solvents were evaporated and the residue was purified by column chromatography (EtOAc: Hexane) to get 0.22 g of 1-(4-(3*H*-spiro[isobenzofuran-1,4'-piperidin]-1'-yl)butyl)-1,3-dihydro-2*H*-benzo[*d*]imidazol-2-one as white-brownish solid in 73% yield. MS (EI) *m/z* 378.66 ($M^+ + 1$). ¹H NMR (400 MHz, DMSO-*d*₆) δ 10.85 (s, 1H), 7.28 (d, *J* = 3.0 Hz, 3H), 7.21 (d, *J* = 4.4 Hz, 1H), 7.14 (d, *J* = 7.0 Hz, 1H), 7.03 – 6.96 (m, 3H), 3.82 (t, *J* = 6.8 Hz, 2H), 3.03 (dd, *J* = 16.9, 9.6 Hz, 2H), 2.69 (d, *J* = 23.3 Hz, 4H), 1.98 (d, *J* = 12.9 Hz, 2H), 1.63 (dq, *J* = 44.1, 7.9, 6.7 Hz, 7H), 1.16 (t, *J* = 7.3 Hz, 1H). ¹³C NMR (101 MHz, DMSO) δ 154.72, 145.11, 139.17, 130.61, 128.72, 128.19, 127.82, 121.76, 121.19, 121.12, 120.92, 109.18, 108.19, 83.39, 70.56, 49.67, 46.10, 39.86, 35.02, 25.89, 22.83.

1-(4-bromobutyl)-5-nitro-3-pentyl-1,3-dihydro-2*H*-benzo[*d*]imidazol-2-one. 471 [(WA419) (WA418A & WA418B)] To a solution of 5-nitro-1,3-dihydro-2*H*-benzo[*d*]imidazol-2-one (WA313) (1 g, 5.58 mmol), potassium carbonate (2.30 g, 16.74 mmol) in DMF (15 ml) was

added 1-iodopentane (2.2 g, 11.16 mmol). Stirring was continued at room temperature for 5 h. Then the mixture extracted with ethyl acetate and water, dried over sodium sulfate and the solvent evaporated using *vacuu* then purified by column chromatography (EtOAc: Hexane) to afford a mixture of (0.4 g, 1.6046 mmol) 5-nitro-1-pentyl-1,3-dihydro-2*H*-benzo[*d*]imidazol-2-one [WA418A] and (0.9 g, 3.61 mmol) of 6-nitro-1-pentyl-1,3-dihydro-2*H*-benzo[*d*]imidazol-2-one [WA418B]. The later was treated with potassium carbonate (1.5 g, 10.86 mmol) and 1,4-dibromobutane (3.119 g, 14.44 mmol) in DMF (15 ml), and the reaction mixture heated at 65 °C for 2 hr, then the mixture extracted with ethyl acetate and water, dried over sodium sulfate and the solvent evaporated using *vacuu*. The remaining residue purified by column chromatography on a silica gel (EtOAc: Hexane) to afford 0.8 g of 1-(4-bromobutyl)-5-nitro-3-pentyl-1,3-dihydro-2*H*-benzo[*d*]imidazol-2-one as yellow oil in 69% yield. MS (ESI) *m/z* 384.56 [M+1]⁺. ¹H NMR (400 MHz, Chloroform-*d*) δ 8.05 – 7.93 (m, 1H), 7.84 (dd, *J* = 10.2, 2.2 Hz, 1H), 7.02 (t, *J* = 9.0 Hz, 1H), 3.93 (t, *J* = 6.4 Hz, 2H), 3.86 (t, *J* = 7.3 Hz, 2H), 3.39 (q, *J* = 5.5, 4.8 Hz, 2H), 1.89 (dq, *J* = 8.8, 4.7 Hz, 4H), 1.71 (d, *J* = 7.3 Hz, 2H), 1.29 (dp, *J* = 8.9, 4.9 Hz, 4H), 0.82 (t, *J* = 6.5 Hz, 3H). ¹³C NMR (101 MHz, CDCl₃) δ 154.35, 142.29, 134.62, 129.07, 118.24, 106.80, 103.24, 41.58, 40.43, 32.76, 29.49, 28.77, 27.93, 26.77, 22.19, 13.85. **WA418A**: ¹H NMR (400 MHz, DMSO-*d*₆) δ 11.39 (s, 1H), 7.97 (dd, *J* = 8.7, 2.3 Hz, 1H), 7.72 (d, *J* = 2.3 Hz, 1H), 7.31 (d, *J* = 8.7 Hz, 1H), 3.82 (t, *J* = 7.1 Hz, 2H), 1.62 (p, *J* = 7.2 Hz, 2H), 1.31 – 1.18 (m, 4H), 0.81 (t, *J* = 6.9 Hz, 3H). ¹³C NMR (101 MHz, DMSO) δ 154.91, 141.78, 136.27, 128.65, 118.09, 107.73, 104.27, 40.74, 28.67, 27.87, 22.17, 14.24. ¹⁵N NMR (51 MHz, DMSO) δ 370.74, 130.81, 119.97. **WA418B**: ¹H NMR (500 MHz, DMSO-*d*₆) δ 11.62 (s, 1H), 8.02 (d, *J* = 2.2 Hz, 1H), 7.96 (dd, *J* = 8.6, 2.2 Hz, 1H), 7.14 (d, *J* = 8.6 Hz, 1H), 3.87 (t, *J* = 7.2 Hz, 2H), 1.64 (p, *J* = 7.3 Hz, 2H), 1.28 (dq, *J* = 14.4, 5.4, 4.2 Hz, 4H), 0.84 (t, *J* = 7.0 Hz, 3H). ¹³C NMR (101 MHz,

DMSO) δ 154.99, 141.94, 134.63, 130.75, 118.32, 108.71, 103.61, 40.58, 28.67, 27.87, 22.18, 14.25. ^{15}N NMR (51 MHz, DMSO) δ 371.36, 125.37, 105.59.

1-(4-(4-(4-fluorophenyl)piperazin-1-yl)butyl)-5-nitro-3-pentyl-1,3-dihydro-2H-benzo

[d]imidazol-2-one. 472 (WA420) To a solution of 3-(4-bromobutyl)-5-nitro-1-pentyl-1,3-dihydro-2H-benzo[d]imidazol-2-one (WA419) (1 g, 3.02 mmol) in 15 mL DMF were added (1.25 g, 9.05 mmol) of potassium carbonate and (0.653g, 3.62 mmol) of 1-(4-fluorophenyl)piperazine, and the reaction mixture heated at 65 °C for 3 hr, then the mixture extracted with ethyl acetate and water, dried over sodium sulfate and the solvent evaporated using *vacuu* then purified by column chromatography (EtOAc: Hexane) to afford 1 g of 1-(4-(4-(4-fluorophenyl)piperazin-1-yl)butyl)-5-nitro-3-pentyl-1,3-dihydro-2H-benzo[d]imidazol-2-one as yellow solid in 76% yield. MS (ESI) m/z 484.69 $[\text{M}+1]^+$. ^1H NMR (400 MHz, Chloroform-*d*) δ 8.08 (dd, $J = 8.6, 2.2$ Hz, 1H), 7.88 (d, $J = 2.2$ Hz, 1H), 7.05 (d, $J = 8.7$ Hz, 1H), 6.99 – 6.91 (m, 2H), 6.91 – 6.80 (m, 2H), 3.95 (dt, $J = 20.4, 7.3$ Hz, 4H), 3.10 (t, $J = 5.0$ Hz, 4H), 2.92 (d, $J = 29.2$ Hz, 2H), 2.63 – 2.54 (m, 4H), 2.44 (t, $J = 7.3$ Hz, 2H), 1.80 (dp, $J = 21.4, 7.2$ Hz, 4H), 1.37 (hept, $J = 4.7, 4.0$ Hz, 4H), 0.95 – 0.86 (m, 3H). ^{13}C NMR (101 MHz, CDCl_3) δ 154.39, 147.89, 142.40, 134.50, 129.40, 118.14, 117.78, 117.71, 115.58, 115.36, 106.63, 103.37, 57.64, 53.16, 50.10, 41.60, 41.35, 28.84, 27.98, 26.19, 23.91, 22.26, 13.91.

5-amino-1-(4-(4-(4-fluorophenyl)piperazin-1-yl)butyl)-3-pentyl-1,3-dihydro-2H-

benzo[d]imidazol-2-one. 473 (WA421) To a solution of 3-(4-(4-(4-fluorophenyl)piperazin-1-yl)butyl)-5-nitro-1-pentyl-1,3-dihydro-2H-benzo[d]imidazol-2-one (WA420) (0.694 g, 1.43 mmol) in methanol (100 ml) was added to 10% Palladium on carbon catalyst (0.150g) and stirred under a hydrogen pressure (50 psi) for 1h. The mixture was filtered through celite and

evaporated in *vacuo* then purified by column chromatography (EtOAc: Hexane) to afford 0.200 g of 5-amino-1-(4-(4-(4-fluorophenyl)piperazin-1-yl)butyl)-3-pentyl-1,3-dihydro-2H-benzo[*d*]imidazol-2-one as brown solid in 31% yield. MS (ESI) m/z 454.73 [M+1]⁺. ¹H NMR (400 MHz, Chloroform-*d*) δ 6.94 (t, J = 8.7 Hz, 2H), 6.85 (dd, J = 9.1, 4.5 Hz, 2H), 6.77 (d, J = 8.1 Hz, 1H), 6.46 – 6.35 (m, 2H), 3.81 (dt, J = 25.5, 7.2 Hz, 4H), 3.67 (s, 2H), 3.09 (t, J = 4.9 Hz, 4H), 2.61 – 2.54 (m, 4H), 2.43 (t, J = 7.5 Hz, 2H), 1.76 (ddd, J = 19.0, 13.2, 7.2 Hz, 4H), 1.58 (ddd, J = 15.1, 8.7, 6.0 Hz, 2H), 1.34 (dt, J = 7.8, 3.7 Hz, 4H), 0.88 (t, J = 6.6 Hz, 3H). ¹³C NMR (101 MHz, CDCl₃) δ 158.27, 155.90, 154.35, 147.96, 147.94, 141.30, 130.50, 122.31, 117.77, 117.70, 115.55, 115.34, 108.15, 107.99, 95.90, 57.83, 53.11, 50.03, 41.04, 40.76, 28.96, 28.03, 26.26, 23.91, 22.36, 13.99.

1-(4-(4-(4-fluorophenyl)piperazin-1-yl)butyl)-5-isothiocyanato-3-pentyl-1,3-dihydro-2H-benzo[*d*]imidazol-2-one. 474 (WA422) To a solution of thiocarbonyldiimidazole (0.047 g, 0.26 mmol) dissolved in DMF (1 mL) at 50 °C was added dropwise a pre-prepared solution of 5-amino-3-(4-(4-(4-fluorophenyl)piperazin-1-yl)butyl)-1-pentyl-1,3-dihydro-2H-benzo[*d*]imidazol-2-one (WA421) (0.100 g, 0.2207 mmol) and triethylamine (0.027 g, 0.2673 mmol) in DMF (1 mL) for 5 min. After the mixture was stirred for 30 min at room temperature, the reaction mixture was diluted with water and extracted with ethylacetate. The combined organic layers were washed with water, brine, dried over sodium sulfate, and filtered. The filtrate was concentrated in *vacuo*, and the residue was purified by column chromatography using Ethylacetate/Hexane (20/80) as an eluent to afford 0.06 g of 1-(4-(4-(4-fluorophenyl)piperazin-1-yl)butyl)-5-isothiocyanato-3-pentyl-1,3-dihydro-2H-benzo[*d*]imidazol-2-one as a white solid in 55% yield. MS (ESI) m/z 496.69 [M+1]⁺. ¹H NMR (400 MHz, Chloroform-*d*) δ 7.04 – 6.89 (m, 4H), 6.89 – 6.81 (m, 3H), 3.91 (q, J = 7.1 Hz, 2H), 3.83 (t, J = 7.4 Hz, 2H), 3.11 (q, J = 5.1 Hz,

4H), 2.60 (q, $J = 6.1, 5.1$ Hz, 4H), 2.45 (s, 2H), 1.84 – 1.68 (m, 4H), 1.63 – 1.54 (m, 2H), 1.34 (tq, $J = 7.0, 4.3, 3.1$ Hz, 4H), 0.89 (dt, $J = 10.5, 6.8$ Hz, 3H). ^{13}C NMR (101 MHz, CDCl_3) δ 158.34, 155.97, 154.25, 147.85, 134.17, 129.98, 128.45, 124.36, 118.92, 117.83, 117.75, 115.59, 115.37, 107.85, 105.26, 57.67, 53.10, 50.01, 41.38, 41.00, 28.88, 27.96, 26.16, 23.80, 22.30, 13.95.

9.4.4 Synthesis of the isothiocyanate derivative of benzofuran

1-(4-(benzofuran-3-yl)butyl)-4-(4-isothiocyanatophenyl)piperazine. 349 (WA255) A solution of 4-(4-(4-(benzofuran-3-yl)butyl)piperazin-1-yl)aniline (WA254) (0.11 g, 0.3151 mmol) in dry DCM 3 mL is added (0.084 g, 0.86 mmol) of TEA, then cooled down to 0 °C and treated with thiophosgene (0.036 g, 0.31 mmol) solution in 2 mL dry DCM. The orange solution was stirred at r.t. under an argon atmosphere for 2hr. Solvents were removed in *vacuo*, and the residue was purified by column chromatography using hexanes/ethylacetate (80/20) eluent to afford 0.06 g of 1-(4-(benzofuran-3-yl)butyl)-4-(4-isothiocyanatophenyl)piperazine as brown residue in 49% yield. MS (ESI) m/z 292.83 $[\text{M}+1]^+$. ^1H NMR (400 MHz, $\text{DMSO}-d_6$) δ 11.55 (s, 1H), 10.66 (s, 1H), 7.82 (s, 1H), 7.63 (d, $J = 7.3$ Hz, 1H), 7.52 (d, $J = 7.9$ Hz, 1H), 7.34 – 7.19 (m, 4H), 7.01 (d, $J = 8.4$ Hz, 2H), 3.85 (d, $J = 13.0$ Hz, 2H), 3.50 (d, $J = 11.7$ Hz, 2H), 3.28 (t, $J = 12.3$ Hz, 2H), 3.11 (dt, $J = 25.0, 7.7$ Hz, 4H), 2.68 (t, $J = 7.3$ Hz, 2H), 1.89 – 1.77 (m, 2H), 1.69 (p, $J = 7.1$ Hz, 2H). ^{13}C NMR (101 MHz, DMSO) δ 155.11, 149.19, 142.51, 132.10, 128.20, 127.36, 124.70, 122.86, 121.13, 120.23, 119.88, 116.62, 111.75, 55.44, 50.65, 45.00, 26.14, 23.09, 22.73.

9.4.5 Synthesis of benzoxazolone derivatives of isothiocyanate

5-nitrobenzo[*d*]oxazol-2(3*H*)-one. 362 (WA391) A solution of 2-amino-4-nitrophenol () (5 g, 32.44 mmol) (**361**) and 1,1'-carbonyldiimidazole (CDI) (7.88 g, 48.66 mmol) in tetrahydrofuran (100 mL) was stirred at 65°C for 6 hours. The reaction mixture was then cooled to 0°C. The resulting precipitate was filtered and dried to give (0.88g, 4mmol, 51.6% yield) of 5-nitrobenzo[*d*]oxazol-2(3*H*)-one as a grey solid. MS (ESI) *m/z* 179.56 [M-1]⁺. ¹H NMR (400 MHz, DMSO-*d*₆) δ 12.09 (s, 1H), 8.00 (d, *J* = 8.7 Hz, 1H), 7.78 (s, 1H), 7.47 (d, *J* = 8.4 Hz, 1H). ¹³C NMR (101 MHz, DMSO) δ 154.43, 148.23, 144.16, 131.62, 118.96, 110.18, 105.37.

3-(4-bromobutyl)-5-nitrobenzo[*d*]oxazol-2(3*H*)-one. 363 (WA392) To a solution of 5-nitrobenzo[*d*]oxazol-2(3*H*)-one (WA391) (4 g, 22.2 mmol) in 25 mL DMF were added (9.19 g, 66.59 mmol) of potassium carbonate and (19,18 g, 88,8 mmol) of 1,4-dibromobutane, and the reaction mixture heated at 60 °C for 4 hr, then the mixture extracted with ethyl acetate and water, dried over sodium sulfate and the solvent evaporated using *vaccu* then purified by column chromatography (EtOAc: Hexane) to get 6.8 g of 3-(4-bromobutyl)-5-nitrobenzo[*d*]oxazol-2(3*H*)-one as a yellow solid in 97 % yield. MS (ESI) *m/z* 337.65 [M+23]⁺. ¹H NMR (400 MHz, DMSO-*d*₆) δ 8.26 (d, *J* = 2.3 Hz, 1H), 8.07 (dd, *J* = 8.8, 2.4 Hz, 1H), 7.56 (d, *J* = 8.6 Hz, 1H), 3.95 (t, *J* = 6.7 Hz, 2H), 3.57 (t, *J* = 6.3 Hz, 2H), 1.87 (ddt, *J* = 16.5, 11.6, 6.9 Hz, 4H). ¹³C NMR (101 MHz, DMSO) δ 154.06, 146.91, 144.55, 132.44, 119.33, 110.45, 105.26, 41.83, 34.82, 29.69, 26.39.

3-(4-(4-(4-fluorophenyl)piperazin-1-yl)butyl)-5-nitrobenzo[*d*]oxazol-2(3*H*)-one. 364 (WA394) To a solution of 3-(4-bromobutyl)-5-nitrobenzo[*d*]oxazol-2(3*H*)-one (WA392) (2 g, 6.35 mmol) in 25 mL DMF were added (2.6 g, 18.84 mmol) of potassium carbonate and (1.37g, 7.6 mmol) of 1-(4-fluorophenyl)piperazine, and the reaction mixture heated at 65 °C for 1 hr,

then the mixture extracted with ethyl acetate and water, dried over sodium sulfate and the solvent evaporated using *vacuo* then purified by column chromatography (EtOAc: Hexane) to get yellow oil, which was washed with methanol to afford 2.6 g of 3-(4-(4-(4-fluorophenyl)piperazin-1-yl)butyl)-5-nitrobenzo[*d*]oxazol-2(3*H*)-one as a yellow solid in 98% yield. MS (ESI) *m/z* 415.94 [M+1]⁺. ¹H NMR (400 MHz, Chloroform-*d*) δ 8.12 (dd, *J* = 8.8, 2.2 Hz, 1H), 7.90 (d, *J* = 2.3 Hz, 1H), 7.32 (d, *J* = 8.7 Hz, 1H), 6.94 (t, *J* = 8.7 Hz, 2H), 6.86 (dd, *J* = 9.2, 4.5 Hz, 2H), 3.95 (t, *J* = 7.3 Hz, 2H), 3.11 (t, *J* = 5.0 Hz, 4H), 2.59 (t, *J* = 5.0 Hz, 4H), 2.46 (t, *J* = 7.2 Hz, 2H), 1.90 (d, *J* = 7.5 Hz, 2H), 1.64 (t, *J* = 7.6 Hz, 2H). ¹³C NMR (101 MHz, CDCl₃) δ 158.30, 155.93, 153.88, 147.91, 146.75, 144.49, 131.75, 119.18, 117.81, 117.74, 115.56, 115.34, 109.96, 104.06, 57.47, 53.23, 50.12, 42.65, 25.48, 23.72.

5-amino-3-(4-(4-(4-fluorophenyl)piperazin-1-yl)butyl)benzo[*d*]oxazol-2(3*H*)-one. 367

(WA396) To a solution of 3-(4-(4-(4-fluorophenyl)piperazin-1-yl)butyl)-5-nitrobenzo[*d*]oxazol-2(3*H*)-one (1.2 g, 2.89 mmol) in methanol (200ml) was added to 10% Palladium on carbon catalyst (0.4 g) and stirred under a hydrogen pressure (40 psi) for 2h. The mixture was filtered through celite and evaporated in *vacuo* to give 0.8 g of 5-amino-3-(4-(4-(4-fluorophenyl)piperazin-1-yl)butyl)benzo[*d*]oxazol-2(3*H*)-one as white crystals in 72% yield. MS (ESI) *m/z* 385.98 [M+1]⁺. ¹H NMR (400 MHz, DMSO-*d*₆) δ 7.06 – 6.83 (m, 5H), 6.46 – 6.37 (m, 1H), 6.33 – 6.23 (m, 1H), 5.03 (d, *J* = 10.9 Hz, 2H), 3.72 (t, *J* = 7.0 Hz, 2H), 3.02 (d, *J* = 5.1 Hz, 4H), 2.44 (t, *J* = 5.0 Hz, 4H), 2.31 (q, *J* = 10.4, 8.8 Hz, 2H), 1.69 (p, *J* = 7.2 Hz, 2H), 1.46 (p, *J* = 7.6 Hz, 2H). ¹³C NMR (101 MHz, DMSO) δ 154.91, 148.39, 146.32, 133.64, 131.89, 117.47, 117.40, 115.75, 115.53, 110.27, 107.44, 95.31, 57.49, 53.11, 49.42, 41.81, 25.47, 23.76.

3-(4-(4-(4-fluorophenyl)piperazin-1-yl)butyl)-5-isothiocyanatobenzo[*d*]oxazol-2(3*H*)-one.

370 (WA397) To a solution of thiocarbonyldiimidazole (0.22 g, 1.24 mmol) dissolved in DMF

(2.5 mL) at 50 °C was added dropwise a pre-prepared solution of 5-amino-3-(4-(4-(4-fluorophenyl)piperazin-1-yl)butyl)benzo[*d*]oxazol-2(3*H*)-one (WA396) (0.4 g, 1.04 mmol) and triethylamine (0.126 g, 1.24 mmol) in DMF (5 mL) for 5 min. After the mixture was stirred for 30 min at room temperature, the reaction mixture was diluted with water and extracted with ethylacetate. The combined organic layers were washed with water, brine, dried over sodium sulfate, and filtered. The filtrate was concentrated in *vacuo*, and the residue was purified by column chromatography using Ethylacetate/Hexane (20/80) eluent to afford 0.4g of 3-(4-(4-(4-fluorophenyl)piperazin-1-yl)butyl)-5-isothiocyanatobenzo[*d*]oxazol-2(3*H*)-one as a white solid in 90% yield. MS (ESI) *m/z* 427.56 [M+1]⁺. ¹H NMR (400 MHz, Chloroform-*d*) δ 7.23 – 7.09 (m, 1H), 6.99 (d, *J* = 15.2 Hz, 3H), 6.89 (s, 3H), 3.86 (s, 2H), 3.14 (s, 4H), 2.62 (s, 4H), 2.47 (s, 2H), 1.86 (s, 2H), 1.63 (s, 2H). ¹³C NMR (101 MHz, CDCl₃) δ 158.36, 154.29, 147.90, 141.17, 131.97, 127.49, 120.08, 117.86, 117.78, 115.59, 115.37, 110.75, 105.88, 57.48, 53.22, 50.14, 42.34, 25.44, 23.72.

3-(4-(3*H*-spiro[isobenzofuran-1,4'-piperidin]-1'-yl)butyl)-5-nitrobenzo[*d*]oxazol-2(3*H*)-one.

365 (WA409) To a solution of 3-(4-bromobutyl)-5-nitrobenzo[*d*]oxazol-2(3*H*)-one (WA392) (0.5 g, 1.58 mmol) in 10 mL DMF were added (0.65 g, 4.71 mmol) of potassium carbonate and (0.33g, 2.39 mmol) of 3*H*-spiro[isobenzofuran-1,4'-piperidine], and the reaction mixture heated at 65 °C for 3 hr, then the mixture extracted with ethyl acetate and water, dried over sodium sulfate and the solvent evaporated using *vacu* then purified by column chromatography (EtOAc: Hexane) to afford 0.4 g of 3-(4-(3*H*-spiro [isobenzofuran-1,4'-piperidin]-1'-yl)butyl)-5-nitrobenzo[*d*]oxazol-2(3*H*)-one as brown residue in 60% yield. MS (ESI) *m/z* 424.57 [M+1]⁺. ¹H NMR (400 MHz, Chloroform-*d*) δ 8.13 (dd, *J* = 8.8, 2.3 Hz, 1H), 7.92 (d, *J* = 2.4 Hz, 1H), 7.33

(d, $J = 8.8$ Hz, 1H), 7.29 – 7.24 (m, 2H), 7.23 – 7.18 (m, 1H), 7.15 (dd, $J = 5.3, 3.3$ Hz, 1H), 5.06 (s, 2H), 3.96 (t, $J = 7.3$ Hz, 2H), 2.95 – 2.86 (m, 2H), 2.55 (t, $J = 7.5$ Hz, 2H), 2.48 (t, $J = 12.3$ Hz, 2H), 2.11 – 1.99 (m, 2H), 1.91 (p, $J = 7.4$ Hz, 2H), 1.78 (dd, $J = 14.1, 2.5$ Hz, 2H), 1.70 (q, $J = 7.5$ Hz, 2H). ^{13}C NMR (101 MHz, CDCl_3) δ 153.90, 146.76, 145.24, 144.51, 138.79, 131.74, 127.66, 127.42, 121.03, 120.84, 119.20, 109.97, 104.11, 84.37, 70.79, 57.70, 50.18, 42.63, 36.27, 25.53, 23.69.

3-(4-(6,7-dimethoxy-3,4-dihydroisoquinolin-2(1H)-yl)butyl)-5-nitrobenzo[*d*]oxazol-2(3H)-one. 366 (WA410) To a solution of 3-(4-bromobutyl)-5-nitrobenzo[*d*]oxazol-2(3H)-one (WA392) (0.6 g, 1.904 mmol) in 10 mL DMF were added (0.788 g, 5.71 mmol) of potassium carbonate and (0.523 g, 2.28 mmol) of 6,7-dimethoxy-1,2,3,4-tetrahydroisoquinoline-HCl, and the reaction mixture heated at 65 °C for 4 hr, then the mixture extracted with ethyl acetate and water, dried over sodium sulfate and the solvent evaporated using *vacuu* then purified by column chromatography (EtOAc: Hexane) to afford 0.7 g of 3-(4-(6,7-dimethoxy-3,4-dihydroisoquinolin-2(1H)-yl)butyl)-5-nitrobenzo [*d*]oxazol-2(3H)-one as yellow solid in 86% yield. MS (ESI) m/z 428.59 $[\text{M}+1]^+$. ^1H NMR (400 MHz, $\text{DMSO}-d_6$) δ 8.24 (d, $J = 2.5$ Hz, 1H), 8.06 (dd, $J = 8.8, 2.5$ Hz, 1H), 7.56 (d, $J = 8.9$ Hz, 1H), 6.58 (d, $J = 19.6$ Hz, 2H), 3.94 (t, $J = 7.2$ Hz, 2H), 3.68 (s, 6H), 3.40 (s, 2H), 3.33 (s, 2H), 2.66 (t, $J = 5.7$ Hz, 2H), 2.44 (t, $J = 7.0$ Hz, 2H), 1.76 (p, $J = 7.4$ Hz, 2H), 1.57 (p, $J = 7.1$ Hz, 2H). ^{13}C NMR (101 MHz, DMSO) δ 154.07, 147.54, 147.29, 146.87, 144.45, 132.44, 126.94, 126.28, 119.29, 112.14, 110.44, 110.31, 105.26, 57.37, 55.88, 55.51, 51.08, 42.54, 28.69, 25.46, 23.85.

5-amino-3-(4-(6,7-dimethoxy-3,4-dihydroisoquinolin-2(1H)-yl)butyl)benzo[*d*]oxazol-2(3H)-one. 368 (WA411) To a solution of 3-(4-(6,7-dimethoxy-3,4-dihydroisoquinolin-2(1H)-yl)butyl)-5-nitrobenzo[*d*]oxazol-2(3H)-one (WA410) (0.6 g, 1.4 mmol) in methanol (150 ml)

was added to 10% Palladium on carbon catalyst (0.2 g) and stirred under a hydrogen pressure (40 psi) for 3h. The mixture was filtered through celite and evaporated in *vacuo* then purified by column chromatography (EtOAc: Hexane) to afford 0.4 g of 5-amino-3-(4-(6,7-dimethoxy-3,4-dihydroisoquinolin-2(1*H*)-yl)butyl)benzo[*d*]oxazol-2(3*H*)-one as yellow solid in 72% yield. MS (ESI) *m/z* 398.63 [M+1]⁺. ¹H NMR (400 MHz, Chloroform-*d*) δ 6.93 (d, *J* = 8.3 Hz, 1H), 6.60 (s, 1H), 6.53 (s, 1H), 6.39 – 6.30 (m, 2H), 3.86 – 3.75 (m, 8H), 3.57 (s, 2H), 3.56 – 3.40 (m, 2H), 2.83 (t, *J* = 5.9 Hz, 2H), 2.72 (t, *J* = 5.9 Hz, 2H), 2.58 (t, *J* = 7.1 Hz, 2H), 1.85 (p, *J* = 7.3 Hz, 2H), 1.68 (q, *J* = 7.2 Hz, 2H). ¹³C NMR (101 MHz, CDCl₃) δ 155.21, 147.60, 147.26, 143.38, 135.59, 131.88, 126.26, 126.00, 111.35, 110.33, 109.49, 108.34, 95.97, 56.85, 55.92, 55.70, 50.73, 41.73, 28.52, 25.22, 23.72.

3-(4-(3*H*-spiro[isobenzofuran-1,4'-piperidin]-1'-yl)butyl)-5-aminobenzo[*d*]oxazol-2(3*H*)-one. 369 (WA412) To a solution of 3-(4-(3*H*-spiro[isobenzofuran-1,4'-piperidin]-1'-yl)butyl)-5-nitrobenzo[*d*]oxazol-2(3*H*)-one (WA409) (0.35 g, 0.827 mmol) in methanol (100 ml) was added to 10% Palladium on carbon catalyst (0.100 g) and stirred under a hydrogen pressure (40 psi) for 3h. The mixture was filtered through celite and evaporated in *vacuo* then purified by column chromatography (EtOAc: Hexane) to afford 0.19 g of 3-(4-(3*H*-spiro[isobenzofuran-1,4'-piperidin]-1'-yl)butyl)-5-aminobenzo[*d*]oxazol-2(3*H*)-one as brown residue in 59% yield. MS (ESI) *m/z* 394.61 [M+1]⁺. ¹H NMR (400 MHz, Chloroform-*d*) δ 7.20 (dq, *J* = 9.9, 5.4, 4.1 Hz, 2H), 7.12 (tt, *J* = 9.1, 4.2 Hz, 2H), 6.86 (dd, *J* = 11.4, 8.1 Hz, 1H), 6.35 (dq, *J* = 12.5, 4.3, 3.3 Hz, 2H), 4.99 (d, *J* = 9.1 Hz, 2H), 4.06 (s, 2H), 3.73 (q, *J* = 8.3, 7.7 Hz, 2H), 3.03 – 2.88 (m, 2H), 2.58 (d, *J* = 9.6 Hz, 4H), 2.10 (ddd, *J* = 16.3, 10.8, 4.0 Hz, 2H), 1.73 (dtt, *J* = 23.2, 15.5, 7.5 Hz, 6H). ¹³C NMR (101 MHz, CDCl₃) δ 155.24, 144.71, 143.81, 138.63, 135.35, 131.69, 127.79,

127.45, 121.06, 120.83, 110.32, 108.48, 95.89, 83.87, 70.83, 57.65, 50.02, 41.72, 35.65, 25.56, 23.23.

3-(4-(6,7-dimethoxy-3,4-dihydroisoquinolin-2(1*H*)-yl)butyl)-5-isothiocyanatobenzo

[*d*]oxazol-2(3*H*)-one. 371 (WA433) To a solution of thiocarbonyldiimidazole (0.110 g, 0.617 mmol) dissolved in DMF (1 mL) at 50 °C was added dropwise a pre-prepared solution of 5-amino-3-(4-(6,7-dimethoxy-3,4-dihydroisoquinolin-2(1*H*)-yl)butyl)benzo [*d*] oxazol-2(3*H*)-one (WA411) (0.200 g, 0.51 mmol) and triethylamine (0.067 g, 0.6633 mmol) in DMF (2 mL) for 5 min. After the mixture was stirred for 30 min at room temperature, the reaction mixture was diluted with water and extracted with ethylacetate. The combined organic layers were washed with water, brine, dried over sodium sulfate, and filtered. The filtrate was concentrated in *vacuo*, and the residue was purified by column chromatography using Ethylacetate/Hexane (20/80) as an eluent to afford 0.110 g of 3-(4-(6,7-dimethoxy-3,4-dihydroisoquinolin-2(1*H*)-yl)butyl)-5-isothiocyanatobenzo [*d*]oxazol -2(3*H*)-one as a yellow solid in 49% yield. MS (ESI) *m/z* 440 [*M*+1]⁺. ¹H NMR (400 MHz, Chloroform-*d*) δ 6.98 (d, *J* = 8.3 Hz, 1H), 6.81 (d, *J* = 11.2 Hz, 2H), 6.41 (d, *J* = 34.2 Hz, 2H), 3.79 – 3.64 (m, 8H), 3.37 (s, 2H), 2.65 (d, *J* = 6.2 Hz, 2H), 2.54 (t, *J* = 5.8 Hz, 2H), 2.41 (t, *J* = 7.1 Hz, 2H), 1.72 (p, *J* = 7.8, 7.2 Hz, 2H), 1.52 (t, *J* = 7.5 Hz, 2H). ¹³C NMR (101 MHz, CDCl₃) δ 154.12, 147.34, 147.02, 140.98, 135.74, 131.84, 127.12, 126.31, 125.98, 119.97, 111.29, 110.48, 109.36, 105.98, 57.14, 55.78, 55.56, 50.92, 42.22, 28.58, 25.30, 23.89.

3-(4-(3*H*-spiro[isobenzofuran-1,4'-piperidin]-1'-yl)butyl)-5-isothiocyanatobenzo[*d*] oxazol-

2(3*H*)-one. 372 (WA434) To a solution of thiocarbonyldiimidazole (0.040 g, 0.2244 mmol) dissolved in DMF (1 mL) at 50 °C was added dropwise a pre-prepared solution of 3-(4-(3*H*-spiro[isobenzofuran-1,4'-piperidin]-1'-yl)butyl)-5-aminobenzo[*d*] oxazol-2(3*H*)-one (WA412)

(0.075 g, 0.2 mmol) and triethylamine (0.025 g, 0.2475 mmol) in DMF (1 mL) for 5 min. After the mixture was stirred for 30 min at room temperature, the reaction mixture was diluted with water and extracted with ethylacetate. The combined organic layers were washed with water, brine, dried over sodium sulfate, and filtered. The filtrate was concentrated in *vacuo*, and the residue was purified by column chromatography using ethylacetate/hexane (20/80) as an eluent to afford 0.050 g of 3-(4-(3*H*-spiro [isobenzofuran-1,4'-piperidin]-1'-yl)butyl)-5-isothiocyanatobenzo[*d*]oxazol-2(3*H*)-one as a yellow solid in 57% yield. MS (ESI) *m/z* 440 [M+1]⁺. ¹H NMR (400 MHz, Methanol-*d*₄) δ 7.32 – 7.21 (m, 3H), 7.17 (tdd, *J* = 8.7, 5.7, 2.5 Hz, 2H), 7.13 – 7.01 (m, 2H), 5.04 (s, 2H), 3.93 (dt, *J* = 19.8, 6.8 Hz, 2H), 3.07 (d, *J* = 12.2 Hz, 2H), 2.73 (dq, *J* = 19.1, 10.9, 9.4 Hz, 4H), 2.14 – 2.02 (m, 2H), 1.81 – 1.68 (m, 4H), 1.28 (d, *J* = 5.4 Hz, 2H). ¹³C NMR (101 MHz, MeOD) δ 144.29, 138.69, 130.04, 128.14, 127.69, 127.18, 121.36, 121.08, 120.86, 120.84, 120.30, 109.43, 109.07, 107.89, 83.29, 70.35, 57.16, 49.52, 39.65, 34.93, 34.77, 25.70, 25.11, 22.55.

9.4.6. Synthesis of benzothiazolone derivatives of isothiocyanate

6-nitrobenzo[*d*]thiazol-2(3*H*)-one. (WA389). (3 g, 20 mmol) of benzo[*d*]thiazol-2(3*H*)-one (**373**) was added 200 mL (10 ml / 1 mmol) of HNO₃ (68%) and stirred for 30 minutes at 50 °C and then was left for 2 hr at room temperature. The HNO₃ was evaporated and the concentrate was purified over column chromatography using hexanes/ethylacetate (50/50) eluent to afford 2 g of 6-nitrobenzo[*d*]thiazol-2(3*H*)-one as a pale yellow solid in 51% yield. MS (ESI) *m/z* 195.32 [M-1]⁺. ¹H NMR (400 MHz, DMSO-*d*₆) δ 12.53 (s, 1H), 8.57 (s, 1H), 8.13 (s, 1H), 7.23 (s, 1H). ¹³C NMR (101 MHz, DMSO) δ 170.96, 142.87, 142.44, 124.93, 123.10, 119.50, 111.83.

3-(4-bromobutyl)-6-nitrobenzo[*d*]thiazol-2(3*H*)-one. 375 (WA408) To a solution of 6-nitrobenzo[*d*]thiazol-2(3*H*)-one (WA389) (3 g, 15.3 mmol) in 35 mL DMF were added (6.3 g, 45.65 mmol) of potassium carbonate and (13.2 g, 61.1 mmol) of 1,4-dibromobutane, and the reaction mixture heated at 65 °C for 2 hr, then the mixture extracted with ethyl acetate and water, dried over sodium sulfate and the solvent evaporated using *vacuu* then purified by column chromatography (EtOAc: Hexane) to afford 3.3 g of 3-(4-bromobutyl)-6-nitrobenzo[*d*]thiazol-2(3*H*)-one as yellow oil in 66% yield. MS (ESI) *m/z* 353.43 [M+23]⁺. ¹H NMR (400 MHz, DMSO-*d*₆) δ 8.68 (d, *J* = 2.4 Hz, 1H), 8.22 (dd, *J* = 9.0, 2.5 Hz, 1H), 7.59 (d, *J* = 9.0 Hz, 1H), 4.03 (t, *J* = 6.9 Hz, 2H), 3.54 (t, *J* = 6.4 Hz, 2H), 1.91 – 1.70 (m, 4H). ¹³C NMR (101 MHz, DMSO) δ 169.91, 143.19, 142.50, 123.16, 123.11, 119.68, 111.79, 42.41, 34.79, 29.78, 26.34.

3-(4-(4-(4-fluorophenyl)piperazin-1-yl)butyl)-6-nitrobenzo[*d*]thiazol-2(3*H*)-one. 376 (WA413) To a solution of 3-(4-bromobutyl)-6-nitrobenzo[*d*]thiazol-2(3*H*)-one (WA408) (1 g, 3.02 mmol) in 15 mL DMF were added (1.25 g, 9.05 mmol) of potassium carbonate and (0.653 g, 3.62 mmol) of 1-(4-fluorophenyl)piperazine, and the reaction mixture heated at 65 °C for 4 hr, then the mixture extracted with ethyl acetate and water, dried over sodium sulfate and the solvent evaporated using *vacuu* then purified by column chromatography (EtOAc: Hexane) to afford 1 g of 3-(4-(4-(4-fluorophenyl)piperazin-1-yl)butyl)-6-nitrobenzo[*d*]thiazol-2(3*H*)-one as yellow solid in 76% yield. MS (ESI) *m/z* 431.58 [M+1]⁺. ¹H NMR (400 MHz, Chloroform-*d*) δ 8.35 (d, *J* = 2.3 Hz, 1H), 8.23 (dd, *J* = 8.9, 2.3 Hz, 1H), 7.21 (d, *J* = 8.9 Hz, 1H), 6.94 (t, *J* = 8.7 Hz, 2H), 6.86 (dd, *J* = 9.2, 4.4 Hz, 2H), 4.05 (t, *J* = 7.4 Hz, 2H), 3.11 (t, *J* = 4.9 Hz, 4H), 2.60 (t, *J* = 4.9 Hz, 4H), 2.46 (t, *J* = 7.2 Hz, 2H), 1.82 (q, *J* = 7.6 Hz, 2H), 1.63 (q, *J* = 7.3 Hz, 2H). ¹³C NMR

(101 MHz, CDCl₃) δ 169.49, 158.32, 155.94, 147.87, 147.85, 143.33, 141.88, 123.61, 122.64, 118.71, 117.78, 117.70, 115.59, 115.38, 110.15, 57.46, 53.19, 50.11, 43.20, 25.38, 23.73.

3-(4-(6,7-dimethoxy-3,4-dihydroisoquinolin-2(1H)-yl)butyl)-6-nitrobenzo[d]thiazol-2(3H)-one. 377 (WA414) To a solution of 3-(4-bromobutyl)-6-nitrobenzo[d]thiazol-2(3H)-one (WA408) (1g, 3.02 mmol) in 15 mL DMF were added (1.25g, 9.05 mmol) of potassium carbonate and (0.824g, 3.59 mmol) of 6,7-dimethoxy-1,2,3,4-tetrahydroisoquinoline-HCl, and the reaction mixture heated at 65 °C for 4 hr, then the mixture extracted with ethyl acetate and water, dried over sodium sulfate and the solvent evaporated using *vacuu* then purified by column chromatography (EtOAc: Hexane) to afford 1g of 3-(4-(6,7-dimethoxy-3,4-dihydroisoquinolin-2(1H)-yl)butyl)-6-nitrobenzo [d]thiazol-2(3H)-one as yellow solid in 74% yield. MS (ESI) *m/z* 444.55 [M+1]⁺. ¹H NMR (400 MHz, Chloroform-*d*) δ 8.32 (d, *J* = 2.3 Hz, 1H), 8.09 – 7.99 (m, 1H), 7.28 (d, *J* = 8.8 Hz, 1H), 6.62 (s, 1H), 6.52 (s, 1H), 4.06 (t, *J* = 7.6 Hz, 2H), 3.85 (d, *J* = 9.7 Hz, 6H), 3.55 (s, 2H), 2.82 (t, *J* = 5.9 Hz, 2H), 2.70 (t, *J* = 5.9 Hz, 2H), 2.58 (t, *J* = 6.9 Hz, 2H), 1.85 (p, *J* = 7.2 Hz, 2H), 1.70 (q, *J* = 7.2 Hz, 2H). ¹³C NMR (101 MHz, CDCl₃) δ 169.49, 147.66, 147.27, 143.31, 141.91, 126.44, 126.03, 123.50, 122.54, 118.57, 111.38, 110.51, 109.49, 56.76, 55.94, 55.87, 50.85, 43.06, 28.72, 25.10, 23.77.

3-(4-(3H-spiro[isobenzofuran-1,4'-piperidin]-1'-yl)butyl)-6-nitrobenzo[d]thiazol-2(3H)-one. 378 (WA415) To a solution of 3-(4-bromobutyl)-6-nitrobenzo[d]thiazol-2(3H)-one (WA408) (0.5 g, 1.5 mmol) in 10 mL DMF were added (0.621 g, 4.5 mmol) of potassium carbonate and (0.324g, 1.8 mmol) of 3H-spiro[isobenzofuran-1,4'-piperidine], and the reaction mixture heated at 65 °C for 6 hr, then the mixture extracted with ethyl acetate and water, dried over sodium sulfate and the solvent evaporated using *vacuu* then purified by column chromatography (EtOAc: Hexane) to afford 0.33 g of 3-(4-(3H-spiro [isobenzofuran-1,4'-piperidin]-1'-yl)butyl)-6-

nitrobenzo[*d*]thiazol-2(3*H*)-one as yellow solid in 50% yield. MS (ESI) *m/z* 440.59 [M+1]⁺. ¹H NMR (400 MHz, Chloroform-*d*) δ 8.35 (t, *J* = 1.8 Hz, 1H), 8.25 (dt, *J* = 8.9, 1.8 Hz, 1H), 7.30 – 7.08 (m, 5H), 5.04 (s, 2H), 4.05 (t, *J* = 7.4 Hz, 2H), 3.44 (d, *J* = 1.4 Hz, 4H), 2.90 (d, *J* = 11.0 Hz, 2H), 2.55 – 2.43 (m, 4H), 2.07 – 1.98 (m, 2H), 1.86 – 1.79 (m, 2H). ¹³C NMR (101 MHz, CDCl₃) δ 169.57, 145.10, 143.35, 141.87, 138.73, 127.70, 127.43, 123.60, 122.66, 121.06, 120.75, 118.71, 110.24, 84.30, 70.78, 57.77, 50.13, 43.18, 36.18, 25.52, 23.66.

6-amino-3-(4-(4-(4-fluorophenyl)piperazin-1-yl)butyl)benzo[*d*]thiazol-2(3*H*)-one. 379

(WA416) To a solution of 3-(4-(4-(4-fluorophenyl)piperazin-1-yl)butyl)-6-nitrobenzo[*d*]thiazol-2(3*H*)-one (WA413) (1 g, 2.32 mmol) in methanol (200 ml) was added to 10% Palladium on carbon catalyst (0.3 g) and stirred under a hydrogen pressure (50 psi) for 2h. The mixture was filtered through celite and evaporated in *vacuo* then purified by column chromatography (EtOAc: Hexane) to afford 0.7 g of 6-amino-3-(4-(4-(4-fluorophenyl)piperazin-1-yl)butyl)benzo[*d*]thiazol-2(3*H*)-one as brown residue in 75% yield. MS (ESI) *m/z* 401.62 [M+1]⁺. ¹H NMR (400 MHz, Methanol-*d*₄) δ 7.00 – 6.76 (m, 6H), 6.76 – 6.65 (m, 1H), 4.70 (s, 2H), 3.87 (q, *J* = 8.9, 8.0 Hz, 2H), 3.01 (dd, *J* = 6.5, 3.6 Hz, 4H), 2.48 (q, *J* = 10.1, 7.6 Hz, 4H), 2.33 (q, *J* = 7.8 Hz, 2H), 1.67 (hept, *J* = 8.6, 7.9 Hz, 2H), 1.53 (ddd, *J* = 15.1, 8.8, 6.0 Hz, 2H). ¹³C NMR (101 MHz, MeOD) δ 169.82, 158.33, 155.97, 147.95, 147.93, 144.30, 128.70, 123.17, 117.68, 117.60, 115.08, 114.86, 114.01, 111.68, 108.54, 57.39, 52.75, 49.48, 42.06, 25.24, 23.19.

6-amino-3-(4-(6,7-dimethoxy-3,4-dihydroisoquinolin-2(1*H*)-yl)butyl)benzo[*d*]thiazol-2(3*H*)-one. 380 (WA417) To a solution of 3-(4-(6,7-dimethoxy-3,4-dihydroisoquinolin-2(1*H*)-yl)butyl)-6-nitrobenzo [*d*]thiazol-2(3*H*)-one (WA414) (1 g, 2.32 mmol) in methanol (300 ml) was added to 10% Palladium on carbon catalyst (0.3 g) and stirred under a hydrogen pressure (50

psi) for 2h. The mixture was filtered through celite and evaporated in *vacuu* then purified by column chromatography (EtOAc: Hexane) to afford 0.75 g of 6-amino-3-(4-(6,7-dimethoxy-3,4-dihydroisoquinolin-2(1*H*)-yl)butyl)benzo[*d*] thiazol-2(3*H*)-one as brown solid in 75% yield. MS (ESI) *m/z* 414 [M+1]⁺. ¹H NMR (400 MHz, Methanol-*d*₄) δ 7.70 (d, *J* = 2.3 Hz, 1H), 7.58 – 7.42 (m, 2H), 6.80 (d, *J* = 8.8 Hz, 2H), 4.69 (d, *J* = 9.5 Hz, 2H), 4.12 (t, *J* = 6.8 Hz, 2H), 3.81 (d, *J* = 2.3 Hz, 8H), 3.36 (dd, *J* = 19.0, 10.7 Hz, 4H), 3.26 – 3.00 (m, 2H), 2.03 – 1.85 (m, 4H). ¹³C NMR (101 MHz, MeOD) δ 170.05, 149.35, 148.54, 137.22, 126.05, 124.10, 123.08, 121.44, 119.32, 117.46, 112.12, 111.47, 109.70, 55.30, 55.20, 52.53, 49.94, 41.81, 24.57, 24.44, 21.14.

3-(4-(3*H*-spiro[isobenzofuran-1,4'-piperidin]-1'-yl)butyl)-6-aminobenzo[*d*]thiazol-2(3*H*)-one. 381 (WA418) To a solution of 3-(4-(3*H*-spiro [isobenzofuran-1,4'-piperidin]-1'-yl)butyl)-6-nitrobenzo[*d*]thiazol-2(3*H*)-one (WA415) (0.2 g, 0.45 mmol) in methanol (75 ml) was added to 10% Palladium on carbon catalyst (0.08 g) and stirred under a hydrogen pressure (50 psi) for 2hr. The mixture was filtered through celite and evaporated in *vacuu* then purified by column chromatography (EtOAc: Hexane) to afford 0.15 g of 3-(4-(3*H*-spiro[isobenzofuran-1,4'-piperidin]-1'-yl)butyl)-6-aminobenzo[*d*] thiazol-2(3*H*)-one as brown solid in 81% yield. MS (ESI) *m/z* 410.56 [M+1]⁺. ¹H NMR (400 MHz, Methanol-*d*₄) δ 7.30 – 7.11 (m, 4H), 7.03 (d, *J* = 8.6 Hz, 1H), 6.88 (d, *J* = 2.3 Hz, 1H), 6.77 (dd, *J* = 8.6, 2.3 Hz, 1H), 5.00 (s, 2H), 4.85 – 4.79 (m, 2H), 3.95 (t, *J* = 7.0 Hz, 2H), 2.82 (d, *J* = 11.6 Hz, 2H), 2.47 – 2.34 (m, 4H), 1.95 (td, *J* = 13.2, 4.4 Hz, 2H), 1.80 – 1.64 (m, 4H), 1.64 – 1.52 (m, 2H). ¹³C NMR (101 MHz, MeOD) δ 170.00, 145.11, 144.27, 138.64, 128.76, 127.43, 127.11, 123.09, 120.75, 120.36, 114.13, 111.66, 108.59, 84.28, 70.16, 57.82, 49.62, 42.01, 35.66, 25.40, 23.35.

3-(4-(6,7-dimethoxy-3,4-dihydroisoquinolin-2(1*H*)-yl)butyl)-6-isothiocyanatobenzo

[*d*]thiazol-2(3*H*)-one. 382 (WA423) To a solution of thiocarbonyldiimidazole (0.047 g, 0.26 mmol) dissolved in DMF (1 mL) at 50 °C was added dropwise a pre-prepared solution of 6-amino-3-(4-(6,7-dimethoxy-3,4-dihydroisoquinolin-2(1*H*)-yl)butyl)benzo [*d*]thiazol-2(3*H*)-one (WA417) (0.100 g, 0.2207 mmol) and triethylamine (0.027 g, 0.2673 mmol) in DMF (1 mL) for 5 min. After the mixture was stirred for 30 min at room temperature, the reaction mixture was diluted with water and extracted with ethylacetate. The combined organic layers were washed with water, brine, dried over sodium sulfate, and filtered. The filtrate was concentrated in *vacuo*, and the residue was purified by column chromatography using Ethylacetate/Hexane (20/80) as an eluent to afford 0.06 g of 3-(4-(6,7-dimethoxy-3,4-dihydroisoquinolin-2(1*H*)-yl)butyl)-6-isothiocyanatobenzo[*d*]thiazol-2(3*H*)-one as a white solid in 55% yield. MS (ESI) *m/z* 496.69 [M+1]⁺. ¹H NMR (400 MHz, Methanol-*d*₄) δ 7.02 (d, *J* = 8.6 Hz, 1H), 6.86 (d, *J* = 2.3 Hz, 1H), 6.73 (dd, *J* = 8.6, 2.3 Hz, 1H), 6.63 (d, *J* = 22.0 Hz, 2H), 3.94 (t, *J* = 7.0 Hz, 2H), 3.77 (d, *J* = 1.6 Hz, 6H), 3.50 (s, 2H), 2.79 (t, *J* = 5.9 Hz, 2H), 2.67 (t, *J* = 5.9 Hz, 2H), 2.51 (dd, *J* = 8.6, 6.6 Hz, 2H), 1.75 (dq, *J* = 14.1, 6.9 Hz, 2H), 1.64 (tt, *J* = 9.8, 5.8 Hz, 2H). ¹³C NMR (101 MHz, MeOD) δ 169.98, 147.69, 147.33, 144.29, 128.72, 126.09, 125.94, 123.04, 114.12, 111.69, 111.50, 109.72, 108.54, 57.22, 55.11, 55.05, 50.55, 41.98, 27.71, 25.31, 23.35.

3-(4-(4-(4-fluorophenyl)piperazin-1-yl)butyl)-5-isothiocyanatobenzo[*d*]thiazol-2(3*H*) -one.

383 (WA435) To a solution of thiocarbonyldiimidazole (0.1067 g, 0.5987 mmol) dissolved in DMF (2 mL) at 50 °C was added dropwise a pre-prepared solution of 6-amino-3-(4-(4-(4-fluorophenyl)piperazin-1-yl)butyl)benzo[*d*]thiazol-2(3*H*)-one (WA416) (0.200 g, 0.499 mmol) and triethylamine (0.025 g, 0.2475 mmol) in DMF (1 mL) for 5 min. After the mixture was

stirred for 30 min at room temperature, the reaction mixture was diluted with water and extracted with ethylacetate. The combined organic layers were washed with water, brine, dried over sodium sulfate, and filtered. The filtrate was concentrated in *vacuo*, and the residue was purified by column chromatography using ethylacetate/hexane (20/80) as an eluent to afford 0.120 g of 3-(4-(4-(4-fluorophenyl) piperazin-1-yl)butyl)-5-isothiocyanatobenzo[*d*]thiazol-2(3*H*)-one as a yellow oil in 54% yield. MS (ESI) *m/z* 443 [M+1]⁺. ¹H NMR (400 MHz, Chloroform-*d*) δ 7.32 (d, *J* = 2.0 Hz, 1H), 7.17 (dd, *J* = 8.6, 2.1 Hz, 1H), 7.05 (d, *J* = 8.6 Hz, 1H), 6.95 (t, *J* = 8.7 Hz, 2H), 6.86 (dd, *J* = 9.1, 4.4 Hz, 2H), 3.97 (t, *J* = 7.3 Hz, 2H), 3.14 (q, *J* = 7.0, 4.8 Hz, 4H), 2.63 (t, *J* = 4.9 Hz, 3H), 2.49 (t, *J* = 7.3 Hz, 2H), 1.79 (p, *J* = 7.6 Hz, 2H), 1.65 (q, *J* = 7.5 Hz, 2H). ¹³C NMR (101 MHz, CDCl₃) δ 169.29, 158.41, 156.03, 147.77, 147.75, 136.29, 135.81, 126.48, 124.05, 119.92, 117.91, 117.83, 115.63, 115.41, 111.13, 57.44, 53.09, 49.95, 42.73, 25.30, 23.54.

3-(4-(3*H*-spiro[isobenzofuran-1,4'-piperidin]-1'-yl)butyl)-6-isothiocyanatobenzo[*d*] thiazol-2(3*H*)-one. 384 (WA436) To a solution of thiocarbonyldiimidazole (0.0522 g, 0.2929 mmol) dissolved in DMF (2 mL) at 50 °C was added dropwise a pre-prepared solution of 3-(4-(3*H*-spiro[isobenzofuran-1,4'-piperidin]-1'-yl)butyl)-6-aminobenzo[*d*] thiazol-2(3*H*)-one (WA418) (0.100 g, 0.244 mmol) and triethylamine (0.032 g, 0.3168 mmol) in DMF (3 mL) for 5 min. After the mixture was stirred for 30 min at room temperature, the reaction mixture was diluted with water and extracted with ethylacetate. The combined organic layers were washed with water, brine, dried over sodium sulfate, and filtered. The filtrate was concentrated in *vacuo*, and the residue was purified by column chromatography using ethylacetate/hexane (20/80) as an eluent to afford 0.065 g of 3-(4-(4-(4-fluorophenyl)piperazin-1-yl)butyl)-5-isothiocyanatobenzo[*d*]thiazol-2(3*H*)-one as yellow oil in 59% yield. MS (ESI) *m/z* 452 [M+1]⁺. ¹H NMR (400 MHz, Chloroform-*d*) δ 7.35 – 7.12 (m, 6H), 7.07 (d, *J* = 8.6 Hz, 1H), 5.06 (s, 2H),

3.98 (dd, $J = 8.3, 6.0$ Hz, 2H), 3.00 (d, $J = 11.0$ Hz, 2H), 2.62 (s, 4H), 2.17 (s, 2H), 1.88 – 1.70 (m, 6H). ^{13}C NMR (101 MHz, CDCl_3) δ 169.35, 138.68, 136.33, 135.76, 127.82, 127.51, 126.53, 124.11, 124.03, 121.07, 120.85, 119.91, 111.17, 83.94, 70.90, 57.61, 50.07, 50.03, 42.62, 35.77, 25.41.

9. 5 Synthesis of CM699 Derivatives

9.5.1 Synthesis of benzo[d]thiazol-2(3H)-one and benzo[d]oxazol-2(3H)-one derivatives

Synthesis of **1-(4-fluorophenyl)thiourea. 386 (WA470)**. 4-Fluoroaniline (11.10 g, 0.1 mmol), hydrochloric acid (9 mL), and water (25 mL) were taken and refluxed for 30 min in a round bottomed flask. The contents were cooled to room temperature and NH_4SCN (7.60 g, 0.1 mmol) was added. The reaction mixture was again refluxed for 4 h. The solid obtained was cooled down, filtered, washed with water, dried and recrystallized from ethanol to give 10.5 g (61 %) of 270 as a yellowish white solid. ^1H NMR (400 MHz, $\text{DMSO}-d_6$) δ 9.62 (s, 1H), 7.39 (dd, $J = 8.8, 5.0$ Hz, 3H), 7.20 – 7.08 (m, 3H). ^{13}C NMR (101 MHz, DMSO) δ 181.80, 160.73, 158.33, 135.86, 135.83, 126.07, 125.99, 115.82, 115.59. MS (EI) m/z 171.33 $[\text{M}+1]^+$.

Synthesis of **6-fluorobenzo[d]thiazol-2-amine. 387 (WA471)**. Bromine (10.8 g, 11.04 mmol) in CHCl_3 (15 mL) was added over 30 min to a stirred solution of compound 270 (6 g, 35.28 mmol) in CHCl_3 (30 mL) at 5 °C. The mixture was held at room temperature for 30 min and was then refluxed for 2 h. Filtration followed by washing the by CHCl_3 and then with ether to give a yellow bromine containing solid which was suspended in acetone (100 mL) to discharge the yellow color. The solid was filtered and washed with acetone and with ether to give HBr salt. The salt was dissolved in hot water (150 mL) and the pH of the cold solution was brought to pH = 9 with 14 N NH_4OH . Filtration followed by washing with H_2O gave 5 g (84 %) of 271 as a

white solid. ^1H NMR (400 MHz, Methanol- d_4) δ 7.84 (dd, $J = 8.9, 4.9$ Hz, 1H), 7.36 – 7.07 (m, 2H). ^{13}C NMR (101 MHz, MeOD) δ 171.49, 163.80, 161.36, 138.74, 138.62, 124.35, 124.25, 118.88, 118.86, 112.64, 112.39, 101.55, 101.27. MS (EI) m/z 169.32 $[\text{M}+1]^+$.

Synthesis of **2-amino-5-fluorobenzenethiol 389 (WA474A)**. Compound 471 (5 g, 29.76), KOH (5 times by weight of thiazole) and H_2O (10 times by weight of thiazole) were transferred into R.B flask and refluxed until evolution of ammonia ceased. The reaction mixture was cooled, filtered and washed with H_2O . The filtrate was neutralized with acetic acid (5N) while vigorous stirring. During neutralization, the temperature of the mixture was maintained below 10°C by adding ice otherwise a decomposed greenish mass is obtained instead of the desired 2-aminobenzenethiol. The resulting mixture was extracted 3 times with ethyl acetate. The organic extract was evaporated, dried and recrystallized from ethanol to give 4 g (93 %) of 474 as a yellow solid. ^1H NMR (400 MHz, DMSO- d_6) δ 6.97 (td, $J = 8.6, 3.1$ Hz, 1H), 6.86 (dq, $J = 8.6, 4.1, 3.0$ Hz, 1H), 6.75 (dd, $J = 8.9, 5.0$ Hz, 1H), 5.41 (s, 2H), 3.38 (s, 1H). ^{13}C NMR (101 MHz, DMSO) δ 154.78, 152.45, 146.70, 146.68, 120.26, 120.04, 118.63, 118.41, 117.18, 117.10, 116.23, 116.15. MS (EI) m/z $[\text{M}+2]^+$; 184 $[\text{M}+39]^+$.

Synthesis of **6-fluorobenzo[d]thiazol-2(3H)-one. 390 (WA474B)**. To a solution of compound 273 (4 g, 29.76 mmol) in THF (30 mL) was added 1,1'-carbonyldiimidazole (5.29 g, 32.69 mmol). The reaction mixture was stirred under reflux for 3 h. The reaction mixture was cooled and the solvent was evaporated. The residue was taken up in 2N HCl solution (30 mL) and extracted with ethyl acetate (2 x 50 mL). The combined organic layers were washed with brine, dried and evaporated. The residue was purified by chromatography on a silica gel column using a gradient of ethyl acetate/hexanes (2 : 8) as eluent to give 4.1 g (81 %) of 274 as a light brown

solid. ^1H NMR (DMSO- d_6): ^1H NMR (400 MHz, DMSO- d_6) δ 11.90 (s, 1H), 7.52 (dd, $J = 8.2$, 2.0 Hz, 1H), 7.16 – 6.99 (m, 3H). ^{13}C NMR (101 MHz, DMSO) δ 170.29, 159.53, 157.16, 133.26, 125.17, 125.06, 114.07, 113.84, 112.85, 112.76, 110.49, 110.22. MS (EI) m/z 170.35 ($\text{M}^+ + 1$).

Synthesis of **3-(4-bromobutyl)-6-fluorobenzo[d]thiazol-2(3H)-one** **391a** (WA151). K_2CO_3 (9.79 g, 71.01 mmol) and 1,4-dibromobutane (25.31 g, 118.34 mmol) were added, while stirring, to a solution of 6-fluorobenzo[d]thiazol-2(3H)-one 274 (4 g, 23.67 mmol) in anhydrous DMF (30 mL). The reaction mixture was heated at 65 °C for 3 h. After cooling, the reaction mixture was poured onto H_2O (100 mL) and extracted with ethyl acetate (3 x 50 mL). The combined organic layers were washed with saturated aqueous NaCl and dried over magnesium sulfate. The solvent was removed in vacuo, and the residue was purified by flash column chromatography (SiO_2) using hexane/ ethyl acetate (8: 2) as eluent to give 5.23 g (73%) of 3-(4-bromobutyl)-6-fluorobenzo[d]thiazol-2(3H)-one as a yellow oil. ^1H NMR (CDCl_3): δ 7.37 – 6.72 (m, 3H), 3.96 (t, $J = 6.8$, 2H), 3.45 (t, $J = 6.1$, 2H), 2.18 – 1.53 (m, 4H). ^{13}C NMR (101 MHz, CDCl_3) δ 169.41, 158.88 (d, $J = 242.8$), 132.81, 123.70, 113.60 (d, $J = 23.8$), 111.14 (d, $J = 8.4$), 110.10 (d, $J = 26.8$), 41.91, 32.91, 29.45, 26.05. MS (EI) m/z 304.27 [M] $^+$; 306.27 [$\text{M} + 2$] $^+$.

Synthesis of **3-(4-bromopentyl)-6-fluorobenzo[d]thiazol-2(3H)-one** **391b** (WA152). K_2CO_3 (9.97 g, 71.01 mmol) and 1,4-dibromopentane (16.18 mL, 71.01 mmol) were added, while stirring, to a solution of 6-fluorobenzo[d]thiazol-2(3H)-one 275 (4.0 g, 23.67 mmol) in anhydrous DMF (30 mL). The reaction mixture was heated at 60 °C for 3 h. After cooling, the reaction mixture was poured onto H_2O (100 mL) and extracted with ethyl acetate (3 x 50 mL).

The combined organic layers were washed with saturated aqueous NaCl and dried over magnesium sulfate. The solvent was removed in vacuo, and the residue was purified by flash column chromatography (SiO₂) using hexane/ ethyl acetate (8: 2) as eluent to give 5.23 g (71%) of 276 as a brown oil. ¹H NMR (CDCl₃) δ 7.19 (dd, *J* = 7.7, 2.4 Hz, 1H), 7.11 – 6.97 (m, 2H), 4.17 (p, *J* = 6.5 Hz, 1H), 4.06 – 3.88 (m, 2H), 2.08 – 1.87 (m, 3H), 1.87 – 1.81 (m, 1H), 1.71 (d, *J* = 6.7 Hz, 3H). ¹³C NMR (101 MHz, CDCl₃) δ 169.40, 160.09, 157.68, 133.11, 133.09, 123.96, 123.86, 113.71, 113.48, 111.18, 111.10, 110.22, 109.95, 50.58, 42.12, 37.72, 26.54, 25.92. MS (EI) *m/z* 318.41 [M]⁺; 320.36 [M+2].

3-(4-(3,5-dimethylpiperazin-1-yl)pentyl)-6-fluorobenzo[*d*]thiazol-2(3*H*)-one. 395 (WA153)

To a solution of 3-(4-bromopentyl)-6-fluorobenzo[*d*]thiazol-2(3*H*)-one (WA152) (0.181 g, 0.57 mmol) in 1.5 mL DMF were added (0.235 g, 1.7 mmol) of potassium carbonate and (0.45 g, 3.94 mmol) of 2,6-dimethylpiperazine, and the reaction mixture heated at 60 °C for 5 h, then the mixture extracted with ethyl acetate and water, washed with brine, dried over magnesium sulfate and the solvent evaporated using *vacuo* then purified by column chromatography (MeOH: DCM) to obtain 0.143 g of 3-(4-(3,5-dimethylpiperazin-1-yl)pentyl)-6-fluorobenzo[*d*]thiazol-2(3*H*)-one as yellow oil in 72% yield. ¹H NMR (400 MHz, Methanol-*d*₄) δ 7.40 (dd, *J* = 8.1, 2.7 Hz, 1H), 7.31 (dd, *J* = 8.9, 4.3 Hz, 1H), 7.15 (td, *J* = 9.0, 2.7 Hz, 1H), 4.01 (dq, *J* = 11.9, 7.1 Hz, 2H), 2.97 – 2.78 (m, 2H), 2.71 – 2.57 (m, 3H), 2.07 (t, *J* = 11.0 Hz, 1H), 1.91 – 1.73 (m, 3H), 1.64 – 1.54 (m, 1H), 1.39 (ddd, *J* = 13.5, 8.5, 6.7 Hz, 1H), 1.14 – 0.94 (m, 9H). ¹³C NMR (101 MHz, MeOD) δ 169.99, 160.25, 157.85, 133.45, 133.43, 123.59, 123.49, 113.45, 113.21, 112.08, 111.99, 109.74, 109.46, 58.07, 56.08, 51.56, 50.90, 42.40, 29.61, 24.07, 17.33, 17.25, 12.59. MS (EI) *m/z* 352.59 [M+1]⁺.

3-(4-(3,5-dimethylpiperazin-1-yl)butyl)-6-fluorobenzo[d]thiazol-2(3H)-one. 394 (WA157)

To a solution of 3-(4-bromobutyl)-6-fluorobenzo[d]thiazol-2(3H)-one (WA151) (0.2 g, 0.66 mmol) in 1 mL DMF were added (0.27 g, 1.6 mmol) of potassium carbonate and (0.52 g, 4.6 mmol) of 2,6-dimethylpiperazine, and the reaction mixture heated at 60 °C for 4 h, then the mixture extracted with ethyl acetate and water, washed with brine, dried over magnesium sulfate and the solvent evaporated using *vacuu* then purified by column chromatography (MeOH: DCM) to obtain 0.160 g of 3-(4-(3,5-dimethylpiperazin-1-yl)pentyl)-6-fluorobenzo[d]thiazol-2(3H)-one as yellow oil in 72% yield. ¹HNMR (400 MHz, Methanol-*d*₄) δ 7.39 (dd, *J* = 8.1, 2.6 Hz, 1H), 7.30 (dd, *J* = 8.9, 4.3 Hz, 1H), 4.03 (t, *J* = 7.1 Hz, 2H), 3.36 (s, 3H), 3.02 – 2.79 (m, 4H), 2.44 – 2.34 (m, 2H), 1.80 – 1.54 (m, 6H), 1.11 (d, *J* = 6.5 Hz, 6H). ¹³C NMR (101 MHz, MeOD) δ 169.97, 160.24, 157.84, 133.37, 123.58, 123.48, 113.48, 113.24, 112.02, 111.93, 109.74, 109.46, 58.56, 57.17, 50.36, 48.44, 48.23, 48.01, 47.80, 47.59, 47.37, 47.16, 46.95, 42.20, 24.91, 22.88, 17.22. MS (EI) *m/z* 338.64 [M+1]⁺.

3-(4-(3H-spiro[isobenzofuran-1,4'-piperidin]-1'-yl)butyl)-6-fluorobenzo[d]thiazol-2(3H)-

one. 396 (WA241) To a solution of 3-(4-bromobutyl)-6-fluorobenzo[d]thiazol-2(3H)-one (WA151) (0.05 g, 0.1644 mmol) in 1 mL DMF were added (0.068 g, 0.4927 mmol) of potassium carbonate and (0.0442 g, 0.1956 mmol) of 3H-spiro[isobenzofuran-1,4'-piperidine]-HCl, and the reaction mixture heated at 60 °C for 4 h, then the mixture extracted with ethyl acetate and water, washed with brine, dried over magnesium sulfate and the solvent evaporated using *vacuu* then purified by column chromatography (MeOH: DCM) to obtain 0.052 g of 3-(4-(3,5-dimethylpiperazin-1-yl)pentyl)-6-fluorobenzo[d]thiazol-2(3H)-one as yellow oil in 77% yield.

^1H NMR (400 MHz, Methanol- d_4) δ 7.39 – 7.12 (m, 7H), 5.04 (s, 2H), 4.05 (t, J = 6.7 Hz, 2H), 3.15 (d, J = 11.5 Hz, 2H), 2.88 – 2.71 (m, 4H), 2.11 (td, J = 13.6, 4.4 Hz, 2H), 1.79 (q, J = 15.5, 11.5 Hz, 6H). ^{13}C NMR (101 MHz, MeOD) δ 170.00, 160.25, 157.85, 144.17, 138.70, 133.30, 127.76, 127.24, 123.50, 120.92, 120.33, 113.33, 112.01, 111.92, 109.80, 109.53, 83.13, 70.46, 56.98, 49.58, 41.98, 34.67, 24.91, 22.36. MS (EI) m/z 413 $[\text{M}+1]^+$.

3-(4-(3*H*-spiro[isobenzofuran-1,4'-piperidin]-1'-yl)pentyl)-6-fluorobenzo[*d*]thiazol-2(3*H*)-one. 397, (WA242) To a solution of 3-(4-bromopentyl)-6-fluorobenzo[*d*]thiazol-2(3*H*)-one (WA152) (0.05 g, 0.1571 mmol) in 1 mL DMF were added (0.065 g, 0.47 mmol) of potassium carbonate and (0.0425 g, 0.1882 mmol) of 3*H*-spiro[isobenzofuran-1,4'-piperidine]-HCl, and the reaction mixture heated at 60 °C for 4 h, then the mixture extracted with ethyl acetate and water, washed with brine, dried over magnesium sulfate and the solvent evaporated using *vacuu* then purified by column chromatography (MeOH: DCM) to obtain 0.045 g of 3-(4-(3,5-dimethylpiperazin-1-yl)pentyl)-6-fluorobenzo[*d*]thiazol-2(3*H*)-one as yellow oil in 67% yield. ^1H NMR (400 MHz, Methanol- d_4) δ 7.43 – 7.14 (m, 7H), 5.07 (s, 2H), 4.07 (t, J = 6.7 Hz, 2H), 3.18 (dd, J = 22.9, 9.5 Hz, 5H), 2.19 (qd, J = 13.3, 5.4 Hz, 2H), 1.94 – 1.56 (m, 6H), 1.28 (d, J = 6.6 Hz, 3H). ^{13}C NMR (101 MHz, MeOD) δ 170.10, 160.29, 157.90, 143.74, 138.66, 133.31, 127.88, 127.30, 123.64, 123.54, 120.97, 120.30, 113.58, 113.34, 112.02, 111.93, 109.82, 109.55, 82.98, 70.56, 60.64, 44.14, 42.11, 34.64, 28.48, 24.22, 12.59. MS (EI) m/z 413 $[\text{M}+1]^+$.

6-fluoro-3-(4-(2'-methyl-3*H*-spiro[isobenzofuran-1,4'-piperidin]-1'-yl)butyl)benzo[*d*]thiazol-2(3*H*)-one. 398 (WA478) To a solution of 3-(4-bromobutyl)-6-fluorobenzo[*d*]thiazol-2(3*H*)-one (WA151) (0.048g, 0.1578 mmol) in 3 mL DMF were added (0.0655g, 0.47 mmol) of potassium carbonate and (0.0455g, 0.19 mmol) of 2'-methyl-3*H*-spiro[isobenzofuran-1,4'-

piperidine]-HCl, and the reaction mixture heated at 65 °C for 2 h, then the mixture extracted with ethyl acetate and water, washed with brine, dried over magnesium sulfate and the solvent evaporated using *vacuu* then purified by column chromatography (EtOAc: Hexane) to obtain 0.04g of 6-fluoro-3-(4-(2'-methyl-3*H*-spiro[isobenzofuran-1,4'-piperidin]-1'-yl)butyl)benzo[*d*]thiazol-2(3*H*)-one as yellow oil in 52% yield. MS (ESI) *m/z* 427.62 [$M^+ + 1$]. ¹H NMR (400 MHz, Methanol-*d*₄) δ 7.37 (dt, *J* = 6.6, 3.3 Hz, 1H), 7.32 (dd, *J* = 9.0, 4.5 Hz, 1H), 7.26 (ddt, *J* = 8.7, 6.4, 3.7 Hz, 4H), 7.15 (td, *J* = 8.9, 2.8 Hz, 1H), 4.85 (d, *J* = 6.3 Hz, 2H), 4.04 (q, *J* = 6.8 Hz, 2H), 3.20 (p, *J* = 5.9 Hz, 1H), 3.03 (ddd, *J* = 12.5, 9.3, 3.6 Hz, 1H), 2.82 – 2.69 (m, 3H), 2.11 – 1.93 (m, 2H), 1.84 – 1.65 (m, 6H), 1.24 (q, *J* = 6.2 Hz, 3H). ¹³C NMR (101 MHz, MeOD) δ 169.99, 163.41, 161.52, 160.25, 157.85, 145.15, 139.06, 133.36, 127.47, 126.96, 123.61, 120.84, 113.53, 113.30, 112.03, 109.79, 109.52, 84.54, 70.17, 52.89, 52.65, 44.32, 42.15, 41.25, 35.22, 25.09, 22.69, 13.88.

3-(4-bromobutyl)benzo[*d*]oxazol-2(3*H*)-one. 393a (WA479) To a solution of benzo[*d*]oxazol-2(3*H*)-one (0.5g, 3.70 mmol) in 10 mL DMF were added (5.59g, 40.50 mmol) of potassium carbonate and (1.53g, 11.08 mmol) of 1,4-dibromobutane, and the reaction mixture heated at 65 °C for 2 h, then the mixture extracted with ethyl acetate and water, treated with brine, dried over magnesium sulfate and the solvent evaporated using *vacuu* then purified by column chromatography (EtOAc: Hexane) to afford 0.65g of 3-(4-bromobutyl)benzo[*d*]oxazol-2(3*H*)-one as clear oil in 65% yield. MS (ESI) *m/z* 292.41 [$M^+ + 23$]. ¹H NMR (400 MHz, Chloroform-*d*) δ 7.20 (t, *J* = 8.4 Hz, 2H), 7.12 (t, *J* = 7.7 Hz, 1H), 7.00 (d, *J* = 7.6 Hz, 1H), 3.87 (t, *J* = 6.3 Hz, 2H), 3.47 (q, *J* = 5.9, 5.4 Hz, 2H), 2.03 – 1.95 (m, 4H). ¹³C NMR (101 MHz, CDCl₃) δ 154.55, 142.67, 130.93, 123.88, 122.49, 110.12, 108.22, 41.28, 32.71, 29.40, 26.31.

3-(4-bromobutyl)benzo[*d*]thiazol-2(3*H*)-one. 392a (WA480) To a solution of benzo[*d*]thiazol-2(3*H*)-one (0.5g, 3.30 mmol) in 5 mL DMF were added (1.4g, 10.14 mmol) of potassium carbonate and (2.85g, 13.2 mmol) of 1,4-dibromobutane, and the reaction mixture heated at 65 °C for 2 h, then the mixture extracted with ethyl acetate and water, treated with brine, dried over magnesium sulfate and the solvent evaporated using *vacuu* then purified by column chromatography (EtOAc: Hexane) to afford 0.7g of 3-(4-bromobutyl)benzo[*d*]thiazol-2(3*H*)-one as clear oil in 74% yield. MS (ESI) *m/z* 308.42 [$M^+ + 23$], 310.43 [$M + 25$]⁺. ¹H NMR (400 MHz, Chloroform-*d*) δ 7.44 (d, *J* = 7.7 Hz, 1H), 7.33 (t, *J* = 7.8 Hz, 1H), 7.17 (t, *J* = 7.6 Hz, 1H), 7.07 (d, *J* = 8.0 Hz, 1H), 4.00 (q, *J* = 6.1 Hz, 2H), 3.47 (q, *J* = 6.0, 5.5 Hz, 2H), 1.95 (qq, *J* = 7.6, 4.2 Hz, 4H). ¹³C NMR (101 MHz, CDCl₃) δ 169.93, 136.86, 126.40, 123.14, 122.78, 122.74, 110.51, 41.68, 32.92, 29.55, 26.15.

3-(4-(2'-methyl-3*H*-spiro[isobenzofuran-1,4'-piperidin]-1'-yl)butyl)benzo[*d*]oxazol-2(3*H*)-one. 399 (WA483) To a solution of 3-(4-bromobutyl)benzo[*d*]oxazol-2(3*H*)-one (WA479) (0.05g, 0.185 mmol) in 2 mL DMF were added (0.0766g, 0.55 mmol) of potassium carbonate and (0.045g, 0.2213 mmol) of 2'-methyl-3*H*-spiro[isobenzofuran-1,4'-piperidine], and the reaction mixture heated at 65 °C for 3 h, then the mixture extracted with ethyl acetate and water, washed with brine, dried over magnesium sulfate and the solvent evaporated using *vacuu* then purified by column chromatography (EtOAc: Hexane) to obtain 0.045g of 3-(4-(2'-methyl-3*H*-spiro[isobenzofuran-1,4'-piperidin]-1'-yl)butyl)benzo[*d*]oxazol-2(3*H*)-one as yellow oil in 62% yield. MS (ESI) *m/z* 393.70 [$M^+ + 1$]. ¹H NMR (400 MHz, Methanol-*d*₄) δ 7.32 – 7.07 (m, 8H), 4.86 (s, 2H), 3.94 (t, *J* = 6.9 Hz, 2H), 3.06 – 2.96 (m, 2H), 2.78 – 2.67 (m, 2H), 2.09 – 1.63 (m,

8H), 1.32 – 1.07 (m, 4H). ¹³C NMR (101 MHz, MeOD) δ 163.41, 155.00, 145.26, 142.64, 139.07, 131.01, 127.41, 126.92, 123.83, 122.29, 120.81, 109.41, 108.74, 84.67, 70.12, 52.88, 52.45, 44.36, 41.48, 35.37, 25.30, 22.77, 13.91.

3-(4-(2'-methyl-3*H*-spiro[isobenzofuran-1,4'-piperidin]-1'-yl)butyl)benzo[*d*]thiazol-2(3*H*)-one. 400 (WA484) To a solution of 3-(4-bromobutyl)benzo[*d*]thiazol-2(3*H*)-one (WA480) (0.05g, 0.1747 mmol) in 2 mL DMF were added (0.0723g, 0.5239 mmol) of potassium carbonate and (0.0426g, 0.21 mmol) of 2'-methyl-3*H*-spiro[isobenzofuran-1,4'-piperidine], and the reaction mixture heated at 65 °C for 3 h, then the mixture extracted with ethyl acetate and water, washed with brine, dried over magnesium sulfate and the solvent evaporated using *vacuo* then purified by column chromatography (EtOAc: Hexane) to obtain 0.05g of 3-(4-(2'-methyl-3*H*-spiro[isobenzofuran-1,4'-piperidin]-1'-yl)butyl)benzo[*d*]thiazol-2(3*H*)-one as yellow oil in 71% yield. MS (ESI) *m/z* 409.66 [*M*⁺+1]. ¹H NMR (400 MHz, Methanol-*d*₄) δ 7.53 (d, *J* = 7.8 Hz, 1H), 7.43 – 7.12 (m, 7H), 4.86 (s, 2H), 4.07 (t, *J* = 7.0 Hz, 2H), 3.23 (dt, *J* = 12.6, 6.4 Hz, 1H), 3.08 – 2.98 (m, 1H), 2.87 – 2.69 (m, 3H), 2.15 – 1.94 (m, 2H), 1.88 – 1.60 (m, 6H), 1.25 (d, *J* = 6.7 Hz, 3H). ¹³C NMR (101 MHz, MeOD) δ 170.50, 145.11, 139.05, 136.97, 127.48, 126.96, 126.42, 123.13, 122.42, 120.83, 111.04, 84.50, 70.18, 52.91, 44.31, 41.89, 41.18, 35.16, 25.12, 22.67, 13.88.

6-fluoro-3-(4-(spiro[isochromane-1,4'-piperidin]-1'-yl)butyl)benzo[*d*]thiazol-2(3*H*)-one. 401 (WA497) To a solution of 3-(4-bromobutyl)-6-fluorobenzo[*d*]thiazol-2(3*H*)-one (WA151) (0.05g, 0.1970 mmol) in 3 mL DMF were added (0.068g, 0.4927 mmol) of potassium carbonate and (0.04g, 0.19 mmol) of spiro[isochromane-1,4'-piperidine]-HCl, and the reaction mixture heated at 65 °C for 2 h, then the mixture extracted with ethyl acetate and water, washed with

brine, dried over magnesium sulfate and the solvent evaporated using *vacuu* then purified by column chromatography (EtOAc: Hexane) to obtain 0.03g of 6-fluoro-3-(4-(spiro[isochromane-1,4'-piperidin]-1'-yl)butyl)benzo[*d*]thiazol-2(3*H*)-one as yellow oil in 43% yield. MS (ESI) *m/z* 427.56 [$M^+ + 1$]. ^1H NMR (400 MHz, Chloroform-*d*) δ 7.24 – 7.12 (m, 4H), 7.12 – 7.03 (m, 3H), 3.99 (t, $J = 7.1$ Hz, 2H), 3.89 (t, $J = 5.5$ Hz, 2H), 2.97 – 2.79 (m, 4H), 2.59 (d, $J = 7.8$ Hz, 4H), 2.22 (s, 2H), 1.93 (d, $J = 13.8$ Hz, 2H), 1.83 (t, $J = 7.0$ Hz, 2H), 1.26 (s, 2H). ^{13}C NMR (101 MHz, CDCl_3) δ 169.43, 160.09, 157.67, 133.62, 133.21, 128.78, 126.40, 126.32, 125.45, 123.99, 123.89, 113.65, 113.41, 111.28, 111.19, 110.18, 109.91, 72.58, 58.93, 57.61, 49.16, 42.58, 36.04, 29.69, 29.59, 25.43.

6-fluoro-3-(4-(2'-methyl-3*H*-spiro[isobenzofuran-1,4'-piperidin]-1'-yl)butyl)benzo[*d*]

thiazol-2(3*H*)-one. 398 (WA478) To a solution of 3-(4-bromobutyl)-6-fluorobenzo[*d*]thiazol-2(3*H*)-one (WA151) (0.048g, 0.1578 mmol) in 3 mL DMF were added (0.0655g, 0.47 mmol) of potassium carbonate and (0.0455g, 0.19 mmol) of 2'-methyl-3*H*-spiro[isobenzofuran-1,4'-piperidine]-HCl, and the reaction mixture heated at 65 °C for 2 h, then the mixture extracted with ethyl acetate and water, washed with brine, dried over magnesium sulfate and the solvent evaporated using *vacuu* then purified by column chromatography (EtOAc: Hexane) to obtain 0.04g of 6-fluoro-3-(4-(2'-methyl-3*H*-spiro[isobenzofuran-1,4'-piperidin]-1'-yl)butyl)benzo[*d*]thiazol-2(3*H*)-one as yellow oil in 52% yield. MS (ESI) *m/z* 427.62 [$M^+ + 1$]. ^1H NMR (400 MHz, Methanol-*d*₄) δ 7.37 (dt, $J = 6.6, 3.3$ Hz, 1H), 7.32 (dd, $J = 9.0, 4.5$ Hz, 1H), 7.26 (ddt, $J = 8.7, 6.4, 3.7$ Hz, 4H), 7.15 (td, $J = 8.9, 2.8$ Hz, 1H), 4.85 (d, $J = 6.3$ Hz, 2H), 4.04 (q, $J = 6.8$ Hz, 2H), 3.20 (p, $J = 5.9$ Hz, 1H), 3.03 (ddd, $J = 12.5, 9.3, 3.6$ Hz, 1H), 2.82 – 2.69 (m, 3H), 2.11 – 1.93 (m, 2H), 1.84 – 1.65 (m, 6H), 1.24 (q, $J = 6.2$ Hz, 3H). ^{13}C NMR (101

MHz, MeOD) δ 169.99, 163.41, 161.52, 160.25, 157.85, 145.15, 139.06, 133.36, 127.47, 126.96, 123.61, 120.84, 113.53, 113.30, 112.03, 109.79, 109.52, 84.54, 70.17, 52.89, 52.65, 44.32, 42.15, 41.25, 35.22, 25.09, 22.69, 13.88.

3-(4-bromobutyl)benzo[*d*]oxazol-2(3*H*)-one. 393a (WA479) To a solution of benzo[*d*]oxazol-2(3*H*)-one (0.5g, 3.70 mmol) in 10 mL DMF were added (5.59g, 40.50 mmol) of potassium carbonate and (1.53g, 11.08 mmol) of 1,4-dibromobutane, and the reaction mixture heated at 65 °C for 2 h, then the mixture extracted with ethyl acetate and water, treated with brine, dried over sodium sulfate and the solvent evaporated using *vacuu* then purified by column chromatography (EtOAc: Hexane) to afford 0.65g of 3-(4-bromobutyl)benzo[*d*]oxazol-2(3*H*)-one as clear oil in 65% yield. MS (ESI) *m/z* 292.41 [$M^{+}+23$]. ¹H NMR (400 MHz, Chloroform-*d*) δ 7.20 (t, *J* = 8.4 Hz, 2H), 7.12 (t, *J* = 7.7 Hz, 1H), 7.00 (d, *J* = 7.6 Hz, 1H), 3.87 (t, *J* = 6.3 Hz, 2H), 3.47 (q, *J* = 5.9, 5.4 Hz, 2H), 2.03 – 1.95 (m, 4H). ¹³C NMR (101 MHz, CDCl₃) δ 154.55, 142.67, 130.93, 123.88, 122.49, 110.12, 108.22, 41.28, 32.71, 29.40, 26.31.

3-(4-bromobutyl)benzo[*d*]thiazol-2(3*H*)-one. (392a, WA480) To a solution of benzo[*d*]thiazol-2(3*H*)-one (0.5 g, 3.30 mmol) in 5 mL DMF were added (1.4 g, 10.14 mmol) of potassium carbonate and (2.85 g, 13.2 mmol) of 1,4-dibromobutane, and the reaction mixture heated at 65 °C for 2 h, then the mixture extracted with ethyl acetate and water, treated with brine, dried over sodium sulfate and the solvent evaporated using *vacuu* then purified by column chromatography (EtOAc: Hexane) to afford 0.7 g of 3-(4-bromobutyl)benzo[*d*]thiazol-2(3*H*)-one as clear oil in 74% yield. MS (ESI) *m/z* 308.42 [$M^{+}+23$], 310.43 [$M+25$]⁺. ¹H NMR (400 MHz, Chloroform-*d*) δ 7.44 (d, *J* = 7.7 Hz, 1H), 7.33 (t, *J* = 7.8 Hz, 1H), 7.17 (t, *J* = 7.6 Hz, 1H), 7.07 (d, *J* = 8.0 Hz, 1H), 4.00 (q, *J* = 6.1 Hz, 2H), 3.47 (q, *J* = 6.0, 5.5 Hz, 2H), 1.95 (qq, *J* = 7.6, 4.2 Hz, 4H). ¹³C

NMR (101 MHz, CDCl₃) δ 169.93, 136.86, 126.40, 123.14, 122.78, 122.74, 110.51, 41.68, 32.92, 29.55, 26.15.

3-(4-(2'-methyl-3*H*-spiro[isobenzofuran-1,4'-piperidin]-1'-yl)butyl)benzo[*d*]oxazol-2(3*H*)-

one. 399 (WA483) To a solution of 3-(4-bromobutyl)benzo[*d*]oxazol-2(3*H*)-one (WA479) (0.05g, 0.185 mmol) in 2 mL DMF were added (0.0766g, 0.55 mmol) of potassium carbonate and (0.045g, 0.2213 mmol) of 2'-methyl-3*H*-spiro[isobenzofuran-1,4'-piperidine], and the reaction mixture heated at 65 °C for 3 h, then the mixture extracted with ethyl acetate and water, washed with brine, dried over sodium sulfate and the solvent evaporated using *vacuu* then purified by column chromatography (EtOAc: Hexane) to obtain 0.045g of 3-(4-(2'-methyl-3*H*-spiro[isobenzofuran-1,4'-piperidin]-1'-yl)butyl)benzo[*d*]oxazol-2(3*H*)-one as yellow oil in 62% yield. MS (ESI) *m/z* 393.70 [M⁺+1]. ¹H NMR (400 MHz, Methanol-*d*₄) δ 7.32 – 7.07 (m, 8H), 4.86 (s, 2H), 3.94 (t, *J* = 6.9 Hz, 2H), 3.06 – 2.96 (m, 2H), 2.78 – 2.67 (m, 2H), 2.09 – 1.63 (m, 8H), 1.32 – 1.07 (m, 4H). ¹³C NMR (101 MHz, MeOD) δ 163.41, 155.00, 145.26, 142.64, 139.07, 131.01, 127.41, 126.92, 123.83, 122.29, 120.81, 109.41, 108.74, 84.67, 70.12, 52.88, 52.45, 44.36, 41.48, 35.37, 25.30, 22.77, 13.91.

3-(4-(2'-methyl-3*H*-spiro[isobenzofuran-1,4'-piperidin]-1'-yl)butyl)benzo[*d*]thiazol-2(3*H*)-

one. 400 (WA484) To a solution of 3-(4-bromobutyl)benzo[*d*]thiazol-2(3*H*)-one (WA480) (0.05g, 0.1747 mmol) in 2 mL DMF were added (0.0723g, 0.5239 mmol) of potassium carbonate and (0.0426g, 0.21 mmol) of 2'-methyl-3*H*-spiro[isobenzofuran-1,4'-piperidine], and the reaction mixture heated at 65 °C for 3 h, then the mixture extracted with ethyl acetate and water, washed with brine, dried over sodium sulfate and the solvent evaporated using *vacuu* then purified by column chromatography (EtOAc: Hexane) to obtain 0.05g of 3-(4-(2'-methyl-3*H*-

spiro[isobenzofuran-1,4'-piperidin]-1'-yl)butyl)benzo[*d*]thiazol-2(3*H*)-one as yellow oil in 71% yield. MS (ESI) *m/z* 409.66 [$M^+ + 1$]. ^1H NMR (400 MHz, Methanol-*d*₄) δ 7.53 (d, *J* = 7.8 Hz, 1H), 7.43 – 7.12 (m, 7H), 4.86 (s, 2H), 4.07 (t, *J* = 7.0 Hz, 2H), 3.23 (dt, *J* = 12.6, 6.4 Hz, 1H), 3.08 – 2.98 (m, 1H), 2.87 – 2.69 (m, 3H), 2.15 – 1.94 (m, 2H), 1.88 – 1.60 (m, 6H), 1.25 (d, *J* = 6.7 Hz, 3H). ^{13}C NMR (101 MHz, MeOD) δ 170.50, 145.11, 139.05, 136.97, 127.48, 126.96, 126.42, 123.13, 122.42, 120.83, 111.04, 84.50, 70.18, 52.91, 44.31, 41.89, 41.18, 35.16, 25.12, 22.67, 13.88.

6-fluoro-3-(4-(spiro[isochromane-1,4'-piperidin]-1'-yl)butyl)benzo[*d*]thiazol-2(3*H*)-one.

401 (WA497) To a solution of 3-(4-bromobutyl)-6-fluorobenzo[*d*]thiazol-2(3*H*)-one (WA151) (0.05g, 0.1970 mmol) in 3 mL DMF were added (0.068g, 0.4927 mmol) of potassium carbonate and (0.04g, 0.19 mmol) of spiro[isochromane-1,4'-piperidine]-HCl, and the reaction mixture heated at 65 °C for 2 h, then the mixture extracted with ethyl acetate and water, washed with brine, dried over sodium sulfate and the solvent evaporated using *vacuu* then purified by column chromatography (EtOAc: Hexane) to obtain 0.03g of 6-fluoro-3-(4-(spiro[isochromane-1,4'-piperidin]-1'-yl)butyl)benzo[*d*] thiazol-2(3*H*)-one as yellow oil in 43% yield. MS (ESI) *m/z* 427.56 [$M^+ + 1$]. ^1H NMR (400 MHz, Chloroform-*d*) δ 7.24 – 7.12 (m, 4H), 7.12 – 7.03 (m, 3H), 3.99 (t, *J* = 7.1 Hz, 2H), 3.89 (t, *J* = 5.5 Hz, 2H), 2.97 – 2.79 (m, 4H), 2.59 (d, *J* = 7.8 Hz, 4H), 2.22 (s, 2H), 1.93 (d, *J* = 13.8 Hz, 2H), 1.83 (t, *J* = 7.0 Hz, 2H), 1.26 (s, 2H). ^{13}C NMR (101 MHz, CDCl₃) δ 169.43, 160.09, 157.67, 133.62, 133.21, 128.78, 126.40, 126.32, 125.45, 123.99, 123.89, 113.65, 113.41, 111.28, 111.19, 110.18, 109.91, 72.58, 58.93, 57.61, 49.16, 42.58, 36.04, 29.69, 29.59, 25.43.

9.5.2 Synthesis of the de-methylated CM699

1-(4-(3*H*-spiro[isobenzofuran-1,4'-piperidin]-1'-yl)butyl)-1,3-dihydro-2*H*-benzo[*d*]

imidazol-2-one. 358 (WA294) To a solution of *tert*-butyl 3-(4-bromobutyl)-2-oxo-2,3-dihydro-1*H*-benzo[*d*]imidazole-1-carboxylate (**353**) (0.5 g, 1.35 mmol) in 10 mL DMF were added (0.56 g, 4 mmol) of potassium carbonate and (0.37 g, 1.63 mmol) of 3*H*-spiro[isobenzofuran-1,4'-piperidine] -HCl, and the reaction mixture heated at 160 °C in microwave reactor for 30 min., then the mixture extracted with ethyl acetate and water, washed with brine and dried over anhydrous magnesium sulfate and the solvent evaporated using *vacuu*. Then the residue was purified by column chromatography (EtOAc: Hexane) to get 0.35 g of 1-(4-(3*H*-spiro[isobenzofuran-1,4'-piperidin]-1'-yl)butyl)-1,3-dihydro-2*H*benzo[*d*]imidazol-2-one as white-yellowish solid in 68 % yield. MS (EI) *m/z* 378.66 (M^+ +1). ¹H NMR (400 MHz, DMSO-*d*₆) δ 10.85 (s, 1H), 7.28 (d, *J* = 3.0 Hz, 3H), 7.21 (d, *J* = 4.4 Hz, 1H), 7.14 (d, *J* = 7.0 Hz, 1H), 7.03 – 6.96 (m, 3H), 3.82 (t, *J* = 6.8 Hz, 2H), 3.03 (dd, *J* = 16.9, 9.6 Hz, 2H), 2.69 (d, *J* = 23.3 Hz, 4H), 1.98 (d, *J* = 12.9 Hz, 2H), 1.63 (dq, *J* = 44.1, 7.9, 6.7 Hz, 7H), 1.16 (t, *J* = 7.3 Hz, 1H). ¹³C NMR (101 MHz, DMSO) δ 154.72, 145.11, 139.17, 130.61, 128.72, 128.19, 127.82, 121.76, 121.19, 121.12, 120.92, 109.18, 108.19, 83.39, 70.56, 49.67, 46.10, 39.86, 35.02, 25.89, 22.83.

9.5.3 Synthesis of 1-methyl-benzo[*d*]imidazol-2-one derivatives of CM699

Synthesis of 5-fluoro-*N*-methyl-2-nitroaniline. 407 (WA374) 5g (31.42 mmol) of 2,4-difluoro-1-nitrobenzene, and 7.68g (40% in water) of methylamine stirred at 0 °C for 30 min and then warmed up to room temperature and left for 1h. The reaction mixture was then filtered and dried to give 5g (93.5%) of 5-fluoro-*N*-methyl-2-nitroaniline as a yellow solid. MS (ESI) *m/z* 171.33 [M^+ +1]. ¹H NMR (400 MHz, DMSO-*d*₆) δ 8.29 (s, 1H), 8.17 – 8.08 (m, 1H), 6.73 (dt, *J* = 12.3, 2.1 Hz, 1H), 6.49 (td, *J* = 8.5, 7.5, 2.1 Hz, 1H), 2.92 (d, *J* = 4.9 Hz, 3H). ¹³C NMR (101 MHz,

DMSO) δ 168.62, 166.11, 148.55, 148.41, 130.14, 130.01, 128.59, 103.82, 103.57, 100.08, 99.80, 30.30.

5-fluoro-*N*¹-methylbenzene-1,2-diamine. 410 (WA375) To a solution of 5-fluoro-*N*-methyl-2-nitroaniline (5g, 29.38 mmol) in methanol (200 ml) was added to 10% Palladium on carbon catalyst (1g) and stirred under a hydrogen atmosphere (40 psi) for 16 h. The mixture was filtered through celite and evaporated in vacuo to give 2.5g of 5-fluoro-*N*¹-methylbenzene-1,2-diamine as reddish-brown residue in 60% yield. MS (ESI) m/z 139.29 [$M^+ - 1$]. ¹H NMR (400 MHz, DMSO-*d*₆) δ 6.51 – 6.45 (m, 1H), 6.20 – 6.13 (m, 2H), 4.94 – 4.85 (m, 1H), 4.27 (s, 2H), 2.69 (d, $J = 4.9$ Hz, 3H). ¹³C NMR (101 MHz, DMSO) δ 158.01, 155.73, 139.44, 139.34, 131.36, 131.34, 114.03, 113.93, 101.28, 101.07, 96.79, 96.52, 30.44.

6-fluoro-1-methyl-1,3-dihydro-2*H*-benzo[*d*]imidazol-2-one. 413 (WA376) A solution of 5-fluoro-*N*¹-methylbenzene-1,2-diamine (2.5 g, 17.85 mmol) and 1,1'-carbonyldiimidazole (CDI) (3.5g, 21.58 mmol) in tetrahydrofuran (100 mL) was stirred at 80°C for 16 h. The reaction mixture was then cooled to 0°C. The resulting precipitate was filtered and dried to give (2 g, 67 % yield) of 6-fluoro-1-methyl-1,3-dihydro-2*H*-benzo[*d*]imidazol-2-one as beige-brown solid. MS (ESI) m/z 189.58 [$M^+ + 1$], 165.52 [$M^+ - 1$]. ¹H NMR (400 MHz, DMSO-*d*₆) δ 10.87 (s, 1H), 7.22 – 6.65 (m, 3H), 3.29 (s, 3H). ¹³C NMR (101 MHz, DMSO) δ 159.30, 156.97, 155.33, 132.26, 132.13, 124.91, 109.33, 109.24, 107.26, 107.02, 96.57, 96.28, 27.07.

1-(4-bromobutyl)-5-fluoro-3-methyl-1,3-dihydro-2*H*-benzo[*d*]imidazol-2-one. 416 (WA377) To a solution of 6-fluoro-1-methyl-1,3-dihydro-2*H*-benzo[*d*]imidazol-2-one (0.93g, 5.6 mmol) in 15 mL DMF were added (2.32g, 16.81 mmol) of potassium carbonate and (4.84g, 22.4 mmol) of

1,4-dibromobutane, and the reaction mixture heated at 65 °C for 2.5 h, then the mixture extracted with CH₂Cl₂ and water, dried over magnesium sulfate and the solvent evaporated using *vacuu* then purified by column chromatography (EtOAc: Hexane) to get 1.4g of 1-(4-bromobutyl)-5-fluoro-3-methyl-1,3-dihydro-2*H*-benzo[*d*]imidazol-2-one as a white solid in 83% yield. MS (ESI) *m/z* 323.61 [M⁺+23]. ¹H NMR (400 MHz, DMSO-*d*₆) δ 7.16 (dd, *J* = 8.6, 4.5 Hz, 1H), 7.10 (dd, *J* = 9.1, 2.5 Hz, 1H), 6.85 (ddd, *J* = 10.2, 8.6, 2.5 Hz, 1H), 3.83 (t, *J* = 6.4 Hz, 2H), 3.54 (t, *J* = 6.2 Hz, 2H), 3.30 (s, 3H), 1.76 (dddd, *J* = 15.4, 10.7, 8.0, 4.6 Hz, 4H). ¹³C NMR (101 MHz, DMSO) δ 159.54, 157.22, 154.40, 130.98, 130.86, 125.63, 108.59, 108.49, 107.37, 107.13, 96.81, 96.52, 40.00, 34.92, 29.83, 27.58, 27.00.

1-(4-(3*H*-spiro[isobenzofuran-1,4'-piperidin]-1'-yl)butyl)-5-fluoro-3-methyl-1,3-dihydro-2*H*-benzo[*d*]imidazol-2-one. 423 (WA378) To a solution of 1-(4-bromobutyl)-5-fluoro-3-methyl-1,3-dihydro-2*H*-benzo[*d*]imidazol-2-one (0.5g, 1.66 mmol) in 5 mL DMF were added (0.687g, 4.97 mmol) of potassium carbonate and (0.38g, 1.68 mmol) of 3*H*-spiro[isobenzofuran-1,4'-piperidine] HCl,, and the reaction mixture heated at 65 °C for 2.5 h, then the mixture extracted with CH₂Cl₂ and water, dried over magnesium sulfate and the solvent evaporated using *vacuu* then purified by column chromatography (EtOAc: Hexane) to get 0.539g of 1-(4-(3*H*-spiro[isobenzofuran-1,4'-piperidin]-1'-yl)butyl)-5-fluoro-3-methyl-1,3-dihydro-2*H*-benzo[*d*]imidazol-2-one as yellow oil in 79% yield. MS (ESI) *m/z* 410.80 [M⁺+1]. ¹H NMR (500 MHz, Methanol-*d*₄) δ 7.25 (dd, *J* = 5.6, 3.1 Hz, 2H), 7.21 – 7.17 (m, 1H), 7.15 (s, 1H), 6.90 (dd, *J* = 8.5, 4.3 Hz, 1H), 6.79 (ddd, *J* = 9.7, 8.5, 2.5 Hz, 1H), 6.72 (dd, *J* = 8.4, 2.5 Hz, 1H), 3.90 (t, *J* = 7.1 Hz, 2H), 2.87 (d, *J* = 11.5 Hz, 2H), 2.54 – 2.37 (m, 5H), 2.00 (td, *J* = 13.1, 4.4 Hz, 3H), 1.92 – 1.70 (m, 6H), 1.71 – 1.56 (m, 3H). ¹³C NMR (126 MHz, CDCl₃) δ 159.57, 157.68,

154.68, 145.43, 138.82, 130.72, 130.62, 127.60, 127.36, 125.38, 121.03, 120.80, 107.73, 107.65, 107.42, 107.23, 96.01, 95.78, 84.51, 70.74, 58.13, 50.12, 41.02, 36.38, 27.27, 26.37, 24.04.

5-fluoro-1-(4-(4-(4-fluorophenyl)piperazin-1-yl)butyl)-3-methyl-1,3-dihydro-2H-

benzo[*d*]imidazol-2-one. 424 (WA379) To a solution of 1-(4-bromobutyl)-5-fluoro-3-methyl-1,3-dihydro-2H-benzo[*d*]imidazol-2-one (0.3g, 0.99 mmol) in 10 mL DMF were added (0.412g, 2.98 mmol) of potassium carbonate and (0.233g, 1.29 mmol) of 1-(4-fluorophenyl)piperazine, and the reaction mixture heated at 65 °C for 3 h, then the mixture extracted with CH₂Cl₂ and water, dried over magnesium sulfate and the solvent evaporated using *vaccu* then purified by column chromatography (EtOAc: Hexane) to get 0.35g of 5-fluoro-1-(4-(4-(4-fluorophenyl)piperazin-1-yl)butyl)-3-methyl-1,3-dihydro-2H-benzo[*d*]imidazol-2-one as yellow oil in 88% yield. MS (ESI) *m/z* 401.67 [*M*⁺+1]. ¹H NMR (400 MHz, Chloroform-*d*) δ 6.99 – 6.92 (m, 2H), 6.92 – 6.84 (m, 3H), 6.82 – 6.71 (m, 2H), 3.91 (t, *J* = 7.1 Hz, 2H), 3.39 (s, 3H), 3.15 – 3.06 (m, 4H), 2.63 – 2.54 (m, 4H), 2.48 – 2.40 (m, 2H), 1.86 – 1.74 (m, 2H), 1.67 – 1.54 (m, 2H). ¹³C NMR (101 MHz, CDCl₃) δ 159.83, 158.32, 157.46, 155.95, 154.69, 147.93, 130.75, 125.38, 117.80, 117.73, 115.58, 115.36, 107.69, 107.60, 107.44, 107.20, 96.04, 95.76, 57.81, 53.17, 50.08, 41.01, 27.27, 26.22, 23.94.

1-(4-(6,7-dimethoxy-3,4-dihydroisoquinolin-2(1*H*)-yl)butyl)-5-fluoro-3-methyl-1,3-dihydro-

2H-benzo[*d*]imidazol-2-one. 425 (WA380) To a solution of 1-(4-bromobutyl)-5-fluoro-3-methyl-1,3-dihydro-2H-benzo[*d*]imidazol-2-one (0.3g, 0.99 mmol) in 10 mL DMF were added (0.412g, 2.98 mmol) of potassium carbonate and (0.3g, 1.31 mmol) of 6,7-dimethoxy-1,2,3,4-tetrahydroisoquinoline, and the reaction mixture heated at 65 °C for 4 h, then the mixture

extracted with CH₂Cl₂ and water, dried over magnesium sulfate and the solvent evaporated using *vacuu* then purified by column chromatography (EtOAc: Hexane) to get 0.3g of 1-(4-(6,7-dimethoxy-3,4-dihydroisoquinolin-2(1*H*)-yl)butyl)-5-fluoro-3-methyl-1,3-dihydro-2*H*-benzo[*d*]imidazol-2-one as yellow oil in 73% yield. MS (ESI) *m/z* 314.69 [M⁺+1]. ¹H NMR (400 MHz, DMSO-*d*₆) δ 7.13 (ddd, *J* = 15.6, 8.8, 3.5 Hz, 2H), 6.82 (ddd, *J* = 11.9, 6.9, 2.5 Hz, 1H), 6.59 (d, *J* = 20.1 Hz, 2H), 3.83 (t, *J* = 7.0 Hz, 2H), 3.67 (d, *J* = 2.6 Hz, 6H), 3.37 (s, 2H), 3.31 – 3.27 (m, 3H), 2.64 (d, *J* = 5.8 Hz, 2H), 2.53 (t, *J* = 5.8 Hz, 2H), 2.40 (t, *J* = 7.1 Hz, 2H), 1.72 – 1.59 (m, 2H), 1.49 (t, *J* = 7.4 Hz, 2H). ¹³C NMR (101 MHz, DMSO) δ 159.49, 157.16, 154.41, 147.54, 147.29, 130.97, 130.84, 127.08, 126.34, 125.71, 112.18, 110.37, 108.67, 108.58, 107.30, 107.06, 96.77, 96.49, 57.40, 55.90, 55.56, 51.07, 40.78, 28.75, 27.57, 26.10, 24.05.

4-fluoro-*N*-methyl-2-nitroaniline. 408 (WA424) 6g (37.71 mmol) of 1,4-difluoro-2-nitrobenzene, and 8.2g (40% in water) of methylamine stirred at 0 °C for 30 min and then warmed up to room temperature and left for 1h. The reaction mixture was then filtered and dried to give 5.5g (85%) of 5-fluoro-*N*-methyl-2-nitroaniline as orange crystals. MS (ESI) *m/z* 171.33 [M⁺+1] ¹H NMR (400 MHz, DMSO-*d*₆) δ 8.09 (s, 1H), 7.80 (dd, *J* = 9.5, 3.2 Hz, 1H), 7.51 (ddd, *J* = 10.2, 7.6, 3.1 Hz, 1H), 7.01 (dd, *J* = 9.5, 4.8 Hz, 1H), 2.94 (d, *J* = 5.0 Hz, 3H). ¹³C NMR (101 MHz, DMSO) δ 153.05, 150.71, 143.83, 129.77, 129.68, 125.88, 125.65, 116.55, 116.48, 111.41, 111.15, 30.31.

4-fluoro-*N*¹-methylbenzene-1,2-diamine. 411 (WA425) To a solution of 4-fluoro-*N*-methyl-2-nitroaniline (5.5g, 32.326 mmol) in methanol (200 ml) was added to 10% Palladium on carbon catalyst (1g) and stirred under a hydrogen atmosphere (45 psi) for 16 h. The mixture was filtered

through celite and evaporated in vacuo to give 4g of 4-fluoro-*N*¹-methylbenzene-1,2-diamine as reddish-brown residue in 88% yield. MS (ESI) *m/z* 141 [*M*⁺+1]. ¹H NMR (400 MHz, Chloroform-*d*) δ 6.61 – 6.50 (m, 2H), 6.47 (dd, *J* = 9.8, 2.7 Hz, 1H), 2.83 (s, 3H). ¹³C NMR (101 MHz, CDCl₃) δ 158.12, 155.79, 136.34, 136.24, 134.35, 134.33, 111.99, 111.90, 105.43, 105.22, 103.22, 102.97, 31.50.

5-fluoro-1-methyl-1,3-dihydro-2*H*-benzo[*d*]imidazol-2-one. 414 (WA426) A solution of 5-fluoro-*N*¹-methylbenzene-1,2-diamine (3g, 28.55 mmol) and 1,1'-carbonyldiimidazole (CDI) (5.55g, 34.25 mmol) in freshly prepared tetrahydrofuran (60 mL) was stirred at 80°C for 5 h. The reaction mixture was then cooled to 0°C. The resulting precipitate was filtered and dried to give (2 g, 66 % yield) of 5-fluoro-1-methyl-1,3-dihydro-2*H*-benzo[*d*]imidazol-2-one as a beige (off-white) solid. MS (ESI) *m/z* 189 [*M*⁺+23], 165 [*M*⁺-1]. ¹H NMR (400 MHz, DMSO-*d*₆) δ 10.98 (s, 1H), 7.04 – 7.00 (m, 1H), 6.84 – 6.78 (m, 2H), 3.24 (s, 3H). ¹³C NMR (101 MHz, DMSO) δ 159.36, 157.04, 155.15, 129.28, 129.15, 127.80, 108.39, 108.29, 107.14, 106.90, 97.27, 96.99, 26.90.

3-(4-bromobutyl)-5-fluoro-1-methyl-1,3-dihydro-2*H*-benzo[*d*]imidazol-2-one. 418 (WA427) To a solution of 5-fluoro-1-methyl-1,3-dihydro-2*H*-benzo[*d*]imidazol-2-one (1.8g, 10.83 mmol) in 15 mL DMF were added (4.43g, 32.10 mmol) of potassium carbonate and (9.36g, 43.33 mmol) of 1,4-dibromobutane, and the reaction mixture heated at 65 °C for 2.5 h, then the mixture extracted with CH₂Cl₂ and water, dried over magnesium sulfate and the solvent evaporated using *vaccu* then purified by column chromatography (EtOAc: Hexane) to get 1.4g of 3-(4-bromobutyl)-5-fluoro-1-methyl-1,3-dihydro-2*H*-benzo[*d*]imidazol-2-one as yellow oil in 82% yield. MS (ESI) *m/z* 301 [*M*⁺+1]. ¹H NMR (400 MHz, Chloroform-*d*) δ 6.89 – 6.73 (m, 3H), 3.92

– 3.86 (m, 2H), 3.48 – 3.42 (m, 2H), 3.40 (s, 3H), 1.92 (q, $J = 3.2$ Hz, 4H). ^{13}C NMR (101 MHz, CDCl_3) δ 159.87, 157.51, 154.66, 129.76, 129.63, 126.18, 107.65, 107.55, 107.31, 96.11, 95.82, 40.27, 32.94, 29.54, 27.22, 26.79.

5-fluoro-3-(4-(4-(4-fluorophenyl)piperazin-1-yl)butyl)-1-methyl-1,3-dihydro-2H-

benzo[*d*]imidazol-2-one. 426 (WA428) To a solution of 3-(4-bromobutyl)-5-fluoro-1-methyl-1,3-dihydro-2H-benzo[*d*]imidazol-2-one (0.8g, 2.657 mmol) in 10 mL DMF were added (0.8g, 5.797 mmol) of potassium carbonate and (0.55g, 1.29 mmol) of 1-(4-fluorophenyl)piperazine, and the reaction mixture heated at 65 °C for 3 h, then the mixture extracted with CH_2Cl_2 and water, dried over magnesium sulfate and the solvent evaporated using *vacuu* then purified by column chromatography (EtOAc: Hexane) to get 0.35g of 5-fluoro-3-(4-(4-(4-fluorophenyl)piperazin-1-yl)butyl)-1-methyl-1,3-dihydro-2H-benzo[*d*]imidazol-2-one as yellow oil in 88% yield. MS (ESI) m/z 401 [$\text{M}^+ + 1$]. ^1H NMR (400 MHz, $\text{DMSO-}d_6$) δ 7.19 (dd, $J = 9.2, 2.5$ Hz, 1H), 7.10 (dd, $J = 8.6, 4.5$ Hz, 1H), 7.01 (t, $J = 8.9$ Hz, 2H), 6.92 – 6.83 (m, 3H), 3.82 (t, $J = 7.1$ Hz, 2H), 3.30 (s, 3H), 3.01 (t, $J = 4.9$ Hz, 4H), 2.43 (t, $J = 4.9$ Hz, 4H), 2.30 (t, $J = 7.2$ Hz, 2H), 1.65 (p, $J = 7.3$ Hz, 2H), 1.45 (p, $J = 7.3$ Hz, 2H). ^{13}C NMR (101 MHz, DMSO) δ 159.58, 157.54, 157.25, 155.20, 154.39, 148.39, 148.37, 130.19, 130.06, 126.48, 117.45, 117.38, 115.74, 115.52, 108.57, 108.47, 107.30, 107.06, 96.81, 96.53, 57.45, 53.10, 49.41, 40.83, 27.43, 25.98, 23.69.

3-(4-(3H-spiro[isobenzofuran-1,4'-piperidin]-1'-yl)butyl)-5-fluoro-1-methyl-1,3-dihydro-

2H-benzo[*d*]imidazol-2-one. 427 (WA429) To a solution of 3-(4-bromobutyl)-5-fluoro-1-methyl-1,3-dihydro-2H-benzo[*d*]imidazol-2-one (0.8g, 2.657 mmol) in 10 mL DMF were added (0.8g, 5.797 mmol) of potassium carbonate and (0.65g, 2.88 mmol) of 3H-spiro[isobenzofuran-

1,4'-piperidine] hydrochloride, and the reaction mixture heated at 65 °C for 3 h, then the mixture extracted with CH₂Cl₂ and water, dried over magnesium sulfate and the solvent evaporated using *vacuu* then purified by column chromatography (EtOAc: Hexane) to get 0.6g of 3-(4-(3*H*-spiro[isobenzofuran-1,4'-piperidin]-1'-yl)butyl)-5-fluoro-1-methyl-1,3-dihydro-2*H*-benzo[*d*]imidazol-2-one as yellow oil in 55% yield. MS (ESI) *m/z* 410 [M⁺+1]. ¹H NMR (400 MHz, Chloroform-*d*) δ 7.26 – 7.18 (m, 2H), 7.13 (dt, *J* = 14.6, 5.0 Hz, 2H), 6.84 – 6.71 (m, 3H), 5.02 (s, 2H), 3.85 (t, *J* = 7.2 Hz, 2H), 3.36 (s, 3H), 2.91 – 2.80 (m, 2H), 2.44 (dt, *J* = 23.9, 9.3 Hz, 4H), 2.00 (td, *J* = 13.3, 4.4 Hz, 2H), 1.75 (ddt, *J* = 14.5, 11.5, 4.9 Hz, 6H). ¹³C NMR (101 MHz, CDCl₃) δ 159.83, 157.47, 154.61, 145.39, 138.80, 129.91, 129.79, 127.56, 127.34, 126.16, 120.98, 120.80, 107.49, 107.40, 107.33, 107.09, 96.19, 95.90, 84.45, 70.72, 57.90, 50.12, 40.95, 36.33, 27.16, 26.06, 23.85.

3-(4-(6,7-dimethoxy-3,4-dihydroisoquinolin-2(1*H*)-yl)butyl)-5-fluoro-1-methyl-1,3-dihydro-2*H*-benzo[*d*]imidazol-2-one. 428 (WA430) To a solution of 3-(4-bromobutyl)-5-fluoro-1-methyl-1,3-dihydro-2*H*-benzo[*d*]imidazol-2-one (0.9g, 2.99 mmol) in 10 mL DMF were added (0.9g, 6.52 mmol) of potassium carbonate and (0.8g, 3.48 mmol) of 6,7-dimethoxy-1,2,3,4-tetrahydroisoquinoline hydrochloride, and the reaction mixture heated at 65 °C for 3 h, then the mixture extracted with CH₂Cl₂ and water, dried over MgSO₄ and the solvent evaporated using *vacuu* then purified by column chromatography (EtOAc: Hexane) to get 0.7g of 3-(4-(6,7-dimethoxy-3,4-dihydroisoquinolin-2(1*H*)-yl)butyl)-5-fluoro-1-methyl-1,3-dihydro-2*H*-benzo[*d*]imidazol-2-one as yellow oil in 63% yield. MS (ESI) *m/z* 414 [M⁺+1]. ¹H NMR (400 MHz, Chloroform-*d*) δ 6.84 (dd, *J* = 8.4, 4.5 Hz, 1H), 6.81 – 6.71 (m, 2H), 6.57 (s, 1H), 6.50 (s, 1H), 3.89 (t, *J* = 7.1 Hz, 2H), 3.82 (d, *J* = 1.3 Hz, 6H), 3.52 (s, 2H), 3.39 (s, 3H), 2.79 (t, *J* = 5.9

Hz, 2H), 2.67 (t, $J = 5.9$ Hz, 2H), 2.56 – 2.49 (m, 2H), 1.87 – 1.77 (m, 2H), 1.65 (q, $J = 7.9$ Hz, 2H). ^{13}C NMR (101 MHz, CDCl_3) δ 159.84, 157.48, 154.69, 147.46, 147.15, 129.93, 129.80, 126.54, 126.17, 126.14, 111.34, 109.46, 107.49, 107.39, 107.34, 107.10, 96.19, 95.91, 57.59, 55.87, 55.73, 51.03, 41.12, 28.65, 27.17, 26.15, 24.33.

1-(4-bromobutyl)-3-methyl-1,3-dihydro-2H-benzo[*d*]imidazol-2-one. 420 (WA318) To a solution of 1-methyl-1,3-dihydro-2H-benzo[*d*]imidazol-2-one (2g, 13.50 mmol) in 10 mL DMF were added (5.59g, 40.50 mmol) of potassium carbonate and (11.66g, 53.98 mmol) of 1,4-dibromobutane, and the reaction mixture heated at 65 °C for 2.5 h, then the mixture extracted with CH_2Cl_2 and water, dried over magnesium sulfate and the solvent evaporated using *vacuo* then purified by column chromatography (EtOAc: Hexane) to afford 2.55g of 1-(4-bromobutyl)-3-methyl-1,3-dihydro-2H-benzo[*d*]imidazol-2-one as colorless oil in 67% yield. MS (ESI) m/z 305.44 [$\text{M}^+ + 23$]; 207.39 [$\text{M}^+ + 25$]. ^1H NMR (400 MHz, Chloroform-*d*) δ 7.13 – 7.07 (m, 2H), 6.99 (ddd, $J = 8.8, 5.1, 2.3$ Hz, 2H), 3.97 – 3.88 (m, 2H), 3.46 (q, $J = 5.5, 4.0$ Hz, 2H), 3.42 (s, 3H), 1.93 (h, $J = 3.5$ Hz, 4H). ^{13}C NMR (101 MHz, CDCl_3) δ 154.40, 130.06, 129.14, 121.24, 121.20, 107.49, 107.47, 40.07, 33.07, 29.62, 27.13, 26.95.

1-methyl-3-(4-(2'-methyl-3H-spiro[isobenzofuran-1,4'-piperidin]-1'-yl)butyl)-1,3-dihydro-2H-benzo[*d*]imidazol-2-one. 429 (WA475) To a solution of 1-(4-bromobutyl)-3-methyl-1,3-dihydro-2H-benzo[*d*]imidazol-2-one (WA318) (0.05g, 0.1765 mmol) in 10 mL DMF were added (0.073g, 0.53 mmol) of potassium carbonate and (0.073g, 0.53 mmol) of 2'-methyl-3H-spiro[isobenzofuran-1,4'-piperidine], and the reaction mixture heated at 65 °C for 3 h, then the mixture extracted with CH_2Cl_2 and water, dried over magnesium sulfate and the solvent

evaporated using *vacuu* then purified by column chromatography (EtOAc: Hexane) to obtain 0.03g of 1-methyl-3-(4-(2'-methyl-3*H*-spiro[isobenzofuran-1,4'-piperidin]-1'-yl)butyl)-1,3-dihydro-2*H*-benzo[*d*]imidazol-2-one as yellow oil in 43% yield. MS (ESI) *m/z* 406.76 [M^+ +1]. ¹H NMR (400 MHz, Methanol-*d*₄) δ 7.31 – 7.18 (m, 5H), 7.16 – 7.08 (m, 3H), 5.04 (d, *J* = 2.3 Hz, 2H), 4.88 (s, 4H), 3.97 (t, *J* = 6.7 Hz, 2H), 3.37 (d, *J* = 12.4 Hz, 3H), 3.18 – 3.02 (m, 3H), 1.91 – 1.73 (m, 6H), 1.44 (d, *J* = 6.9 Hz, 3H). ¹³C NMR (101 MHz, MeOD) δ 154.62, 144.22, 138.84, 129.75, 128.77, 127.87, 127.26, 121.44, 120.96, 120.72, 107.91, 107.75, 83.30, 70.60, 54.20, 52.84, 43.88, 39.90, 39.05, 33.75, 26.14, 25.50, 21.72, 13.20.

5-fluoro-3-methyl-1-(4-(2'-methyl-3*H*-spiro[isobenzofuran-1,4'-piperidin]-1'-yl)butyl)-1,3-dihydro-2*H*-benzo[*d*]imidazol-2-one. 430 (WA476) To a solution of 1-(4-bromobutyl)-5-fluoro-3-methyl-1,3-dihydro-2*H*-benzo[*d*]imidazol-2-one (WA377) (0.05g, 0.166 mmol) in 10 mL DMF were added (0.07g, 0.507 mmol) of potassium carbonate and (0.048g, 0.24 mmol) of 2'-methyl-3*H*-spiro[isobenzofuran-1,4'-piperidine], and the reaction mixture heated at 65 °C for 3 h, then the mixture extracted with CH₂Cl₂ and water, washed with brine, dried over magnesium sulfate and the solvent evaporated using *vacuu* then purified by column chromatography (EtOAc: Hexane) to obtain 0.04g of 1-methyl-3-(4-(2'-methyl-3*H*-spiro[isobenzofuran-1,4'-piperidin]-1'-yl)butyl)-1,3-dihydro-2*H*-benzo[*d*]imidazol-2-one as yellow oil in 55% yield. MS (ESI) *m/z* 424.64 [M^+ +1]. ¹H NMR (400 MHz, Methanol-*d*₄) δ 7.38 – 7.21 (m, 4H), 7.19 (dd, *J* = 8.6, 4.3 Hz, 1H), 7.01 (dd, *J* = 8.7, 2.5 Hz, 1H), 6.89 (ddd, *J* = 10.7, 8.7, 2.5 Hz, 1H), 5.06 (d, *J* = 2.2 Hz, 2H), 4.00 (t, *J* = 6.7 Hz, 2H), 3.42 (s, 3H), 3.30 (s, 2H), 3.02 (d, *J* = 13.1 Hz, 3H), 2.25 (dd, *J* = 14.4, 5.2 Hz, 1H), 2.12 (td, *J* = 12.5, 11.0, 4.2 Hz, 1H), 1.92 – 1.69 (m, 6H), 1.41 (d, *J* = 6.8 Hz, 3H). ¹³C NMR (101 MHz, MeOD) δ 163.42, 160.16, 157.81, 155.08, 144.45, 138.93, 130.64,

127.75, 127.14, 125.07, 120.90, 120.69, 108.40, 108.30, 107.58, 107.34, 96.15, 95.86, 83.66, 70.45, 53.79, 52.83, 43.99, 40.08, 35.53, 30.24, 26.24, 25.53, 22.01.

1-(4-bromopentyl)-3-methyl-1,3-dihydro-2H-benzo[d]imidazol-2-one. 421 (WA477) To a solution of 1-methyl-1,3-dihydro-2H-benzo[d]imidazol-2-one (1g, 6.75 mmol) in 10 mL DMF were added (2.8g, 20.28 mmol) of potassium carbonate and (6.207g, 26.99 mmol) of 1,4-dibromopentane, and the reaction mixture heated at 65 °C for 3 h, then the mixture extracted with ethyl acetate and water, washed with brine, dried over magnesium sulfate and the solvent evaporated using *vacuu* then purified by column chromatography (EtOAc: Hexane) to afford 1.5g of 1-(4-bromopentyl)-3-methyl-1,3-dihydro-2H-benzo[d]imidazol-2-one as clear oil in 75% yield. MS (ESI) *m/z* 319.45 [$M^+ + 23$]. ¹H NMR (400 MHz, Chloroform-*d*) δ 7.10 (dt, *J* = 8.1, 4.1 Hz, 2H), 7.03 – 6.96 (m, 2H), 4.17 (h, *J* = 6.6 Hz, 1H), 3.91 (p, *J* = 6.9 Hz, 2H), 3.42 (s, 3H), 2.08 – 1.84 (m, 4H), 1.70 (d, *J* = 6.6 Hz, 3H). ¹³C NMR (101 MHz, CDCl₃) δ 154.39, 130.06, 129.17, 121.23, 121.17, 107.50, 107.46, 50.87, 40.31, 37.90, 27.13, 26.80, 26.53.

1-(4-(3H-spiro[isobenzofuran-1,4'-piperidin]-1'-yl)pentyl)-3-methyl-1,3-dihydro-2H-benzo[d]imidazol-2-one. 431 (WA481) To a solution of 1-(4-bromopentyl)-3-methyl-1,3-dihydro-2H-benzo[d]imidazol-2-one (WA477) (0.15g, 0.5047 mmol) in 3 mL DMF were added (0.209g, 1.51 mmol) of potassium carbonate and (0.115g, 0.6 mmol) of 3H-spiro[isobenzofuran-1,4'-piperidine], and the reaction mixture heated at 65 °C for 2 h, then the mixture extracted with ethyl acetate and water, washed with brine, dried over magnesium sulfate and the solvent evaporated using *vacuu* then purified by column chromatography (EtOAc: Hexane) to obtain 0.1g of 6-fluoro-3-(4-(2'-methyl-3H-spiro[isobenzofuran-1,4'-piperidin]-1'-

yl)butyl)benzo[*d*]thiazol-2(3*H*)-one as yellow oil in 50% yield. MS (ESI) *m/z* 406.67 [$M^+ + 1$]. ^1H NMR (400 MHz, Methanol-*d*₄) δ 7.34 – 7.23 (m, 5H), 7.18 – 7.14 (m, 3H), 5.10 (s, 2H), 4.02 (td, *J* = 6.4, 2.5 Hz, 2H), 3.53 – 3.38 (m, 10H), 2.37 (dd, *J* = 13.3, 6.6 Hz, 2H), 1.97 (ddt, *J* = 14.8, 6.5, 2.9 Hz, 4H), 1.41 (d, *J* = 6.6 Hz, 3H). ^{13}C NMR (101 MHz, MeOD) δ 154.73, 142.78, 138.67, 129.80, 128.75, 128.21, 127.44, 121.52, 121.48, 121.12, 120.26, 107.81, 81.85, 70.84, 62.00, 46.41, 44.84, 39.94, 33.57, 27.79, 26.07, 24.81, 12.35.

5-fluoro-1-methyl-3-(4-(2'-methyl-3*H*-spiro[isobenzofuran-1,4'-piperidin]-1'-yl)butyl)-1,3-dihydro-2*H*-benzo[*d*]imidazol-2-one. 432 (WA486) To a solution of 3-(4-bromobutyl)-5-fluoro-1-methyl-1,3-dihydro-2*H*-benzo[*d*]imidazol-2-one (WA427) (0.05g, 0.166 mmol) in 2 mL DMF were added (0.069g, 0.5036 mmol) of potassium carbonate and (0.0426g, 0.197 mmol) of 2'-methyl-3*H*-spiro[isobenzofuran-1,4'-piperidine], and the reaction mixture heated at 65 °C for 4 h, then the mixture extracted with ethyl acetate and water, washed with brine, dried over magnesium sulfate and the solvent evaporated using *vacuu* then purified by column chromatography (EtOAc: Hexane) to obtain 0.055g of 5-fluoro-1-methyl-3-(4-(2'-methyl-3*H*-spiro[isobenzofuran-1,4'-piperidin]-1'-yl)butyl)-1,3-dihydro-2*H*-benzo[*d*]imidazol-2-one as yellow oil in 78% yield. MS (ESI) *m/z* 424.70 [$M^+ + 1$]. ^1H NMR (400 MHz, Methanol-*d*₄) δ 7.23 (qt, *J* = 8.3, 4.6 Hz, 4H), 7.04 (dd, *J* = 8.6, 4.2 Hz, 2H), 4.98 (s, 2H), 3.91 (t, *J* = 7.0 Hz, 2H), 3.37 (s, 3H), 2.81 – 2.54 (m, 4H), 2.08 – 1.90 (m, 2H), 1.83 – 1.57 (m, 7H), 1.20 (d, *J* = 6.7 Hz, 3H). ^{13}C NMR (101 MHz, MeOD) δ 160.07, 157.72, 154.89, 145.26, 139.07, 129.69, 129.56, 127.43, 126.95, 125.99, 120.93, 120.83, 108.13, 108.04, 107.51, 107.27, 96.26, 95.97, 84.62, 70.14, 52.94, 52.46, 44.31, 41.39, 40.54, 35.34, 26.18, 25.81, 22.76, 13.88.

1-(4-bromopentyl)-5-fluoro-3-methyl-1,3-dihydro-2H-benzo[d]imidazol-2-one. 417

(WA488) To a solution of 6-fluoro-1-methyl-1,3-dihydro-2H-benzo[d]imidazol-2-one (WA376) (0.1g, 0.6 mmol) in 3 mL DMF were added (0.248g, 1.8 mmol) of potassium carbonate and (0.554g, 2.4 mmol) of 1,4-dibromopentane, and the reaction mixture heated at 65 °C for 2 h, then the mixture extracted with ethyl acetate and water, treated with brine, dried over magnesium sulfate and the solvent evaporated using *vacuu* then purified by column chromatography (EtOAc: Hexane) to afford 0.09g of 1-(4-bromopentyl)-5-fluoro-3-methyl-1,3-dihydro-2H-benzo[d]imidazol-2-one as clear oil in 48% yield. MS (ESI) m/z 315.30 [$M^+ + 1$]. ^1H NMR (400 MHz, Methanol- d_4) δ 7.12 (dd, $J = 8.6, 4.3$ Hz, 1H), 6.97 (dd, $J = 8.7, 2.5$ Hz, 1H), 6.86 (ddd, $J = 9.9, 8.6, 2.5$ Hz, 1H), 4.21 (h, $J = 6.5$ Hz, 1H), 3.92 (td, $J = 6.5, 2.2$ Hz, 2H), 3.39 (s, 3H), 2.01 – 1.78 (m, 4H), 1.66 (d, $J = 6.6$ Hz, 3H). ^{13}C NMR (101 MHz, MeOD) δ 160.09, 157.74, 154.95, 130.57, 130.44, 125.07, 108.26, 108.17, 107.52, 107.27, 96.09, 95.80, 50.40, 39.96, 37.66, 26.40, 26.20, 25.53.

3-(4-bromopentyl)-5-fluoro-1-methyl-1,3-dihydro-2H-benzo[d]imidazol-2-one. 419

(WA489) To a solution of 5-fluoro-1-methyl-1,3-dihydro-2H-benzo[d]imidazol-2-one (WA426) (0.08g, 0.5 mmol) in 3 mL DMF were added (0.207g, 1.5 mmol) of potassium carbonate and (0.443g, 1.92 mmol) of 3H-spiro[isobenzofuran-1,4'-piperidine]-HCl, and the reaction mixture heated at 65 °C for 6 h, then the mixture extracted with ethyl acetate and water, treated with brine, dried over magnesium sulfate and the solvent evaporated using *vacuu* then purified by column chromatography (EtOAc: Hexane) to afford 0.06g of 3-(4-bromopentyl)-5-fluoro-1-methyl-1,3-dihydro-2H-benzo[d]imidazol-2-one as clear oil in 38% yield. MS (ESI) m/z 315.30 [$M^+ + 1$]. ^1H NMR (400 MHz, Methanol- d_4) δ 7.07 (dd, $J = 8.6, 4.4$ Hz, 1H), 7.01 (dd, $J = 8.8, 2.5$ Hz, 1H), 6.89 – 6.82 (m, 1H), 4.21 (q, $J = 6.6$ Hz, 1H), 3.90 (ddd, $J = 9.6, 5.5, 2.8$ Hz, 2H), 3.40

(s, 3H), 2.01 – 1.78 (m, 4H), 1.66 (d, $J = 6.6$ Hz, 3H). ^{13}C NMR (101 MHz, MeOD) δ 160.10, 157.75, 154.93, 129.62, 129.49, 125.98, 108.15, 108.06, 107.54, 107.29, 96.14, 95.85, 50.40, 40.05, 37.63, 26.33, 26.11, 25.53.

1-(4-(3*H*-spiro[isobenzofuran-1,4'-piperidin]-1'-yl)pentyl)-5-fluoro-3-methyl-1,3-dihydro-2*H*-benzo[*d*]imidazol-2-one. 434 (WA490) To a solution of 1-(4-bromopentyl)-5-fluoro-3-methyl-1,3-dihydro-2*H*-benzo[*d*]imidazol-2-one (WA488) (0.074g, 0.235 mmol) in 3 mL DMF were added (0.0972g, 0.7043 mmol) of potassium carbonate and (0.064g, 0.2835 mmol) of 3*H*-spiro[isobenzofuran-1,4'-piperidine]-HCl, and the reaction mixture heated at 65 °C for 6 h, then the mixture extracted with ethyl acetate and water, treated with brine, dried over magnesium sulfate and the solvent evaporated using *vacuu* then purified by column chromatography (EtOAc: Hexane) to afford 0.06g of 1-(4-(3*H*-spiro[isobenzofuran-1,4'-piperidin]-1'-yl)pentyl)-5-fluoro-3-methyl-1,3-dihydro-2*H*-benzo[*d*]imidazol-2-one as clear oil in 50% yield. MS (ESI) m/z 424.83 [$\text{M}^+ + 1$]. ^1H NMR (400 MHz, Methanol- d_4) δ 7.32 – 7.22 (m, 3H), 7.20 – 7.12 (m, 2H), 6.99 (dd, $J = 8.7, 2.5$ Hz, 1H), 6.88 (ddd, $J = 9.9, 8.6, 2.5$ Hz, 1H), 5.04 (s, 2H), 3.96 (t, $J = 6.7$ Hz, 2H), 3.41 (s, 3H), 2.95 (q, $J = 14.4, 13.7$ Hz, 5H), 2.15 – 1.98 (m, 2H), 1.93 – 1.70 (m, 5H), 1.58 – 1.44 (m, 1H), 1.18 (d, $J = 6.6$ Hz, 3H). ^{13}C NMR (101 MHz, MeOD) δ 160.12, 157.77, 155.03, 144.32, 138.64, 130.61, 127.68, 127.19, 125.13, 120.87, 120.30, 108.28, 107.31, 95.84, 83.64, 70.37, 59.97, 46.21, 43.62, 40.54, 35.12, 29.04, 26.24, 25.17, 12.71.

3-(4-(3*H*-spiro[isobenzofuran-1,4'-piperidin]-1'-yl)pentyl)-5-fluoro-1-methyl-1,3-dihydro-2*H*-benzo[*d*]imidazol-2-one. 433 (WA491) To a solution of 3-(4-bromopentyl)-5-fluoro-1-methyl-1,3-dihydro-2*H*-benzo[*d*]imidazol-2-one (WA489) (0.1g, 0.317 mmol) in 3 mL DMF

were added (0.131g, 0.9492 mmol) of potassium carbonate and (0.085g, 0.3765 mmol) of 3*H*-spiro[isobenzofuran-1,4'-piperidine]-HCl, and the reaction mixture heated at 65 °C for 8 h, then the mixture extracted with ethyl acetate and water, treated with brine, dried over magnesium sulfate and the solvent evaporated using *vacuu* then purified by column chromatography (EtOAc: Hexane) to afford 0.09g of 3-(4-(3*H*-spiro[isobenzofuran-1,4'-piperidin]-1'-yl)pentyl)-5-fluoro-1-methyl-1,3-dihydro-2*H*-benzo[*d*]imidazol-2-one as yellow oil in 67% yield. MS (ESI) *m/z* 424.77 [$M^+ + 1$]. Free base: ^1H NMR (400 MHz, Methanol-*d*₄) δ 7.31 – 7.23 (m, 3H), 7.20 – 7.14 (m, 1H), 7.10 (td, *J* = 8.6, 3.5 Hz, 2H), 6.94 – 6.82 (m, 1H), 5.05 (s, 2H), 3.96 (t, *J* = 6.8 Hz, 2H), 3.42 (d, *J* = 6.5 Hz, 3H), 3.36 (s, 2H), 2.98 (q, *J* = 14.1, 11.6 Hz, 4H), 2.14 – 1.97 (m, 2H), 1.84 (ddt, *J* = 24.4, 12.6, 8.1 Hz, 4H), 1.57 – 1.49 (m, 1H), 1.18 (d, *J* = 6.6 Hz, 3H). HCl salt: ^1H NMR (400 MHz, Methanol-*d*₄) δ 7.38 – 7.31 (m, 2H), 7.26 (td, *J* = 17.0, 16.3, 9.5 Hz, 3H), 7.13 (dq, *J* = 8.0, 3.0, 2.5 Hz, 2H), 6.91 (t, *J* = 9.4 Hz, 1H), 4.86 (d, *J* = 2.6 Hz, 6H), 4.00 (dt, *J* = 8.7, 4.2 Hz, 2H), 3.47 – 3.41 (m, 6H), 2.36 (s, 2H), 2.01 (d, *J* = 3.1 Hz, 2H), 1.96 (s, 2H), 1.42 (dd, *J* = 6.9, 2.6 Hz, 3H). ^{13}C NMR (101 MHz, MeOD) δ 157.84, 155.08, 142.77, 138.68, 129.55, 129.42, 128.21, 127.44, 126.08, 121.12, 120.25, 108.33, 108.23, 107.73, 107.49, 96.27, 95.98, 81.85, 70.85, 62.01, 46.40, 44.88, 40.19, 33.59, 27.73, 26.18, 24.71, 12.35.

1'-(4-(benzofuran-3-yl)butyl)spiro[isochromane-1,4'-piperidine]. 314 (WA496) To a solution of 3-(4-bromobutyl)benzofuran (WA208) (0.05g, 0.1382 mmol) in 3 mL DMF were added (0.06g, 0.4347 mmol) of potassium carbonate and (0.034g, 0.1674 mmol) of spiro[isochromane-1,4'-piperidine]-HCl, and the reaction mixture heated at 65 °C for 3 h, then the mixture extracted with ethyl acetate and water, treated with brine, dried over magnesium sulfate and the solvent evaporated using *vacuu* then purified by column chromatography (EtOAc: Hexane) to afford

0.034g of 1'-(4-(benzofuran-3-yl)butyl)spiro[isochromane-1,4'-piperidine] as yellow oil in 67% yield. MS (ESI) m/z 376 [$M^+ + 1$]. ^1H NMR (400 MHz, Methanol- d_4) δ 7.62 – 7.57 (m, 1H), 7.55 (s, 1H), 7.46 – 7.41 (m, 1H), 7.31 – 7.19 (m, 2H), 7.19 – 7.05 (m, 4H), 3.87 (t, $J = 5.5$ Hz, 2H), 2.77 (dt, $J = 13.9, 6.4$ Hz, 6H), 2.51 – 2.39 (m, 4H), 2.03 (td, $J = 13.5, 4.4$ Hz, 2H), 1.86 (dd, $J = 14.4, 2.6$ Hz, 2H), 1.80 – 1.61 (m, 4H). ^{13}C NMR (101 MHz, MeOD) δ 155.50, 141.41, 141.23, 133.56, 128.44, 128.05, 125.87, 124.88, 123.75, 121.89, 120.05, 119.22, 110.75, 72.68, 58.43, 58.30, 48.90, 35.88, 29.18, 26.90, 25.96, 22.82.

9.6 Synthesis of the heterocycle substituents

9.6.1 Synthesis of 3*H*-spiro[isobenzofuran-1,4'-piperidine]

1-benzyl-4-(3-(4,4-dimethyl-4,5-dihydrooxazol-2-yl)phenyl)piperidin-4-ol. 477 (WA186) A solution of 4,4-dimethyl-2-phenyl-4,5-dihydrooxazole (**475**) (6.4g, 36.5 mmol) in anhydrous THF (100 mL) was stirred and cooled to -70 °C under argon. At this temperature (-70 °C), 17.78 mL of *n*-butyllithium (2.5 M) was added slowly and stirred for 25 min. at -70 °C. After that, *N*-benzyl-4-piperidone (**476**) (7 g, 37 mmol) in 50 mL anhydrous THF was added slowly with maintaining the temperature below -65 °C, and the reaction mixture was stirred for more 20 min. at 70 °C. After that the reaction mixture left at room temperature for 1 h. Then the mixture was poured into saturated solution of NH_4Cl and extracted (3x) with ethyl acetate. The combined organic layers were washed with brine, dried over magnesium sulfate and evaporated. The residue was purified by chromatography on a silica gel column using a gradient of ethyl acetate/hexanes (2 : 8) as eluent to give 4.0 g (70 %) of 1-benzyl-4-(3-(4,4-dimethyl-4,5-dihydrooxazol-2-yl)phenyl)piperidin-4-ol as a brown solid that was analyzed by the Mass Spectrometer and immediately used in the next step without further characterization. MS (EI)

m/z 365.76 $[M+1]^+$.

1'-benzyl-3*H*-spiro[isobenzofuran-1,4'-piperidin]-3-one. 478, (WA188) A solution of 1-benzyl-4-(3-(4,4-dimethyl-4,5-dihydrooxazol-2-yl)phenyl)piperidin-4-ol (**477**) (4.0 g, 11 mmol) in 85 mL of 3 *N* HCl was refluxed for 5 h and then evaporated in vacuo to yield a white solid. This was layered between CHCl₃ and water and the pH of the aqueous layer was adjusted to 10 with saturated KOH solution. The layers were separated and the aqueous phase was extracted with CHCl₃. The combined extracts were washed with brine, dried over magnesium sulfate, and evaporated in vacuo to give an oil which was crystallized from ether to yield 2.2 g (68%) of 1'-benzyl-3*H*-spiro[isobenzofuran-1,4'-piperidin]-3-one as a white crystals that was analyzed by the Mass Spectrometer and directly used in the next step without further characterization. MS (EI) m/z 294.61 $[M^++1]^+$.

1'-benzyl-3*H*-spiro[isobenzofuran-1,4'-piperidine]. 479 (WA190) To a solution of 1'-benzyl-3*H*-spiro[isobenzofuran-1,4'-piperidin]-3-one, in 35 mL of anhydrous THF cooled to 0 °C was added dropwise 13.73 mL of 1M Borane-THF with stirring. After addition was completed the mixture was kept at room temperature for 30 min. and then refluxed overnight. The reaction mixture cooled to 0 °C and 15 mL of 6N HCl was added dropwise. The reaction mixture was then refluxed for 5 h. After that, the reaction mixture pH adjusted to 10 and extracted with ethyl acetate (3x), treated with brine, dried over magnesium sulfate, and concentrated. The residue was purified by chromatography on a silica gel column using a gradient of methanol/dichloromethane (1: 9) as eluent to give 2.2 g (69 %) of 1'-benzyl-3*H*-spiro[isobenzofuran-1,4'-piperidine] as a white solid that was analyzed by the Mass Spectrometer and directly used in the next step without further characterization. MS (EI) m/z 280.79 $[M+1]^+$.

3*H*-spiro[isobenzofuran-1,4'-piperidine]. 480 (WA201) To a suspension of 0.17 g of 10% Pd/C in water/acetic acid (6: 4, 100 mL), and 2 mL of conc. HCl was added (1.7 g, 6 mmol) of 1'-benzyl-3*H*-spiro[isobenzofuran-1,4'-piperidine]. The mixture was hydrogenated at 45 (psi) for 5 h. Filtration, extraction with DCM, drying and evaporation of the filtrate gave clear oil, which triturated with ether to yield pure compound, 0.8 g (60%) of 3*H*-spiro[isobenzofuran-1,4'-piperidine] as a white solid. MS (EI) m/z 204.56 [M+23]⁺. ¹H NMR (400 MHz, DMSO-*d*₆) δ 9.39 (d, J = 31.4 Hz, 1H), 7.31 (d, J = 2.8 Hz, 3H), 7.15 (dd, J = 5.4, 2.6 Hz, 1H), 5.01 (s, 2H), 3.30 – 3.21 (m, 2H), 3.05 (s, 2H), 2.24 (td, J = 13.8, 4.6 Hz, 2H), 1.75 (d, J = 14.0 Hz, 2H). ¹³C NMR (101 MHz, DMSO) δ 144.45, 138.98, 128.51, 128.03, 121.97, 120.89, 82.53, 70.89, 40.69, 32.77.

9.6.2 Synthesis of 3*H*-spiro[isobenzofuran-1,4'-piperidine] (Second route)

1'-benzyl-3*H*-spiro[isobenzofuran-1,4'-piperidin]-3-one. 478 (WA281) A solution of 2-bromobenzoic acid (**481**) (20.00 g, 0.1 mol) in THF (200 mL) was treated dropwise with n-BuLi (2.5 M, 80 mL) at -78°C. The mixture was stirred at this temperature for 40 min, followed by dropwise addition of a solution of N-benzylpiperidine-4-one (**476**) (26 g, 137 mmol) in THF (100 mL). The resulting mixture was stirred at -78°C for 30 min, and was then allowed to warm up to room temperature and stirred overnight. The reaction was quenched with water (100 mL) and the resulting mixture was washed with ether (100 mL). The aqueous layer was refluxed for 1 h and then acidified to pH 2.5. The mixture was extracted with CHCl₃ (3x), the combined organic layers were washed with brine, dried over magnesium sulfate and concentrated to dryness to obtain 8 g of 1'-benzyl-3*H*-spiro[isobenzofuran-1,4'-piperidin]-3-one as yellow oil that was used

in the next step without further purification .

1'-benzyl-3*H*-spiro[isobenzofuran-1,4'-piperidine]. 479 (WA282) Under argon atmosphere 8 g (30 mmol) of 1'-benzyl-3*H*-spiro[isobenzofuran-1,4'-piperidin]-3-one were suspended in freshly distilled THF (70 mL), the reaction mixture cooled at 0 °C and under vigorously stirring (CH₃)₂S * BH₃ (5.70 mL, 60 mmol) was added drop wise. The reaction mixture was heated at reflux overnight. After this time the reaction was acidified (HCl 10%) until pH 2 and heated again at reflux for 4 h. The reaction was quenched with NaOH 2 N until pH 12, the THF was removed in vacuo and the aqueous layer extracted with ethyl acetate (3x). The organic layer was washed with brine, dried over magnesium sulfate, concentrated in vacuo and purified by column chromatography using ethyl acetate/hexane as an eluent to afford 6 g of 1'-benzyl-3*H*-spiro[isobenzofuran-1,4'-piperidine] as a white solid in 78% yield. MS (EI) m/z 280.58 (M⁺+1). ¹H NMR (400 MHz, Chloroform-*d*) δ 7.40 – 7.30 (m, 4H), 7.30 – 7.24 (m, 3H), 7.22 – 7.14 (m, 2H), 3.63 (s, 2H), 2.96 – 2.84 (m, 4H), 2.47 (td, *J* = 12.1, 2.6 Hz, 2H), 2.03 (td, *J* = 13.2, 4.6 Hz, 2H), 1.77 (dd, *J* = 14.2, 2.5 Hz, 2H). ¹³C NMR (101 MHz, CDCl₃) δ 145.67, 138.91, 138.03, 129.41, 128.24, 127.54, 127.32, 127.10, 121.03, 120.82, 84.67, 70.72, 63.32, 50.07, 36.50.

3*H*-spiro[isobenzofuran-1,4'-piperidine]. 480 (WA290) To a solution of 1'-benzyl-3*H*-spiro[isobenzofuran-1,4'-piperidin] (6 g, 21.5 mmol) in dichloromethane (30 mL) was added dropwise 1-chloroethyl chloroformate (3 g, 20.9 mmol). The mixture was stirred at 25°C for 5 h and then was concentrated to dryness under reduced pressure. The residue was dissolved in methanol and the mixture was heated to reflux for 35 min. The mixture was concentrated to dryness and ether was added. The precipitated solid was collected by filtration and washed with ether, dried in air to obtain 4 g of 3*H*-spiro[isobenzofuran-1,4'-piperidine] as a white solid (HCl

salt) in 83% yield. MS (EI) m/z 190.53 (M^{+1}). ^1H NMR (400 MHz, $\text{DMSO-}d_6$) δ 9.43 (s, 1H), 9.35 (s, 1H), 7.31 (d, $J = 2.8$ Hz, 3H), 7.15 (dd, $J = 5.4, 2.6$ Hz, 1H), 5.01 (s, 2H), 3.30 – 3.21 (m, 2H), 3.05 (s, 2H), 2.24 (td, $J = 13.8, 4.6$ Hz, 2H), 1.75 (d, $J = 14.0$ Hz, 2H). ^{13}C NMR (101 MHz, DMSO) δ 144.45, 138.98, 128.51, 128.03, 121.97, 120.89, 82.53, 70.89, 40.69, 40.59, 40.38, 40.17, 39.97, 39.76, 39.55, 39.34, 32.77.

9.6.3 Synthesis of 2'-methyl-3H-spiro[isobenzofuran-1,4'-piperidine] (WA469)

***tert*-butyl-2'-methyl-3-oxo-3H-spiro[isobenzofuran-1,4'-piperidine]-1'-carboxylate. (485, WA460)** To a solution of bromobenzoic acid (1 g, 4.97 mmol) in freshly distilled THF (5 mL) at -20°C was added BuMgCl (2.249 mL, 2M, 4.50 mmol), followed by slowly addition of $n\text{-BuLi}$ (2.65 mL, 2.5M). The reaction mixture was then stirred for 40 min at -10°C and added (1g, 4.75 mmol) of *tert*-butyl 2-methyl-4-oxopiperidine-1-carboxylate in 1.5 mL THF dropwise over 20 min. After stirring at -5°C for 1 h, acetic acid (1.5 mL) and water (3 mL) were added, and the reaction mixture was then heated at 40°C for 18 h, and then extracted with methyl *tert*-butyl ether (3x), and the combined organic layer were washed with NaOH (1N, 50mL), saturated solution of K_2CO_3 , brine, dried over magnesium sulfate, and concentrated. The residue was treated with hexane to give a white precipitate of *tert*-butyl-2'-methyl-3-oxo-3H-spiro[isobenzofuran-1,4'-piperidine]-1'-carboxylate that was filtered and dried (0.6g). MS (EI) m/z 340.52 [$M+1$] $^+$. ^1H NMR (400 MHz, $\text{DMSO-}d_6$) δ 7.80 (dd, $J = 22.1, 5.9$ Hz, 3H), 7.59 (dt, $J = 8.4, 4.2$ Hz, 1H), 4.43 (s, 1H), 3.98 (s, 1H), 3.14 (s, 1H), 2.37 (dd, $J = 14.9, 6.7$ Hz, 1H), 2.12 (td, $J = 13.8, 5.1$ Hz, 1H), 1.60 (t, $J = 13.2$ Hz, 2H), 1.43 (s, 9H), 1.27 (d, $J = 7.0$ Hz, 3H). ^{13}C NMR (101 MHz, DMSO) δ 169.18, 154.24, 135.03, 129.98, 125.53, 125.02, 122.58, 85.19, 79.36, 38.98, 35.29, 35.26, 28.56, 20.23, 18.06.

2'-methyl-3H-spiro[isobenzofuran-1,4'-piperidin]-3-one. 486 (WA461) A solution of *tert*-

butyl-2'-methyl-3-oxo-3*H*-spiro[isobenzofuran-1,4'-piperidine]-1'-carboxylate (600 mg, 1.9 mmol) in DCM (5 mL) was treated with TFA (10 mL) for 2 h. The solvent was removed in vacuo and the crude was dissolved in Chloroform, washed with saturated NaHCO₃, brine, dried over anhydrous magnesium sulfate, filtered, concentrated, and purified by chromatography on a silica gel column using MeOH/DCM (1:9) as an eluent to provide 0.4 g of 2'-methyl-3*H*-spiro[isobenzofuran-1,4'-piperidin]-3-one as a white solid. MS (EI) *m/z* 218.54 (M⁺+1). [Salt] ¹H NMR (400 MHz, DMSO-*d*₆) δ 10.16 (s, 1H), 8.95 (s, 1H), 7.89 (dd, *J* = 11.2, 7.7 Hz, 2H), 7.83 (t, *J* = 7.5 Hz, 1H), 7.66 (t, *J* = 7.4 Hz, 1H), 3.83 (s, 1H), 3.48 – 3.37 (m, 2H), 2.26 (dd, *J* = 14.3, 4.2 Hz, 1H), 2.16 (t, *J* = 6.0 Hz, 2H), 2.03 (dd, *J* = 14.3, 8.3 Hz, 1H), 1.37 (d, *J* = 6.6 Hz, 3H). [Free base] ¹H NMR (400 MHz, Methanol-*d*₄) δ 7.89 (d, *J* = 7.6 Hz, 1H), 7.82 (d, *J* = 4.2 Hz, 2H), 7.65 (dq, *J* = 9.0, 5.1, 4.6 Hz, 1H), 3.98 (h, *J* = 6.6 Hz, 1H), 3.63 (ddd, *J* = 13.0, 8.1, 4.3 Hz, 1H), 3.54 (ddd, *J* = 13.3, 7.6, 4.3 Hz, 1H), 2.44 (dd, *J* = 14.8, 4.7 Hz, 1H), 2.34 (ddd, *J* = 13.2, 8.3, 4.3 Hz, 1H), 2.27 – 2.15 (m, 1H), 2.09 (dd, *J* = 14.8, 6.8 Hz, 1H), 1.57 (d, *J* = 6.9 Hz, 3H). ¹³C NMR (101 MHz, MeOD) δ 169.05, 151.87, 134.76, 129.90, 125.65, 125.01, 121.82, 82.32, 48.31, 37.81, 37.53, 31.91, 16.42.

1'-benzyl-2'-methyl-3*H*-spiro[isobenzofuran-1,4'-piperidin]-3-one. 487 (WA462) To a solution of 2'-methyl-3*H*-spiro[isobenzofuran-1,4'-piperidin]-3-one (0.4 g, 1.97 mmol) in anhydrous DMF (5 mL) was added anhydrous K₂CO₃ (0.68g, 4.9 mmol) and benzylbromide (0.4 g, 2.34 mmol). The reaction mixture was stirred at 65°C for 1 h, cooled down and poured into water and extracted (4x) with ethyl acetate, washed with brine, dried over magnesium sulfate, and concentrated. The residue was purified by chromatography on a silica gel column using ethyl acetate/hexane (5:5) as an eluent to provide 0.35 g (58%) of 1'-benzyl-2'-methyl-3*H*-

spiro[isobenzofuran-1,4'-piperidin]-3-one as clear oil. MS (EI) m/z 308.55 ($M^+ + 1$). ^1H NMR (400 MHz, Methanol- d_4) δ 7.84 (dt, $J = 7.7, 1.0$ Hz, 1H), 7.72 (td, $J = 7.5, 1.2$ Hz, 1H), 7.63 (dt, $J = 7.8, 1.0$ Hz, 1H), 7.57 (td, $J = 7.5, 1.0$ Hz, 1H), 7.43 – 7.38 (m, 2H), 7.35 – 7.31 (m, 2H), 7.27 – 7.23 (m, 1H), 3.86 (d, $J = 13.2$ Hz, 1H), 3.66 (d, $J = 13.2$ Hz, 1H), 3.18 (dt, $J = 6.9, 5.0$ Hz, 1H), 2.93 (ddd, $J = 12.6, 9.3, 3.4$ Hz, 1H), 2.65 (ddd, $J = 12.5, 5.9, 4.3$ Hz, 1H), 2.29 – 2.22 (m, 1H), 2.10 – 2.00 (m, 1H), 1.77 (dddd, $J = 14.0, 11.9, 4.8, 2.1$ Hz, 2H), 1.28 (d, $J = 6.7$ Hz, 3H). ^{13}C NMR (101 MHz, MeOD) δ 170.10, 154.07, 138.36, 134.14, 129.12, 128.86, 127.97, 127.93, 126.85, 126.57, 125.22, 125.18, 121.88, 85.77, 57.88, 51.54, 48.26, 48.05, 47.84, 47.63, 47.41, 47.20, 46.99, 43.37, 41.26, 35.26, 13.62.

1'-benzyl-2'-methyl-3*H*-spiro[isobenzofuran-1,4'-piperidine]. 488 (WA463) Under argon atmosphere 0.335 g (1.08 mmol) of 1'-benzyl-2'-methyl-3*H*-spiro[isobenzofuran-1,4'-piperidin]-3-one were suspended in freshly distilled THF (70 mL), the reaction mixture cooled at 0 °C and under vigorously stirring $(\text{CH}_3)_2\text{S} \cdot \text{BH}_3$ (5.70 mL, 60 mmol) was added drop wise. The reaction mixture was heated at reflux overnight. After this time the reaction was acidified (HCl 10%) until pH 2 and heated again at reflux for 4 h. The reaction was quenched with NaOH 2 N until pH 12, the THF was removed in vacuo and the aqueous layer extracted with ethyl acetate (3x). The organic layer was washed with brine, dried over magnesium sulfate, concentrated in vacuo and purified by column chromatography using methanol/DCM (1:9) as an eluent to afford 0.23 g of 1'-benzyl-2'-methyl-3*H*-spiro[isobenzofuran-1,4'-piperidine] as clear oil in 76.6% yield. MS (EI) m/z 294.61 ($M^+ + 1$). ^1H NMR (400 MHz, Methanol- d_4) δ 7.45 – 7.37 (m, 2H), 7.36 – 7.30 (m, 2H), 7.29 – 7.17 (m, 5H), 5.00 (s, 1H), 4.88 (s, 1H), 3.88 (d, $J = 13.1$ Hz, 1H), 3.60 (d, $J = 13.1$ Hz, 1H), 3.06 (td, $J = 6.6, 4.6$ Hz, 1H), 2.88 (ddd, $J = 12.2, 8.2, 3.7$ Hz, 1H), 2.57 (ddd, $J =$

12.0, 7.3, 4.1 Hz, 1H), 2.04 (ddd, $J = 13.6, 4.7, 1.5$ Hz, 1H), 1.89 (dddd, $J = 12.4, 8.3, 4.2, 1.4$ Hz, 1H), 1.83 – 1.69 (m, 2H), 1.27 (d, $J = 6.5$ Hz, 3H). ^{13}C NMR (101 MHz, MeOD) δ 145.58, 139.16, 137.98, 129.17, 127.90, 127.24, 126.84, 126.75, 121.10, 120.76, 85.23, 69.96, 57.86, 52.22, 48.24, 48.03, 47.81, 47.60, 47.39, 47.18, 46.96, 44.50, 42.54, 35.91, 14.93.

2'-methyl-3*H*-spiro[isobenzofuran-1,4'-piperidine]. 489 (WA469) To a solution of 1'-benzyl-2'-methyl-3*H*-spiro[isobenzofuran-1,4'-piperidine] (0.23 g, 0.785 mmol) in methanol (30 ml) was hydrogenated in the Parr apparatus (40 psi) in the presence of 10% palladium on charcoal (0.035 g) for 16 h. Filtration of the catalyst, concentrated and washed with ether, dried in air to afford 0.14 g (88%) of 2'-methyl-3*H*-spiro [isobenzofuran-1,4'-piperidine] as clear oil. MS (EI) m/z 204.47 ($\text{M}^+ + 1$). ^1H NMR (400 MHz, Methanol- d_4) δ 7.53 – 7.43 (m, 1H), 7.33 – 7.22 (m, 3H), 5.02 (d, $J = 9.0$ Hz, 2H), 3.14 (tdd, $J = 17.5, 9.7, 4.7$ Hz, 2H), 2.42 (s, 1H), 2.03 – 1.84 (m, 4H), 1.61 (dd, $J = 13.3, 9.8$ Hz, 1H), 1.24 – 1.17 (m, 3H). ^{13}C NMR (101 MHz, MeOD) δ 144.89, 139.36, 127.48, 126.84, 121.35, 121.04, 84.98, 69.95, 48.07, 43.45, 40.34, 36.00, 19.98.

9.6.4 Synthesis of spiro[isochromane-1,4'-piperidine] (493)

1-benzyl-4-(2-(2-hydroxyethyl)phenyl)piperidin-4-ol. 491 (WA485a) To a solution of 2-bromophenyl ethyl alcohol (6g, 30 mmol) in freshly distilled THF (75 mL) was added 1.6M *n*-butyl lithium solution in *n*-hexane (49 ml, 70 mmol) at - 60° C. After stirring for 30 min a solution of 1-benzyl-4-piperidone (7.8 g, 41.24 mmol) in THF (30 ml) was added over a period of 20 min at - 40° C. The cooling bath was removed and the reaction mixture was stirred for 72 h at room temperature. The mixture was quenched with saturated aqueous ammonium chloride solution (75 ml). Basification to pH 11 with 2 M aqueous sodium carbonate solution, followed by extraction (3x) with tert-butyl methyl ether. The combined organic layers were dried over

anhydrous magnesium sulfate and concentrated in *vacuo*. The residue was purified by chromatography on a silica gel column using methanol/DCM (2:8) as an eluent to provide 4.0 g (43%) of 1-benzyl-4-(2-(2-hydroxyethyl)phenyl)piperidin-4-ol as brown oil. MS (EI) m/z 312.51 ($M^+ + 1$). ^1H NMR (400 MHz, $\text{DMSO-}d_6$) δ 7.37 (dd, $J = 7.2, 2.1$ Hz, 1H), 7.32 (d, $J = 4.4$ Hz, 4H), 7.24 (ddt, $J = 8.7, 6.2, 3.6$ Hz, 1H), 7.20 – 7.07 (m, 3H), 4.76 (d, $J = 17.8$ Hz, 2H), 3.60 (t, $J = 7.4$ Hz, 2H), 3.50 (s, 2H), 3.37 (s, 2H), 3.14 (t, $J = 7.4$ Hz, 2H), 2.61 (d, $J = 10.4$ Hz, 2H), 1.98 (td, $J = 12.7, 4.3$ Hz, 2H), 1.79 (d, $J = 12.8$ Hz, 2H). ^{13}C NMR (101 MHz, DMSO) δ 147.31, 139.10, 138.34, 132.37, 129.32, 128.54, 127.21, 126.78, 125.90, 125.70, 71.00, 63.69, 62.84, 49.41, 37.96, 37.35.

1'-Benzyl-3,4-dihydrospiro[isochromene-1,4'-piperidine]. 492 (WA485b) To a solution of 1-benzyl-4-(2-(2-hydroxyethyl)phenyl)piperidin-4-ol (4g, 12.8 mmol) and triethylamine (4 mL, 28 mmol) in freshly distilled THF (100 mL) was added methanesulfonyl chloride (0.96 g, 12.6 mmol) at 0 C for a period of 10 min and then warmed up to room temperature for 15 min. The reaction mixture was then refluxed for 5 h, after that was cooled down and quenched with water and basified with 1M aqueous NaOH solution, followed by extraction (3x) with ethyl acetate. The combined organic layers were dried over anhydrous magnesium sulfate and concentrated in *vacuo*. The residue was purified by chromatography on a silica gel column using ethyl acetate/hexane (3:7) as an eluent to provide 1.6 g (42%) of 1'-Benzyl-3,4-dihydrospiro[isochromene-1,4'-piperidine] as yellow oil. MS (EI) m/z 294.48 ($M^+ + 1$). ^1H NMR (400 MHz, Methanol- d_4) δ 7.40 – 7.21 (m, 5H), 7.20 – 7.12 (m, 2H), 7.12 – 7.02 (m, 2H), 3.85 (t, $J = 5.5$ Hz, 2H), 3.57 (s, 2H), 2.80 – 2.68 (m, 4H), 2.53 – 2.41 (m, 2H), 2.03 (td, $J = 13.4, 4.5$ Hz, 2H), 1.83 (dd, $J = 14.4, 2.5$ Hz, 2H). ^{13}C NMR (101 MHz, MeOD) δ 141.53, 136.96, 133.56, 129.56, 128.45, 127.94, 127.09, 125.89, 125.87, 124.92, 72.70, 62.94, 58.40, 48.80, 35.94, 29.21.

3,4-dihydrospiro[isochromane-1,4'-piperidine]. 493 (WA485c) To a solution of 1'-Benzyl-3,4-dihydrospiro[isochromene-1,4'-piperidine] (1g, 3.4 mmol) in methanol (100 mL) was hydrogenated in the Parr apparatus (45 psi) in the presence of 10% palladium on charcoal (0.1 g) for 72 h. Filtration of the catalyst, concentrated and washed with ether, dried in air to afford 0.45 g (65%) of spiro[isochromane-1,4'-piperidine] as clear oil. MS (EI) m/z 204.53 ($M^+ + 1$) ^1H NMR (400 MHz, Methanol- d_4) δ 7.20 (d, $J = 4.1$ Hz, 2H), 7.14 (dt, $J = 13.6, 7.5$ Hz, 2H), 3.91 (t, $J = 5.5$ Hz, 2H), 3.20 (td, $J = 12.7, 2.9$ Hz, 2H), 3.08 (dd, $J = 12.6, 4.5$ Hz, 2H), 2.81 (t, $J = 5.5$ Hz, 2H), 2.09 (td, $J = 13.7, 4.7$ Hz, 2H), 1.94 (dd, $J = 14.9, 2.6$ Hz, 2H). ^{13}C NMR (101 MHz, MeOD) δ 140.71, 133.45, 128.61, 126.22, 126.05, 124.82, 72.05, 58.81, 40.61, 34.73, 29.06.

9.7 Synthesis of Spiro[isochromane-1,4'-piperidine] derivatives

1-methyl-3-(4-(spiro[isochromane-1,4'-piperidin]-1'-yl)butyl)-1,3-dihydro-2H-

benzo[d]imidazol-2-one. 435 (WA514) To a solution of 1-(4-bromobutyl)-3-methyl-1,3-dihydro-2H-benzo[d]imidazol-2-one (WA318) (0.03 g, 0.106 mmol) in 4 mL DMF were added (0.044 g, 0.3188 mmol) of potassium carbonate and (0.03 g, 0.1251 mmol) of spiro[isochromane-1,4'-piperidine]-HCl, and the reaction mixture heated at 65 °C for 2 h, then the mixture extracted with ethyl acetate and water, washed with brine, dried over MgSO_4 and the solvent evaporated using *vacuu* then purified by column chromatography (EtOAc: Hexane) to obtain 0.03 g of 1-methyl-3-(4-(spiro[isochromane-1,4'-piperidin]-1'-yl)butyl)-1,3-dihydro-2H-benzo[d]imidazol-2-one as yellow oil in 70% yield. MS (ESI) m/z 406.48 [$M^+ + 1$]. ^1H NMR (400 MHz, Chloroform- d) δ 10.38 (s, 1H), 7.25 – 7.03 (m, 6H), 6.97 (ddd, $J = 13.2, 5.8, 3.2$ Hz, 2H), 3.87 (dt, $J = 20.7, 5.7$ Hz, 4H), 3.39 (d, $J = 1.7$ Hz, 3H), 3.19 – 3.10 (m, 2H), 2.91 – 2.75 (m,

6H), 2.41 (td, $J = 13.8, 4.2$ Hz, 2H), 1.92 (d, $J = 14.3$ Hz, 2H), 1.80 (tt, $J = 10.6, 5.9$ Hz, 4H). ^{13}C NMR (101 MHz, CDCl_3) δ 154.43, 140.09, 133.39, 130.00, 129.02, 128.73, 126.62, 126.57, 125.52, 121.32, 121.26, 107.54, 107.51, 71.74, 59.18, 56.84, 48.58, 40.24, 34.61, 29.44, 27.12, 25.99, 21.84.

3-(4-(spiro[isochromane-1,4'-piperidin]-1'-yl)butyl)benzo[*d*]oxazol-2(3*H*)-one. 436 (WA515)

To a solution of 3-(4-bromobutyl)benzo[*d*]oxazol-2(3*H*)-one (WA479) (0.03 g, 0.11 mmol) in 4 mL DMF were added (0.046 g, 0.33 mmol) of potassium carbonate and (0.032 g, 0.1334 mmol) of spiro[isochromane-1,4'-piperidine]-HCl, and the reaction mixture heated at 65 °C for 2 h, then the mixture extracted with ethyl acetate and water, washed with brine, dried over MgSO_4 and the solvent evaporated using *vacuu* then purified by column chromatography (EtOAc: Hexane) to obtain 0.025 g of 3-(4-(spiro[isochromane-1,4'-piperidin]-1'-yl)butyl)benzo[*d*]oxazol-2(3*H*)-one as yellow oil in 58% yield. MS (ESI) m/z 393.51 [$\text{M}^+ + 1$]. ^1H NMR (400 MHz, Chloroform-*d*) δ 7.24 – 7.01 (m, 8H), 3.93 – 3.84 (m, 4H), 2.83 (t, $J = 5.5$ Hz, 4H), 2.63 – 2.43 (m, 4H), 2.14 (s, 2H), 1.96 – 1.83 (m, 4H), 1.71 (q, $J = 7.6$ Hz, 2H). ^{13}C NMR (101 MHz, CDCl_3) δ 154.61, 142.71, 133.69, 131.10, 128.78, 126.30, 126.21, 125.45, 123.79, 122.37, 110.07, 108.30, 72.81, 58.83, 57.80, 49.25, 42.01, 36.41, 29.62, 25.74, 23.69.

5-fluoro-3-methyl-1-(4-(spiro[isochromane-1,4'-piperidin]-1'-yl)butyl)-1,3-dihydro-2*H*-

benzo[*d*]imidazol-2-one. 437 (WA516) To a solution of 1-(4-bromobutyl)-5-fluoro-3-methyl-1,3-dihydro-2*H*-benzo[*d*]imidazol-2-one (WA377) (0.03 g, 0.0996 mmol) in 4 mL DMF were added (0.041 g, 0.30 mmol) of potassium carbonate and (0.0286 g, 0.1195 mmol) of spiro[isochromane-1,4'-piperidine]-HCl, and the reaction mixture heated at 65 °C for 3 h, then the mixture extracted with ethyl acetate and water, washed with brine, dried over MgSO_4 and the

solvent evaporated using *vacuu* then purified by column chromatography (EtOAc: Hexane) to obtain 0.02 g of 5-fluoro-3-methyl-1-(4-(spiro[isochromane-1,4'-piperidin]-1'-yl)butyl)-1,3-dihydro-2*H*-benzo[*d*]imidazol-2-one as yellow oil in 48% yield. MS (ESI) *m/z* 424.44 [$M^+ + 1$]. ^1H NMR (400 MHz, Chloroform-*d*) δ 7.26 – 7.05 (m, 4H), 6.92 (ddd, $J = 7.8, 5.0, 2.7$ Hz, 1H), 6.87 – 6.70 (m, 2H), 4.03 – 3.83 (m, 4H), 3.45 – 3.37 (m, 3H), 2.98 (d, $J = 8.0$ Hz, 2H), 2.83 (q, $J = 4.7$ Hz, 2H), 2.29 (s, 2H), 2.10 – 1.66 (m, 7H), 1.26 (s, 2H), 0.87 (s, 1H). ^{13}C NMR (101 MHz, CDCl_3) δ 159.88, 157.52, 154.73, 133.54, 130.62, 128.75, 126.49, 126.40, 125.51, 125.26, 107.76, 107.66, 107.59, 107.35, 96.10, 95.82, 72.34, 59.01, 57.53, 49.05, 40.69, 35.61, 29.55, 27.30, 26.18, 22.95.

5-fluoro-1-methyl-3-(4-(spiro[isochromane-1,4'-piperidin]-1'-yl)butyl)-1,3-dihydro-2*H*-

benzo[*d*]imidazol-2-one. 438 (WA517) To a solution of 3-(4-bromobutyl)-5-fluoro-1-methyl-1,3-dihydro-2*H*-benzo[*d*]imidazol-2-one. (WA427) (0.03 g, 0.0996 mmol) in 3 mL DMF were added (0.041 g, 0.30 mmol) of potassium carbonate and (0.0286 g, 0.1195 mmol) of spiro[isochromane-1,4'-piperidine]-HCl, and the reaction mixture heated at 65 °C for 3 h, then the mixture extracted with ethyl acetate and water, washed with brine, dried over MgSO_4 and the solvent evaporated using *vacuu* then purified by column chromatography (EtOAc: Hexane) to obtain 0.025 g of 5-fluoro-1-methyl-3-(4-(spiro[isochromane-1,4'-piperidin]-1'-yl)butyl)-1,3-dihydro-2*H*-benzo[*d*]imidazol-2-one as yellow oil in 59% yield. MS (ESI) *m/z* 424.51 [$M^+ + 1$]. ^1H NMR (400 MHz, Chloroform-*d*) δ 7.21 – 7.10 (m, 3H), 7.07 (d, $J = 7.5$ Hz, 1H), 6.88 – 6.77 (m, 3H), 3.93 – 3.87 (m, 4H), 3.40 (s, 3H), 2.86 – 2.74 (m, 4H), 2.52 – 2.37 (m, 4H), 2.11 – 2.00 (m, 2H), 1.89 (dd, $J = 14.3, 2.5$ Hz, 2H), 1.85 – 1.77 (m, 2H), 1.67 – 1.58 (m, 2H). ^{13}C NMR (101 MHz, CDCl_3) δ 159.88, 157.52, 154.68, 141.83, 133.70, 129.96, 129.84, 128.75, 126.23, 126.19, 126.10, 125.43, 107.51, 107.41, 107.38, 107.14, 96.21, 95.93, 73.00, 58.74, 57.92, 49.17,

41.08, 36.60, 29.65, 27.19, 26.19, 23.92.

1-methyl-3-(4-(spiro[isochromane-1,4'-piperidin]-1'-yl)pentyl)-1,3-dihydro-2H-

benzo[d]imidazol-2-one. 439 (WA518) To a solution of 1-(4-bromopentyl)-3-methyl-1,3-dihydro-2H-benzo[d]imidazol-2-one. (WA477) (0.03 g, 0.1 mmol) in 3 mL DMF were added (0.042 g, 0.30 mmol) of potassium carbonate and (0.0286 g, 0.1209 mmol) of spiro[isochromane-1,4'-piperidine]-HCl, and the reaction mixture heated at 65 °C for 3 h, then the mixture extracted with ethyl acetate and water, washed with brine, dried over MgSO₄ and the solvent evaporated using *vacuo* then purified by column chromatography (EtOAc: Hexane) to obtain 0.028 g of 1-methyl-3-(4-(spiro[isochromane-1,4'-piperidin]-1'-yl)pentyl)-1,3-dihydro-2H-benzo[d]imidazol-2-one as yellow oil in 67% yield. MS (ESI) *m/z* 420.49 [M⁺+1]. ¹H NMR (400 MHz, Chloroform-*d*) δ 7.26 – 6.97 (m, 8H), 4.00 – 3.85 (m, 4H), 3.43 (s, 2H), 2.83 (q, *J* = 5.7, 5.3 Hz, 5H), 2.72 (s, 1H), 2.58 (t, *J* = 12.3 Hz, 1H), 2.45 (s, 1H), 2.31 – 2.12 (m, 2H), 2.00 – 1.78 (m, 5H), 1.31 – 1.22 (m, 2H), 1.12 (s, 2H). ¹³C NMR (101 MHz, CDCl₃) δ 154.40, 133.67, 130.09, 128.78, 128.70, 126.39, 126.27, 125.67, 125.44, 121.17, 121.08, 107.59, 107.41, 72.13, 58.89, 51.18, 46.35, 42.05, 41.07, 36.23, 29.60, 27.11, 25.69, 13.77.

5-fluoro-1-methyl-3-(4-(spiro[isochromane-1,4'-piperidin]-1'-yl)pentyl)-1,3-dihydro-2H-

benzo[d]imidazol-2-one. 440 (WA519) To a solution of 3-(4-bromopentyl)-5-fluoro-1-methyl-1,3-dihydro-2H-benzo[d]imidazol-2-one. (WA489) (0.03 g, 0.0951 mmol) in 3 mL DMF were added (0.039 g, 0.2826 mmol) of potassium carbonate and (0.027 g, 0.1126 mmol) of spiro[isochromane-1,4'-piperidine]-HCl, and the reaction mixture heated at 65 °C for 4 h, then the mixture extracted with ethyl acetate and water, washed with brine, dried over MgSO₄ and the

solvent evaporated using *vacuu* then purified by column chromatography (EtOAc: Hexane) to obtain 0.02 g of 5-fluoro-1-methyl-3-(4-(spiro[isochromane-1,4'-piperidin]-1'-yl)pentyl)-1,3-dihydro-2*H*-benzo[*d*]imidazol-2-one as yellow oil in 49% yield. MS (ESI) *m/z* 438.52 [M^+ +1]. ¹H NMR (400 MHz, Chloroform-*d*) δ 7.33 (d, *J* = 7.8 Hz, 1H), 7.24 – 7.05 (m, 3H), 6.88 (dd, *J* = 9.0, 4.4 Hz, 1H), 6.81 (ddd, *J* = 9.0, 6.7, 2.5 Hz, 2H), 3.98 – 3.82 (m, 4H), 3.40 (s, 5H), 3.38 – 3.22 (m, 4H), 2.90 – 2.72 (m, 4H), 2.04 (d, *J* = 14.8 Hz, 2H), 1.39 (d, *J* = 6.5 Hz, 3H), 1.31 (s, 1H), 1.25 (s, 2H). ¹³C NMR (101 MHz, CDCl₃) δ 159.97, 157.60, 154.72, 138.74, 133.12, 128.69, 127.06, 126.97, 126.14, 125.78, 107.88, 107.61, 96.20, 95.91, 77.37, 77.12, 71.22, 61.57, 59.57, 45.82, 43.85, 40.60, 33.68, 29.36, 28.15, 27.27, 25.14, 13.50.

3-(4-(spiro[isochromane-1,4'-piperidin]-1'-yl)butyl)benzo[*d*]thiazol-2(3*H*)-one. 441

(WA520) To a solution of 3-(4-bromobutyl)benzo[*d*]thiazol-2(3*H*)-one (WA480) (0.03 g, 0.1048 mmol) in 3 mL DMF were added (0.044 g, 0.3188 mmol) of potassium carbonate and (0.03 g, 0.1251 mmol) of spiro[isochromane-1,4'-piperidine]-HCl, and the reaction mixture heated at 65 °C for 3 h, then the mixture extracted with ethyl acetate and water, washed with brine, dried over MgSO₄ and the solvent evaporated using *vacuu* then purified by column chromatography (EtOAc: Hexane) to obtain 0.023 g of 3-(4-(spiro[isochromane-1,4'-piperidin]-1'-yl)butyl)benzo[*d*]thiazol-2(3*H*)-one as yellow oil in 55% yield. MS (ESI) *m/z* 409.53 [M^+ +1]. ¹H NMR (400 MHz, Chloroform-*d*) δ 7.42 (d, *J* = 7.7 Hz, 1H), 7.33 (t, *J* = 7.8 Hz, 1H), 7.15 (ddt, *J* = 29.3, 18.5, 8.6 Hz, 6H), 4.00 (t, *J* = 7.1 Hz, 2H), 3.88 (t, *J* = 5.5 Hz, 2H), 2.99 – 2.75 (m, 4H), 2.59 (q, *J* = 13.0, 10.0 Hz, 4H), 2.21 (t, *J* = 13.5 Hz, 2H), 1.92 (d, *J* = 13.8 Hz, 2H), 1.84 (q, *J* = 7.3 Hz, 2H), 1.78 – 1.69 (m, 2H). ¹³C NMR (101 MHz, CDCl₃) δ 169.95, 141.24, 136.98, 133.63, 128.78, 126.38, 126.34, 126.29, 125.47, 123.08, 122.78, 122.68, 110.65, 72.60,

58.90, 57.71, 49.22, 42.31, 36.10, 29.59, 25.46, 23.36.

5-fluoro-3-methyl-1-(4-(spiro[isochromane-1,4'-piperidin]-1'-yl)pentyl)-1,3-dihydro-2H-

benzo[*d*]imidazol-2-one. 442 (WA522) To a solution of 1-(4-bromopentyl)-5-fluoro-3-methyl-1,3-dihydro-2H-benzo[*d*]imidazol-2-one (WA488) (0.03 g, 0.0942 mmol) in 3 mL DMF were added (0.039 g, 0.2826 mmol) of potassium carbonate and (0.027 g, 0.1126 mmol) of spiro[isochromane-1,4'-piperidine]-HCl, and the reaction mixture heated at 65 °C for 4 h, then the mixture extracted with ethyl acetate and water, washed with brine, dried over magnesium sulfate and the solvent evaporated using *vacuo* then purified by column chromatography (EtOAc: Hexane) to obtain 0.018 g of 3-(4-(spiro[isochromane-1,4'-piperidin]-1'-yl)butyl)benzo[*d*]thiazol-2(3*H*)-one as yellow oil in 43% yield. MS (ESI) *m/z* 438.45 [$M^+ + 1$]. ¹H NMR (400 MHz, Chloroform-*d*) δ 7.37 (d, *J* = 7.7 Hz, 1H), 7.18 (dt, *J* = 25.4, 7.4 Hz, 2H), 7.06 (d, *J* = 7.6 Hz, 1H), 6.94 (dd, *J* = 8.6, 4.3 Hz, 1H), 6.83 – 6.71 (m, 2H), 3.95 – 3.83 (m, 4H), 3.38 (s, 3H), 3.30 – 3.09 (m, 5H), 2.81 (t, *J* = 5.4 Hz, 4H), 2.21 (s, 1H), 2.00 (d, *J* = 14.6 Hz, 2H), 1.93 – 1.77 (m, 2H), 1.61 – 1.49 (m, 1H), 1.34 (d, *J* = 6.6 Hz, 3H). ¹³C NMR (101 MHz, CDCl₃) δ 159.93, 157.56, 154.68, 139.21, 133.16, 130.70, 130.58, 128.65, 126.94, 126.82, 125.87, 125.07, 107.87, 107.78, 107.55, 96.22, 95.93, 71.54, 61.24, 59.44, 46.10, 43.38, 40.65, 34.13, 34.02, 29.40, 28.56, 27.33, 25.34, 13.44.

9.8 Synthesis of CM304 derivatives

6-(2-chloroacetyl)benzo[*d*]thiazol-2(3*H*)-one. 443 (WA309) DMF (10 ml) was slowly added to AlCl₃ (44.1 g, 330.73 mmol) under vigorous stirring. The mixture was heated at 45⁰C and 2(3*H*)-benzothiazole (5 g, 33.07 mmol) was added. After 20 min chloroacetyl chloride (5.6 g,

49.58 mmol) was added and the reaction mixture was heated at 85⁰C for 3h. The hot mixture was then carefully poured onto ice and stirred for 30 min then the crude product was collected by filtration, washed with water and air-dried. The solid was crystallized from ethanol to give 9 g of 6-(2-chloroacetyl)benzo[*d*]thiazol-2(3*H*)-one as a chocolate solid in 99% yield. MS (ESI) *m/z* 226.32 [M+1]⁺. H NMR (400 MHz, DMSO-*d*₆) δ 12.43 – 12.29 (m, 1H), 8.23 (s, 1H), 7.94 – 7.88 (m, 1H), 7.26 – 7.19 (m, 1H), 5.12 (s, 2H). ¹³C NMR (101 MHz, DMSO) δ 190.36, 170.81, 141.31, 129.34, 127.81, 124.33, 124.03, 111.82, 47.76.

6-(3-chloropropanoyl)benzo[*d*]thiazol-2(3*H*)-one. 444 (WA310) Anhydrous DMF (10 ml) was slowly added to AlCl₃ (52.91 g, 396.80 mmol) under vigorous stirring. The mixture was heated at 45⁰C and 2(3*H*)-benzothiazole (6 g, 39.68 mmol) was added. After 20 min chloropropionyl chloride (7.55 g, 59.46 mmol) was added and the reaction mixture was heated at 85⁰C for 3h. The hot mixture was then carefully poured onto ice and stirred for 30 min then the crude product was collected by filtration, washed with water and air-dried. The solid was crystallized from ethanol to give 8 g of 6-(3-chloropropanoyl)benzo[*d*]thiazol-2(3*H*)-one as a grey solid in 83% yield. MS (ESI) *m/z* 240.33 [M-1]⁺. ¹H NMR (400 MHz, DMSO-*d*₆) δ 12.28 (s, 1H), 8.24 (s, 1H), 7.89 (d, *J* = 8.6 Hz, 1H), 7.19 (d, *J* = 8.0 Hz, 1H), 3.95 – 3.87 (m, 2H), 3.57 – 3.45 (m, 2H). ¹³C NMR (101 MHz, DMSO) δ 195.58, 170.90, 141.01, 131.41, 127.40, 124.27, 123.77, 111.71, 40.88, 40.03.

6-(2-chloroethyl)benzo[*d*]thiazol-2(3*H*)-one. 445 (WA311) Triethylsilane (10.57 g, 90.90 mmol) was added to the stirred solution of 6-(2-chloroacetyl)benzo[*d*]thiazol-2(3*H*)-one (WA309)(9 g, 39.53 mmol) in (30 mL) trifluoroacetic acid. The mixture was vigorously stirred at room temperature for 16h, and then the mixture was evaporated over the *vacuu*. The residue

was purified by column chromatography using (3:7) ethyl acetate in hexanes to give 3.5 g 6-(2-chloroethyl)benzo[*d*]thiazol-2(3*H*)-one as a white solid in 41% yield. MS (ESI) *m/z* 212.30 [M-1]⁺. ¹H NMR (400 MHz, DMSO-*d*₆) δ 11.82 (s, 1H), 7.47 (s, 1H), 7.16 (s, 1H), 7.06 – 7.02 (m, 1H), 3.83 – 3.80 (m, 2H), 3.00 (s, 2H). ¹³C NMR (101 MHz, DMSO) δ 170.25, 135.26, 133.18, 127.64, 123.70, 123.26, 111.70, 45.91, 38.22.

6-(3-chloropropyl)benzo[*d*]thiazol-2(3*H*)-one. 446 (WA315) Triethylsilane (8.57 g, 71.29 mmol) was added to the stirred solution of 6-(3-chloropropanoyl)benzo[*d*]thiazol-2(3*H*)-one (WA310)(7.5 g, 31.03 mmol) in (30 mL) trifluoroacetic acid. The mixture was vigorously stirred at room temperature for 18h, and then the mixture was evaporated over the *vacuo*. The residue was purified by column chromatography using (3:7) ethyl acetate in hexanes to give 4.5 g 6-(3-chloropropyl)benzo[*d*]thiazol-2(3*H*)-one as a white solid in 41% yield. MS (ESI) *m/z* 226.32 [M-1]⁺. ¹H NMR (400 MHz, Methanol-*d*₄) δ 7.35 – 7.29 (m, 1H), 7.14 (dt, *J* = 7.6, 2.7 Hz, 1H), 7.06 (dd, *J* = 8.3, 5.0 Hz, 1H), 3.54 (q, *J* = 6.2 Hz, 2H), 2.78 (td, *J* = 7.6, 5.1 Hz, 2H), 2.12 – 1.99 (m, 2H).

3-(2-(azepan-1-yl)ethyl)-6-(3-chloropropyl)benzo[*d*]thiazol-2(3*H*)-one. 448 (WA323) 6-(3-chloropropyl)benzo[*d*]thiazol-2(3*H*)-one (WA315) (1 g, 4.39 mmol) was dissolved in 25 mL DMF and was added (4.35 g, 21.95 mmol) 1-(2-chloroethyl)azepane-HCl and heated at 120 °C. Then the (3.68 g, 43.81 mmol) sodium bicarbonate was added slowly and the reaction left at 120 °C for 30 min. The reaction mixture was cooled to room temperature and poured into water. It was extracted in ethyl acetate and the organic layer was washed with brine. The solvent was evaporated under reduced pressure and the product was purified by column chromatography over silica gel using ethyl acetate in hexanes to give 0.8 g of 3-(2-(azepan-1-yl)ethyl)-6-(3-

chloropropyl)benzo[*d*]thiazol-2(3*H*)-one as yellow oil in 51% yield. MS (ESI) *m/z* 353.59 [M+1]⁺. ¹H NMR (400 MHz, Methanol-*d*₄) δ 7.36 (d, *J* = 1.6 Hz, 1H), 7.21 – 7.14 (m, 2H), 4.04 (t, *J* = 7.1 Hz, 2H), 3.53 (t, *J* = 6.5 Hz, 2H), 2.78 (t, *J* = 6.9 Hz, 4H), 2.73 – 2.69 (m, 4H), 2.10 – 1.98 (m, 2H), 1.66 – 1.60 (m, 4H), 1.56 (d, *J* = 3.8 Hz, 4H). ¹³C NMR (101 MHz, MeOD) δ 170.26, 136.34, 135.34, 126.71, 122.36, 122.19, 110.85, 55.38, 54.37, 43.47, 40.38, 34.07, 31.94, 27.56, 26.54.

3-(2-(azepan-1-yl)ethyl)-6-(2-chloroethyl)benzo[*d*]thiazol-2(3*H*)-one. 447 (WA324) 6-(2-chloroethyl)benzo[*d*]thiazol-2(3*H*)-one (WA311) (1 g, 4.67 mmol) was dissolved in 25 mL DMF and was added (4.63 g, 23.36 mmol) 1-(2-chloroethyl)azepane-HCl and heated at 120 °C. Then the (3.93 g, 46.78 mmol) sodium bicarbonate was added slowly and the reaction left at 120 °C for 30 min. The reaction mixture was cooled to room temperature and poured into water. It was extracted in ethyl acetate and the organic layer was washed with brine. The solvent was evaporated over *vacuo* and the product was purified by column chromatography over silica gel using ethyl acetate in hexanes to give 1.3 g of 3-(2-(azepan-1-yl)ethyl)-6-(2-chloroethyl)benzo[*d*]thiazol-2(3*H*)-one as yellow oil in 82% yield. MS (ESI) *m/z* 339.49 [M+1]⁺. ¹H NMR (400 MHz, Methanol-*d*₄) δ 7.40 (dd, *J* = 5.7, 1.7 Hz, 1H), 7.30 – 7.14 (m, 2H), 4.03 (q, *J* = 6.4, 5.8 Hz, 2H), 3.73 (q, *J* = 6.4, 5.8 Hz, 2H), 3.06 (t, *J* = 6.9 Hz, 2H), 2.78 (t, *J* = 7.1 Hz, 2H), 2.71 (q, *J* = 5.3 Hz, 4H), 1.60 (dq, *J* = 18.9, 4.3, 3.8 Hz, 8H). ¹³C NMR (101 MHz, MeOD) δ 170.26, 135.80, 133.84, 127.14, 122.69, 122.31, 110.80, 55.38, 54.35, 44.57, 40.39, 38.16, 27.52, 26.54.

3-(2-(azepan-1-yl)ethyl)-6-(3-(methylthio)propyl)benzo[*d*]thiazol-2(3*H*)-one. 450 (WA325)
A mixture of 3-(2-(azepan-1-yl)ethyl)-6-(3-chloropropyl)benzo[*d*]thiazol-2(3*H*)-one

(WA323)(0.250 g, 0.7 mmol), and sodium thiomethoxide (0.300 g, 4.28 mmol), in ethanol (2 ml) was stirred at room temperature for 16 h. Then, the reaction mixture was poured into water and extracted with ethyl acetate (3x20 ml). The combined organic layers were washed with water (20 ml) and brine (20 ml), and then concentrated over vacuo. The residue was purified by column chromatography over silica gel using ethyl acetate in hexanes to afford 0.160 g of 3-(2-(azepan-1-yl)ethyl)-6-(3-(methylthio)propyl)benzo[*d*]thiazol-2(3*H*)-one as viscous oil, in 62 % yield. MS (ESI) *m/z* 365.55 [M+1]⁺. ¹H NMR (400 MHz, Methanol-*d*₄) δ 7.32 (s, 1H), 7.18 (s, 2H), 4.08 (t, *J* = 7.1 Hz, 2H), 2.90 – 2.81 (m, 6H), 2.70 (t, *J* = 7.6 Hz, 2H), 2.45 (t, *J* = 7.2 Hz, 2H), 2.04 (d, *J* = 2.7 Hz, 3H), 1.87 (q, *J* = 7.5 Hz, 2H), 1.67 – 1.63 (m, 4H), 1.58 (p, *J* = 3.1 Hz, 4H). ¹³C NMR (101 MHz, MeOD) δ 170.23, 137.28, 135.02, 126.77, 122.25, 122.21, 110.77, 55.34, 54.32, 39.95, 33.82, 32.92, 30.63, 26.97, 26.47, 14.08.

3-(2-(azepan-1-yl)ethyl)-6-(2-(methylthio)ethyl)benzo[*d*]thiazol-2(3*H*)-one. 449 (WA327) A mixture of 3-(2-(azepan-1-yl)ethyl)-6-(2-chloroethyl)benzo[*d*]thiazol-2(3*H*)-one (WA324)(0.5 g, 1.47 mmol), and sodium thiomethoxide (0.450 g, 6.42 mmol), in ethanol (5 ml) was stirred at room temperature for 18 h. Then, the reaction mixture was poured into water and extracted with ethyl acetate (3x25 ml). The combined organic layers were washed with water (25 ml) and brine (25 ml), and then concentrated over vacuo. The residue was purified by column chromatography over silica gel using ethyl acetate in hexanes to afford 0.45 g of 3-(2-(azepan-1-yl)ethyl)-6-(2-(methylthio)ethyl)benzo[*d*]thiazol-2(3*H*)-one as viscous oil, in 87 % yield. MS (ESI) *m/z* 351.55 [M+1]⁺. ¹H NMR (500 MHz, Methanol-*d*₄) δ 7.42 (d, *J* = 1.7 Hz, 1H), 7.29 – 7.15 (m, 2H), 4.08 (t, *J* = 7.1 Hz, 2H), 2.92 (dd, *J* = 8.6, 6.6 Hz, 2H), 2.83 (t, *J* = 7.1 Hz, 2H), 2.76 (dd, *J* = 10.4, 5.2

Hz, 6H), 2.11 (s, 3H), 1.69 – 1.57 (m, 8H). ¹³C NMR (126 MHz, MeOD) δ 170.42, 136.28, 135.42, 126.83, 122.34, 122.22, 110.77, 55.39, 54.37, 40.37, 35.40, 34.95, 27.52, 26.54, 14.12.

3-(2-(azepan-1-yl)ethyl)-6-(2-azidoethyl)benzo[*d*]thiazol-2(3*H*)-one. 453 (WA329) A solution of 3-(2-(azepan-1-yl)ethyl)-6-(2-chloroethyl)benzo[*d*]thiazol-2(3*H*)-one (WA324) (0.5 g, 1.47mmol) in 3 mL anhydrous DMF was added a solution of NaN₃ (0.192 g, 2.95 mmol) in 2 mL anhydrous DMF at room temperature. The mixture was stirred for 3 h, then was added a catalytic amount of potassium iodide and left until all the starting material had been consumed after 36 h, as observed by TLC. The reaction was quenched with water (50mL) and extracted with ethyl acetate (3x30mL), and washed with brine (50mL). The organic layer was dried over sodium sulfate, filtered, and the solvent removed over vacuo. The residue was purified by column chromatography over silica gel using ethyl acetate in hexanes to afford 0.4 g of 3-(2-(azepan-1-yl)ethyl)-6-(2-azidoethyl)benzo[*d*]thiazol-2(3*H*)-one as brown oil in 78 % yield. MS (ESI) *m/z* 346.62 [M+1]⁺. ¹H NMR (400 MHz, Methanol-*d*₄) δ 7.30 – 7.18 (m, 2H), 4.08 (t, *J* = 7.0 Hz, 2H), 3.53 (t, *J* = 6.9 Hz, 2H), 2.91 (t, *J* = 6.9 Hz, 2H), 2.85 – 2.77 (m, 2H), 2.77 – 2.69 (m, 4H), 1.67 – 1.55 (m, 8H). ¹³C NMR (101 MHz, MeOD) δ 170.38, 135.75, 134.00, 127.07, 122.61, 122.41, 110.91, 55.37, 54.34, 52.17, 40.37, 34.42, 27.52, 26.51.

6-(2-aminoethyl)-3-(2-(azepan-1-yl)ethyl)benzo[*d*]thiazol-2(3*H*)-one. 455 (WA343) To a solution of 3-(2-(azepan-1-yl)ethyl)-6-(2-azidoethyl)benzo[*d*]thiazol-2(3*H*)-one (WA329) (0.232 g, 0.67 mmol) in methanol (75 mL) was added to 10% Palladium on carbon catalyst (0.027 g) and stirred under a hydrogen atmosphere (30 psi) for 3 h. The mixture was filtered through celite and evaporated under *vacuo*. The residue was purified by column chromatography over silica gel using ethyl acetate in hexanes to afford 0.160 g of 6-(2-aminoethyl)-3-(2-(azepan-1-

yl)ethyl)benzo[*d*]thiazol-2(3*H*)-one as brown residue in 74% yield. MS (ESI) *m/z* 320.65 [M+1]⁺. ¹H NMR (400 MHz, Methanol-*d*₄) δ 7.39 (d, *J* = 1.7 Hz, 1H), 7.27 – 7.16 (m, 2H), 4.05 (t, *J* = 7.0 Hz, 2H), 2.95 – 2.85 (m, 2H), 2.79 (t, *J* = 7.1 Hz, 4H), 2.72 (t, *J* = 5.4 Hz, 4H), 1.63 – 1.54 (m, 8H). ¹³C NMR (101 MHz, MeOD) δ 170.30, 135.50, 134.93, 126.97, 122.47, 122.39, 110.92, 63.60, 55.37, 54.37, 42.65, 40.38, 27.55, 26.54.

3-(2-(azepan-1-yl)ethyl)-6-(3-azidopropyl)benzo[*d*]thiazol-2(3*H*)-one. 454 (WA345) A solution of 3-(2-(azepan-1-yl)ethyl)-6-(3-chloropropyl)benzo[*d*]thiazol-2(3*H*)-one (WA323) (0.69 g, 1.955 mmol) in 15 mL anhydrous acetonitrile was added a solution of NaN₃ (0.254 g, 3.9 mmol) in 5 mL anhydrous acetonitrile at room temperature. Then was added a catalytic amount of potassium iodide (33 mg) and heated at 75 °C until all the starting material had been consumed after 36 h, as observed by TLC. The reaction mixture was quenched with water (50mL) and extracted with ethyl acetate (3x30mL), and washed with brine (50mL). The organic layer was dried over sodium sulfate, filtered, and the solvent removed under vacuo. The residue was purified by column chromatography over silica gel using ethyl acetate in hexanes to afford 0.45 g of 3-(2-(azepan-1-yl)ethyl)-6-(3-azidopropyl)benzo[*d*]thiazol-2(3*H*)-one as brown oil in 64 % yield. MS (ESI) *m/z* 360.69 [M+1]⁺. ¹H NMR (400 MHz, Methanol-*d*₄) δ 8.28 (s, 1H), 8.05 (dt, *J* = 25.5, 12.5 Hz, 2H), 4.77 (t, *J* = 6.7 Hz, 2H), 4.13 (t, *J* = 6.9 Hz, 2H), 3.53 (t, *J* = 6.7 Hz, 2H), 3.46 (t, *J* = 7.6 Hz, 2H), 3.41 (d, *J* = 5.6 Hz, 2H), 2.64 (q, *J* = 7.2 Hz, 2H), 2.28 (d, *J* = 14.9 Hz, 6H), 2.03 (d, *J* = 7.1 Hz, 2H), 1.63 (dt, *J* = 10.5, 6.6 Hz, 2H). ¹³C NMR (101 MHz, MeOD) δ 169.81, 137.18, 136.51, 127.90, 123.57, 122.72, 112.57, 56.24, 55.64, 51.29, 42.03, 32.94, 31.36, 29.37, 27.69.

6-(3-aminopropyl)-3-(2-(azepan-1-yl)ethyl)benzo[d]thiazol-2(3H)-one. 456 (WA351) To a solution of 3-(2-(azepan-1-yl)ethyl)-6-(3-azidopropyl)benzo[d]thiazol-2(3H)-one (WA345) (0.350 g, 0.99 mmol) in methanol (100 mL) was added to 10% Palladium on carbon catalyst (0.040 g) and stirred under a hydrogen atmosphere (30 psi) for 3 h. The mixture was filtered through celite and evaporated under *vacuo*. The residue was purified by column chromatography over silica gel using ethyl acetate in hexanes to afford 0.250 g of 6-(2-aminoethyl)-3-(2-(azepan-1-yl)ethyl)benzo[d]thiazol-2(3H)-one as brown residue in 75% yield. MS (ESI) m/z 334.64 $[M+1]^+$. ^1H NMR (400 MHz, DMSO- d_6) δ 7.44 (s, 1H), 7.25 – 7.14 (m, 2H), 3.96 (t, $J = 6.9$ Hz, 2H), 3.16 – 2.96 (m, 4H), 2.73 (t, $J = 6.8$ Hz, 2H), 2.55 (t, $J = 7.3$ Hz, 2H), 2.49 (s, 2H), 1.66 (q, $J = 7.5$ Hz, 2H), 1.48 (d, $J = 10.8$ Hz, 10H). ^{13}C NMR (101 MHz, DMSO) δ 169.01, 137.61, 135.44, 127.08, 122.70, 121.75, 111.67, 55.42, 54.81, 41.20, 41.16, 35.05, 32.45, 28.55, 26.89.

3-(2-(azepan-1-yl)ethyl)-6-(3-mercaptopropyl)benzo[d]thiazol-2(3H)-one. 452 (WA353) A mixture of thiourea (0.060 g, 0.788 mmol) and 3-(2-(azepan-1-yl)ethyl)-6-(3-chloropropyl)benzo[d]thiazol-2(3H)-one (WA323) (0.25 g, 0.709 mmol) were dissolved in ethanol (15 mL) under an atmosphere of argon. After stirring for 24 h at 80°C, the the solvent was evaporated and the residue was dissolved in water (5 mL) and treated with aqueous solution of sodium hydroxide (40% in water, 10 mL). After a further 2 h of stirring at room temperature, the reaction mixture was extracted with ethyl acetate (3 X 20 mL). The organic phase was washed with sodium bicarbonate and brine, dried over anhydrous sodium sulfate, and the solvent was removed under *vacuo*. The residue was purified by column chromatography over silica gel using ethyl acetate in hexanes to afford 0.2 g of 3-(2-(azepan-1-yl)ethyl)-6-(3-mercaptopropyl)benzo[d]thiazol-2(3H)-one as brown oil in 80 % yield. MS (ESI) m/z 350.70

[M+1]⁺. ¹H NMR (400 MHz, DMSO-*d*₆) δ 7.40 (s, 1H), 7.21 (d, *J* = 8.2 Hz, 1H), 7.13 (d, *J* = 8.2 Hz, 1H), 3.93 (t, *J* = 6.9 Hz, 2H), 2.70 (t, *J* = 6.7 Hz, 2H), 2.64 (q, *J* = 8.6, 7.7 Hz, 4H), 2.59 (d, *J* = 5.8 Hz, 4H), 1.89 (p, *J* = 7.5 Hz, 2H), 1.48 (s, 2H), 1.46 (s, 1H), 1.43 (s, 6H). ¹³C NMR (101 MHz, DMSO) δ 168.98, 136.53, 135.60, 127.05, 122.72, 121.92, 111.66, 55.39, 54.75, 41.10, 37.59, 33.61, 30.79, 28.39, 26.86.

3-(2-(azepan-1-yl)ethyl)-6-(2-mercaptoethyl)benzo[*d*]thiazol-2(3*H*)-one. 451 (WA354) A mixture of thiourea (0.062 g, 0.814 mmol) and 3-(2-(azepan-1-yl)ethyl)-6-(2-chloroethyl)benzo[*d*]thiazol-2(3*H*)-one (WA324) (0.25 g, 0.739 mmol) were dissolved in ethanol (15 mL) under an atmosphere of argon. After stirring for 24 h at 80°C, the solvent was evaporated and the residue dissolved in water (5 mL) and treated with aqueous solution of sodium hydroxide (40% in water, 10 mL). After a further 2 h of stirring at room temperature, the reaction mixture was extracted with ethyl acetate (3 X 20 mL). The organic phase was washed with sodium bicarbonate and brine, dried over anhydrous sodium sulfate, and the solvent was removed under *vacuo*. The residue was purified by column chromatography over silica gel using ethyl acetate in hexanes to afford 0.21 g of 3-(2-(azepan-1-yl)ethyl)-6-(2-mercaptoethyl)benzo[*d*]thiazol-2(3*H*)-one as brown oil in 84 % yield. MS (ESI) *m/z* 339.49 [M+1]⁺. ¹H NMR (400 MHz, DMSO-*d*₆) δ 7.54 (s, 1H), 7.27 (t, *J* = 5.5 Hz, 2H), 3.98 (t, *J* = 6.7 Hz, 2H), 3.84 (t, *J* = 7.0 Hz, 2H), 3.03 (t, *J* = 7.0 Hz, 2H), 2.74 (t, *J* = 6.7 Hz, 2H), 2.63 (t, *J* = 5.4 Hz, 4H), 1.51 (s, 1H), 1.48 (s, 2H), 1.46 (d, *J* = 5.6 Hz, 6H). ¹³C NMR (101 MHz, DMSO) δ 169.01, 136.38, 136.16, 133.59, 127.72, 123.38, 121.81, 111.74, 55.39, 54.74, 45.87, 41.15, 38.11, 28.40, 26.87.

6-(2-bromopropanoyl)benzo[*d*]thiazol-2(3*H*)-one. 457 (WA437) DMF (4.5 ml) was slowly added to AlCl₃ (26.6 g, 200 mmol) under vigorous stirring. The mixture was heated at 45⁰C and 2(3*H*)-benzothiazole (3 g, 20 mmol) was added. After 20 min 2-bromobutyryl chloride (5.42 g, 31.61 mmol) was added and the reaction mixture was heated at 65⁰C for 45 min. The hot mixture was then carefully poured onto ice and stirred for 30 min then the crude product was collected by filtration, washed with water and air-dried. The solid was purified by column chromatography over silica gel using ethyl acetate in hexanes to afford 4 g of 6-(2-bromopropanoyl)benzo[*d*]thiazol-2(3*H*)-one as a white solid in 70% yield. MS (ESI) *m/z* 286.37; 288.38 [M, M+2]⁺. ¹H NMR (400 MHz, DMSO-*d*₆) δ 12.34 (s, 1H), 8.27 (s, 1H), 7.99 – 7.92 (m, 1H), 7.22 (d, *J* = 8.4 Hz, 1H), 5.71 (dq, *J* = 13.2, 6.5 Hz, 1H), 1.75 (d, *J* = 6.5 Hz, 3H), 1.60 (d, *J* = 6.5 Hz, 1H). ¹³C NMR (101 MHz, DMSO) δ 192.45, 170.98, 141.23, 128.74, 128.36, 124.38, 124.36, 111.85, 43.36, 20.47.

6-(2-bromopropyl)benzo[*d*]thiazol-2(3*H*)-one. 458 (WA438) Triethylsilane (1.87 g, 16.08 mmol) was added to the stirred solution of 6-(2-bromopropanoyl)benzo[*d*]thiazol-2(3*H*)-one (WA437) (2 g, 7 mmol) in (15 mL) trifluoroacetic acid. The mixture was vigorously stirred at room temperature for 16 h, and then the mixture was evaporated over the *vacuu*. The residue was purified by column chromatography using (4:6) ethyl acetate in hexanes to give 1.7 g 6-(2-bromopropyl)benzo[*d*]thiazol-2(3*H*)-one as a white solid in 89 % yield. MS (ESI) *m/z* 272.37; 274.38 [M, M+1]⁺. ¹H NMR (400 MHz, Chloroform-*d*) δ 10.19 (s, 1H), 7.28 (s, 1H), 7.14 (d, *J* = 1.2 Hz, 2H), 4.33 – 4.16 (m, 1H), 3.24 – 3.06 (m, 2H), 1.73 (d, *J* = 6.7 Hz, 3H). ¹³C NMR (101 MHz, CDCl₃) δ 173.58, 134.12, 133.99, 127.72, 124.00, 123.06, 111.79, 50.44, 46.92, 25.72.

1-(2-oxo-2,3-dihydrobenzo[*d*]thiazol-6-yl)propan-2-yl benzoate. 459 (WA442) Anhydrous potassium carbonate (3.042 g, 22.04 mmol) and benzoic acid (4.48 g, 36.68 mmol) were added successively to a stirred solution of 6-(2-bromopropyl)benzo[*d*]thiazol-2(3*H*)-one (WA338) (2 g, 7.35 mmol) in anhydrous DMF (60 mL). The reaction mixture was heated at 110 °C for 9 h. After cooling the mixture was poured into 50 mL of HCl (2N) solution in water, extracted with ethyl acetate (3 x 50 mL) and the organic layer was washed several times with saturated sodium bicarbonate solution to remove excess benzoic acid. The organic layer was washed with brine, dried over anhydrous sodium sulfate, and evaporated under vacuo. The residue was purified by column chromatography (silica gel) using a mobile phase consisting of (2:98) methanol/diethyl ether to afford 1.7 g of 1-(2-oxo-2,3-dihydrobenzo[*d*]thiazol-6-yl)propan-2-yl benzoate as a white solid in 74% yield. MS (ESI) *m/z* 336.31 [M+23]⁺. ¹H NMR (400 MHz, Chloroform-*d*) δ 10.47 (d, *J* = 16.1 Hz, 1H), 8.19 – 8.08 (m, 1H), 8.03 – 8.00 (m, 1H), 7.62 – 7.54 (m, 1H), 7.49 – 7.43 (m, 2H), 7.27 (d, *J* = 2.9 Hz, 1H), 7.17 (dd, *J* = 8.2, 1.6 Hz, 1H), 7.11 (t, *J* = 7.4 Hz, 1H), 5.37 (q, *J* = 6.3 Hz, 1H), 3.11 – 2.90 (m, 2H), 1.37 (d, *J* = 6.3 Hz, 3H). ¹³C NMR (101 MHz, CDCl₃) δ 173.47, 166.09, 134.12, 132.94, 130.45, 130.12, 129.48, 128.44, 128.37, 127.85, 124.05, 123.21, 111.78, 72.06, 41.97, 19.50.

1-(3-(2-(azepan-1-yl)ethyl)-2-oxo-2,3-dihydrobenzo[*d*]thiazol-6-yl)propan-2-yl benzoate. 460 (WA448) Benzoic acid (1 g, 8.18 mmol) was dissolved in 10 mL HMPA and added 25% aqueous solution of sodium hydroxide (0.197 g, 4.925 mmol) and stirred for 15 minutes before adding a solution of 3-(2-(azepan-1-yl)ethyl)-6-(2-bromopropyl)benzo[*d*]thiazol-2(3*H*)-one (WA444a) (0.655 g, 1.65 mmol) in 5 mL HMPA. After that, the reaction mixture was then heated at 100 °C for 36 h. After cooling the mixture was poured into 30 mL water, extracted with

ethyl acetate (3 x 25 mL) and the organic layer was washed with brine, dried over anhydrous sodium sulfate, and evaporated under *vacuo*. The residue was purified by column chromatography over silica gel using ethyl acetate in hexanes to afford 0.7 g of 1-(3-(2-(azepan-1-yl)ethyl)-2-oxo-2,3-dihydrobenzo[*d*]thiazol-6-yl)propan-2-yl benzoate as yellow oil in 96 % yield. MS (ESI) *m/z* 339.62 [M+1]⁺. ¹H NMR (400 MHz, Methanol-*d*₄) δ 7.95 – 7.91 (m, 1H), 7.58 – 7.48 (m, 1H), 7.47 – 7.36 (m, 3H), 7.27 (tdd, *J* = 16.5, 7.9, 3.7 Hz, 2H), 7.15 (d, *J* = 8.4 Hz, 1H), 4.55 (d, *J* = 2.2 Hz, 1H), 4.03 (dt, *J* = 9.4, 6.0 Hz, 2H), 3.02 (ddt, *J* = 17.0, 11.4, 5.7 Hz, 2H), 2.85 – 2.79 (m, 2H), 2.73 (dd, *J* = 6.8, 4.1 Hz, 2H), 2.71 – 2.67 (m, 2H), 1.61 – 1.51 (m, 8H), 1.37 (d, *J* = 6.3 Hz, 3H). ¹³C NMR (101 MHz, MeOD) δ 170.45, 166.09, 135.79, 133.20, 132.67, 129.80, 128.96, 128.07, 127.57, 125.02, 124.20, 123.18, 122.27, 119.36, 110.84, 110.78, 72.21, 55.43, 54.45, 41.35, 40.61, 27.56, 26.47, 18.53.

3-(2-(azepan-1-yl)ethyl)-6-(2-hydroxypropyl)benzo[*d*]thiazol-2(3*H*)-one. 462 (WA449) To a solution of 3-(3-(2-(azepan-1-yl)ethyl)-2-oxo-2,3-dihydrobenzo[*d*]thiazol-6-yl) propyl benzoate (WA448) (1 g, 2.3 mmol) in 20 mL of methanol/H₂O (6:4) was added 25 ml of freshly prepared aqueous sodium hydroxide (0.228 g, 5.7 mmol) solution. The mixture was heated at 90°C for 1 h. The reaction mixture was cooled to room temperature, and the residue concentrated in *vacuo* to remove methanol. The residue was acidified with 1N HCl while cooling in an ice bath and the aqueous layer was extracted initially with 30 mL of ethyl acetate. The pH of the aqueous layer was adjusted to pH=10 with aqueous potassium carbonate solution and the product extracted with ethyl acetate (25 mL x 3). The combined organic layers were washed with brine, dried over sodium sulfate, filtered and evaporated under *vacuo*. The residue was purified by column chromatography using 2.5 % methanol/diethyl ether as the eluent to obtain 0.7 g of 3-(2-(azepan-

1-yl)ethyl)-6-(2-hydroxypropyl)benzo[*d*]thiazol-2(3*H*)-one as yellow oil in 91 % yield. MS (ESI) m/z 335.60 [M+1]⁺. ¹H NMR (400 MHz, Methanol-*d*₄) δ 8.50 (s, 1H), 7.42 (d, *J* = 1.7 Hz, 1H), 7.37 – 7.21 (m, 2H), 4.37 (t, *J* = 6.8 Hz, 2H), 3.96 (h, *J* = 6.2 Hz, 1H), 3.43 – 3.31 (m, 6H), 2.75 (qd, *J* = 13.6, 6.4 Hz, 2H), 1.99 – 1.85 (m, 4H), 1.79 – 1.67 (m, *J* = 4.8, 4.3 Hz, 4H), 1.16 (d, *J* = 6.2 Hz, 3H). ¹³C NMR (101 MHz, MeOD) δ 170.86, 135.22, 134.59, 127.96, 123.33, 122.09, 110.54, 68.23, 55.05, 53.81, 44.53, 37.93, 25.97, 24.27, 21.65.

3-(2-(azepan-1-yl)ethyl)-6-(3-methyloxiran-2-yl)benzo[*d*]thiazol-2(3*H*)-one. (464, (WA458)
(0.460 g, 1.45 mmol) of 3-(2-(azepan-1-yl)ethyl)-6-(prop-1-en-1-yl)benzo[*d*]thiazol-2(3*H*)-one (WA444b) was dissolved in 15 mL freshly distilled THF and added 15 mL of 2 M solution of 9-BBN in THF and refluxed overnight. After that, then were added 10 mL of 3N NaOH and 10 mL of 50 % solution of H₂O₂ and stirred for 1 h. The mixture was extracted with ethyl acetate (3 x 25 mL) and the organic layer was washed with brine, dried over anhydrous sodium sulfate, and evaporated under vacuo. The residue was purified by column chromatography over silica gel using ethyl acetate in hexanes to afford 0.200 g of 3-(2-(azepan-1-yl)ethyl)-6-(3-methyloxiran-2-yl)benzo[*d*]thiazol-2(3*H*)-one as a white solid in 41 % yield. MS (ESI) m/z 333.65 [M+1]⁺. ¹H NMR (400 MHz, Methanol-*d*₄) δ 7.50 (dd, *J* = 19.3, 1.6 Hz, 1H), 7.47 – 7.31 (m, 2H), 6.40 (dd, *J* = 15.6, 2.0 Hz, 1H), 6.26 (dq, *J* = 15.8, 6.5 Hz, 1H), 4.52 (q, *J* = 8.3, 7.6 Hz, 2H), 3.59 (dt, *J* = 14.7, 9.1 Hz, 4H), 3.52 – 3.42 (m, 2H), 2.18 – 2.04 (m, 2H), 1.88 (td, *J* = 6.2, 1.8 Hz, 3H), 1.75 (d, *J* = 16.4 Hz, 4H). ¹³C NMR (101 MHz, MeOD) δ 170.33, 135.04, 134.28, 129.64, 125.27, 124.47, 122.53, 119.50, 110.83, 69.67, 64.56, 36.46, 26.52, 21.31, 17.18. Note: The intention at first was to break the epoxide ring and get the alcohol (462); however, breaking the ring didn't happen and I was curious to test this compound against sigma receptors.

(E)-3-(2-(azepan-1-yl)ethyl)-6-(prop-1-en-1-yl)benzo[d]thiazol-2(3H)-one. 461 (WA459)

This compound was obtained as a result of benzoate hydrolysis (460) where the elimination take place in stead of forming alcohol in compound (462). ¹H NMR (400 MHz, Methanol-*d*₄) δ 7.42 (d, *J* = 1.7 Hz, 1H), 7.28 (dd, *J* = 8.4, 1.8 Hz, 1H), 7.10 (d, *J* = 8.4 Hz, 1H), 6.34 (dd, *J* = 15.8, 1.9 Hz, 1H), 6.20 (dq, *J* = 15.7, 6.5 Hz, 1H), 3.98 (t, *J* = 7.1 Hz, 2H), 2.82 – 2.61 (m, 6H), 1.84 (dt, *J* = 11.5, 5.7 Hz, 3H), 1.65 – 1.50 (m, 8H). ¹³C NMR (101 MHz, MeOD) δ 170.17, 135.64, 133.77, 129.78, 124.93, 124.22, 122.51, 119.36, 110.76, 55.35, 54.34, 40.34, 27.50, 26.53, 17.31.

3-(2-(azepan-1-yl)ethyl)-6-(2-fluoropropyl)benzo[d]thiazol-2(3H)-one. 463 (WA466) To a solution of 3-(2-(azepan-1-yl)ethyl)-6-(2-hydroxypropyl)benzo[d]thiazol-2(3H)-one (WA449) (0.1 g, 0.3 mmol) in anhydrous DCM 7.5 mL at -78 °C was added Deoxo-Fluor (0.0795 g, 36 mmol). After that, the reaction mixture was warmed up to room temperature and stirred for 1 h. The reaction mixture was poured onto water 15 mL and extracted (3 x 25 mL) with methylene chloride and the organic layer was washed with brine, dried over anhydrous sodium sulfate, and evaporated under vacuo. The residue was purified by column chromatography over silica gel using ethyl acetate in hexanes to afford 0.065 g of 3-(2-(azepan-1-yl)ethyl)-6-(2-fluoropropyl)benzo[d]thiazol-2(3H)-one as yellow oil in 65 % yield. MS (ESI) *m/z* 337.61 [M+1]⁺. ¹H NMR (400 MHz, Chloroform-*d*) δ 7.29 (d, *J* = 1.7 Hz, 1H), 7.17 (d, *J* = 7.9 Hz, 1H), 7.07 (d, *J* = 8.3 Hz, 1H), 4.21 (q, *J* = 6.6 Hz, 1H), 4.05 (t, *J* = 7.4 Hz, 2H), 3.12 – 2.96 (m, 2H), 2.84 (t, *J* = 7.4 Hz, 2H), 2.75 (d, *J* = 5.7 Hz, 2H), 1.61 (d, *J* = 22.8 Hz, 8H), 1.54 (d, *J* = 6.5 Hz, 3H), 1.27 (s, 2H). ¹³C NMR (101 MHz, CDCl₃) δ 169.79, 135.95, 132.22, 127.43, 123.32, 122.90, 110.52, 91.74, 90.07, 55.73, 54.72, 42.85, 42.63, 41.26, 28.24, 26.92, 20.67, 20.45.

3-(2-(azepan-1-yl)ethyl)-6-(2-bromopropyl)benzo[*d*]thiazol-2(3*H*)-one. 494(WA444a) & 3-(2-(azepan-1-yl)ethyl)-6-(prop-1-en-1-yl)benzo[*d*]thiazol-2(3*H*)-one. 461 (WA444b)

A solution of 6-(2-bromopropyl)benzo[*d*]thiazol-2(3*H*)-one (WA438) (1.3 g, 4.77 mmol) and 1-(2-chloroethyl) azepane hydrochloride (4.1 g, 20.69 mmol) in anhydrous DMF (35 mL) was heated at 110 °C and added sodium bicarbonate (2.4 g, 28.62 mmol) slowly over 5 minutes. Then, the temperature was raised to 120 °C and the reaction left for 30 min. After cooling the mixture was poured into 50 mL water, extracted with ethyl acetate (3 x 25 mL) and the organic layer was washed with brine, dried over anhydrous sodium sulfate, and evaporated under vacuo. The residue was purified by column chromatography over silica gel using ethyl acetate in hexanes to afford 0.7 g of 3-(2-(azepan-1-yl)ethyl)-6-(2-bromopropyl)benzo[*d*]thiazol-2(3*H*)-one as yellow oil that was used in the next step without further characterization. Also, bromine elimination afforded 0.4 g of 3-(2-(azepan-1-yl)ethyl)-6-(prop-1-en-1-yl)benzo[*d*]thiazol-2(3*H*)-one as yellow solid. MS (ESI) m/z 317.57 [M+1]⁺. ¹H NMR (400 MHz, Chloroform-*d*) δ 7.36 (d, J = 1.7 Hz, 1H), 7.30 – 7.19 (m, 1H), 7.01 (d, J = 8.4 Hz, 1H), 6.35 (dd, J = 15.7, 2.0 Hz, 1H), 6.16 (dq, J = 15.8, 6.6 Hz, 1H), 4.01 (q, J = 7.9 Hz, 2H), 2.82 (q, J = 7.2, 6.5 Hz, 2H), 2.73 (q, J = 5.6, 4.9 Hz, 4H), 1.88 (td, J = 7.2, 6.6, 2.0 Hz, 3H), 1.64 – 1.55 (m, 8H). ¹³C NMR (101 MHz, CDCl₃) δ 169.73, 135.92, 133.41, 129.88, 125.35, 124.15, 123.04, 119.57, 110.60, 55.69, 54.73, 41.24, 28.23, 26.91, 18.44.

CHAPTER X: CONCLUSION

Since the discovery of sigma receptors and their roles in various diseases have been widely demonstrated and documented in the literature. Similarly, an increasing number of research indicated the involvement of sigma receptors in the toxic and locomotor effects of cocaine and methamphetamine. In fact, several reports confirmed the association of sigma receptors with a number of CNS functions and disorders including: anxiety, convulsions, schizophrenia, regulation of motor behavior, and psychostimulatory effects from drugs of abuse. Interestingly, sigma receptor antagonists have been shown to attenuate cocaine-induced convulsions and locomotor stimulation. With this, sigma receptor ligands are being studied as a possible means to treat drug addiction. On the other hand, it has been reported that sigma-2 receptors have a 10-fold higher density in proliferating tumor cells than in quiescent tumor cells, and that sigma-2 receptor agonists are capable of killing tumor cells via apoptotic and non-apoptotic mechanisms. Thus the development of ligands with high affinity and selectivity would greatly assist in the determination of the specific roles of the sigma receptor subtypes.

In an effort to determine the basis for sigma activity and selectivity, a series of original benzofuran-based analogs were synthesized and characterized and their affinities for sigma receptors are being determined using *in vitro* radioligand binding assays. Most of the tested molecules exhibited preference for sigma-1 receptors over sigma-2 receptors. Among the tested compounds, **287** (W224) displayed the best selectivity towards sigma-1 receptors with 73 σ_2/σ_1 selectivity ratio. Introducing a nitro group or isothiocyanate group at para position on the phenyl ring of **(274)**, and **(379)** the phenyl piperazine motif does not show any preference to any of sigma receptors, whereas the 1-methyl-4-phenethylpiperazine substituent in **272** (WA205) displayed good affinity toward both subtypes with some preference to sigma-1 receptors. Both **(273)** and **(279)** showed high affinity for both subtypes. In general, the benzofuran-based analogs

showed good to moderate binding affinity towards sigma receptors and warrant further modification upon receiving the results for the rest of the compounds.

Also, in the search for a highly selective sigma-2 receptor ligand, which cannot only act as a probe to explore unknown biochemical mechanisms in cancer and other related diseases, but also be used as a radioligand in sigma-2 receptor binding assays. In this regard, we have synthesized and incorporated the isothiocyanate moiety in the heterocyclic aromatic ring of a series of selective sigma-2 ligands that were developed in our laboratory. This has resulted in producing novel selective irreversible sigma-2 ligands with little to no irreversible binding to sigma-1 receptors. Among these tested compounds, **345** (WA350) and **346** (WA352) produced selective irreversible inhibition of sigma-2 binding over sigma-1 binding. Nevertheless, **345** (WA350) showed higher affinity and selectivity for sigma-2 over sigma-1 than the other compounds irreversibly. Compound **344** (WA349), interestingly, has a higher binding affinity for sigma-2 receptors and is one of the best synthesized and tested compounds in the series so far; however, the irreversible data for this compound is still under investigation and will be presented in detail in the near future.

Additionally, in the search for an effective drug for the treatment of cocaine abuse and addiction, and based on our previous work on **240** CM699 that showed high affinity for sigma-1 and DAT, and its ability to attenuate the cocaine self-administration. We have decided to make more analogs of **240** (CM699) in order to enhance blockade of cocaine self-administration and metabolic stability. The **240** (CM699) analogs were synthesized and their affinities toward sigma receptors and dopamine transporter measured using radioligand binding assays. Several compounds have retained the dual affinity towards sigma receptors and DAT. Subsequently; some of these compounds were subjected to metabolic stability study in liver microsomes assays.

Interestingly, all the tested analogs showed superior metabolic stability to CM699. We successfully improved the metabolic stability of our lead **240** (CM699) through designing of a new series while blocking the vulnerable sites of metabolism.

The last part of my research was to make more derivatives of the highly selective sigma-1 ligand **23** (CM304) to assess its pharmacokinetic issues. The very lipophilic, **23** (CM304) has shown a short half life in rat liver microsomes ($t_{1/2} = 12.6$ min;) as well as poor oral bioavailability in rats (0.7%). In this regard, several analogs have been synthesized and characterized and their affinities toward sigma receptor subtypes have not been completed. These analogs were designed in attempt to reduce the lipophilicity by introducing several polar groups to the alkyl side chain.

BIBLIOGRAPHY

1. Martin, W.R.; Eades, C.G.; Thompson, J.A.; Huppler, R.E.; Gilbert, P.E. The effects of morphine- and nalorphine-like drugs in the nondependent and morphine-dependent chronic spinal dog. *J. Pharmacol. Exp. Ther.* 1976, *197*, 517-532.
2. Vaupel, D.B. Naltrexone fails to antagonize the sigma effects of PCP and SKF 10,047 in the dog. *Eur. J. Pharmacol.* 1983, *92*, 269-274.
3. Young GA, Khazan N. Differential neuropharmacological effects of mu, kappa and sigma opioid agonists on cortical EEG power spectra in the rat. Stereospecificity and naloxone antagonism. *Neuropharmacology* 1984, *23*, 1161-1165.
4. Berzetei-Gurske IP, Toll L. The mu-opioid activity of kappa-opioid receptor agonist compounds in the guinea pig ileum. *Eur J Pharmacol* 1992, *212*, 283-286.
5. Khazan N, Young GA, El-Fakany EE, Hong O, Caliigaro D. Sigma receptors mediated the psychotomimetic effects of N-allylnormetazocine (SKF-10,047), but not its opioid agonistic-antagonistic properties. *Neuropharmacology* 1984, *23*, 983-987.
6. Matsumoto, R.R.; Bowen, W.D.; Su, T.P. *Sigma Receptors: Chemistry, Cell Biology and Clinical Implications*. Springer Science + Business Media, LLC: New York, NY, USA, 2007, 1-23.
7. Maurice, T.; Su, T.P. The pharmacology of sigma-1 receptors. *Pharmacol. Ther.* 2009, *124*, 195-206.
8. Hellewell, S.B., Bowen, W.D. A sigma-like binding site in rat pheochromocytoma PC12-cells: decreased affinity for (+)-benzomorphans, and lower molecular weight suggest a different sigma receptor form from that in guinea pig brain. *Brain Res.* 1990, *527*, 244–253.

9. Quirion, R., Bowen, W.D., Itzhak, Y., Junien, J.L., Musacchio, J.M., Rothman, R.B., Su, T.-P., Tam, S.W., Taylor, D.P. A proposal for the classification of sigma binding sites. *Trends Pharmacol Sci.* 1992, 13, 85–86.
10. Hanner M, Moebius FF, Flandorfer A, Knaus HG, Striessnig J, Kempner E, et al. Purification, molecular cloning, and expression of the mammalian sigma-1 binding site. *Proc Natl Acad Sci USA* 1996, 93, 8072–8077.
11. Seth P, Fei YJ, Li HW, Huang W, Leibach FH, Ganapathy V. Cloning and functional characterization of a sigma receptor from rat brain. *J Neurochem* 1998, 70, 922–931.
12. Mei J, Pasternak GW. Molecular cloning and pharmacological characterization of the rat σ_1 receptor. *Biochem Pharmacol.* 2001, 62, 349–355.
13. Gebreselassie, D., Bowen, W.D. Sigma-2 receptors are specifically localized to lipid rafts in rat liver membranes. *Eur. J. Pharmacol.* 2004, 493, 19–28.
14. Uyen B, Chu1, Timur A, Mavlyutov, Ming-Liang Chu, Huan Yang, Amanda Schulman, Christophe Mesangeau, Christopher R. McCurdy, Lian-Wang Guo, Arnold E. Ruoho. The Sigma-2 Receptor and Progesterone Receptor Membrane Component 1 are Different Binding Sites Derived From Independent Genes. *EBioMedicine.* 2015, 2, 11, 1806–1813
15. Jinbin Xu, Chenbo Zeng, Wenhua Chu, Fenghui Pan, Justin M. Rothfuss, Fanjie Zhang, Zhude Tu, Dong Zhou, Dexing Zeng, Suwanna Vangveravong, Fabian Johnston, Dirk Spitzer, Katherine C. Chang, Richard S. Hotchkiss, William G. Hawkins, Kenneth T. Wheeler & Robert H. Mach. "Identification of the PGRMC1 protein complex as the putative sigma-2 receptor binding site". *Nature Communications.* 2011, 380 (2).
16. Aydar E, Palmer CP, Klyachko VA, Jackson MB. The σ receptor as a ligand-regulated auxiliary potassium channel subunit. *Neuron.* 2002, 34, 399-410.

17. Jbilo O, Vidal H, Paul R, De Nys N, Bensaid M, Silve S, Carayon P, Davi D, Galiegue S, Bourrie B, Guillemot J-C, Ferrara P, Loison G, Maffrand J-P, Le Fur G, Casellas P. Purification and characterization of the human SR 31747A-binding protein. A nuclear membrane protein related to yeast sterol isomerase. *J Biol Chem*. 1997, 272(43), 27107-15.
18. Monassier, L., & Bousquet, P. Sigma receptors: From discovery to highlights of their implications in the cardiovascular system. *Fundamental & Clinical Pharmacology*. 2002, 16(1), 1–8.
19. Bourrie, B., Bribes, E., Derocq, J. M., Vidal, H., & Casellas, P. Sigma receptor ligands: Applications in inflammation and oncology. *Current Opinion in Investigational Drugs*. 2004, 5(11), 1158–1163.
20. Su, T. P., London, E. D., Jaffe, J. H. Steroid binding at sigma receptors suggests a link between endocrine, nervous, and immune systems. *Science*. 1988, 240(4849), 219–221.
21. Wolfe, S. A., Jr., Kulsakdinun, C., Battaglia, G., Jaffe, J. H., & De Souza, E. B. Initial identification and characterization of sigma receptors on human peripheral blood leukocytes. *The Journal of Pharmacology and Experimental Therapeutics*. 1988, 247(3), 1114–1119.
22. Hellewell, S. B., & Bowen, W. D. (1990). A sigma-like binding site in rat pheochromocytoma (PC12) cells: Decreased affinity for (b)-benzomorphans and lower molecular weight suggest a different sigma receptor form from that of guinea pig brain. *Brain Researc*. 1990, 527(2), 244–253.
23. Hellewell, S. B., Bruce, A., Feinstein, G., Orringer, J., Williams, W., & Bowen, W. D. Rat liver and kidney contain high densities of sigma 1 and sigma 2 receptors:

- Characterization by ligand binding and photoaffinity labeling. *European Journal of Pharmacology*. 1994, 268(1), 9–18.
24. M. E. Ganapathy, P. D. Prasad, W. Huang, P. Seth, F. H. Leibach, V. Ganapathy, J. *Pharmacol. Exp. Ther.* 1999, 289, 251.
 25. H. Yamamoto, R. Miura, T. Yamamoto, K. Shinohara, M. Watanabe, S. Okuyama, A. Nakazato, T. Nukada, *FEBS Lett.* 1999, 445, 19.
 26. P. Seth, M. E. Ganapathy, S. J. Conway, C. D. Bridges, S. B. Smith, P. Casellas, V. Ganapathy, *Biochim. Biophys. Acta* 2001, 1540, 59.
 27. Madhura Manohar, Samuel D. Banister, Corinne Beinat, James O'Brien-Brown, and Michael Kassiou, Recent Advances in the Development of Sigma-1 Receptor Ligands. *Aust. J. Chem.* 2015, 68, 600–609.
 28. Hayashi, T.; Su, T.P. Sigma-1 receptor chaperones at the ER-mitochondrion interface regulate Ca(2+) signaling and cell survival. *Cell.* 2007, 131, 596-610.
 29. Maurice T, Roman FJ, Privat A. Modulation by neurosteroids of the in vivo (+)-[3H]SKF 10,047 binding to sigma1 receptors in the mouse forebrain. *J Neurosci Res* 1996, 46, 734–743.
 30. McCann DJ, Su T-P. Solubilization and characterization of haloperidol-sensitive (+)-[3H]SKF 10,047 binding sites (sigma sites) from rat liver membranes. *J Pharmacol Exp Ther* 1991, 257, 547– 554.
 31. Fontanilla D, Johannessen M, Hajipour AR, Cozzi NV, Jackson MB, Ruoho AE. The Hallucinogen *N,N*-Dimethyltryptamine (DMT) Is an Endogenous Sigma-1 Receptor Regulator. *Science (New York, NY)*. 2009, 323(5916), 934-937.
 32. Hayashi, T., & Su, T. P. (2004). Sigma-1 receptor ligands: Potential in the treatment of

- neuropsychiatric disorders. *CNS Drugs*. 2004, 18(5), 269–284.
33. Hayashi, T., Tsai, S. Y., Mori, T., Fujimoto, M., & Su, T. P. (2011). Targeting ligand-operated chaperone sigma-1 receptors in the treatment of neuropsychiatric disorders. *Expert Opinion on Therapeutic Targets*. 2011, 15(5), 557–577.
 34. Kaushal, N., Seminerio, M. J., Robson, M. J., McCurdy, C. R., & Matsumoto, R. R. Pharmacological evaluation of SN79, a sigma (σ) receptor ligand, against methamphetamine-induced neurotoxicity in vivo. *European Neuropsychopharmacology*. 2013, 23, 960–971.
 35. Aydar, R., Palmer, C. P., & Djamgoz, M. B. (2004). Sigma receptors and cancer: Possible involvement of ion channels. *Cancer Research*. 2004, 64(15), 5029–5035.
 36. Van Waarde, A., Rybczynska, A. A., Ramakrishnan, N., Ishiwata, K., Elsinga, P. H., & Dierckx, R. A. Sigma receptors in oncology: Therapeutic and diagnostic applications of sigma ligands. *Current Pharmaceutical Design*. 2010, 16(31), 3519–3537.
 37. Ahmed, I. S., Chamberlain, C., & Craven, R. J. S2R(Pgrmc1): The cytochrome-related sigma-2 receptor that regulates lipid and drug metabolism and hormone signaling. *Expert Opinion on Drug Metabolism & Toxicology*. 2012, 8(3), 361–370.
 38. Crawford, K. W., Coop, A., & Bowen, W. D. Sigma2 Receptors regulate changes in sphingolipid levels in breast tumor cells. *European Journal of Pharmacology* 2002, 443(1–3), 207–209.
 39. Vilner B. J., de Costa B.R., Bowen W. D. Cytotoxic effects of sigma ligands: Sigma receptor-mediated alterations in cellular morphology and viability. *J Neurosci* 1995, 15, 117–134.
 40. Zeng, C., Vangveravong, S., Xu, J., Chang, K. C., Hotchkiss, R. S., Wheeler, K. T., et al.

- (2007). Subcellular localization of sigma-2 receptors in breast cancer cells using two-photon and confocal microscopy. *Cancer Research*. 2007, 67(14), 6708–6716.
41. Basile, A. S., Paul, I. A., & de Costa, B. Differential effects of cytochrome P-450 induction on ligand binding to sigma receptors. *European Journal of Pharmacology*. 1992, 227(1), 95–98.
 42. Kaushal, N., & Matsumoto, R. R. Role of sigma receptors in methamphetamine- induced neurotoxicity. *Current Neuropharmacology*. 2011, 9(1), 54–57.
 43. Aanonsen, L.M., Seybold, V.S. Phencyclidine and sigma receptors in rat spinal cord: binding characterization and quantitative autoradiography. *Synapse*. 1989, 4, 1–10.
 44. Bouchard, P., Quirion, R., 1997. [³H]1,3-Di(2-tolyl)guanidine and [³H](+)pentazocine binding sites in the rat brain: autoradiographic visualization of the putative sigma₁ and sigma₂ receptor subtypes. *Neuroscience* 76, 467 – 477.
 45. Walker, J.M., Bowen, W.D., Goldstein, S.R., Roberts, A.H., Patrick, S.L., Hohmann, A.G., DeCosta, B., 1992. Autoradiographic distribution of [³H](+)pentazocine and [³H]1,3-di-o-tolylguanidine (DTG) binding sites in guinea pig brain: a comparative study. *Brain Res*. 581, 33–38.
 46. McCann DJ, Weissman AD, Su TP (1994) Sigma-1 and sigma-2 sites in rat brain: comparison of regional ontogenic and subcellular patterns. *Synapse* 17:182–189.
 47. Matsumoto, R. R.; Pouw, B. Correlation between neuroleptic binding to σ_1 and σ_2 receptors and acute dystonic reactions. *Eur. J. Pharmacol*. 2000, 401, 155-160.
 48. Graybiel, A.M., Besson, M.-J., Weber, E., 1989. Neuroleptic-sensitive binding sites in the nigrostriatal system: evidence for differential distribution of sigma sites in the substantia nigra, pars compacta of the cat. *J. Neurosci*. 1989, 9, 326–338.

49. Gundlach, A.L., Largent, B.L., Snyder, S.H. Autoradiographic localization of sigma receptor binding sites in guinea pig and rat central nervous system with (+)³H-3-(3-hydroxyphenyl)-N-(1-propyl)piperidine. *J. Neurosci.* 1986, 6, 1757–1770.
50. Jansen, K.L.R., Faull, R.L.M., Dragunow, M., Leslie, R.A., 1991. Auto- radiographic distribution of sigma receptors in human neocortex, hippo- campus, basal ganglia, cerebellum, pineal and pituitary glands. *Brain Res.* 1991, 559, 172–177.
51. Mash, D.C., Zabetian, C.P. Sigma receptors are associated with cortical limbic areas in the primate brain. *Synapse.* 1992, 12, 195–205.
52. McLean, S., Weber, E. Autoradiographic visualization of haloperidol-sensitive sigma receptors in guinea-pig brain. *Neuroscience.* 1988, 25, 259 – 269.
53. James, M. L.; Shen, B.; Zavaleta, C. L.; Nielsen, C. H.; Mesangeau, C.; Vuppala, P. K.; Chan, C.; Avery, B. A.; Fishback, J. A.; Matsumoto, R. R.; Gambhir, S. S.; McCurdy, C. R.; Chin, F. T. New positron emission tomography (PET) radioligand for imaging sigma-1 receptors in living subjects. *J Med Chem.* 2012, 55, 8272-8282
54. James, M. L.; Shen, B.; Nielsen, C. H.; Behera, D.; Buckmaster, C. L.; Mesangeau, C.; Zavaleta, C.; Vuppala, P. K.; Jamalapuram, S.; Avery, B. A.; Lyons, D. M.; McCurdy, C. R.; Biswal, S.; Gambhir, S. S.; Chin, F. T. Evaluation of s-1 receptor radioligand ¹⁸F-FTC-146 in rats and squirrel monkeys using PET. *J Nucl Med.* 2014, 55, 147-153.
55. Samoilova NN, Nagornaya LV, Vinogradov VA (1988) (+)-[³H] SKF 10,047 binding sites in rat liver. *Eur J Pharmacol.* 1988, 147, 259–264.
56. Dumont M, Lemaire S. Interaction of 1,3-di(2-[5-³H]tolyl) guanidine with σ-2 binding sites in rat heart membrane preparations. *Eur J Pharmacol* 1991, 209, 245–248 .
57. Jansen KL, Elliot M, Leslie RA (1992) Sigma receptors in rat brain and testes show

- similar reductions in response to chronic haloperidol. *Eur J Pharmacol.* 1992, 214, 281–283
58. Ela C, Barg J, Vogel Z, Hasin Y, Eliam Y. Sigma receptor ligands modulate contractility Ca^{+2} influx and beating rate in cultured cardiac myocytes. *J Pharmacol Exp Ther.* 1994, 269:1300– 1309
59. Wolfe, S. A. Jr.; Keun, H. B.; Whitlock, B. B.; Saini, P. Differential localization of three distinct binding sites for sigma receptor ligands in rat spleen. *J. Neuroimmun.* 1997, 72, 45-58.
60. Novakova, M.; Ela, C.; Barg, J.; Vogel, E.; Hasin, Y.; Eilam, Y. Iontropic action of sigma receptor ligands in isolated cardiac myocytes from adult rats. *Eur. J. Pharmacol.* 1995, 286, 19-30.
61. Kawamura, K.; Ishiwata, K.; Tajima, H.; Ishii, S.; Matsuno, S.; Homma, Y.; Senda, M. In vivo evaluation of [^{11}C]SA4503 as a PET ligand for mapping CNS sigma₁ receptors. *Nucl. Med. Biol.* 2000, 27, 255-261.
62. Seth P, Leibach FH, Ganapathy V. Cloning and structural analysis of the cDNA and the gene encoding the murine type 1 sigma receptor. *Biochem. Biophys. Res. Commun.* 1997, 241, 535–540.
63. Cagnotto A, Bastone A, Mennini T. [3H](+)-pentazocine binding to rat brain sigma₁ receptors. *Eur. J. Pharmacol.* 1994, 266, 131–138.
64. Cobos EJ, del Pozo E, Baeyens JM. Irreversible blockade of sigma-1 receptors by haloperidol and its metabolites in guinea pig brain and SH-SY5Y human neuroblastoma cells. *J. Neurochem.* 2007, 102, 812–825.
65. Itzhak Y, Stein I, Zhang SH, Kassim CO, Cristante D. Binding of σ -ligands to C57BL/6

- mouse brain membranes: effects of monoamine oxidase inhibitors and subcellular distribution studies suggest the existence of σ -receptor subtypes. *J. Pharmacol. Exp. Ther.* 1991, 257, 141–148.
66. Palacios G, Muro A, Vela JM, Molina-Holgado E, Guitart X, Ovalle S, Zamanillo D. Immunohistochemical localization of the σ_1 -receptor in oligodendrocytes in the rat central nervous system. *Brain Res.* 2003, 961, 92–99.
67. Alonso G, Phan V, Guillemain I, Saunier M, Legrand A, Anol M, Maurice T. Immunocytochemical localization of the sigma1 receptor in the adult rat central nervous system. *Neuroscience.* 2000, 97, 155–170.
68. Dussosoy D, Carayon P, Belugou S, Feraut D, Bord A, Goubet C, Roque C, Vidal H, Combes T, Loison G, Casellas P. Colocalization of sterol isomerase and sigma1 receptor at endoplasmic reticulum and nuclear envelope level. *Eur. J. Biochem.* 1999, 263, 377–386.
69. Jiang G, Mysona B, Dun Y, Gnana-Prakasam JP, Pabla N, Li W, Dong Z, Ganapathy V, Smith SB. Expression, subcellular localization, and regulation of sigma receptor in retinal muller cells. *Invest. Ophthalmol. Vis. Sci.* 2006, 47, 5576–5582.
70. Hayashi T, Su TP. The potential role of sigma-1 receptors in lipid transport and lipid raft reconstitution in the brain: implication for drug abuse. *Life Sci.* 2005, 77, 1612–1624.
71. Szabadkai, G., Bianchi, K., Varnai, P., De Stefani, D., Wieckowski, M.R., Cavagna, D., Nagy, A.I., Balla, T., and Rizzuto, R. (2006). Chaperone-mediated coupling of endoplasmic reticulum and mitochondrial Ca^{2+} channels. *J. Cell Biol.* 2006, 175, 901–911.
72. Hayashi, T.; Su, T.P. Intracellular dynamics of sigma-1 receptors (sigma(1) binding sites)

- in NG108-15 cells. *J. Pharmacol. Exp. Ther.* 2003, 306, 726-733.
73. Navarro, G., Moreno, E., Aymerich, M., Marcellino, D., McCormick, P. J., Mallol, J., et al. Direct involvement of sigma-1 receptors in the dopamine D₁ receptor-mediated effects of cocaine. *Proceedings of the National Academy of Sciences of the United States of America.* 2010, 107(43), 18676–18681.
74. Balasuriya, D., Stewart, A. P., Crottes, D., Borgese, F., Soriani, O., & Edwardson, J. M. The sigma-1 receptor binds to the Nav1.5 voltage-gated Na⁺ channel with 4-fold symmetry. *The Journal of Biological Chemistry.* 2012, 287(44), 37021–37029.
75. Gemma Navarro, Estefania Moreno, Jordi Bonaventura, Marc Brugarolas, Daniel Farré, David Aguinaga, Josefa Mallol, Antoni Cortés, Vicent Casadó, Carmen Lluís, Enric Canela, Peter J. McCormick. Cocaine inhibits dopamine D₂ receptor signaling via sigma-1-D₂ receptor heteromers. Published: April 18, 2013
76. Kourrich, S., Hayashi, T., Chuang, J. Y., Tsai, S. Y., Su, T. P., & Bonci, A. Dynamic interaction between sigma-1 receptor and Kv1.2 shapes neuronal and behavioral responses to cocaine. *Cell.* 2013, 152(1–2), 236–247.
77. Bowen W D: "Sigma receptors: recent advances and new clinical potentials " *Pharmaceutica Acta Helvetiae.* 2000 (2000-03), 74,2-3, 211-218.
78. Baulieu EE. Neurosteroids: a novel function of the brain. *Psychoneuroendocrinology* 1998; 23: 963-87.
79. H. Ishiguro, T. Ohtsuke, M. Toru, M. Itokawa, J. Aoki, H. Shibuya, A. Kurumaji, Y. Okubo, A. Iwawaki, K. Ota, H. Shimizu, H. Hamaguchi and T. Arinami, *Neurosci. Lett.*, 1998, 257.
80. J. L. Diaz, D. Zamanillo, J. Corbera, J. M. Baeyens, R. Maldonado, M. A. Pericàs, J. M.

- Vela and A. Torrens, *Cent. Nerv. Syst. Agents Med. Chem.*, 2009, 9, 172.
81. Bem WT, Thomas GE, Mamone JY *et al.* Overexpression of σ receptors in nonneural human tumors. *Cancer Res.* 1991, 51, 6558–6562.
 82. Vilner BJ, Bowen WD. Characterization of σ -like binding sites of NB41A3, S-20Y, and N1E-115 neuroblastomas, C6 glioma, and NG108–15 neuroblastoma-glioma hybrid cells: further evidence for σ -2 receptors. In: *Mult. Sigma PCP Recept. Ligands: Mech. Neuromodulation Neuroprot., Proc. Jt. Fr.-U.S. Semin, CNRS-NSF, 3rd.* Kamenka, Jean-Marc, Domino, Edward F (Eds). American chemical society. 1992, 341–353.
 83. Mach RH, Smith CR, Al-Nabulsi I, Whirrett BR, Childers SR, Wheeler KT. σ 2 receptors as potential biomarkers of proliferation in breast cancer. *Cancer Res.* 1997, 57, 156–161.
 84. Mach RH, Wheeler KT: Development of molecular probes for imaging sigma-2 receptors in vitro and in vivo. *Cent Nerv Syst Agents Med Chem* 2009, 9, 230-45.
 85. Xu J, Zeng C, Chu W, Pan F, Rothfuss JM, Zhang F, *et al.* Identification of the PGRMC1 protein complex as the putative sigma-2 receptor binding site. *Nature Comm* 2011, 2, 380.
 86. Rohe HJ, Ahmed IS, Twist KE, Craven RJ. PGRMC1 (progesterone receptor membrane component 1): A targetable protein with multiple functions in steroid signaling, P450 activation, and drug binding. *Pharmacol Ther.* 2009, 121, 14–19.
 87. Ahmed IS, Rohe HJ, Twist KE, Mattingly MN, Craven RJ. Progesterone receptor membrane component 1 (Pgrmc1): A heme-1 domain protein that promotes tumorigenesis and is inhibited by a small molecule. *J Pharmacol Exp Ther.* 2010, 333, 564–573.
 88. Yun-Sheng Huang, He-Lin Lu, Lang-Jun Zhang, and Zongwen Wu. Sigma-2 Receptor

- Ligands and Their Perspectives in Cancer Diagnosis and Therapy. *Medicinal Research Reviews*. 2014, 34, 3, 532–566.
89. Tsung-Ping Su, Teruo Hayashi, Tangui Maurice, Shilpa Buch, and Arnold E. Ruoho. The sigma-1 receptor chaperone as an inter- organelle signaling modulator. *Trends Pharmacol. Sci*. 2010, 31, 557– 566
 90. James A. Fishback, Matthew J. Robson, Yan-Tong Xu, and Rae R. Matsumoto. Sigma receptors: potential targets for a new class of antidepressant drug. *Pharmacol. Ther*. 2010, 127, 271–282 .
 91. Maurice T, Urani A, Phan VL, Romieu P. The interaction between neuroactive steroids and the sigma1 receptor function: behavioral consequences and therapeutic opportunities. *Brain Res. Brain Res. Rev*. 2001, 37, 116–132
 92. Maurice, T., Martin-Fardon, R., Romieu, P., Matsumoto, R. R. Sigma1 (σ_1) receptor antagonists represent a new strategy against cocaine addiction and toxicity. *Neurosci Biobehav Rev*. 2002, 26, 499–527.
 93. Matsumoto, R. R., Liu, Y., Lerner, M., Howard, E. W., & Brackett, D. J. Sigma receptors: Potential medications development target for anti-cocaine agents. *Eur J Pharmacol*. 2003, 469, 1–12.
 94. Maurice, T., Romieu, P. Involvement of the sigma1 receptor in the appetitive effects of cocaine. *Pharmacopsychiatry*. 2004, 37, S198–207.
 95. Guitart, X., Codony, X., Monroy, X. Sigma receptors: Biology and therapeutic potential. *Psychopharmacology (Berl)*. 2004, 174, 301–319.
 96. National Institute of Drug Abuse, 2012; National Survey on Drug Use and Health: Summary of National Findings.(Retrieved November 16, 2015).

[\(http://www.samhsa.gov/data/\)](http://www.samhsa.gov/data/)

97. - Redila VA1, Chavkin C. Stress-induced reinstatement of cocaine seeking is mediated by the kappa opioid system. *Psychopharmacology (Berl)*. 2008, 200(1), 59-70. doi: 10.1007/s00213-008-1122-y. Epub 2008 Jun 25.
98. Sperling RE1, Gomes SM, Sypek EI, Carey AN, McLaughlin JP. Endogenous kappa-opioid mediation of stress-induced potentiation of ethanol-conditioned place preference and self-administration. *Psychopharmacology (Berl)*. 2010, 210(2), 199-209. doi: 10.1007/s00213-010-1844-5. Epub 2010 Apr 17.
99. Toni S Shippenberg. The dynorphin/kappa opioid receptor system: a new target for the treatment of addiction and affective disorders? *Neuropsychopharmacology*. 2009, 34, 247; doi:10.1038/npp.2008.165.
100. Charles Chavkin. The Therapeutic Potential of κ -Opioids for Treatment of Pain and Addiction. *Neuropsychopharmacology*. 2011, 36, 369–370; doi:10.1038/npp.2010.137.
101. Diana Martinez, MD, and Pierre Trifilieff, PhD. Targeting the Brain Stress System to Treat Addiction, *ASAM Magazine*. June 12, 2015.]
<http://www.asam.org/magazine/read/article/2015/06/12/targeting-the-brain-stress-system-to-treat-addiction>. [Retrieved Nov.,15, 2015]
102. Igor Bazov, Olga Kononenko, Hiroyuki Watanabe, Vesna Kuntić, Daniil Sarkisyan, Malik M. Taqi, Muhammad Z. Hussain, Fred Nyberg, Tatjana Yakovleva and Georgy Bakalkin. The endogenous opioid system in human alcoholics: molecular adaptations in brain areas involved in cognitive control of addiction. *Addiction Biology*. 2013,18,1, 161–169.
103. Sharkey, J., Glen, K. A., Wolfe, S., & Kuhar, M. J. Cocaine binding at sigma receptors.

- Eur J Pharmacol. 1988, 149, 171–174.
104. Romieu, P., Martin-Fardon, R., & Maurice, T. Involvement of the sigma1 receptor in the cocaine-induced conditioned place preference. *Neuroreport*. 2000, 11, 2885–2888.
105. Romieu, P., Phan, V. L., Martin-Fardon, R., & Maurice, T. Involvement of the sigma1 receptor in cocaine-induced conditioned place preference: Possible dependence on dopamine uptake blockade. *Neuropsychopharmacology*. 2002, 26, 444–455.
106. Matsumoto, R. R., McCracken, K. A., Pouw, B., Zhang, Y., & Bowen, W. D. Involvement of sigma receptors in the behavioral effects of cocaine: Evidence from novel ligands and antisense oligodeoxynucleotides. *Neuropharmacology*. 2002, 42, 1043–1055.
107. Nidhi Kaushal, Matthew J. Robson, Harsha Vinnakota, Sanju Narayanan, Bonnie A. Avery, Christopher R. McCurdy, and Rae R. Matsumoto. Synthesis and Pharmacological Evaluation of 6-Acetyl-3-(4-(4-(4-fluorophenyl) piperazin-1-yl)butyl)benzo[d]oxazol-2(3H)-one (SN79), a Cocaine Antagonist, in Rodents. *The AAPS Journal*. 2011, 13, 3.
108. Yan-Tong Xu, Nidhi Kaushal, Jamaluddin Shaikh, Lisa L. Wilson, Christophe Mésangeau, Christopher R. McCurdy and Rae R. Matsumoto. A novel substituted piperazine, CM156, attenuates the stimulant and toxic effects of cocaine in mice. *The Journal of Pharmacology and Experimental Therapeutics*. 2010, 333(2), 491–500.
109. Xu YT, Robson MJ, Szeszel-Fedorowicz W, Patel D, Rooney R, McCurdy CR, Matsumoto RR. CM156, a sigma receptor ligand, reverses cocaine induced place conditioning and transcriptional responses in the brain. *Pharmacology, Biochemistry and Behavior*. 2012, 101(1), 174–180.
110. Matsumoto, R. R.; McCracken, K. A.; Friedman, M. J.; Pouw, B.; De Costa, B. R.; Bowen, W. D. Conformationally restricted analogs of BD1008 and an antisense

- oligodeoxynucleotide targeting sigma1 receptors produce anti-cocaine effects in mice. *Eur. J. Pharmacol.* 2001, 419, 163-74.
111. Martin-Fardon, R., Maurice, T., Aujla, H., Bowen, W. D., & Weiss, F. Blockade of σ_1 receptors attenuates conditioned reinstatement but not self-administration maintained by cocaine or a potent conventional reinforcer. *Neuropsychopharmacology*. 2007, 32, 1967–1973.
112. Takato Hiranita; Jianjing Cao; Stephen J Kohut; Theresa A Kopajtic; Amy Hauck Newman; Paul Levi Soto; Gianluigi Tanda; Jonathan L Katz. Decreases in cocaine self-administration with dual inhibition of the dopamine transporter and σ receptors. *The Journal of pharmacology and experimental therapeutics* 2011, 339 (2), 662-77.
113. Jupp, B., & Lawrence, A. J. New horizons for therapeutics in drug and alcohol abuse. *Pharmacology & Therapeutics*. 2010, 125(1), 138–168.
114. Nguyen, E. C., McCracken, K. A., Liu, Y., Pouw, B., & Matsumoto, R. R. Involvement of sigma (sigma) receptors in the acute actions of methamphetamine: Receptor binding and behavioral studies. *Neuropharmacology*. 2005, 49(5), 638–645.
115. Ujike, H.; Kanzaki, A.; Okumura, K.; Akiyama, K.; Otsuki, S. Sigma (σ) antagonist BMY 14802 prevents methamphetamine-induced sensitization. *Life Sci*. 1992, 50, PL129-132.
116. Takashi, S.; Miwa, T.; Hirikomi, K. Involvement of sigma-1 receptors in methamphetamine-induced behavioral sensitization in rats. *Neurosci. Lett.* 2000, 289, 21-24.
117. Matsumoto, R.R.; Shaikh, J.; Wilson, L.L.; Vedam, S.; Coop, A. Attenuation of methamphetamine-induced effects through the antagonism of sigma (σ) receptors:

- evidence from in vivo and in vitro studies. *Eur. Neuropsychopharmacol.* 2008, 18, 871-881.
118. Nidhi Kaushal, Michael J. Seminerio, Jamaluddin Shaikh , Mark A. Medina, Christophe Mesangeau, Lisa L. Wilson, Christopher R. McCurdy, Rae R. Matsumoto. CM156, a high affinity sigma ligand, attenuates the stimulant and neurotoxic effects of methamphetamine in mice. *Neuropharmacology.* 2011, 61, 992-1000.
119. Matthew J. Robson, Ryan C. Turner, Zachary J. Naser, Christopher R. McCurdy, Jason D. Huber, Rae R. Matsumoto. SN79, a sigma receptor ligand, blocks methamphetamine-induced microglial activation and cytokine upregulation. *Experimental Neurology.* 2013, 247, 134–142.
120. Seminerio MJ1, Robson MJ, Abdelazeem AH, Mesangeau C, Jamalapuram S, Avery BA, McCurdy CR, Matsumoto RR.. (2012). Synthesis and pharmacological characterization of a novel sigma receptor ligand with improved metabolic stability and antagonistic effects against methamphetamine. *American Association of Pharmaceutical Scientists Journal.* 2012, 14, 43–51.
121. Michael J. Seminerio, Matthew J. Robson, Ahmed H. Abdelazeem, Christophe Mesangeau, Seshulatha Jamalapuram, Bonnie A. Avery, Christopher R. McCurdy, and Rae R. Matsumoto. Synthesis and pharmacological characterization of a novel sigma receptor ligand with improved metabolic stability and antagonistic effects against methamphetamine. *The AAPS Journal.* 2012, 14, (1).
122. Alcohol Use Disorder AUD's certain criteria outlined in the Diagnostic and Statistical Manual of Mental Disorders (DSM). Link: <http://www.niaaa.nih.gov/alcohol-health/overview-alcohol-consumption/alcohol-use-disorders> [Retrieved, Oct. 15, 2015]

123. Substance Use and Mental Health Estimates from the 2013 National Survey on Drug Use and Health-Overview of Findings. The NSDUH Report, September 4, 2014. <http://store.samhsa.gov/product/Substance-Use-and-Mental-Health-Estimates-from-the-2013-National-Survey-on-Drug-Use-and-Health-Overview-of-Findings/NSDUH14-0904>.
124. Maurice, T., Casalino, M., Lacroix, M., & Romieu, P. Involvement of the sigma-1 receptor in the motivational effects of ethanol in mice. *Pharmacol Biochem Behav.* 2003, 74, 869–876.
125. Sabino V.; Cottone P.; Zhao Y.; et al. The sigma-receptor antagonist BD-1063 decreases ethanol intake and reinforcement in animal models of excessive drinking. *Neuropsychopharmacology.* 2008, 34, 1482–1493.
126. Miyatake, R., Furukawa, A., Matsushita, S., Higuchi, S., & Suwaki, H. Functional polymorphisms in the σ_1 receptor gene associated with alcoholism. *Biol Psychiatry.* 2004, 55, 85–90.
127. Alonso G, Phan V, Guillemain I, Saunier M, Legrand A, Anoaal M, Maurice T. Immunocytochemical localization of the sigma1 receptor in the adult rat central nervous system. *Neuroscience.* 2000, 97, 155–170.
128. Kitaichi K, Chabot JG, Moebius FF, Flandorfer A, Glossmann H, Quirion R. Expression of the purported sigma1 (σ_1) receptor in the mammalian brain and its possible relevance in deficits induced by antagonism of the NMDA receptor complex as revealed using an antisense strategy. *J. Chem. Neuroanat.* 2000, 20, 375–387.
129. King, M., Pan, Y. X., Mei, J., Chang, A., Xu, J., & Pasternak, G.W. Enhanced kappaopioid receptor-mediated analgesia by antisense targeting the sigma-1 receptor. *Eur*

- J Pharmacol 1997, 331, R5–6.
130. Mei, J., Pasternak, G. W. σ 1 Receptor modulation of opioid analgesia in the mouse. J Pharmacol Exp Ther 2002, 300, 1070–1074.
131. Chien CC, Pasternak GW. Functional antagonism of morphine analgesia by (+)-pentazocine: evidence for an anti-opioid σ 1 system. Eur. J. Pharmacol. 1993, 250, R7–R8.
132. Chien CC, Pasternak GW. Sigma antagonists potentiate opioid analgesia in rats. Neurosci. Lett. 1995, 190, 137–139
133. Cendan, C.M., Pujalte, J.M., Portillo-Salido, E., Montoliu, L., & Baeyens, J.M. Formalin-induced pain is reduced in sigma-1 receptor knockout mice. Eur J Pharmacol 2005, 511, 73–74.
134. Kim, H. W., Kwon, Y. B., Roh, D. H., Yoon, S. Y., Han, H. J., Beitz, A. J., et al. Intrathecal treatment with sigma-1 receptor antagonists reduces formalin-induced phosphorylation of NMDA receptor subunit 1 and the second phase of formalin test in mice. Br J Pharmacol 2006, 148, 490–498.
135. Kibaly, C., Meyer, L., Patte-Mensah, C., & Mensah-Nyagan, A. G. Biochemical and functional evidence for the control of pain mechanisms by dehydroepiandrosterone endogenously synthesized in the spinal cord. FASEB J 2008, 22, 93–104.
136. Tseng LF, Hogan QH, Wu HE: (+)-Morphine attenuates the (-)-morphine-produced tail-flick inhibition via the sigma-1 receptor in the mouse spinal cord. Life Sci. 2011, 89, 875-877.
137. Terashvili M, Wu HE, Moore RM, Harder DR, Tseng LF: (+)-Morphine and (-)-morphine stereoselectively attenuate the (-)-morphine-produced tail-flick inhibition via

- the naloxone-sensitive sigma receptor in the ventral periaqueductal gray of the rat. *Eur J Pharmacol* 2007, 571, 1-7.
138. Wu HE, Hong JS, Tseng LF: Stereoselective action of (+)-morphine over (-)-morphine in attenuating the (-)-morphine-produced antinociception via the naloxone-sensitive sigma receptor in the mouse. *Eur J Pharmacol* 2007, 571, 145-151.
139. Chien CC, Pasternak GW: Selective antagonism of opioid analgesia by a sigma system. *J Pharmacol Exp Ther*. 1994, 271, 1583-1590. II) Chien CC, Pasternak GW: Sigma antagonists potentiate opioid analgesia in rats. *Neurosci Lett* 1995, 190, 137-139.
140. Mei J, Pasternak GW: Sigma1 receptor modulation of opioid analgesia in the mouse. *J Pharmacol Exp Ther* 2002, 300, 1070-1074.
141. Mei J, Pasternak GW: Modulation of brainstem opiate analgesia in the rat by sigma 1 receptors: a microinjection study. *J Pharmacol Exp Ther* 2007, 322, 1278-1285.
142. L Romero, D Zamanillo, X Nadal, R Sánchez-Arroyos, I Rivera-Arconada, A Dordal, A Montero, A Muro, A Bura, C Segalés, M Laloya, E Hernández, E Portillo-Salido, M Escriche, X Codony, G Encina, J Burgueño, M Merlos, JM Baeyens, J Giraldo, JA López-García, R Maldonado, CR Plata-Salamán, and JM Vela. Pharmacological properties of S1RA, a new sigma-1 receptor antagonist that inhibits neuropathic pain and activity-induced spinal sensitization. *Br J Pharmacol* 2012, 166, 2289-2306.
143. Roh DH, Kim HW, Yoon SY, Seo HS, Kwon YB, Kim KW, Han HJ, Beitz AJ, Lee JH: Intrathecal administration of sigma-1 receptor agonists facilitates nociception: Involvement of a protein kinase C-dependent pathway. *J Neurosci Res* 2008, 86, 3644-3654.
144. Roh DH, Choi SR, Yoon SY, Kang SY, Moon JY, Kwon SG, Han HJ, Beitz AJ, Lee JH:

- Spinal nNOS activation mediates sigma-1 receptor-induced mechanical and thermal hypersensitivity in mice: involvement of PKC-dependent NR1 phosphorylation. *Br J Pharmacol* 2011, 163,1707-1720.
145. Yoon SY, Roh DH, Seo HS, Kang SY, Han HJ, Beitz AJ, Lee JH: Intrathecal injection of the neurosteroid, DHEAS, produces mechanical allodynia in mice: involvement of spinal sigma-1 and GABA receptors. *Br J Pharmacol* 2009, 157, 666-673.
146. Rigaud M, Gemes G, Weyker PD, Cruikshank JM, Kawano T, Wu HE, Hogan QH: Axotomy depletes intracellular calcium stores in primary sensory neurons. *Anesthesiology*. 2009, 111, 381-392.
147. Hogan QH, McCallum JB, Sarantopoulos C, Aason M, Mynlieff M, Kwok WM, Bosnjak ZJ: Painful neuropathy decreases membrane calcium current in mammalian primary afferent neurons. *Pain* 2000, 86, 43-53.
148. McCallum JB, Kwok WM, Sapunar D, Fuchs A, Hogan QH: Painful peripheral nerve injury decreases calcium current in axotomized sensory neurons. *Anesthesiology*. 2006, 105, 160-168.
149. Hayashi T, Maurice T, Su TP: Ca(2+) signaling via sigma(1)-receptors: novel regulatory mechanism affecting intracellular Ca(2+) concentration. *J Pharmacol Exp Ther*. 2000, 293, 788-798.
150. Fishback JA, Robson MJ, Xu YT, Matsumoto RR Sigma receptors: potential targets for a new class of antidepressant drug. *Pharmacol Ther*. 2010, 127, 271-282. doi: 10.1016/j.pharmthera.2010.04.003.
151. Skuza G, Rogoz Z. A potential antidepressant activity of SA4503, a selective σ 1 receptor agonist. *Behav. Pharmacol*. 2002, 13, 537-543.

152. Urani A, Roman FJ, Phan VL, Su TP, Maurice T. The antidepressant-like effect induced by σ 1-receptor agonists and neuroactive steroids in mice submitted to the forced swimming test. *J. Pharmacol. Exp. Ther.* 2001, 298, 1269–1279.
153. Urani A, Romieu P, Portales-Casamar E, Roman FJ, Maurice T. The antidepressant-like effect induced by the sigma1 (σ 1) receptor agonist igmesine involves modulation of intracellular calcium mobilization. *Psychopharmacology (Berl.)* 2002, 163, 26–35.
154. Wang J, Mack AL, Coop A, Matsumoto RR. Novel sigma (σ) receptor agonists produce antidepressant-like effects in mice. *Eur. Neuropsychopharmacol.* 2007, 17, 708–716.
155. Ukai M, Maeda H, Nanya Y, Kameyama T, Matsuno K. Beneficial effects of acute and repeated administrations of σ receptor agonists on behavioral despair in mice exposed to tail suspension. *Pharmacol. Biochem. Behav.* 1998;61:247–252.
156. Sanchez C, Papp M. The selective sigma(2) ligand Lu 28-179 has an antidepressant-like profile in the rat chronic mild stress model of depression. *Behav Pharmacol.* 2000 11, 117–124.
157. Bergeron, R., Debonnel, G., & De Montigny, C. Modification of the N-methyl-D-aspartate response by antidepressant sigma receptor ligands. *Eur J Pharmacol.* 1993, 240, 319–323.
158. Maurice T, Meunier J, Feng B, Ieni J, Monaghan DT. Interaction with σ 1 protein, but not N-methyl-D-aspartate receptor, is involved in the pharmacological activity of donepezil. *J. Pharmacol. Exp. Ther.* 2006, 317, 606–614.
159. Narita, N., Hashimoto, K., Tomitaka, S., & Minabe, Y. Interactions of selective serotonin reuptake inhibitors with subtypes of sigma receptors in rat brain. *Eur J Pharmacol.* 1996, 307, 117–119.

160. Villard, V. Vanessa Villard, Julie Espallergues, Emeline Keller, Alexandre Vamvakides and Tangui Maurice. Antiamnesic and neuroprotective effects of the aminotetrahydrofuran derivative anavex1-41 against amyloid b25- 35-induced toxicity in mice. *Neuropsychopharmacology*. 2009, 34, 1552–1566
161. Villard V, Espallergues J, Keller E, Vamvakides A, Maurice T. Anti-amnesic and neuroprotective potentials of the mixed muscarinic receptor/sigma1 (σ 1) ligand ANAVEX2-73, a novel aminotetrahydrofuran derivative. *J. Psychopharmacol*. 2011, 25(8), 1101-17.
162. Selkoe DJ. Molecular pathology of amyloidogenic proteins and the role of vascular amyloidosis in Alzheimer's disease. *Neurobiol Aging* 1989, 10, 387–395.
163. Selkoe DJ. Cell biology of protein misfolding: the examples of Alzheimer's and Parkinson's diseases. *Nat Cell Biol*. 2004, 6, 1054–1061.
164. Maurice, T., Su, T. P., & Privat, A. (1998). Sigma1 (σ 1) receptor agonists and neurosteroids attenuate β 25–35-amyloid peptide-induced amnesia in mice through a common mechanism. *Neuroscience* 83, 413–428.
165. Meunier, J., Ieni, J., Maurice, T. The anti-amnesic and neuroprotective effects of donepezil against amyloid β 25–35 peptide-induced toxicity in mice involve an interaction with the σ 1 receptor. *Br J Pharmacol*. 2006 (b) 149, 998–1012.
166. Marrazzo, A., Caraci, F., Salinaro, E. T., Su, T. P., Copani, A., & Ronsisvalle, G. Neuroprotective effects of sigma-1 receptor agonists against β -amyloid-induced toxicity. *Neuroreport*. 2005, 16, 1223–1226.
167. Liang Li; Bingzhong Xu; Ying Zhu; Lei Chen; Masahiro Sokabe; Ling Chen. DHEA prevents Ab25-35-impaired survival of newborn neurons in the dentate gyrus

- through a modulation of PI3K-Akt-mTOR signaling. *Neuropharmacology*. 2010, 59, 323–333.
168. Depatie L, Lal S. Apomorphine and the dopamine hypothesis of schizophrenia: a dilemma? *J. Psychiatry. Neurosci.* 2001, 26, 203–220.
169. Chavez-Noriega LE, Marino MJ, Schaffhauser H, Campbell HUC, Conn PJ. Novel potential therapeutics for schizophrenia: focus on the modulation of metabotropic glutamate receptor function. *Curr. Neuropharmacol.* 2005, 3, 9–34.
170. Miyamoto S, Duncan GE, Marx CE, Lieberman JA. Treatments for schizophrenia: a critical review of pharmacology and mechanisms of action of antipsychotic drugs. *Mol Psychiatry*. 2005, 10, 79-104.
171. Skuza G, Rogoz Z. Effect of BD 1047, a sigma receptor antagonist, in the animal models predictive of antipsychotic activity. *Pharmacol. Rep.* 2006, 58, 626–635
172. Guitart X, Codony X, Ballarín M, Dordal A, Farré AJ. E-5842: a new potent and preferential σ ligand: preclinical pharmacological profile. *CNS Drug Rev.* 1998, 4, 201–224.
173. Takahashi S, Sonehara K, Takagi K, Miwa T, Horikomi K, Mita N, Nagase H, Iizuka K, Sakai K. Pharmacological profile of MS-377, a novel antipsychotic agent with selective affinity for σ receptors. *Psychopharmacology (Berl)* 1999, 145, 295–302.
174. Taylor DP, Eison MS, Moon SL, Schlemmer RF Jr, Shukla UA, VanderMaelen CP, Yocca FD, Gallant DJ, Behling SH, Boissard CG. A role for σ binding in the antipsychotic profile of BMY 14802? *NIDA. Res. Monogr.* 1993, 133, 125–157.
175. Poncelet M, Santucci V, Paul R, Gueudet C, Lavastre S, Guitard J, Steinberg R, Terranova JP, Breliere JC, Soubrie P. Neuropharmacological profile of a novel and

- selective ligand of the sigma site: SR 31742A. *Neuropharmacology*. 1993, 32, 605–615.
176. Rückert NG, Schmidt WJ. The σ receptor ligand 1,3-di-(2-tolyl)guanidine in animal models of schizophrenia. *Eur. J. Pharmacol.* 1993, 233, 261–267.
177. Davidson, J.; Miller, R.; Wingfield, M.; Zung, W.; Dren A. T. The first clinical study of BW-234U in schizophrenia, *Psychopharmacol. Bull.* 1982, 18, 1159-1166.
178. Chouinard, G.; Annable, L. An early phase II clinical trial of BW-234U in the treatment of acute schizophrenia in newly admitted patients. *Psychopharmacology* 1984, 84, 282-284.
179. Wojciech, T. B., Thomas, G. E., Mamone, J. Y., Homan, S. M., Levy, B. K., Johnson, and Carmine J. Coscia. Overexpression of sigma receptors in nonneural human tumors. *Cancer Research*, 1991, 51, 6558–6562.
180. Vilner, B. J., John, C. S., Bowen, W. D. Sigma-1 and sigma-2 receptors are expressed in a wide variety of human and rodent tumor cell lines. *Cancer Res*, 1995, 55, 408–413.
181. Spruce BA, Campbell LA, McTavish N, Cooper MA, Appleyard MV, O'Neill M, Howie J, Samson J, Watt S, Murray K, McLean D, Leslie NR, Safrany ST, Ferguson MJ, Peters JA, Prescott AR, Box G, Hayes A, Nutley B, Raynaud F, Downes CP, Lambert JJ, Thompson AM, Eccles S. Small molecule antagonists of the sigma-1 receptor cause selective release of the death program in tumor and self-reliant cells and inhibit tumor growth in vitro and in vivo. *Cancer Res*, 2004, 64, 4875–4886.
182. Wang B, Rouzier R, Albarracin CT, Sahin A, Wagner P, Yang Y, Smith TL, Meric-Bernstam F, Marcelo Aldaz C, Hortobagyi GN, Puztai L.. Expression of sigma-1 receptor in human breast cancer. *Breast Cancer Res Treat*, 2006, 87, 205–214.
183. Aydar, E., Omganer, P., Perrett, R., Djamgoz, M. B., & Palmer, C. P. The expression and

- functional characterization of sigma-1 receptors in breast cancer cell lines. *Cancer Lett*, 2006, 242, 245–257.
184. Wheeler, K. T.; Wang, L. M.; Wallen, C. A.; Childers, S. R.; Cline, J. M.; Keng, P. C.; Mach, R. H. Sigma-2 receptors as a biomarker of proliferation in solid tumours. *Br. J. Cancer* 2000, 82, 1223–1232.
185. Crawford, K. W., & Bowen, W. D. (2002). Sigma-2 receptor agonists activate a novel apoptotic pathway and potentiate antineoplastic drugs in breast tumor cell line. *Cancer Res*, 2002, 62, 313–322. B
186. Crawford, K. W., Bittman, R., Chun, J., Byun, H. S., & Boiwen, W. D. Novel ceramide analogs display selective cytotoxicity in drug-resistant breast tumor cell lines compared to normal breast epithelial cells. *Cell Mol Biol*, 2003, 49, 1017–1023.
187. Ostefeld, M. S., Fehrenbacher, N., Høyer-Hansen, M., Thomsen, C., Farkas, T., Jäättelä, M. Effective tumor cell death by sigma-2 receptor ligand siramesine involves lysosomal leakage and oxidative stress. *Cancer Res*. 2005, 65, 8975–8983.
188. Ostefeld MS, Høyer-Hansen M, Bastholm L, Fehrenbacher N, Olsen OD, Groth-Pedersen L, Puustinen P, Kirkegaard-Sørensen T, Nylandsted J, Farkas T, Jäättelä M. Anti-cancer agent siramesine is a lysosomotropic detergent that induces cytoprotective autophagosome accumulation. *Autophagy*. 2008, 16, 487–499.
189. Jodi L. Haller, Irina Panyutin, Aneeka Chaudhry, Chenbo Zeng, Robert H. Mach, Joseph A. Frank. Sigma-2 Receptor as Potential Indicator of Stem Cell Differentiation *Molecular Imaging and Biology*. 2012, 14, (3), 325-335.
190. Robert H. Mach, Chenbo Zeng, and William G. Hawkins. The σ_2 Receptor: A Novel Protein for the Imaging and Treatment of Cancer. *J. Med. Chem*. 2013, 56, 7137–7160.

191. Moebius, F. F.; Reiter, R. J.; Hanner, M.; Glossmann, H. High affinity of sigma-1 binding sites for sterol isomerization inhibitors: Evidence for a pharmacological relationship with the yeast sterol C8-C7 isomerase. *Br. J. Pharmacol.*, 1997, 121,1-6.
192. Matsuno, K.; Matsunaga, K.; Mita, S. Increase of extracellular acetylcholine level in rat 160 frontal cortex induce by (+)-N-allylnormetazocineas measured by brain microdialysis. *Brain. Res.* 1992, 265, 851-859.
193. Kobayashi, T.; Matsuno, K.; Nakata, K.; Mita, S. Enhancement of acetylcholine release by SA4503, a novel sigma 1 receptor agonist, in the rat brain. *J. Pharmacol. Exp. Ther.* 1996, 279, 106-113.
194. Ablordeppey, S. Y.; Fischer, J. B.; Glennon, R. A. Is a Nitrogen Atom an Important Pharmacophoric Element in Sigma Ligand Binding? *Bioorganic & Medicinal Chemistry* 2000, 8, 2105-2111.
195. Largent, B. L.; Wikstroem, H.; Gundlach, A. L.; Snyder, S. H. Structural determinants of sigma receptor affinity. *Mol. Pharmacol.* 1987, 32, 772-784.
196. Abou-Gharbia, M.; Ablordeppey, S. Y.; Glennon, R. A. Sigma receptors and their 266 ligands: the sigma enigma. *Annu. Rep. Med. Chem.* 1993, 28, 1-10.
197. Walker JM, Bowen WD, Walker FO, Matsumoto RR, de Costa B, Rice KC. Sigma receptors: biology and function. *Pharmacol Rev* 1990, 42:355-402.
198. De Costa BR, He X. Structure-activity relationships and evolution of σ receptor ligands. In: Itzhak, Y., ed. *Sigma Receptors*, Academic Press, London, 1994. pp. 45-111.
199. Nakazato, A.; Ohta, K.; Sekiguchi, Y.; Okuyama, S.; Chaki, S.; Kawashima, Y.; Hatayama, K. Design, synthesis, structure-activity relationships, and biological characterization of novel arylalkoxyphenylalkylamines ligands as potential antipsychotic

- drugs. *J. Med. Chem.* 1999, 42, 1076-1087.
200. Maeda, D. Y.; Williams, W.; Kim, W. E.; Thatcher, L. N.; Bowen, W. D.; Coop, A. N- Arylalkylpiperidines as High-Affinity Sigma-1 and Sigma-2 Receptor Ligands: Phenylpropylamines as Potential Leads for Selective Sigma-2 Agents. *Bioorganic & Medicinal Chemistry Letters* 2002, 12, 497-500.
201. Van de Waterbeemd, H.; El Tayar, N.; Testa, B.; Wikstroem, H.; Largent, B. Quantitative structure-activity relationships and eudismic analyses of the presynaptic dopaminergic activity and dopamine D2 and σ receptor affinities of 3-(3- hydroxyphenyl)piperidines and octahydrobenzo[f]quinolines. *J. Med. Chem.* 1987, 30, 2175-81.
202. Gilligan PJ, Cain GA, Christos TE, Cook L, Drummond S, Johnson AL, Kergaye AA, McElroy JF, Rohrbach KW, Schmidt WK, Tam S W. Novel piperidine sigma receptor ligands as potential antipsychotic drugs. *J Med Chem* 1992, 35:4344-4361.
203. Glennon, R. A.; Ismaiel, A. M.; Smith, J. D.; Yousif, M.; El-Ashmawy, M.; Herndon, J. L.; Fischer, J. B.; Howie, K. J. B.; Server, A. C. Binding of substituted and conformationally restricted derivatives of N-(3-phenyl-n-propyl)-1-phenyl-2-aminopropane at σ -receptors. *J. Med. Chem.* 1991, 34, 1855-9.
204. Glennon, R. A.; El-Ashmawy, M. B.; Fischer, J. B.; Burke-Howie, K. B.; Ismaiel, A. M. N-Substituted 5-phenylpentylamines: a new class of sigma ligands. *Med. Chem. Res.* 1991, 1, 207-212.
205. El-Ashmawy, M. B.; Ablordeppey, S. Y.; Hassan, I. Gad, L.; Fischer, J. B.; Burke-Howie, K. B.; Glennon, R. A. Further investigation of 5-phenyl ethylamines derivatives as novel sigma receptor ligands. *Med. Chem. Res.* 1992, 2, 119-126.
206. Glennon RA, Yousif MY, Ismaiel AM, El-Ashmawy MB, Herndon JL Fischer JB, Server

- AC, Burke-Howie KJ. Novel 1-phenylpiperazine and 4-phenylpiperidine derivatives as high affinity sigma ligands. *J. Med. Chem* 1991, 34:3360-3365.
207. Ablordeppey SY, Issa H, Fischer JB, Burke-Howie KB, Glennon RA. Synthesis and structure-affinity relationship studies of sigma ligands related to haloperidol. *Med Chem Res* 1993, 3:131-138.
208. Su, T. P.; Wu, X. Z.; Cone, E. J.; Shukla, K.; Gund, T. M.; Dodge, A. L.; Parish, D. W. Sigma compounds derived from phencyclidine: identification of PRE-084, a new, selective sigma ligand. *J. Pharmacol. Exp. Ther.* 1991, 259, 543-550.
209. Ablordeppey, S. Y.; Fischer, J. B.; Glennon, R. A. Is a Nitrogen Atom an Important Pharmacophoric Element in Sigma Ligand Binding? *Bioorganic & Medicinal Chemistry* 2000, 8, 2105-2111.
210. Zamoieri, D.; Mamolo, M. G.; Laurini, E.; Florio, C.; Zanette, C.; Fermeglia, M.; Posocco, P.; Paneni, M. S.; Pricl, S.; Vio, L. Synthesis, biological evaluation, and three dimensional in silico pharmacophore model for σ_1 receptor ligands based on a series of substituted Benzo[d]oxazol-2(3H) one derivatives. *J. Med. Chem.* 2009, 52, 5380-5393.
211. Gund, T. M.; Floyd, J.; Jung, D. Molecular modeling of σ_1 receptor ligands: a model of binding conformational and electrostatic considerations. *J. Mol Graph. Mod.* 2004, 22, 221-230.
212. Bowen WD, de Costa BR, Hellewell SB, Walker JM, Rice KC. [3 H](+)-Pentazocine: A potent and highly selective benzomorphan-based probe for sigma-1 receptors. *Mol Neuropharmacol* 1993, 3:117-126.
213. Ablordeppey SY, Fischer JB, Burke Howie KJ, Glennon RA. Design, synthesis and binding of sigma receptor ligands derived from butaclamol. *Med Chem Res* 1992, 2:368-

375.

214. Bowen WD, Moses EL, Tolentino PJ, Walker JM. Metabolites of haloperidol display preferential activity at sigma receptors compared to dopamine D-2 receptors. *Eur J Pharmacol* 1990, 177:111-118.
215. Guitart, X.; Farre, A. J. The effect of E-5842, a σ receptor ligand and potential atypical antipsychotic, on Fos expression in rat forebrain. *Eur. J. Pharmacol.* 1998, 363, 127-130.
216. Guitart, X.; Ballarin, M.; Codony, X.; Dordal, A.; Farre, A. J.; Frigola, J.; Merce, R. E-5842: antipsychotic σ -receptor ligand. *Drugs of the Future.* 1999, 24, 386-392.
217. Huang, Y.; Hammond, P. S.; Whirrett, B. R.; Kuhner, R. J.; Wu, L.; Childers, S. R.; Mach, R. H. Synthesis and Quantitative Structure-Activity Relationships of N-(1-Benzylpiperidin-4-yl)phenylacetamides and Related Analogs as Potent and Selective σ_1 Receptor Ligands. *J. Med. Chem.* 1998, 41, 2361-2370.
218. Huang, Y.; Hammond, P. S.; Wu, L.; Mach, R. H. Synthesis and structure-activity relationships of N-(1-benzylpiperidin-4-yl)arylamide analogues as potent sigma-1 receptor ligands. *J. Med. Chem.* 2001, 44, 4404-4415.
219. Chaki, S.; Tanaka, M.; Muramatsu, M.; Otomo, S. NE-100, a novel potent σ ligand, preferentially binds to σ_1 binding sites in guinea pig brain. *Eur. J. Pharmacol.* 1994, 251, R1-R2.
220. T. Schlaeger, D. Schepmann, K. Lehmkuhl, J. Holenz, J. M. Vela, H. Buschmann, B. Wuensch, *J. Med. Chem.* 2011, 54, 6704.
221. C. Oberdorf, D. Schepmann, J. M. Vela, H. Buschmann, J. Holenz, B. Wuensch, *J. Med. Chem.* 2012, 55, 5350.
222. Maeda, D. Y.; Williams, W.; Bowen, W. D.; Coop, A. A sigma-1 receptor selective

- analogue of BD1008. A potential substitute for (+)-opioids in sigma receptor binding assays. *Bioorg. Med. Chem. Lett.* 2000, 10, 17-18.
223. Quaglia, W.; Giannella, M.; Piergentili, A.; Pignini, M.; Brasili, L.; Di Toro, R.; Rossetti, L.; Spampinato, S.; Melchiorre, C. 1'-Benzyl-3,4-dihydrospiro[2H-1- benzothiopyran-2,4'-piperidine] (Spipethiane), a Potent and Highly Selective σ_1 Ligand. *J. Med. Chem.* 1998, 41, 1557-1560.
224. Beradi, F.; Santoro, S.; Perrone, R.; Tortorella, V.; Govoni, S.; Lucchi, L. N-[ω -(Tetralin-1-yl)alkyl] Derivatives of 3,3-Dimethylpiperidine Are Highly Potent and Selective σ_1 or σ_2 Ligands. *J. Med. Chem.* 1998, 41, 3940-3947.
225. Beradi, F.; Ferorelli, S.; Abate, C.; Pedone, M. P.; Colabufo, N. A.; Contino, M.; Perrone, R. Methyl Substitution on the Piperidine Ring of N-[ω -(6- Methoxynaphtalen-1-yl)alkyl] Derivatives as a Probe for selective Binding and Activity at the σ_1 Receptor. *J. Med. Chem.* 2005, 48, 8237- 8244.
226. Beradi, F.; Ferorelli, S.; Abate, C.; Colabufo, N. A.; Contino, M.; Perrone, R.; Tortorella, V. 4- (Tetralin-1-yl)- and 4-(Naphthalen-1-yl) alkyl Derivatives of 1-Cyclohexylpiperazine as Receptor Ligands with Agonist σ Activity *J. Med. Chem.* 2004, 47, 2308- 2317.
227. Yous, S.; Wallez, V.; Belloir, M.; Caignard, D. H.; McCurdy, C. R.; Poupaert, J. H. Novel 2(3H)-Benzothiazolones as highly potent and selective sigma-1 receptor ligands. *Med. Chem. Res.* 2005, 14, 158-168.
228. R. Bhat, J. A. Fishback, R. R. Matsumoto, J. H. Poupaert, C. R. McCurdy, *Bioorg. Med. Chem. Lett.* 2013, 23, 5011.
229. Bowen WD, Bertha CM, Vilner BJ, Rice KC. CB-64D and CB- 184: ligands with high "2

- receptor affinity and subtype selectivity. *Eur J Pharmacol* 1995; 278: 257-60.
230. Bertha CM, Mattson MV, Flippen-Anderson JL, et al. A marked change of receptor affinity of the 2-methyl-5-(3- hydroxyphenyl) morphans upon attachment of an (E)-8-benzylidene moiety: synthesis and evaluation of a new class of sigma receptor ligands. *J Med Chem* 1994; 37: 3163-70.
231. Carmen Abate, Roberto Perrone and Francesco Berardi. Classes of Sigma2 (σ_2) Receptor Ligands: Structure Affinity Relationship (SAfiR) Studies and Antiproliferative Activity. *Current Pharmaceutical Design*, 2012, 18, 938-949.
232. Bowen WD, Vilner BJ, Williams W, Bertha CM, Kuehne ME, Jacobson AE. Ibogaine and its congeners are σ_2 receptor-selective ligands with moderate affinity. *Eur J Pharmacol* 1995; 279: R1-R3.
233. Bowen, W. D. Sigma receptors and iboga alkaloids. *Alkaloids (Academic Press)* 2001, 56,173-191.
234. Moltzen, E. K.; Perregaard, J.; Meier, E. σ Ligands with Subnanomolar Affinity and Preference for the σ_2 Binding Site. 2. Spiro-Joined Benzofuran, Isobenzofuran, and Benzopyran Piperidines. *J. Med. Chem.* 1995, 38, 2009-2017.
235. Perregaard J, Moltzen EK, Meier E, Sanchez C. " Ligands with subnanomolar affinity and preference for the σ_2 binding site. 1. 3 (w-Aminoalkyl)-1H-indoles. *J Med Chem* 1995; 38: 1998-2008.
236. Mach RH, Vangveravong S, Huang Y, Yang B, Blair JB, Wu L. Synthesis of *N*-substituted 9- azabicyclo[3.3.1]nonan-3a-yl phenylcarbamate analogs as sigma-2 receptor ligands. *Med Chem Res* 2003,11:380-398.
237. Mach RH, Wu L, West T, Whirrett BR, Childers SR. The analgesic tropane analogue (+/-

-)-SM 21 has a high affinity for sigma-2 receptors. *Life Sci* 1999, 64:PL131-PL137.
238. Matsumoto RR, Mack AL. (+/-)-SM 21 attenuates the convulsive and locomotor stimulatory effects of cocaine. *Eur J Pharmacol* 2001, 417:R1-R2.
239. Mach RH, Huang Y, Freeman RA, Wu L, Vangveravong S, Luedtke RR. Conformationally-flexible benzamide analogues as dopamine D3 and s2 receptor ligands. *Bioorg Med Chem* 2004; 14: 195-202.
240. Xu R, Lever JR, Lever SZ. Synthesis and in vitro evaluation of tetrahydroisoquinolinyll benzamides as ligands for receptors. *Bioorg Med Chem Lett* 2007; 17: 2594-97.
241. Fan KF, Lever JR, Lever SZ. Effect of structural modification on amine portion of substituted aminobutyl-benzamides as ligands for binding s1 and s2 receptors. *Bioorg Med Chem* 2011; 19: 1852-59.
242. Menkel M, Terry P, Pontecorvo M, Katz JL, Witkin JM. Selective sigma ligands block stimulant effects of cocaine. *Eur J Pharmacol* 1991, 201:251-252.
243. Ujike H, Kuroda S, Otsuki S. Sigma receptor antagonist block the development of sensitization to cocaine. *Eur J Pharmacol* 1996, 296:123-128.
244. Contreras PC, Bremer ME, Rao TS. GBR-12909 and fluspirilene potently inhibited binding of [³H] (+) 3-PPP to sigma receptors in rat brain. *Life Sci* 1990, 47:133-137.
245. Husbands SM, Izenwasser S, Loeloff RJ, Katz JL, Bowen WD, Vilner BJ, Newman AH. Isothiocyanate derivatives of 9-[3-(*cis*-3,5-dimethyl-1-piperazinyll)propyl]-carbazole (rimcazole): irreversible ligands for the dopamine transporter. *J Med Chem* 1997, 40:4340-4346.
246. Husbands SM, Isenwasser S, Kopajtic T, Bowen WD, Vilner BJ, Katz JL, Newman AH. Structure-activity relationships at the monoamine transporters and sigma receptors for a

- novel series of 9-[3-*cis*-3,5-dimethyl-1-piperazinyl)-propyl]carbazole (rimcazole) analogues. *J Med Chem* 1999, 42:4446-4455.
247. Cao JJ, Husbands SM, Kopajtic T, Katz JL, Newman AH. [3-*cis*-3,5-Dimethyl-(1-piperazinyl)alkyl]-bis-(4'-fluorophenyl)amine analogues as novel probes for the dopamine transporter. *Bioorg Med Chem Lett* 2001, 11:3169-3173.
248. Cao JJ, Kulkarni SS, Husbands SM, Bowen WD, Williams W, Kopajtic T, Katz JL, George C, Newman AH. Dual probes for the dopamine transporter and sigma-1 receptors: novel piperazinyl alkyl-*bis*-(4'-fluorophenyl)amine analogues as potential cocaine-abuse therapeutic agents. *J Med Chem* 2003, 46:2589-2598.
249. De Costa, B. R.; Bowen, W. D.; Hellewell, S. B.; Walker, J. M.; Thurkauf, A.; Jacobson, A. E.; Rice, K. C. Synthesis and evaluation of optically pure [3H]-(+)-pentazocine, a highly potent and selective radioligand for σ receptors. *FEBS Lett.* 1989, 251, 53-8.
250. S. Banister, D. Roeda, F. Dollé, M. Kassiou, Fluorine-18 Chemistry for PET: A Concise Introduction *Curr. Radiopharm.* 2010, 3, 68.
251. Ishiwata, K.; Tsukada, H.; Kawamura, K.; Kimura, Y.; Nishiyama, S.; Kobayashi, T.; VMatsuno, K.; Senda, M. Mapping of CNS sigma1 receptors in the conscious monkey: Preliminary PET study with [11C]SA4503. *Synapse.* 2001, 40, 235-237.
252. Kawamura, K.; Kimura, Y.; Tsukada, H.; Kobayashi, T.; Nishiyama, S.; Kakiuchi, T.; Ohba, H.; Harada, N.; Matsuno, K.; Ishii, K.; Ishiwata, K. An increase in sigma-1 receptors in aged monkey brain. *Neurobiol. Ageing.* 2003, 24, 745-752.
253. Ishikawa, M.; Ishiwata, K.; Ishii, K.; Kimura, Y.; Sakata, M.; Naganawa, M.; Oda, K.; Miyatake, R.; Fujisaki, M.; Shimizu, E.; Shiramaya, Y.; Iyo, M.; Hashimoto, K. High occupancy of sigma-1 receptors in human brain after single oral administration of

- fluvoxamine: a positron emission tomography study using [11C]SA4503. *Biol. Psychiatry*. 2007, 62, 878-883.
254. Kawamura, K.; Tsukada, H.; Shiba, K.; Tsuji, C.; Harada, N.; Kimura, Y.; Ishiwata, K. Synthesis and evaluation of fluorine-18-labeled SA4503 as a selective sigma1 receptor ligand for positron emission tomography. *Nucl. Med. Biol.* 2007, 34, 571-577.
255. Maestrup, E. G.; Fischer, S.; Wiese, C.; Schepmann, D.; Hiller, A.; Deuther-Conrad, W.; Steinbach, J.; Wunsch, B.; Burst, P. Evaluation of spirocyclic 3-(3-Fluoropropyl)-2-benzofuran as σ_1 receptor ligands for neuroimaging with positron imaging tomography. *J. Med. Chem.* 2009, 52, 6062-6072.
256. James A. Fishback, Christophe Mesangeau, Jacques H. Poupaert, Christopher R. McCurdy, Rae R. Matsumoto. Synthesis and characterization of [3H]-SN56, a novel radioligand for the σ_1 receptor. *European Journal of Pharmacology* 653 (2011) 1–7.
257. Weber, E.; Sonders, M.; Quarum, M.; McLean, S.; Pou, S.; Keana, J. F. W. 1,3-Di(2-[5-3H]tolyl)guanidine: a selective ligand that labels σ -type receptors for psychotomimetic opiates and antipsychotic drugs. *Proc. Natl. Acad. Sci. U. S. A.* 1986, 83, 8784-8788.
258. Rowland, D. J.; Tu, Z.; Xu, J.; Ponde, D.; Mach, R. H.; Welch, M. J. Synthesis and in vivo evaluation of 2 high-affinity ⁷⁶Br-labeled σ_2 -receptor ligands. *J. Nucl. Med.* 2006, 47, 1041-1048.
259. Xu J, Tu Z, Jones LA, Wheeler KT, Mach RH. [3H]N-[4-(3,4-dihydro-6,7-dimethoxyisoquinolin-2(1H)-yl)butyl]-2-methoxy-5-methylbenzamide: a novel sigma-2 receptor probe. *Eur J Pharmacol* 2005; 525: 8-17.
260. Phase I Clinical Trial. [ClinicalTrials.gov Identifier: NCT00968656](https://clinicaltrials.gov/ct2/show/study/NCT00968656). Assessment of Cellular Proliferation in Tumors by Positron Emission Tomography (PET) Using

[18F]ISO-1 (PET/CT).

261. Tu, Z.; Xu, J.; Jones, L. A.; Li, S.; Zeng, D.; Kung, M. P.; Kung, H. F.; Mach, R. H. Radiosynthesis and biological evaluation of a promising σ_2 receptor ligand radiolabeled with fluorine-18 or iodine-125 as a PET/SPECT probe for imaging breast cancer. *Appl. Radiat. Isot.* 2010, 68, 2268-2273
262. WHO; GLOBOCAN 2012: Estimated Incidence, Mortality and Prevalence Worldwide in 2012. Accessed 08/06/2015. http://globocan.iarc.fr/Pages/fact_sheets_cancer.aspx.
263. Cancer chemotherapy: Wikipedia;
https://en.wikipedia.org/wiki/Chemotherapy#cite_ref-psk_61-0
264. Vadhan-Raj S (Jan 2009). "Management of chemotherapy-induced thrombocytopenia: current status of thrombopoietic agents". *Seminars in Hematology* 46 (1 Suppl 2): S26–32.
265. "Coriolus Versicolor". Cancer.org. 2008-06-10. Accessed 7 August 2015. http://www.cancer.org/docroot/ETO/content/ETO_5_3X_Coriolous_Versicolor.asp
266. Lemieux J (Oct 2012). "Reducing chemotherapy-induced alopecia with scalp cooling". *Clinical Advances in Hematology & Oncology*, 2012, 10, 681–682.
267. Volz HP, Stoll KD. Clinical trials with sigma ligands. *Pharmacopsychiatry* 2004, 37, S214–S220.
268. Kunitachi S, Fujita Y, Ishima T, Kohno M, Horio M, Tanibuchi Y, Shirayama Y, Iyo M, Hashimoto K. Phencyclidine-induced cognitive deficits in mice are ameliorated by subsequent subchronic administration of donepezil: Role of sigma-1 receptors. *Brain Res* 2009, 1279, 189–196.
269. Maurice T, Su TP. The pharmacology of sigma-1 receptors. *Pharmacol Ther* 2009, 124,

195–206.

270. C. Meyer, K. Schmieding, E. Falkenstein, M. Wehling, Are high-affinity progesterone binding site(s) from porcine liver microsomes members of the sigma receptor family? *Eur. J. Pharmacol.* 1998, 347, 293–299.
271. Ahmed IS, Rohe HJ, Twist KE, Craven RJ. Pgrmc1 (progesterone receptor membrane component 1) associates with epidermal growth factor receptor and regulates erlotinib sensitivity. *J Biol Chem*, 2010, 285, 24775–24782.
272. Mir SUR, Jin L, Craven RJ. Neutrophil gelatinase-associated lipocalin (NGAL) expression is dependent on the tumor-associated sigma-2 receptor S2RPgrmc1. *J Biol Chem* 2012, 287, 14494–14501.
273. Cahill MA. Progesterone receptor membrane component 1: an integrative review. *J Steroid Biochem Mol Biol.* 2007;105:16–36.
274. Peluso JJ, Liu X, Gawkowska A, Lodde V, Wu CA. Progesterone inhibits apoptosis in part by PGRMC1-regulated gene expression. *Mol Cell Endocrinol.* 2010, 320, 153–161.
275. Chen JI, et al. Proteomic characterization of midproliferative and midsecretory human endometrium. *J Proteome Res.* 2009, 8, 2032–2044.
276. Intlekofer KA, Petersen SL. Distribution of mRNAs encoding classical progestin receptor, progesterone membrane components 1 and 2, serpine mRNA binding protein 1, and progestin and ADIPOQ receptor family members 7 and 8 in rat forebrain. *Neuroscience.* 2011, 172, 55–65.
277. Suchanek M, Radzikowska A, Thiele C. Photo-leucine and photo-methionine allow identification of protein-protein interactions in living cells. *Nat Methods.* 2005, 2, 261–267.

278. Szczesna-Skorupa E, Kemper B. Progesterone receptor membrane component 1 inhibits the activity of drug-metabolizing cytochromes P450 and binds to cytochrome P450 reductase. *Mol Pharmacol.* 2011, 79, 340–350.
279. Yang T, et al. Crucial step in cholesterol homeostasis: sterols promote binding of SCAP to INSIG-1, a membrane protein that facilitates retention of SREBPs in ER. *Cell.* 2002,110, 489–500.
280. Peluso JJ, Pappalardo A, Losel R, Wehling M. Progesterone membrane receptor component 1 expression in the immature rat ovary and its role in mediating progesterone's antiapoptotic action. *Endocrinology.* 2006, 147, 3133–3140.
281. Al-Nabulsi I, et al. Effect of ploidy, recruitment, environmental factors, and tamoxifen treatment on the expression of sigma-2 receptors in proliferating and quiescent tumour cells. *Br J Cancer.* 1999;81:925–33.
282. Peluso JJ, Lodde V, Liu X. Progesterone regulation of progesterone receptor membrane component 1 (PGRMC1) sumoylation and transcriptional activity in spontaneously immortalized granulosa cells. *Endocrinology* 2012, 153(8):3929–3939.
283. Peluso JJ, DeCerbo J, Lodde V. Evidence for a genomic mechanism of action for progesterone receptor membrane component-1. *Steroids* 2012, 77, 1007–1012.
284. Groth Pedersen L, Ostenfeld MS, Hoyer Hansen M, Nylandsted J, Jaattela M. Vincristine induces dramatic lysosomal changes and sensitizes cancer cells to lysosome destabilizing siramisine. *Cancer Res* 2007, 67, 2217–2225.
285. Zeng C, Rothfuss J, Zhang J, Chu W, Vangveravong S, Tu Z, Pan F, Chang KC, Hotchkiss R, Mach RH. Sigma-2 ligands induce tumour cell death by multiple signaling pathways. *Br J Cancer* 2012, 106, 693–701.

286. Vilner BJ, Bowen WD, Modulation of cellular calcium by sigma-2 receptors: Release from intracellular stores in human SK-N-SH neuroblastoma cells. *J Pharmacol Exp Ther* 2000, 292, 900–911.
287. Cassano G, Gasparre G, Contino M, Niso M, Berardi F, Perrone R, Colabufo NA. The sigma-2 receptor agonist PB28 inhibits calcium release from the endoplasmic reticulum on SK-N-SH neuroblastoma cells. *Cell Calcium* 2006, 40, 23–28
288. Cassano G, Gasparre G, Niso M, Contino M, Scalera V, Colabufo NA. F281, synthetic agonist of the sigma-2 receptor, induces Ca^{2+} efflux from the endoplasmic reticulum and mitochondria in SK-N-SH cells. *Cell Calcium* 2009, 45, 340–345.
289. Monassier L, Manoury B, Bellocq C, Weissenburger J, Greney H, Zimmermann D, Ehrhardt JD, Jaillon P, Baro I, Bousquet P. Sigma-2 receptor ligand-mediated inhibition of inwardly rectifying K^+ channels in the heart. *J Pharmacol Exp Ther* 2007, 322, 341–350.
290. Hornick JR, Vangveravong S, Spitzer D, Abate C, Berardi F, Goedegebuur P, Mach RH, Hawkins WG. Lysosomal membrane permeabilization is an early event in sigma-2 receptor ligand mediated cell death in pancreatic cancer. *J Exp Clin Cancer Res* 2012, 31, 41.
291. Colabufo NA, Berardi F, Contino M, Ferorelli S, Niso M, Perrone R, et al. Correlation between sigma2 receptor protein expression and histopathologic grade in human bladder cancer. *Cancer Lett.* 2006, 237, 83-88.
292. Mach RH, Wheeler KT. Imaging the proliferative status of tumors with PET. *J. Labelled Compd. Radiopharm.* 2007; 50: 366-369.
293. Tu Z, Dence CS, Ponde DE, Jones L, Wheeler KT, Welch MJ, Mach RH. Carbon-11

- labeled sigma-2 receptor ligands for imaging breast cancer. *Nucl Med Biol* 2005, 32, 423–430.
294. Kashiwagi H, McDunn JE, Simon PO, Jr., Goedegebuure PS, Xu J, Jones L, Chang K, Johnston F, Trinkaus K, Hotchkiss RS, Mach RH, Hawkins WG. Selective sigma-2 ligands preferentially bind to pancreatic adenocarcinomas: Applications in diagnostic imaging and therapy. *Mol Cancer* 2007, 6, 48.
295. Szabadkai G, Rizzuto R. Participation of endoplasmic reticulum and mitochondrial calcium handling in apoptosis: More than just neighborhood? *FEBS Lett* 2004, 567, 111–115.
296. John CS, Vilner BJ, Geyer BC, Moody T, Bowen WD. Targeting sigma receptor-binding benzamides as in vivo diagnostic and therapeutic agents for human prostate tumors. *Cancer Res* 1999, 59, 4578–4583.
297. Brent PJ, Pang GT. Sigma binding site ligands inhibit cell proliferation in mammary and colon carcinoma cell lines and melanoma cells in culture. *Eur J Pharmacol* 1995, 278, 151-60.
298. Jonhede S, Peterson A, Zetterberg M, Karlsson JO. Acute effects of the sigma-2 receptor agonist siramesine on lysosomal and extra-lysosomal proteolytic systems in lens epithelial cells. *Mol Vision* 2010,16, 819–827.
299. Megalizzi V, Le Mercier M, Decaestecker C. Sigma receptors and their ligands in cancer biology: overview and new perspectives for cancer therapy. *Med Res Rev.* 2012, 32, 410-427.
300. Hornick JR, Spitzer D, Goedegebuure P, Mach RH, Hawkins WG. Therapeutic targeting of pancreatic cancer utilizing sigma-2 ligands. *Surgery.* 2012, 152, S152-156.

301. Abate C, Ferorelli S, Niso M, Lovicario C, Infantino V, Convertini P, et al. 2-Aminopyridine derivatives as potential σ (2) receptor antagonists. *ChemMedChem*. 2012, 7, 1847-1857.
302. Hornick JR, Xu JB, Vangveravong S, Tu Z, Mitchem JB, Spizer D, Goedegebuure P, Mach RH, Hawkins WG. The novel sigma-2 receptor ligand SW43 stabilizes pancreas cancer progression in combination with gemcitabine. *Mol Cancer*. 2010, 9, 298.
303. Kashiwagi H, McDunn JE, Simon PO, Jr., Goedegebuure PS, Vangeravong S, Chang K, Hotchkiss RS, Mach RH, Hawkins WG. Sigma-2 receptor ligands potentiate conventional chemotherapies and improve survival in models of pancreatic adenocarcinoma. *J Transl Med*. 2009,7, 24.
304. Azzariti A, Colabufo NA, Berardi F, Porcelli L, Niso M, Simone GM, et al. Cyclohexylpiperazine derivative PB28, a sigma2 agonist and sigma1 antagonist receptor, inhibits cell growth, modulates P-glycoprotein, and synergizes with anthracyclines in breast cancer. *Mol Cancer Ther*. 2006, 5, 1807-1816.
305. Abate C, Niso M, Contino M, Colabufo NA, Ferorelli S, Perrone R, et al. 1-Cyclohexyl-4-(4-arylcyclohexyl)piperazines: Mixed s and human $\Delta(8)$ - $\Delta(7)$ sterol isomerase ligands with antiproliferative and P-glycoprotein inhibitory activity. *Chem Med Chem*. 2011, 6, 73-80.
306. Spitzer D, Simon PO Jr, Kashiwagi H, Xu J, Zeng C, Vangveravong S, et al. Use of multifunctional sigma-2 receptor ligand conjugates to trigger cancer-selective cell death signaling. *Cancer Res*. 2012, 72, 201-209.
307. Kashiwagi H, McDunn JE, Goedegebuure PS, Gaffney MC, Chang K, Trinkaus K, et al. TAT-Bim induces extensive apoptosis in cancer cells. *Ann Surg Oncol*. 2007, 14, 1763-

- 1771.
308. Torchilin VP Passive and active drug targeting: drug delivery to tumors as an example. *Handb Exp Pharmacol*. 2010, 197, 3–53.
309. van Waarde, A., Rybczynska, A. A., Ramakrishnan, N. K., Ishiwata, K., Elsinga, P. H., & Dierckx, R. A. (2014). Potential applications for sigma receptor ligands in cancer diagnosis and therapy. *Biochimica et Biophysica Acta (BBA)-Biomembranes*. <https://dx.doi.org/10.1016/j.bbamem.2014.08.022>.
310. Zhang Y, Huang Y, Zhang P, Gao X, Gibbs RB, Li S. Incorporation of a selective sigma-2 receptor ligand enhances uptake of liposomes by multiple cancer cells. *Int J Nanomed*. 2012, 7:4473–4485.
311. Hilary Nicholson, Anthony Comeau, Christophe Mesangeau, Christopher R. McCurdy, and Wayne D. Bowen. Characterization of CM572, a Selective Irreversible Partial Agonist of the Sigma-2 Receptor with Antitumor Activity. *J Pharmacol Exp Ther*. 354:203–212, August 2015.
312. <http://en.wikipedia.org/wiki/Stimulant> (Accessed 10/15/2015)
313. Research Report: <http://www.drugabuse.gov/publications/research-reports/> (Accessed 10/15/2015).
314. Lexicon of alcohol and drug terms. WHO; Geneva 1994. 1) Substance abuse-terminology. ISBN 92 4 154468 6.
<http://whqlibdoc.who.int/publications/9241544686.pdf?ua=1>(Accessed 10/15/2015).
315. World Drug Report 2012; United Nations Office On Drugs And Crime (Vienna). (www.unodc.org)
316. Hardman, Joel G., and Limbird, Lee E., eds. (1996). Goodman & Gilman's The

Pharmacological Basis of Therapeutics, 9th edition. New York: McGraw-Hill, Health Professions Division.

317. Voet, Donald, and Voet, Judith G. (1995). Biochemistry, 2nd edition. New York: Wiley

318. Robert C. Peterson, Ph.D. (May 1977). ["NIDA research monograph #13: Cocaine 1977, Chapter I"](#) . Retrieved 06/06/2015.

319. Perrine, D. M. The chemistry of mind-alerting drugs; history, pharmacology and cultural context. American chemical society, Washington, DC. 1996, 181-182.

320. Cocaine and Methamphetamine Addiction: Treatment, Recovery, and Relapse Prevention Arnold M. Washton and Joan E. Zweben, W.W. Norton & Co, 2009. Book Chapter: Chapter 2; "Understanding Stimulant Drugs"

321. Leikin, J. B.; Morris, R. W.; Warren, M.; Erickson, T. Trends in a decade of drug abuse presentation to an inner city ED. Am. J. Emerg. Med. 2001, 19, 37-9.

322. Boghdadi, M. S.; Henning, R. J. Cocaine: pathophysiology and clinical toxicology. Heart Lung 1997, 26, 466-83; quiz 484-5.

323. Jatlow, P., Cocaine: analysis, pharmacokinetics, and metabolic disposition. Yale J Biol Med 1988, 61 (2), 105-13.

324. Gold, M. S., Substance Abuse: A Comprehensive Textbook, Lippincott Williams & Wilkins: Baltimore, 2005, 218-251.

325. Cooper, J.; Bloom, F.; and Roth, R. The Biochemical Basis of Neuropharmacology, 6th ed. New York: Oxford University Press, 1991.

326. Book Chapter: 2. Treatment Improvement Protocol (TIP) Series, No. 33.Center for Substance Abuse Treatment. Rockville (MD): [Substance Abuse and Mental Health Services Administration \(US\)](#); 1999.

327. Taylor, D.; Ho, B., Comparison of inhibition of monoamine uptake by cocaine, methylphenidate and amphetamine. *Res Commun Chem Pathol Pharmacol.* 1978, 21 (1), 67.
328. Harris, J. E.; Baldessarini, R. J., Uptake of (3H)-catecholamines by homogenates of rat corpus striatum and cerebral cortex: effects of amphetamine analogues. *Neuropharmacology* 1973, 12 (7), 669-79.
329. Gawin, F. H.; Kleber, H. D.; Byck, R.; Rounsaville, B. J.; Kosten, T. R.; Jatlow, P. I.; Morgan, C., Desipramine facilitation of initial cocaine abstinence. *Arch Gen Psychiatry* 1989, 46 (2), 117-21.
330. Cregler, L. L.; Mark, H. Relation of stroke to cocaine abuse; United States, 1987, 128-9.
331. Self, D., and Nestler, E. Molecular mechanisms of drug reinforcement and addiction. *Annual Review of Neuroscience.* 1995, 18, 463-495.
332. Selden, L.S. Neurotoxicity of methamphetamine: Mechanisms of action and issues related to aging. In: Miller, M.A., and Kozel, N.J., eds. *Methamphetamine Abuse: Epidemiologic Issues and Implications.* NIDA Research Monograph Series, Number 115. DHHS Pub. No. (ADM) 91-1836. Rockville, MD: National Institute on Drug Abuse, 1991, 24-32.
333. F. Ivy Carroll, Leonard L. Howell, and, and Michael J. Kuhar. Pharmacotherapies for Treatment of Cocaine Abuse: Preclinical Aspects. *Journal of Medicinal Chemistry* 1999 42 (15), 2721-2736.
334. Di Chiara, G. The role of dopamine in drug abuse viewed from the perspective of its role in motivation. *Drug and Alcohol Dependence.* 1995; 38:95-137

335. Weis, D.A. "Stimulant use disorder (adult)." Unpublished report. Minneapolis, MN: Institute for Healthcare Quality/Health Risk Management. 1997.
336. Robbins, T.W.; Cador, M.; Taylor, J.R.; and Everitt, B.J. Limbic striatal interactions in reward-related processes. *Neuroscience and Biobehavioral Reviews*. 1989, 13, 155-162
337. Nash, J.M. Addicted. *Time*. 1997, 149(18), 69–76.
338. Snyder, S. *Drugs and the Brain*. New York: Scientific American Library, 1986.
339. Volkow, N.D.; Wang, G.J.; Fischman, M.W.; Foltin, R.W.; Fowler, J.S.; Abumrad, N.N.; Vitkum, S.; Logan, J.; Gatley, S.J.; Pappas, N.; Hitzemann, R.; and Shea, C.E. Relationship between subjective effects of cocaine and dopamine transporter occupancy. *Nature*. 1997a, 386, 827-830
340. Church, W. H.; Justice Jr, J. B.; Byrd, L. D., Extracellular dopamine in rat striatum following uptake inhibition by cocaine, nomifensine and benztropine. *Eur J Pharmacol*. 1987, 139 (3), 345-348.
341. Ritz, M. C.; Lamb, R. J.; Goldberg, S. R.; Kuhar, M. J. Cocaine receptors on dopamine transporters are related to self-administration of cocaine. *Science* 1987, 237, 1219–1223.
342. Kuhar, M. J.; Ritz, M. C.; Boja, J. W. The dopamine hypothesis of the reinforcing properties of cocaine. *Trends Neurosci*. 1991, 14, 299–302.
343. Koob, G. F.; Bloom, F. E. Cellular and molecular mechanisms of drug dependence. *Science* 1988, 242, 715–723.
344. Robinson, T.; Barridge, K. C. The neural basis of drug craving: An incentive-sensitization theory of addiction. *Brain Res. Rev*. 1993, 18, 249–291.
345. Kuhar, M. J.; Pilotte, N. S. Neurochemical changes in cocaine withdrawal. *Trends Pharmacol. Sci*. 1996, 17, 260–264.

346. Parham, W. E.; Egberg, D. C.; Sayed, Y. A.; Thraikill, R. W.; Keyser, G. E.; Neu, M.; Montgomery, W. C.; Jones, L. D., Spiro piperidines. 1. Synthesis of spiro[isobenzofuran-1(3H),4'-piperidin]-3-ones, spiro[isobenzofuran-1(3H),4'-piperidines], and spiro[isobenzotetrahydrothio phene-1(3H),4'-piperidines]. *J Org Chem.* 1976, 41 (15), 2628-2633.
347. Ritz, M. C.; Kuhar, M.; Psychostimulant drugs and a dopamine hypothesis regarding addiction: update on recent research. *Biochem. Soc. Symp.* 1993, 59, 51-64.
348. Carroll, F. I.; Howell, L. L.; Kuhar, M. J. Pharmacotherapies for treatment of cocaine abuse: preclinical aspects. *J. Med. Chem.* 1999, 42, 2721-2736.
349. Nader, M. A.; Grant, K. A.; Davies, H. M.; Mach, R. H.; Childers, S. R. The reinforcing and discriminative stimulus effects of the novel cocaine analog 2beta- propanoyl-3beta-(4-tolyl)-tropane in rhesus monkeys. *J. Pharmacol. Exp. Ther.* 1997, 280, 541-550.
350. Villemagne, V. L.; Rothman, R. B.; Yokoi, F.; Rice, K. C.; Matecka, D.; Dannals, R. F.; Wong, D. F. Doses of GBR12909 that suppress cocaine self-administration in non-human primates substantially occupy dopamine transporters as measured by [^{11}C] WIN35,428 PET scans. *Synapse.* 1999, 32, 44-50.
351. Rothman, R. B.; Glowa, J. R. A review of the effects of dopaminergic agents on humans, animals, and drug-seeking behavior, and its implications for medication development. *Mol. Neurobiol.* 1995, 11, 1-19.
352. Cristina Missale, S. Russel Nash, Susan W. Robinson, Mohamed Jaber, And Marc G. Caron Dopamine Receptors: From Structure to Function. *Physiological Reviews* Vol. 78, No. 1, January 1998

353. Kleven, M. S.; Woolverton, W. L. Effects of bromocriptine and desipramine on behavior maintained by cocaine or food presentation in rhesus monkeys. *Psychopharmacology* 1990, 101, 208–213.
354. Woolverton, W. L.; Goldberg, L. I.; Ginos, J. Z. Intravenous self-administration of dopamine receptor agonists by rhesus monkeys. *J. Pharmacol. Exp. Ther.* 1984, 230, 678–683.
355. Baxter, B. L.; Gluckman, M. I.; Stein, L.; Scerni, R. A. Self-injection of apomorphine in the rat: Positive reinforcement by a dopamine receptor stimulant. *Pharmacol. Biochem. Behav.* 1974, 2, 387–391.
356. Yokel, R. A.; Wise, R. A. Amphetamine-type reinforcement by dopaminergic agonists in the rat. *Psychopharmacology (Berlin)* 1978, 58, 289–296.
357. Grech, D. M.; Spealman, R. D.; Bergman, J. Self-administration of D1 receptor agonists by squirrel monkeys. *Psychopharmacology (Berlin)* 1996, 125, 97–104.
358. Le Foll, B.; Schwartz, J. C.; Sokoloff, P., Dopamine D3 receptor agents as potential new medications for drug addiction. *Eur Psychiatry* 2000, 15 (2), 140-6.
359. Caine, S. B.; Koob, G. F., Effects of dopamine D-1 and D-2 antagonists on cocaine self-administration under different schedules of reinforcement in the rat. *J Pharmacol Exp Ther.* 1994, 270 (1), 209-18.
360. Melia, K. F.; Spealman, R. D. Pharmacological characterization of the discriminative-stimulus effects of GBR 12909. *J. Pharmacol. Exp. Ther.* 1991, 258, 626-32.
361. Witkin, J. M.; Nichols, D. E.; Terry, P.; Katz, J. L. Behavioral effects of selective dopaminergic compounds in rats discriminating cocaine injections. *J. Pharmacol. Exp. Ther.* 1991, 257, 706-13.

362. Jaerbe, T . U. C. Discriminative stimulus properties of cocaine. Effects of apomorphine, haloperidol, procaine and other drugs. *Neuropharmacology* 1984, 23, 899-907.
363. De Wit, H.; Wise, R. A. Blockade of cocaine reinforcement in rats with the dopamine receptor blocker pimozide, but not with the noradrenergic blockers phentolamine or phenoxybenzamine. *Can. J. Psychol.* 1977, 31, 195-20.
364. Woolverton, W. L. Effects of a D₁ and a D₂ dopamine antagonist on the self-administration of cocaine and piribedil by rhesus monkeys. *Pharmacol., Biochem. Behav.* 1986, 24, 531-5.
365. Scheel-Kruger, J.; Braestrup, C.; Nielson, M.; Golembiowska, K.; Mogilnicka, E. Cocaine: discussion on the role of dopamine in the biochemical mechanism of action. *Adv. Behav. Biol.* 1977, 21, 373-407.
366. Barrett, R. L.; Appel, J. B. Effects of stimulation and blockade of dopamine receptor subtypes on the discriminative stimulus properties of cocaine. *Psychopharmacology (Berlin)* 1989, 99, 13-16.
367. Colpaert, F. C.; Niemegeers, C. J. E.; Janssen, P. A. J. Discriminative stimulus properties of cocaine: neuropharmacological characteristics as derived from stimulus generalization experiments. *Pharmacol. Biochem. Behav.* 1979, 10, 535-46.
368. Vanover, K. E.; Kleven, M. S.; Woolverton, W. L. Blockade of the discriminative stimulus effects of cocaine in rhesus monkeys with the D₁ dopamine antagonists SCH-39166 and A-66359. *Behav. Pharmacol.* 1991, 2, 151-159.
369. Goeders, N. E.; Smith, J. E. Reinforcing properties of cocaine in the medial prefrontal cortex: Primary action on presynaptic dopaminergic terminals. *Pharmacol. Biochem. Behav.* 1986, 25, 191-199.

370. Madras, B. K.; Elmaleh, D. R.; Meltzer, P. C.; Liang, A. Y.; Brownell, G. L.; Brownell, A. L. Positron emission tomography of cocaine binding sites on the dopamine transporter. *NIDA Res. Monogr.* 1994, 138, 57–69.
371. Carroll, F. I.; Lewin, A. H.; Boja, J. W.; Kuhar, M. J. Cocaine receptor: Biochemical characterization and structure–activity relationships for the dopamine transporter. *J. Med. Chem.* 1992, 35, 969–981.
372. Carroll, F. I.; Lewin, A. H.; Kuhar, M. J. Dopamine Transporter Uptake Blockers: Structure–Activity Relationships. In *Neurotransmitter Transporters: Structure, Function, and Regulation*; Reith, M. E. A., Ed.; Humana: Totowa, NJ, 1997; 263–295.
373. Bennett, B. A.; Wichems, C. H.; Hollingsworth, C. K.; Davies, H. M. L.; Thornley, C.; Sexton, T.; Childers, S. R. Novel 2-substituted cocaine analogues: Uptake and ligand binding studies at dopamine, serotonin and norepinephrine transport sites in the rat brain. *J. Pharmacol. Exp. Ther.* 1995, 272, 1176–1186.
374. Meltzer, P. C.; Liang, A. Y.; Madras, B. K. The discovery of an unusually selective and novel cocaine analog: Difluoropine. Synthesis and inhibition of binding at cocaine recognition sites. *J. Med. Chem.* 1994, 37, 2001–2010.
375. Deutsch, H. M.; Shi, Q.; Gruszecka-Kowalik, E.; Schweri, M. M. Synthesis and pharmacology of potential cocaine antagonists. 2. Structure–activity relationship studies of aromatic ring-substituted methylphenidate analogues. *J. Med. Chem.* 1996, 39, 1201–1209.
376. Davies, H. M. L.; Saikali, E.; Sexton, T.; Childers, S. R. Novel 2-substituted cocaine analogues: Binding properties at dopamine transport sites in rat striatum. *Eur. J. Pharmacol. Mol. Pharmacol. Sec.* 1993, 244, 93–97.

377. Van der Zee, P.; Koger, H. S.; Gootjes, J.; Hesse, W. Aryl 1,4-dialk(en)ylpiperazines as selective and very potent inhibitors of dopamine uptake. *Eur. J. Med. Chem.* 1980, 15, 363–370.
378. Wang, S.; Gao, Y.; Laruelle, M.; Baldwin, R. M.; Scanley, B. E.; Innis, R. B.; Neumeier, J. L. Enantioselectivity of cocaine recognition sites: binding of (1S)- and (1R)-2 β -carbomethoxy-3 β -(4-iodophenyl)tropane (β -CIT) to monoamine transporters. *J. Med. Chem.* 1993, 36, 1914–1917.
379. Kline, R. H., Jr.; Wright, J.; Fox, K. M.; Eldefrawi, M. E. Synthesis of 3-aryleugonine analogues as inhibitors of cocaine binding and dopamine uptake. *J. Med. Chem.* 1990, 33, 2024–2027.
380. Simoni, D.; Stoelwinder, J.; Kozikowski, A. P.; Johnson, K. M.; Bergmann, J. S.; Ball, R. G. Methoxylation of cocaine reduces binding affinity and produces compounds of differential binding and dopamine uptake inhibitory activity: Discovery of a weak cocaine “antagonist”. *J. Med. Chem.* 1993, 36, 3975–3977.
381. Goodman, M. M.; Kung, M.-P.; Kabalka, G. W.; Kung, H. F.; Switzer, R. Synthesis and characterization of radioiodinated *N*-(3-iodopropen-1-yl)-2 β -carbomethoxy-3 β -(4-chlorophenyl)tropanes: Potential dopamine reuptake site imaging agents. *J. Med. Chem.* 1994, 37, 1535–1542.
382. Newman, A. H.; Allen, A. C.; Izenwasser, S.; Katz, J. L. Novel 3 α -(diphenylmethoxy)tropane analogues: Potent dopamine uptake inhibitors without cocaine-like behavioral profiles. *J. Med. Chem.* 1994, 37, 2258–2261.

383. Bergman, J.; Madras, B. K.; Johnson, S. E.; Spealman, R. D. Effects of cocaine and related drugs in nonhuman primates. III. Self-administration by squirrel monkeys. *J. Pharmacol. Exp. Ther.* 1989, 251, 150–155.
384. Howell, L. L.; Byrd, L. D. Characterization of the effects of cocaine and GBR 12909, a dopamine uptake inhibitor, on behavior in the squirrel monkey. *J. Pharmacol. Exp. Ther.* 1991, 258, 178–185.
385. P. Leone, D. Pocock, R.A. Wise. Morphine-dopamine interaction: ventral tegmental morphine increases nucleus accumbens dopamine release. *Pharmacol Biochem Behav.* 1991, 39, 469–472.
386. R.A. Wise, P. Leone, R. Rivest, K. Leeb. Elevations of nucleus accumbens dopamine and DOPAC levels during intravenous heroin self-administration. *Synapse.* 1995, 21, 140–148
387. A. Herz. Opioid reward mechanisms: a key role in drug abuse. *Can J Physiol Pharmacol.* 76, 1998, 252–258.
388. Mello, N. K.; Negus, S. S. Preclinical evaluation of pharmacotherapies for treatment of cocaine and opioid abuse using drug self-administration procedures. *Neuropsychopharmacology.* 1996, 14, 375–424.
389. Comer, S. D.; Lac, S. T.; Wyvell, C. L.; Carroll, M. E. Combined effects of buprenorphine and a nondrug alternative reinforcer on i.v. cocaine self-administration in rats maintained under FR schedules. *Psychopharmacology (Berlin)* 1996, 125, 355–360.
390. Tech, S. K.; Mello, N. K.; Mendelson, J. H.; Kuehnle, J.; Gastfriend, D. R. Buprenorphine effects on heroin-and cocaine-induced subjective responses by drug dependent men. *J. Clin. Pharmacol.* 1994, 14, 15–77.

391. Schottenfeld, R. S.; Pakes, J.; Ziedonis, D.; Kosten, T. R. Buprenorphine: Dose-related effect on cocaine and opioid use in cocaine-abusing opioid-dependent humans. *Biol. Psychiatry* 1993, 34, 66–74.
392. Bronwyn M. Kivell, Amy W.M. Ewald, Thomas E. Prisinzano. Chapter Twelve – Salvinorin A Analogs and Other Kappa-Opioid Receptor Compounds as Treatments for Cocaine Abuse. Available online; 30 January 2014.
393. Katherine M. Prevatt-Smith, Kimberly M. Lovell, Denise S. Simpson, Victor W. Day, Justin T. Douglas, Peter Bosch, Christina M. Dersch, Richard B. Rothman, Bronwyn Kivell and Thomas E. Prisinzano. Potential drug abuse therapeutics derived from the hallucinogenic natural product salvinorin A. *Med. Chem. Commun.*, 2011, 2, 1217-1222.
394. Kosten TR1. Future of anti-addiction vaccines. *Stud Health Technol Inform.* 2005;118:177-85.
395. Montoya I. Immunotherapies for drug addictions. *Adicciones.* 2008, 20, (2),111-5.
396. Zalewska-Kaszubska J1. Is immunotherapy an opportunity for effective treatment of drug addiction? *Vaccine.* 2015 Oct 2. pii: S0264-410X(15)01369-9.
397. Matsumoto R. R.; Coop, A. Ethylamines with high affinity and selectivity for sigma receptors attenuate cocaine-induced behaviors in mice. *The FASEB Journal* 2007, 21, 715.14.
398. Derlet, R. W., & Albertson, T. E. Anticonvulsant modification of cocaine-induced toxicity in the rat. *Neuropharmacology.* 1990, 29(3), 255–259.

399. Ushijima I, Kobayashi T, Suetsugi M, Watanabe K, Yamada M and Yamaguchi K. Cocaine: evidence for NMDA-, B-carboline- and dopaminergic-mediated seizures in mice. *Brain Res.* 1998, 797, 347-350.
400. Matsumoto R. R., Hewett K. L., Pouw B., Bowen W. D., Husbands S. M., Cao J. J., and Hauck N. A., Rimcazole analogs attenuate the convulsive effects of cocaine: correlation with binding to sigma receptors rather than dopaminetransporters. *Neuropharmacology* 2001, 41, 878-886,.
401. Noorbakhsh, B., Seminerio, M. J., Xu, Y.-T., Beatty, C., Mesangeau, C., McCurdy, C. R., et al. (2011). Synthesis and pharmacological characterization of sigma-2 preferring compounds: Implications for cocaine-induced behaviors. *Society for Neuroscience Abstract*, #896.02.
402. R.R Matsumoto, K.A McCracken, B Pouw, J Miller, W.D Bowen, W Williams, B.R de Costa. N-alkyl substituted analogs of the σ receptor ligand BD1008 and traditional σ receptor ligands affect cocaine-induced convulsions and lethality in mice. *Eur. J. Pharmacol.*, 2001, 411, 261–273.
403. Rae R. Matsumoto, Linda Nguyen, Nidhi Kaushal, Matthew J. Robson. Sigma (σ) Receptors as Potential Therapeutic Targets to Mitigate Psychostimulant Effects. *Book Chapter*; Nine.
404. Gilmore D. L.; Coop A.; Bowen W. D.; Pouw B.; Matsumoto R. R. AC927, a putative sigma-2 receptor antagonist, attenuates cocaine-induced behaviors. In *Society for Neuroscience annual meeting*, November 2002.
405. Matsumoto, R. R., Gilmore, D. L., Pouw, B., Bowen, W. D., Williams, W., Kausar, A., Coop A. Novel analogs of the sigma receptor ligand BD1008 attenuate cocaine- induced

- toxicity in mice. *European Journal of Pharmacology* 2004, 492, (1), 21–26.
406. Matsumoto, R. R., Li, S. M., Katz, J. L., Fantegrossi, W. E., & Coop, A.. Effects of the selective sigma receptor ligand, 1-(2-phenethyl)piperidine oxalate (AC927), on the behavioral and toxic effects of cocaine. *Drug and Alcohol Dependence*, 2011, 118, (1), 40–47.
407. K.A McCracken, W.D Bowen, B.R De Costa, R.R Matsumoto Two novel σ receptor ligands, BD1047 and LR172, attenuate cocaine-induced toxicity and locomotor activity. *Eur. J. Pharmacol.*, 1999, 370, 225–232
408. G Skuza. Effect of sigma ligands on the cocaine-induced convulsions in mice. *Pol. J. Pharmacol.*, 51 (1999), pp. 477–483
409. M Witkin, P Terry, M Menkel, P Hickey, M Pontecorvo, J Ferkany, J.L Katz. Effects of the selective sigma receptor ligand, 6-[6-(4-hydroxypiperidinyl)hexyloxy]-3-methylflavone (NPC 16377), on behavioral and toxic effects of cocaine. *J. Pharmacol. Exp. Ther.*, 1993, 266, 473–482.
410. Romieu, P., Martin-Fardon, R., Bowen, W. D., & Maurice, T. (2003). Sigma1 receptor-related neuroactive steroids modulate cocaine-induced reward. *The Journal of Neuroscience*. 2003, 23, (9), 3572–3576
411. Mori, T., Rahmadi, M., Yoshizawa, K., Itoh, T., Shibasaki, M., & Suzuki, T. (2012). Inhibitory effects of SA4503 on the rewarding effects of abused drugs. *Addiction Biology*. 2014,19, (3), 362-9
412. Slifer, B.L.; Balster, R.L. Reinforcing properties of stereoisomers of the putative sigma agonists. N-allylnormetazocine and cyclazocine in rhesus monkeys. *J. Pharmacol. Exp. Ther.* 1983, 225,522-528.

413. Takato Hiranita, Paul L. Soto, Gianluigi Tanda, and Jonathan L. Katz. Reinforcing Effects of Receptor Agonists in Rats Trained to Self-Administer Cocaine. *JPET* 332:515–524, 2010.
414. Izenwasser S, Newman AH, and Katz JL (1993) Cocaine and several sigma receptor ligands inhibit dopamine uptake in rat caudate-putamen. *Eur J Pharmacol* 243:201–205.
415. Loland CJ, Desai RI, Zou MF, Cao J, Grundt P, Gerstbrein K, Sitte HH, Newman AH, Katz JL, and Gether U (2008) Relationship between conformational changes in the dopamine transporter and cocaine-like subjective effects of uptake inhibitors. *Mol Pharmacol* 2008, 73, 813–823.
416. Reith ME, Berfield JL, Wang LC, Ferrer JV, and Javitch JA (2001) The uptake inhibitors cocaine and bupropion differentially alter the conformation of the human dopamine transporter. *J Biol Chem* 2001, 276, 29012–29018.
417. Garcés-Ramírez L, Green JL, Hiranita T, et al. Sigma receptor agonists: Receptor binding and effects on mesolimbic dopamine neurotransmission assessed by microdialysis. *Biological psychiatry*. 2011, 69, (3), 208-217.
418. Borison RL, Diamond BI, and Dren AT. Does receptor antagonism predict clinical antipsychotic efficacy? *Psychopharmacol Bull* 1991, 27,103–106.
419. Methamphetamine: Wikipedia, <http://en.wikipedia.org/wiki/Methamphetamine>. (Accessed 10/15/2015).
420. Grollman A. *Pharmacology and Therapeutics: a Textbook for Students and Practitioners of Medicine*. Lea & Febiger. 1954, pp. 209.
421. Freye, E.; Levy, J. V. *Pharmacology and Abuse of Cocaine, Amphetamines, Ecstasy and Related Designer Drugs; A Comprehensive Review on their Mode of Action, Treatment*

of Abuse and Intoxication. Springer Dordrecht Heidelberg, London, New York, 2009, 50-63

422. Durrel TM, Kroutil LA, Crits-Christoph P, et al. Prevalence of nonmedical methamphetamine use in the United States. *Subst Abuse Treat Prev Policy*. 2008, 3, 19
423. Cook, C.E. Pyrolytic characteristics, pharmacokinetics, and bioavailability of smoked heroin, cocaine, phencyclidine, and methamphetamine. In: Miller, M.A., and Kozel, N.J., eds. *Methamphetamine Abuse: Epidemiologic Issues and Implications*. NIDA Research Monograph Series, Number 115. DHHS Pub. No. (ADM) 91-1836. Rockville, MD: National Institute on Drug Abuse, 1991, 6-23.
424. Office of National Drug Control Policy (ONDCP), Office of Justice Programs, Department of Justice. *Methamphetamine: Facts and Figures*. ONDCP Drug Policy Information Clearinghouse. Pub. No. PK 29. Rockville, MD: Office of National Drug Control Policy, 1998b.
425. Lyness WH, Friedle NM, Moore KE. Increased self-administration of d-amphetamine after destruction of 5-hydroxytryptaminergic neurons. *Pharmacol Biochem Behav*. 1980, 12, 937-941.
426. Yu DSL, Smith FL, Smith DG. Fluoxetine-induced attenuation of amphetamine self-administration in rats. *Life Sci*. 1986, 39, 1383-1388.
427. Peck JA, Reback CJ, Yang X, et al. Sustained reductions in drug use and depression symptoms from treatment for drug abuse in methamphetamine-dependent gay and bisexual men. *J Urban Health*. 2005, 82, 100-10.
428. Galloway GP, Newmeyer J, Knapp T, et al. A controlled trial of imipramine for the treatment of methamphetamine dependence. *J Subst Abuse Treat*. 1996, 13, 493-497.

429. Elkashef AM, Rawson RA, Anderson AL, Li SH, Holmes T, Smith EV, Chiang N, Kahn R, Vocci F, Ling W, Pearce VJ, McCann M, Campbell J, Gorodetzky C, Haning W, Carlton B, Mawhinney J, Weis D. Bupropion for the treatment of methamphetamine dependence *Neuropsychopharmacology* 2008, 33, (5), 1162-70. Epub 2007 Jun 20.
430. Jittiwutikan J, Srisurapanont M, Jarusuraisin N. Amineptine in the treatment of amphetamine withdrawal: a placebo-controlled, randomised, double-blind study. *J Med Assoc Thai.* 1997, 80, 587-591.
431. Srisurapanont M, Jarusuraisin N, Jittiwutikan J. Amphetamine withdrawal: II. A placebo-controlled, randomised, double-blind study of amineptine treatment. *Aust N Z J Psychiatry.* 1999, 33, 94-98.
432. Johnson BA1, Ait-Daoud N, Elkashef AM, Smith EV, Kahn R, Vocci F, Li SH, Bloch DA; Methamphetamine Study Group. A preliminary randomized, double-blind, placebo-controlled study of the safety and efficacy of ondansetron in the treatment of methamphetamine dependence. *Int J Neuropsychopharmacol.* 2008, Feb, 11(1), 1-14. Epub 2007 May 1.
433. McGregor C, White JM, Srisurapanont M, et al. Open-label pilot trials of mirtazapine and modafinil in inpatient methamphetamine withdrawal: symptoms and sleep patterns. Presented at: 67th Annual Scientific Meeting of the College on Problems of Drug Dependence; June 18-23, 2005; Orlando, Fla.
434. Batki SL, Moon J, Bradley M, et al. Fluoxetine in methamphetamine dependence--a controlled trial: preliminary analysis. In: LS Harris, ed. *Problems of Drug Dependence 1999. Proceedings of the 61st Annual Scientific Meeting of the College on Problems of Drug Dependence, Inc.* Washington, DC: US Government Printing Office. 2000:235.

NIDA research monograph 180, NIH publication 00-4737.

435. Piasecki MP, Steinagel GM, Thienhaus OJ. An exploratory study: the use of paroxetine for methamphetamine craving. *J Psychoactive Drugs*. 2003, 34, 301-304.
436. Shoptaw S, Huber A, Peck J, et al. Randomized, placebo-controlled trial of sertraline and contingency management for the treatment of methamphetamine dependence. *Drug Alcohol Depend*. 2006, 85, 12-18.
437. Meredith CW, Jaffe C, Yanasak E, et al. An open-label pilot study of risperidone in the treatment of methamphetamine dependence. *J Psychoactive Drugs*. 2007, 39, 167-172.
438. Malcom, Robert, et al. "Clinical Applications of Modafinil in Stimulant Abusers: Low Abuse Potential." *The American Journal on Addictions* 2002, 11, 247-249.
439. Shearer, J., Sherman, J., Wodak, A., and van Beek, I. Substitution therapy for amphetamine users. *Drug and Alcohol Review* 2002, 21, (2), 179-185.
440. Okuyama S, Nakazato A. NE-100: a novel sigma receptor antagonist. *CNS Drug Rev*. 1996, 2, 226-237.
441. Takahashi S, Miwa T, Horikomi K., Involvement of sigma 1 receptors in methamphetamine induced behavioral sensitization in rats. *Neurosci Lett*. 2000 Jul 28, 289(1), 21-4.
442. Akiyama K, Kanzaki A, Tsuchida K, Ujike H., Methamphetamine-induced behavioral sensitization and its implications for relapse of schizophrenia. *Schizophr Res*. 1994 Jun, 12(3), 251-7.
443. Stefanski, R.; Justinova, Z.; Hayashi, T.; Takebayashi, M.; Goldberg, S.R.; Su, T.P. Sigma 1 receptor upregulation after chronic methamphetamine self-administration in rats: A study with yoked controls. *Psychopharmacology (Berl)* 2004, 175, 68-75.

444. Hayashi, T., Justinova, Z., Hayashi, E., Cormaci, G., Mori, T., Tsai, S. Y., et al. (2010). Regulation of sigma-1 receptors and endoplasmic reticulum chaperones in the brain of methamphetamine self-administering rats. *The Journal of Pharmacology and Experimental Therapeutics*, 332, (3), 1054–1063.
445. Stefanski, R.; Ladenheim, B.; Lee, S.H.; Cadet, J.L.; Goldberg, S.R. Neuroadaptations in the dopaminergic system after active self-administration but not after passive administration of methamphetamine. *Eur. J. Pharmacol.* 1999, 371, 123-135.
446. Chen, J. C., Chen, P. C., and Chiang, Y. C. (2009). Molecular mechanisms of psychostimulant addiction. *Chang Gung Medical Journal*. 2009, 32, (2), 148–154.
447. Hyman, S. E., and Malenka, R. C. Addiction and the brain: the neurobiology of compulsion and its persistence. *Nature Reviews Neuroscience*. 2001, 2(10), 695–703.
448. Jonathan L. Katz, Tsung-Ping Su, Takato Hiranita, Teruo Hayashi, Gianluigi Tanda, Theresa Kopajtic and Shang-Yi Tsai. A Role for Sigma Receptors in Stimulant Self-administration and Addiction. *Pharmaceuticals*. 2011, 4, 880-914.
449. Thomas, G. E.; Szucs, M.; Iiviamone, J. Y.; Bem, W. T.; Rush, M. D.; Johnson, F. E.; Coscia, C. J. Sigma and opioid receptors in human brain tumors. *Life Sci* 1990, 46, 1279-1286.
450. Baker BR. *Design of Active-Site-Directed Irreversible Enzyme Inhibitors*. New York: John Wiley and Sons, 1976.
451. Book: *Sigma Receptors; Cell biology and clinical implications*. Chapter 3: Irreversible s compounds. Ronsisvalle Giuseppe and Prezzavento Orazio. [Related to ref. 6]
452. Rafferty MF, Mattson M, Jacobson AE, Rice KC. A specific acylating agent for the [³H]phencyclidine receptors in rat brain. *FEBS Lett* 1985, 181:318-322.

453. Rice KC, Rafferty MF, Jacobson AE, Contreras P, O'Donohue TL, Lessor RA, Mattson MV. Metaphit, a specific acylating agent for the [³H]-phencyclidine receptors. 1986, U.S. Patent 4,598,153, 8 pp.
454. Rice KC, Rafferty MF, Jacobson AE, Contreras PC, O'Donohue TL. Metaphit and related compounds as acylating agents for the [³H]phencyclidine receptors. 1988, U. S. Patent 4,762,846, 29 pp.
455. Contreras PC, Rafferty MF, Lessor RA, Rice KC, Jacobson AE, O'Donohue TL. A specific alkylating ligand for phencyclidine (PCP) receptors antagonizes PCP behavioral effects. *Eur J Pharmacol* 1985, 111:405-406.
456. French ED, Jacobson AE, Rice KC. Metaphit, a proposed phencyclidine (PCP) antagonist, prevents PCP-induced locomotor behavior through mechanisms unrelated to specific blockade of PCP receptors. *Eur J Pharmacol* 1987, 140:267-274.
457. Berger P, Jacobsen AE, Rice KC, Lessor RA, Reith MA. Metaphit, a receptor acylator, inactivates cocaine binding sites in striatum and antagonizes cocaine-induced locomotor stimulation in rodents. *Neuropharmacology* 1986,25, 931-933.
458. Nabeshima T, Tohyama K, Noda A, Maeda Y, Hiramatsu M, Harrer SM, Kameyama T, Furukawa H, Jacobson AE, Rice KC. Effects of metaphit on phencyclidine and serotonin₂ receptors. *Neurosci Lett* 1989, 102, 303-308.
459. Haertzen CA. Subjective effects of narcotic antagonists cyclazocine and nalorphine on the Addiction Research Center Inventory (ARCI). *Psychopharmacologia* 1970, 18, 366-377.
460. Allen RM, Young SJ. Phencyclidine-induced psychosis. *Am J Psychiatry* 1978, 135, 1081-1084.

461. Sonders MS, Keana JF, Weber E. Phencyclidine and psychotomimetic sigma opiates: recent insights into their biochemical and physiological sites of action. *Trends Neurosci* 1988, 11, 37-40.
462. Teal JJ, Holtzman SG. Stereoselectivity of the stimulus effects of morphine and cyclazocine in the squirrel monkey. *J Pharmacol Exp Ther* 1980, 215:369-376.
463. Holtzman SG. Phencyclidine-like discriminative effects of opioids in the rat. *J Pharmacol Exp Ther* 1980, 214, 614-619.
464. Sircar R, Nichtenhauser R, Ieni JR, Zukin SR. Characterization and autoradiographic visualization of (+)-[³H]SKF10,047 binding in rat and mouse brain: further evidence for phencyclidine/"sigma opiate" receptor commonality. *J Pharmacol Exp Ther* 1986, 237, 681-688.
465. Gundlach AL, Largent BL, Snyder SH. Phencyclidine and sigma opiate receptors in brain: biochemical and autoradiographical differentiation. *Eur J Pharmacol* 1985, 113, 465-466.
466. Carroll FI, Abraham P, Parham K, Bai X, Zhang X, Brine GA, Mascarella S.W, Martin BR, May EL, Sauss C, Di Paolo L, Wallace P, Walker JM, Bowen WD. Enantiomeric N-substituted N-normetazocines: a comparative study of affinities at Sigma, PCP, and mu opioid receptors. *J Med Chem* 1992, 35, 2812-2818.
467. Bluth LS, Rice KC, Jacobson AE, Bowen WD. Acylation of sigma receptors by Metaphit, an isothiocyanate derivative of phencyclidine. *Eur J Pharmacol* 1989, 161, 273-277.
468. Bowen WD, Hellewell SB, McGarry KA. Evidence for a multi-site model of the rat brain sigma receptor. *Eur J Pharmacol* 1989, 163, 309-318.

469. Reid AA, Kim CH, Thurkauf A, Monn JA, de Costa B, Jacobson AE, Rice KC, Bowen WD, Rothman RB. Wash-resistant inhibition of phencyclidine- and haloperidol-sensitive sigma receptor sites in guinea pig brain by putative affinity ligands: determination of selectivity. *Neuropharmacology* 1990, 29:1047-1053.
470. Zhang H, Cuevas J. Sigma receptors inhibit high-voltage-activated calcium channels in rat sympathetic and parasympathetic neurons. *J Neurophysiol* 2002, 87, 2867-2879.
471. Weber E, Sonders M, Quarum M, McLean S, Pou S, Keana JF. 1,3-Di(2-[5-³H]tolyl)guanidine: a selective ligand that labels sigma-type receptors for psychotomimetic opiates and antipsychotic drugs. *Proc Natl Acad Sci USA*. 1986, 83, 8784-8788.
472. Rothman RB, Reid A, Mahboubi A, Kim CH, De Costa BR, Jacobson AE, Rice KC. Labeling by [³H]1,3-di(2-tolyl)guanidine of two high affinity binding sites in guinea pig brain:evidence for allosteric regulation by calcium channel antagonists and pseudoallosteric modulation by sigma ligands. *Mol Pharmacol* 1991, 39, 222-232
473. Adams JT, Teal PM, Sonders MS, Tester B, Esherick JS, Scherz MW, Keana JF, Weber E. Synthesis and characterization of an affinity label for brain receptors to psychotomimetic benzomorphans: differentiation of sigma-type and phencyclidine receptors. *Eur J Pharmacol* 1987, 142, 61-71.
474. Campbell BG, Scherz MW, Keana JFW, Weber E. Sigma receptors regulate contractions of the guinea pig ileum longitudinal muscle/myenteric plexus preparation elicited by both electrical stimulation and exogenous serotonin. *J Neurosci* 1989, 9, 3380-3391.
475. Mascarella SW, Bai X, Williams W, Sine B, Bowen WD, Carroll FI. (+)-*cis*-N-(para-, meta-, and ortho-substituted benzyl)-N-normetazocines: synthesis and binding affinity at

- the [³H]-(+)-pentazocine-labeled (sigma-1) site and quantitative structure-affinity relationship studies. *J Med Chem* 1995, 38, 565-569.
476. Ronsisvalle G, Prezzavento O, Marrazzo A, Vittorio F, Massimino M, Murari G, Spampinato S. Synthesis of (+)-cis-N-(4-isothiocyanatobenzyl)-N-normetazocine, an isothiocyanate derivative of N-benzylnormetazocine as acylant agent for the sigma(1) receptor. *J Med Chem* 2002, 45, 2662-2665.
477. Dubinsky, L.; Krom, B.P.; Meijler, M.M. Diazirine based photoaffinity labeling. *Bioorg. Med. Chem.* 2012, 20, 554–570.
478. Leslie, B.J.; Hergenrother, P.J. Identification of the cellular targets of bioactive small organic molecules using affinity reagents. *Chem. Soc. Rev.* 2008, 37, 1347–1360.
479. Mizuhara, T.; Oishi, S.; Ohno, H.; Shimura, K.; Matsuoka, M.; Fujii, N. Design and synthesis of biotin- or alkyne-conjugated photoaffinity probes for studying the target molecules of PD 404182. *Bioorg. Med. Chem.* 2013, 21, 2079–2087.
480. Lapinsky, D.J. Tandem photoaffinity labeling-bioorthogonal conjugation in medicinal chemistry. *Bioorg. Med. Chem.* 2012, 20, 6237–6247.
481. Das, J. Aliphatic diazirines as photoaffinity probes for proteins: Recent developments. *Chem. Rev.* 2011, 111, 4405–4444.
482. Leyva, E.; de Loera, D.; Leyva, S. Photochemistry of 7-azide-1-ethyl-3-carboxylate-6,8-difluoroquinolone: A novel reagent for photoaffinity labeling. *Tetrahedron Lett.* 2008, 49, 6759–6761.
483. Peng, Q.; Xia, Y.; Qu, F.; Wu, X.; Campese, D.; Peng, L. Synthesis of a photoactivatable phospholipidic probe containing tetrafluorophenylazide. *Tetrahedron Lett.* 2005, 46, 5893–5897.

484. Vodovozova, E.L. Photoaffinity labeling and its application in structural biology. *Biochemistry-Moscow* 2007, 72, 1–20.
485. Hilbold, B.; Perrault, M.; Ehret, C.; Niu, S.L.; Frisch, B.; Pécheur, E.I.; Bourel-Bonnet, L. Benzophenone-containing fatty acids and their related photosensitive fluorescent new probes: Design, physico-chemical properties and preliminary functional investigations. *Bioorg. Med. Chem.* 2011, 19, 7464–7473.
486. Qvit, N.; Monderer-Rothkoff, G.; Ido, A.; Shalev, D.E.; Amster-Choder, O.; Gilon, C. Development of bifunctional photoactivatable benzophenone probes and their application to glycoside substrates. *Biopolymers* 2008, 90, 526–536.
487. Kahoun JR, Ruoho AE. (¹²⁵I)iodoazidococaine, a photoaffinity label for the haloperidol-sensitive sigma receptor. *Proc Natl Acad Sci USA* 1992, 89:1393-1397.
488. Williams WE, Wu R, De Costa BR, Bowen WD. [³H](+)-Azidophenazocine: characterization as a selective photoaffinity probe for sigma-1 receptors. *Soc Neurosci Abstr* 1993, 19, 1553, 638.17.
489. Garza HH Jr, Mayo S, Bowen WD, DeCosta BR, Carr DJJ. Characterization of a (+)-azidophenazocine-sensitive sigma receptor on splenic lymphocytes. *J Immunol* 1993, 151, 4672-4680.
490. M P Kavanaugh, B C Tester, M W Scherz, J F Keana, and E Weber. Identification of the binding subunit of the sigma-type opiate receptor by photoaffinity labeling with 1-(4-azido-2-methyl[6-3H]phenyl)-3-(2-methyl[4,6-3H]phenyl)guanidine.. *Proc Natl Acad Sci U S A.* 1988 Apr; 85(8), 2844–2848.
491. Thomas N. Thompson. Optimization of Metabolic Stability as a Goal of Modern Drug Design. *Medicinal Research Reviews*, Vol. 21, No. 5, 412-449, 2001.

492. Graham R. Jang, Robert Z. Harris, David T. Lau. Pharmacokinetics and Its Role in Small Molecule Drug Discovery Research. Medicinal Research Reviews, Vol. 21, No. 5, 382-396, 2001.
493. Gondi N. Kumar, Sekhar Surapaneni. Role of Drug Metabolism in Drug Discovery and Development. Medicinal Research Reviews, 2001, 21, 5, 397- 411.
494. Rane A, Wilkinson GR, Shand DG. Prediction of hepatic extraction ratio from in vitro measurements of intrinsic clearance. J Pharmacol Exp Ther 1977, 200 (2), 420-424.
495. Houston JB. Utility of in vitro drug metabolism data in predicting in vivo metabolic clearance. Biochem Pharmacol 1994, 47(9), 1469-1479.
496. Houston JB, Carlile DJ. Prediction of hepatic clearance from microsomes, hepatocytes, and liver slices. Drug Metab Rev 1997, 29(4), 891-922.
497. Ito K, Iwatsubo T, Kanamitsu S, Nakajima Y, Sugiyama Y. Quantitative prediction of in vivo drug clearance and drug interactions from in vitro data on metabolism, together with binding and transport. Ann Rev Pharmacol Toxicol 1998, 38, 461-499.
498. Iwatsubo T, Hirota N, Ooie T, Suzuki H, Shimada N, Chiba K, Ishizaki T, Green CE, Tyson CA, Sugiyama Y. Prediction of in vivo drug metabolism in the human liver from in vitro metabolism data. Pharmacol Ther 1997, 73(2), 147-171.
499. Lave T, Dupin S, Schmitt C, Valles B, Ubeaud G, Chou RC, Jaeck D, Coassolo P. The use of humanm hepatocytes to select compounds based on their expected hepatic extraction ratios in humans. Clinm Pharmacokinet 1999, 36(3), 211-231.
500. Segel, I.H. et al. Kinetics of Unireactant Enzymes. In Enzyme Kinetics. 1993, 18–89, John Wiley & Sons.
501. Obach RS, Baxter JG, Liston TE, Silber BM, Jones BC, MacIntyre F, Rance DJ, Wastall

- P. The prediction of human pharmacokinetic parameters from preclinical and in vitro metabolism data. *J Pharmacol Exp Ther* 1997, 283(1), 46-58.
502. Donglu, Z., Mingshe, Z., Griffith, H. *Drug Metabolism in Drug Design and Development; Basic Concepts and Practice*, John Wiley & Sons, INC., 2007, 239-245.
503. Testa, B. and Meyer, J.M. *Drug metabolism and pharmacokinetics: implications for drug design*. *Acta Pharm. Jugosl.* 1990, 40, 315–350 26. II) M. J. Humphreya and D. A. Smitha. *Role of metabolism and pharmacokinetic studies in the discovery of new drugs - present and future perspectives*. *Xenobiotica*. 1992, 22, 743–755
504. Peter S. Dragovich , Thomas J. Prins , Ru Zhou , Theodore O. Johnson , Ye Hua , Hiep T. Luu , Sylvie K. Sakata , Edward L. Brown , Fausto C. Maldonado , Tove Tuntland , Caroline A. Lee , Shella A. Fuhrman , Leora S. Zalman, Amy K. Patick , David A. Matthews , Ellen Y. Wu , Ming Guo , Bennett C. Borer , Naresh K. Nayyar , Terence Moran , Lijian Chen , Paul A. Rejto , Peter W. Rose , Mark C. Guzman , Elena Z. Dovalsantos , Steven Lee , Kevin McGee, Michael Mohajeri , Andreas Liese , Junhua Tao , Maha B. Kosa , Bo Liu , Minerva R. Batugo , Jean-Paul R. Gleeson , Zhen Ping Wu , Jia Liu , James W. Meador , III, and Rose Ann Ferre. *Structure-based design, synthesis, and biological evaluation of irreversible human rhinovirus 3C protease inhibitors*. 8. *Pharmacological optimization of orally bioavailable 2- pyridone-containing peptidomimetics*. *J. Med. Chem.* 2003, 46, 4572–4585
505. Tagat JR1, Steensma RW, McCombie SW, Nazareno DV, Lin SI, Neustadt BR, Cox K, Xu S, Wojcik L, Murray MG, Vantuno N, Baroudy BM, Strizki JM. *Piperazine-based CCR5 antagonists as HIV-1 inhibitors*. II. *Discovery of 1-[(2,4-dimethyl-3-pyridinyl)carbonyl]-4-methyl-4-[3(S)-methyl-4-[1(S)-[4-(trifluoromethyl)phenyl]ethyl]-*

- 1- piperazinyl]- piperidine N1-oxide (Sch-350634), an orally bioavailable, potent CCR5 antagonist. *J. Med. Chem.* 2001, 44, 3343–3346
506. Imamura S., Ichikawa T., Nishikawa Y., Kanzaki N., Takashima K., Niwa S., Iizawa Y., Baba M., Sugihara Y. Discovery of a Piperidine-4-carboxamide CCR5 Antagonist (TAK-220) with Highly Potent Anti-HIV-1 Activity. *J. Med. Chem.* 2006, 49, 2784-2793.
507. Stratford RE, Clay MP, Heinz BA, Kuhfeld MT, Osborne SJ, Phillips DL, Sweetana SA, Tebbe MJ, Vasudevan V, Zornes LL, Lindstrom TD. Application of oral bioavailability surrogates in the design of orally active inhibitors of rhinovirus replication. *J Pharm Sci* 1999, 88(8), 747-753.
508. Victor F, Brown TJ, Campanale K, Heinz, BA Shipley LA, Su KS, Tang J, Vance LM, Spitzer WA. Synthesis, antiviral activity, and biological properties of vinylacetylene analogs of enviroxime. *J Med Chem* 1997, 40(10), 1511-1518.
509. Wayne E. C., Jr., Lisa M. H., Magda A., James J. B., Dan C. C., George T. G., Zhongqi S., Magid, A. A-G., Alvin, C. B., Harrison, Natasha K., Teresa K., Ronald M., Vasilios M., Albert J. R., Annmarie L. S., Mei-Yi Z., Terrance H., Susan H. A., Chad B., Thomas A. C., Mark D., Rizzo K. M., Sullivan, A. A., Christine H., Warren D. H. The Synthesis and Biological Evaluation of Quinolyl piperazinyl Piperidines
510. Jeffrey J. R., Marina A. P., Bryan K. S., Dariusz W., Jiahong W., Steven F., Katina M. M., William J. C., Liping P., Xiaoqing D., Linda E. C., Atul R., Mark M., Rodger F. H., Michael E. B., Heidi S. C., Hing L. S., Peer B. J., and J. T. L. Discovery and Metabolic Stabilization of Potent and Selective 2-Amino-N-(adamant-2-yl) Acetamide 11 α -Hydroxysteroid Dehydrogenase Type1 Inhibitors. *J. Med. Chem.* 2007, 50, 149-164.
511. Nan-Horng Lin, David E. Gunn, Keith B. Ryther, David S. Garvey, Diana L. Donnelly-

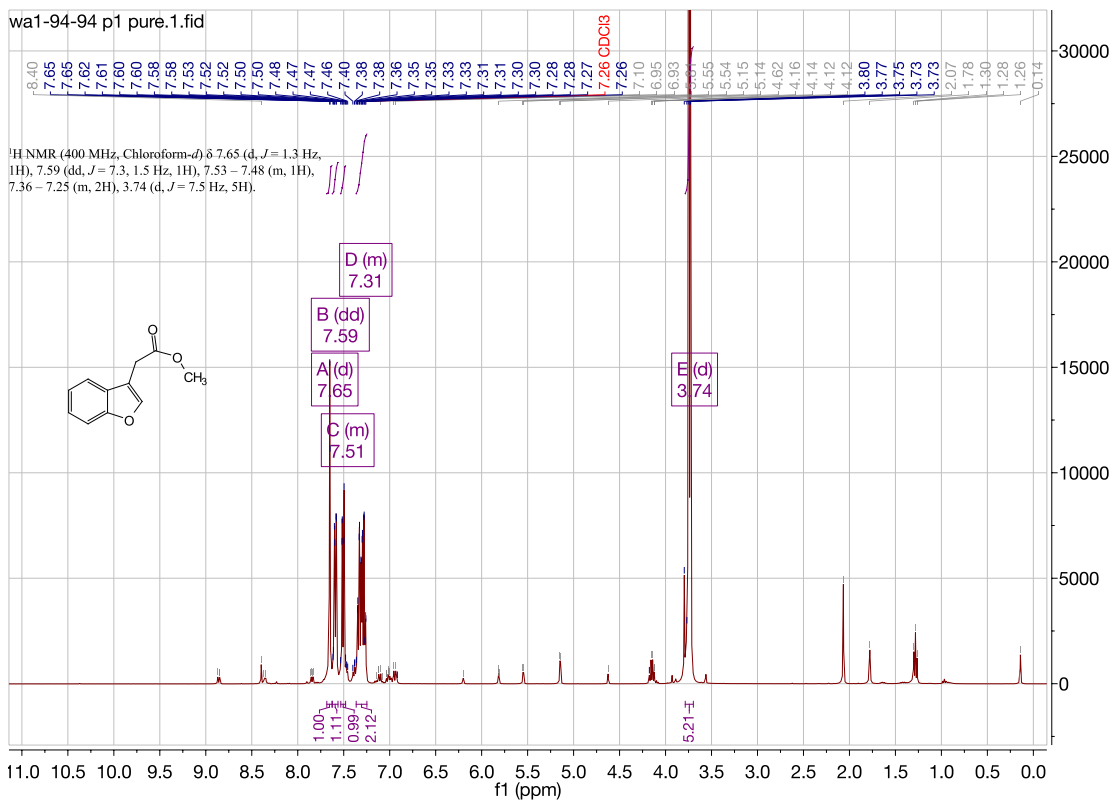
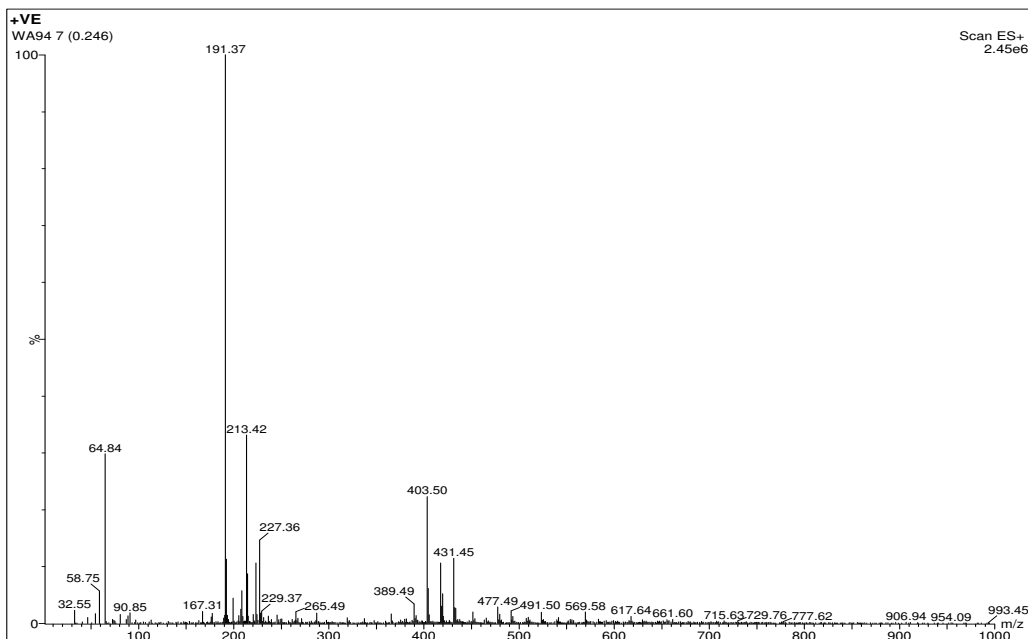
- Roberts, Michael W. Decker, Jorge D. Brioni, Michael J. Buckley, A. David Rodrigues, Kennan G. Marsh, David J. Anderson, Jerry J. Buccafusco, Mark A. Prendergast, James P. Sullivan, Michael Williams, Stephen P. Arneric, and Mark W. Holladay. Structure-activity studies on 2-methyl-3-(2(S)-pyrrolidinylmethoxy) pyridine (ABT-089): an orally bioavailable 3-pyridyl ether nicotinic acetylcholine receptor ligand with cognition enhancing properties. *J. Med. Chem.* 1997, 40, 385–390.
512. Michael J. Genin, Toni J. Poel, Yoshihiko Yagi, Carolyn Biles, Irene Althaus, Barbara J. Keiser, Laurice A. Kopta, Jan M. Friis, Fritz Reusser, Wade J. Adams, Robert A. Olmsted, Richard L. Voorman, Richard C. Thomas, and Donna L. Romero. Synthesis and bioactivity of novel bis(heteroaryl)piperazine reverse transcriptase inhibitors: structure-activity relationships and increased metabolic stability of novel substituted pyridine analogs. *J. Med. Chem.* 1996, 39, 5267–5275.
513. Steven G. Blanchard, Robert C. Andrews, Peter J. Brown, Liang-Shang L. Gan, Frank W. Lee, Achintya K. Sinhababu, Thomas N. Wheeler. Discovery of bioavailable inhibitors of secretory phospholipase A2. *Pharm. Biotechnol.* 1998, 11, 445–463.
514. Zhi-Ping Zhuang, Mei-Ping Kung, Mu Mu, and Hank F. Kung. Isoindol-1-one analogues of 4-(2'-methoxyphenyl)-1-[2'-[N-(2''-pyridyl)-piodobenzamido] ethyl]piperazine (p-MPPI) as 5-HT_{1A} receptor ligands. *J. Med. Chem.* 1998, 41, 157–166.
515. Jennifer J. Bouska, Randy L. Bell, Carole L. Goodfellow, Andrew O. Stewart, Clint D. W. Brooks and George W. Carter. Improving the in vivo duration of 5-lipoxygenase inhibitors: application of an in vitro glucuronosyltransferase assay. *Drug Metab. Dispos.* 1997, 25, 1032–1038.
516. C. Mesangeau, S. Narayanan, A.M. Green, J. Shaikh, N. Kaushal, E. Viard, Y.T. Xu, J.A.

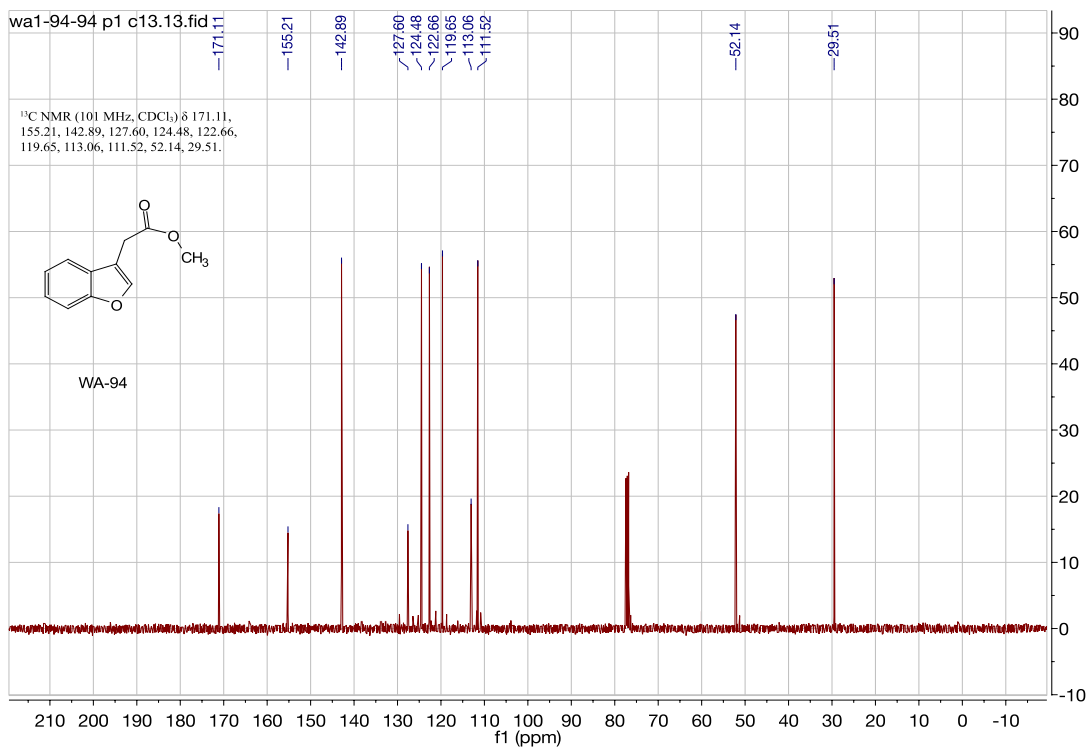
- Fishback, J.H. Poupaert, R.R. Matsumoto, C.R. McCurdy, *J. Med. Chem.* 2008, 51, 1482-1486.
517. Christophe Mésangeau, Emanuele Amata, Walid Alsharif, Michael J. Seminerio, Matthew J. Robson, Rae R. Matsumoto, Jacques H. Poupaert, Christopher R. McCurdy. Synthesis and pharmacological evaluation of indole-based sigma receptor ligands. *European Journal of Medicinal Chemistry.* 2011, 46, 5154-5161
518. Portoghese PS, Takemori AE. Affinity labels as probes for opioid receptor types and subtypes. *NIDA Res Monogr* 1986, 69, 157-68.

LIST OF APPENDICES

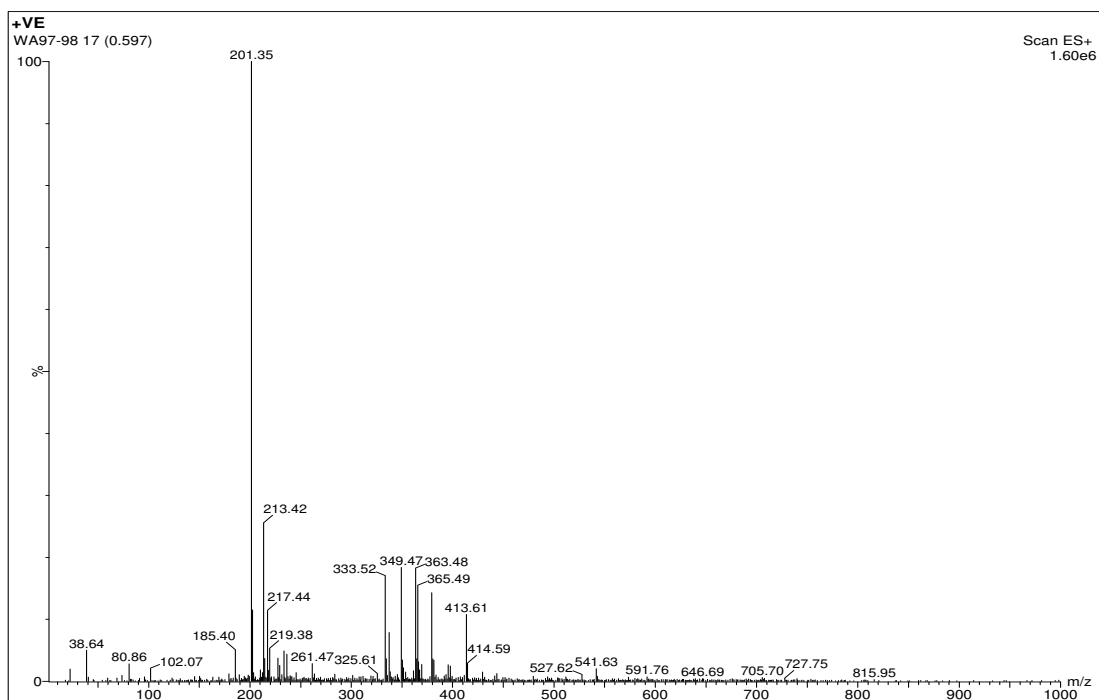
**MASS SPECTRA, ¹H NMR, ¹³C NMR, AND DEPT-135 NMR SPECTRA
OF THE SYNTHESIZED COMPOUNDS**

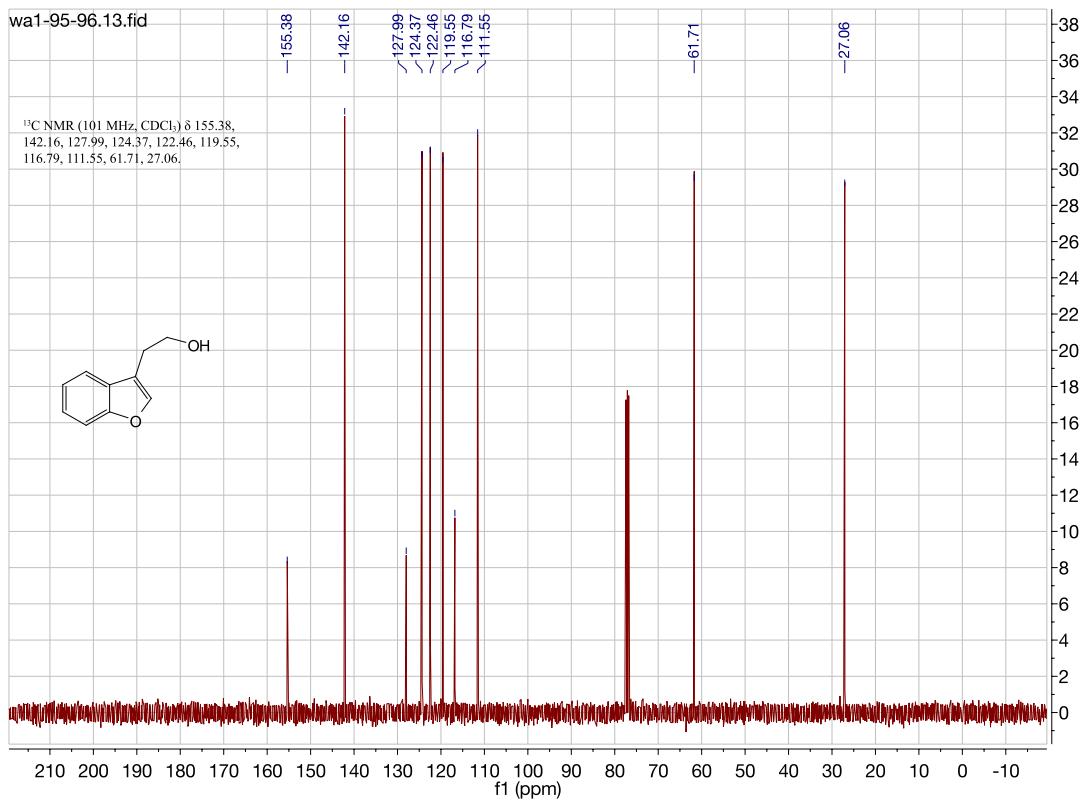
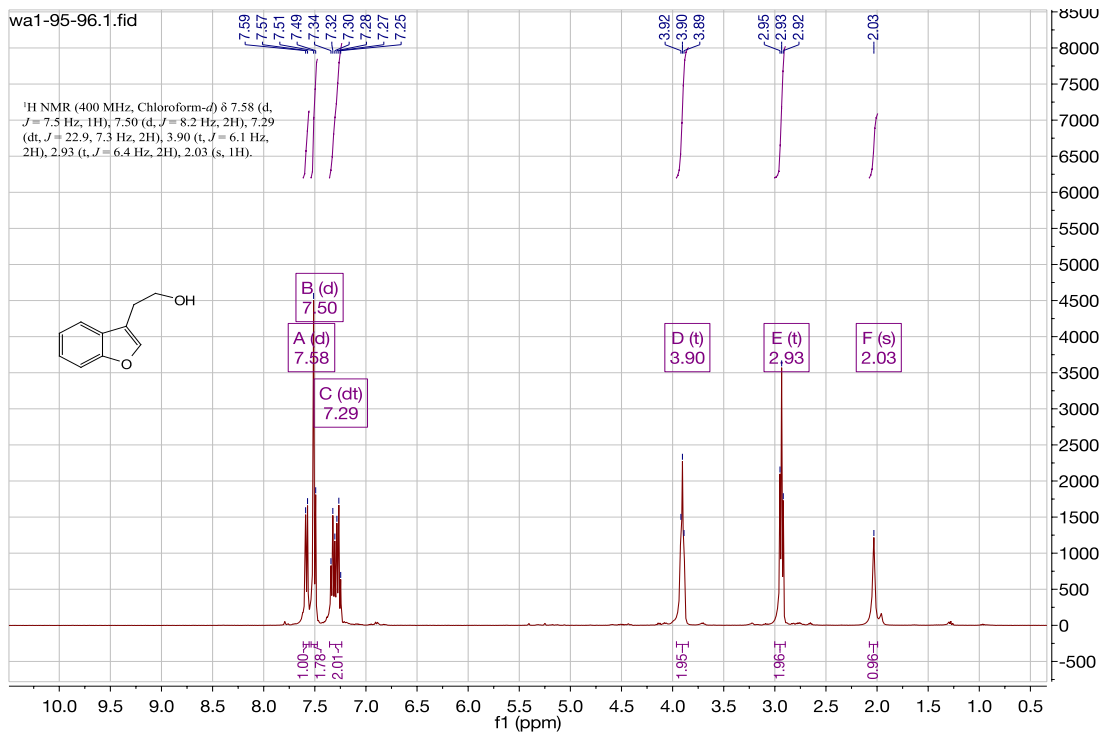
Methyl 2-(benzofuran-3-yl) ac etate. (WA94)



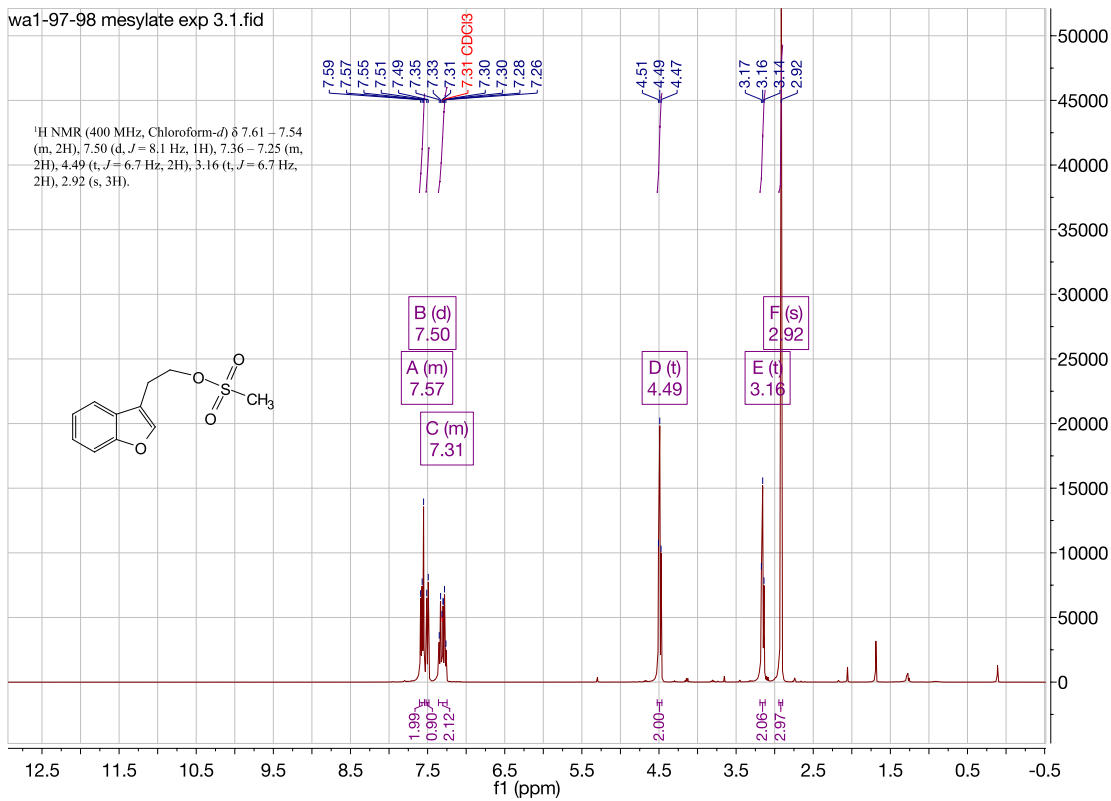
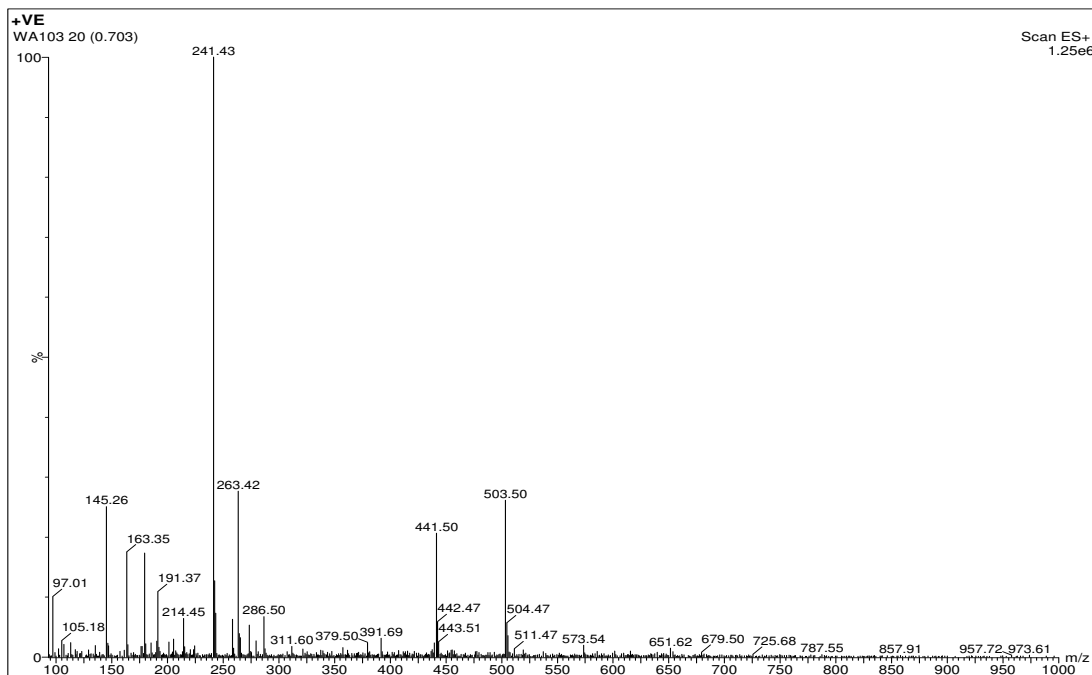


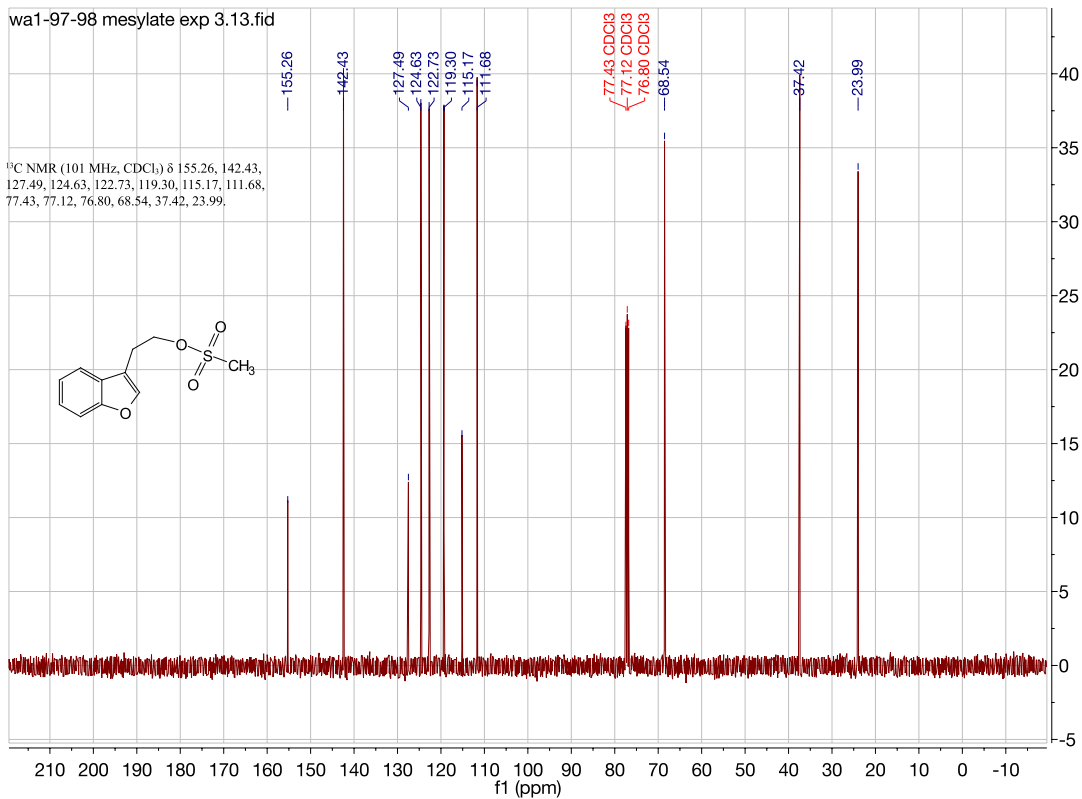
2-(benzofuran-3-yl)ethan-1-ol. (WA95)



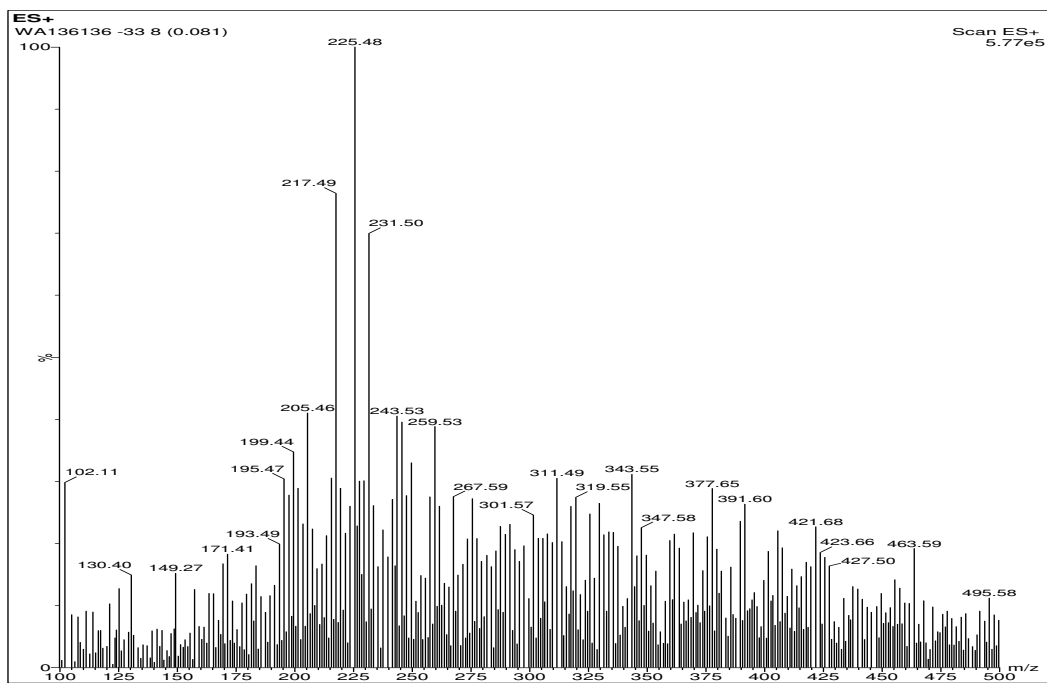


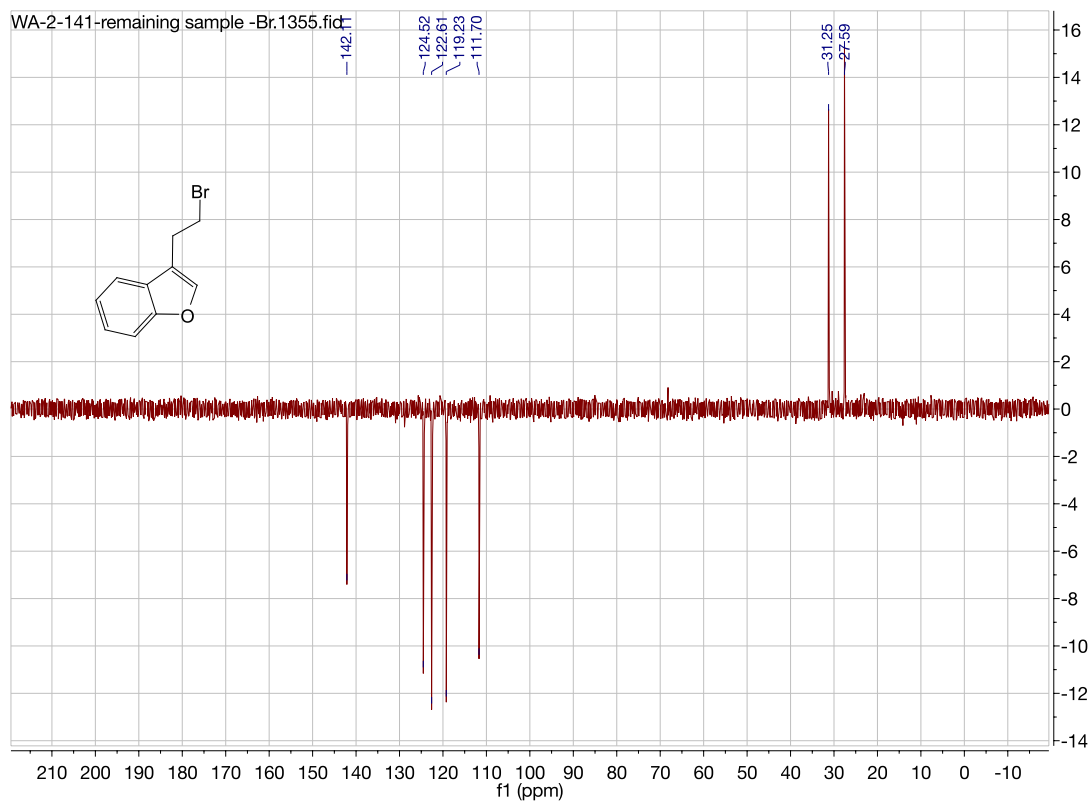
2-(benzofuran-3-yl)ethyl methanesulfonate. (WA98/WA103)



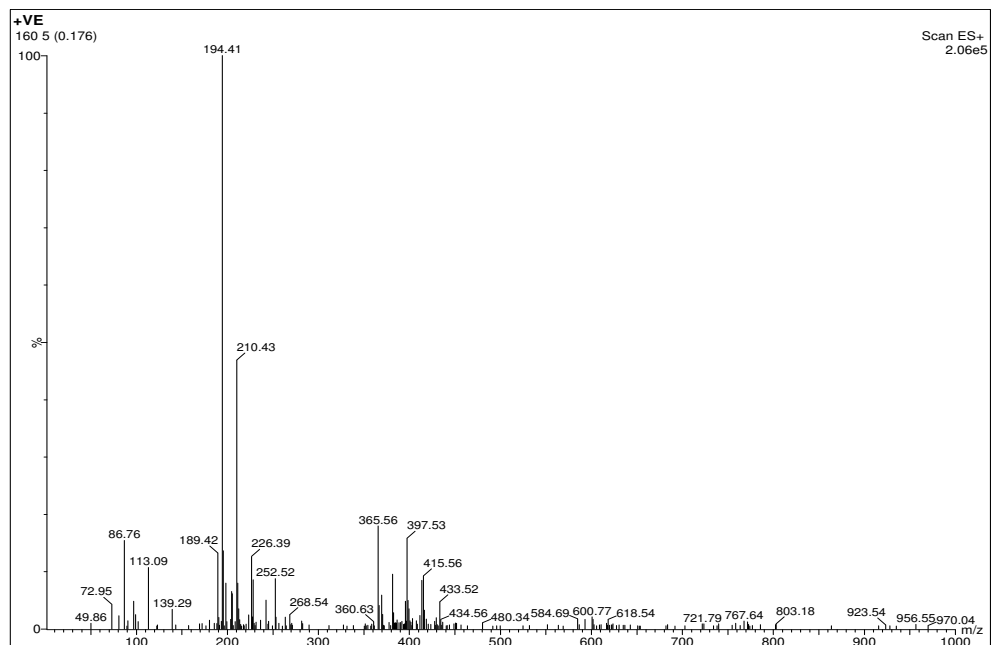


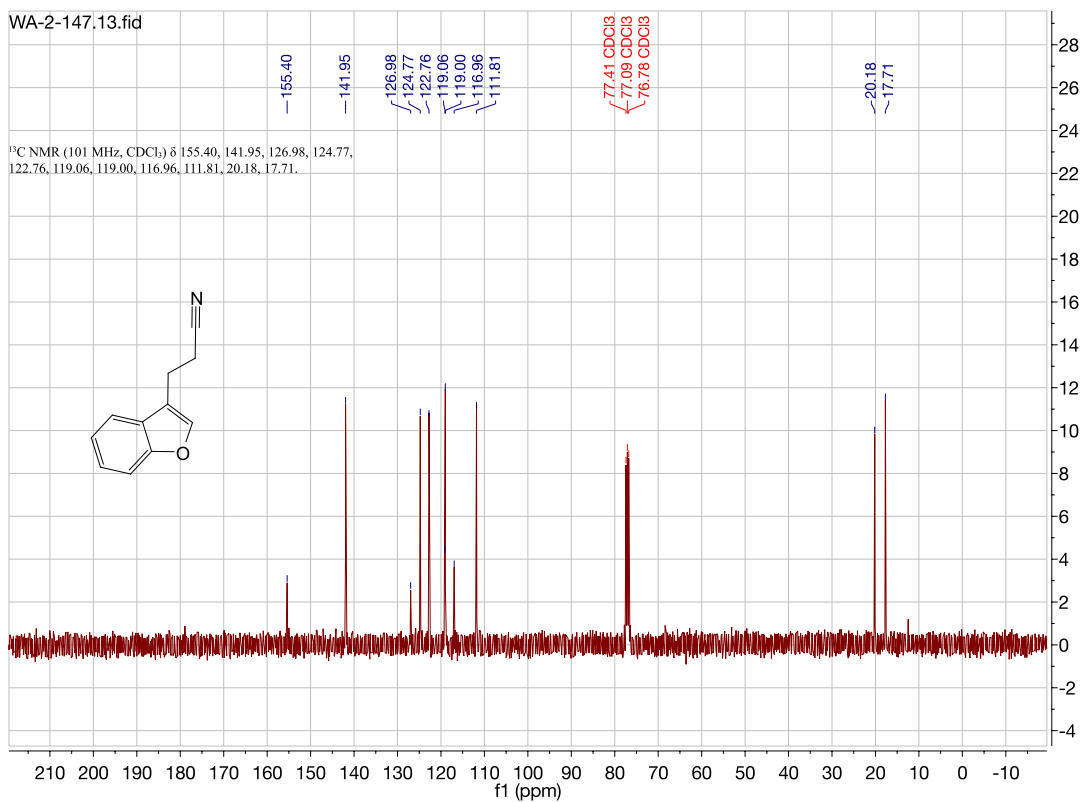
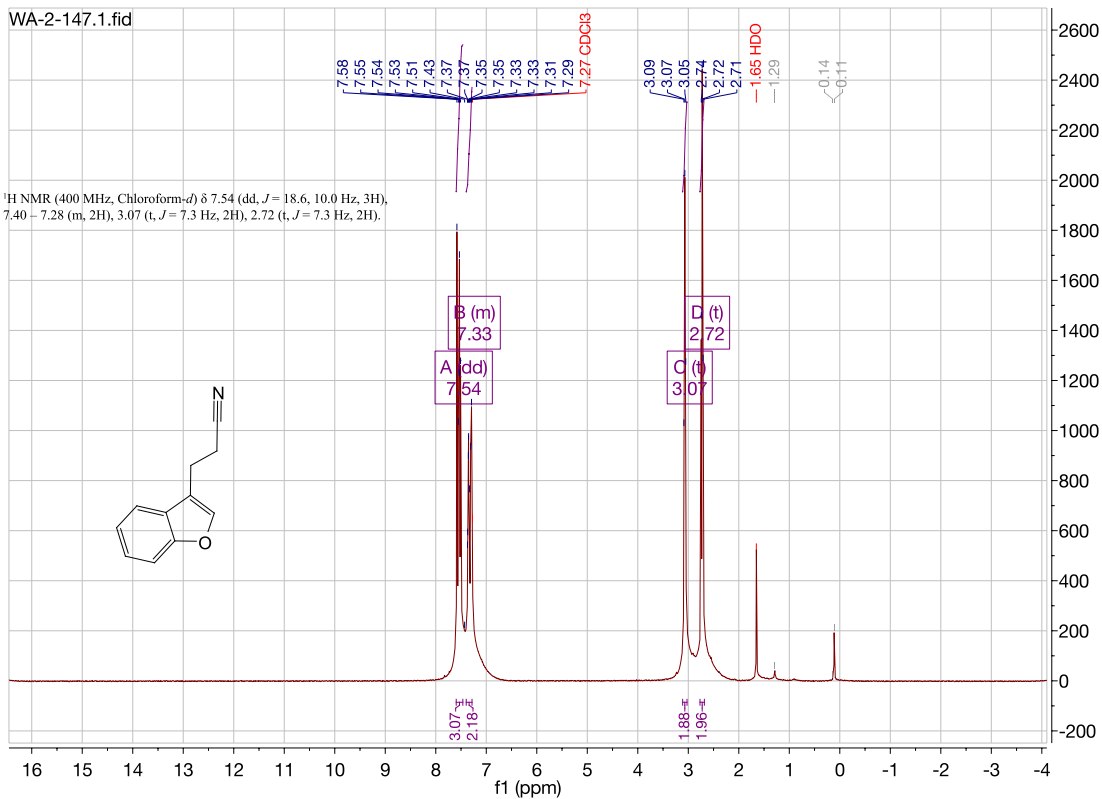
3-(2-bromoethyl)benzofuran. (WA136/141)

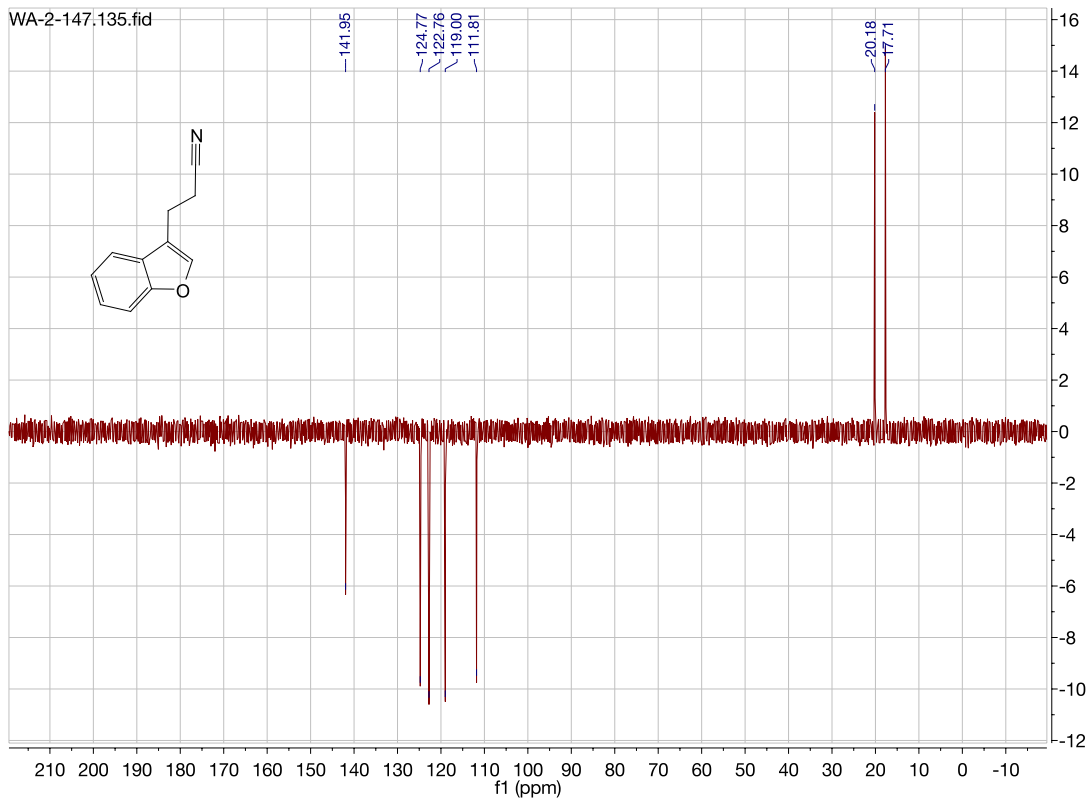




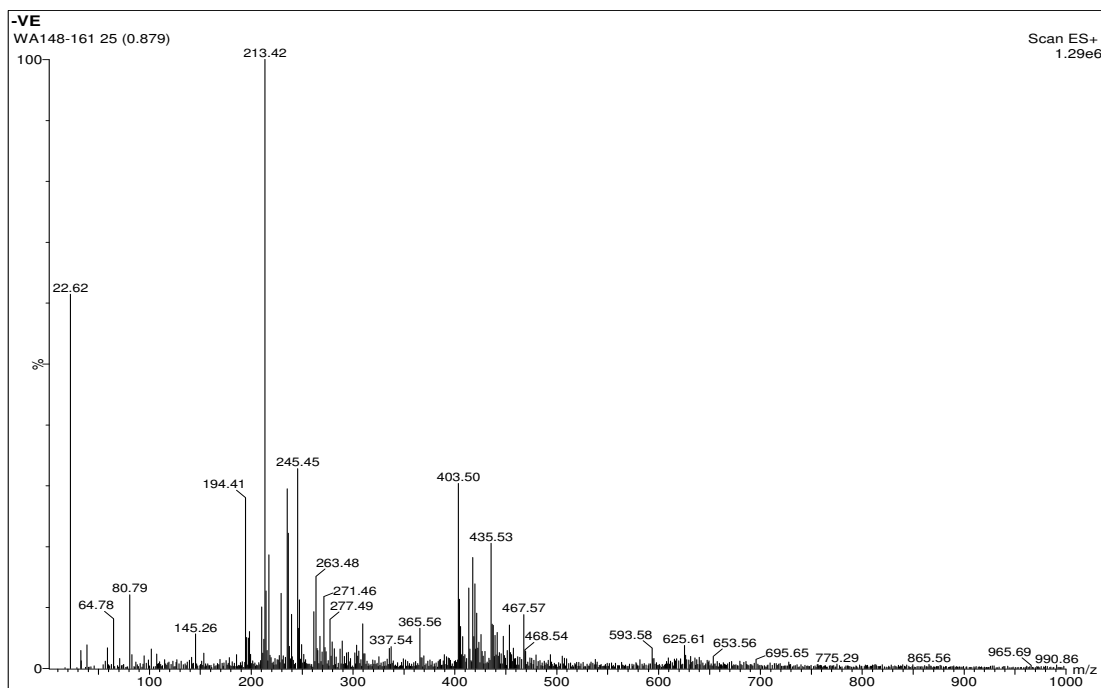
3-(benzofuran-3-yl)propanenitrile. (WA147/160/191)

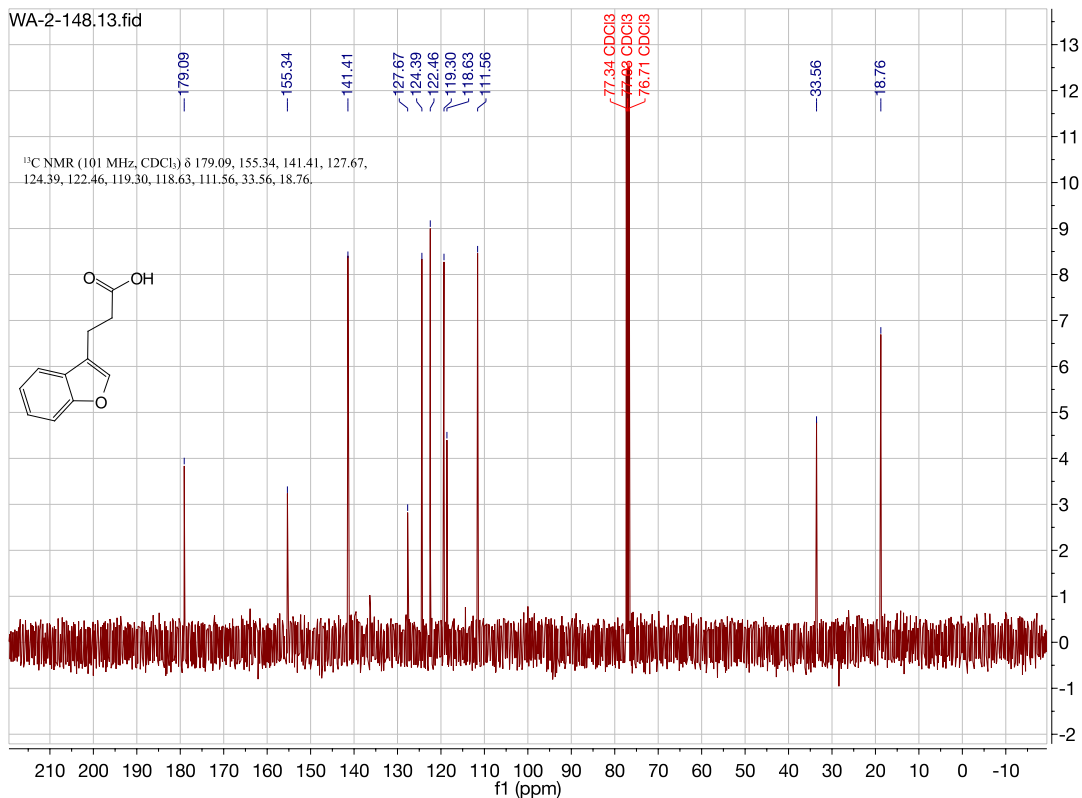
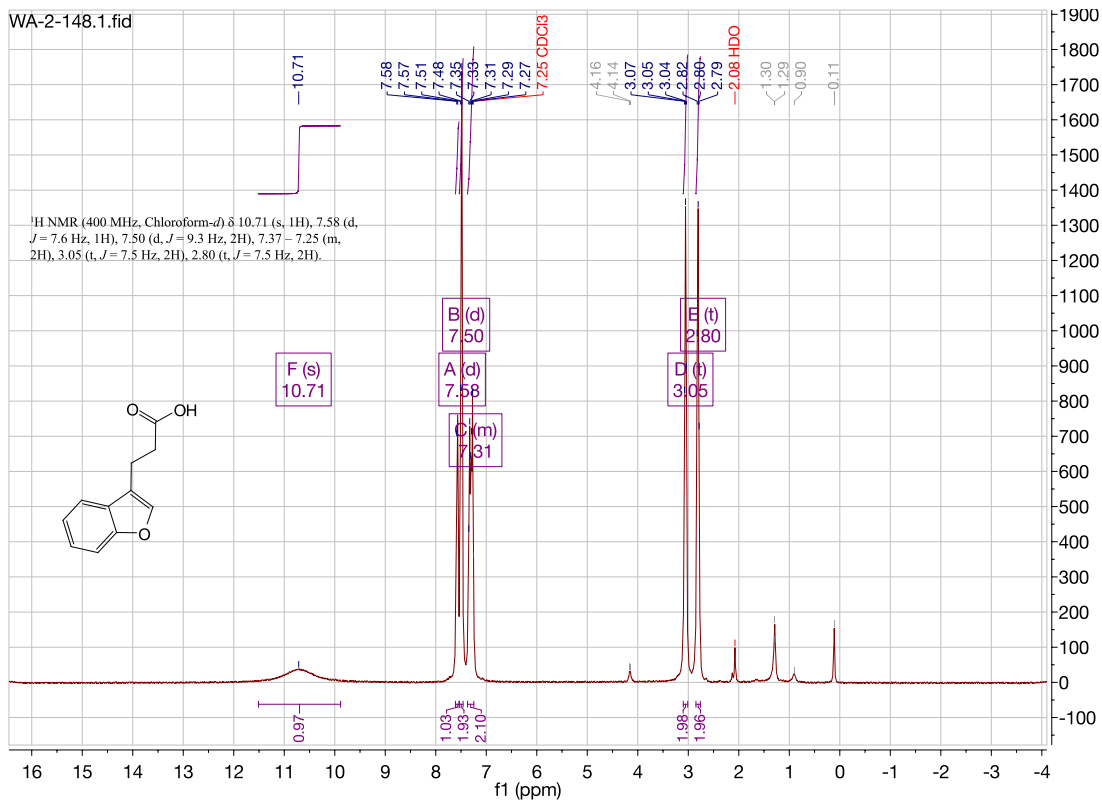


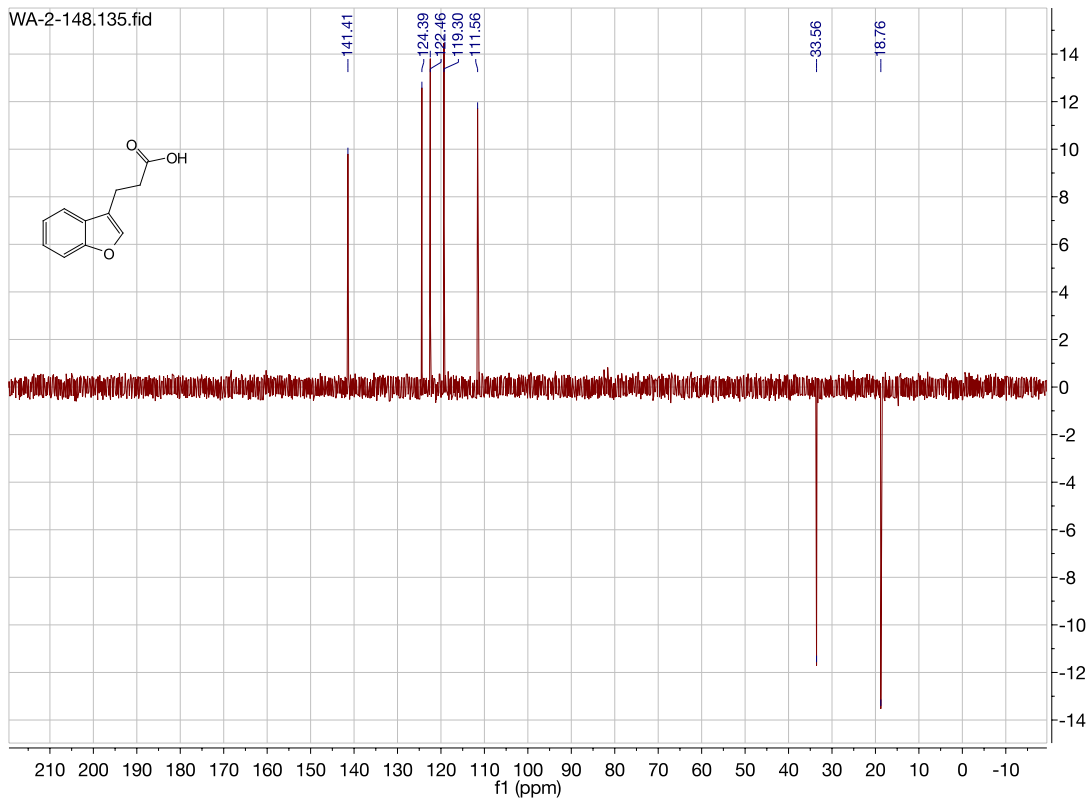




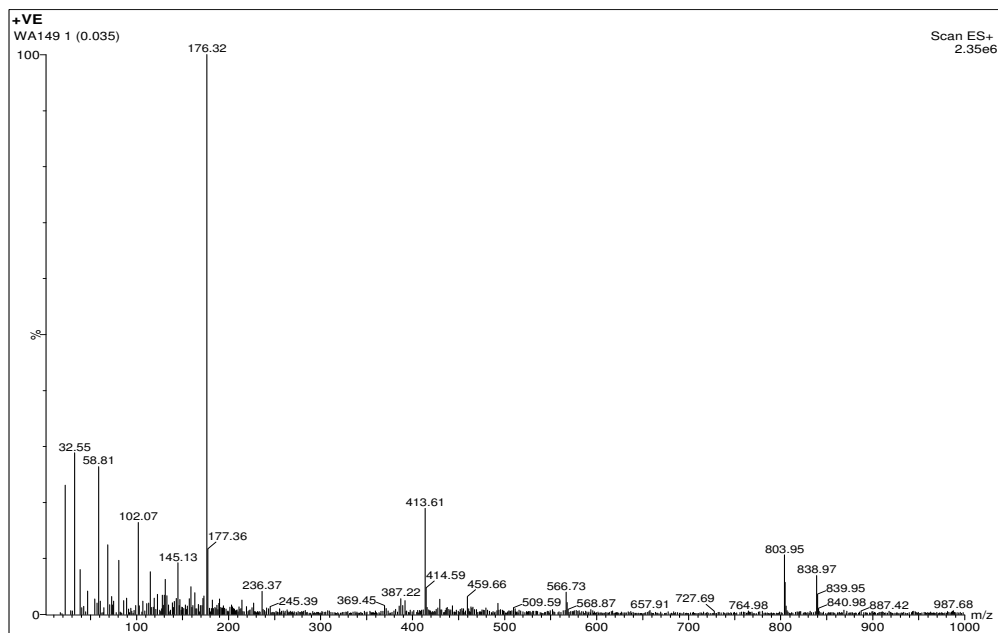
3-(benzofuran-3-yl)propanoic acid. (WA148/161/191)

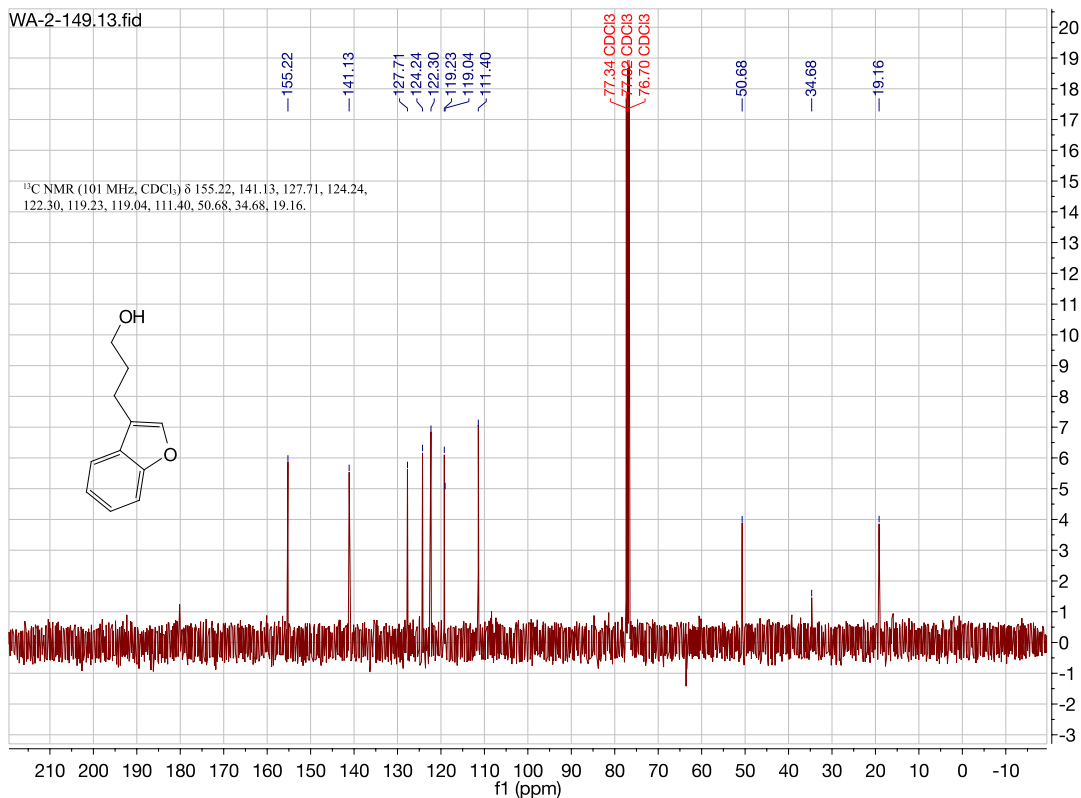
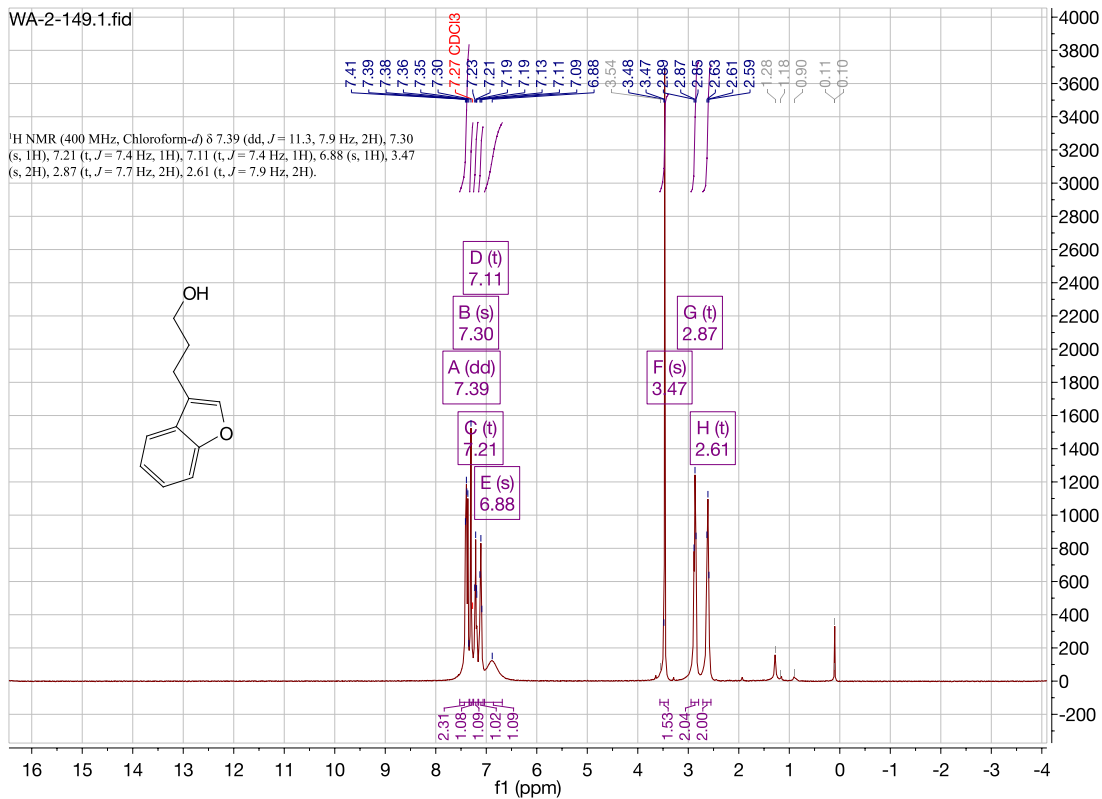




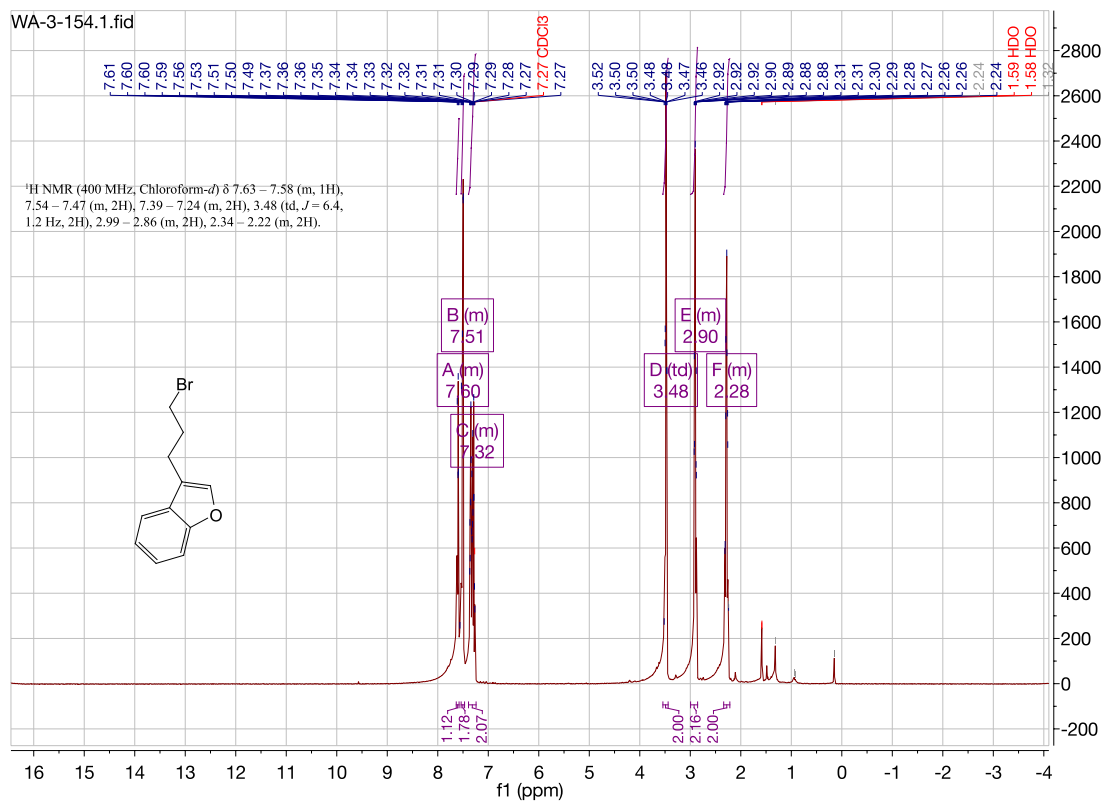
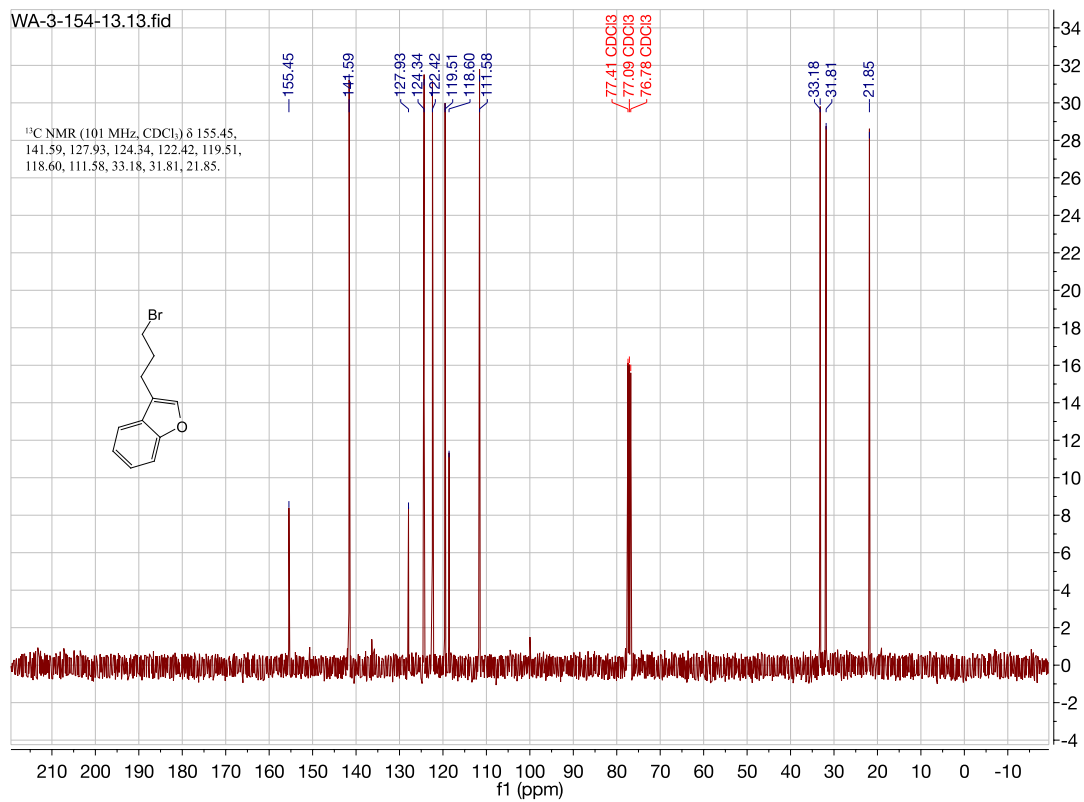


3-(benzofuran-3-yl)propan-1-ol. (WA149/162/192)

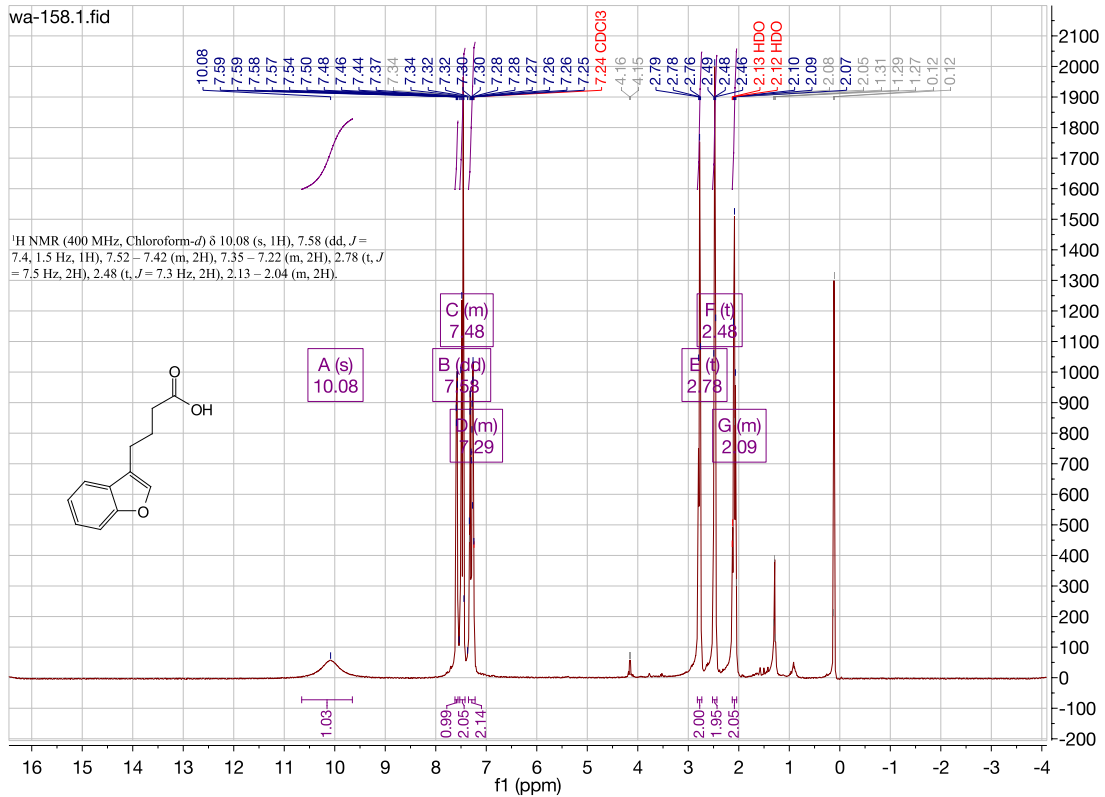
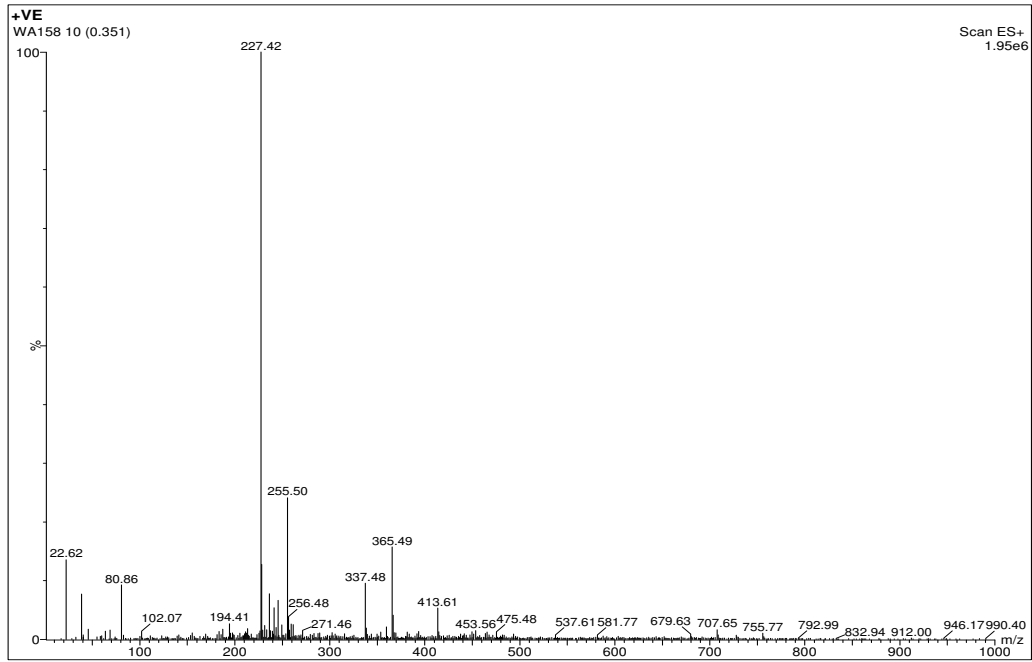


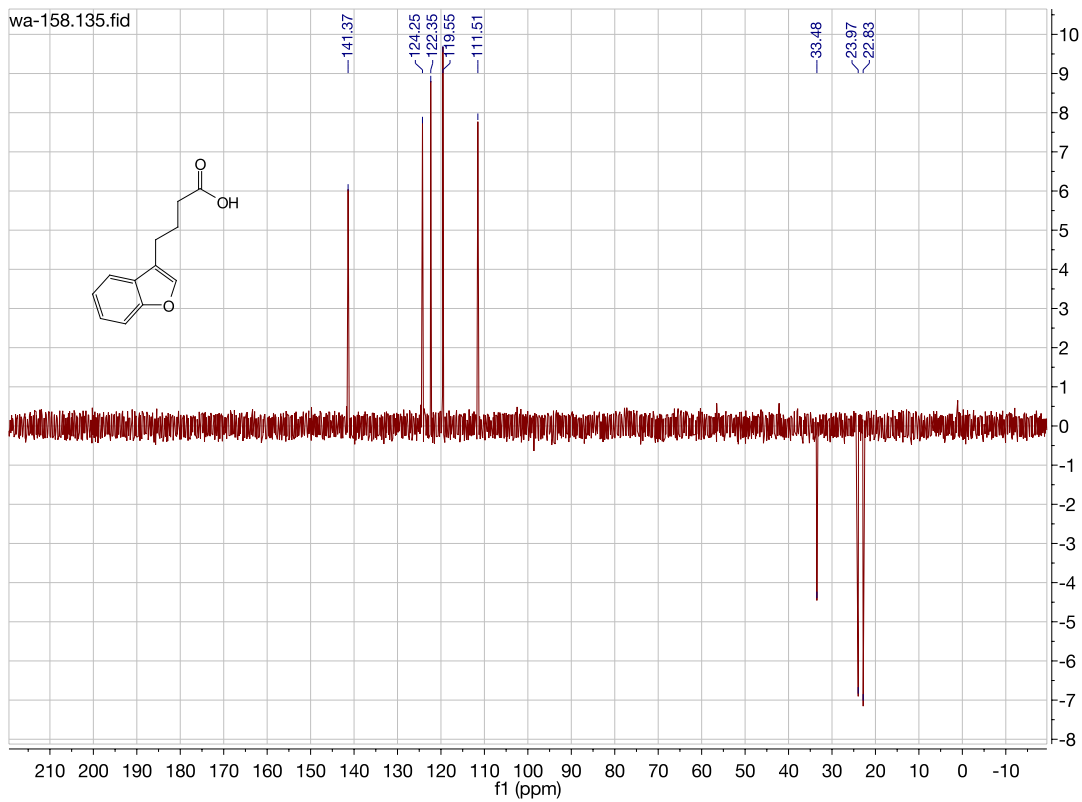
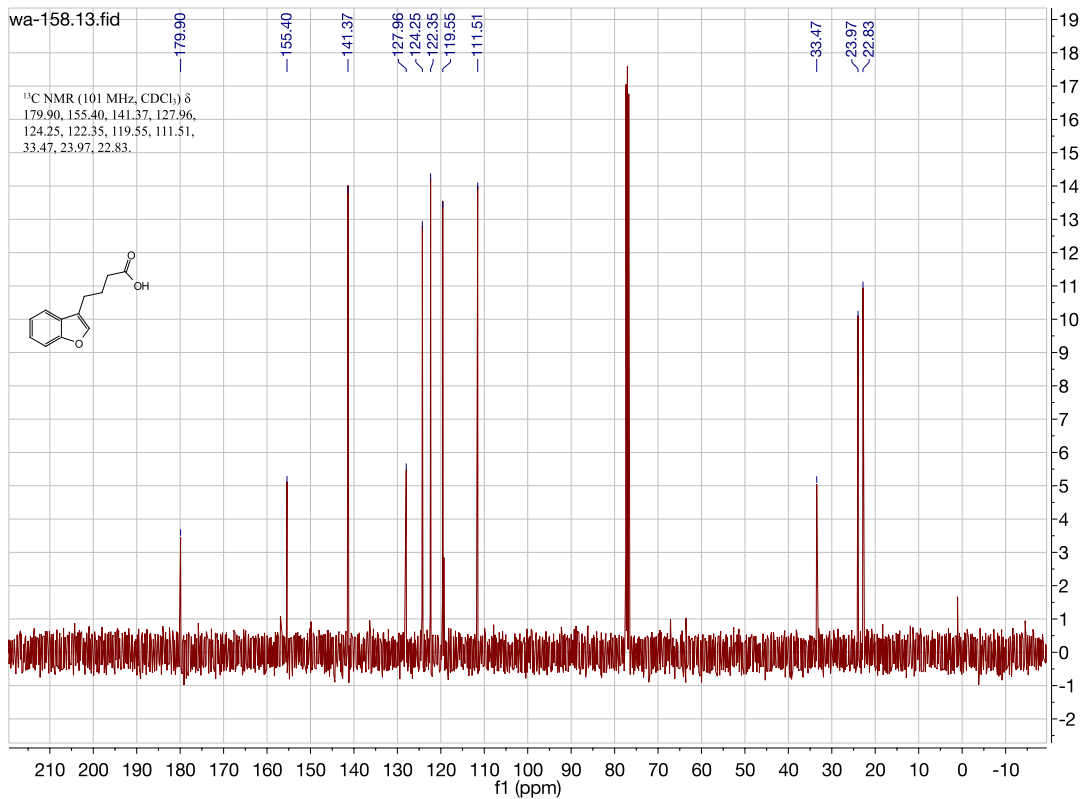


3-(3-bromopropyl)benzofuran. (WA154/164/197)

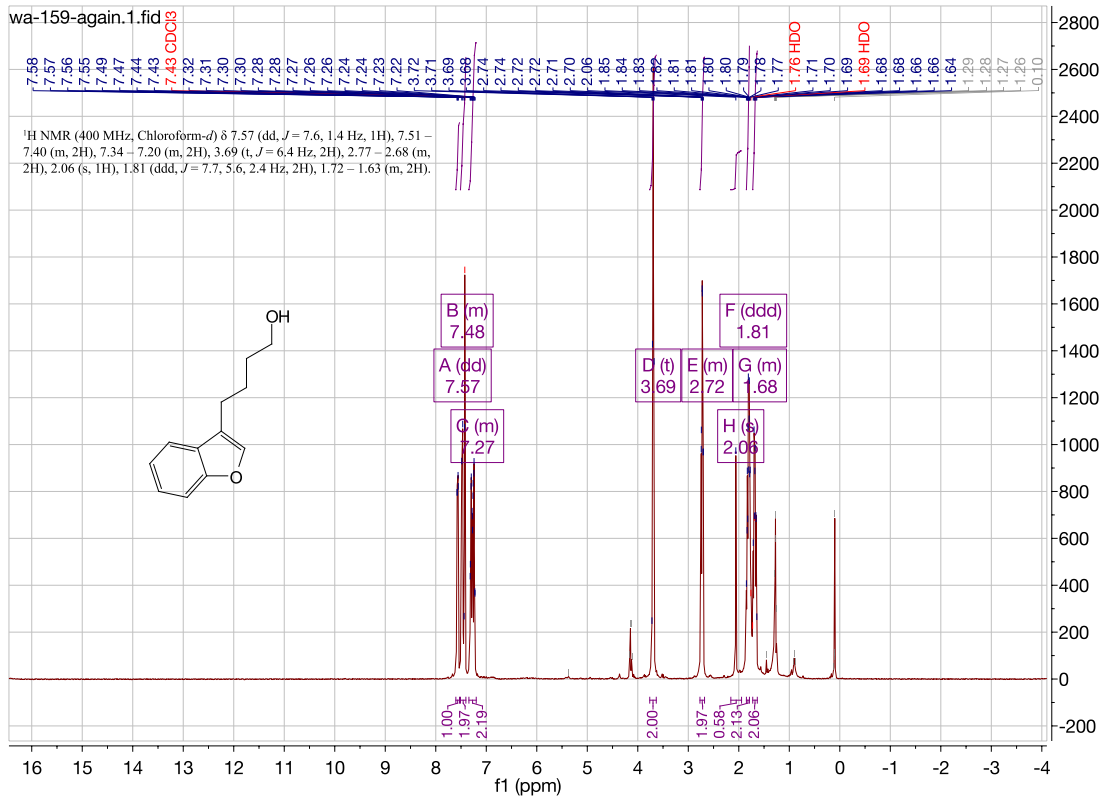
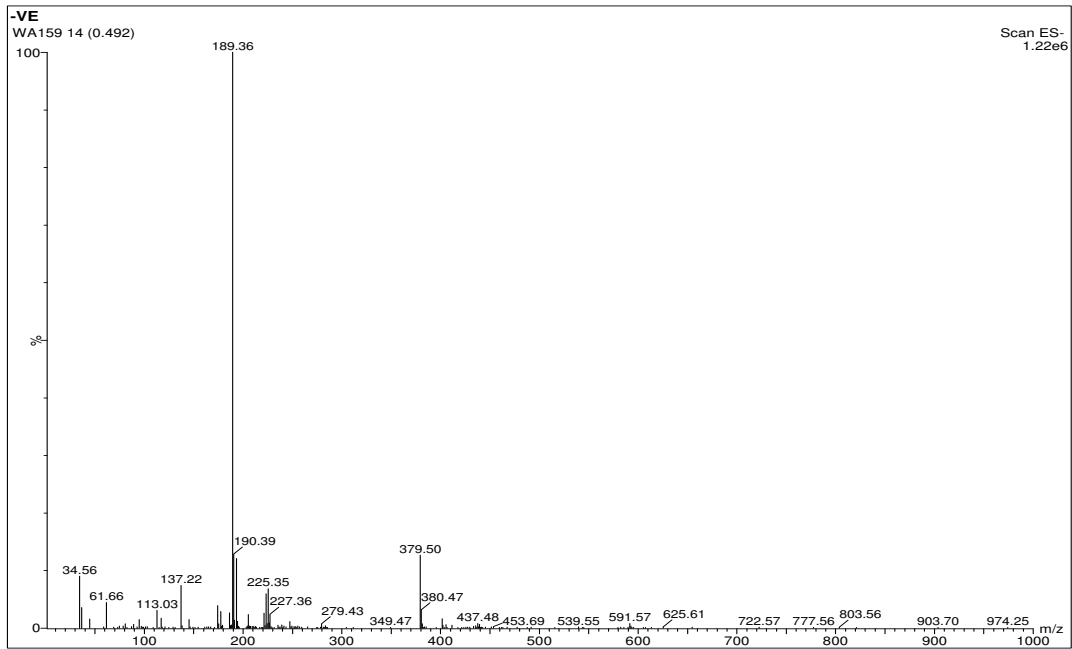


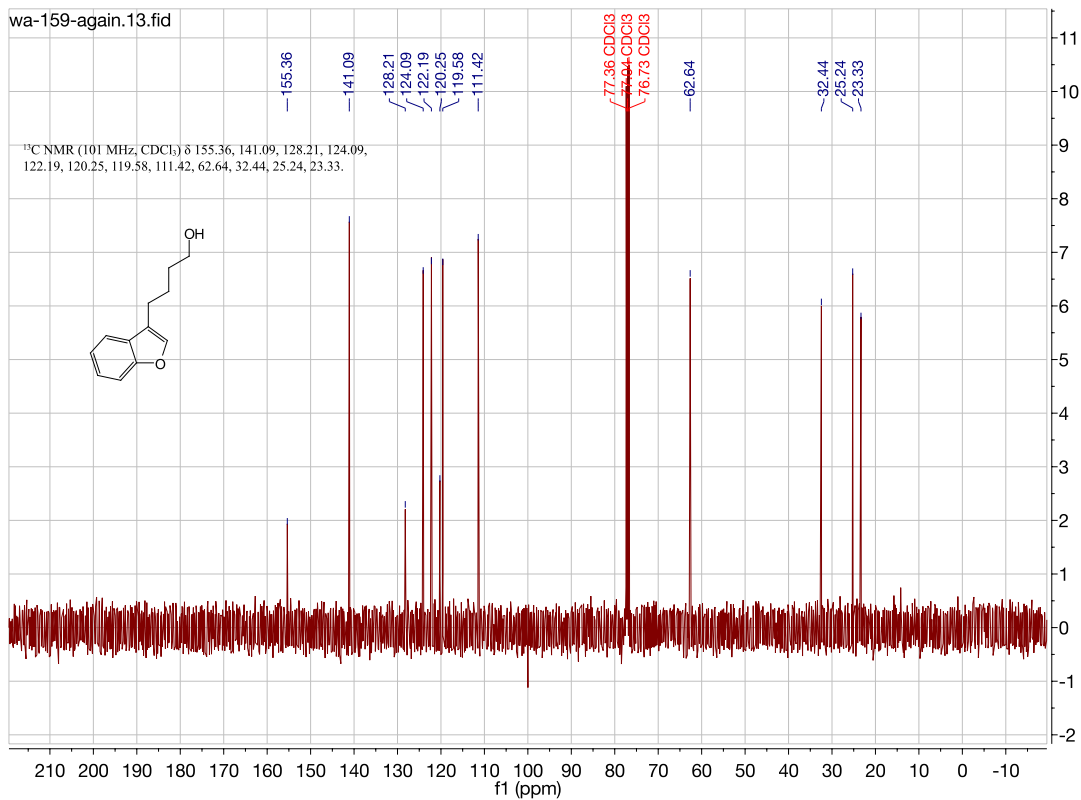
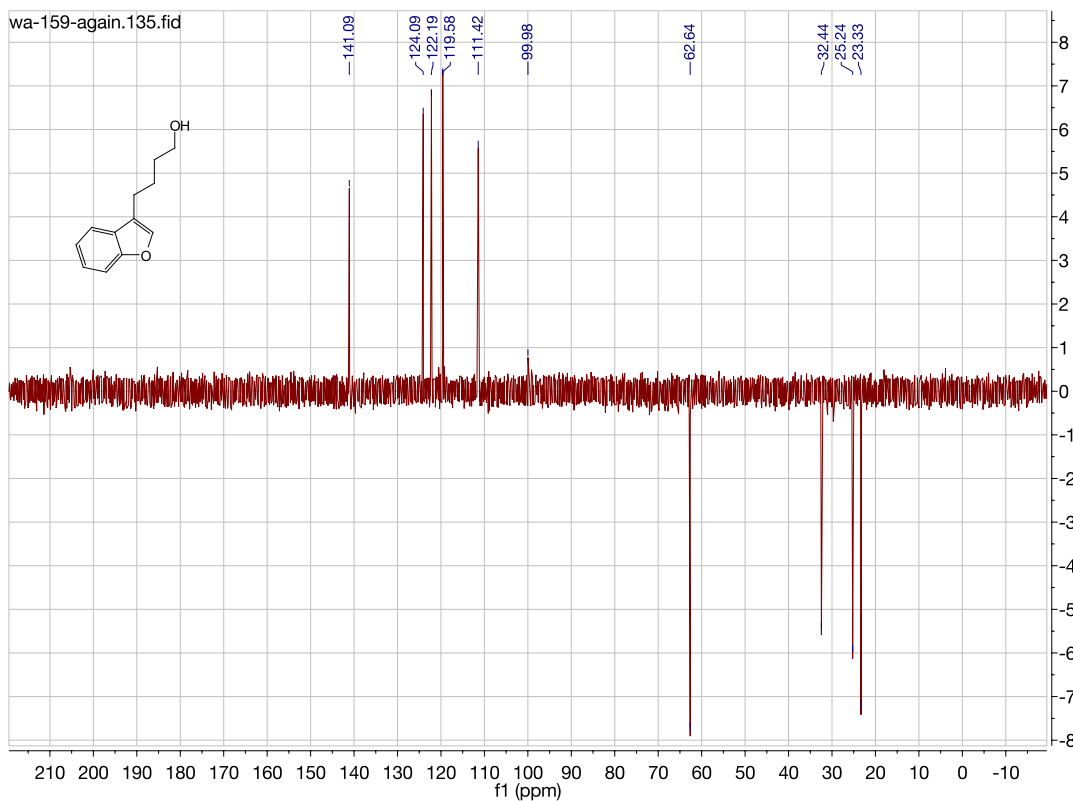
4-(benzofuran-3-yl)butanoic acid. (WA166/158/202)



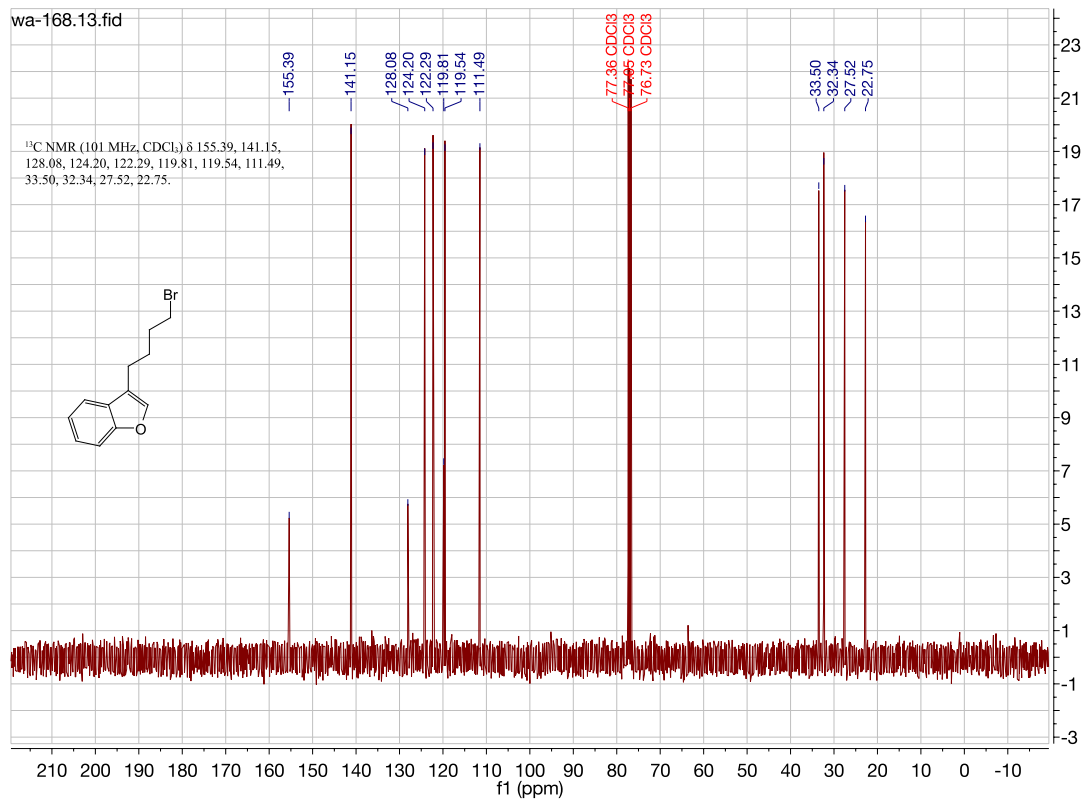
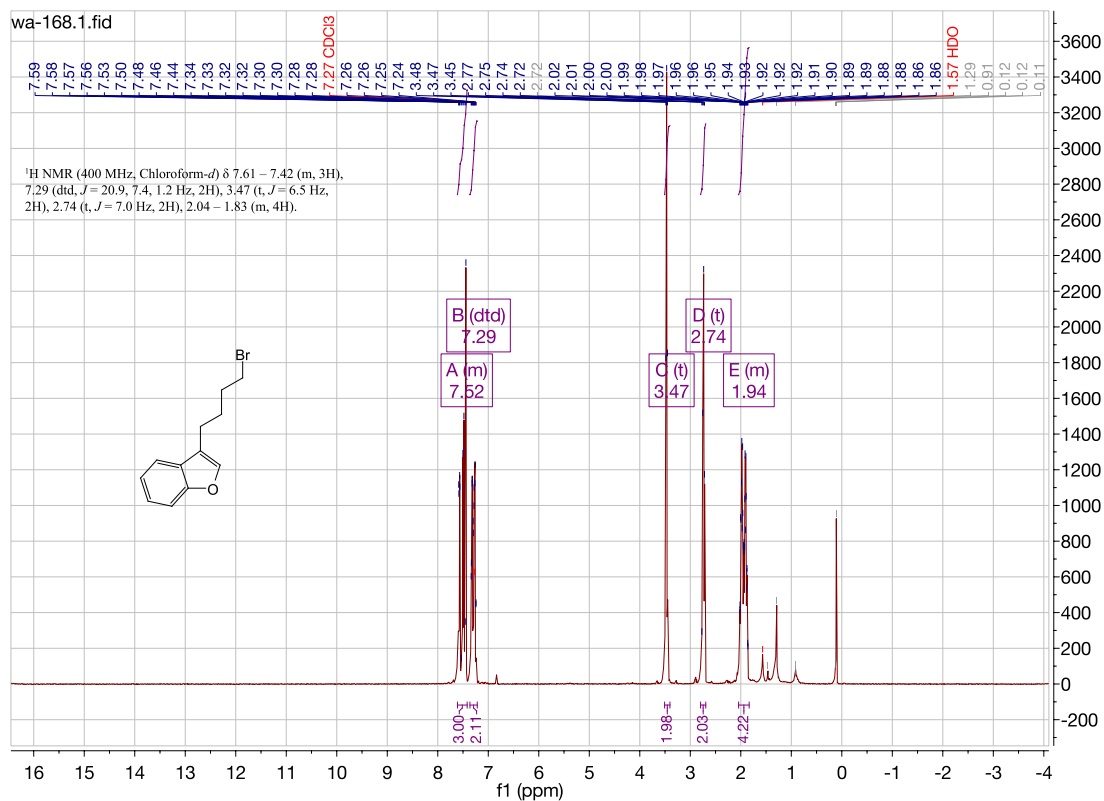


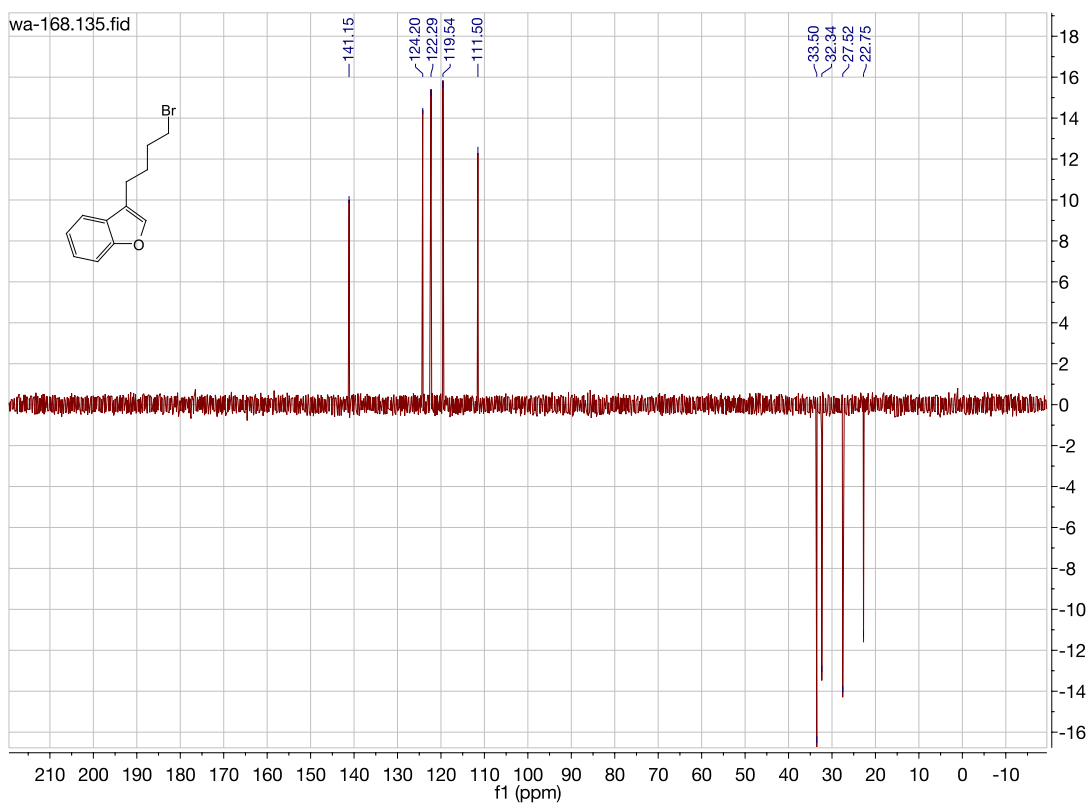
4-(benzofuran-3-yl) butan-1-ol. (WA159/167)



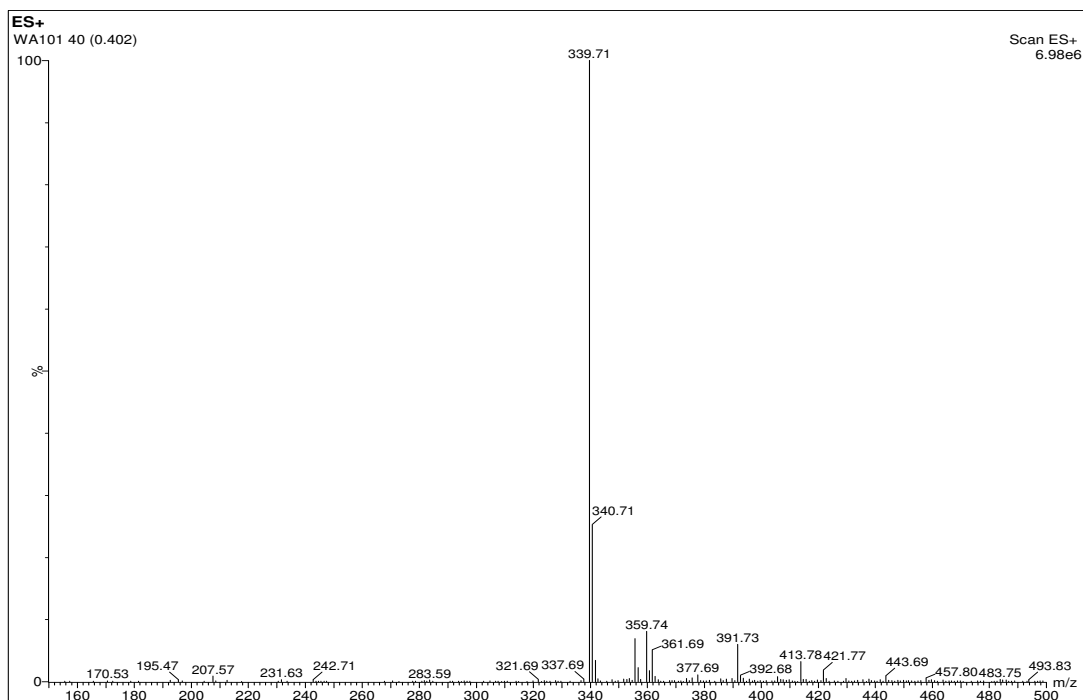


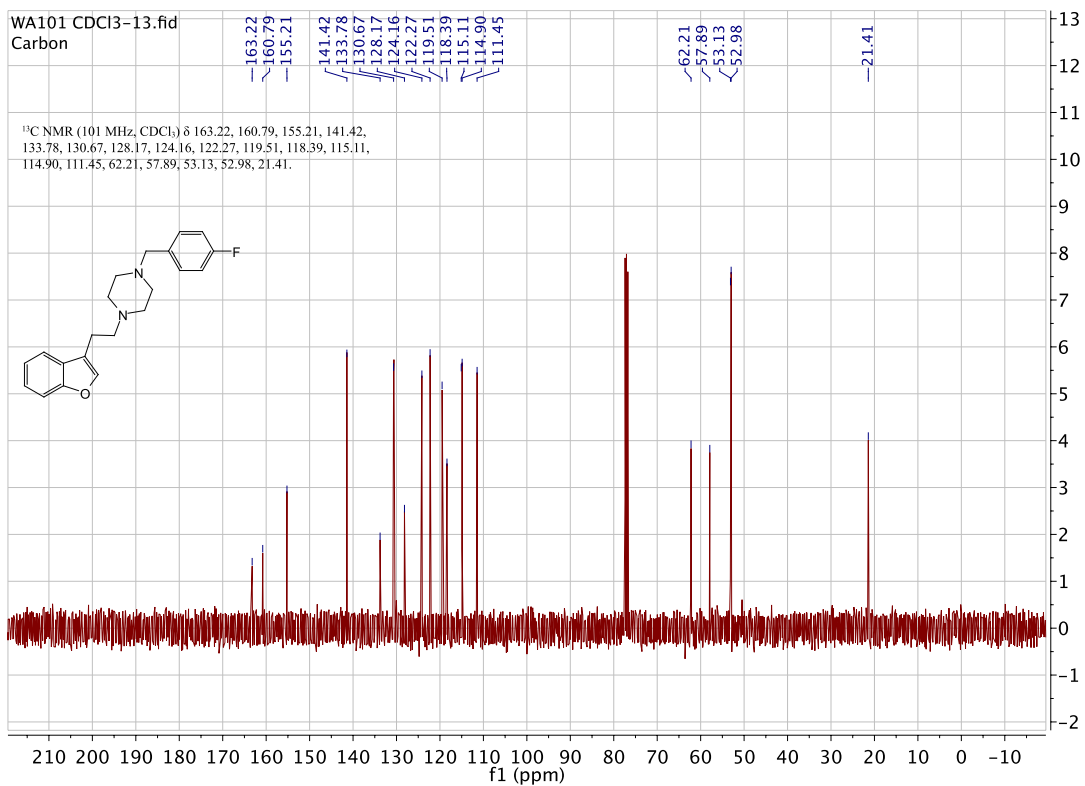
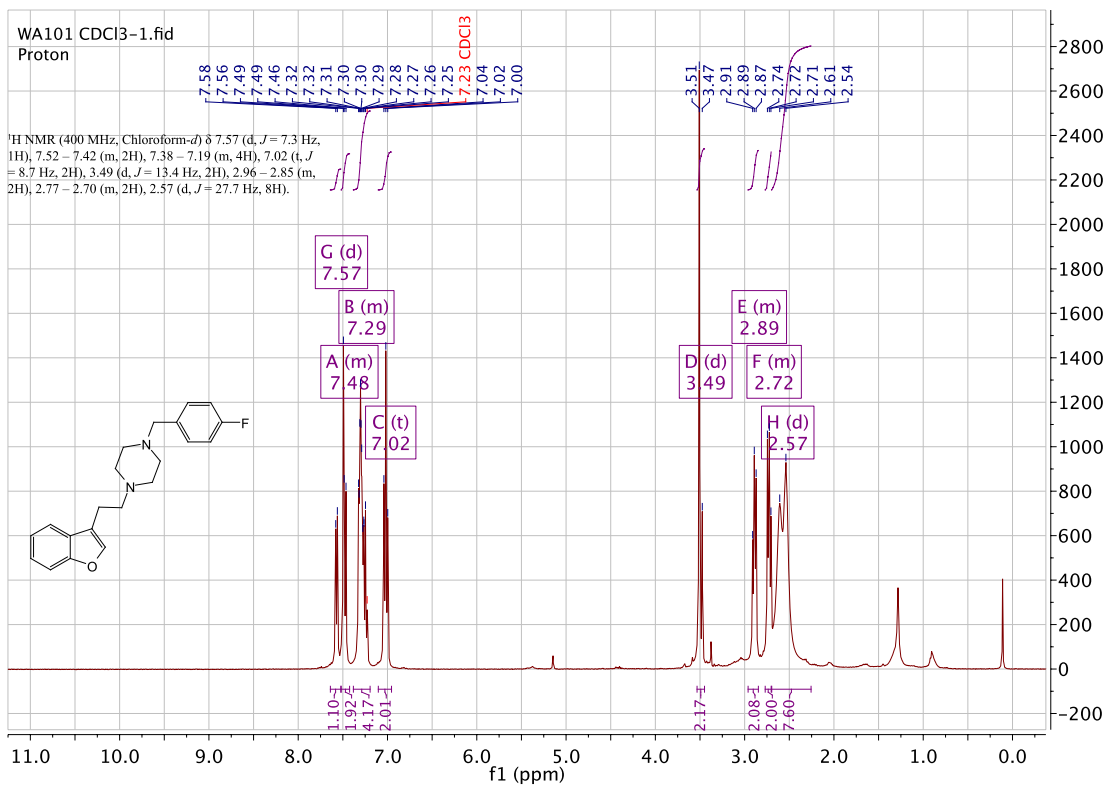
3-(4-bromobutyl)benzofuran. (WA163/168)

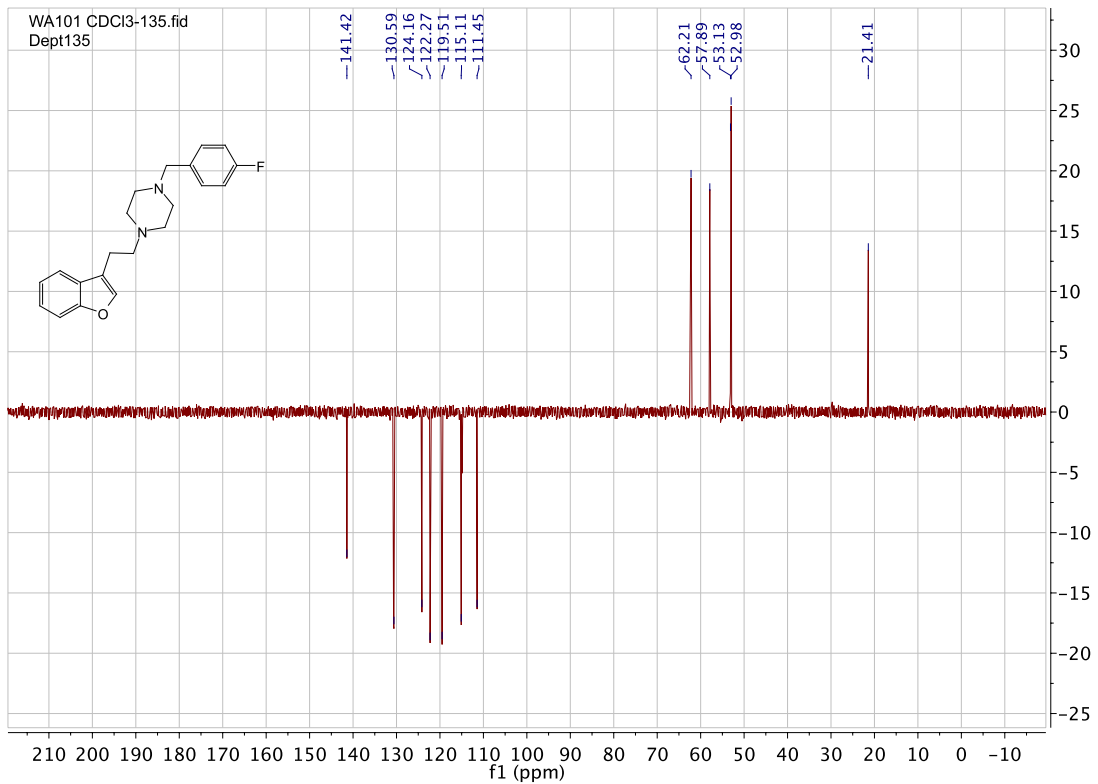




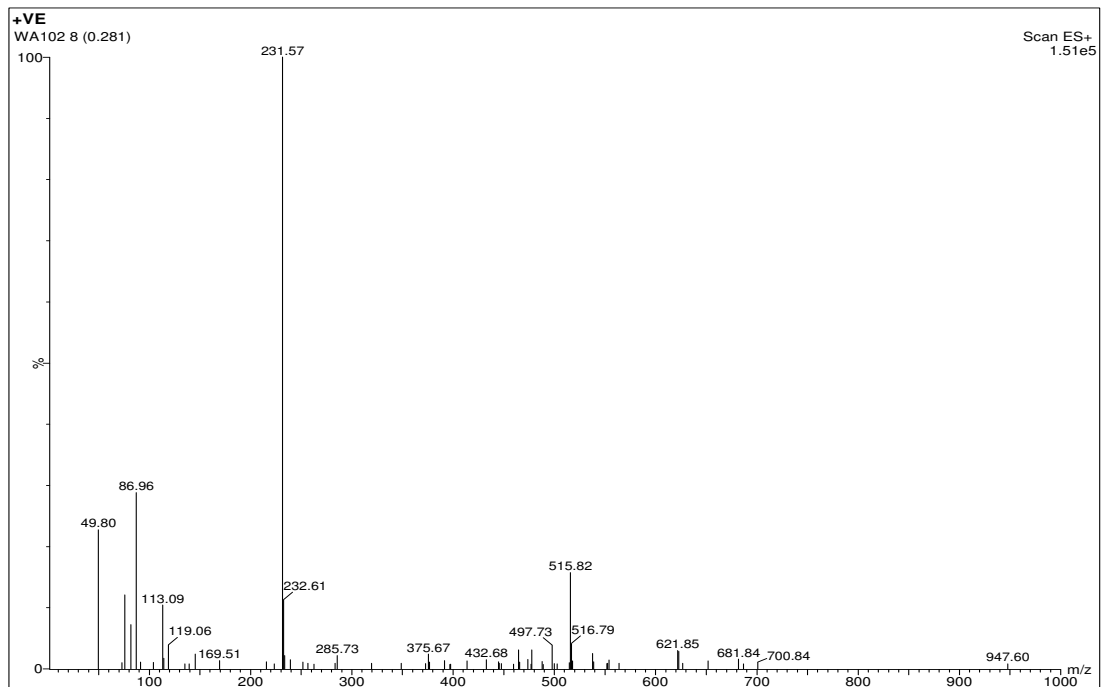
1-(2-(benzofuran-3-yl)ethyl)-4-(4-fluorobenzyl)piperazine. (WA101)

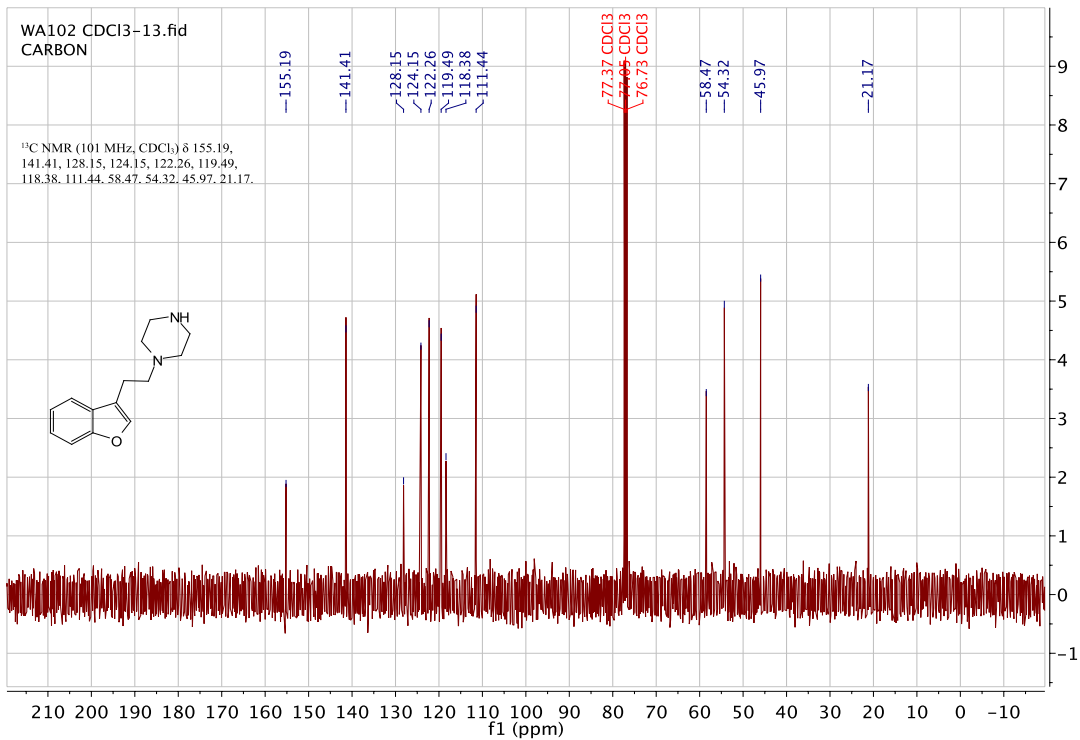
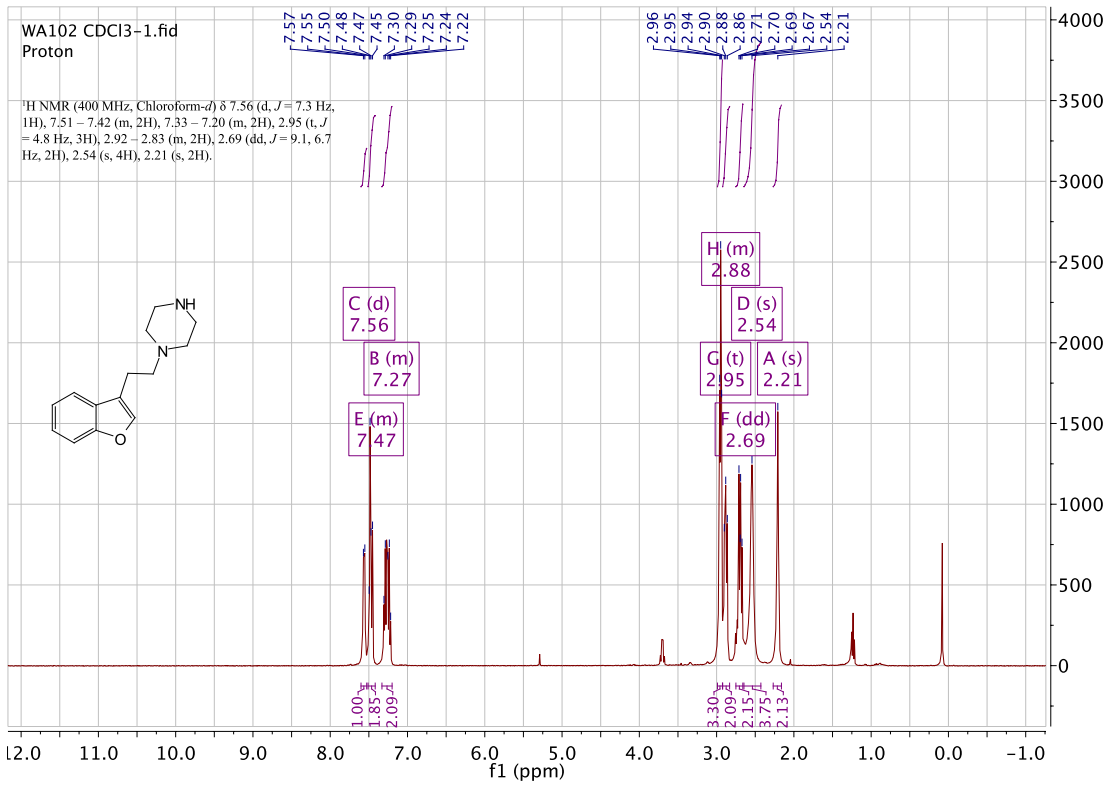




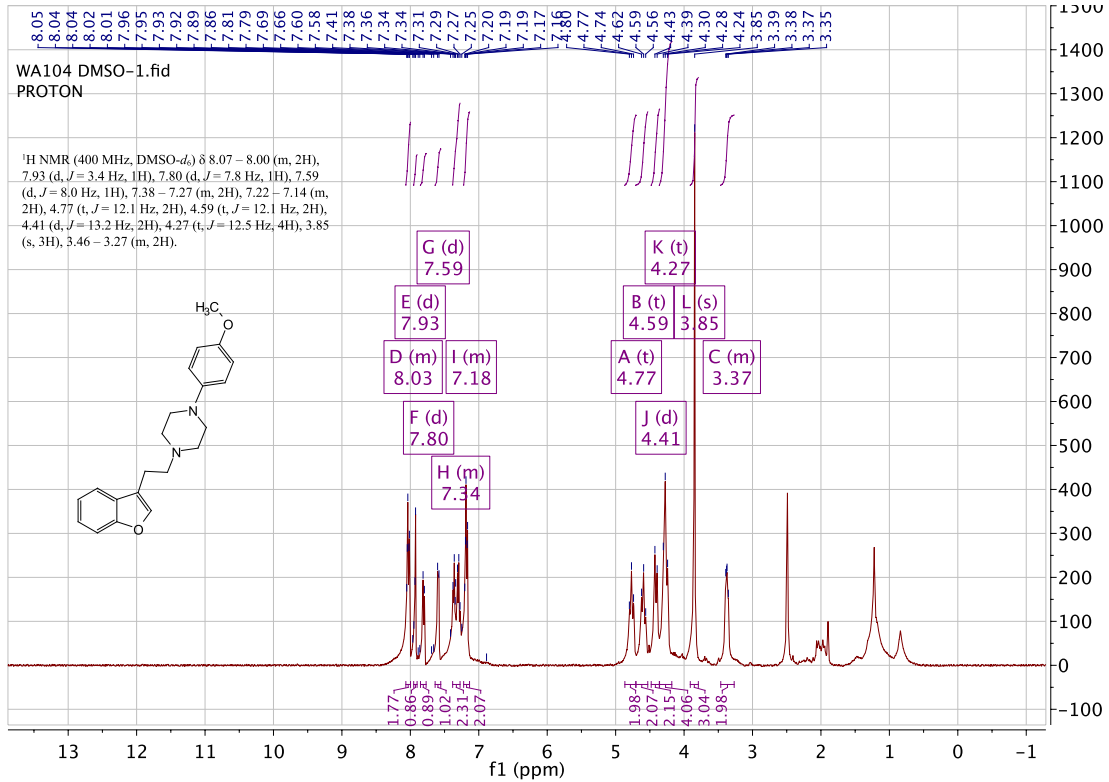
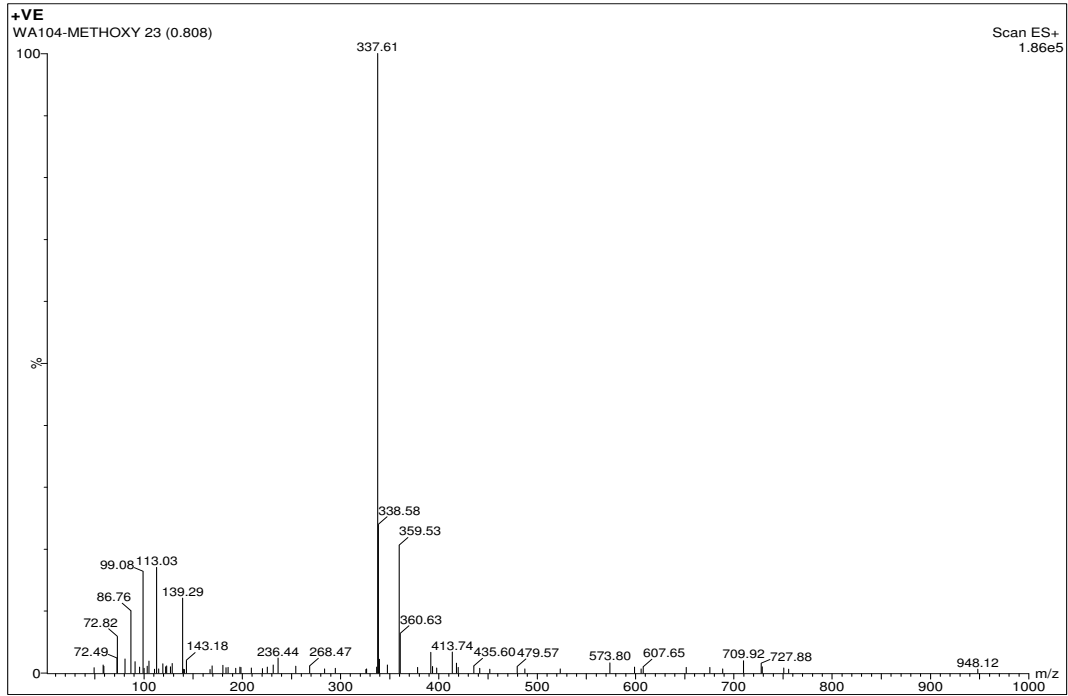


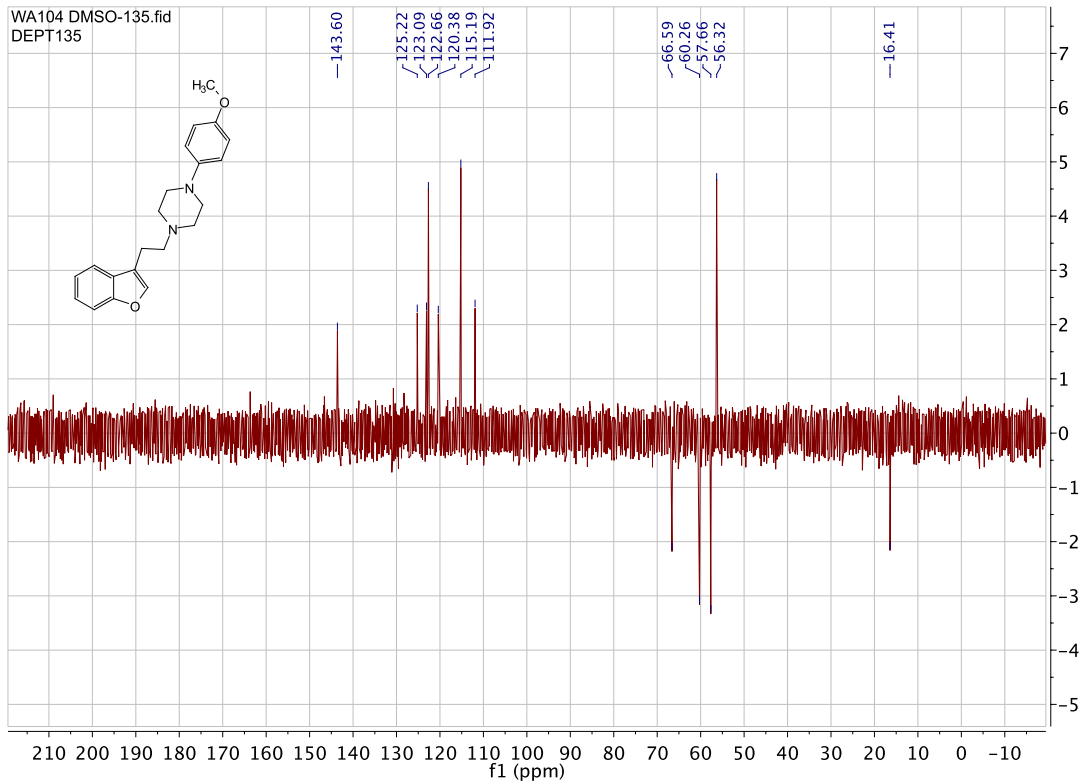
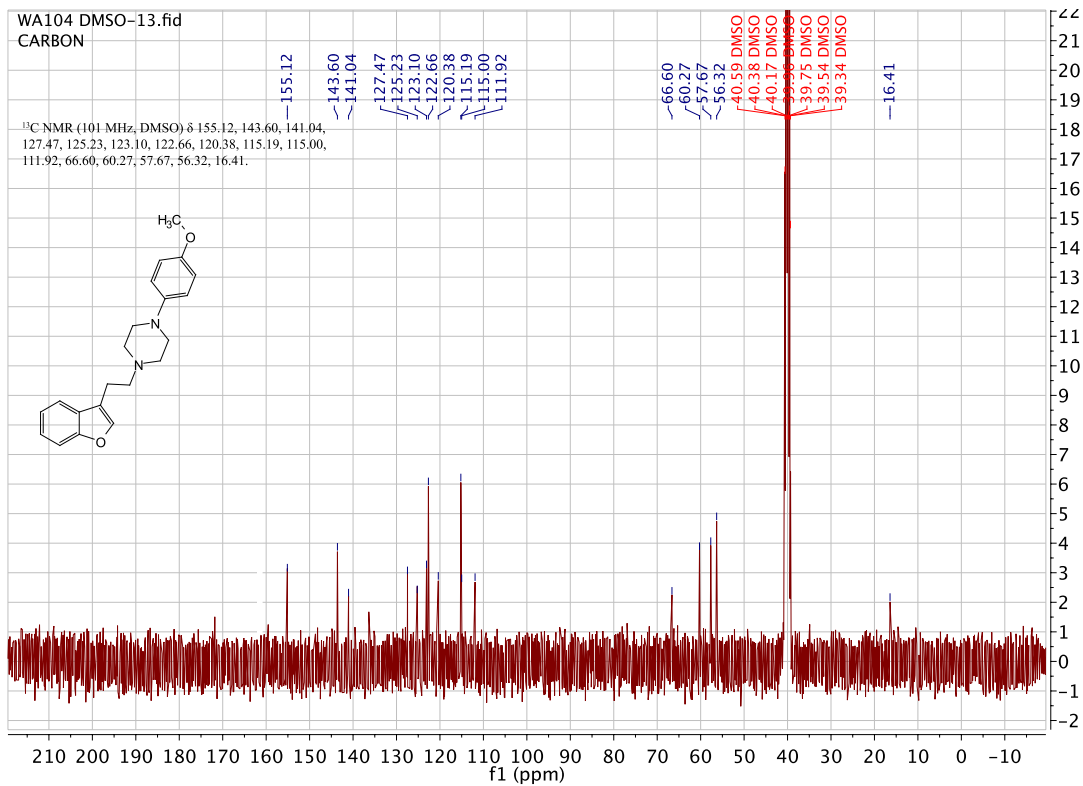
1-(2-(benzofuran-3-yl)ethyl)piperazine. (WA102)



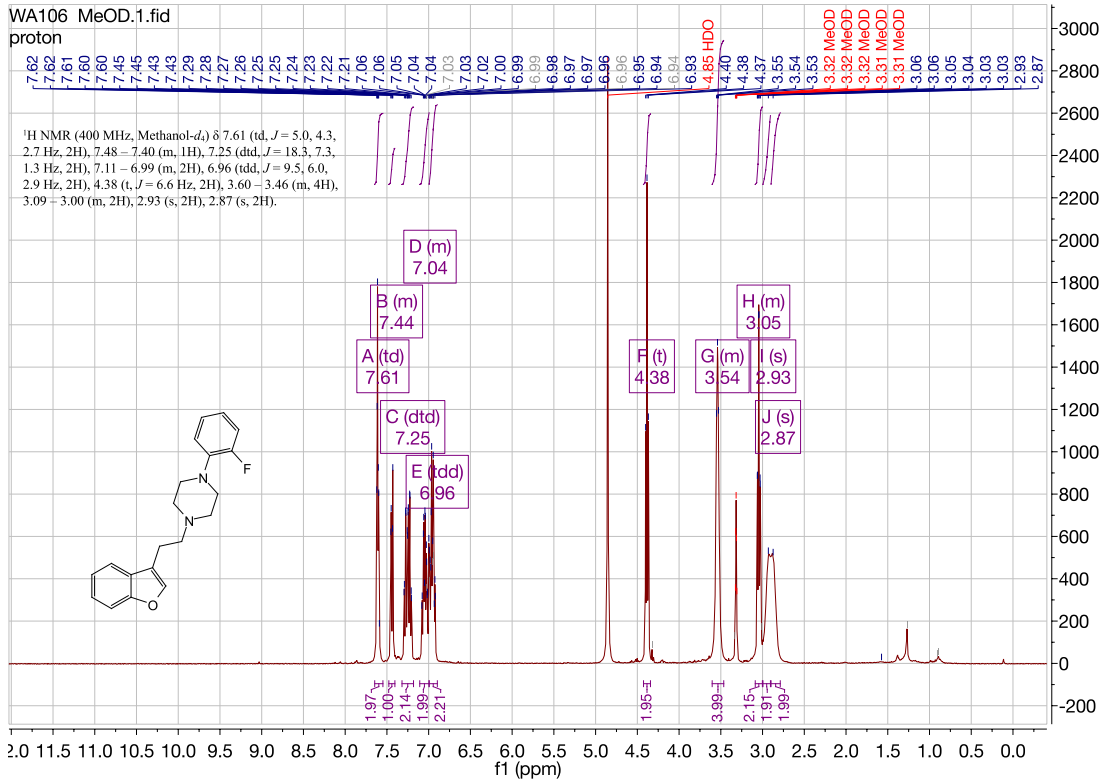
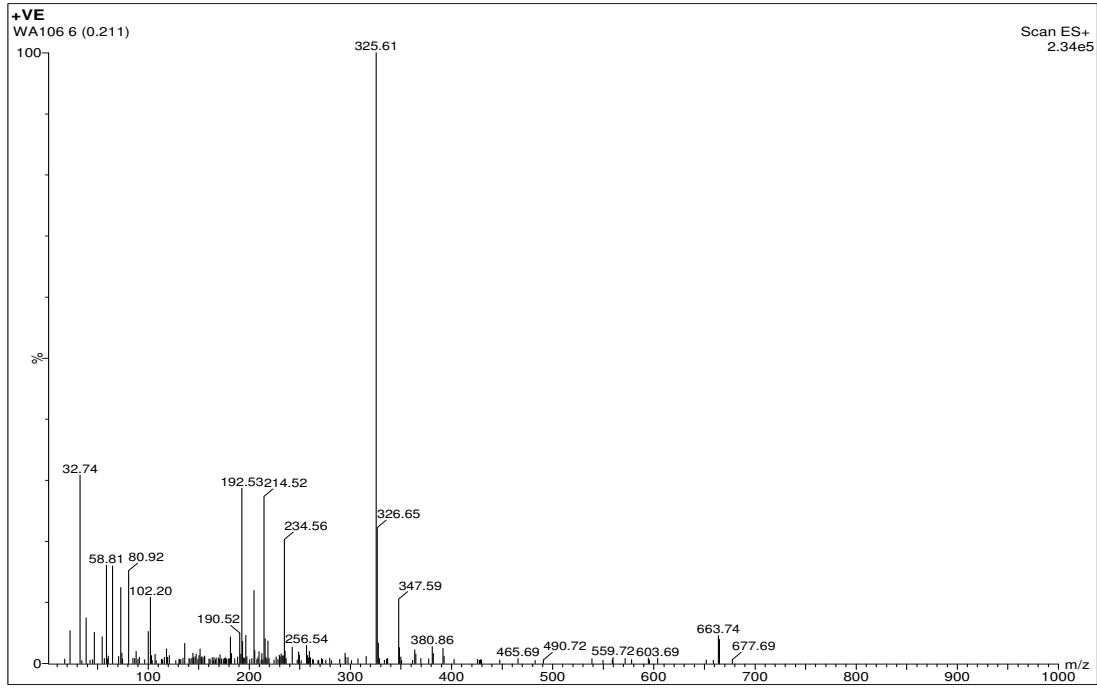


1-(2-(benzofuran-3-yl)ethyl)-4-(4-methoxyphenyl)piperazine. (WA104)

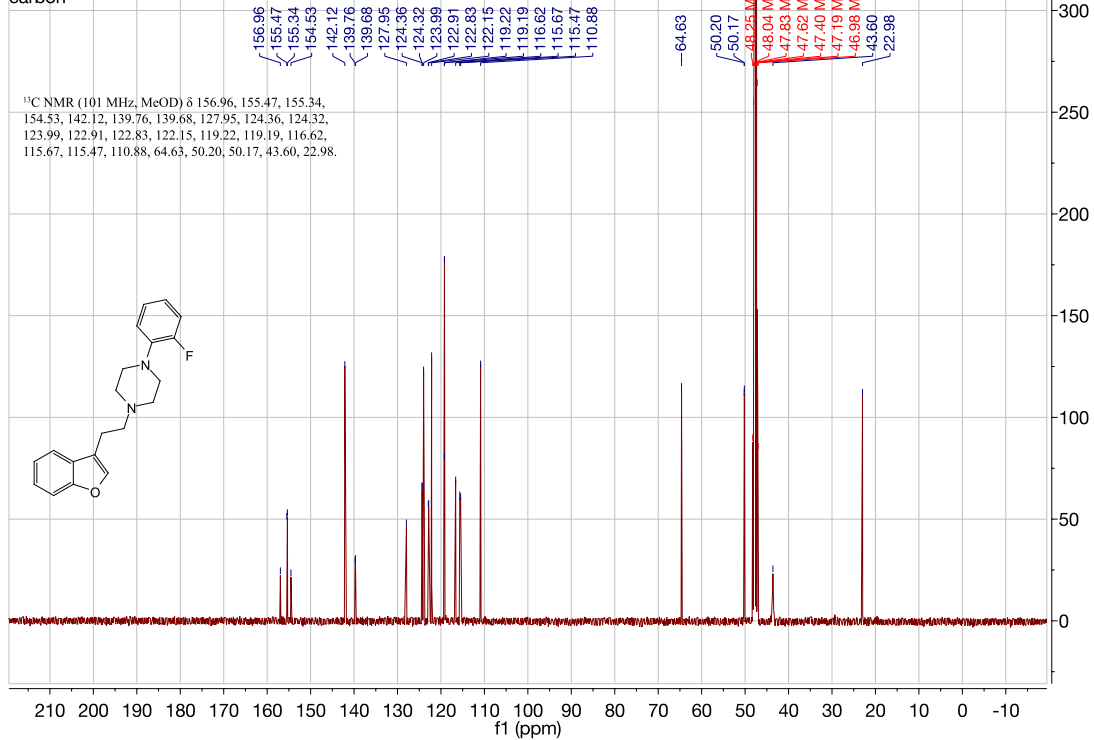




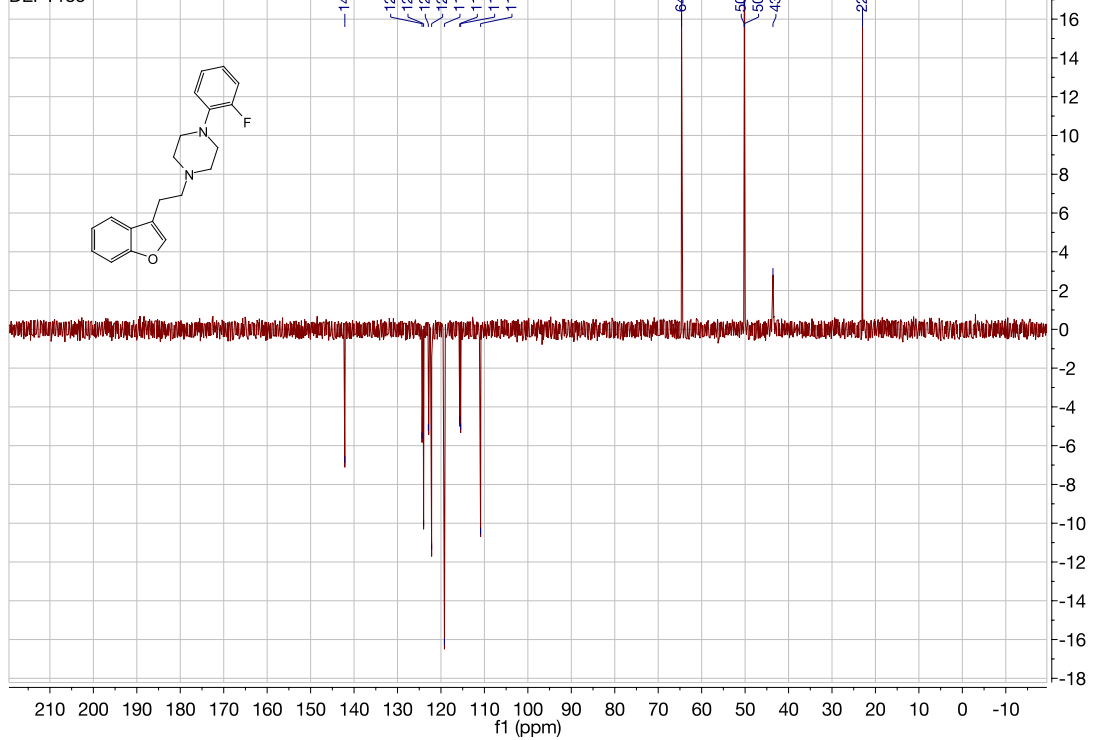
1-(2-(benzofuran-3-yl)ethyl)-4-(2-fluorophenyl)piperazine.(WA106/110/180)



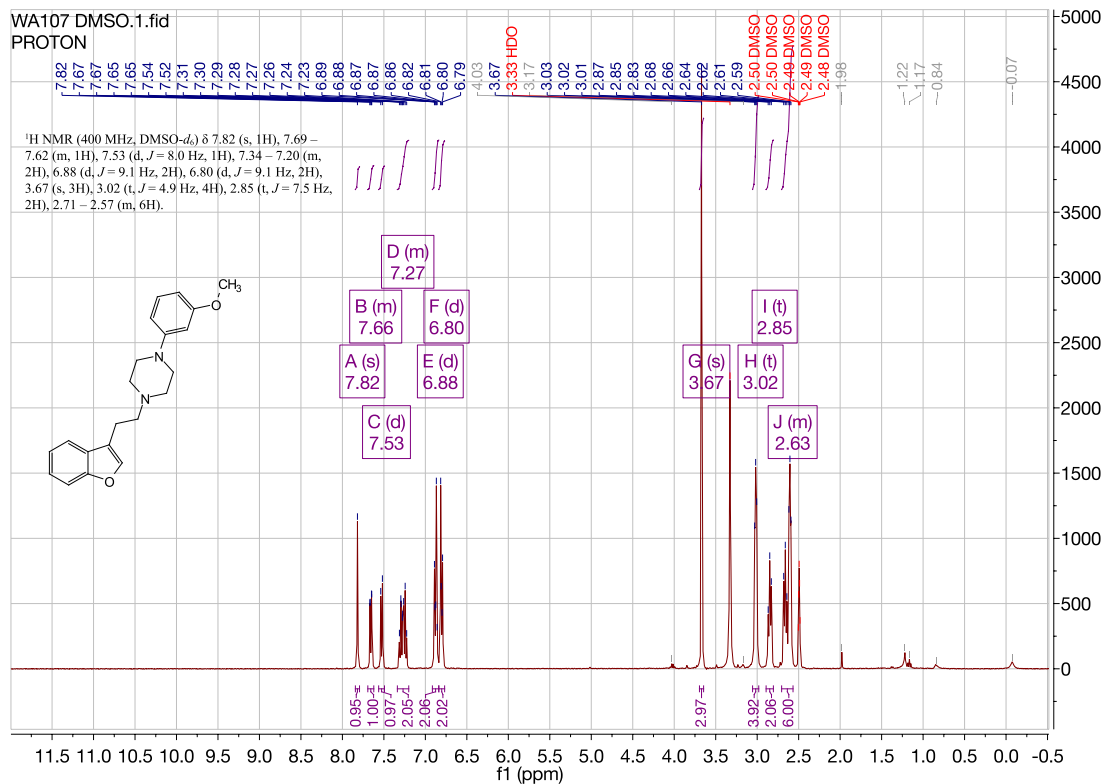
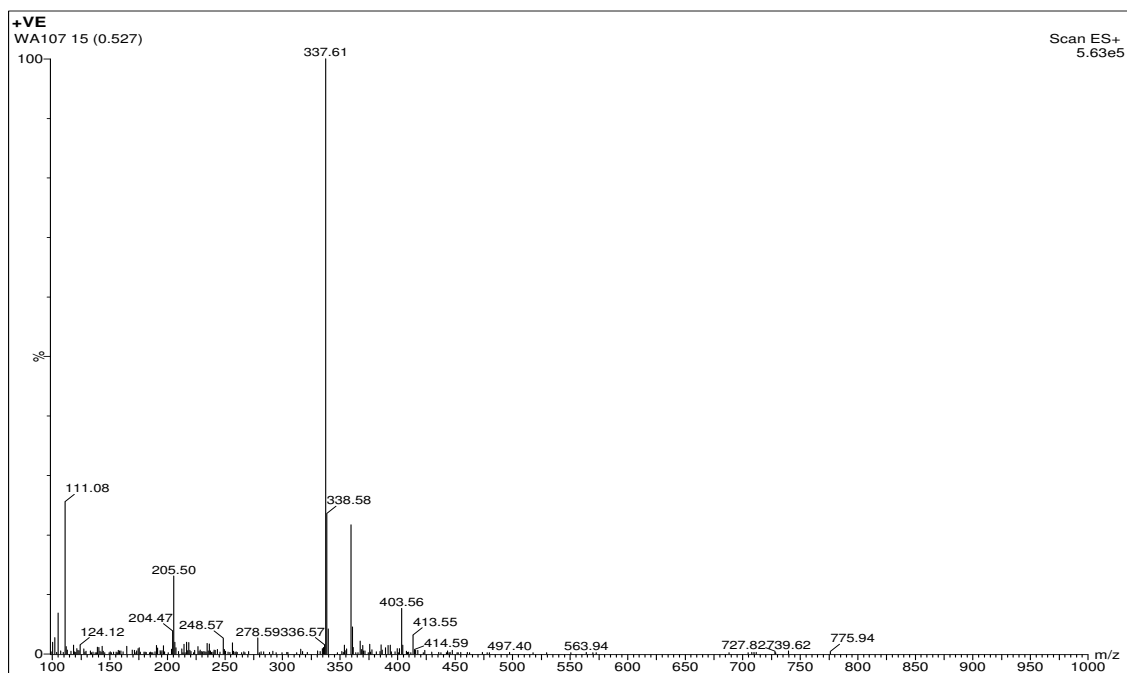
WA106 MeOD.13.fid
carbon

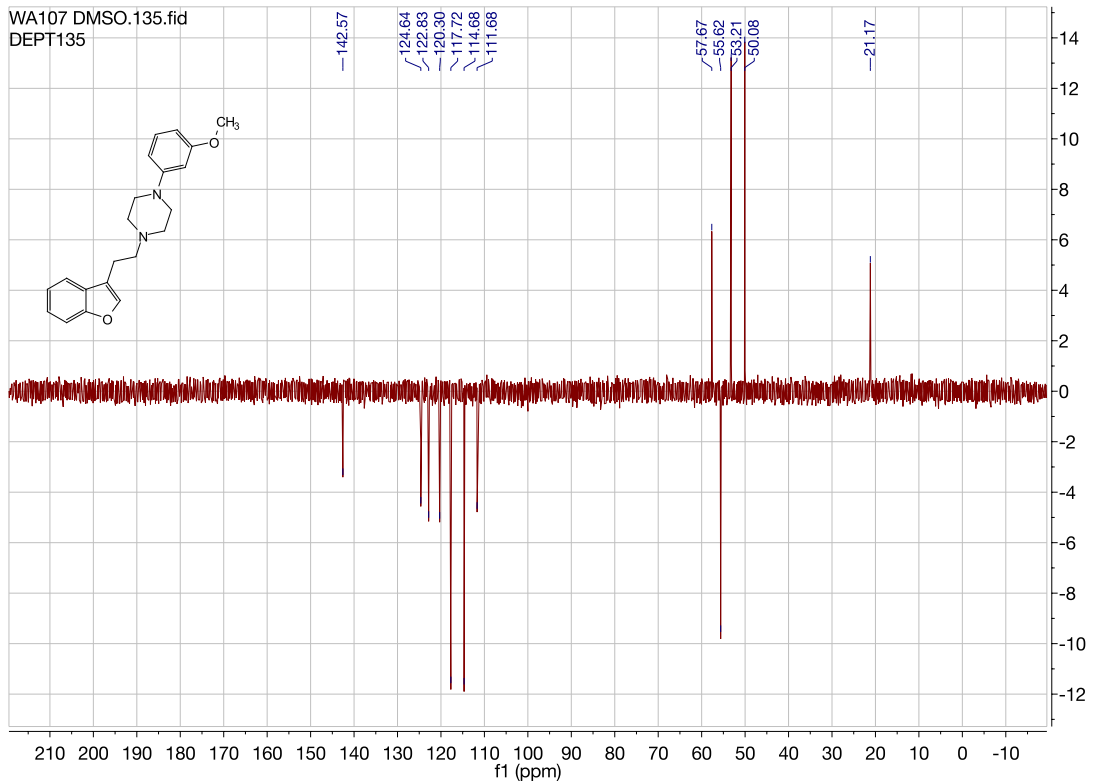
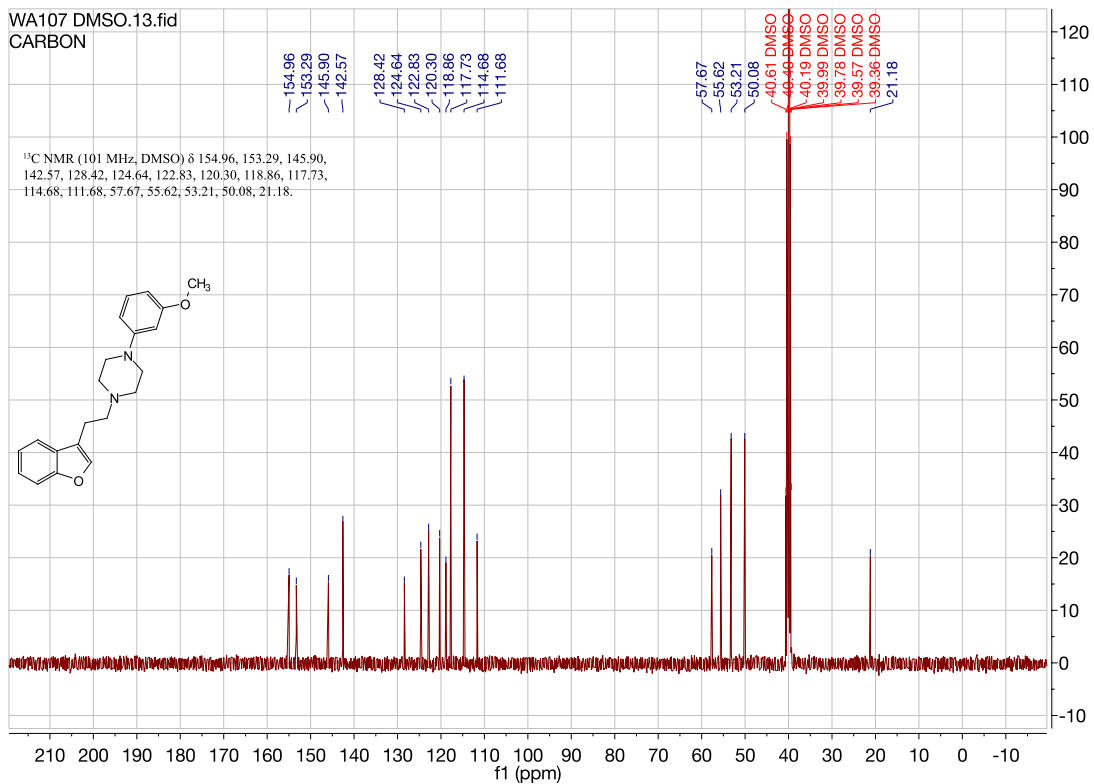


WA106 MeOD.135.fid
DEPT135

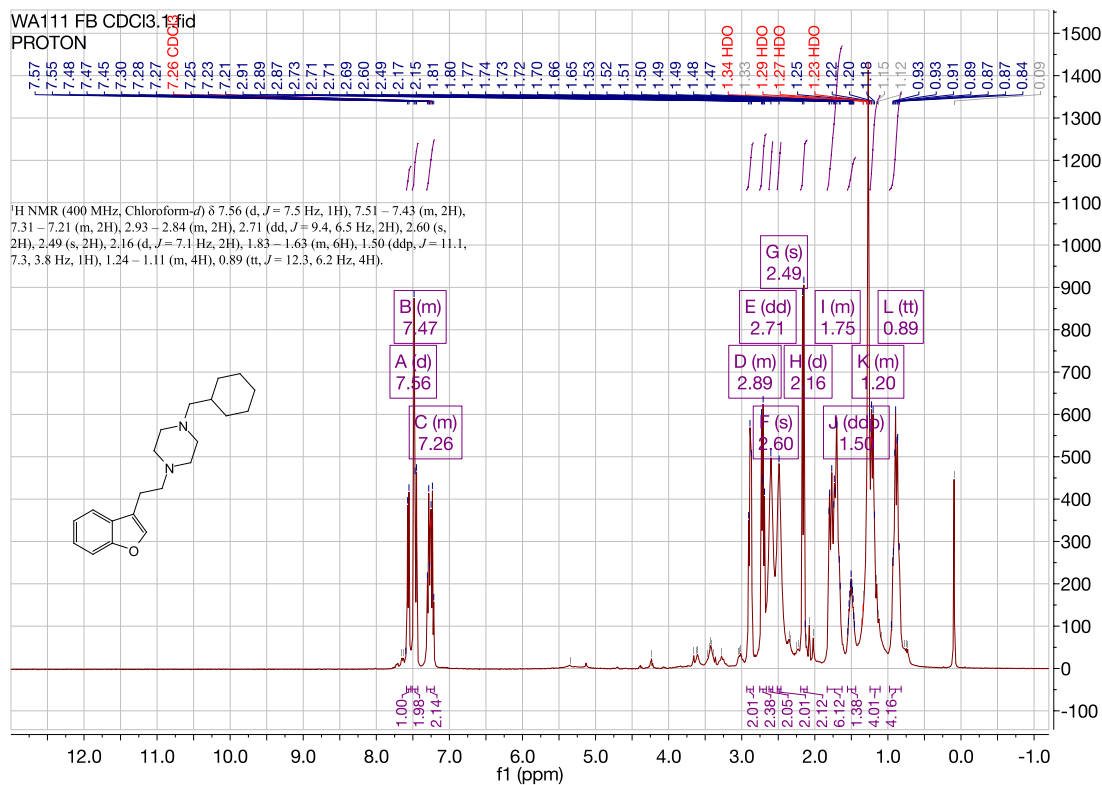
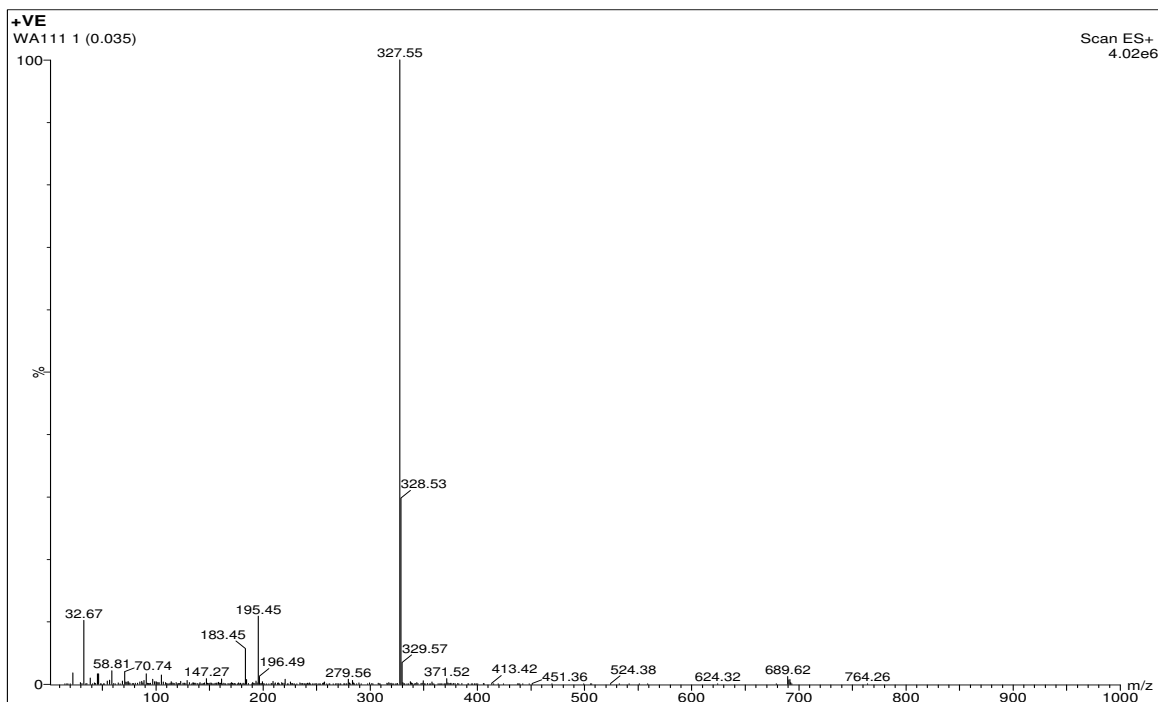


1-(2-(benzofuran-3-yl)ethyl)-4-(3-methoxyphenyl)piperazine. (WA107/182)



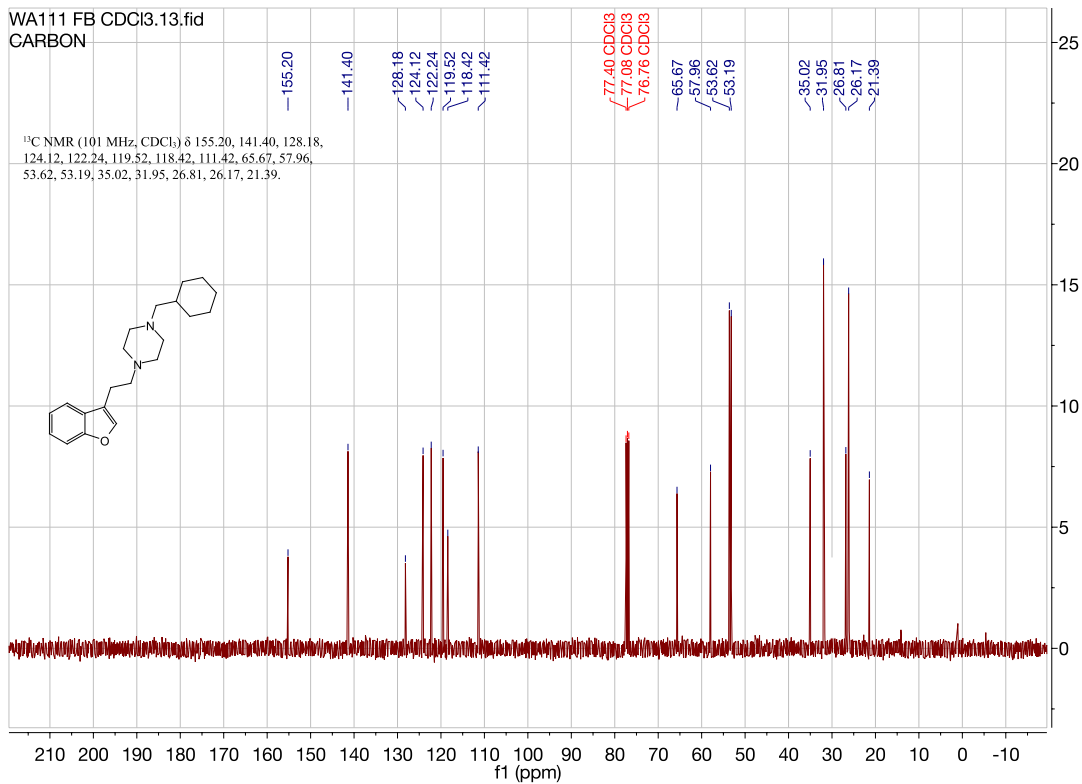


1-(2-(benzofuran-3-yl)ethyl)-4-(cyclohexylmethyl)piperazine. (WA111)

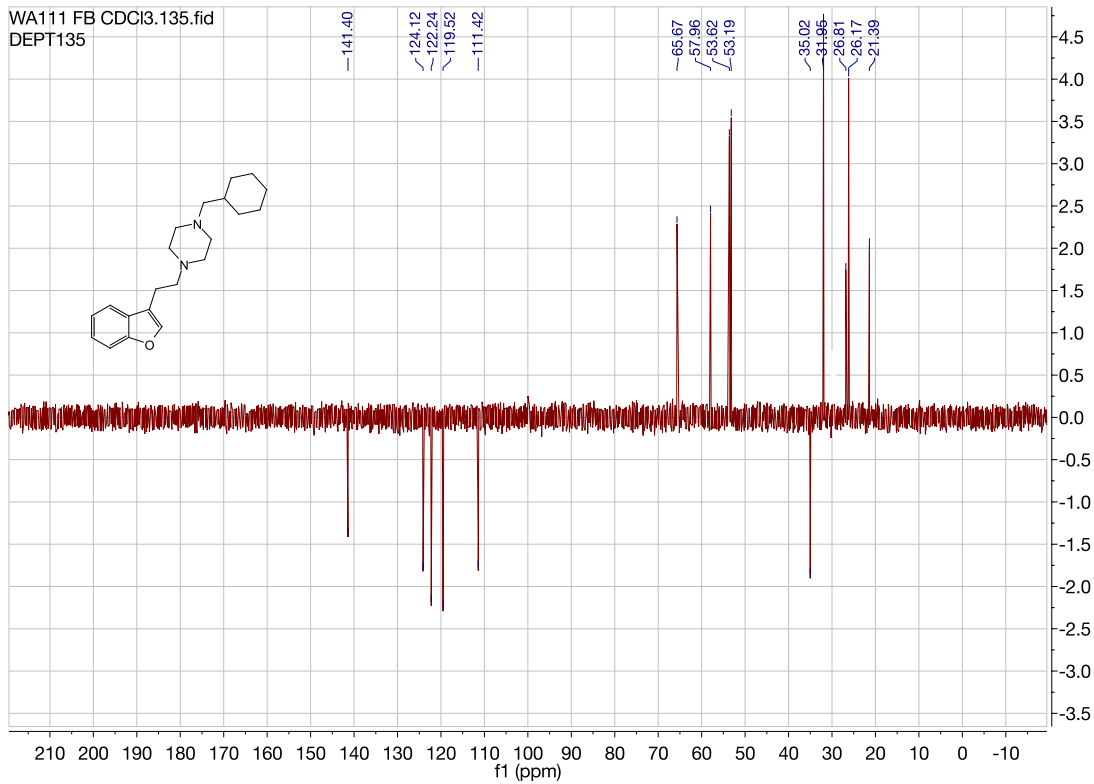


WA111 FB CDCI3.13.fid
CARBON

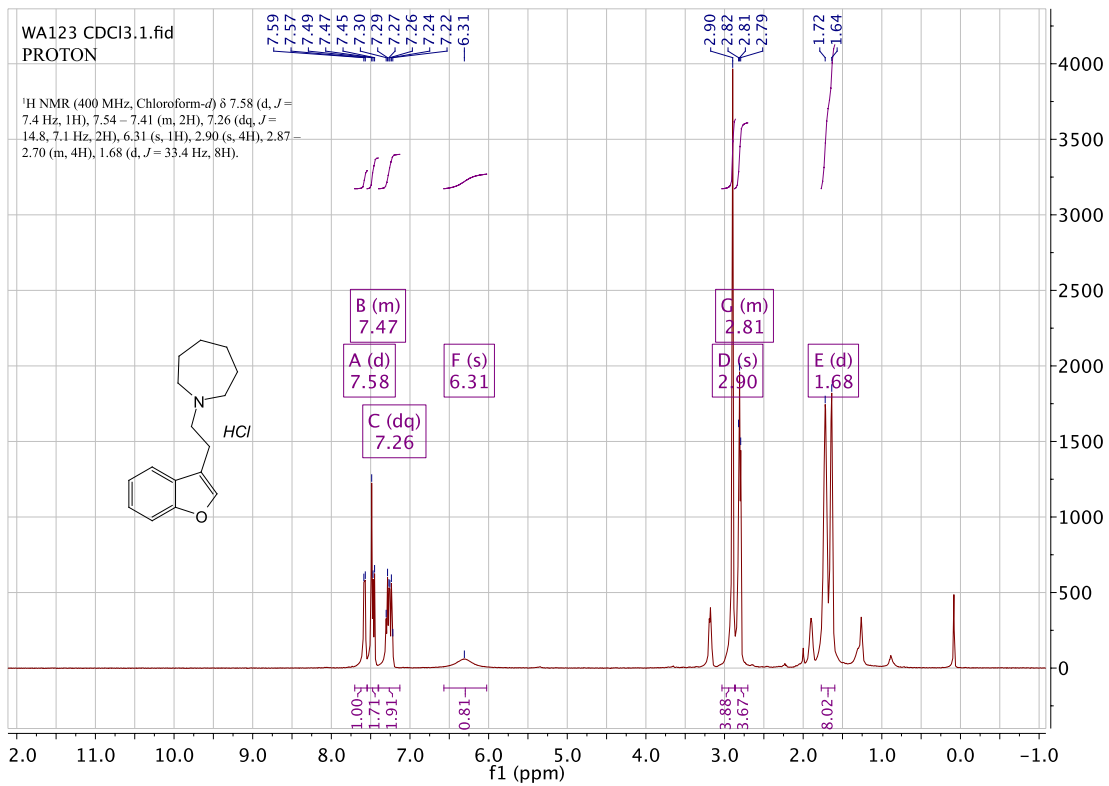
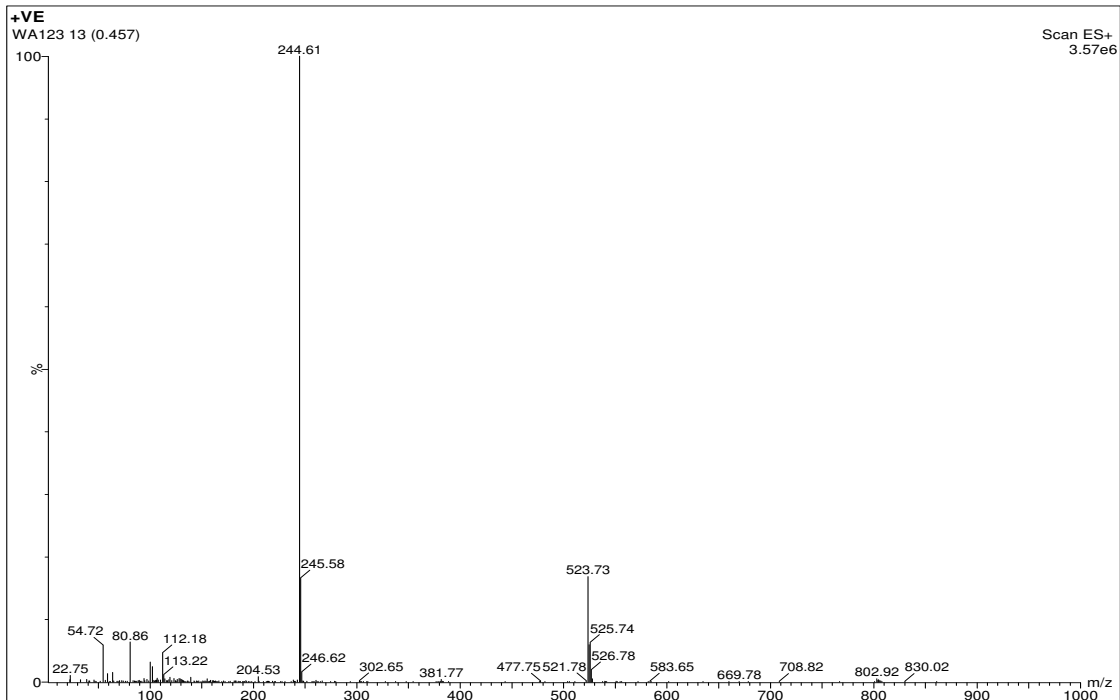
¹³C NMR (101 MHz, CDCl₃) δ 155.20, 141.40, 128.18, 124.12, 122.24, 119.52, 118.42, 111.42, 77.40, 77.08, 76.76, 65.67, 57.96, 53.62, 53.19, 35.02, 31.95, 26.81, 26.17, 21.39.

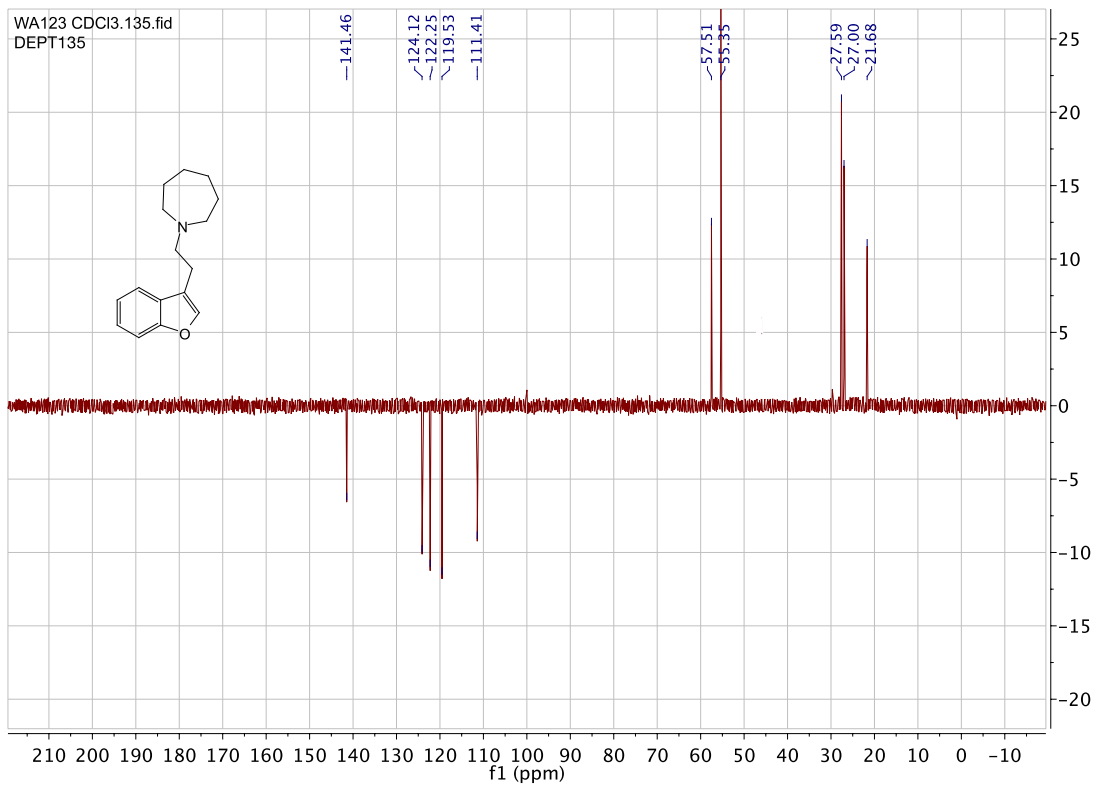
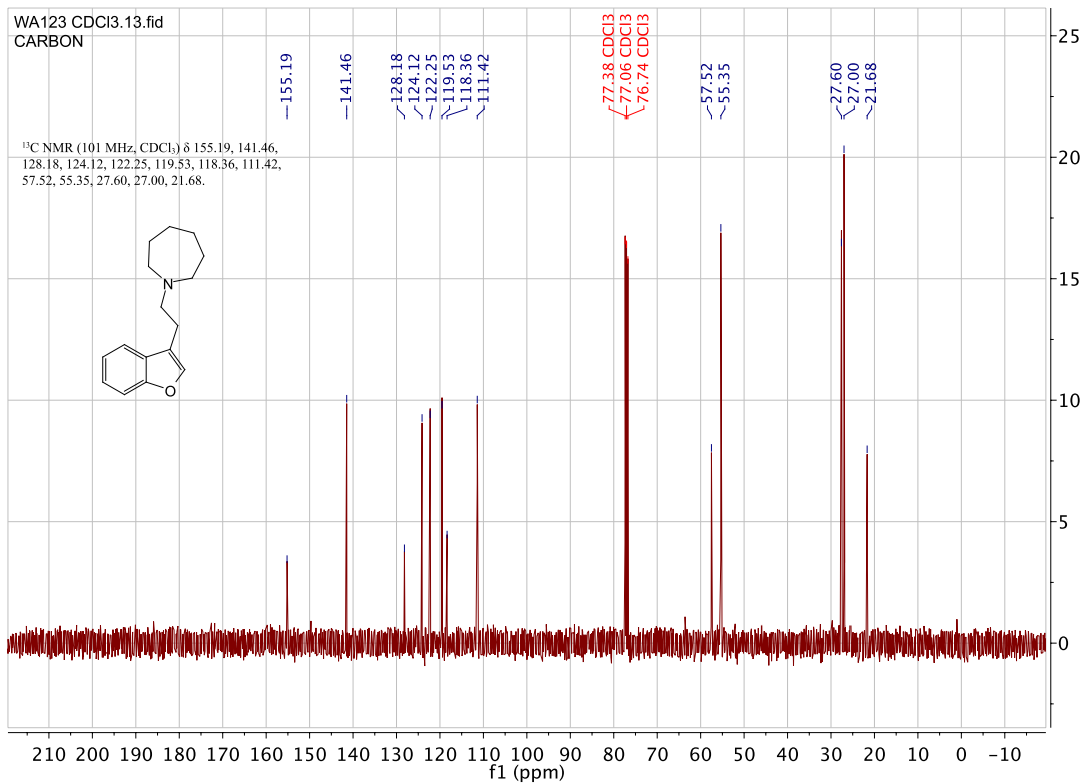


WA111 FB CDCI3.135.fid
DEPT135

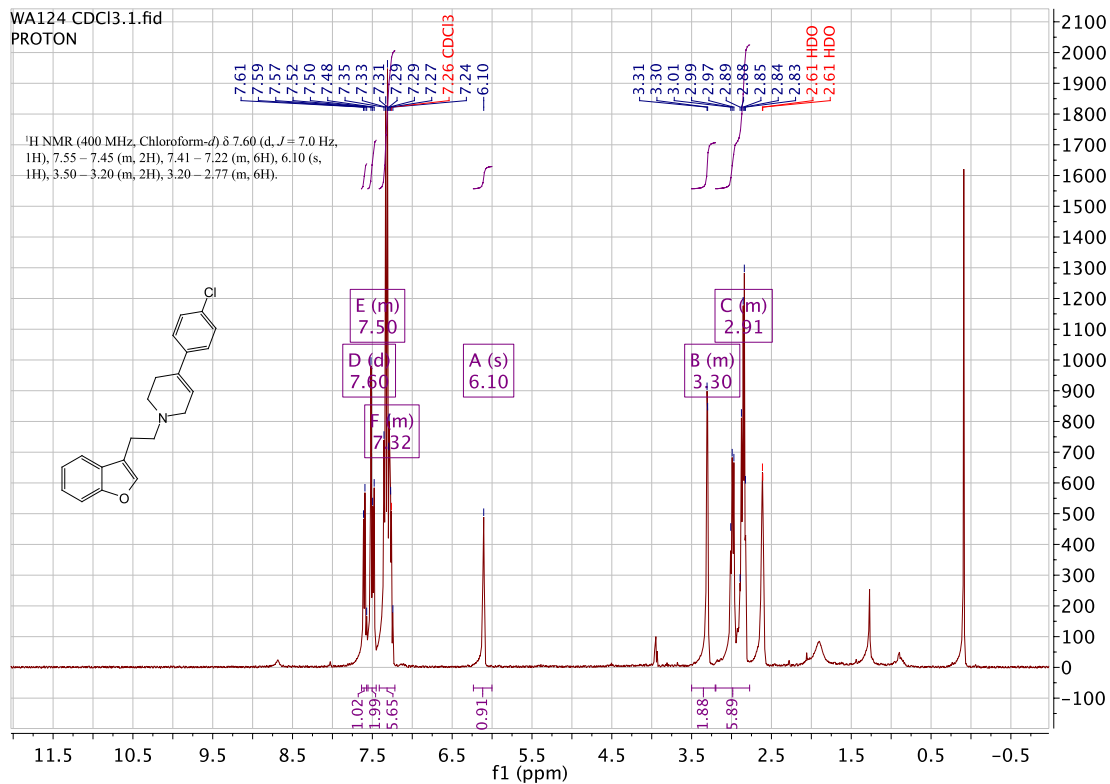
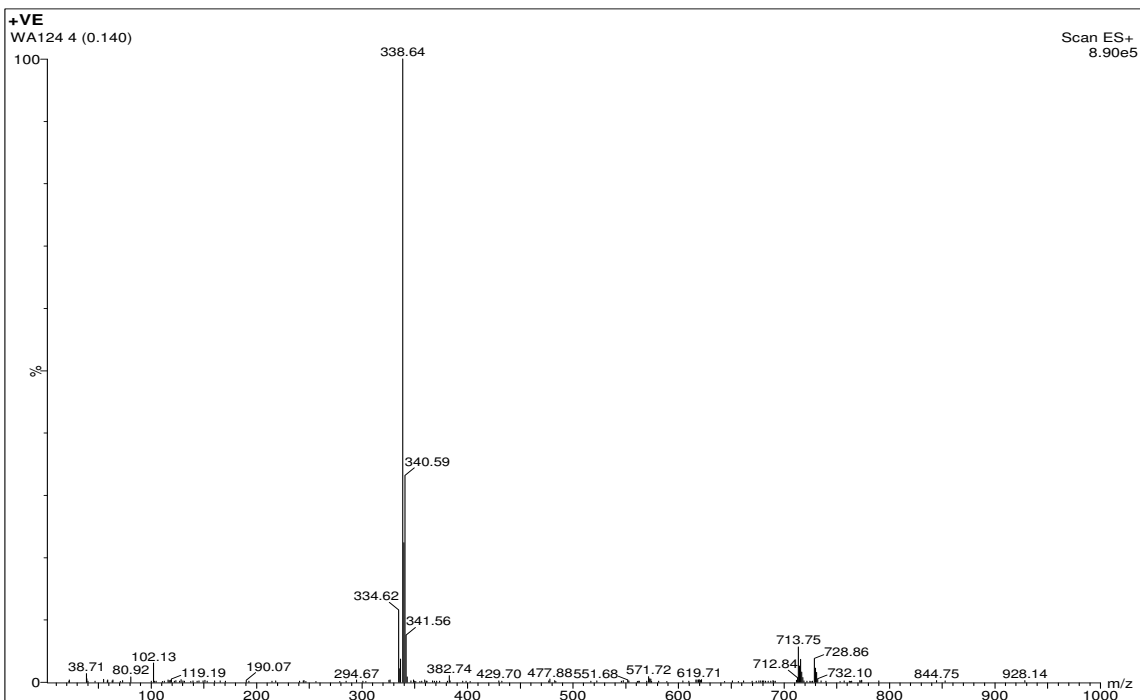


1-(2-(benzofuran-3-yl)ethyl)azepane. (WA123)

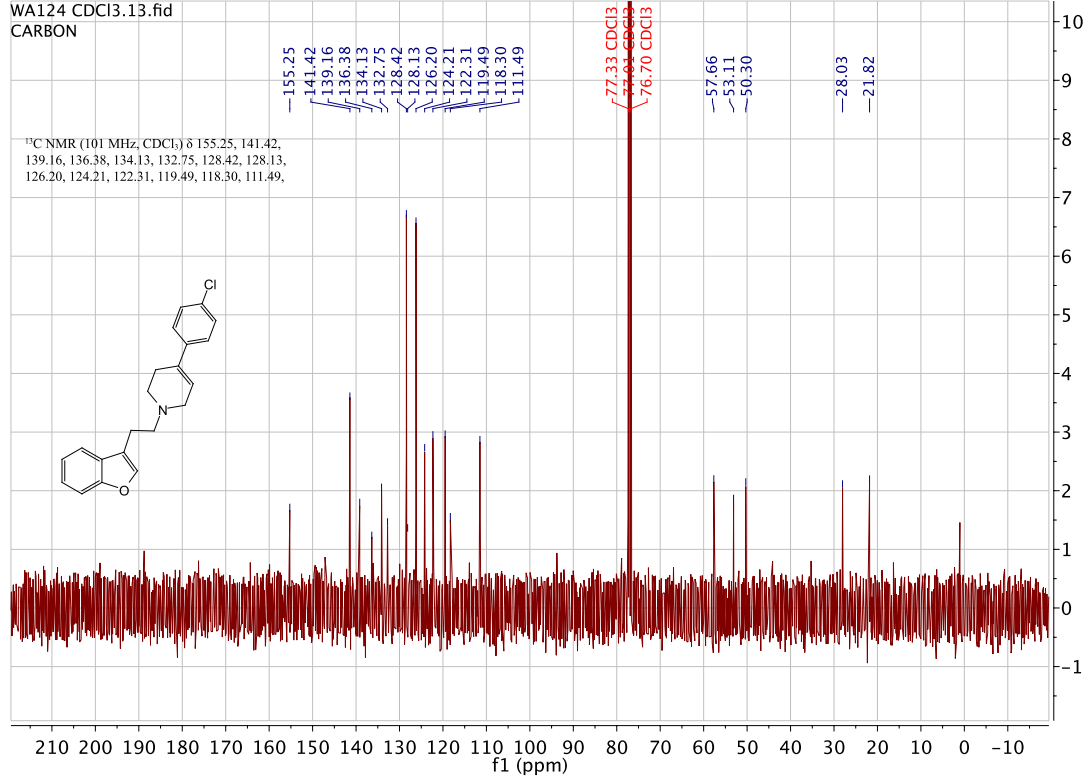




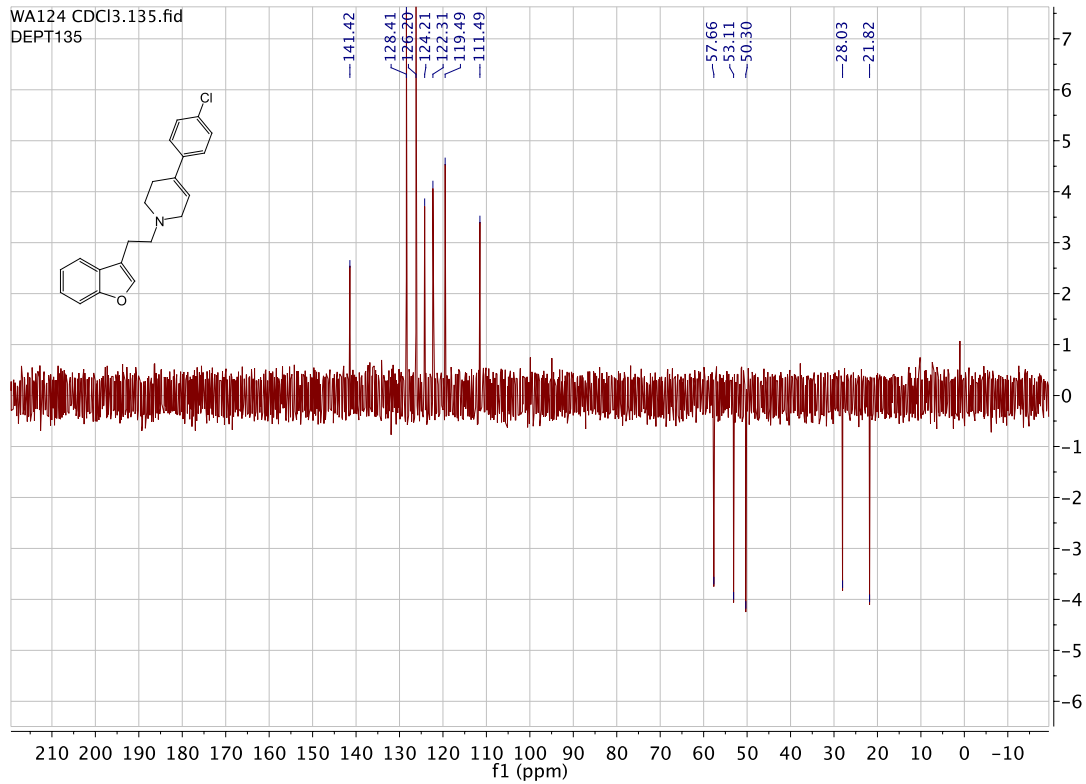
1-(2-(benzofuran-3-yl)ethyl)-4-(4-chlorophenyl)-1,2,3,4-tetrahydropyridine.(WA124)



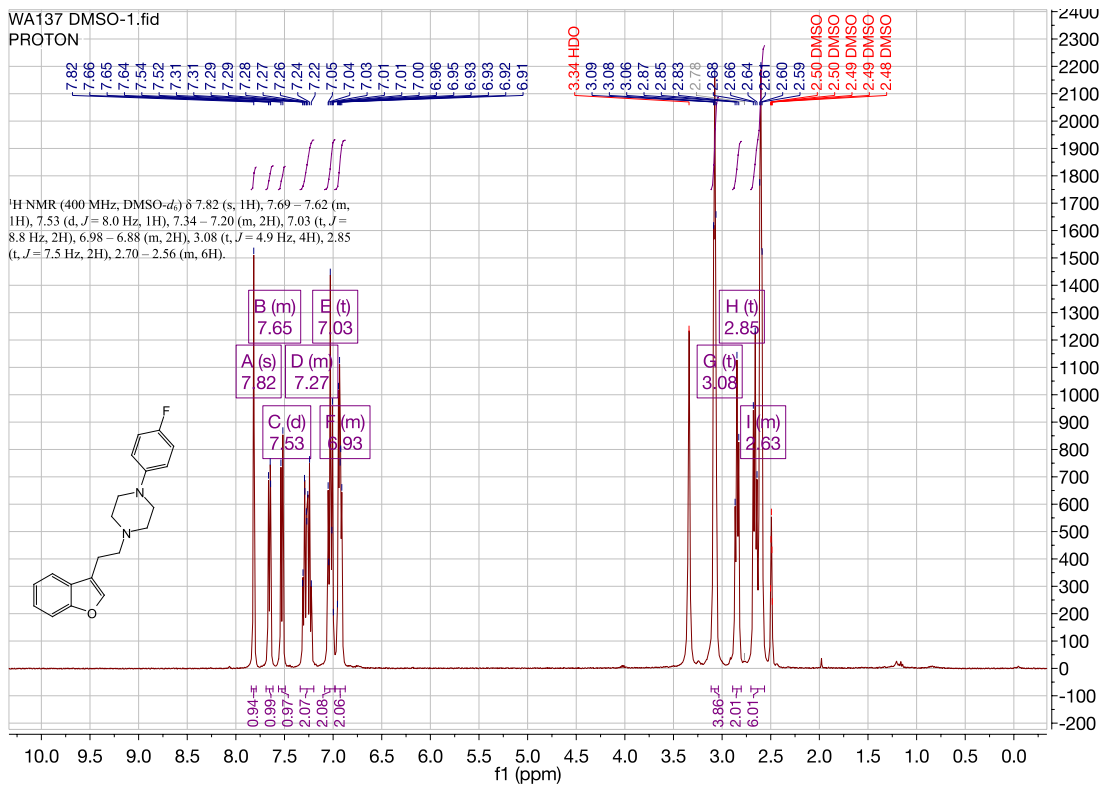
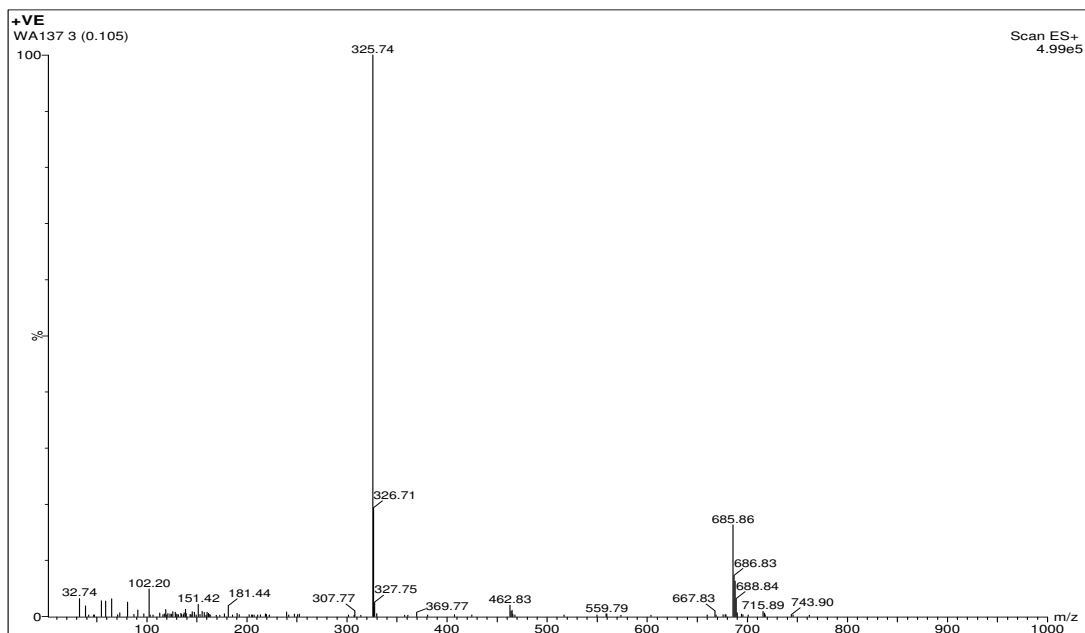
WA124 CDCl3.13.fid
CARBON

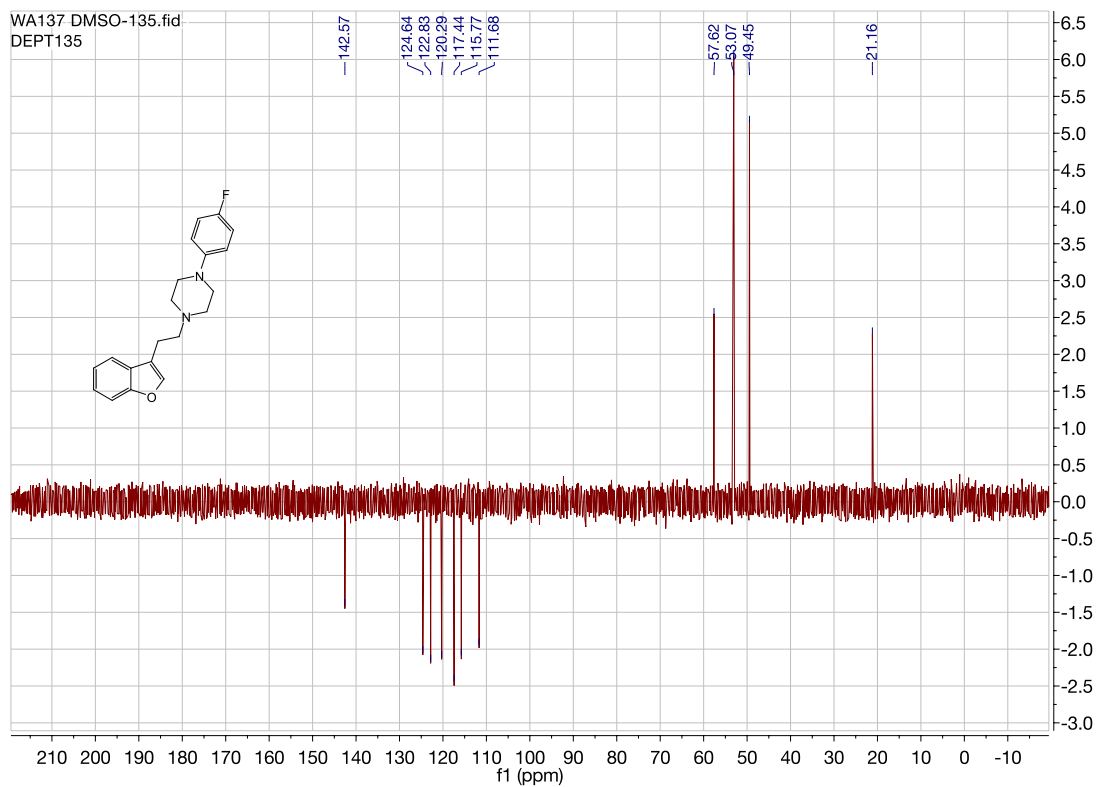
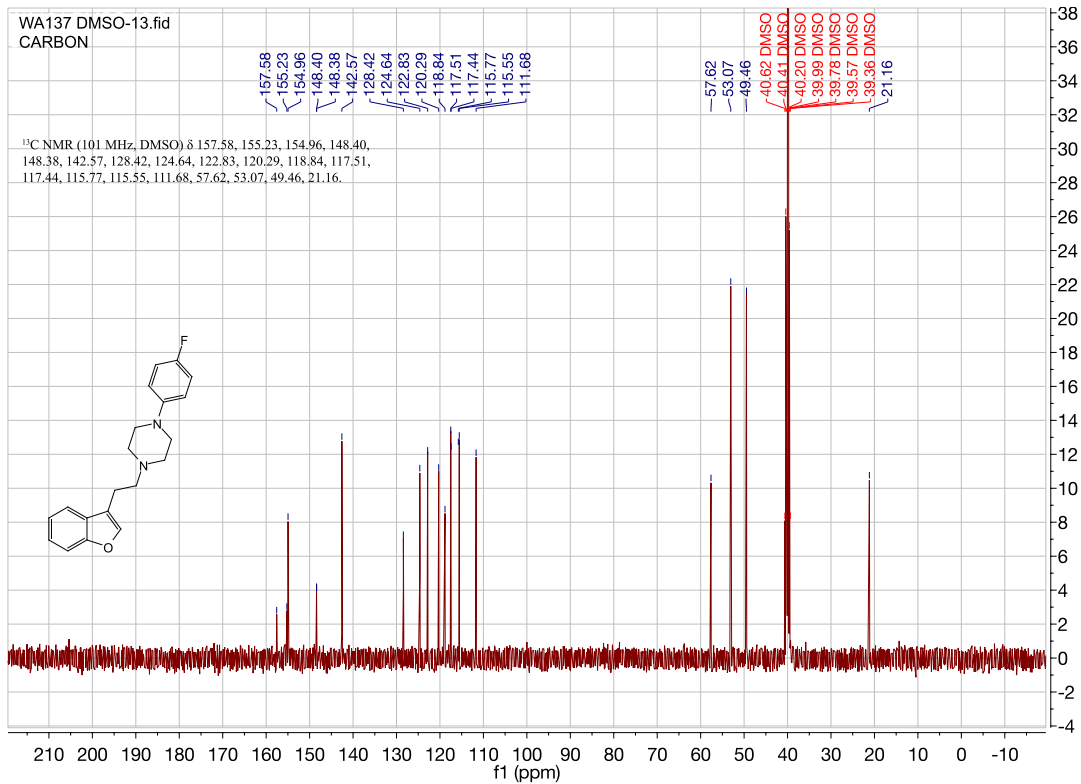


WA124 CDCl3.135.fid
DEPT135

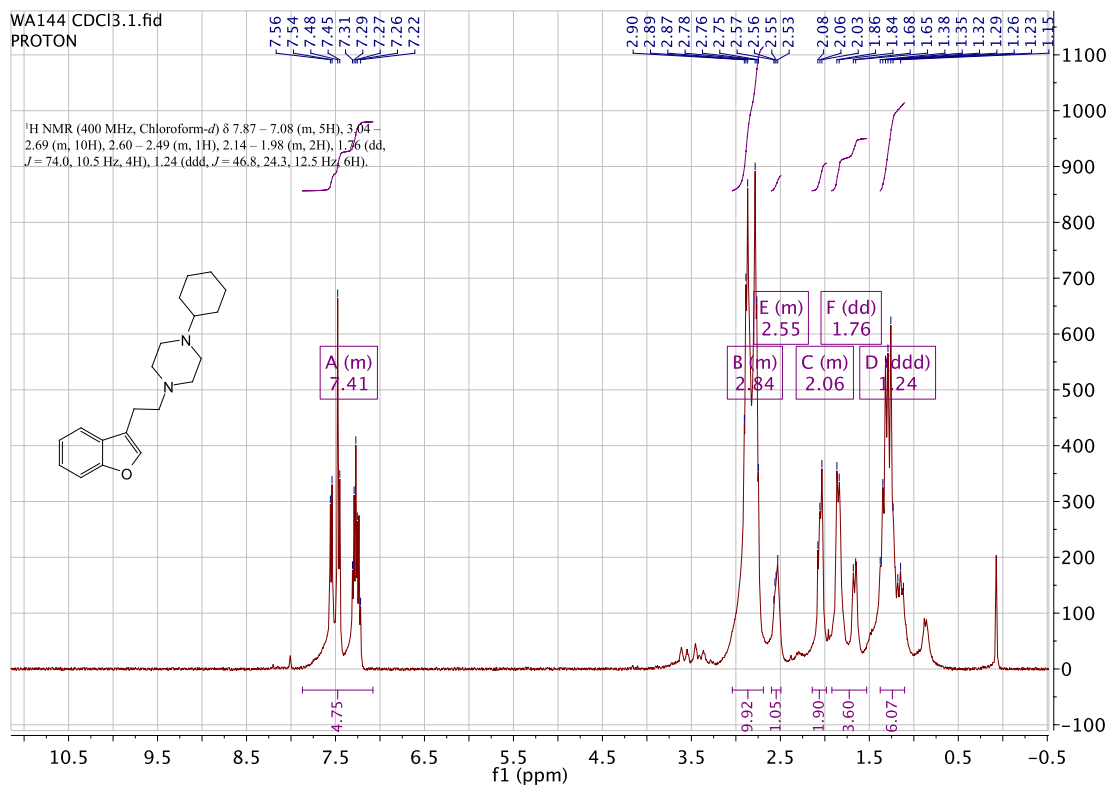
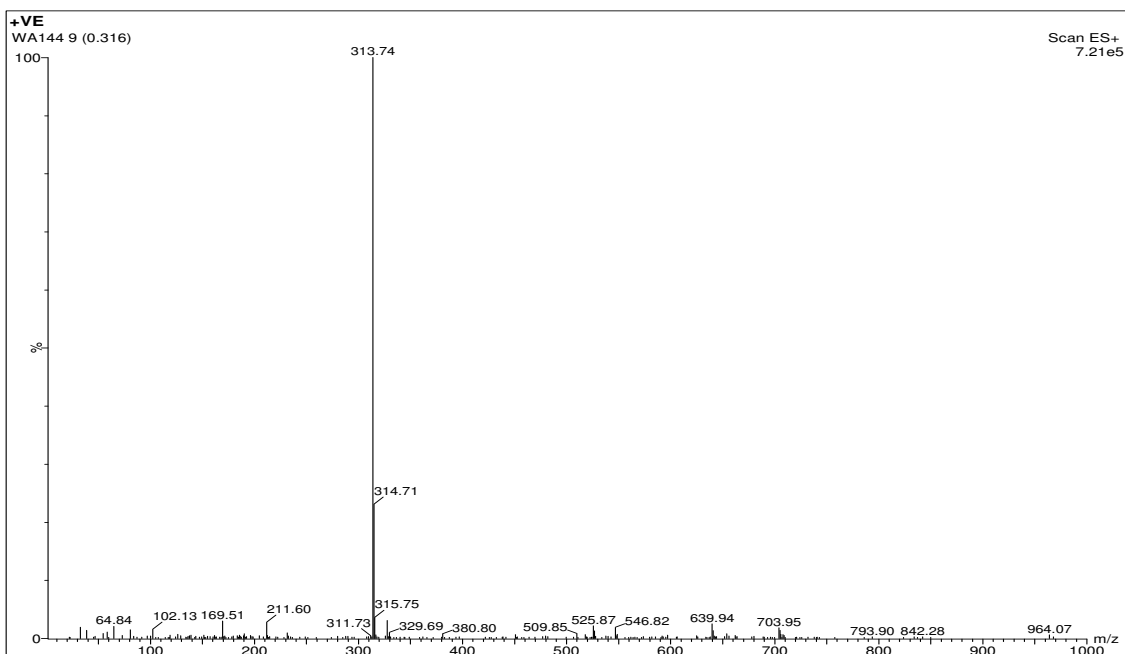


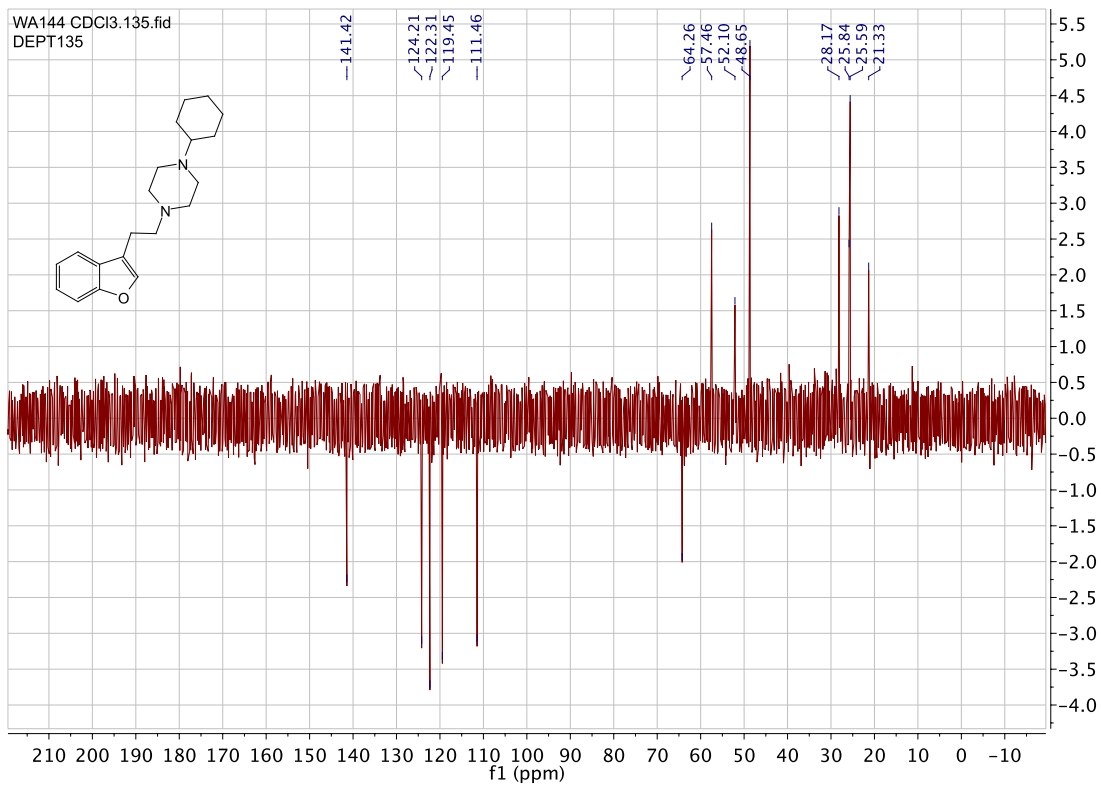
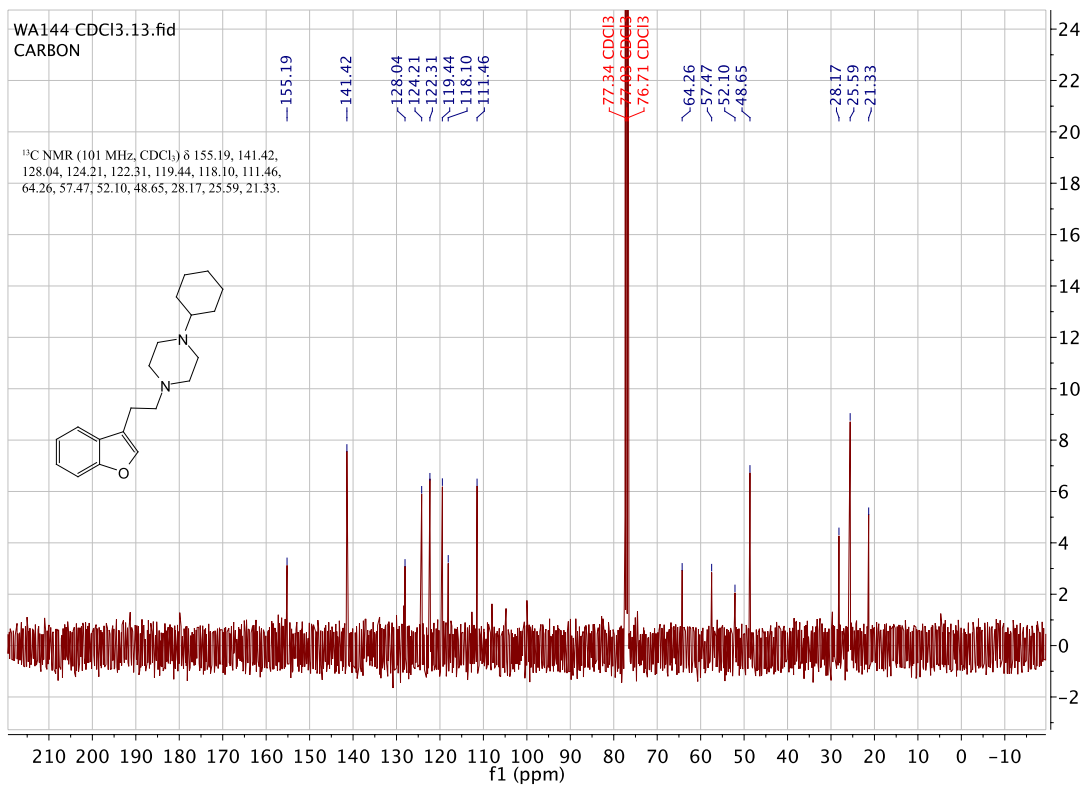
1-(2-(benzofuran-3-yl)ethyl)-4-(4-fluorophenyl)piperazine. (WA137)



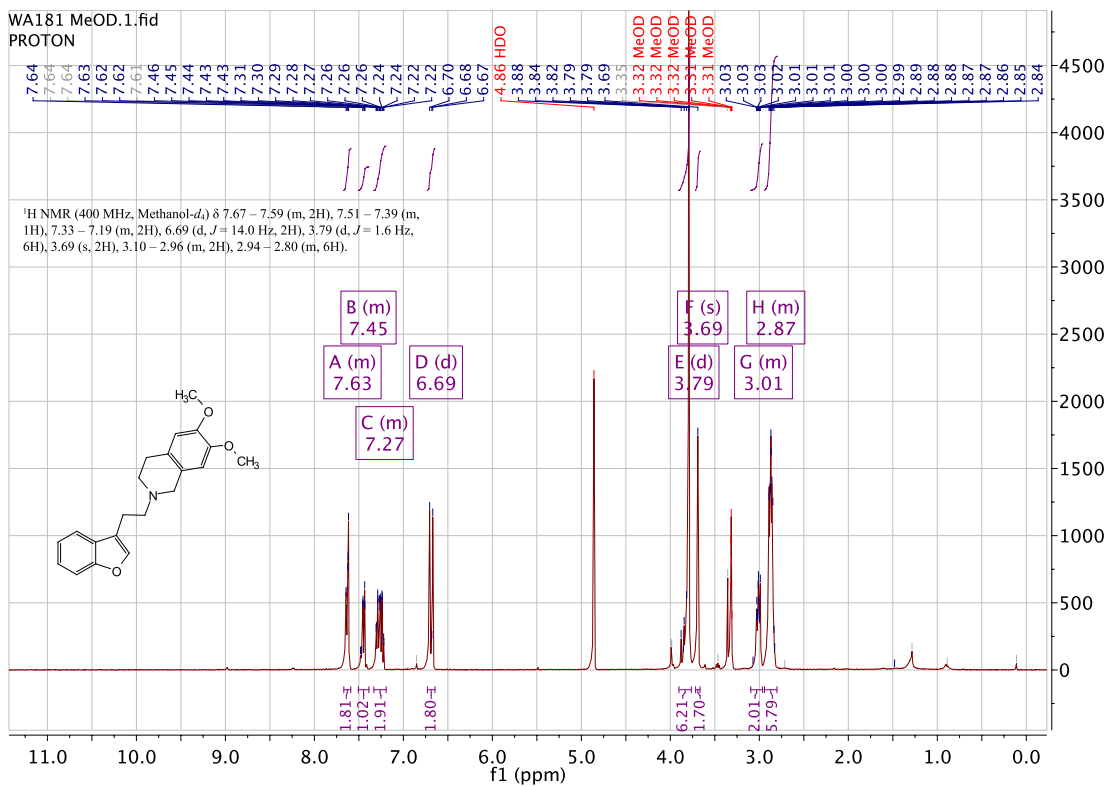
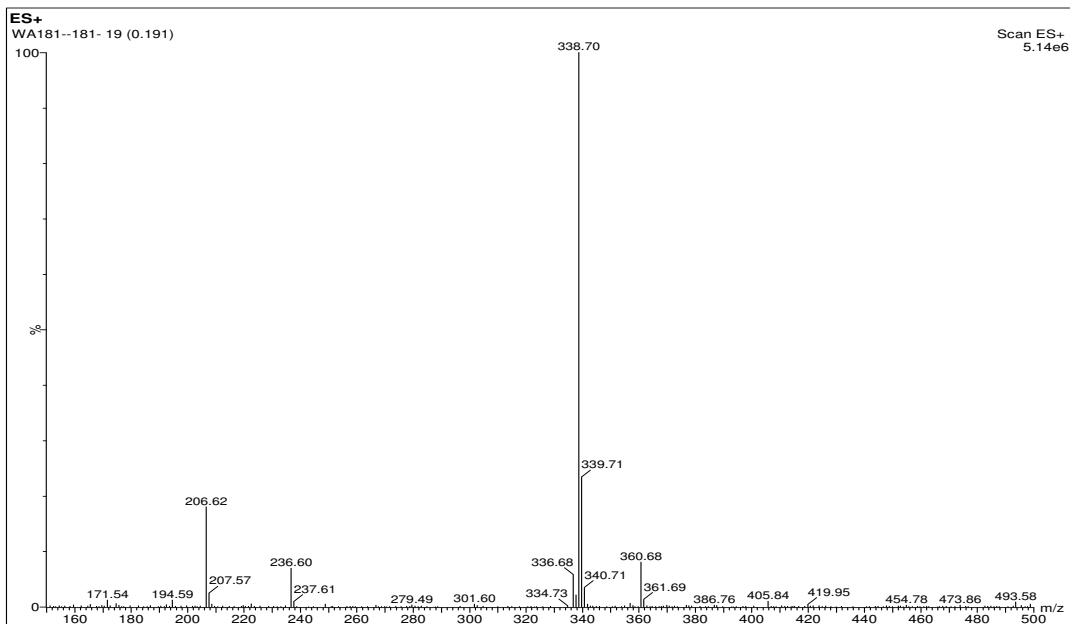


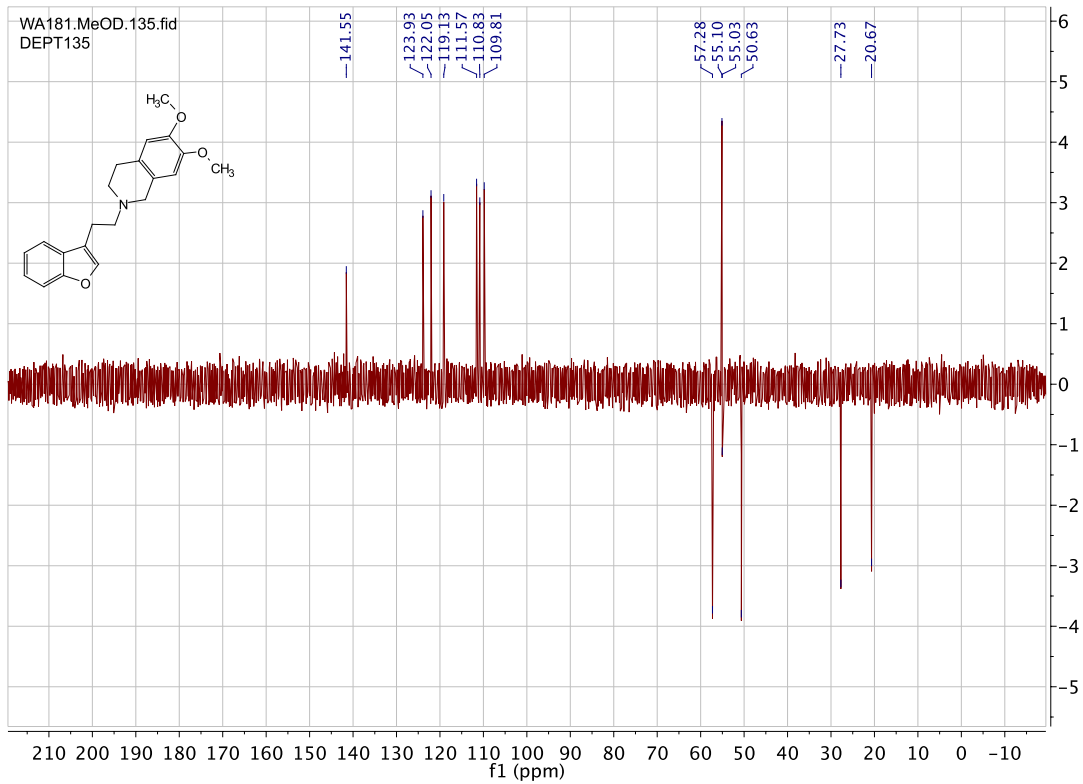
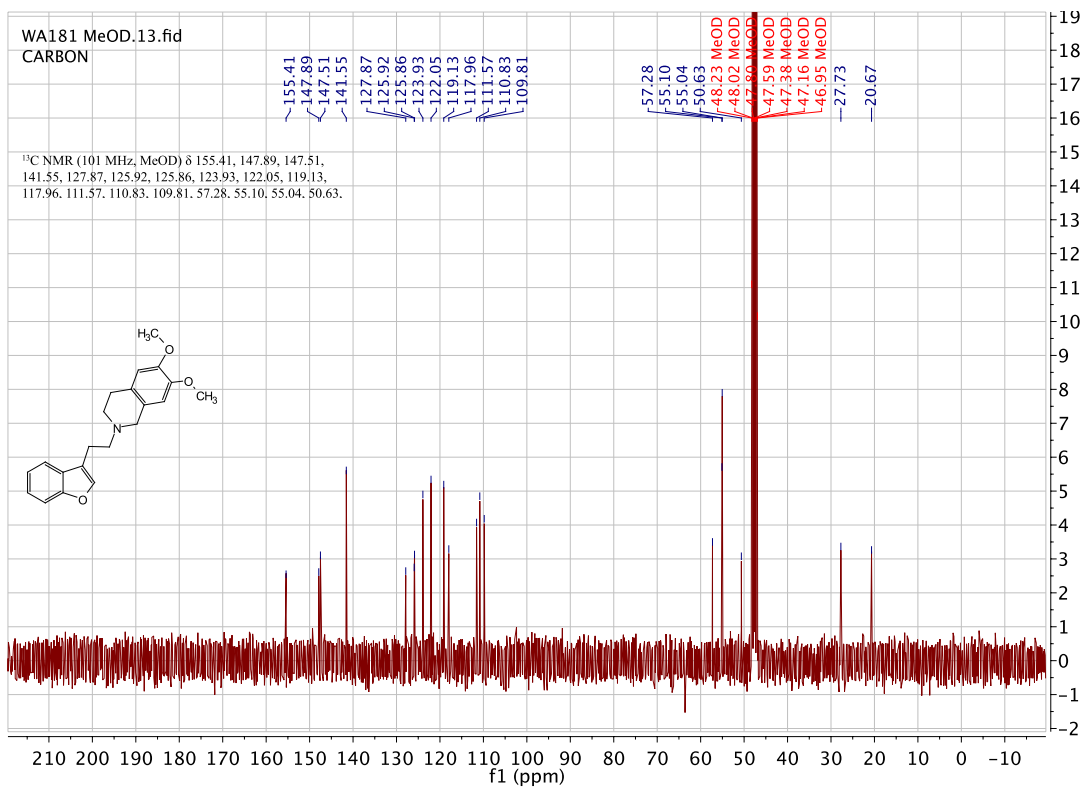
1-(2-(benzofuran-3-yl)ethyl)-4-cyclohexylpiperazine. (WA144)



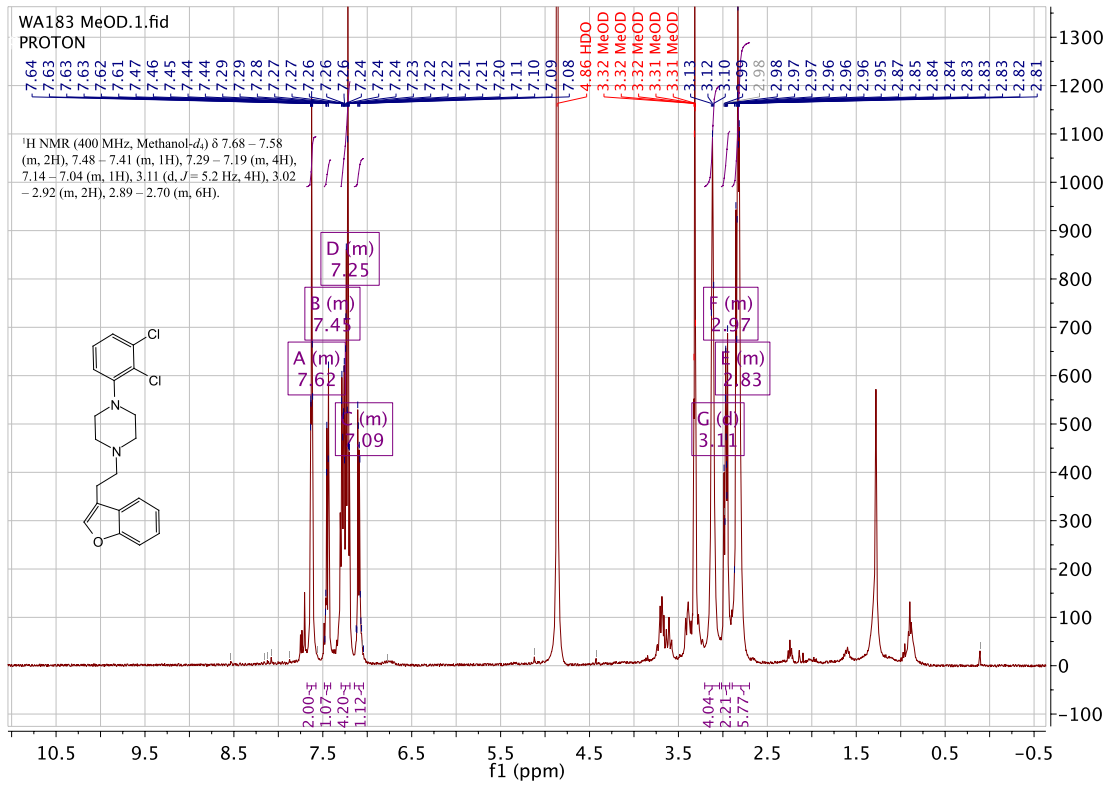
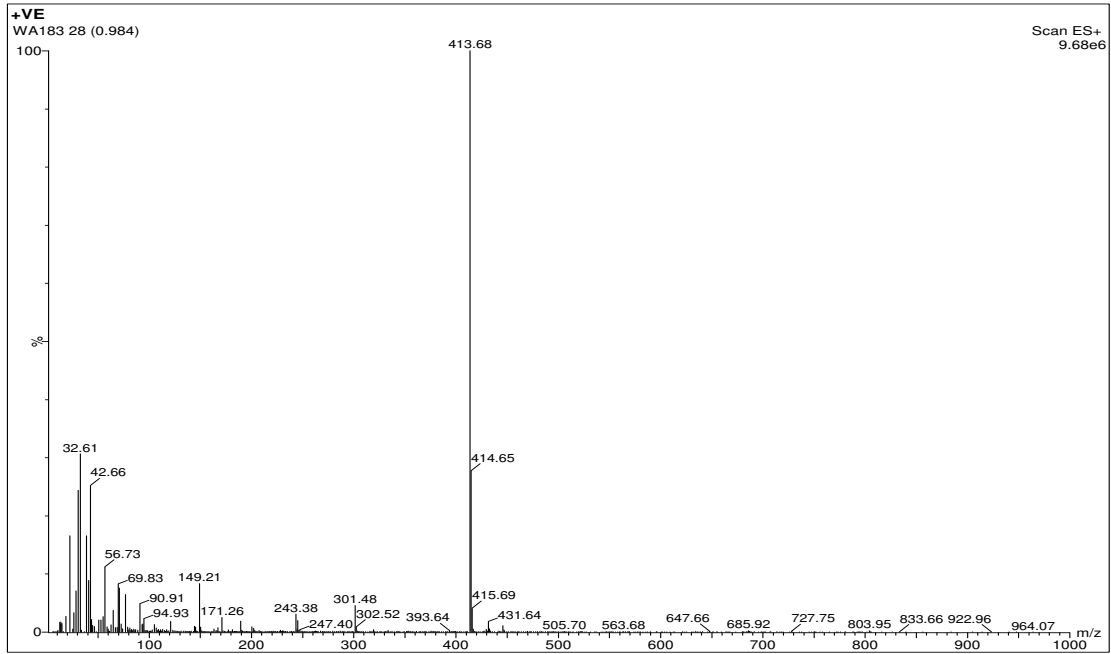


2-(2-(benzofuran-3-yl)ethyl)-6,7-dimethoxy-1,2,3,4-tetrahydroisoquinoline. (WA181)

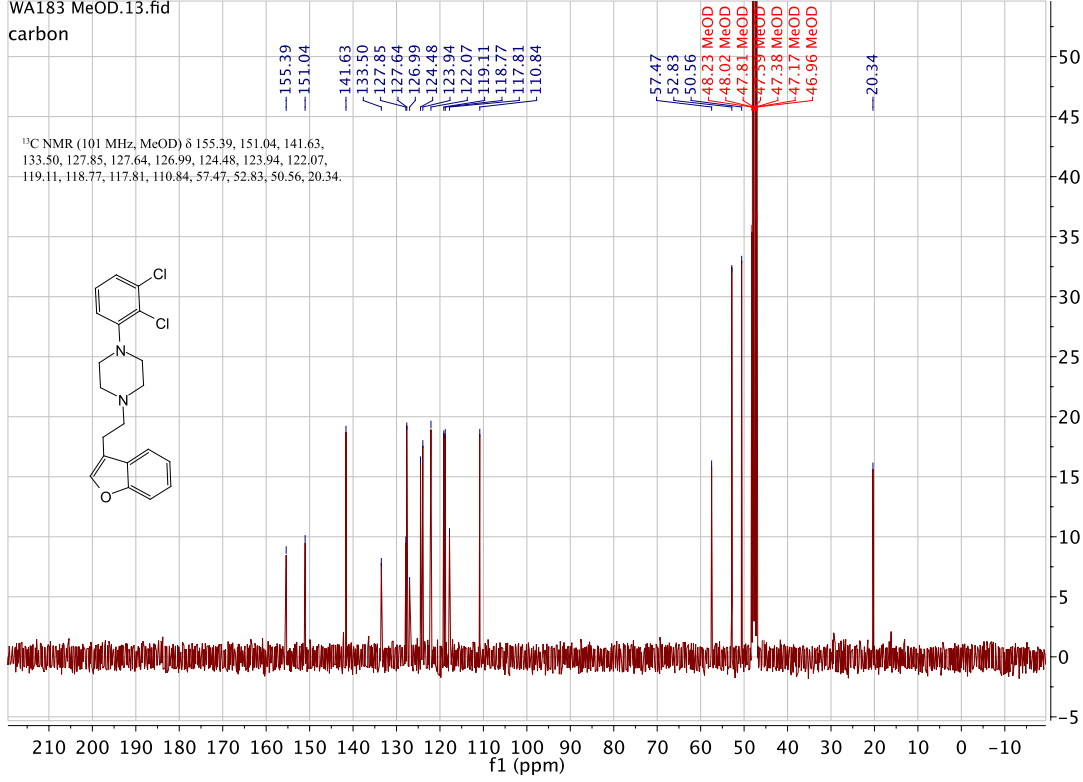




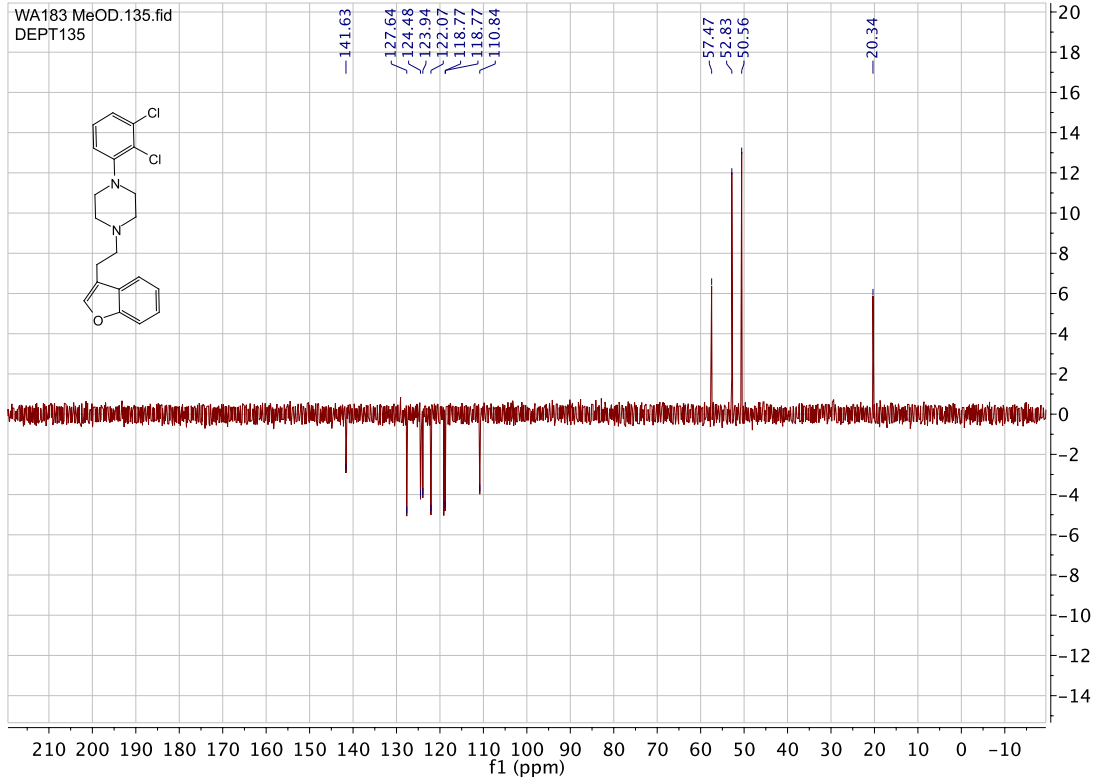
1-(2-(benzofuran-3-yl)ethyl)-4-(2,3-dichlorophenyl)piperazine. (WA183)



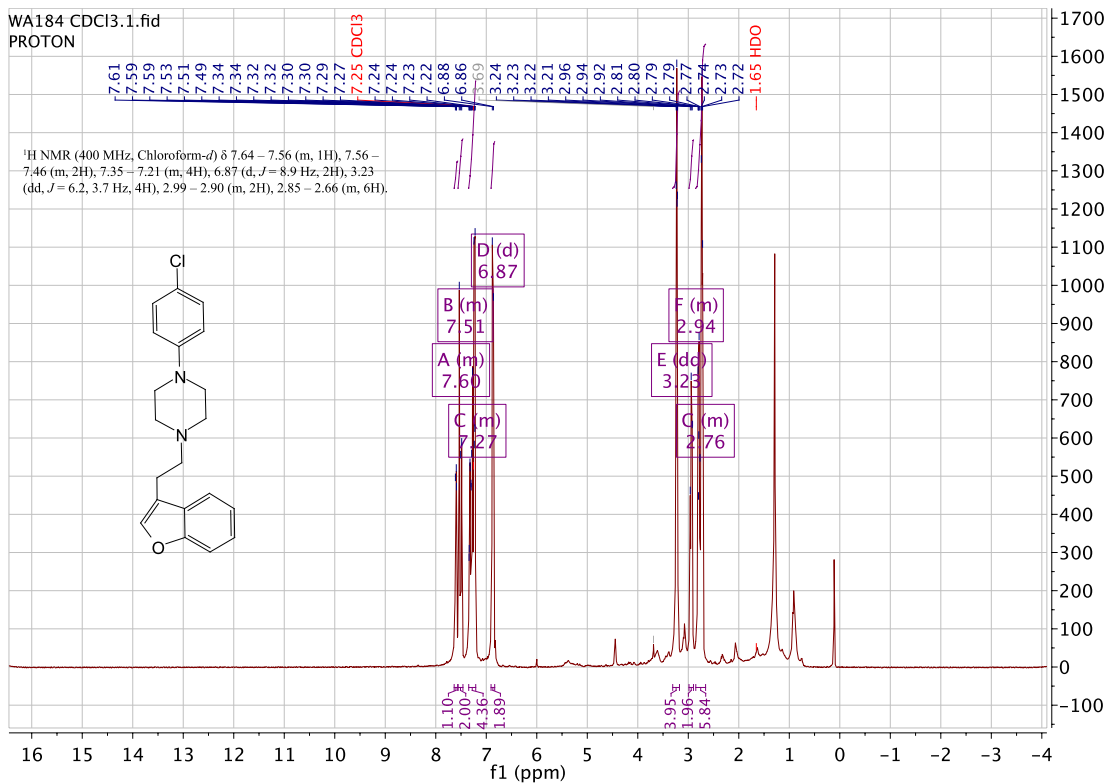
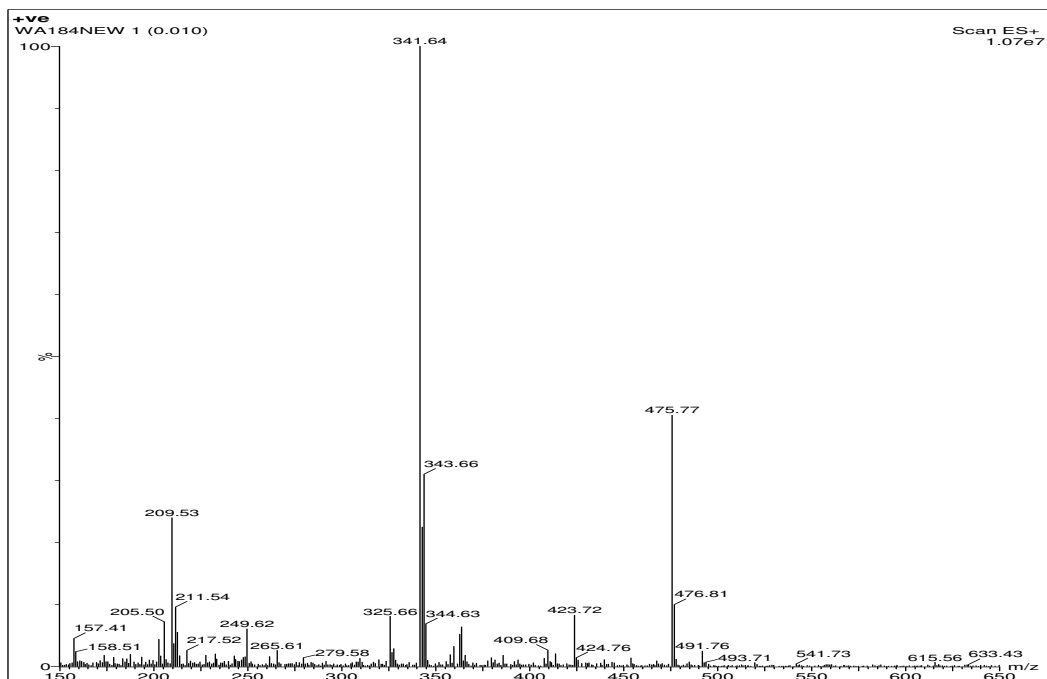
WA183 MeOD.13.fid
carbon

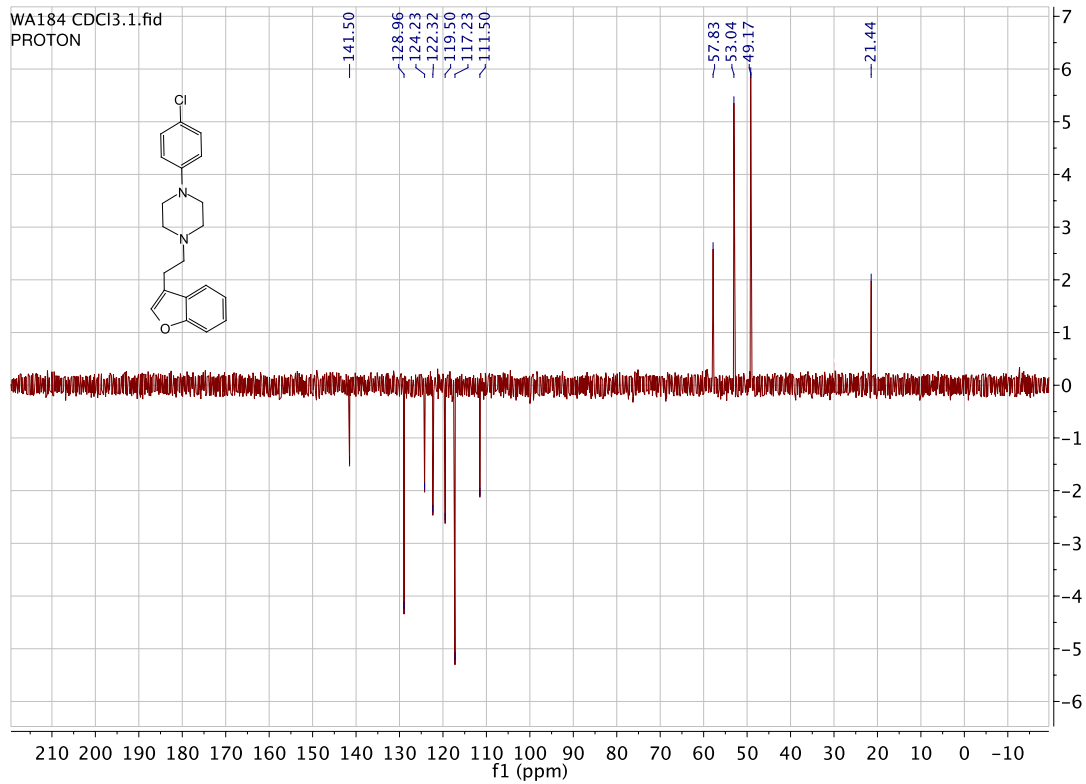
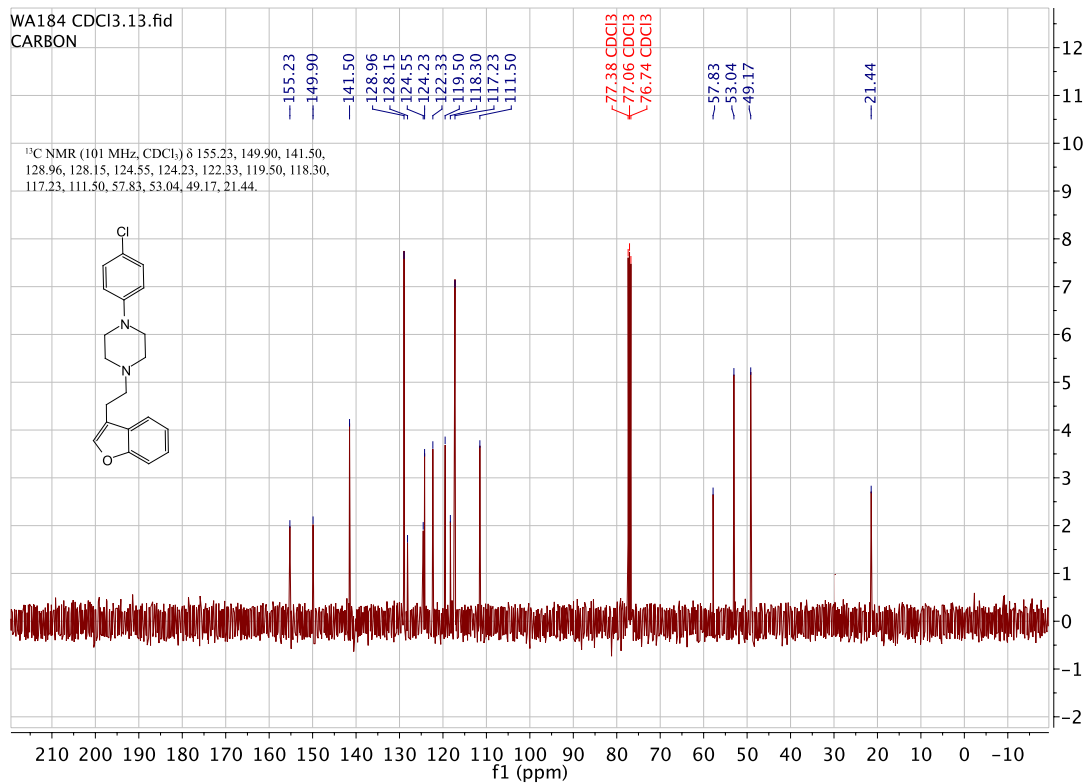


WA183 MeOD.135.fid
DEPT135

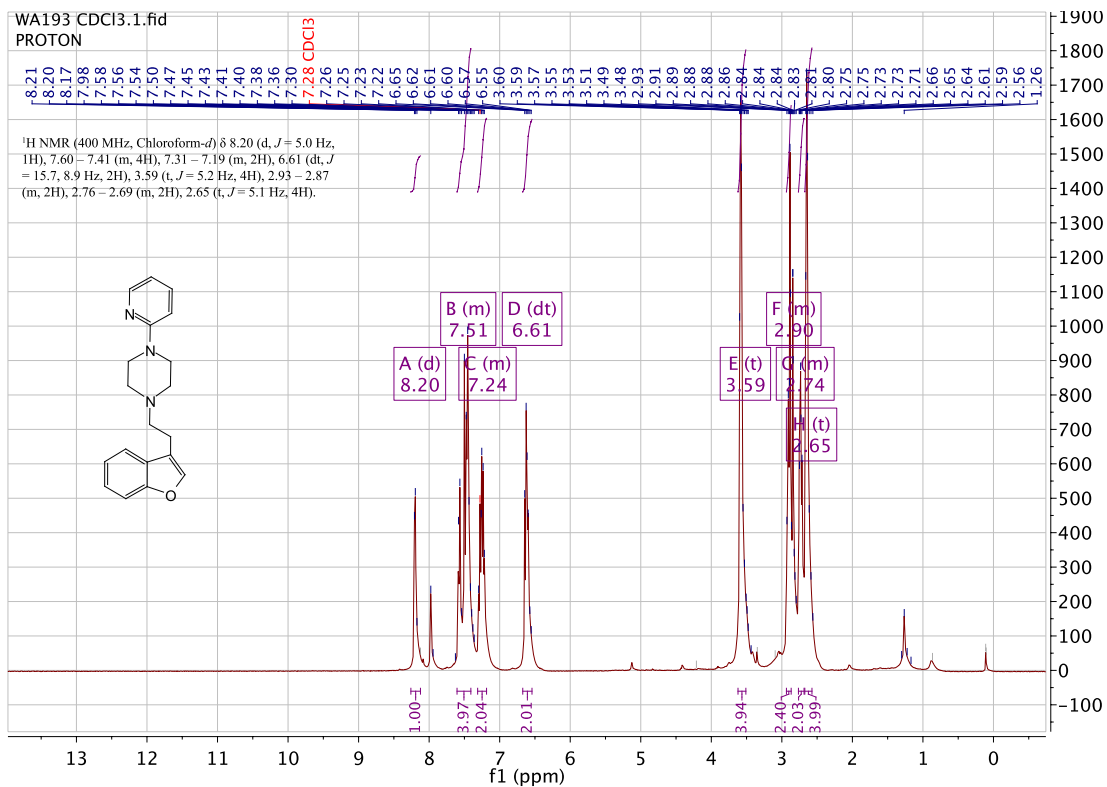
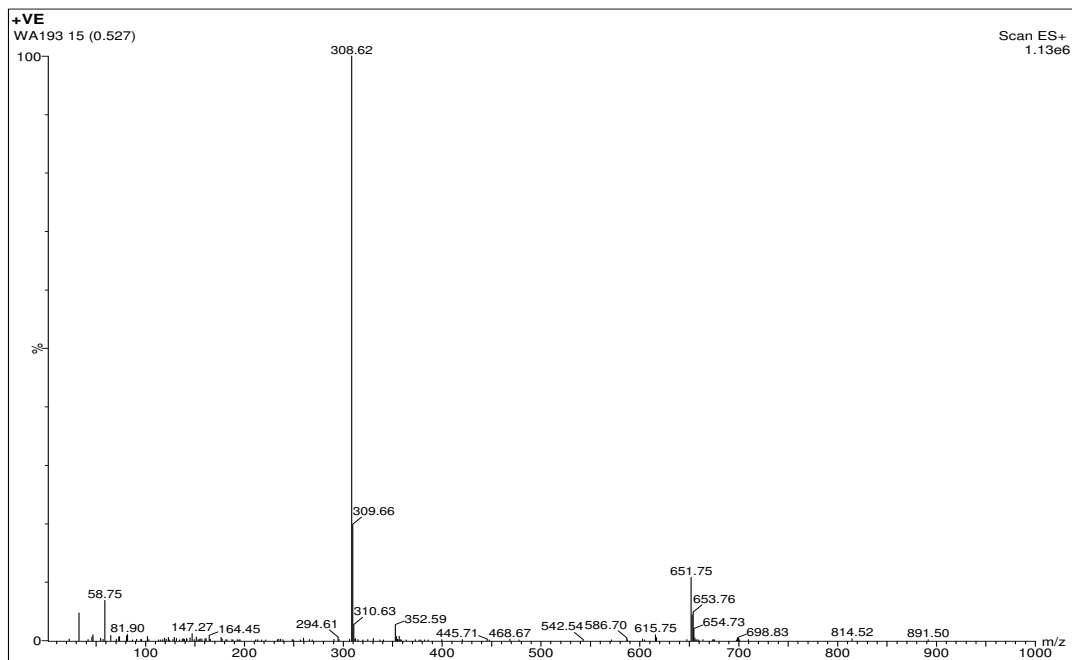


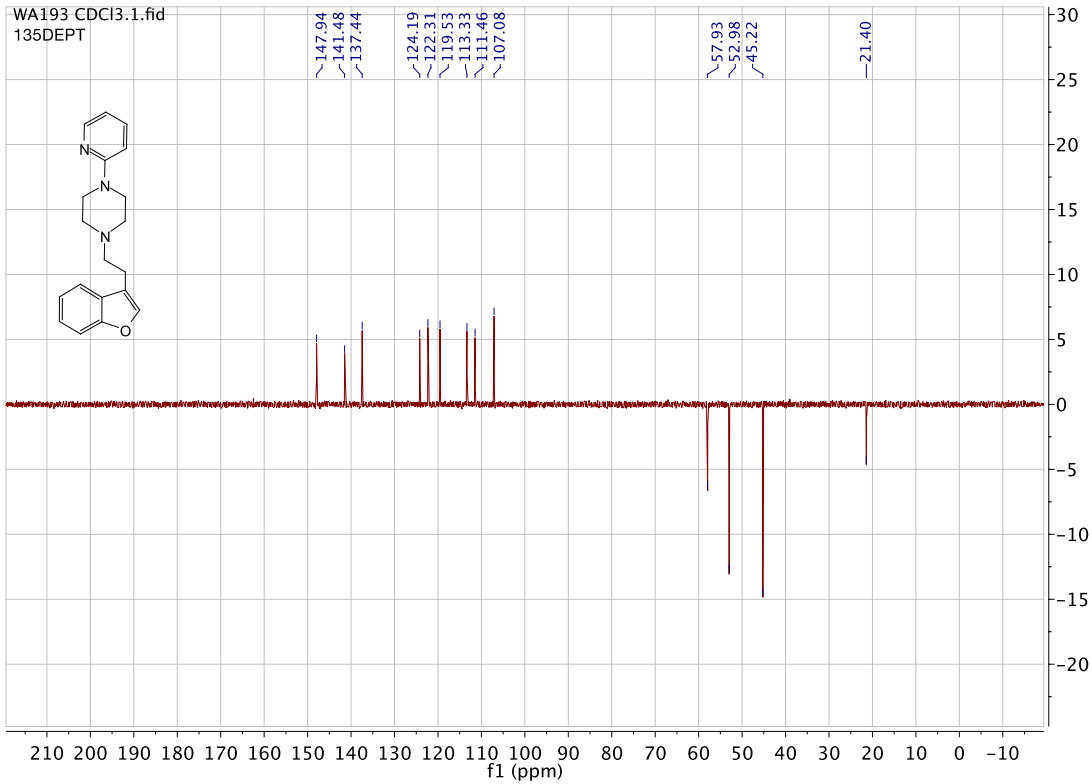
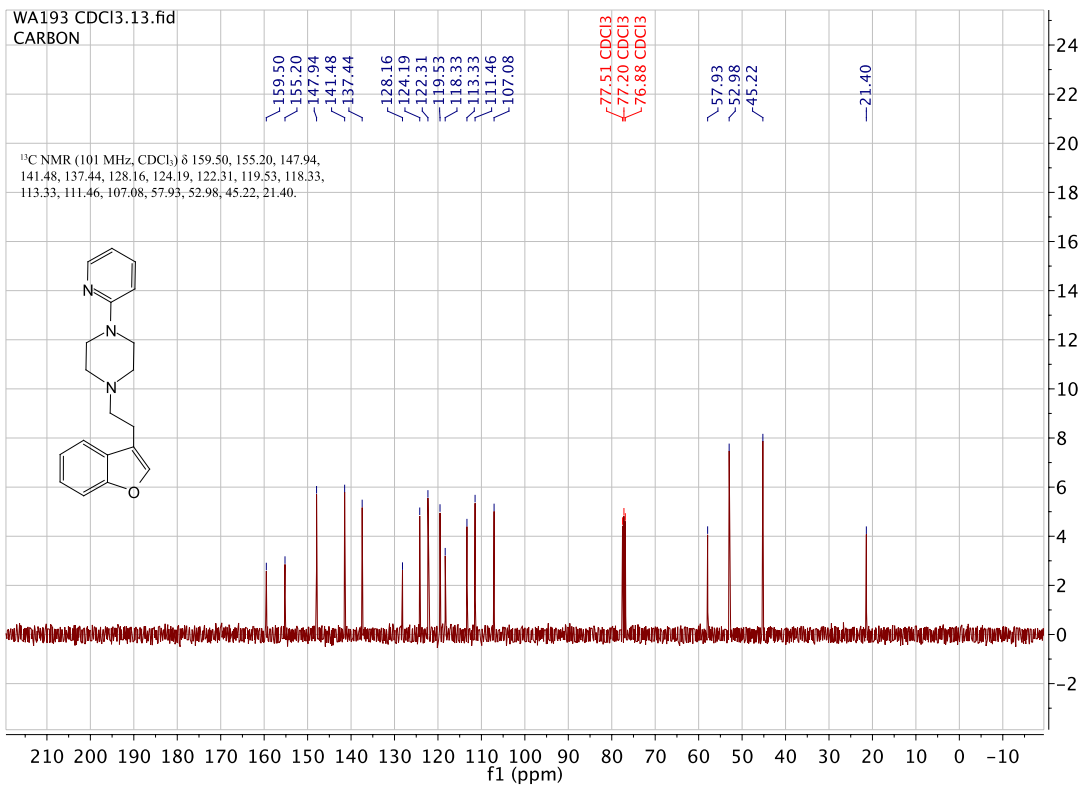
1-(2-(benzofuran-3-yl)ethyl)-4-(4-chlorophenyl)piperazine. (WA184)



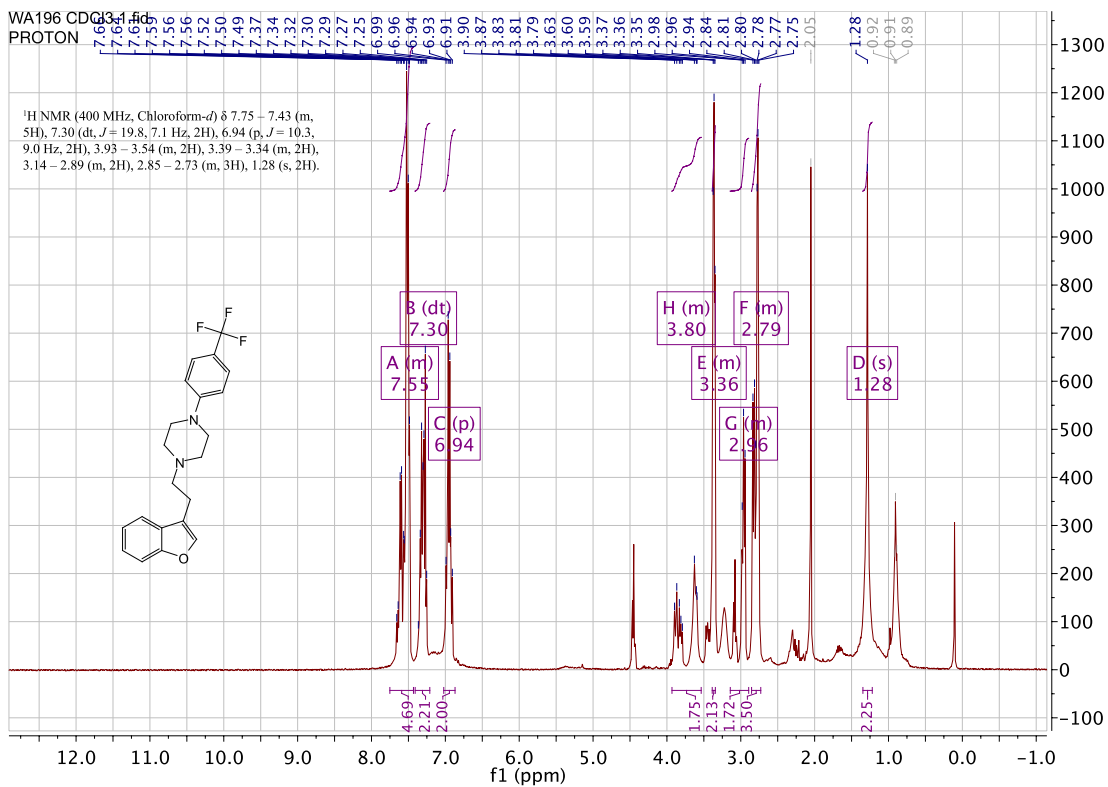
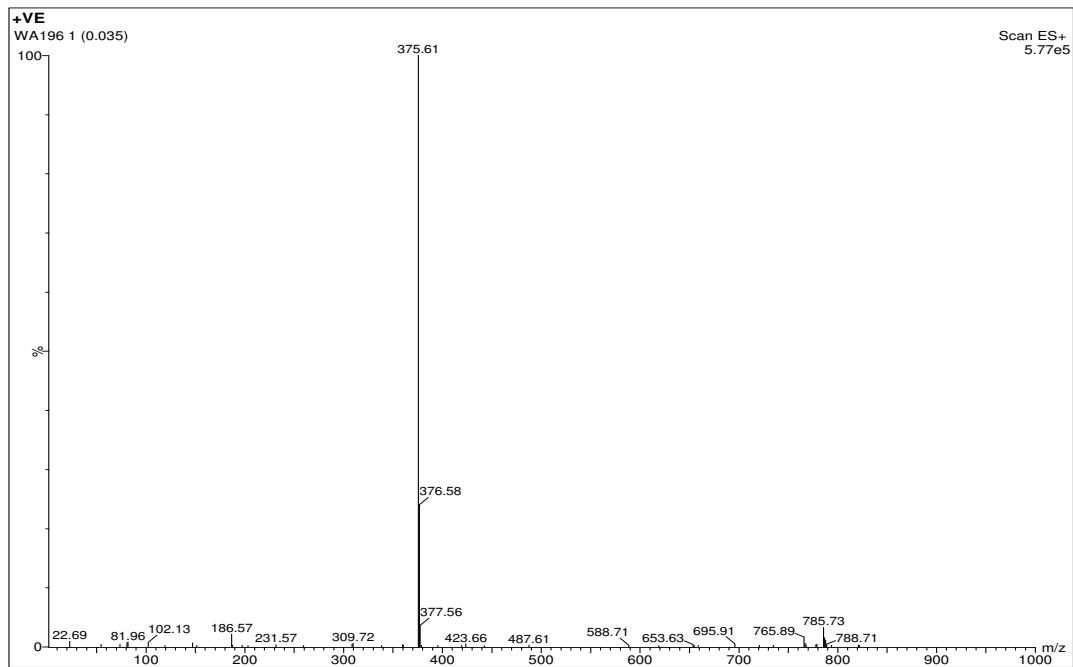


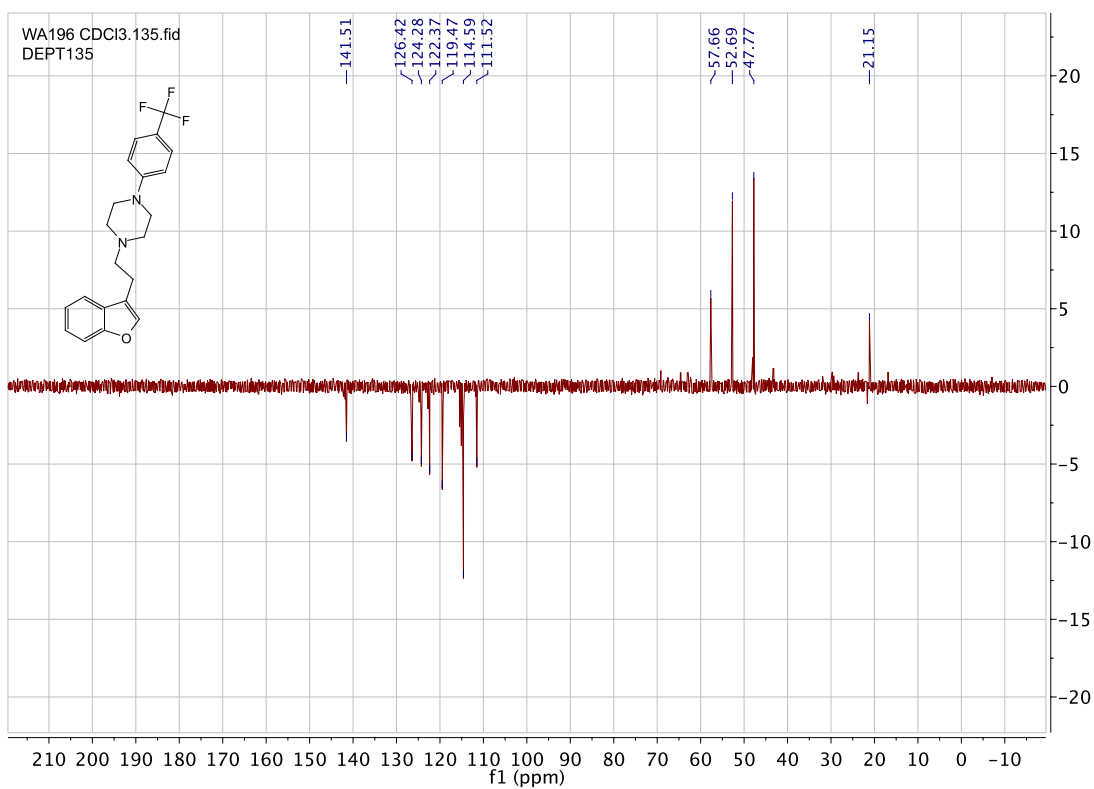
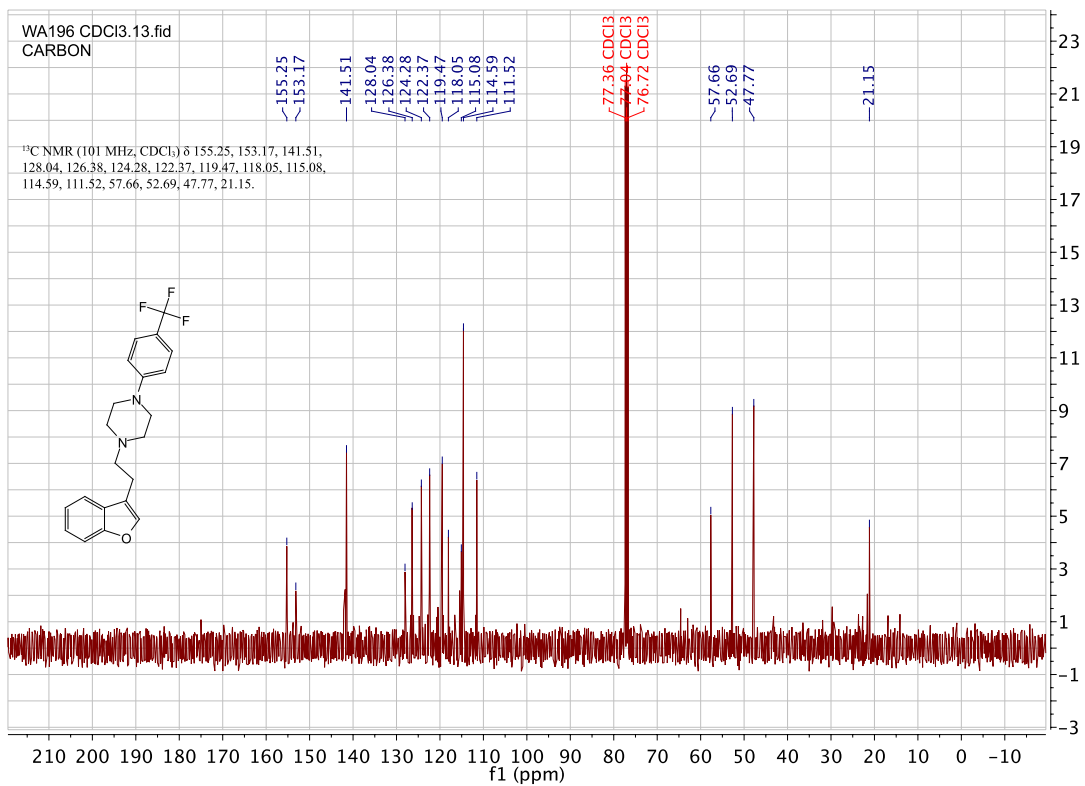
1-(2-(benzofuran-3-yl)ethyl)-4-(pyridin-2-yl)piperazine. (WA193)



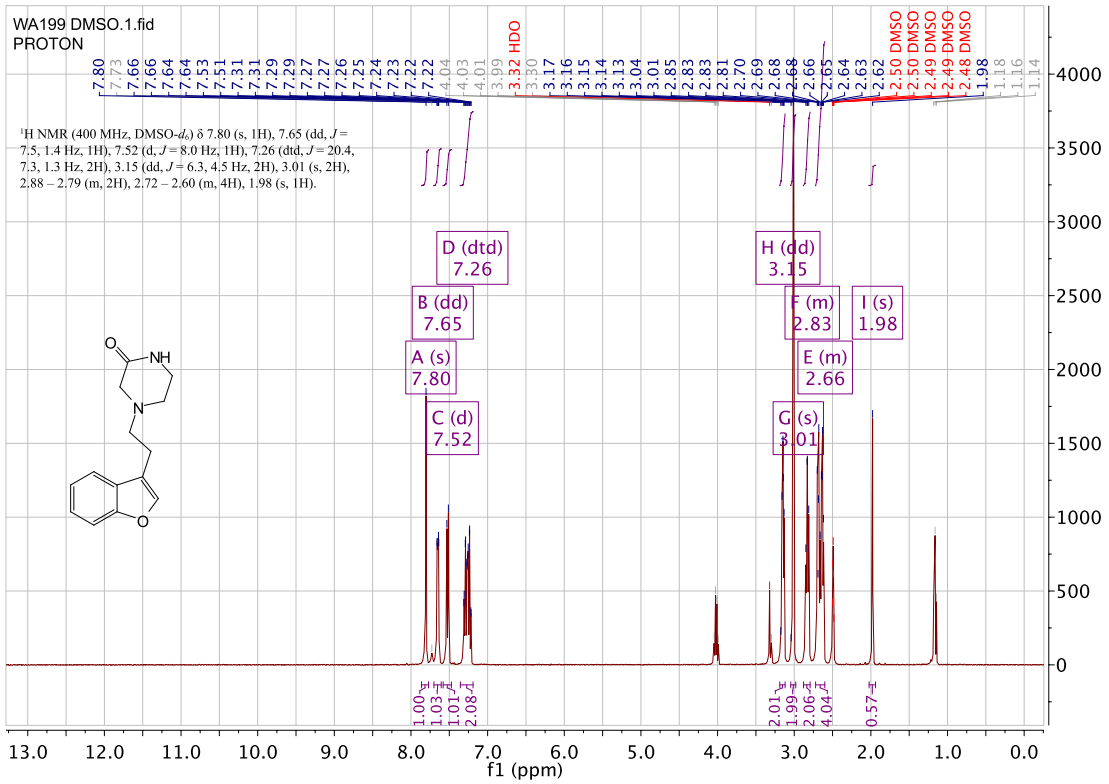
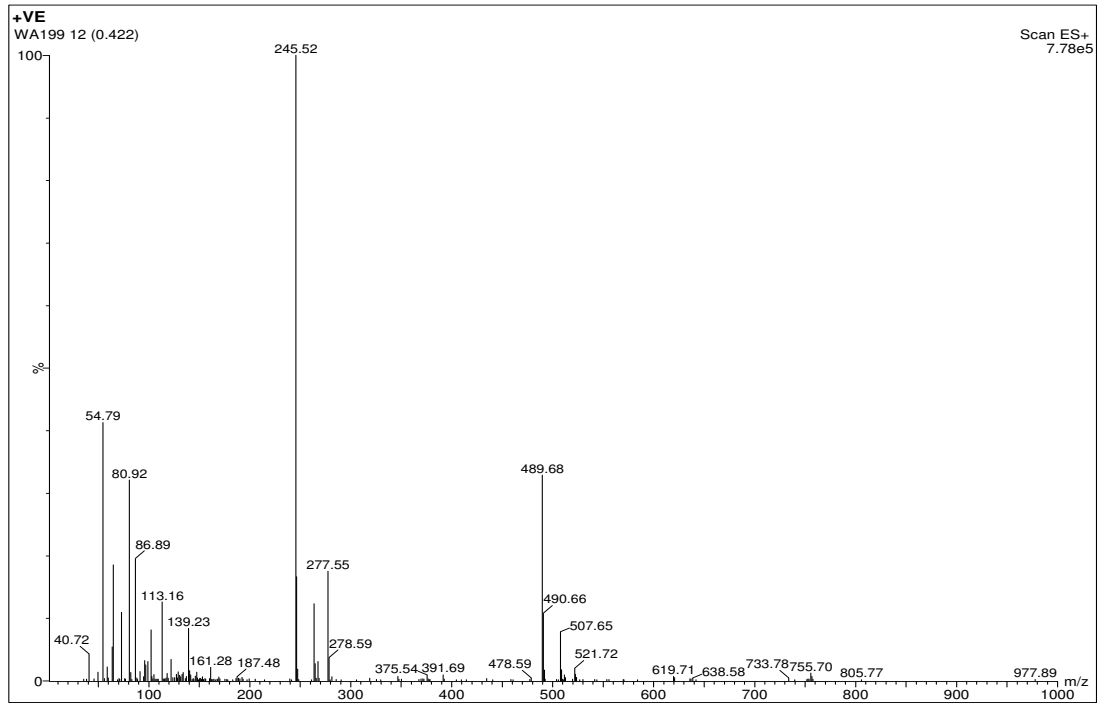


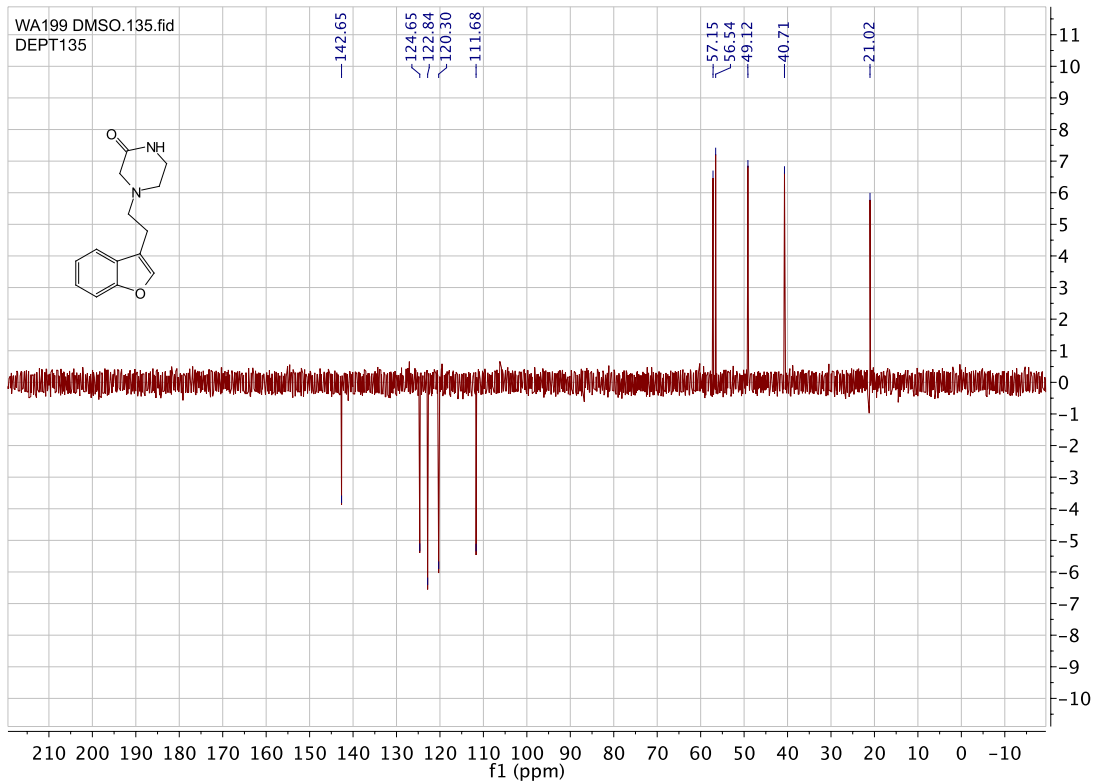
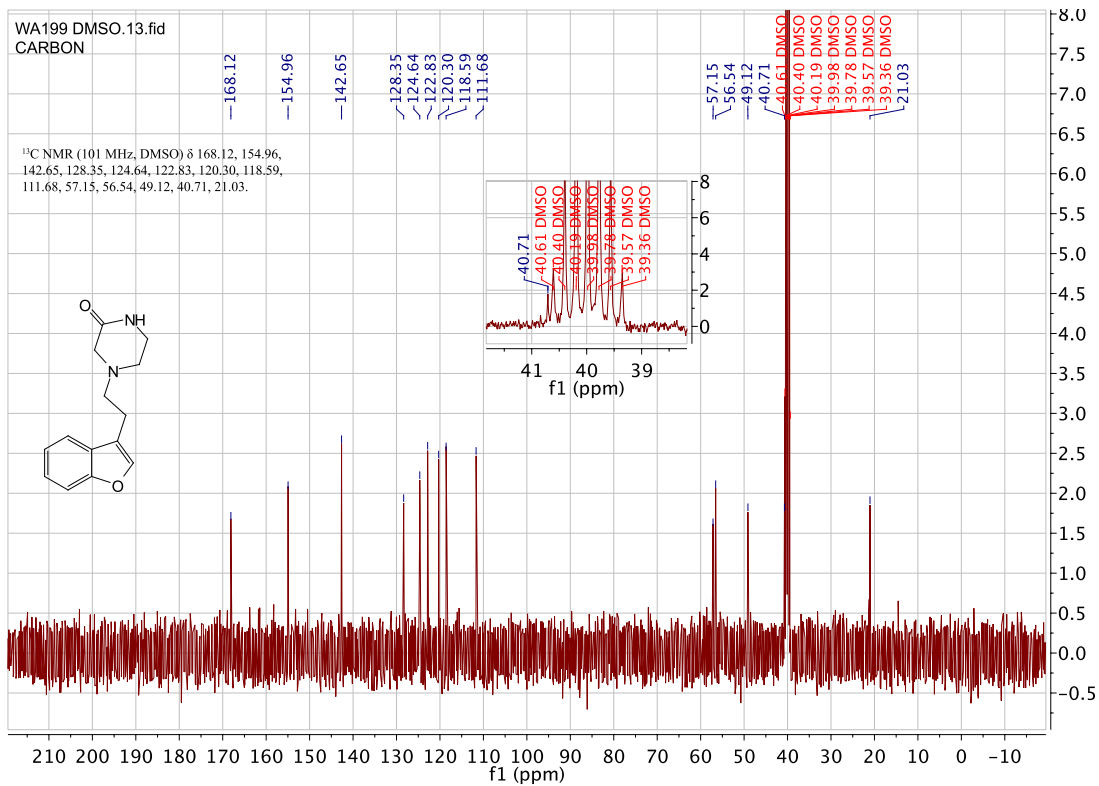
1-(2-(benzofuran-3-yl)ethyl)-4-(4-(trifluoromethyl)phenyl)piperazine. (WA196)



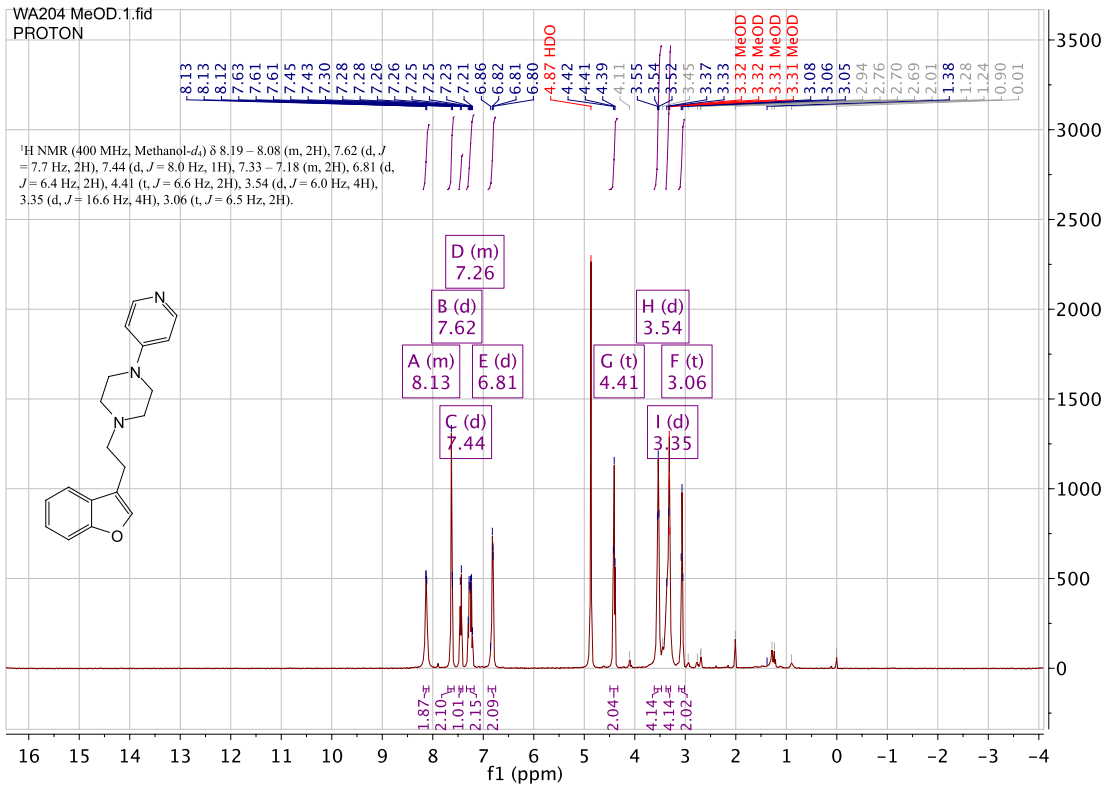
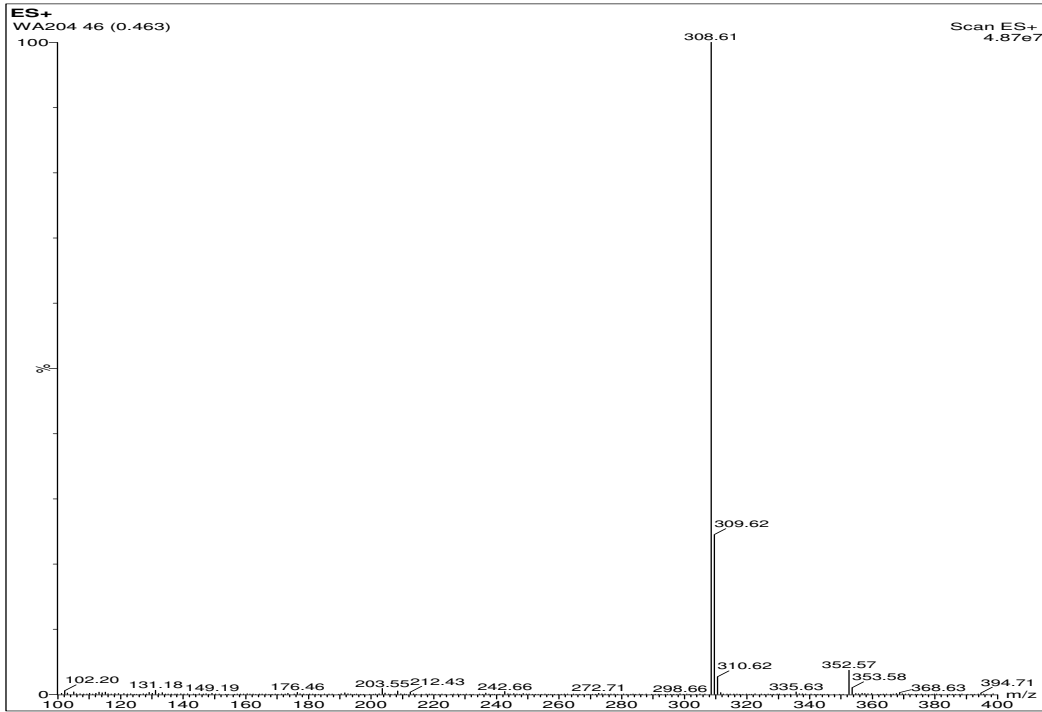


4-(2-(benzofuran-3-yl)ethyl)piperazin-2-one. (WA199)

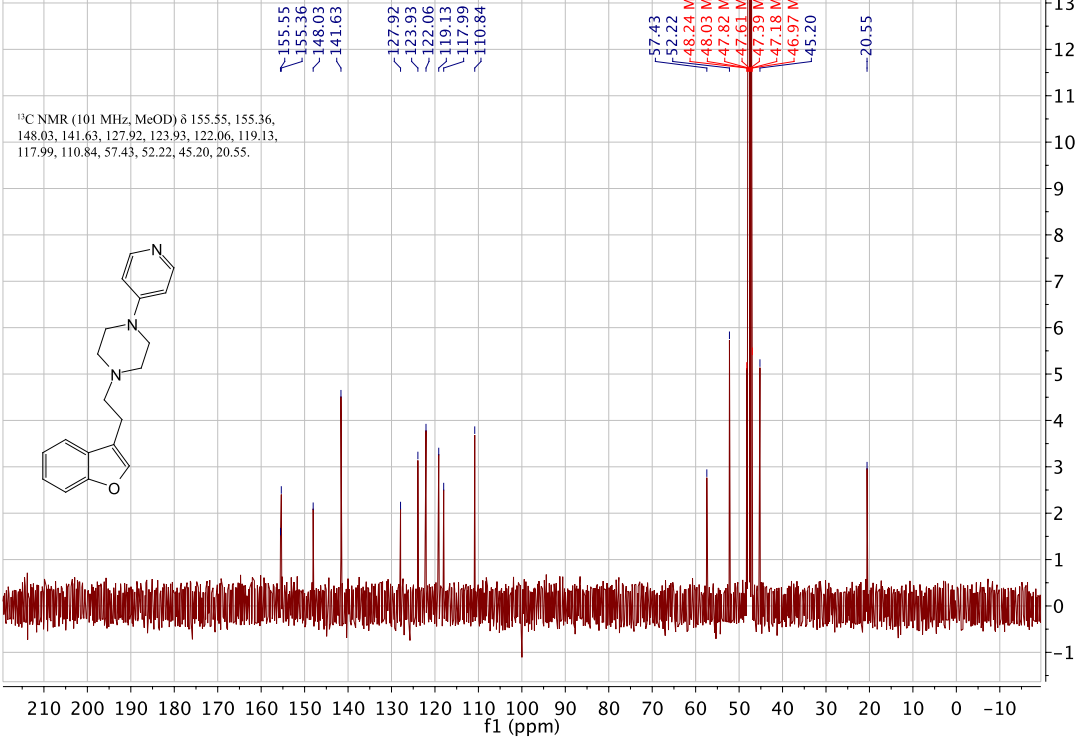




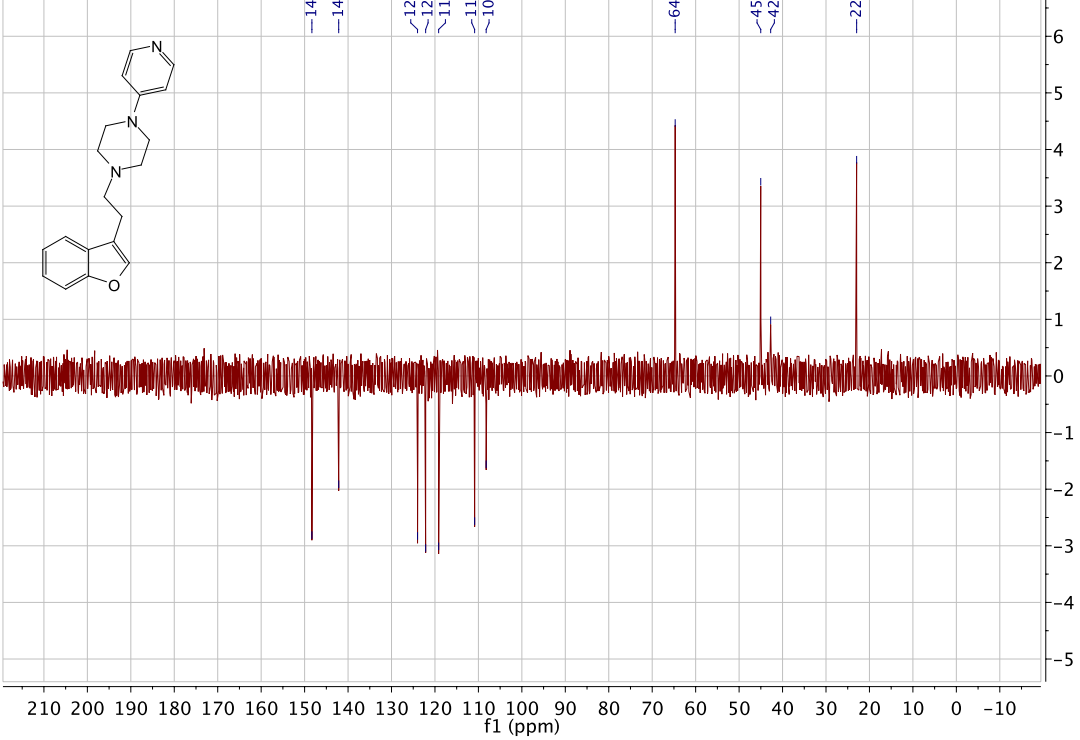
1-(2-(benzofuran-3-yl)ethyl)-4-(pyridin-4-yl)piperazine. (WA204)



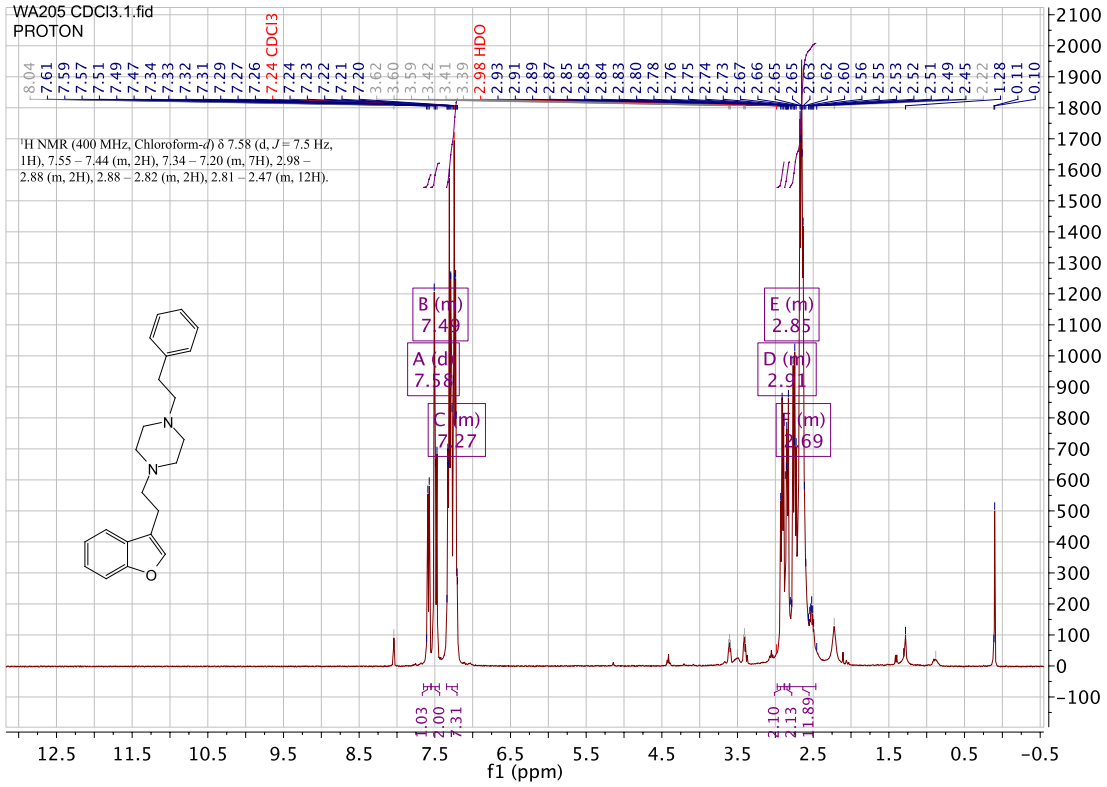
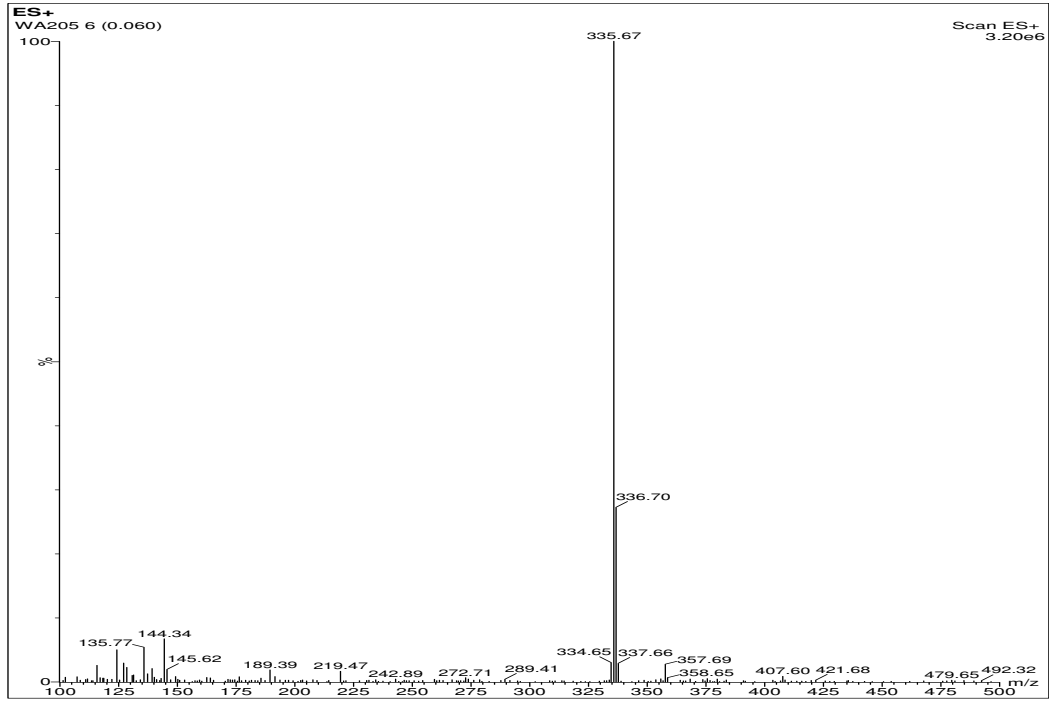
WA204 MeOD.13.fid
CARBON

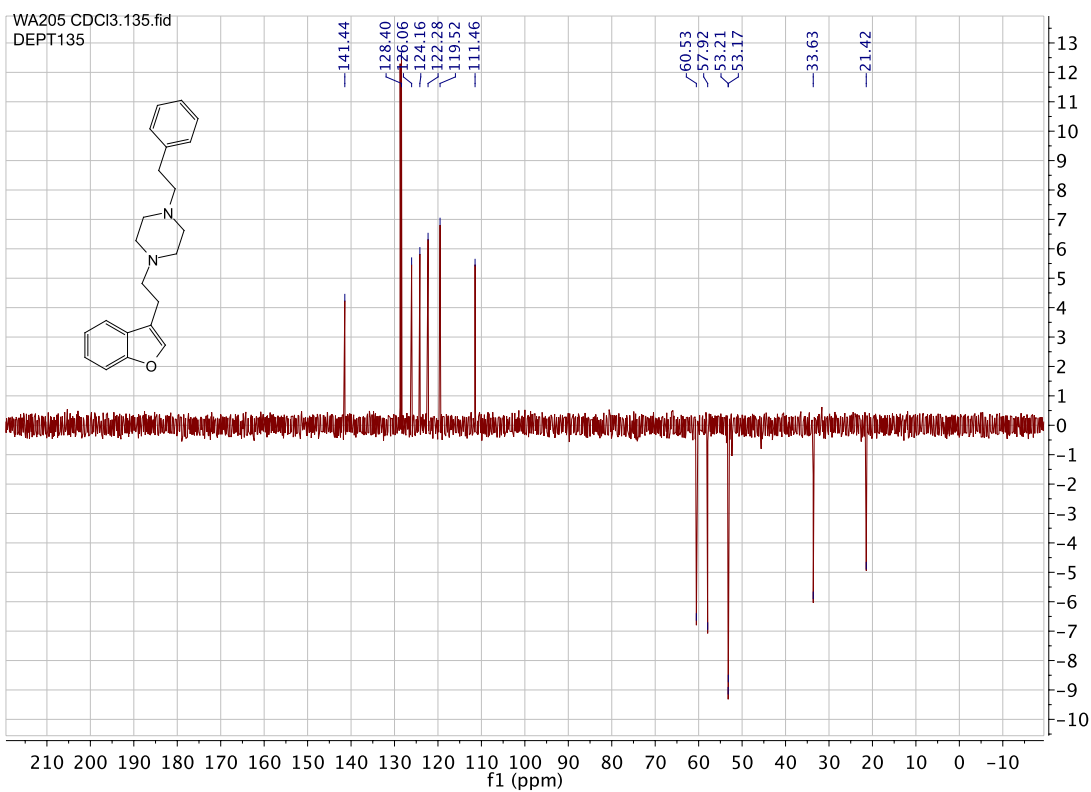
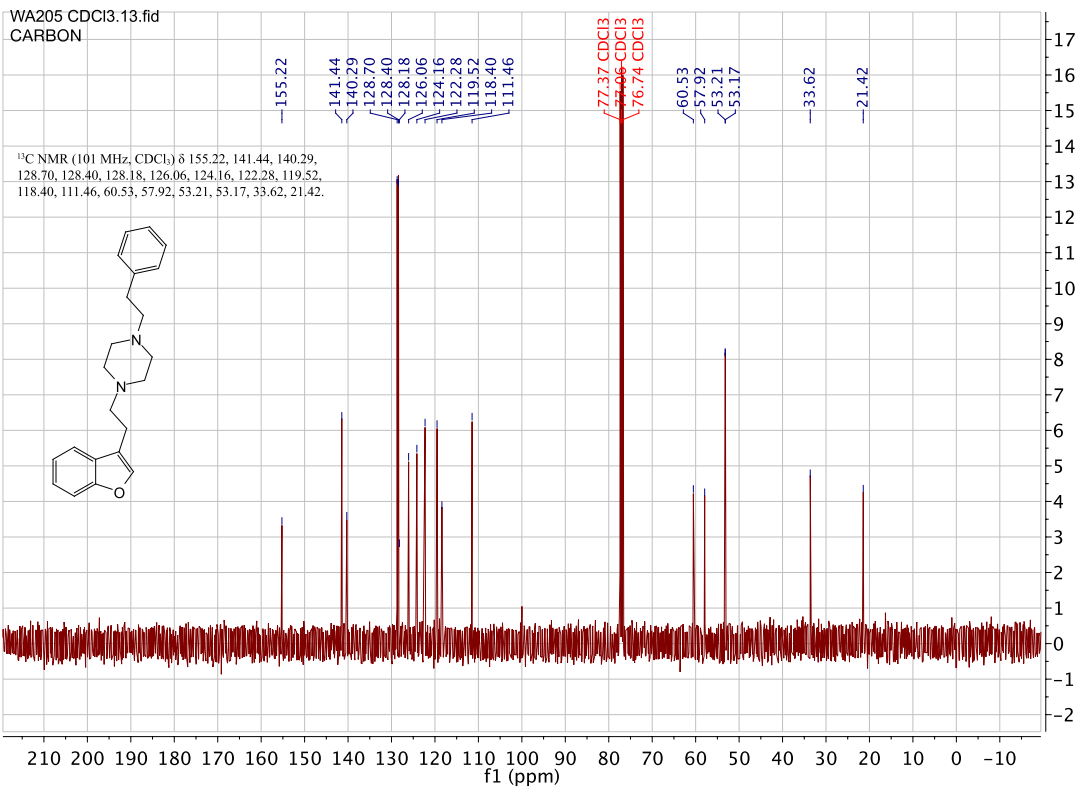


WA204 MeOD.135.fid
DEPT135

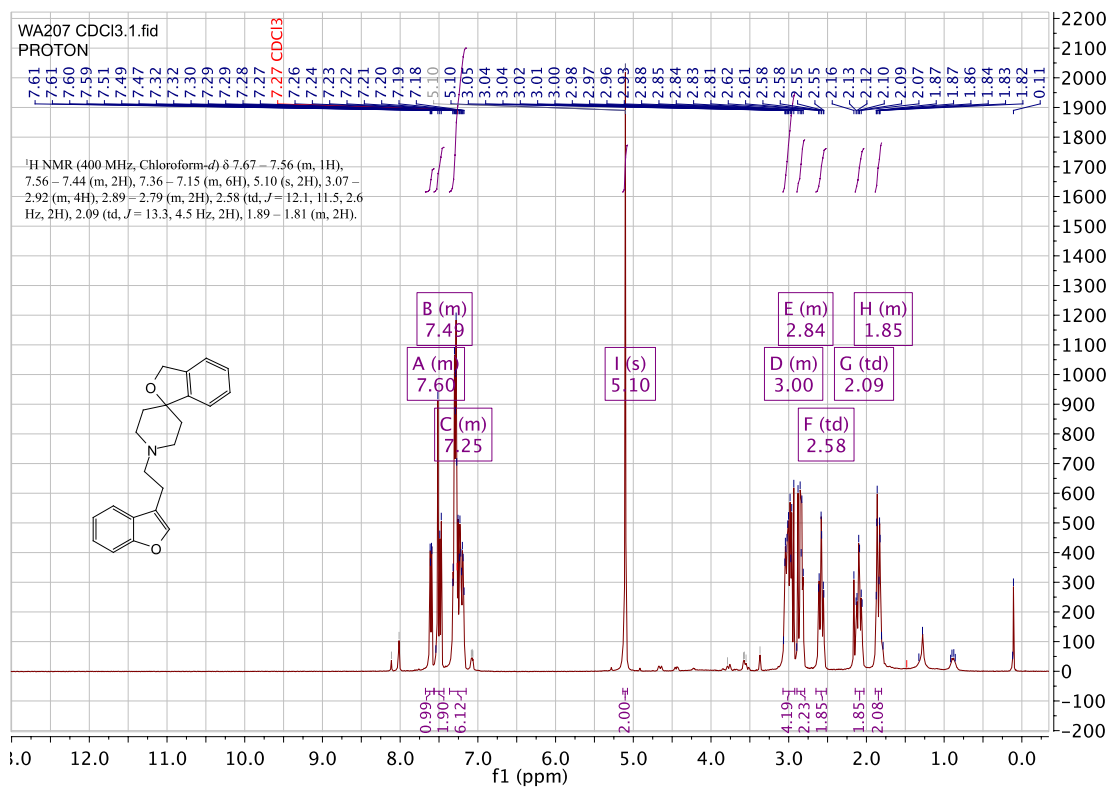
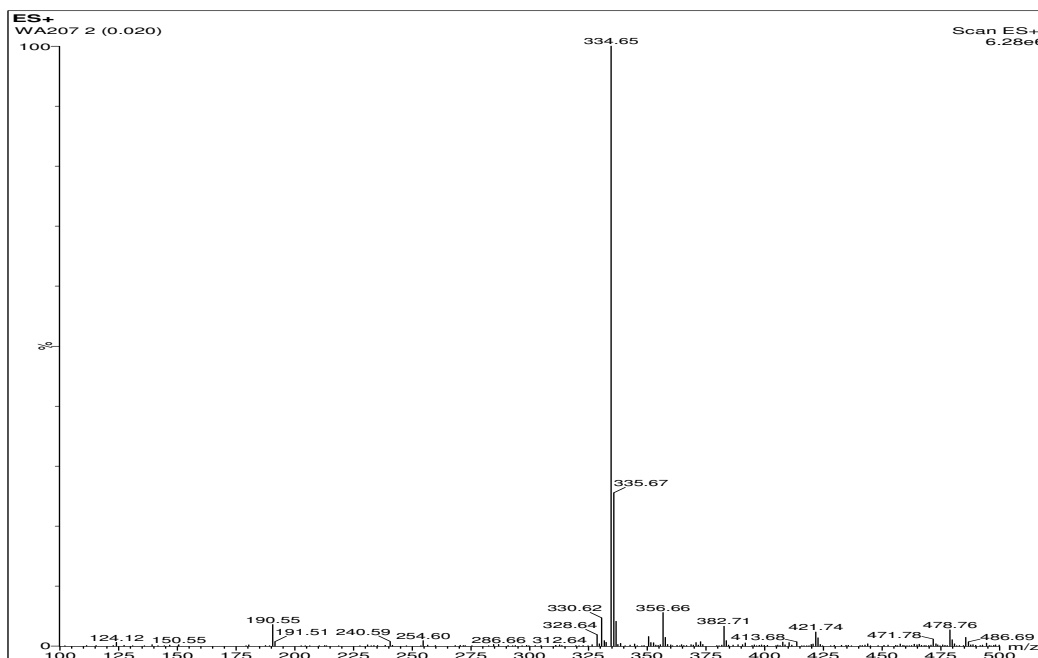


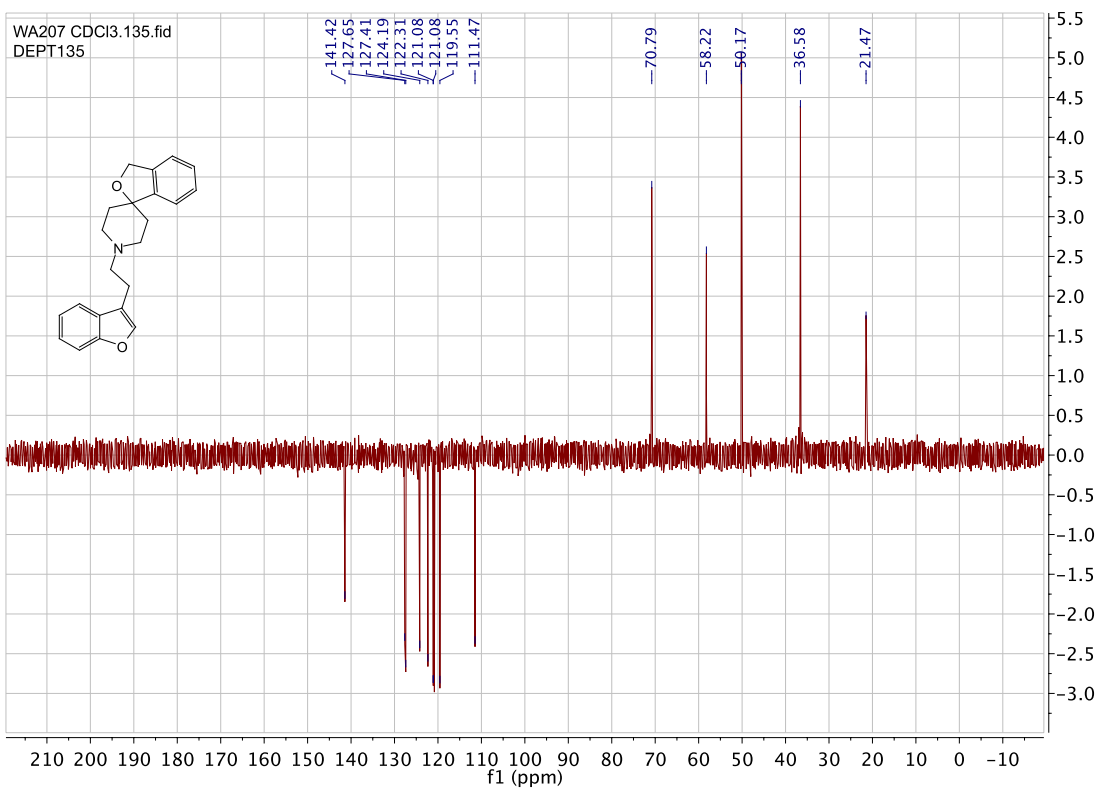
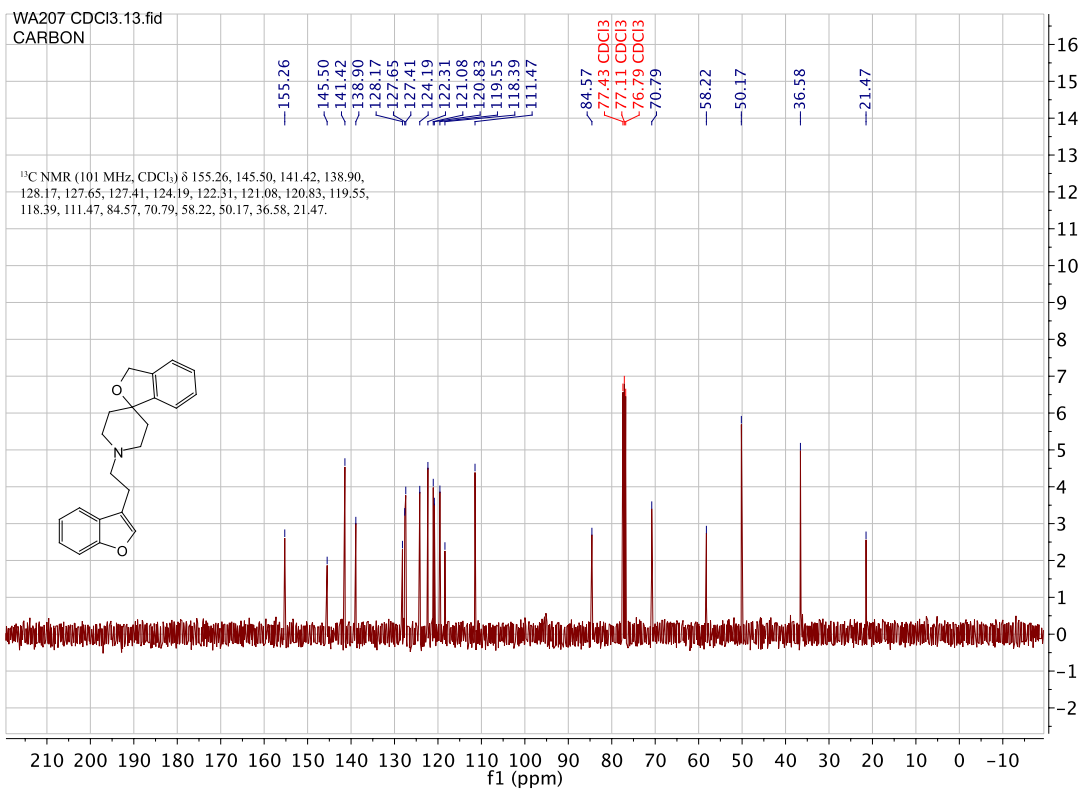
1-(2-(benzofuran-3-yl)ethyl)-4-phenethylpiperazine. (WA205)



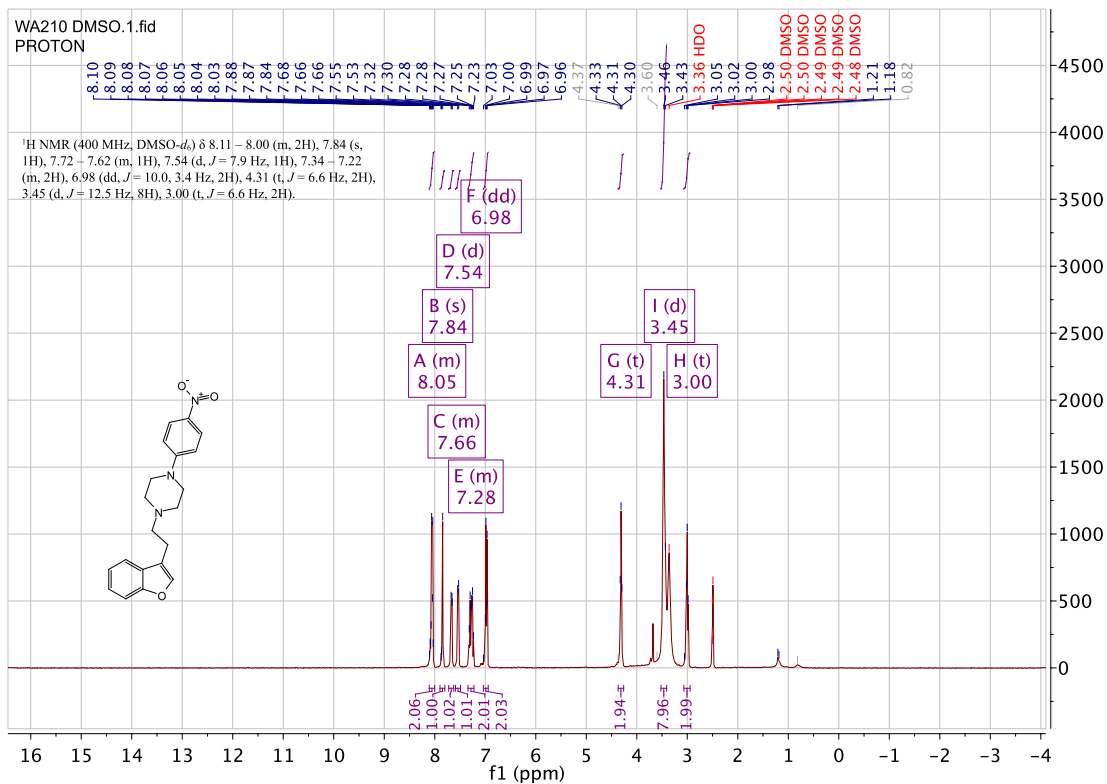
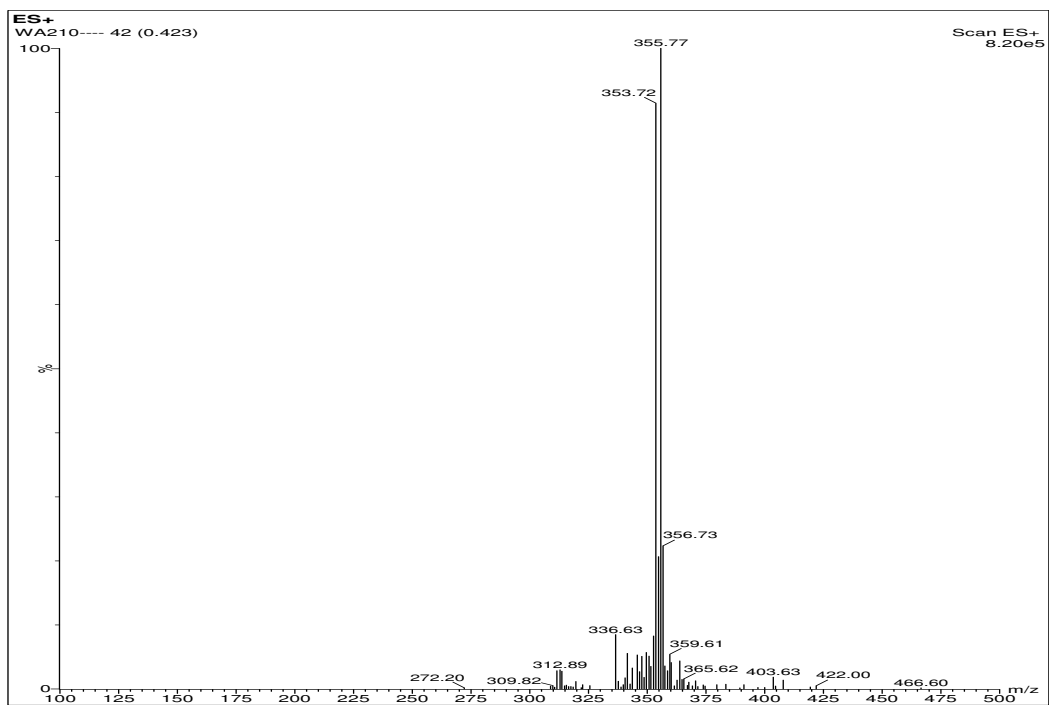


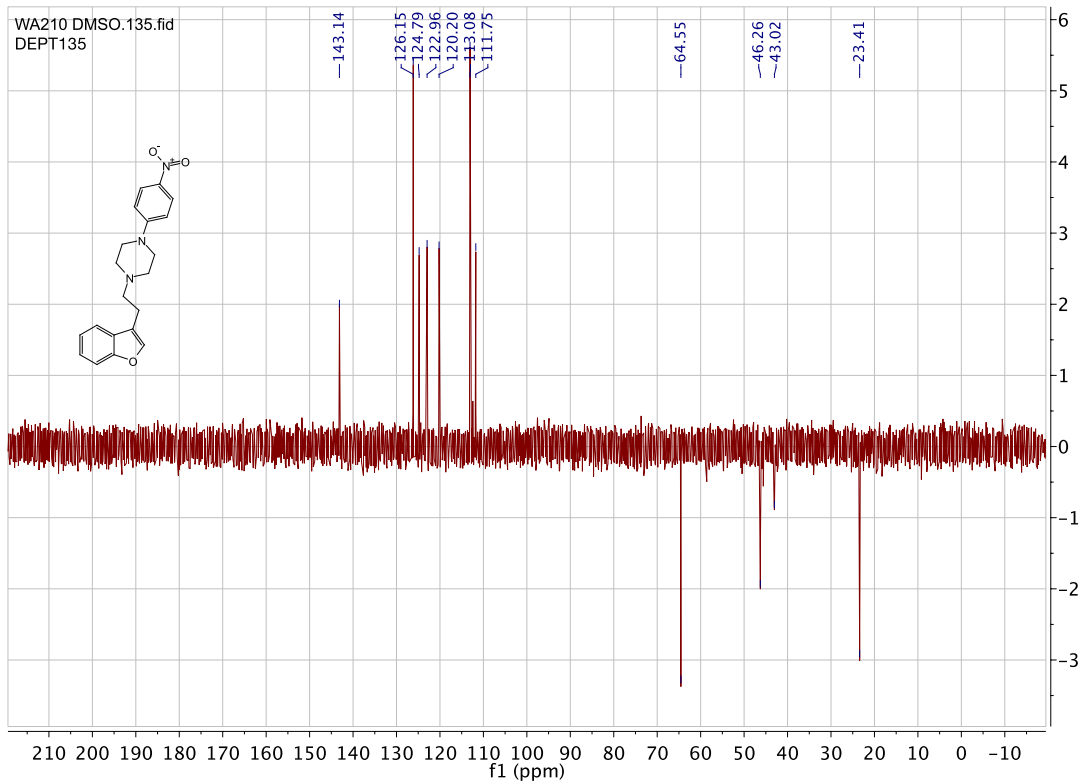
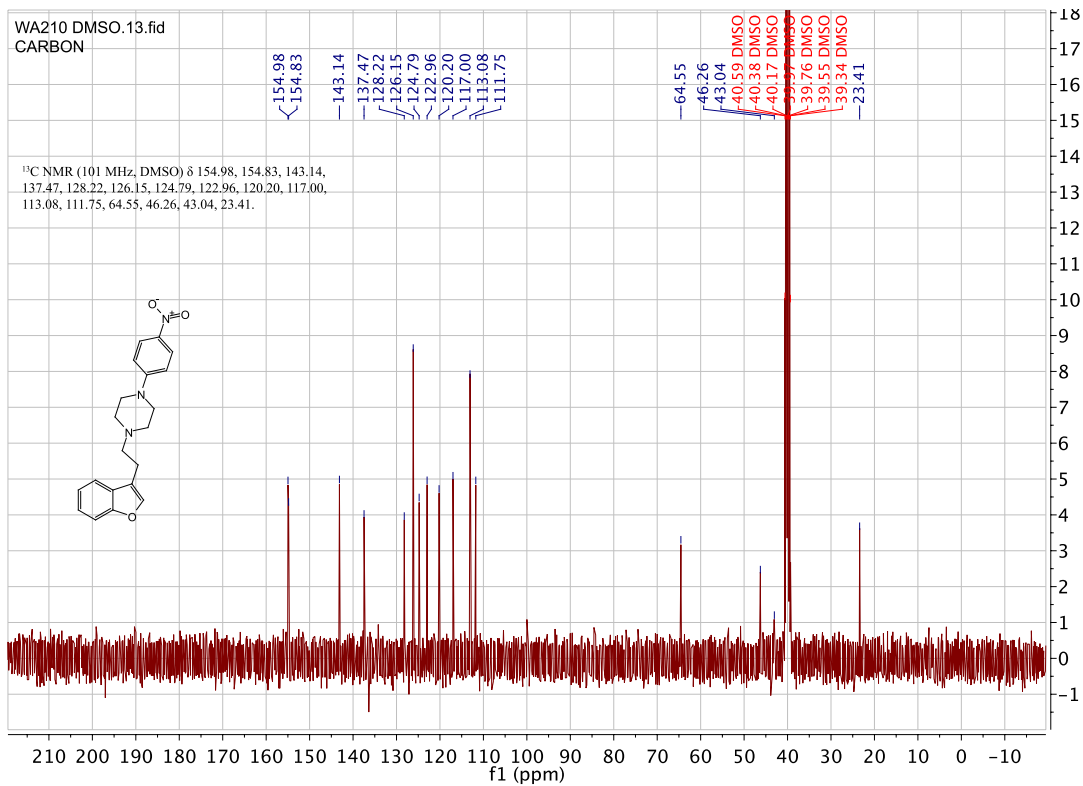
1'-(2-(benzofuran-3-yl)ethyl)-3H-spiro[isobenzofuran-1,4'-piperidine]. (WA207)



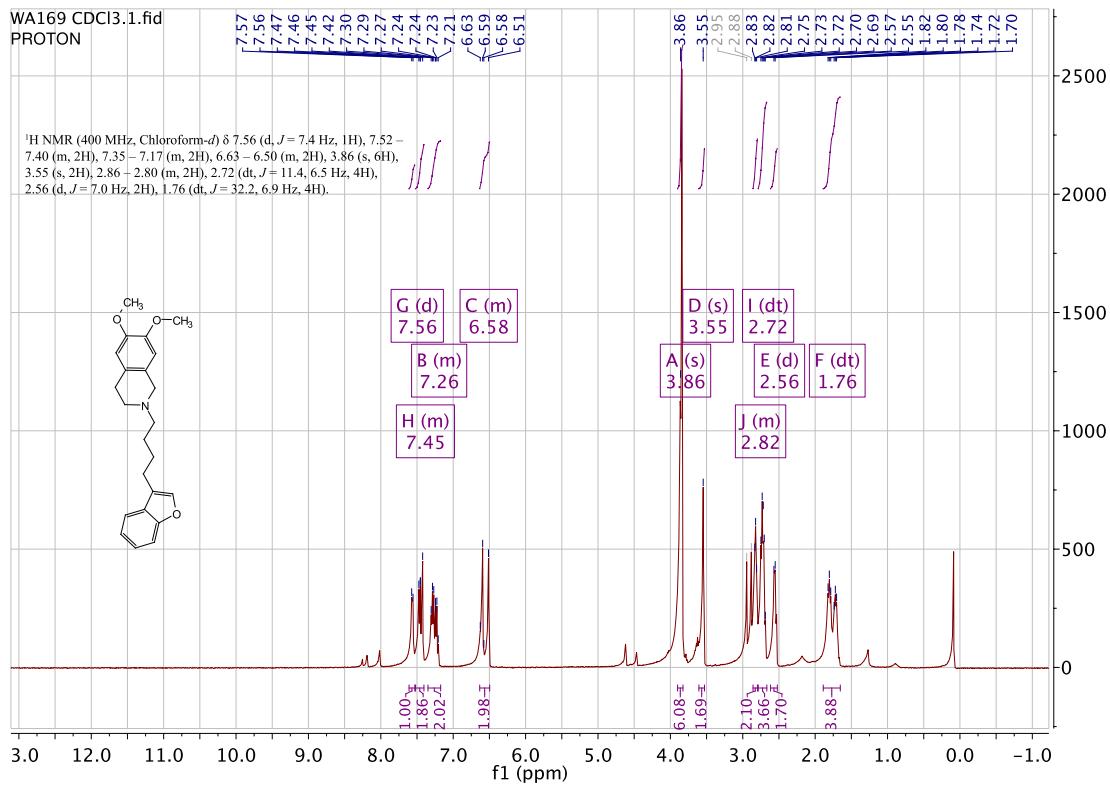
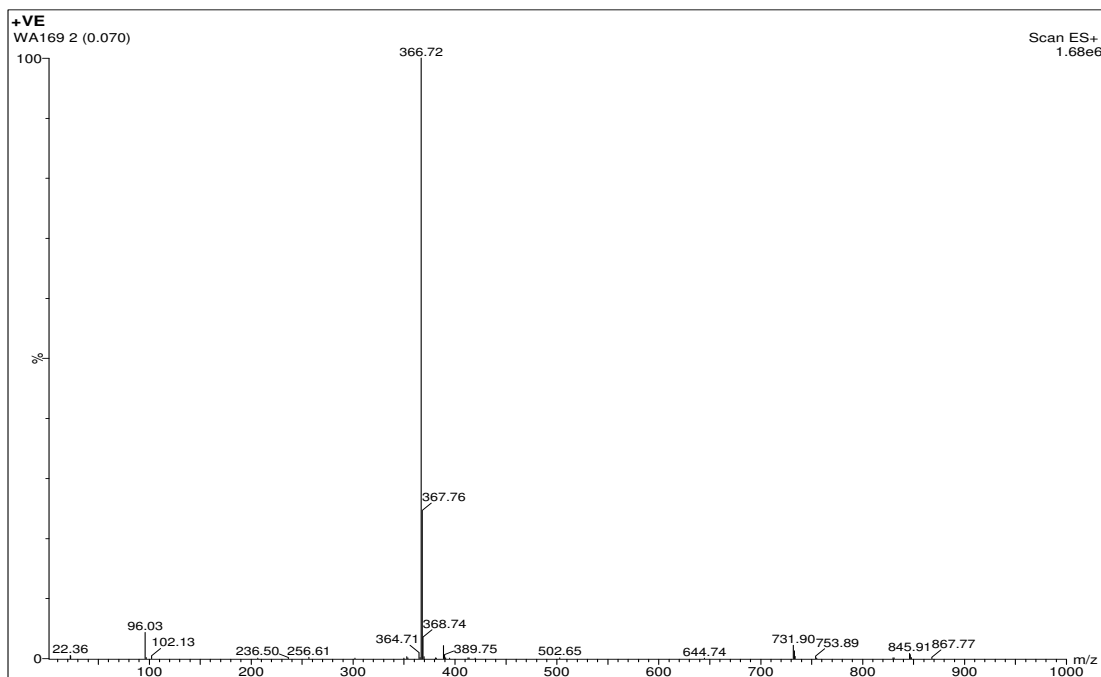


1-(2-(benzofuran-3-yl)ethyl)-4-(4-nitrophenyl)piperazine. (WA210)

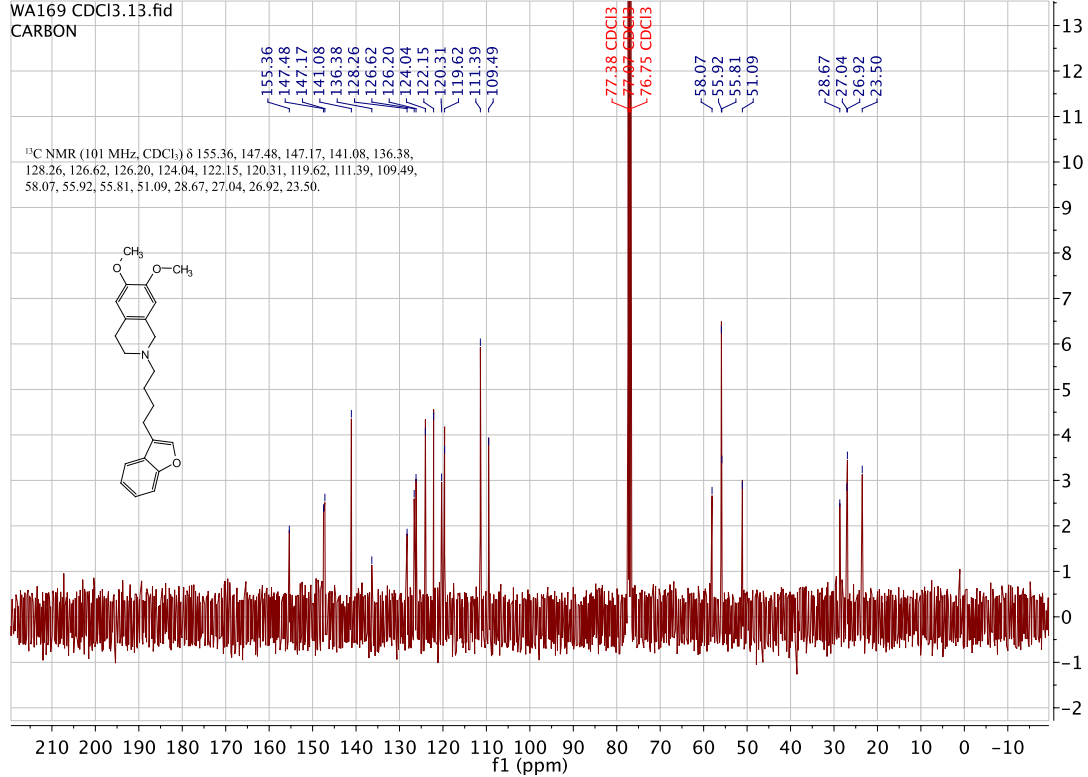




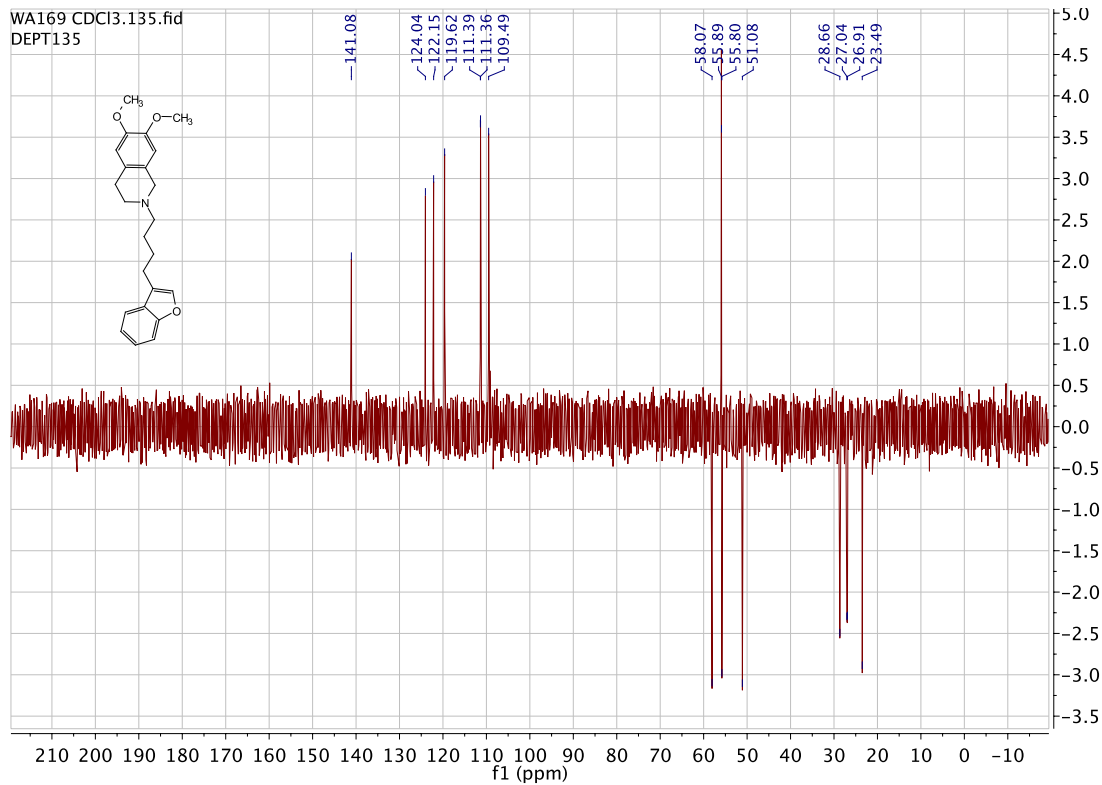
2-(4-(benzofuran-3-yl)butyl)-6,7-dimethoxy-1,2,3,4-tetrahydroisoquinoline. (WA169)



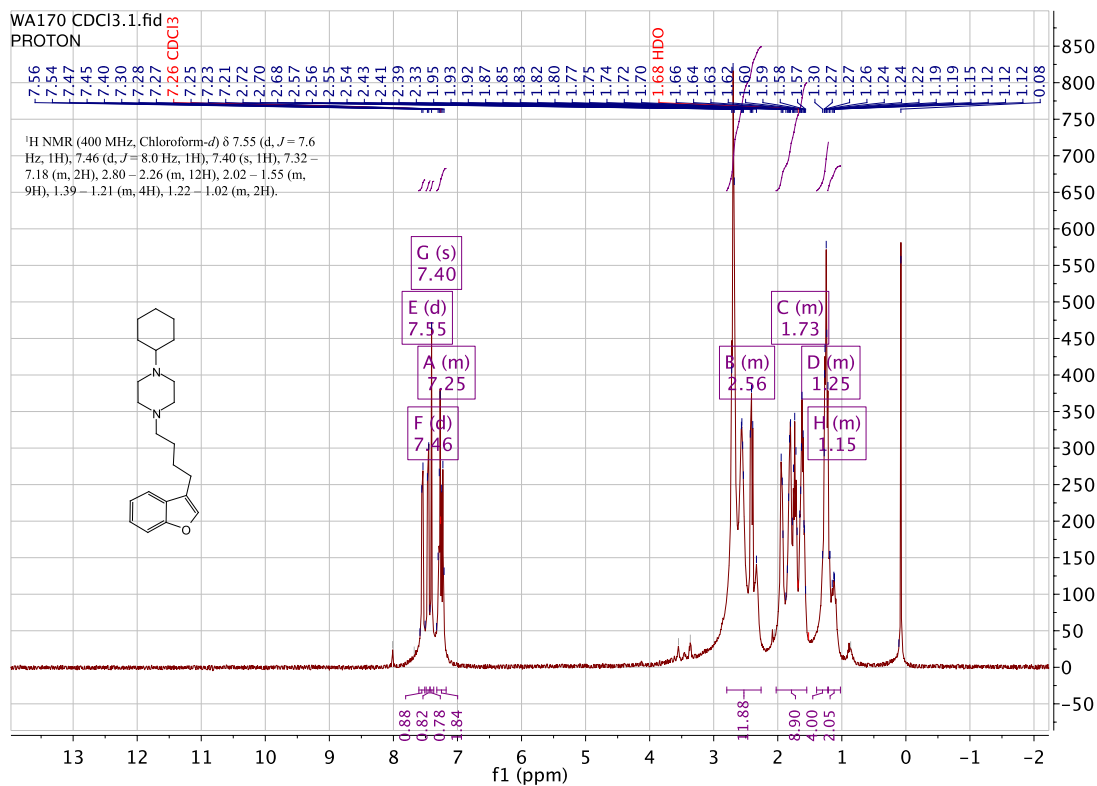
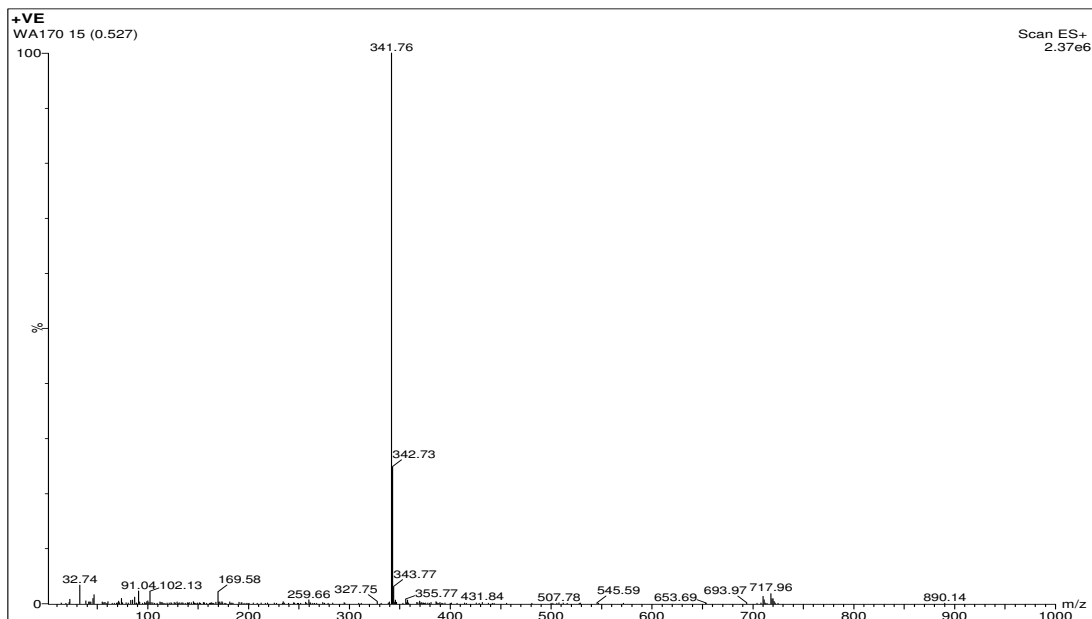
WA169 CDCl3.13.fid
CARBON



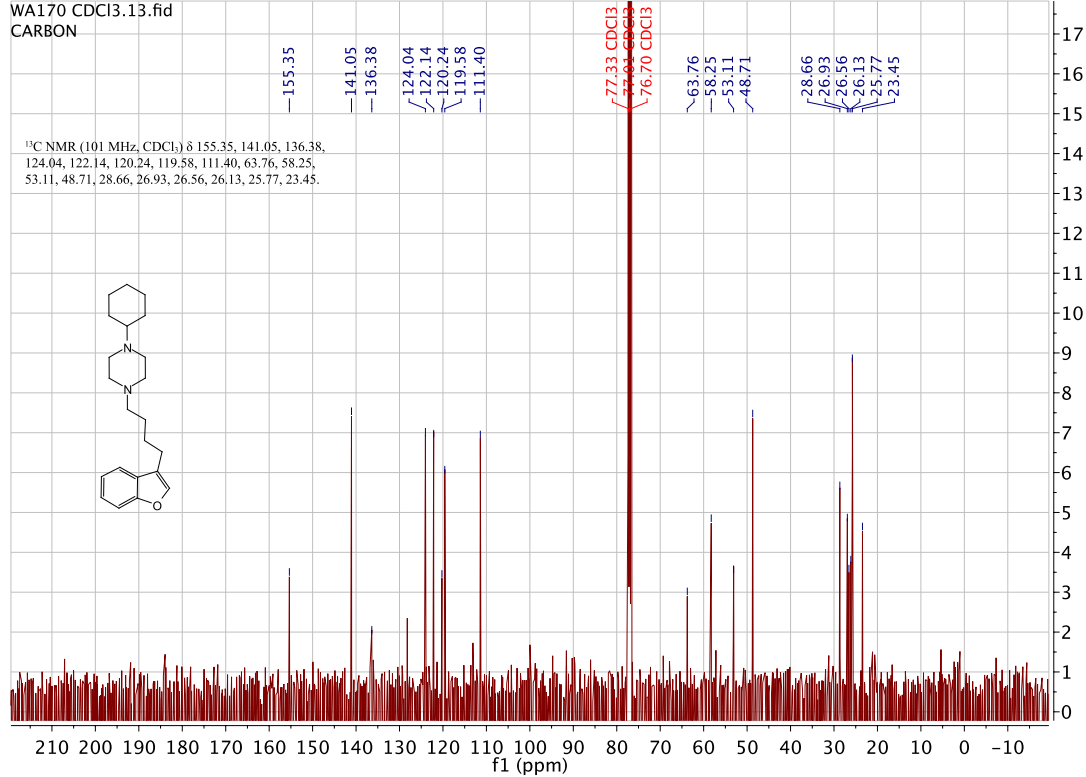
WA169 CDCl3.135.fid
DEPT135



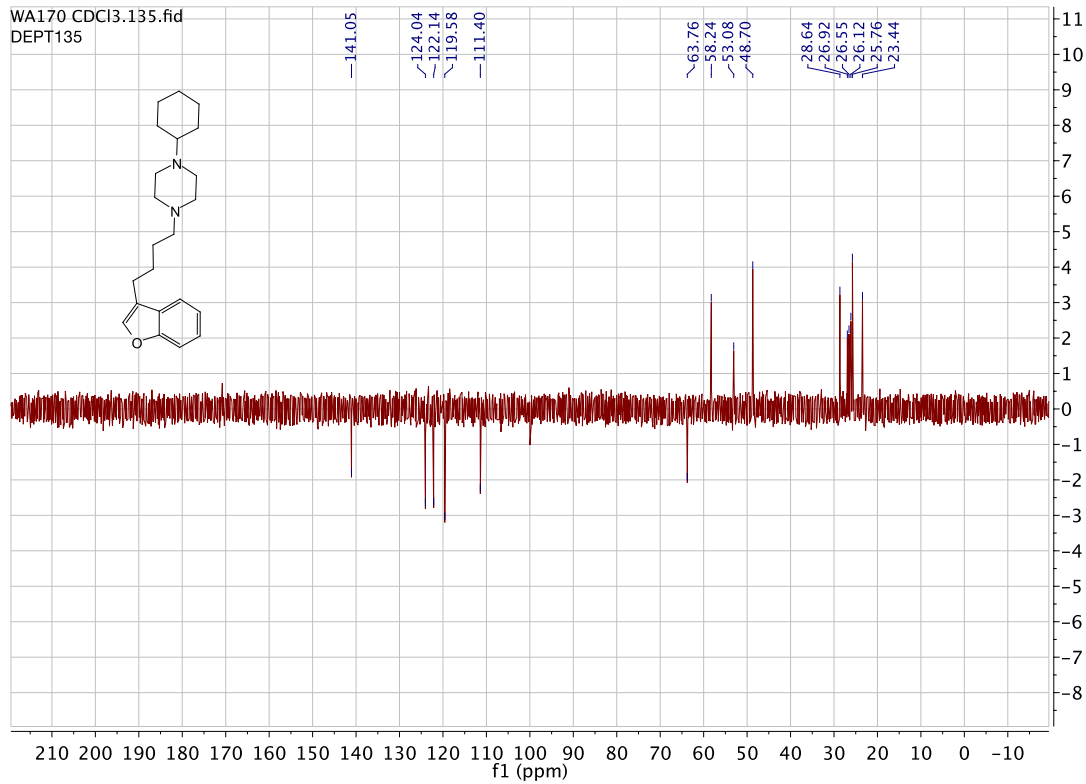
1-(4-(benzofuran-3-yl)butyl)-4-cyclohexylpiperazine. (WA170)



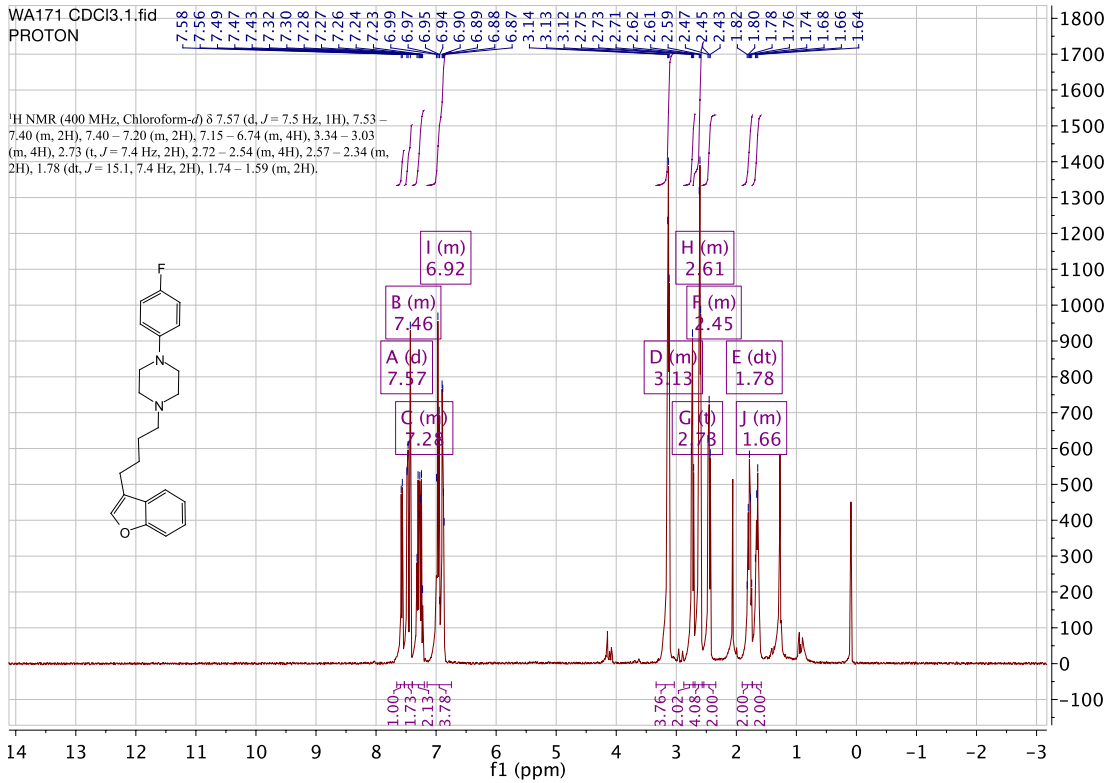
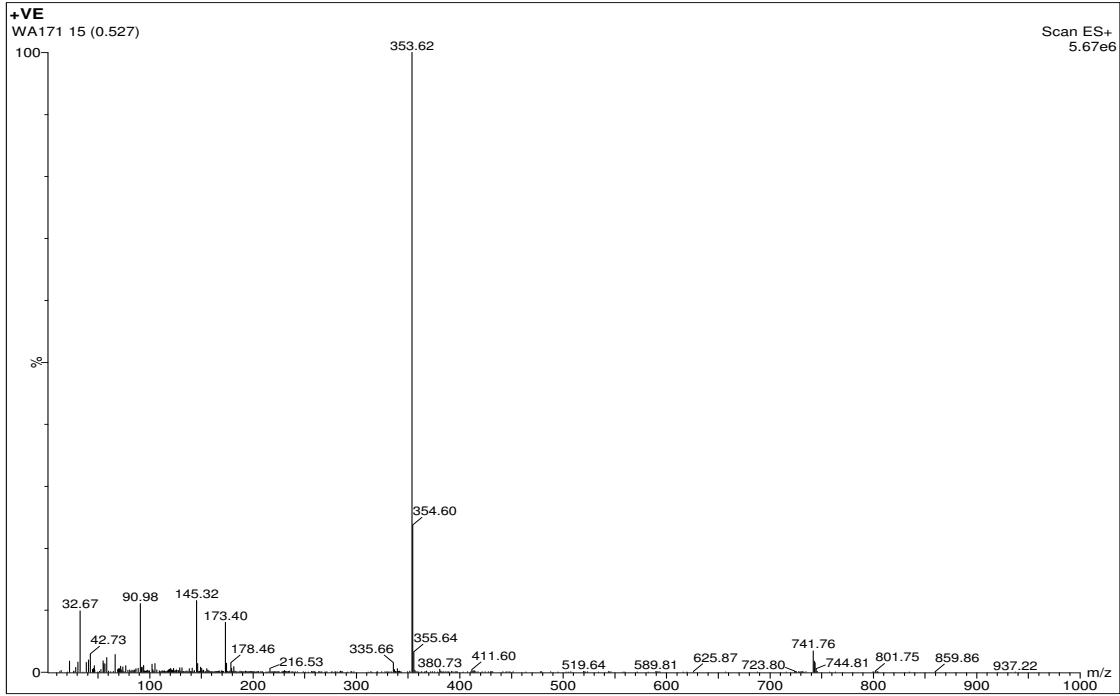
WA170 CDCl3.13.fid
CARBON

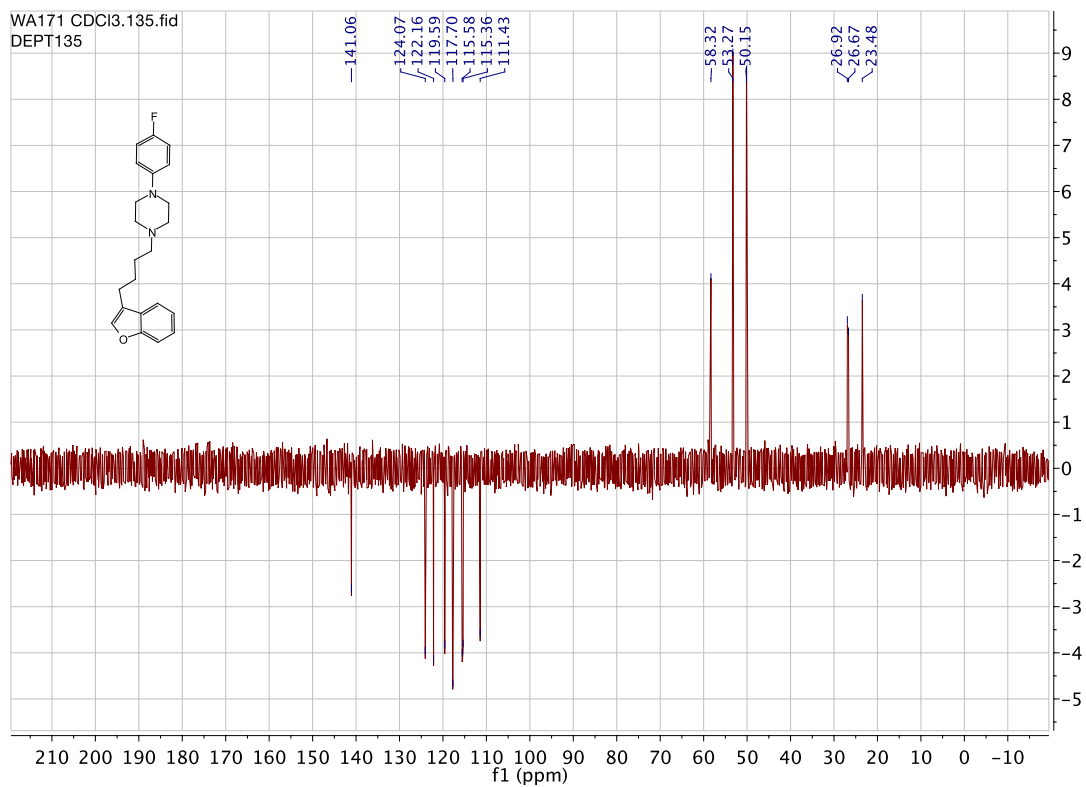
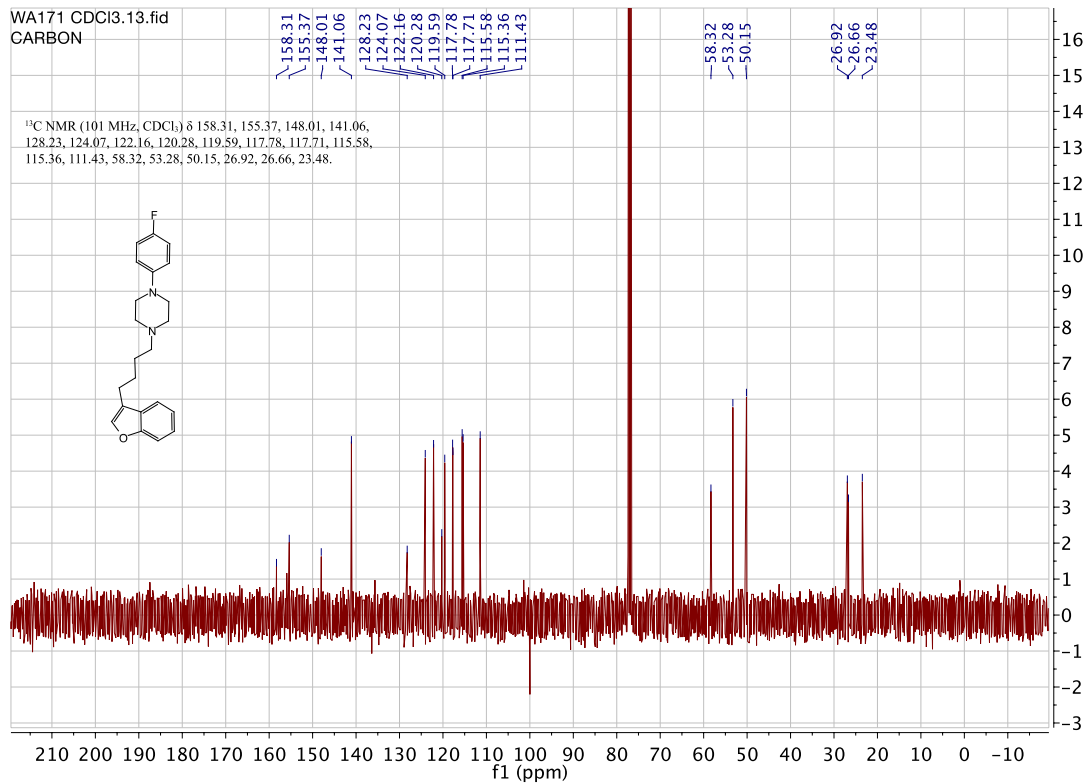


WA170 CDCl3.135.fid
DEPT135

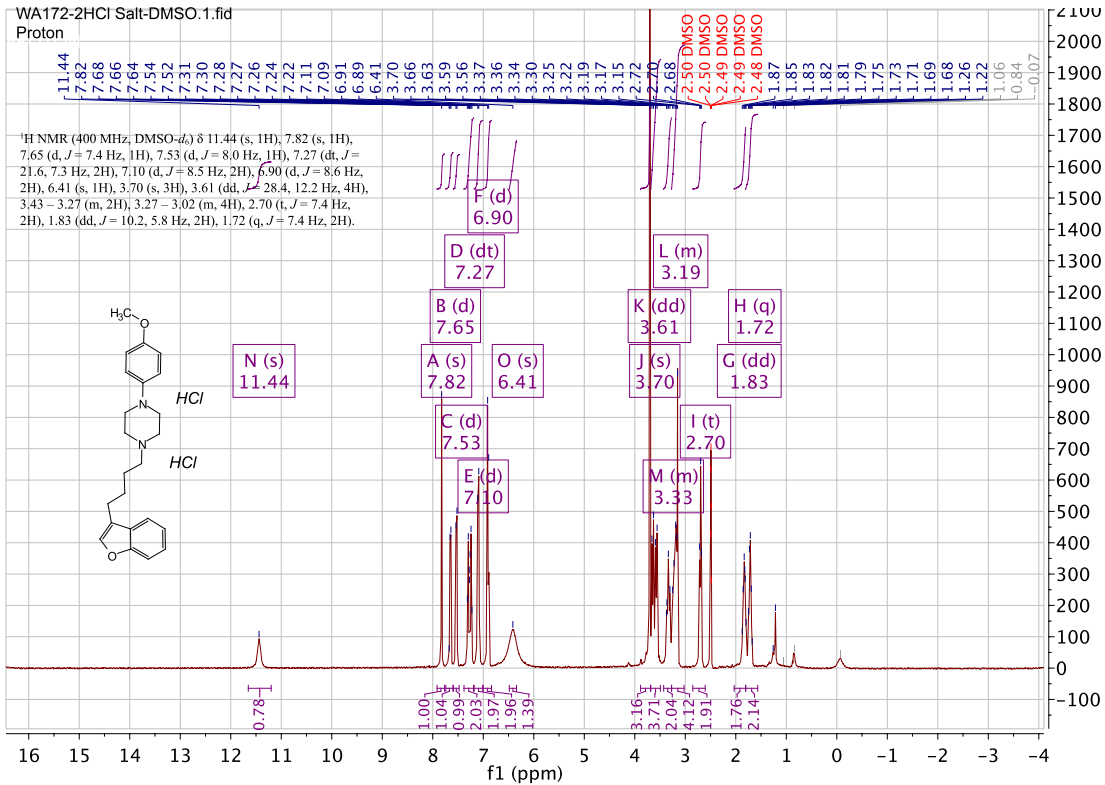
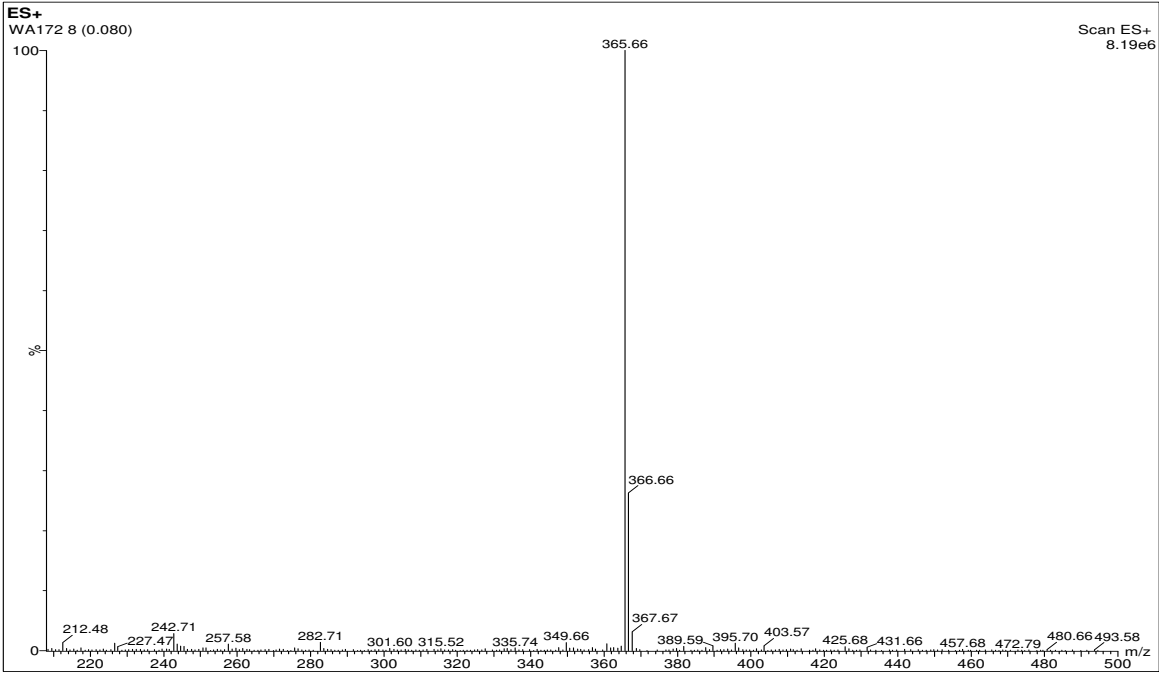


1-(4-(benzofuran-3-yl)butyl)-4-(4-fluorophenyl)piperazine. (WA171)

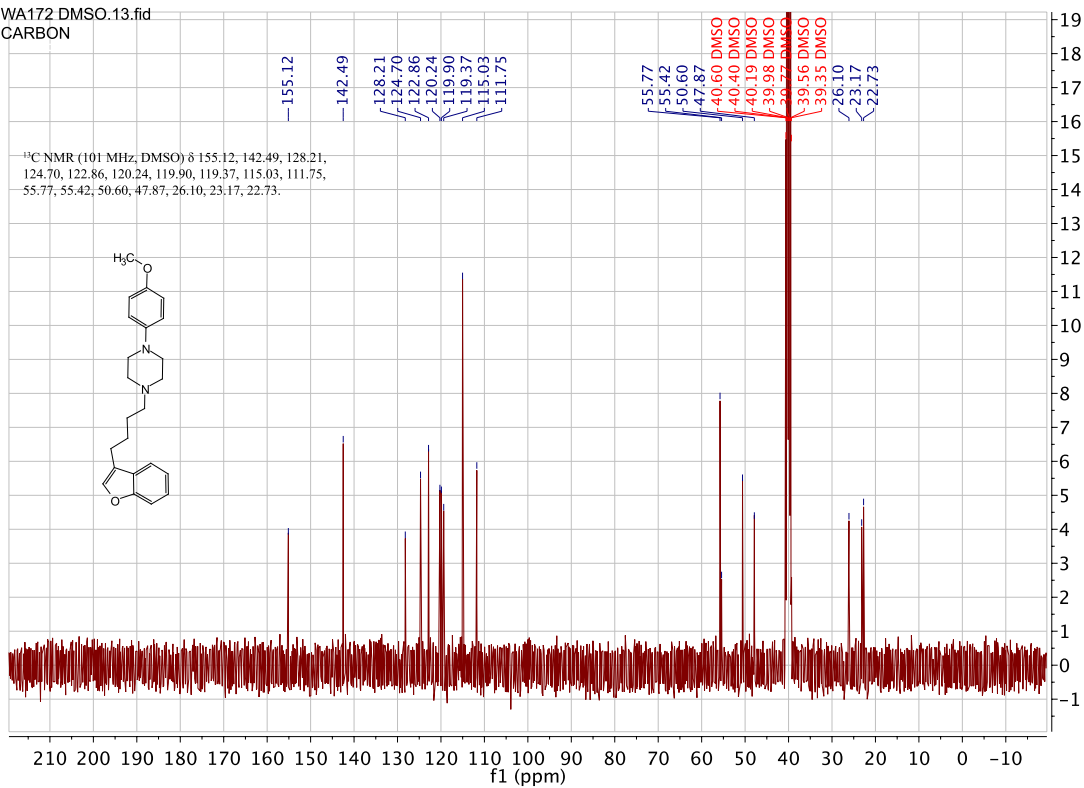




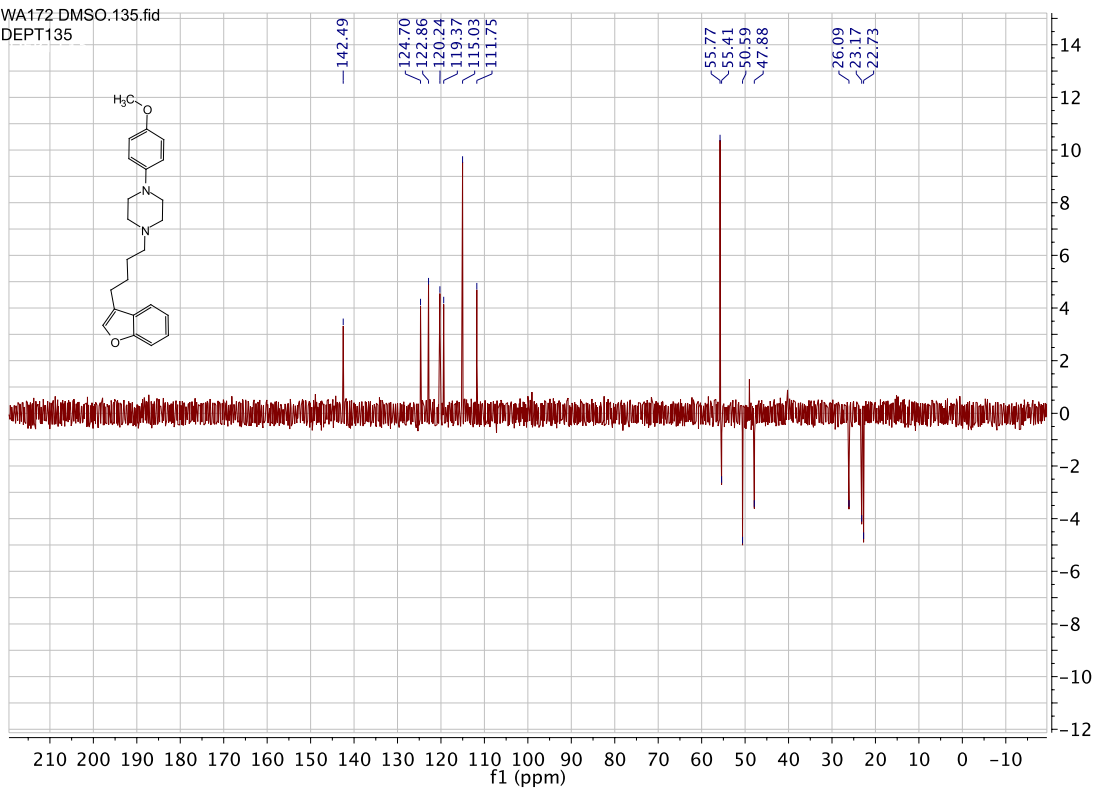
1-(4-(benzofuran-3-yl)butyl)-4-(4-methoxyphenyl)piperazine. (WA172)



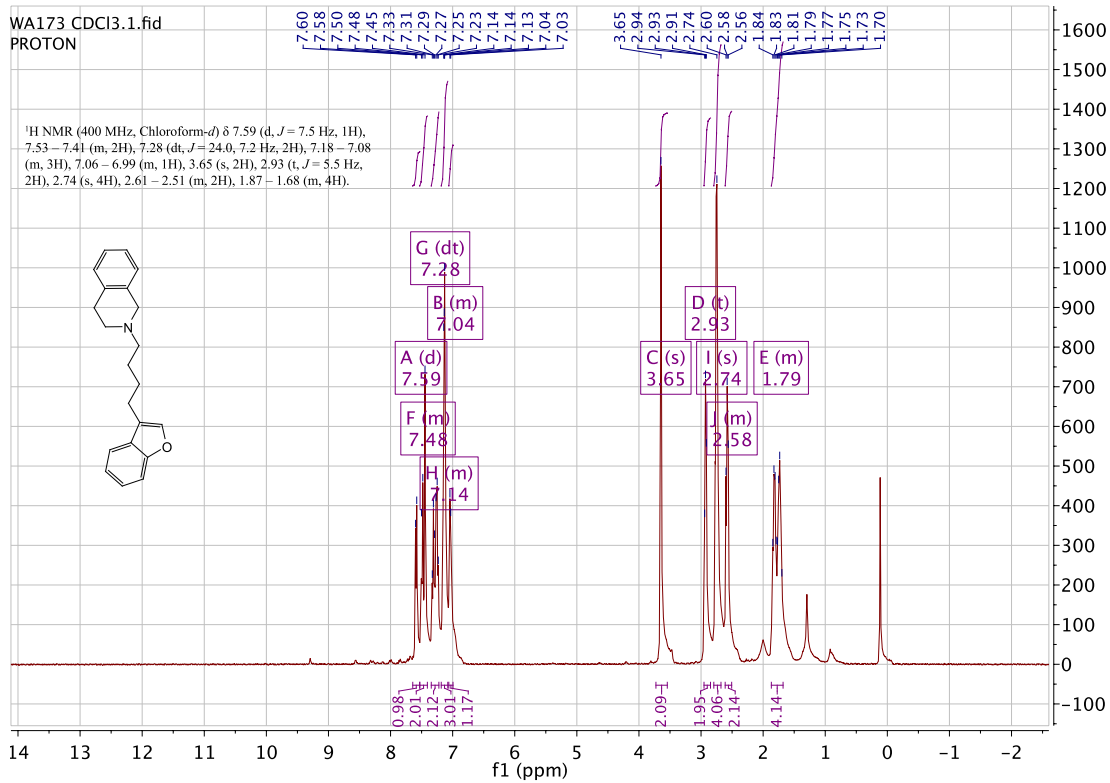
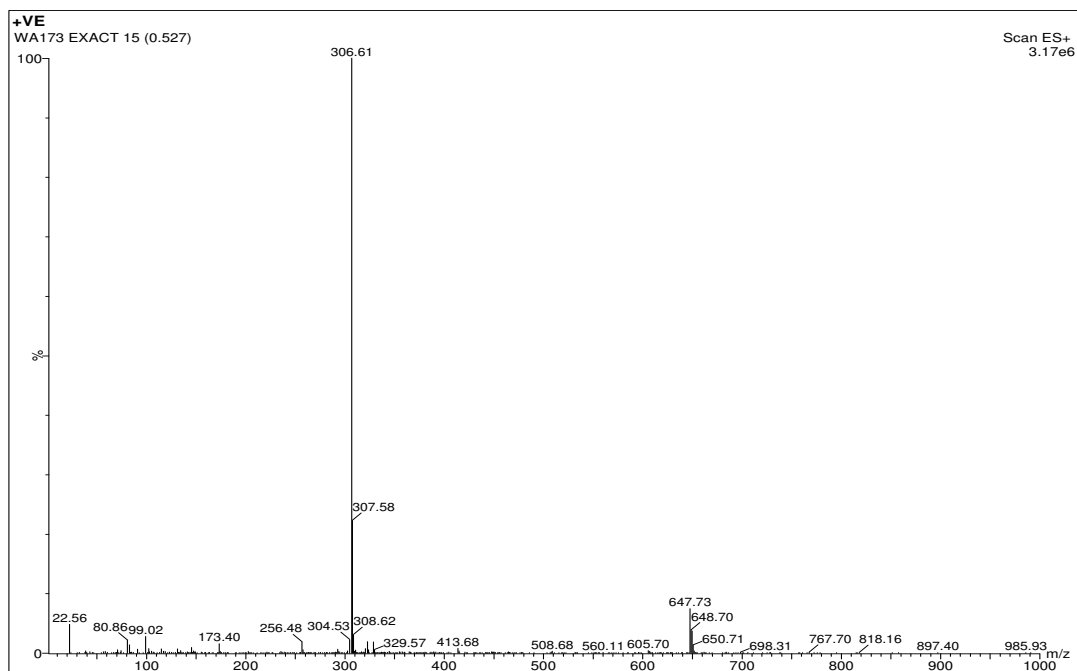
WA172 DMSO.13.fid
CARBON

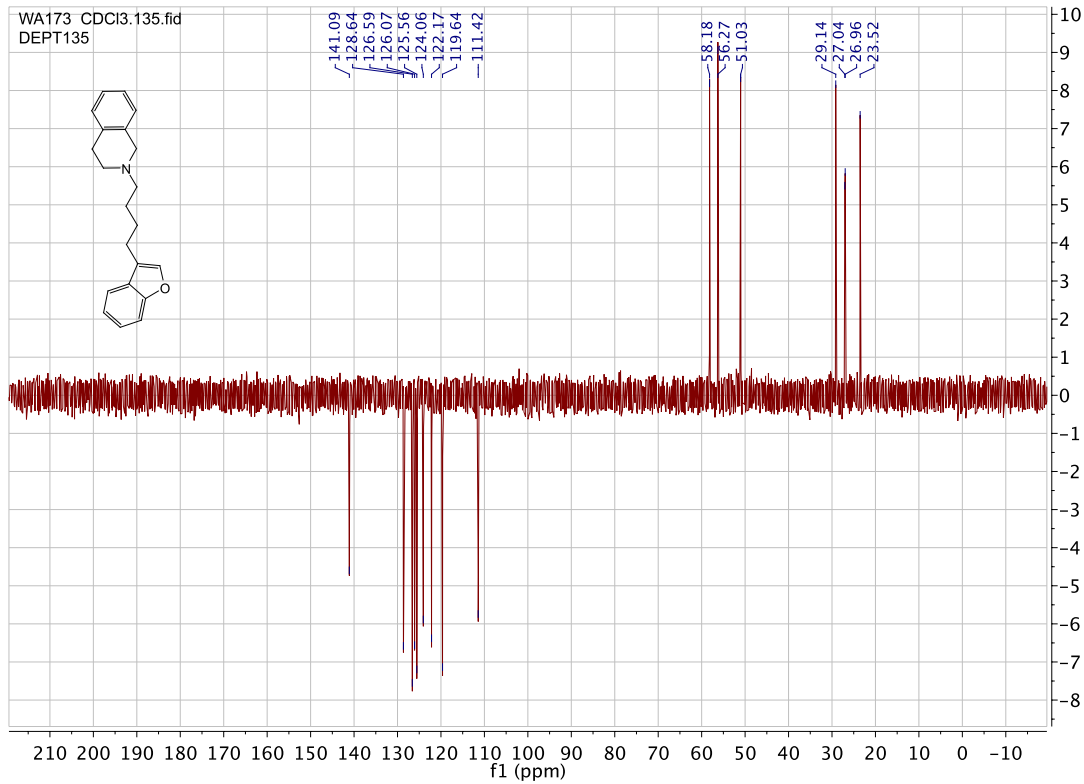
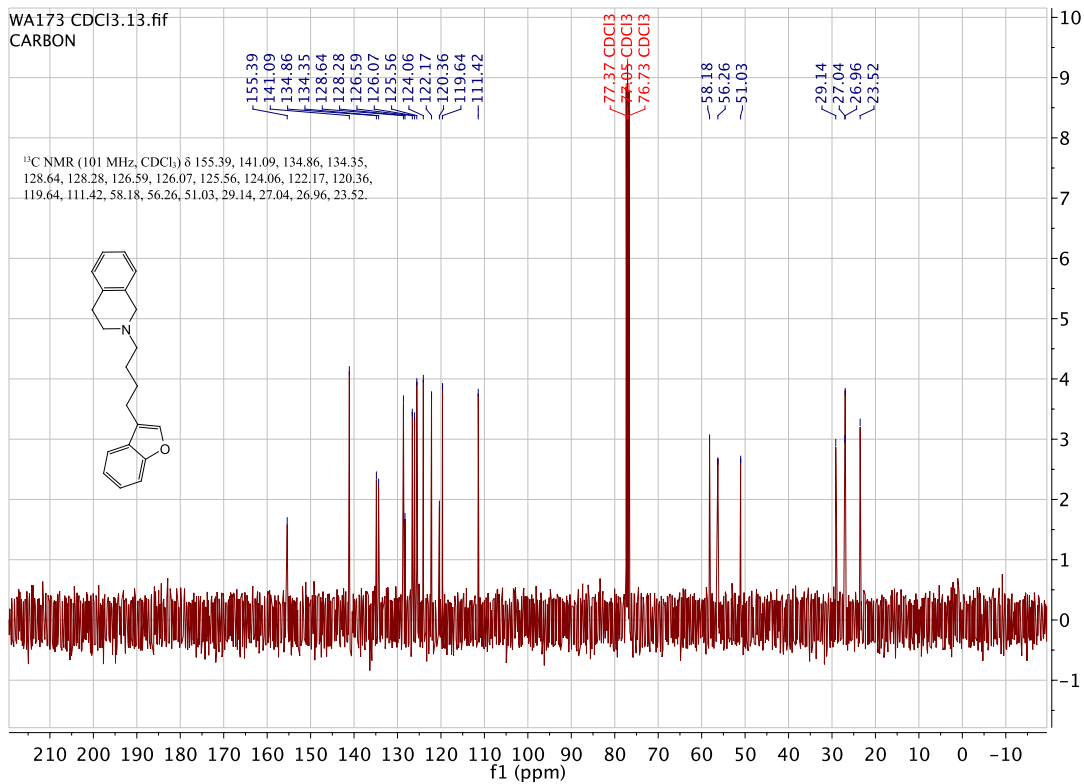


WA172 DMSO.135.fid
DEPT135

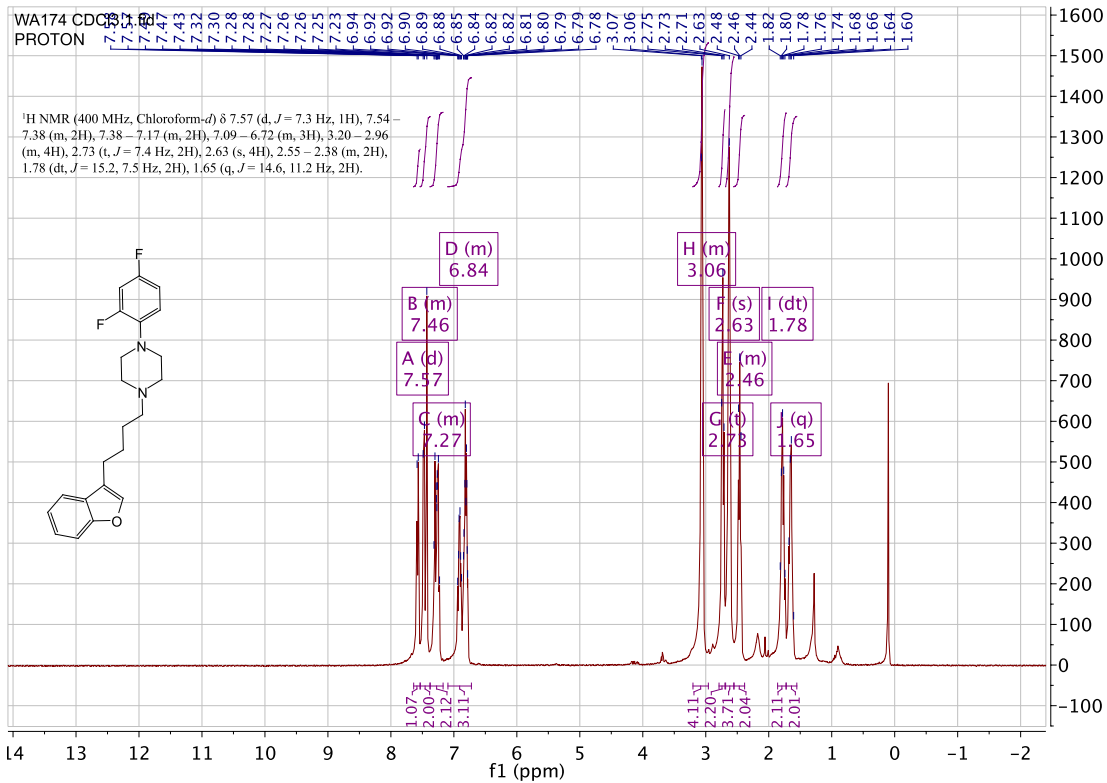
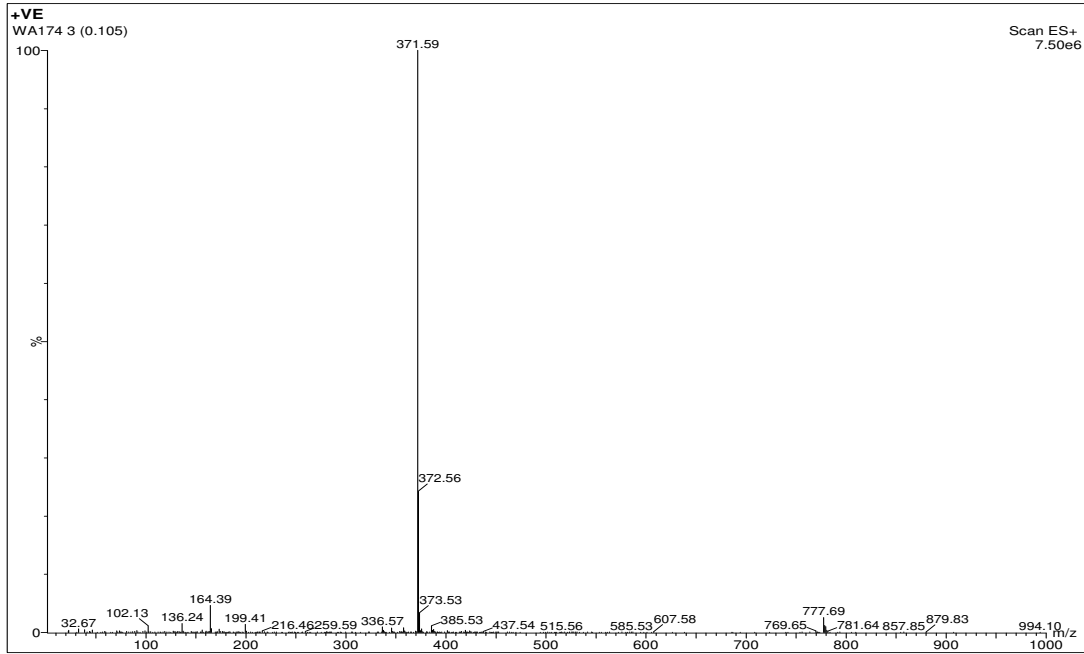


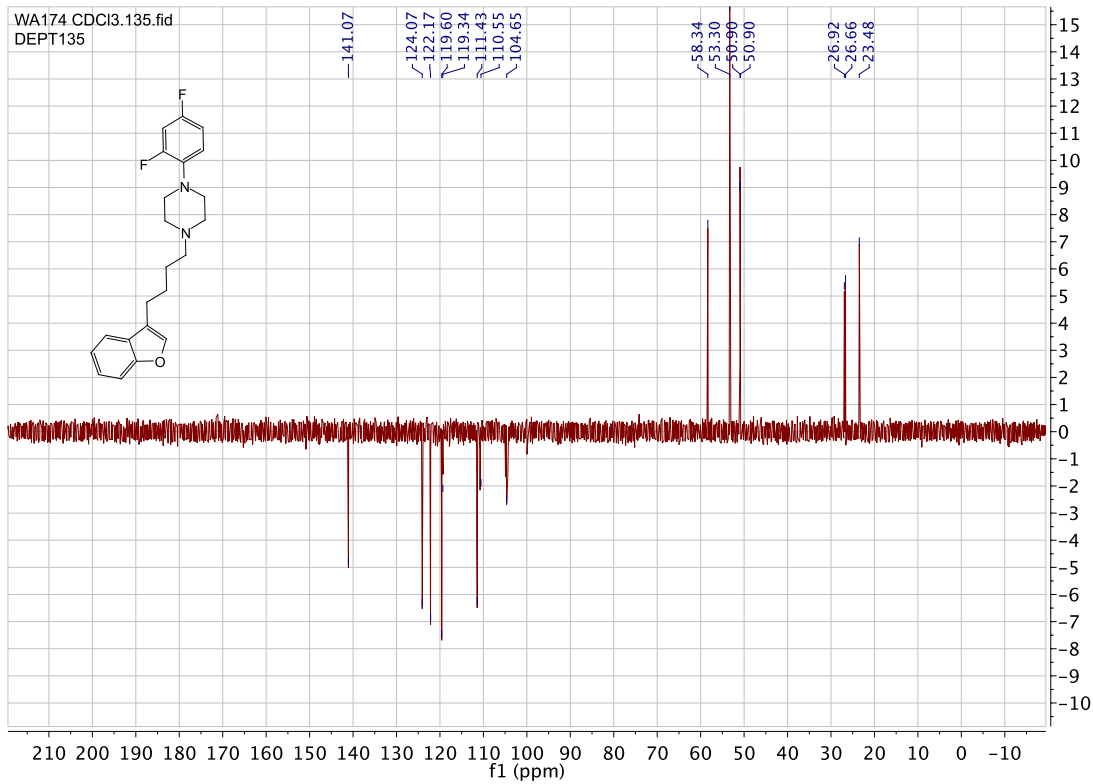
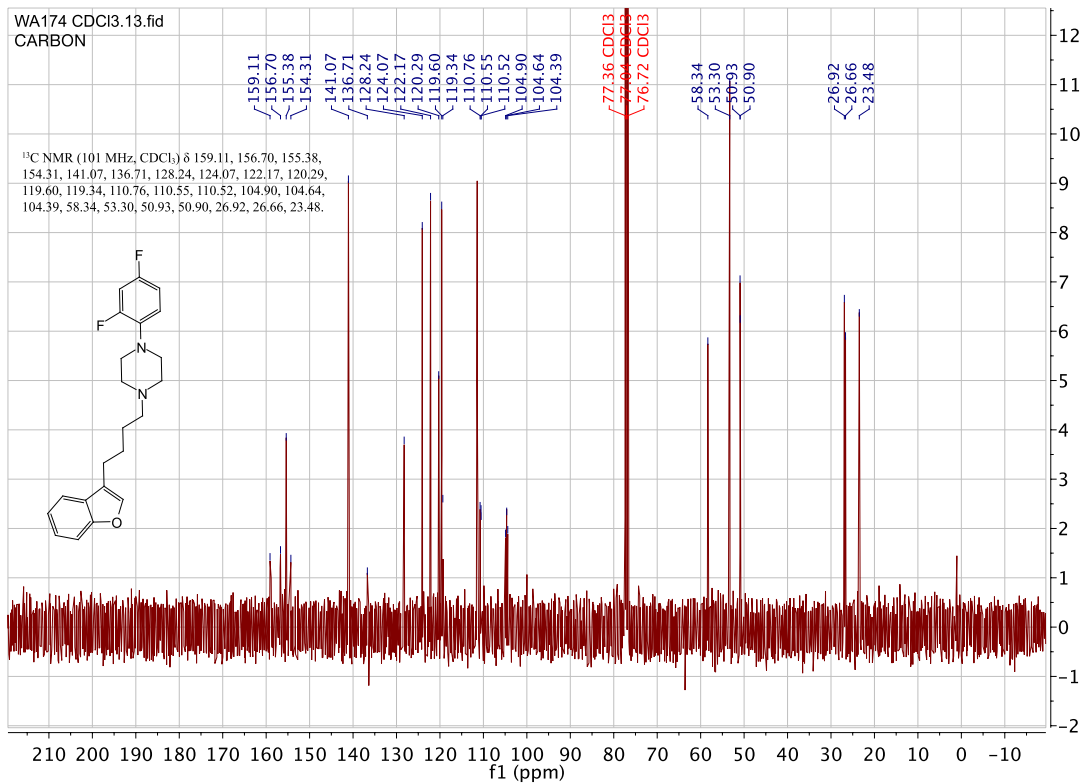
2-(4-(benzofuran-3-yl)butyl)-1,2,3,4-tetrahydroisoquinoline. (WA173)



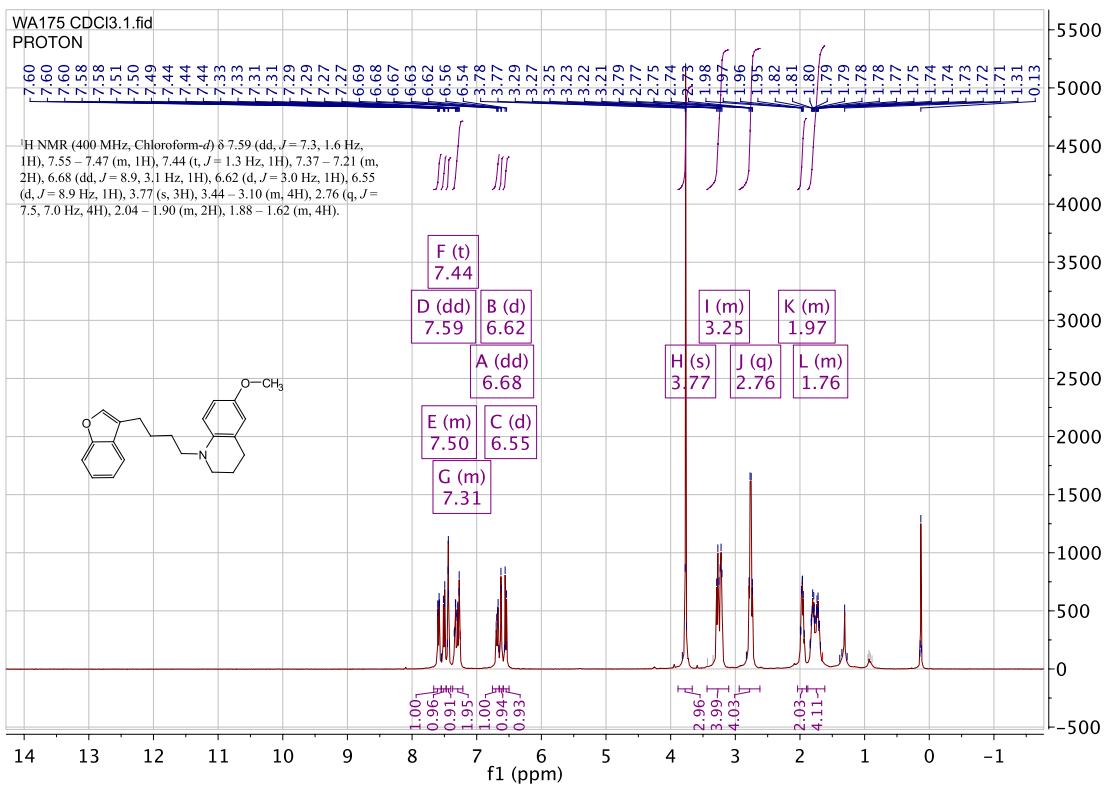
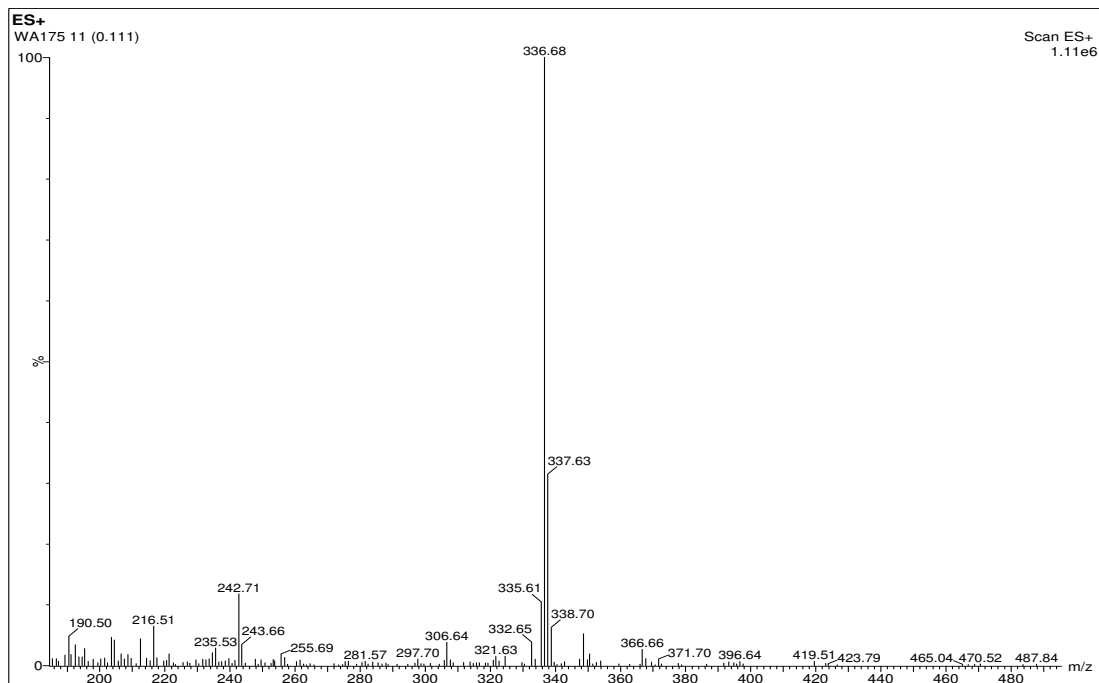


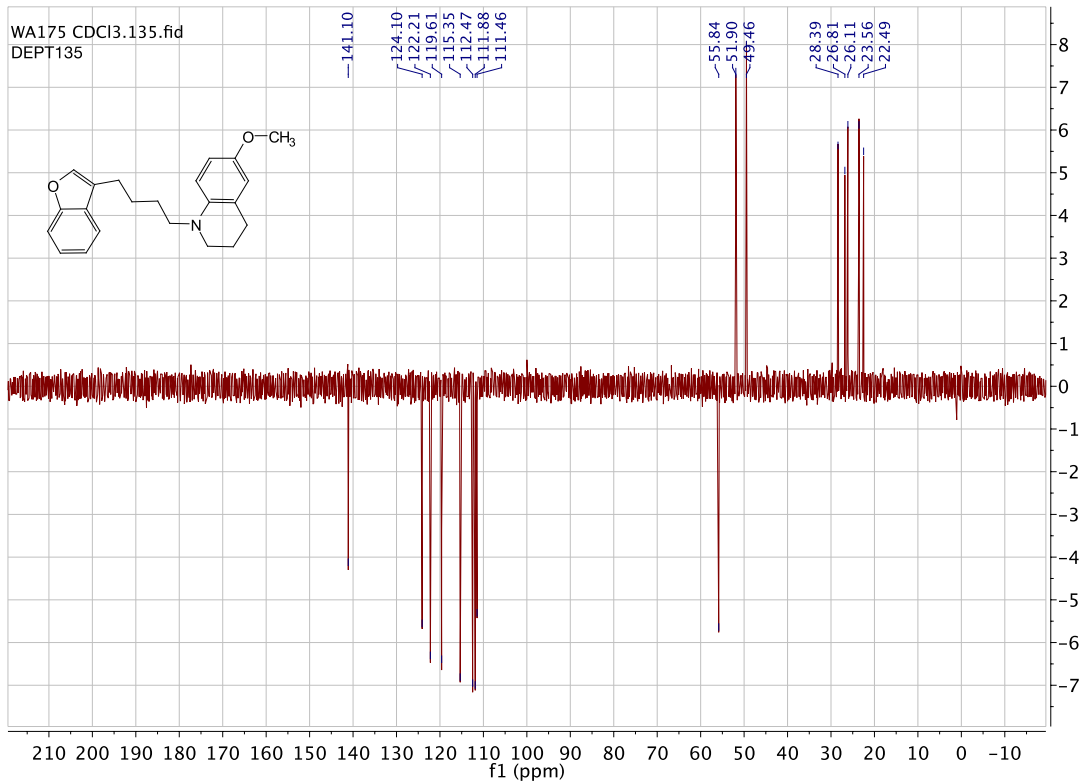
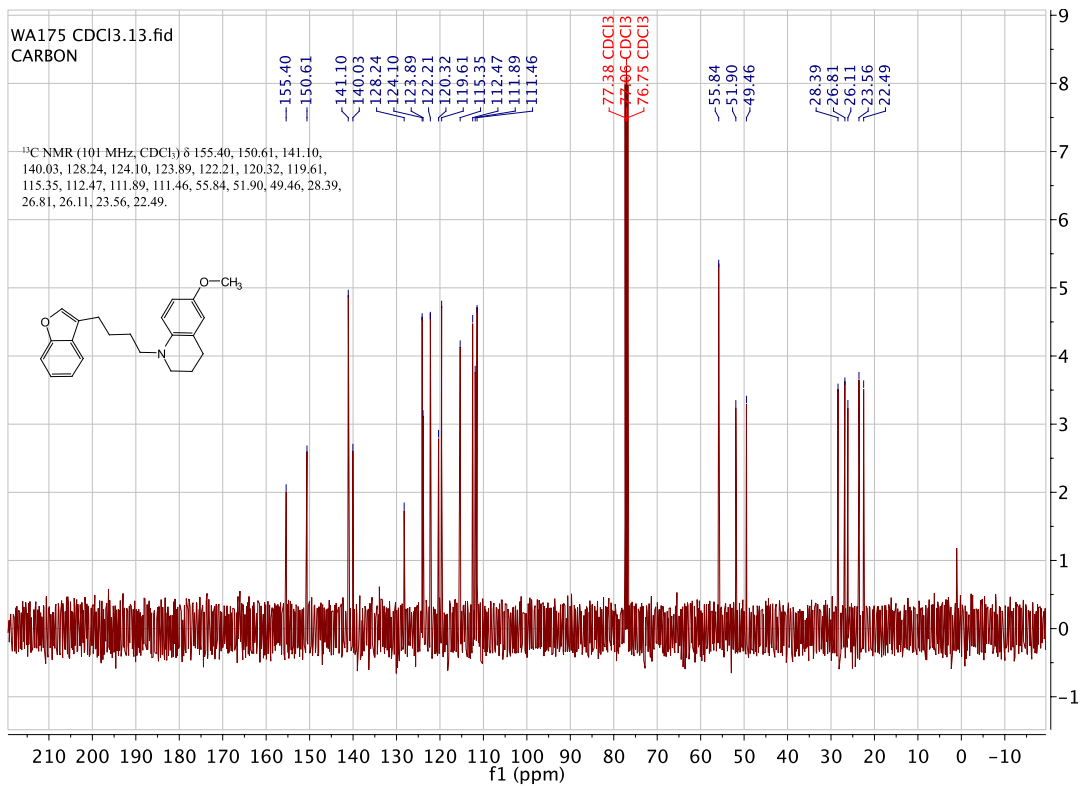
1-(4-(benzofuran-3-yl)butyl)-4-(2,4-difluorophenyl)piperazine. (WA174)



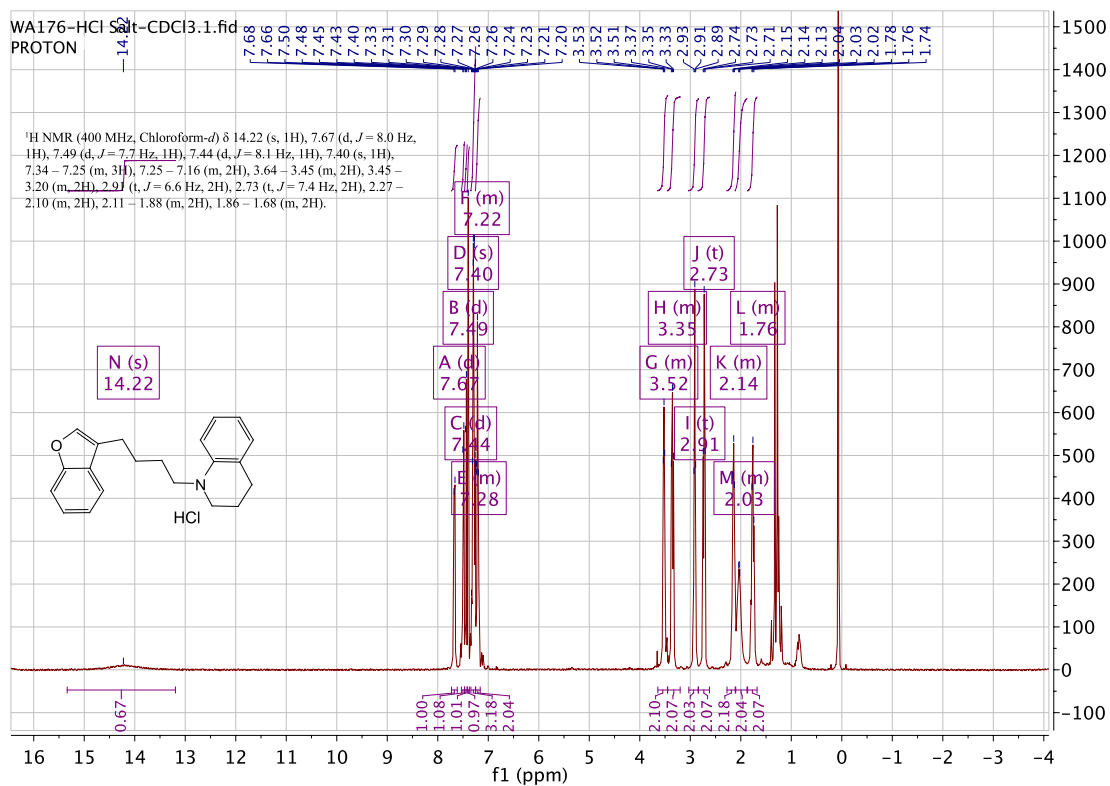
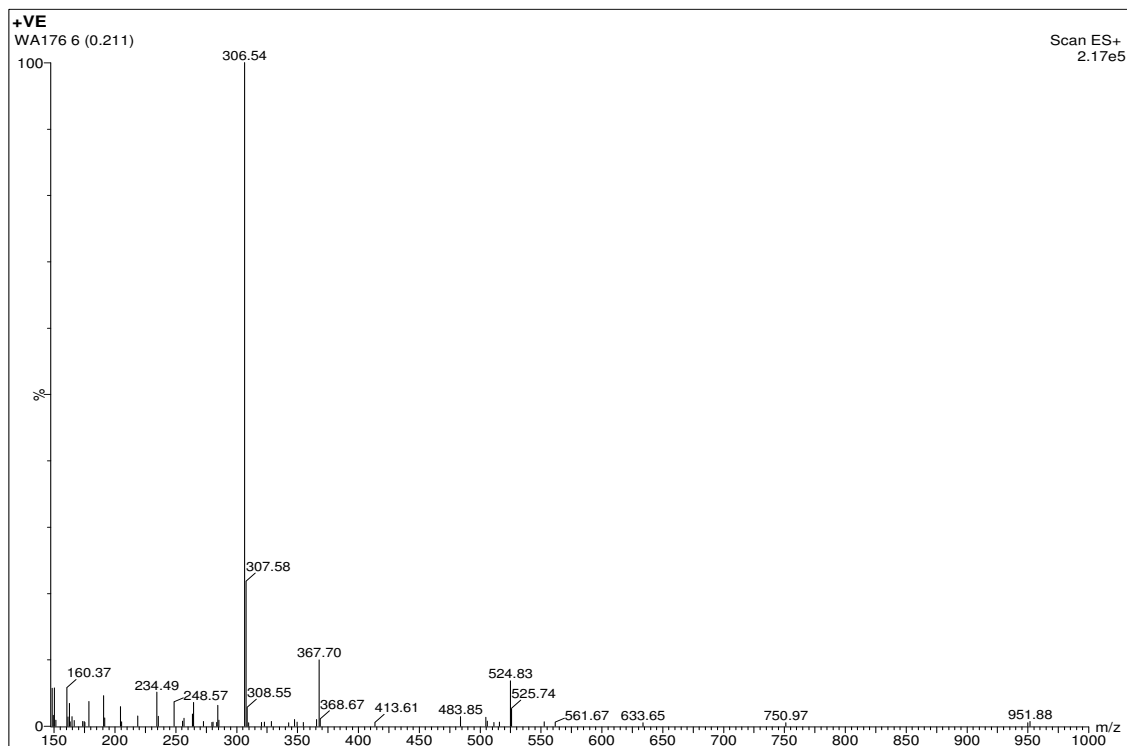


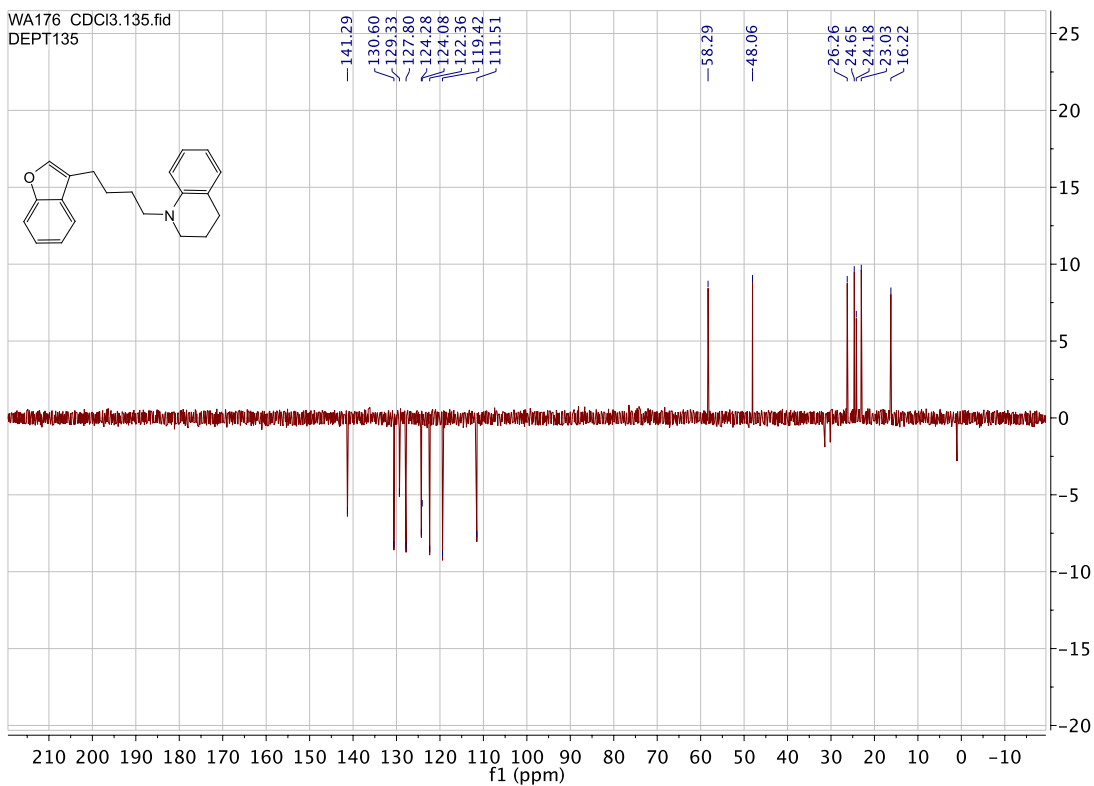
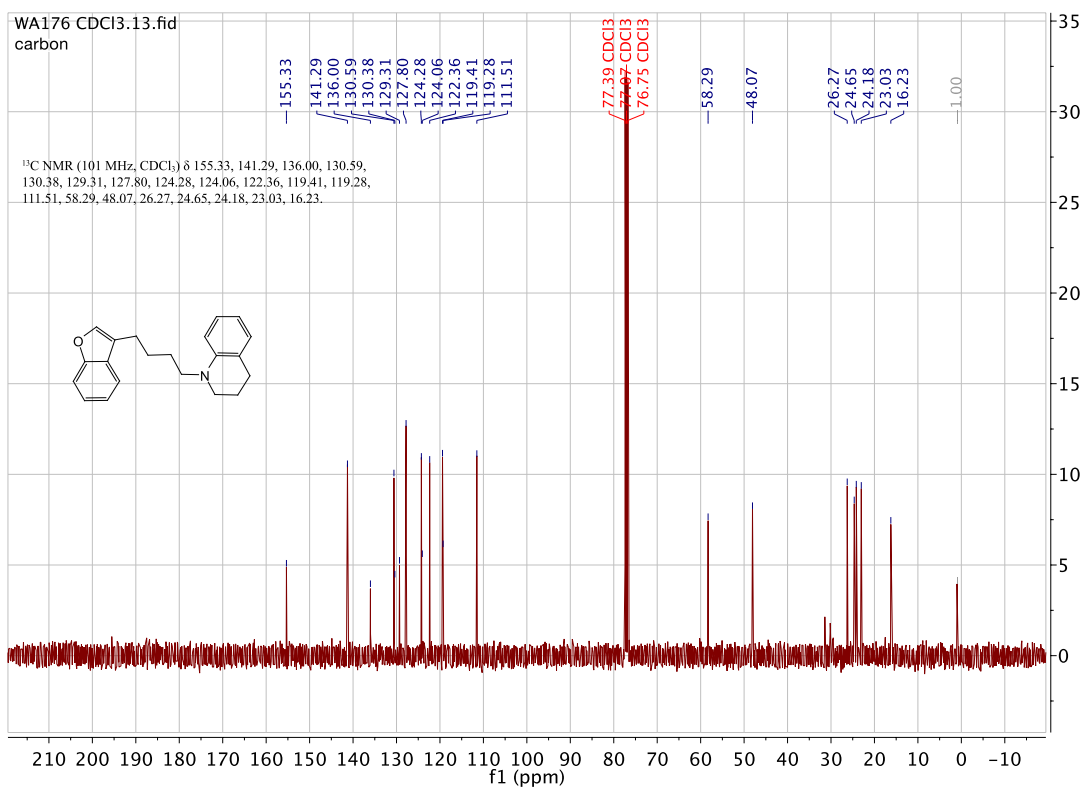
1-(4-(benzofuran-3-yl)butyl)-6-methoxy-1,2,3,4-tetrahydroquinoline. (WA175)



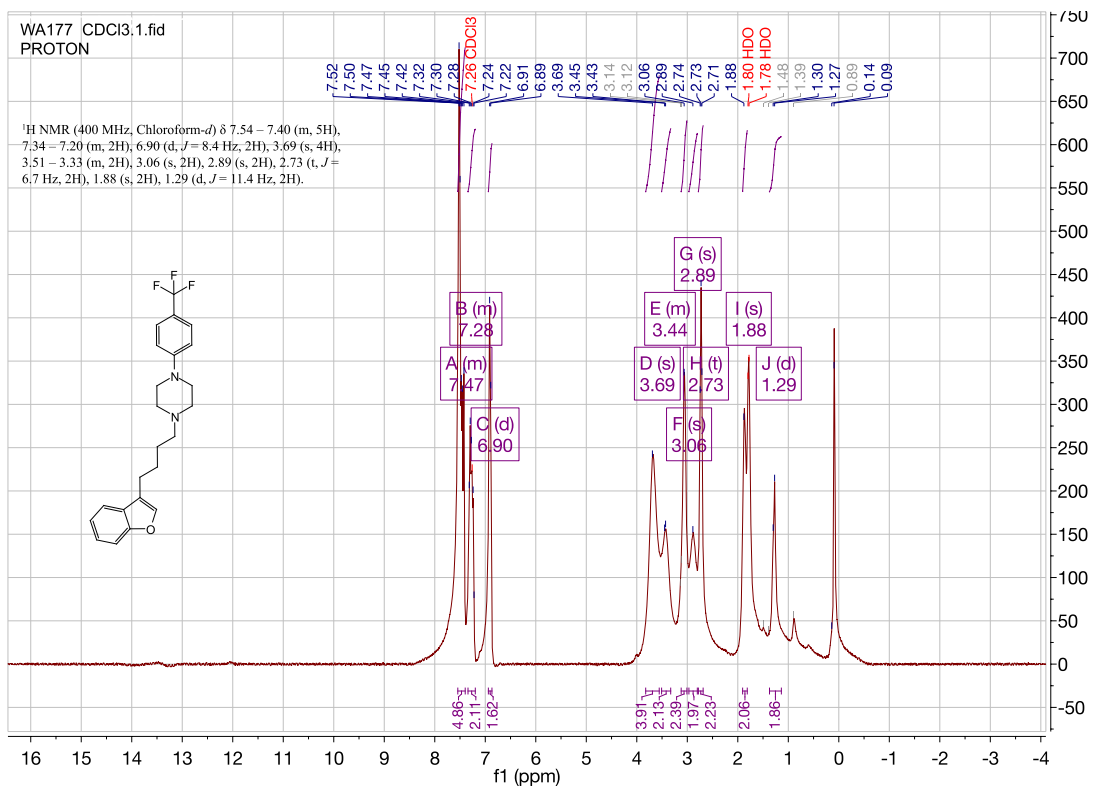
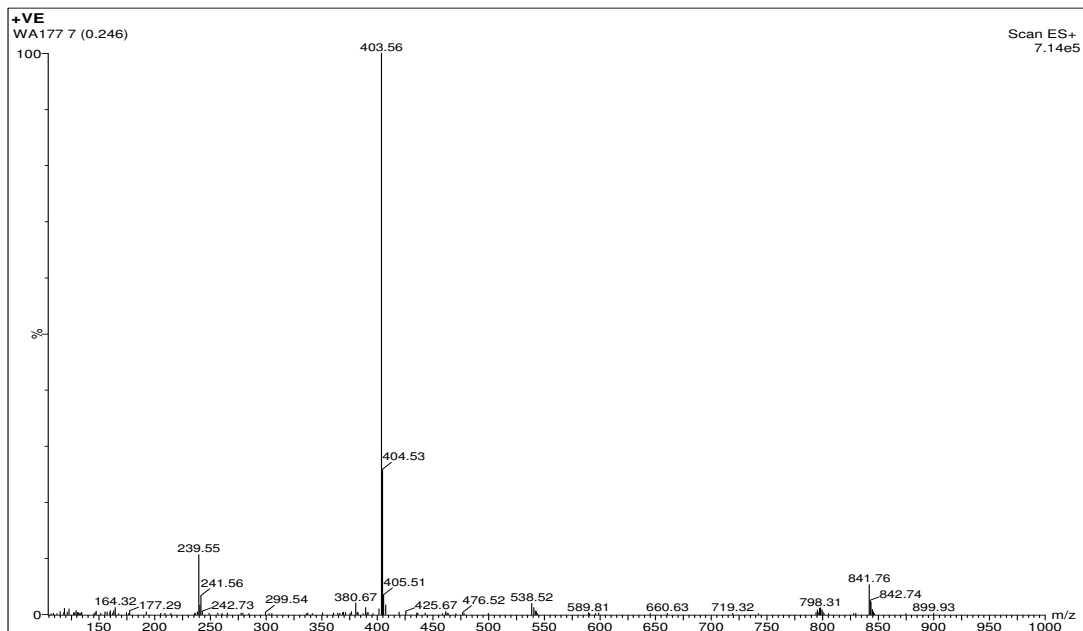


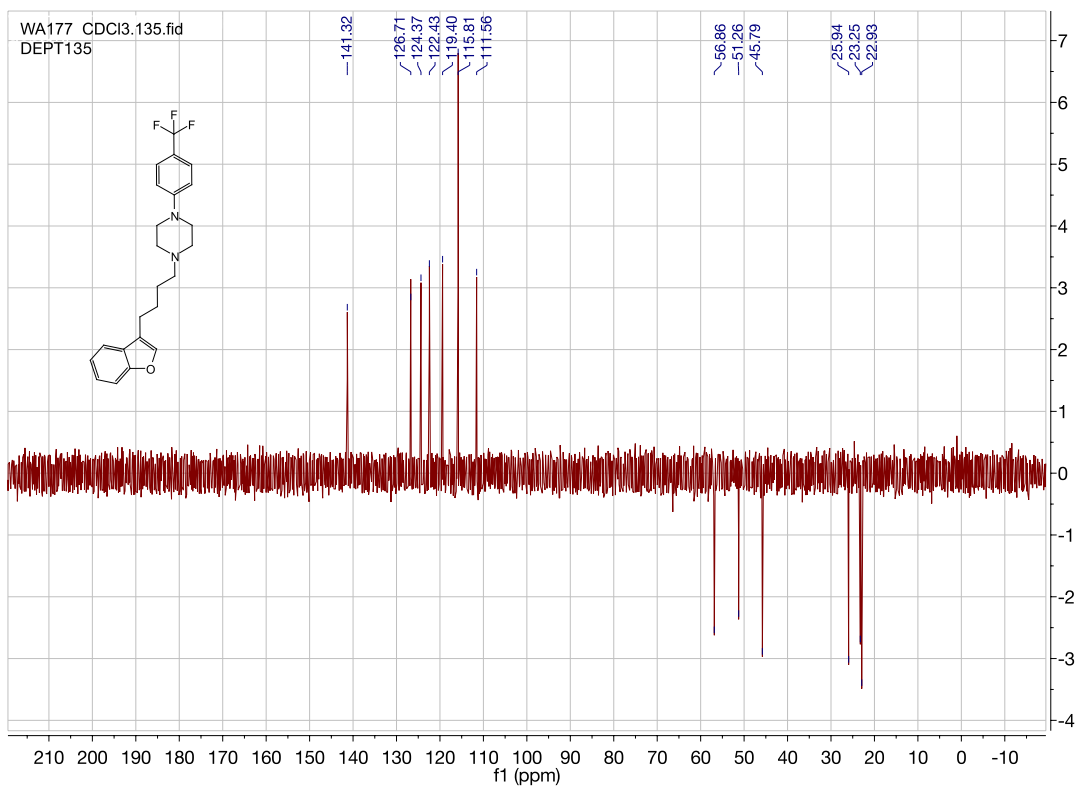
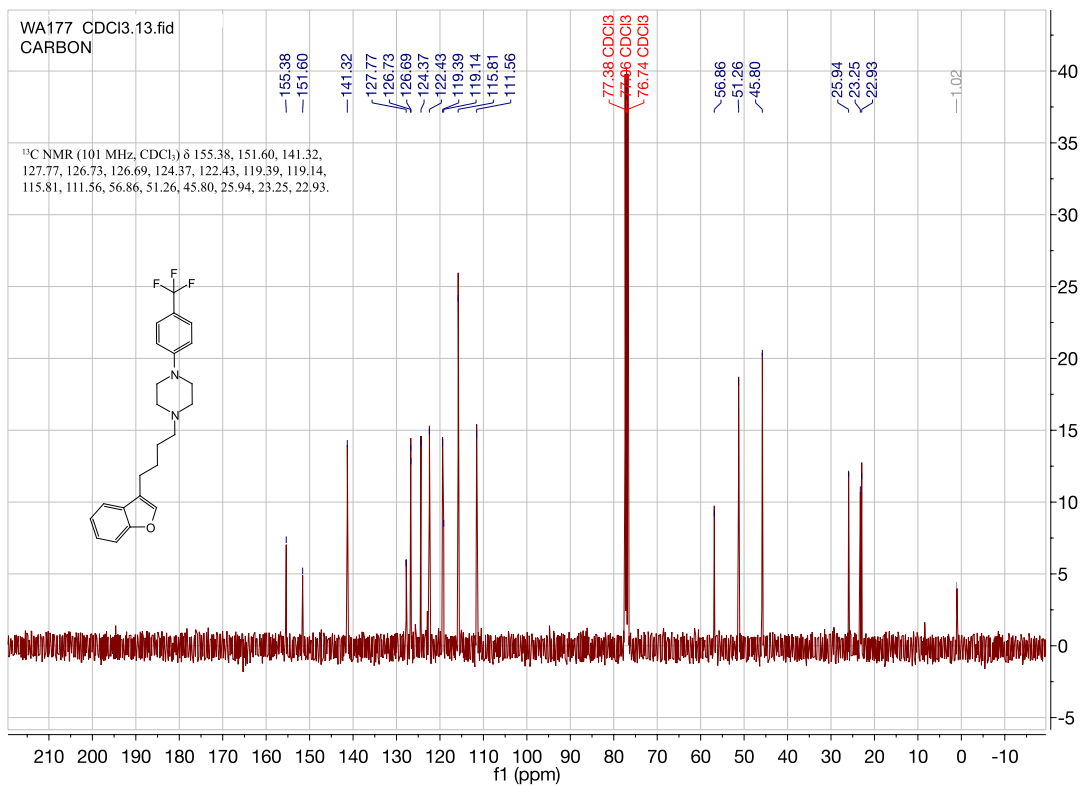
1-(4-(benzofuran-3-yl)butyl)-1,2,3,4-tetrahydroquinoline. (WA176)



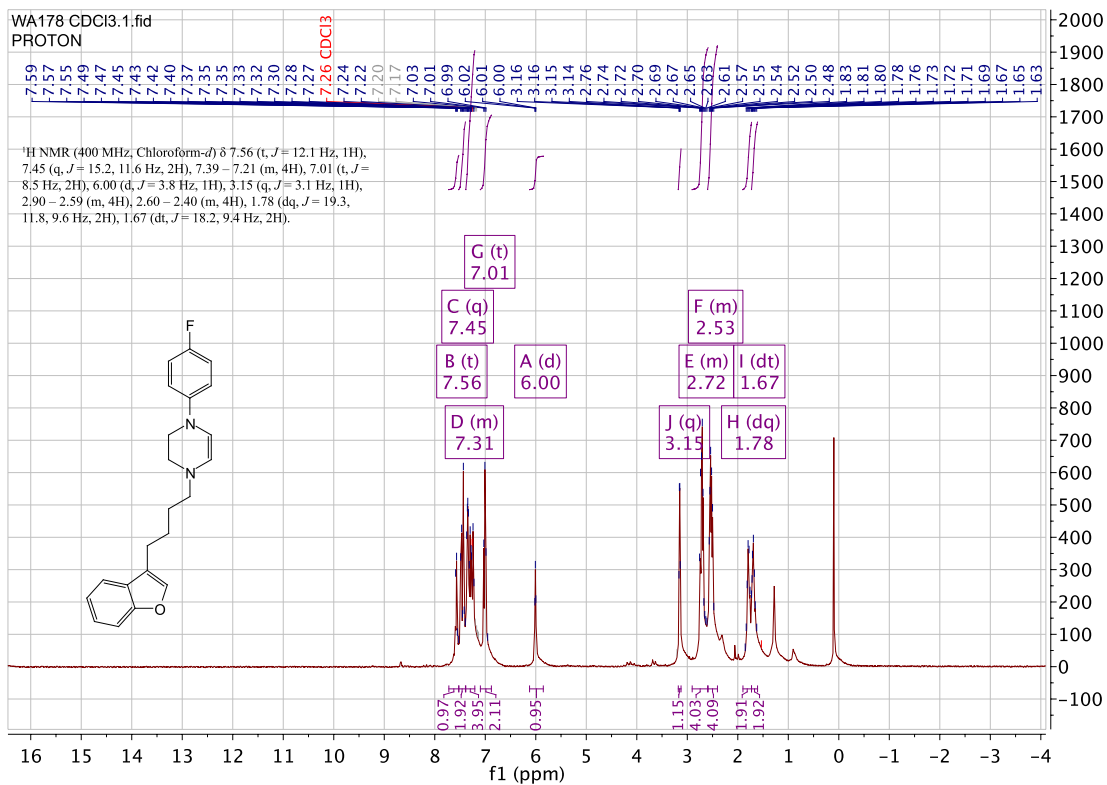
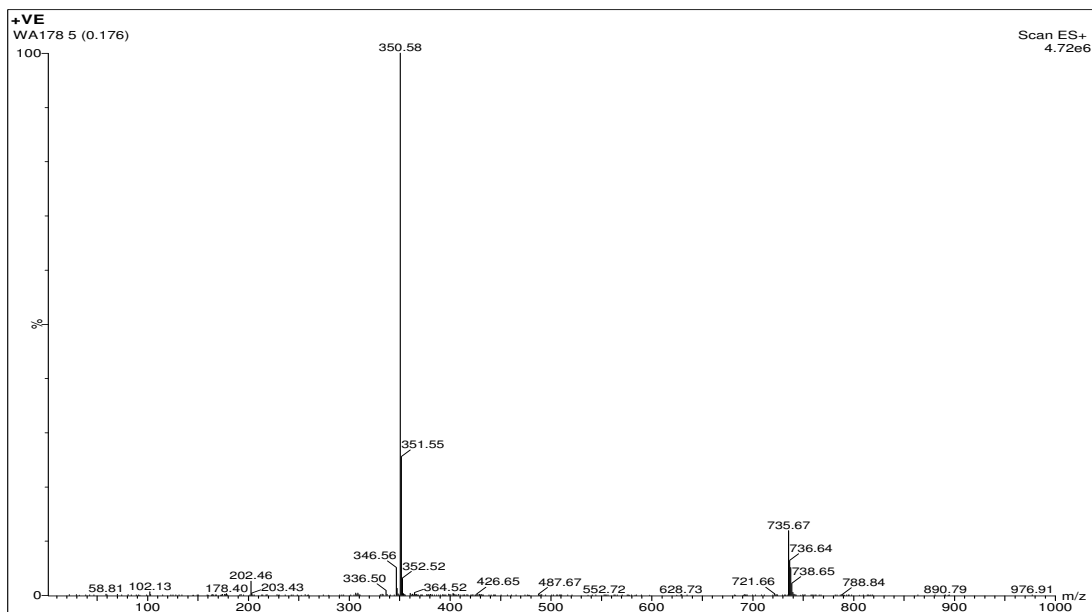


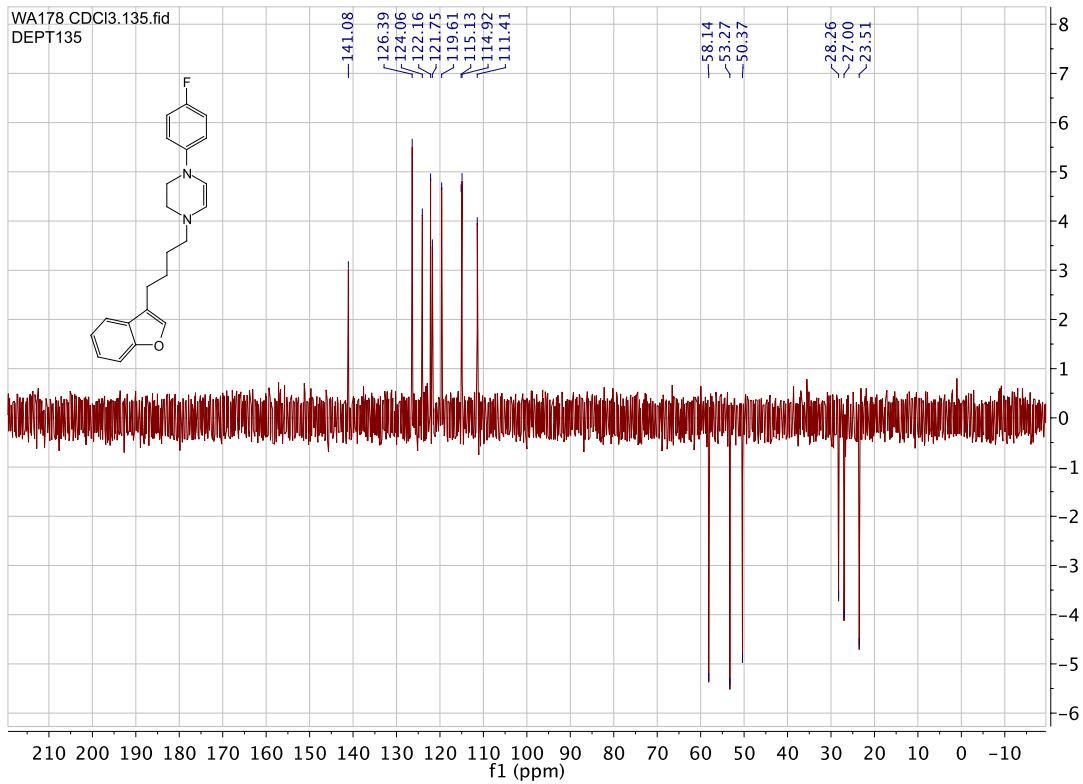
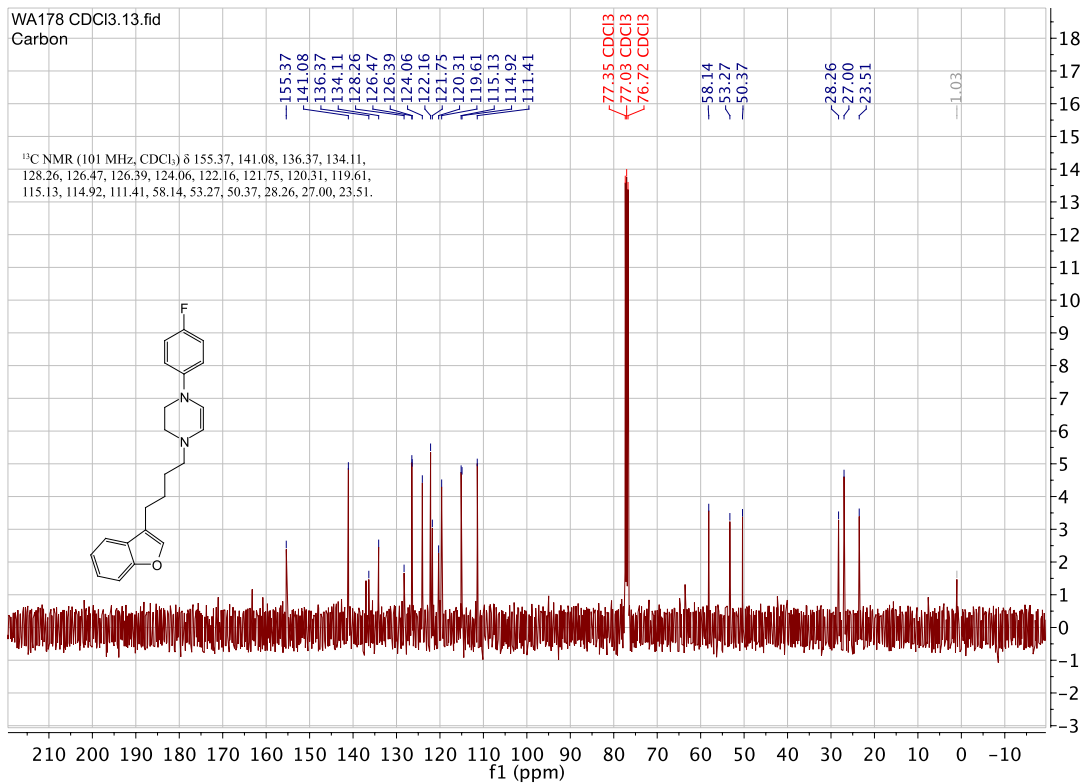
1-(4-(benzofuran-3-yl)butyl)-4-(4-(trifluoromethyl)phenyl)piperazine. (WA177)



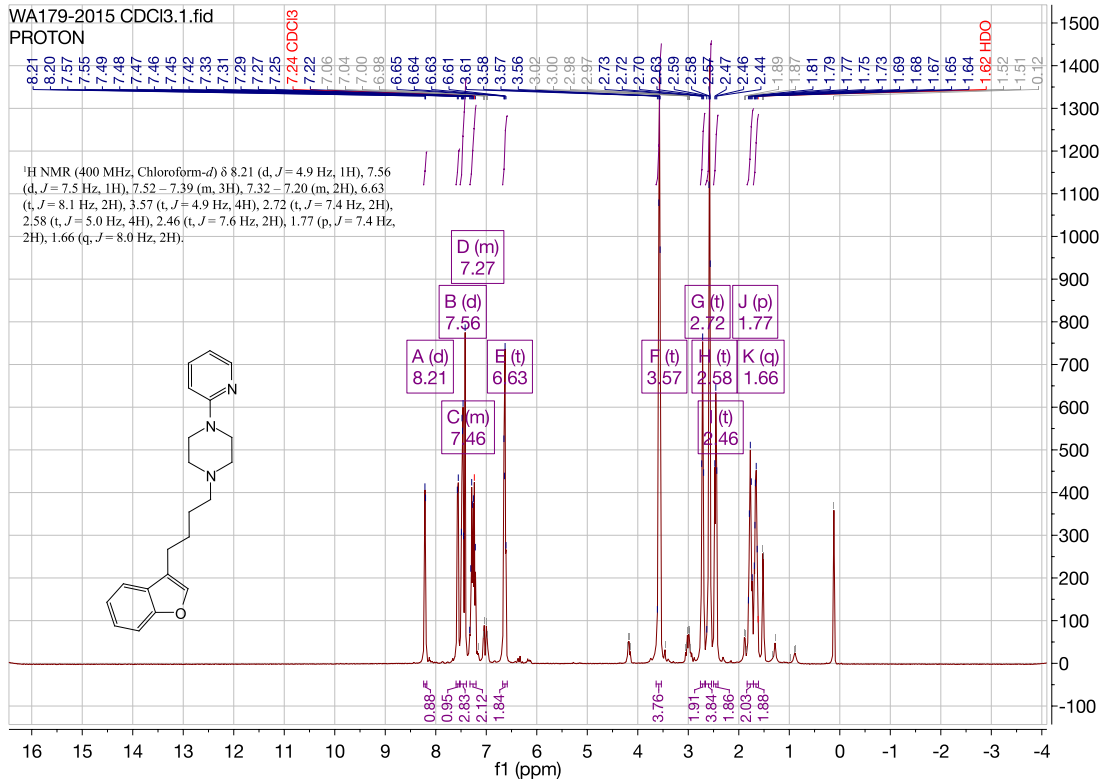
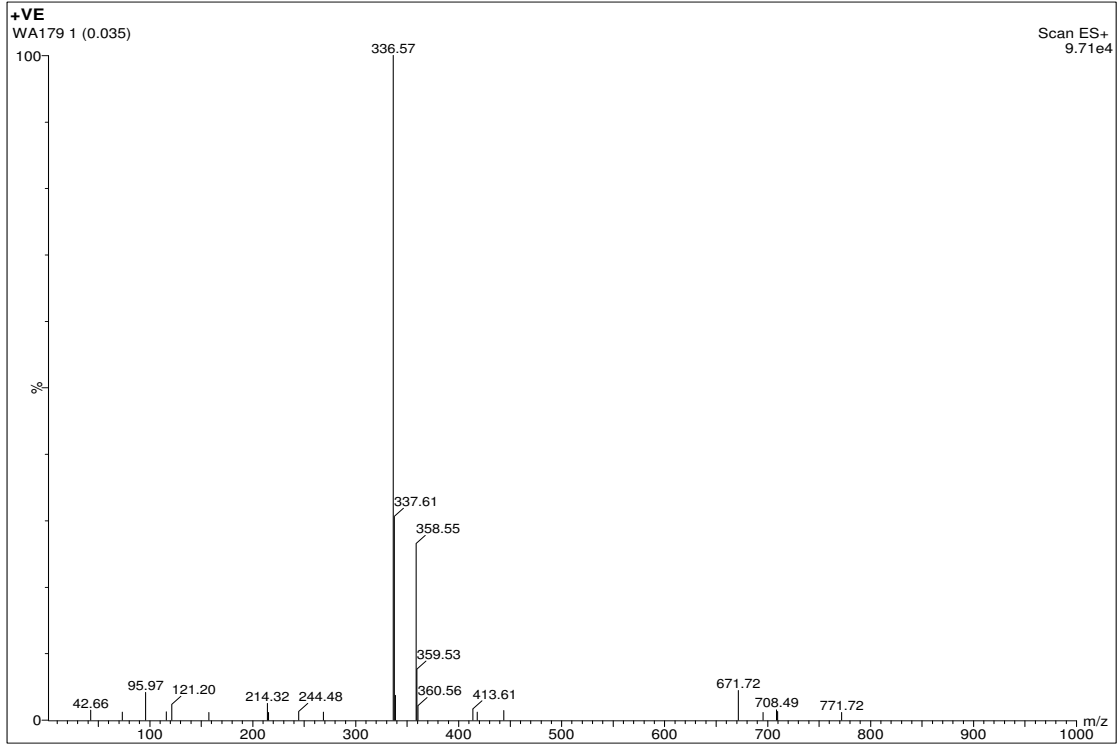


1-(4-(benzofuran-3-yl)butyl)-4-(4-fluorophenyl)-1,2,3,4-tetrahydropyrazine. (WA178)

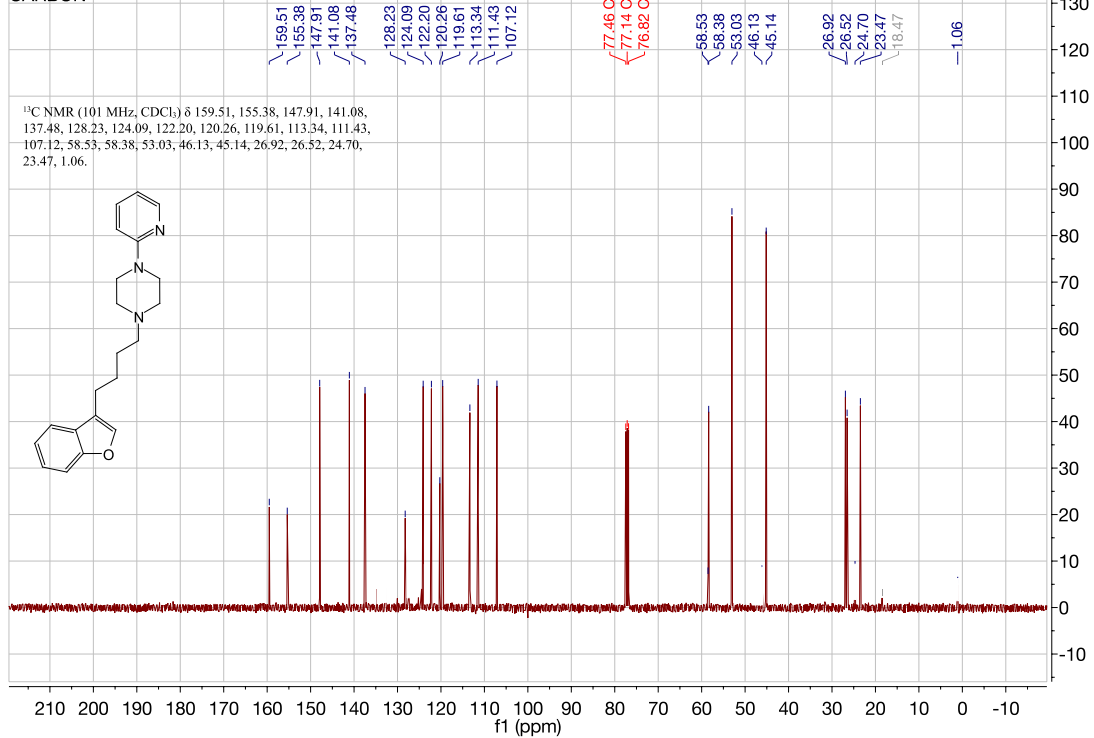




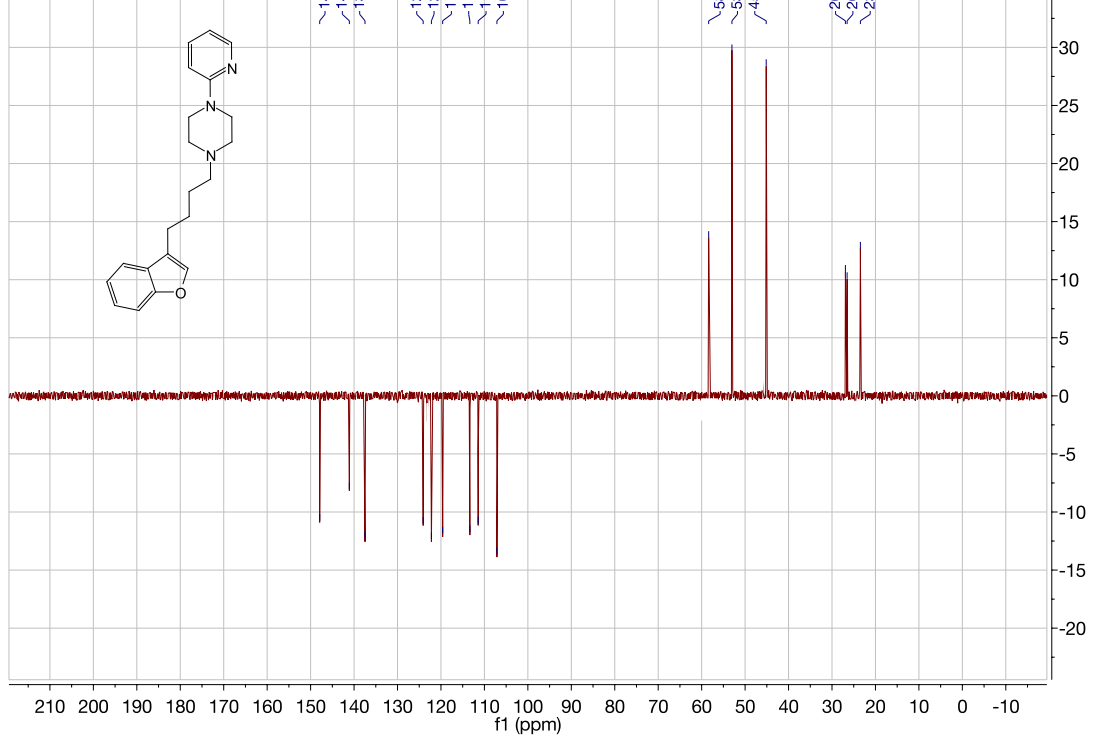
1-(4-(benzofuran-3-yl)butyl)-4-(pyridin-2-yl)piperazine. (WA179)



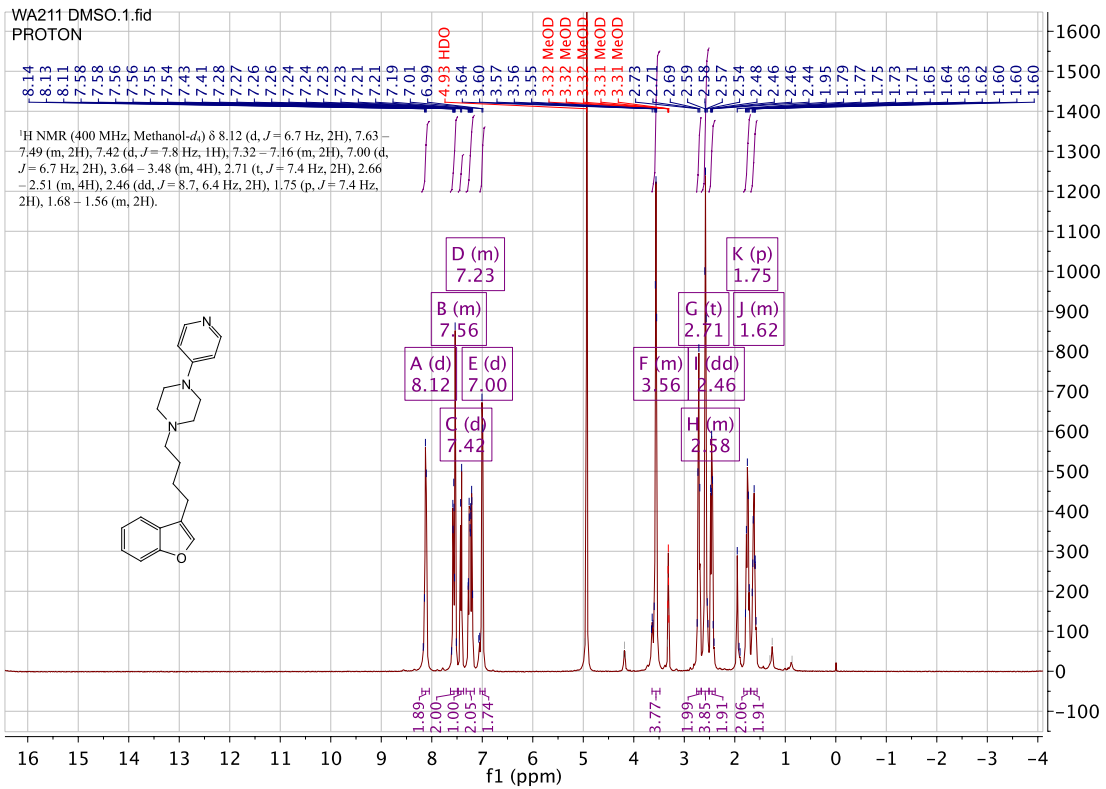
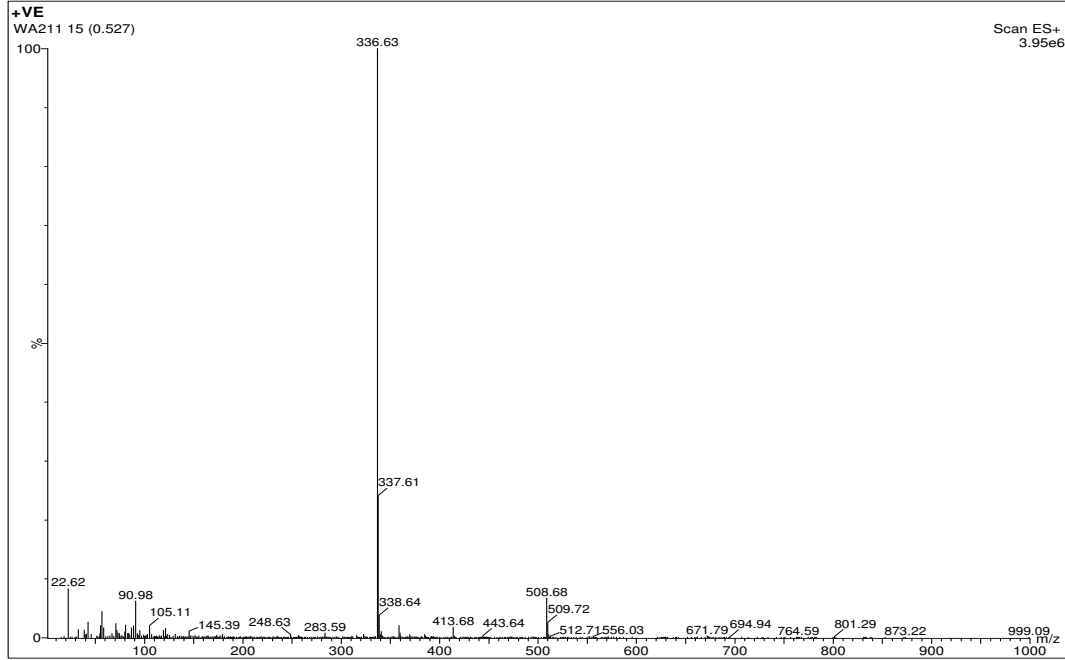
WA179-2015 CDCl3.13.fid
CARBON

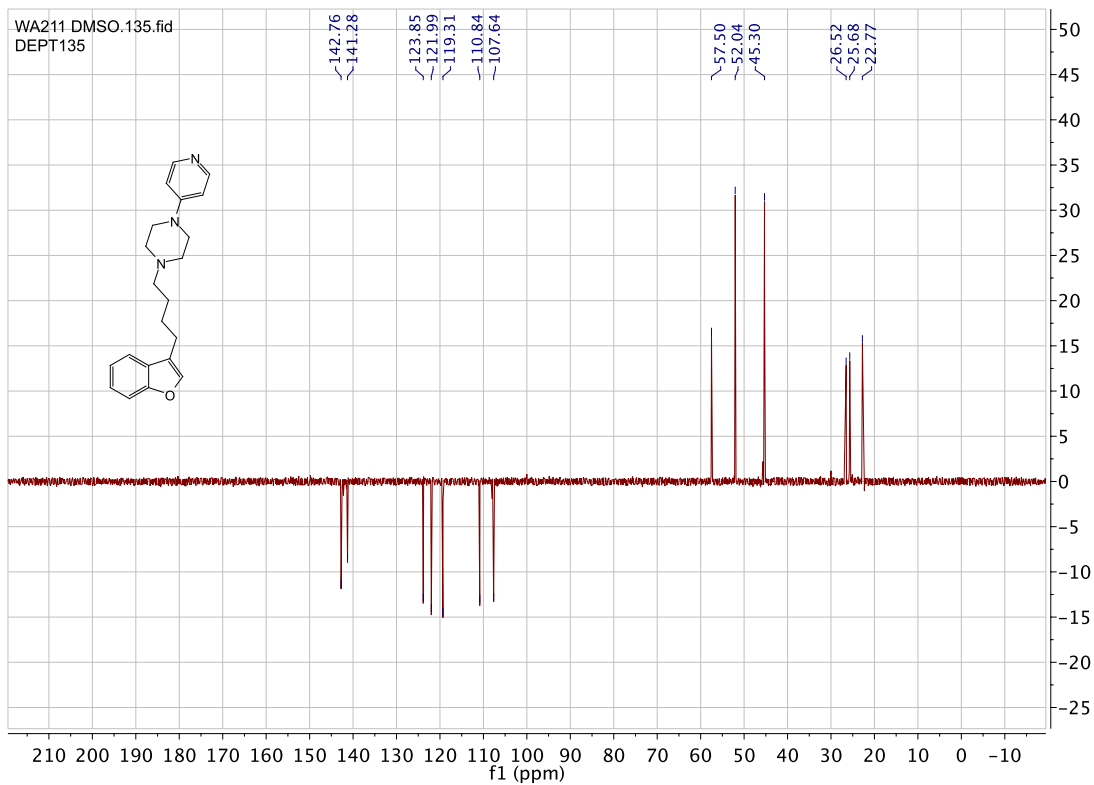
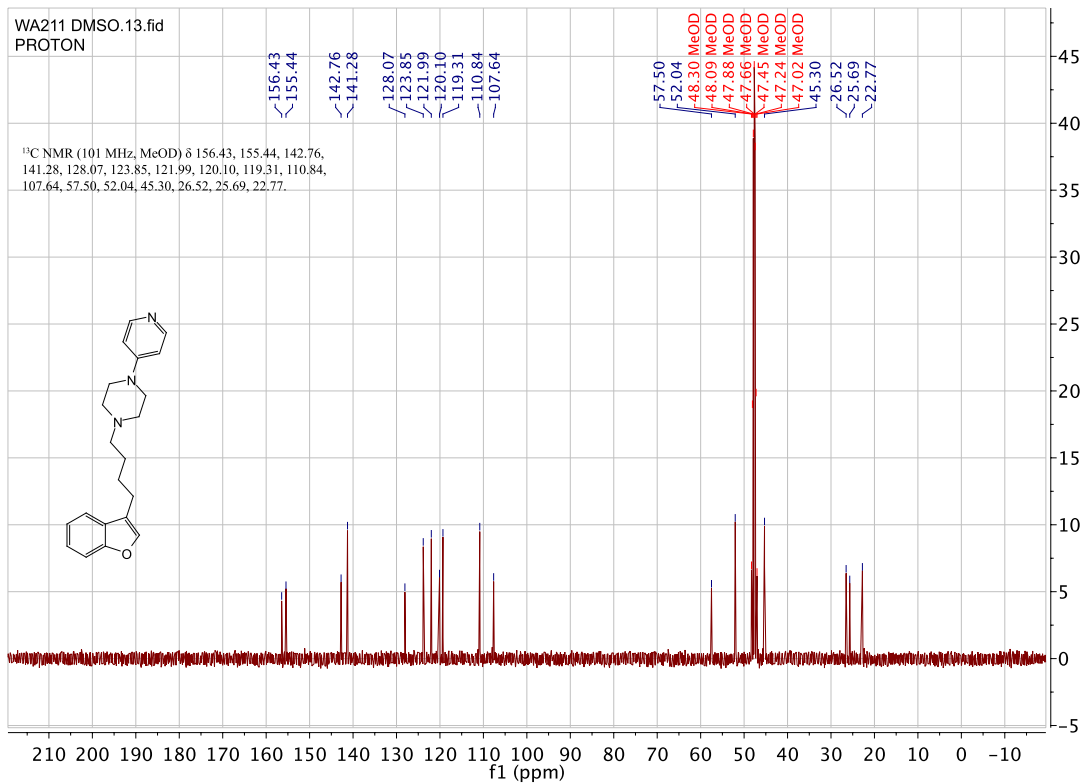


WA179-2015 CDCl3.135.fid
DEPT135

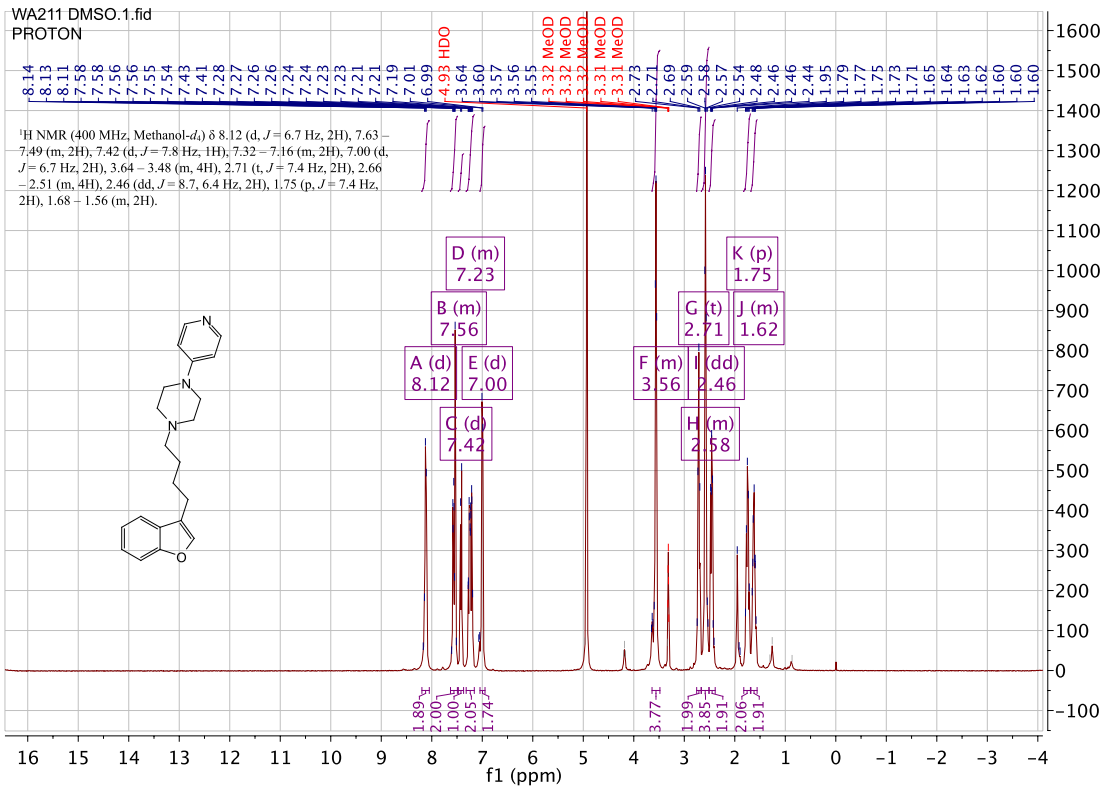
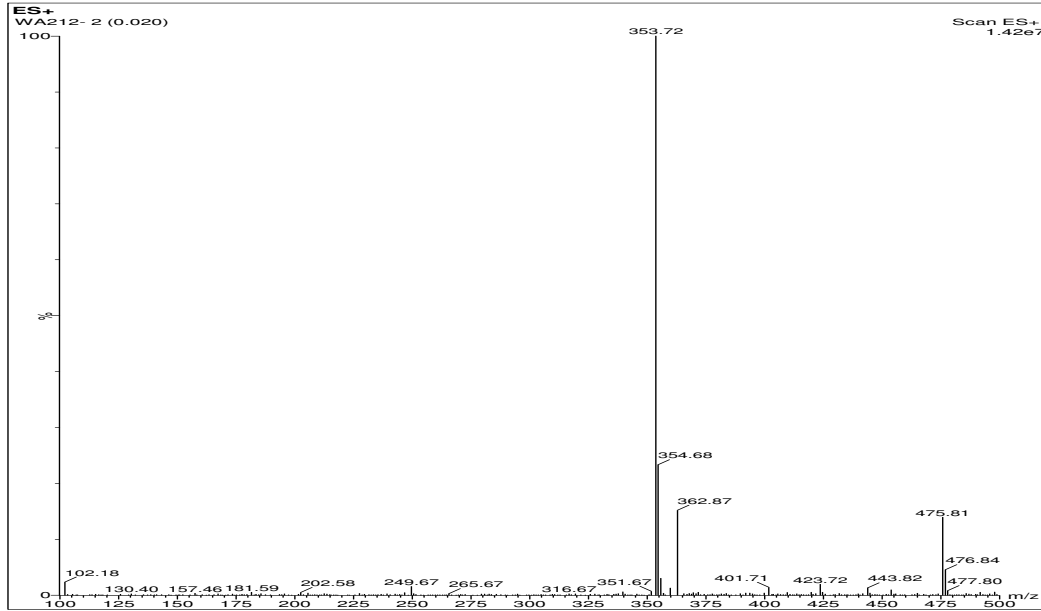


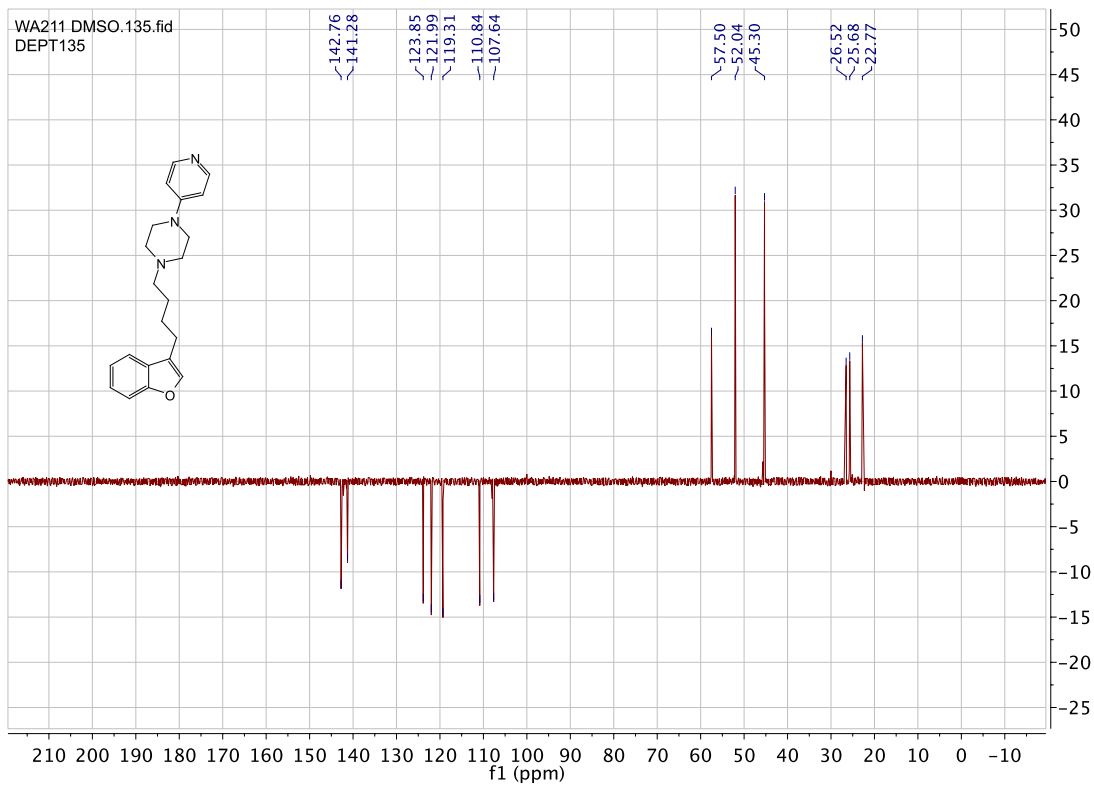
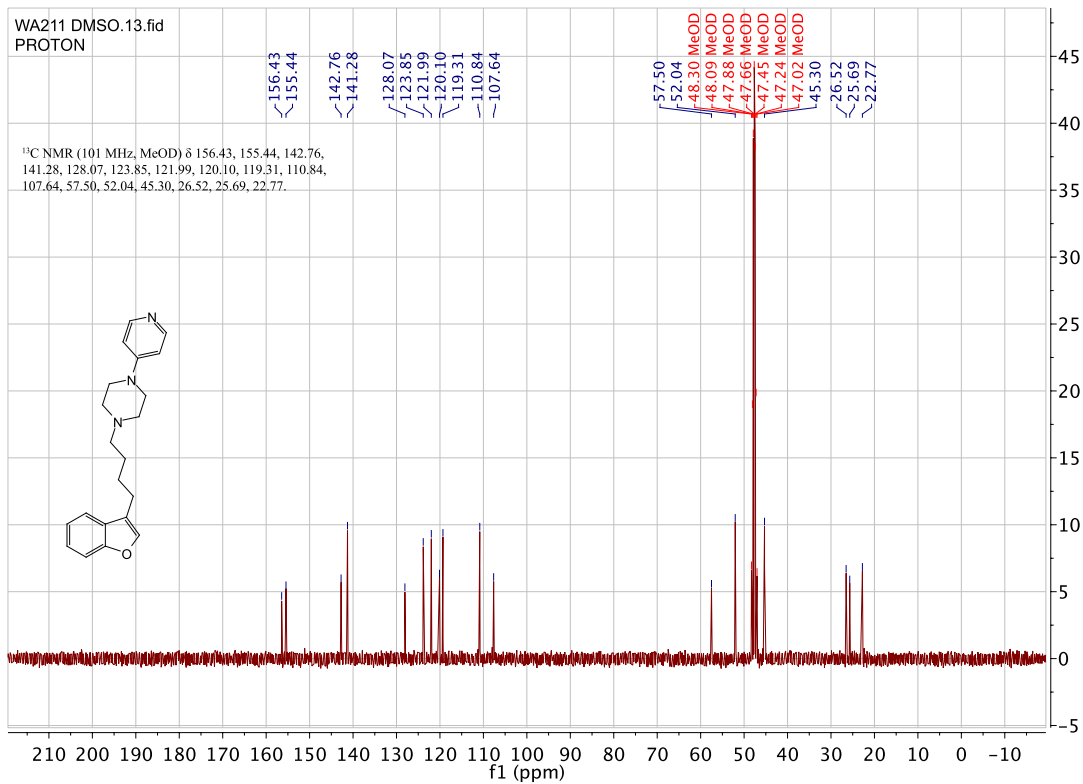
1-(4-(benzofuran-3-yl)butyl)-4-(pyridin-4-yl)piperazine. (WA211)



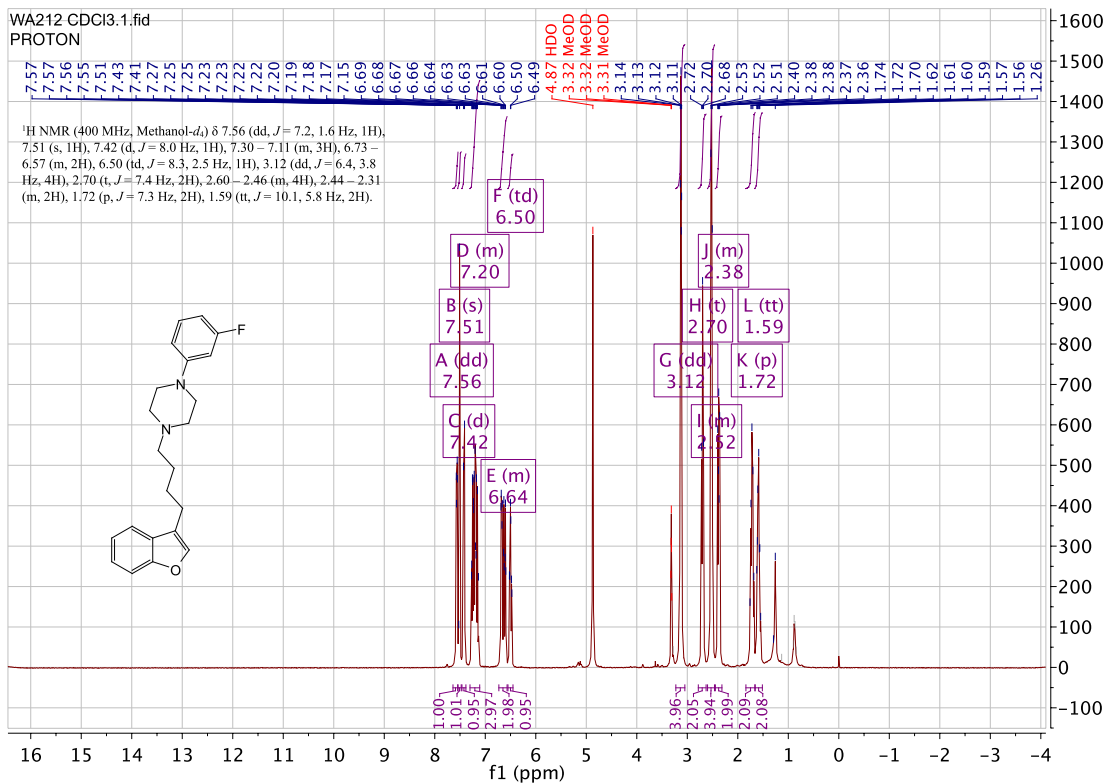
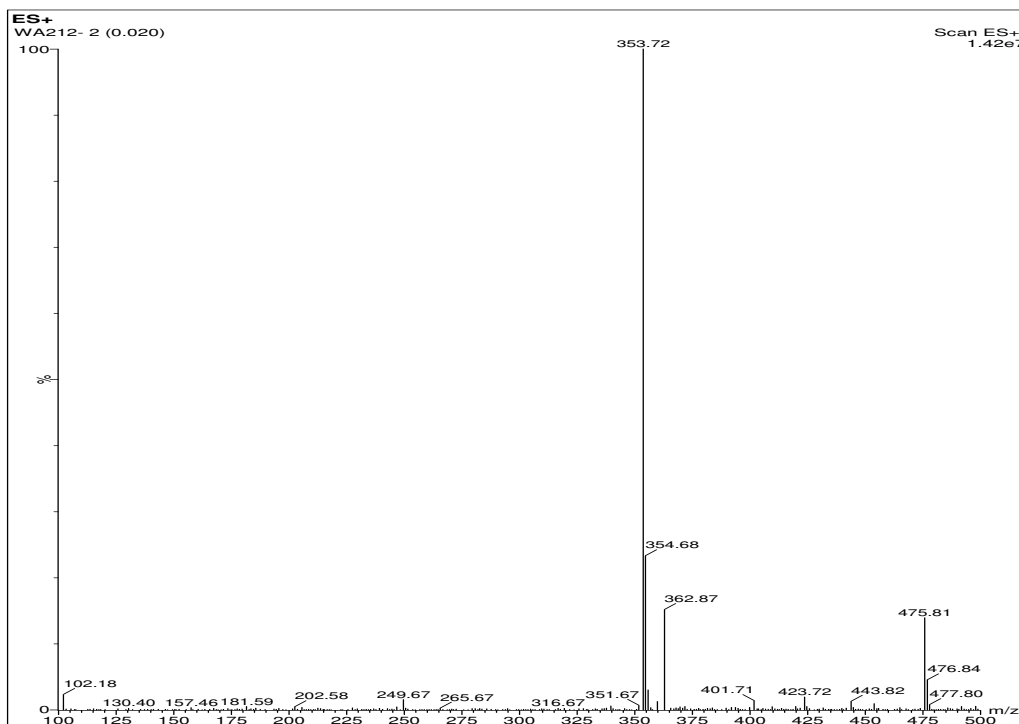


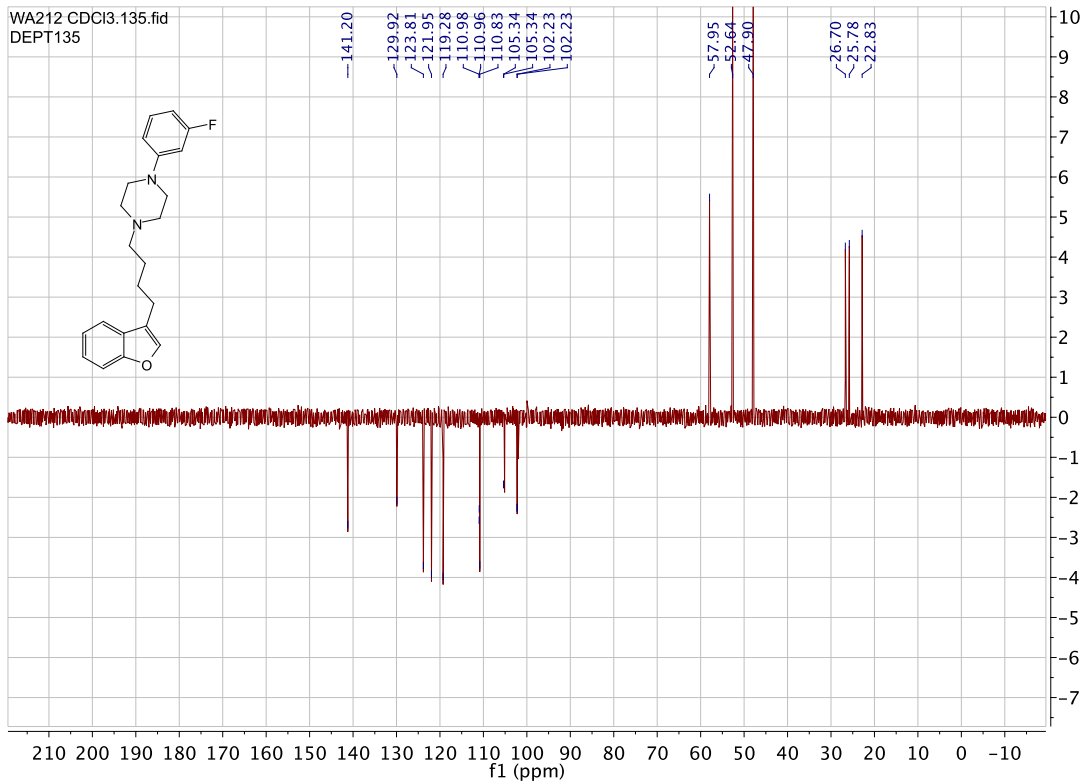
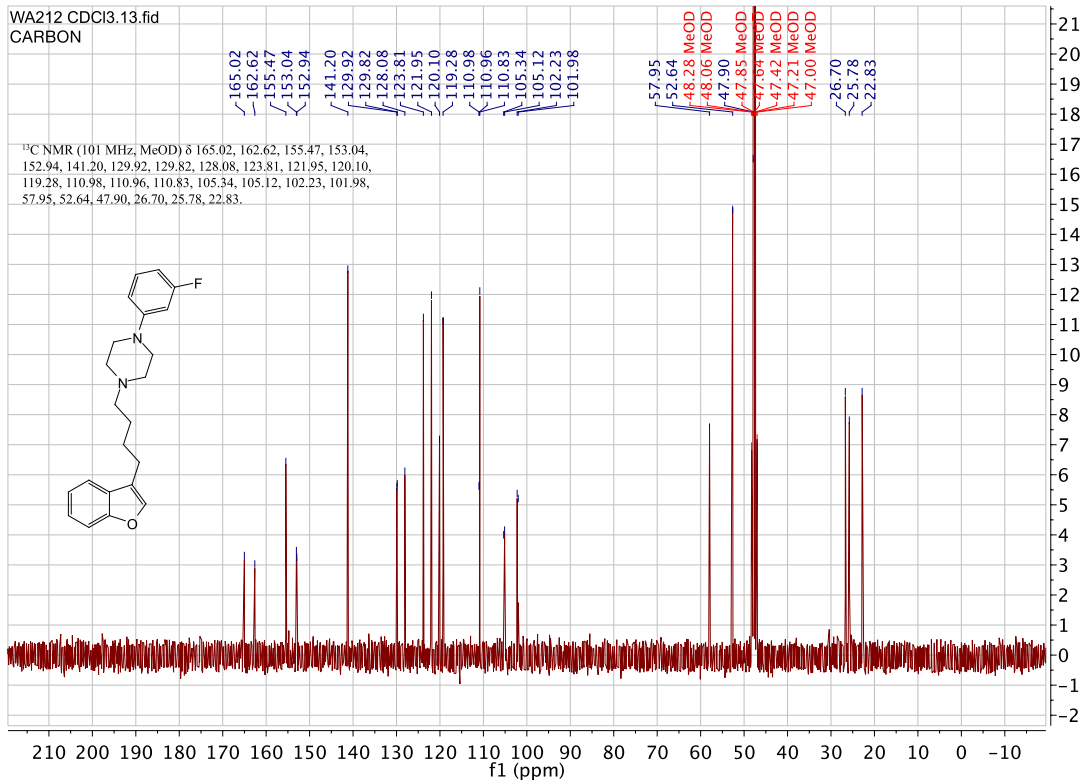
1-(4-(benzofuran-3-yl)butyl)-4-(3-fluorophenyl)piperazine. (WA212)



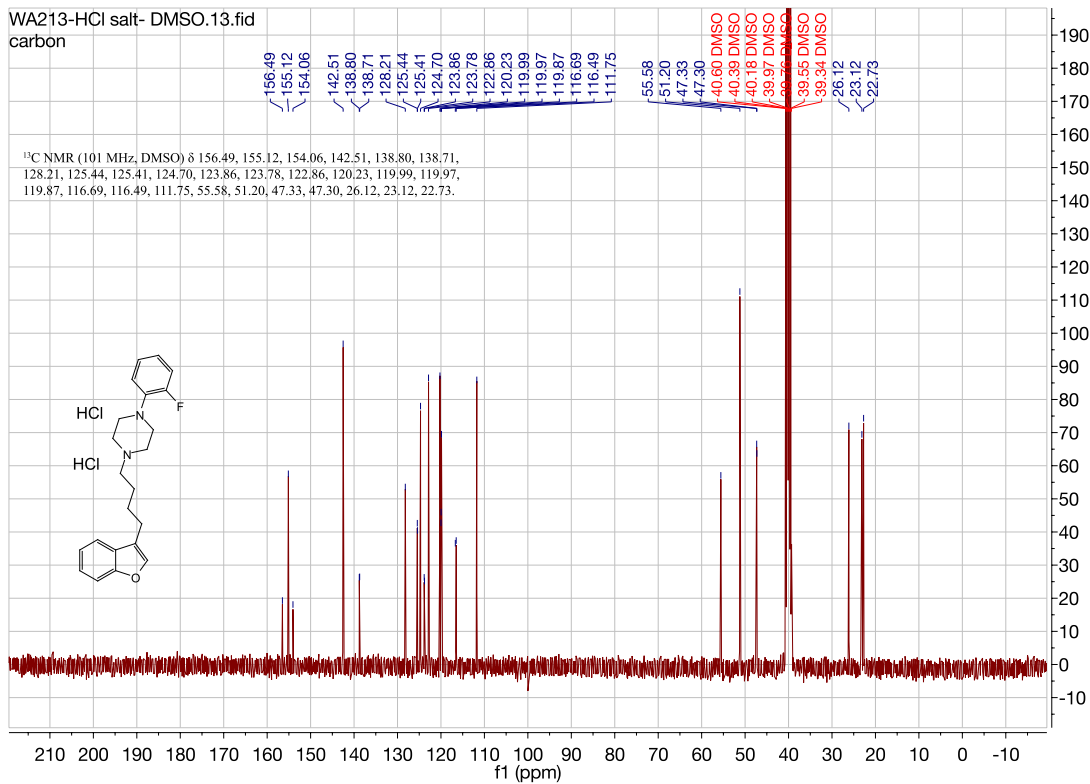


1-(4-(benzofuran-3-yl)butyl)-4-(3-fluorophenyl)piperazine. (WA212)

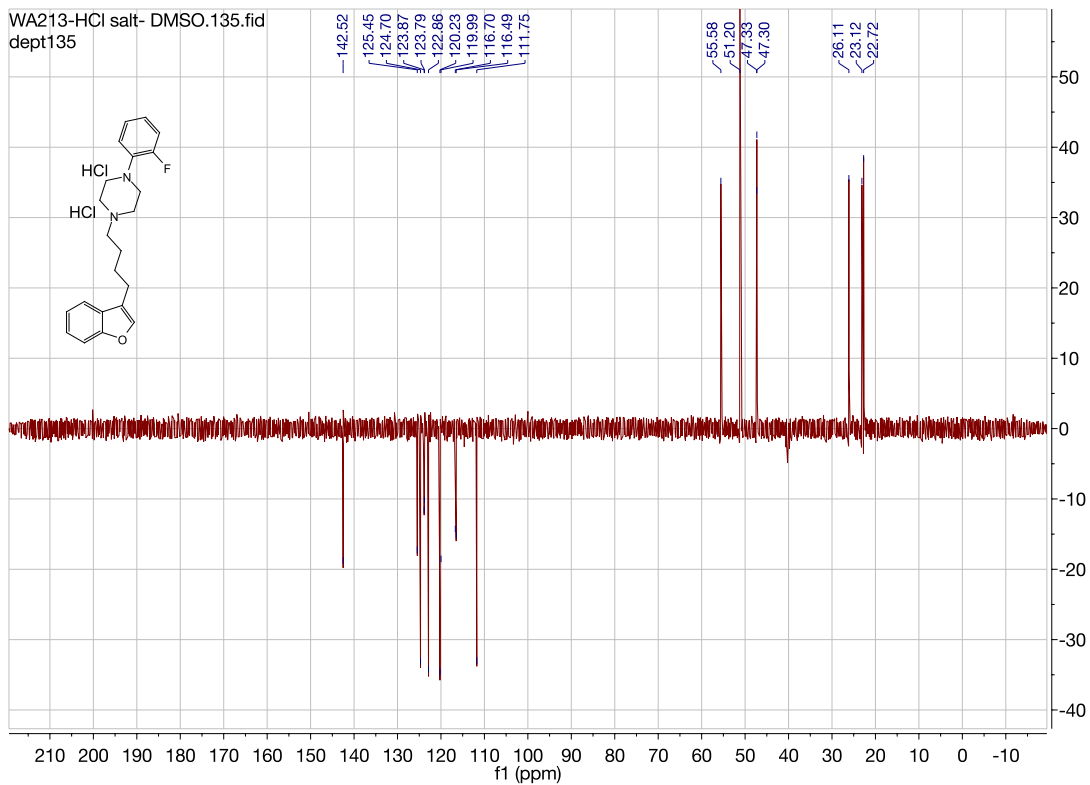




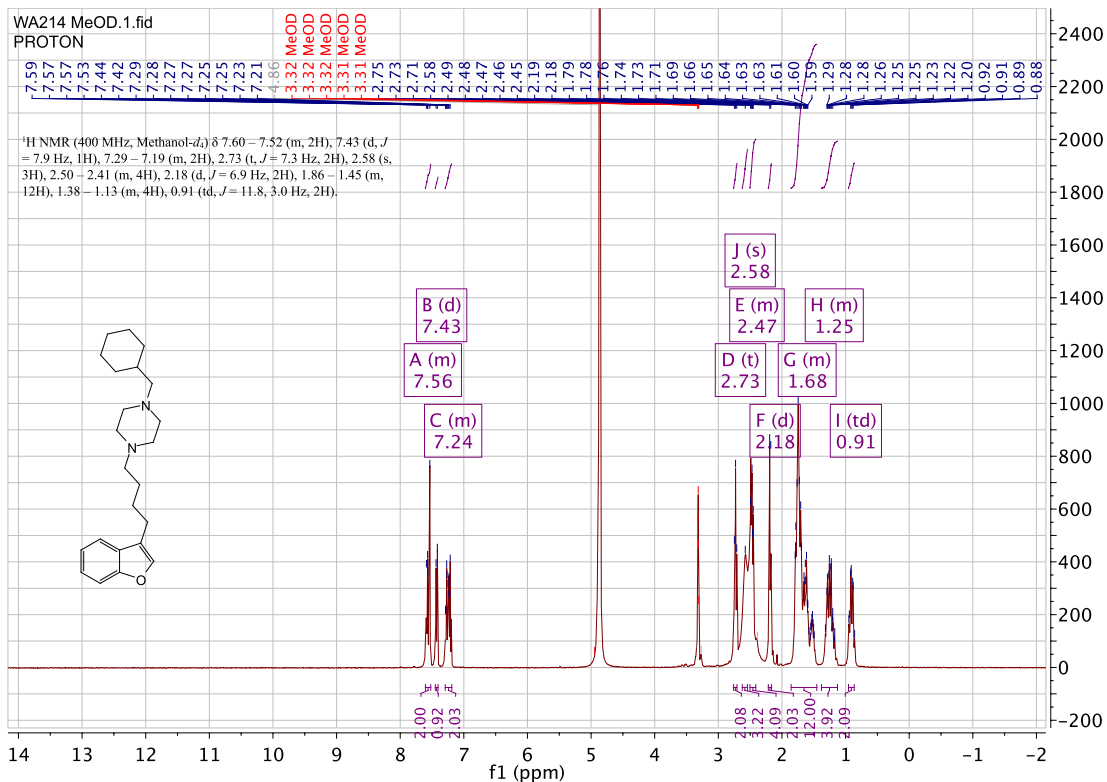
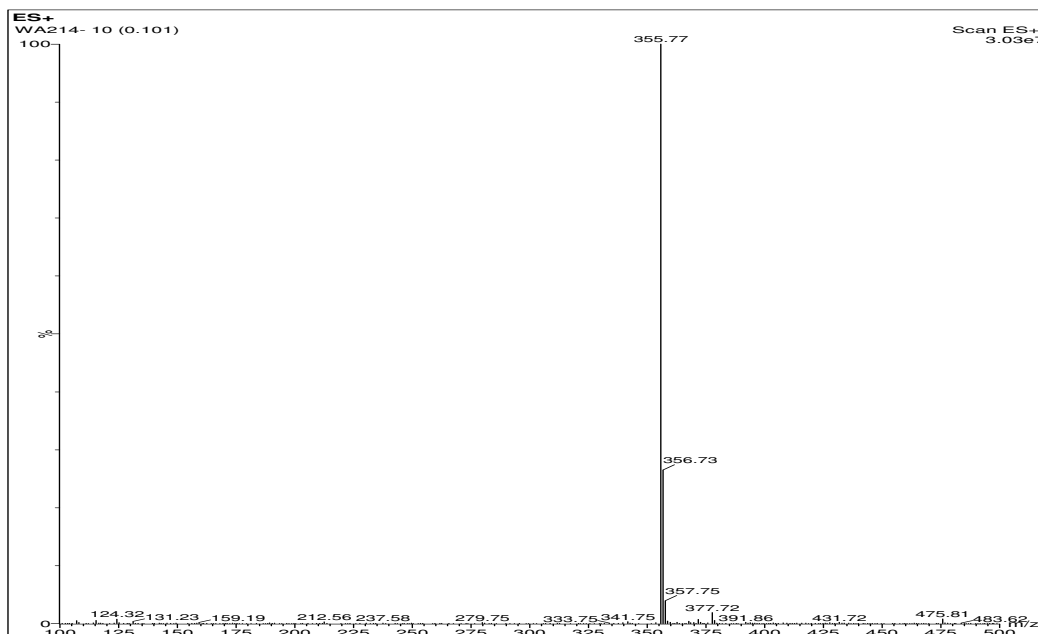
WA213-HCl salt- DMSO.13.fid
carbon

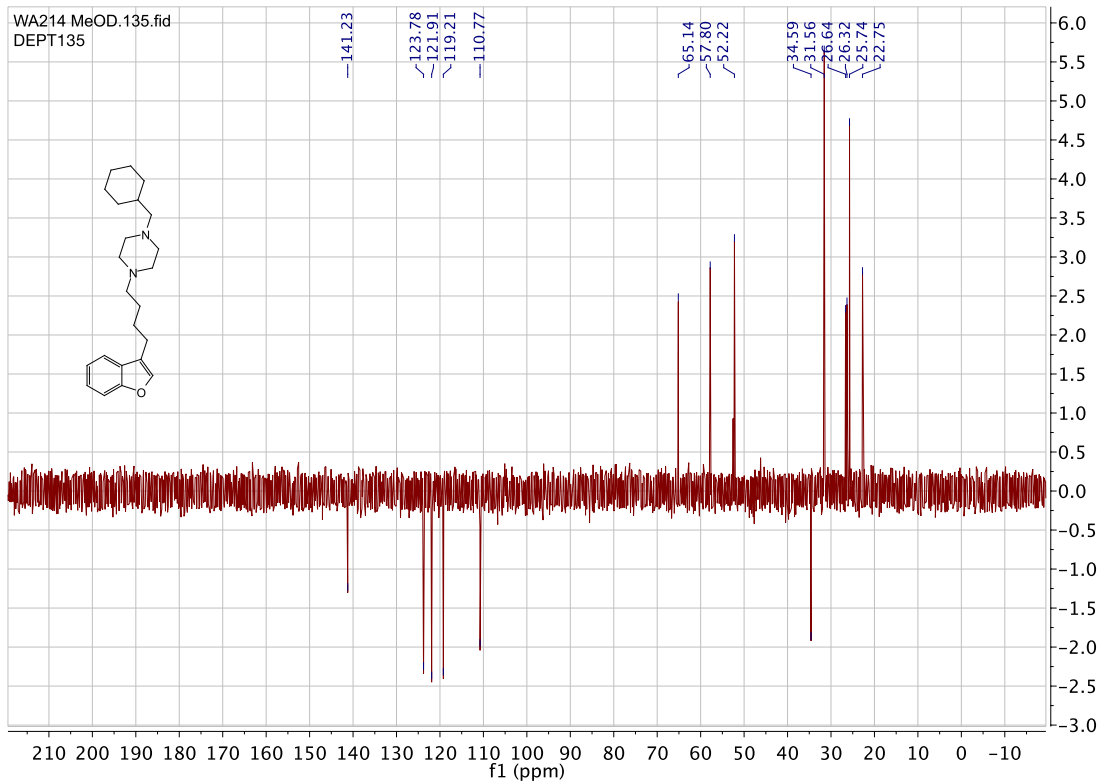
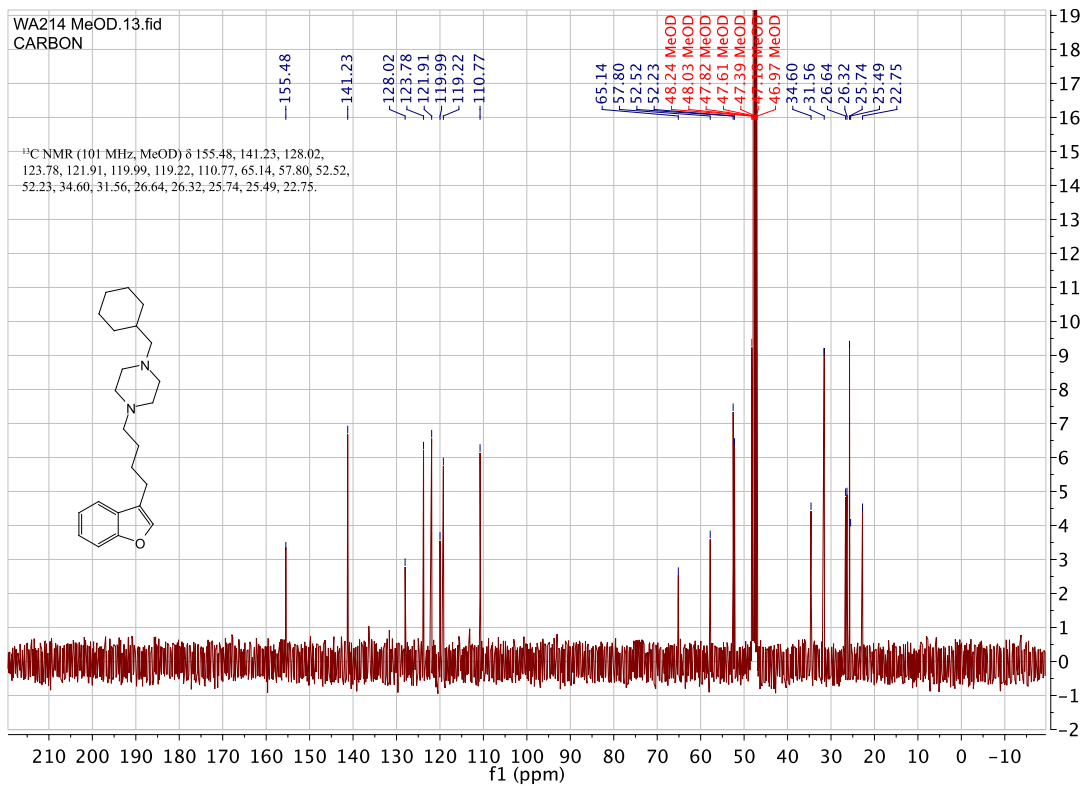


WA213-HCl salt- DMSO.135.fid
dept135

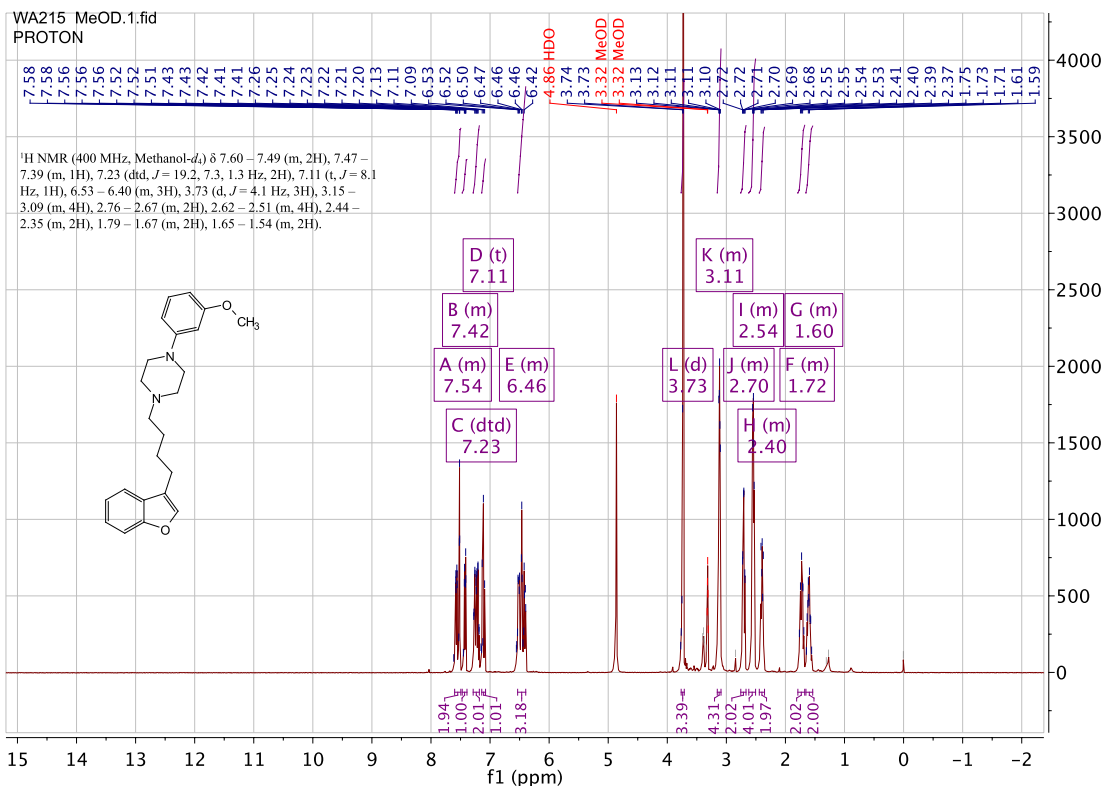
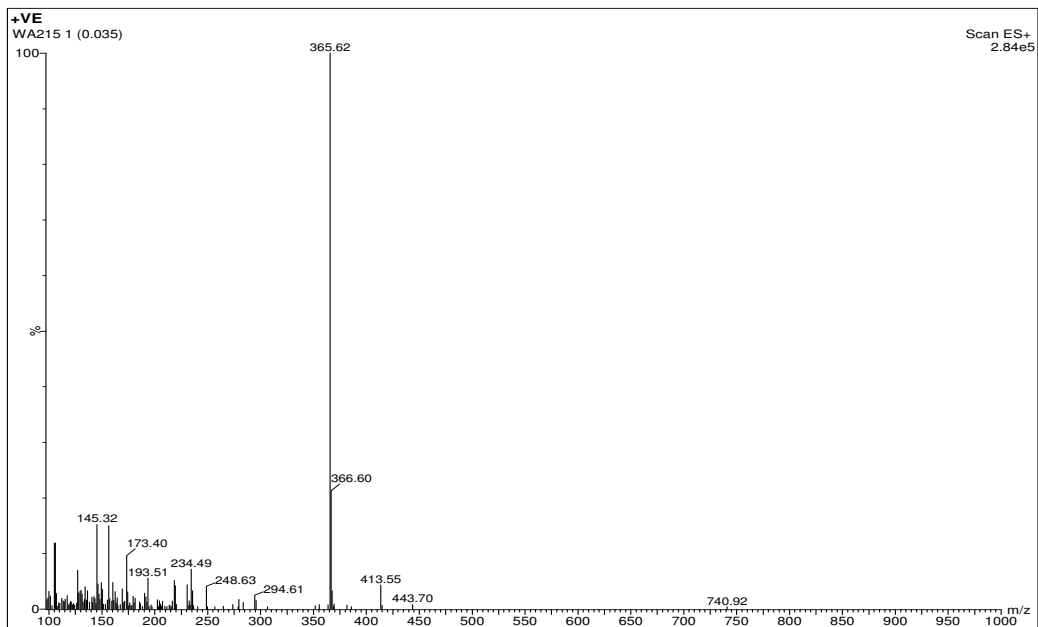


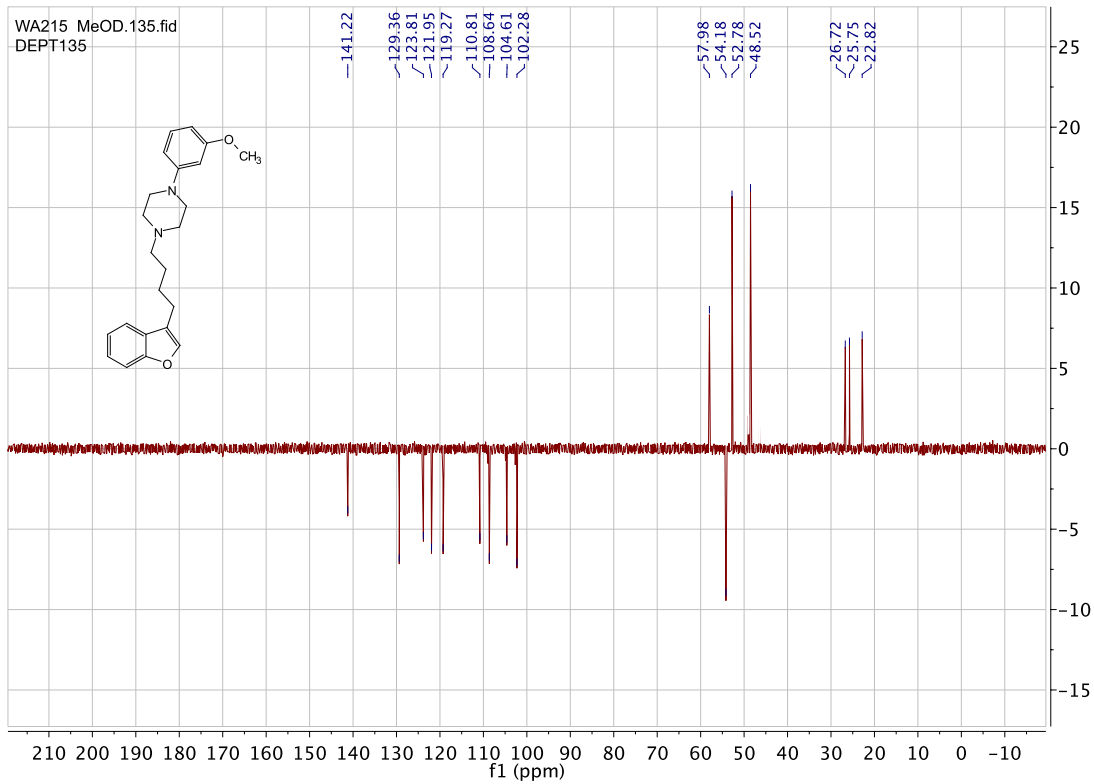
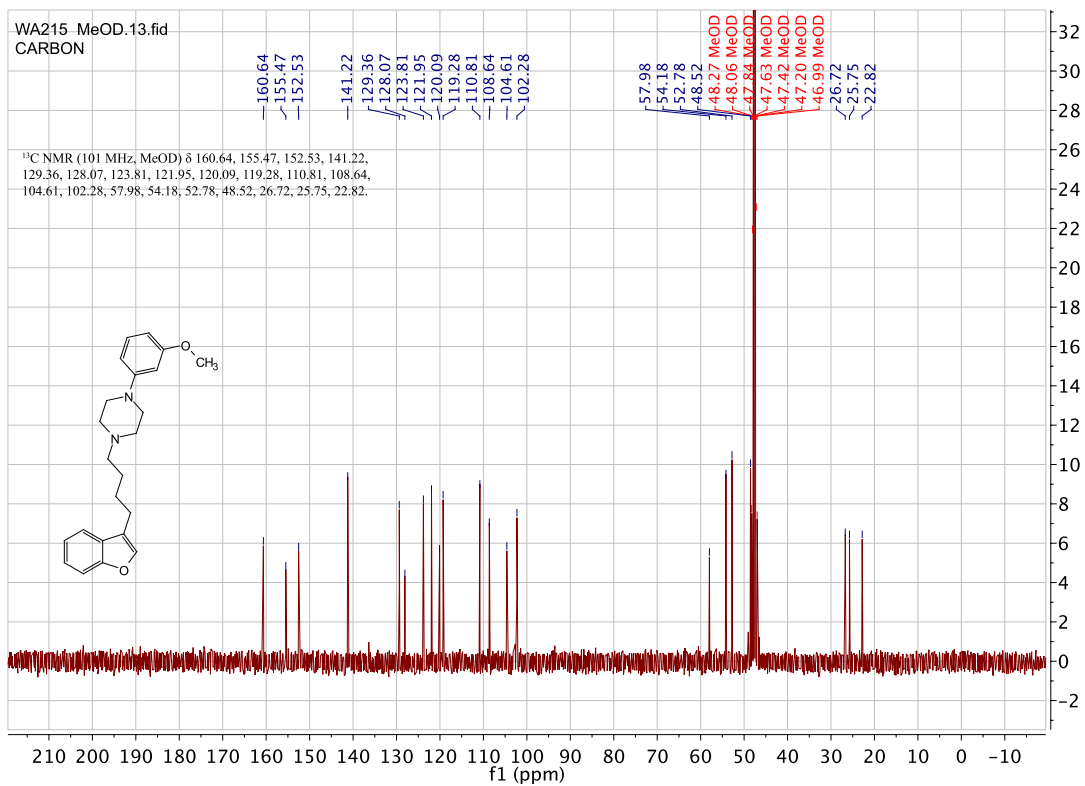
1-(4-(benzofuran-3-yl)butyl)-4-(cyclohexylmethyl)piperazine. (WA214)



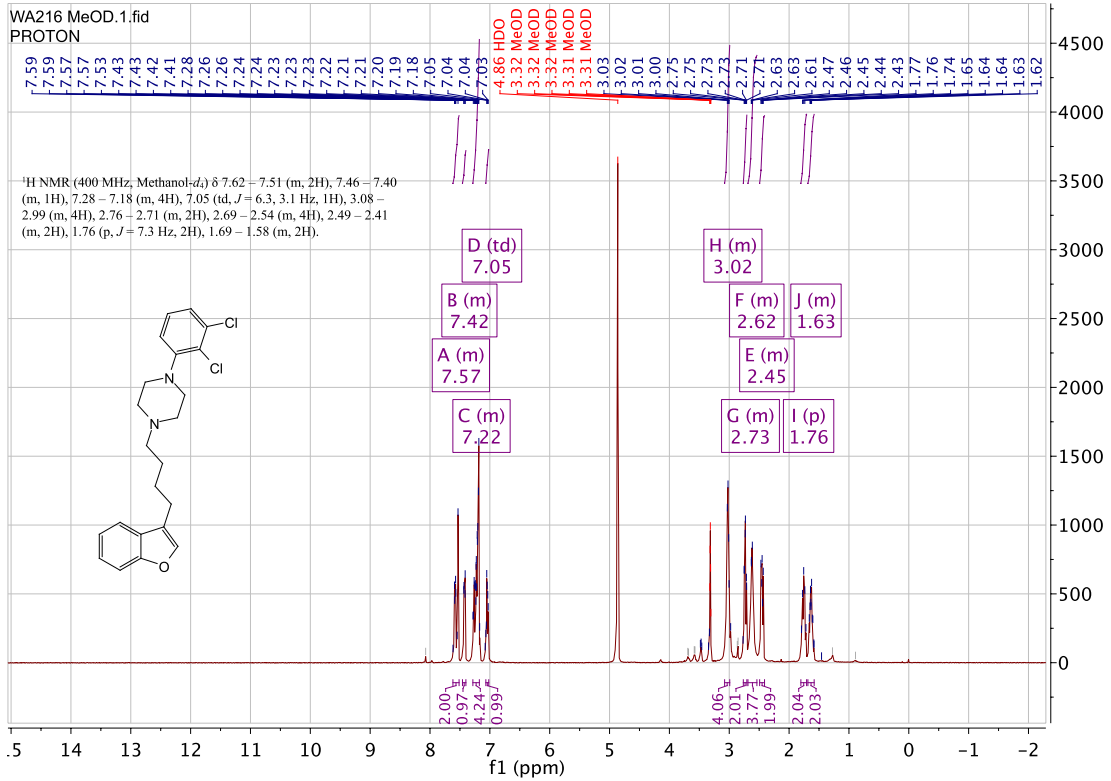
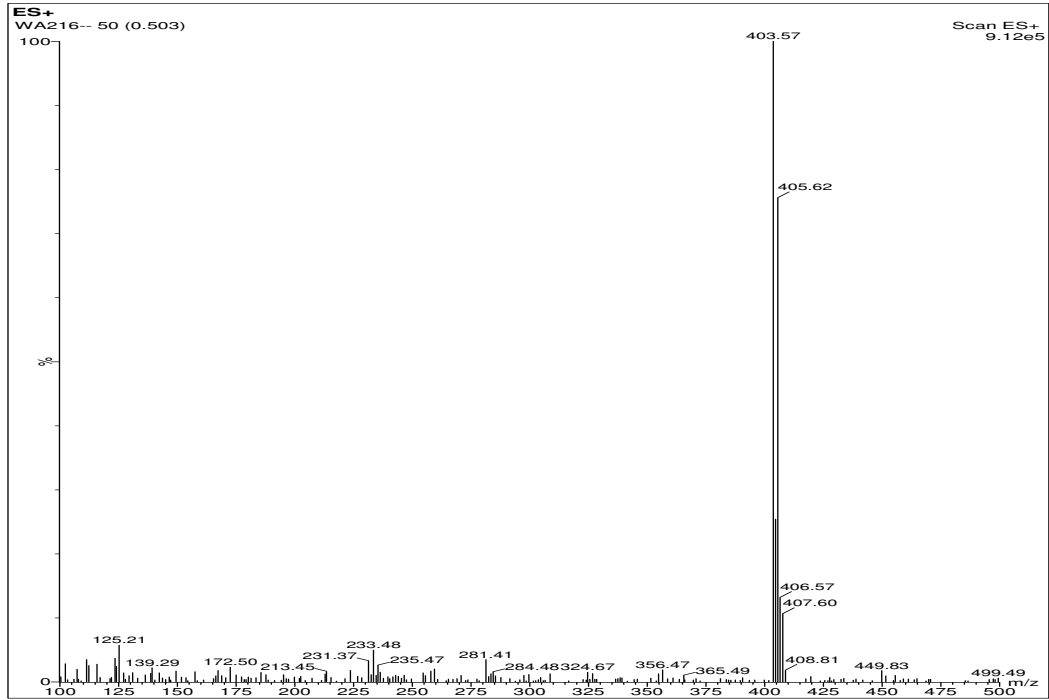


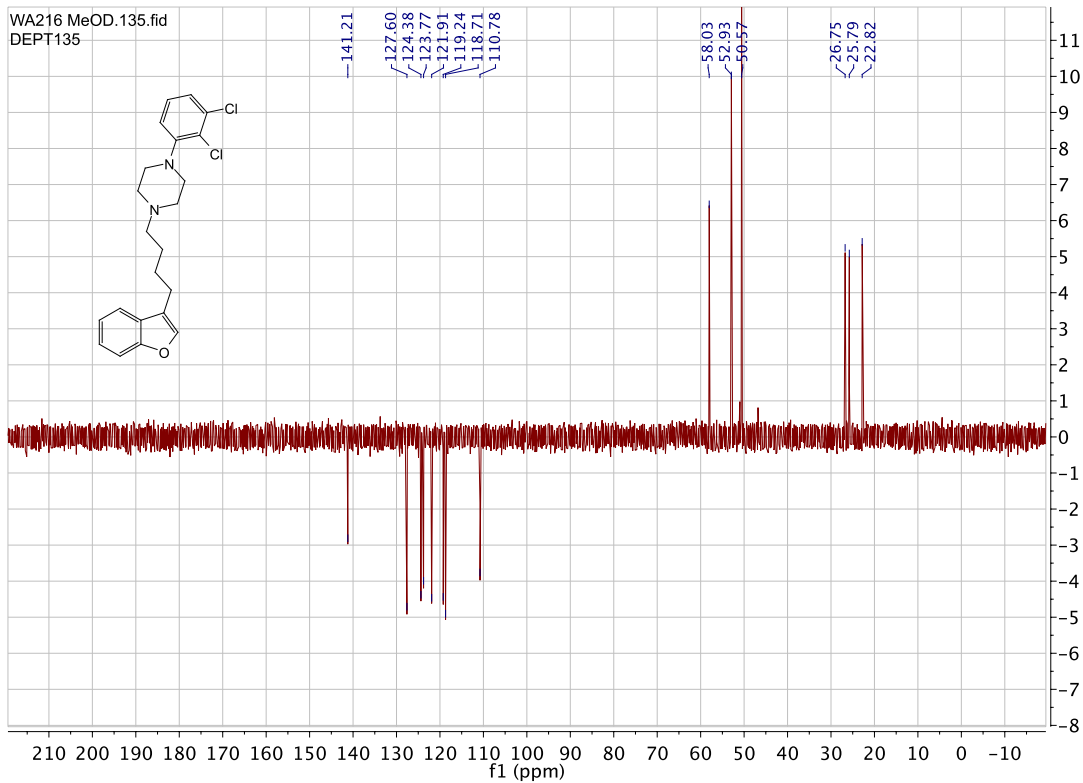
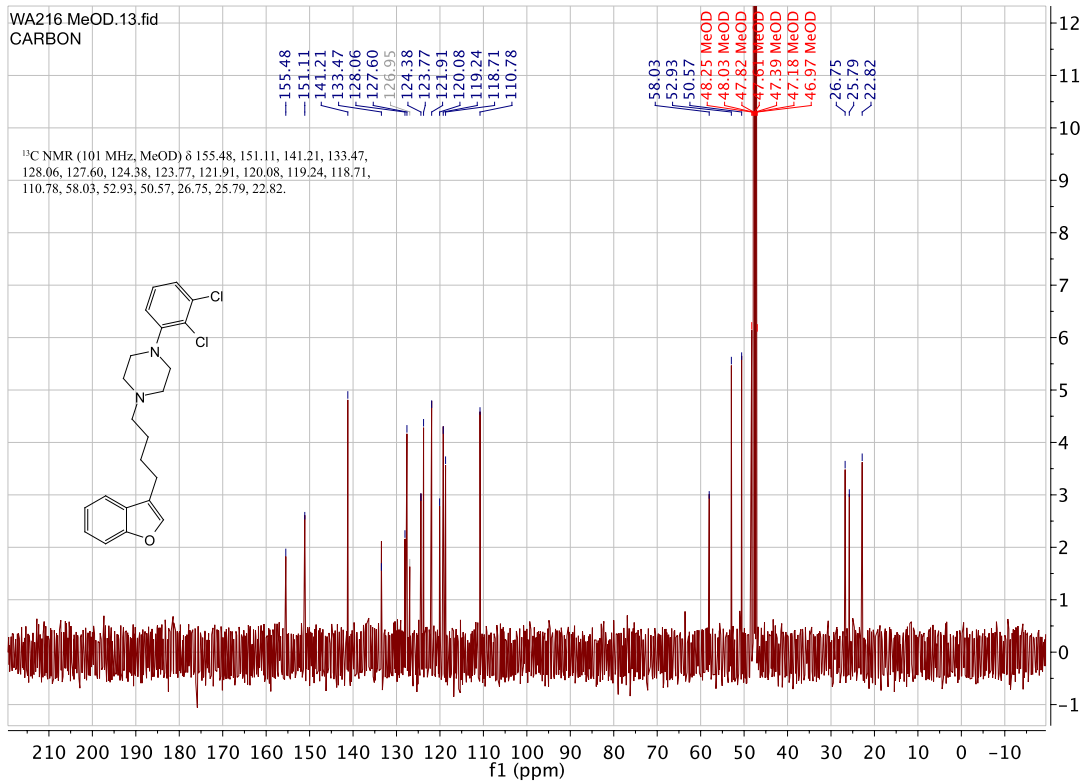
1-(4-(benzofuran-3-yl)butyl)-4-(3-methoxyphenyl)piperazine. (WA215)



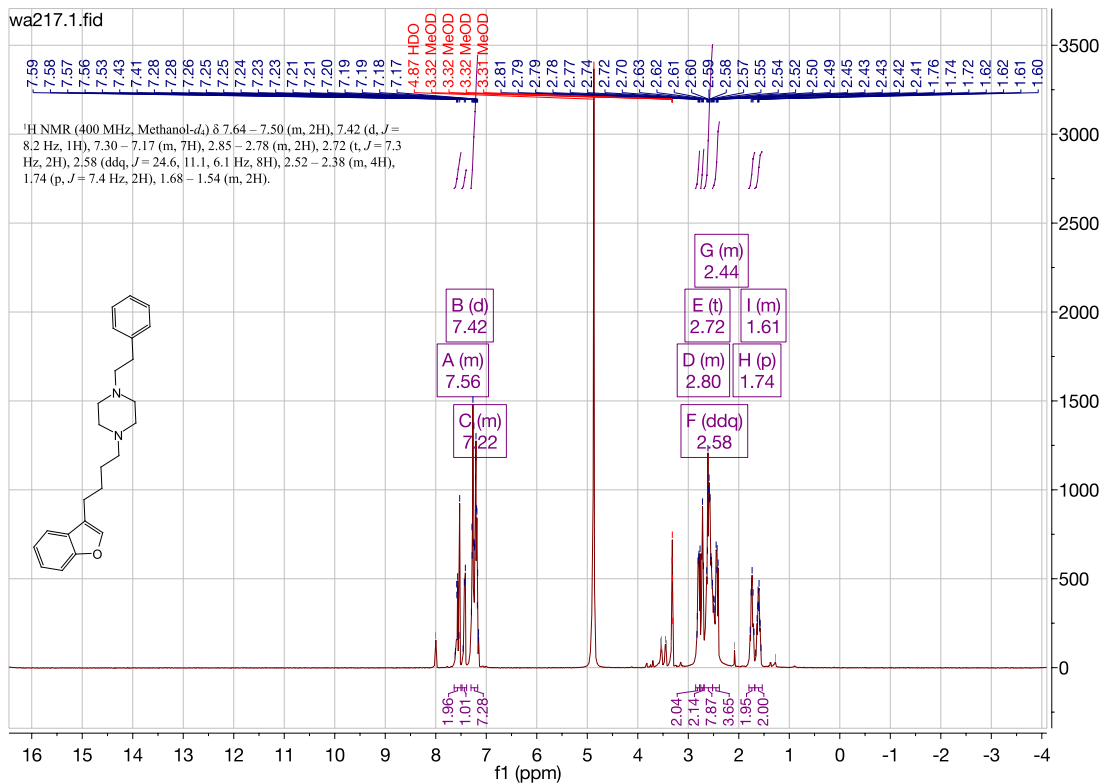
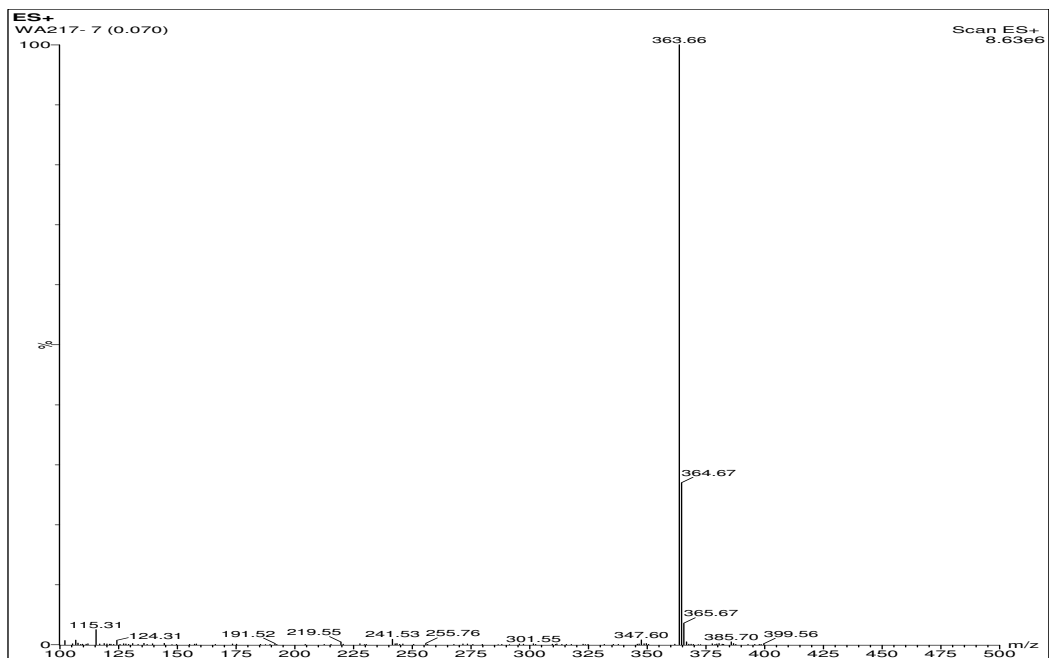


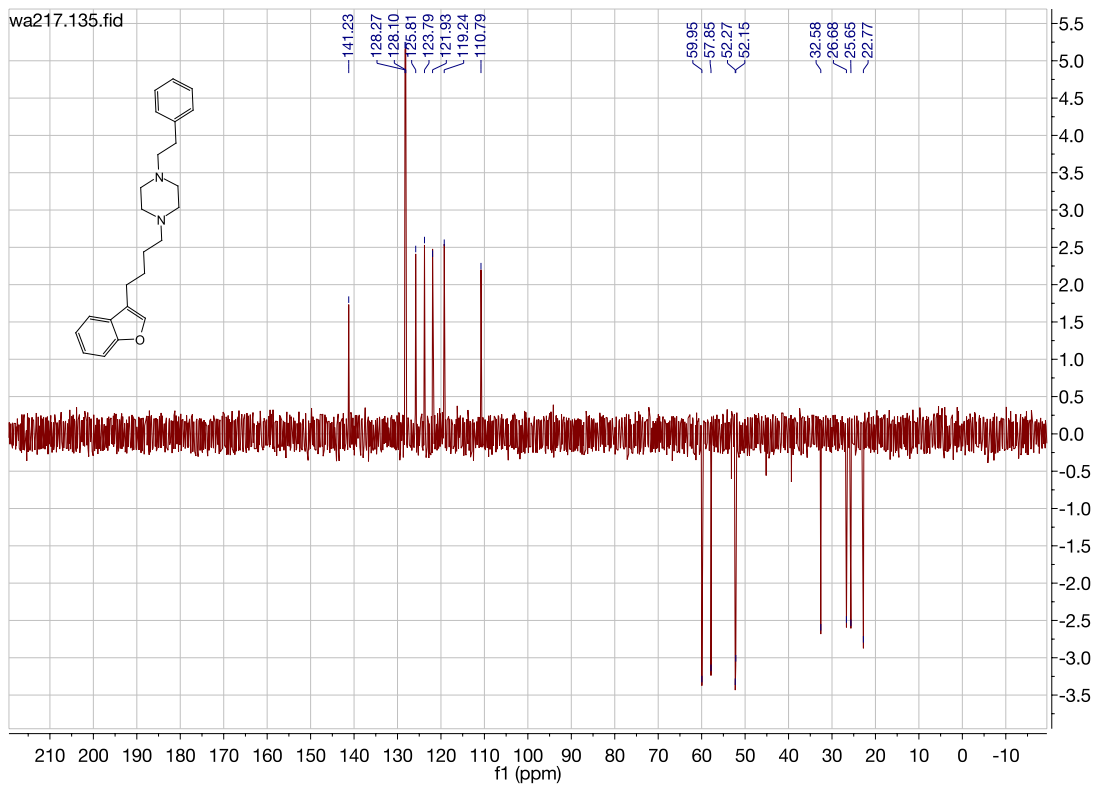
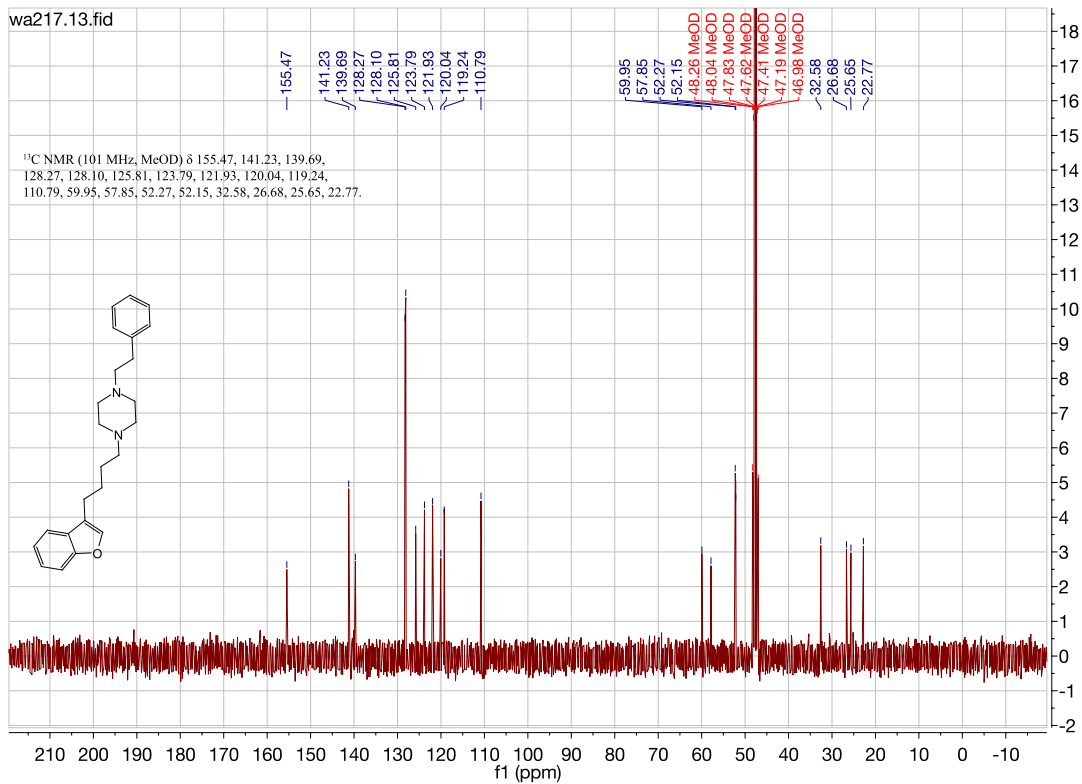
1-(4-(benzofuran-3-yl)butyl)-4-(2,3-dichlorophenyl)piperazine. (WA216)



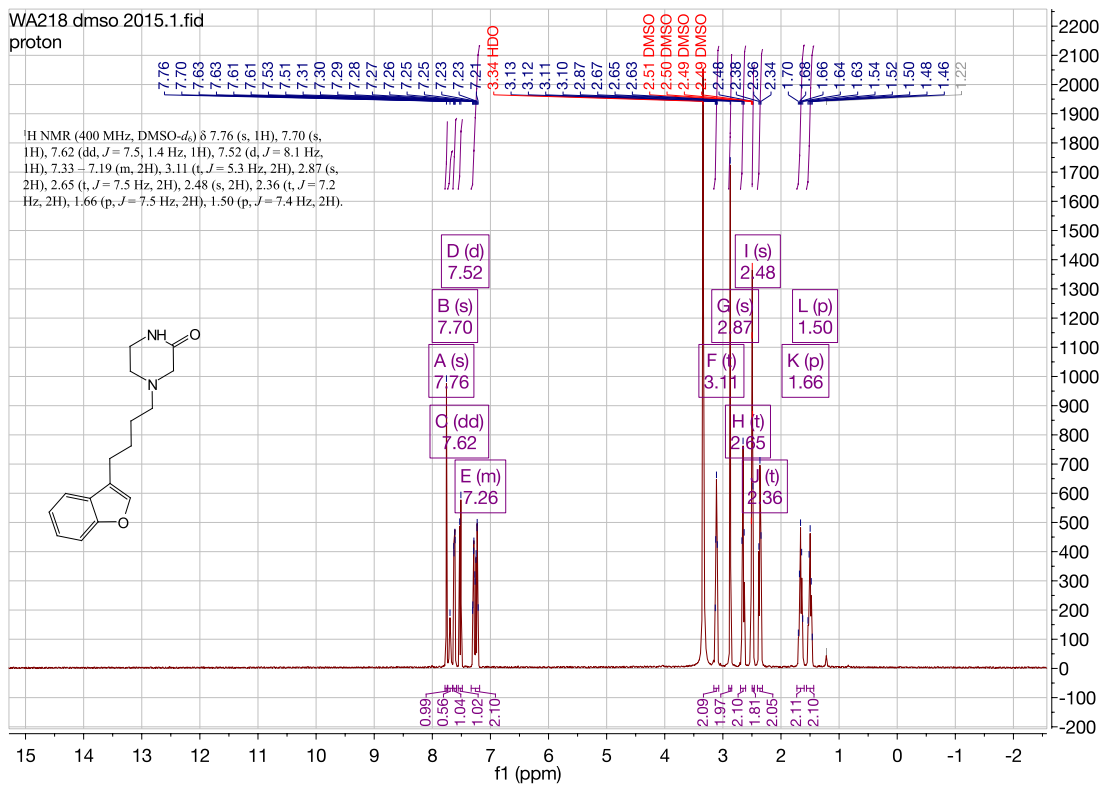
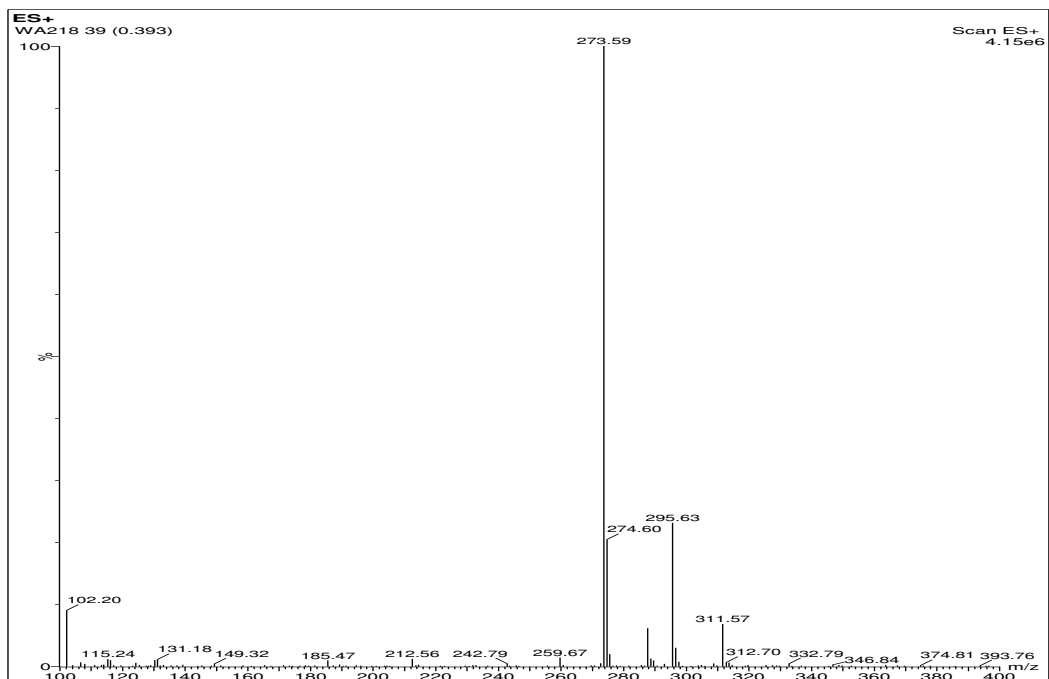


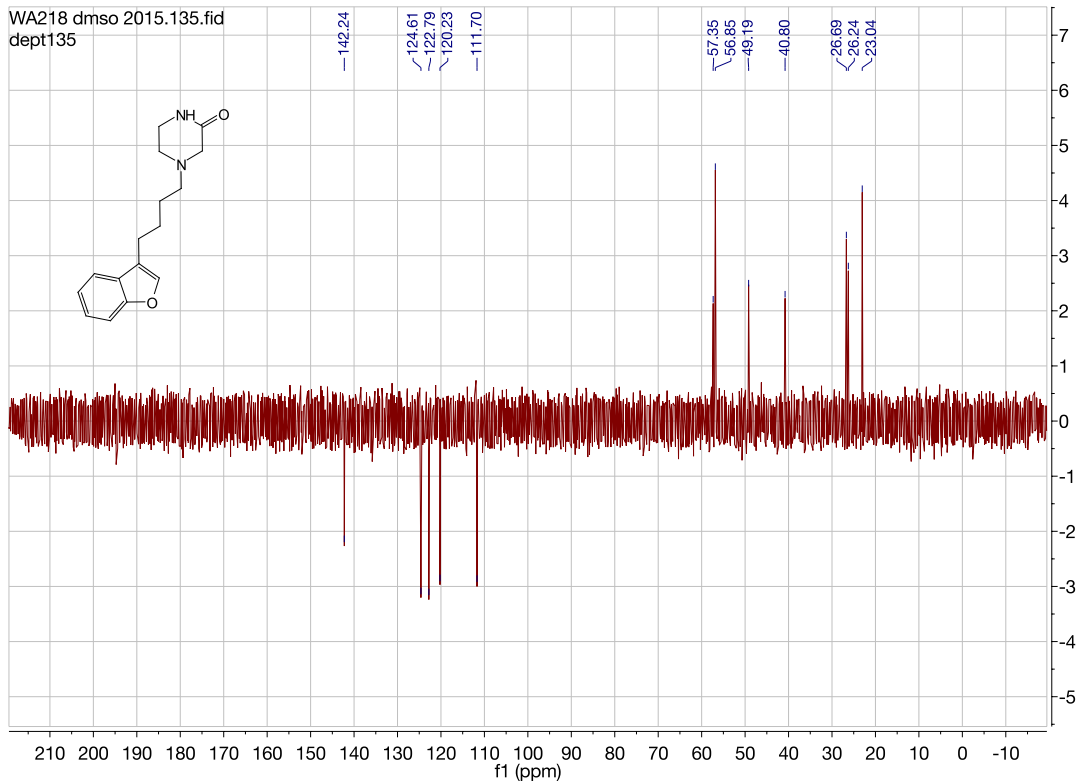
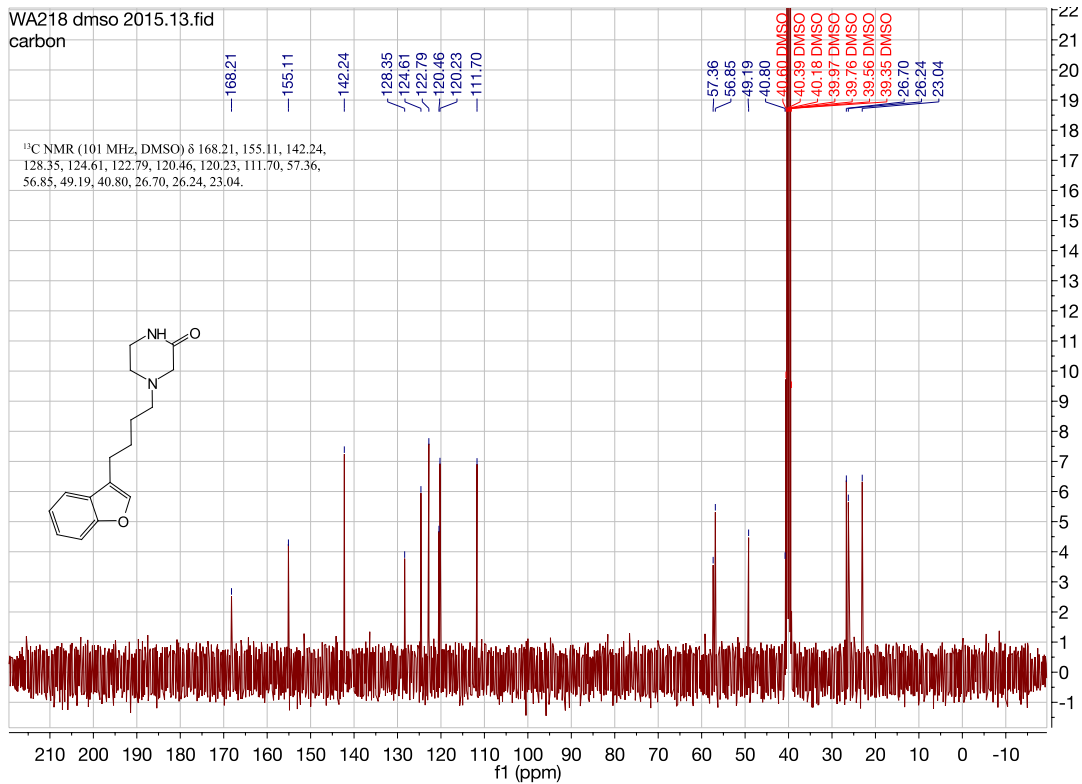
1-(4-(benzofuran-3-yl)butyl)-4-phenethylpiperazine. (WA217)



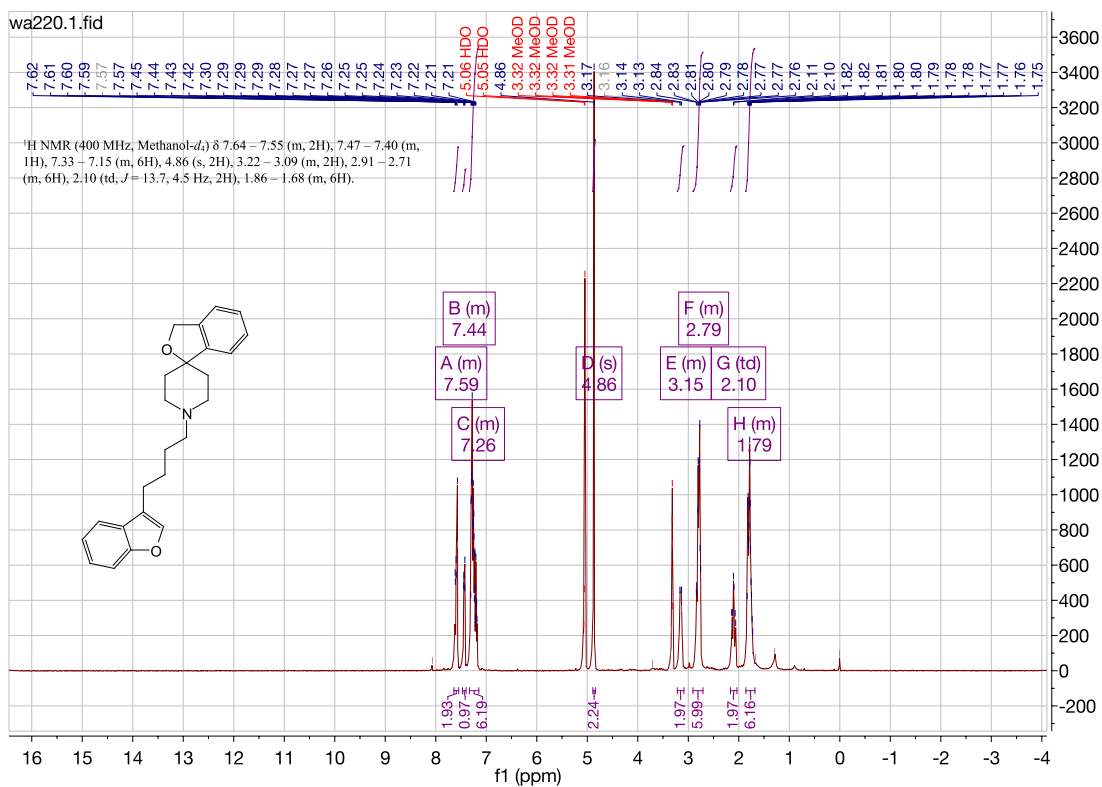
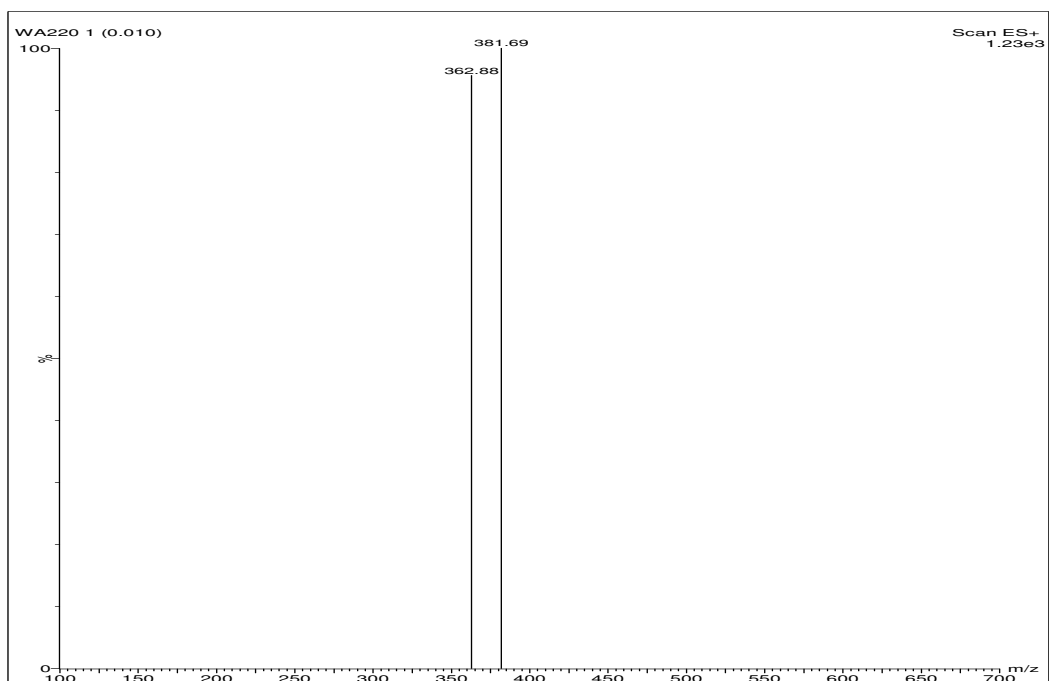


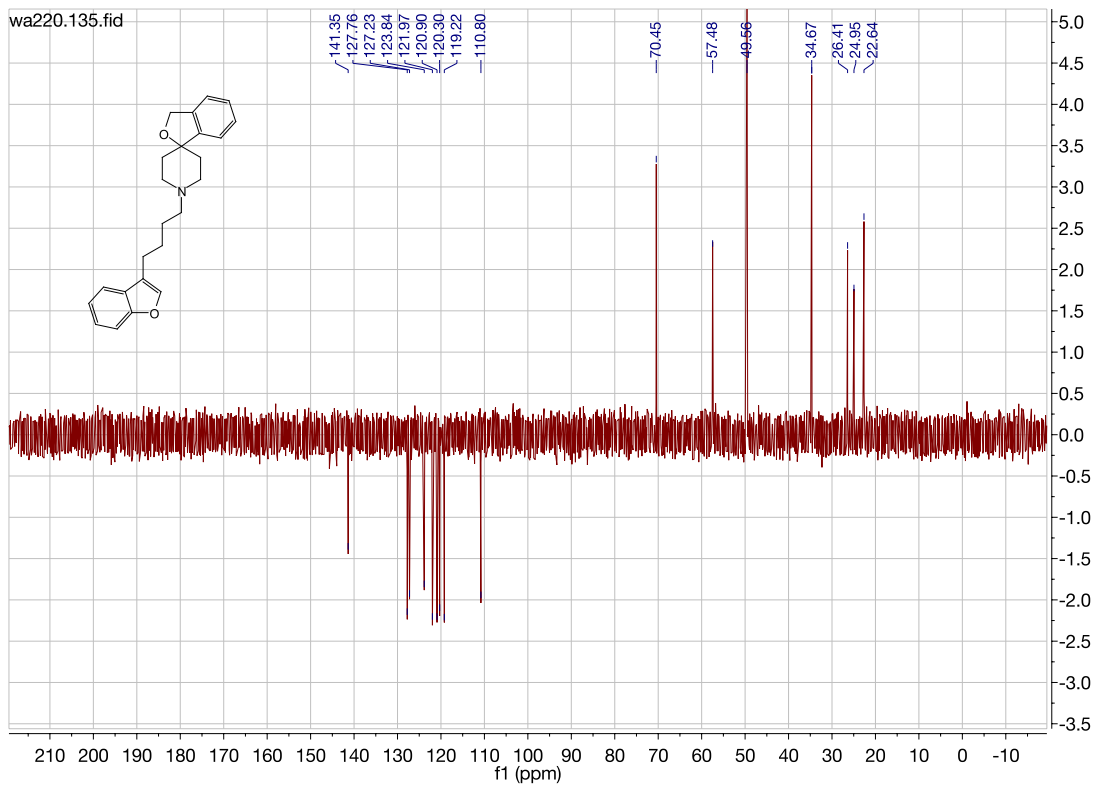
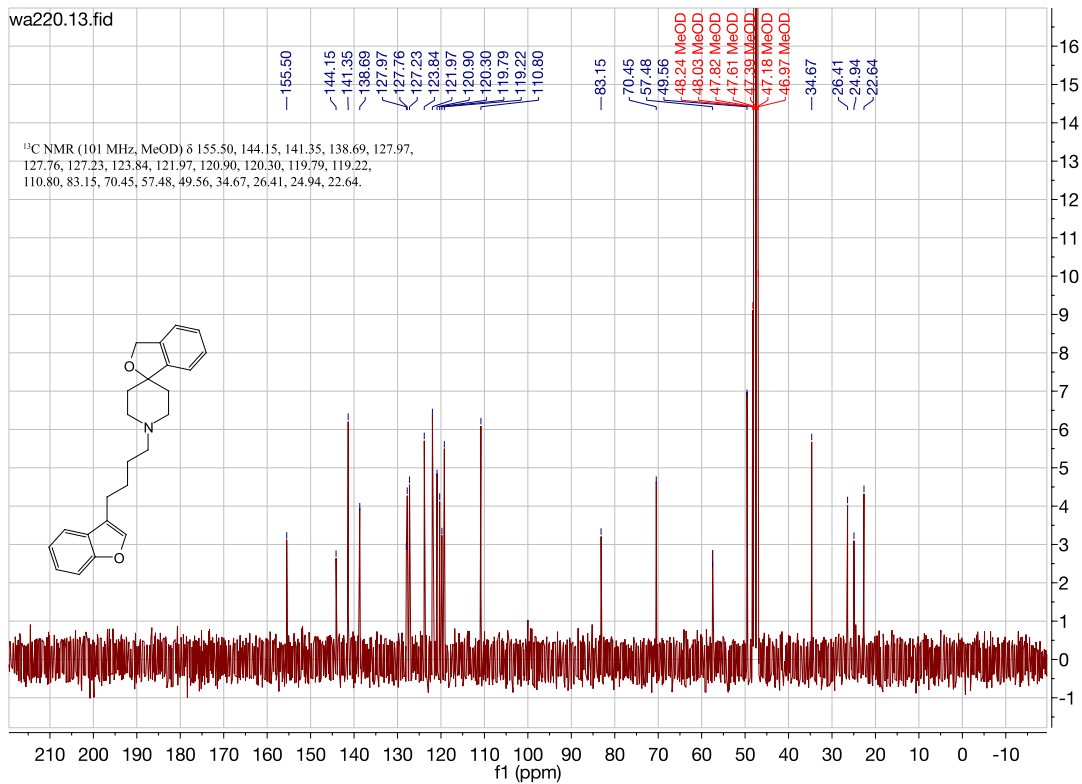
4-(4-(benzofuran-3-yl)butyl)piperazin-2-one. (WA218)



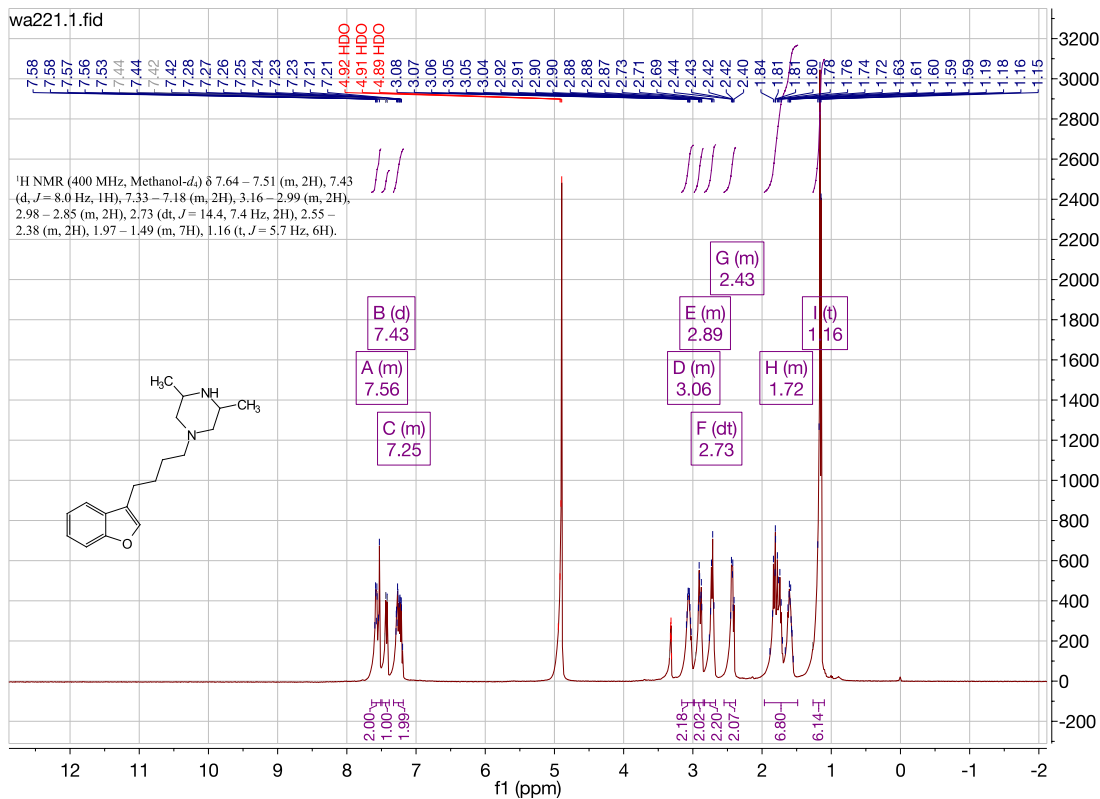
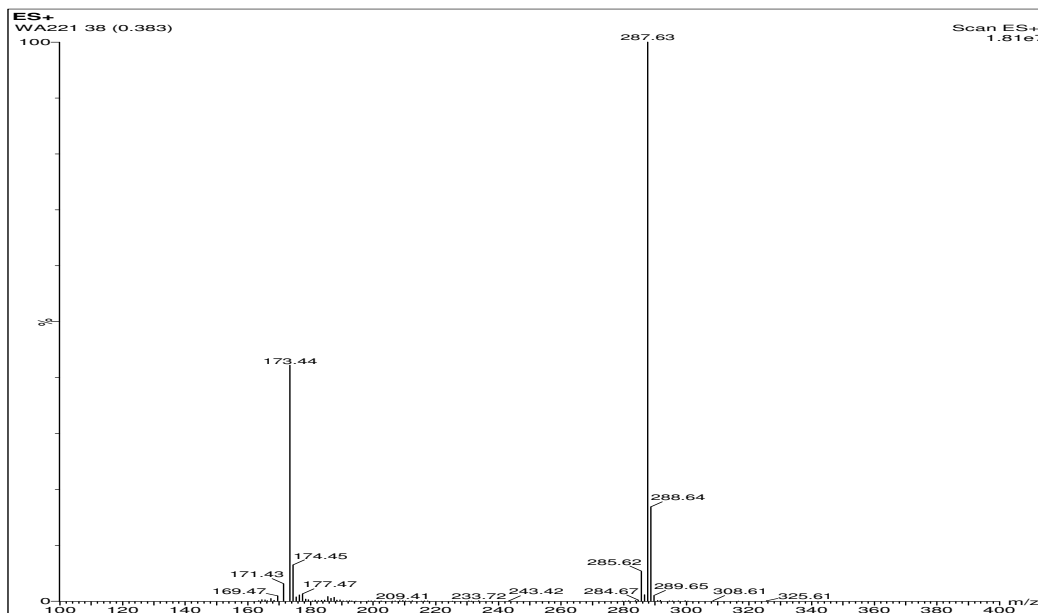


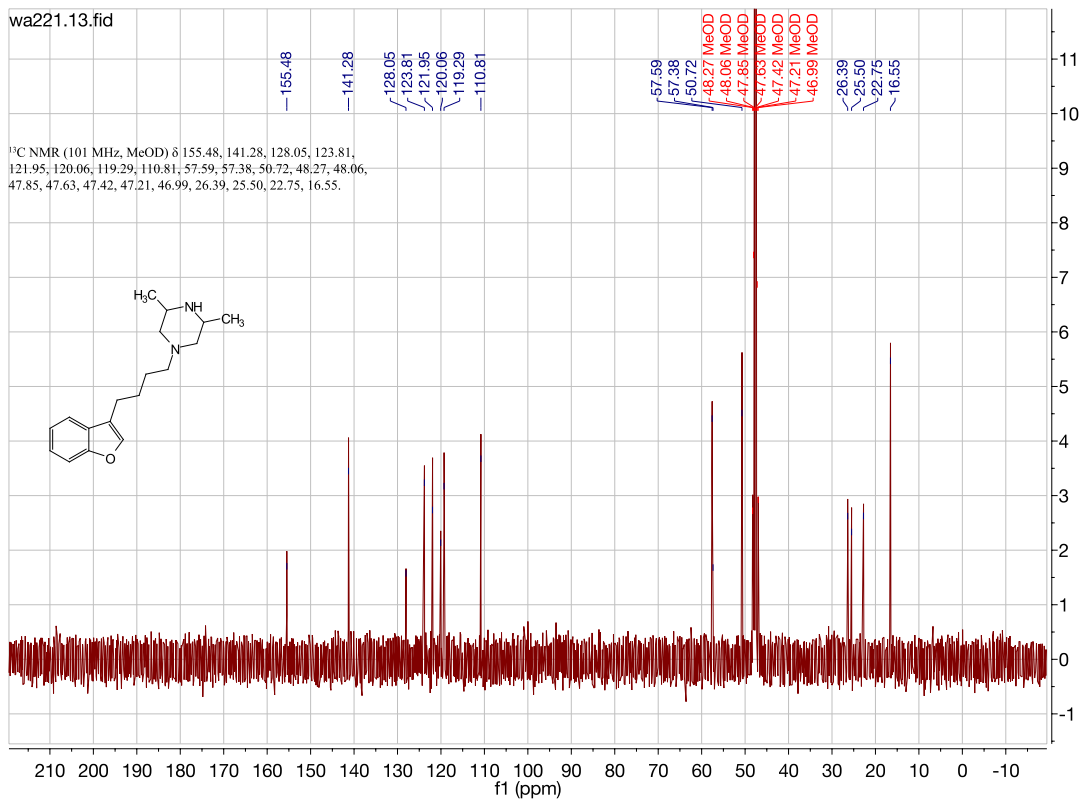
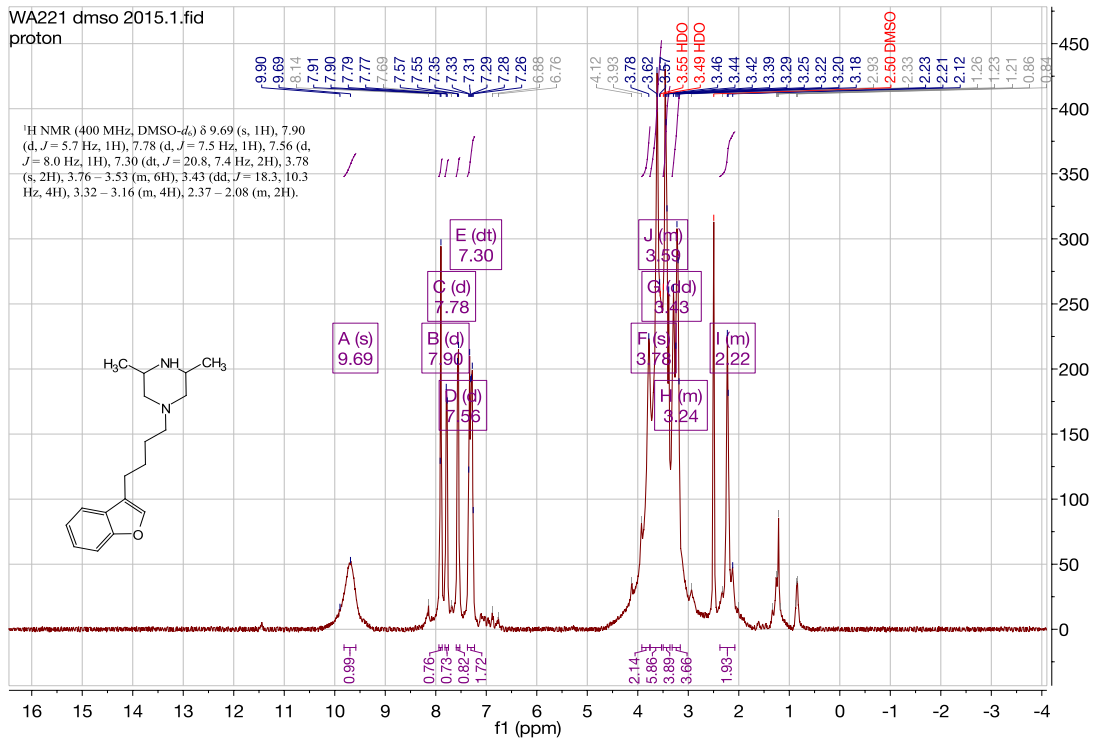
1'-(4-(benzofuran-3-yl)butyl)-3H-spiro[isobenzofuran-1,4'-piperidine]. (WA220)

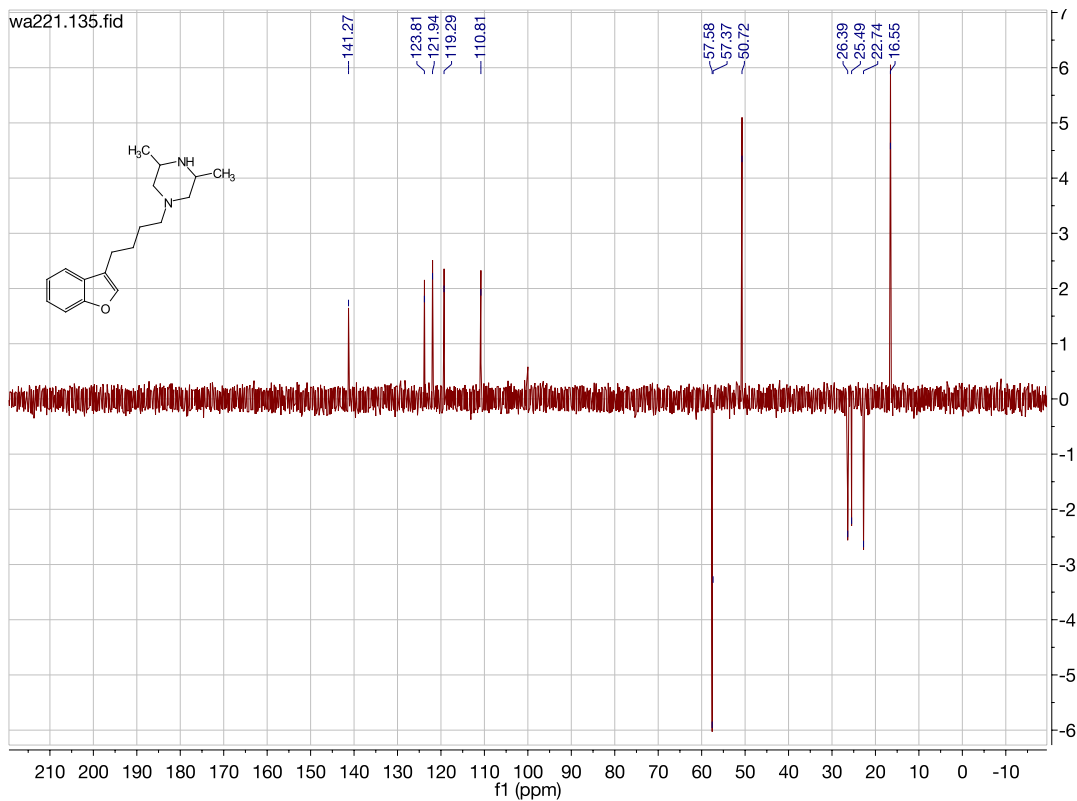




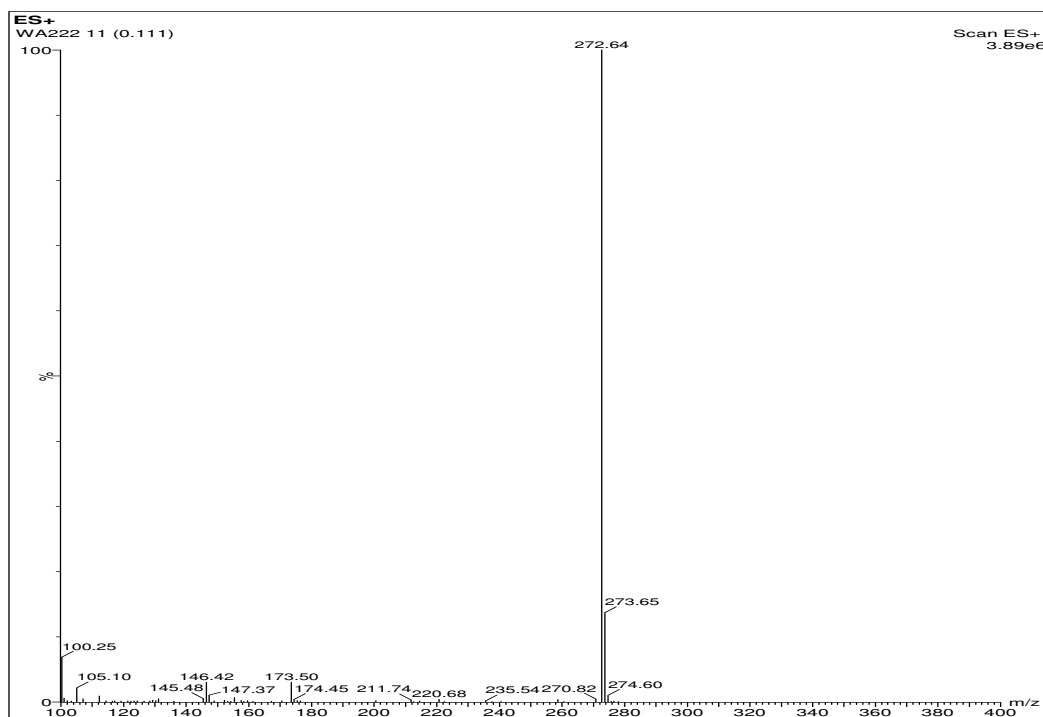
1-(4-(benzofuran-3-yl)butyl)-3,5-dimethylpiperazine. (WA221)

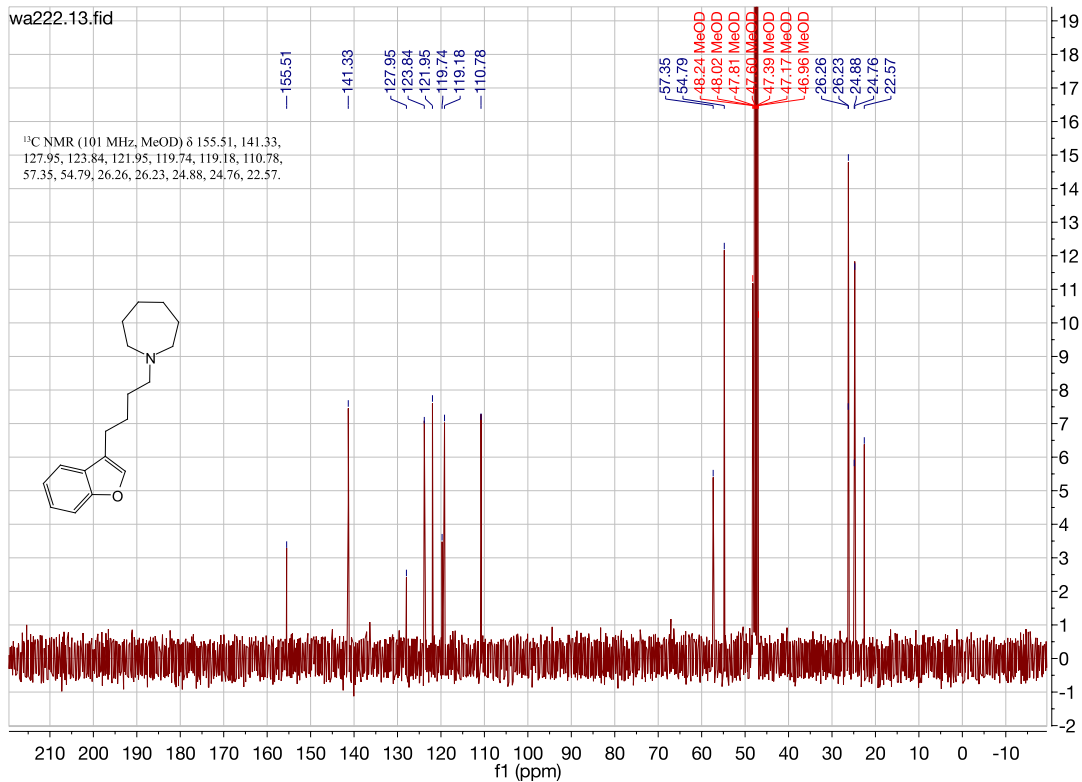
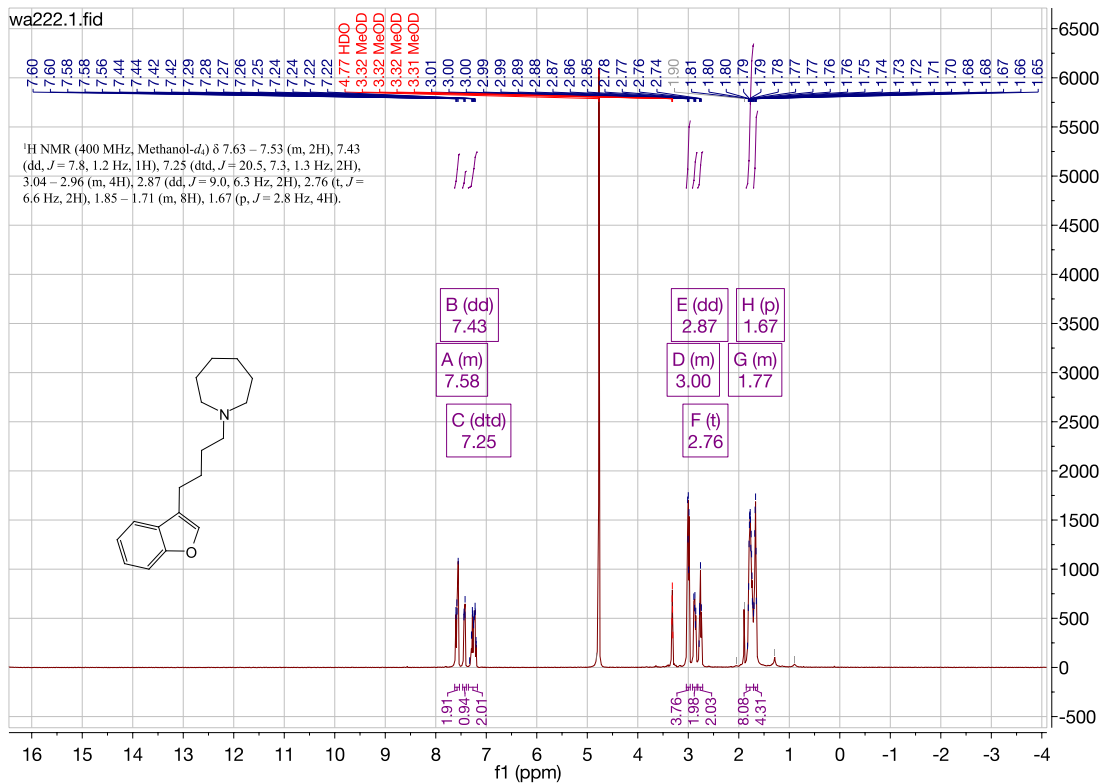


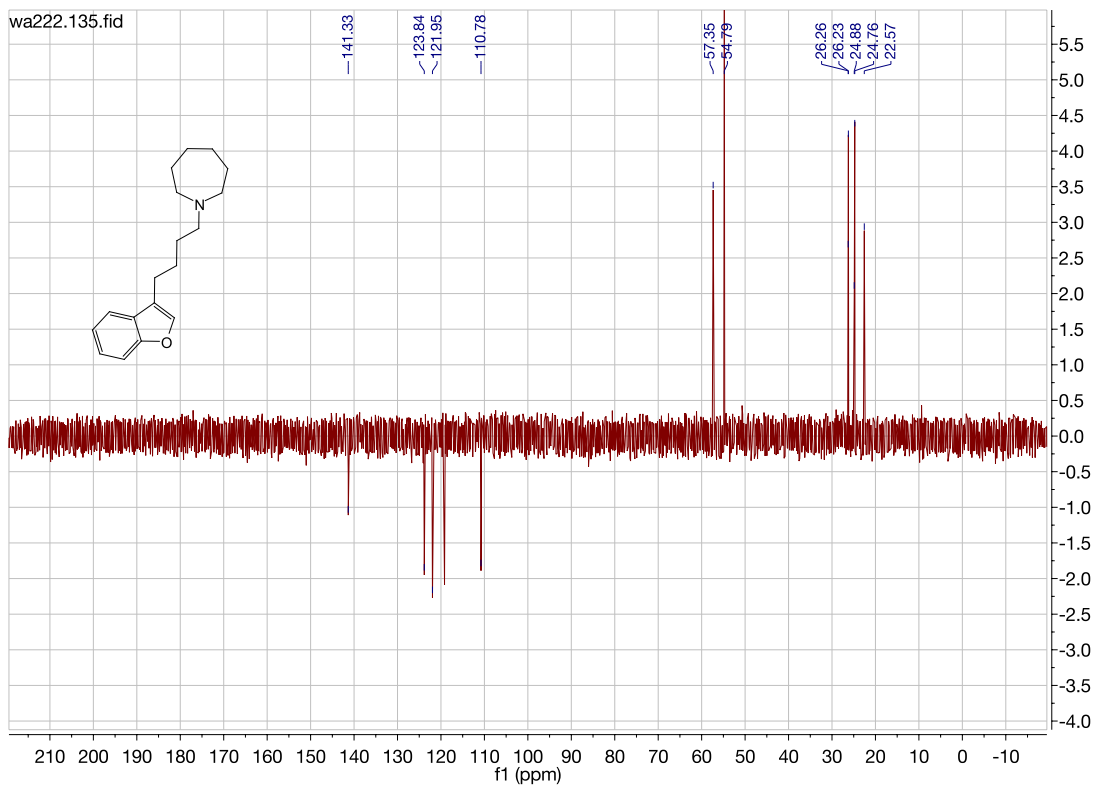




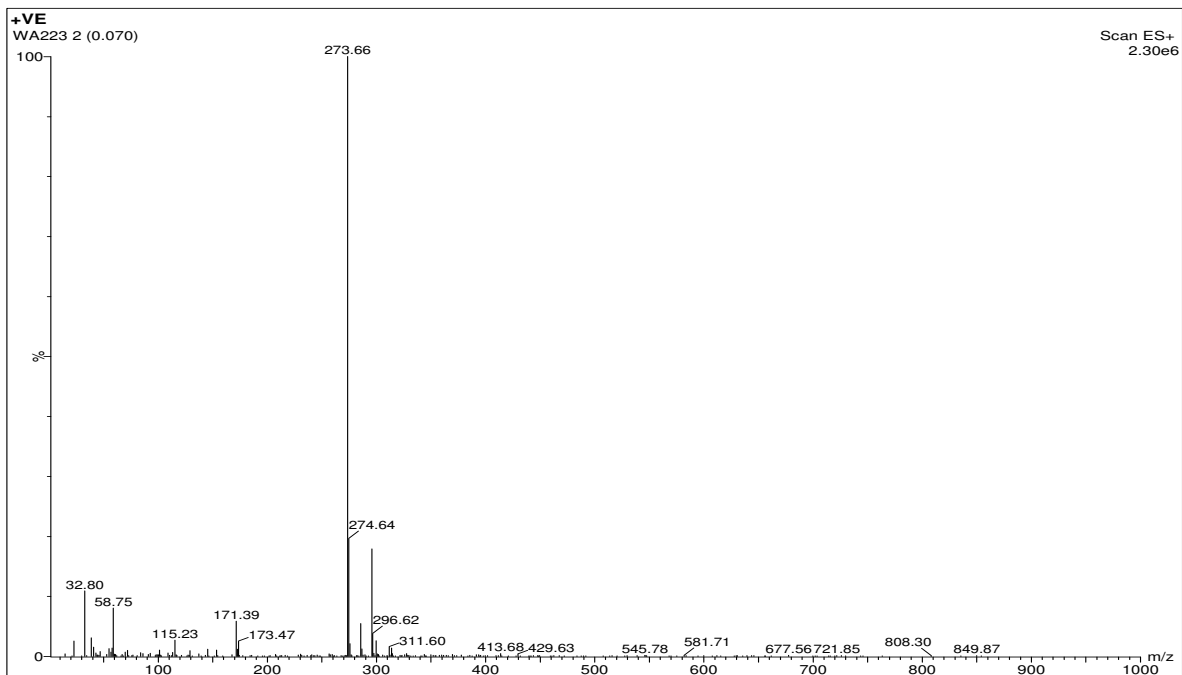
1-(4-(benzofuran-3-yl)butyl)azepane. (WA222)

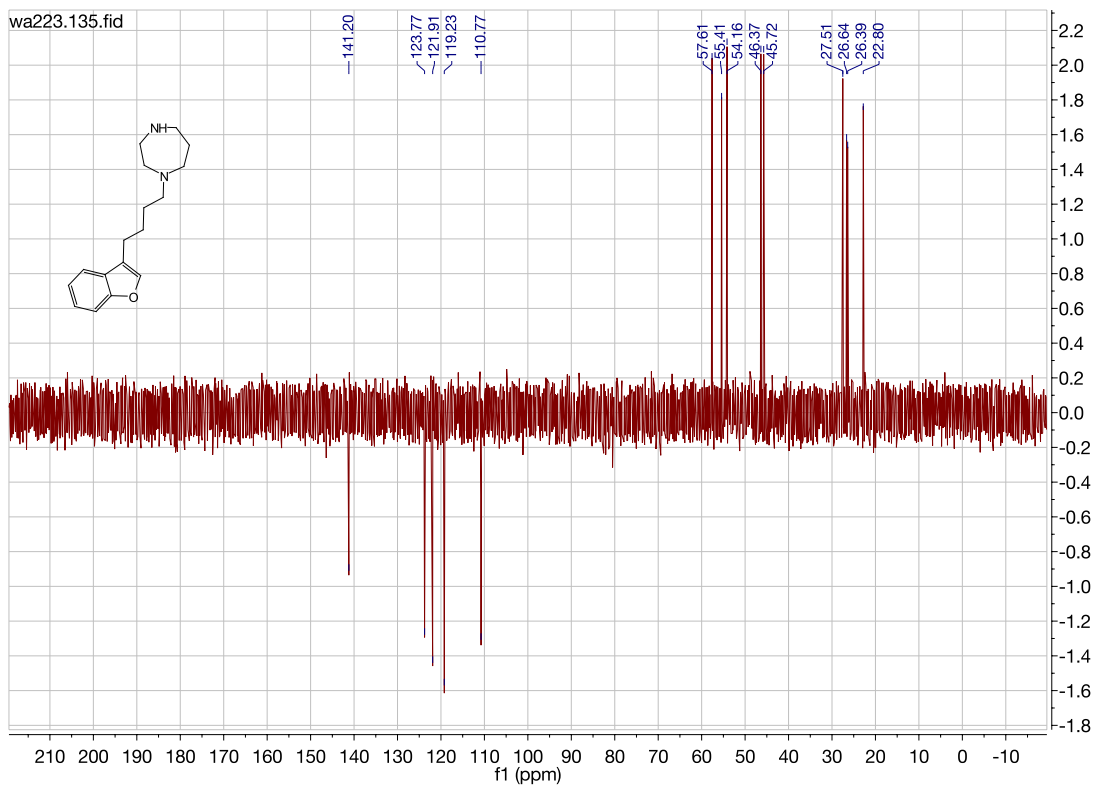




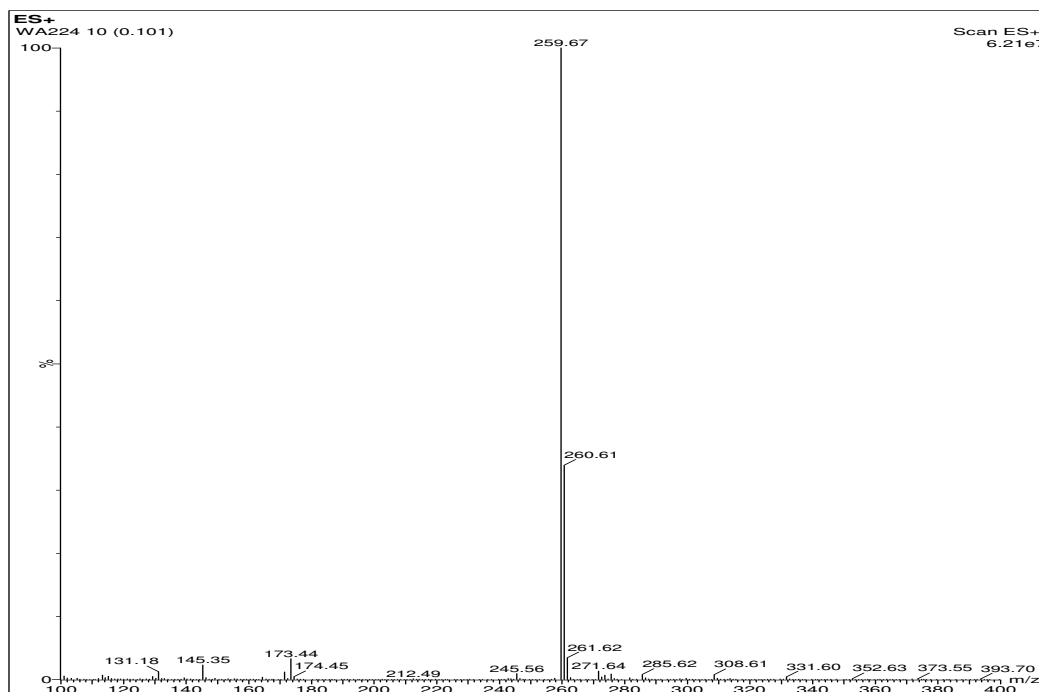


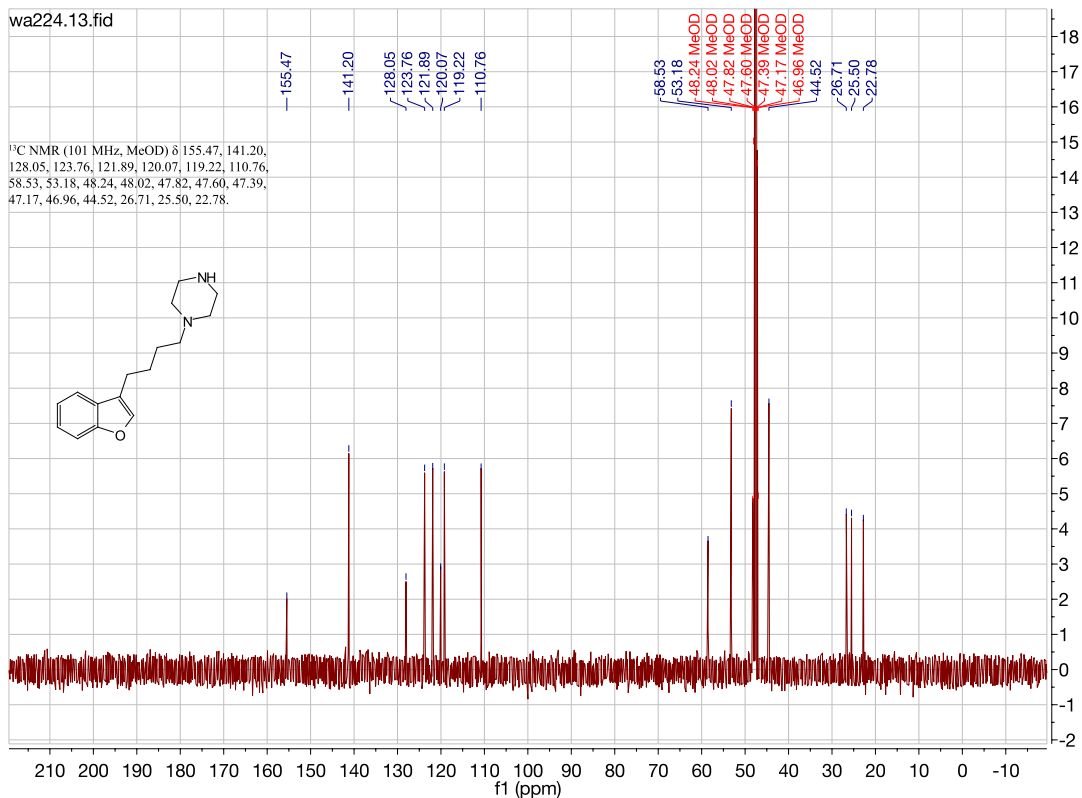
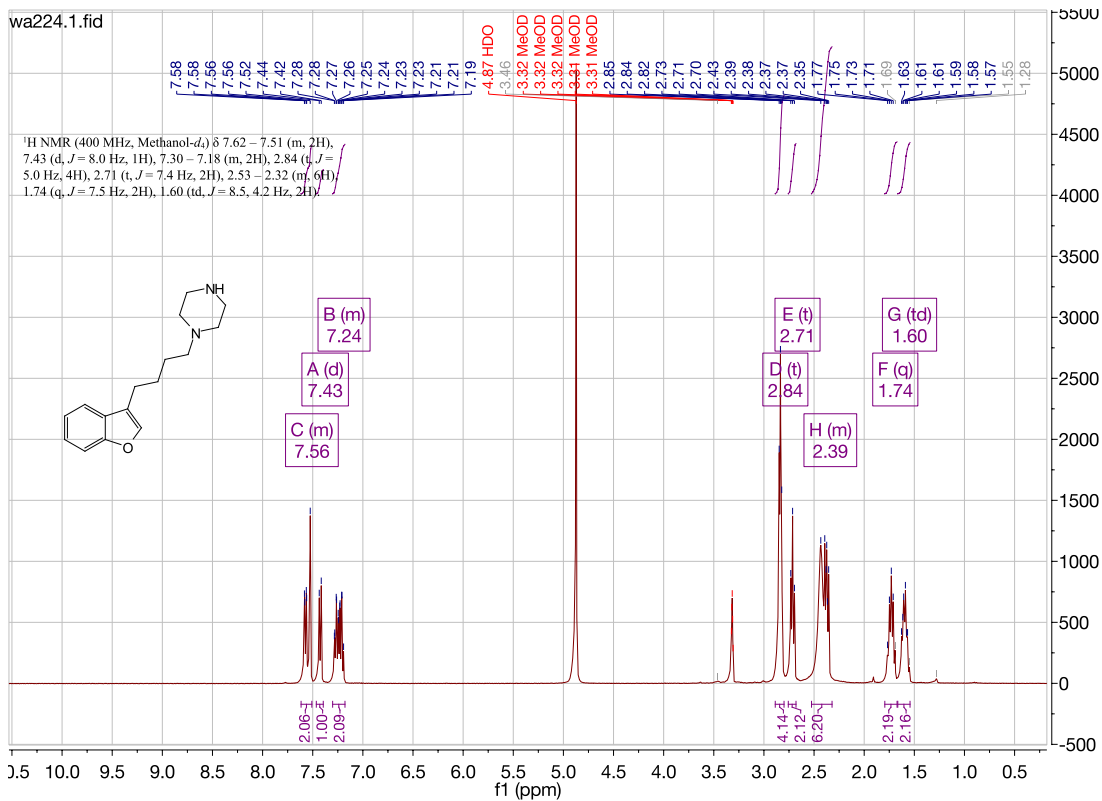
1-(4-(benzofuran-3-yl)butyl)-1,4-diazepane. (WA223)

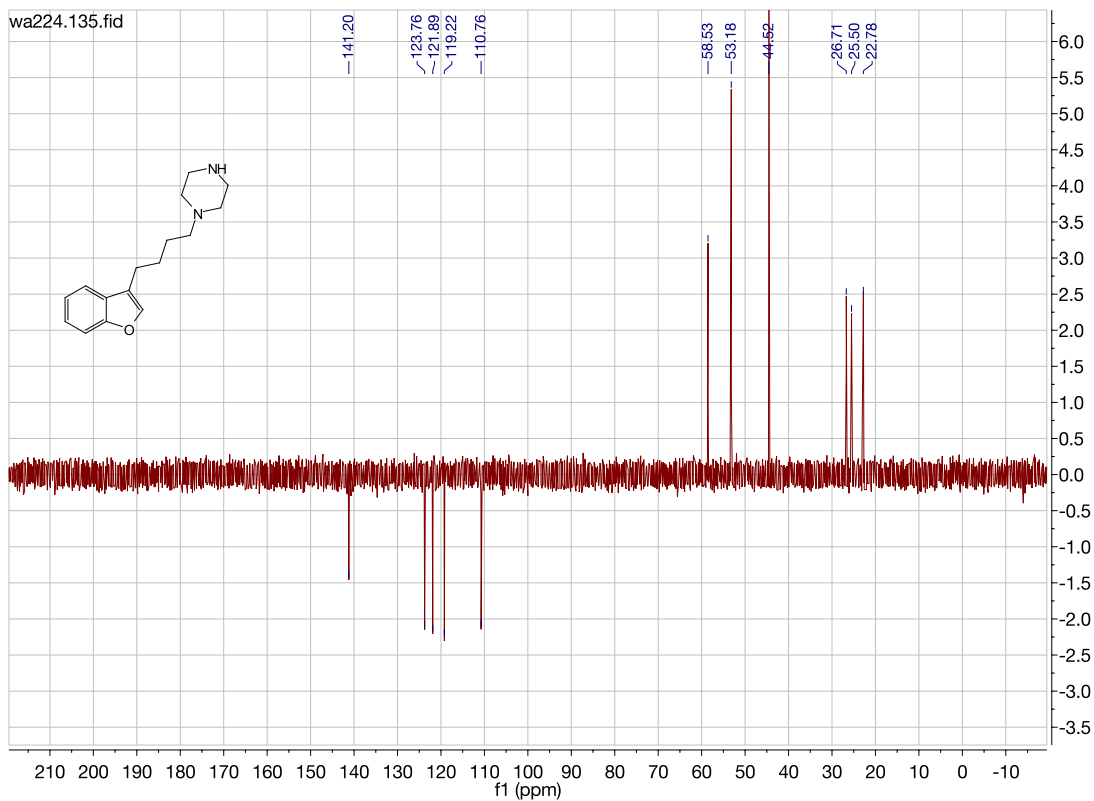




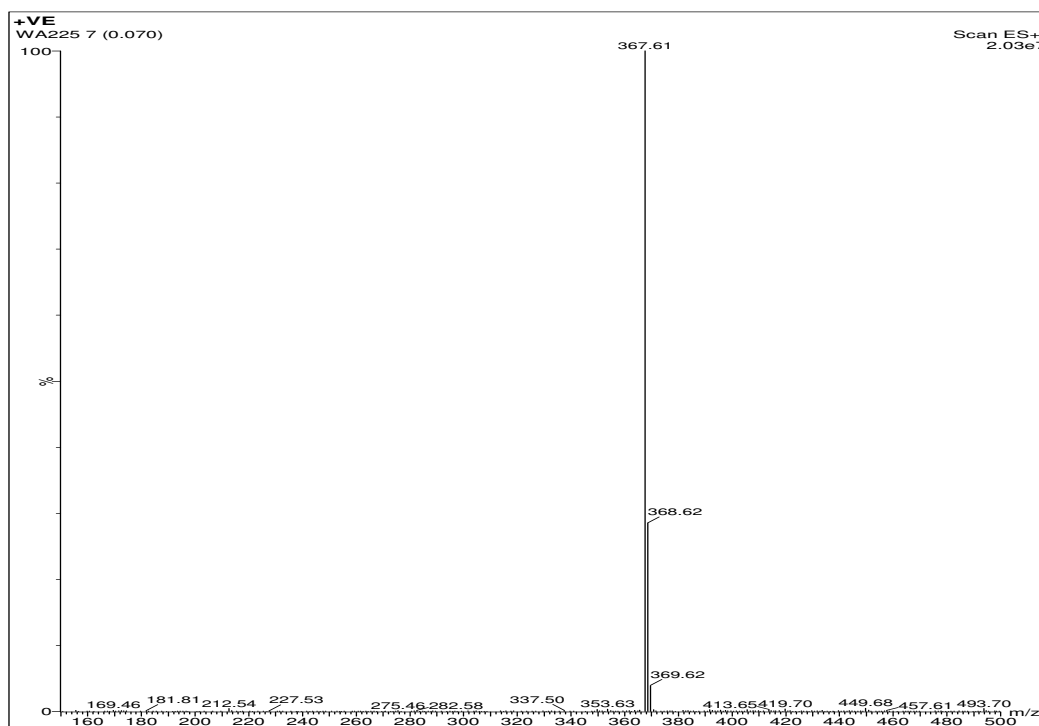
1-(4-(benzofuran-3-yl)butyl)piperazine. (WA224)

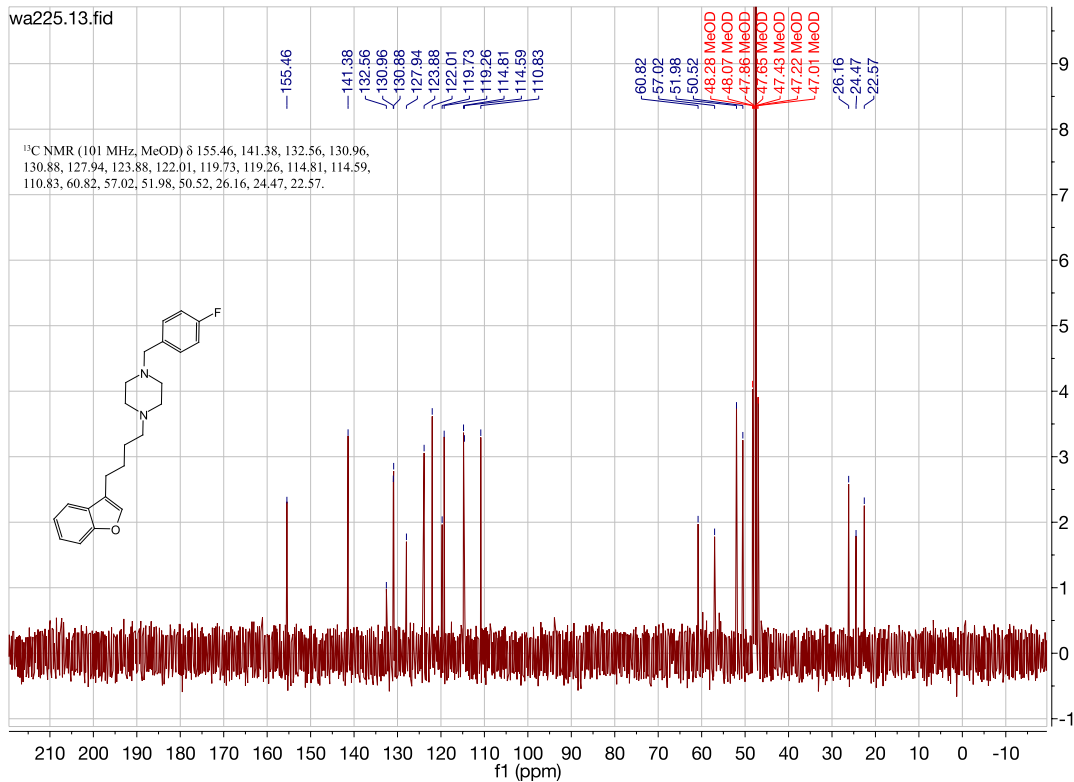
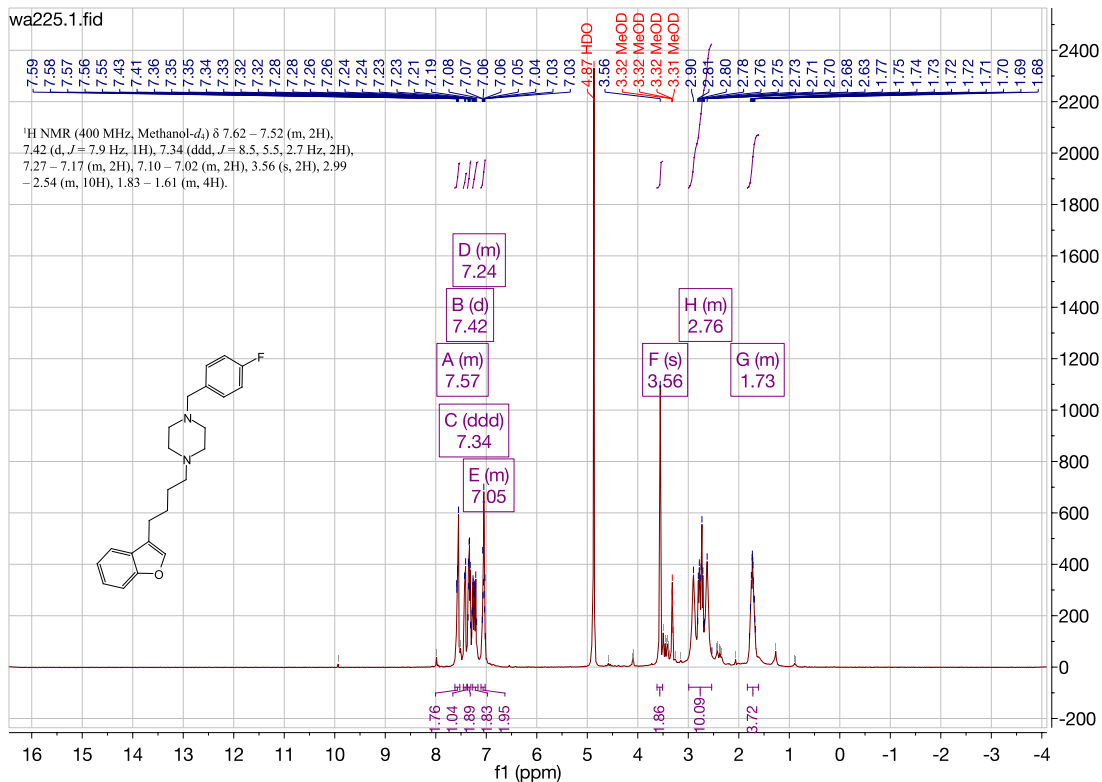


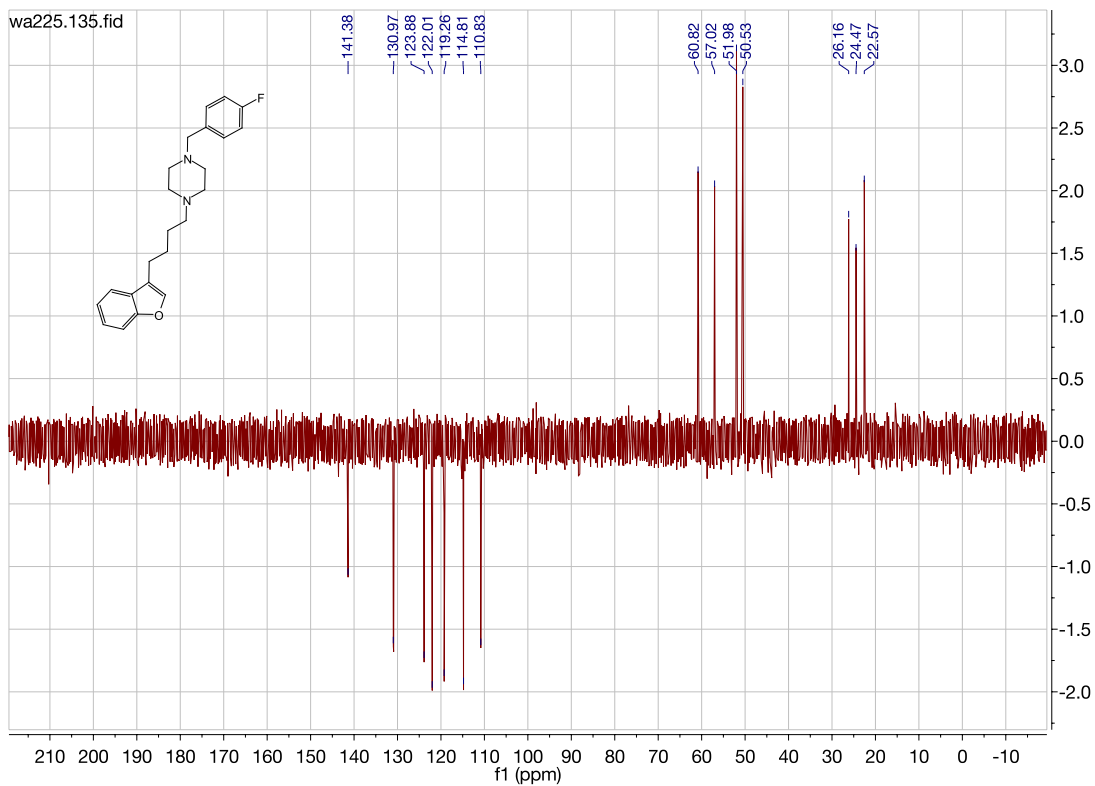




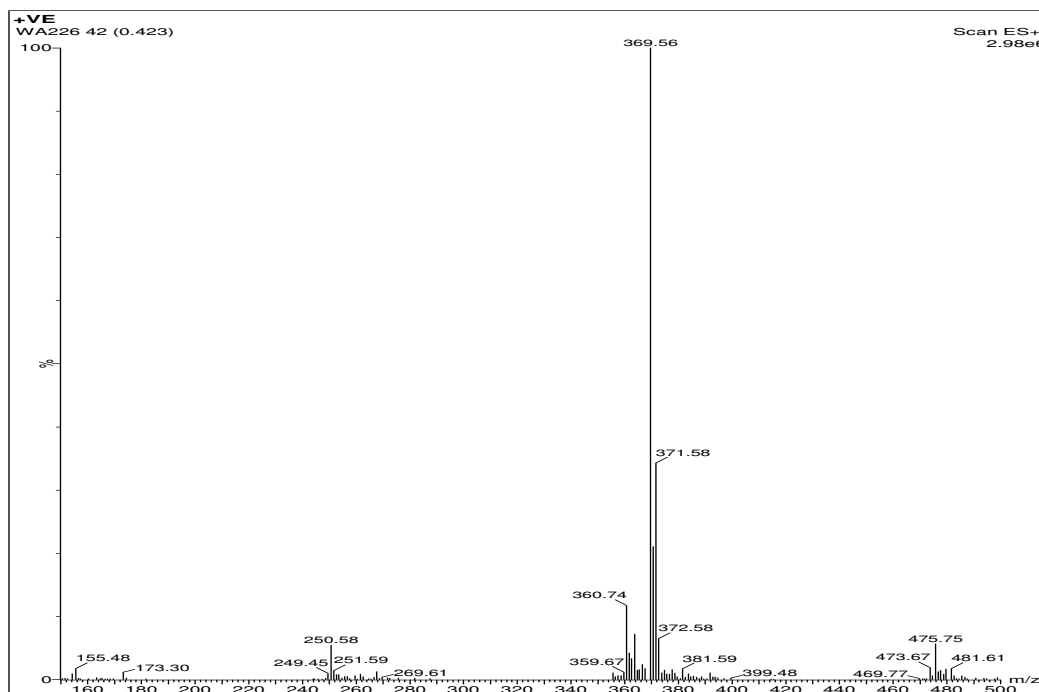
1-(4-(benzofuran-3-yl)butyl)-4-(4-fluorobenzyl)piperazine. (WA225)

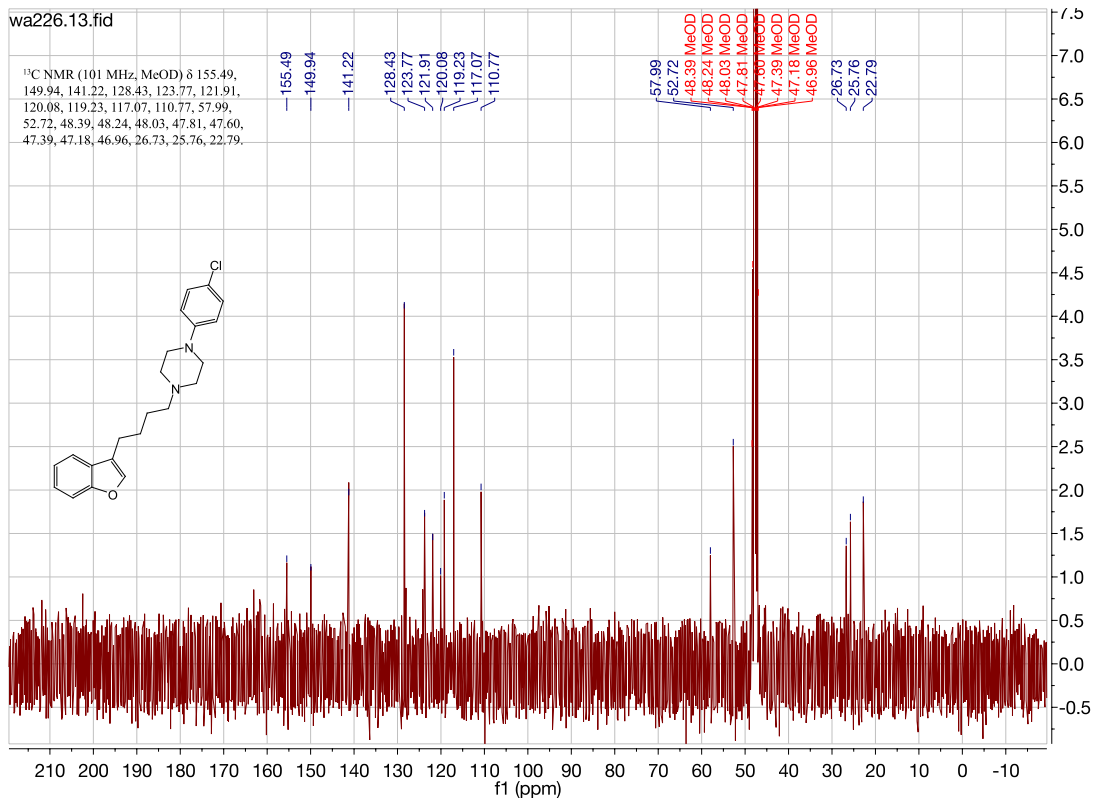
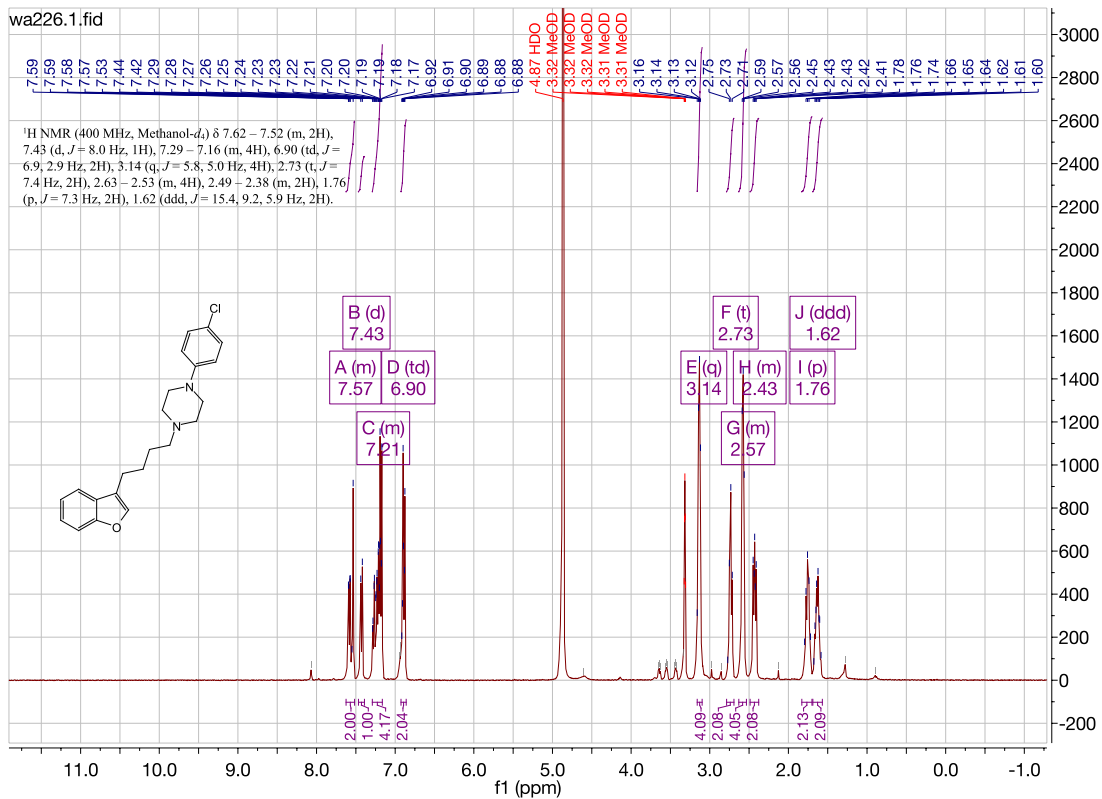


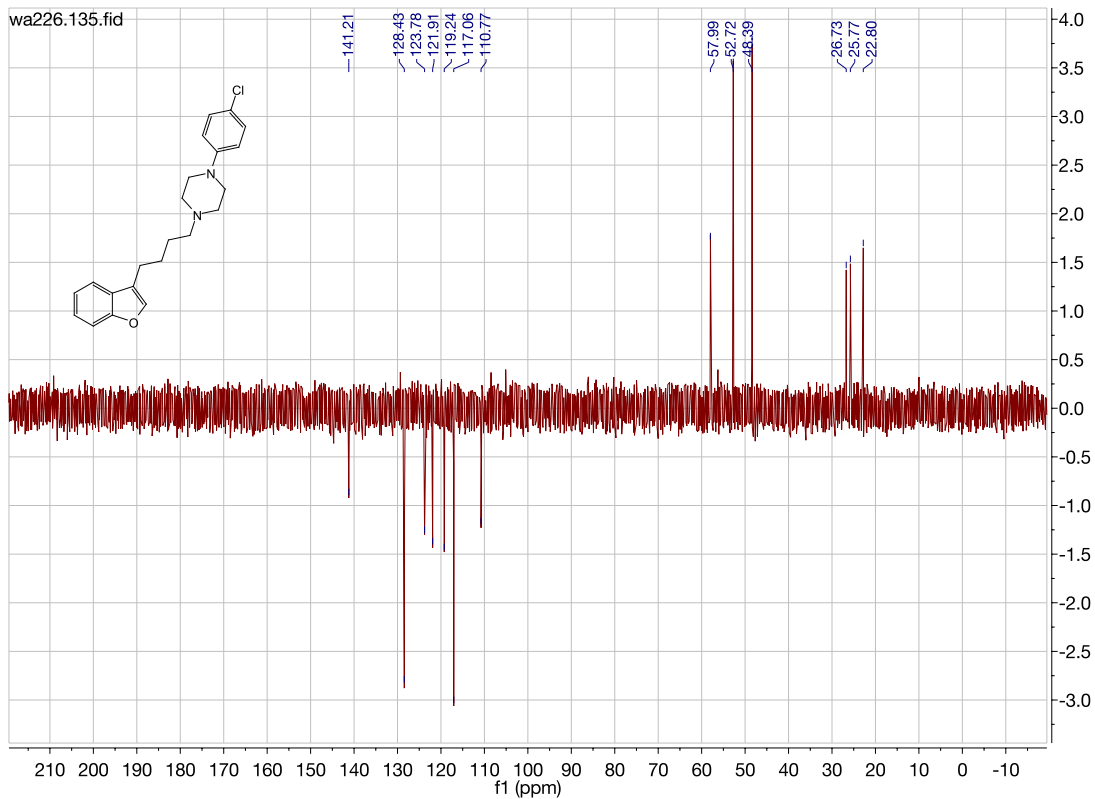




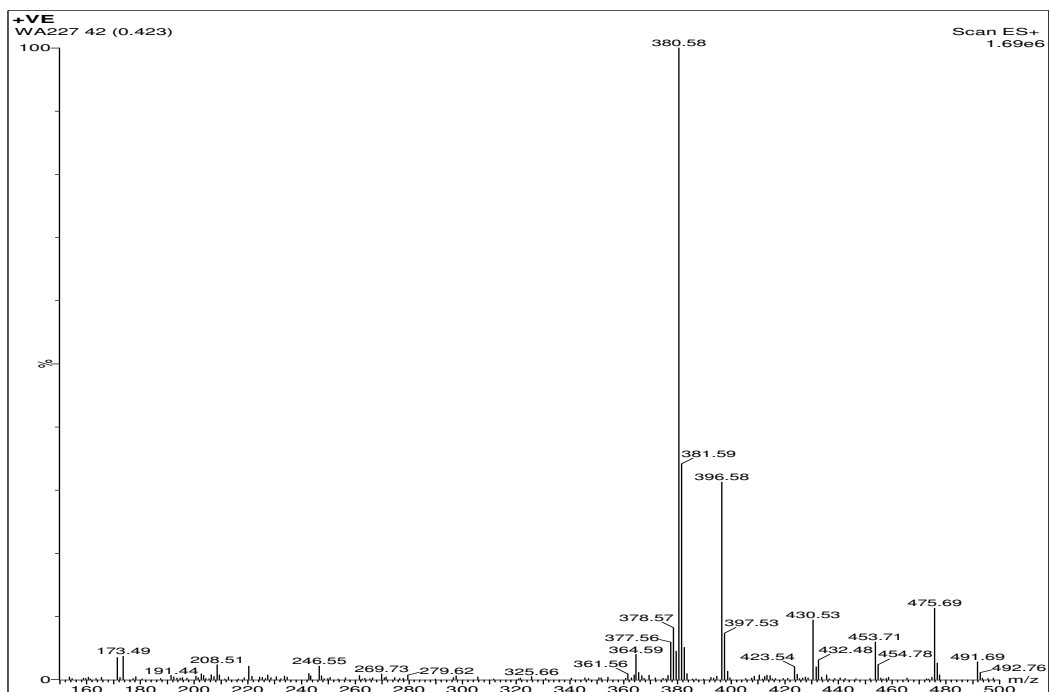
1-(4-(benzofuran-3-yl)butyl)-4-(4-chlorophenyl)piperazine. (WA226)

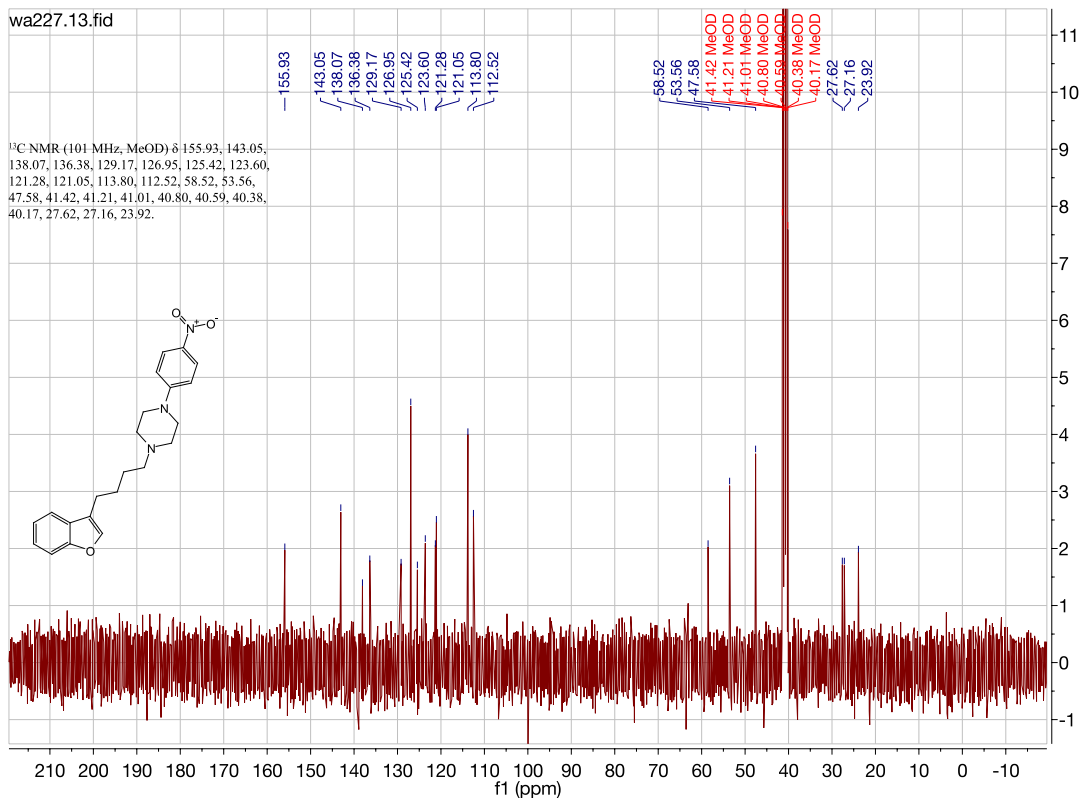
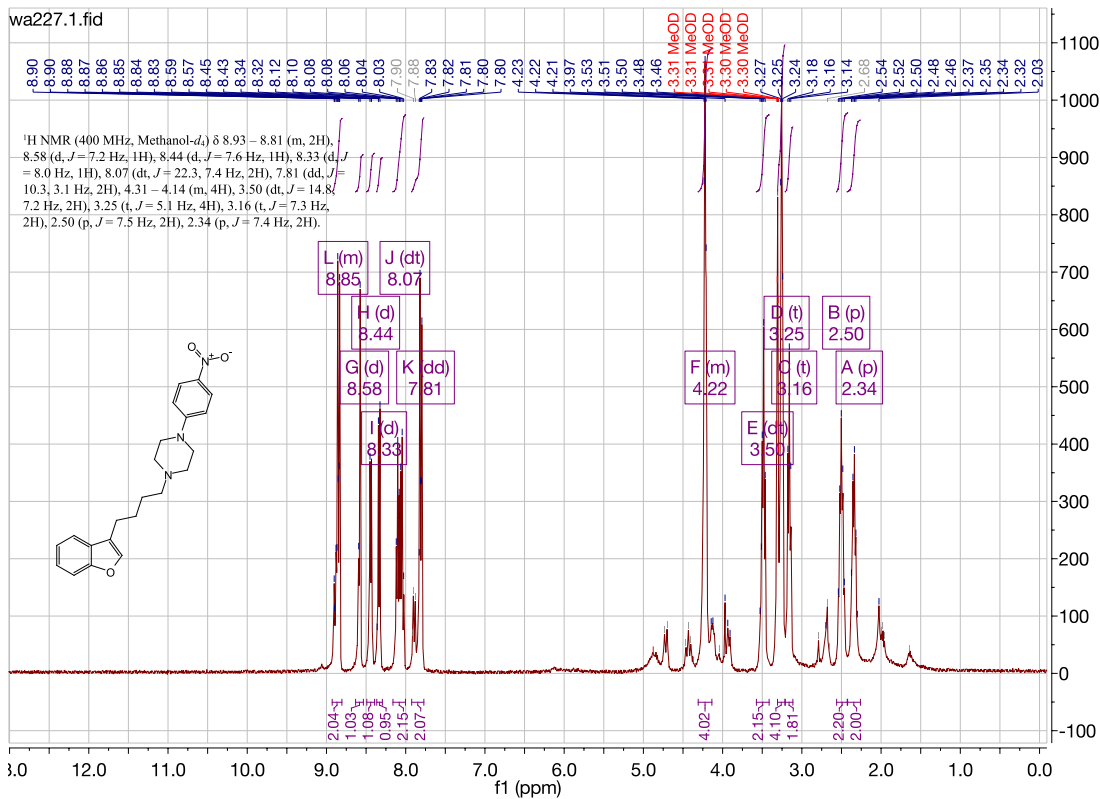


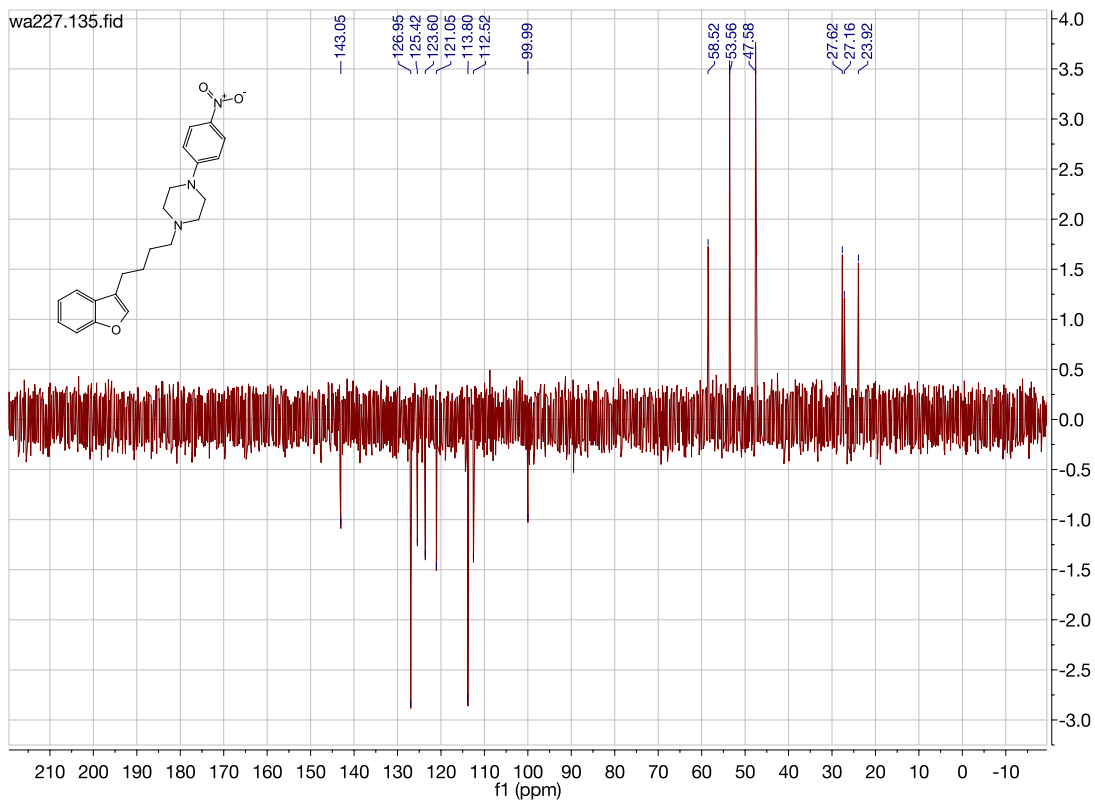




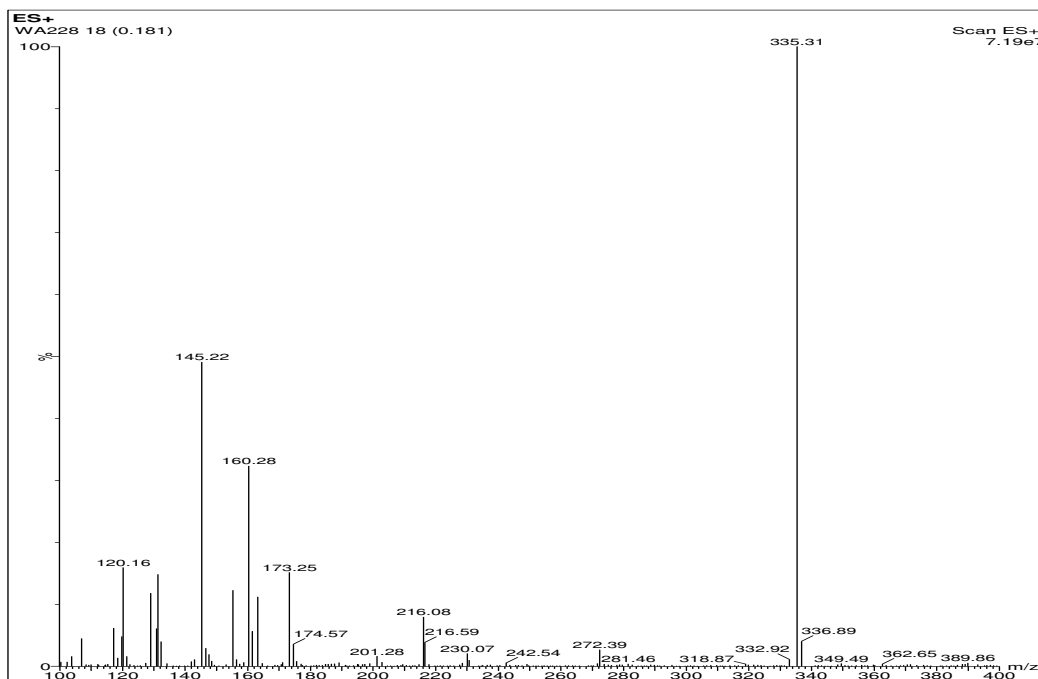
1-(4-(benzofuran-3-yl)butyl)-4-(4-nitrophenyl)piperazine. (WA227)

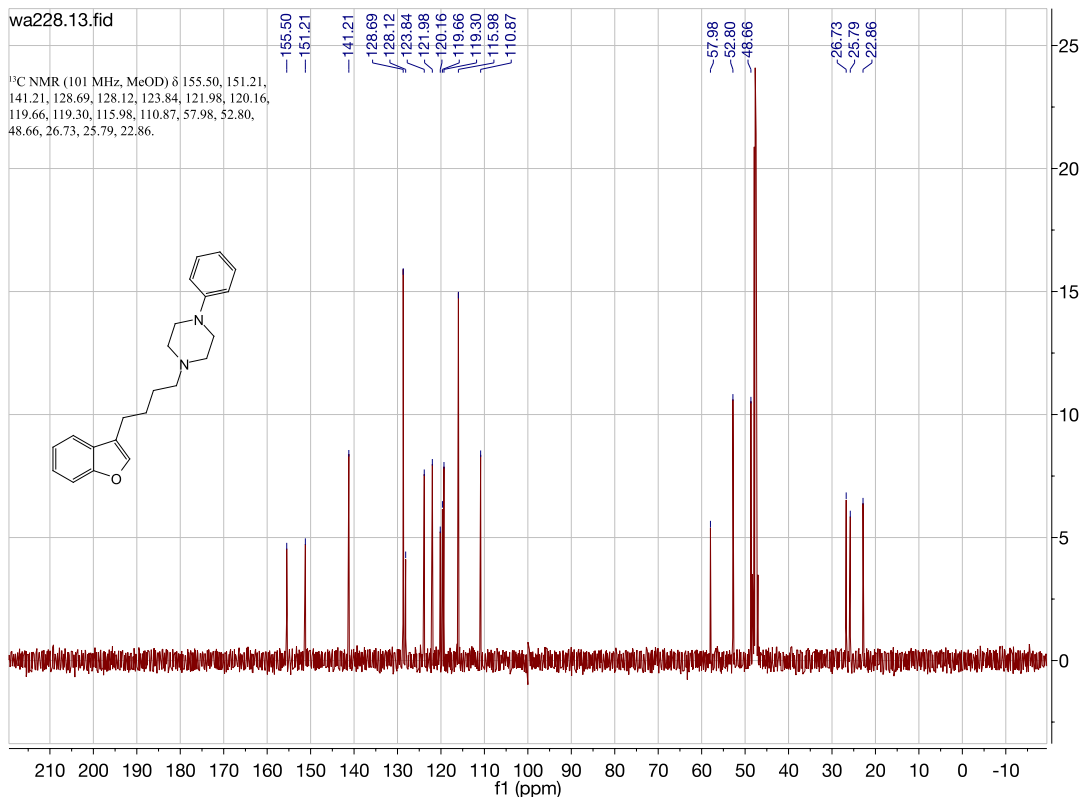
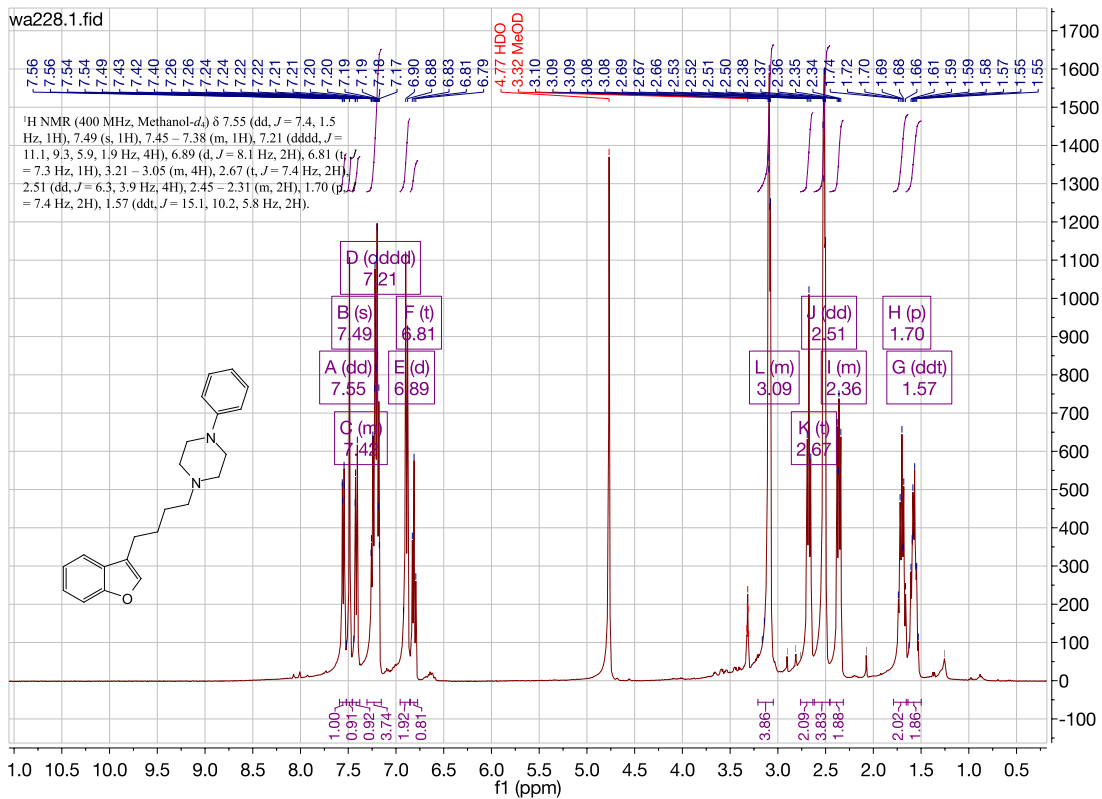


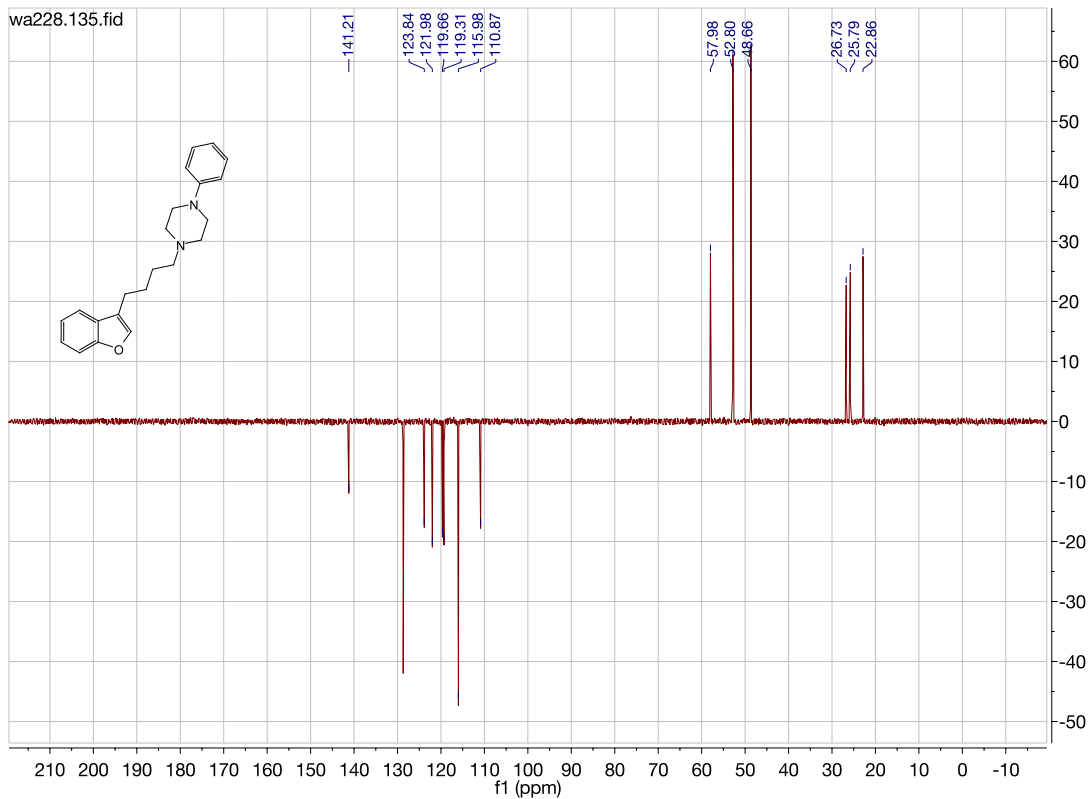




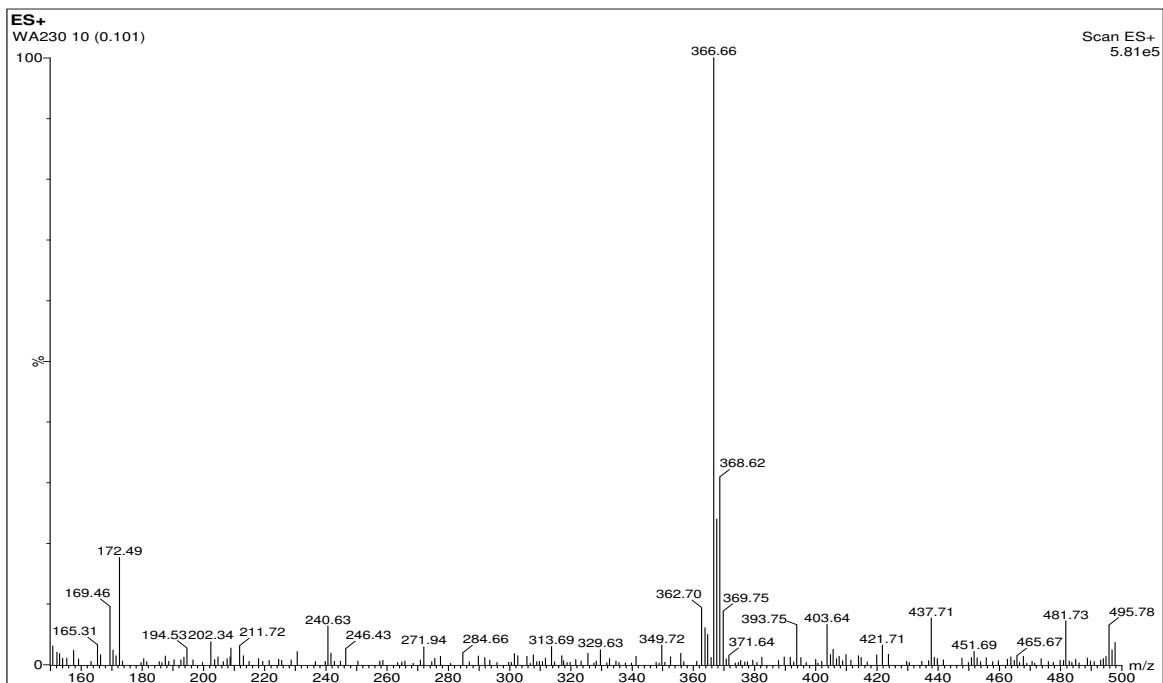
1-(4-(benzofuran-3-yl)butyl)-4-phenylpiperazine. (WA228)

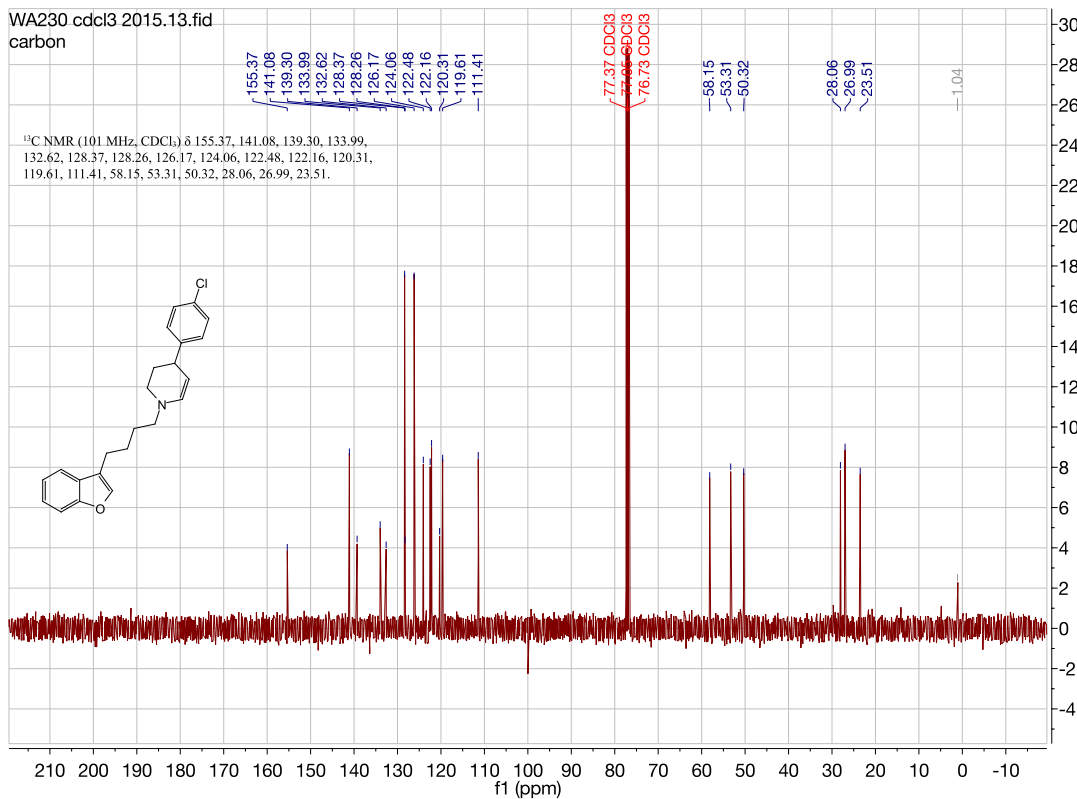
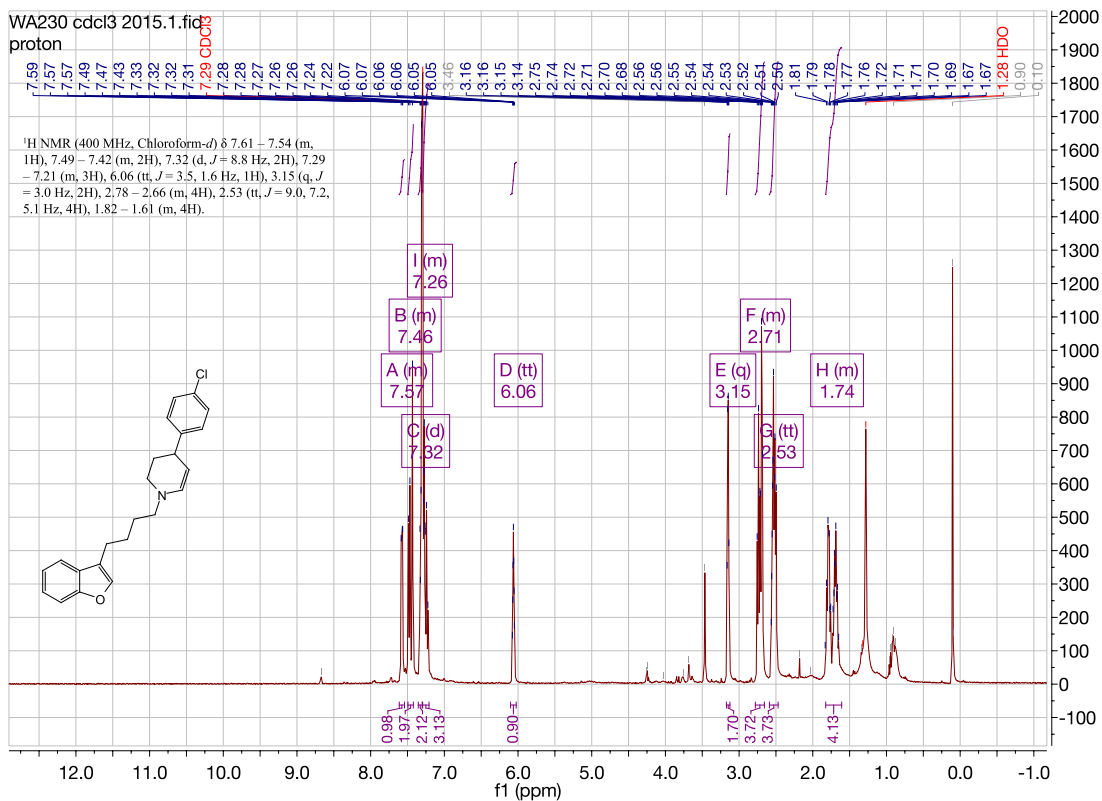


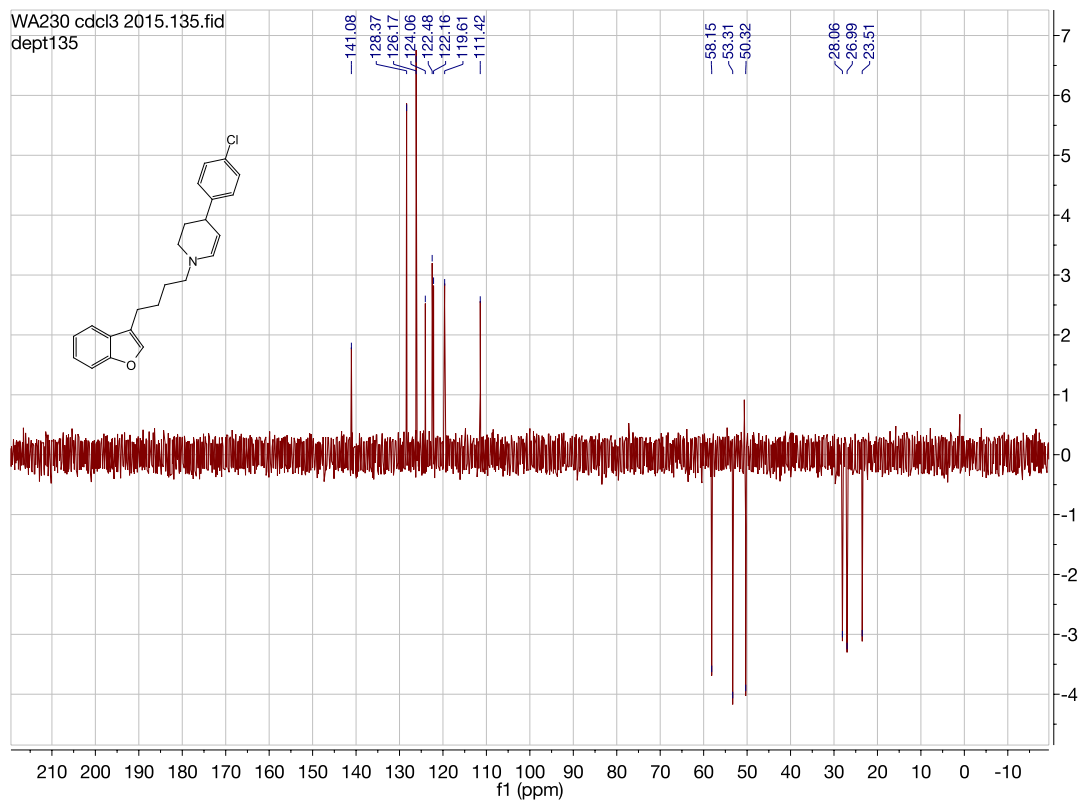




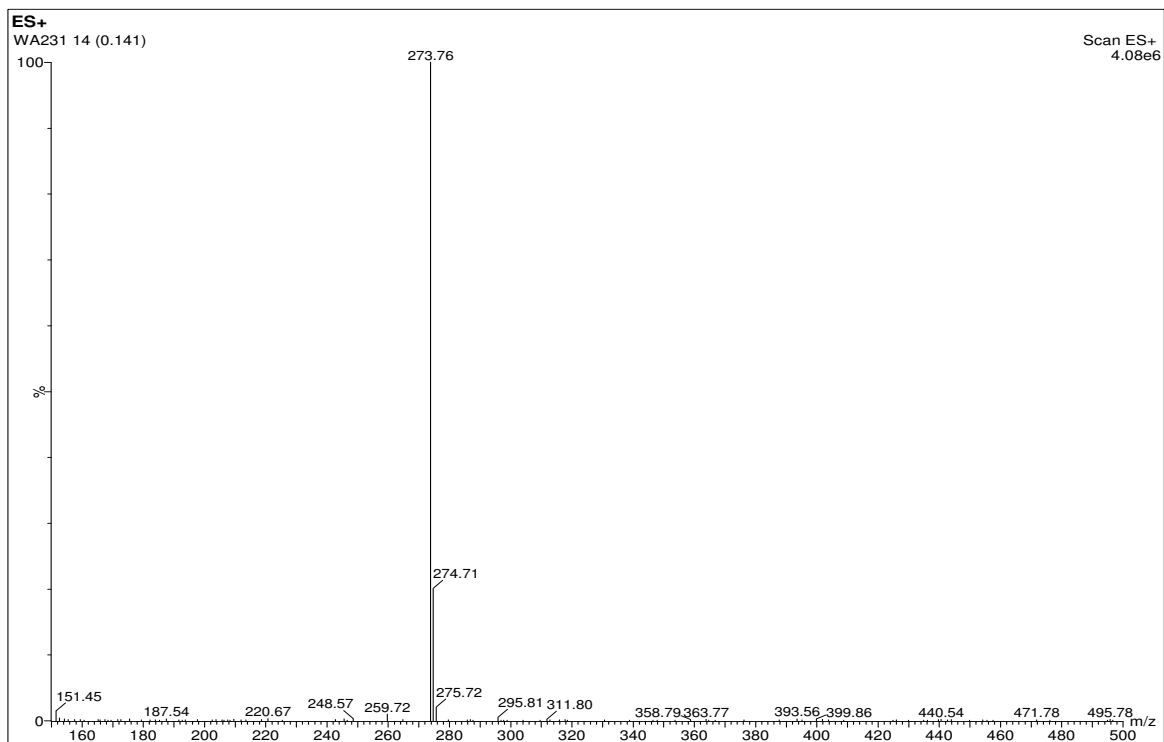
1-(4-(benzofuran-3-yl)butyl)-4-(4-chlorophenyl)-1,2,3,4-tetrahydropyridine. (WA230)

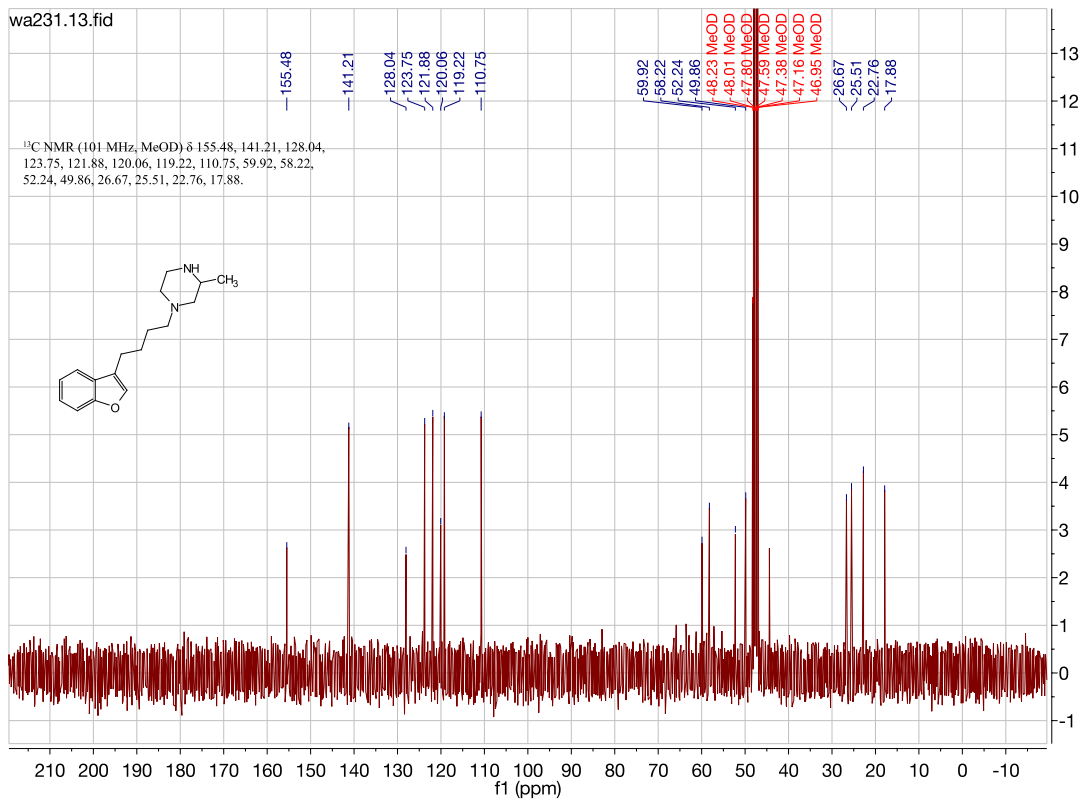
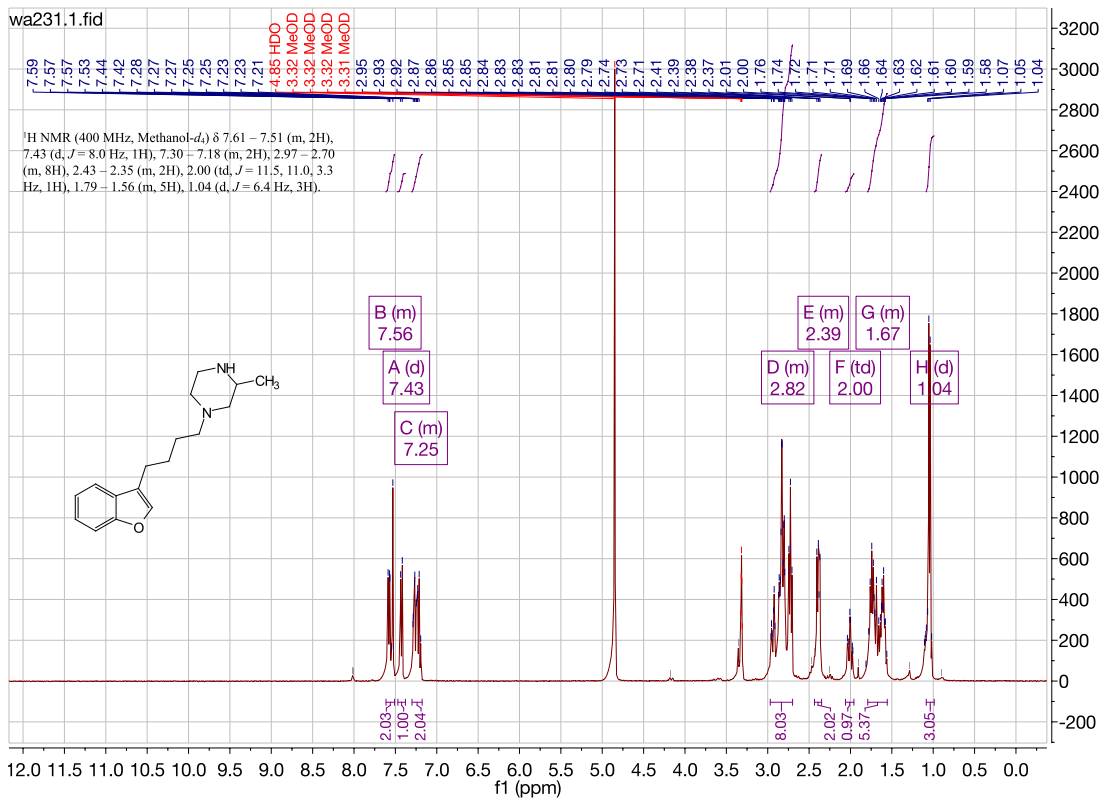


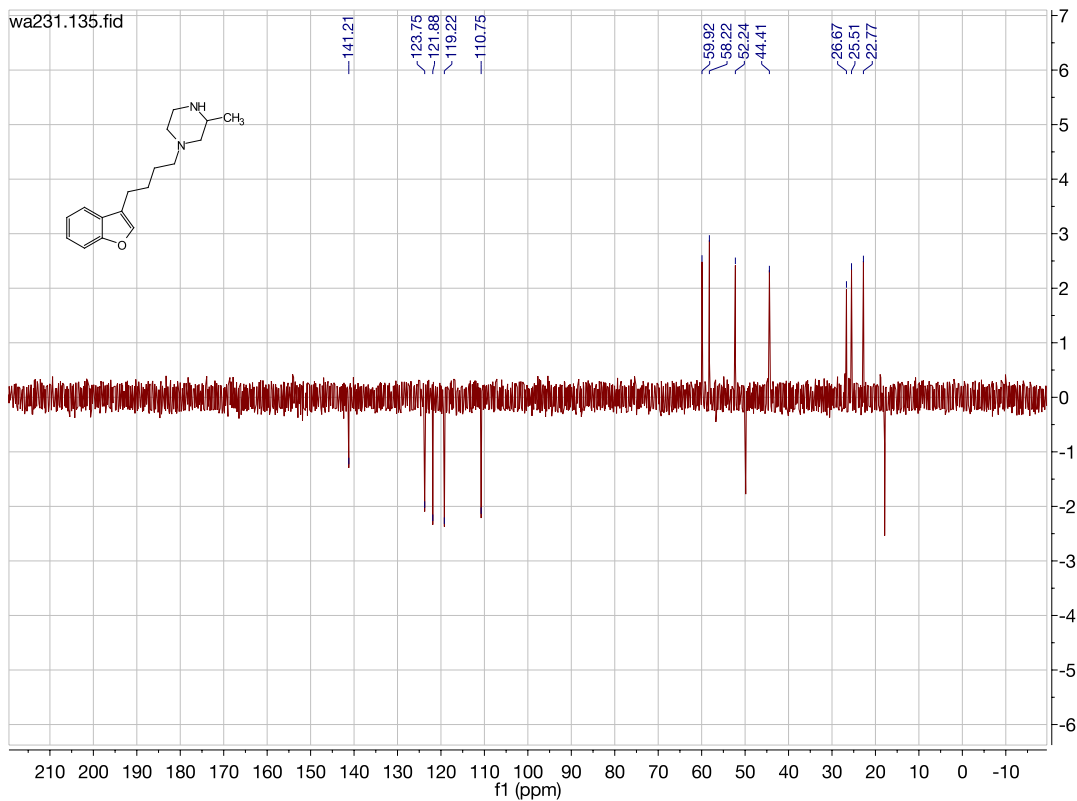




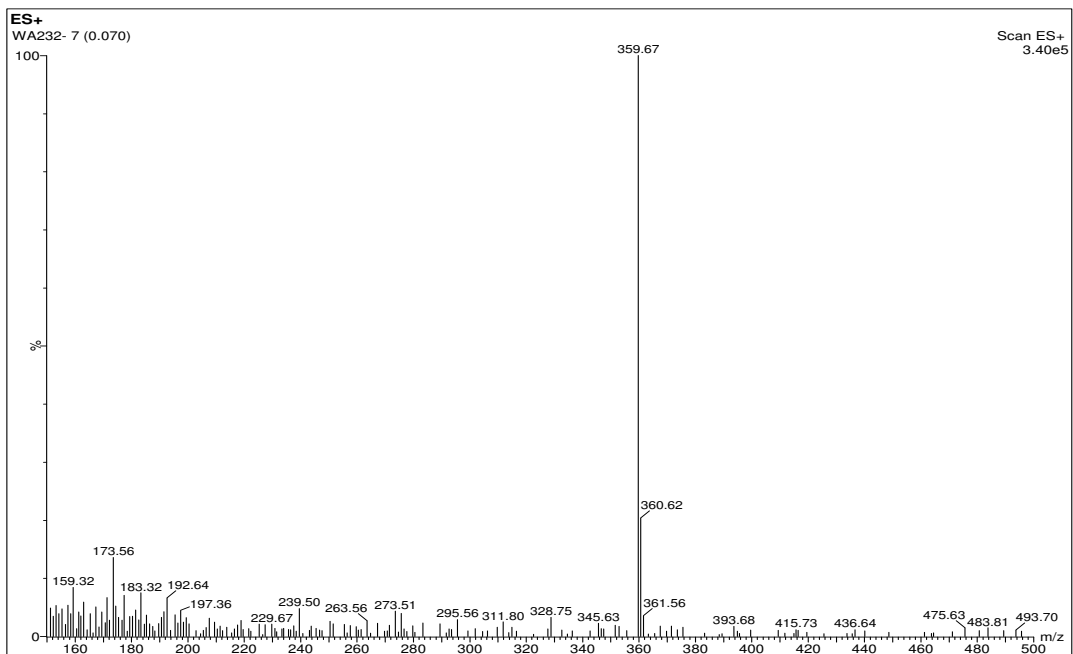
1-(4-(benzofuran-3-yl)butyl)-3-methylpiperazine. (WA231)

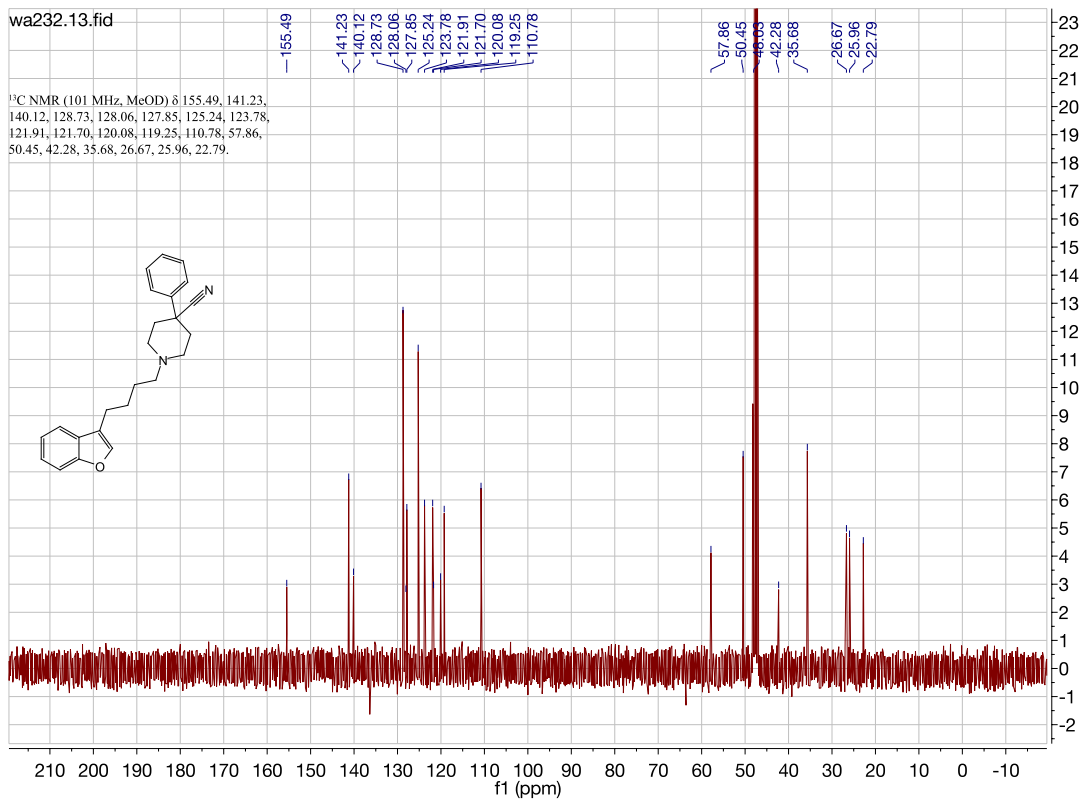
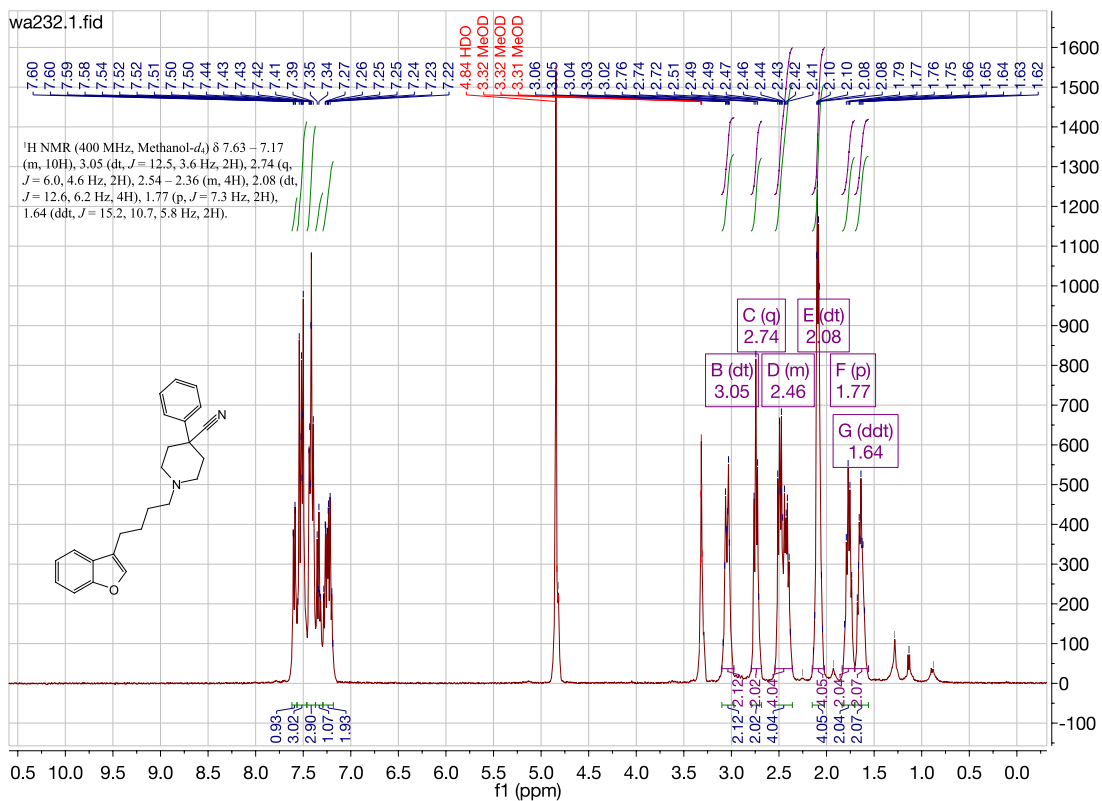


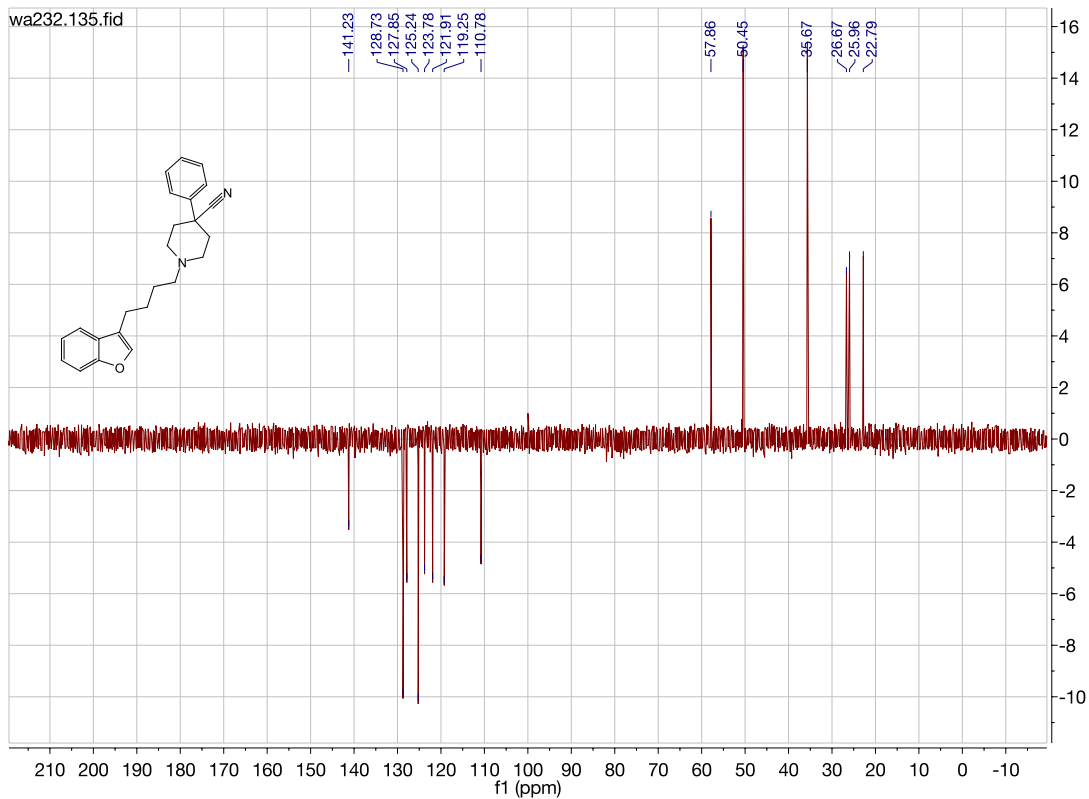




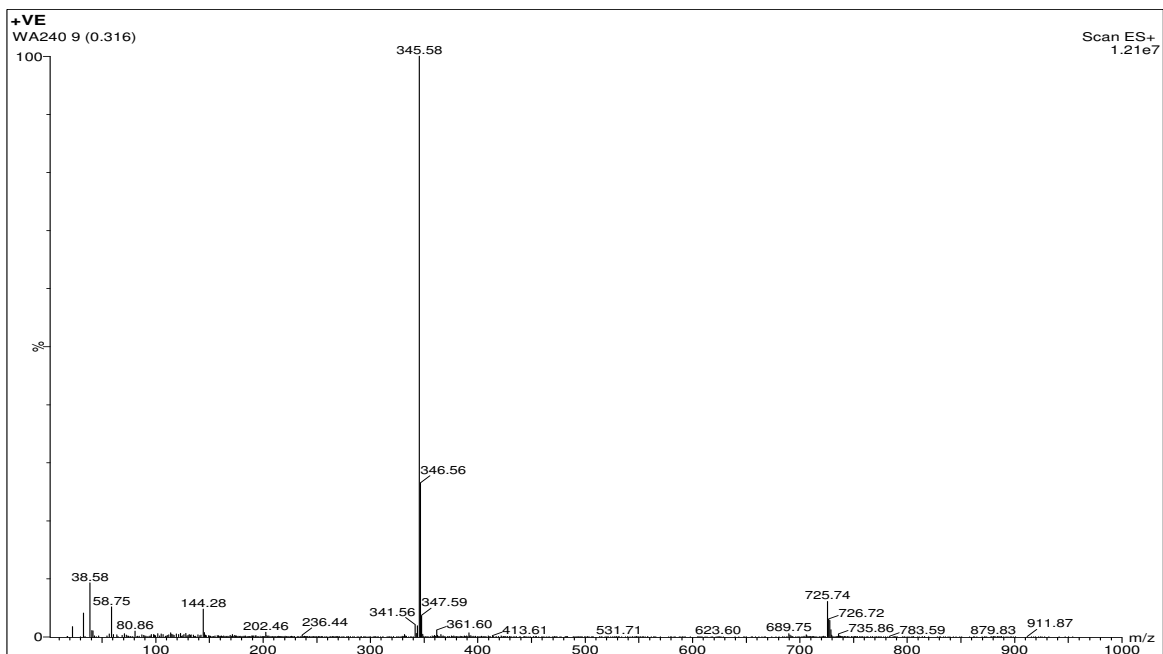
1-(4-(benzofuran-3-yl)butyl)-4-phenylpiperidine-4-carbonitrile. (WA232)

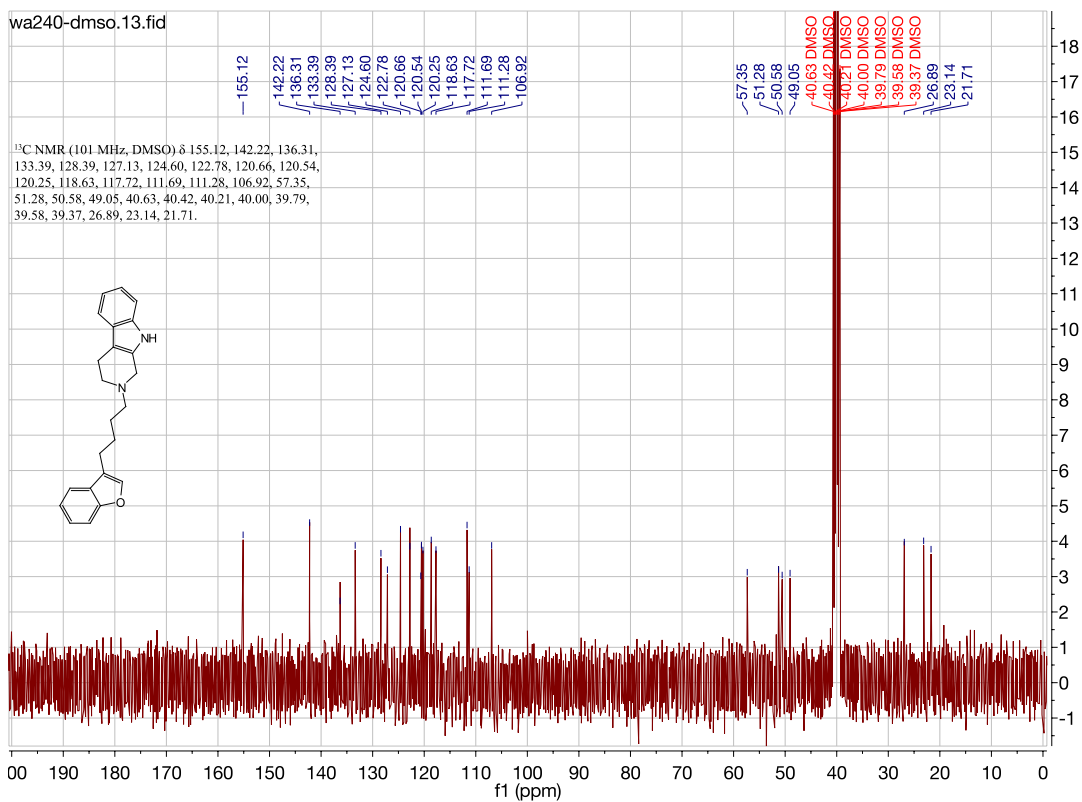
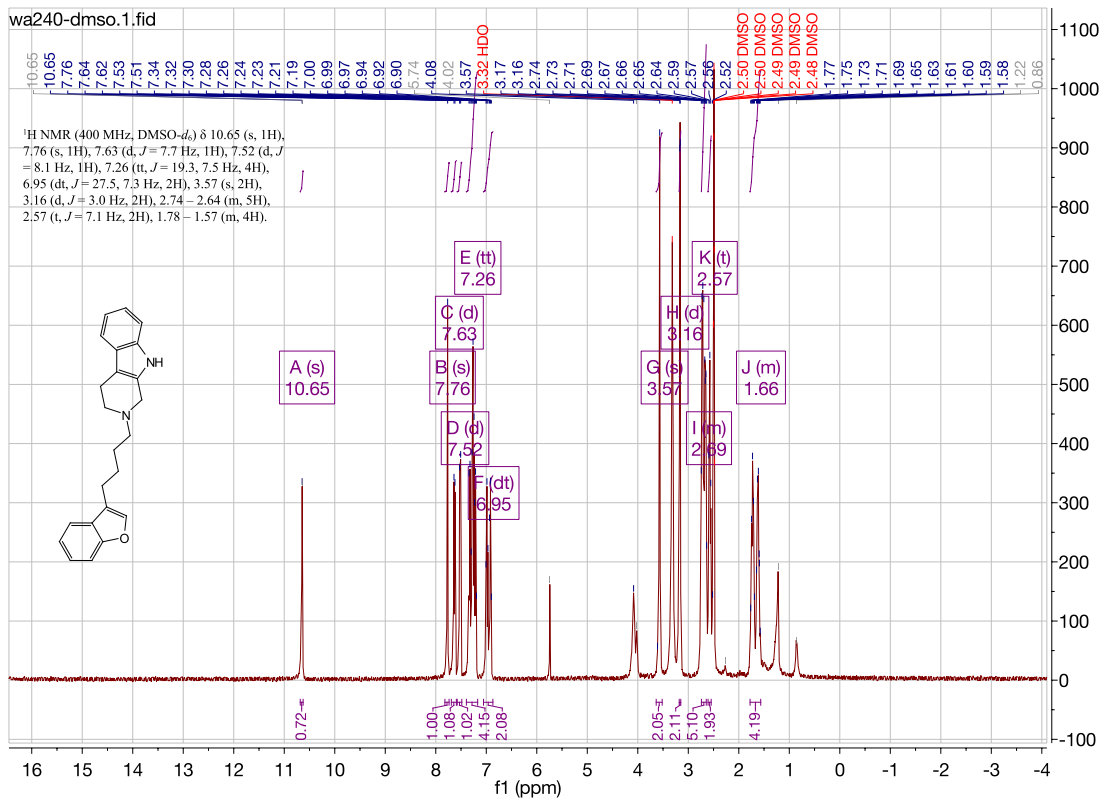


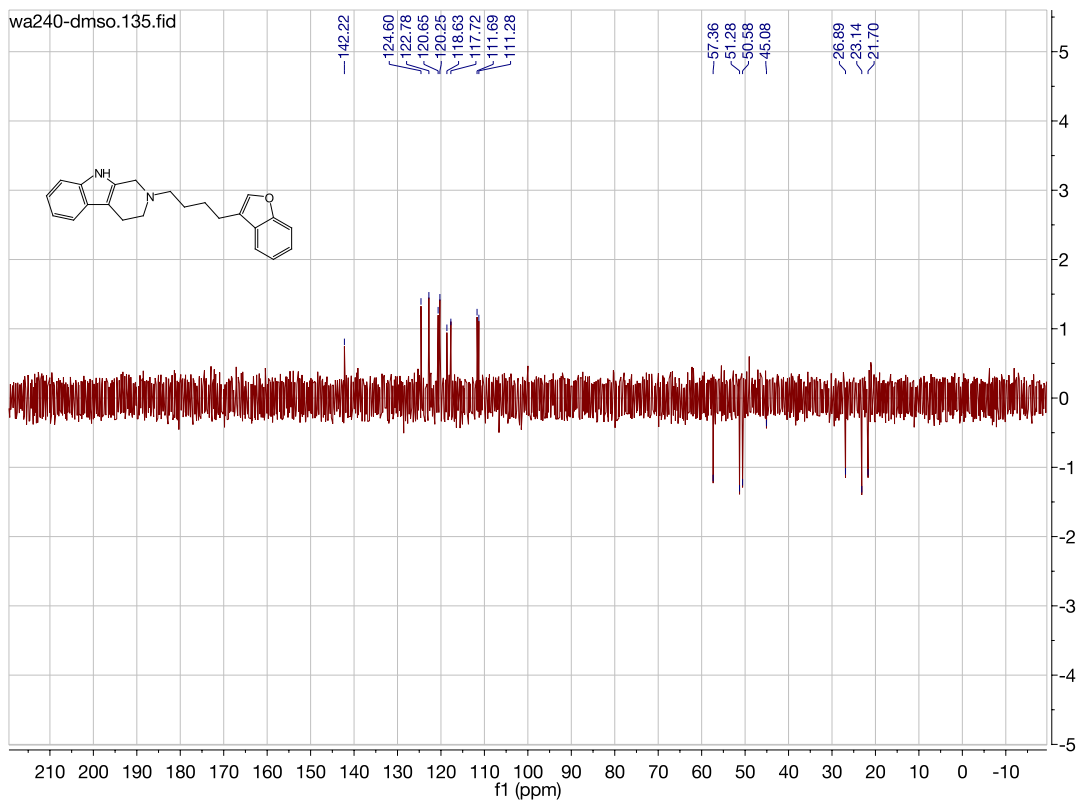




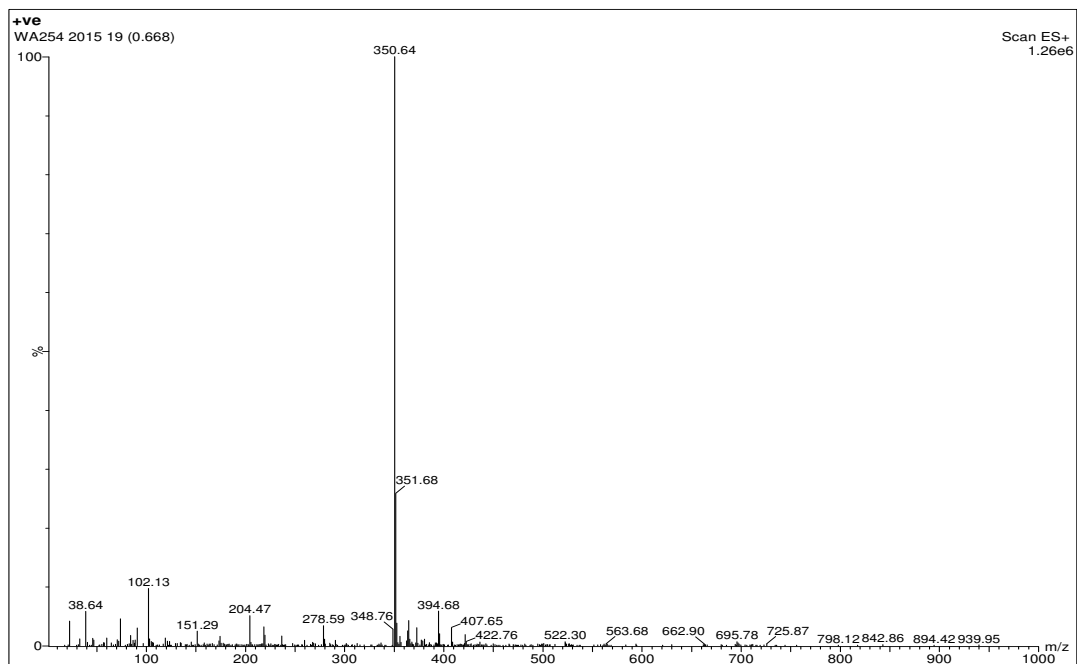
2-(4-(benzofuran-3-yl)butyl)-2,3,4,9-tetrahydro-1H-pyrido[3,4-b]indole. (WA240)

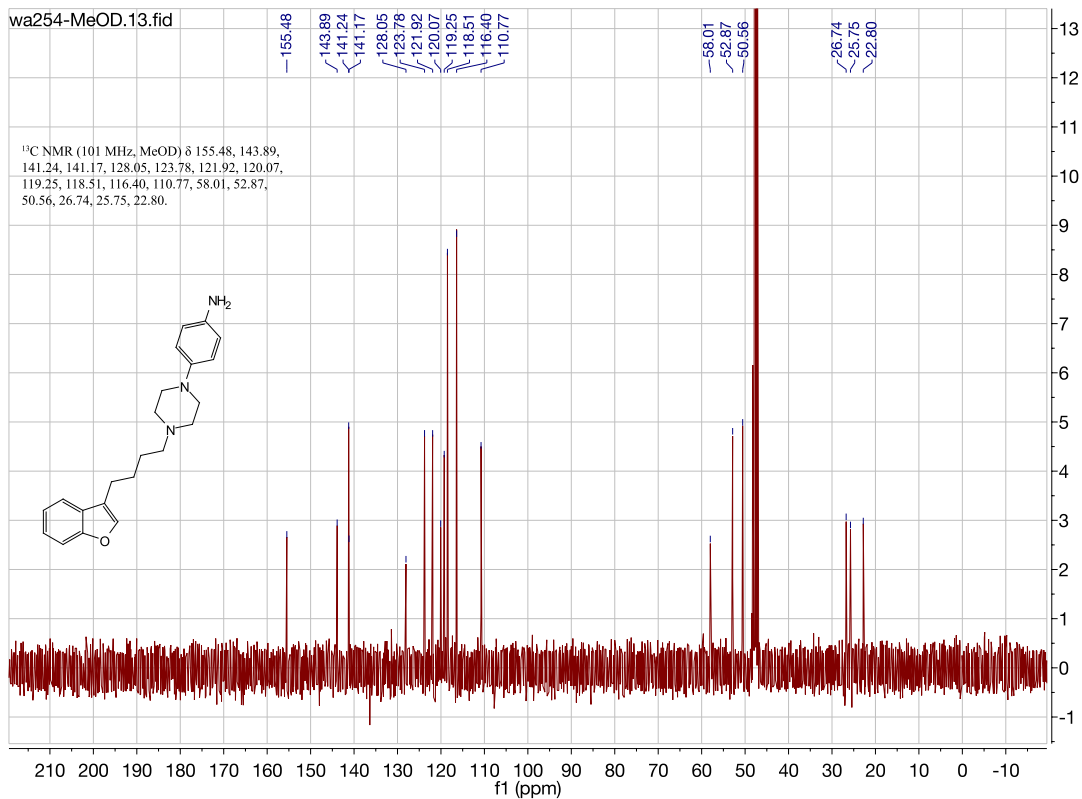
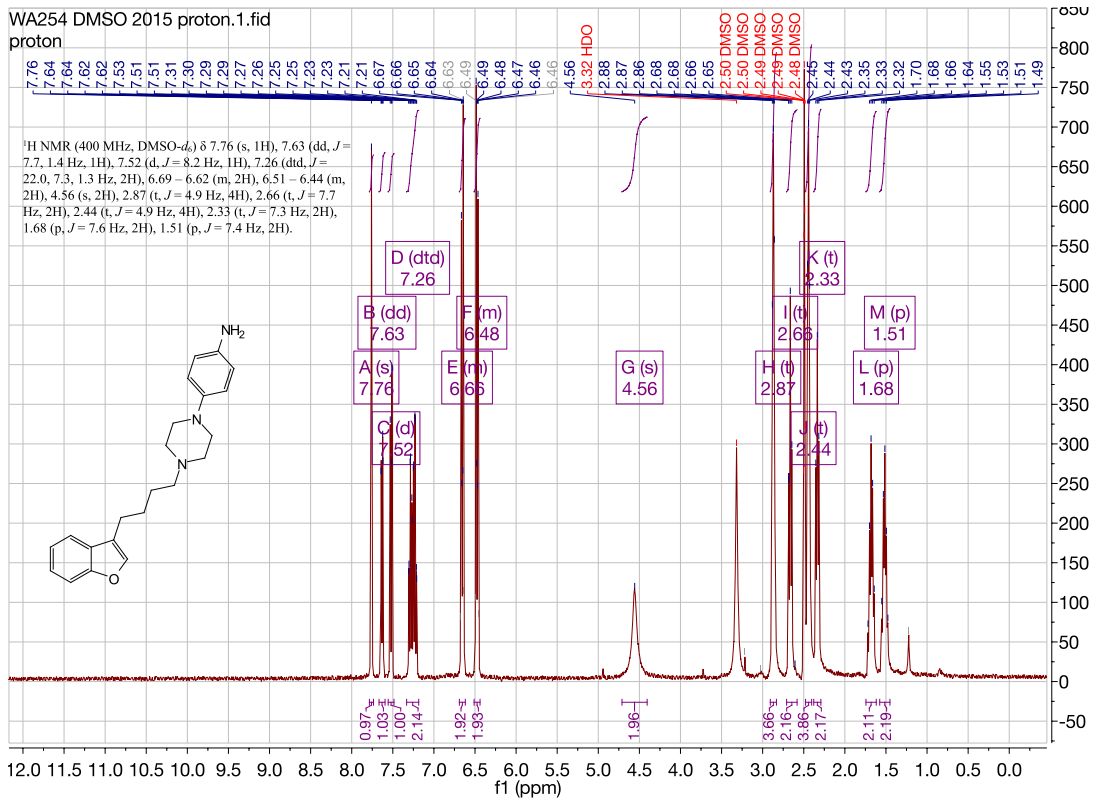


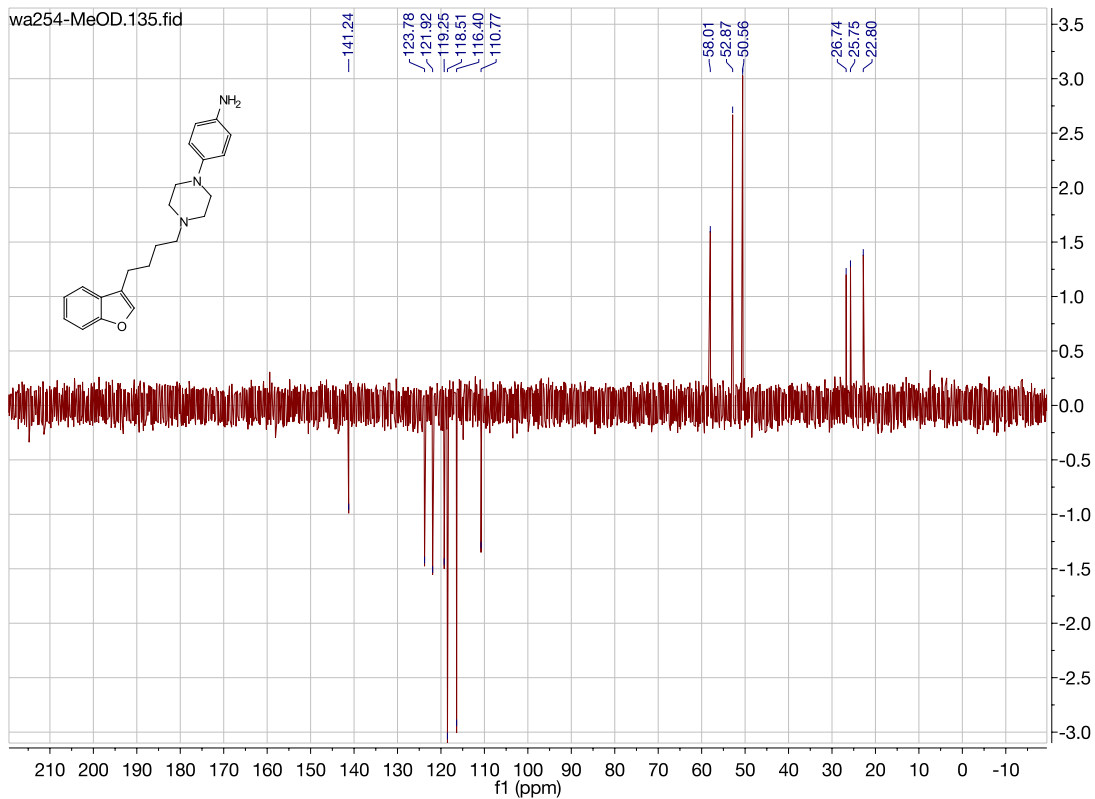




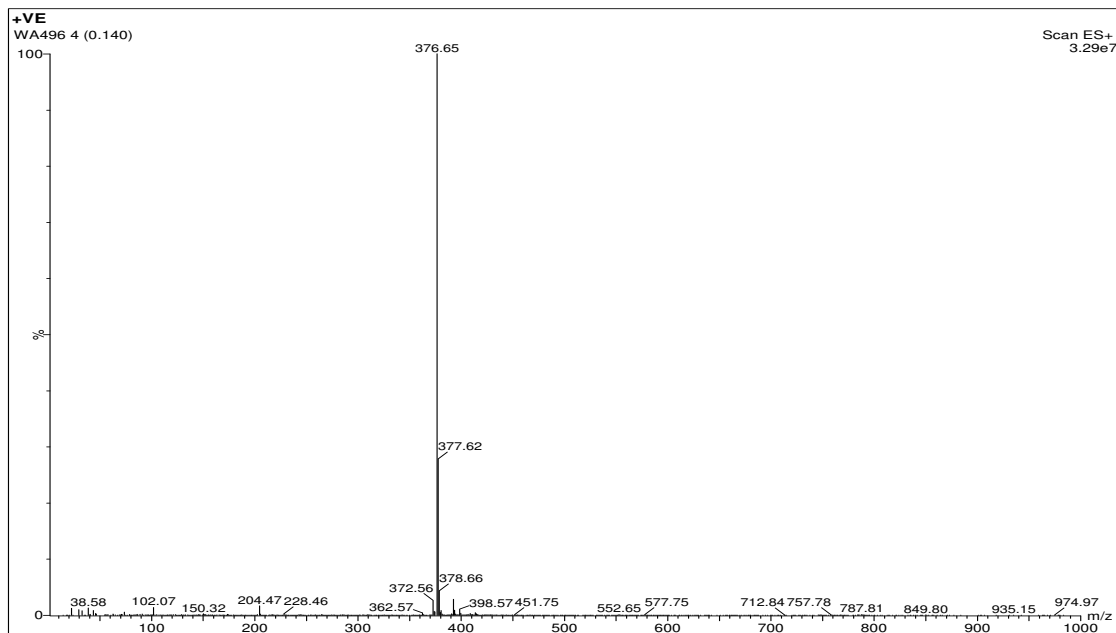
4-(4-(4-(benzofuran-3-yl)butyl)piperazin-1-yl)aniline. (WA254)

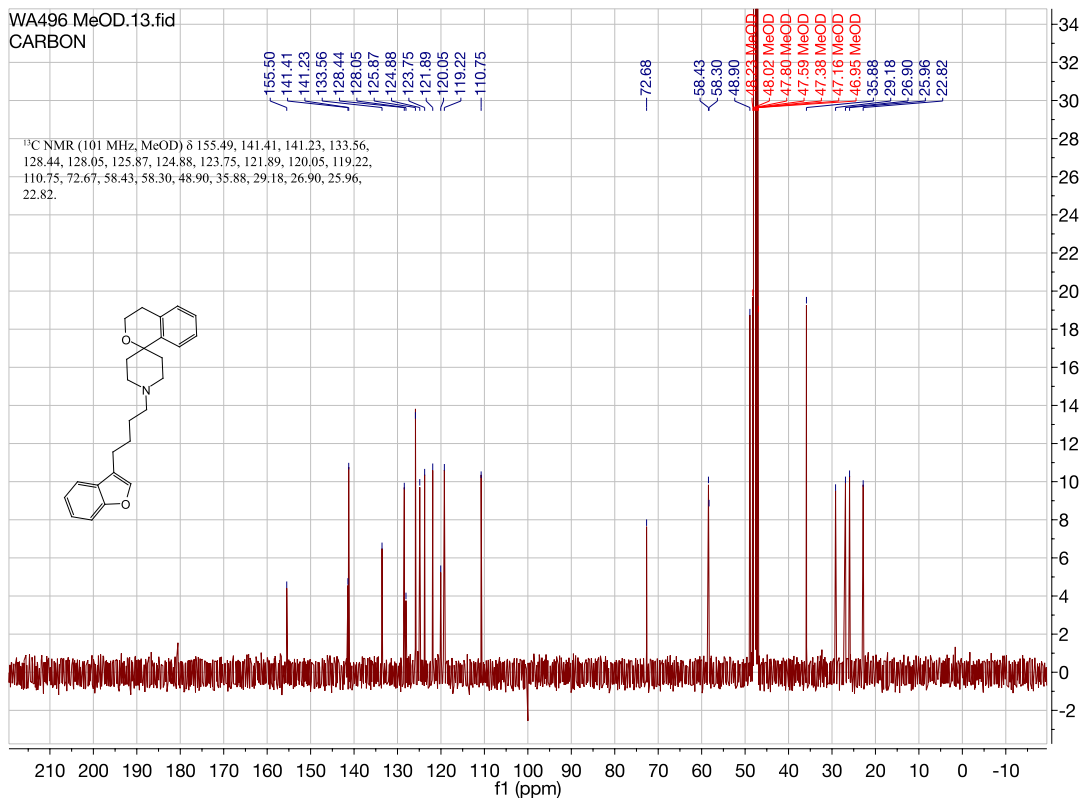
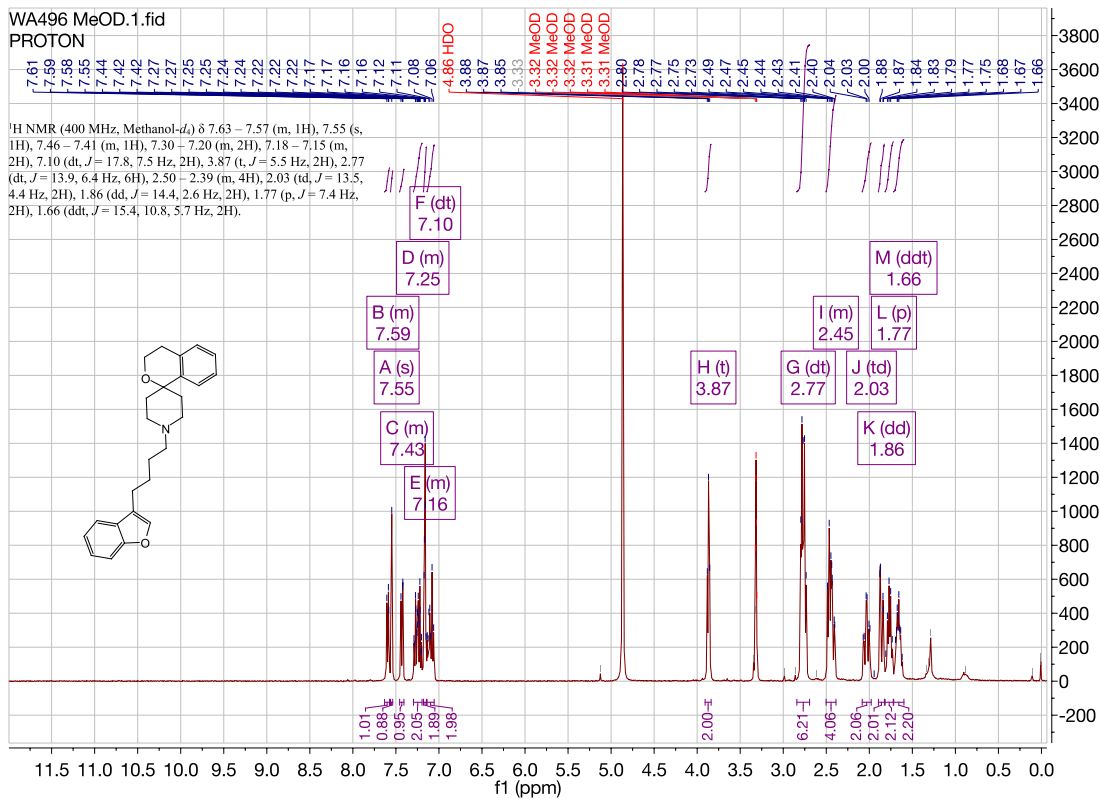




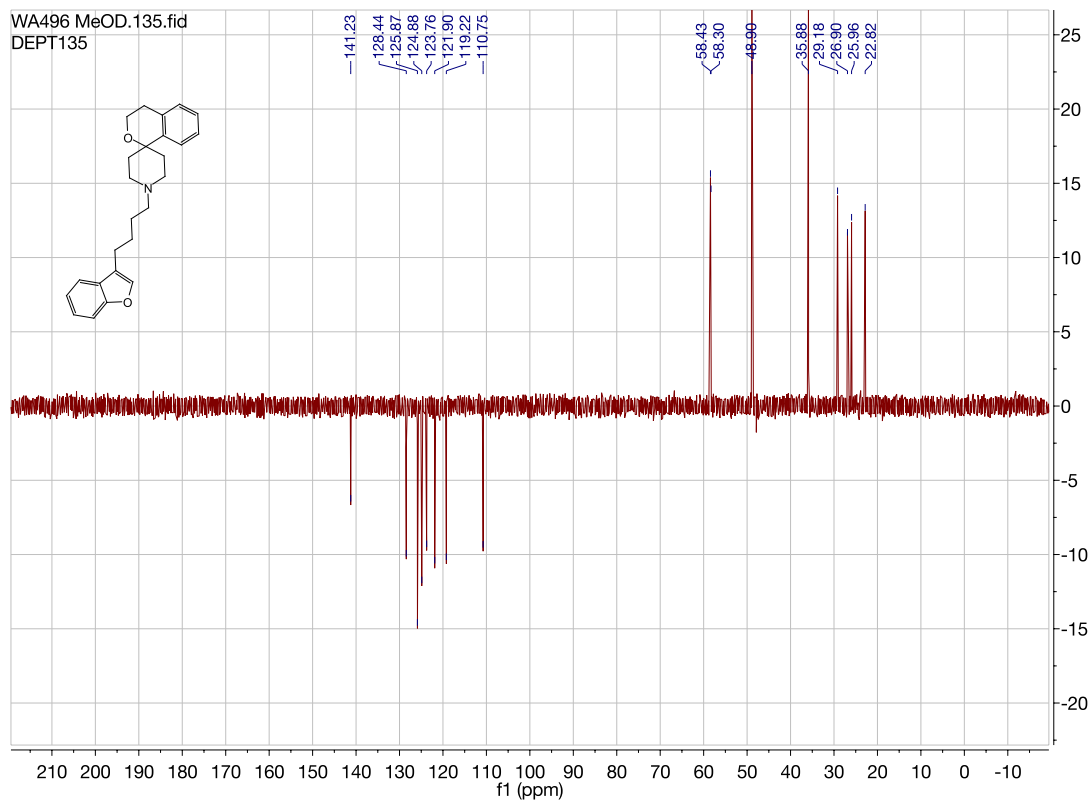


1'-(4-(benzofuran-3-yl)butyl)spiro[isochromane-1,4'-piperidine]. (WA496)

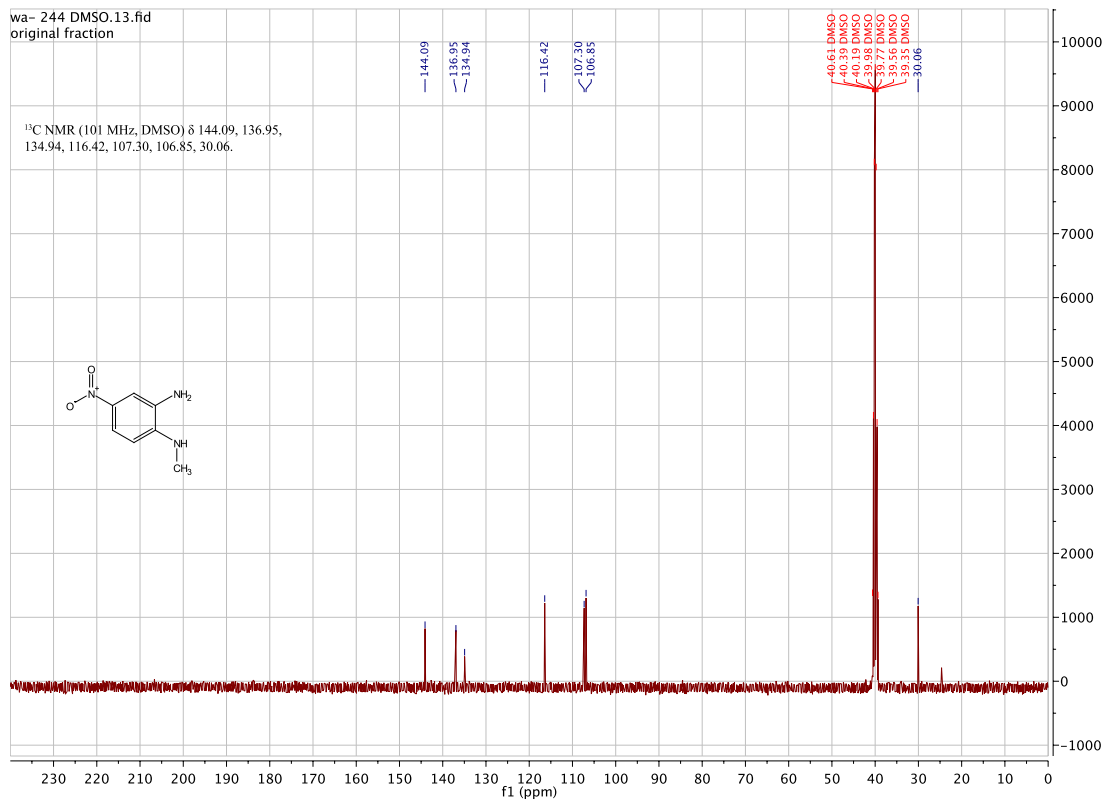
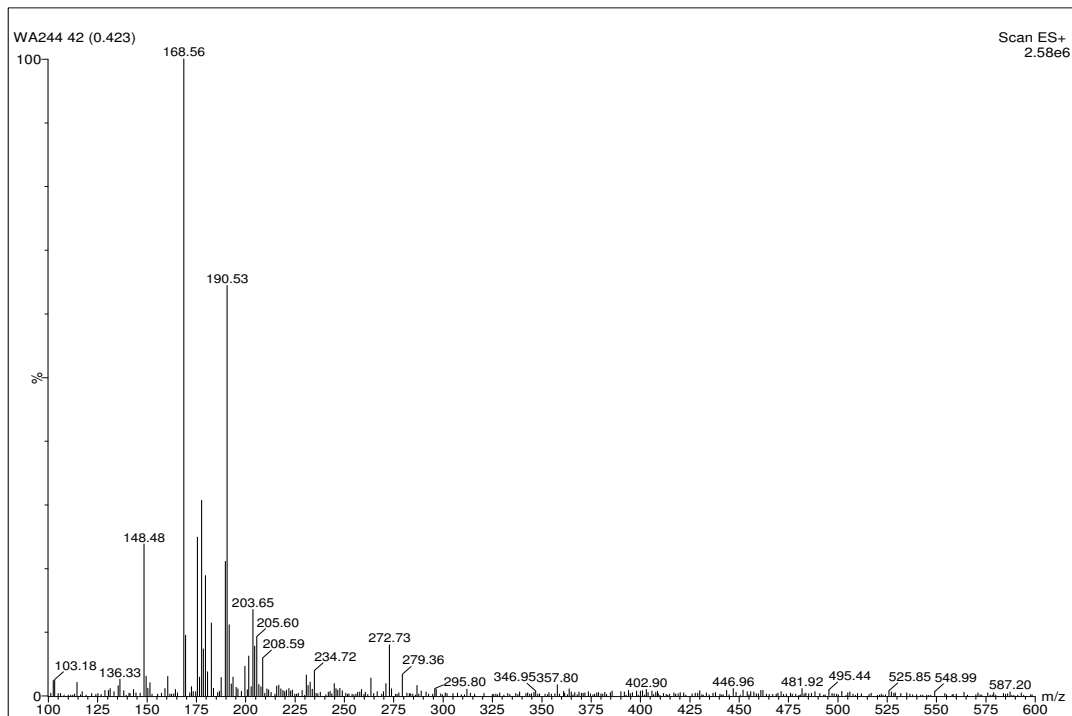


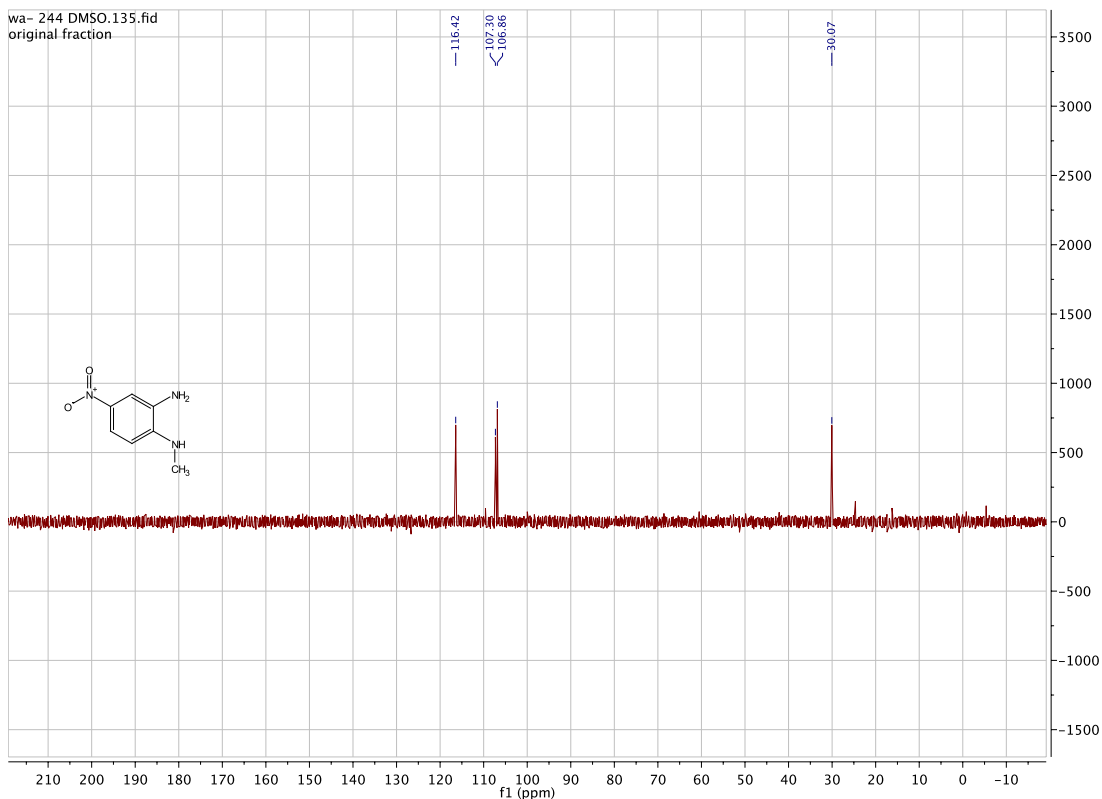
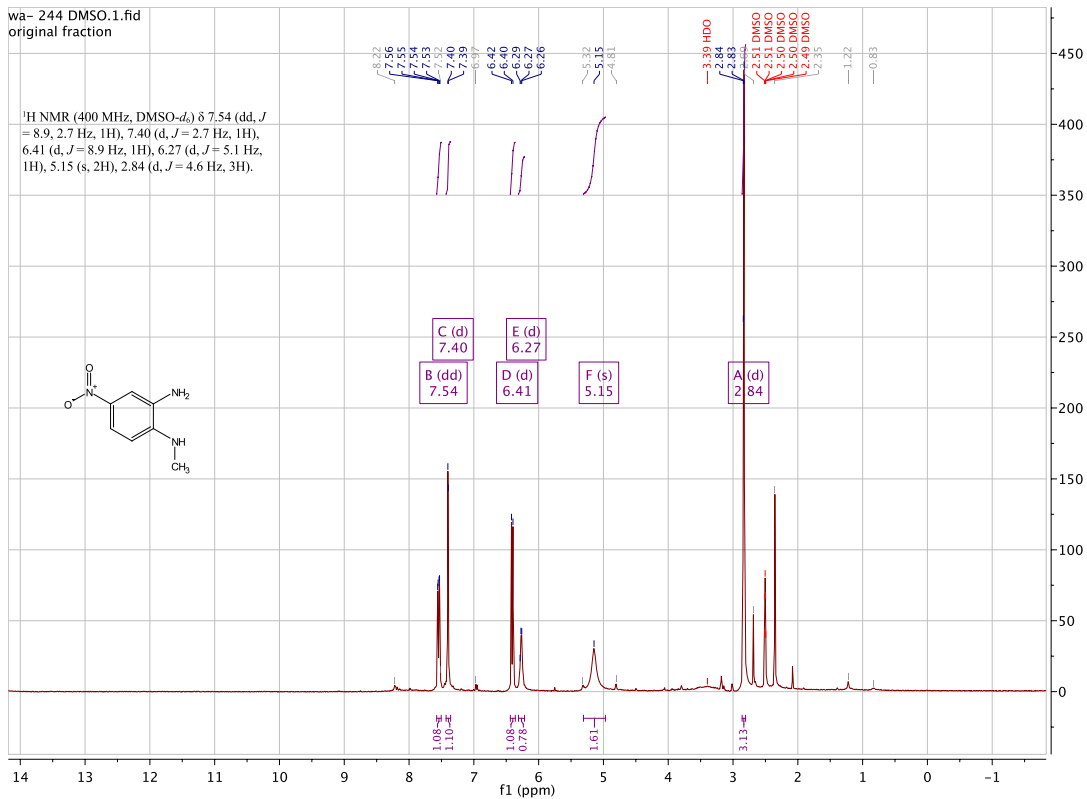


WA496 MeOD.135.fid
DEPT135

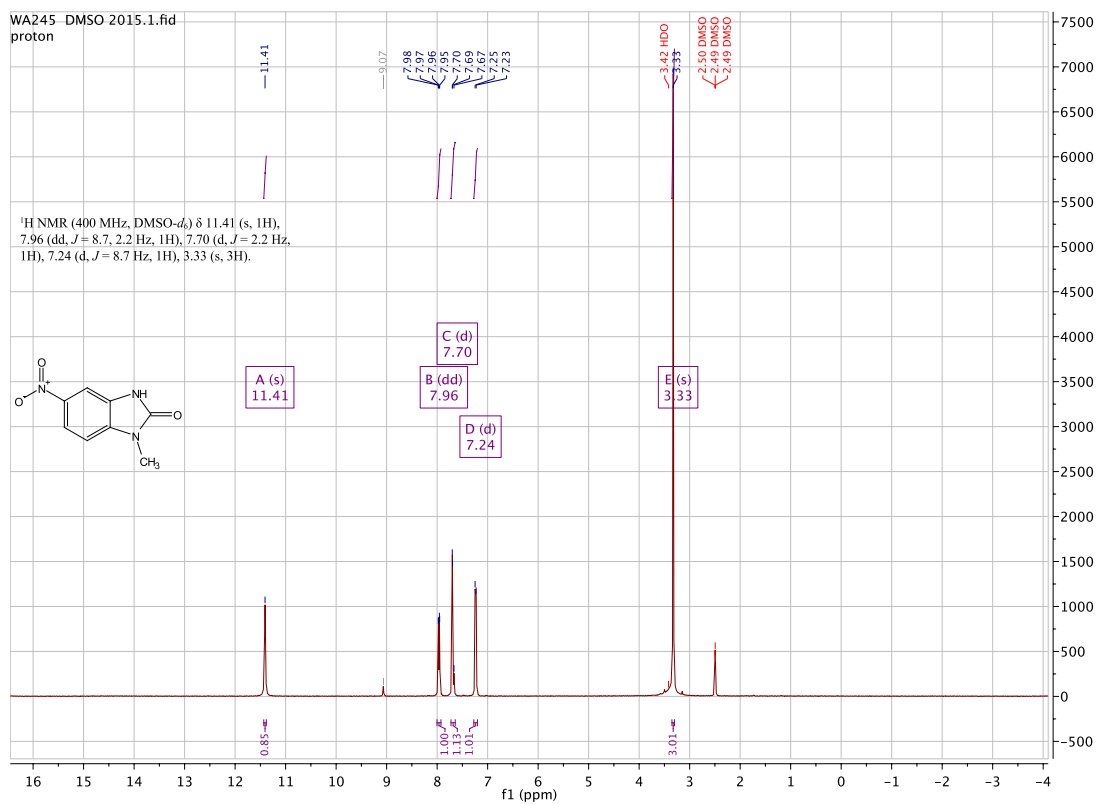
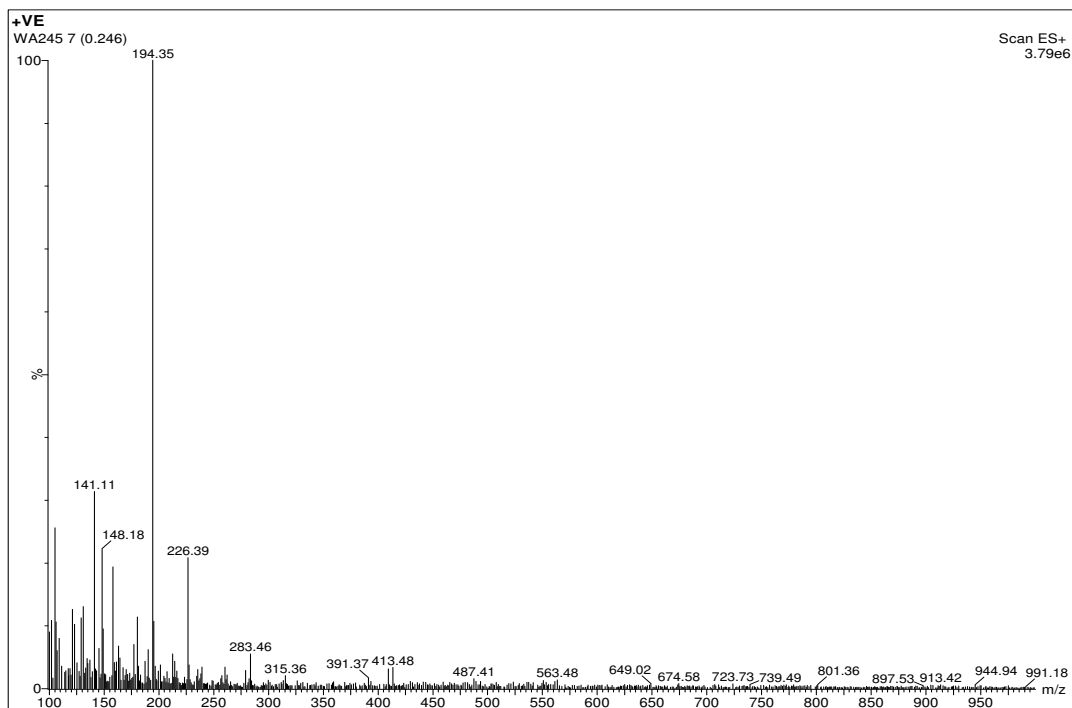


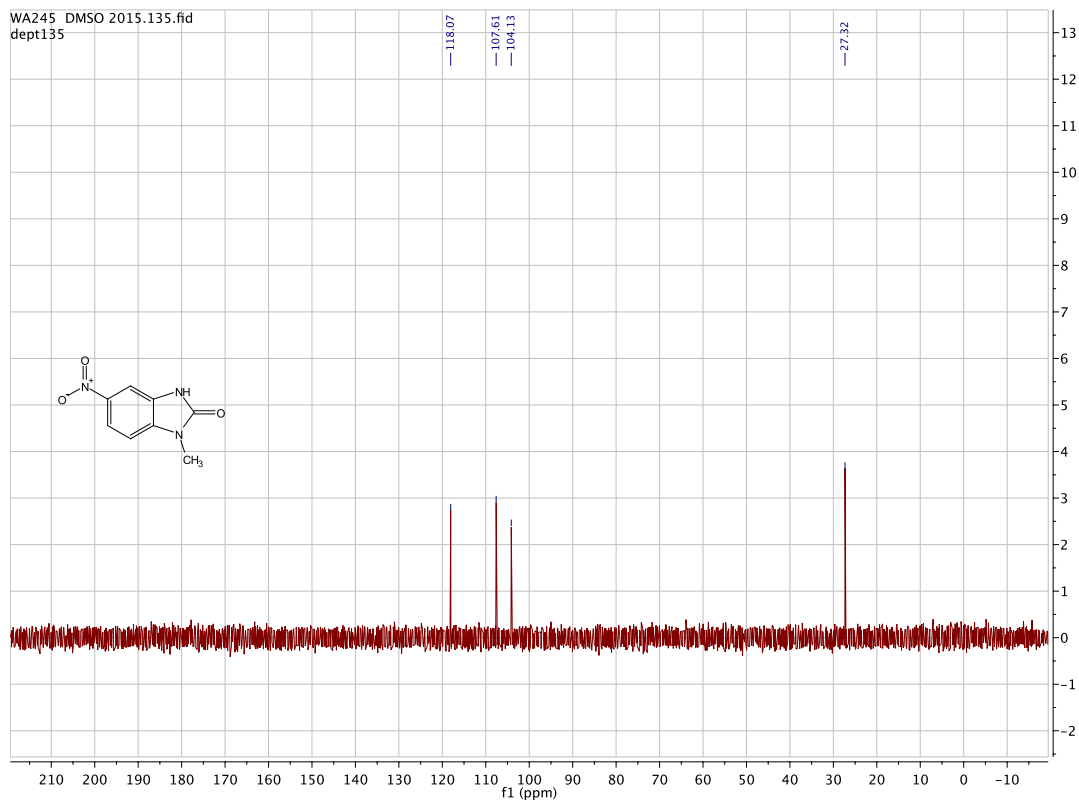
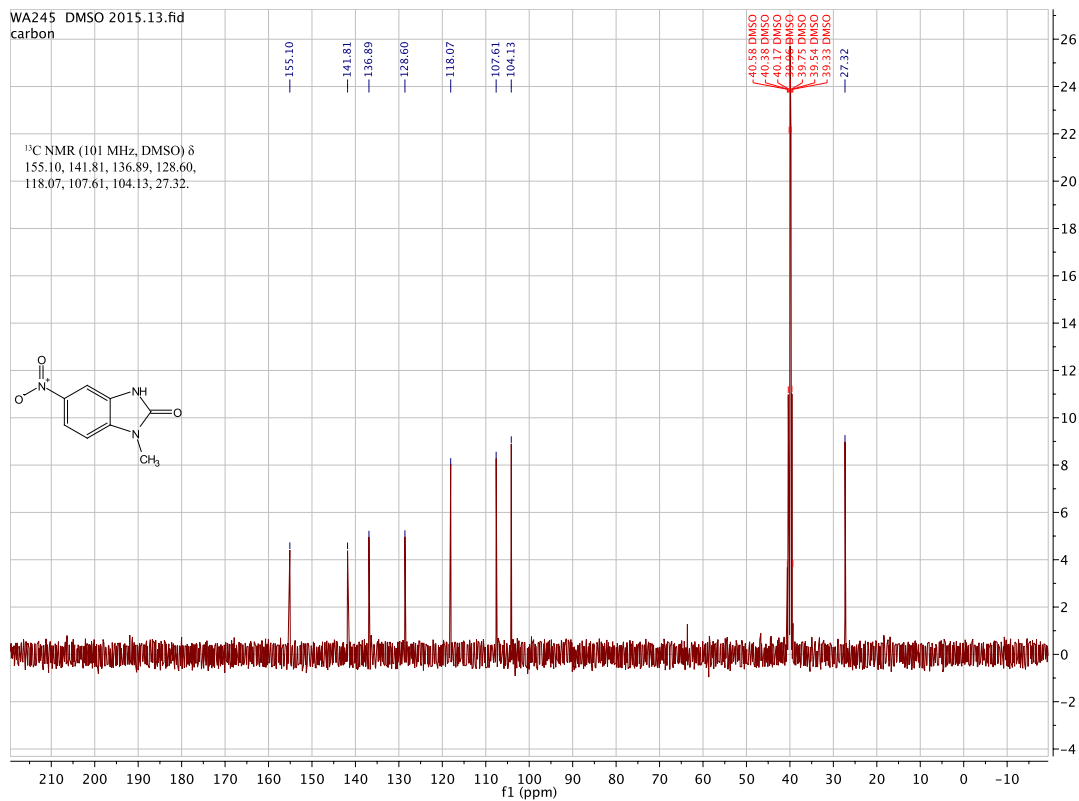
N-methyl-4-nitrobenzene-1,2-diamine:[WA244]



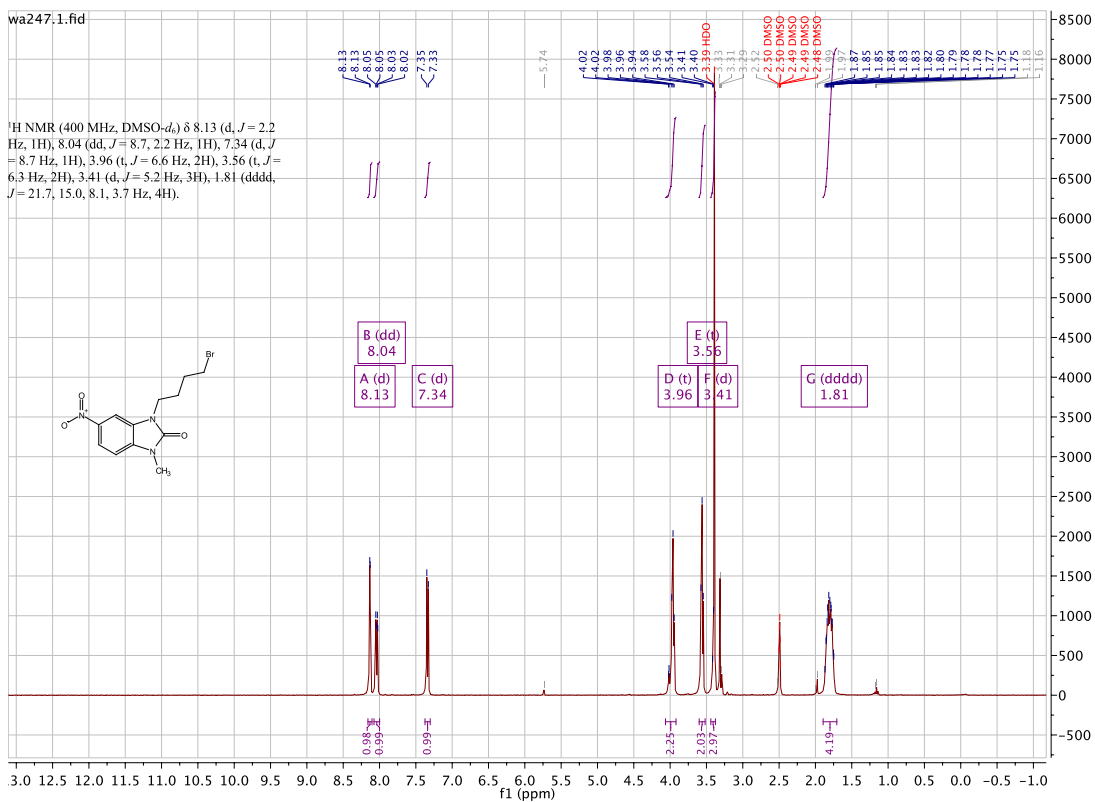
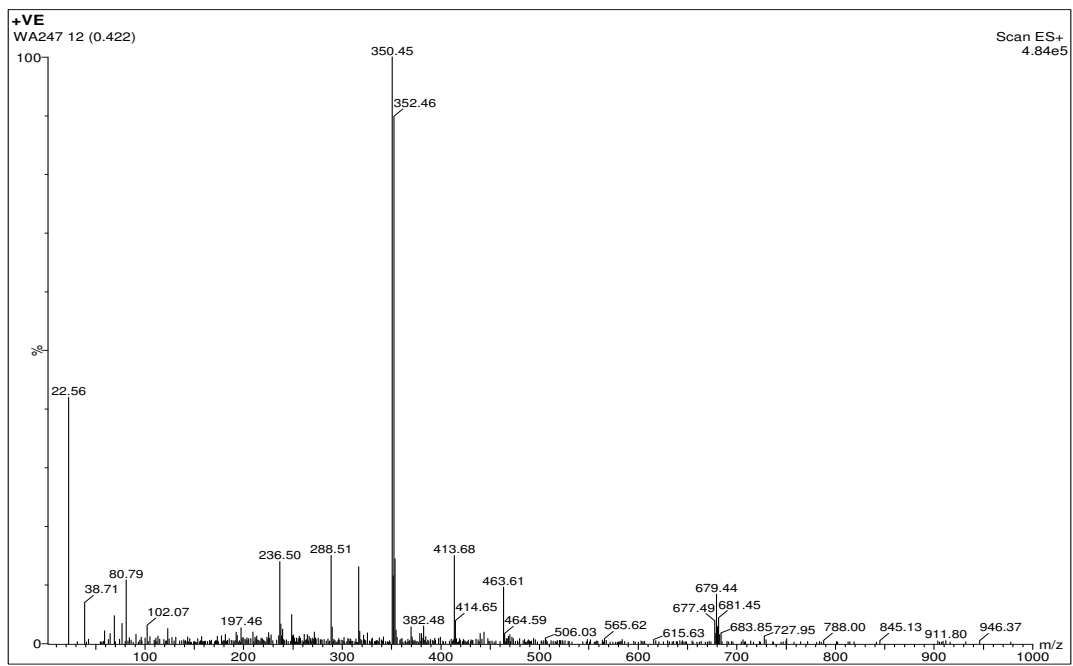


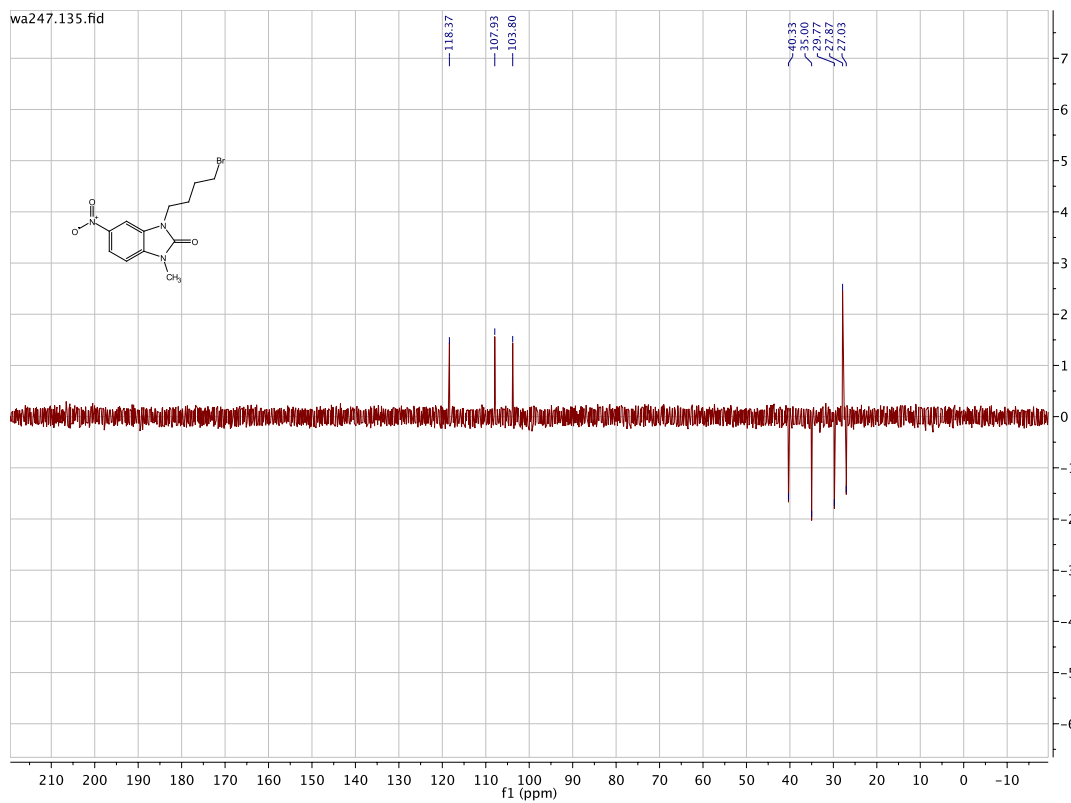
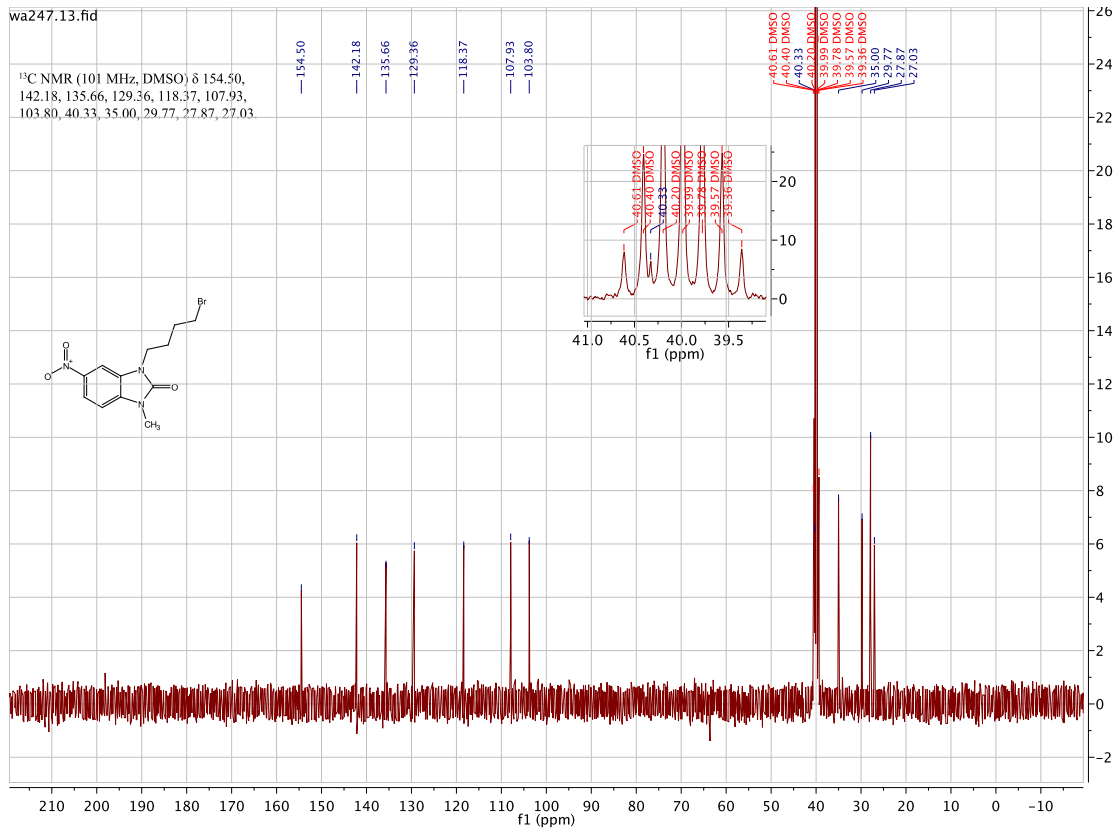
1-methyl-5-nitro-1,3-dihydro-2H-benzo[d]imidazol-2-one: [WA245]



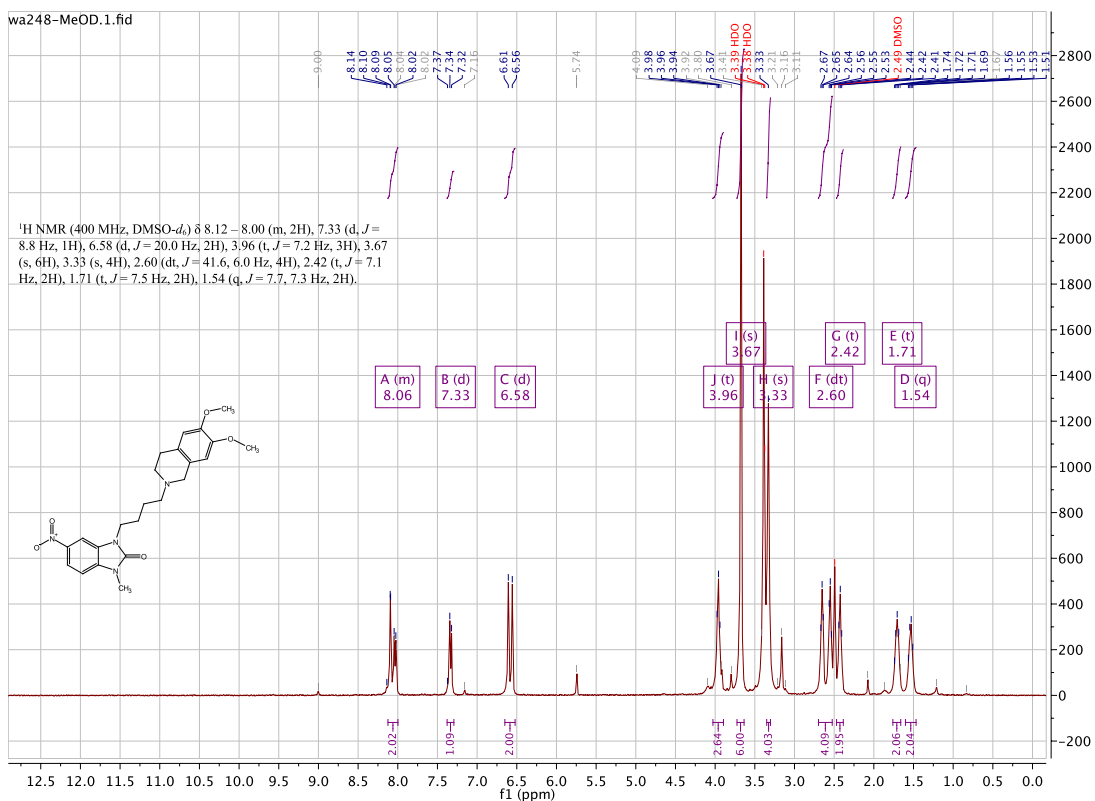
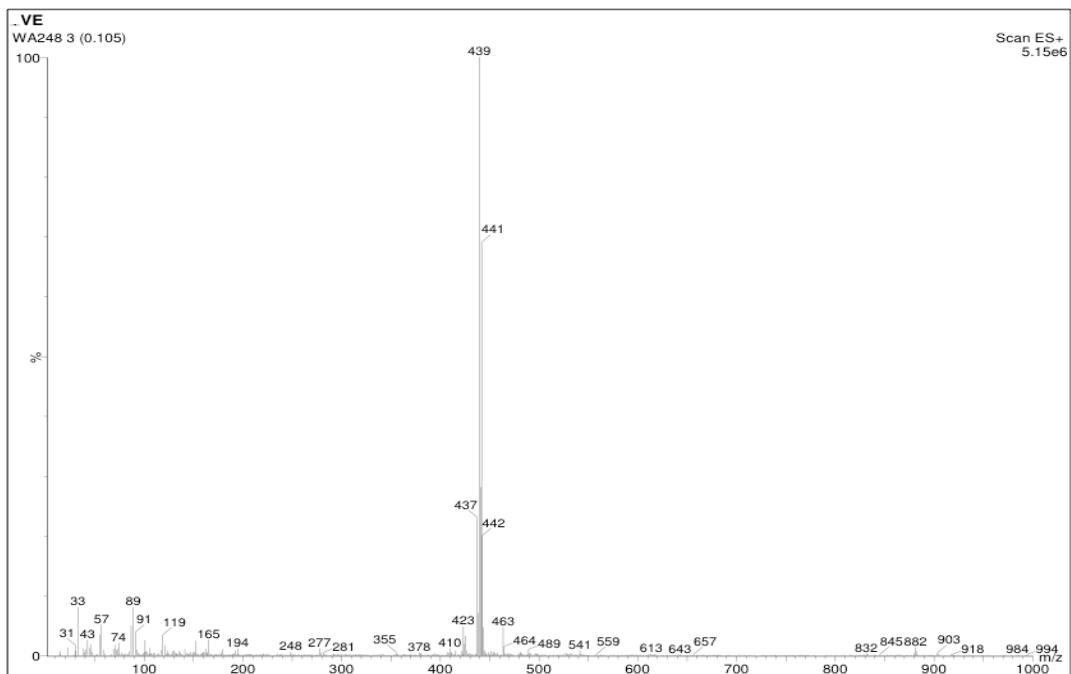


3-(4-bromobutyl)-1-methyl-5-nitro-1,3-dihydro-2H-benzo[d]imidazol-2-one:[WA247]

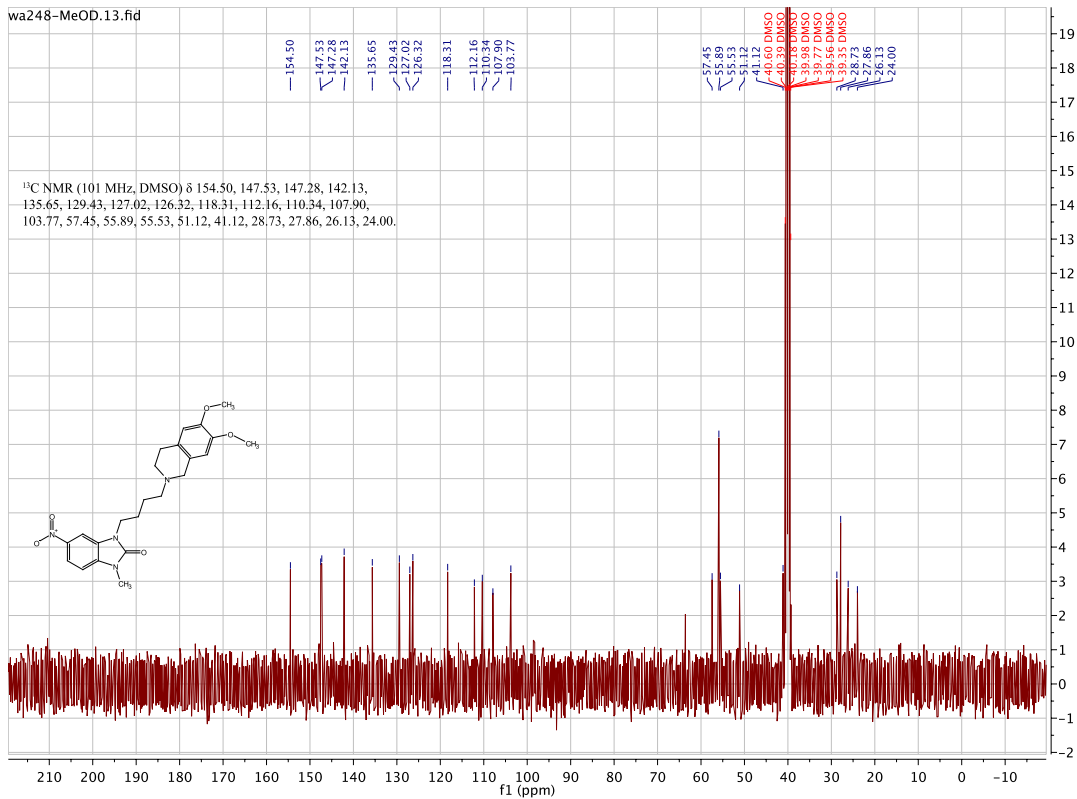




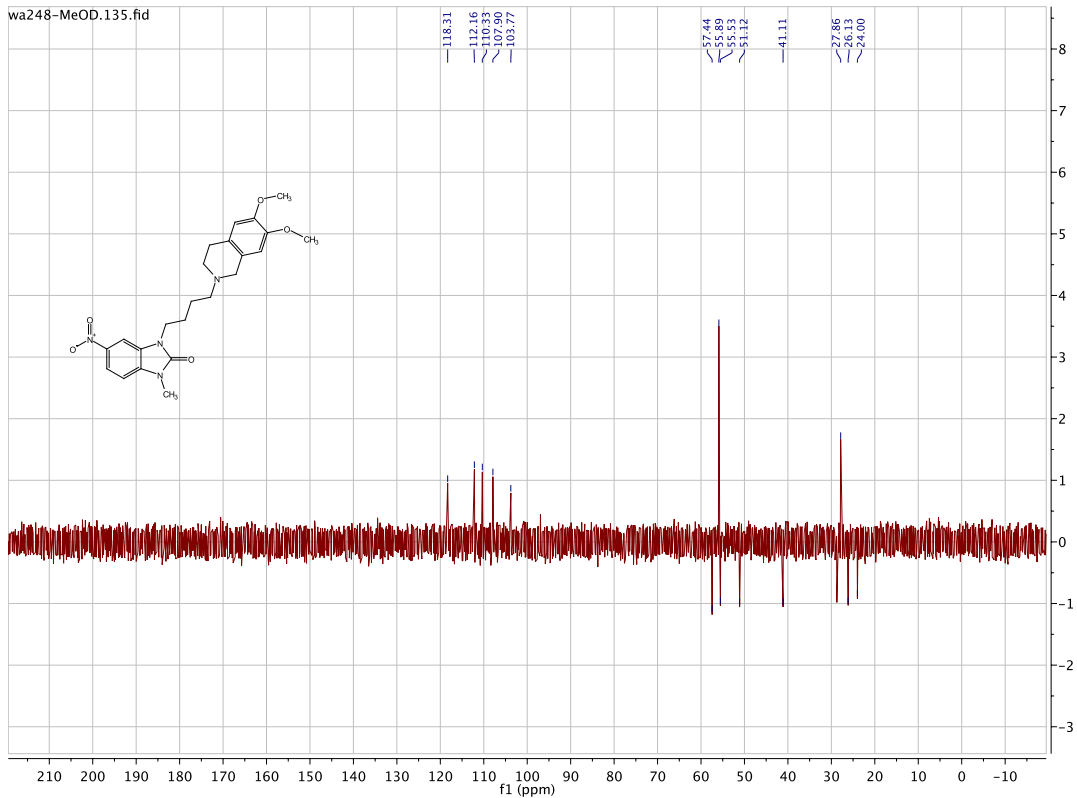
3-(4-(6,7-dimethoxy-3,4-dihydroisoquinolin-2(1H)-yl)butyl)-1-methyl-5-nitro-1,3-dihydro-2H-benzo[d]imidazol-2-one:[WA248]



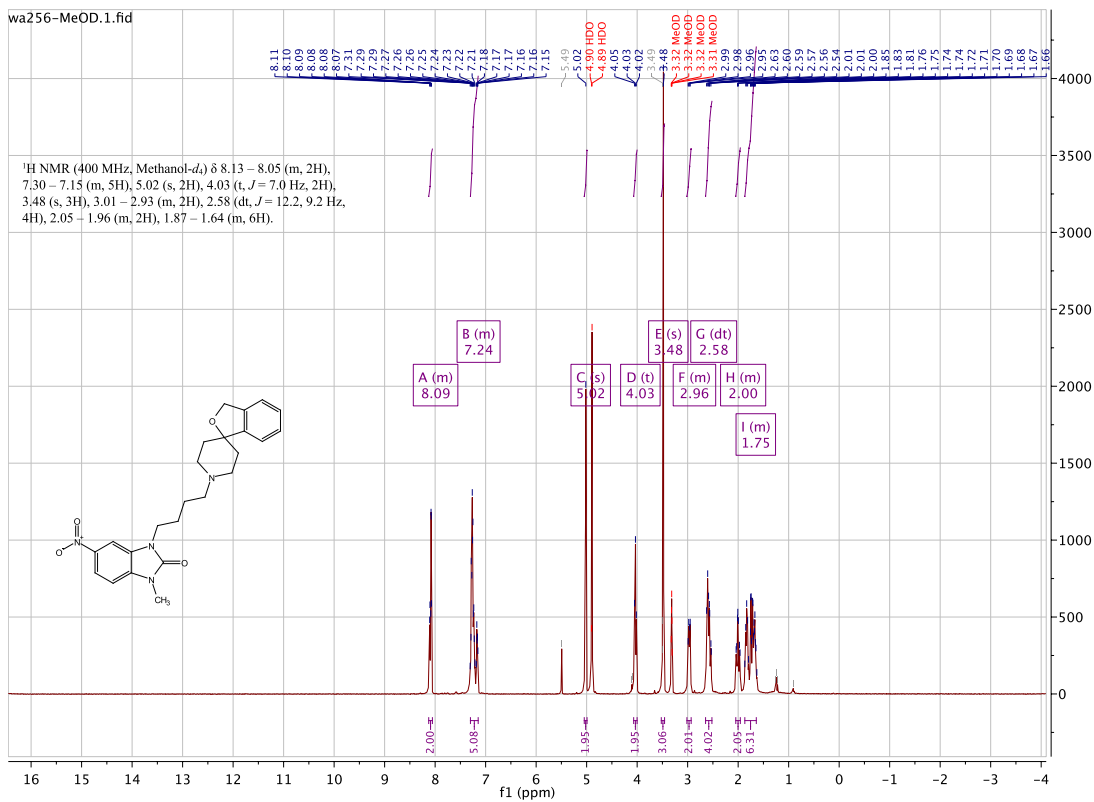
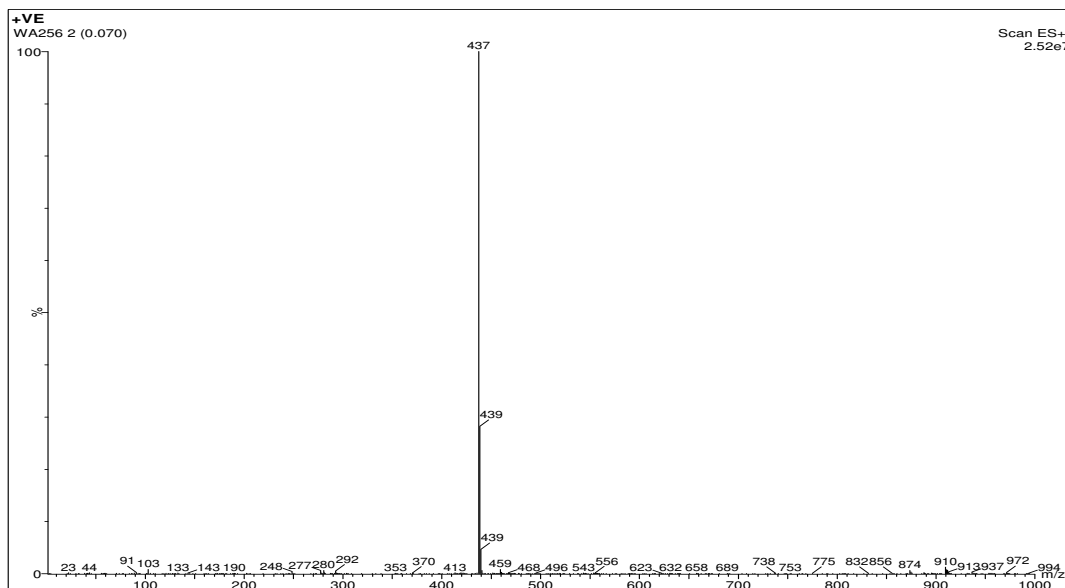
wa248-MeOD.13.fid

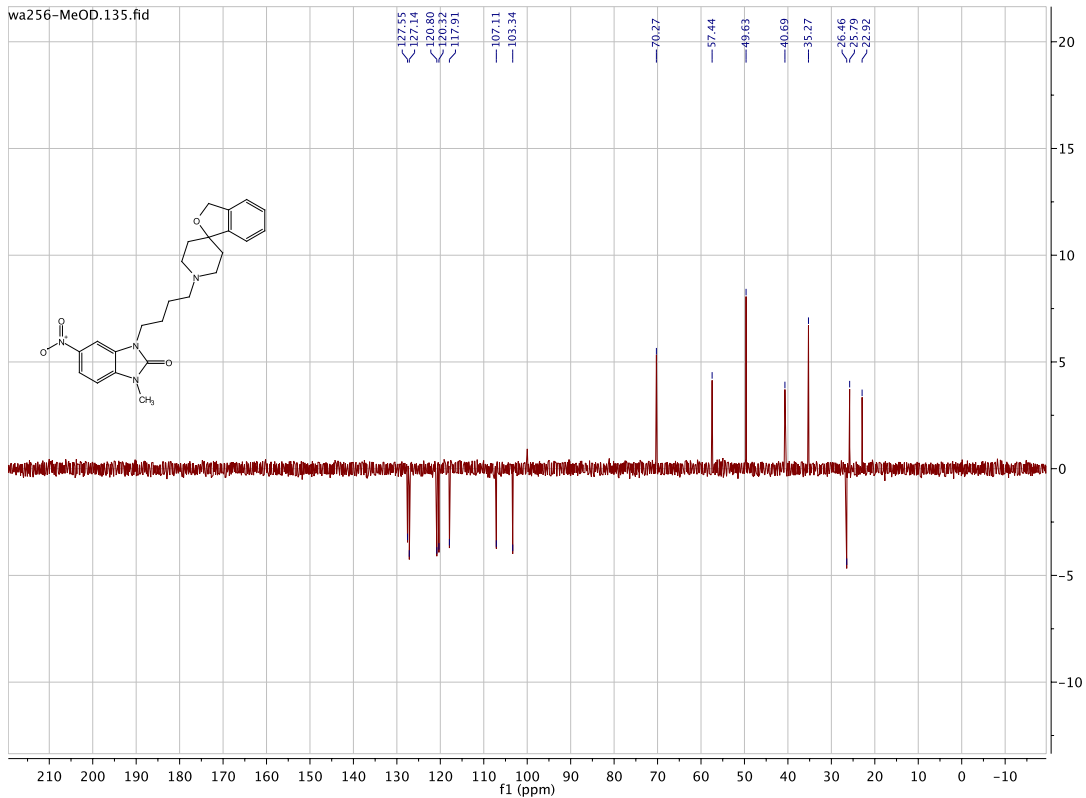
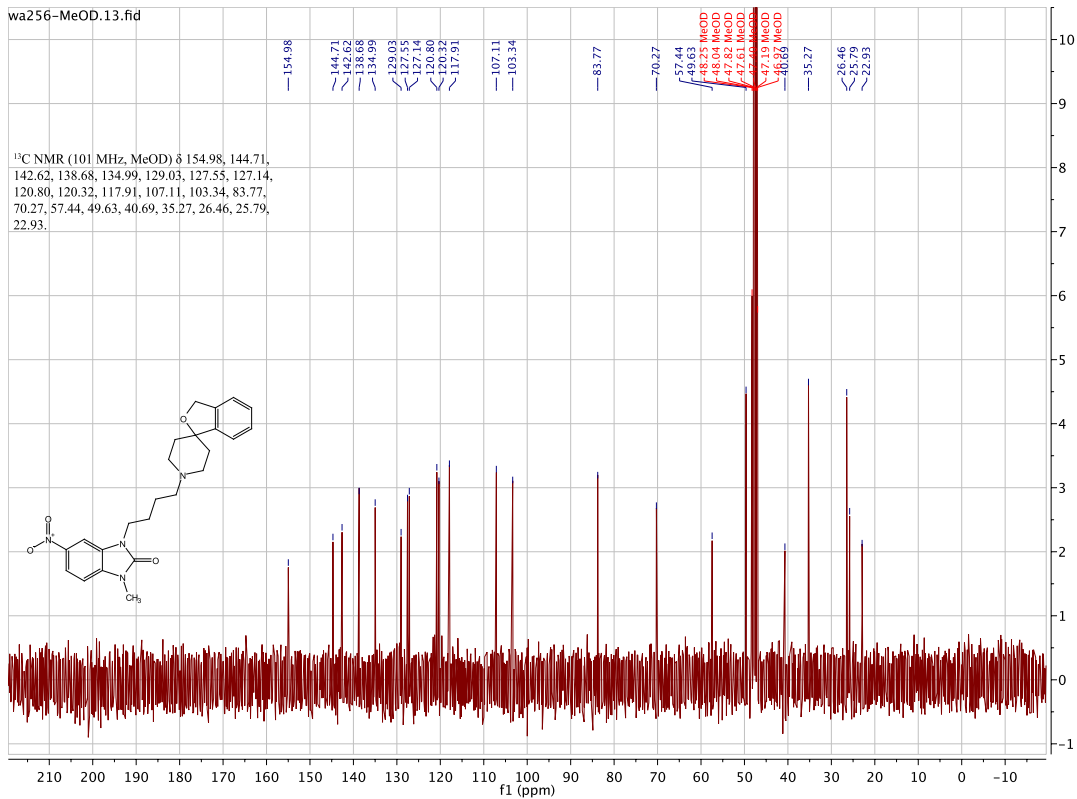


wa248-MeOD.135.fid

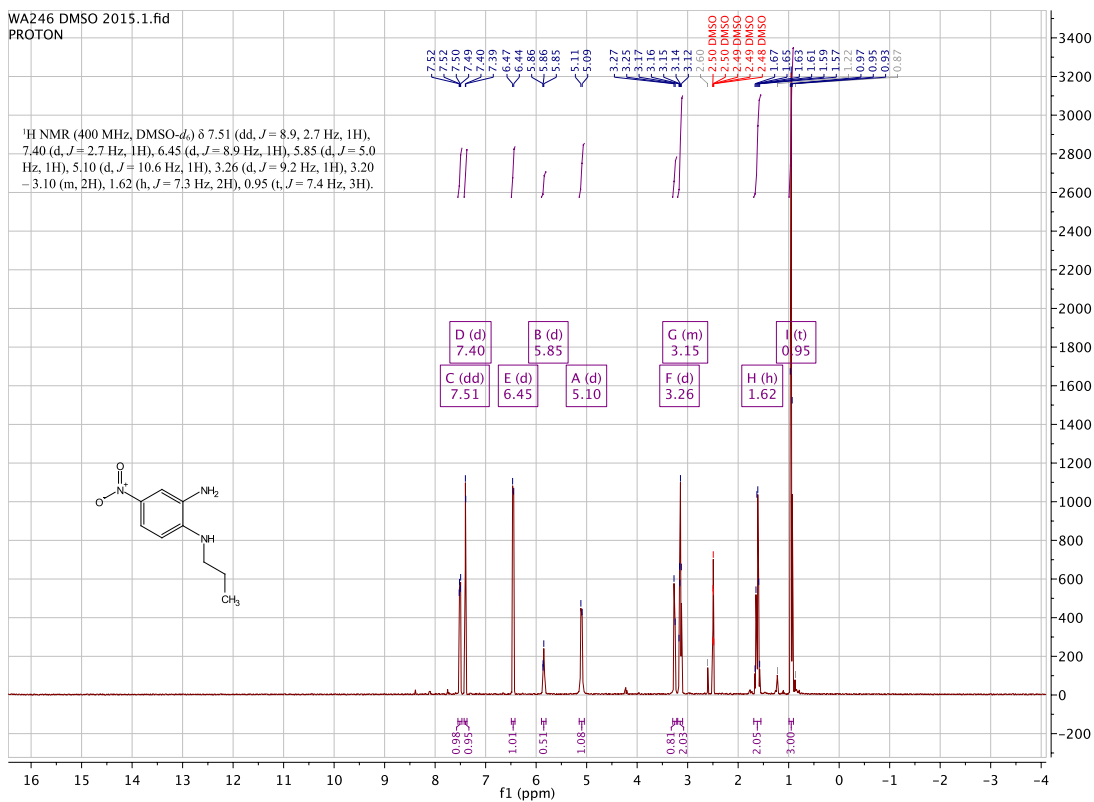
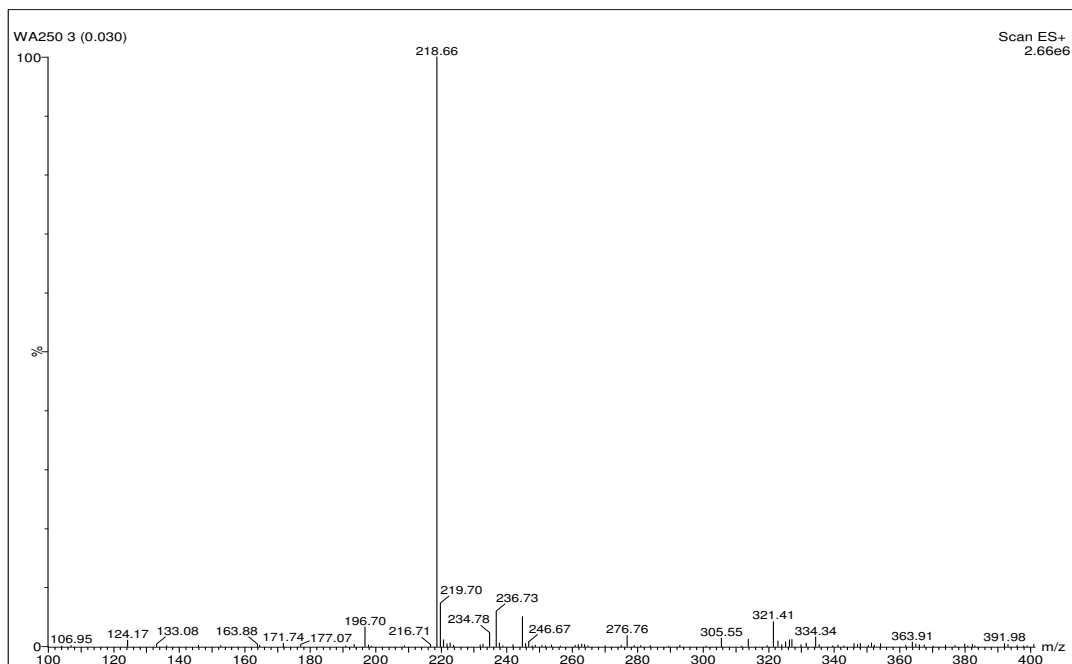


3-(4-(3H-spiro[isobenzofuran-1,4'-piperidin]-1'-yl)butyl)-1-methyl-5-nitro-1,3-dihydro-2H-benzo[d]imidazol-2-one:[WA256]

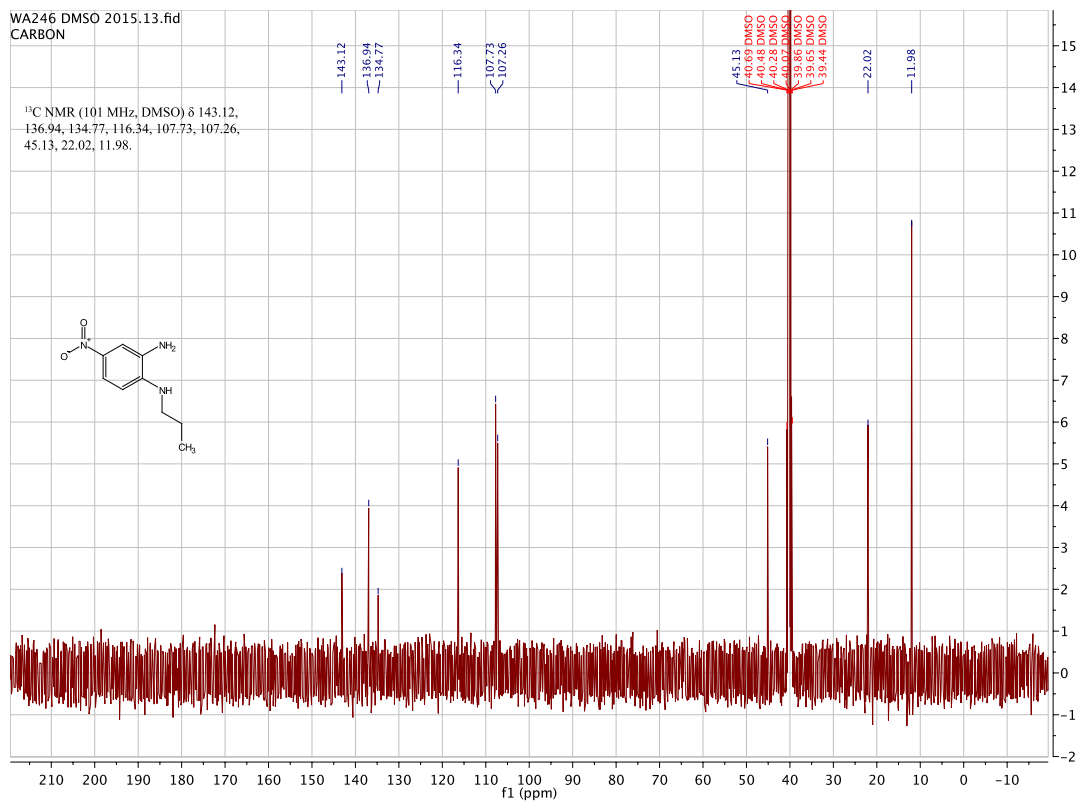




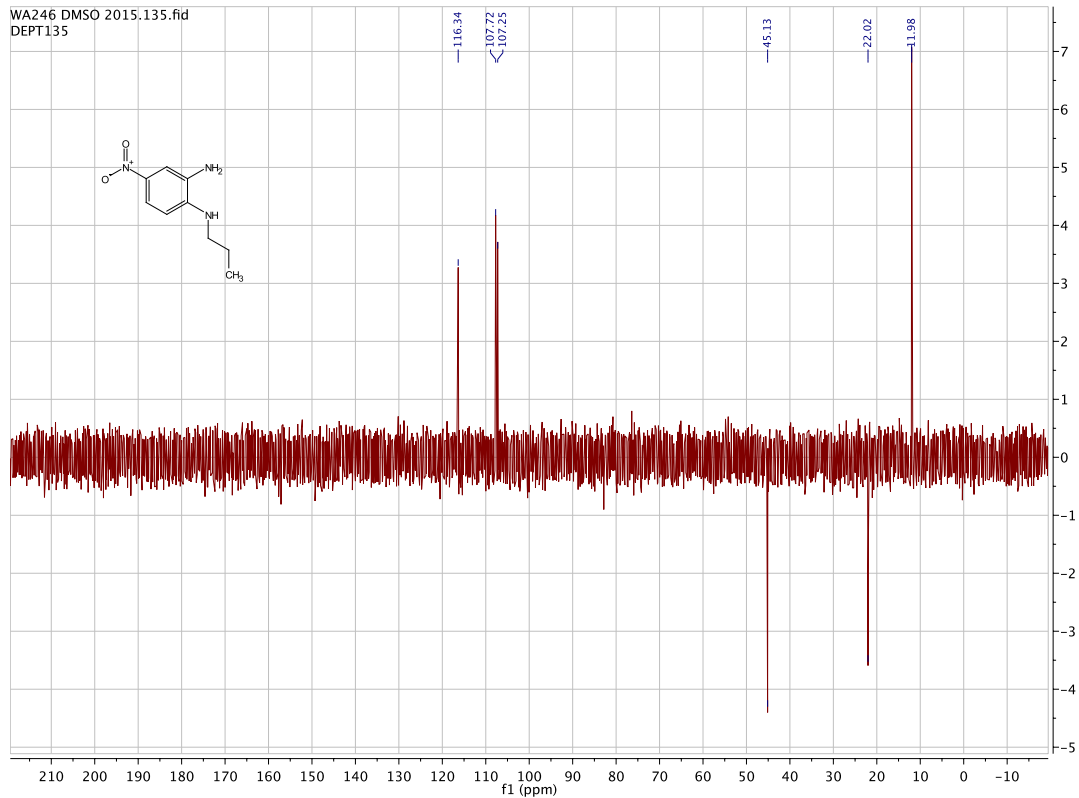
4-nitro-N¹-propylbenzene-1,2-diamine: [WA246]



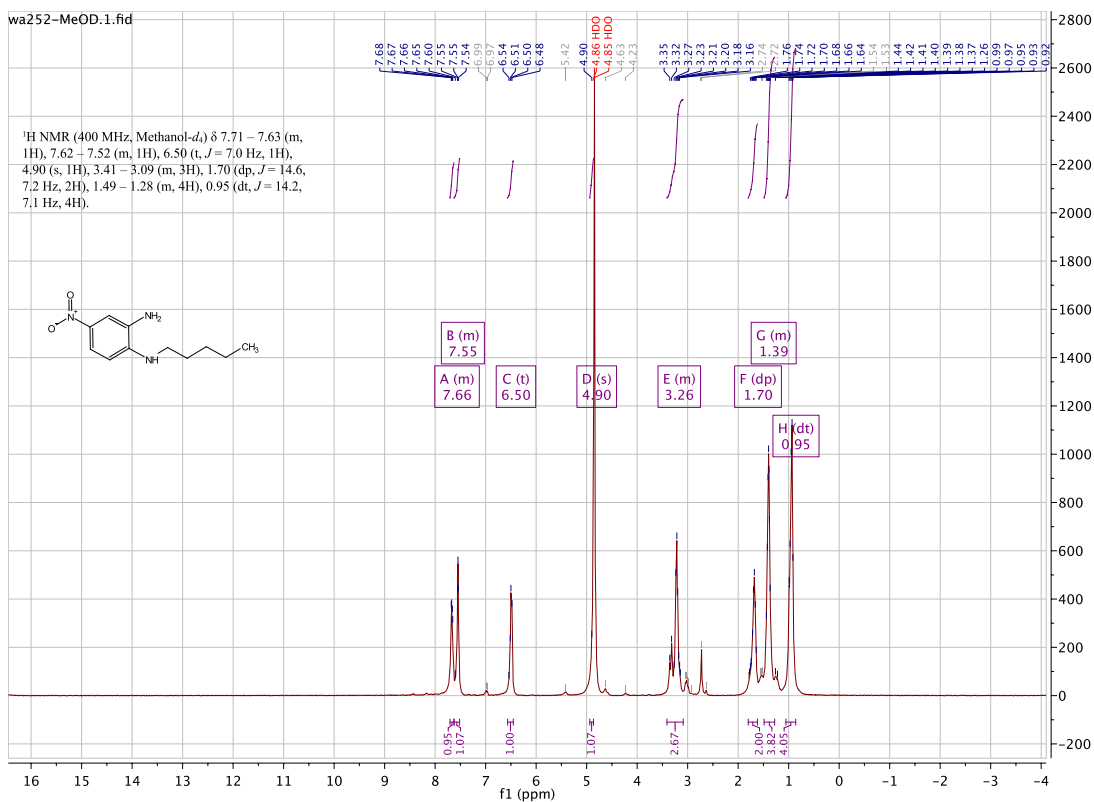
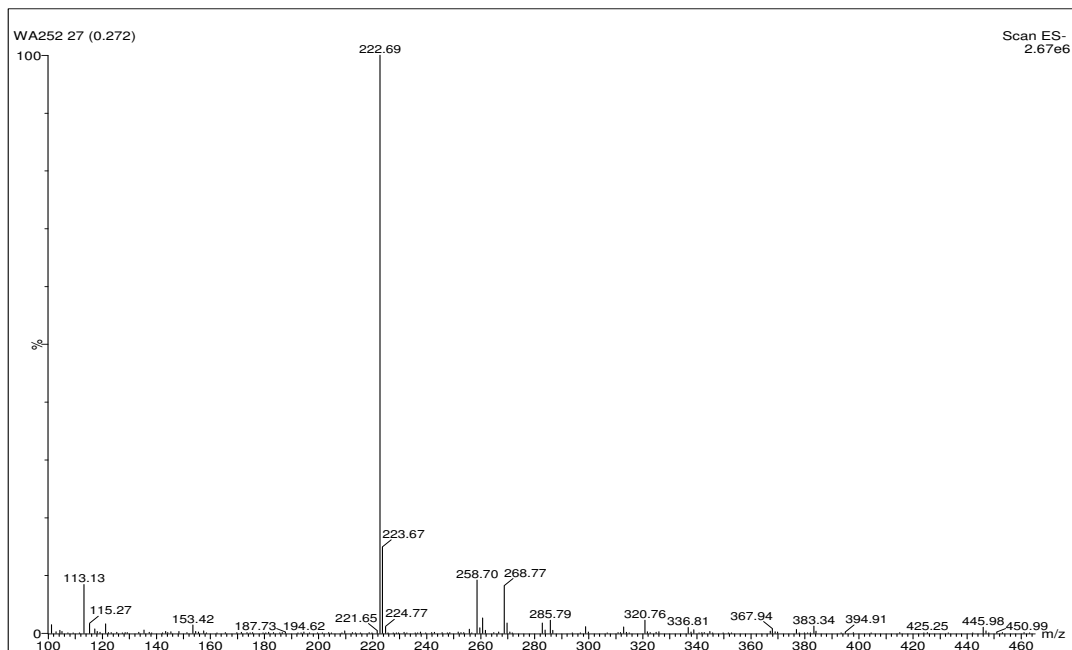
WA246 DMSO 2015.13.fid
CARBON

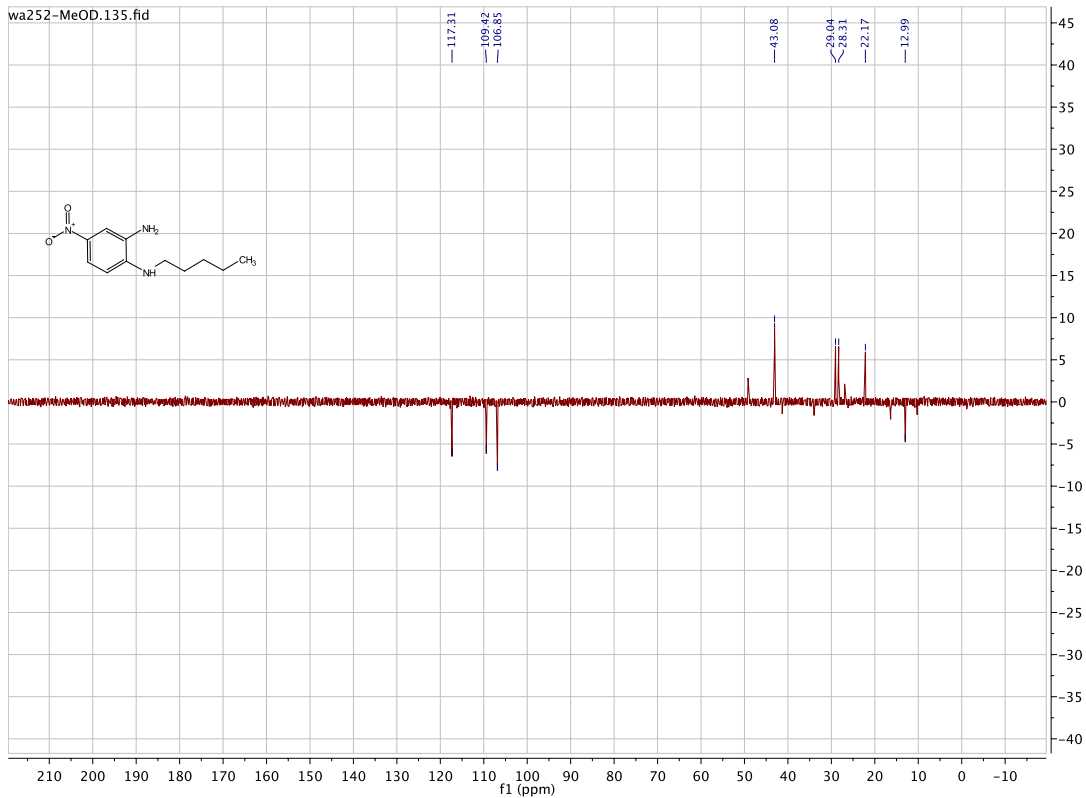
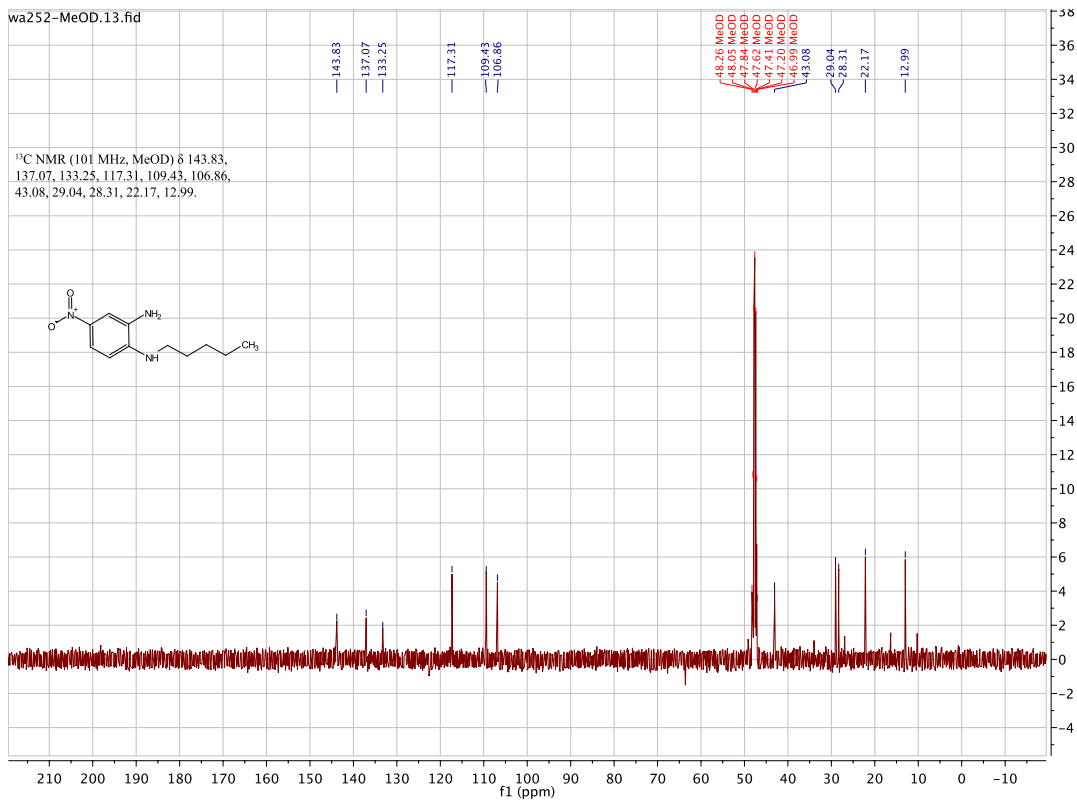


WA246 DMSO 2015.135.fid
DEPT135

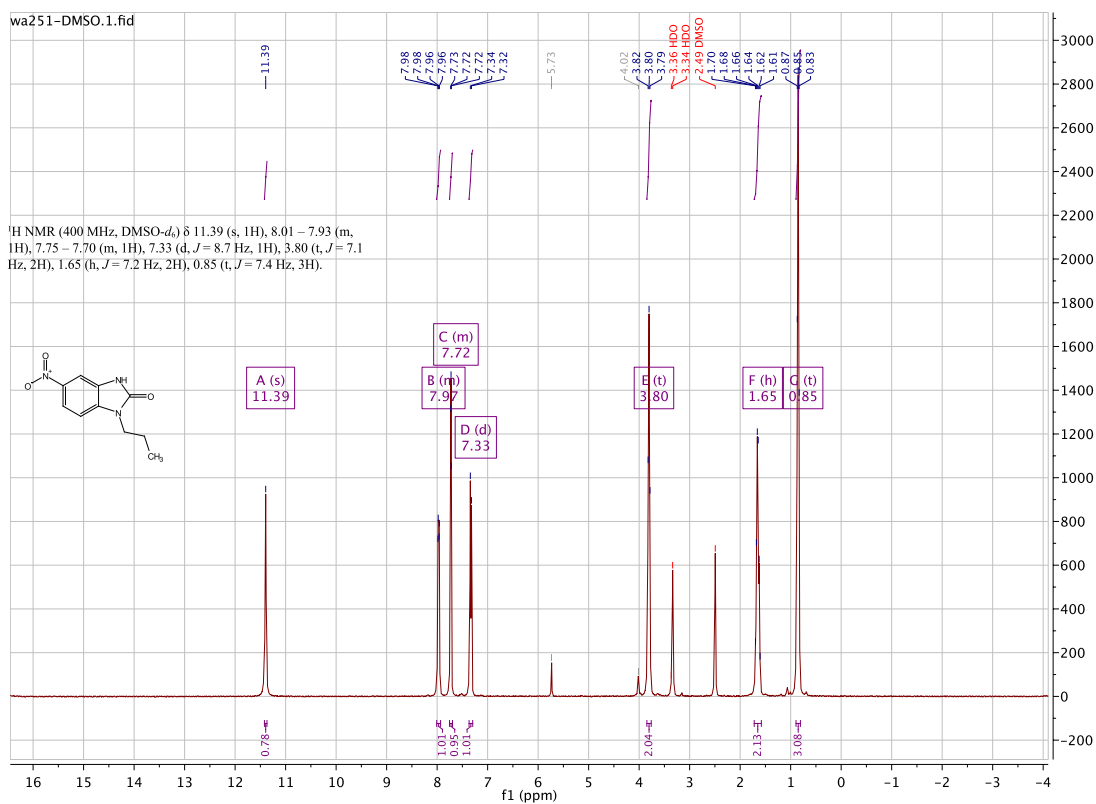
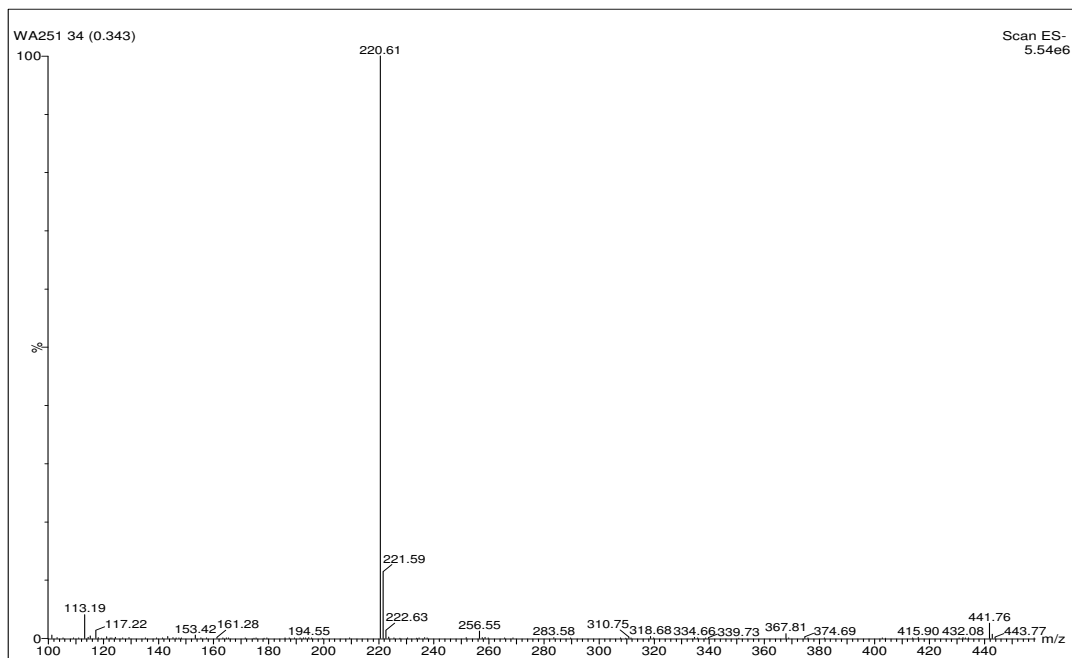


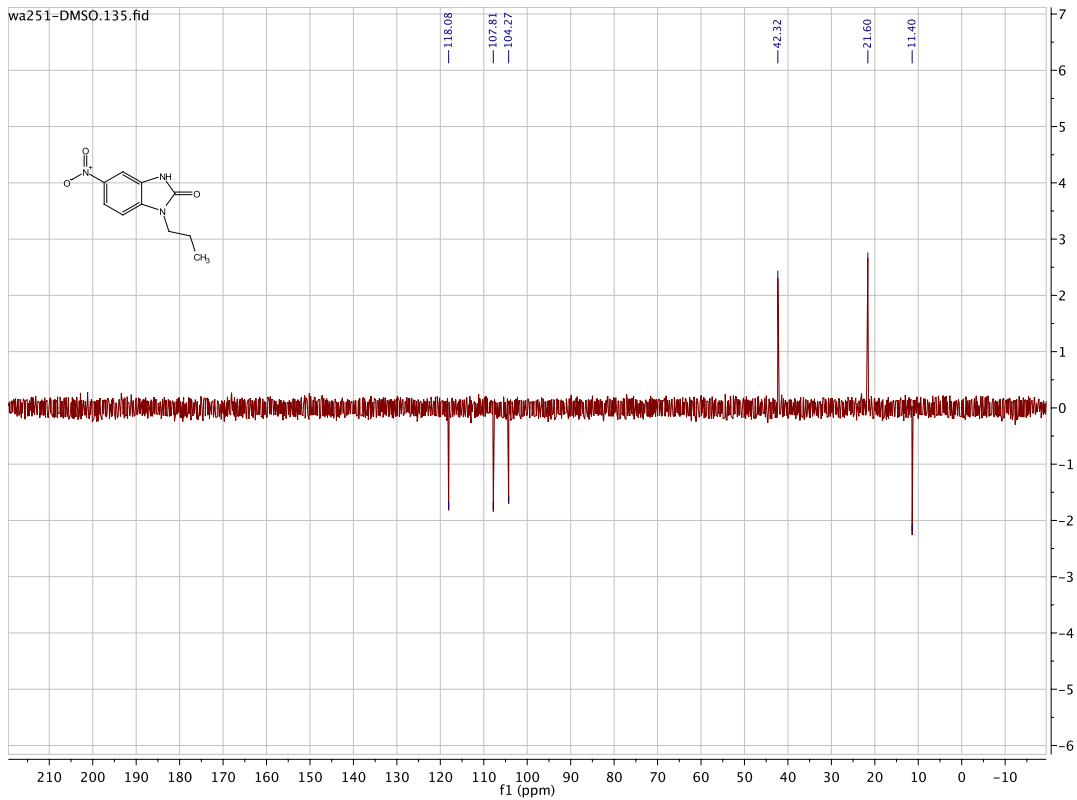
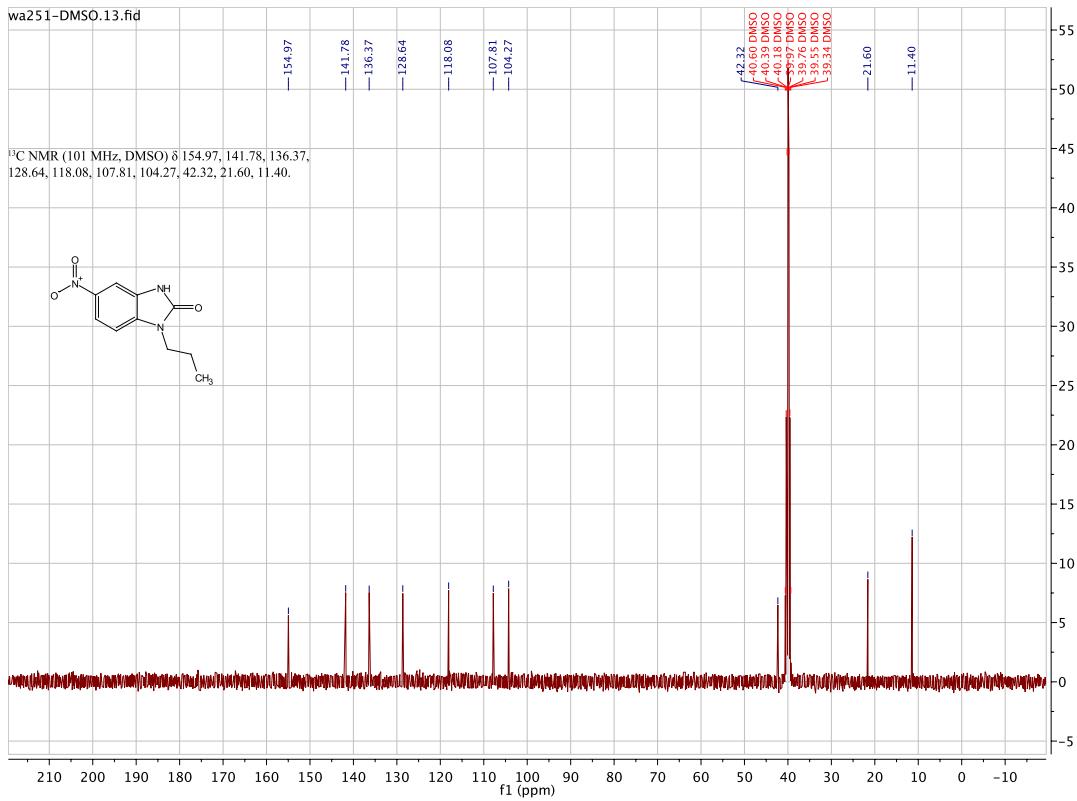
4-nitro-N¹-pentylbenzene-1,2-diamine: [WA252]



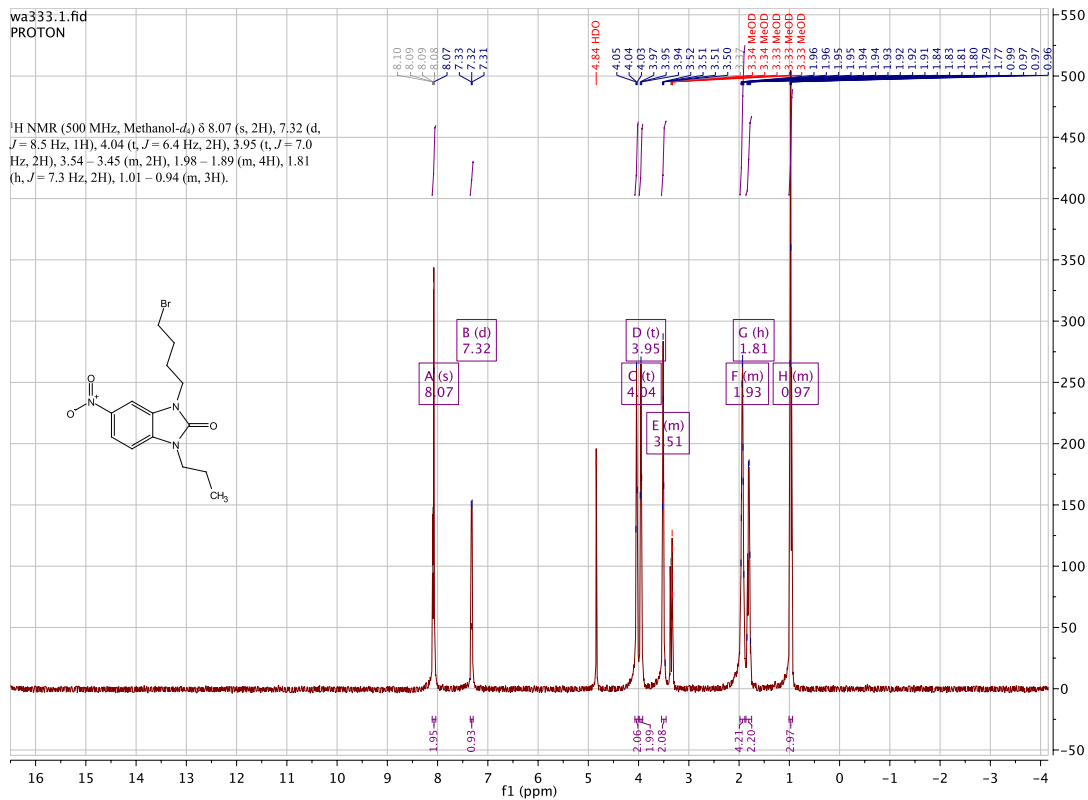
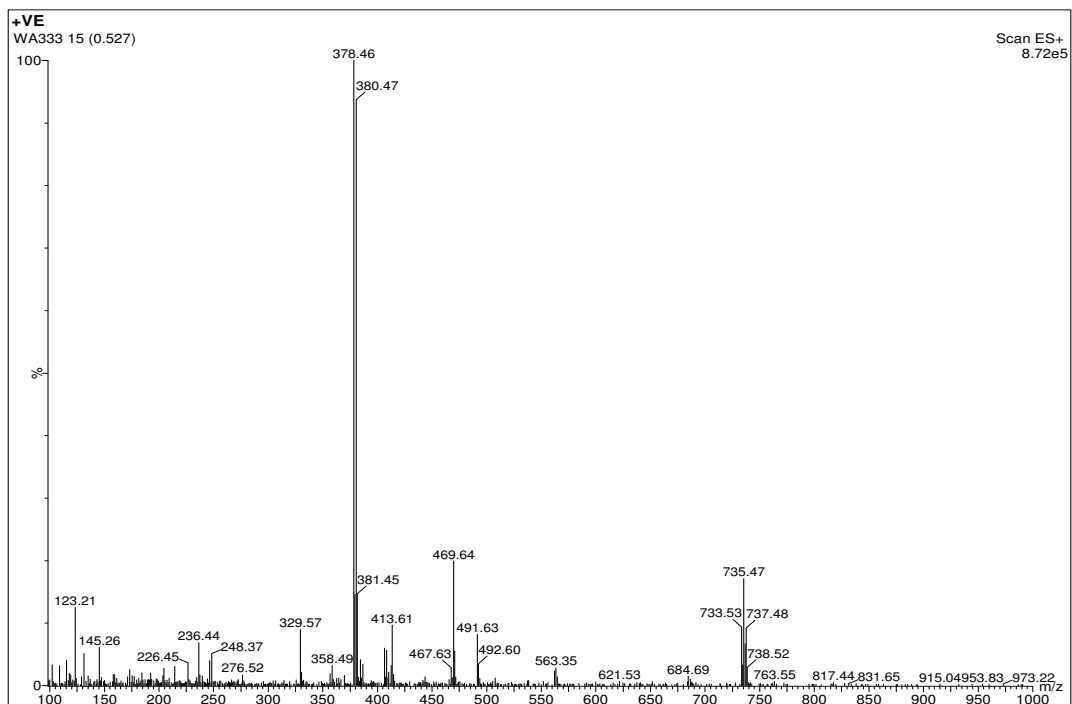


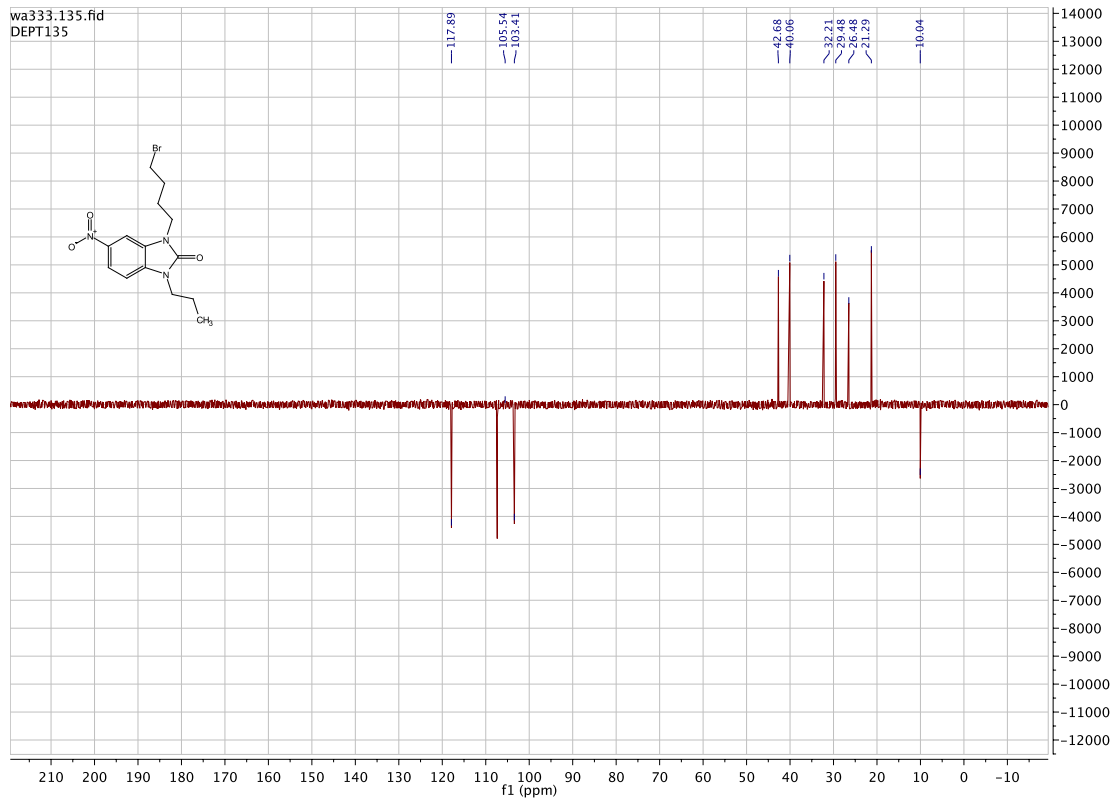
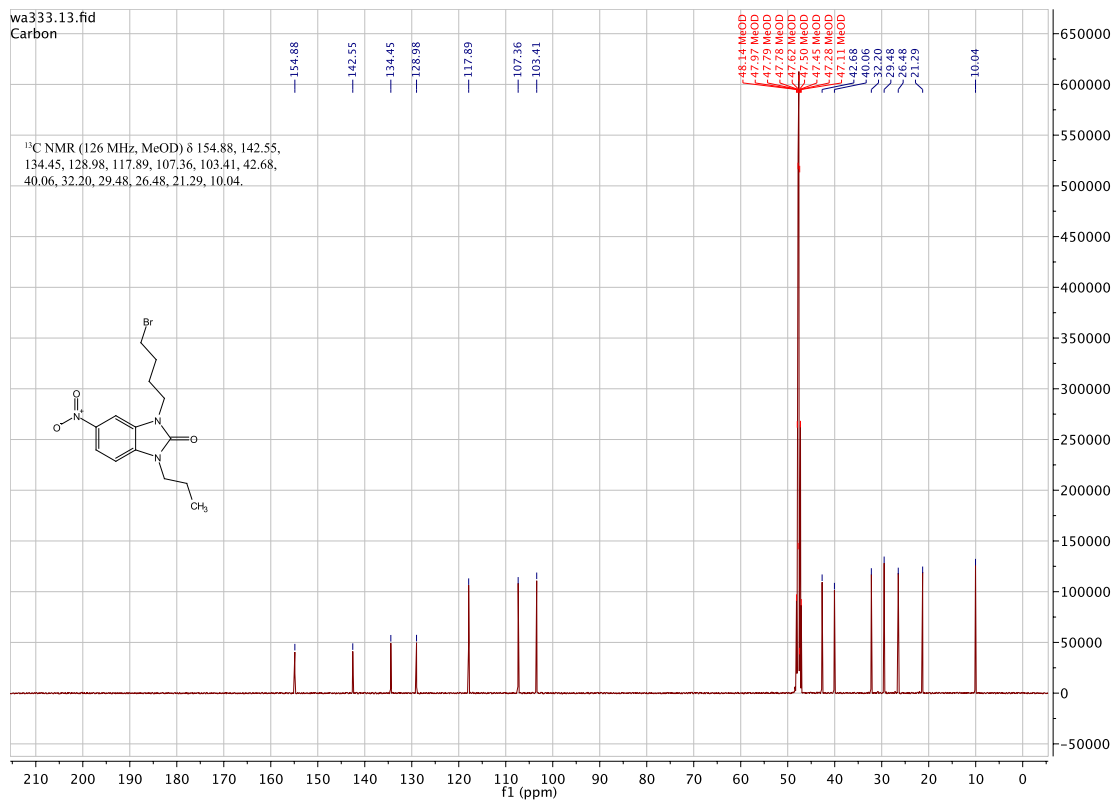
5-nitro-1-propyl-1,3-dihydro-2H-benzo[d]imidazol-2-one: [WA251]



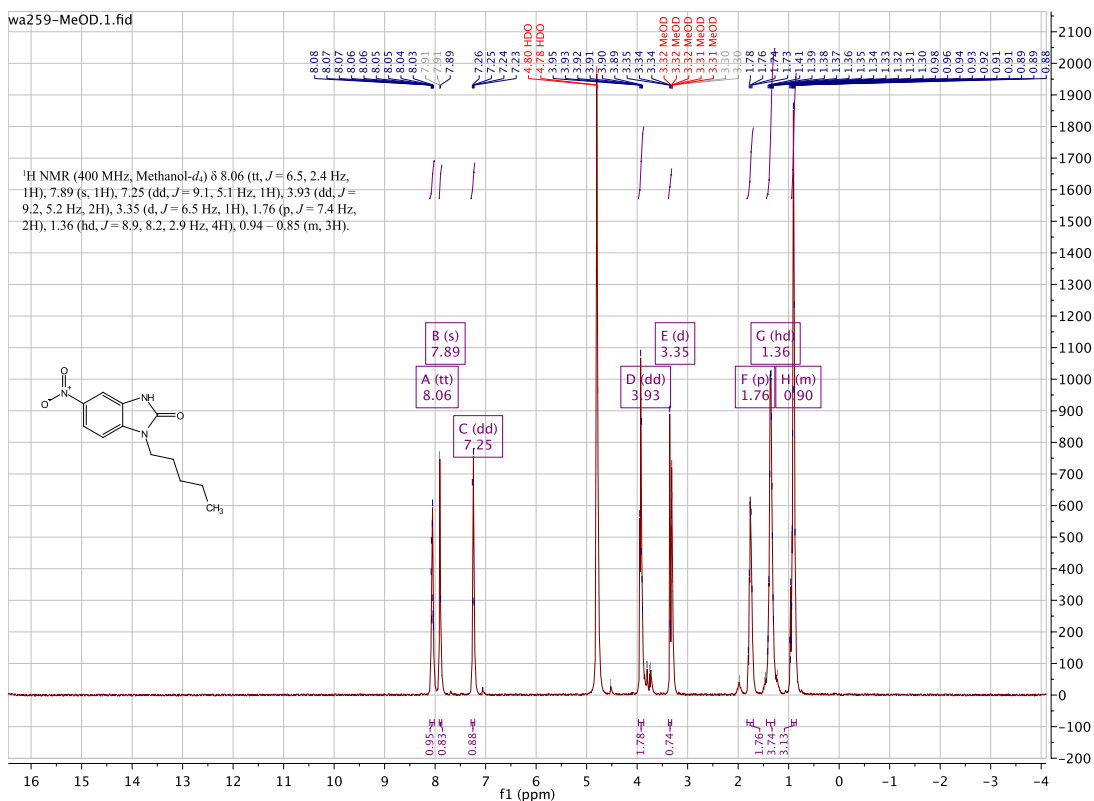
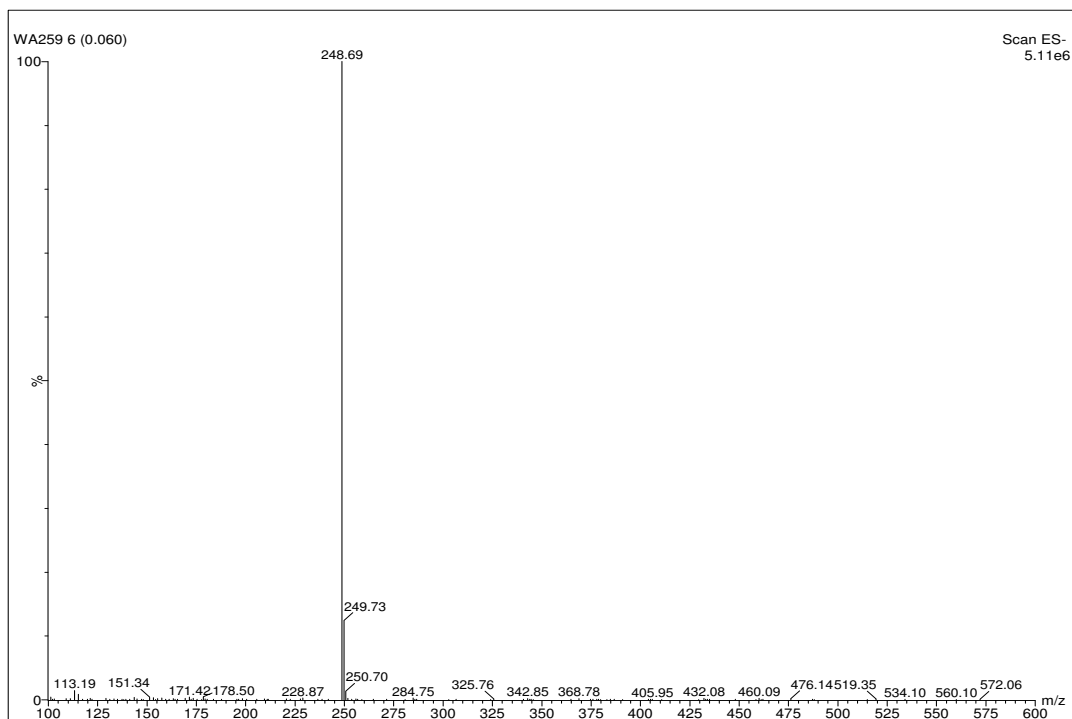


3-(4-bromobutyl)-5-nitro-1-propyl-1,3-dihydro-2H-benzo[d]imidazol-2-one: [WA333]



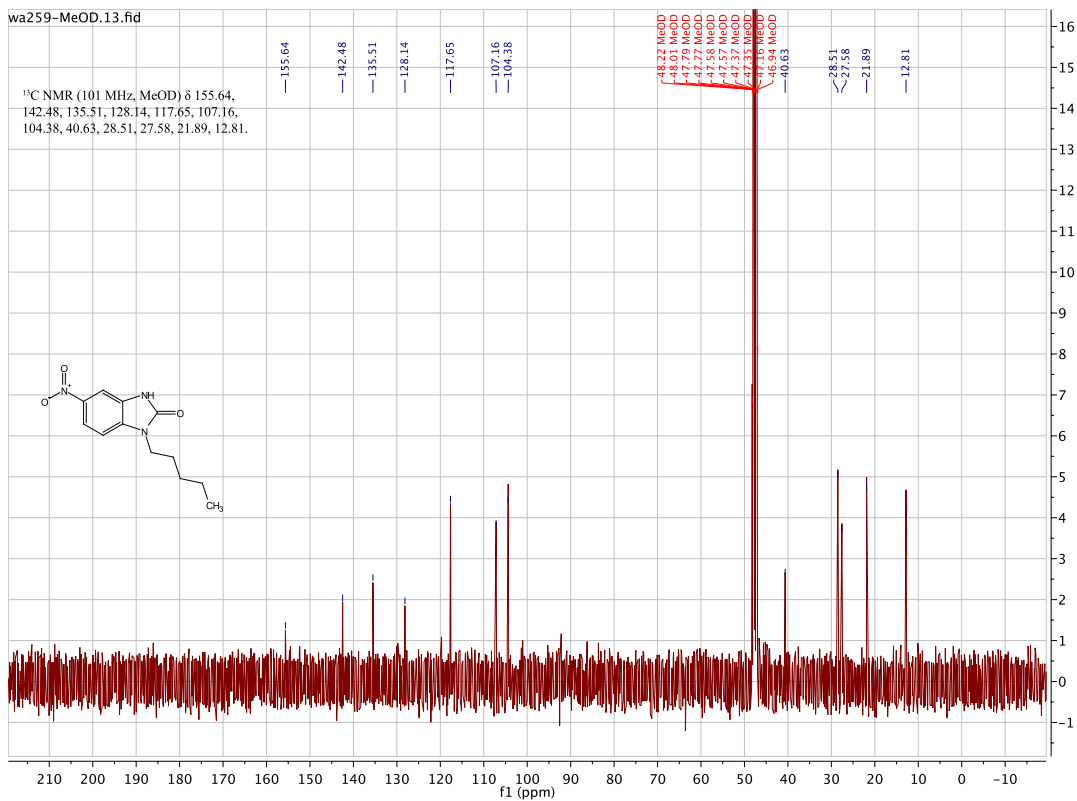


5-nitro-1-pentyl-1,3-dihydro-2H-benzo[d]imidazol-2-one: [WA259]

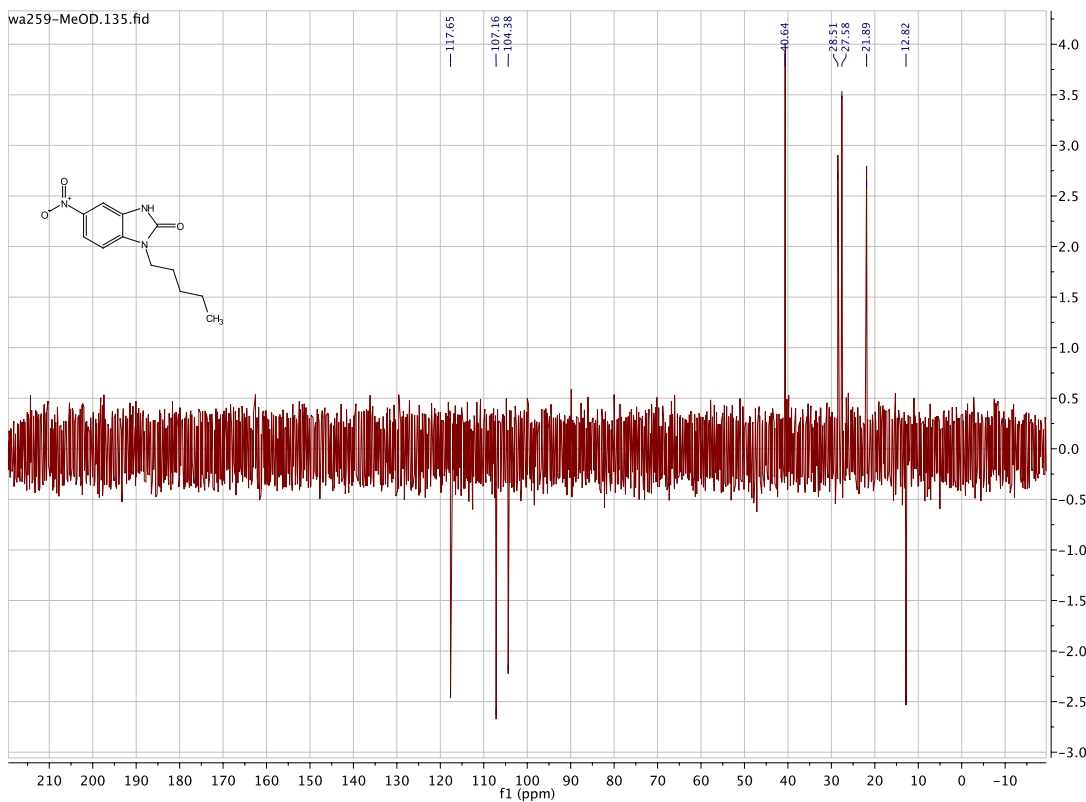


wa259-MeOD.13.fid

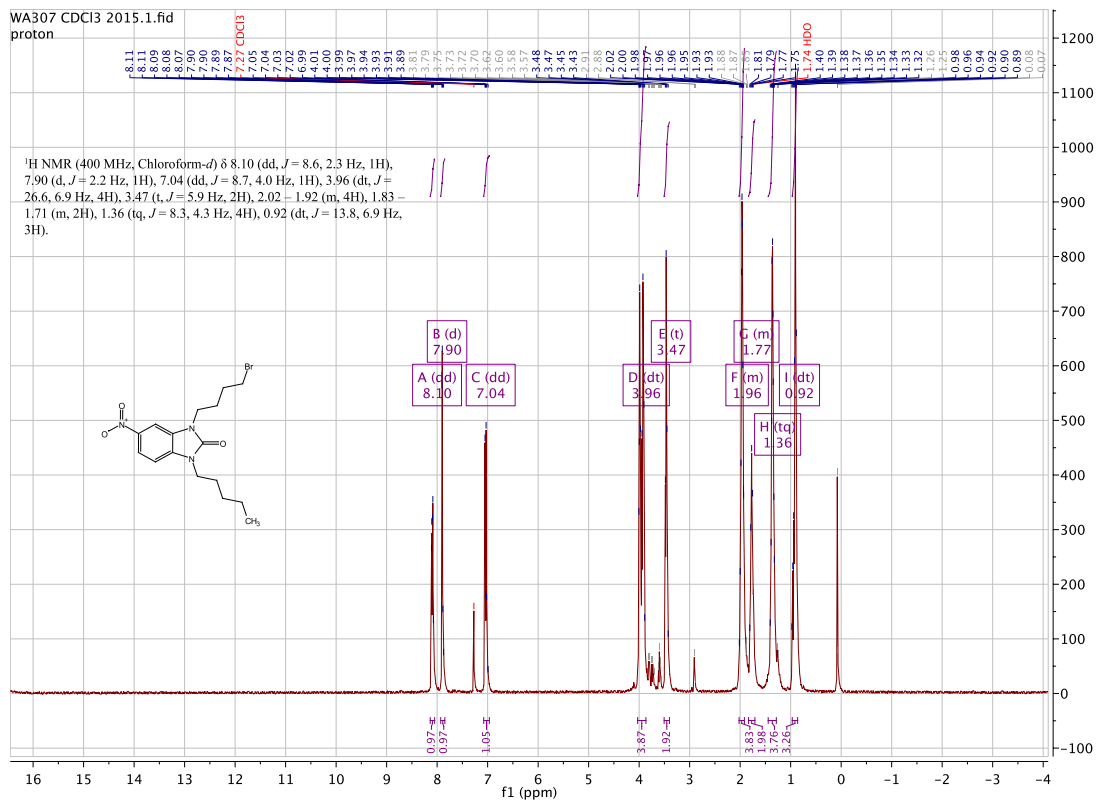
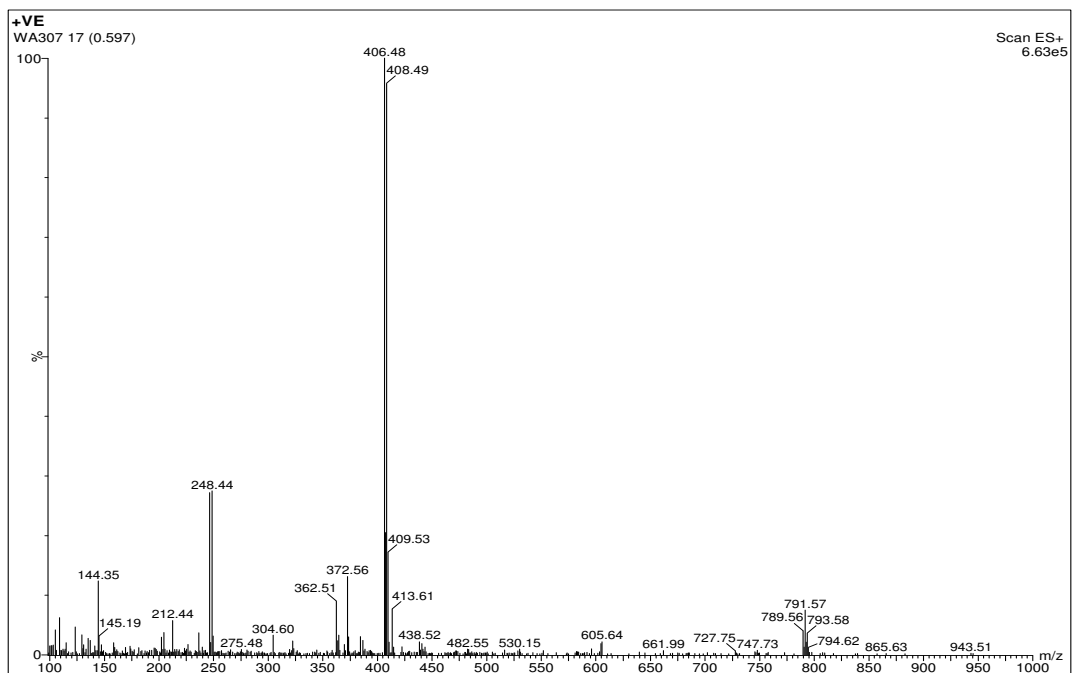
^{13}C NMR (101 MHz, MeOD) δ 155.64, 142.48, 135.51, 128.14, 117.65, 107.16, 104.38, 40.63, 28.51, 27.58, 21.89, 12.81.

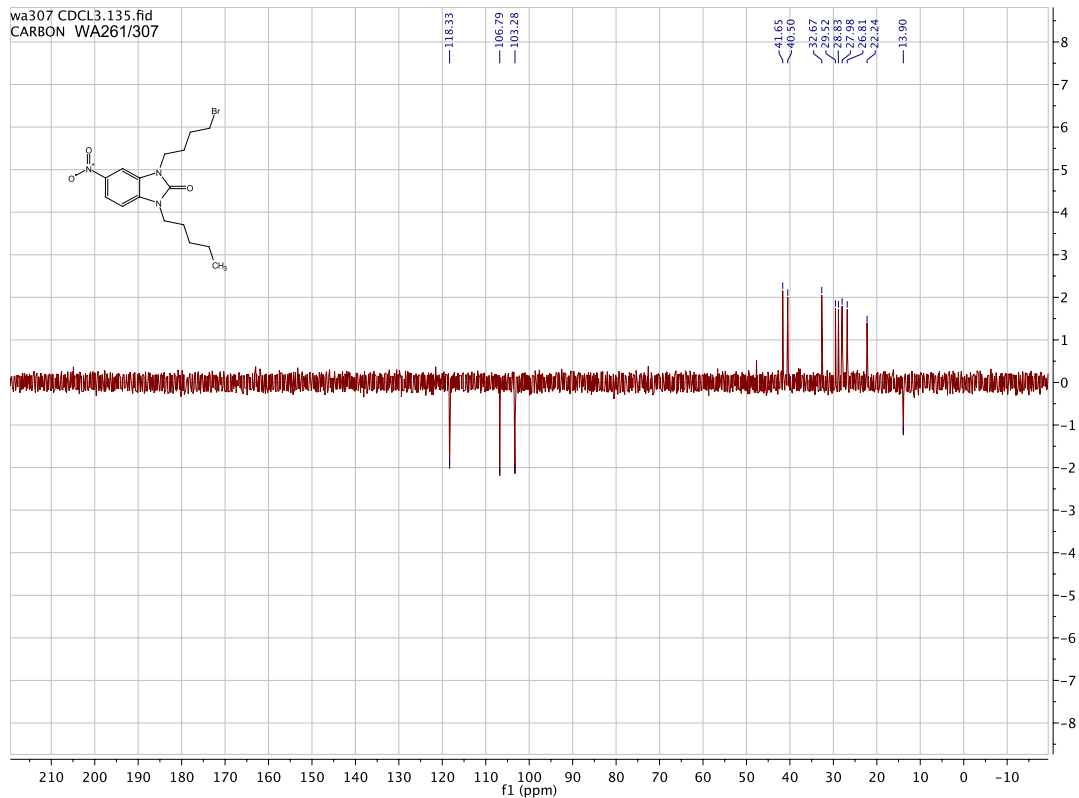
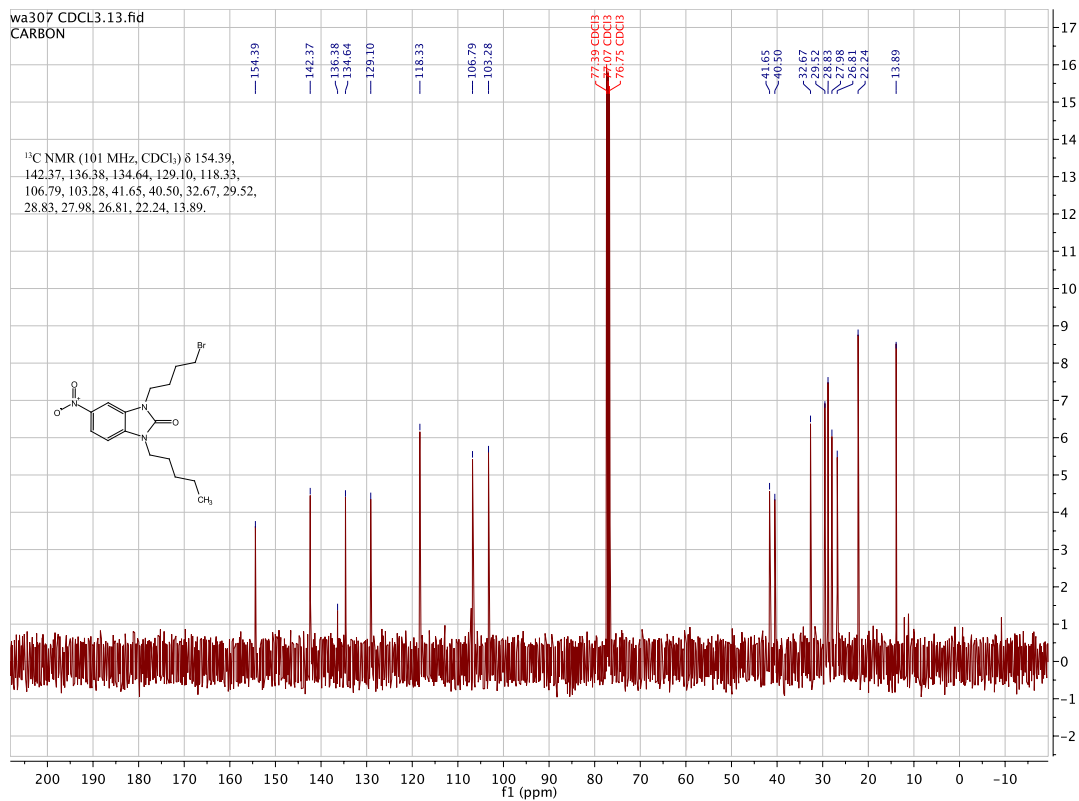


wa259-MeOD.135.fid

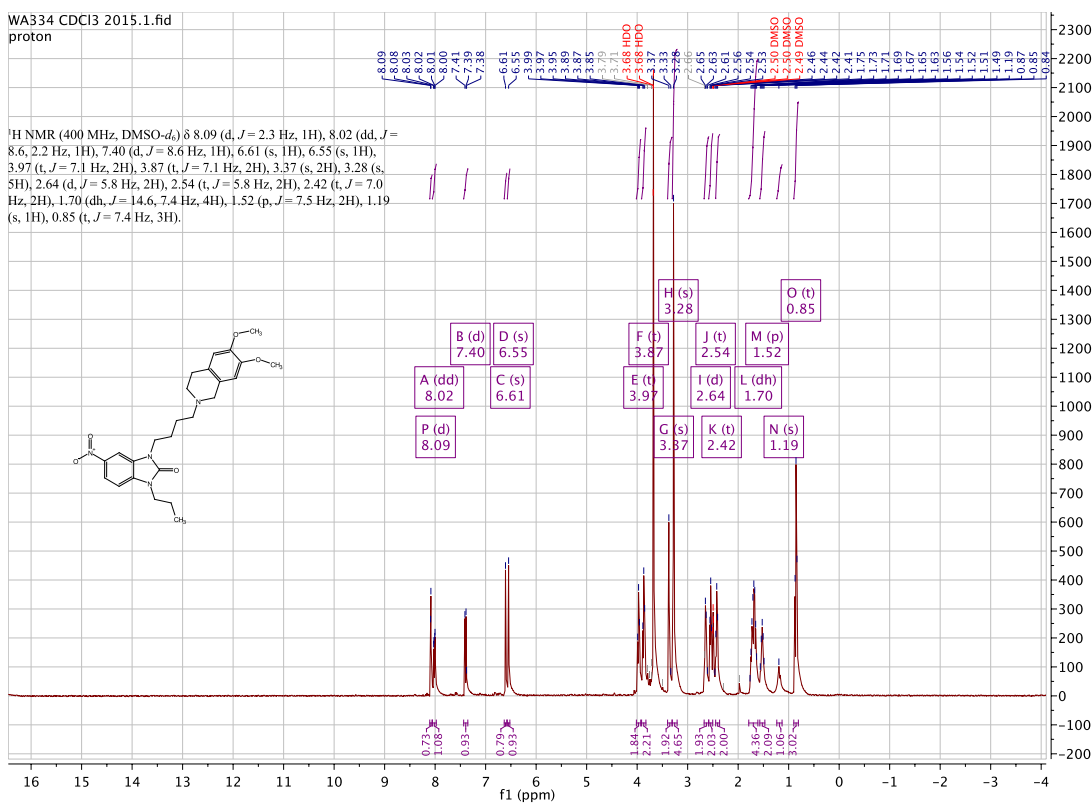
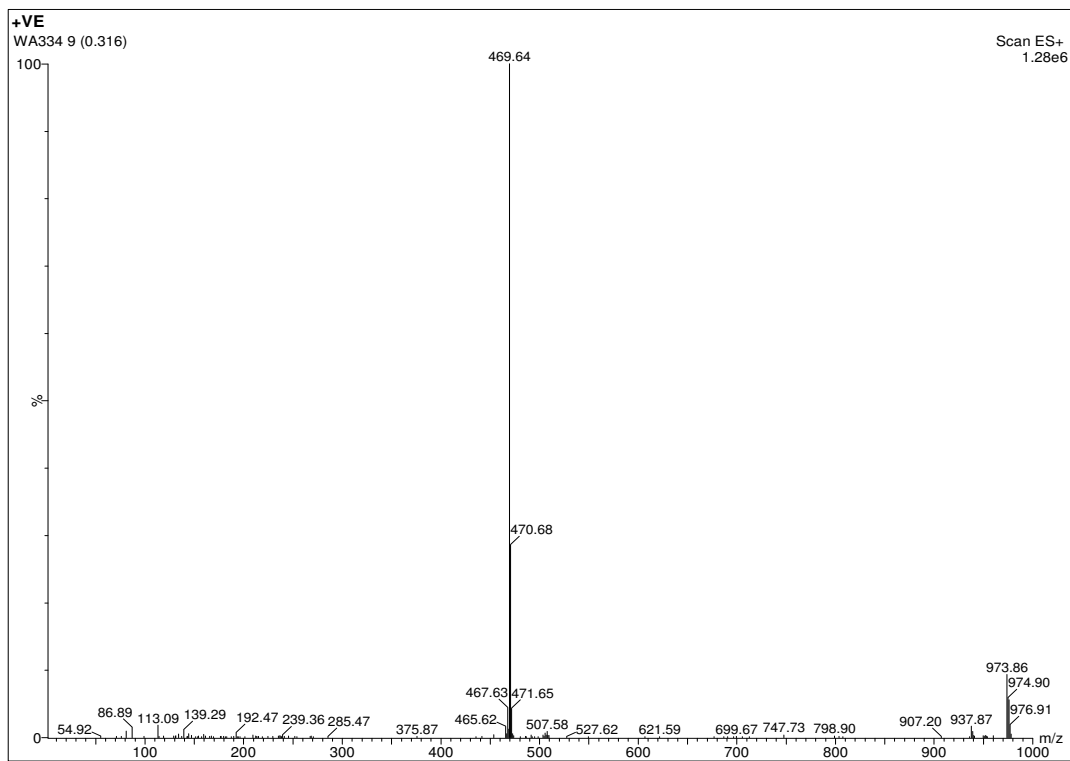


3-(4-bromobutyl)-5-nitro-1-pentyl-1,3-dihydro-2H-benzo[d]imidazol-2-one:
[WA261/WA307]



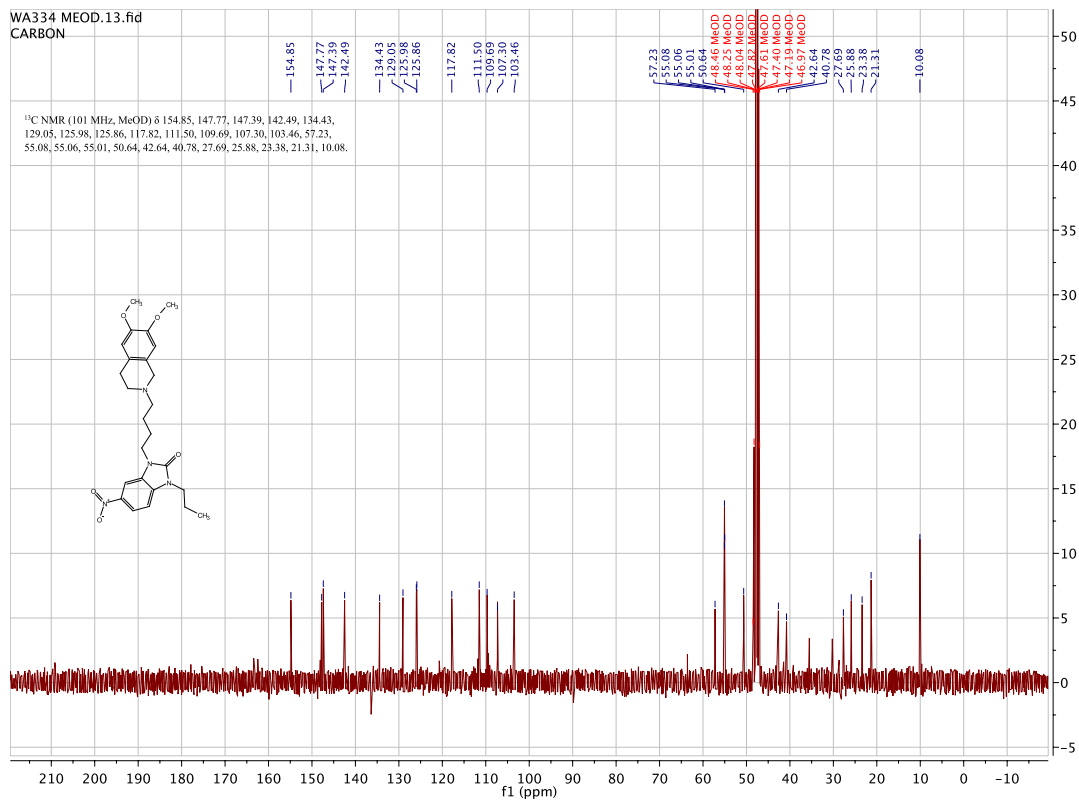


3-(4-(6,7-dimethoxy-3,4-dihydroisoquinolin-2(1H)-yl)butyl)-5-nitro-1-propyl-1,3-dihydro-2H-benzo[d]imidazol-2-one: [WA334]

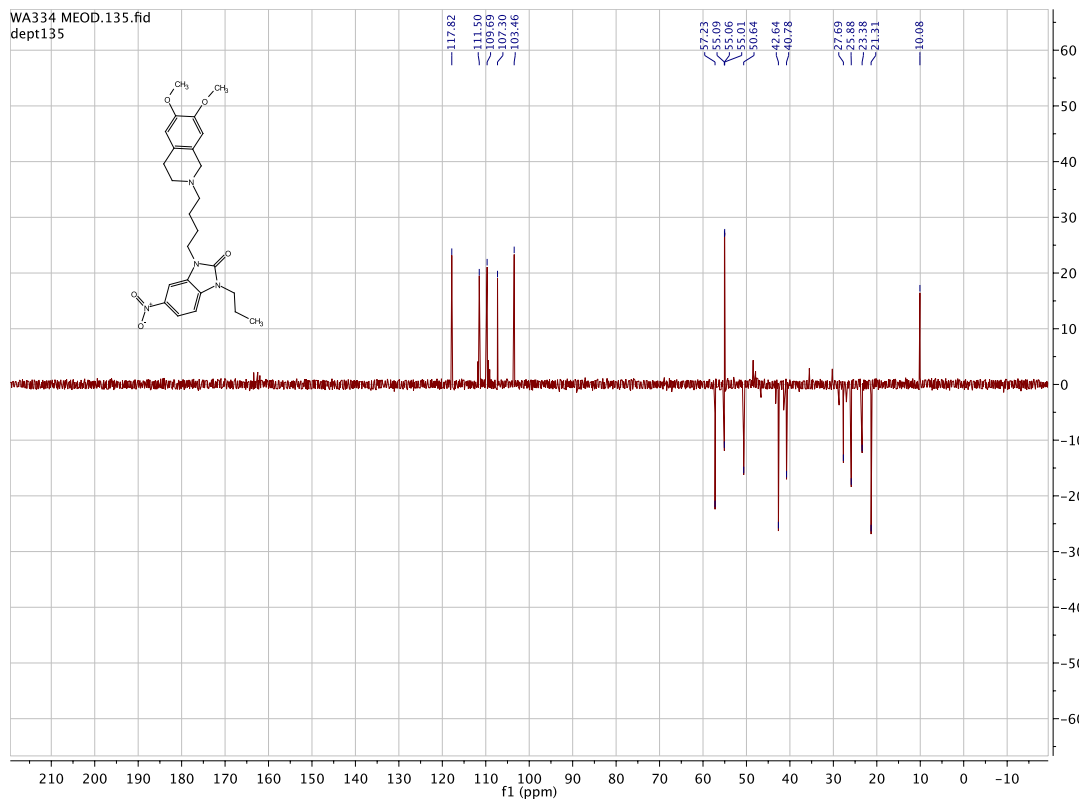


WA334 MEOD.13.fid
CARBON

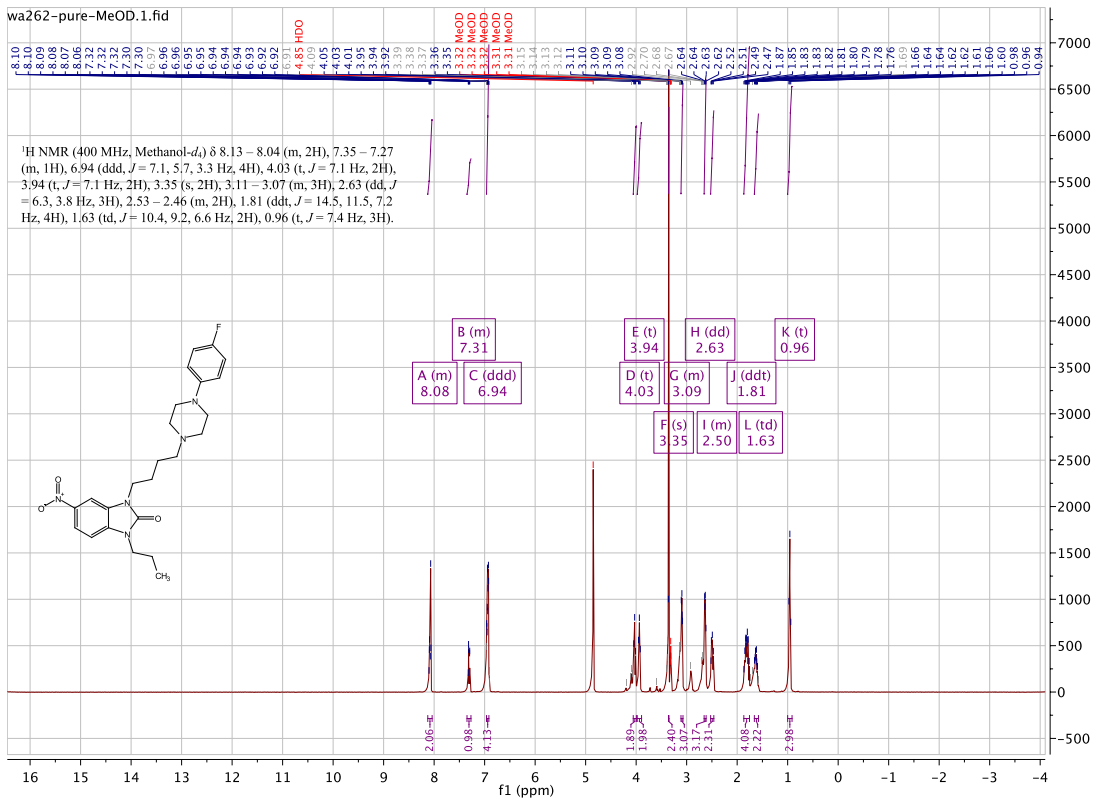
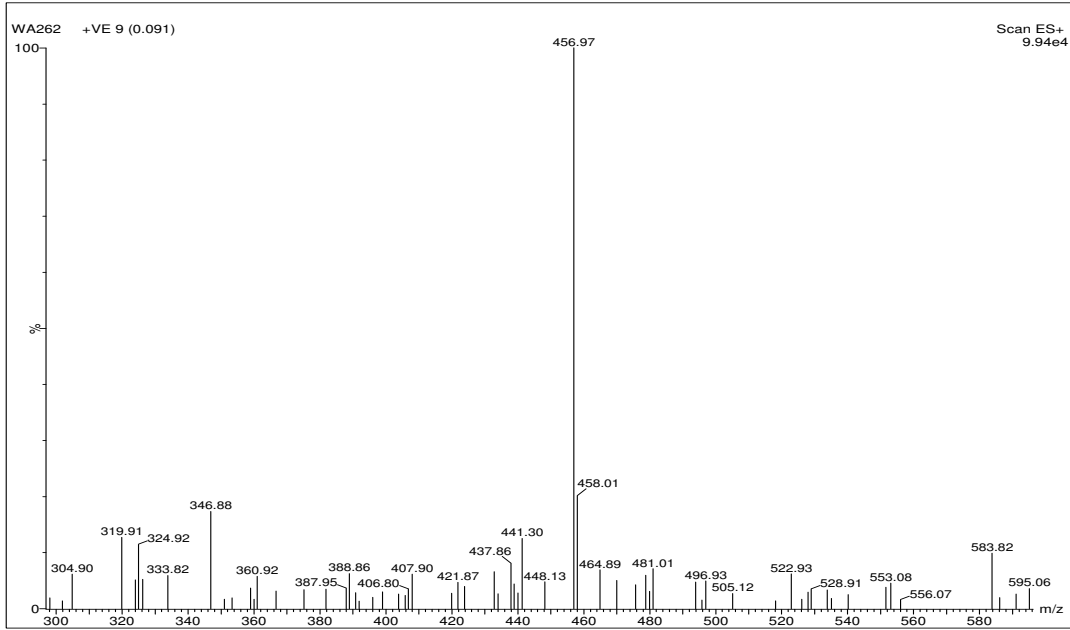
¹³C NMR (101 MHz, MeOD) δ 154.85, 147.77, 147.39, 142.49, 134.43,
129.05, 125.98, 125.86, 117.82, 111.50, 109.69, 107.30, 103.46, 57.23,
55.08, 55.06, 55.01, 50.64, 42.64, 40.78, 27.69, 25.88, 23.38, 21.31, 10.08.

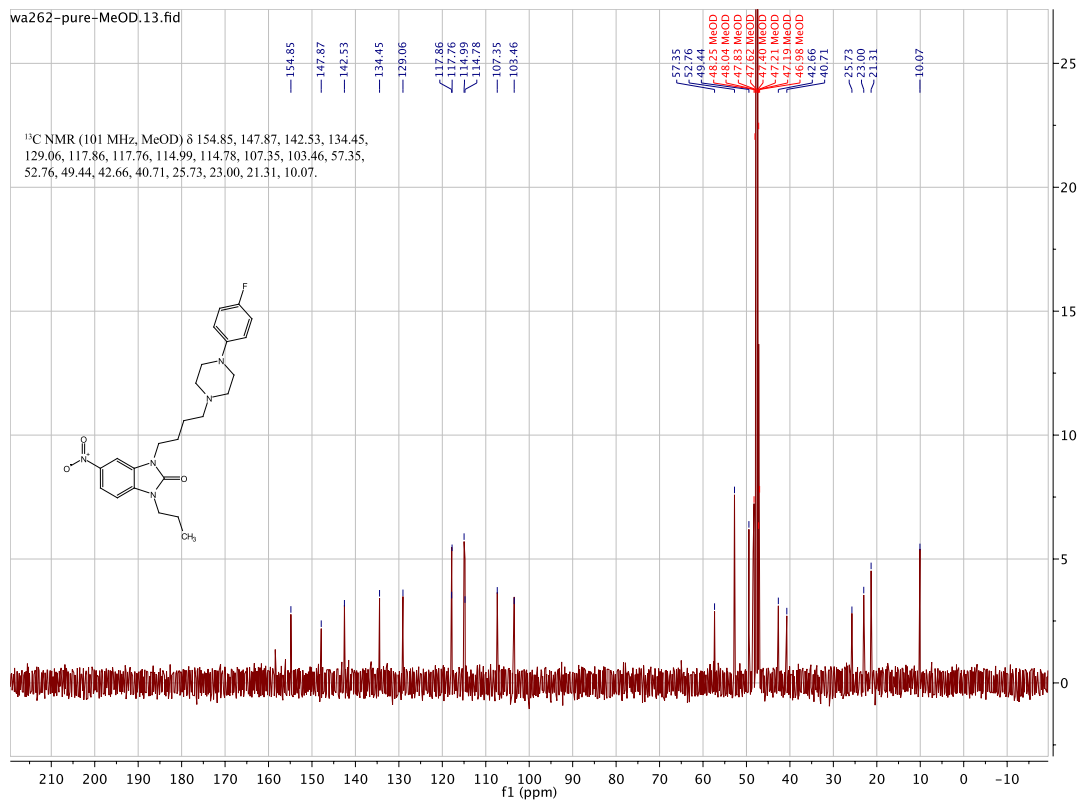


WA334 MEOD.135.fid
dept135

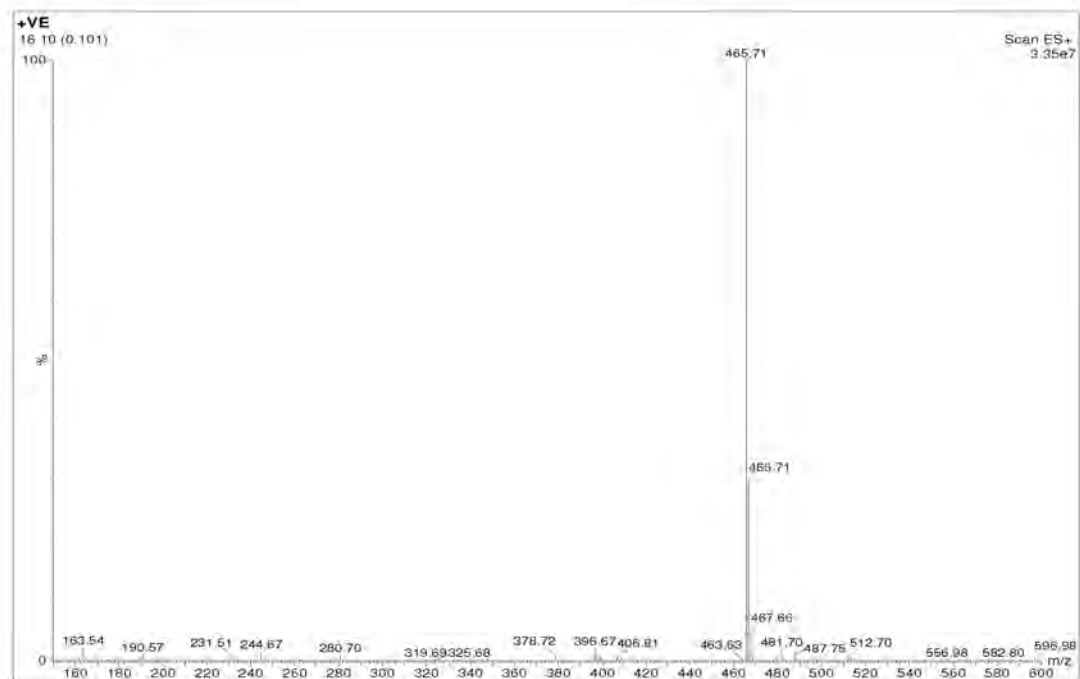


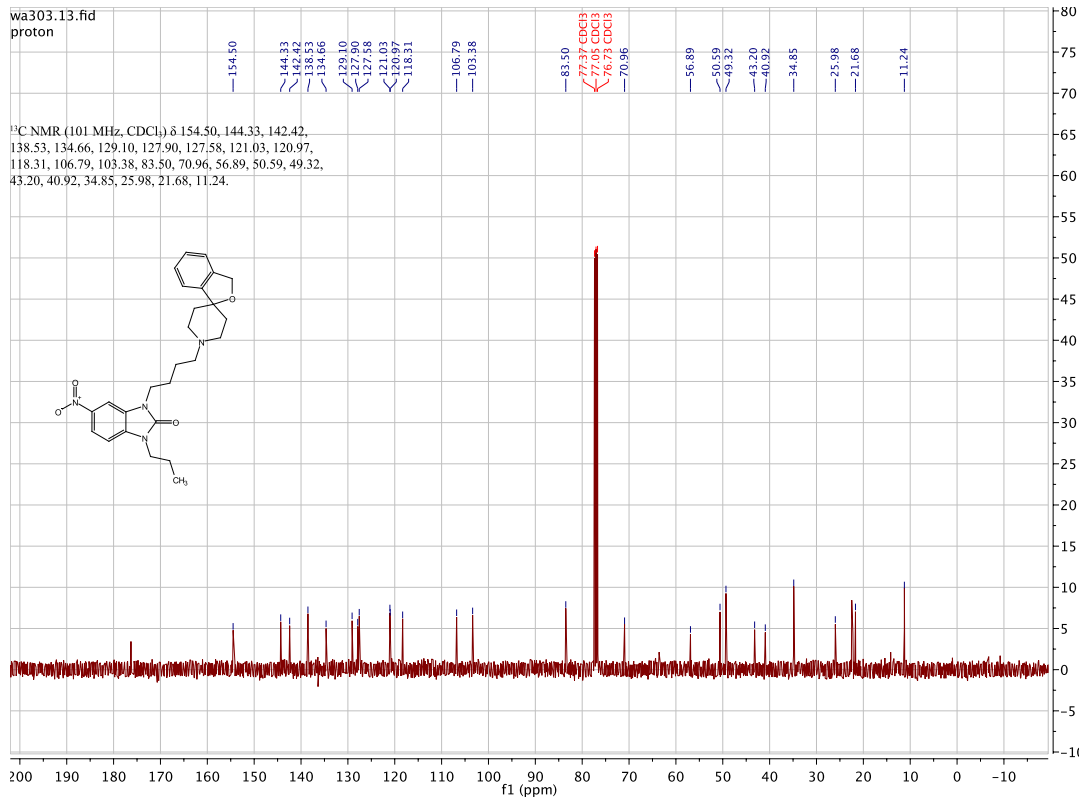
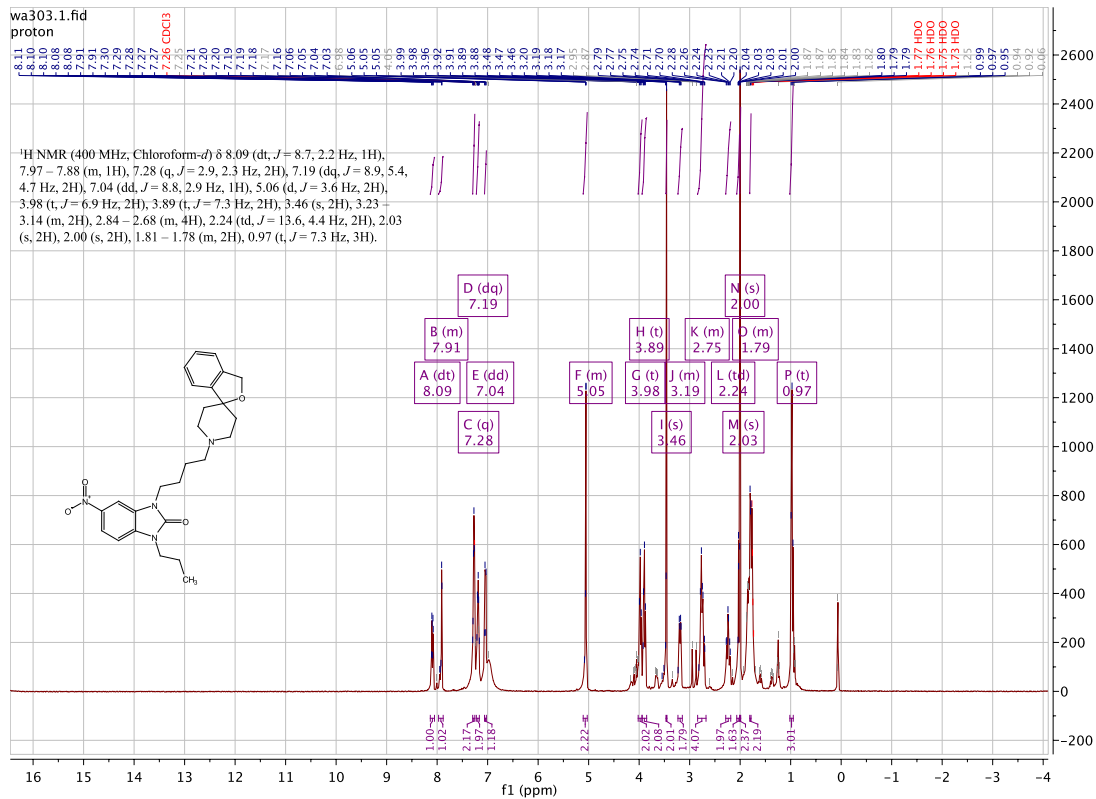
3-(4-(4-(4-fluorophenyl)piperazin-1-yl)butyl)-5-nitro-1-propyl-1,3-dihydro-2H-benzof[d]imidazol-2-one: [WA262]



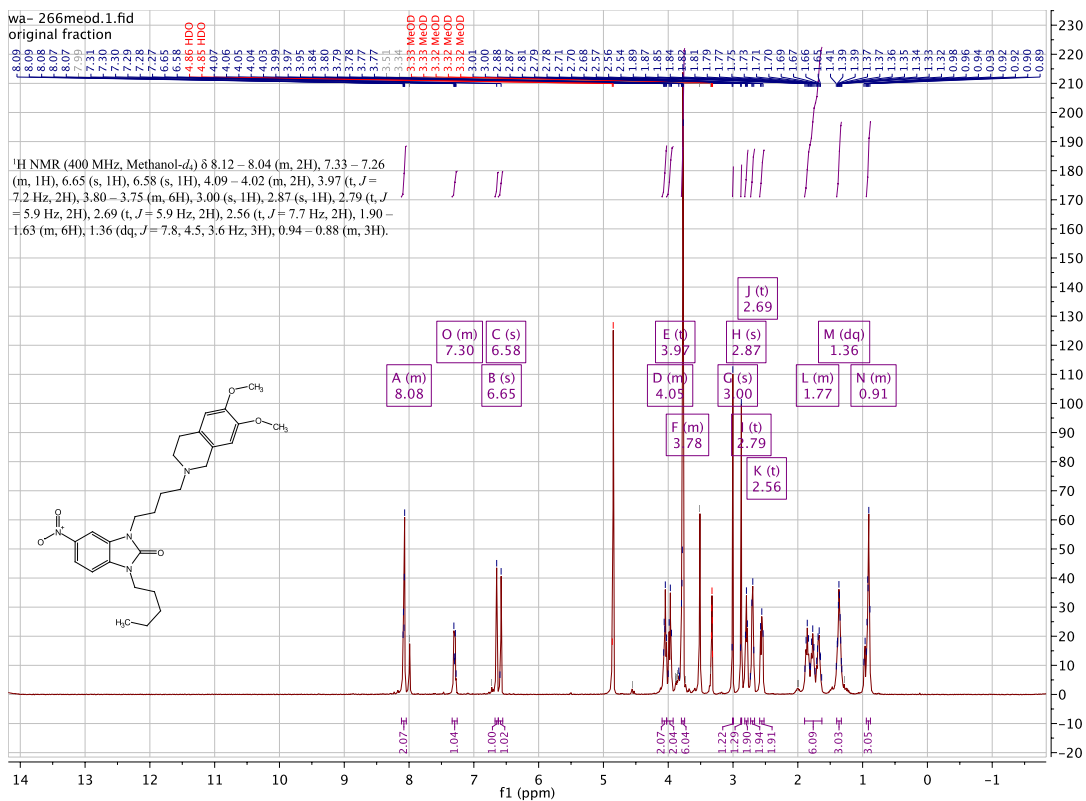
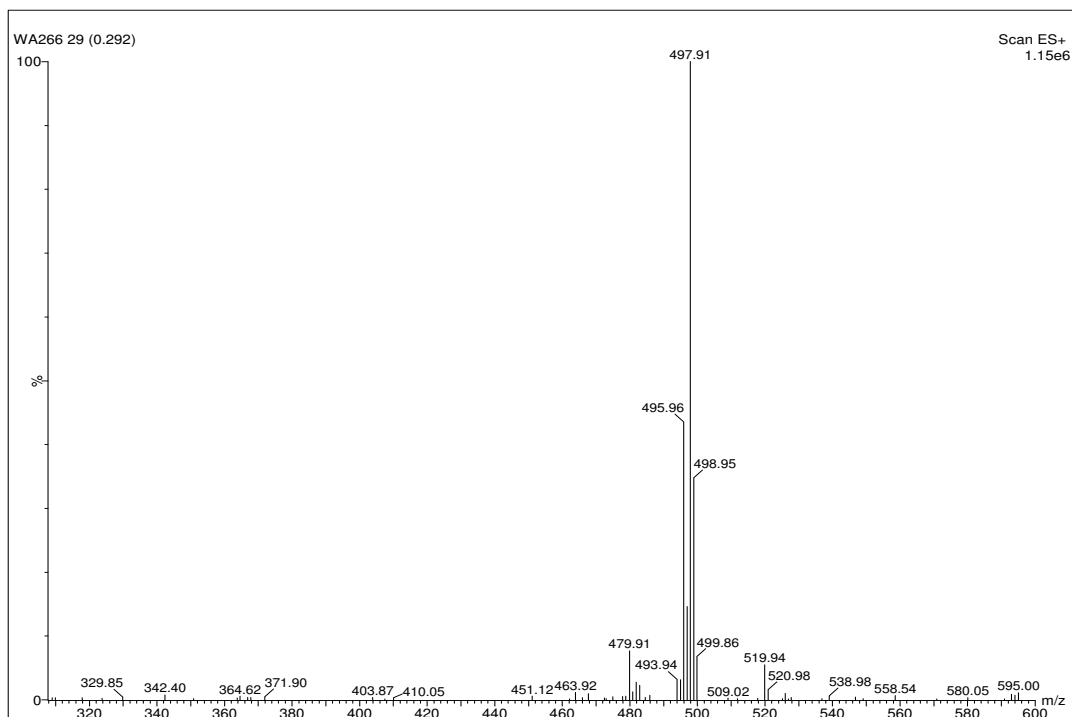


3-(4-(3H-spiro[isobenzofuran-1,4'-piperidin]-1'-yl)butyl)-5-nitro-1-propyl-1,3-dihydro-2H-benzo[d]imidazol-2-one: [WA303]



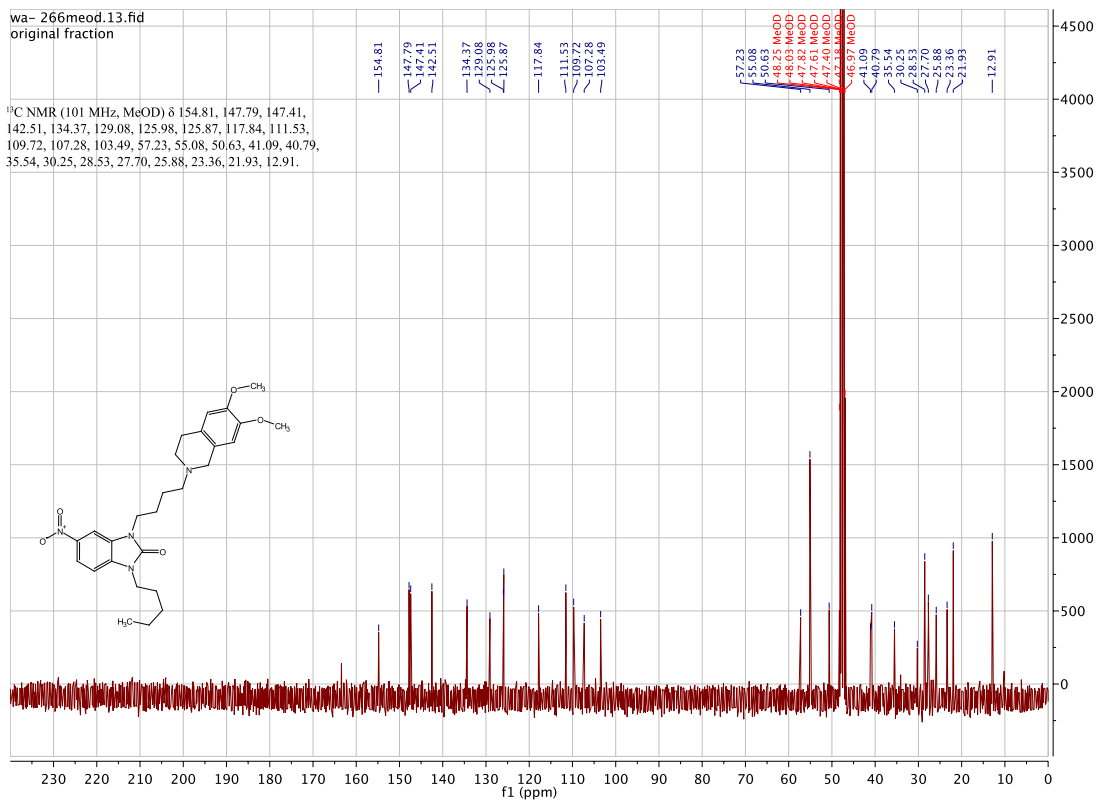


3-(4-(6,7-dimethoxy-3,4-dihydroisoquinolin-2(1H)-yl)butyl)-5-nitro-1-pentyl-1,3-dihydro-2H-benzo[d]imidazol-2-one:[WA266/299/308]

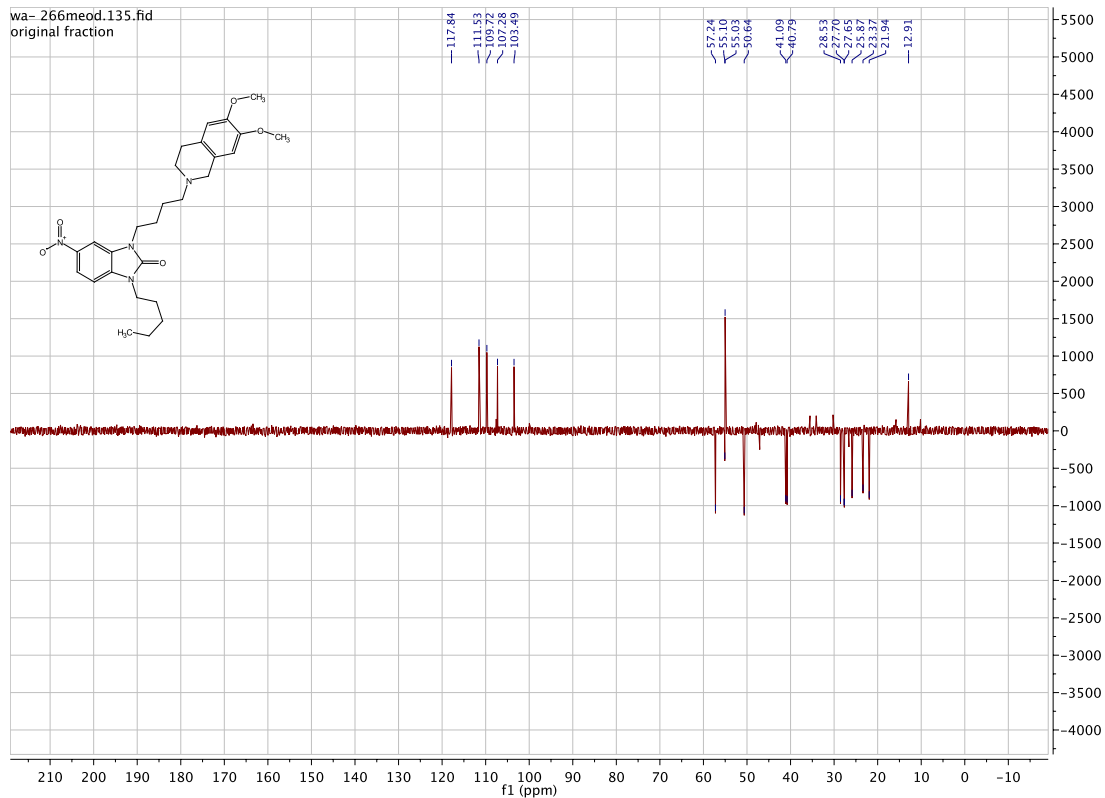


wa- 266meod.13.fid
original fraction

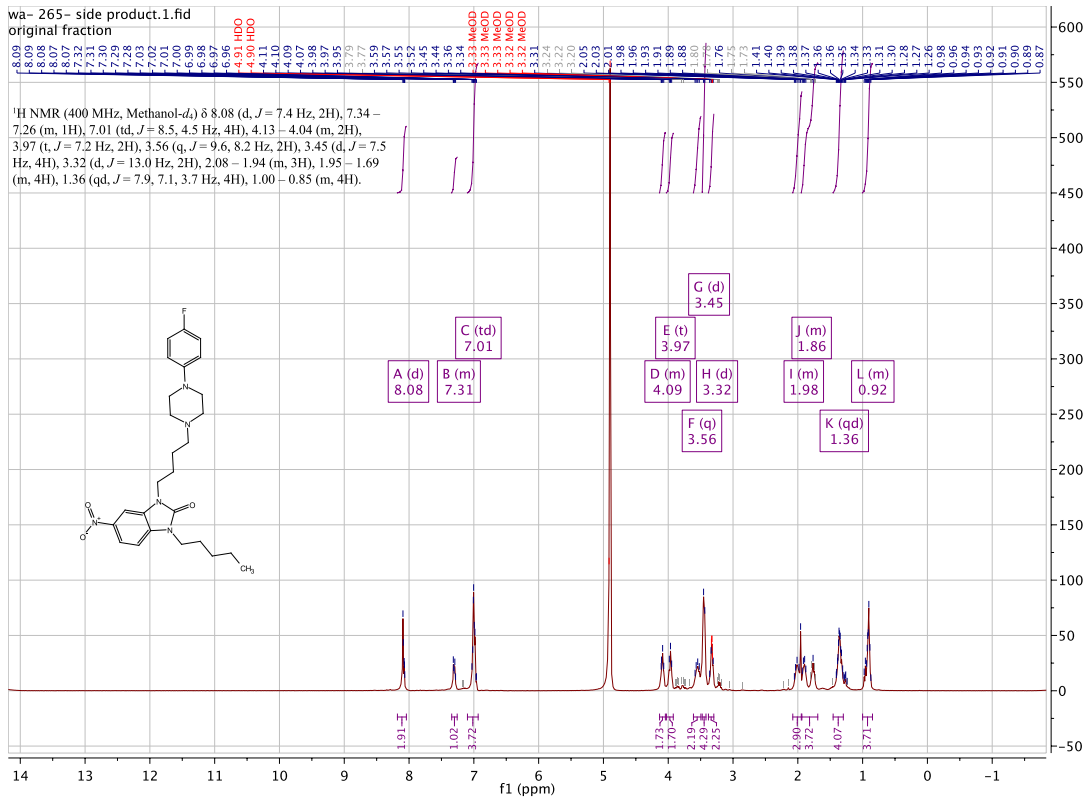
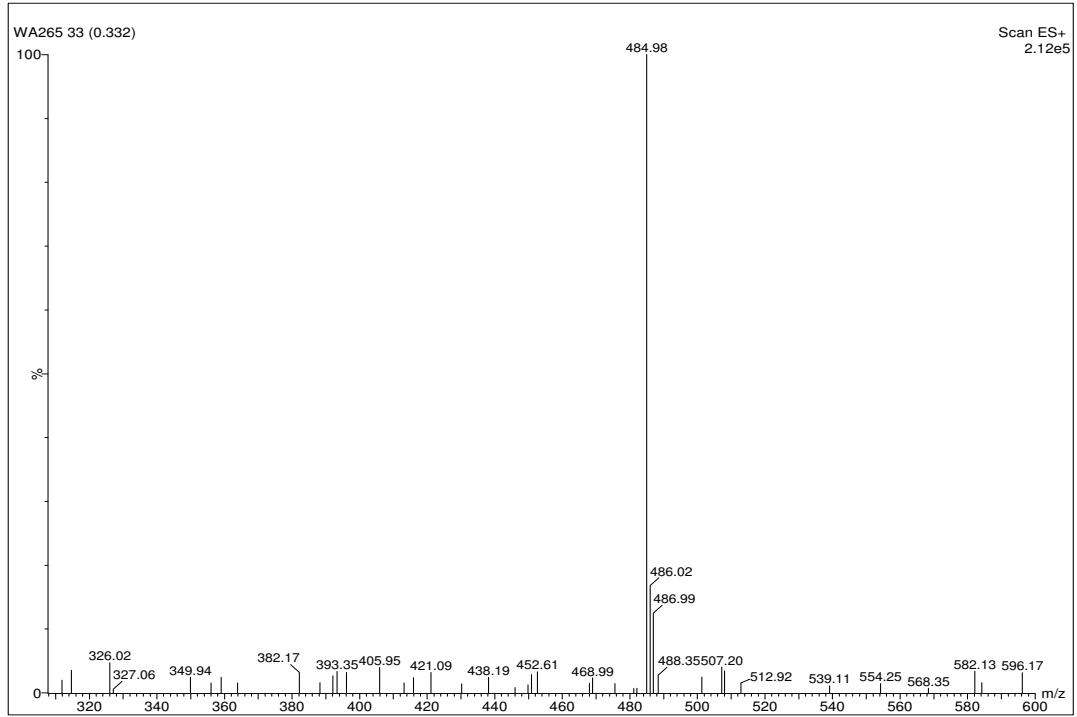
¹³C NMR (101 MHz, MeOD) δ 154.81, 147.79, 147.41, 142.51, 134.37, 129.08, 125.98, 125.87, 117.84, 111.53, 109.72, 107.28, 103.49, 57.23, 55.08, 50.63, 41.09, 40.79, 35.54, 30.25, 28.53, 27.70, 25.88, 23.36, 21.93, 12.91.

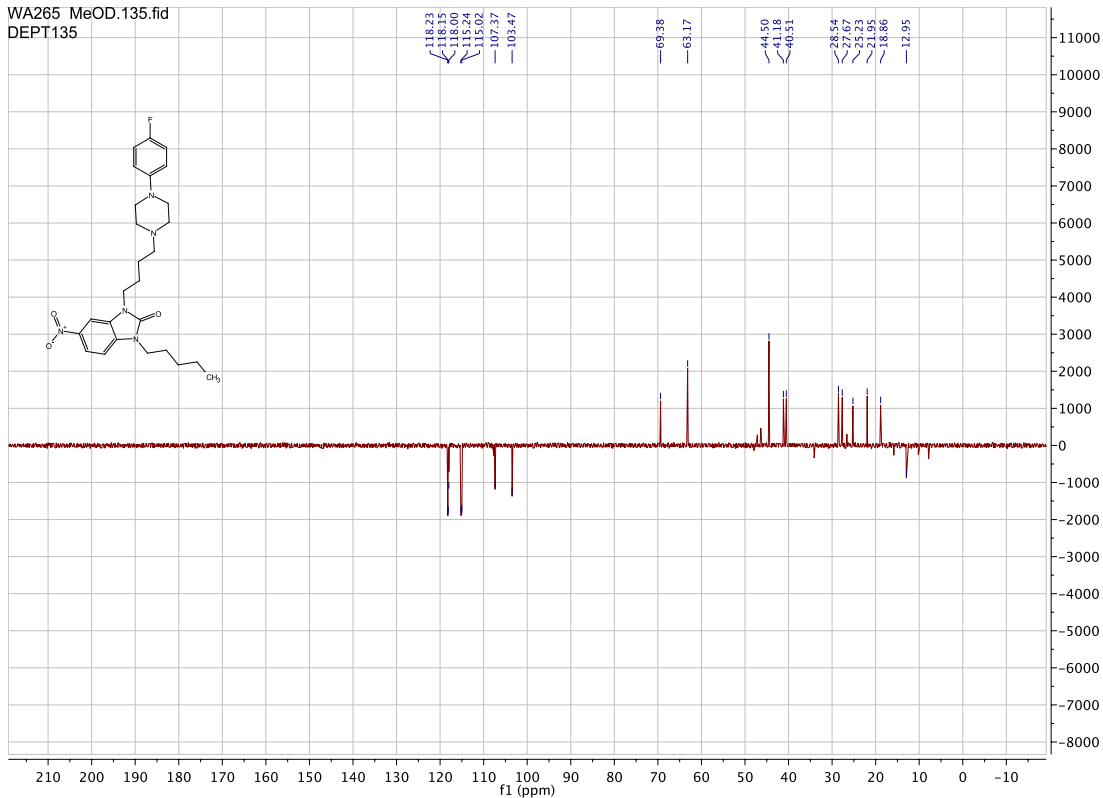
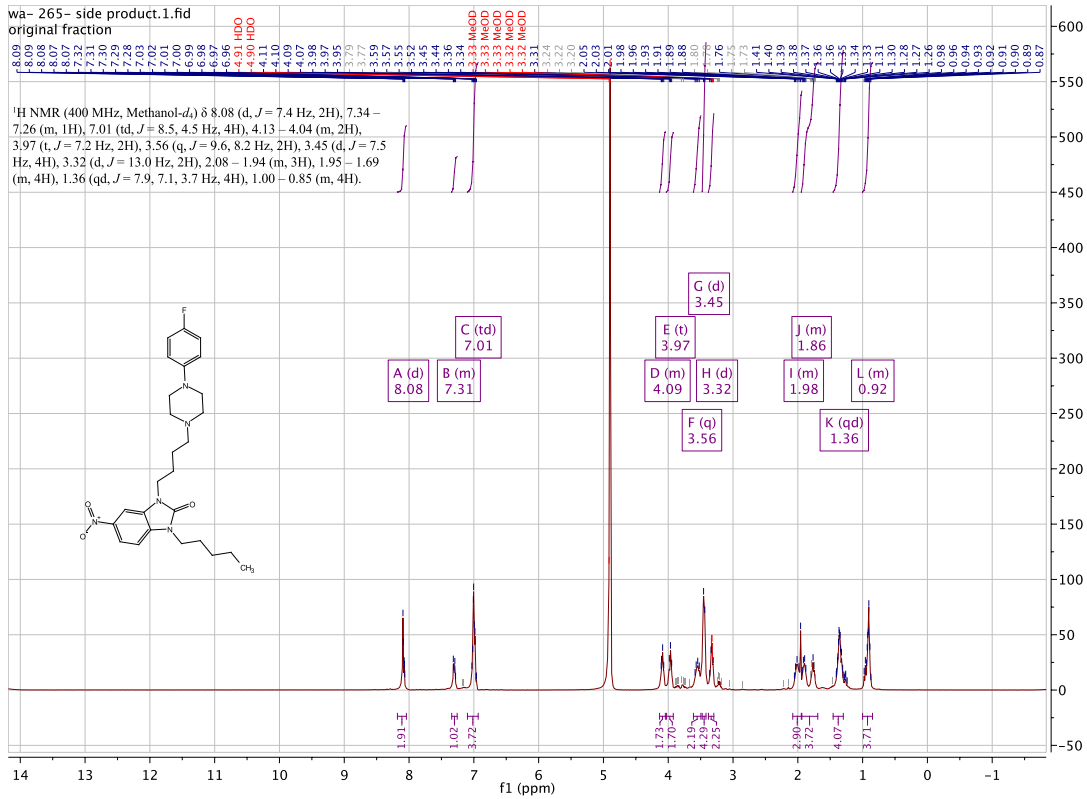


wa- 266meod.135.fid
original fraction

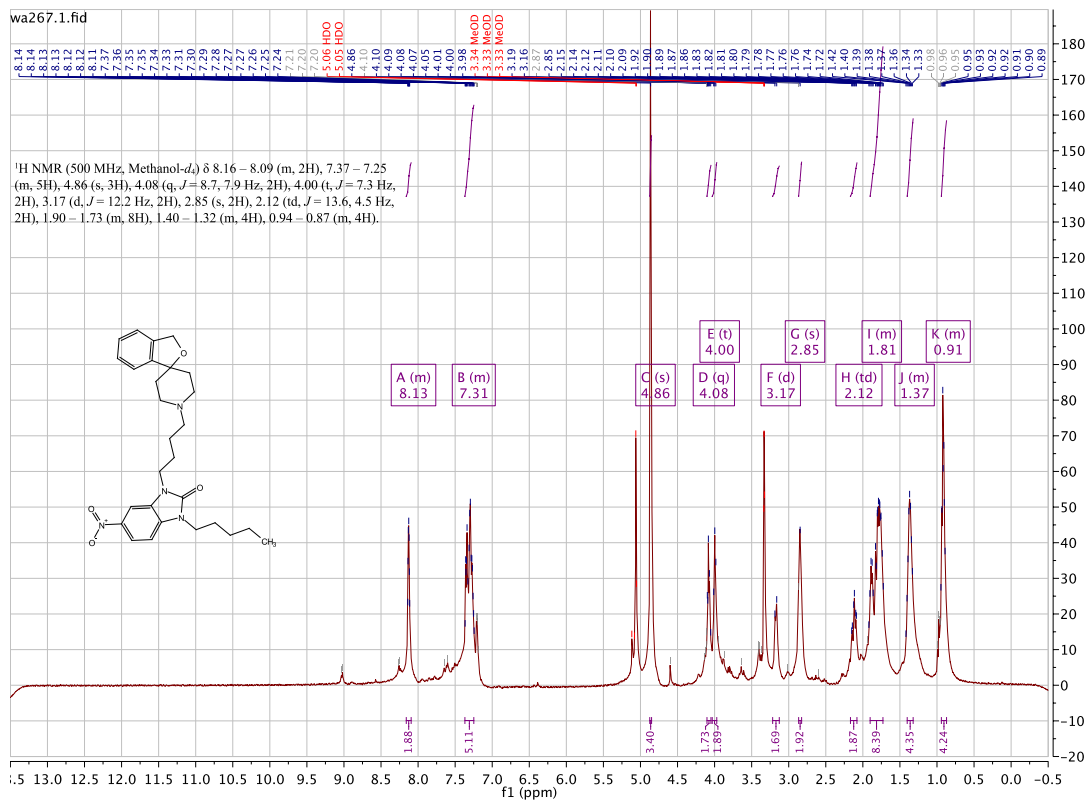
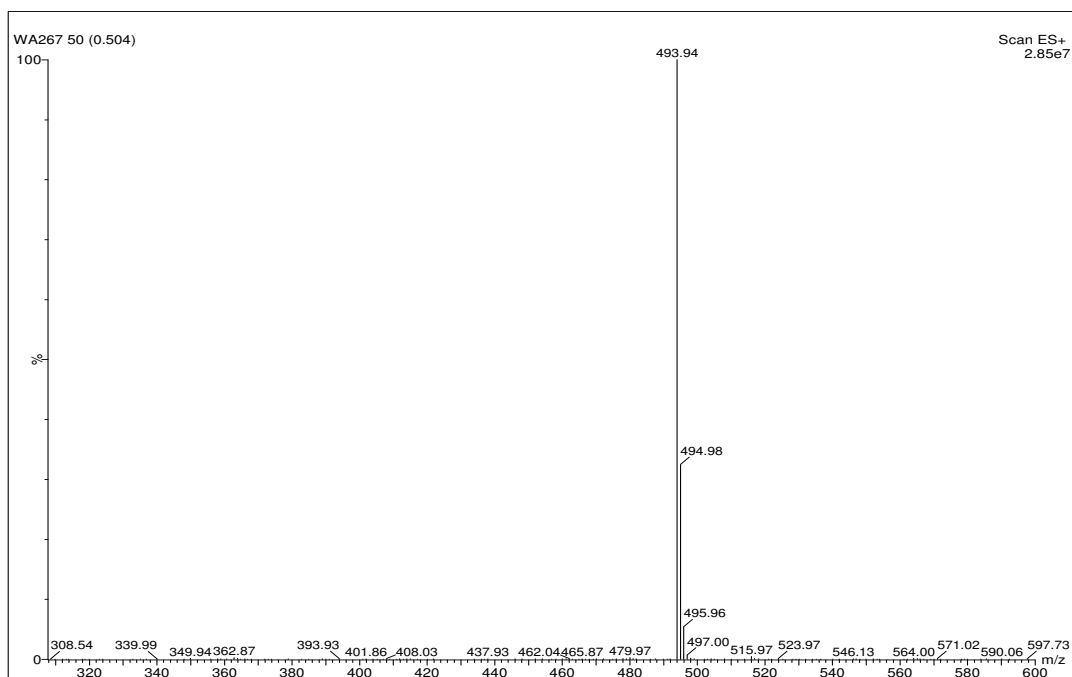


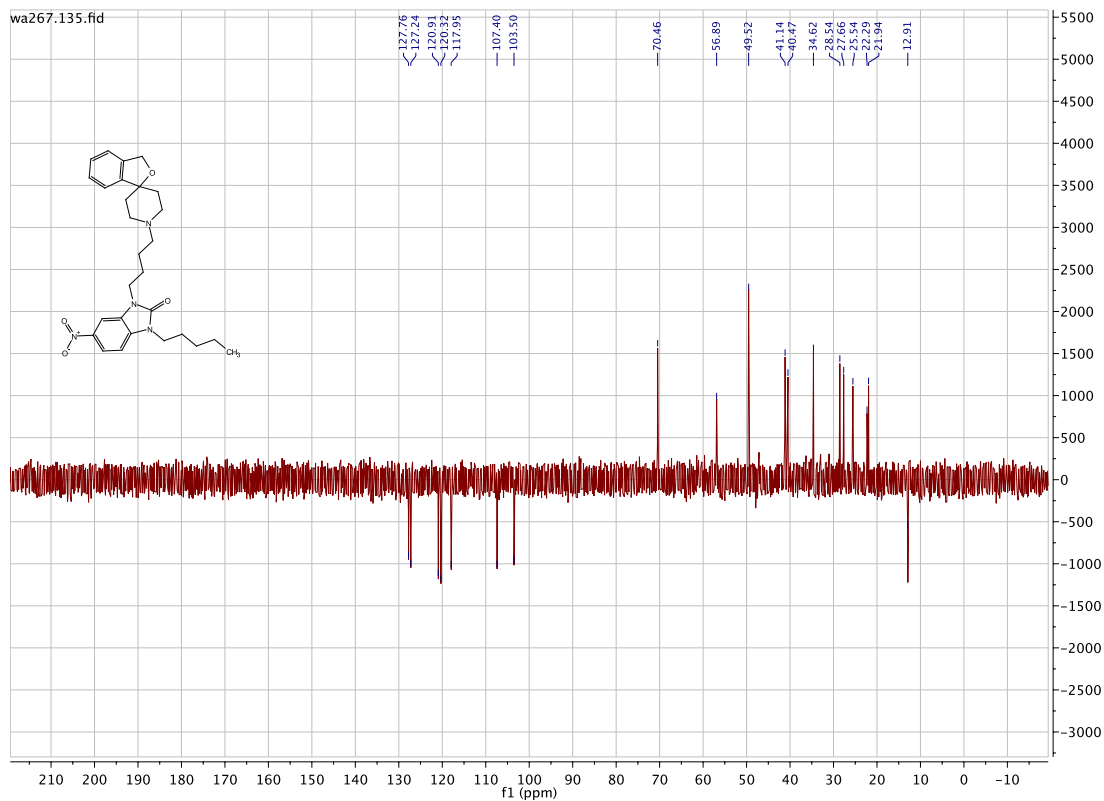
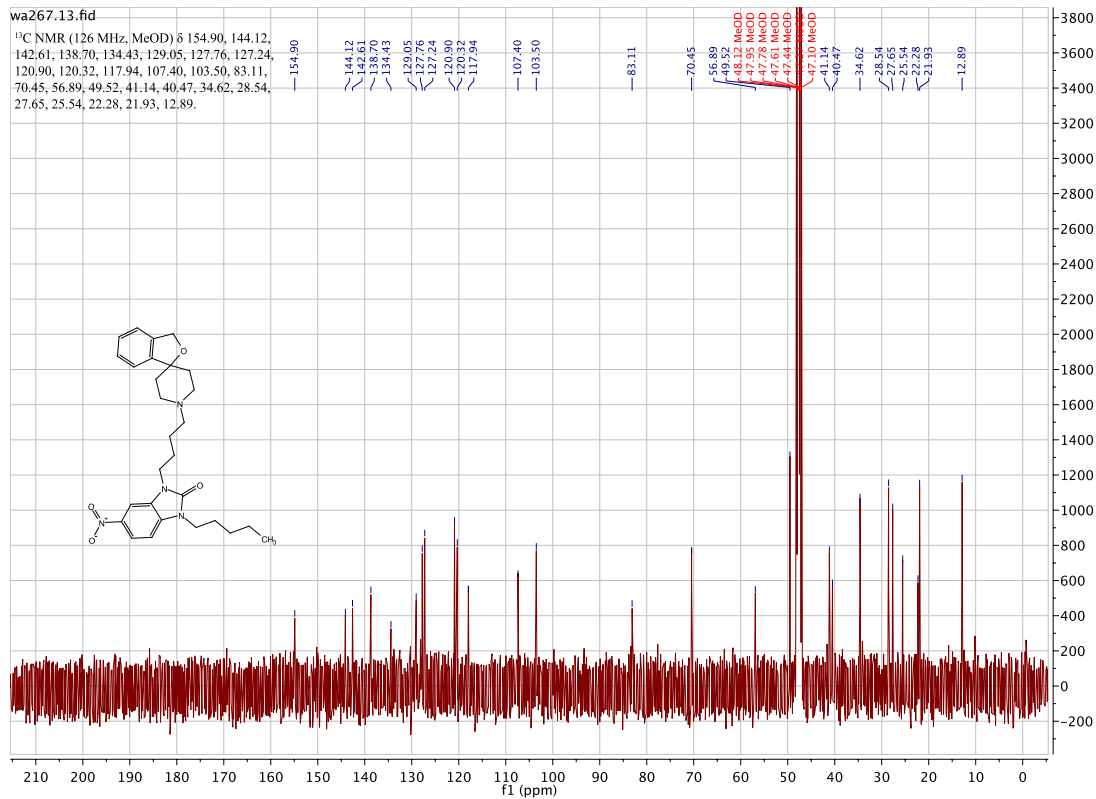
3-(4-(4-(4-fluorophenyl)piperazin-1-yl)butyl)-5-nitro-1-pentyl-1,3-dihydro-2H-benzof[d]imidazol-2-one: [WA336/265]



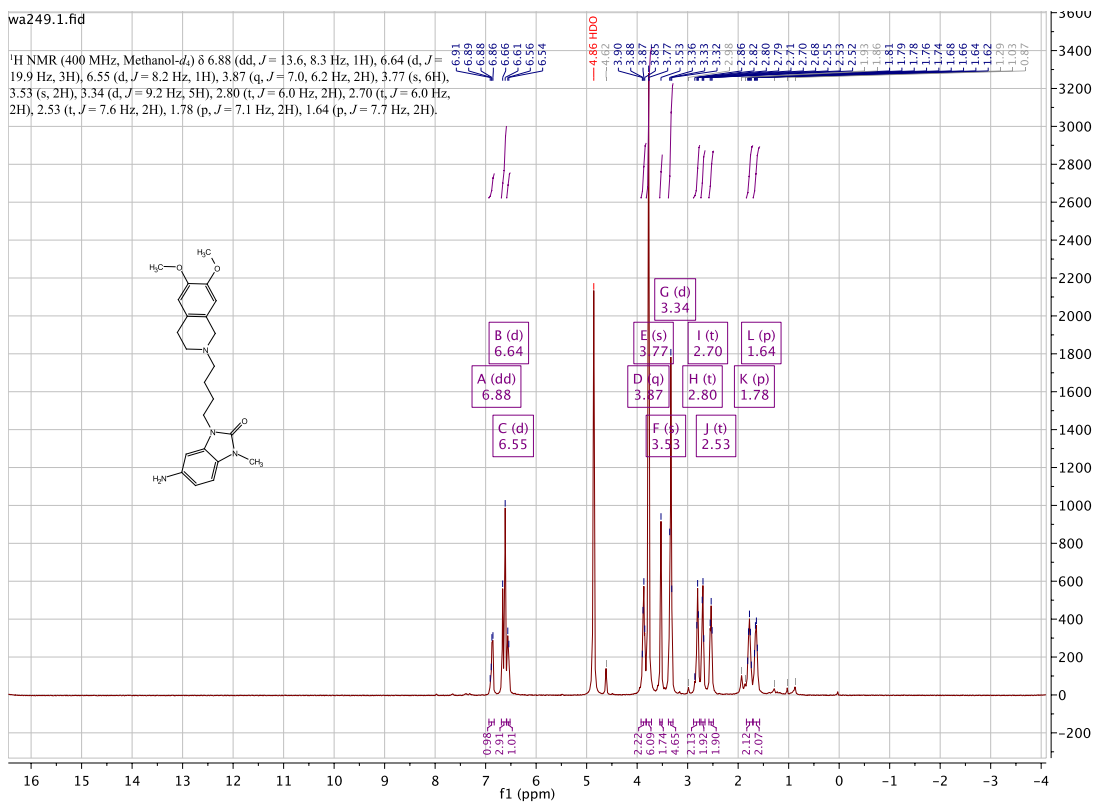
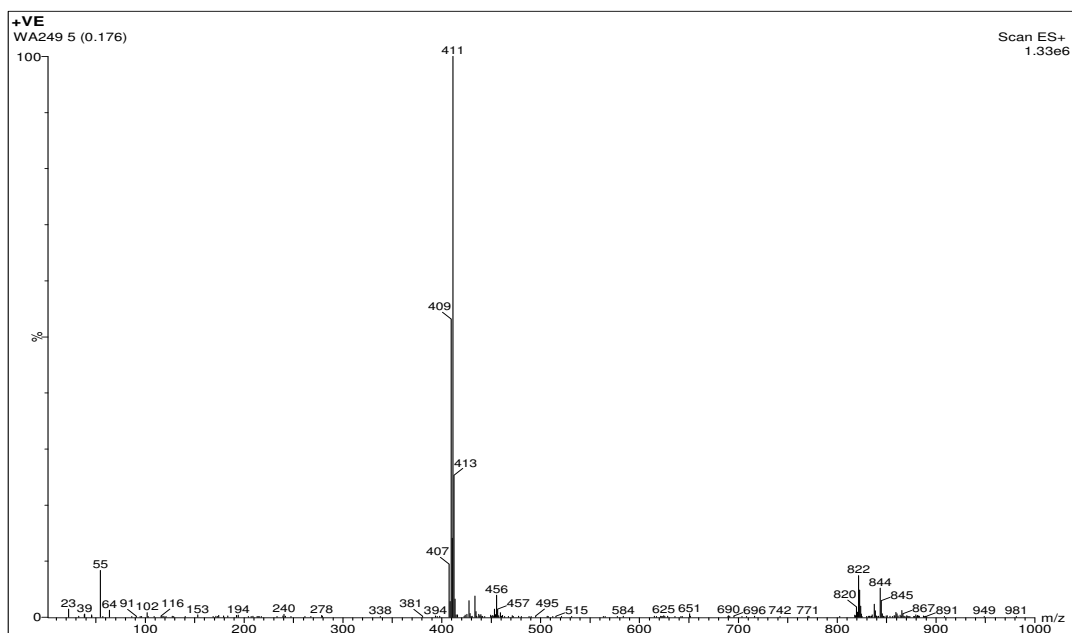


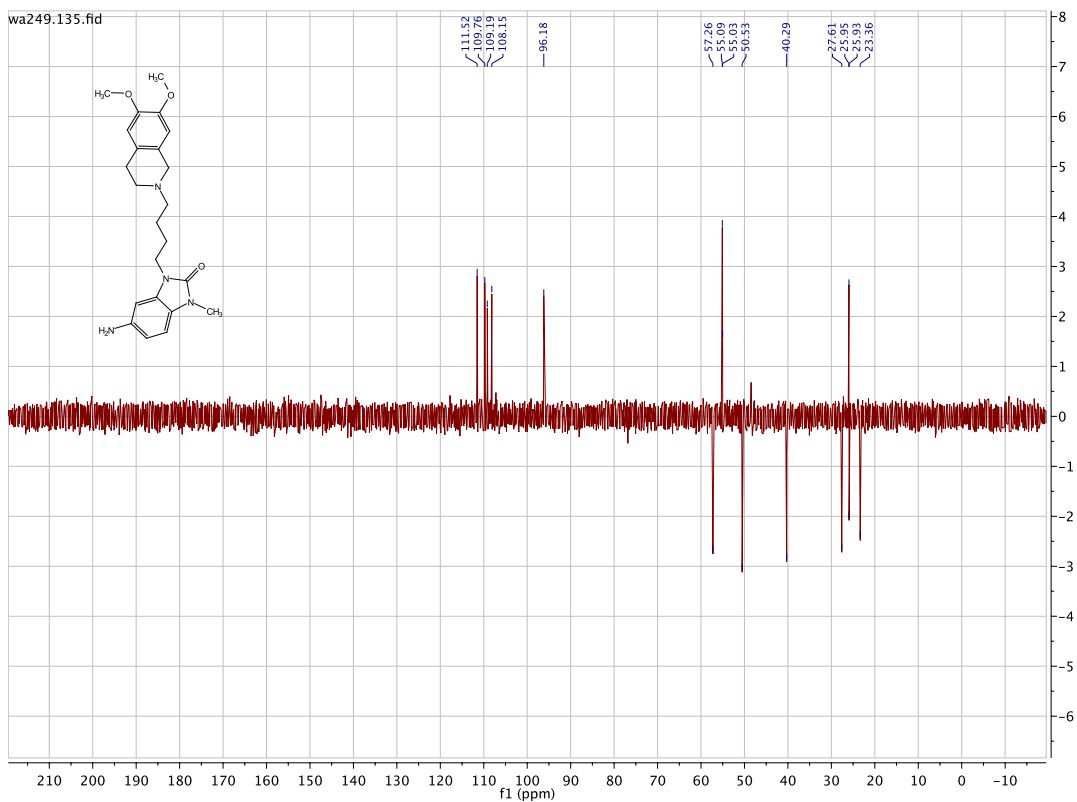
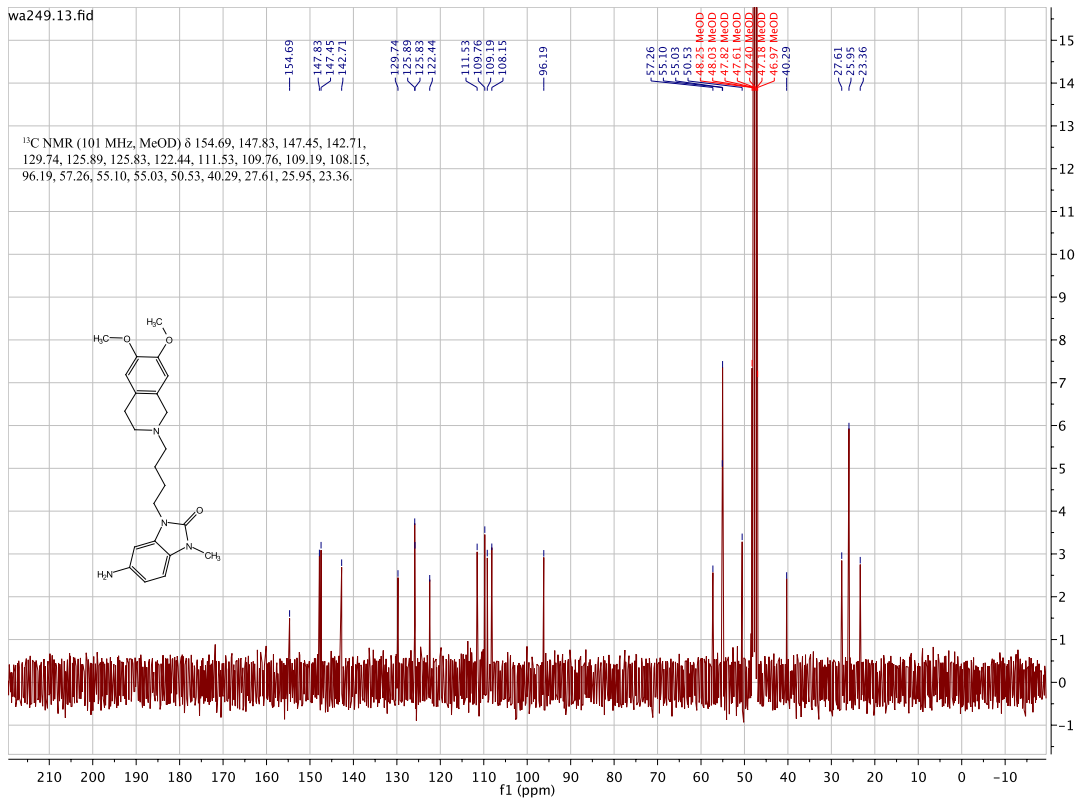
3-(4-(3H-spiro[isobenzofuran-1,4'-piperidin]-1'-yl)butyl)-5-nitro-1-pentyl-1,3-dihydro-2H-benzo[d]imidazol-2-one: [WA267]



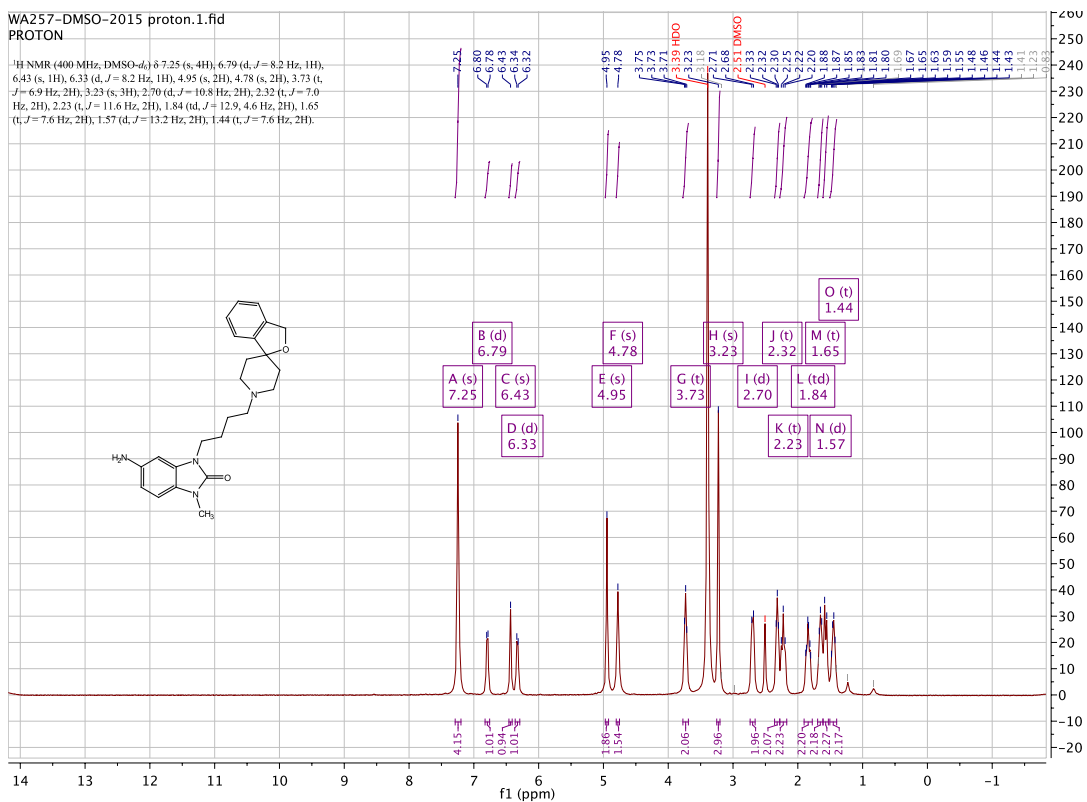
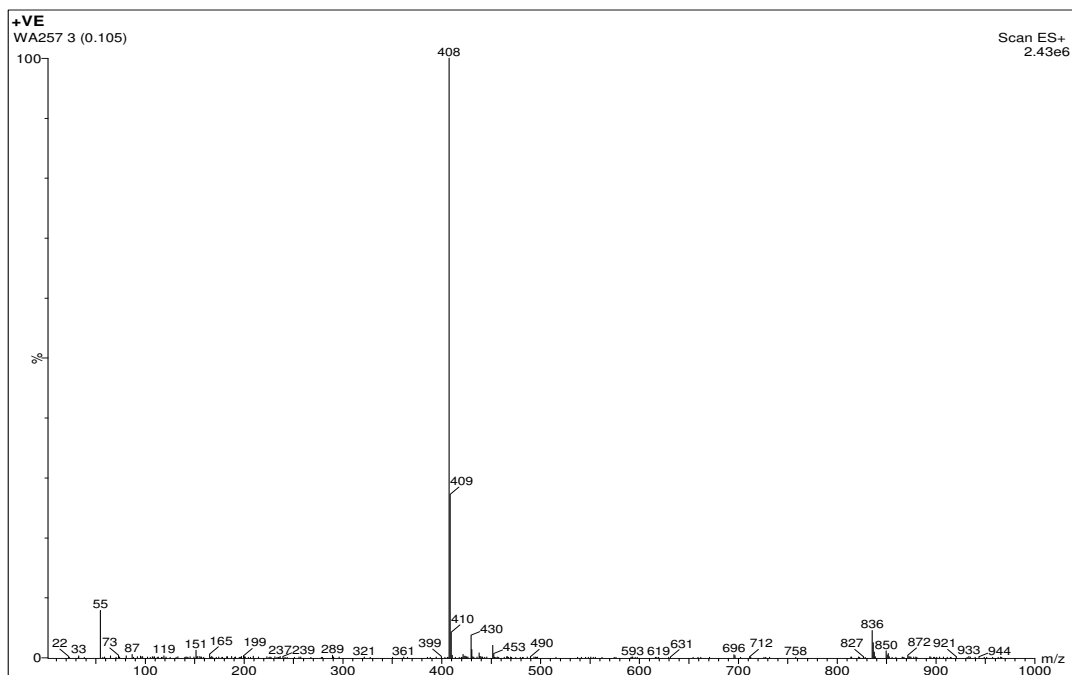


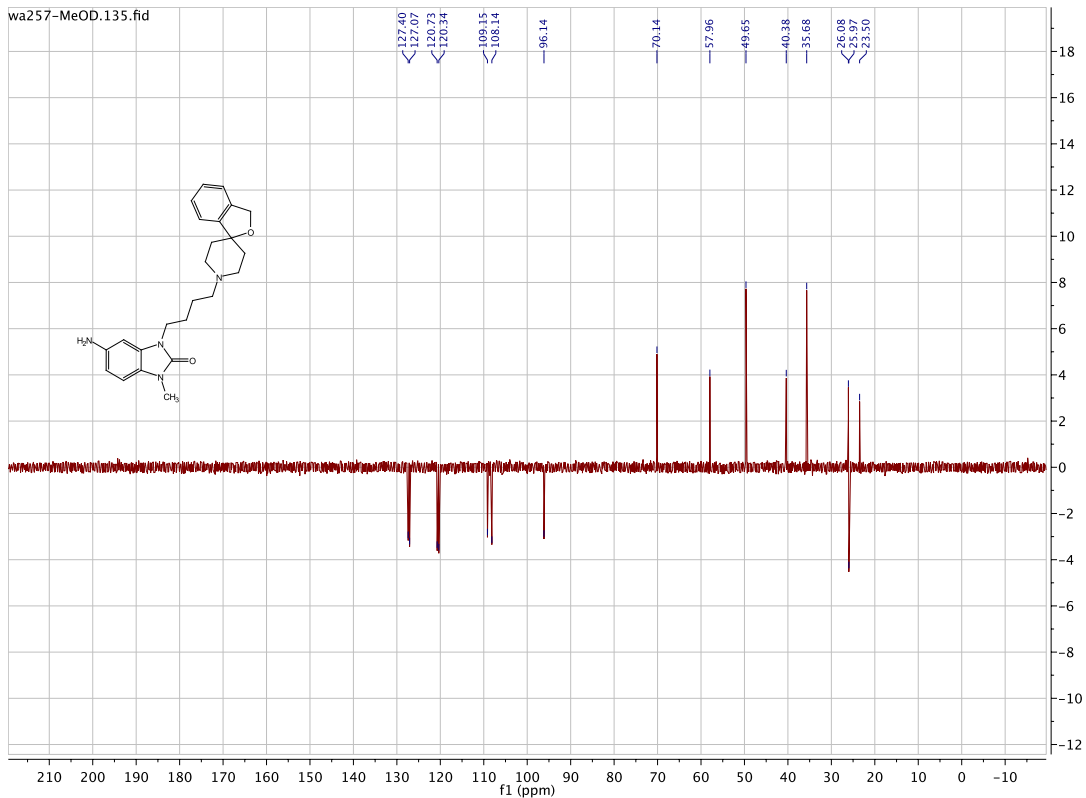
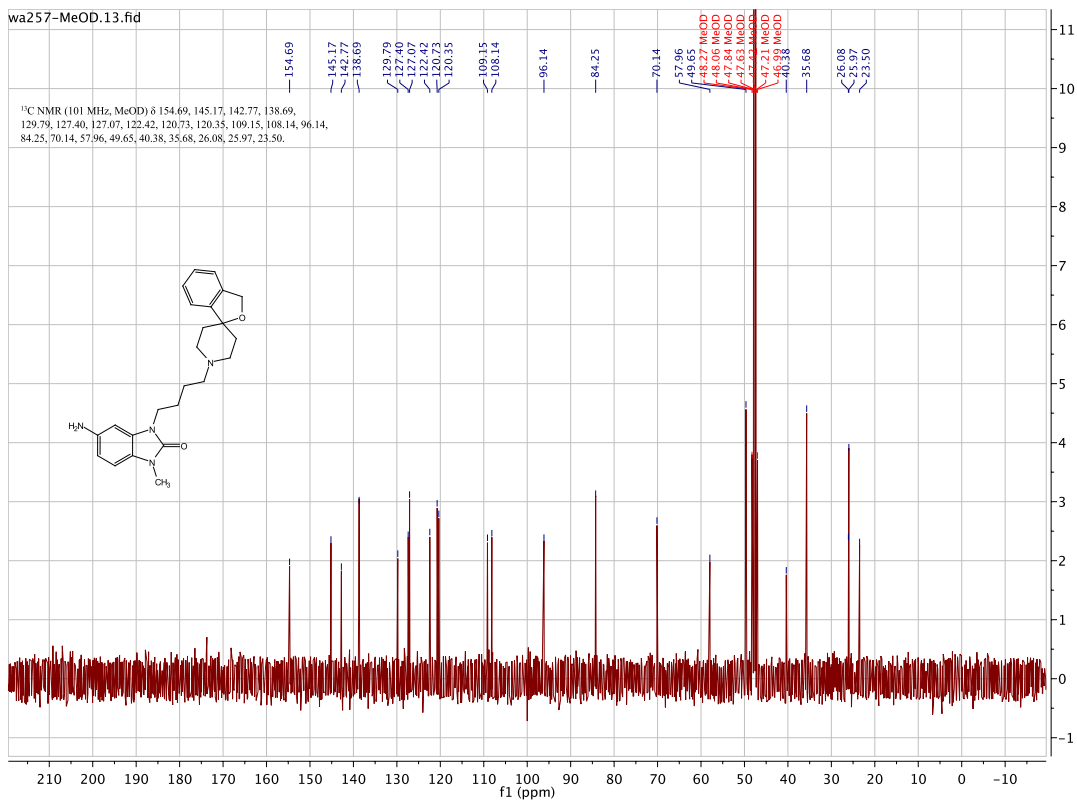
5-amino-3-(4-(6,7-dimethoxy-3,4-dihydroisoquinolin-2(1H)-yl)butyl)-1-methyl-1,3-dihydro-2H-benzo[d]imidazol-2-one: [WA249]



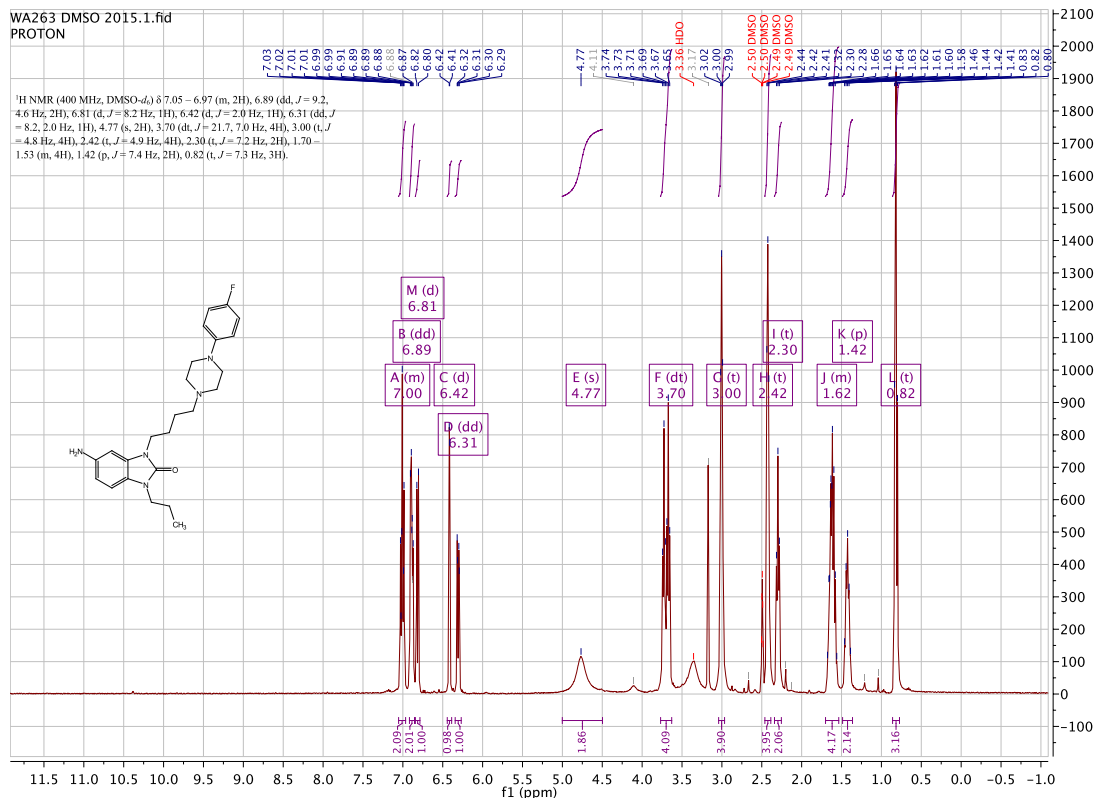
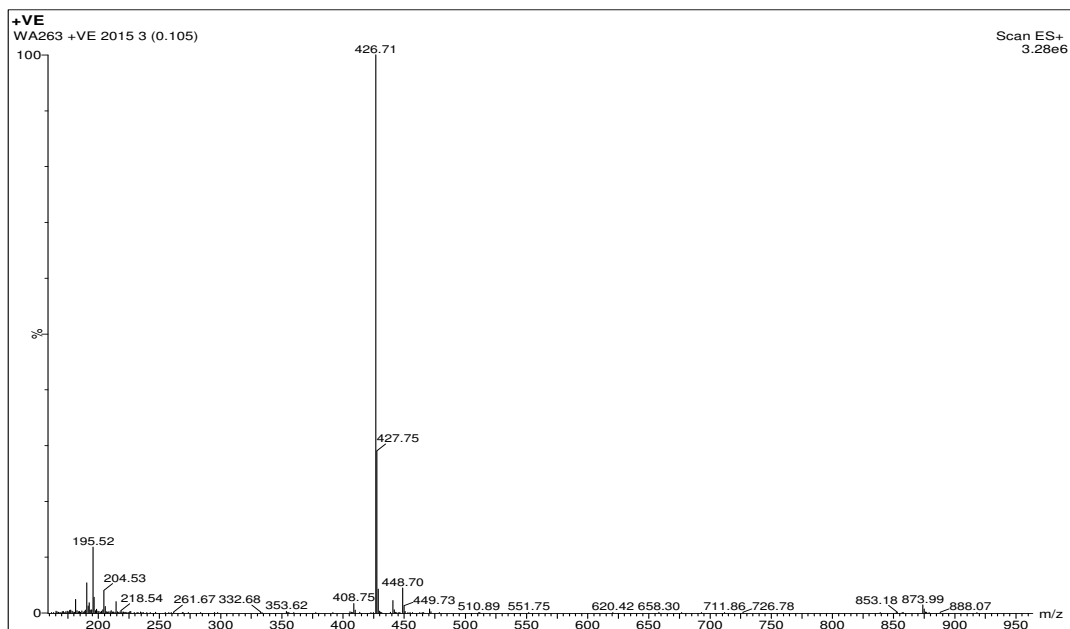


3-(4-(3H-spiro[isobenzofuran-1,4'-piperidin]-1'-yl)butyl)-5-amino-1-methyl-1,3-dihydro-2H-benzo[d]imidazol-2-one:[WA257]

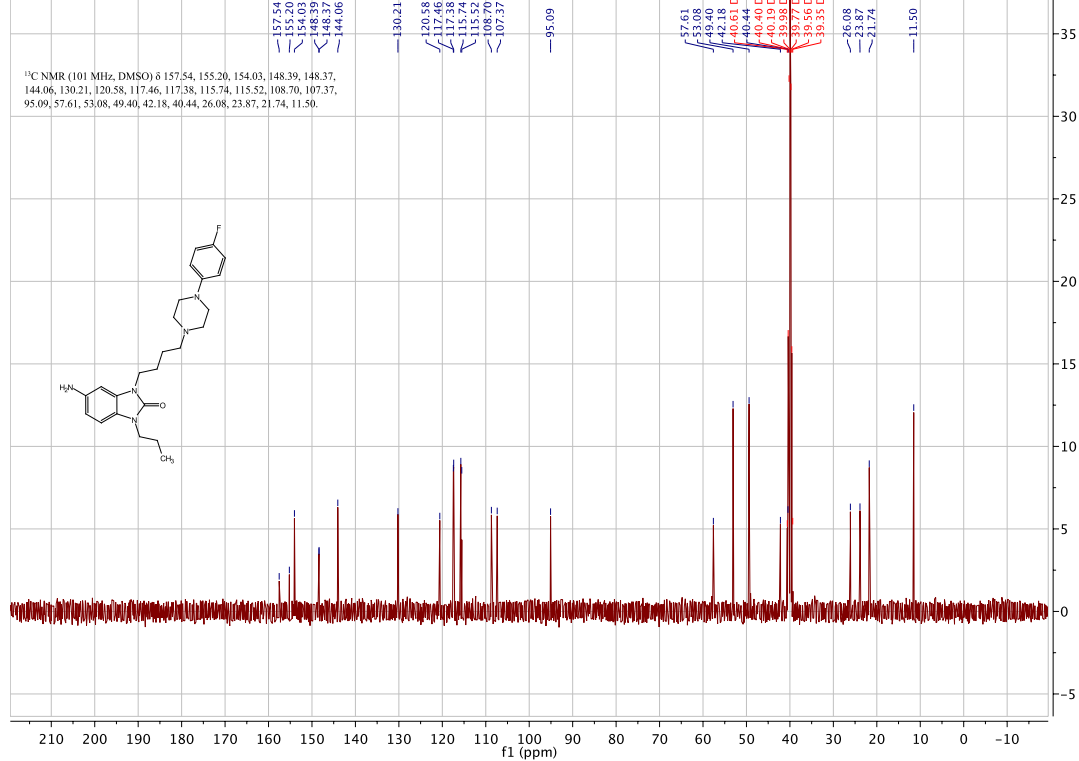




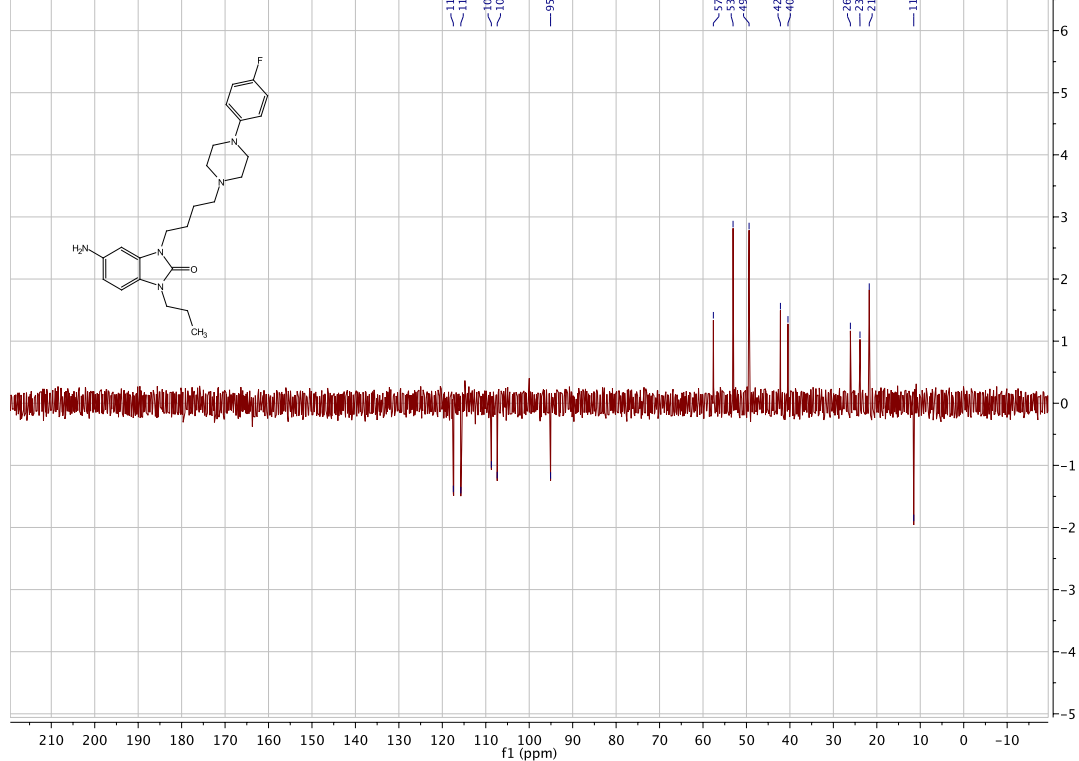
5-amino-3-(4-(4-(4-fluorophenyl)piperazin-1-yl)butyl)-1-propyl-1,3-dihydro-2H-benzof[d]imidazol-2-one: [WA263]



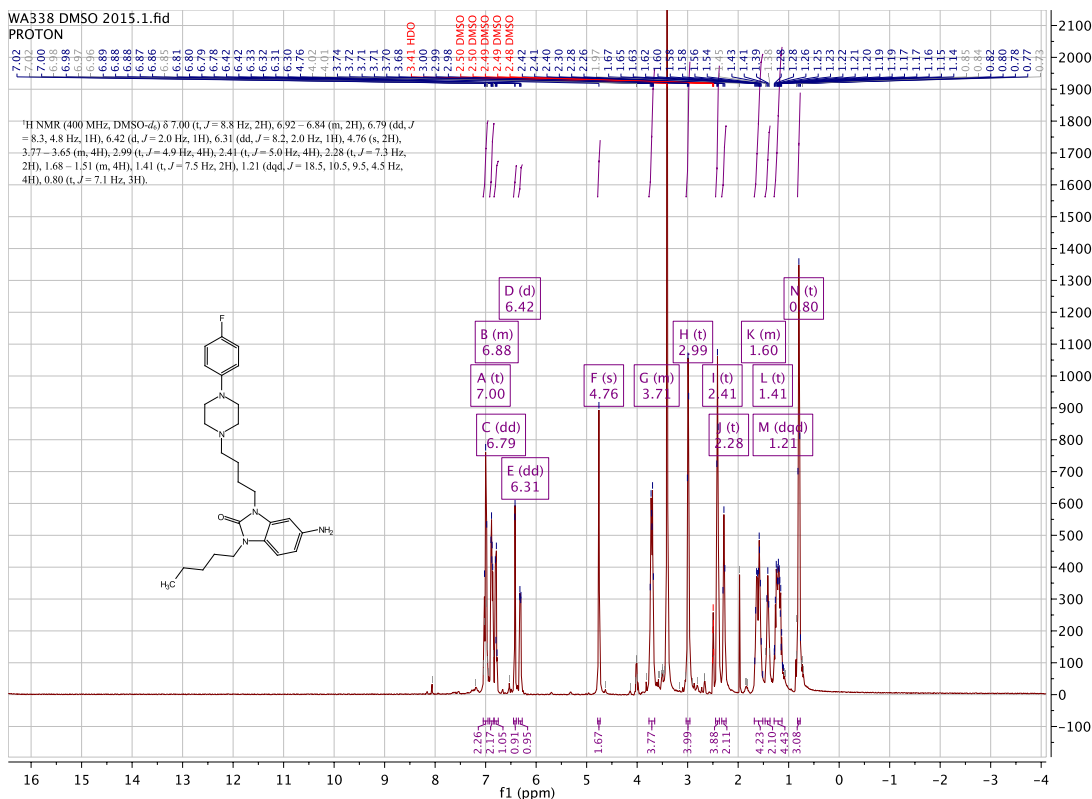
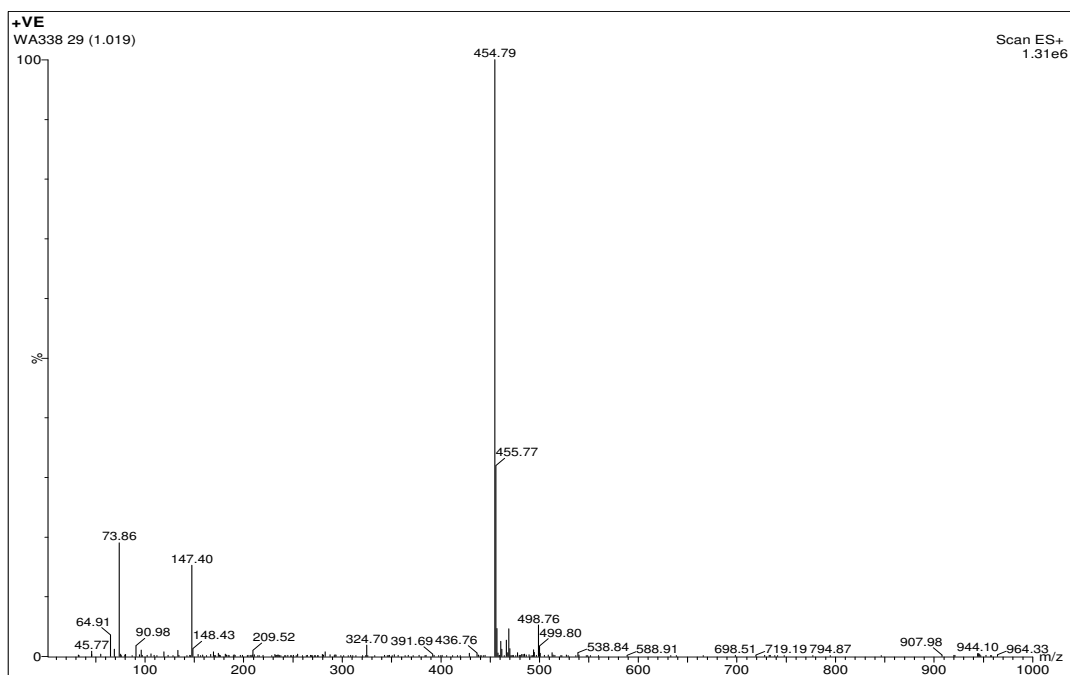
WA263 DMSO 2015.13.fid
CARBON



WA263 DMSO 2015.135.fid
DEPT135

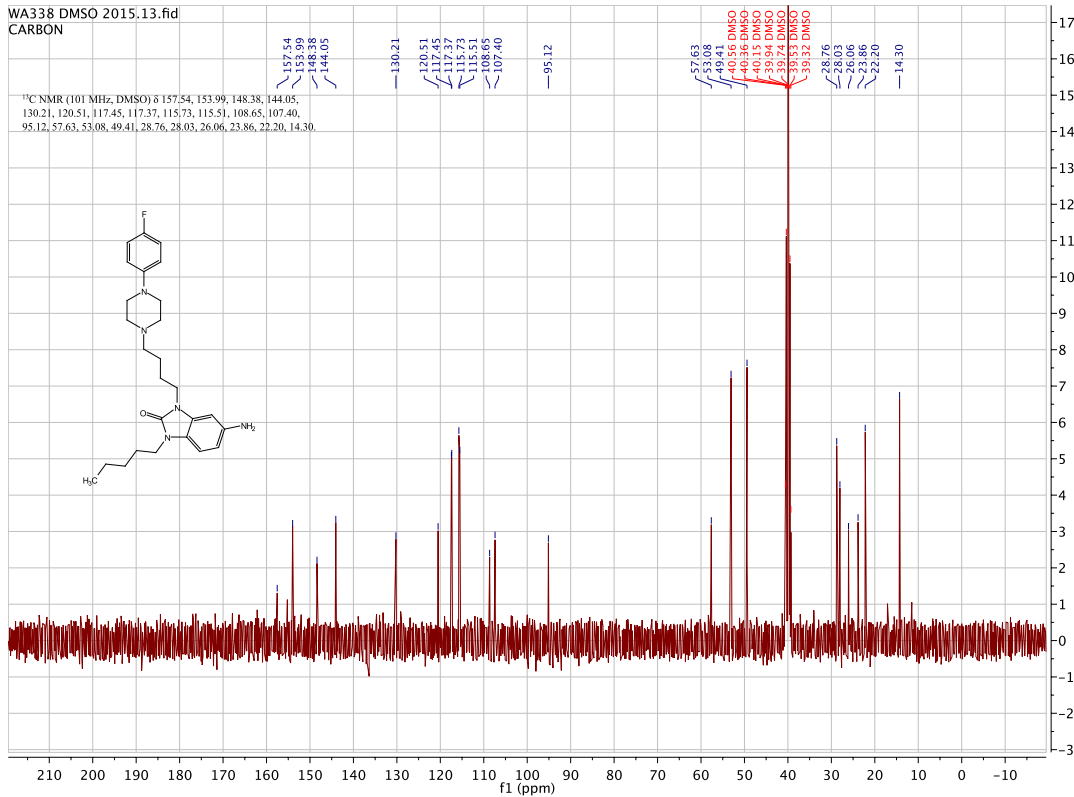


5-amino-3-(4-(4-(4-fluorophenyl)piperazin-1-yl)butyl)-1-pentyl-1,3-dihydro-2H-benzo[d]imidazol-2-one: [WA338]

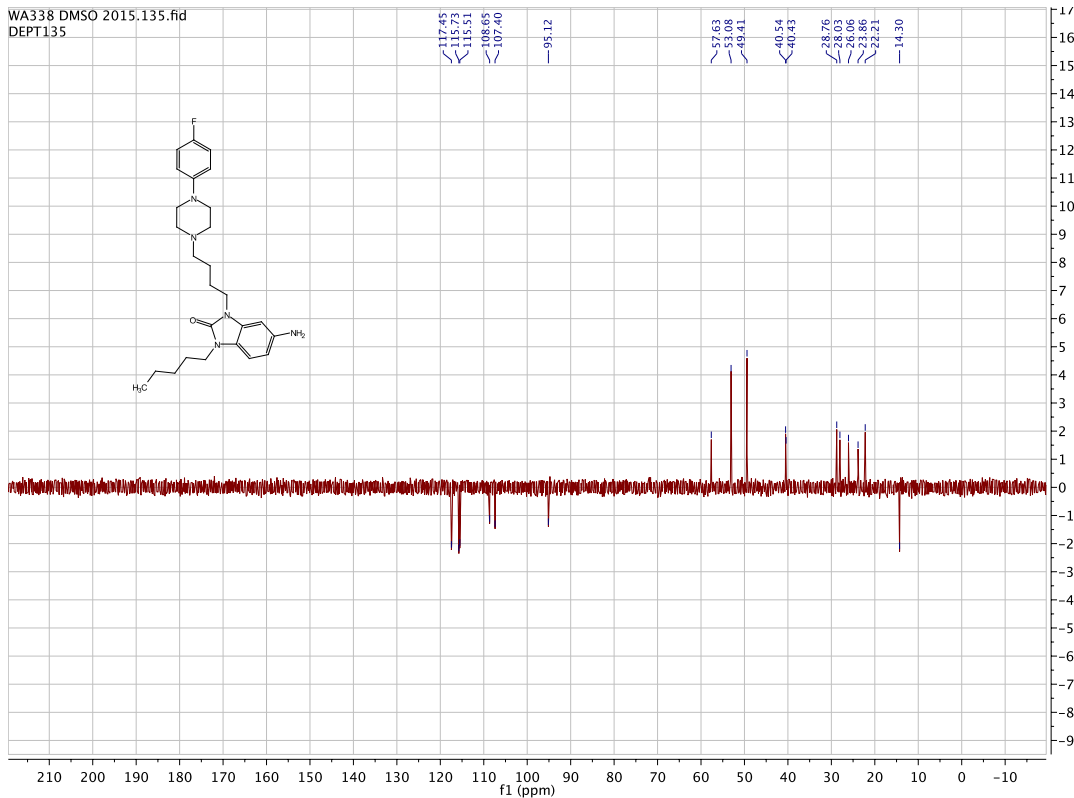


WA338 DMSO 2015.13.fid
CARBON

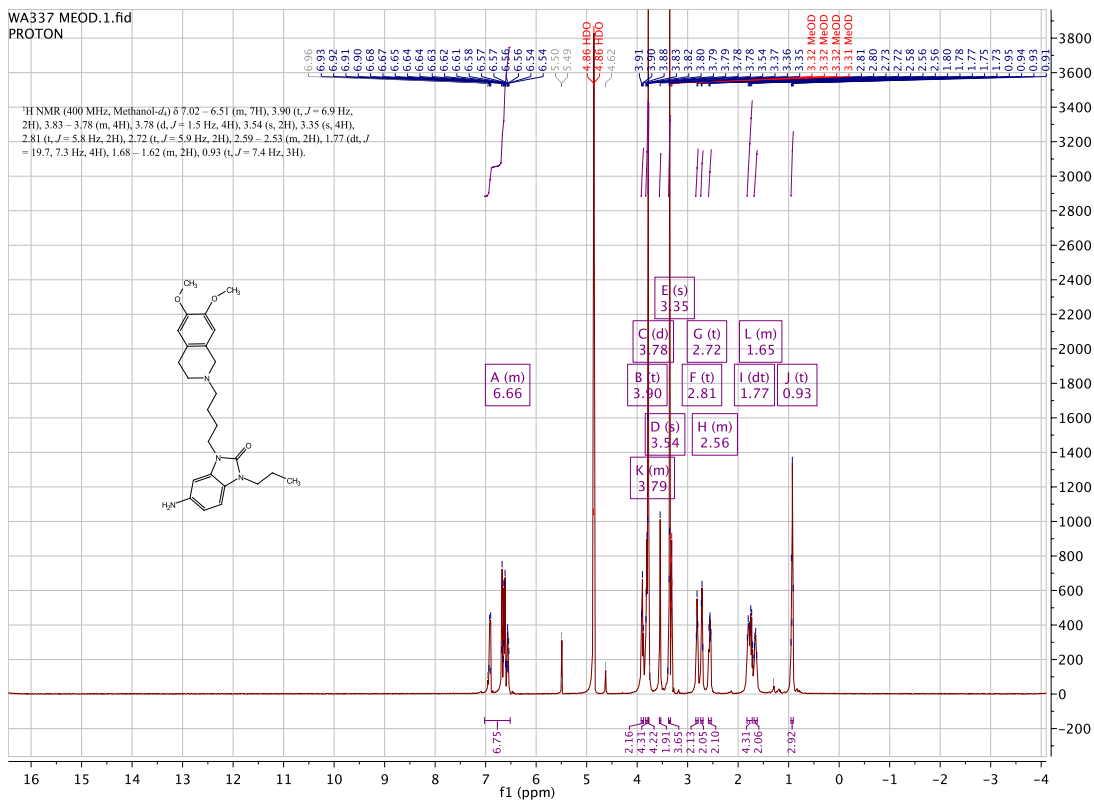
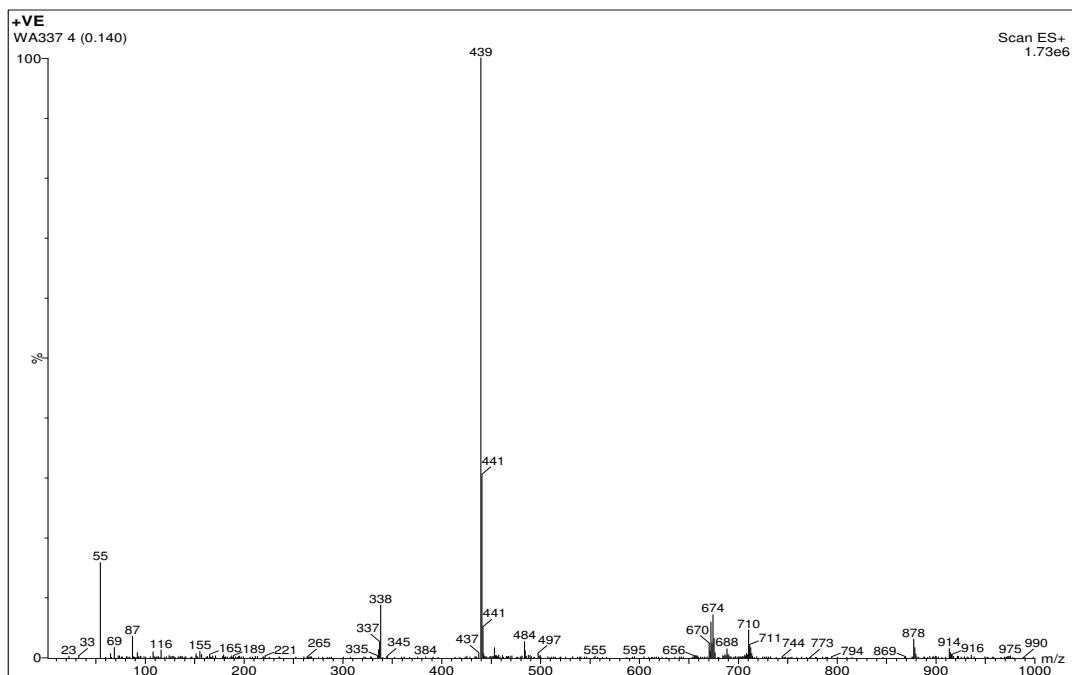
¹³C NMR (101 MHz, DMSO) δ 157.54, 153.99, 148.38, 144.05, 130.21, 120.51, 117.45, 117.37, 115.73, 115.51, 108.65, 107.40, 95.12, 57.63, 53.08, 49.41, 28.76, 28.03, 26.06, 23.86, 22.20, 14.30.

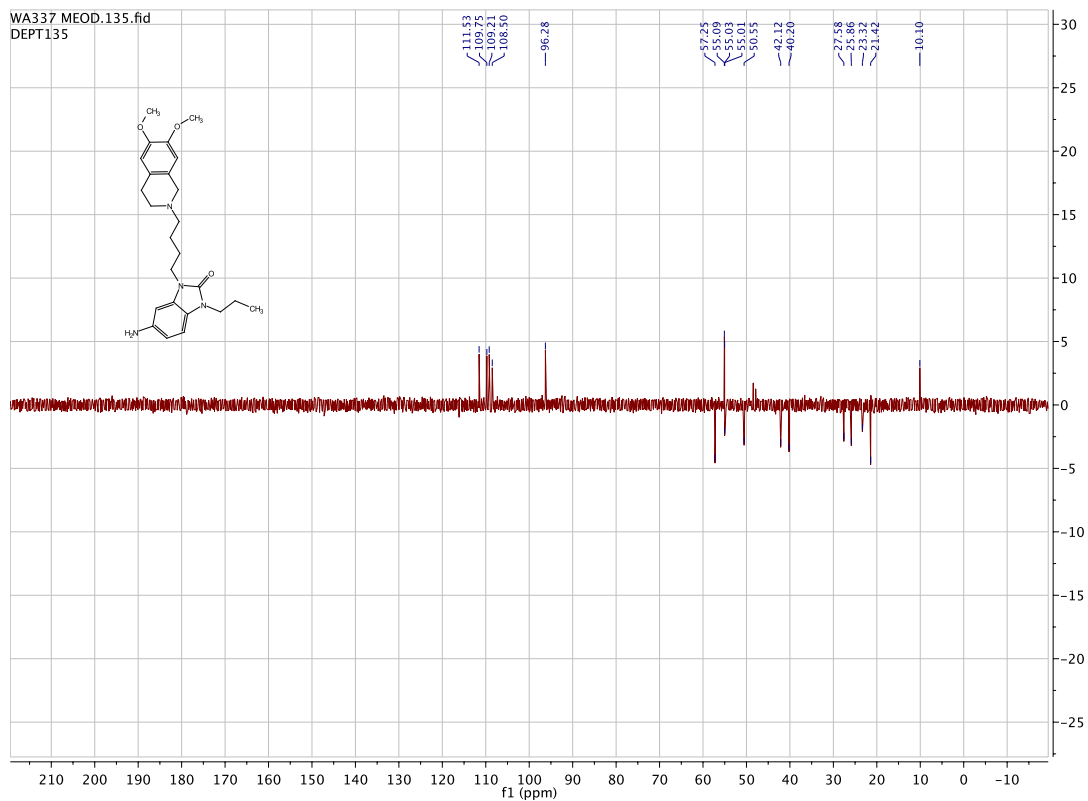
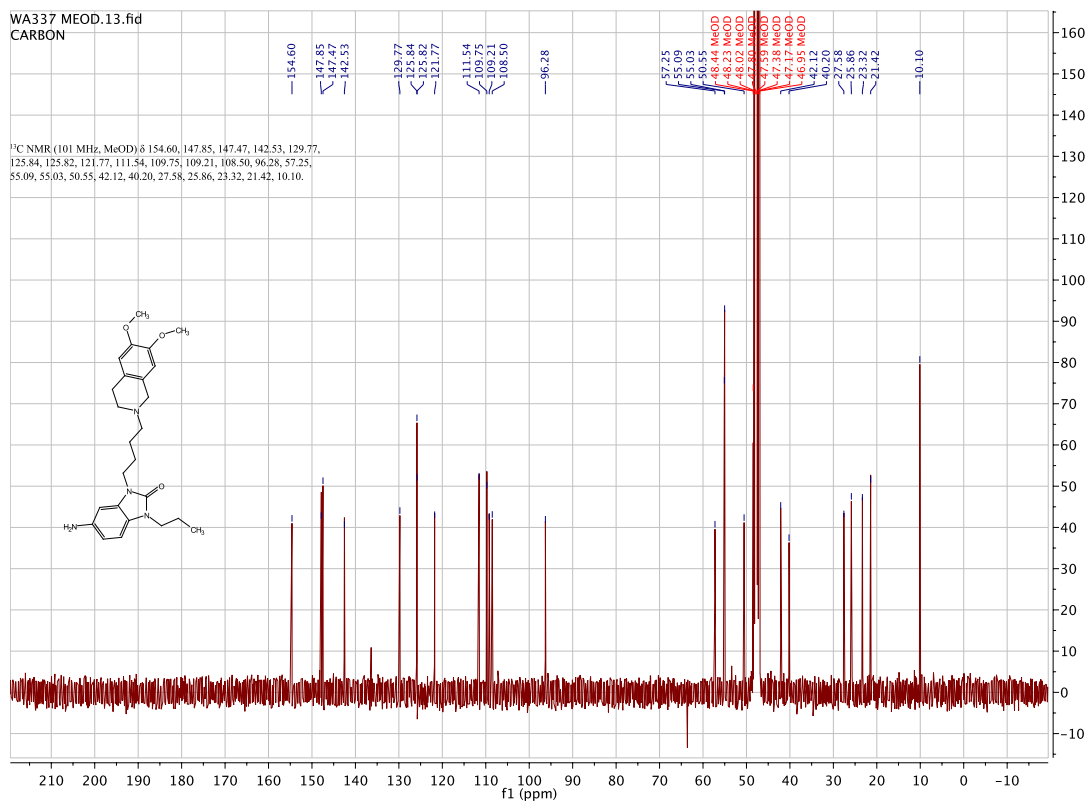


WA338 DMSO 2015.135.fid
DEPT135

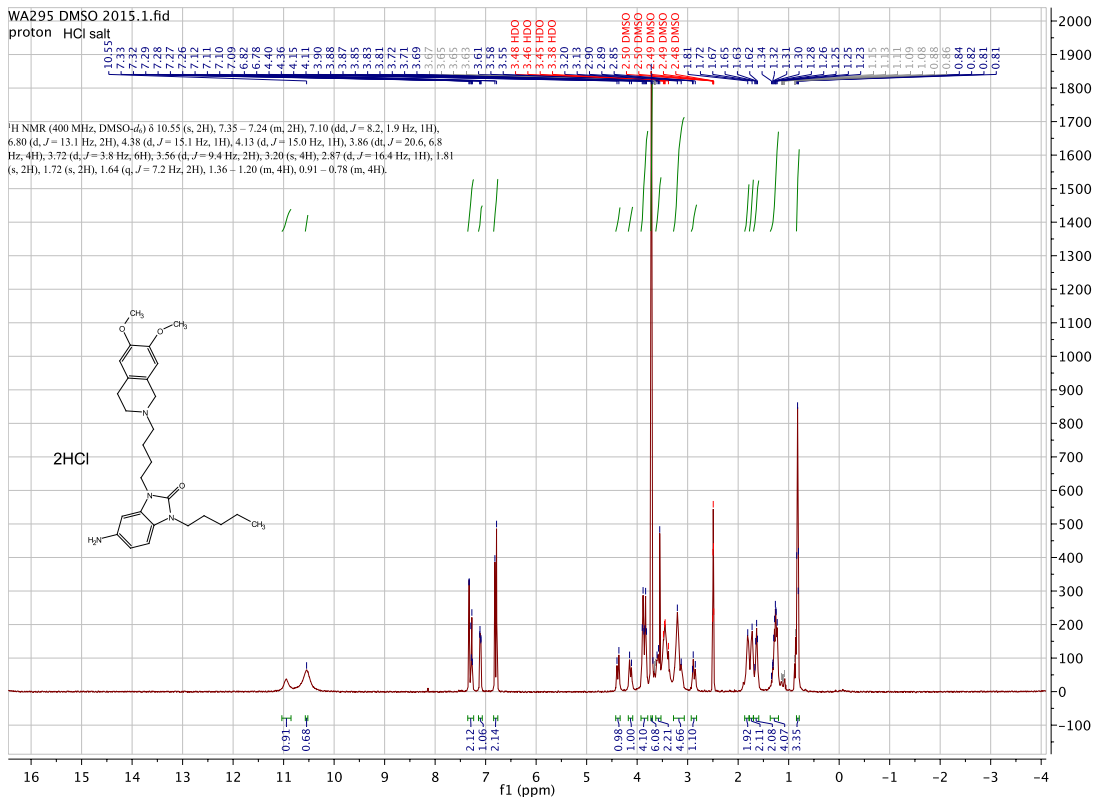
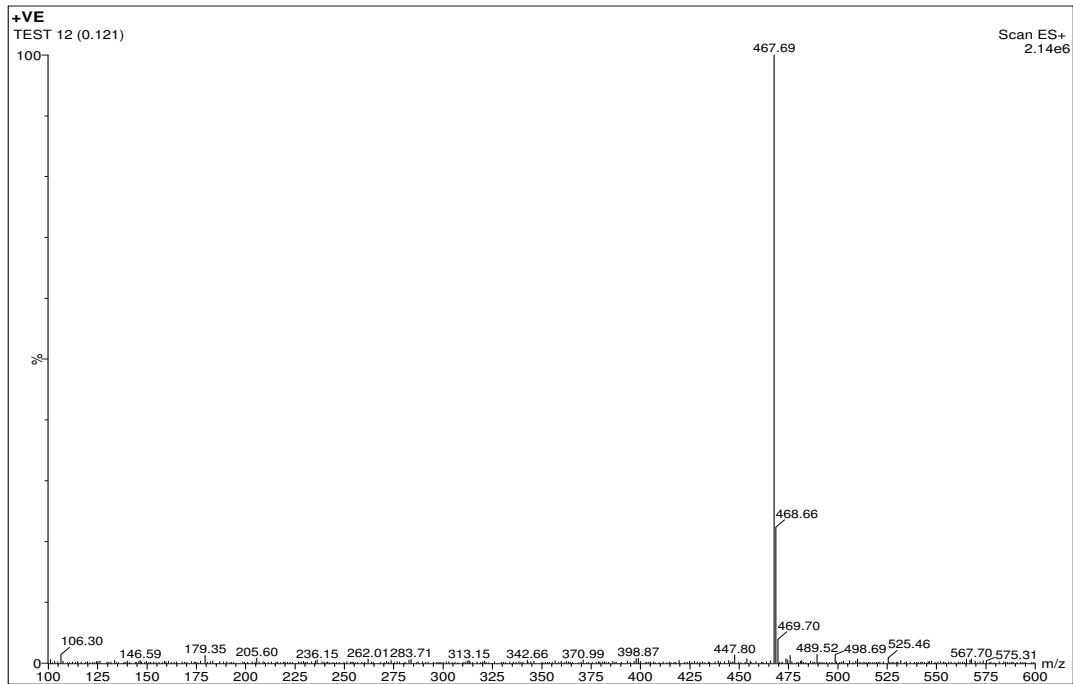


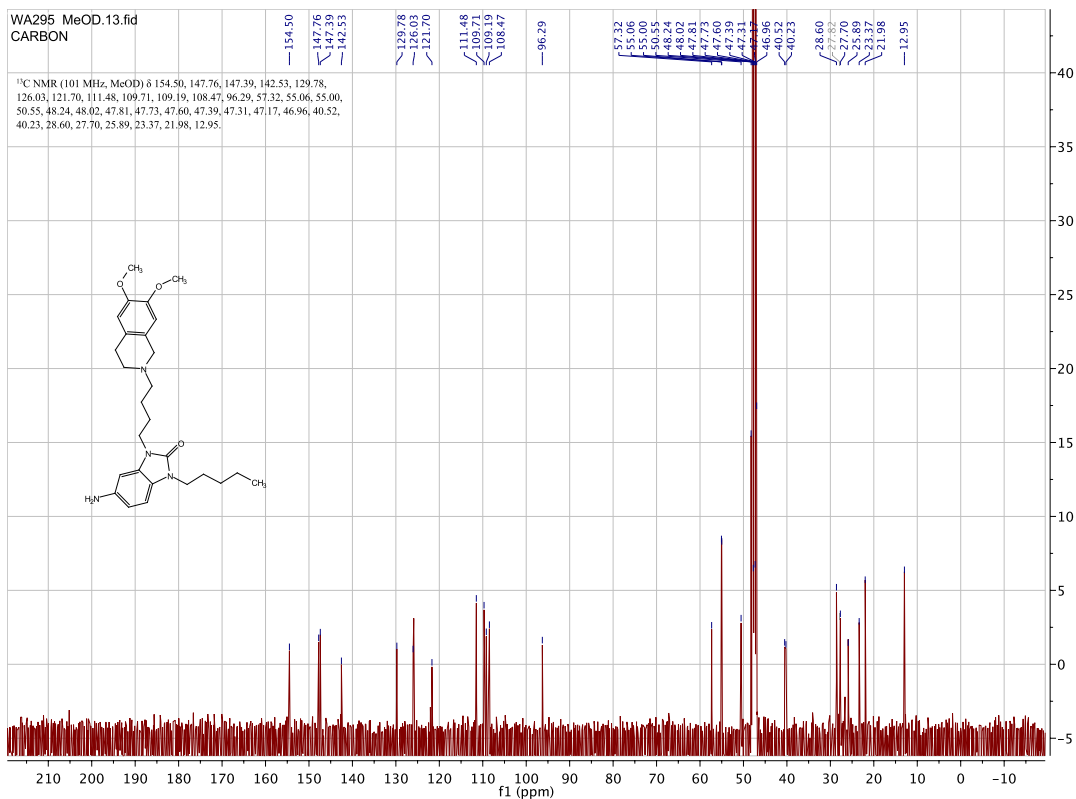
5-amino-3-(4-(6,7-dimethoxy-3,4-dihydroisoquinolin-2(1H)-yl)butyl)-1-propyl-1,3-dihydro-2H-benzo[d]imidazol-2-one:[WA337]



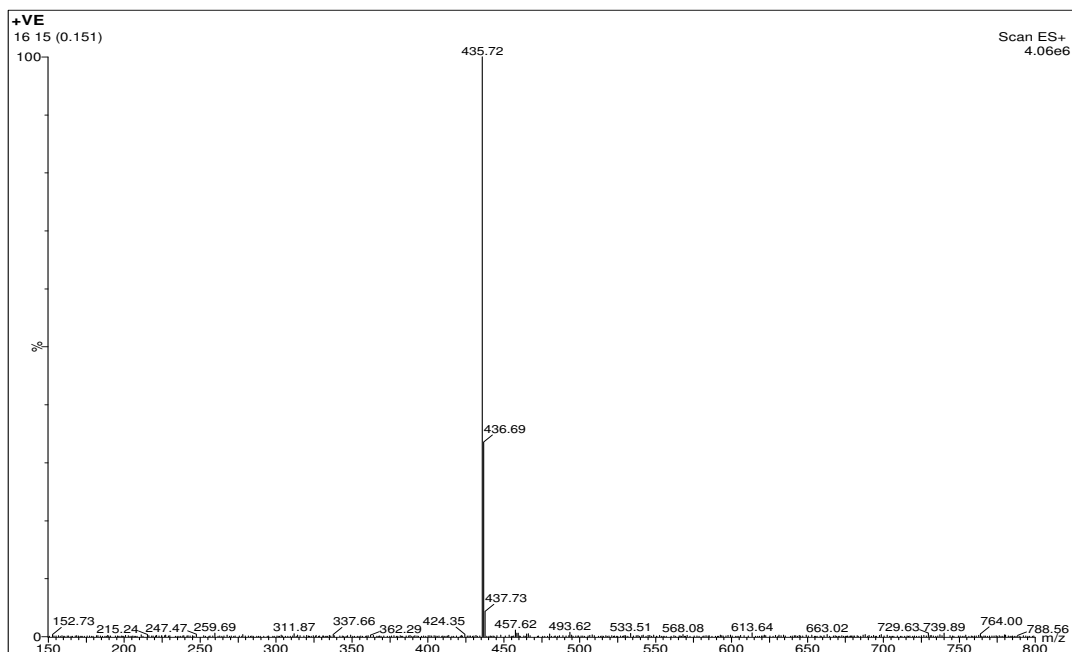


5-amino-3-(4-(6,7-dimethoxy-3,4-dihydroisoquinolin-2(1H)-yl)butyl)-1-pentyl-1,3-dihydro-2H-benzof[d]imidazol-2-one:[WA295/300/312]



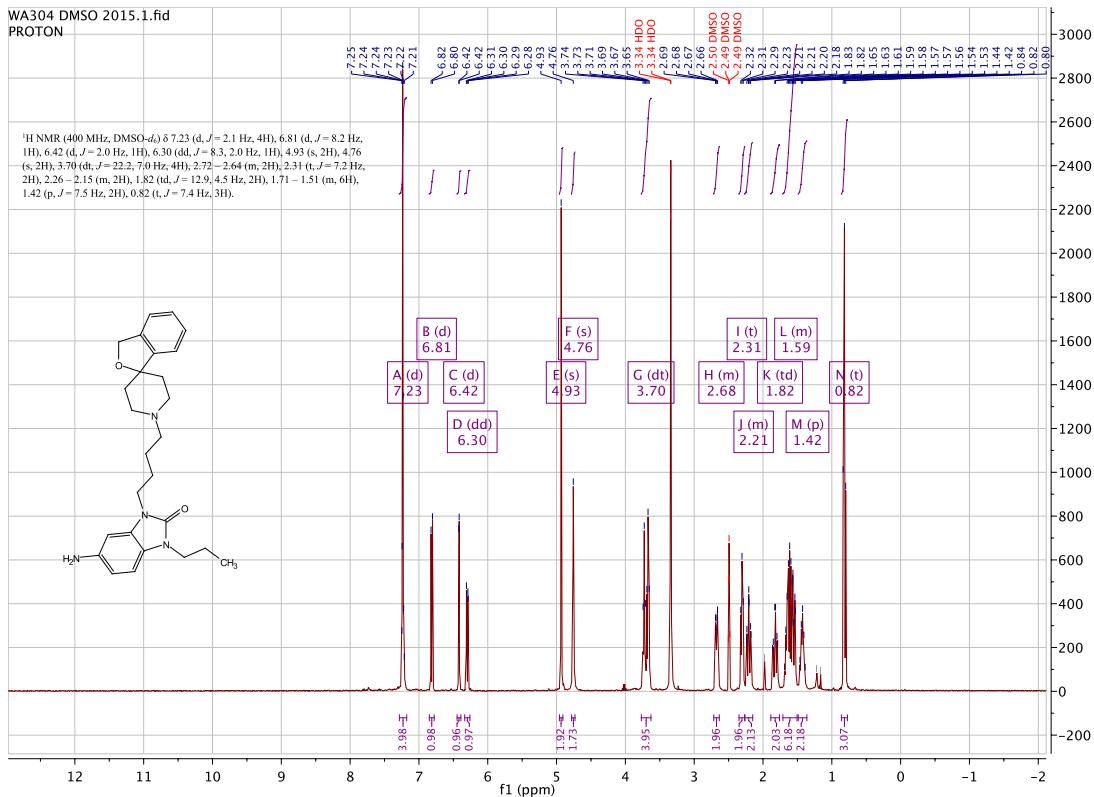
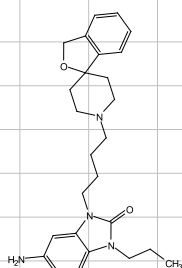


3-(4-(3H-spiro[isobenzofuran-1,4'-piperidin]-1'-yl)butyl)-5-amino-1-propyl-1,3-dihydro-2H-benzod[imidazol-2-one]:[WA304]



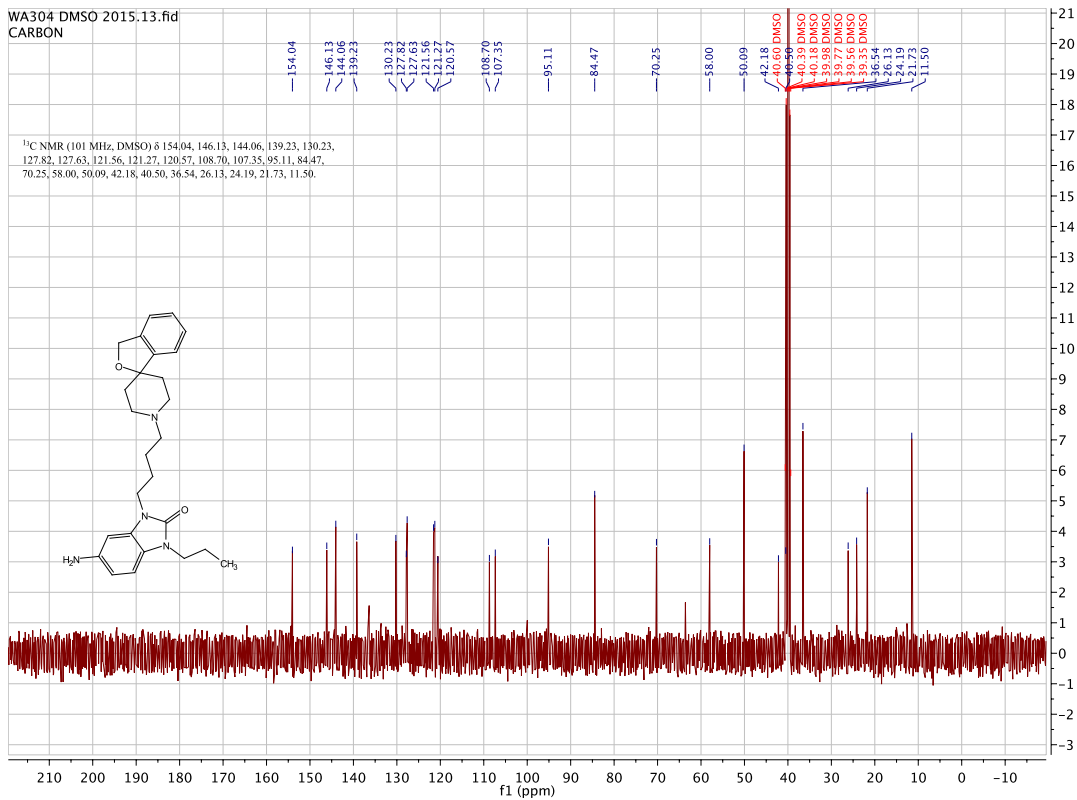
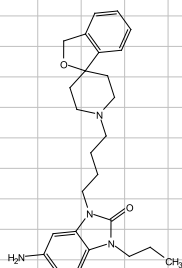
WA304 DMSO 2015.1.fid
 PROTON

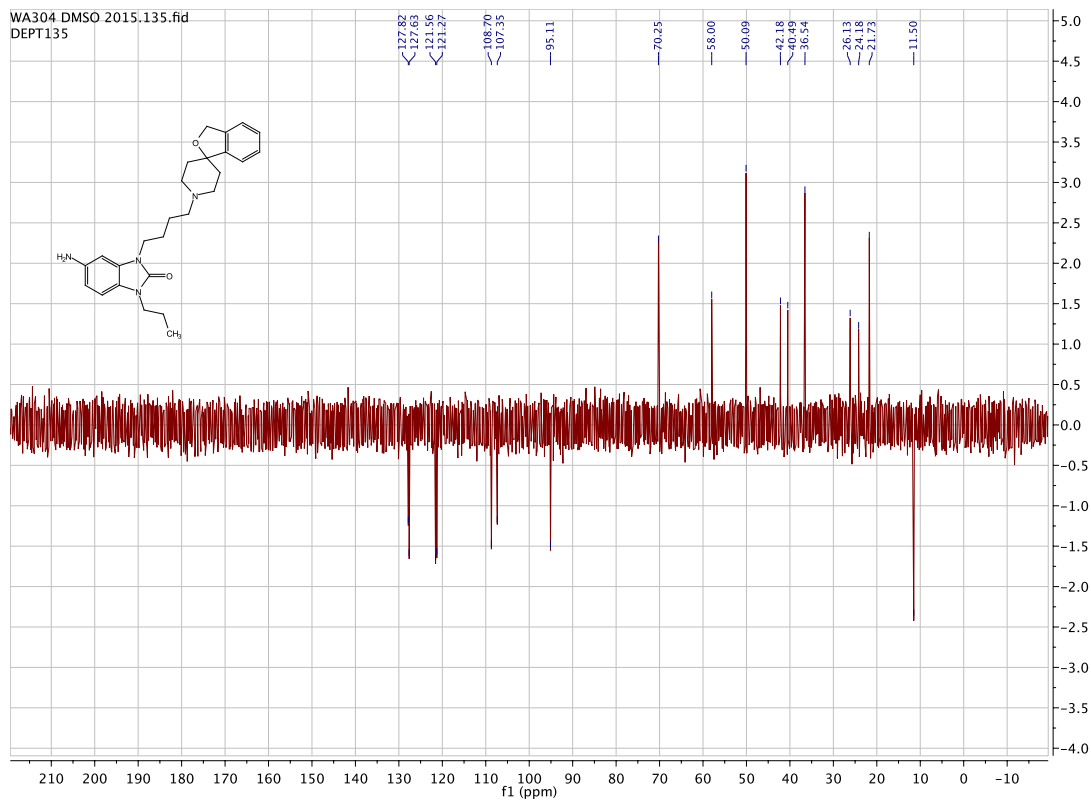
¹H NMR (400 MHz, DMSO-*d*₆) δ 7.23 (d, *J* = 2.1 Hz, 4H), 6.81 (d, *J* = 8.2 Hz, 1H), 6.42 (d, *J* = 2.0 Hz, 1H), 6.30 (dd, *J* = 8.3, 2.0 Hz, 1H), 4.93 (s, 2H), 4.76 (s, 2H), 3.70 (dt, *J* = 22.2, 7.0 Hz, 4H), 2.73 – 2.64 (m, 2H), 2.31 (t, *J* = 7.2 Hz, 2H), 2.26 – 2.15 (m, 2H), 1.82 (dt, *J* = 12.9, 4.5 Hz, 2H), 1.71 – 1.51 (m, 6H), 1.42 (p, *J* = 7.5 Hz, 2H), 0.82 (t, *J* = 7.4 Hz, 3H).



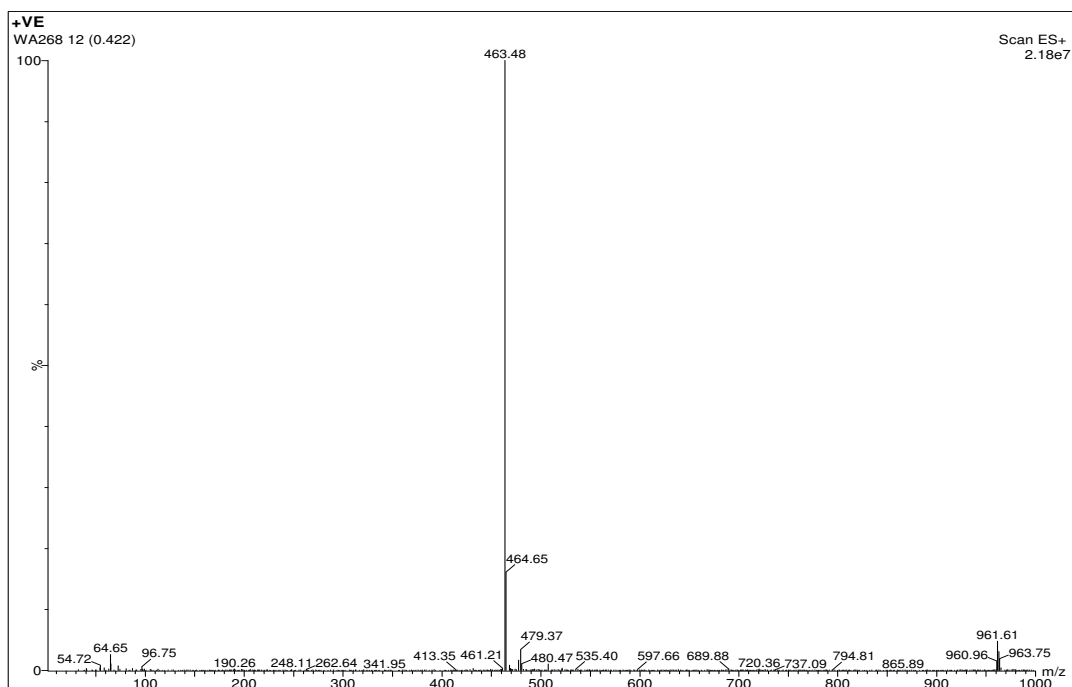
WA304 DMSO 2015.13.fid
 CARBON

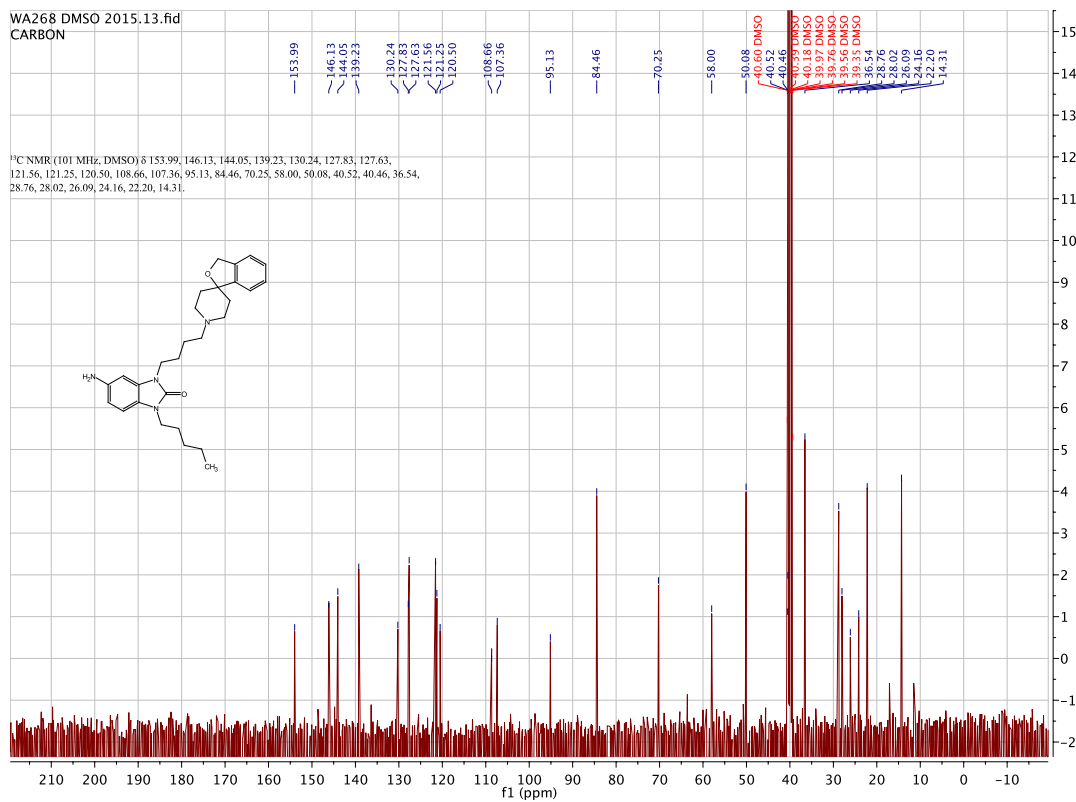
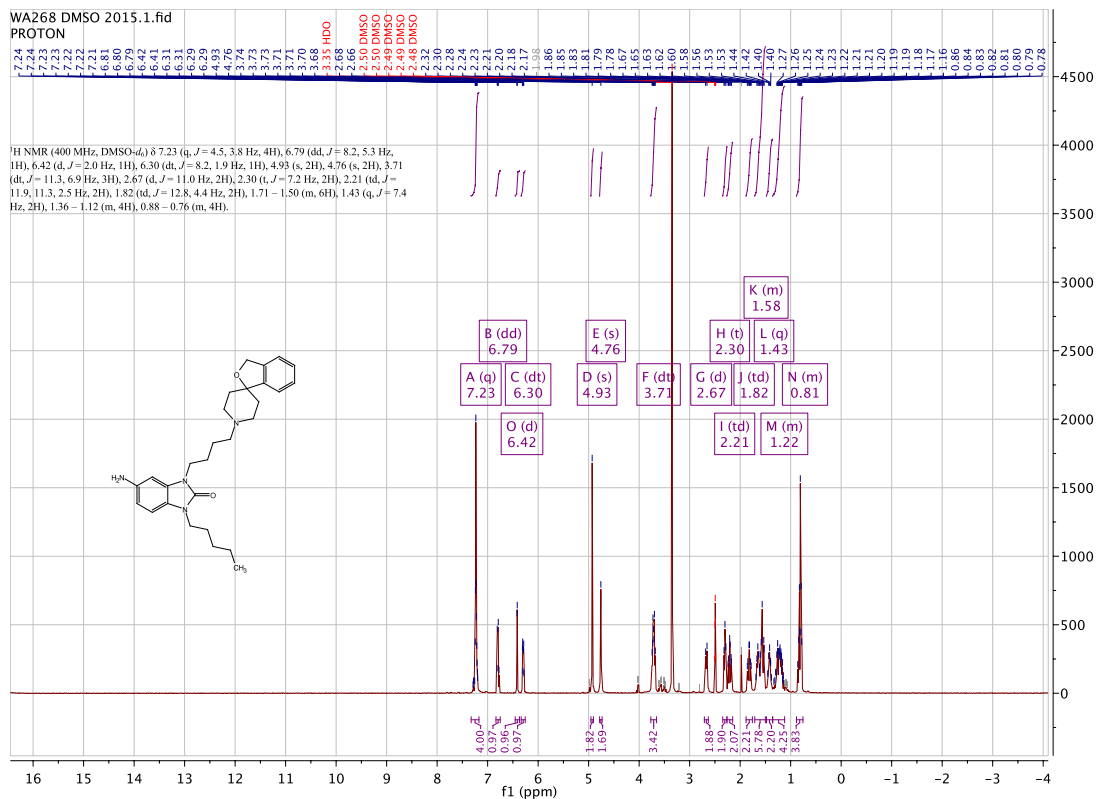
¹³C NMR (101 MHz, DMSO) δ 154.04, 146.13, 144.06, 139.23, 130.23, 127.82, 127.63, 121.56, 121.27, 120.57, 108.70, 107.35, 95.11, 84.47, 70.25, 58.00, 50.09, 42.18, 40.50, 36.54, 26.13, 24.19, 21.73, 11.50.

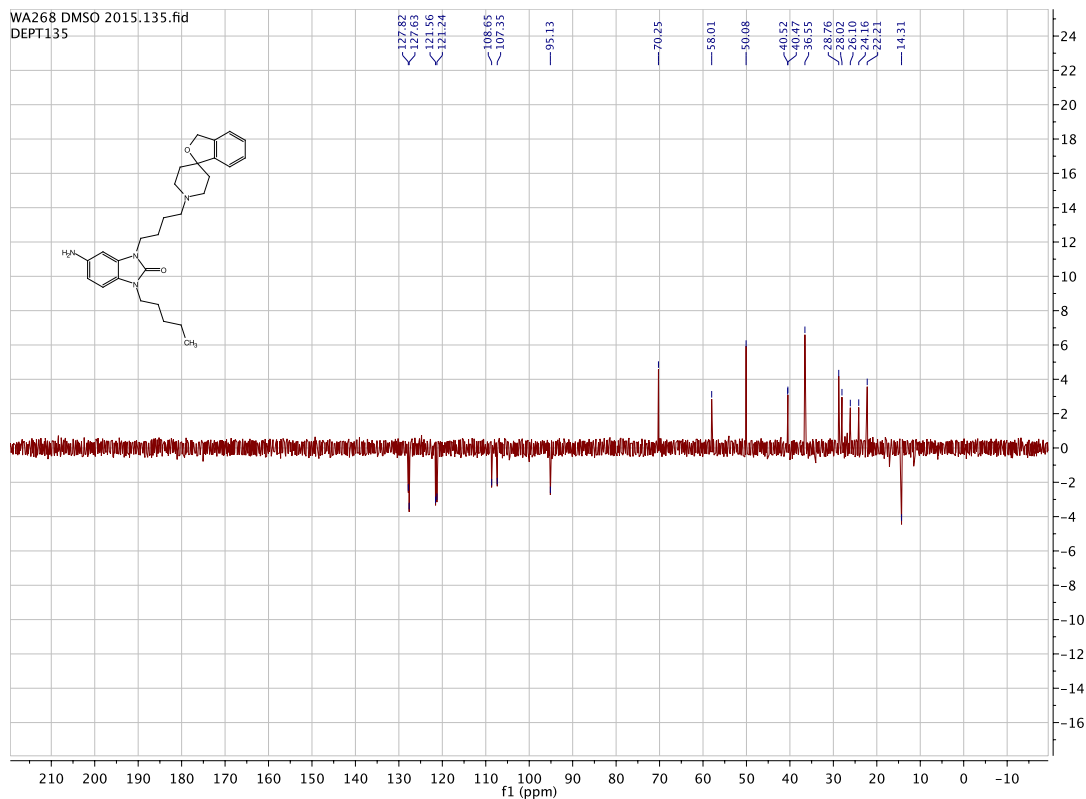




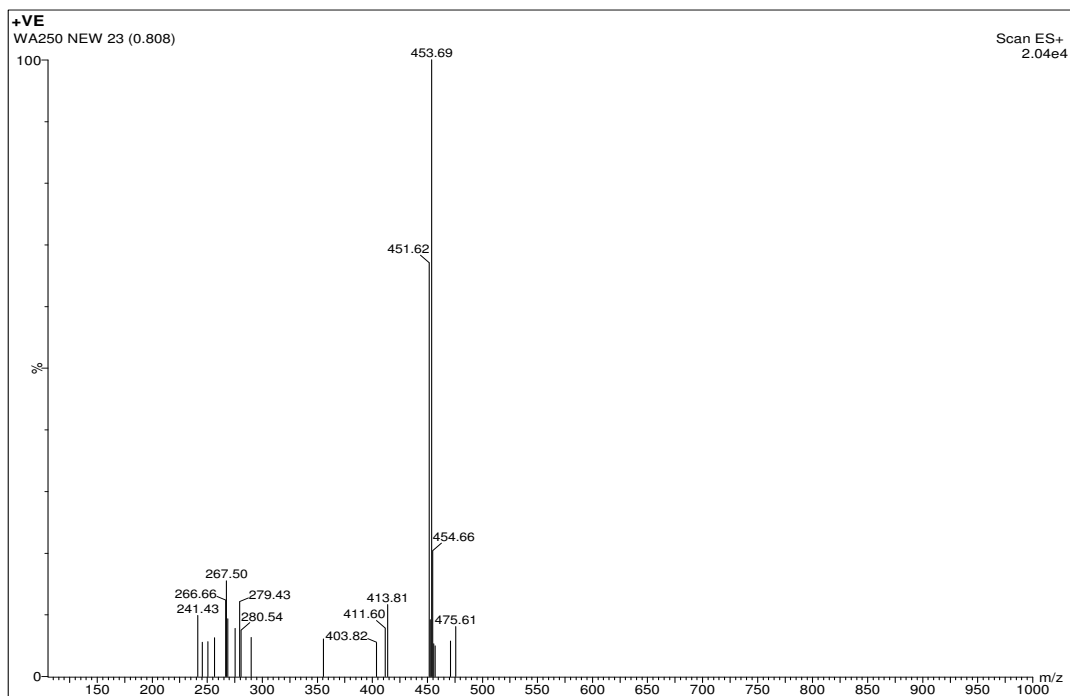
3-(4-(3H-spiro[isobenzofuran-1,4'-piperidin]-1'-yl)butyl)-5-amino-1-pentyl-1,3-dihydro-2H-benzod[imidazol-2-one]:[WA268]

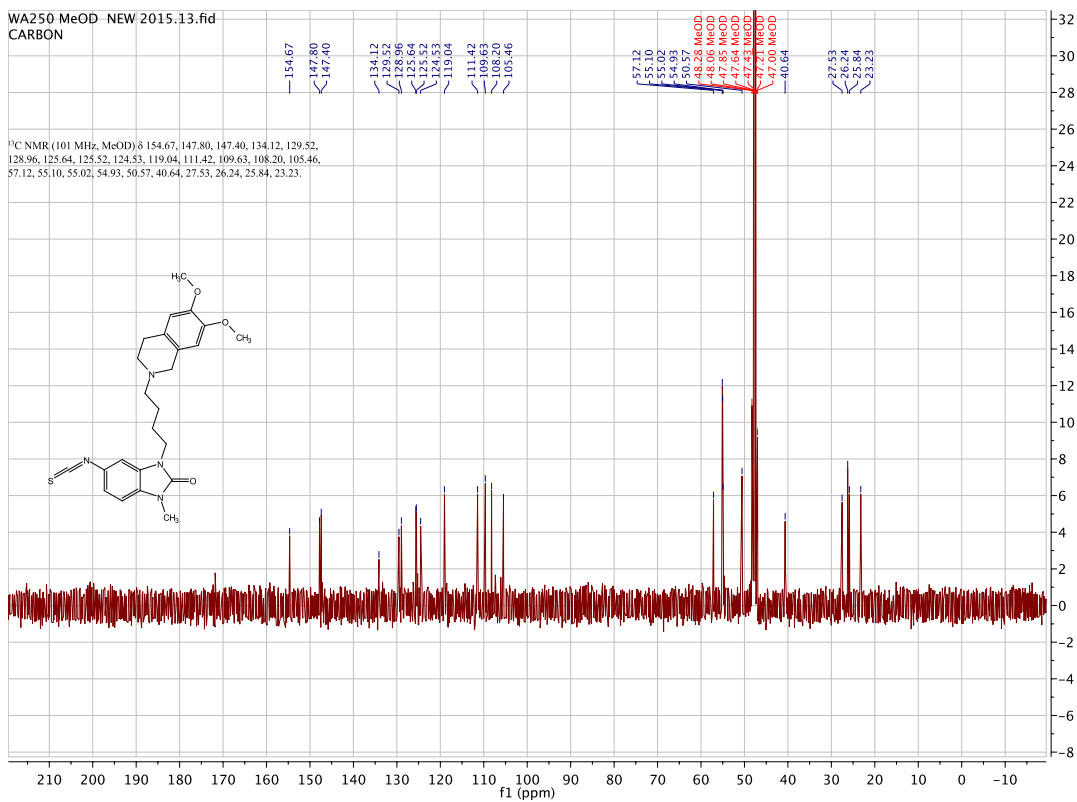
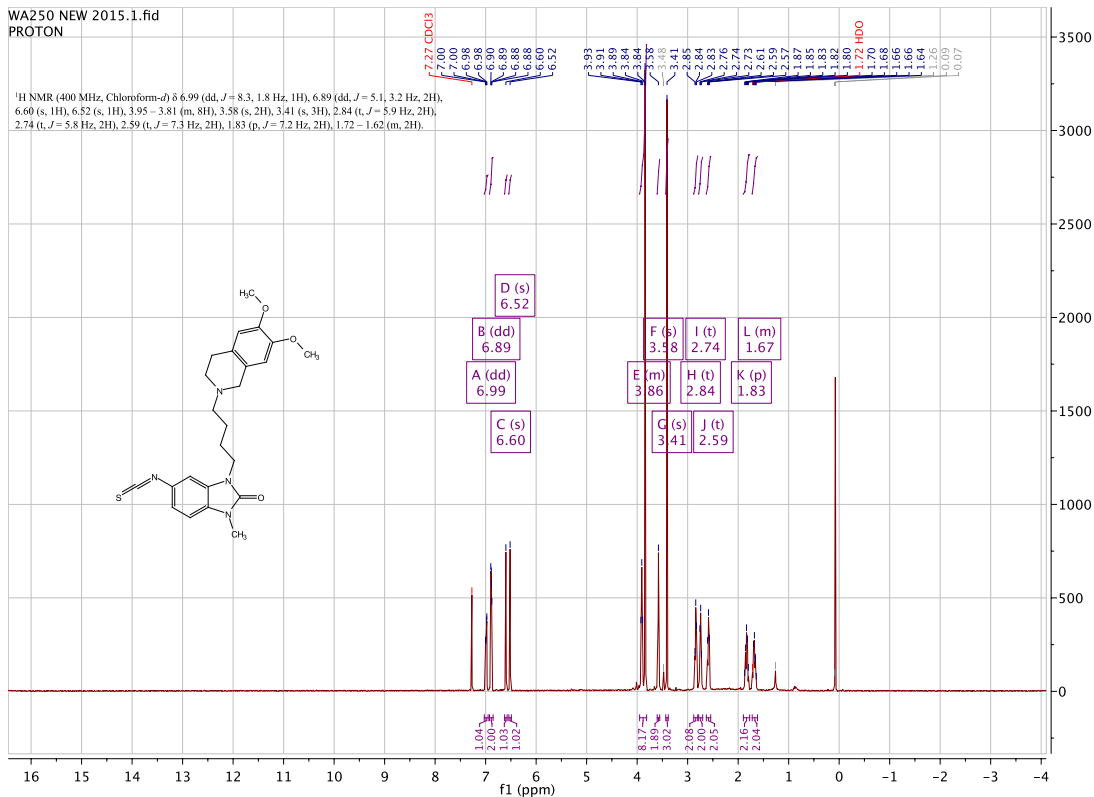


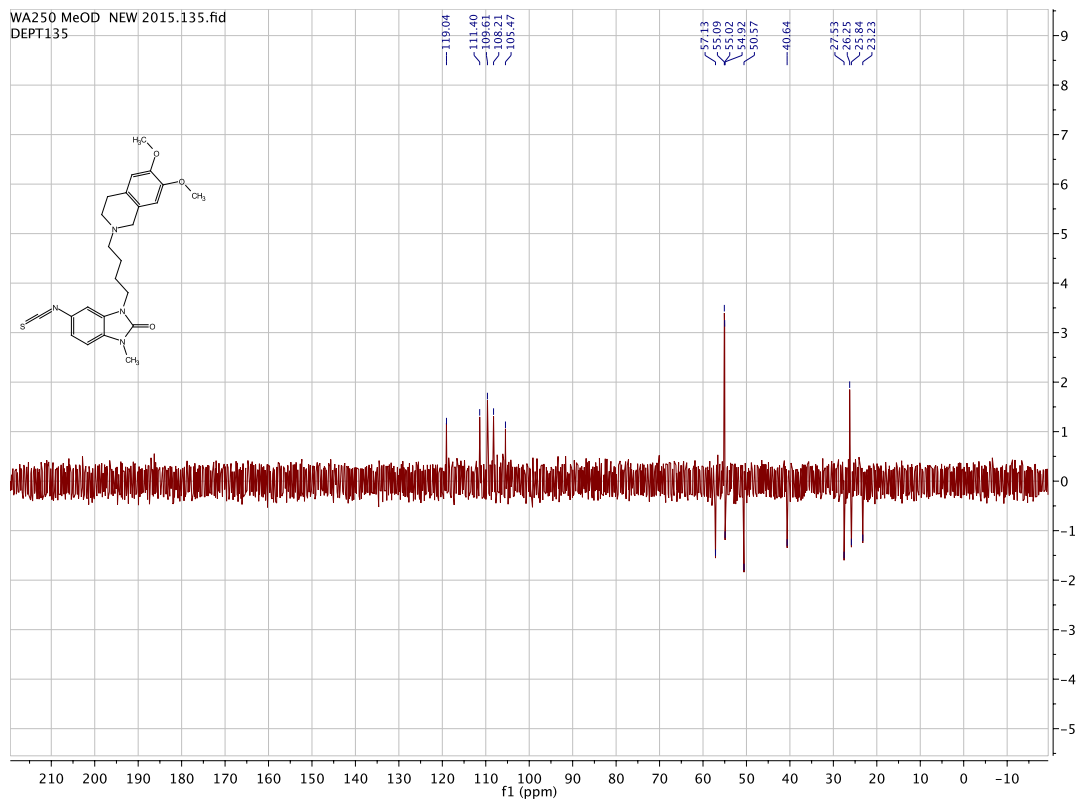




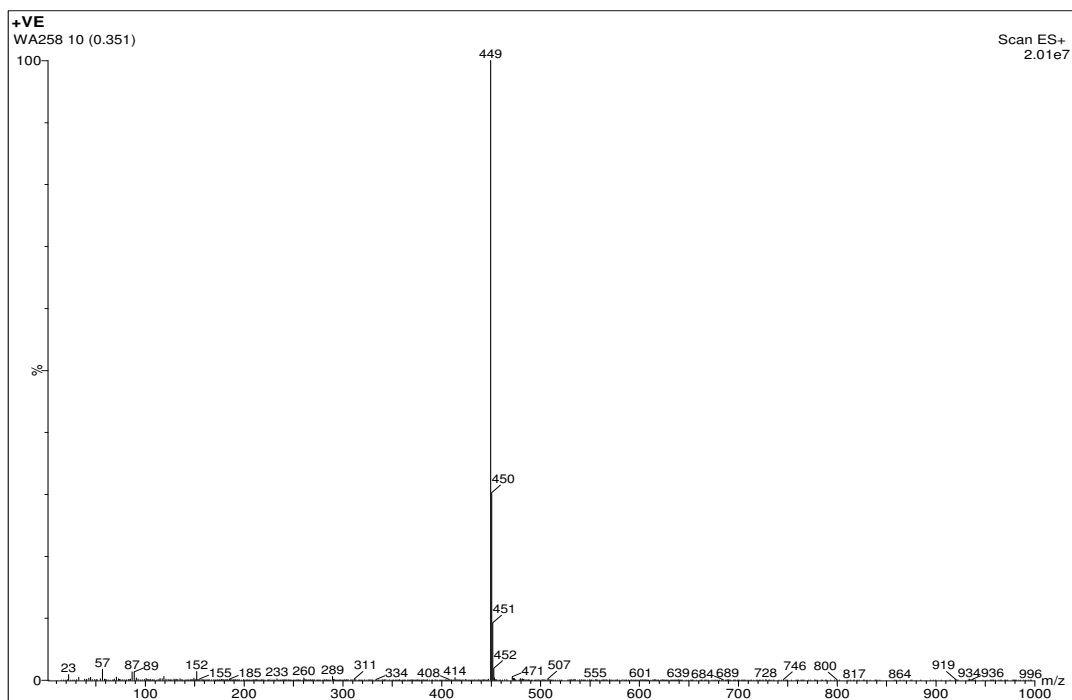
3-(4-(6,7-dimethoxy-3,4-dihydroisoquinolin-2(1H)-yl)butyl)-5-isothiocyanato-1-methyl-1,3-dihydro-2H-benzo[d]imidazol-2-one: [WA250]



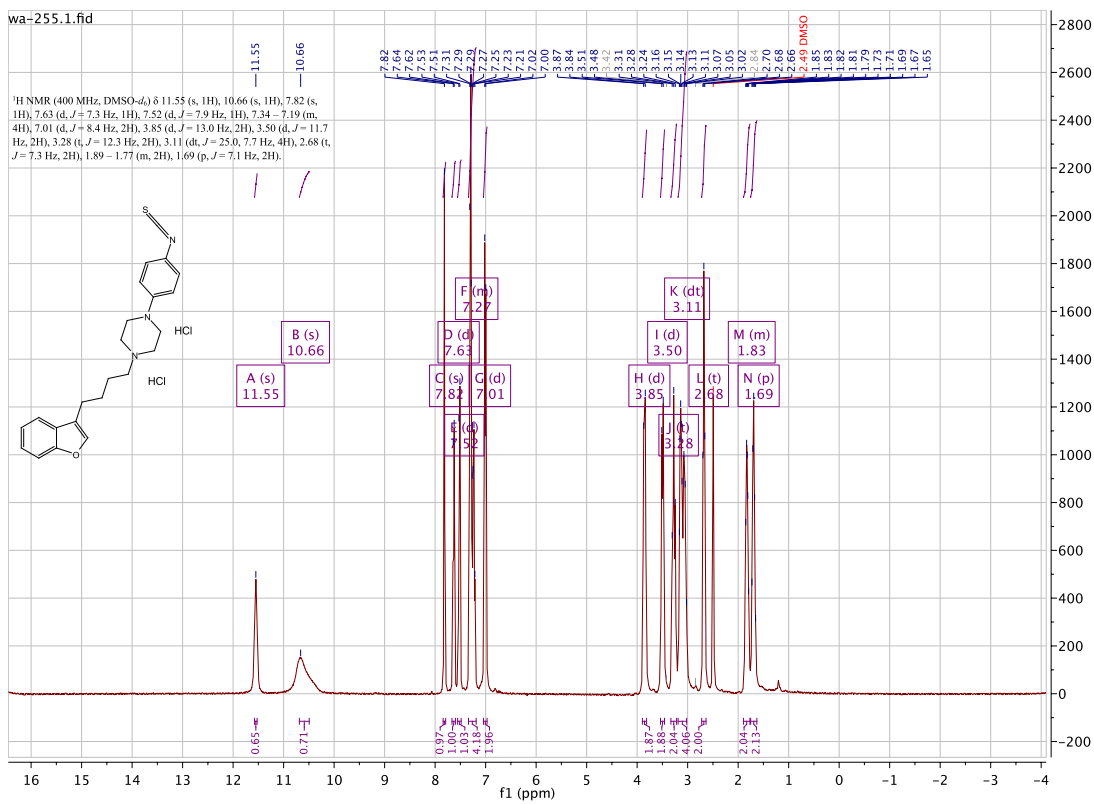
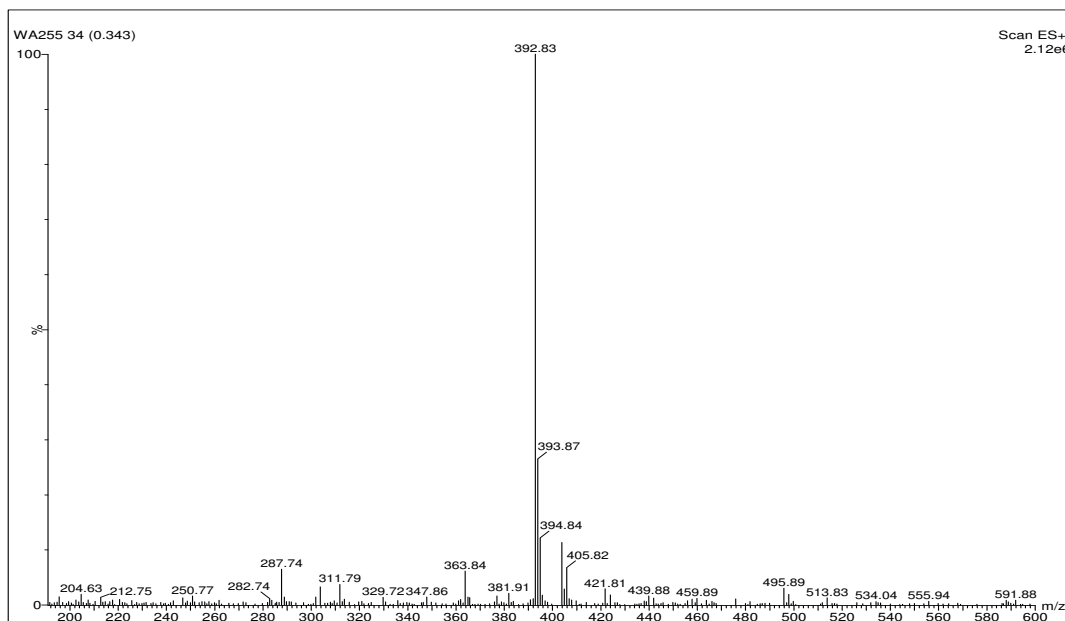


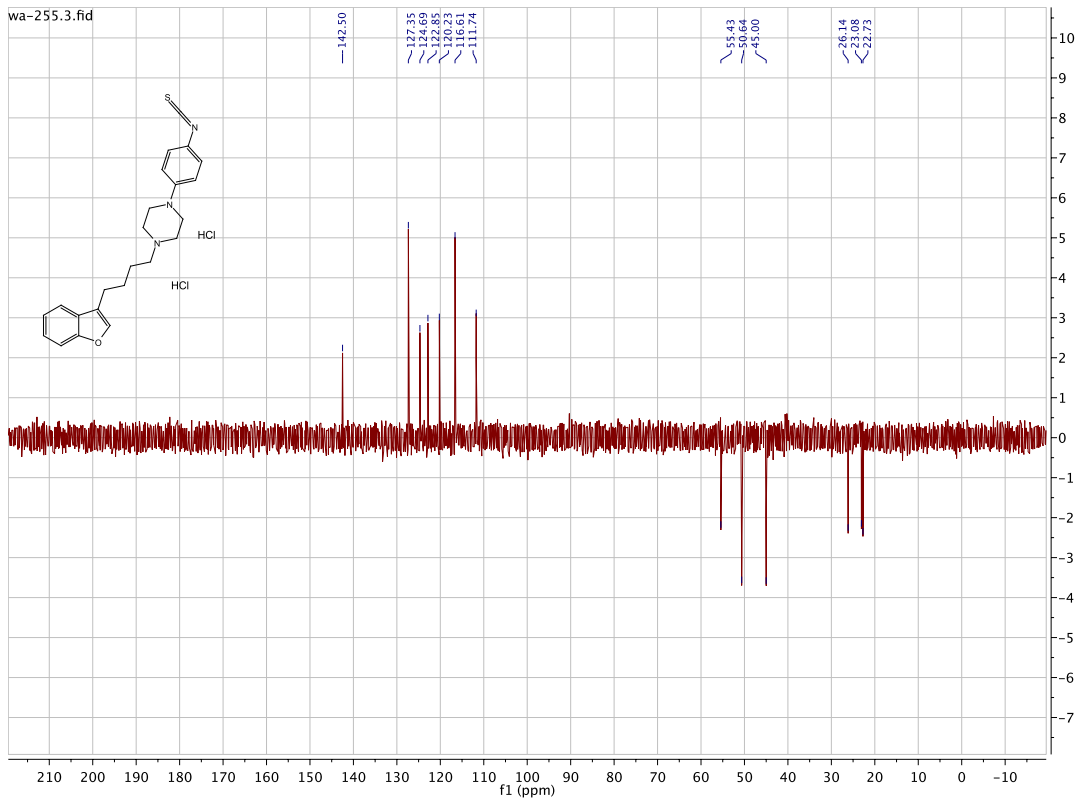
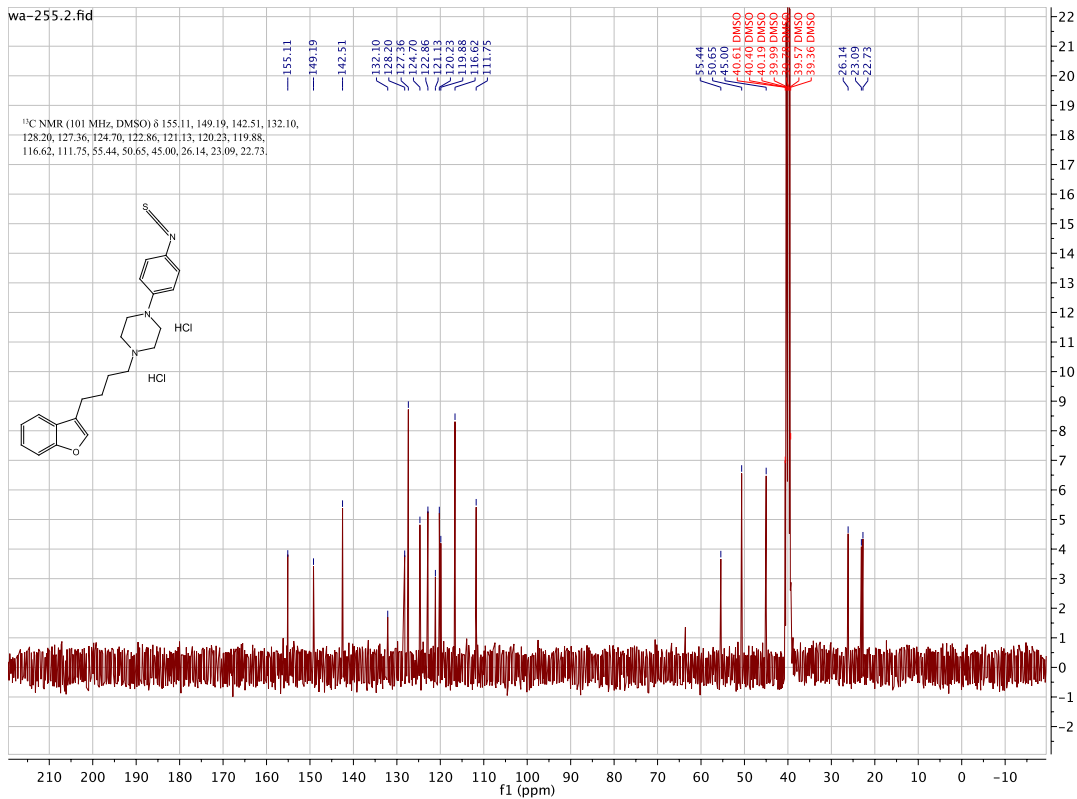


3-(4-(3H-spiro[isobenzofuran-1,4'-piperidin]-1'-yl)butyl)-5-isothiocyanato-1-methyl-1,3-dihydro-2H-benzo[d]imidazol-2-one:[WA258]

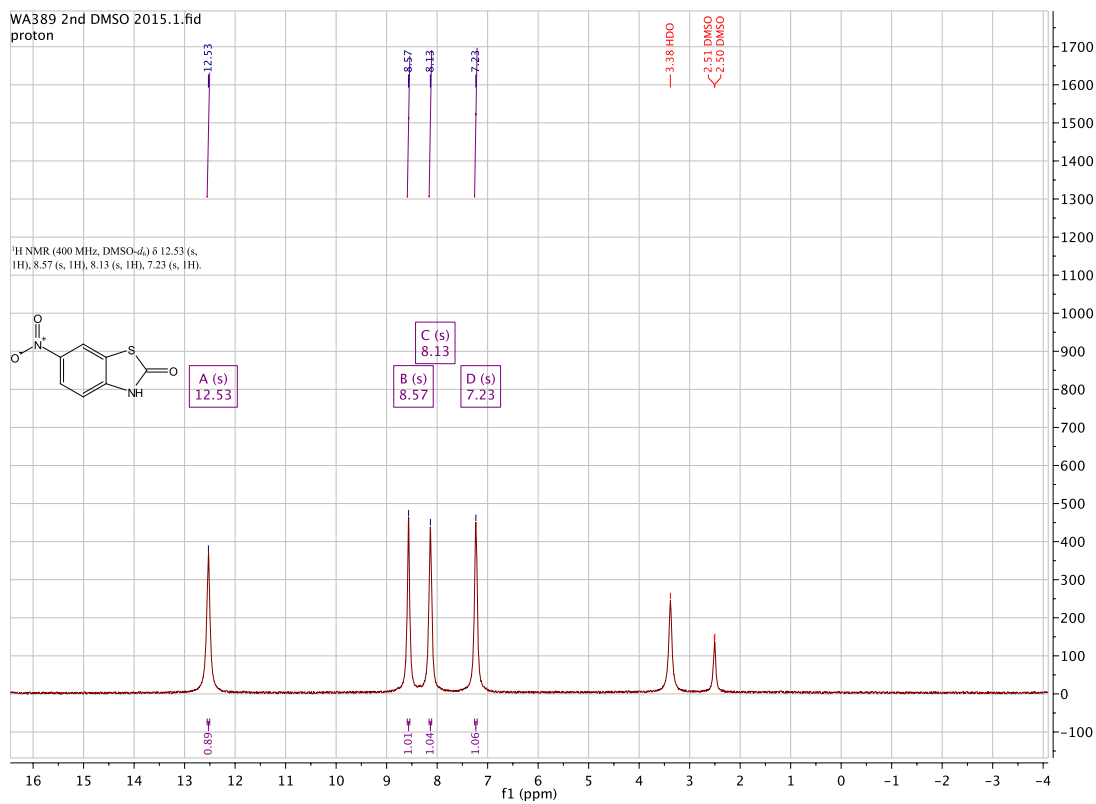
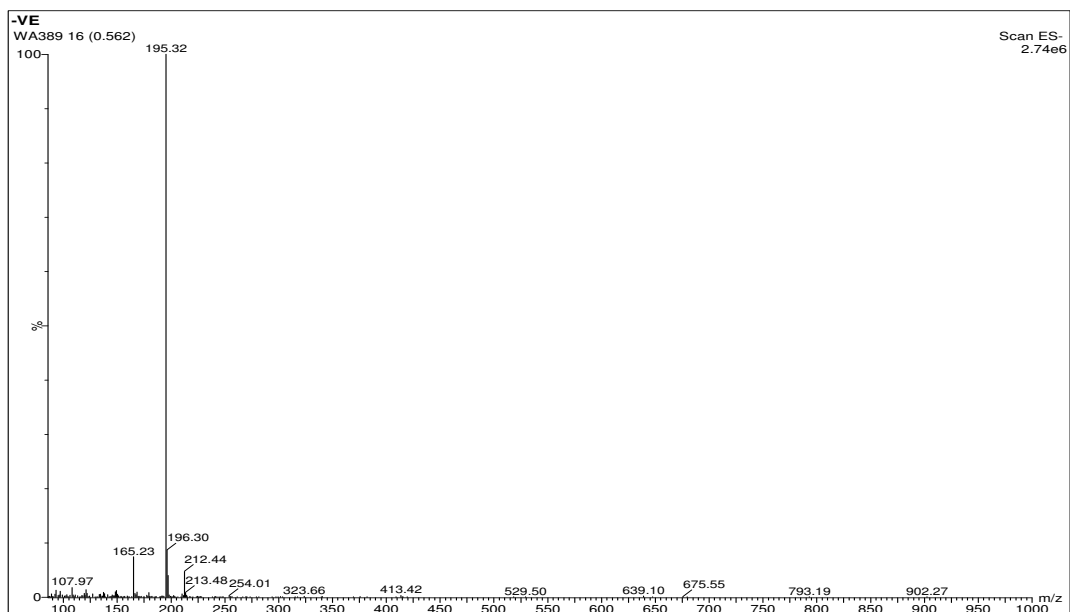


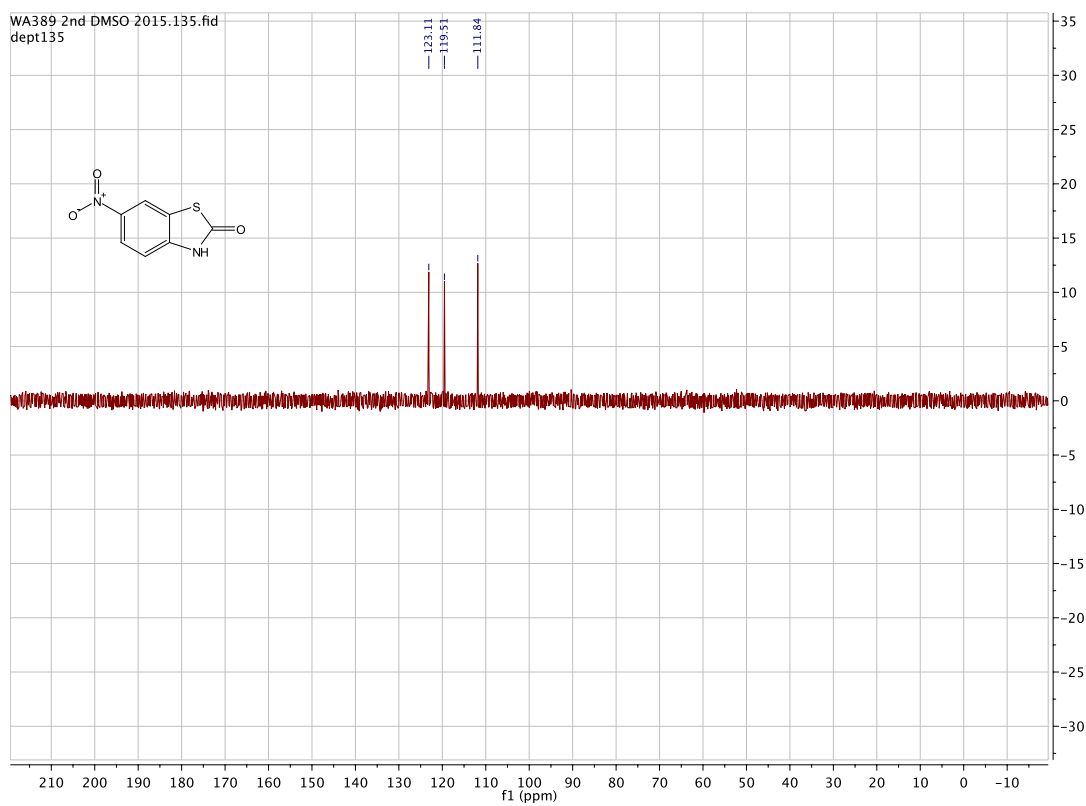
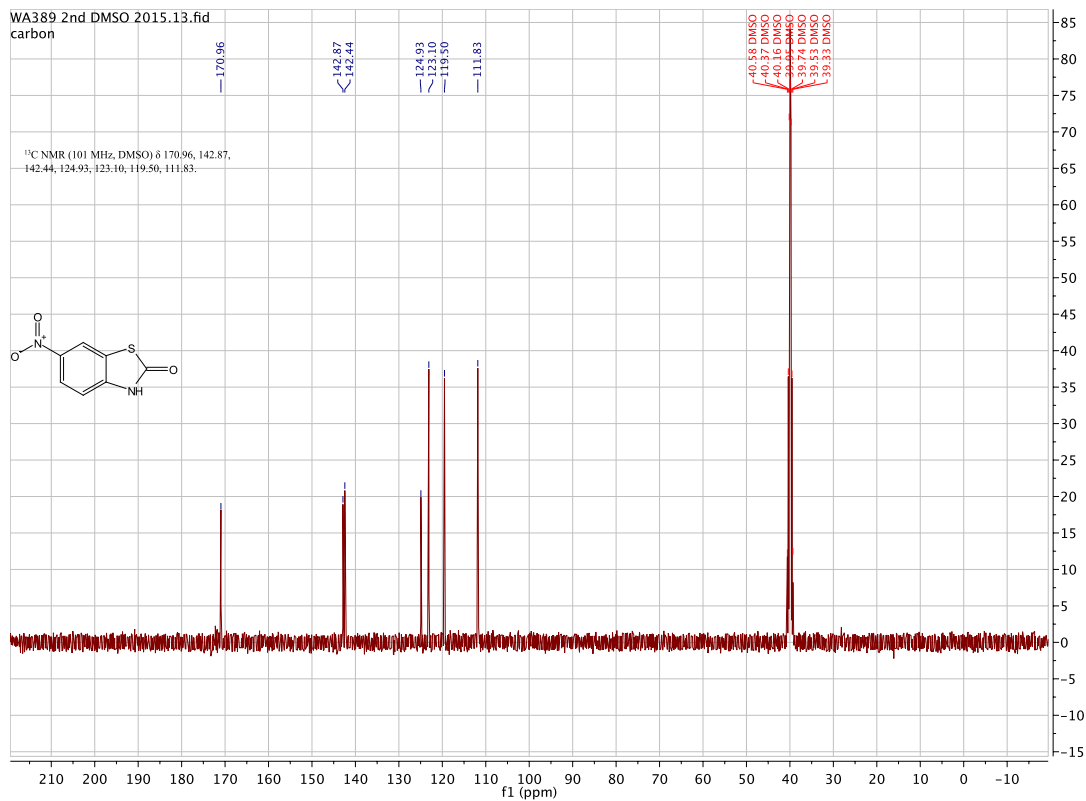
1-(4-(benzofuran-3-yl)butyl)-4-(4-isothiocyanatophenyl)piperazine. (349, WA255)



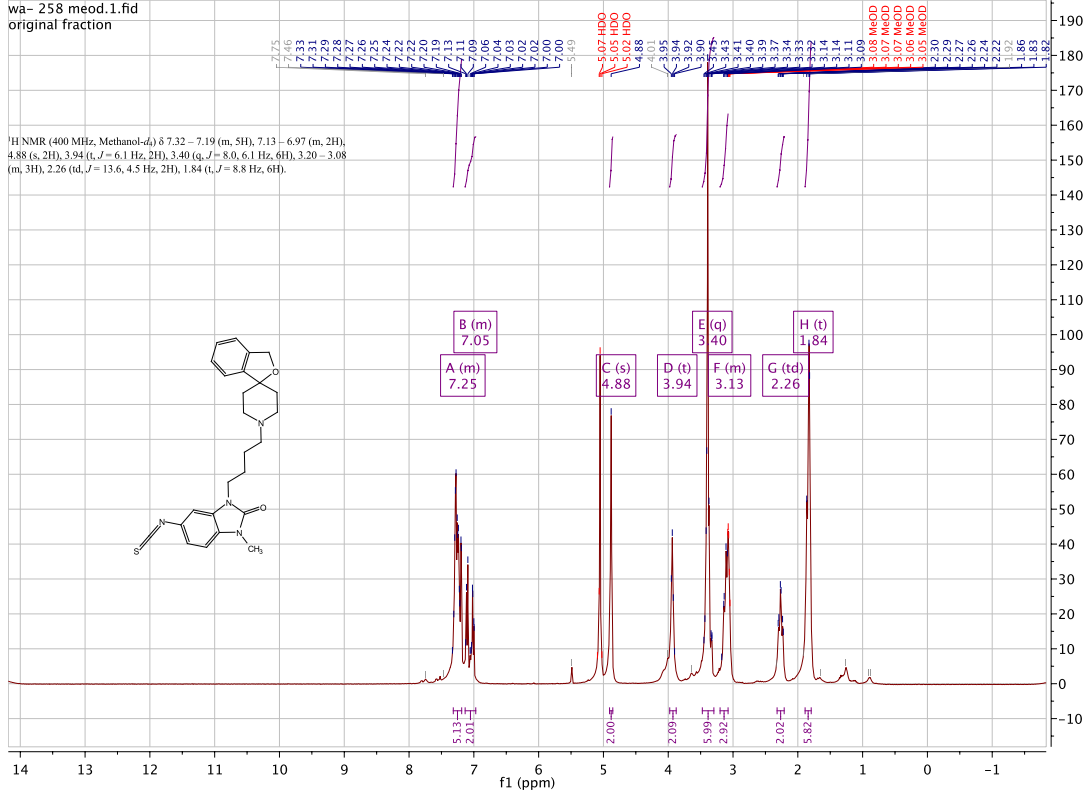


6-nitrobenzo[d]thiazol-2(3H)-one (WA389)

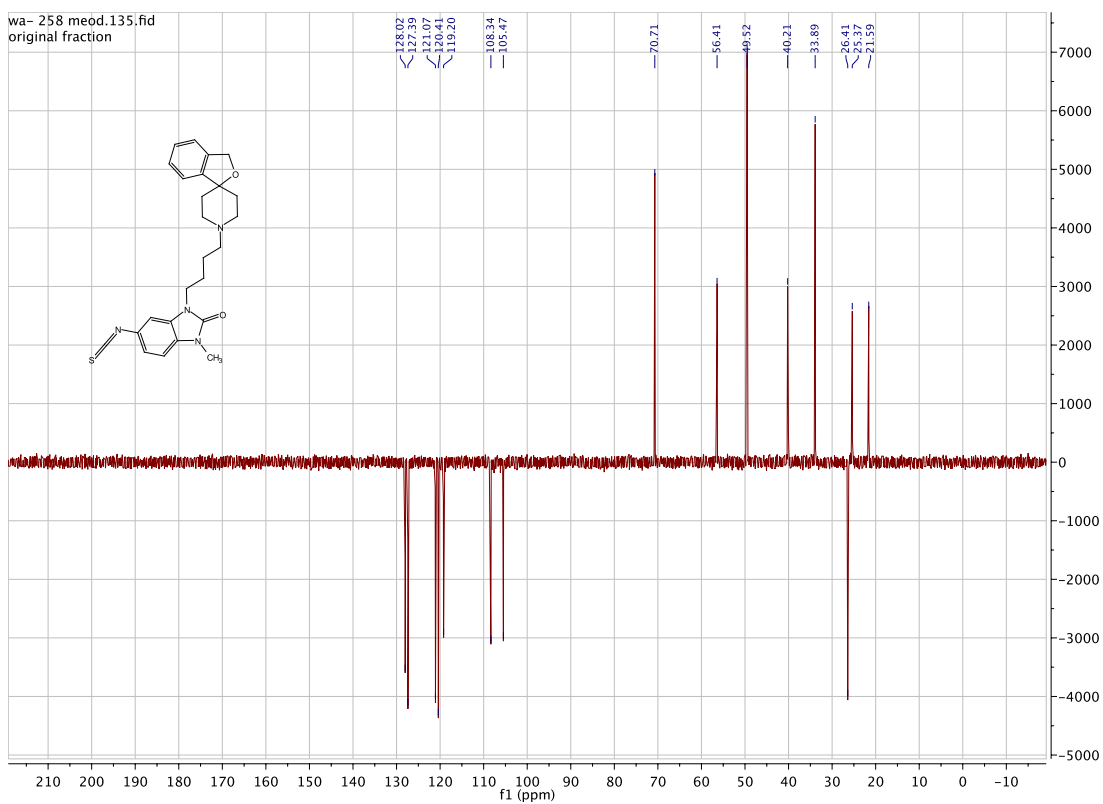


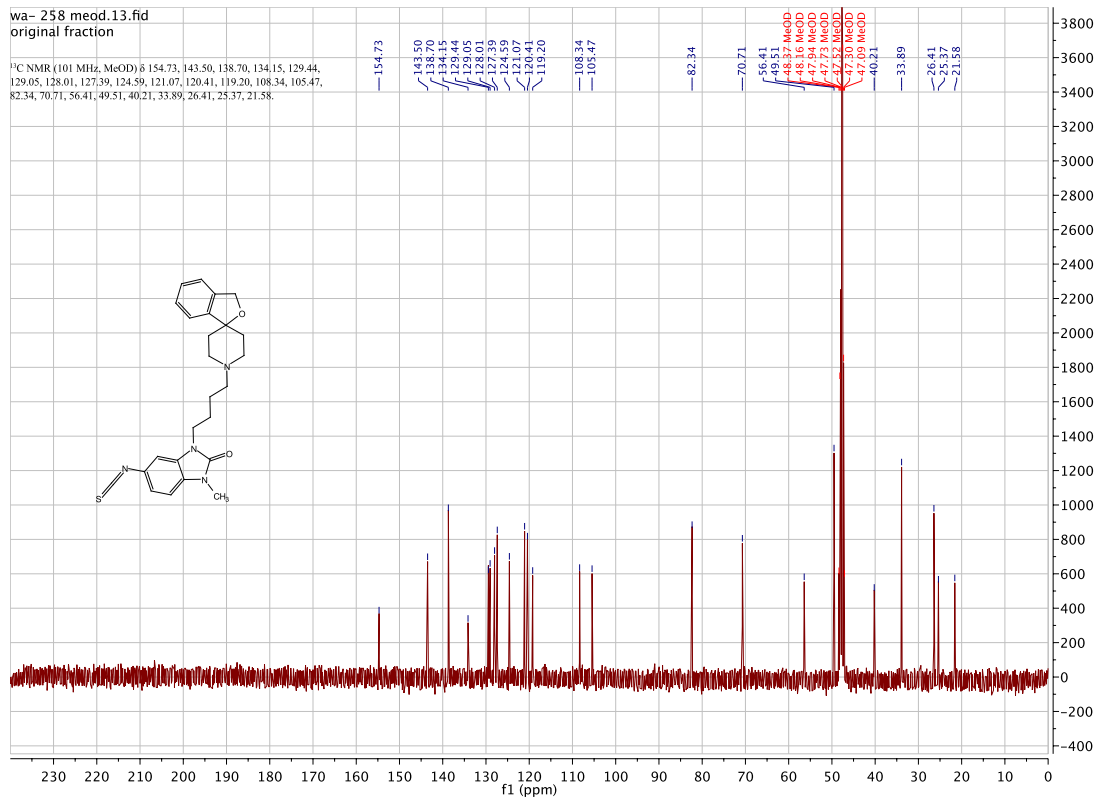


wa- 258 meod.1.fid
original fraction

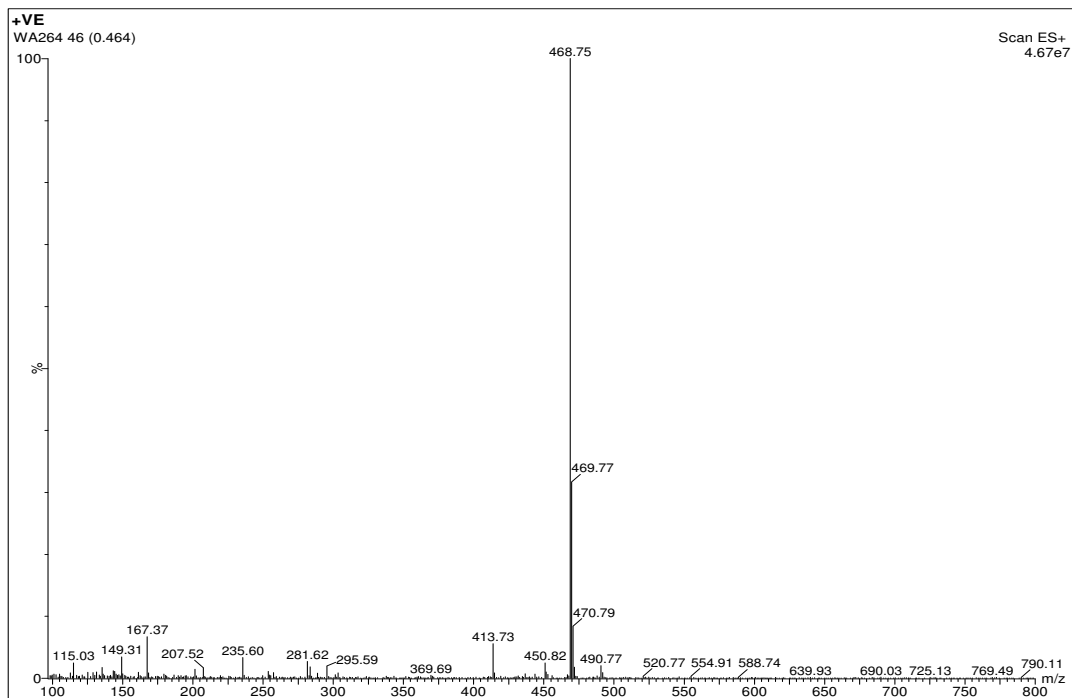


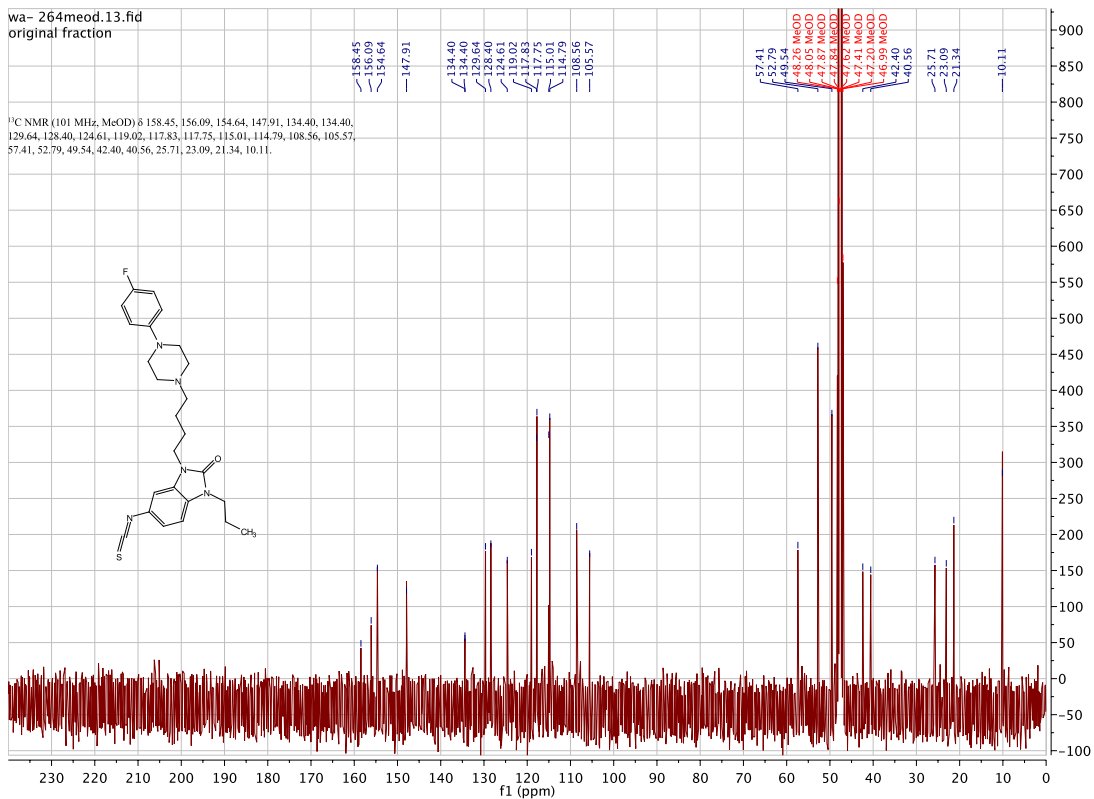
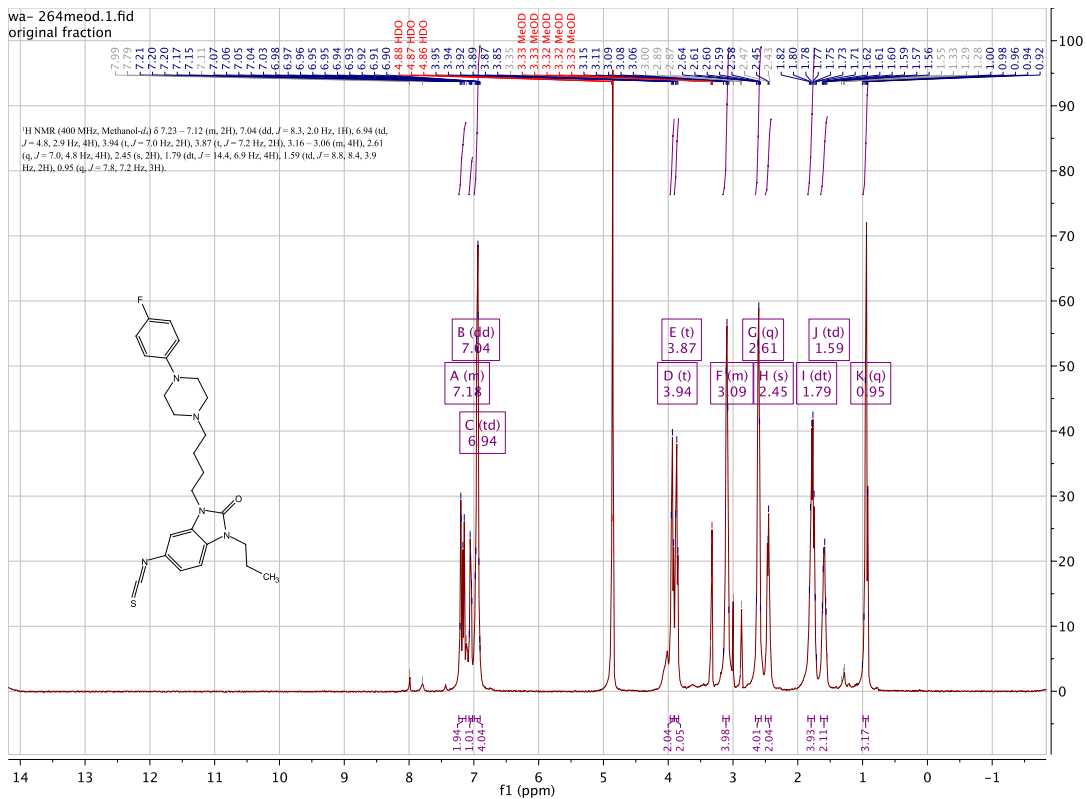
wa- 258 meod.135.fid
original fraction

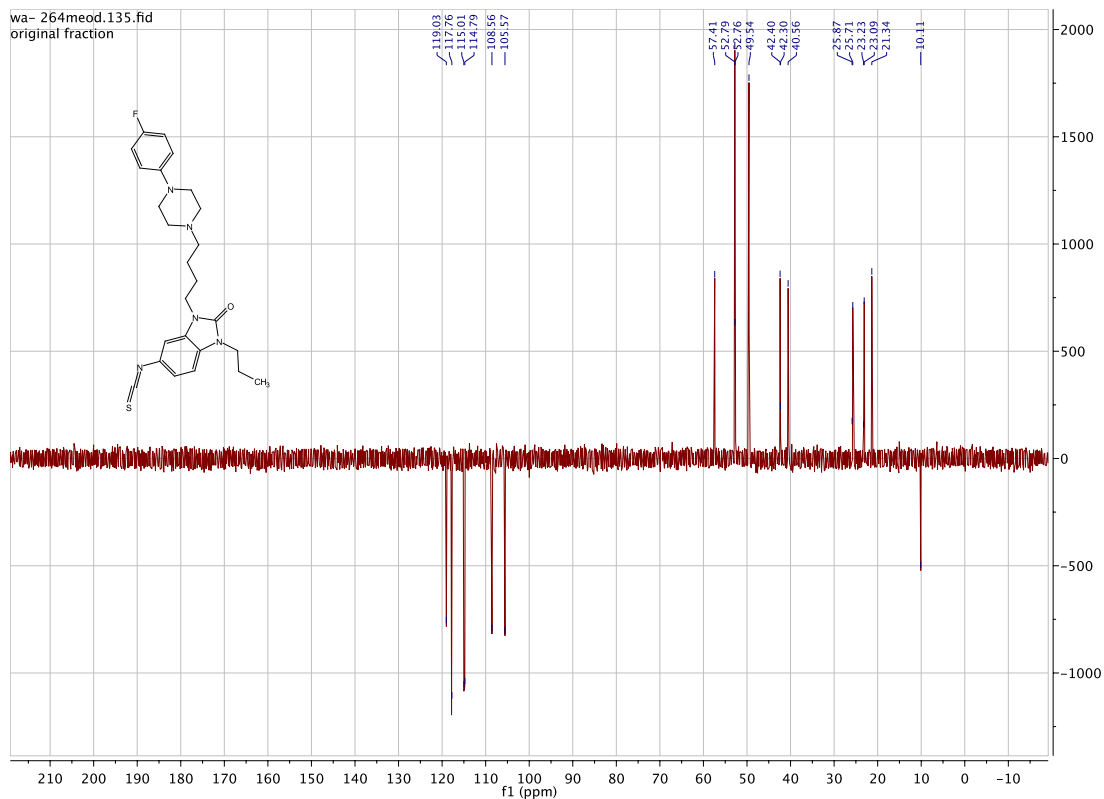




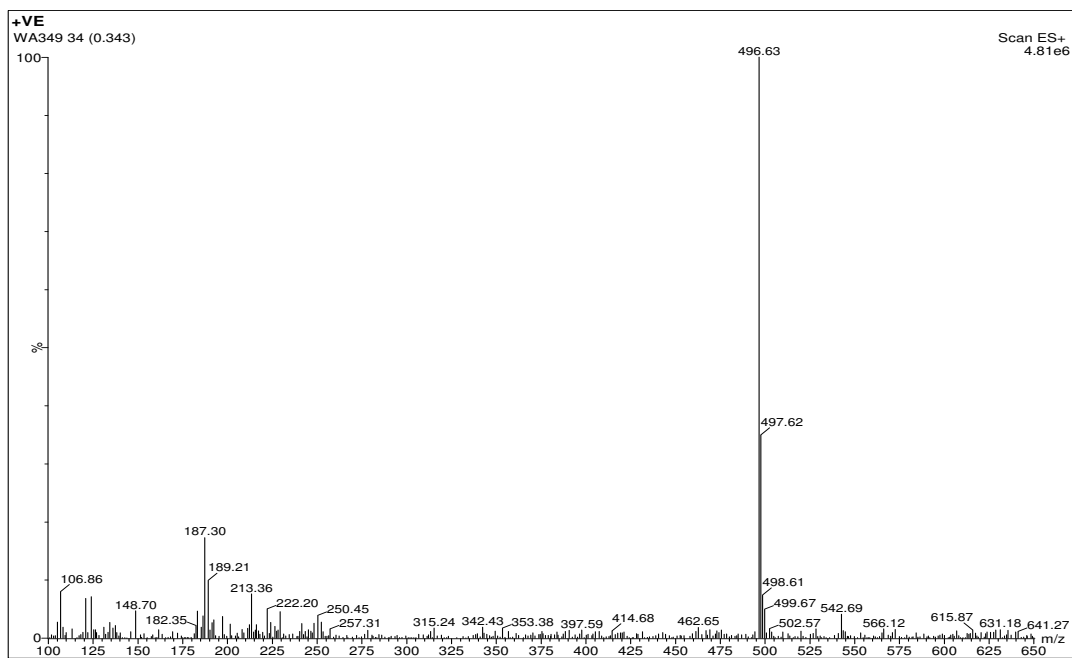
3-(4-(4-(4-fluorophenyl)piperazin-1-yl)butyl)-5-isothiocyanato-1-propyl-1,3-dihydro-2H-benzod[imidazol-2-one:[WA264]

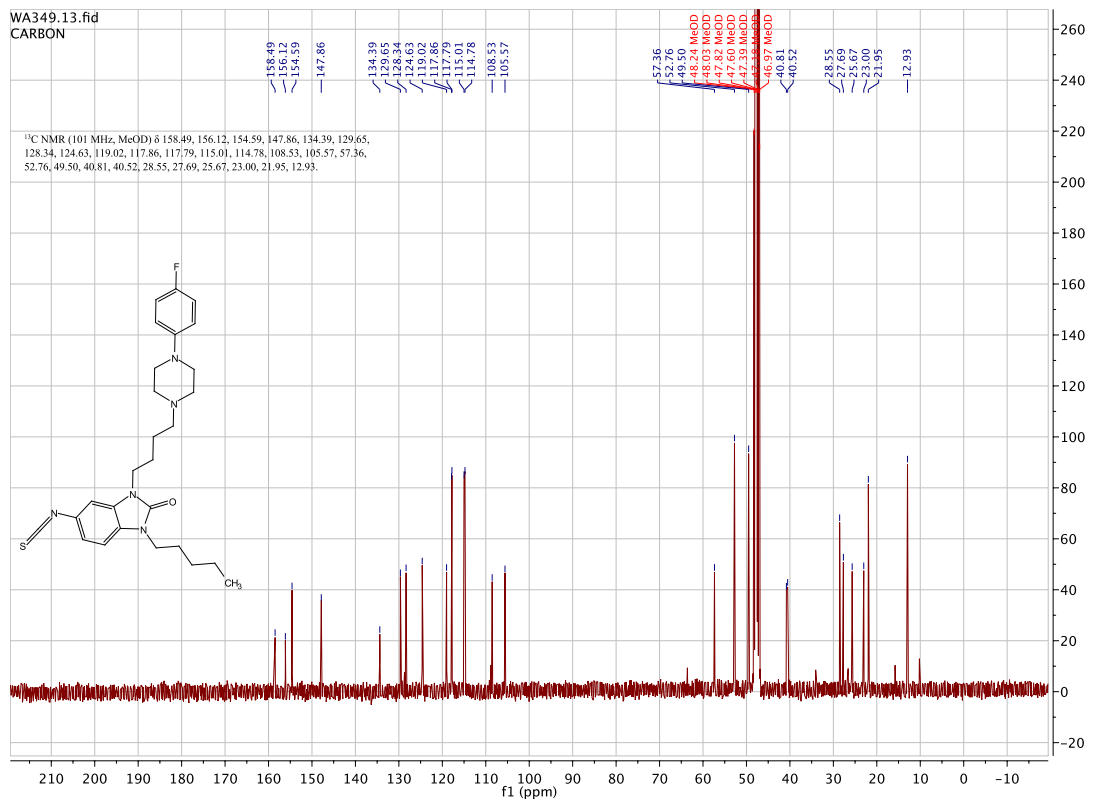
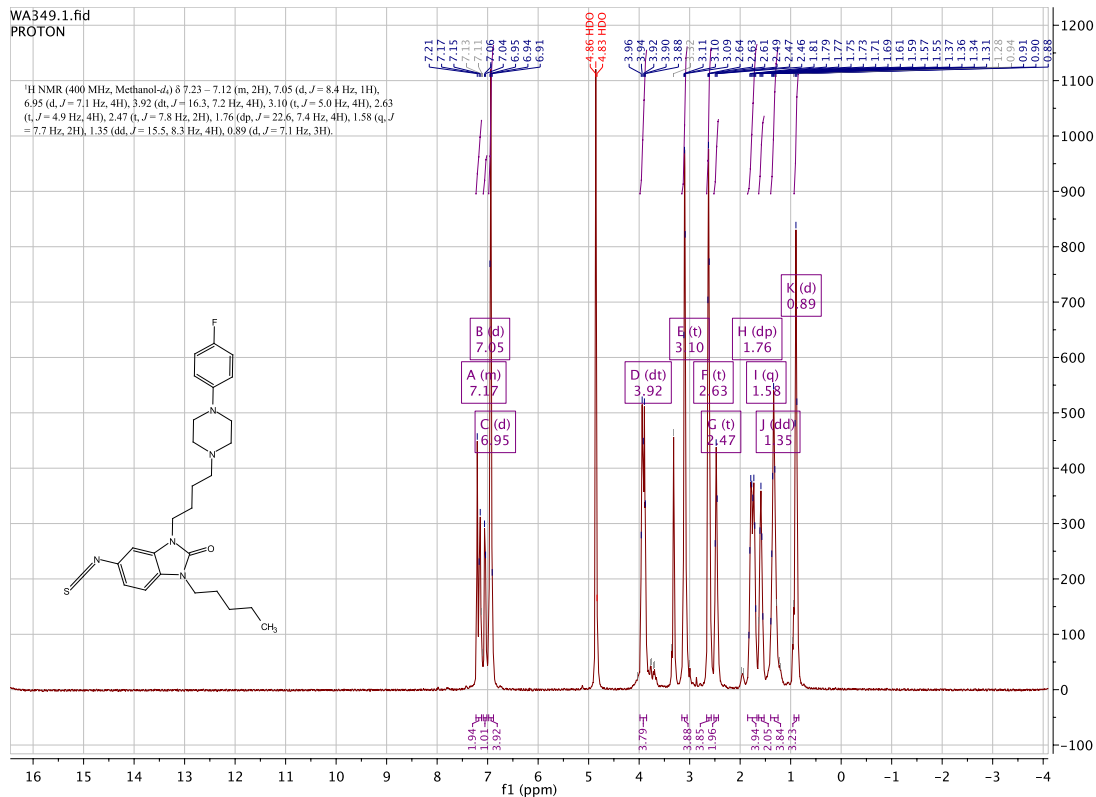


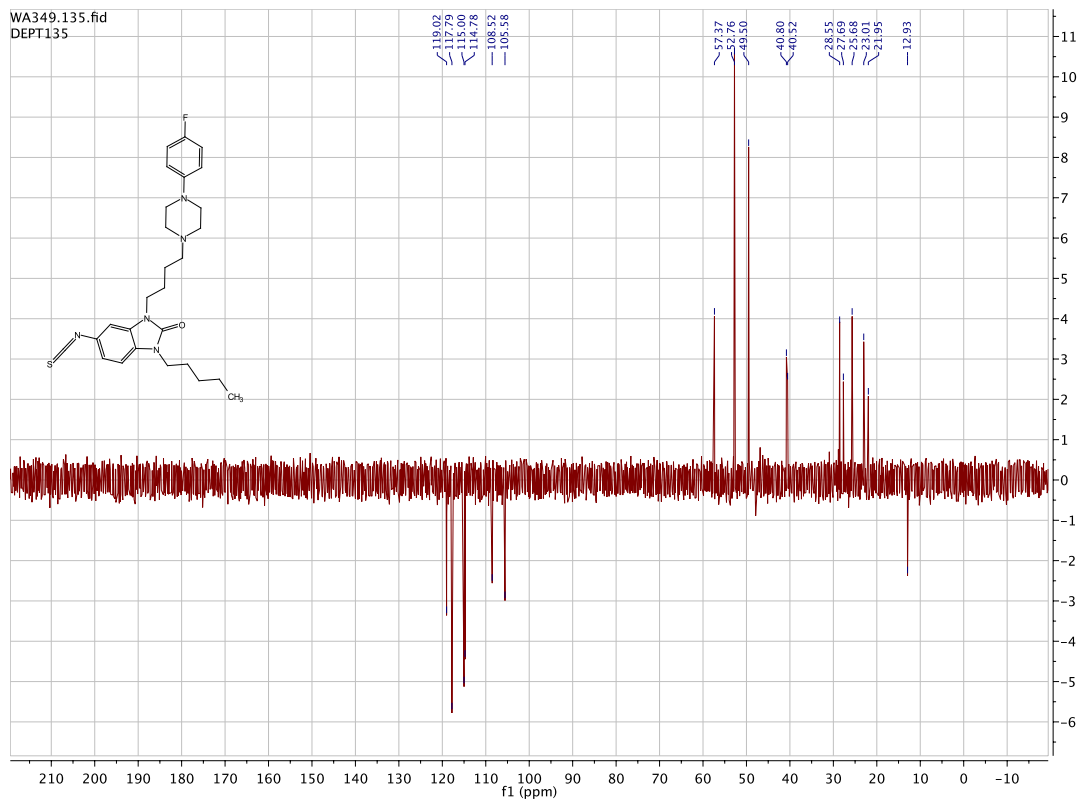




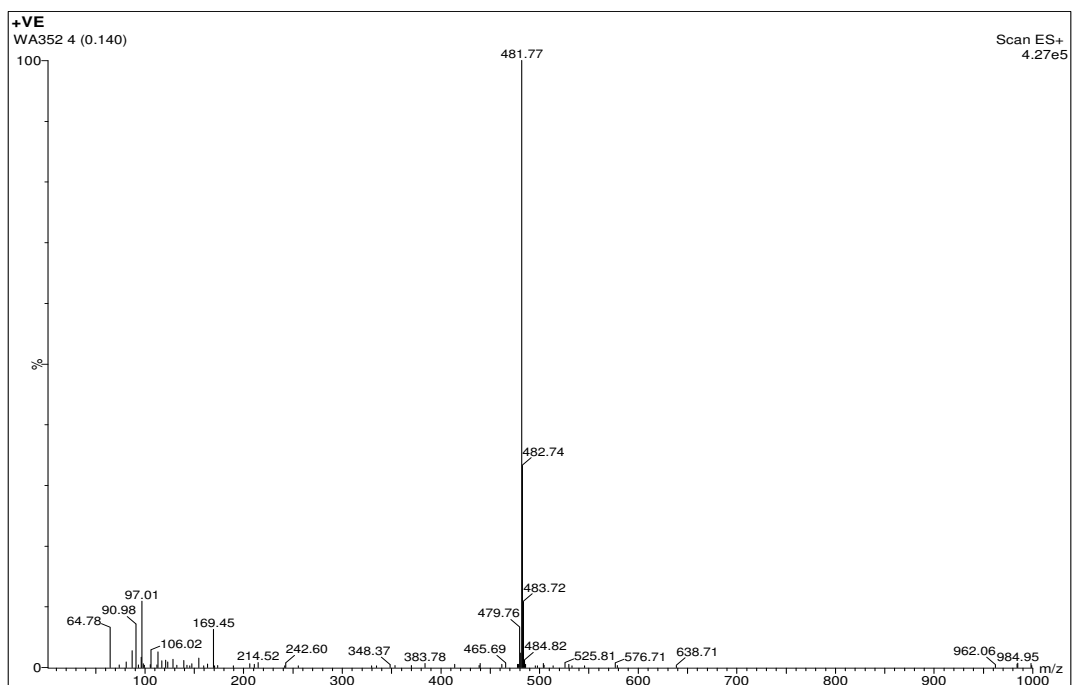
3-(4-(4-(4-fluorophenyl)piperazin-1-yl)butyl)-5-isothiocyanato-1-pentyl-1,3-dihydro-2H-benzod[imidazol-2-one:[WA349]

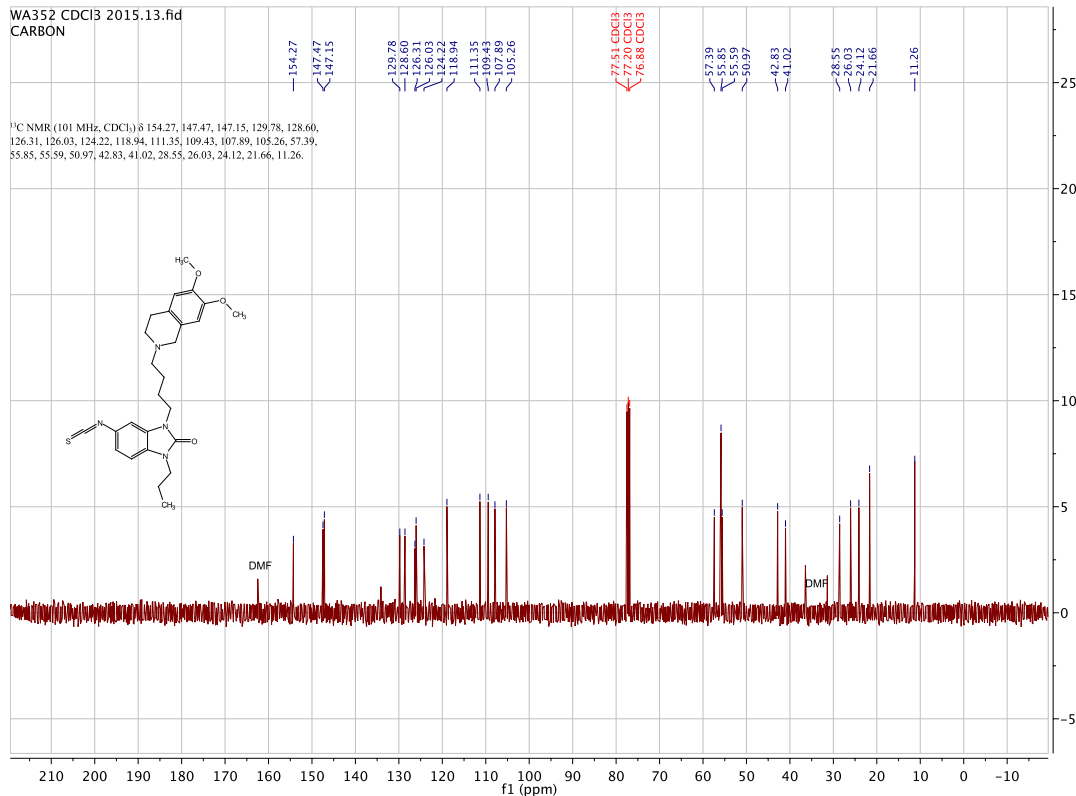
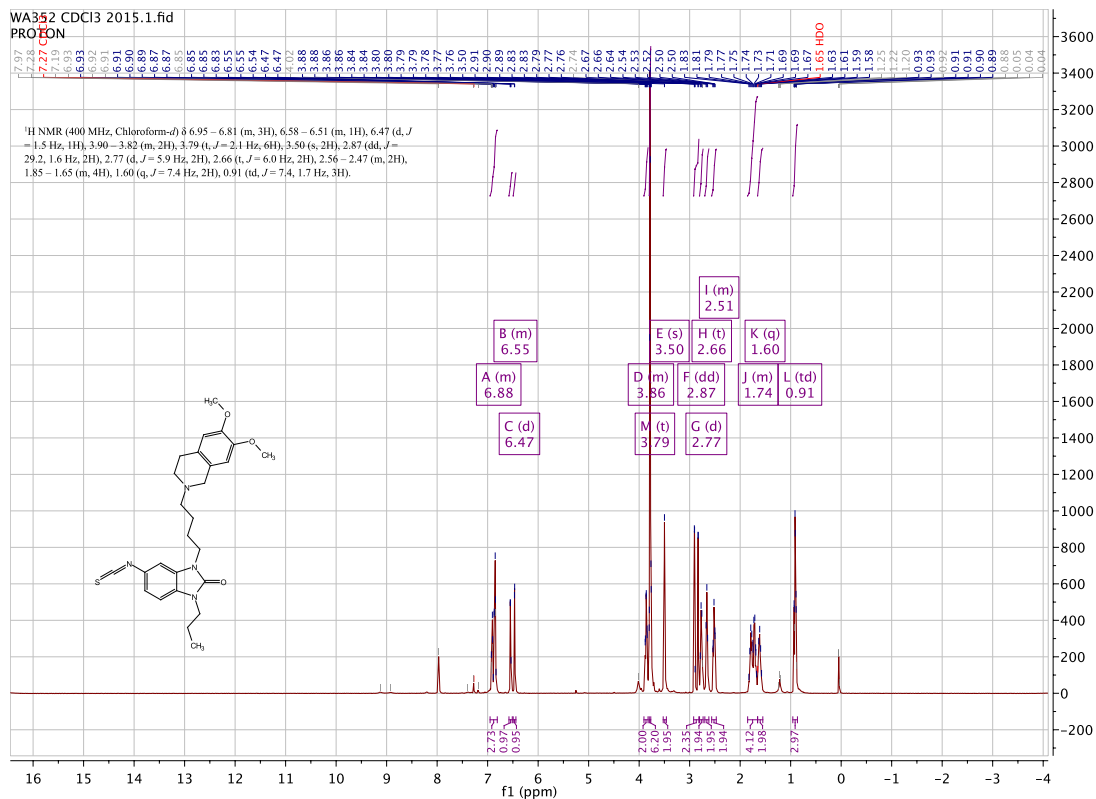


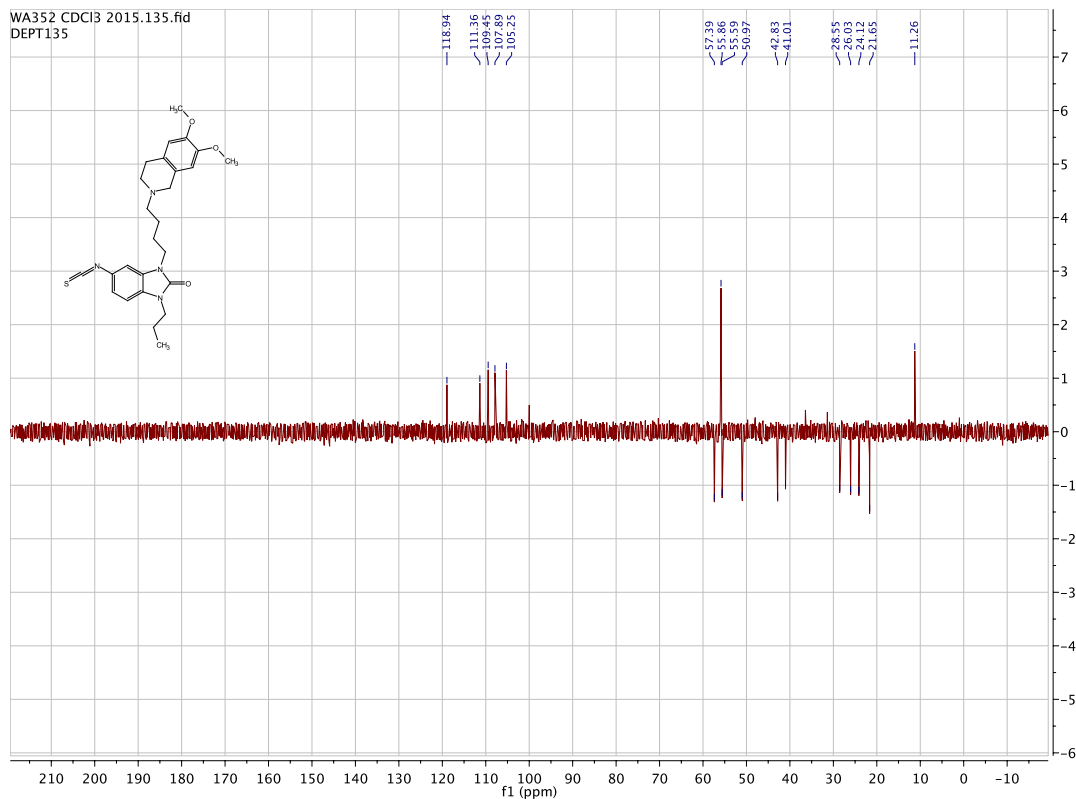




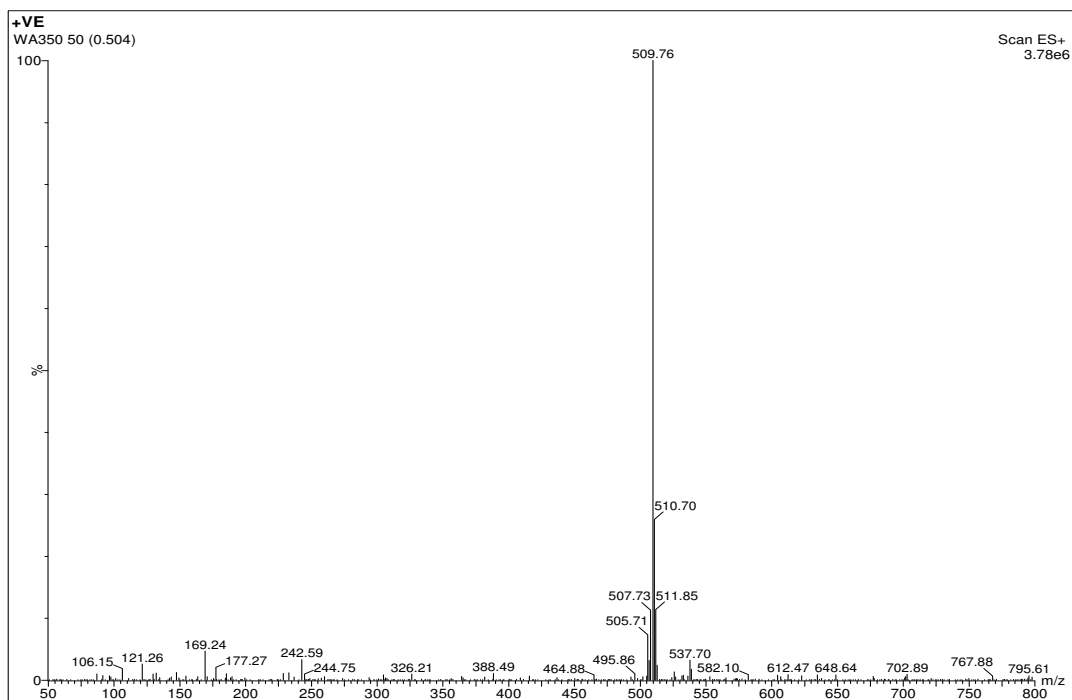
3-(4-(6,7-dimethoxy-3,4-dihydroisoquinolin-2(1H)-yl)butyl)-5-isothiocyanato-1-propyl-1,3-dihydro-2H-benzo[d]imidazol-2-one:[WA352]

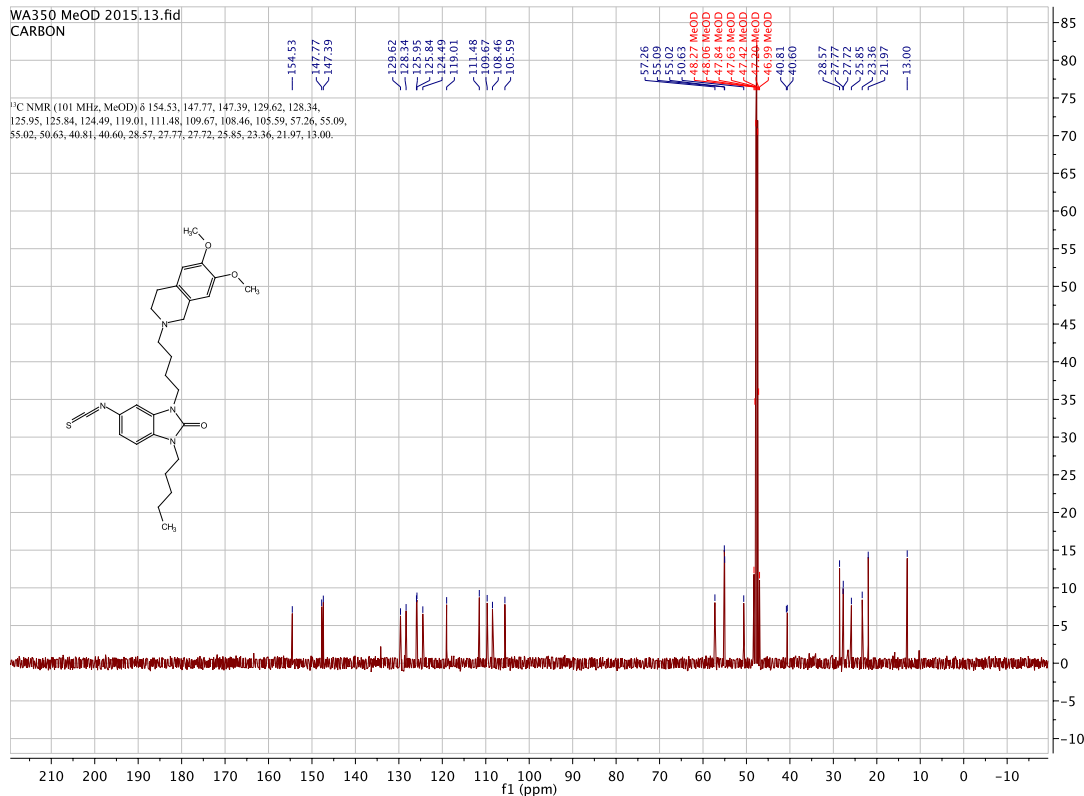
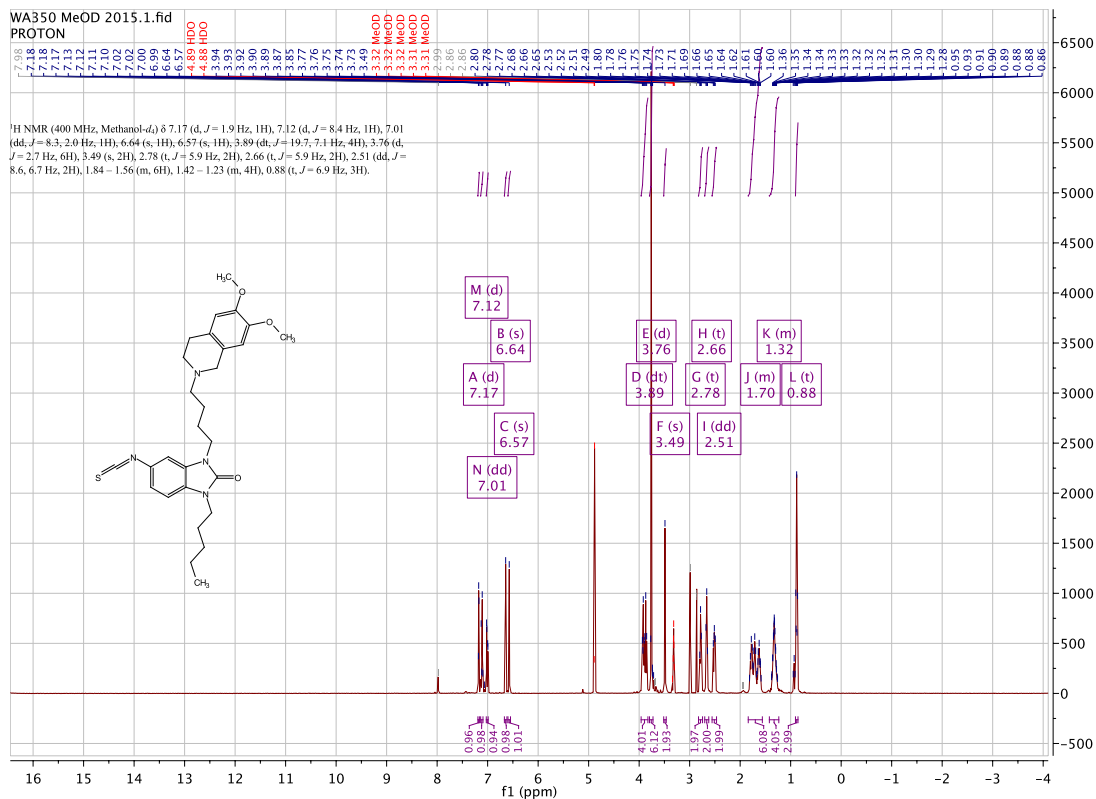


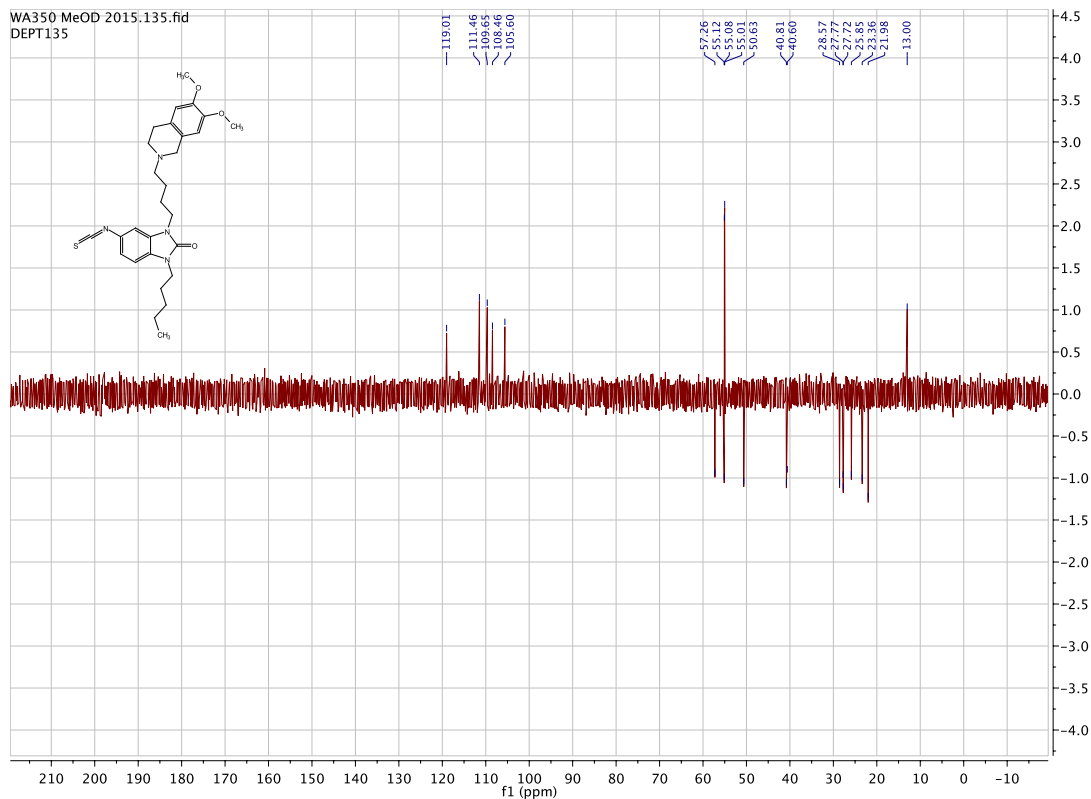




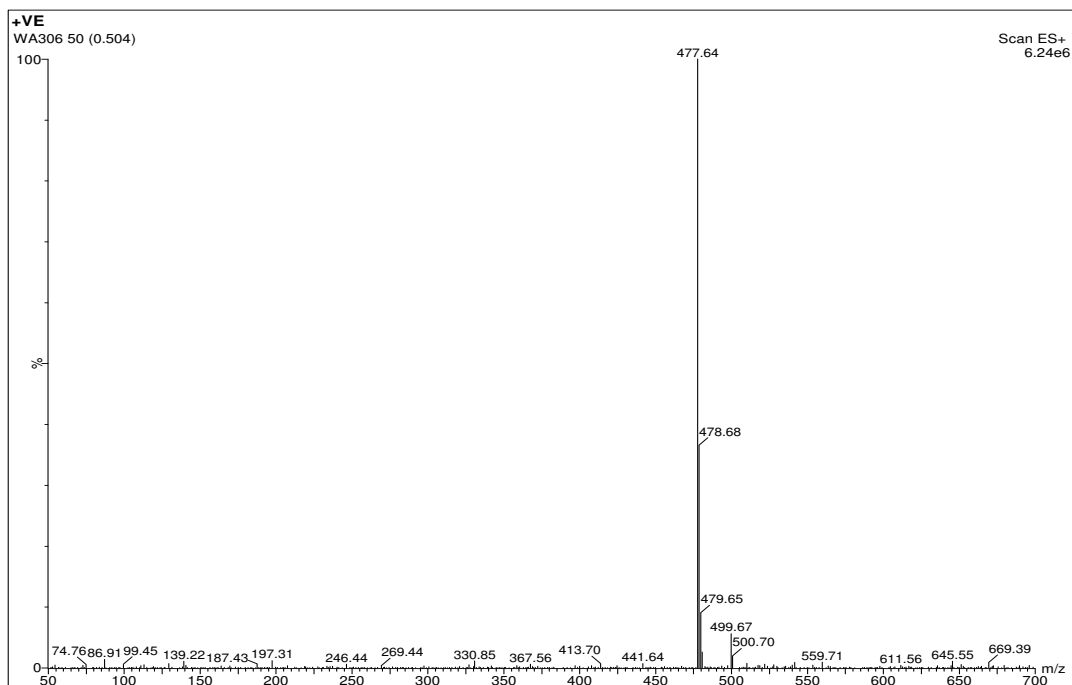
3-(4-(6,7-dimethoxy-3,4-dihydroisoquinolin-2(1H)-yl)butyl)-5-isothiocyanato-1-pentyl-1,3-dihydro-2H-benzo[d]imidazol-2-one: [WA350]

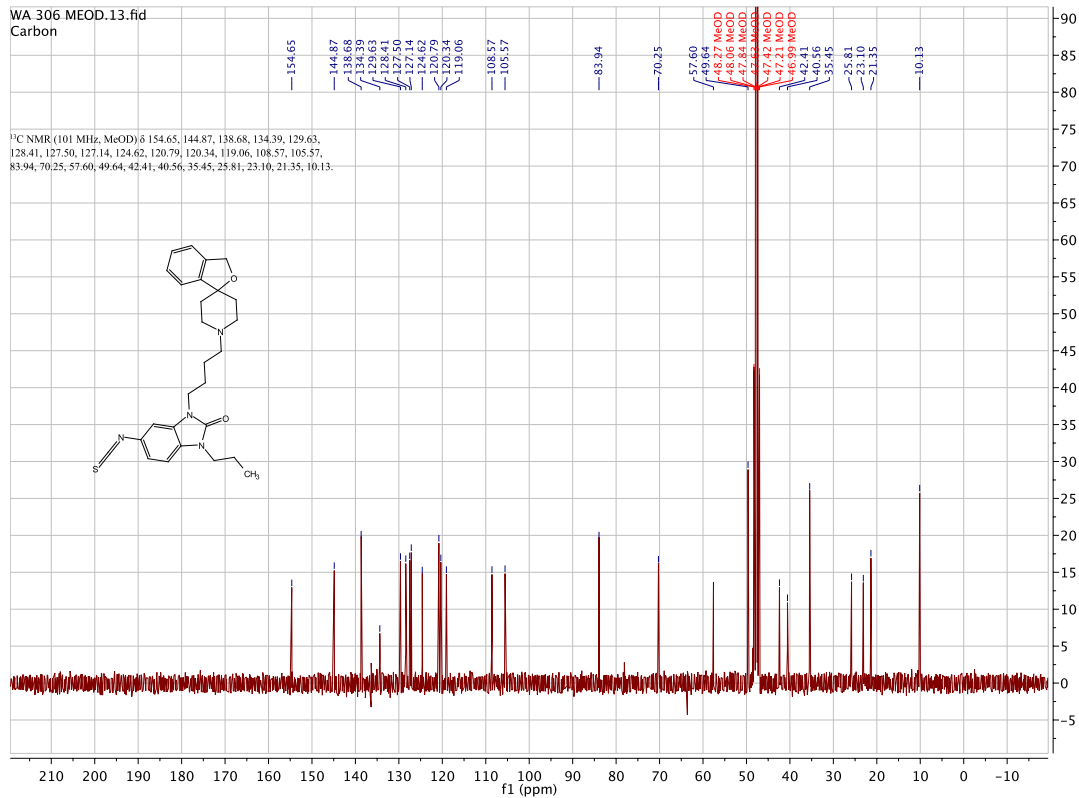
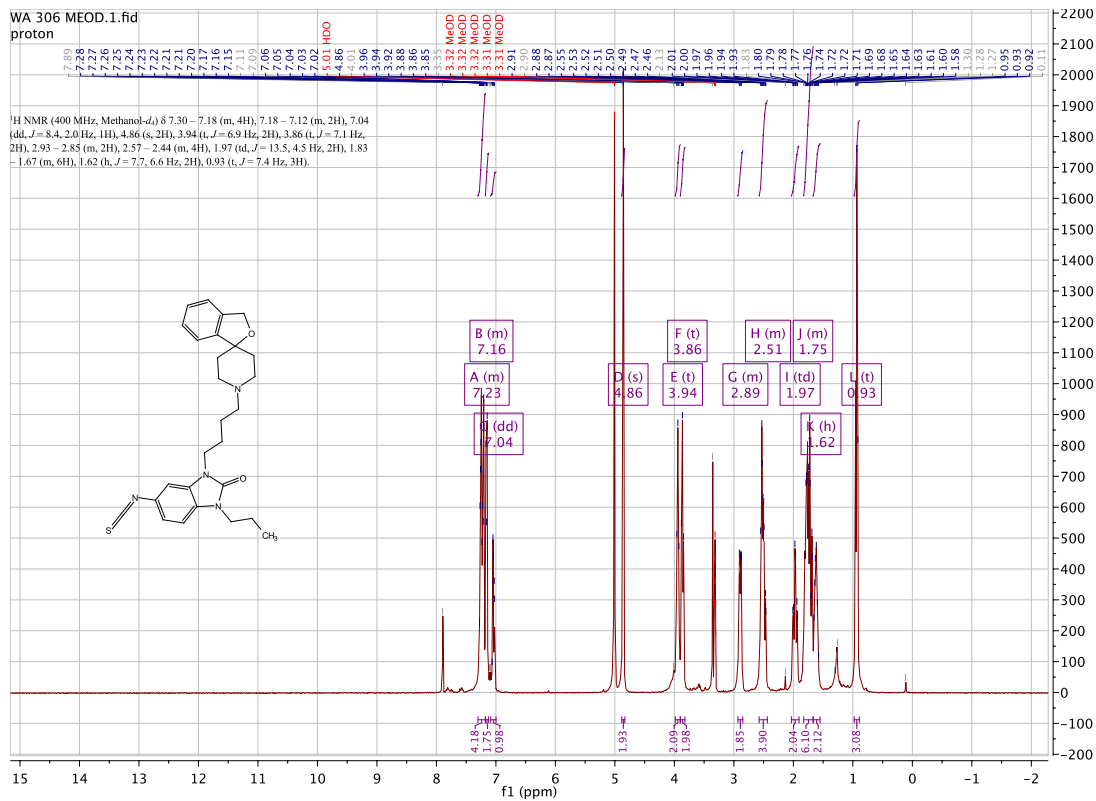


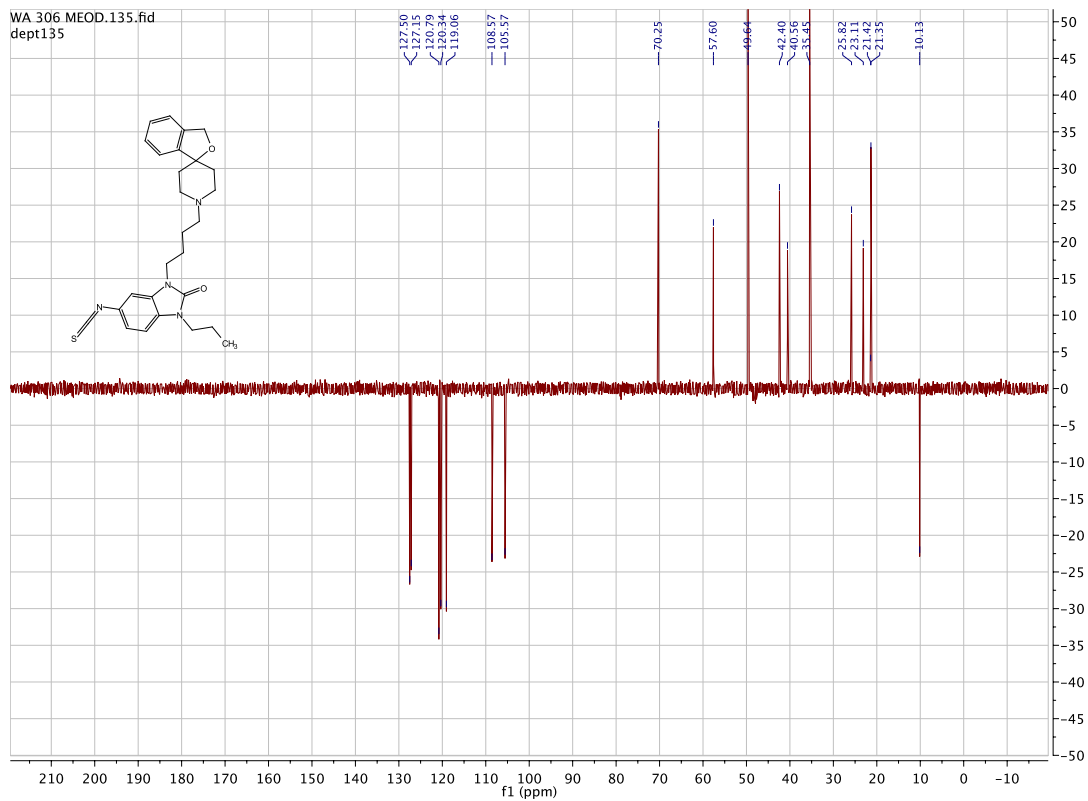




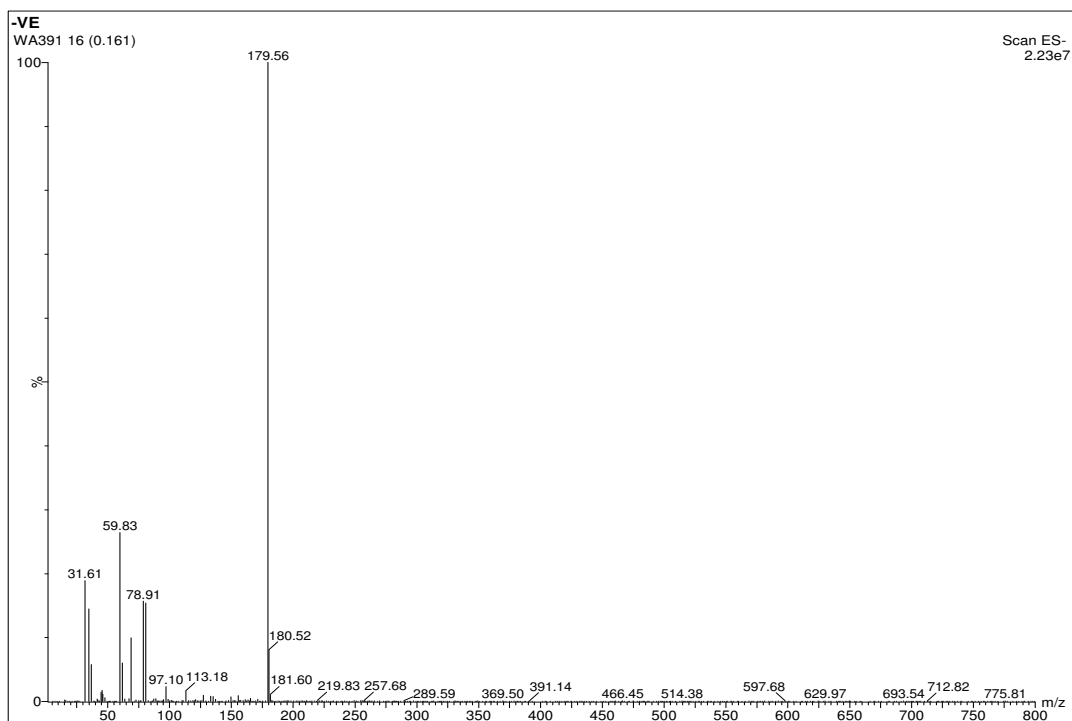
3-(4-(3H-spiro[isobenzofuran-1,4'-piperidin]-1'-yl)butyl)-5-isothiocyanato-1-propyl-1,3-dihydro-2H-benzo[d]imidazol-2-one: [WA306]

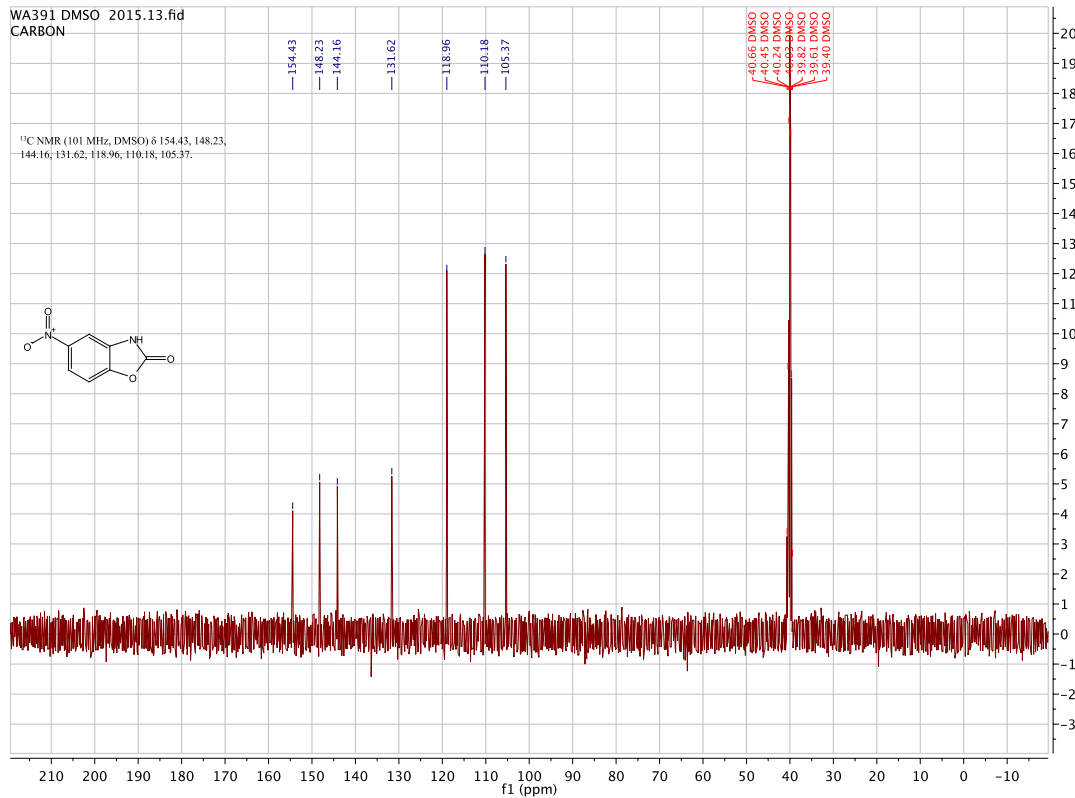
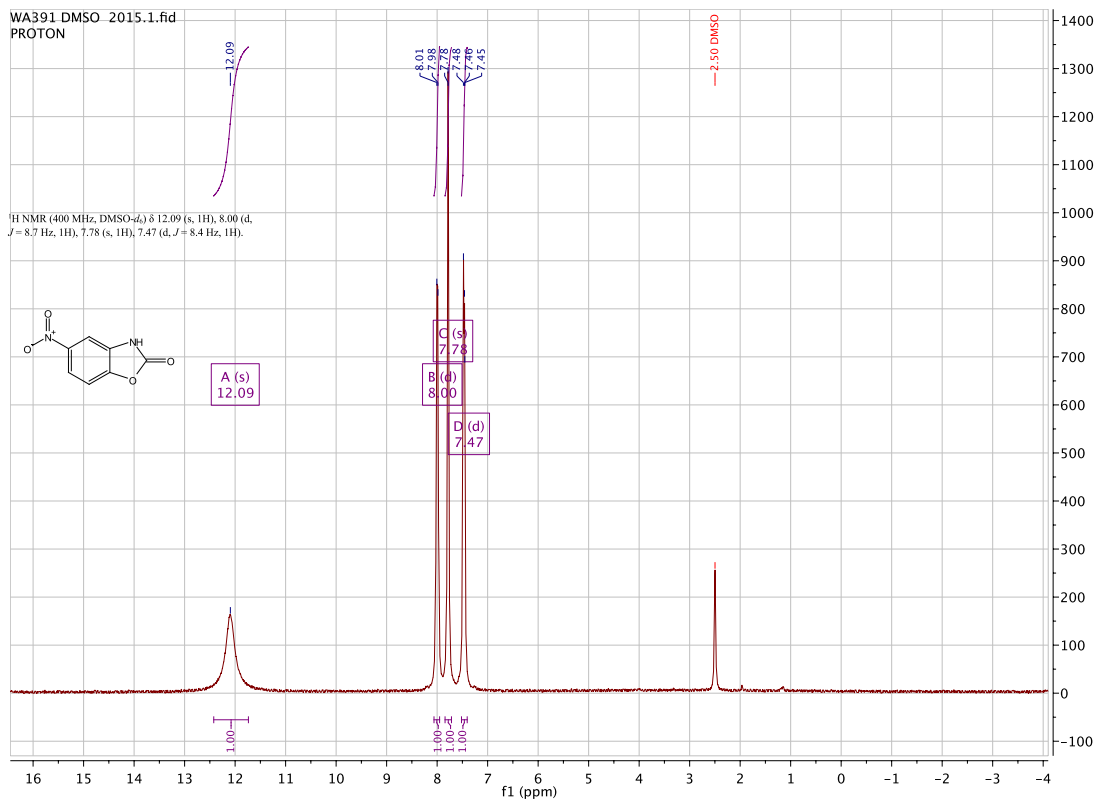


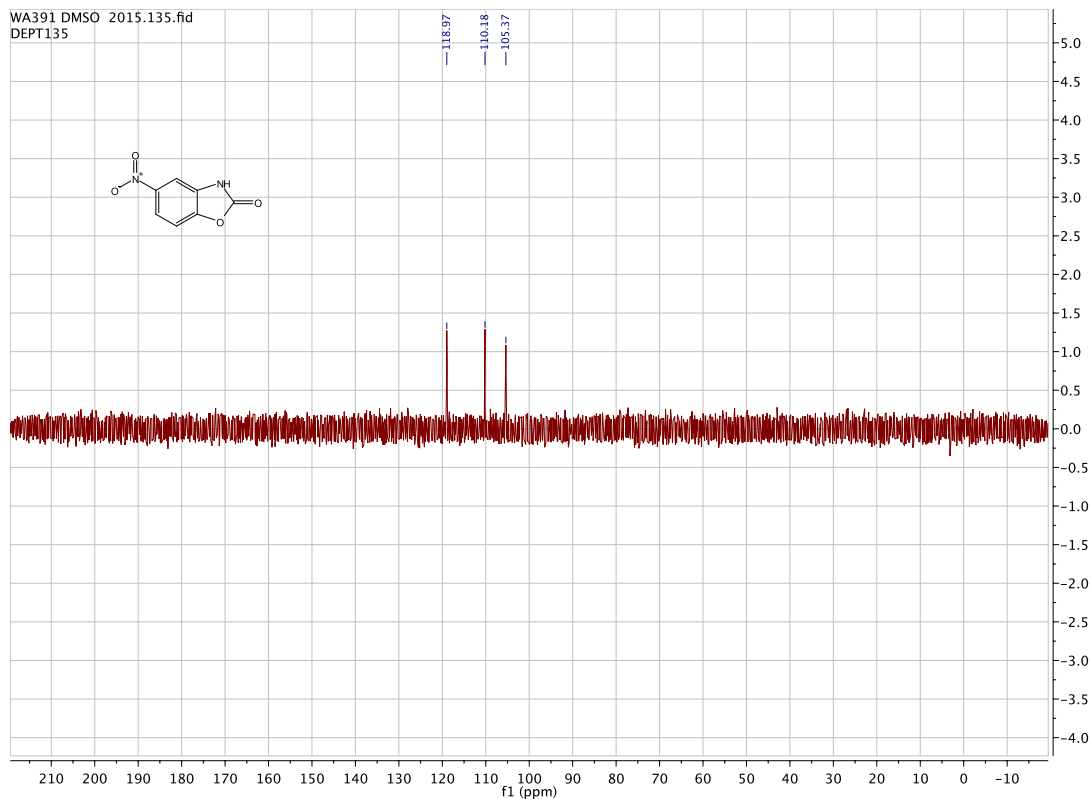




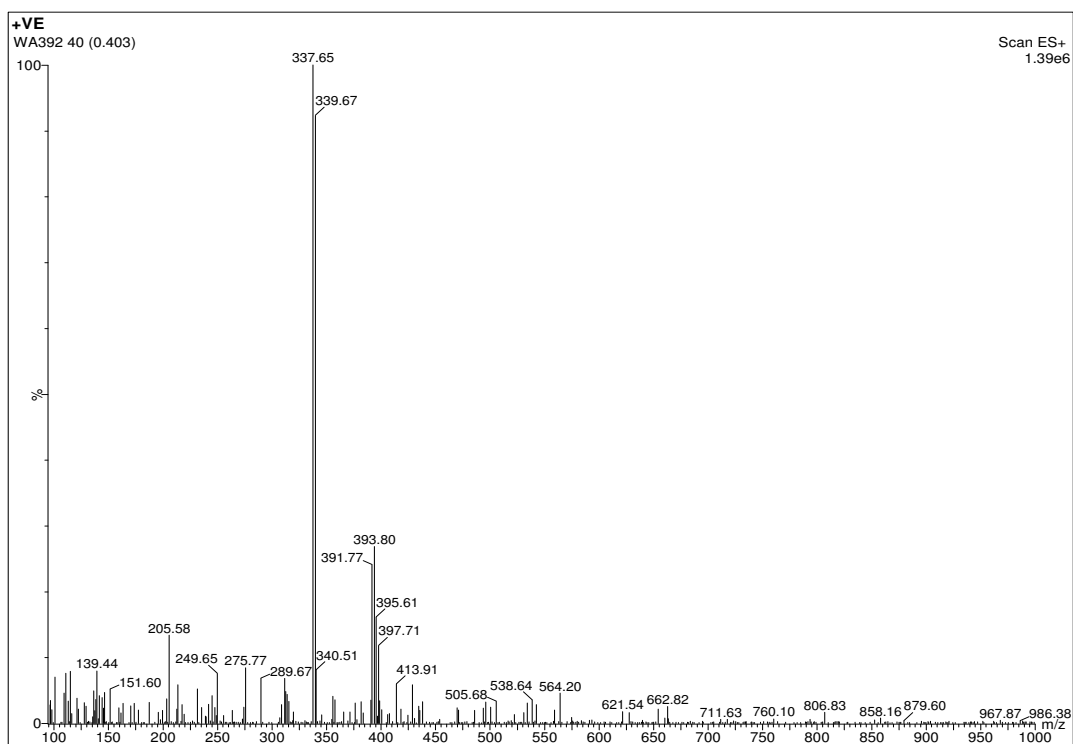
5-nitrobenzo[d]oxazol-2(3H)-one.[WA391]

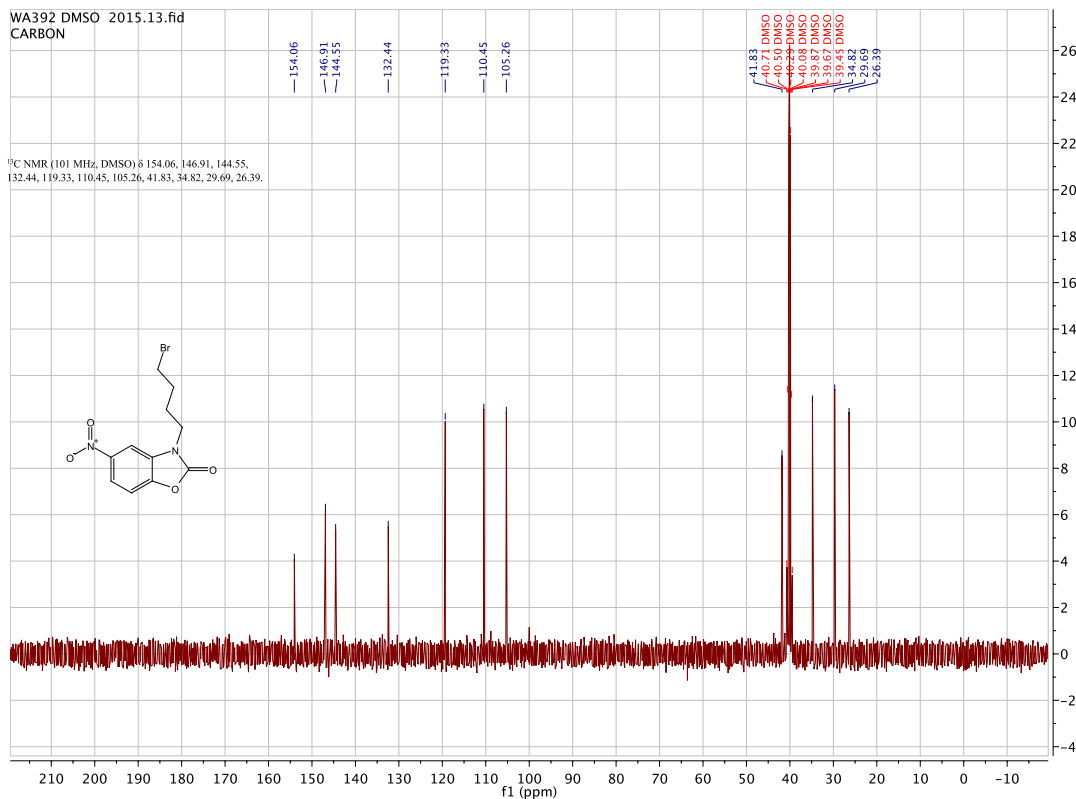
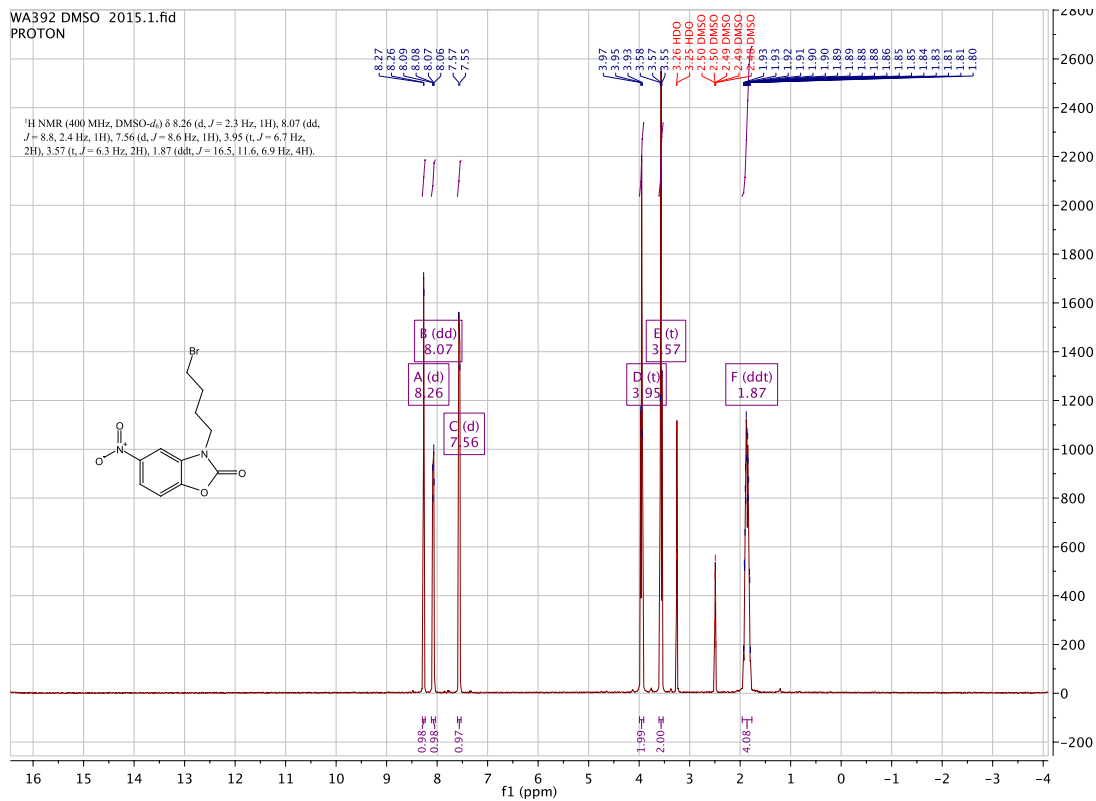


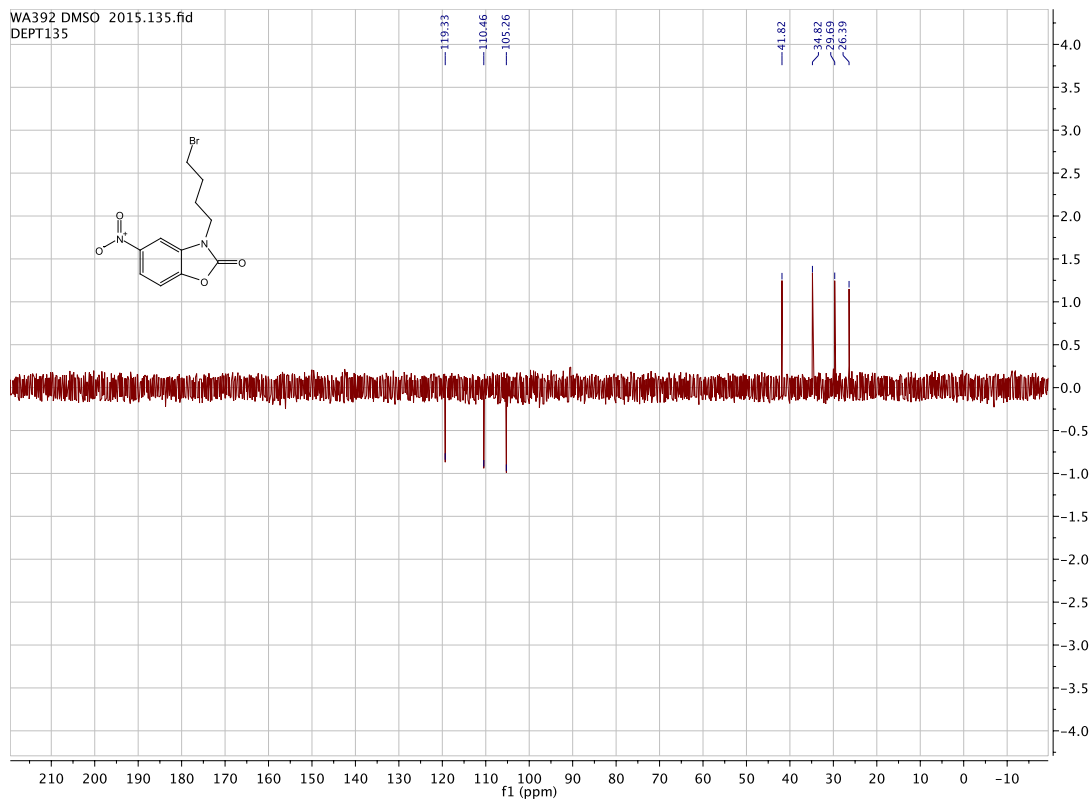




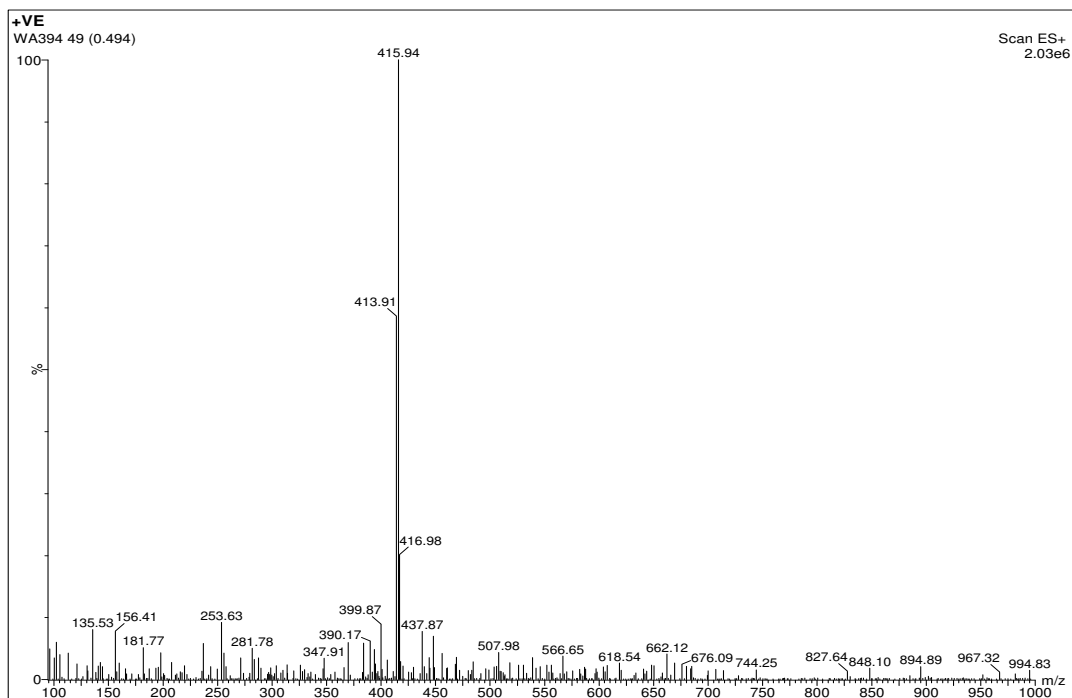
3-(4-bromobutyl)-5-nitrobenzo[d]oxazol-2(3H)-one.[WA392]



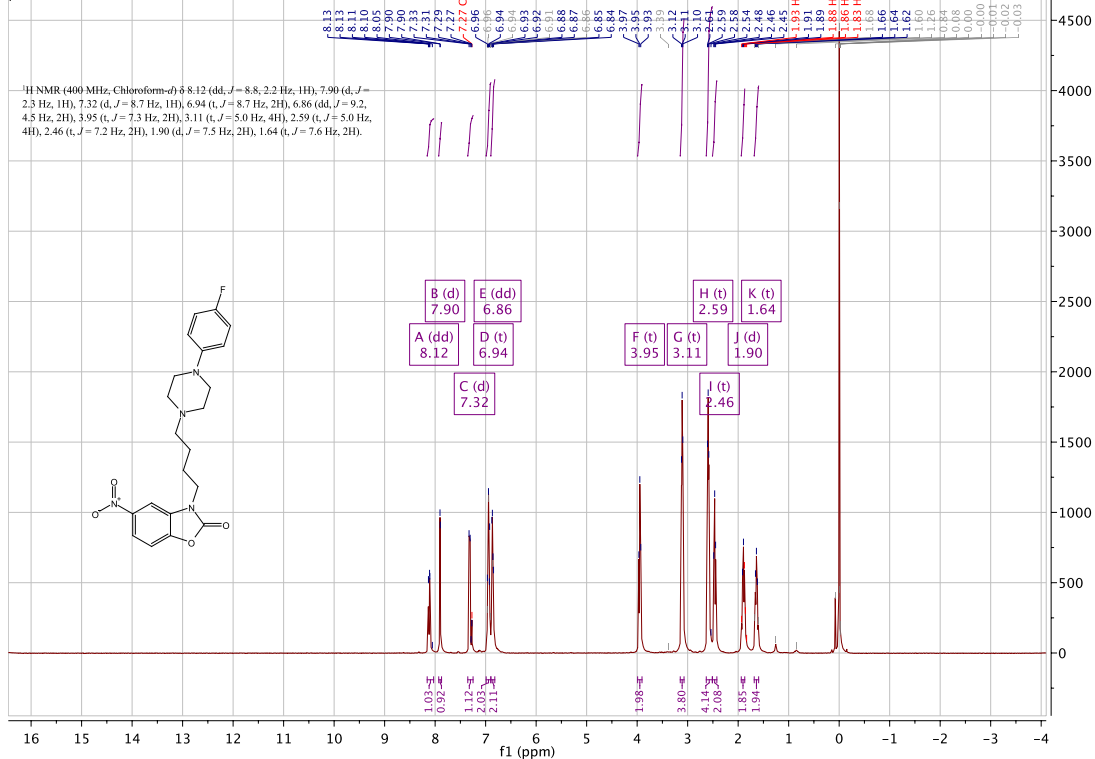




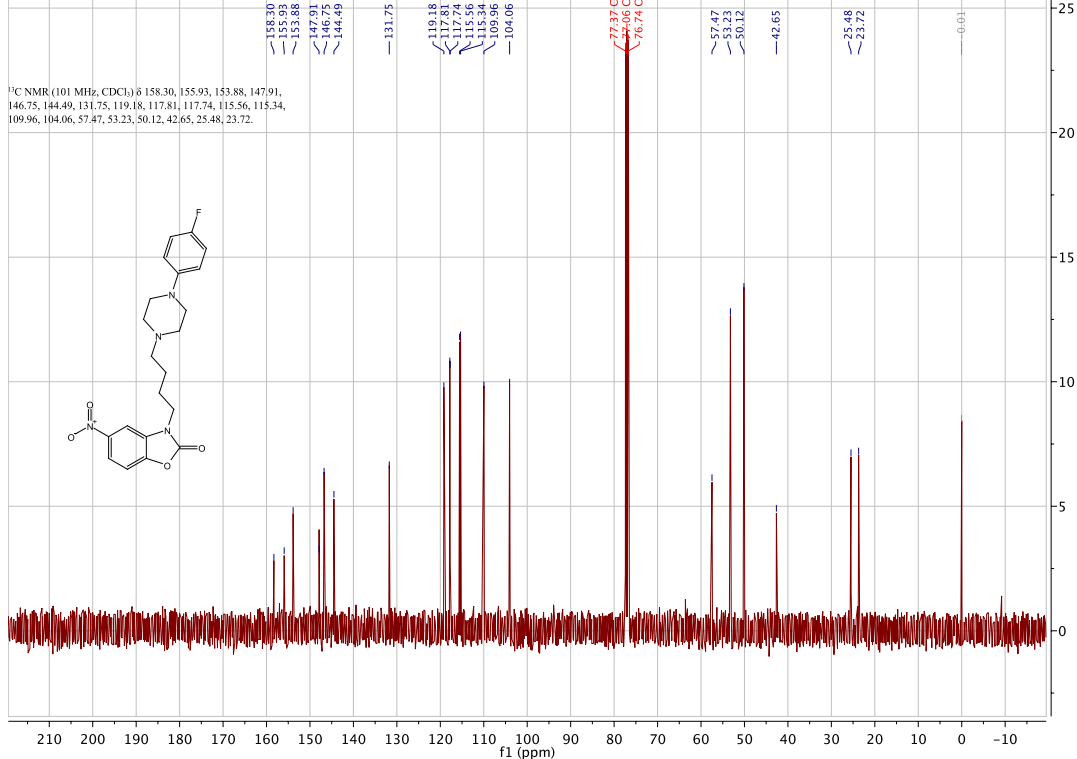
3-(4-(4-(4-fluorophenyl)piperazin-1-yl)butyl)-5-nitrobenzo[d]oxazol-2(3H)-one.
[WA394]

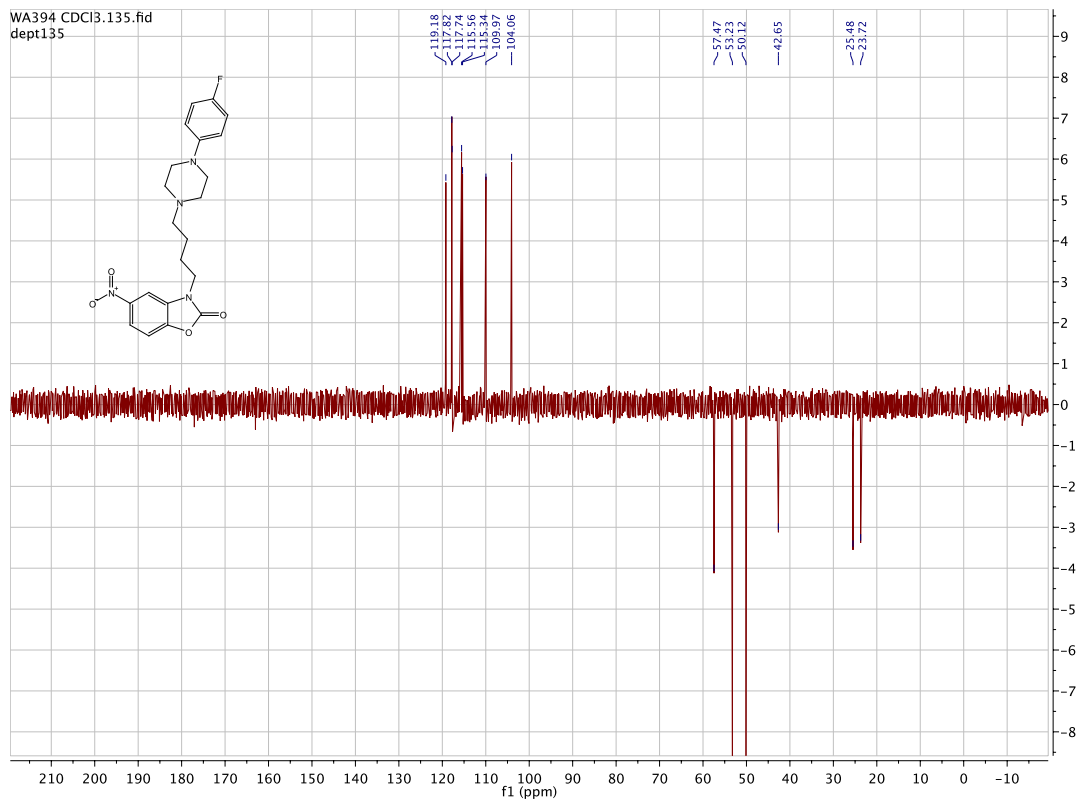


WA394 CDCl₃.1.fid
proton

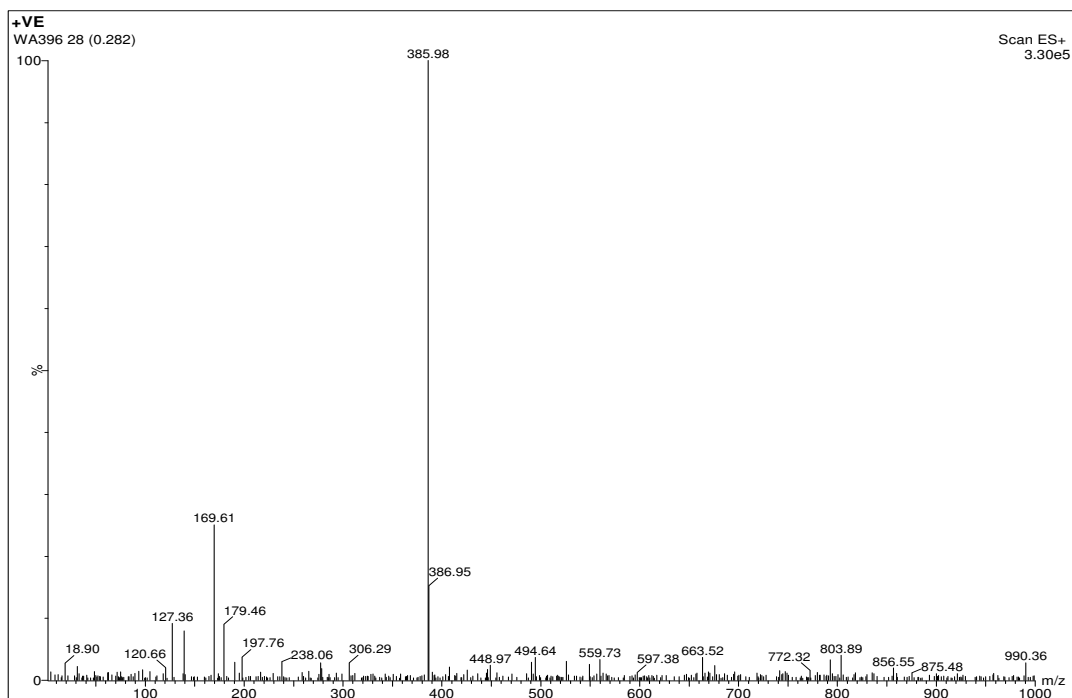


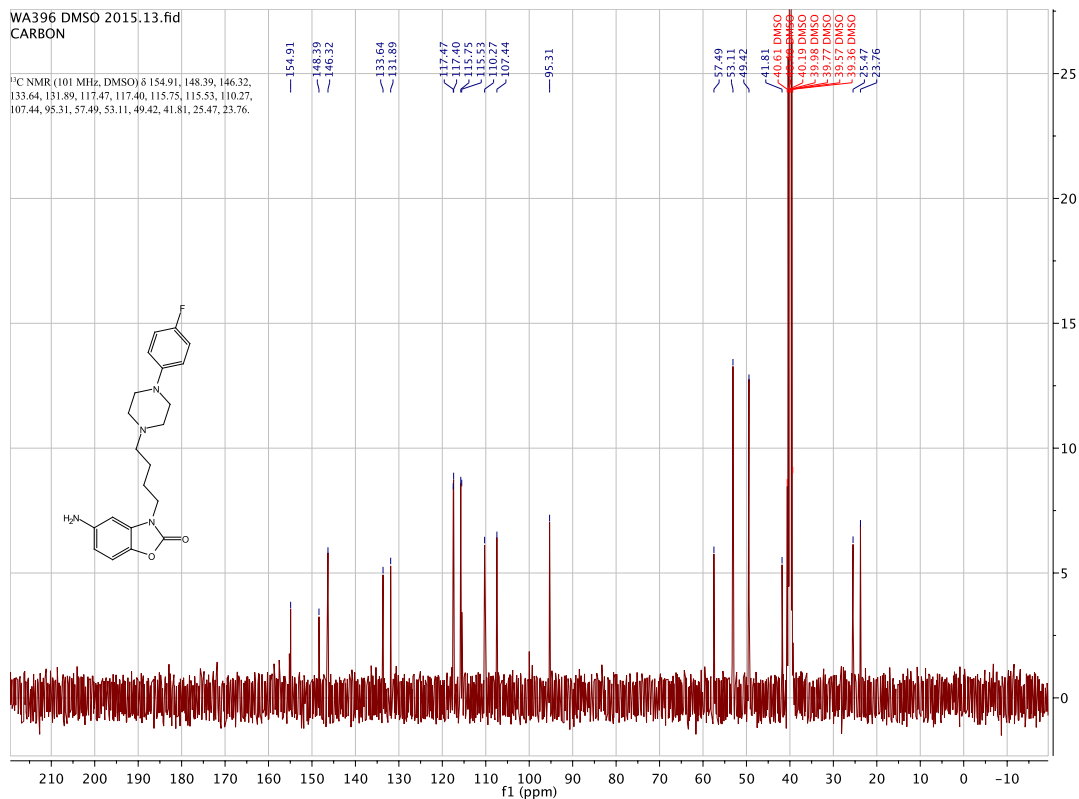
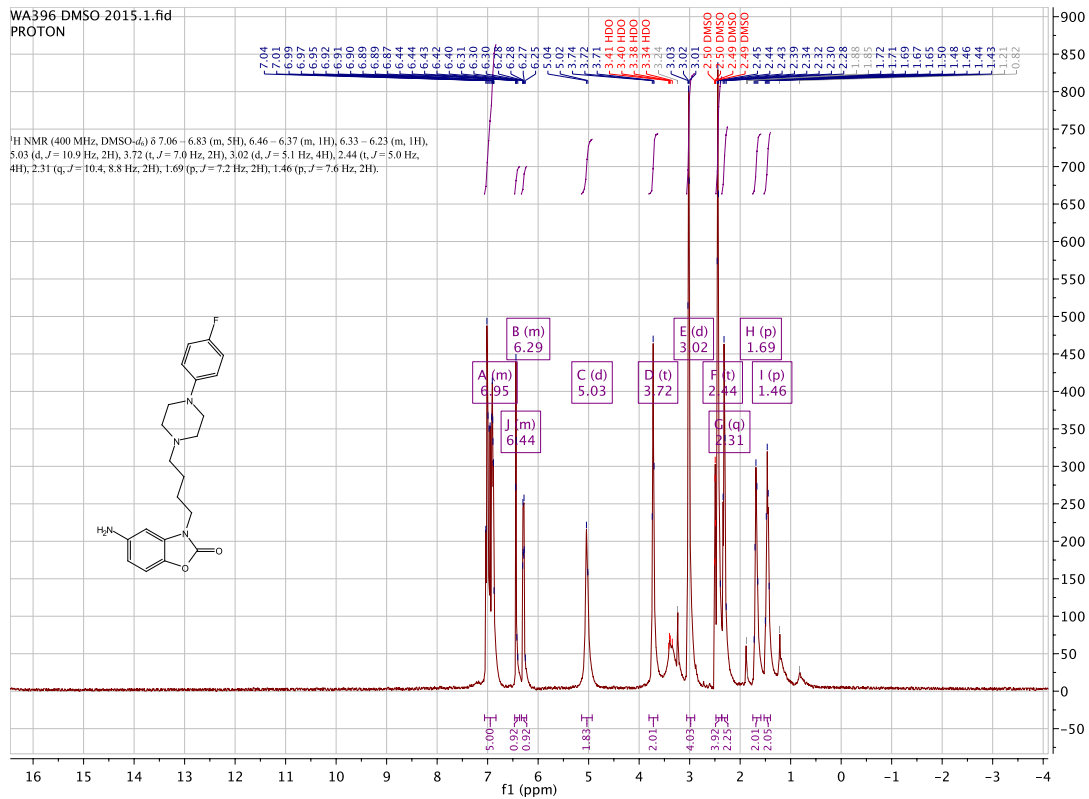
WA394 CDCl₃.13.fid
carbon

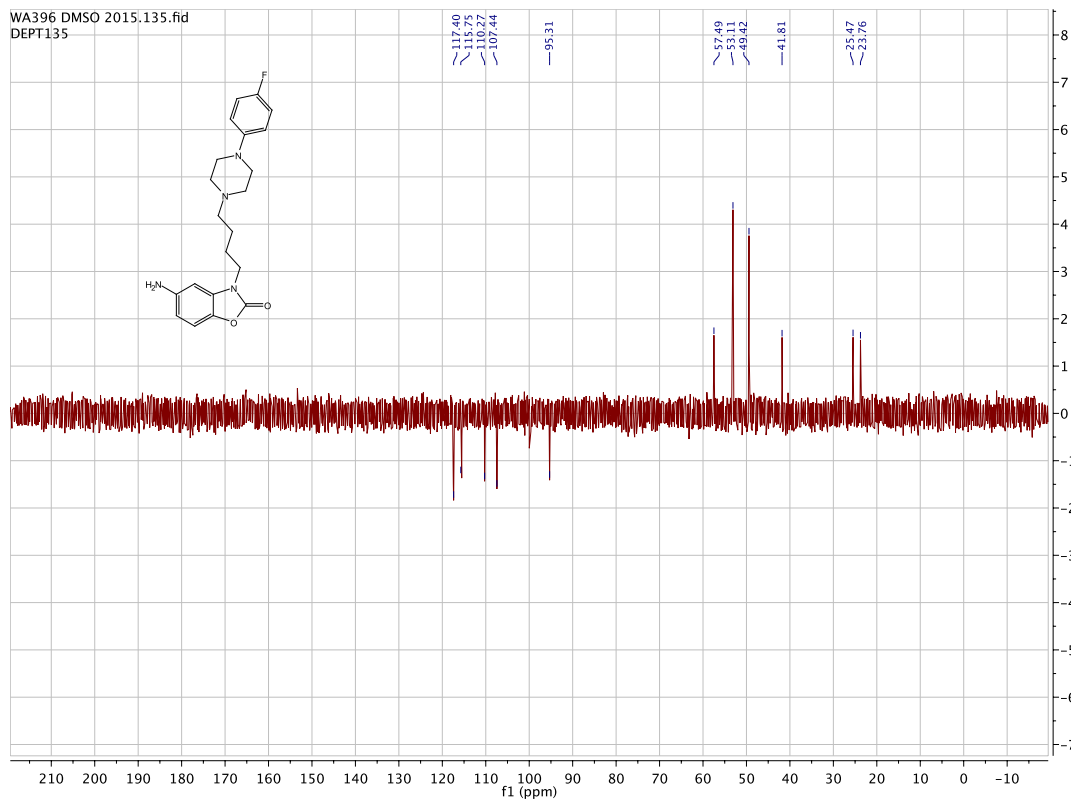




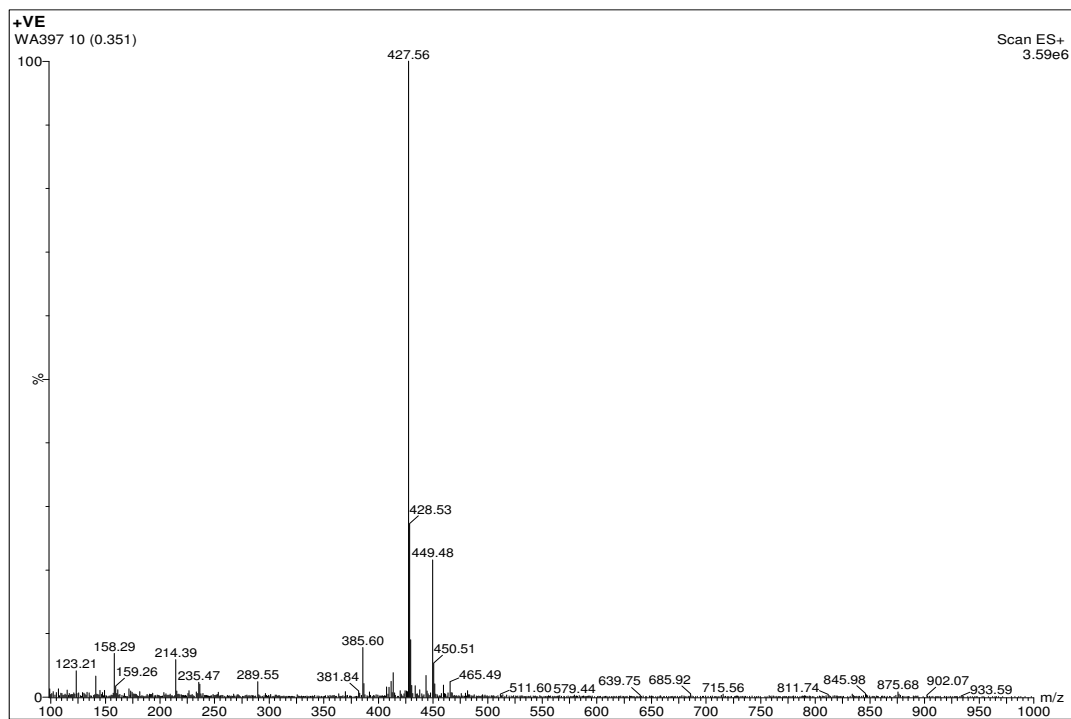
5-amino-3-(4-(4-(4-fluorophenyl)piperazin-1-yl)butyl)benzo[d]oxazol-2(3H)-one.[WA396]

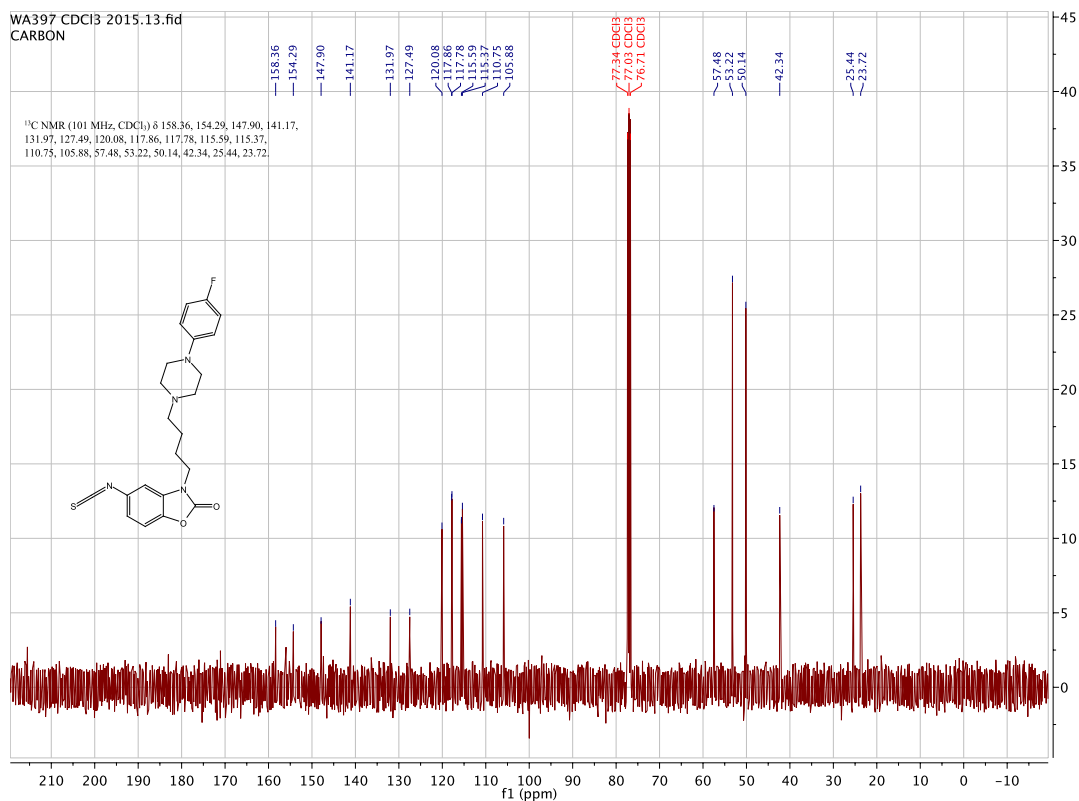
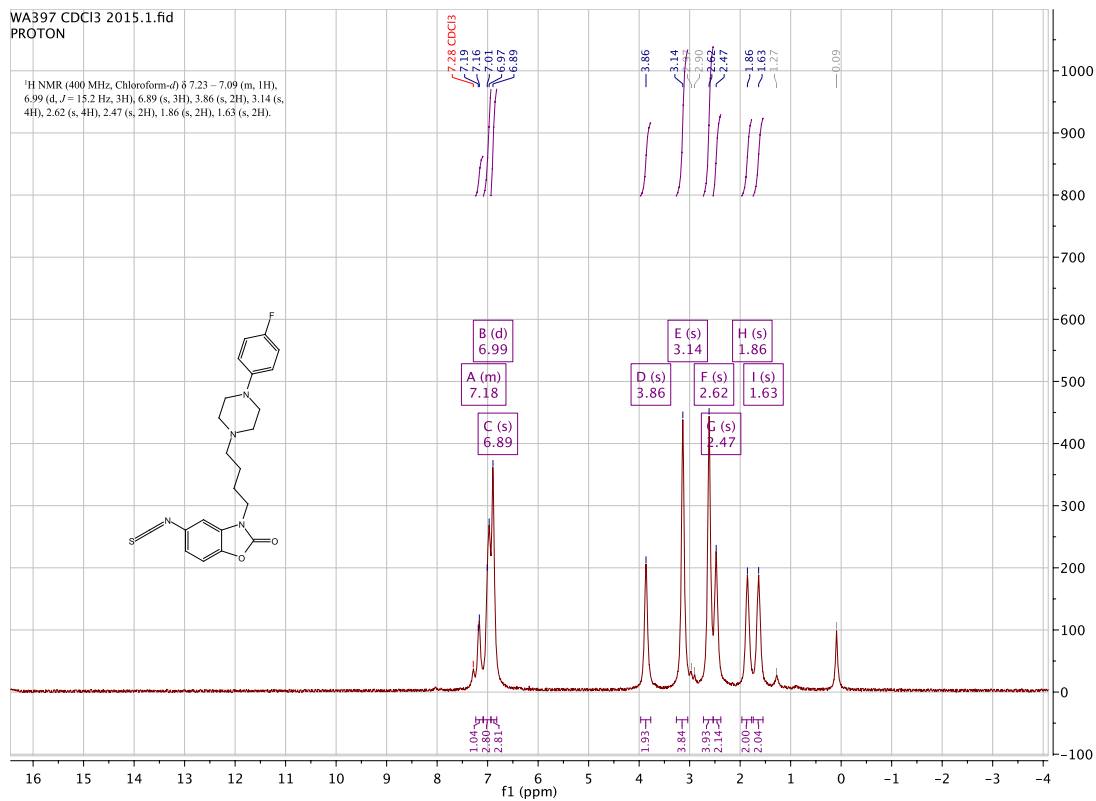


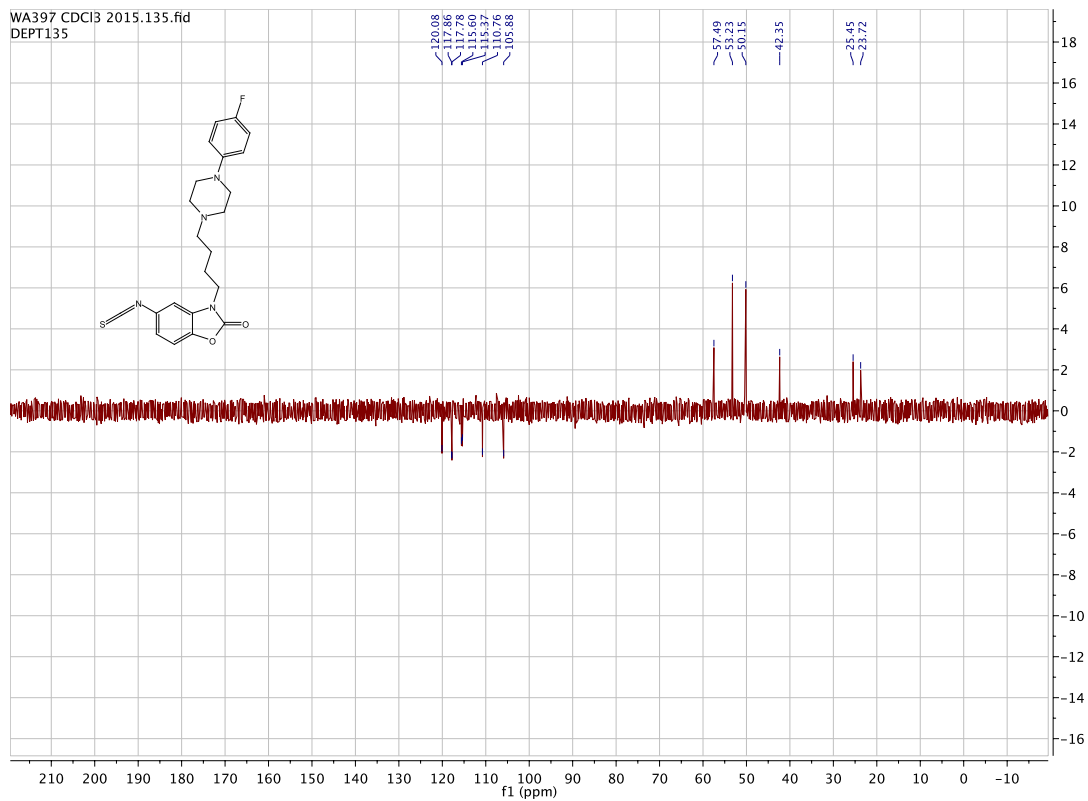




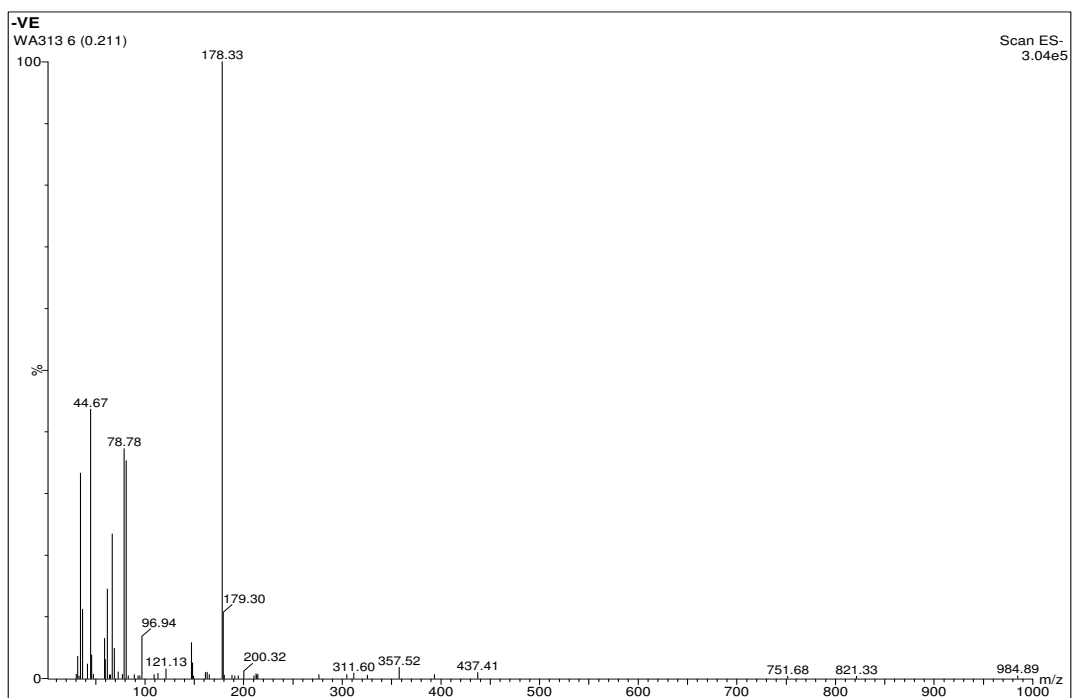
3-(4-(4-(4-fluorophenyl)piperazin-1-yl)butyl)-5-isothiocyanatobenzo[d]oxazol-2(3H)-one. [WA397]





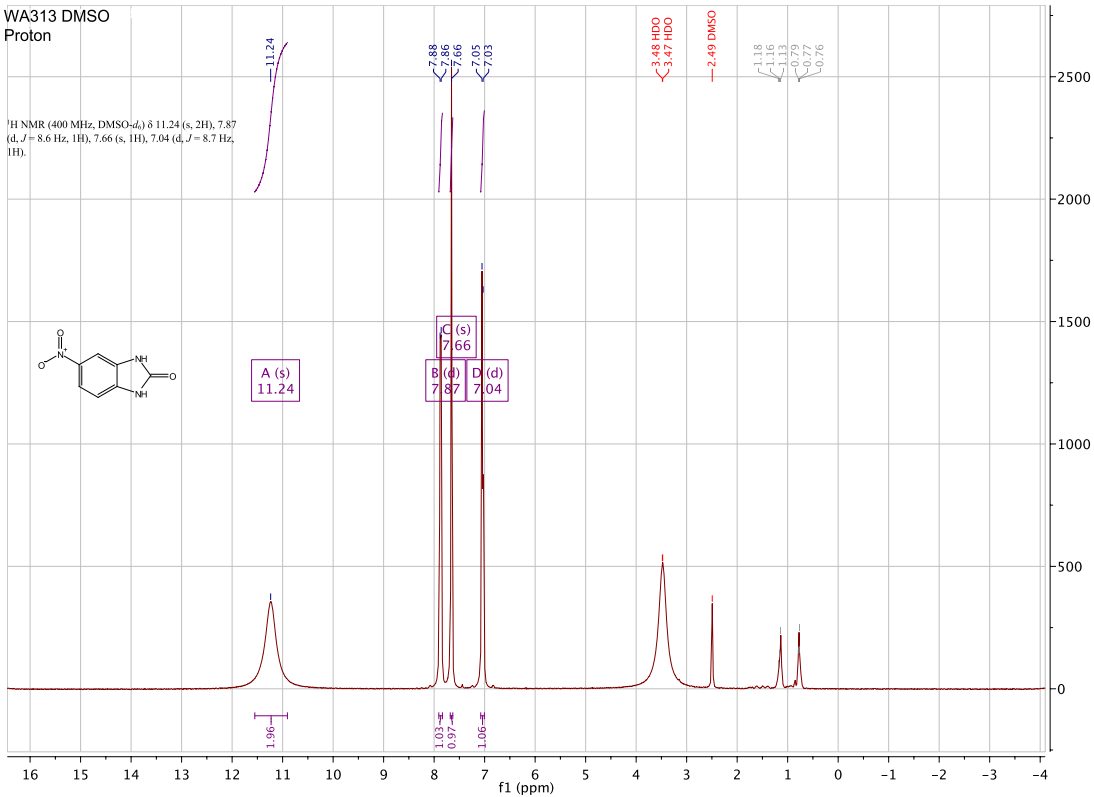


5-nitro-1,3-dihydro-2H-benzo[d]imidazol-2-one. (WA313)



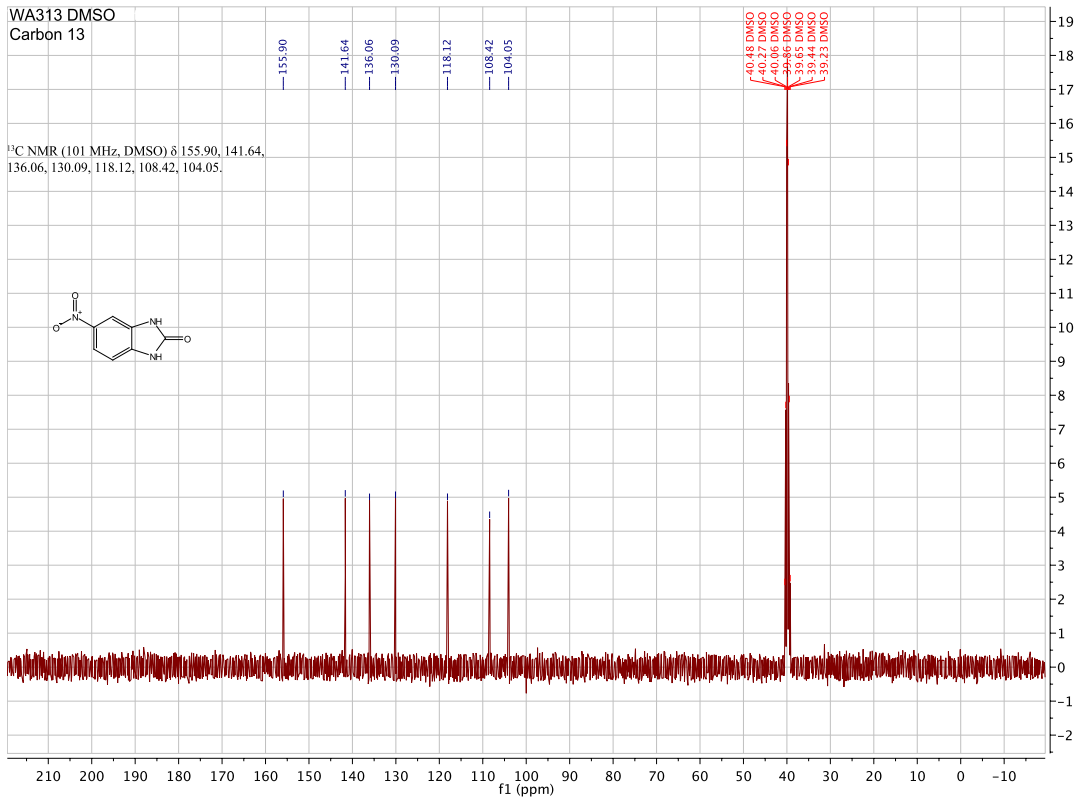
WA313 DMSO
Proton

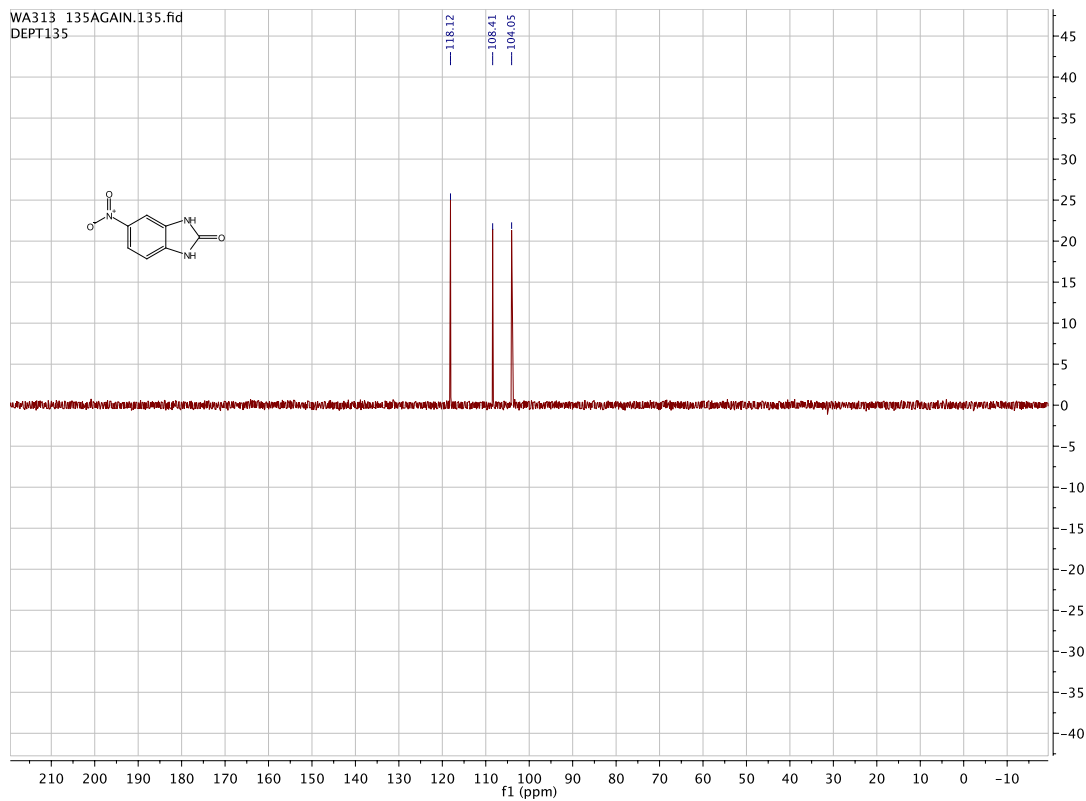
¹H NMR (400 MHz, DMSO-d₆) δ 11.24 (s, 2H), 7.87 (d, J = 8.6 Hz, 1H), 7.66 (s, 1H), 7.04 (d, J = 8.7 Hz, 1H).



WA313 DMSO
Carbon 13

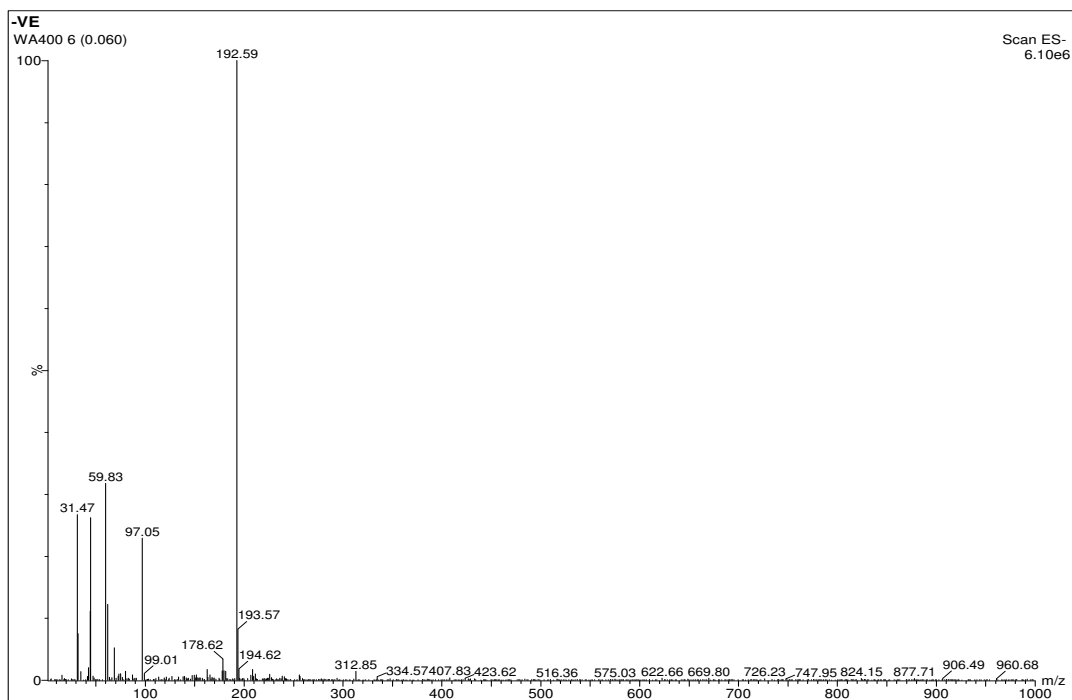
¹³C NMR (101 MHz, DMSO) δ 155.90, 141.64, 136.06, 130.09, 118.12, 108.42, 104.05.

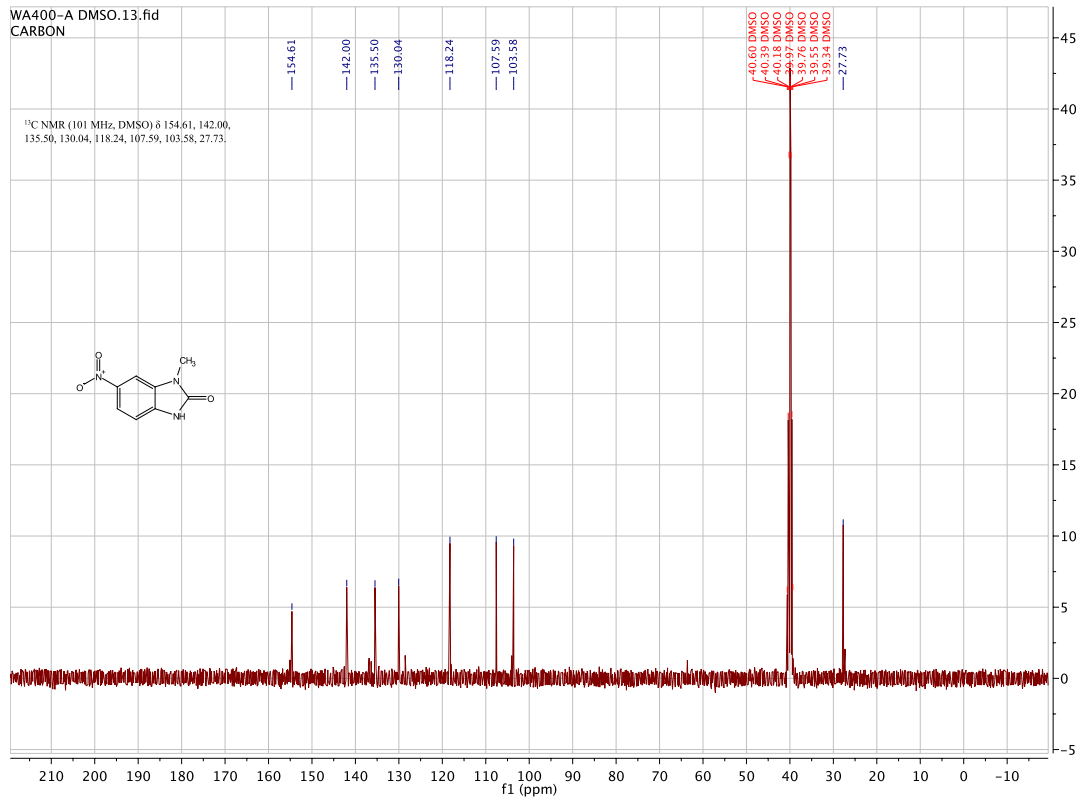
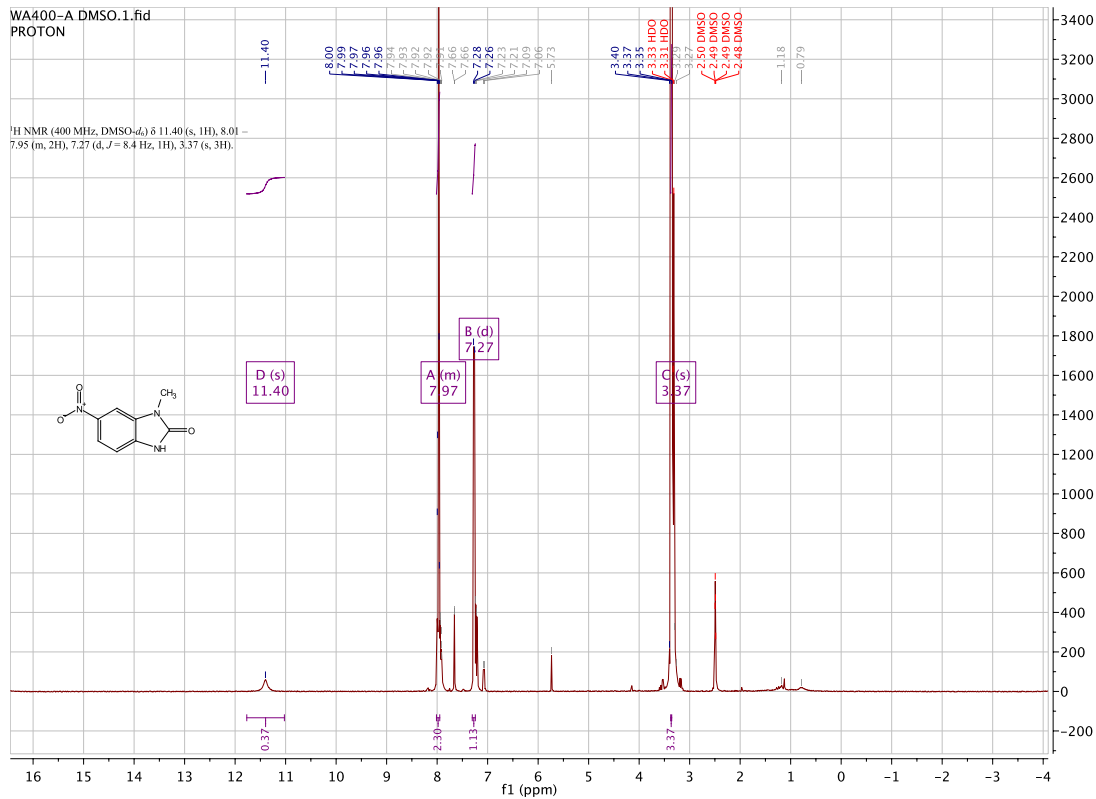


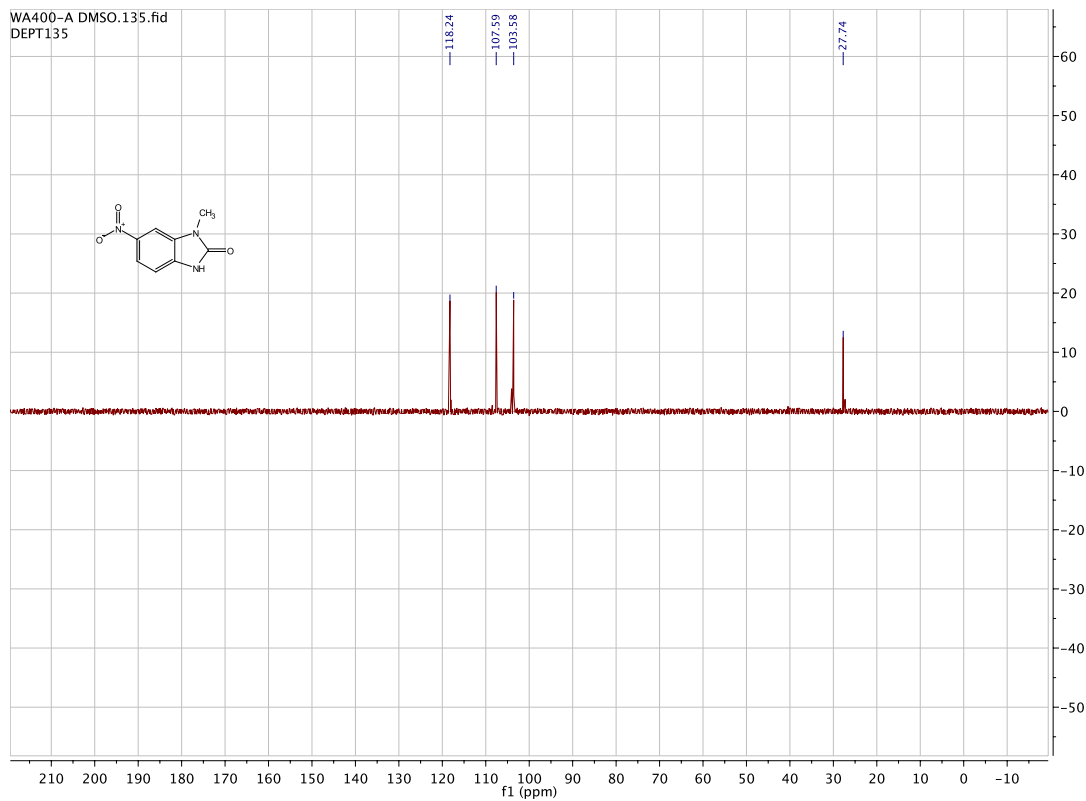


1-methyl-6-nitro-1,3-dihydro-2H-benzo[d]imidazol-2-one. (WA400)

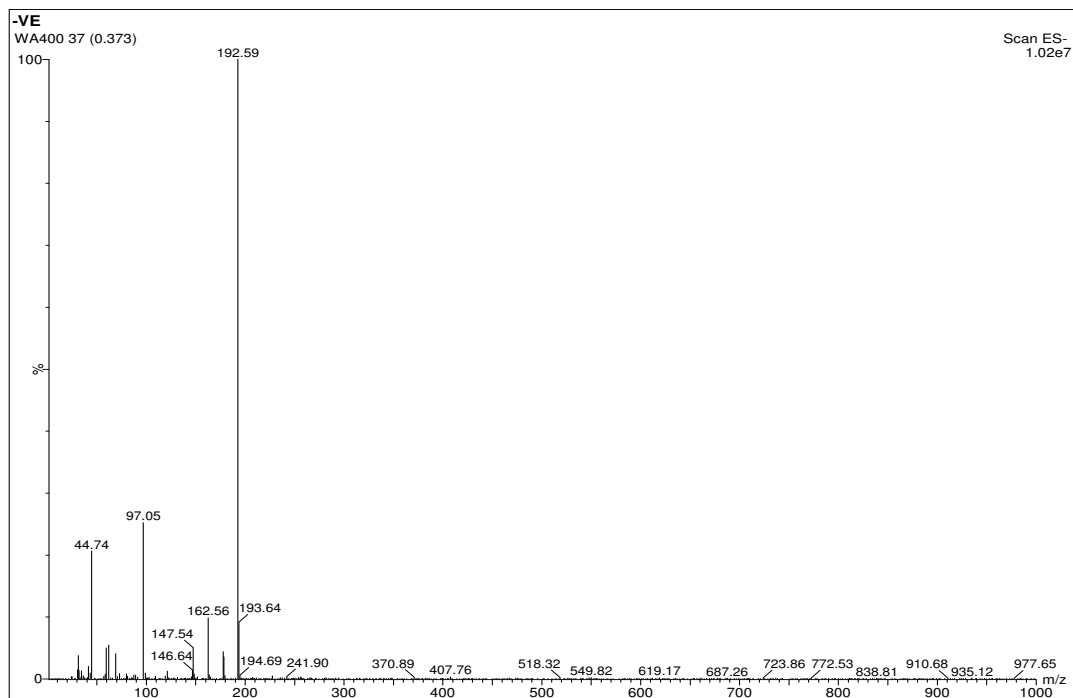
WA400A:

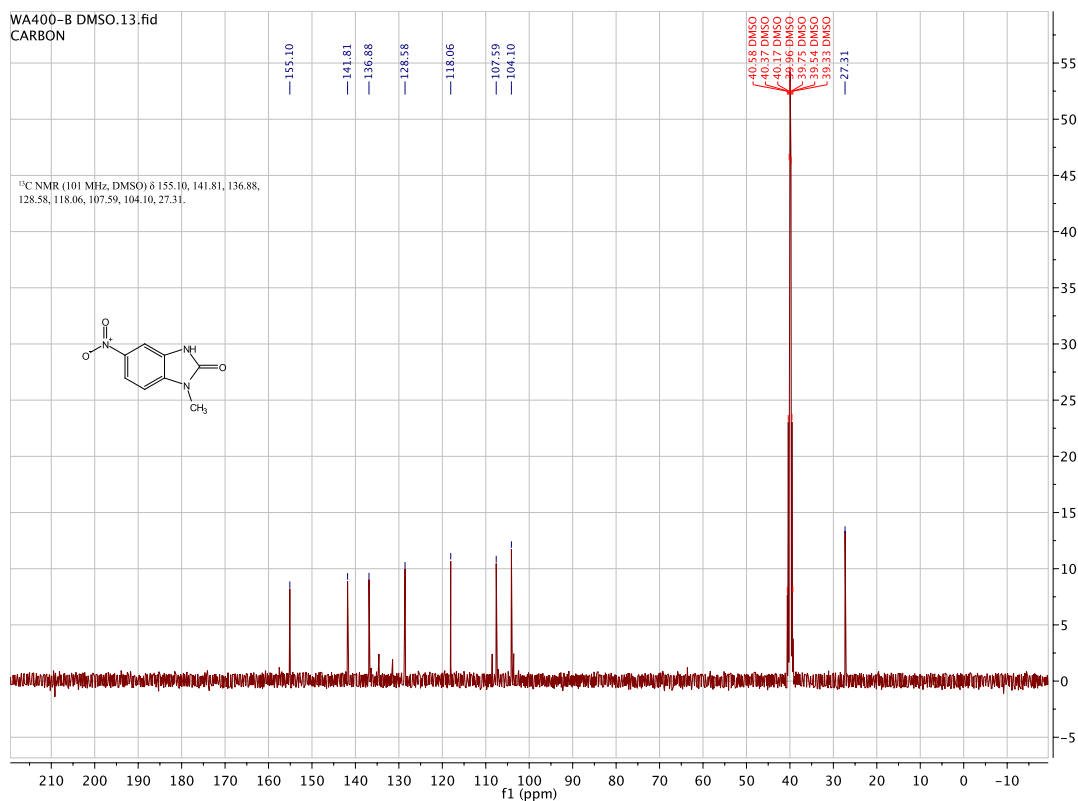
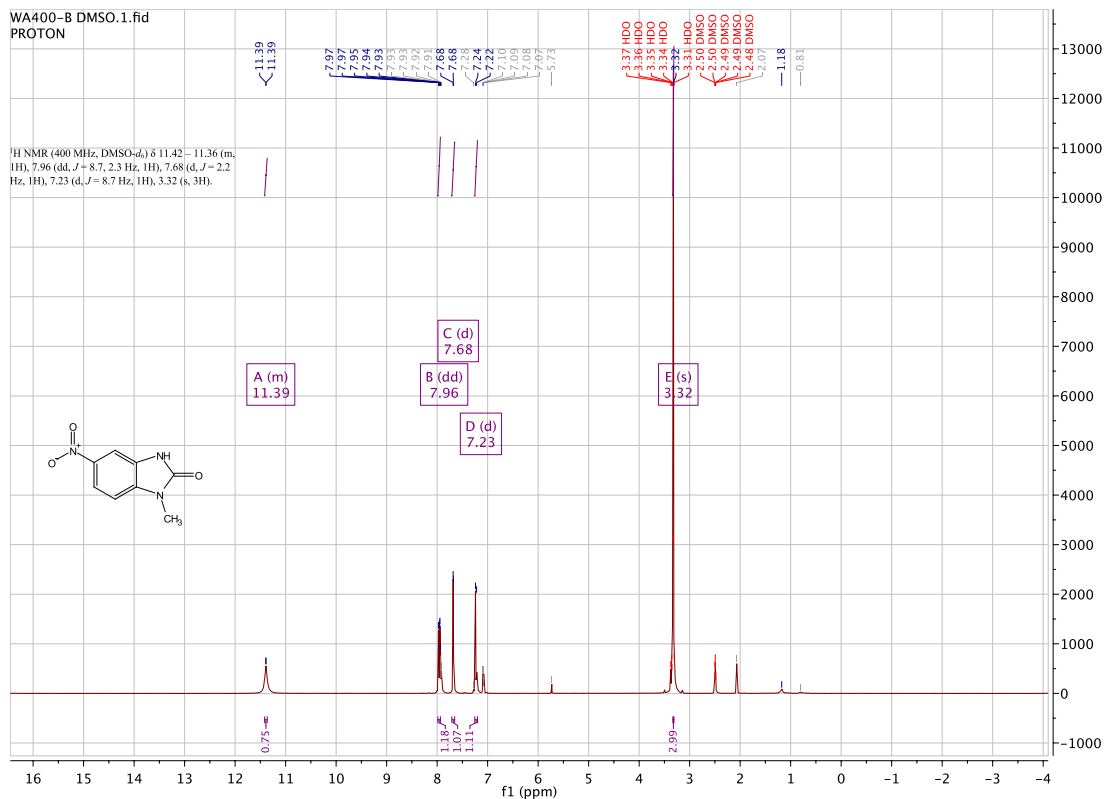


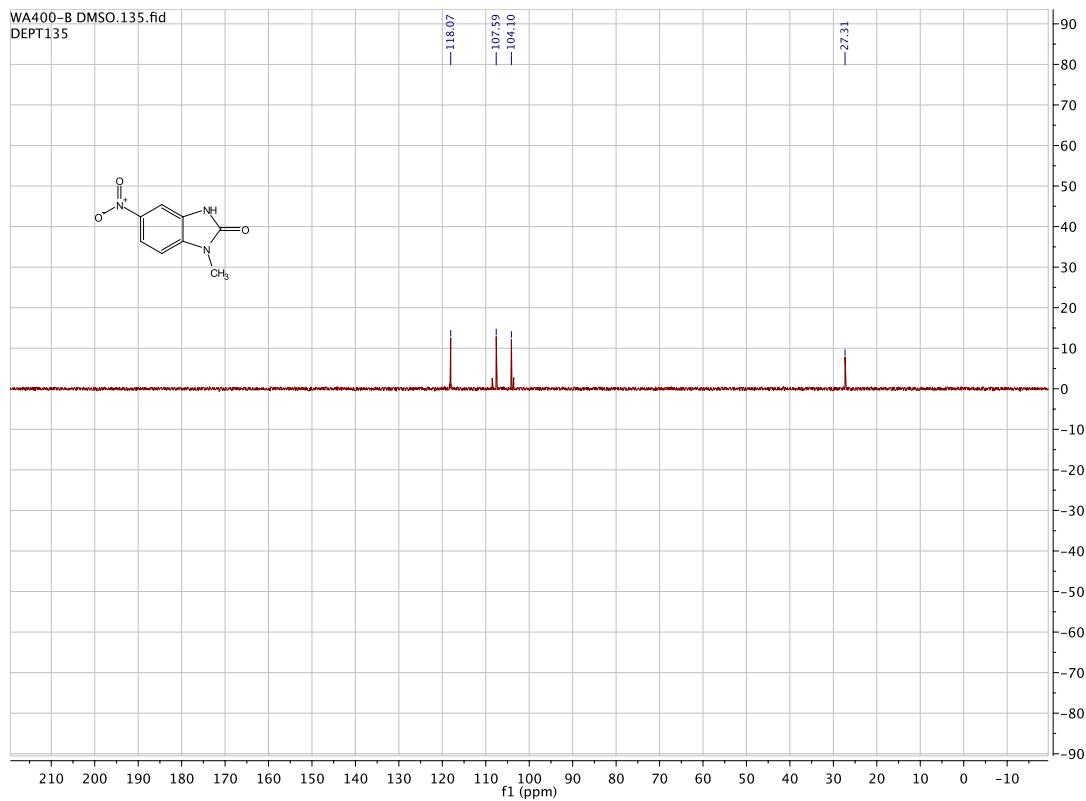




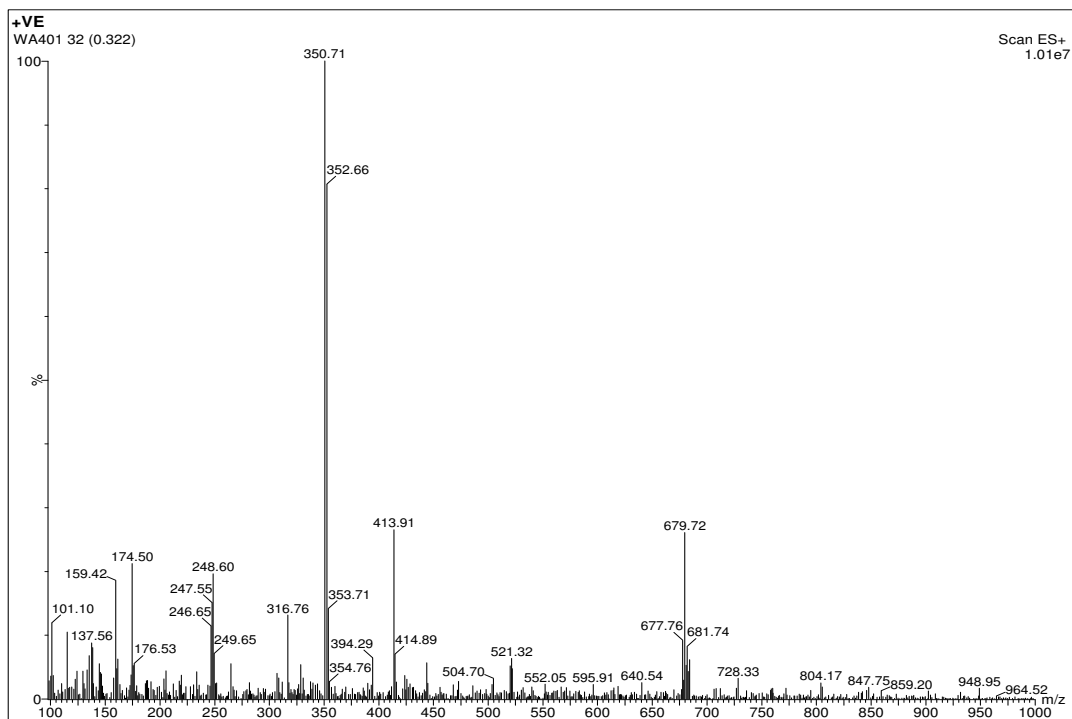
WA404B:

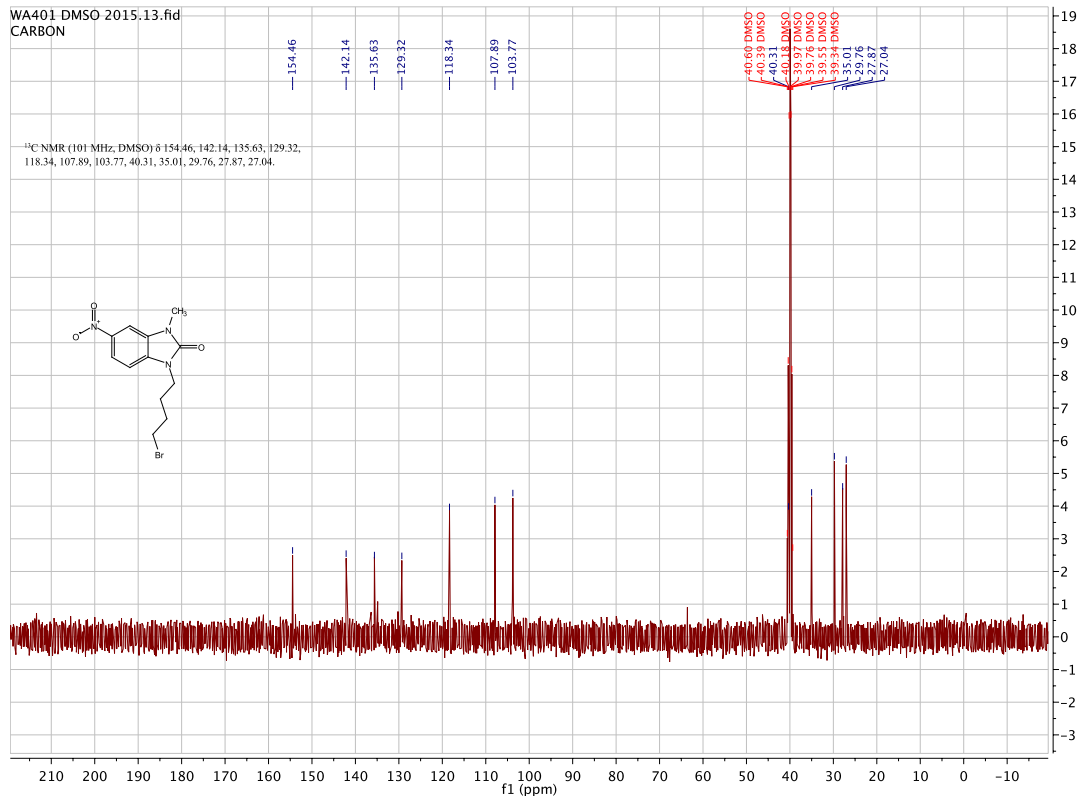
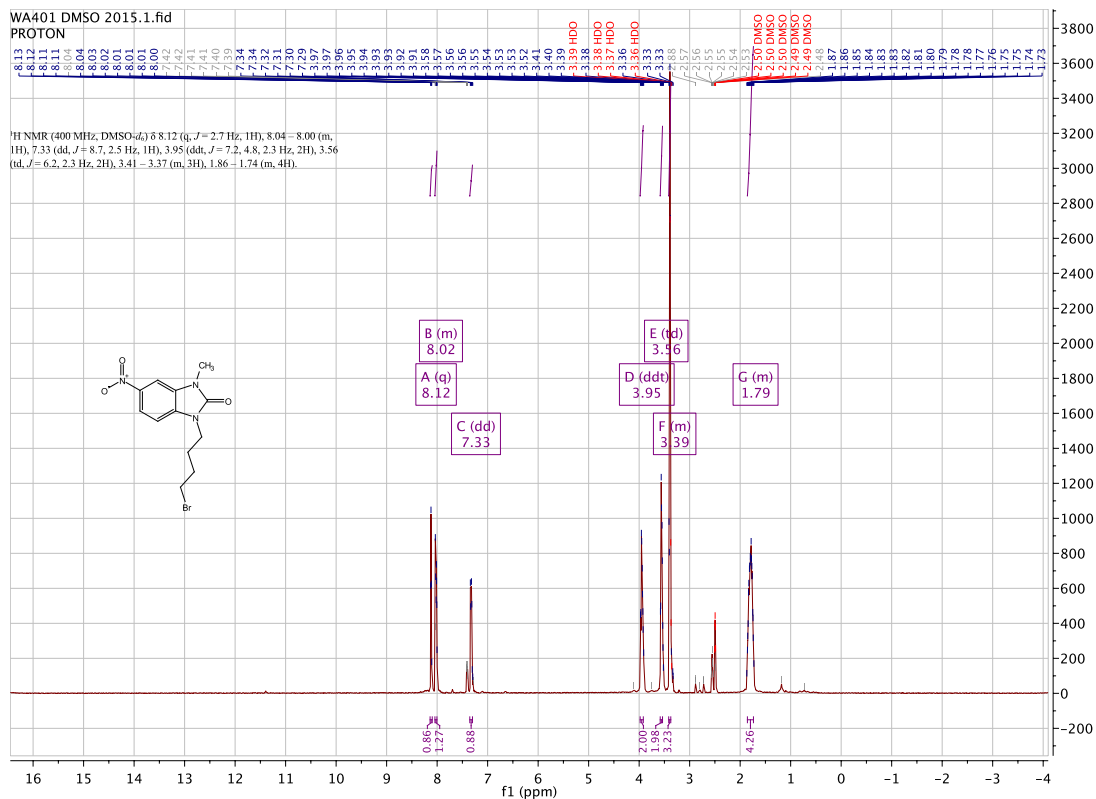


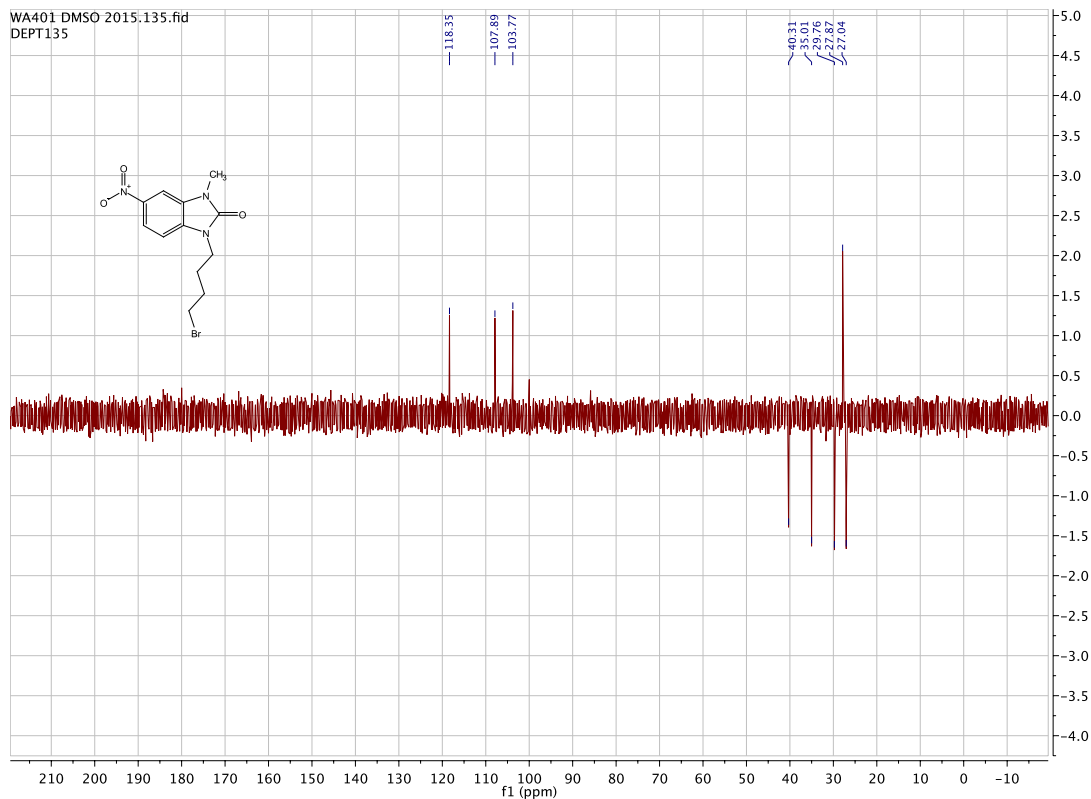




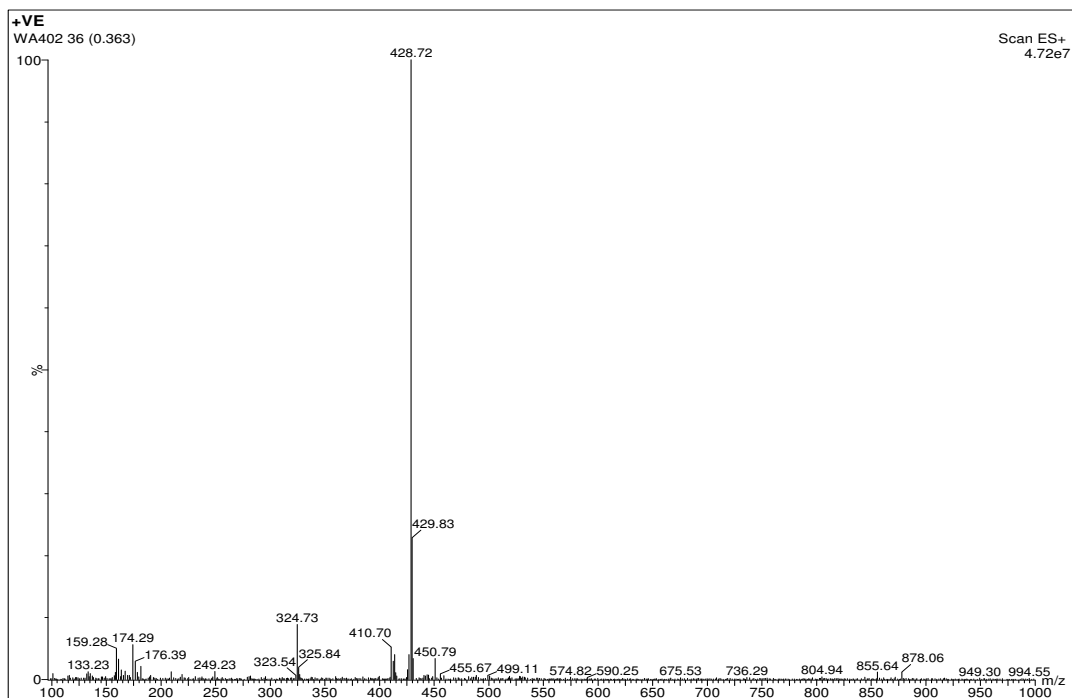
**1-(4-bromobutyl)-3-methyl-5-nitro-1,3-dihydro-2H-benzo[d]imidazol-2-one.
(WA401/WA406)**

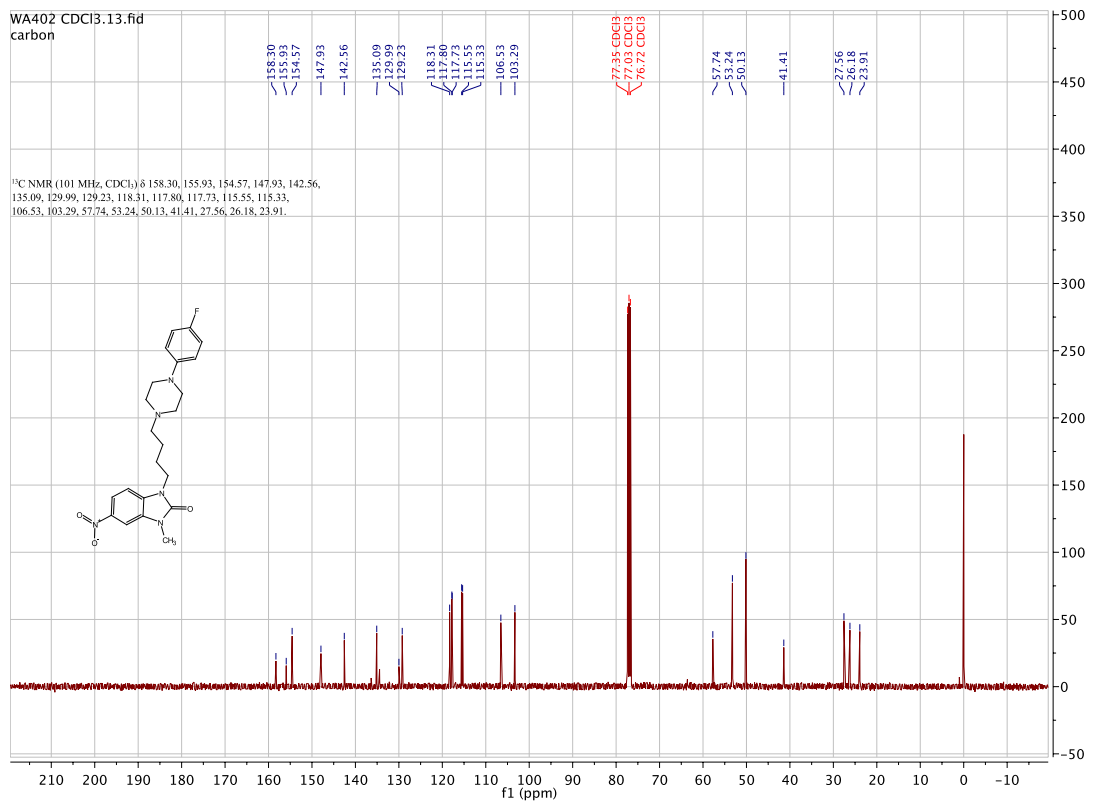
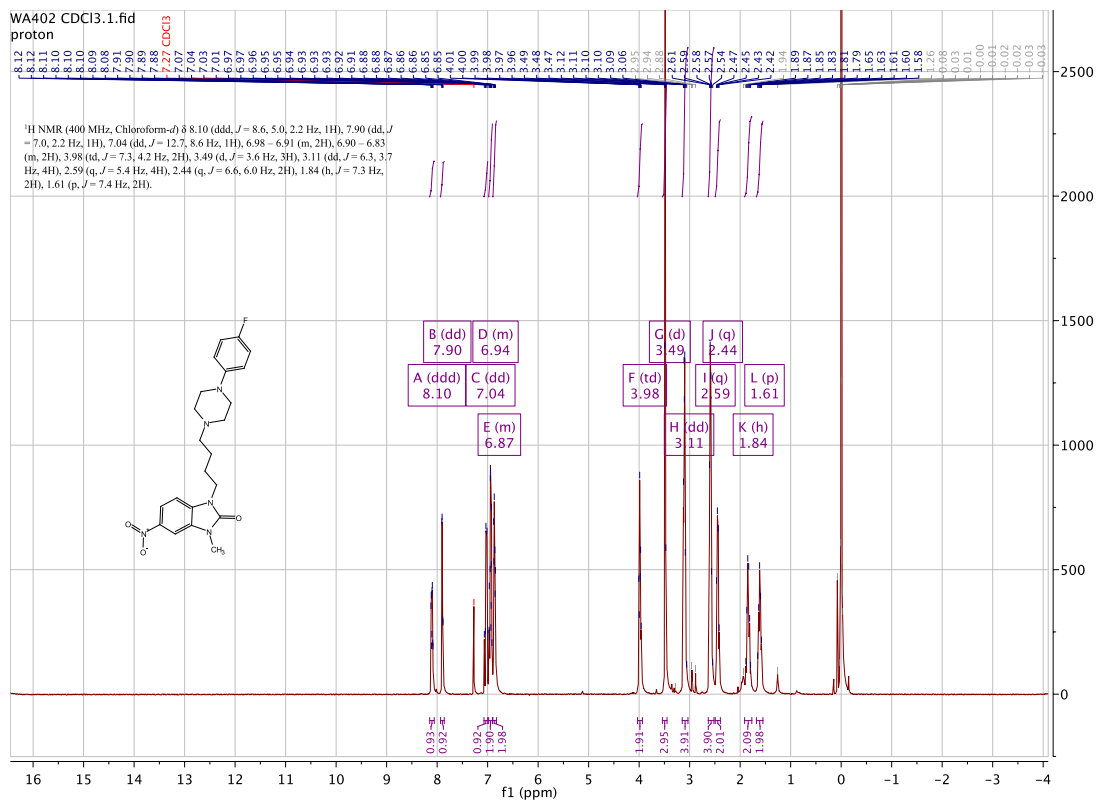


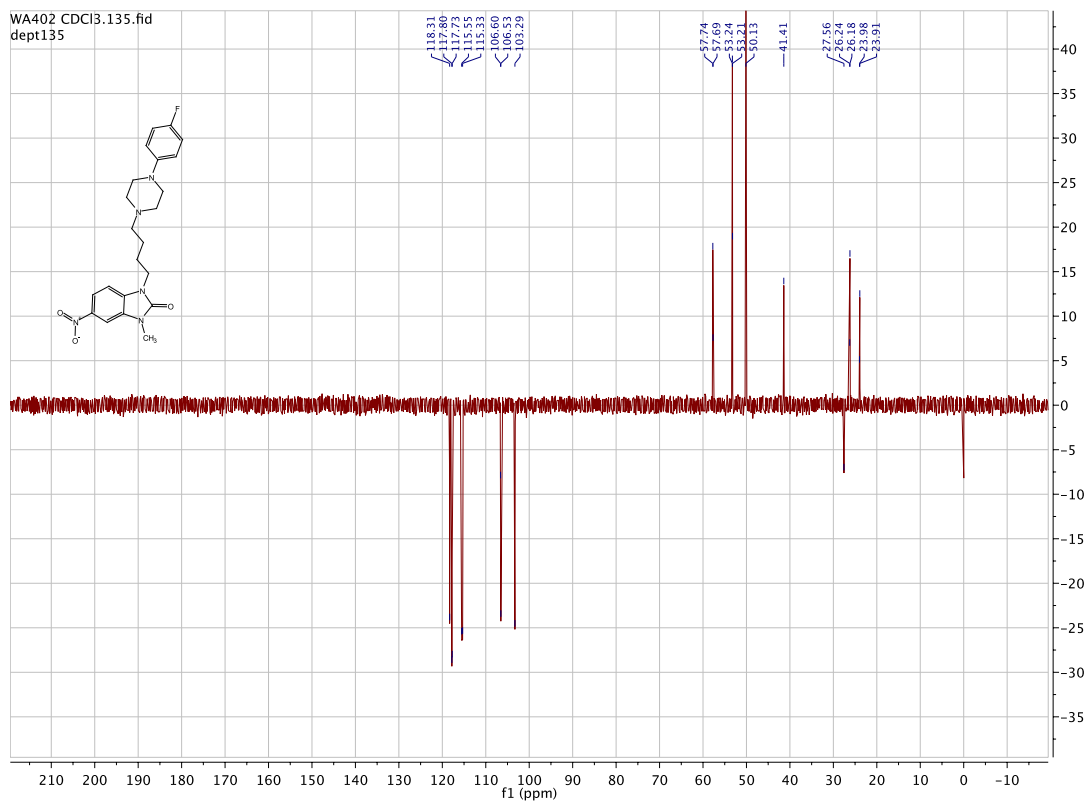




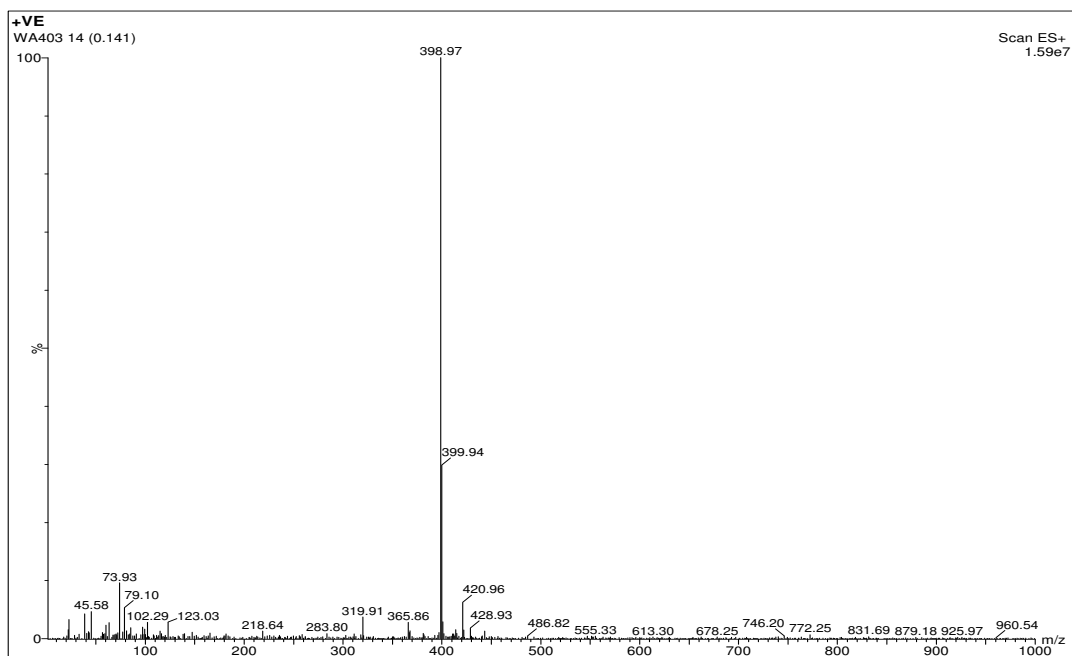
1-(4-(4-(4-fluorophenyl)piperazin-1-yl)butyl)-3-methyl-5-nitro-1,3-dihydro-2H-benzo[d]imidazol-2-one. [WA402]

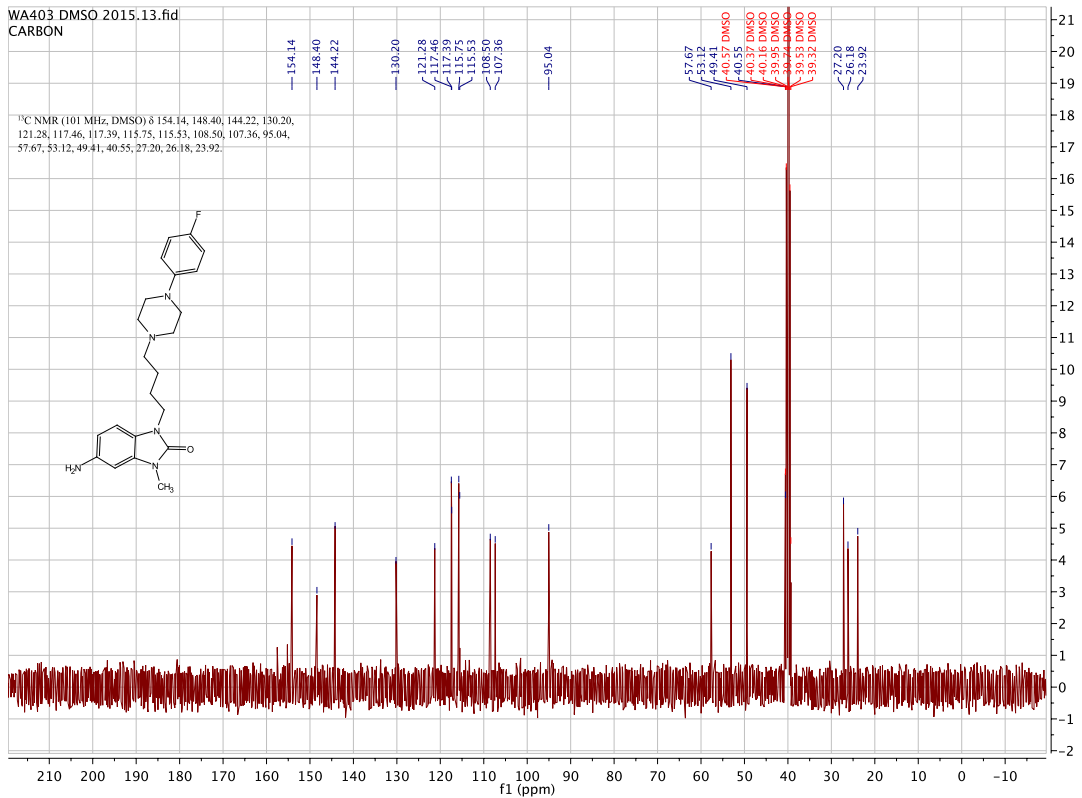
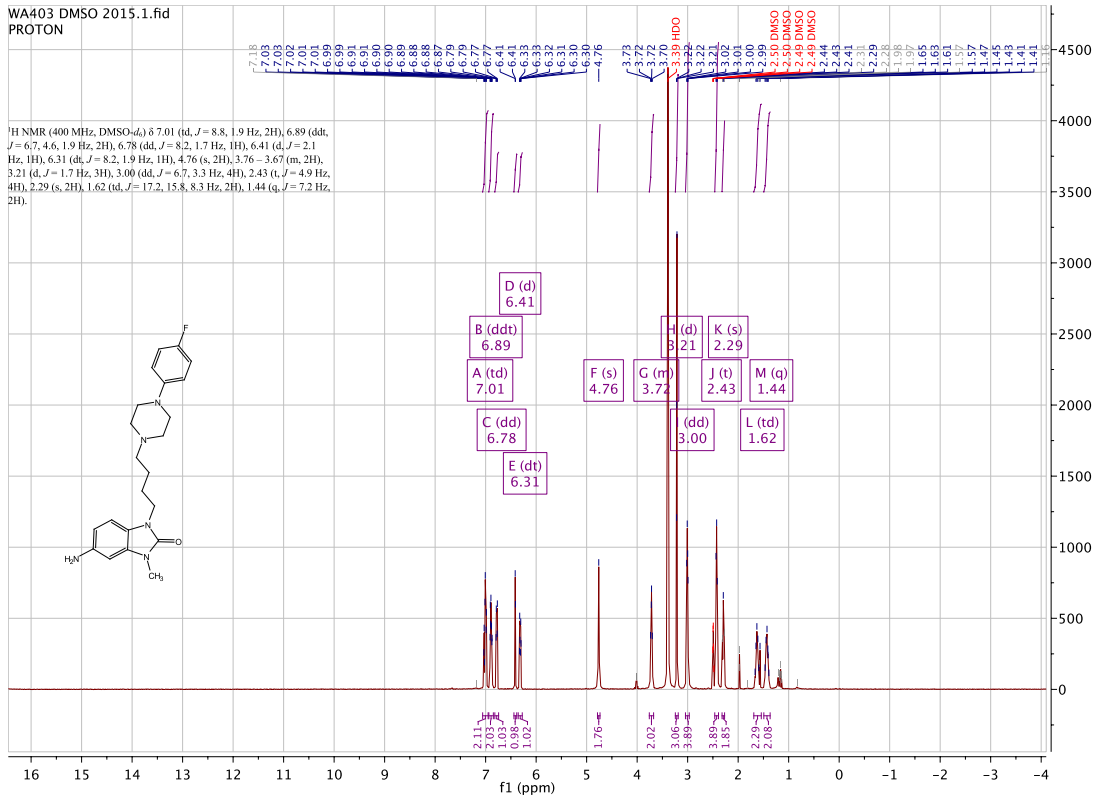


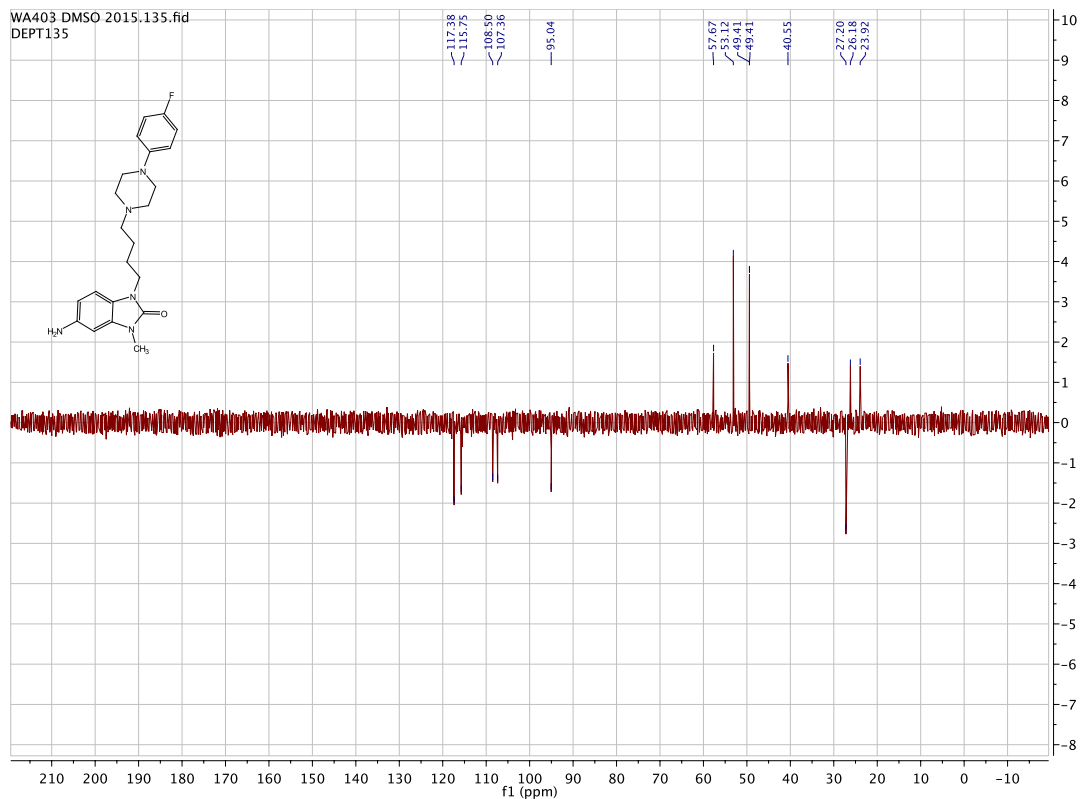




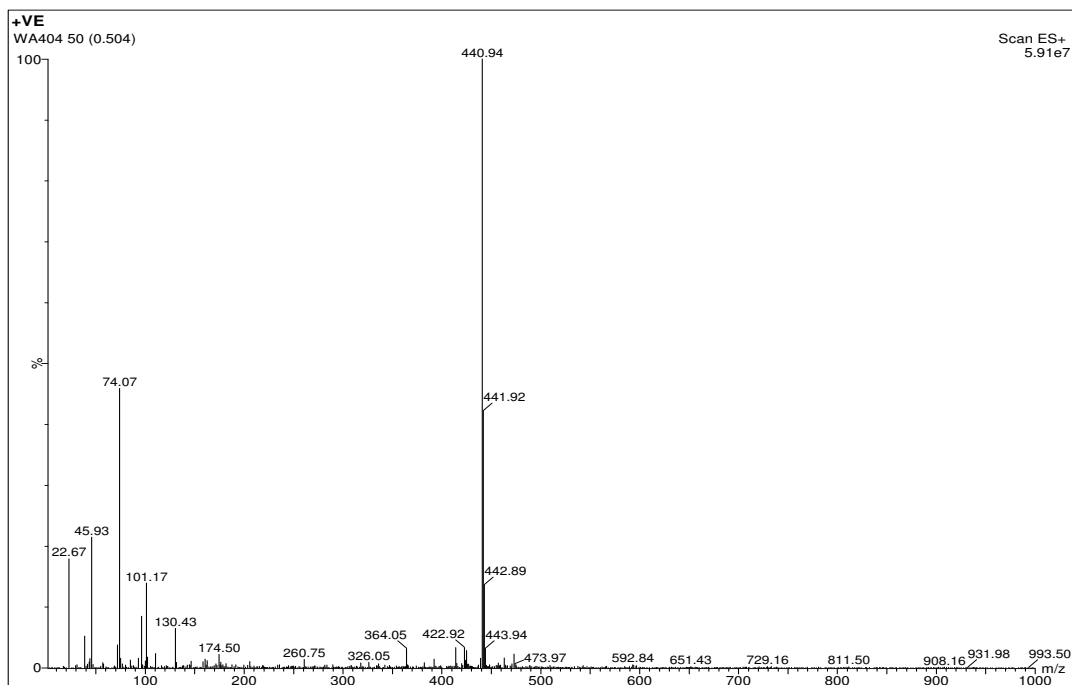
5-amino-1-(4-(4-(4-fluorophenyl)piperazin-1-yl)butyl)-3-methyl-1,3-dihydro-2H-benzo[d]imidazol-2-one. [WA403]

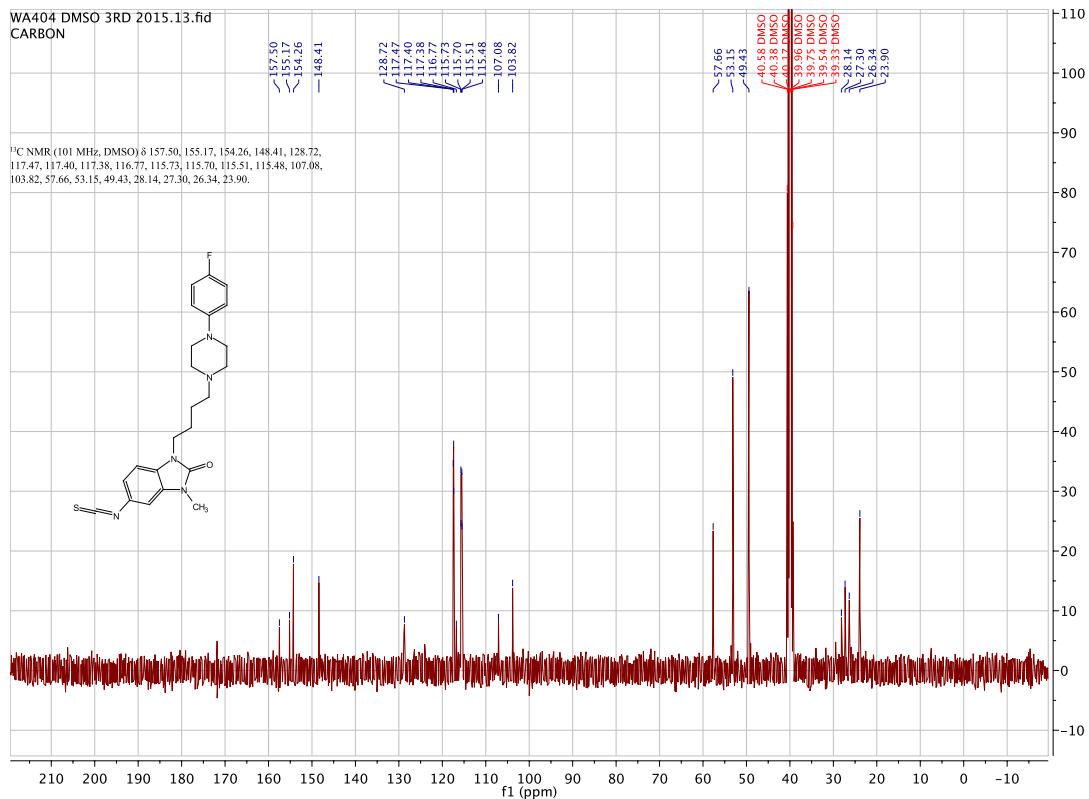
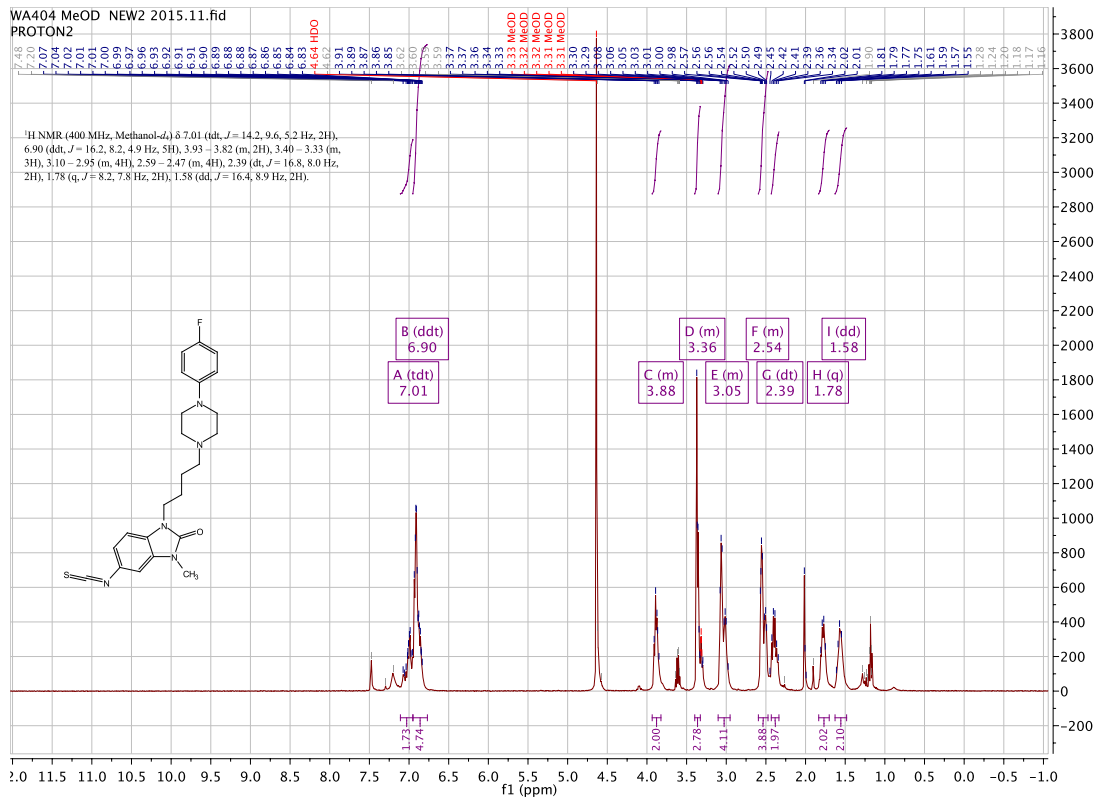


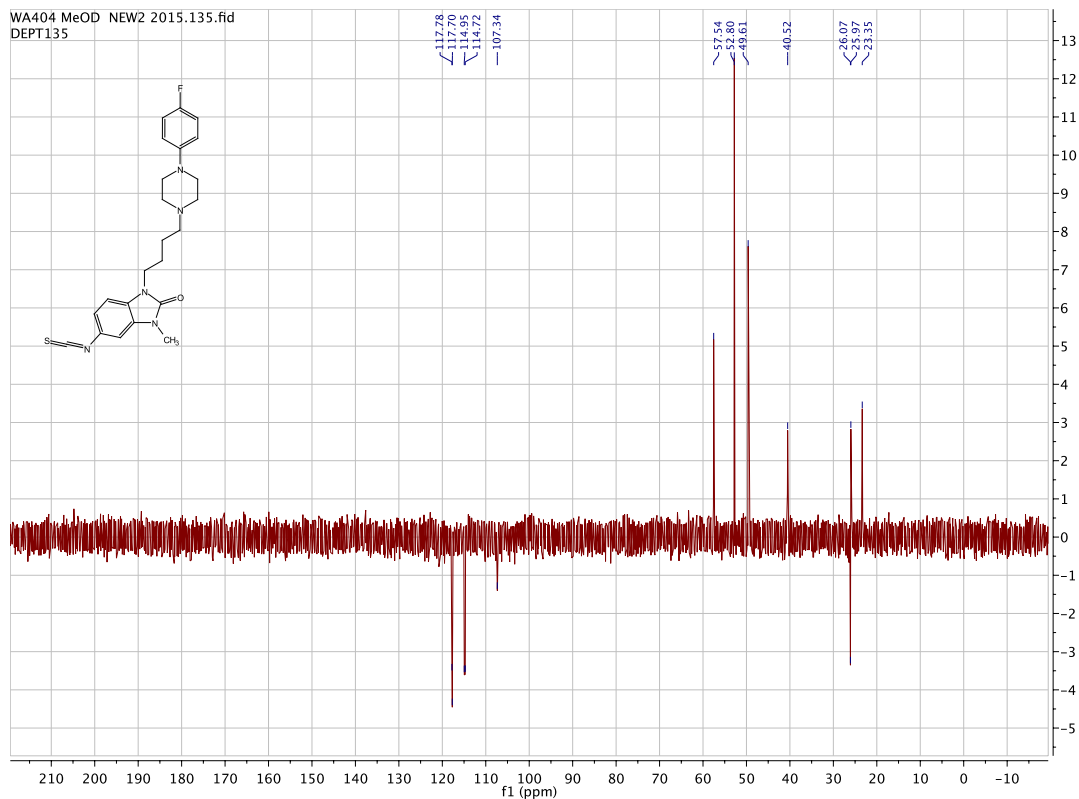




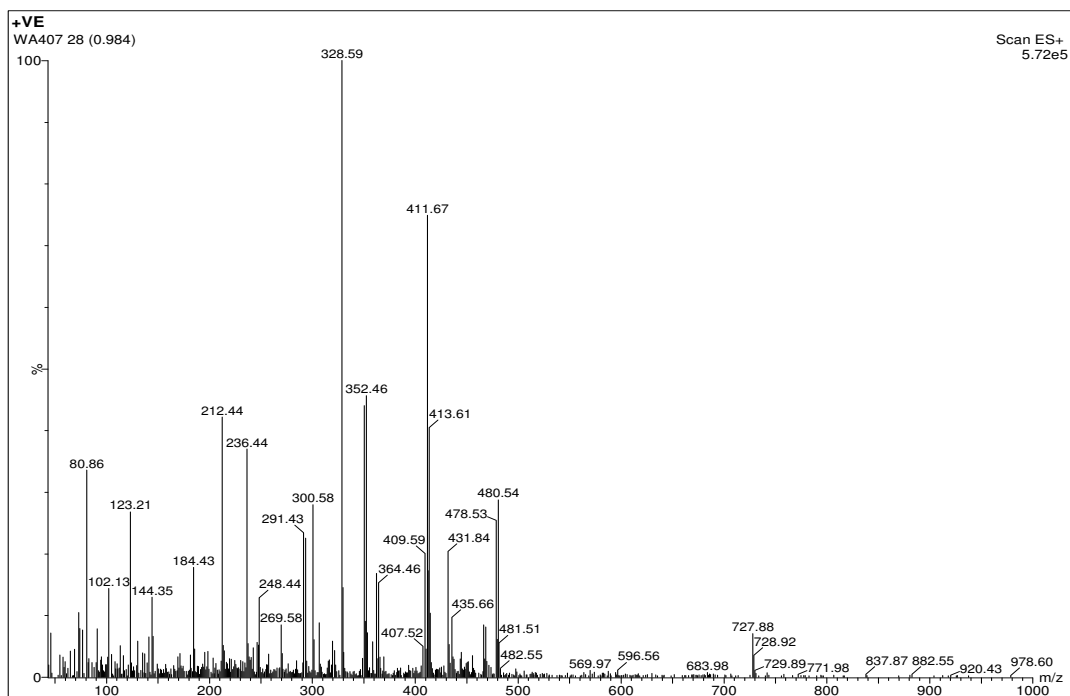
1-(4-(4-(4-fluorophenyl)piperazin-1-yl)butyl)-5-isothiocyanato-3-methyl-1,3-dihydro-2H-benzo[d]imidazol-2-one. [WA404]

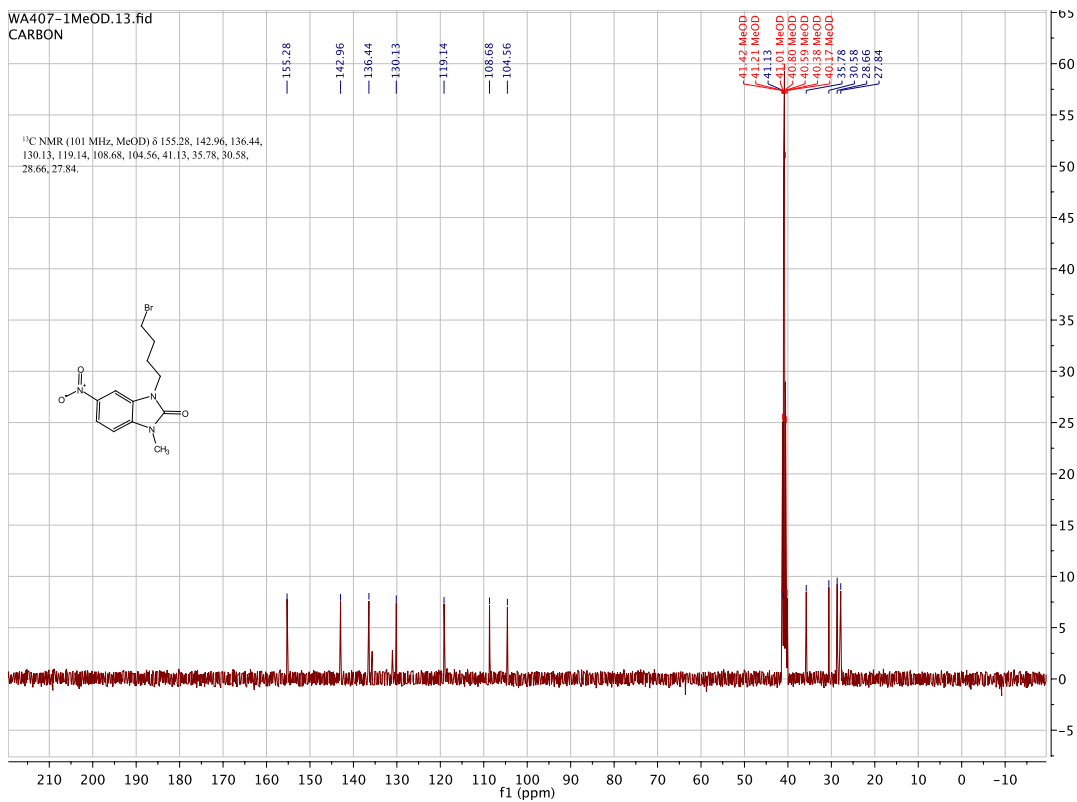
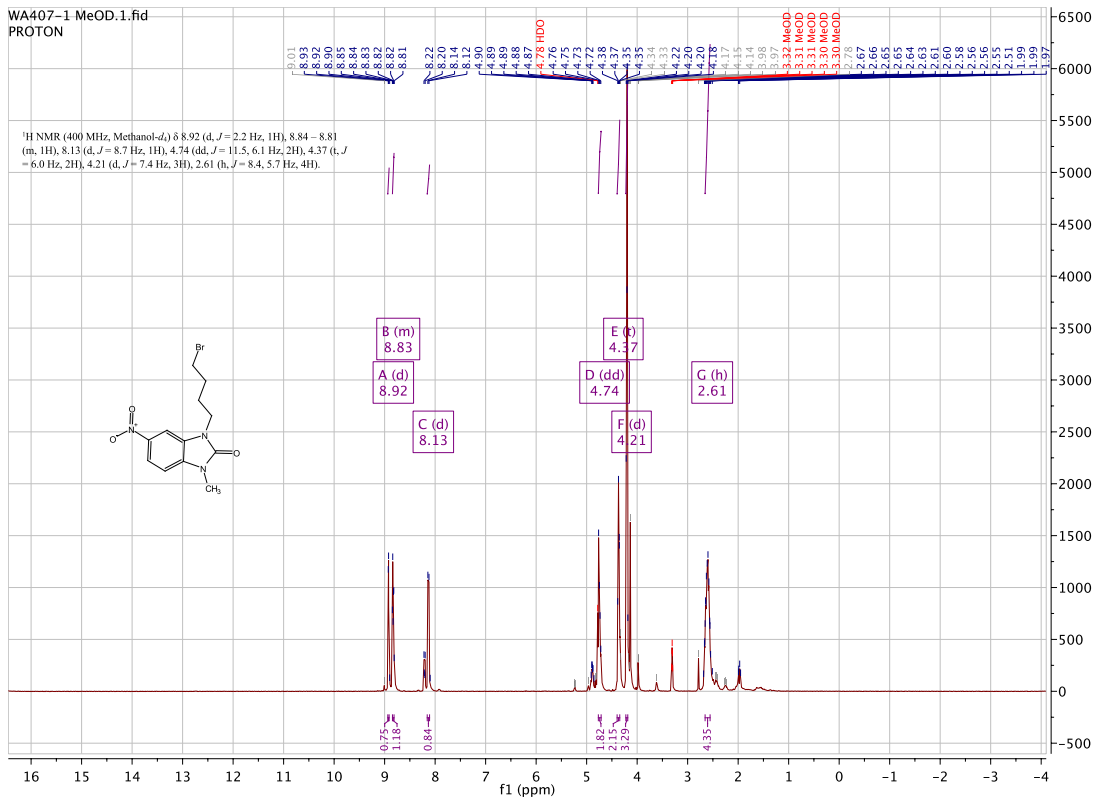


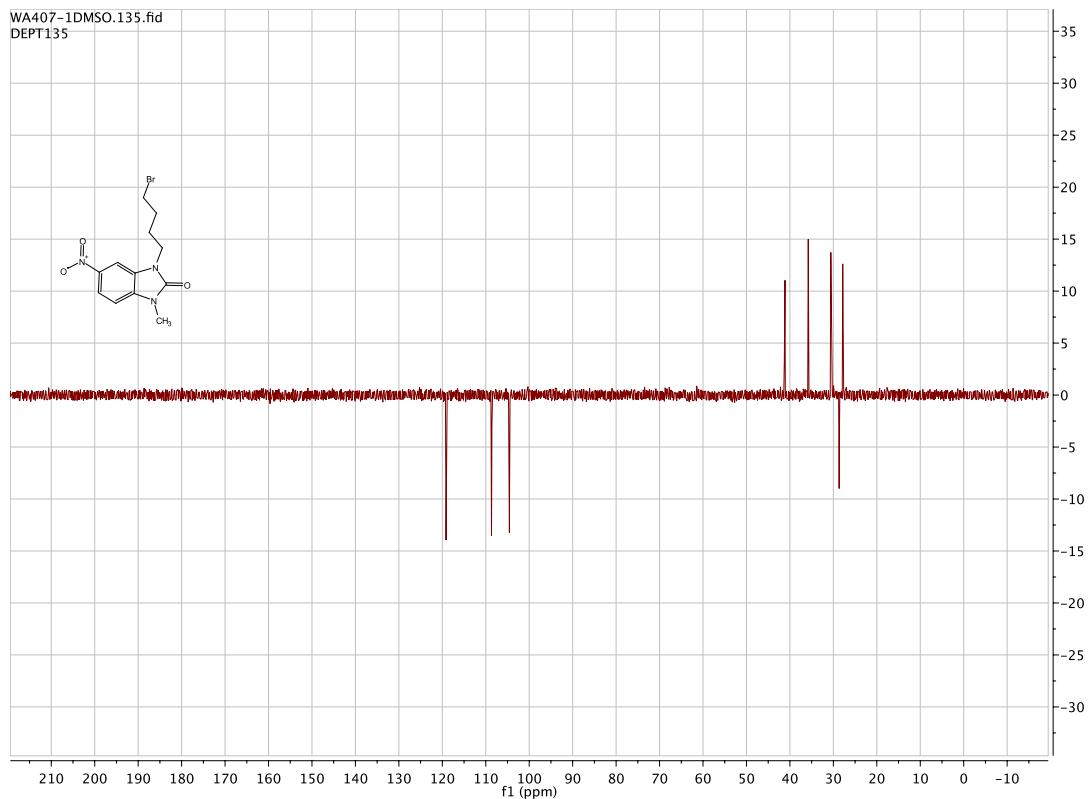




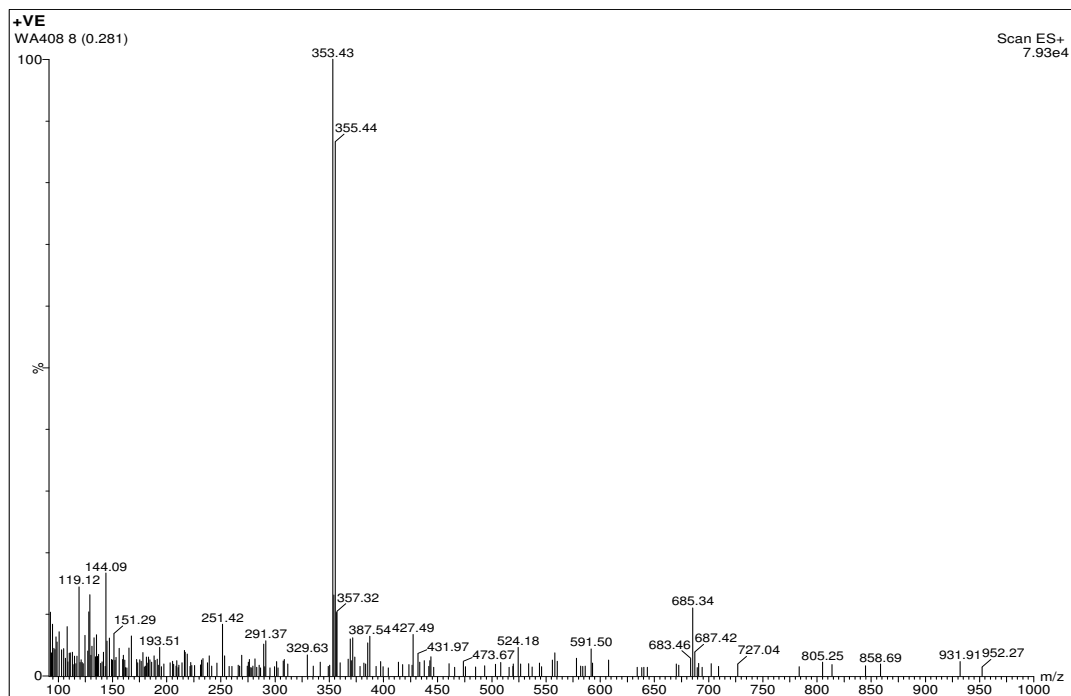
**3-(4-bromobutyl)-1-methyl-5-nitro-1,3-dihydro-2H-benzo[d]imidazol-2-one.
[WA407]**

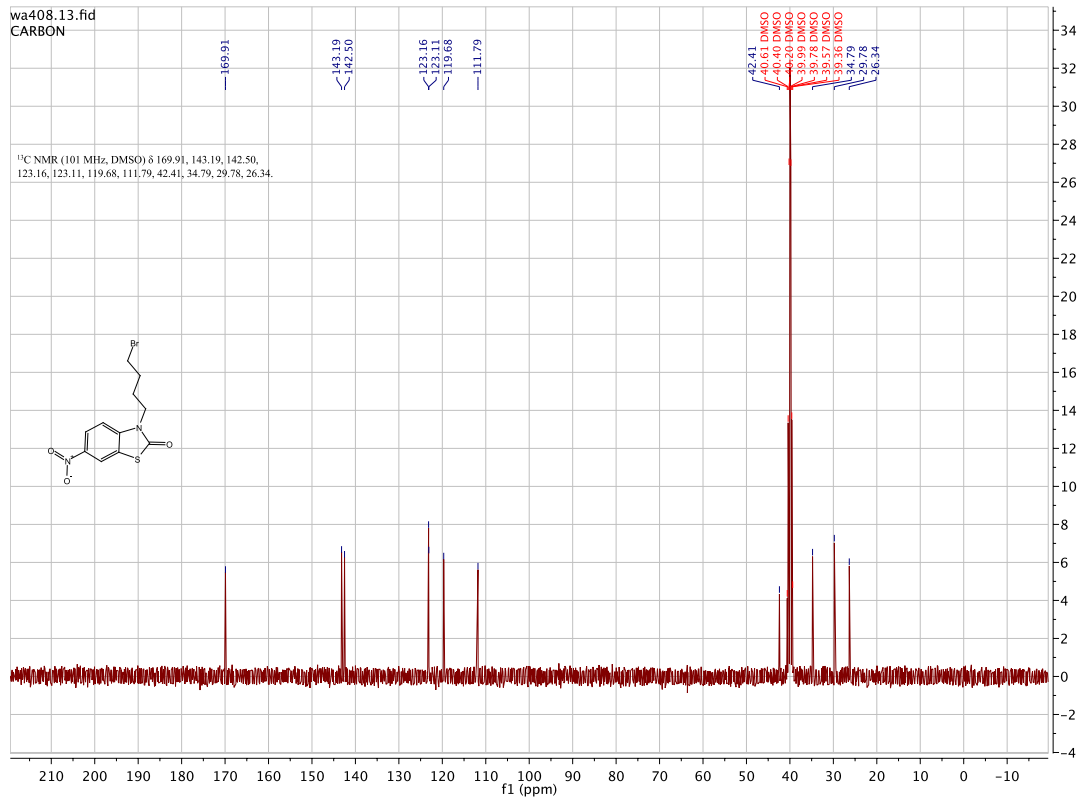
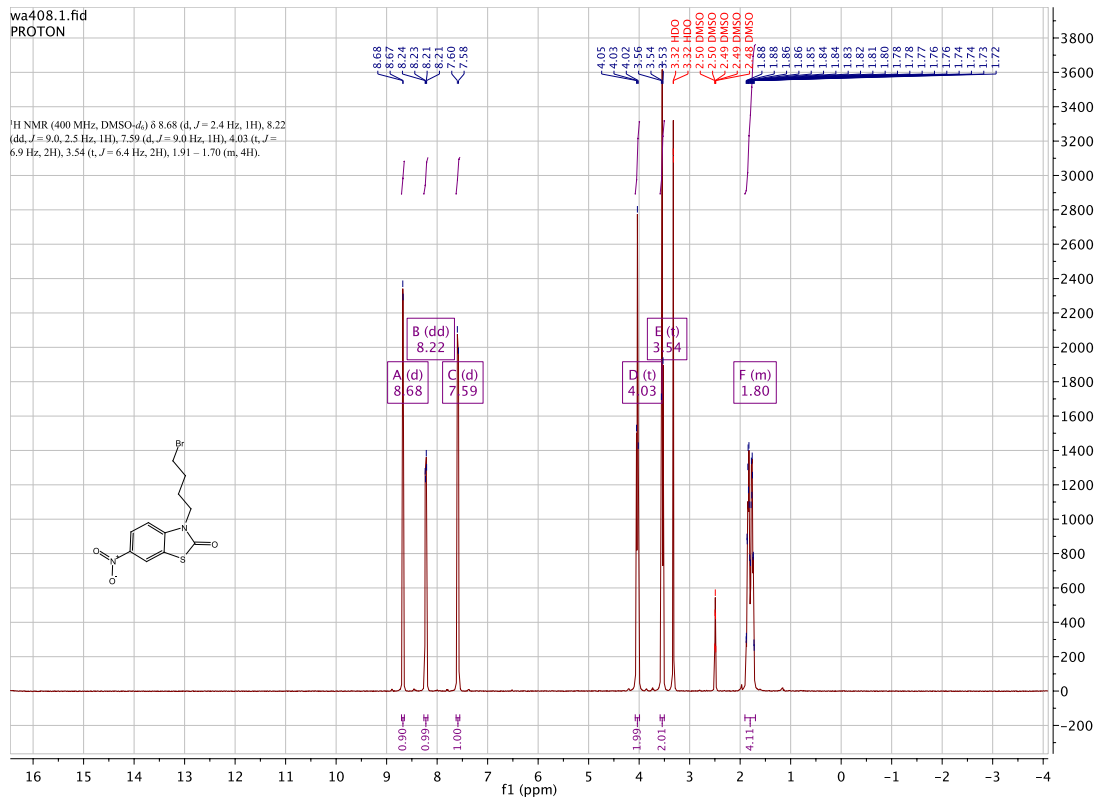


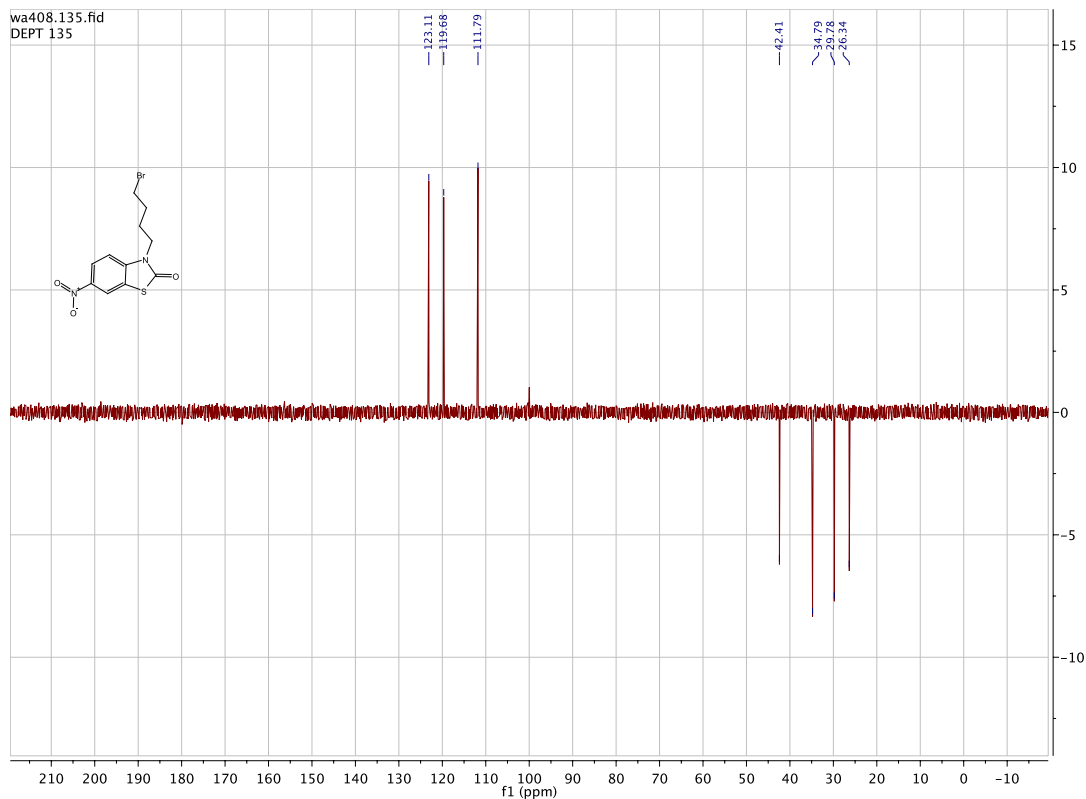




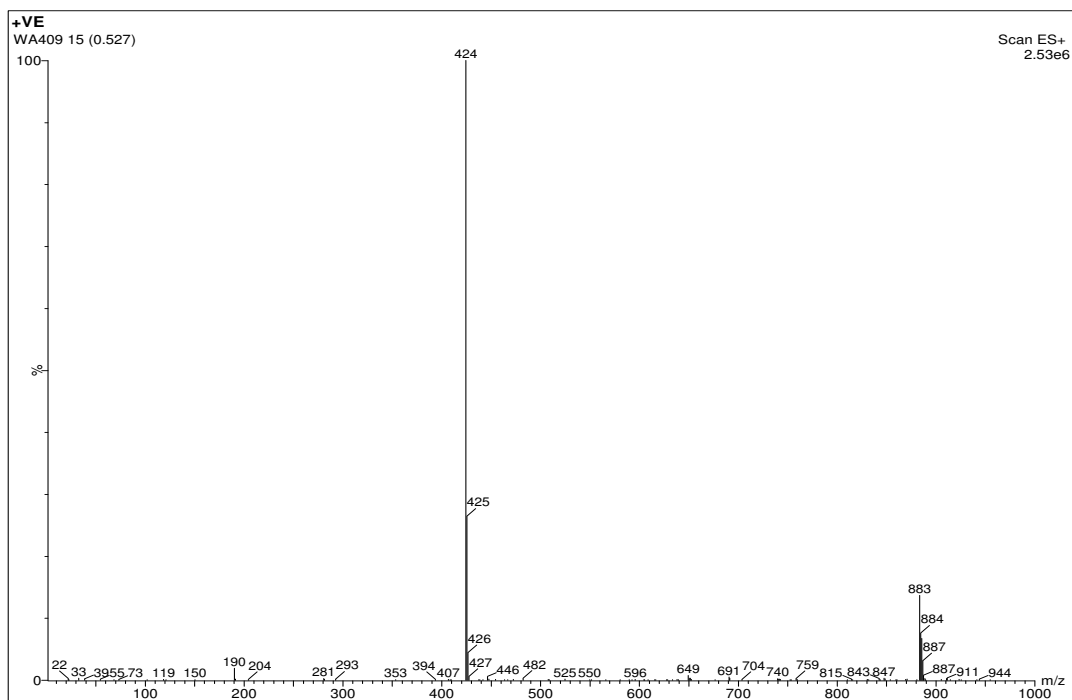
3-(4-bromobutyl)-6-nitrobenzo[*d*]thiazol-2(3*H*)-one. [WA408]

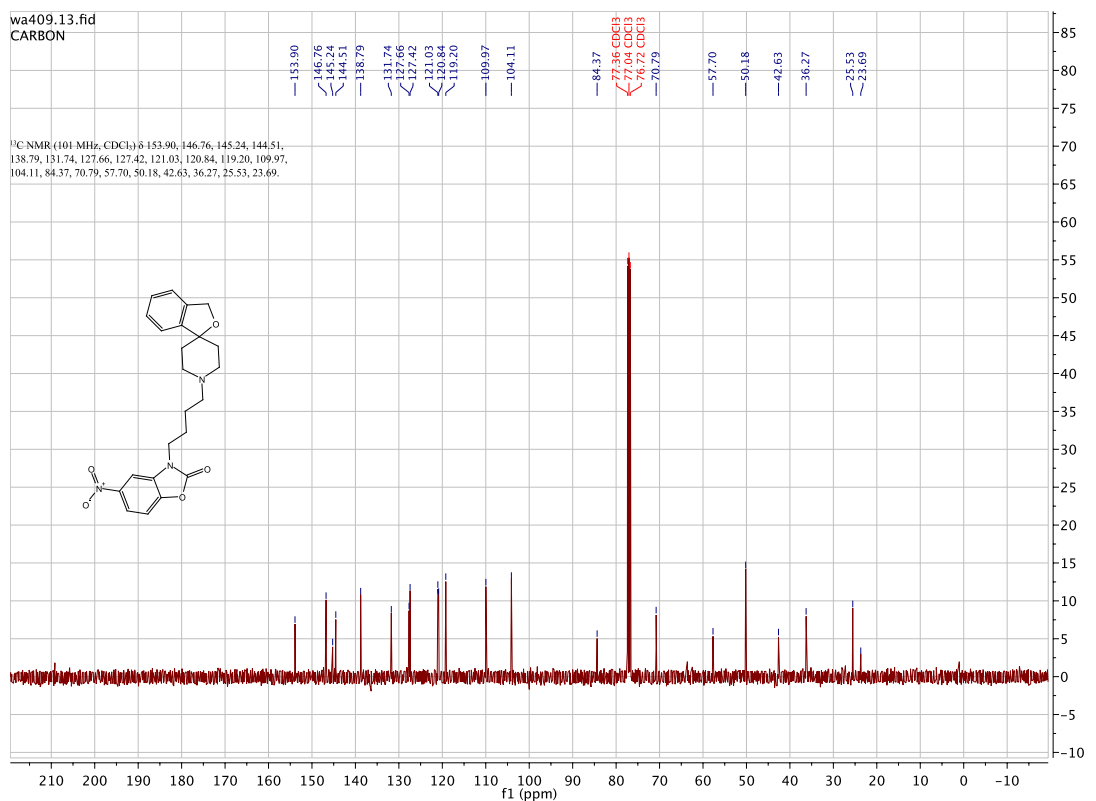
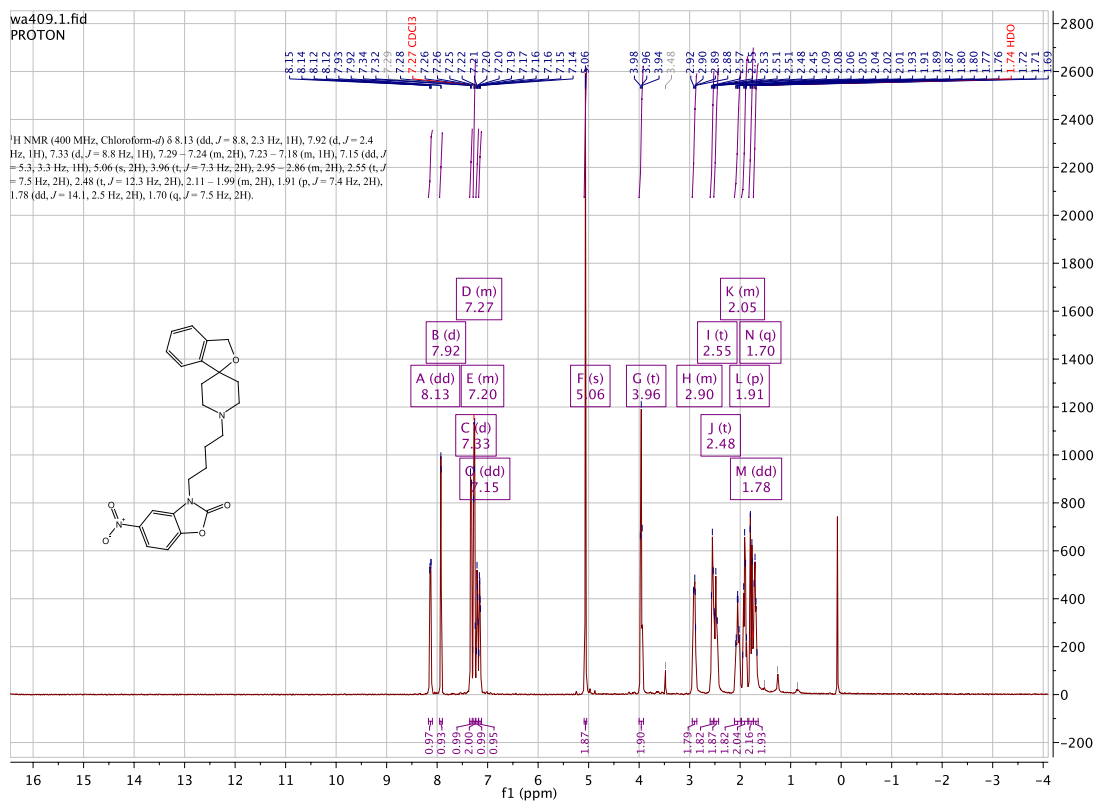


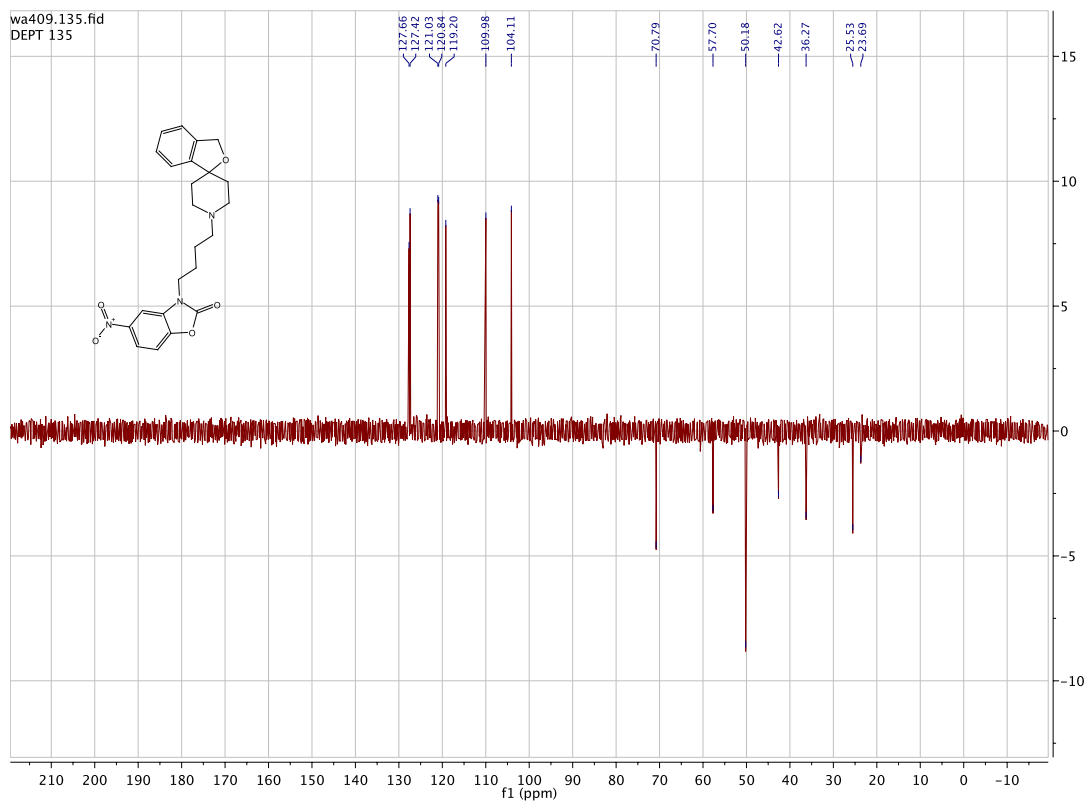




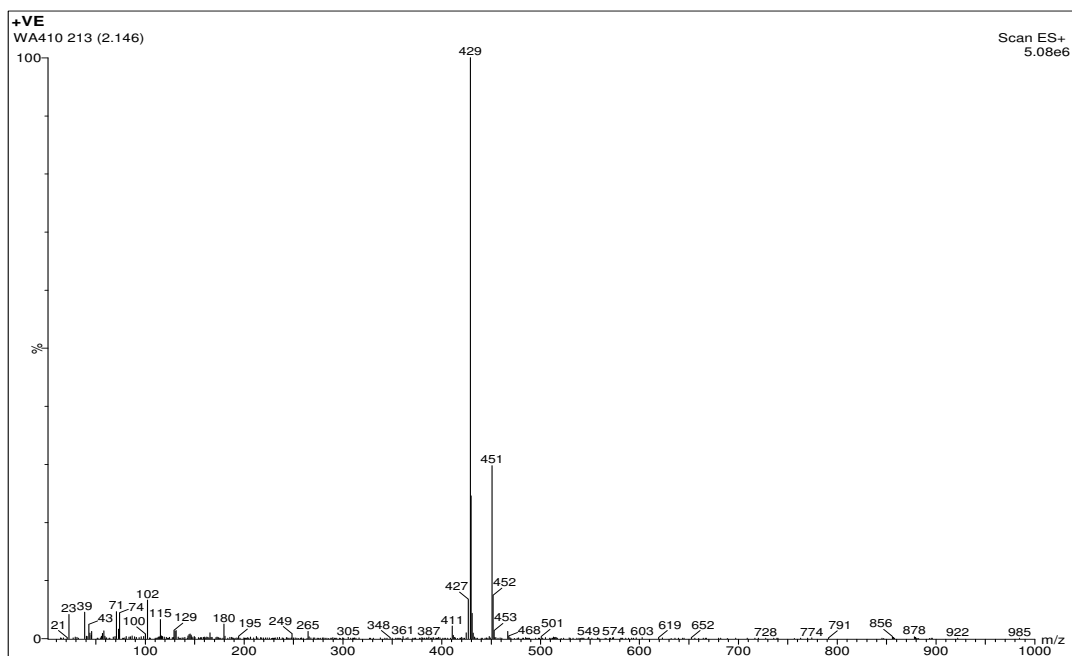
3-(4-(3H-spiro[isobenzofuran-1,4'-piperidin]-1'-yl)butyl)-5-nitrobenzo[d]oxazol-2(3H)-one. [WA409]

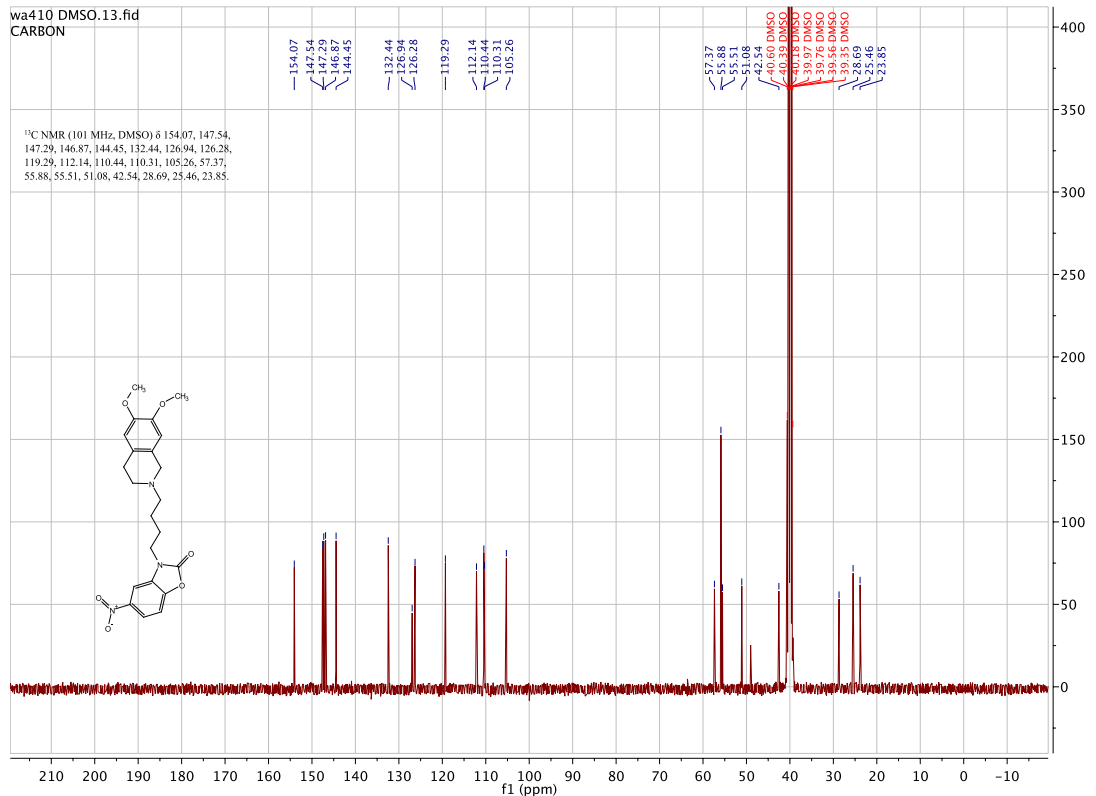
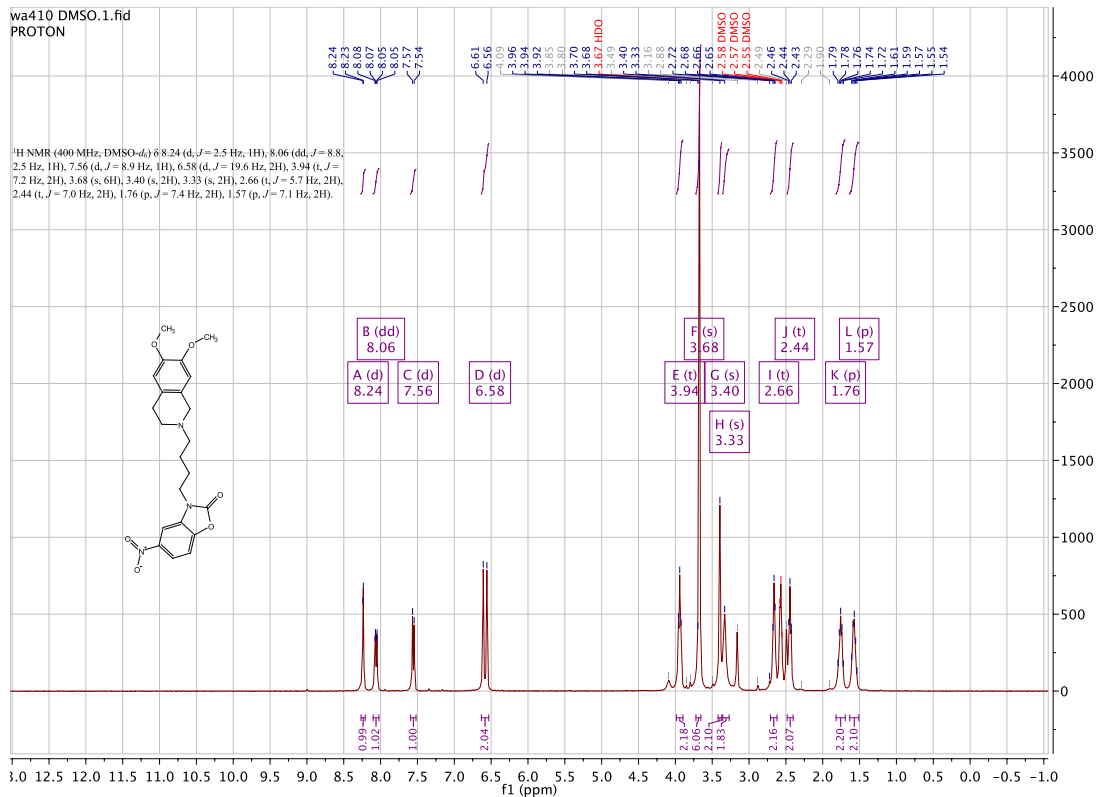


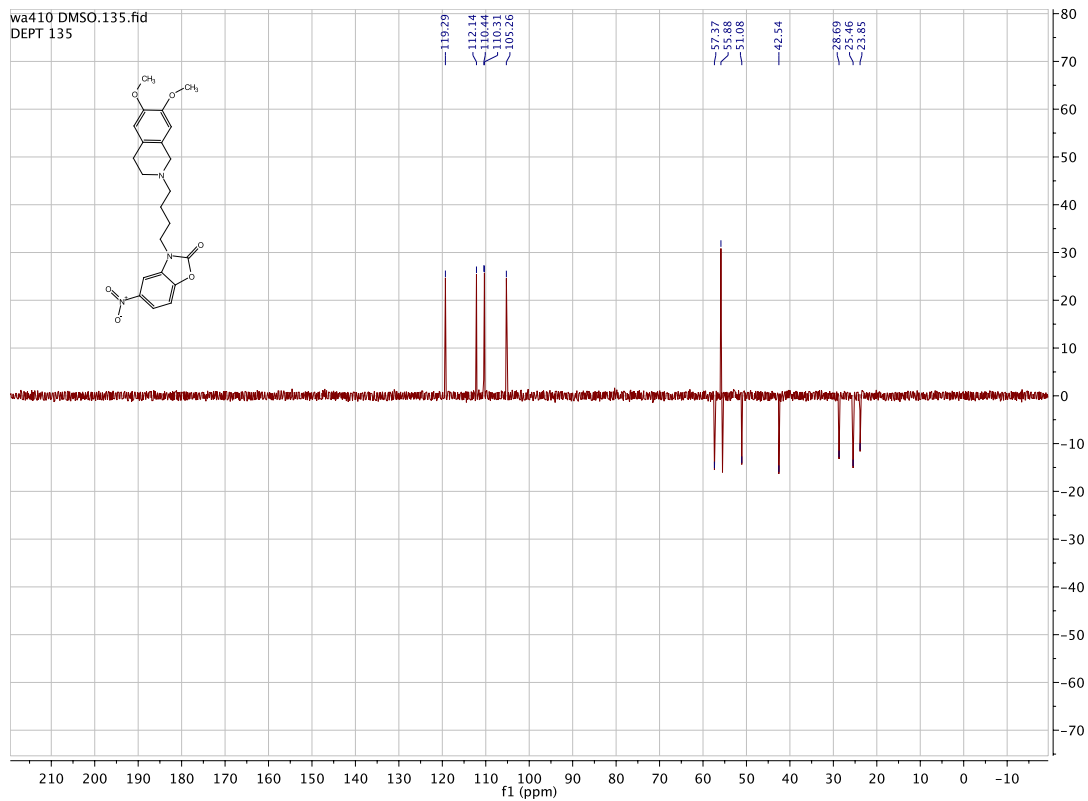




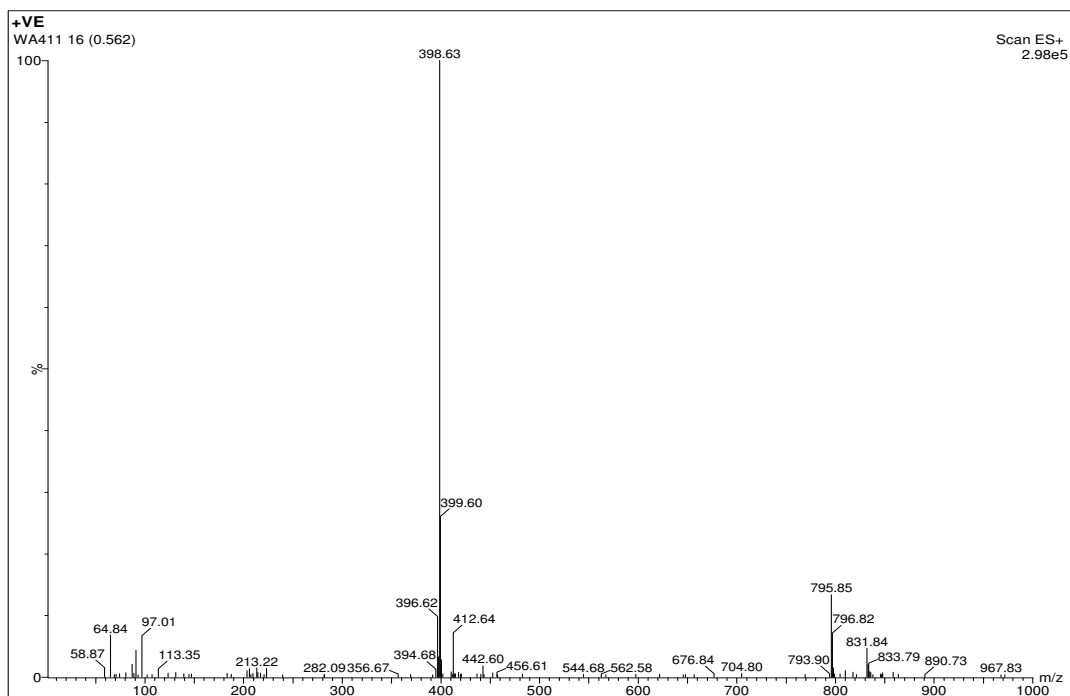
3-(4-(6,7-dimethoxy-3,4-dihydroisoquinolin-2(1H)-yl)butyl)-5-nitrobenzo[d]oxazol-2(3H)-one. [WA410]





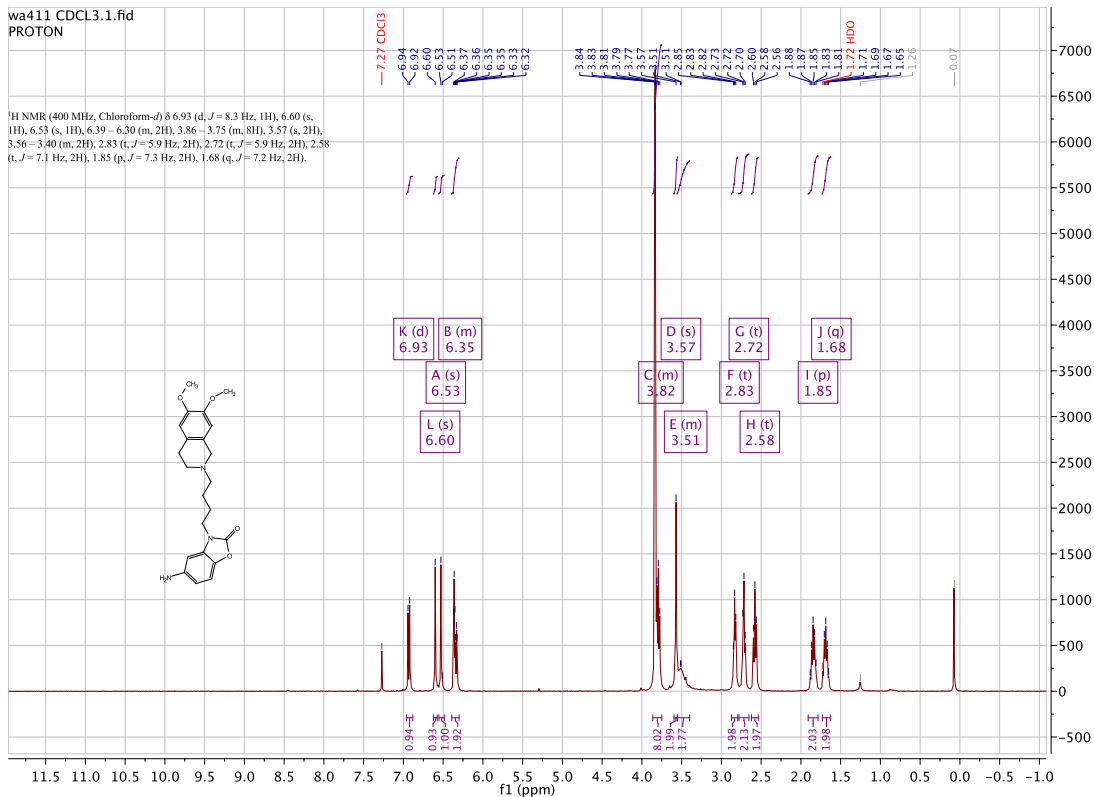


5-amino-3-(4-(6,7-dimethoxy-3,4-dihydroisoquinolin-2(1H)-yl)butyl)benzo[d]oxazol-2(3H)-one. [WA411]



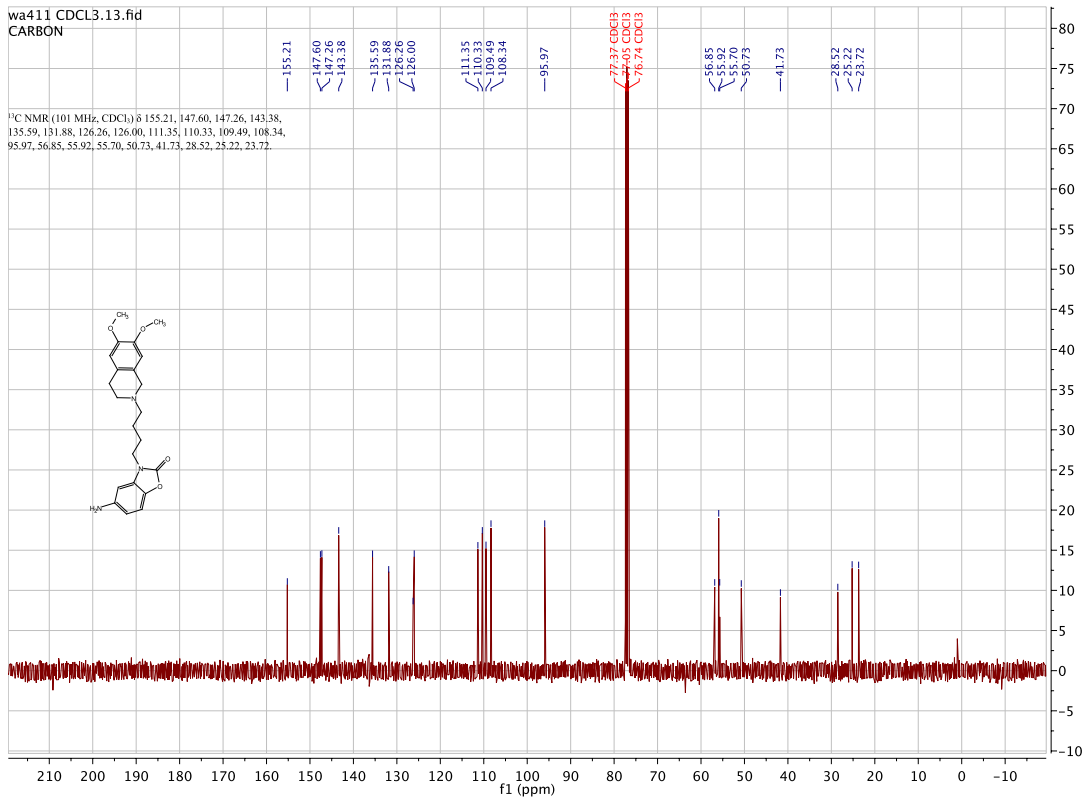
wa411 CDCL3.1.fid
PROTON

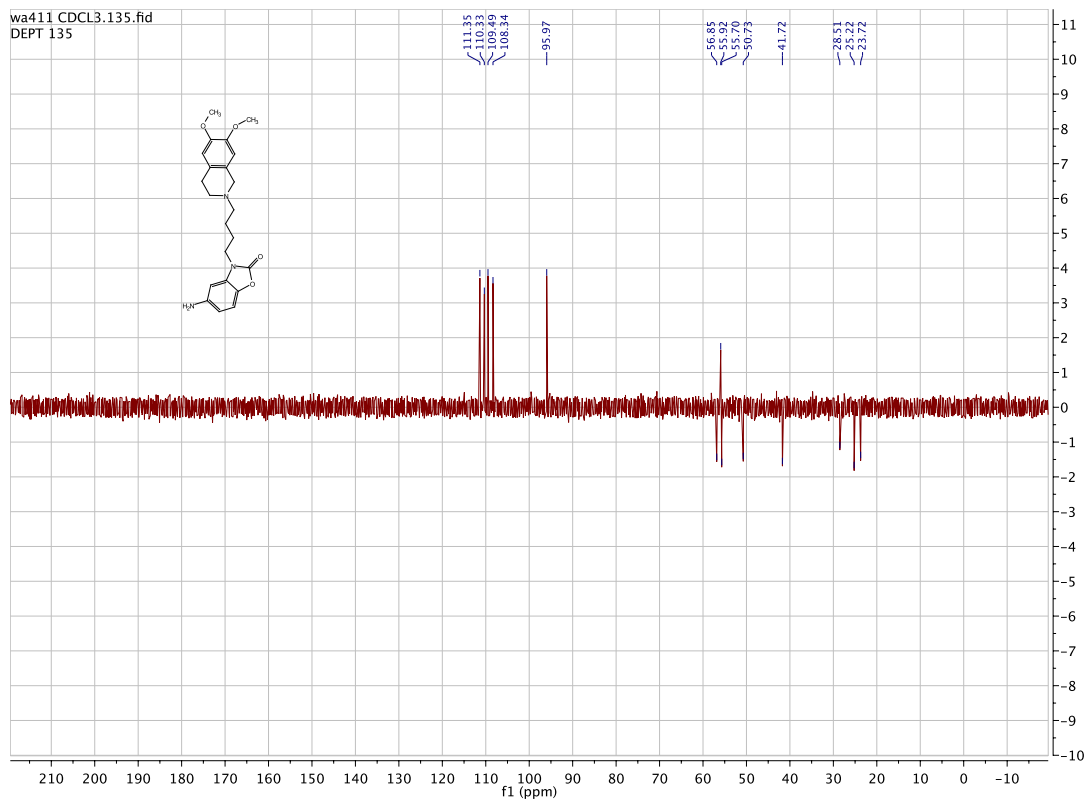
¹H NMR (400 MHz, Chloroform-d) δ 6.93 (d, *J* = 8.3 Hz, 1H), 6.60 (s, 1H), 6.53 (s, 1H), 6.39 – 6.30 (m, 2H), 3.86 – 3.75 (m, 8H), 3.57 (s, 2H), 3.56 – 3.40 (m, 2H), 2.83 (t, *J* = 5.9 Hz, 2H), 2.72 (t, *J* = 5.9 Hz, 2H), 2.58 (t, *J* = 7.1 Hz, 2H), 1.85 (p, *J* = 7.3 Hz, 2H), 1.68 (q, *J* = 7.2 Hz, 2H).



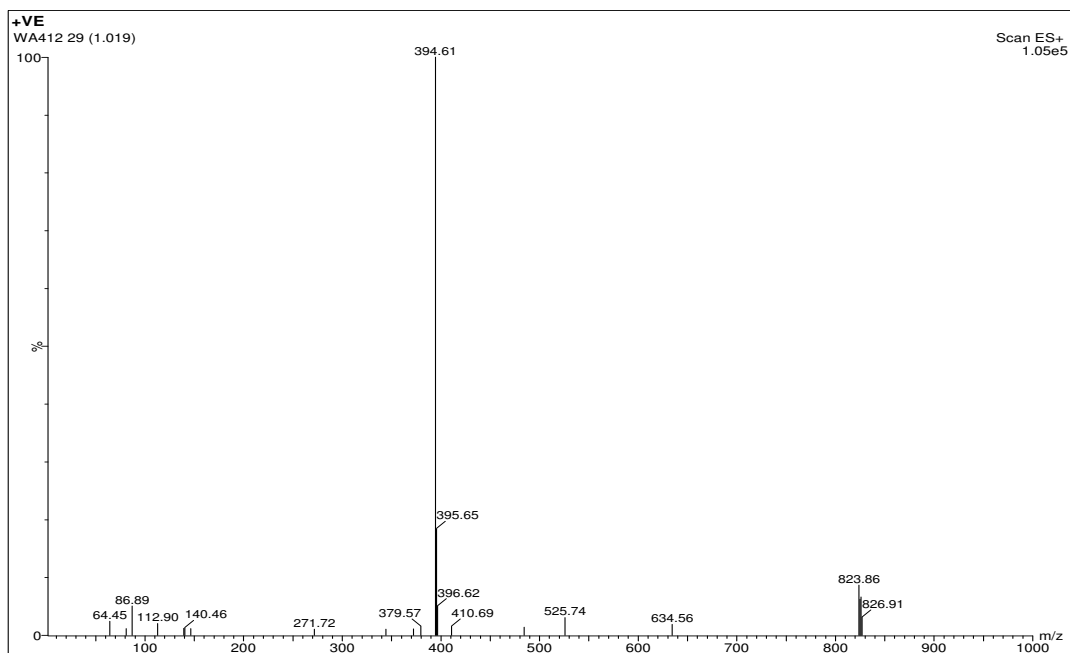
wa411 CDCL3.13.fid
CARBON

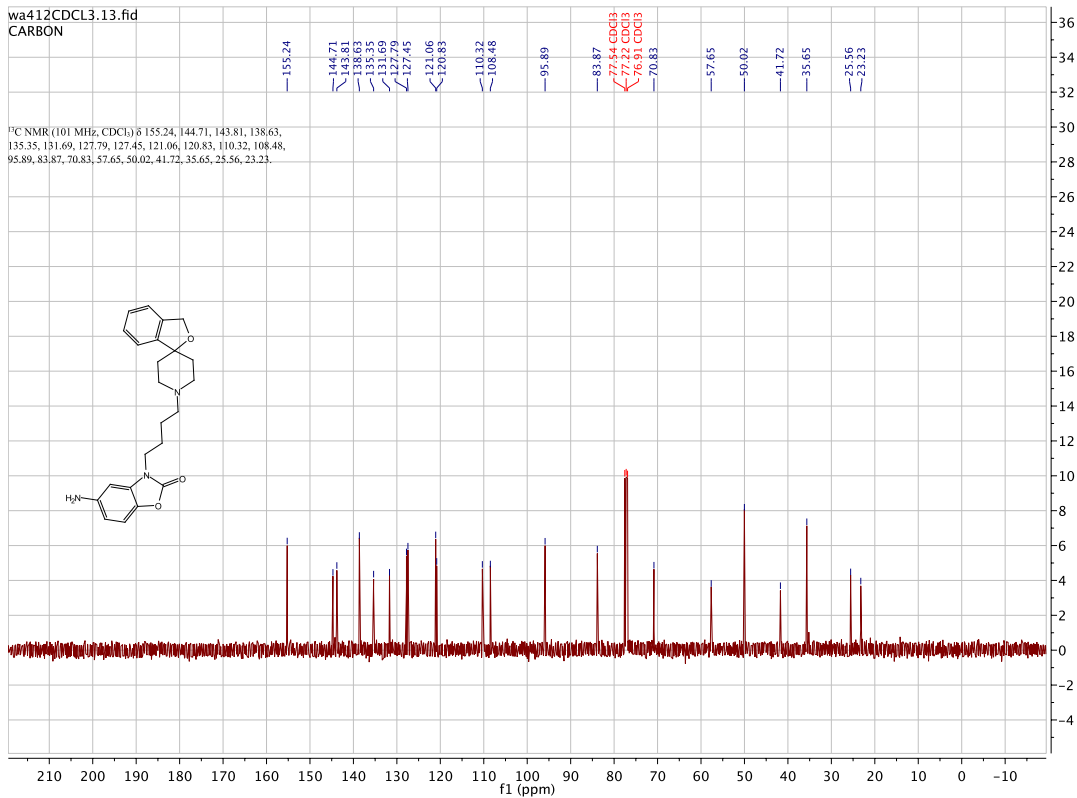
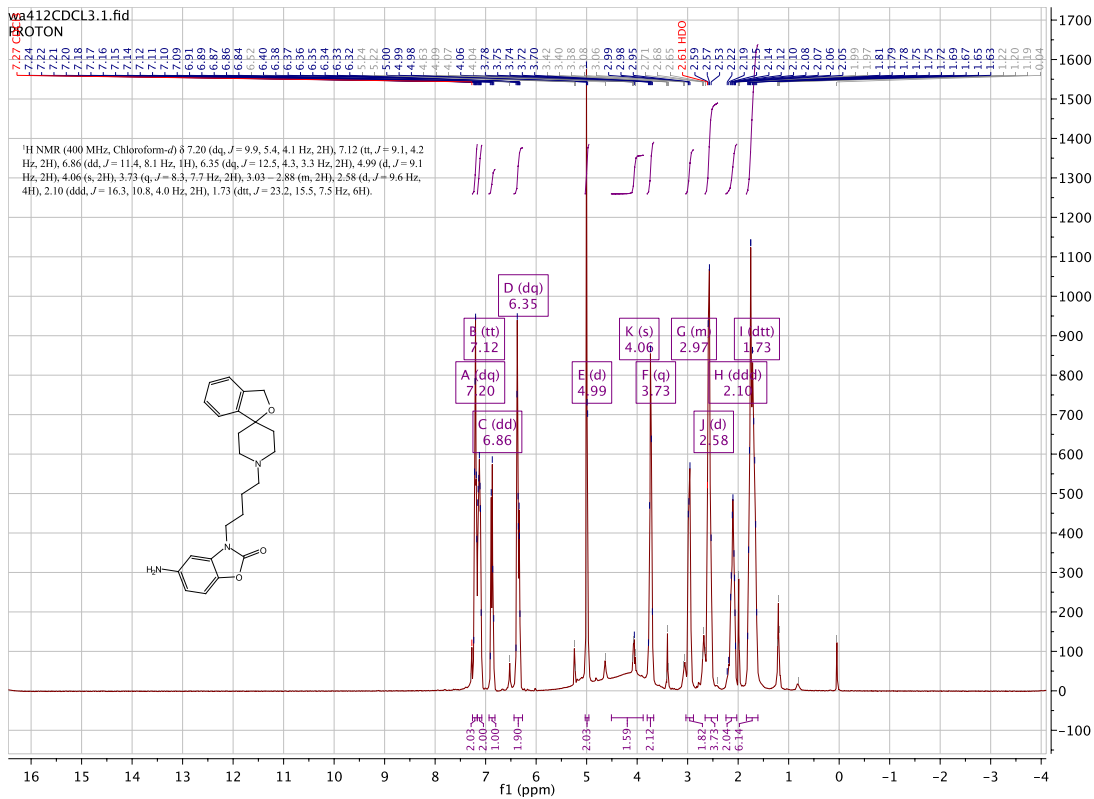
¹³C NMR (101 MHz, CDCl₃) δ 155.21, 147.60, 147.26, 143.38, 135.59, 131.88, 126.26, 126.00, 111.35, 110.33, 109.49, 108.34, 95.97, 56.85, 55.92, 55.70, 50.73, 41.73, 28.52, 25.22, 23.72.

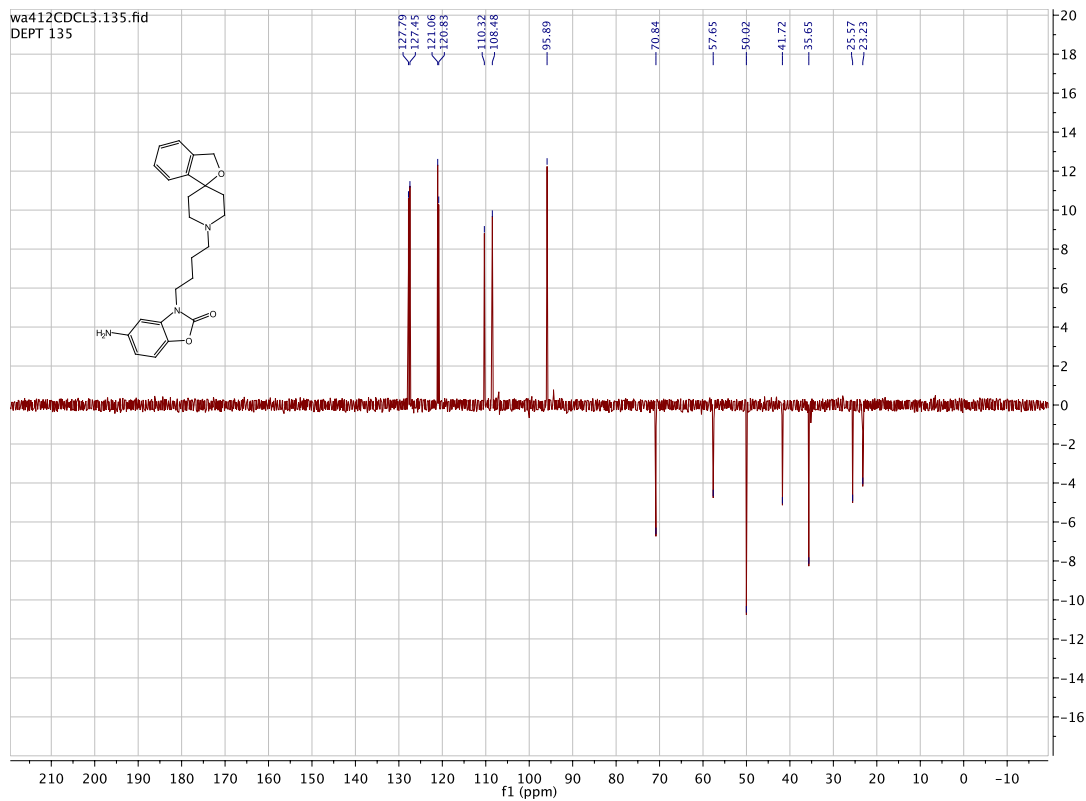




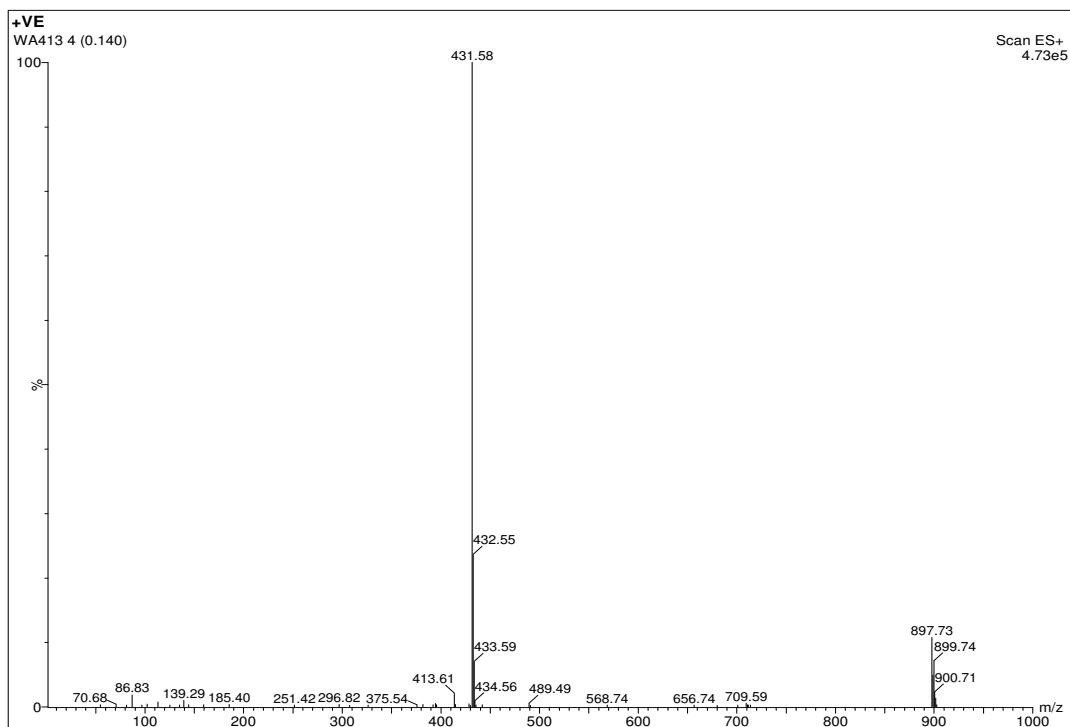
3-(4-(3H-spiro[isobenzofuran-1,4'-piperidin]-1'-yl)butyl)-5-aminobenzo[d]oxazol-2(3H)-one. [WA412]





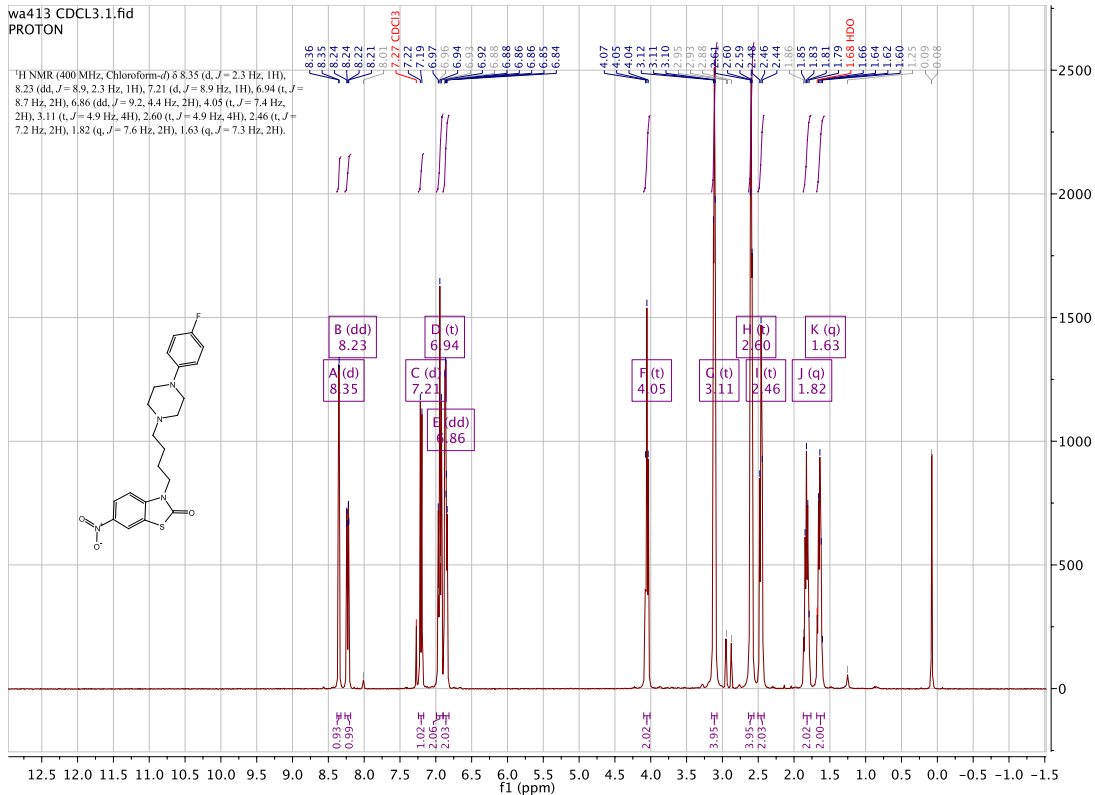


**3-(4-(4-(4-fluorophenyl)piperazin-1-yl)butyl)-6-nitrobenzo[d]thiazol-2(3H)-one.
[WA413]**



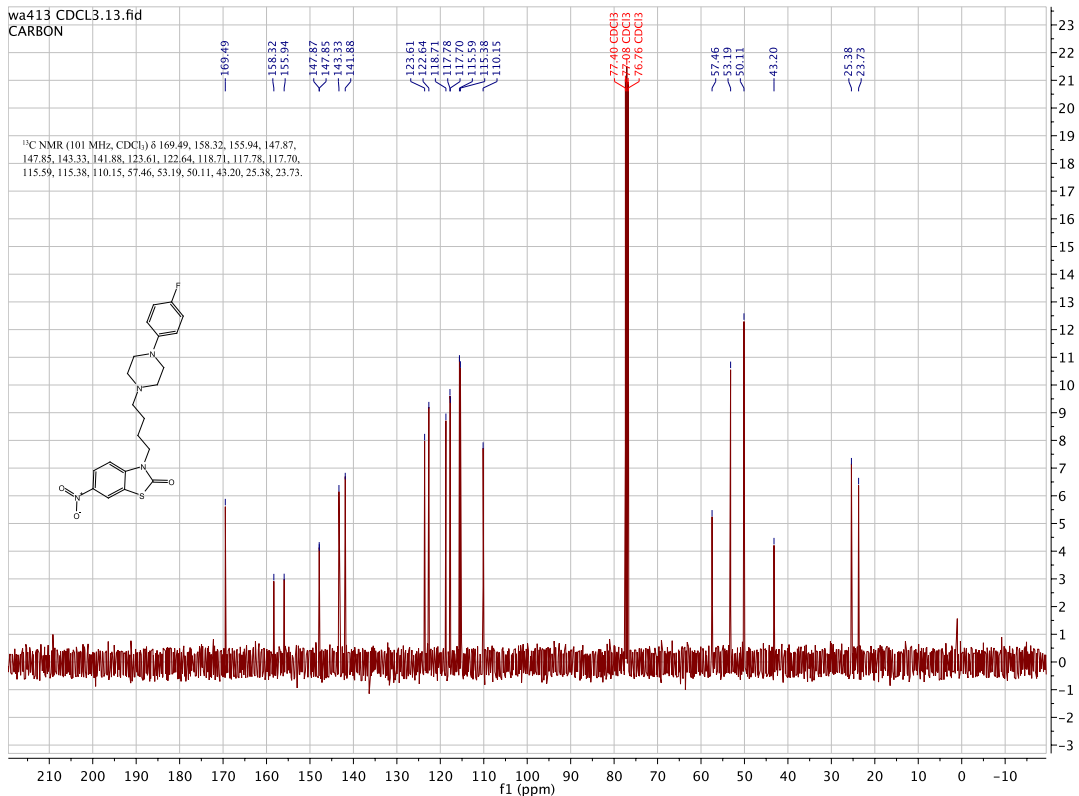
wa413 CDCL3.1.fid
PROTON

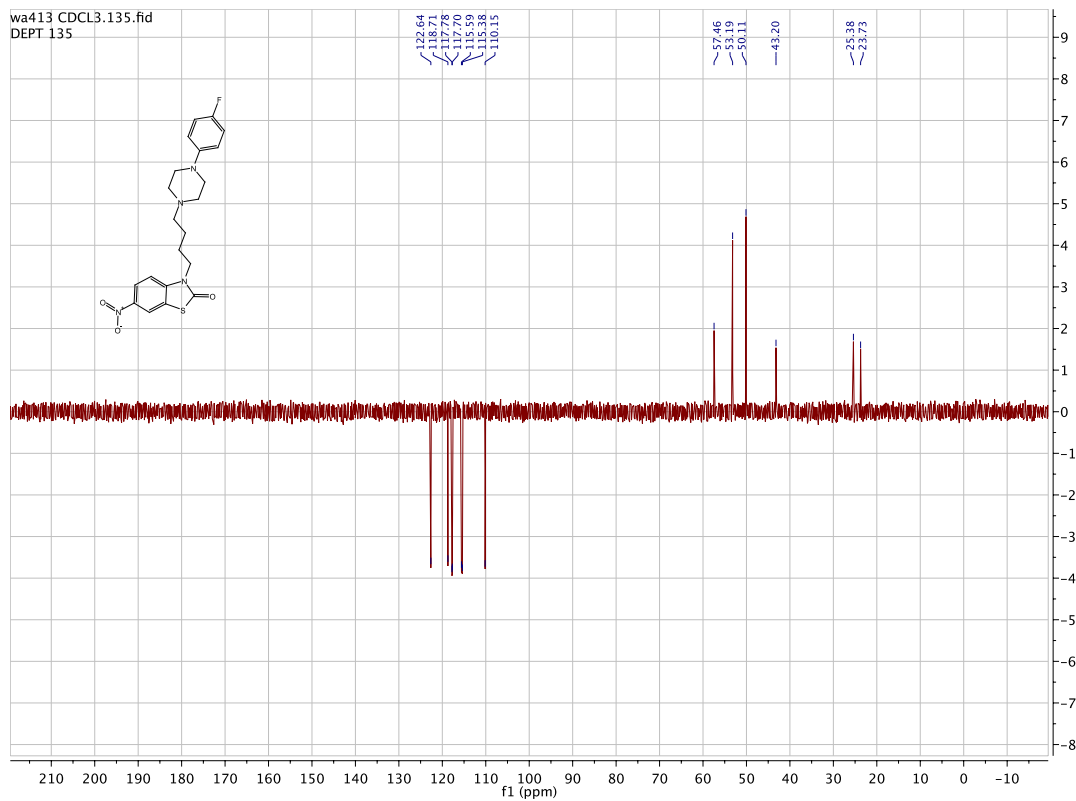
¹H NMR (400 MHz, Chloroform-*d*) δ 8.35 (d, *J* = 2.3 Hz, 1H), 8.23 (dd, *J* = 8.9, 2.3 Hz, 1H), 7.21 (d, *J* = 8.9 Hz, 1H), 6.94 (t, *J* = 8.7 Hz, 2H), 6.86 (dd, *J* = 9.2, 4.4 Hz, 2H), 4.05 (t, *J* = 7.4 Hz, 2H), 3.11 (t, *J* = 4.9 Hz, 4H), 2.60 (t, *J* = 4.9 Hz, 4H), 2.46 (t, *J* = 7.2 Hz, 2H), 1.82 (q, *J* = 7.6 Hz, 2H), 1.63 (q, *J* = 7.3 Hz, 2H).



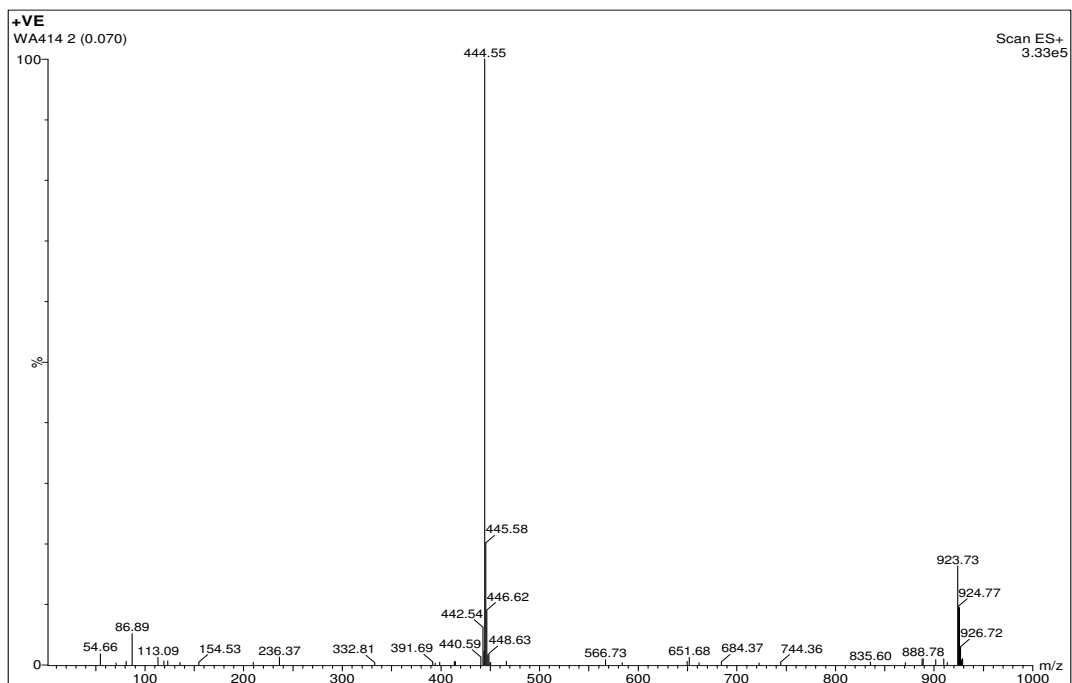
wa413 CDCL3.13.fid
CARBON

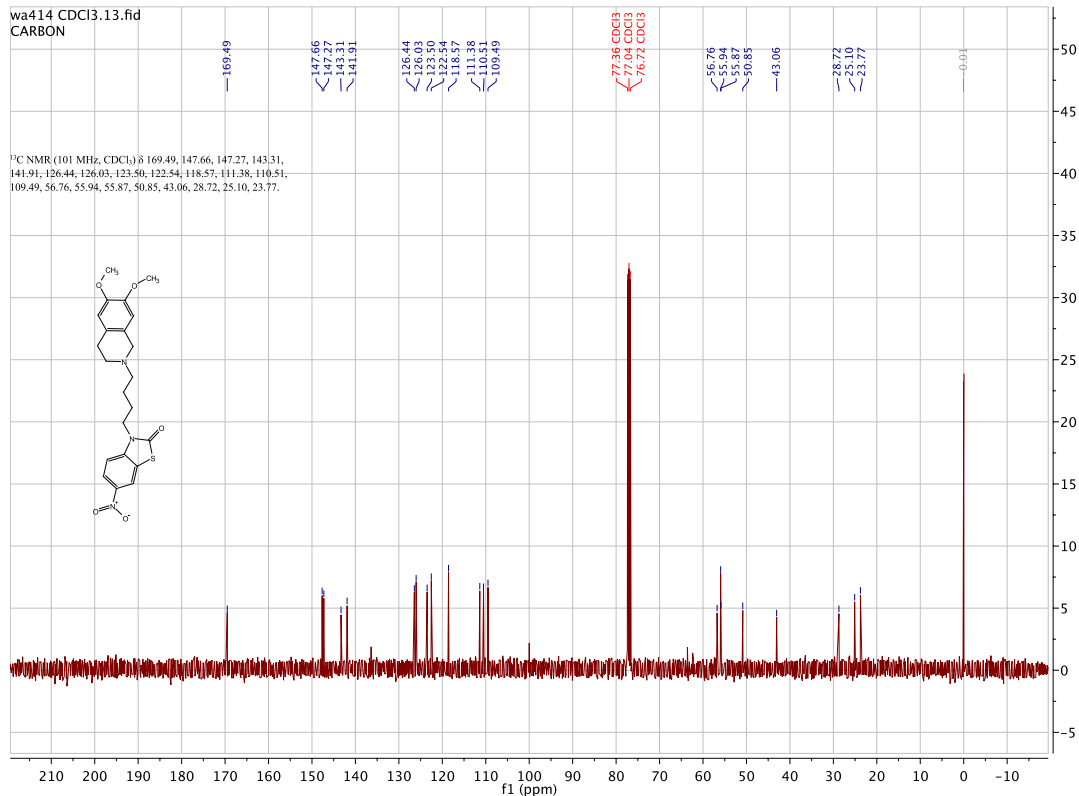
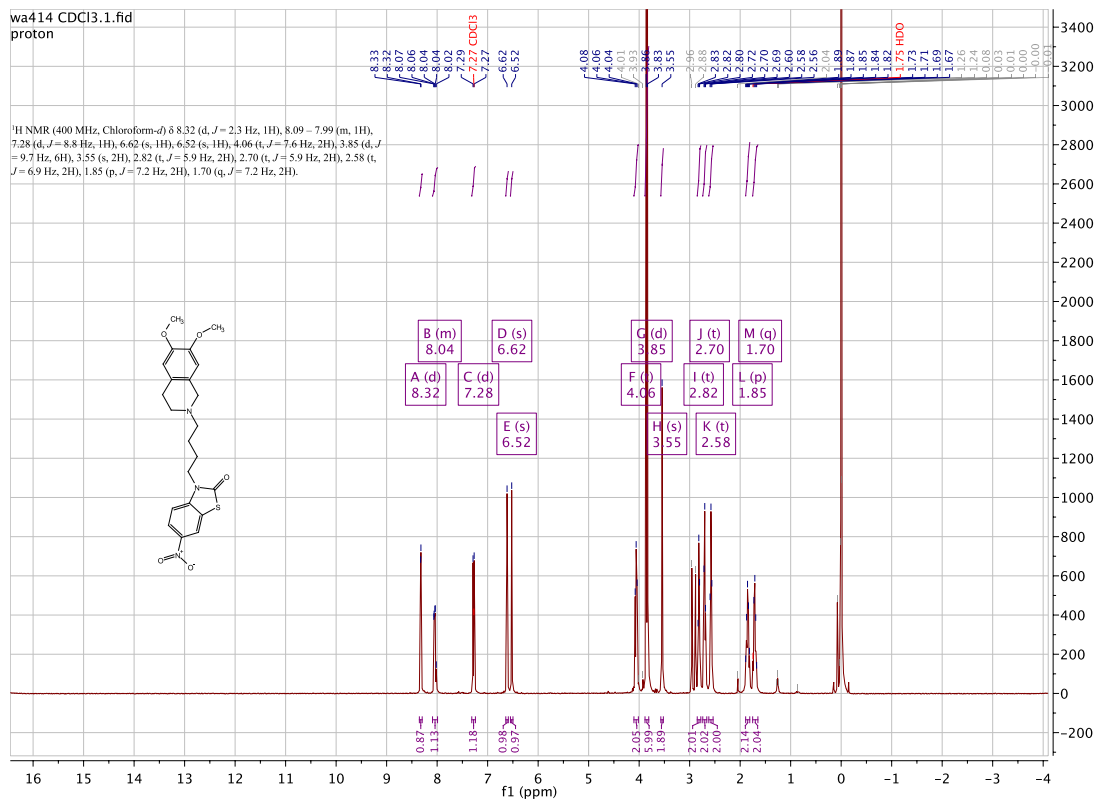
¹³C NMR (101 MHz, CDCl₃) δ 169.49, 158.32, 155.94, 147.87, 147.85, 143.33, 141.88, 123.61, 122.64, 118.71, 117.78, 117.70, 115.59, 115.38, 110.15, 57.46, 53.19, 50.11, 43.20, 25.38, 23.73.

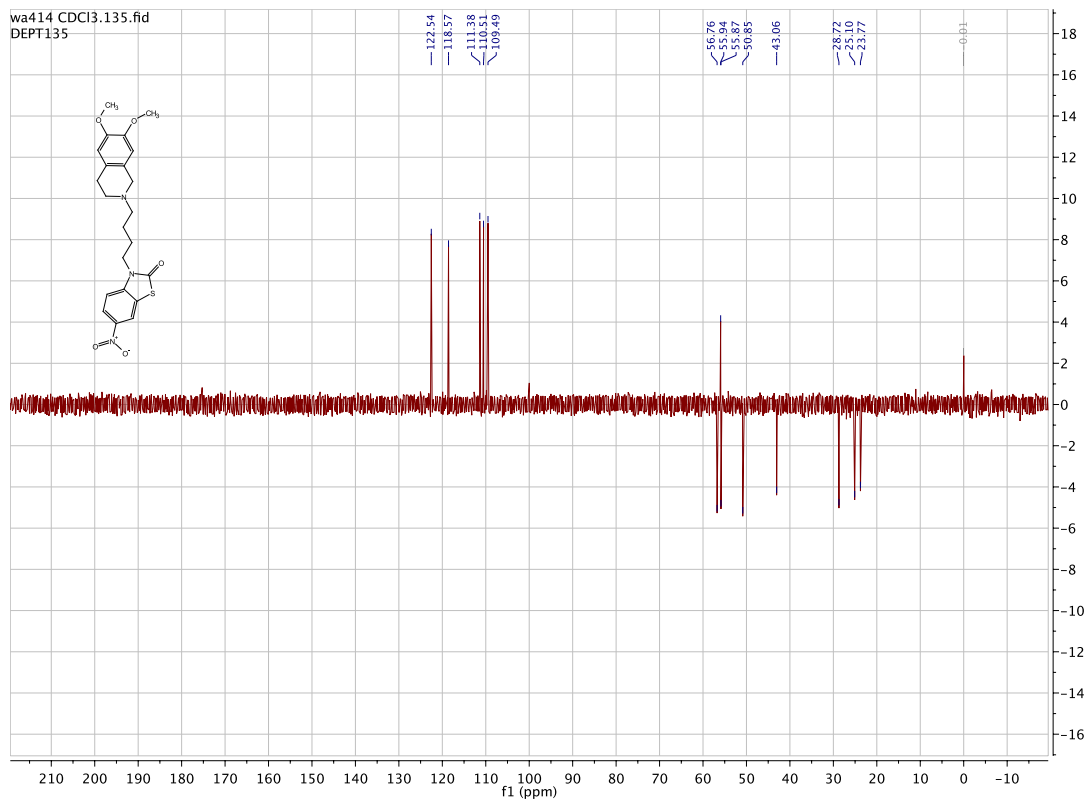




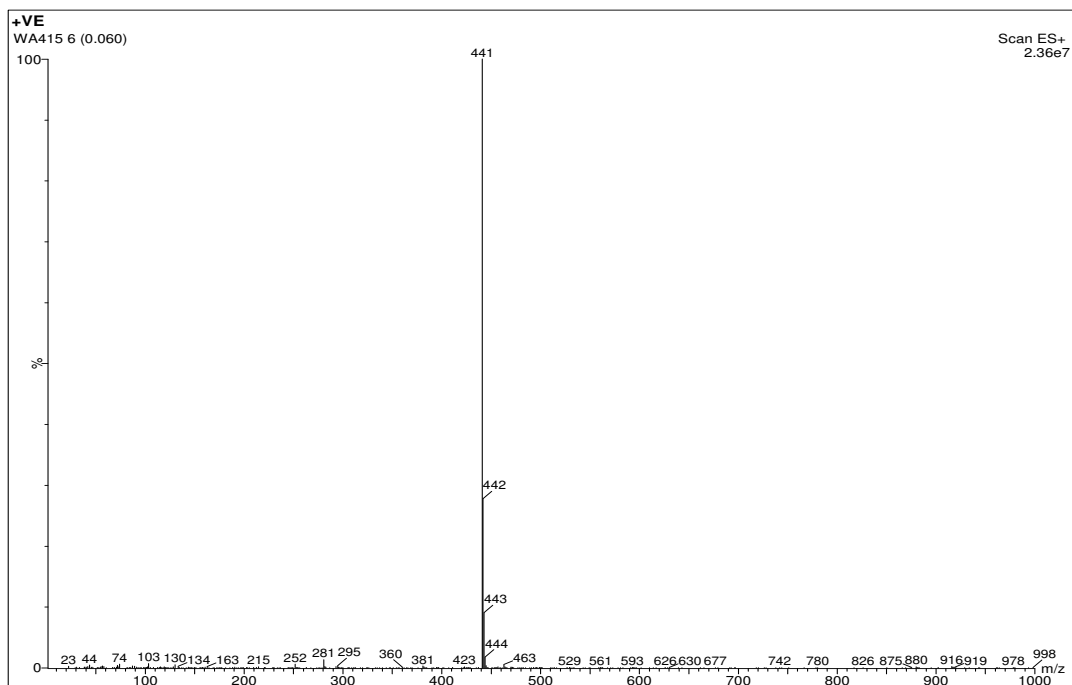
3-(4-(6,7-dimethoxy-3,4-dihydroisoquinolin-2(1H)-yl)butyl)-6-nitrobenzo[d]thiazol-2(3H)-one. [WA414]

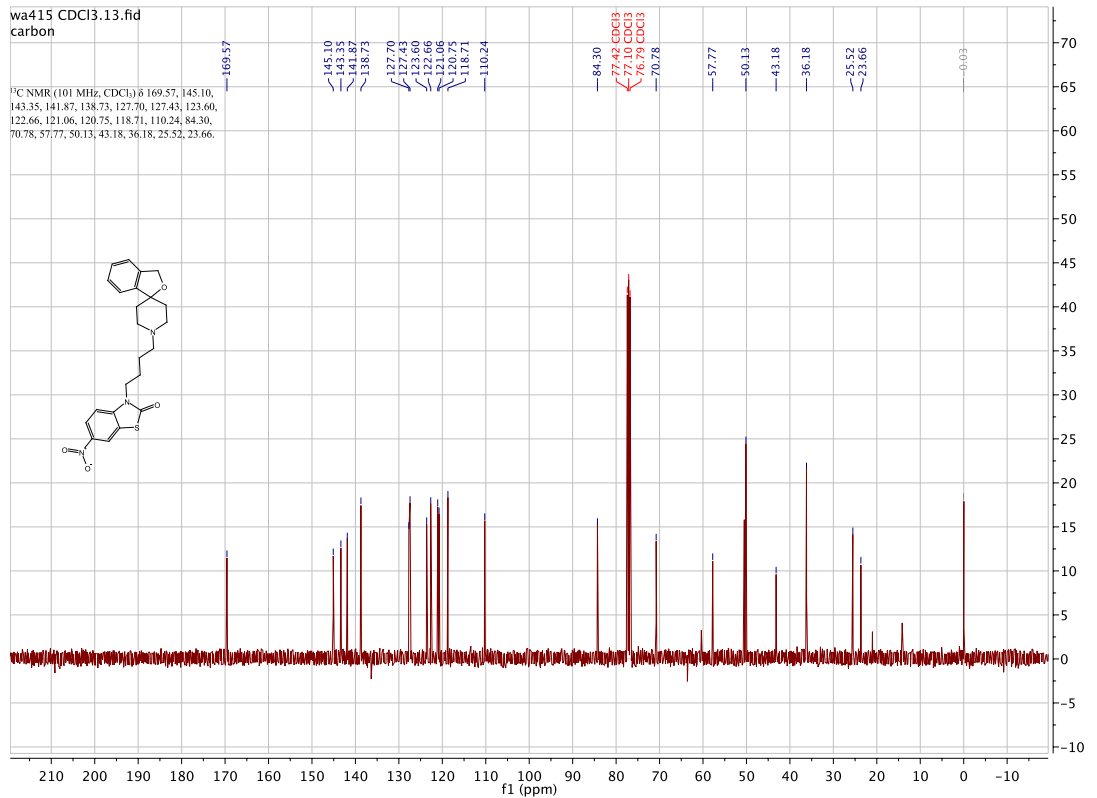
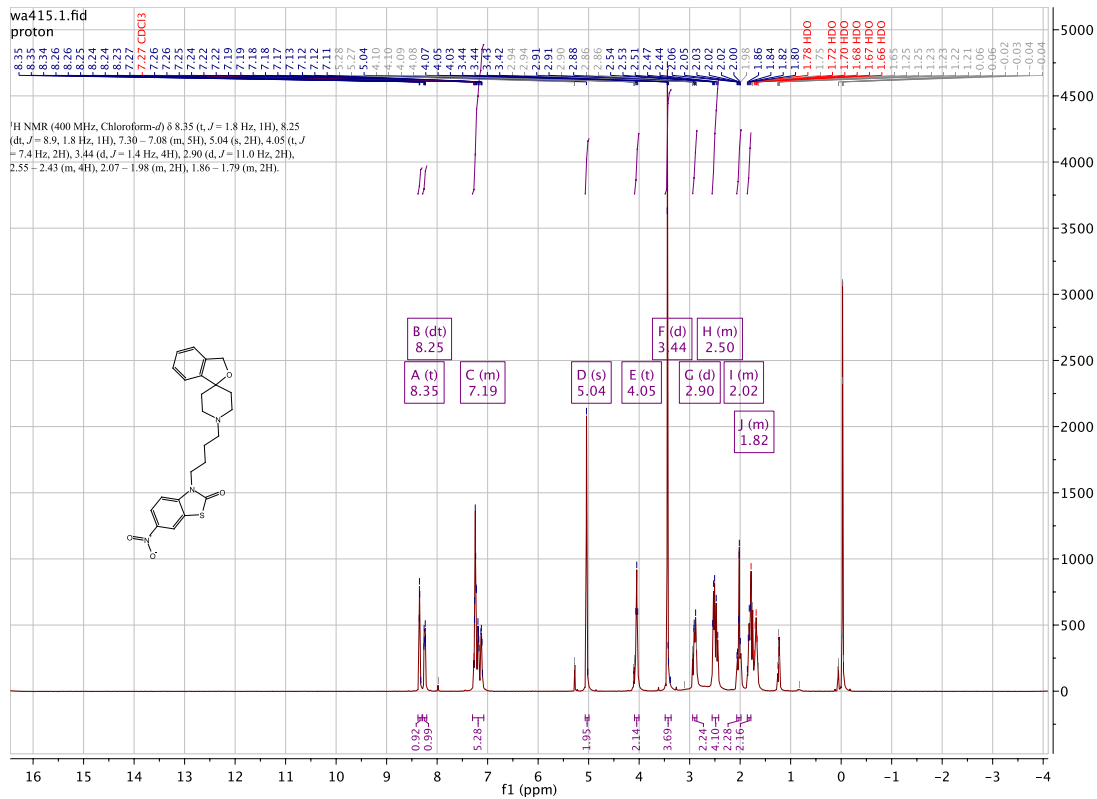


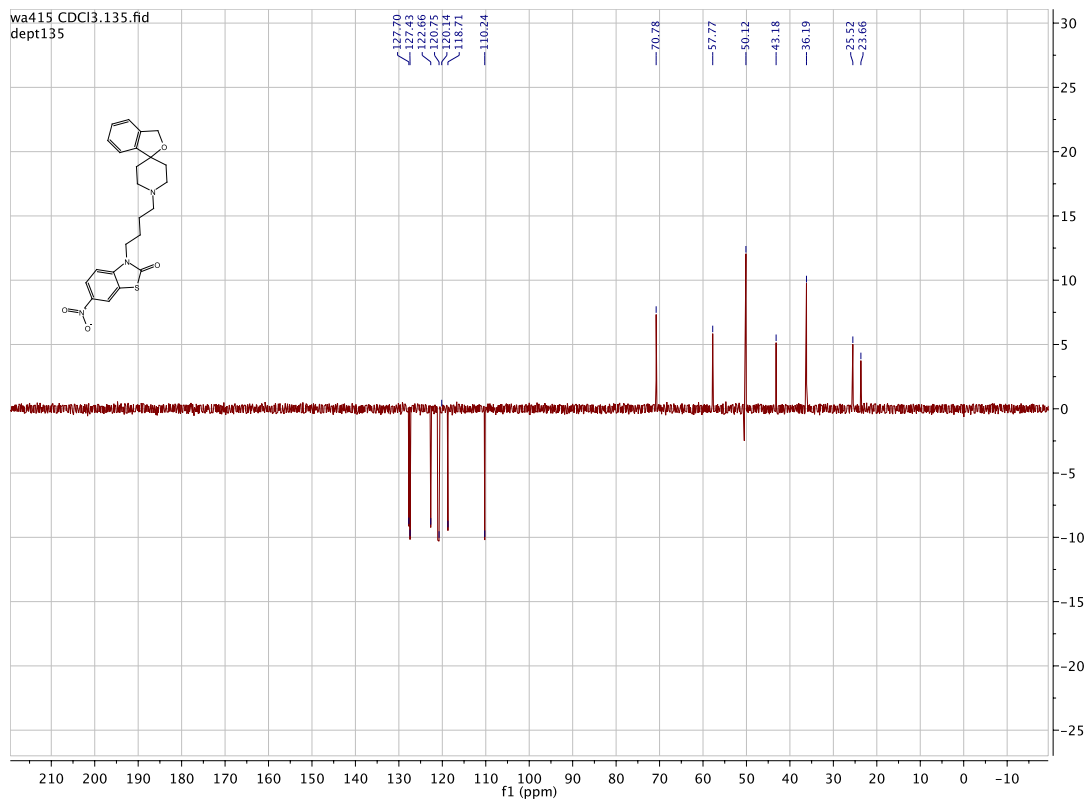




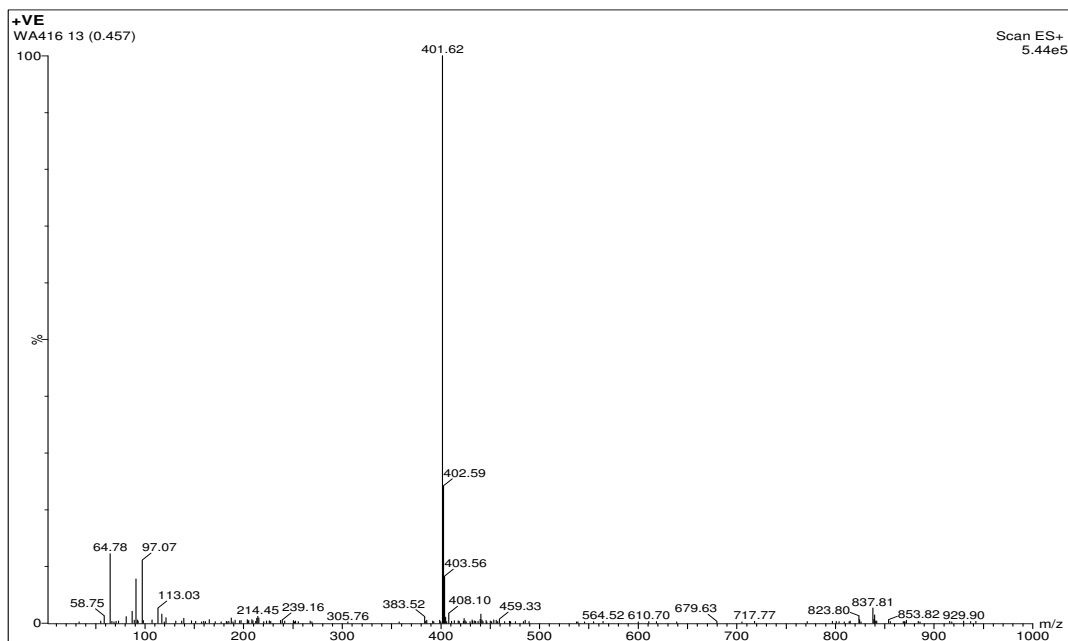
3-(4-(3H-spiro[isobenzofuran-1,4'-piperidin]-1'-yl)butyl)-6-nitrobenzo[d]thiazol-2(3H)-one. [WA415]



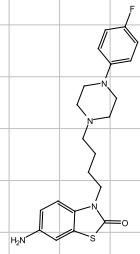
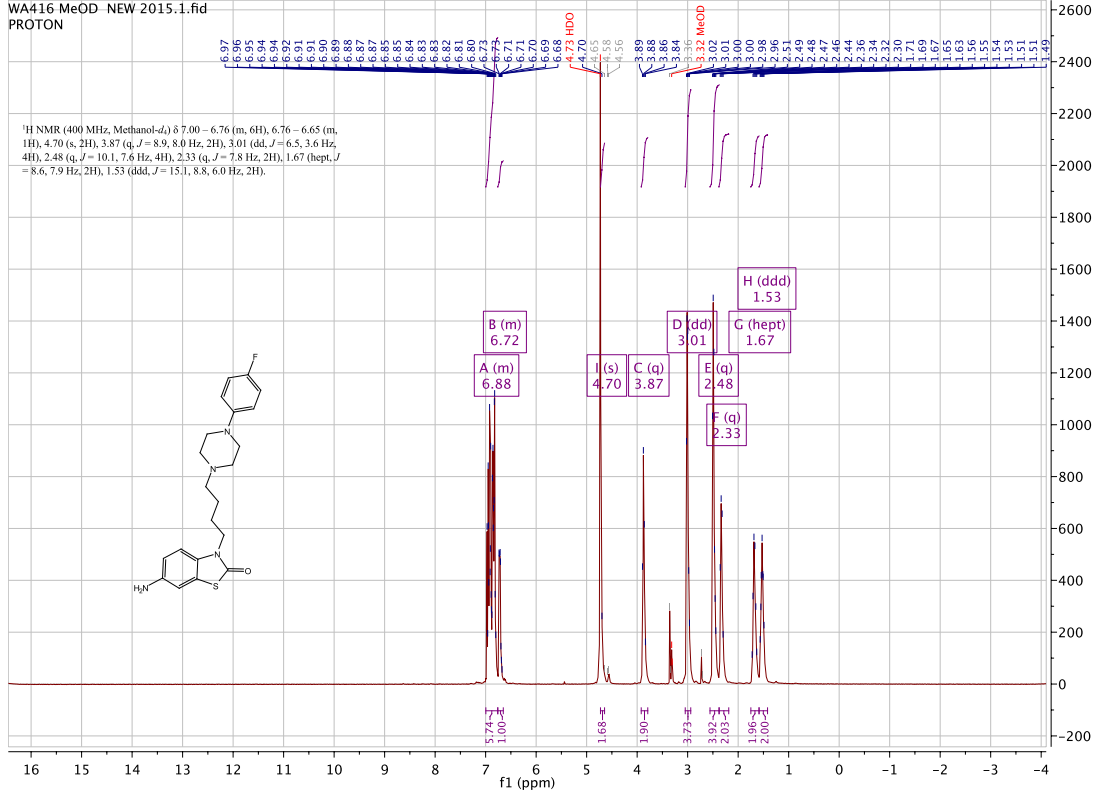




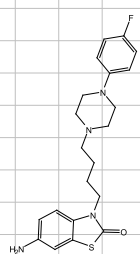
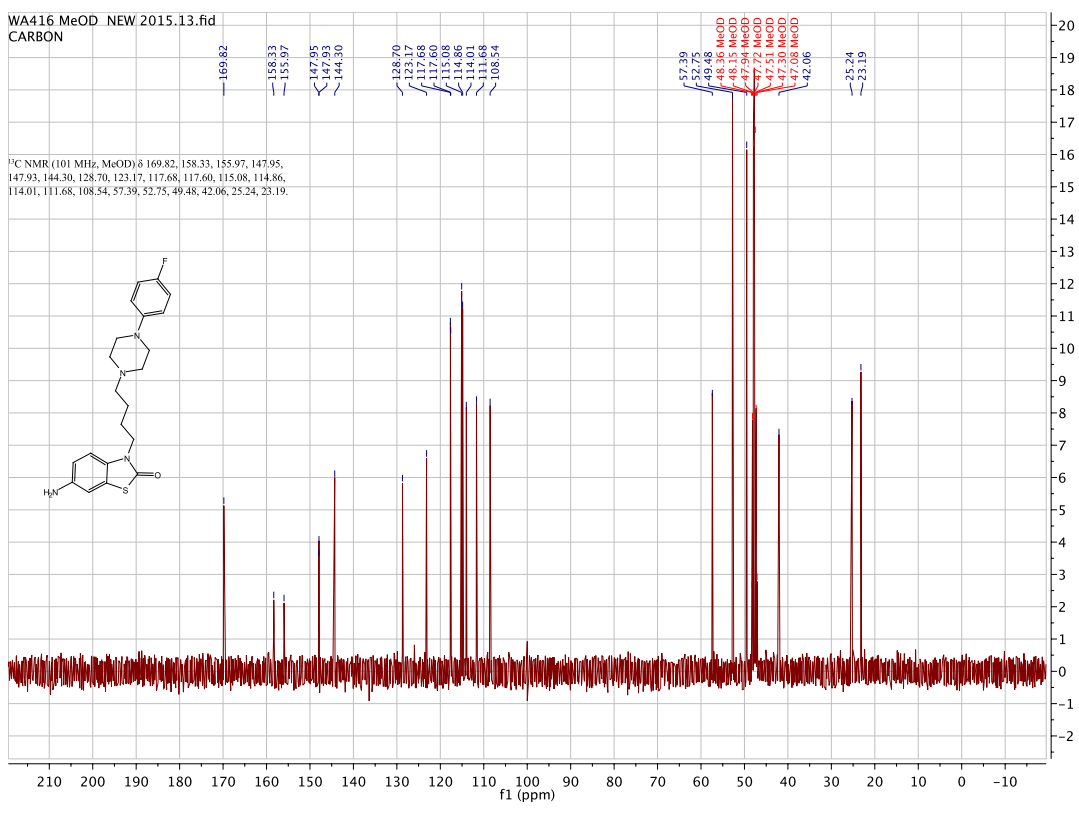
6-amino-3-(4-(4-(4-fluorophenyl)piperazin-1-yl)butyl)benzo[d]thiazol-2(3H)-one. [WA416]

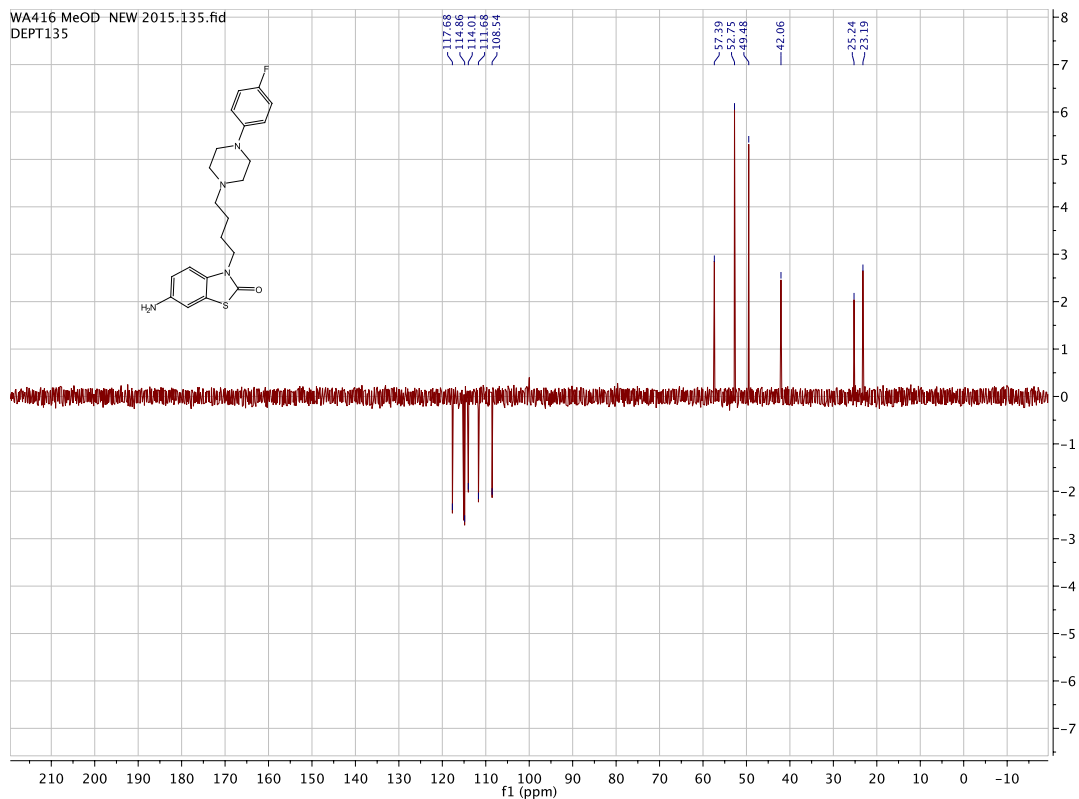


WA416 MeOD - NEW 2015.1.fid
 PROTON

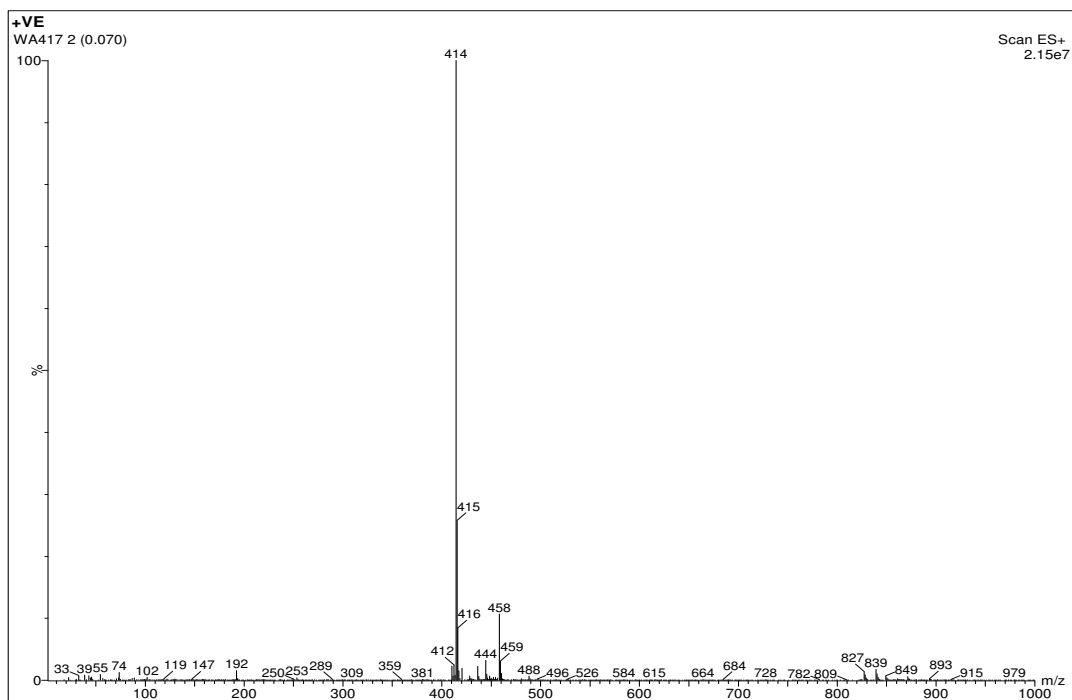


WA416 MeOD - NEW 2015.13.fid
 CARBON



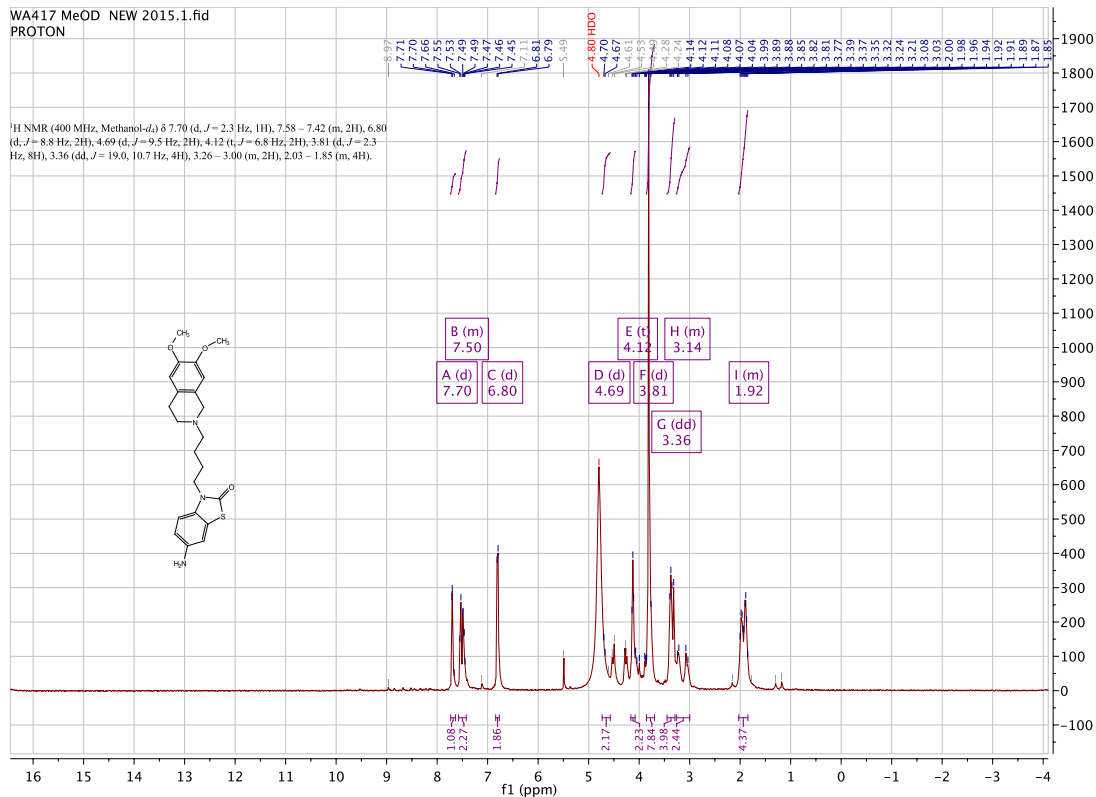


6-amino-3-(4-(6,7-dimethoxy-3,4-dihydroisoquinolin-2(1H)-yl)butyl)benzo[d]thiazol-2(3H)-one. [WA417]



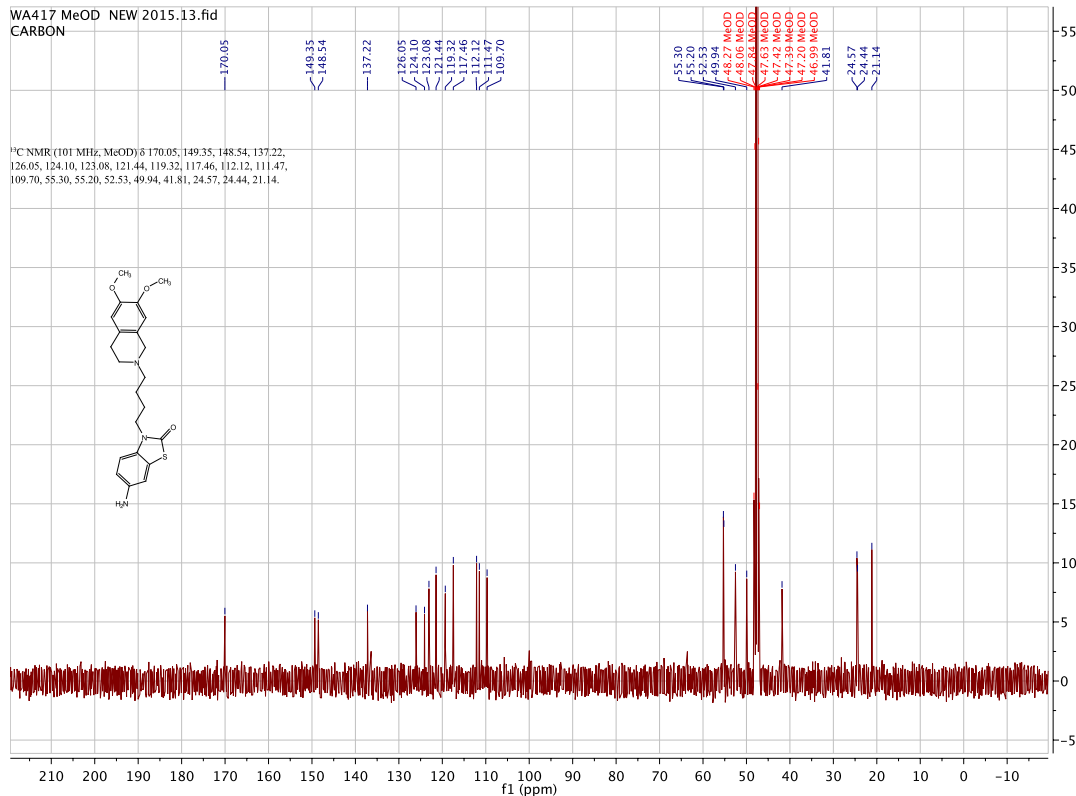
WA417 MeOD NEW 2015.1.fid
 PROTON

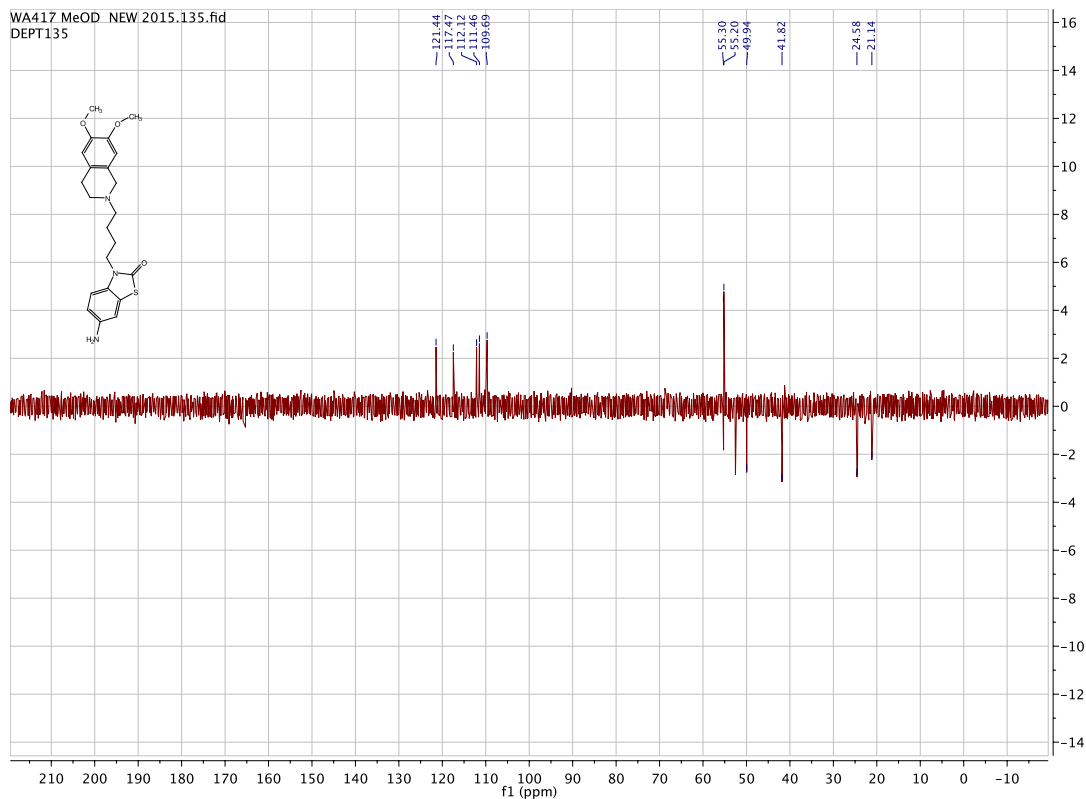
¹H NMR (400 MHz, Methanol-d₄) δ 7.70 (d, *J* = 2.3 Hz, 1H), 7.58 – 7.42 (m, 2H), 6.80 (d, *J* = 8.8 Hz, 2H), 4.69 (d, *J* = 9.5 Hz, 2H), 4.12 (t, *J* = 6.8 Hz, 2H), 3.81 (d, *J* = 2.3 Hz, 8H), 3.36 (dd, *J* = 19.0, 10.7 Hz, 4H), 3.26 – 3.00 (m, 2H), 2.03 – 1.85 (m, 4H).



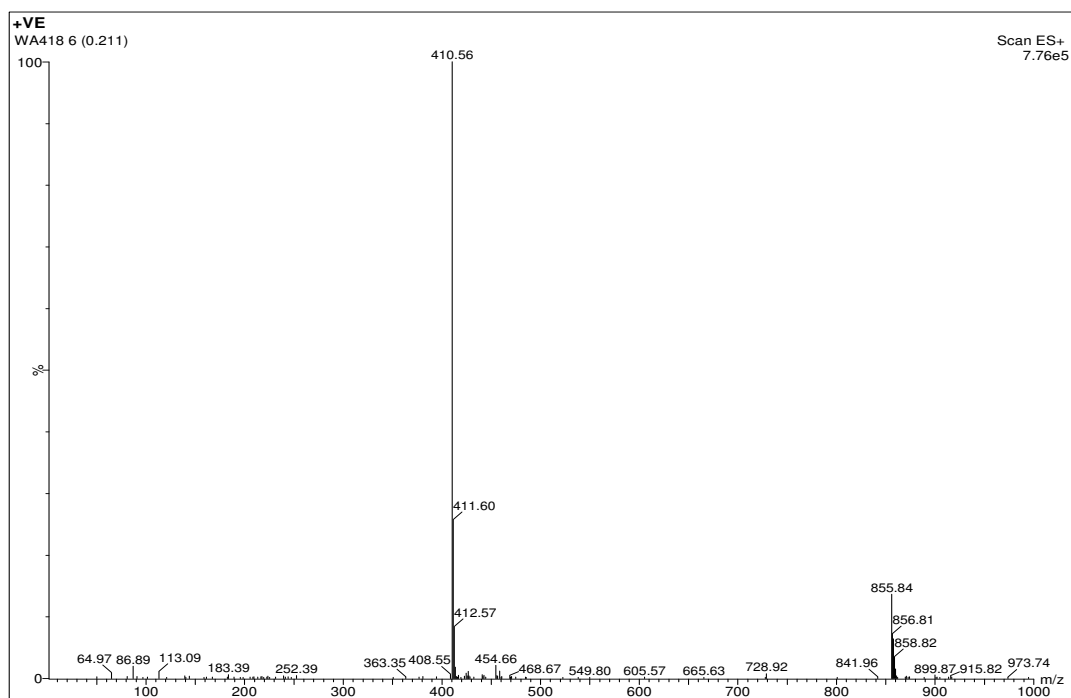
WA417 MeOD NEW 2015.13.fid
 CARBON

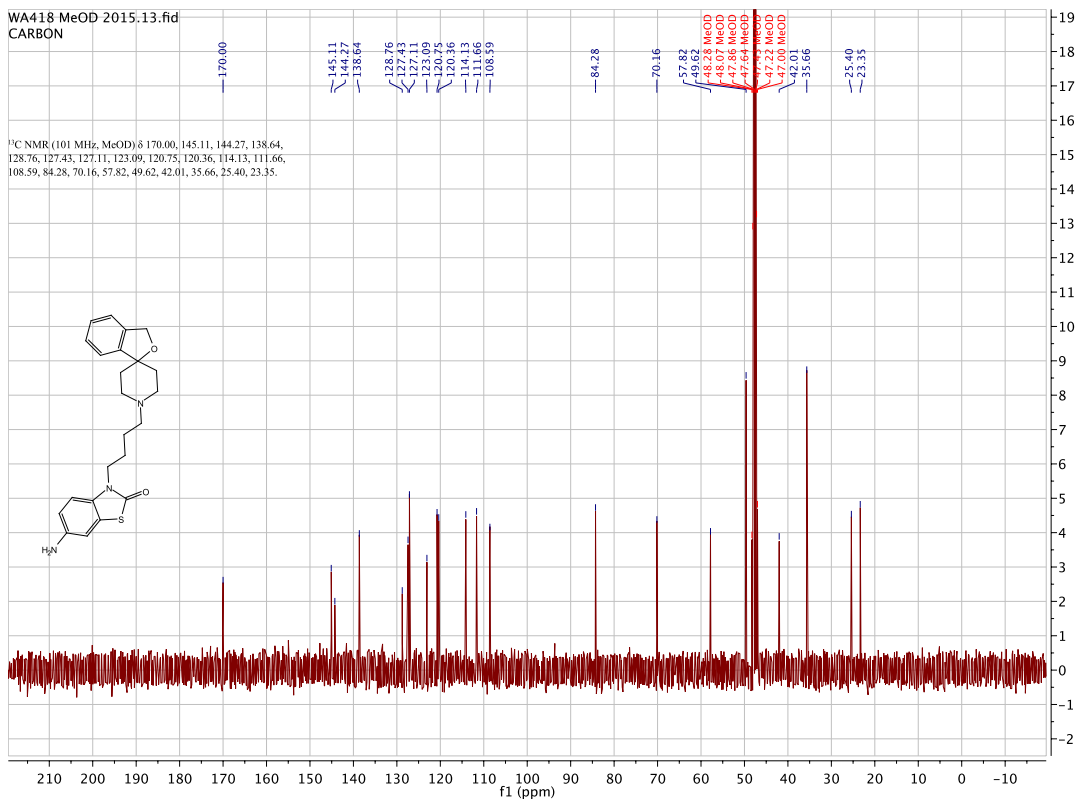
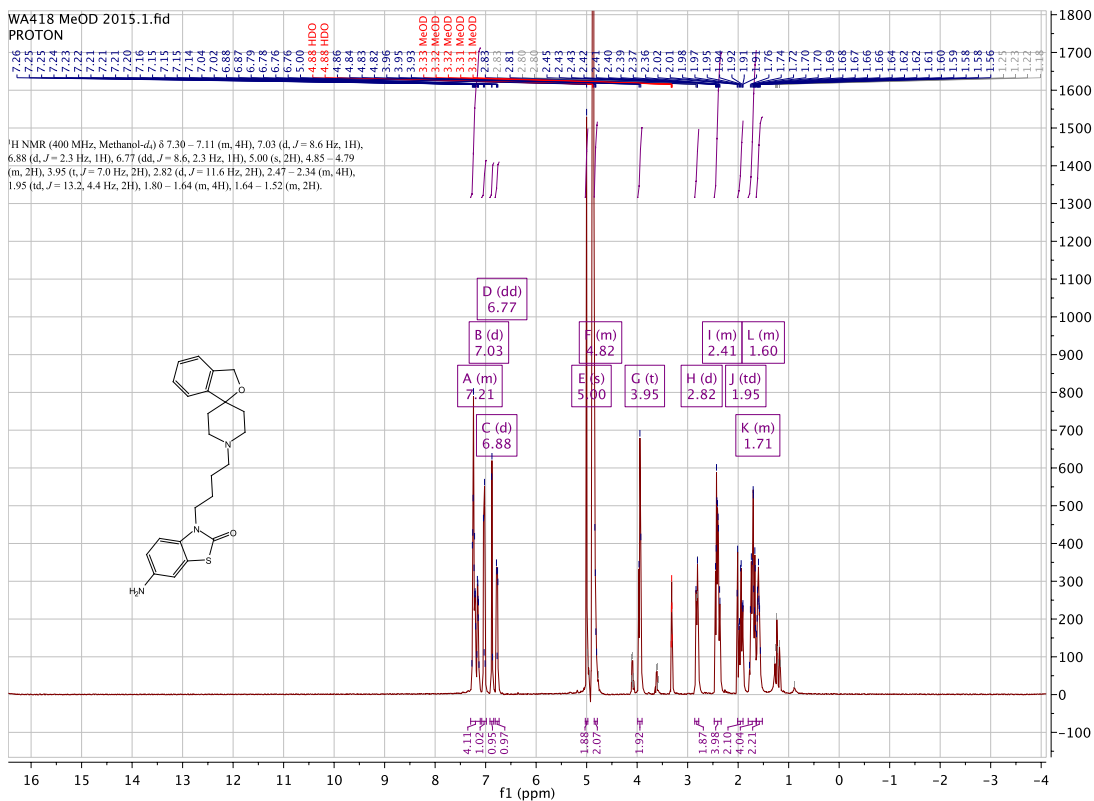
¹³C NMR (101 MHz, MeOD) δ 170.05, 149.35, 148.54, 137.22, 126.05, 124.10, 123.08, 121.44, 119.32, 117.46, 112.12, 111.47, 109.70, 55.30, 55.20, 52.53, 49.94, 41.81, 24.57, 24.44, 21.14.

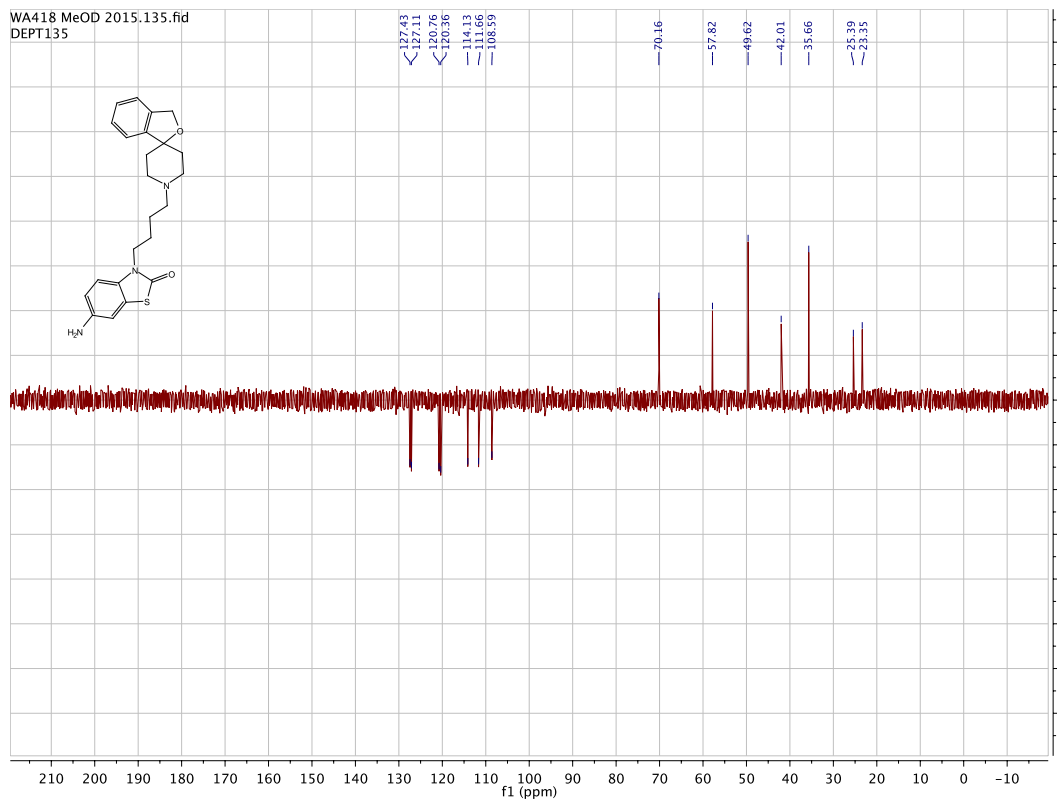




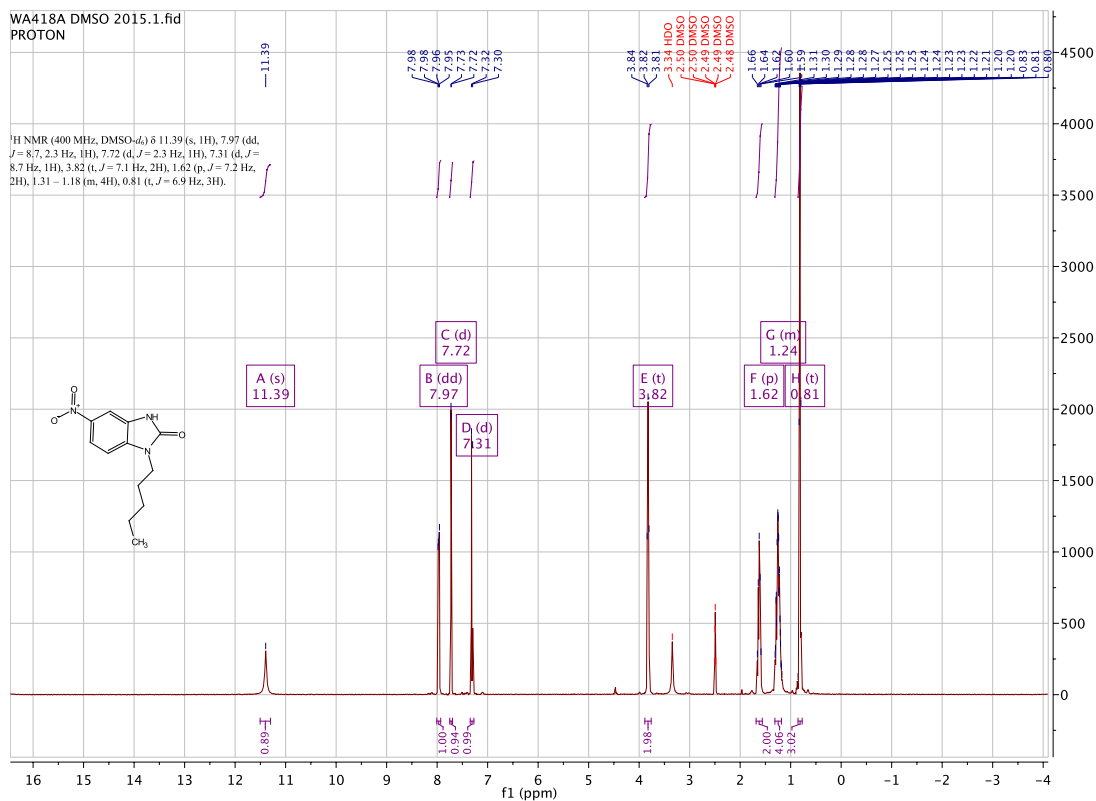
3-(4-(3H-spiro[isobenzofuran-1,4'-piperidin]-1'-yl)butyl)-6-aminobenzo[d]thiazol-2(3H)-one. [WA418]





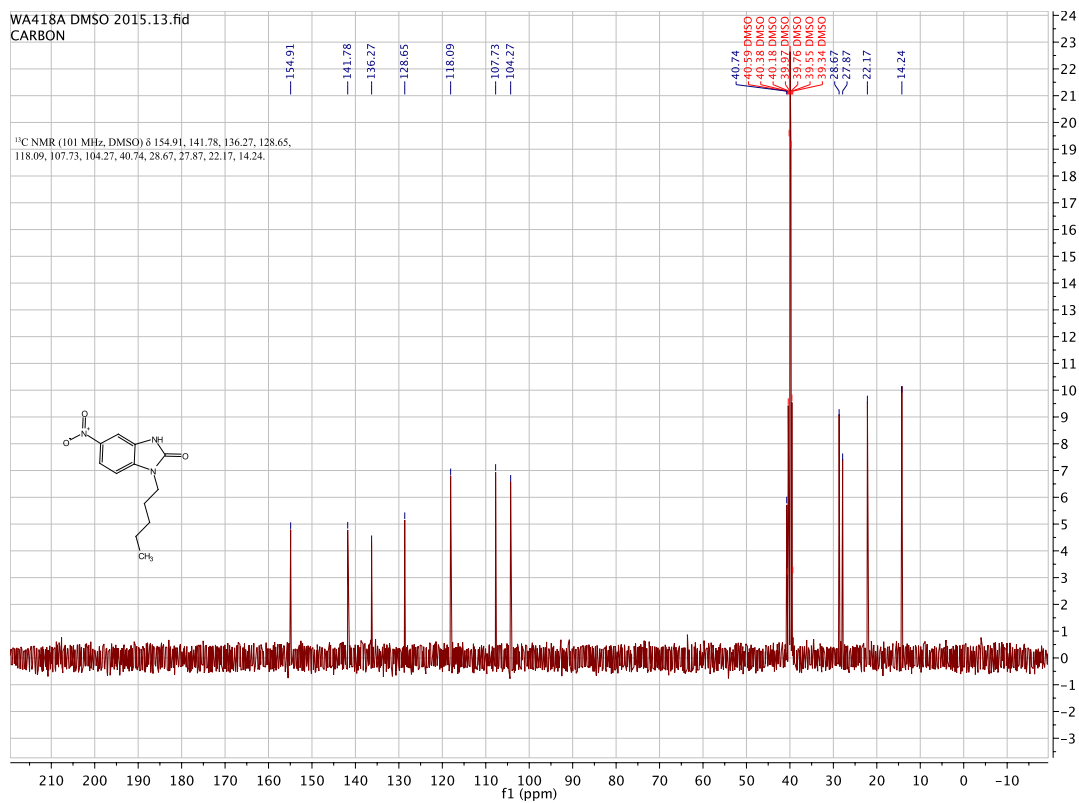


6-nitro-1-pentyl-1,3-dihydro-2H-benzo[d]imidazol-2-one. [WA418A]

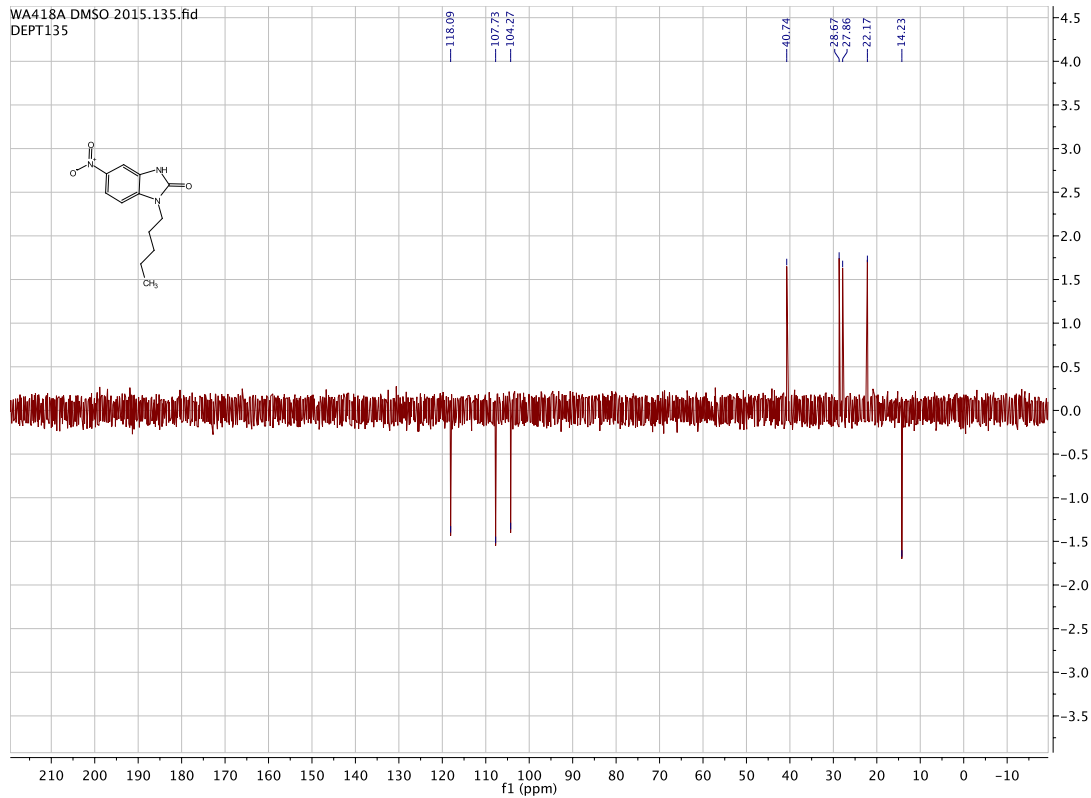


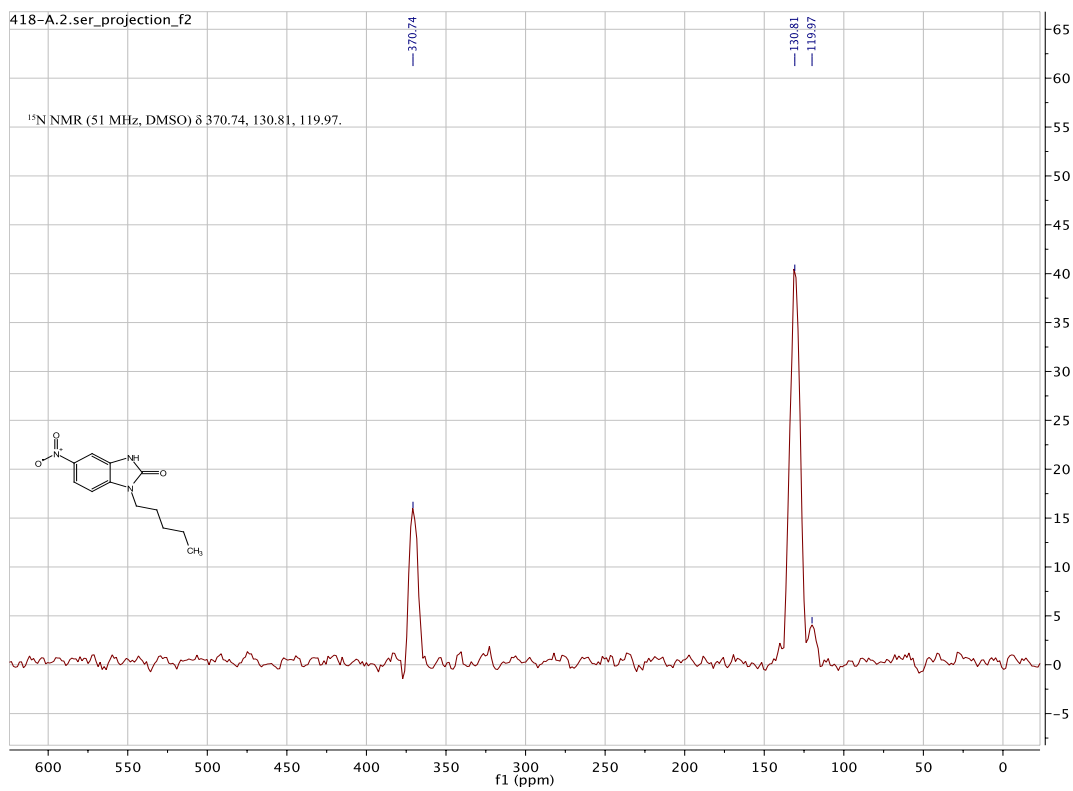
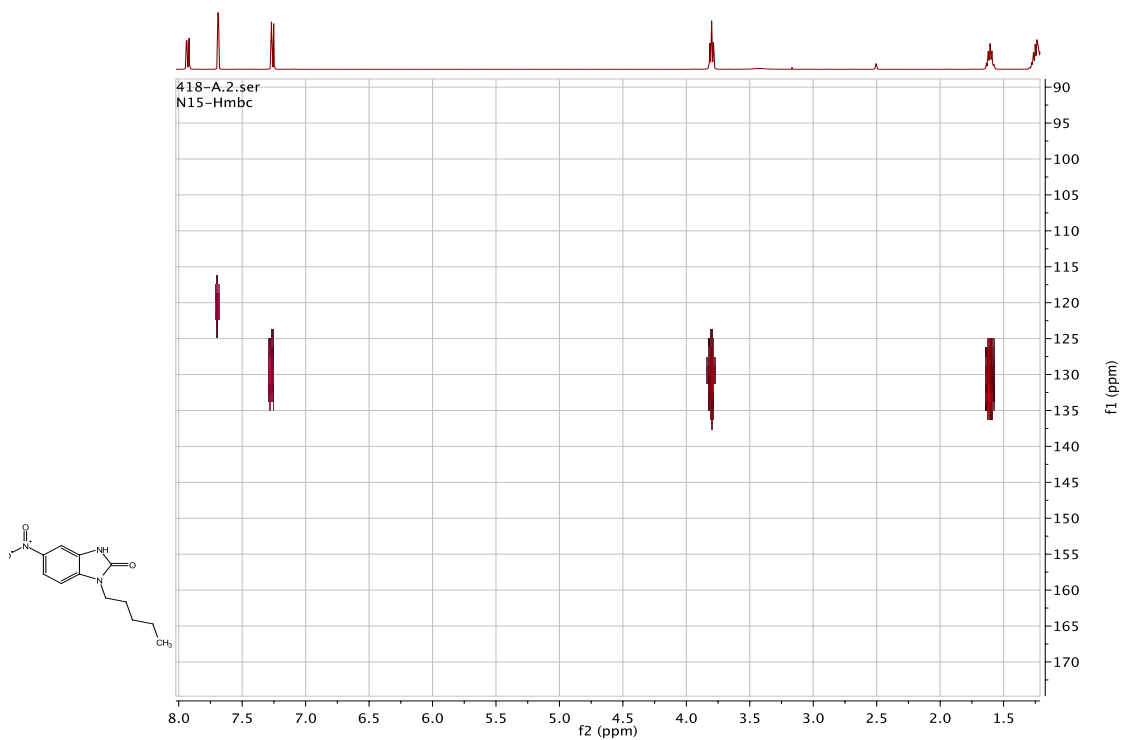
WA418A DMSO 2015.13.fid
CARBON

¹³C NMR (101 MHz, DMSO) δ 154.91, 141.78, 136.27, 128.65,
118.09, 107.73, 104.27, 40.74, 28.67, 27.87, 22.17, 14.24.

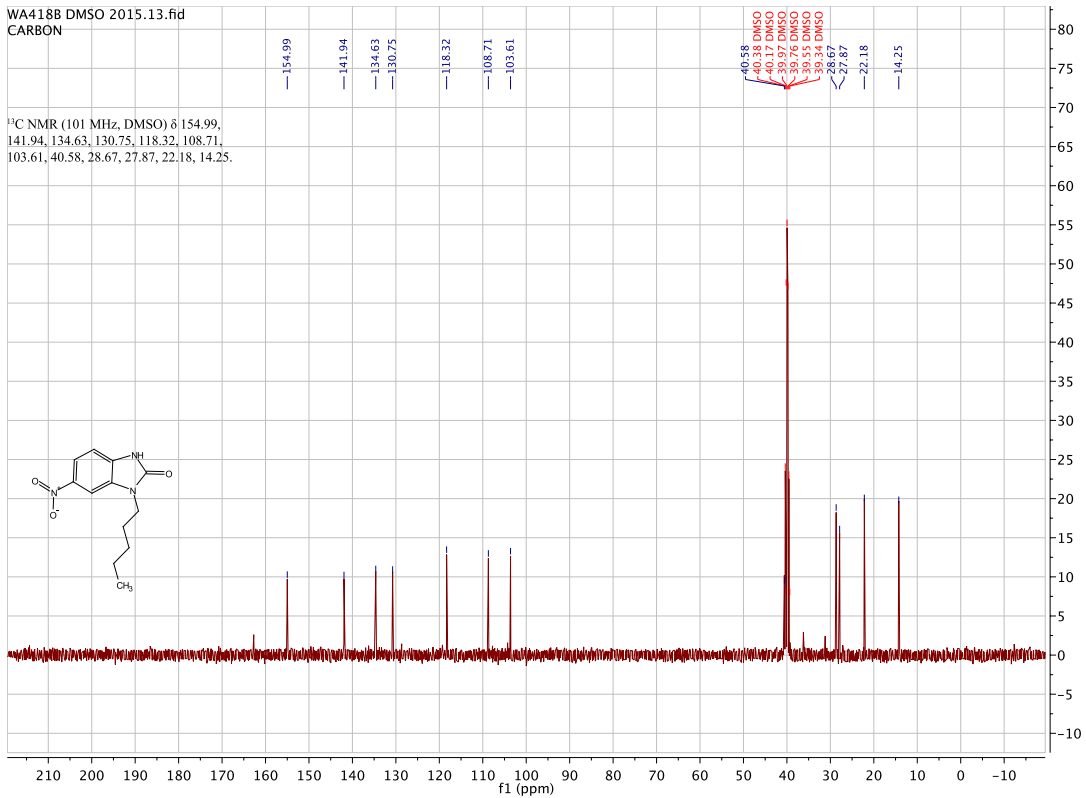
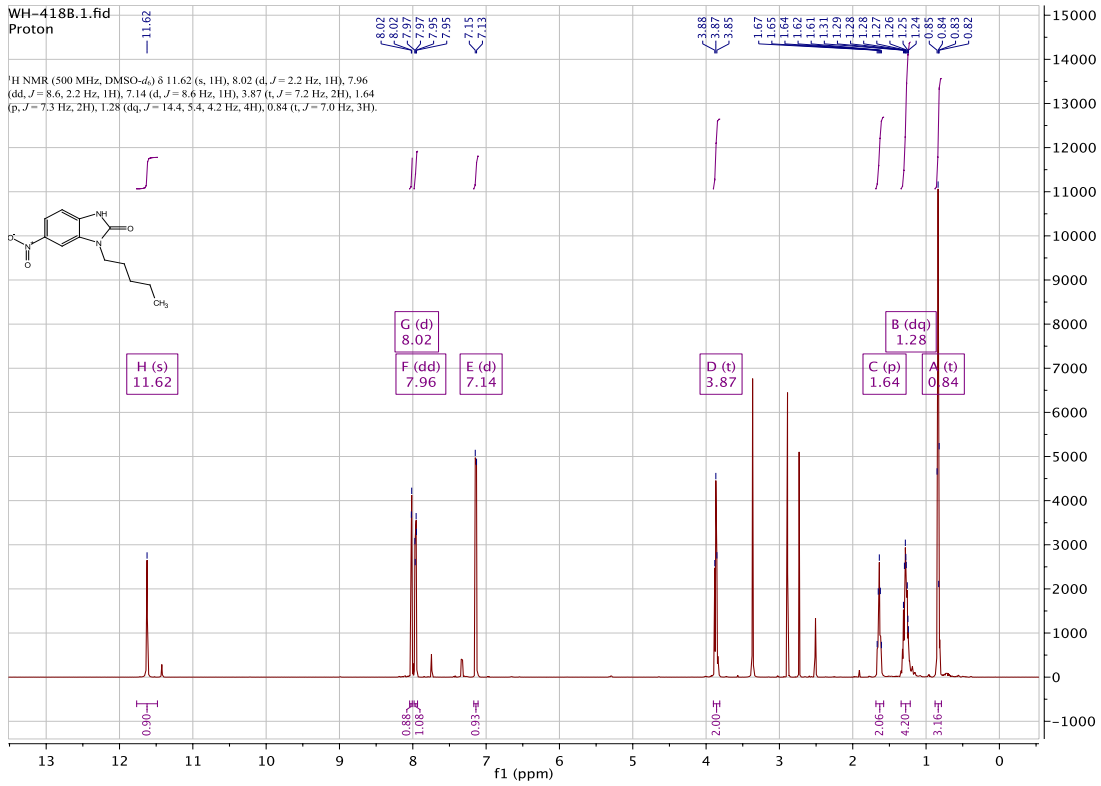


WA418A DMSO 2015.135.fid
DEPT135

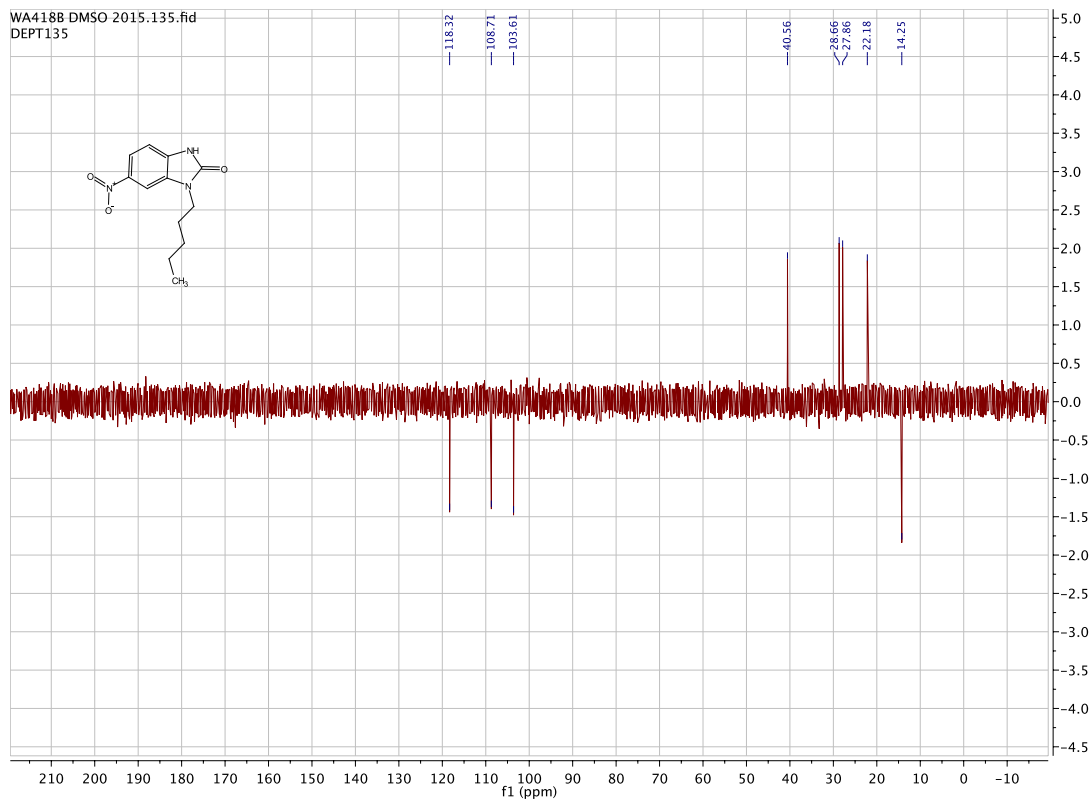




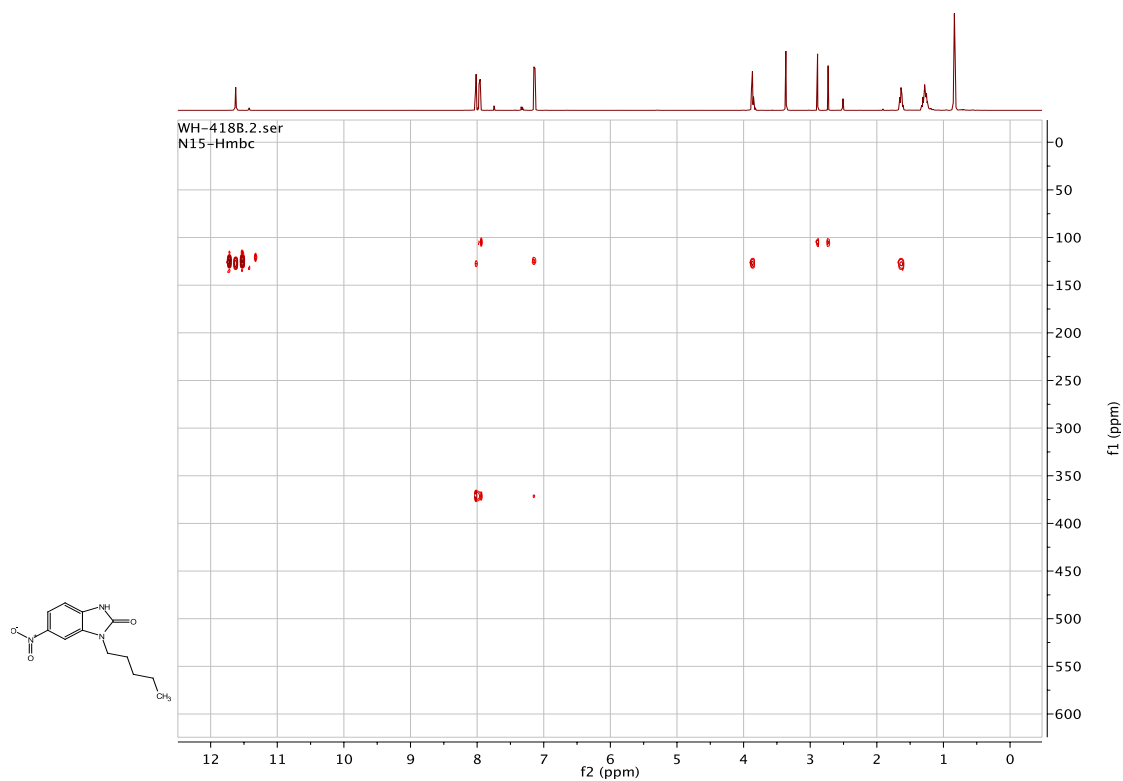
5-nitro-1-pentyl-1,3-dihydro-2H -benzo[d]imidazol-2-one. [WA418B]

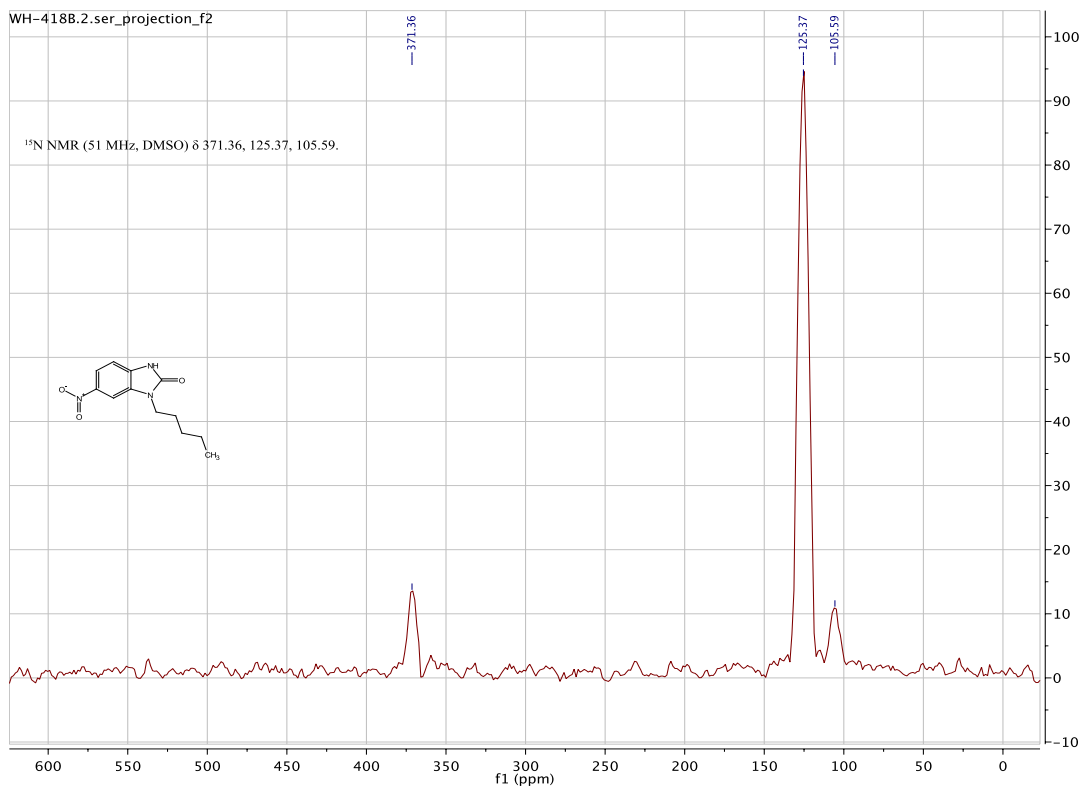


WA4188 DMSO 2015.135.fid
DEPT135

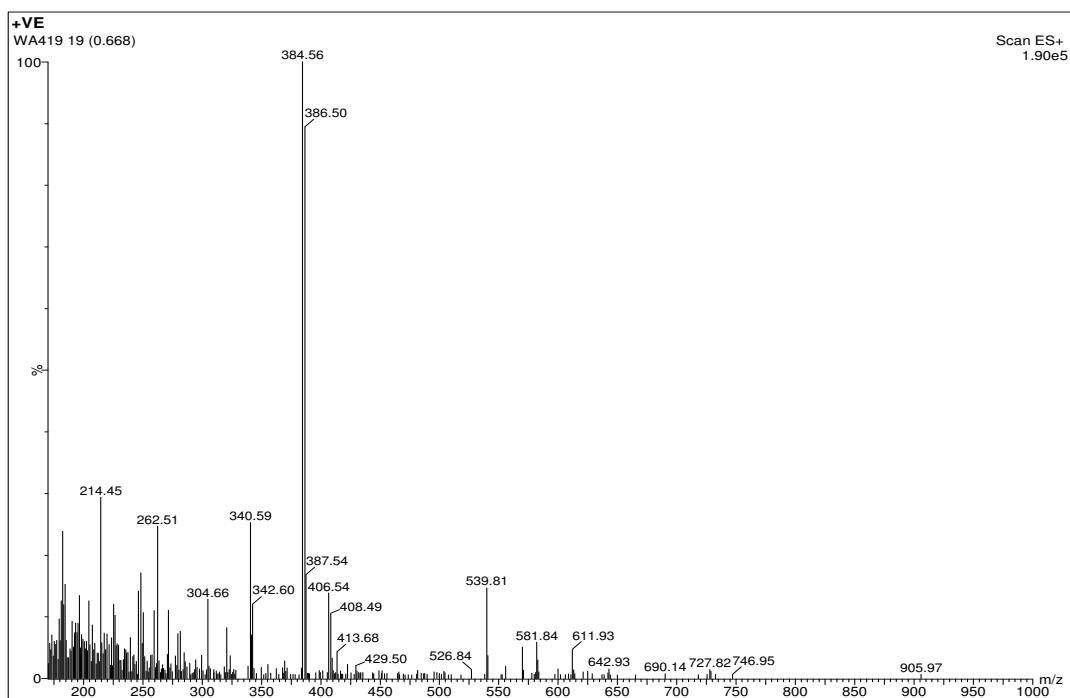


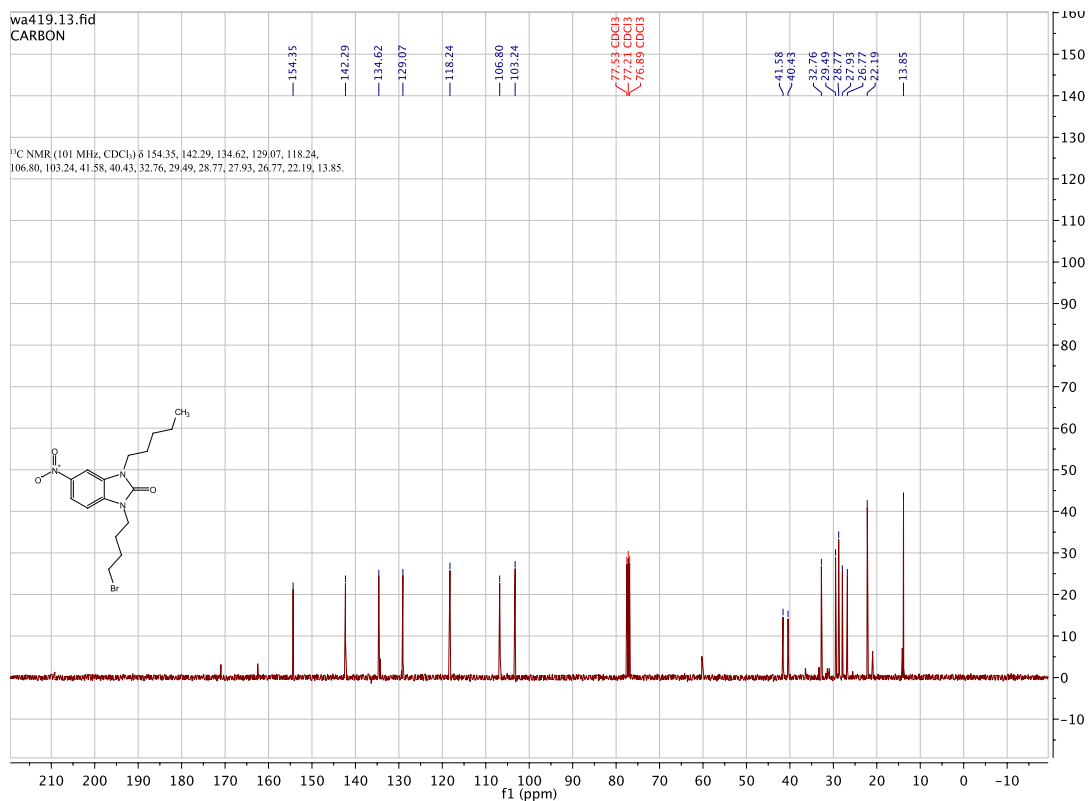
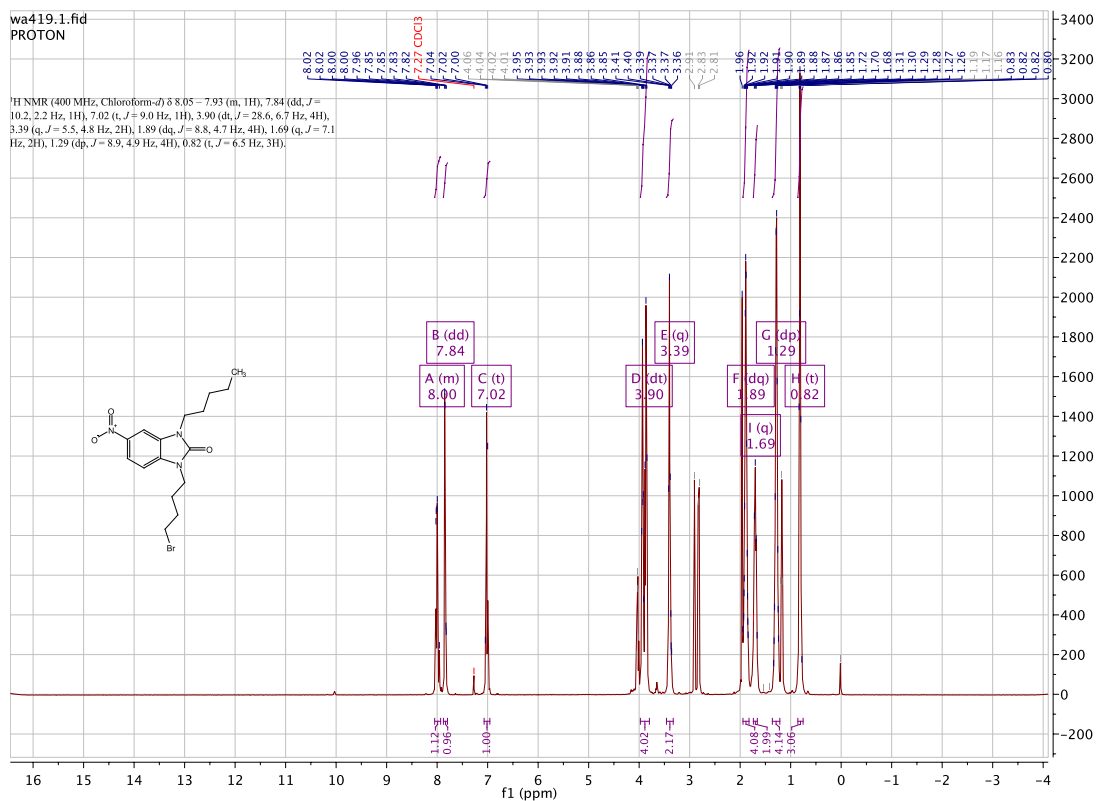
WH-4188.2.ser
N15-Hmbc

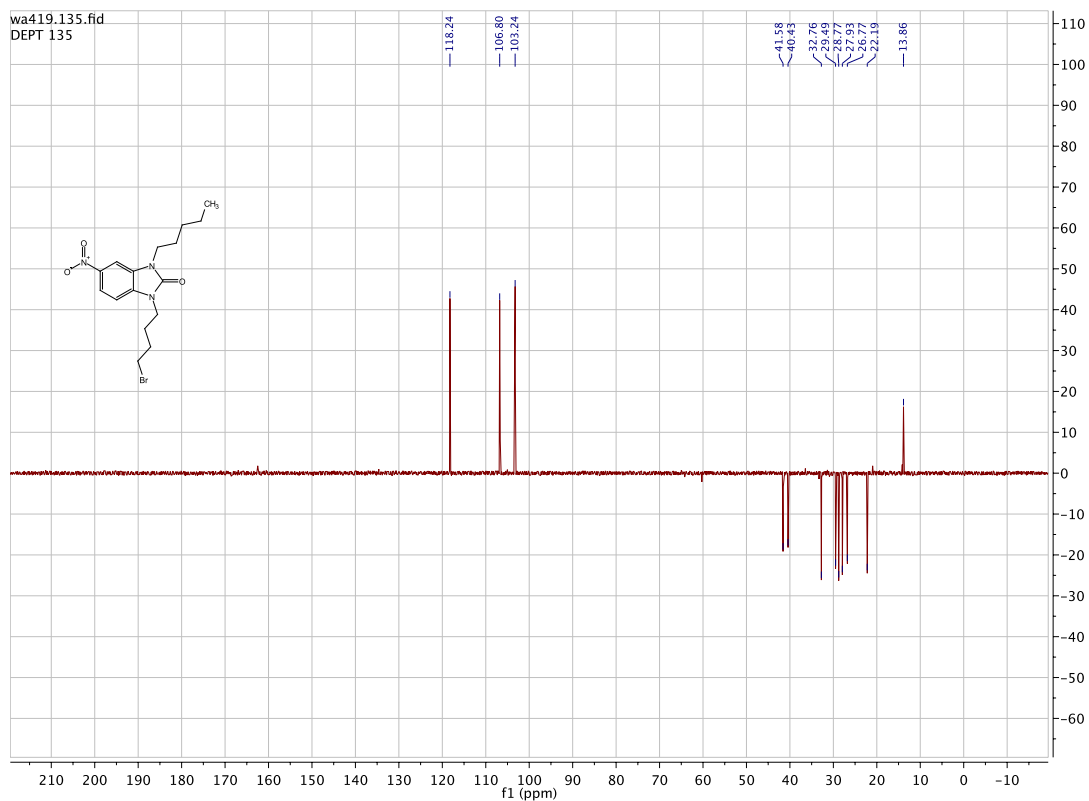




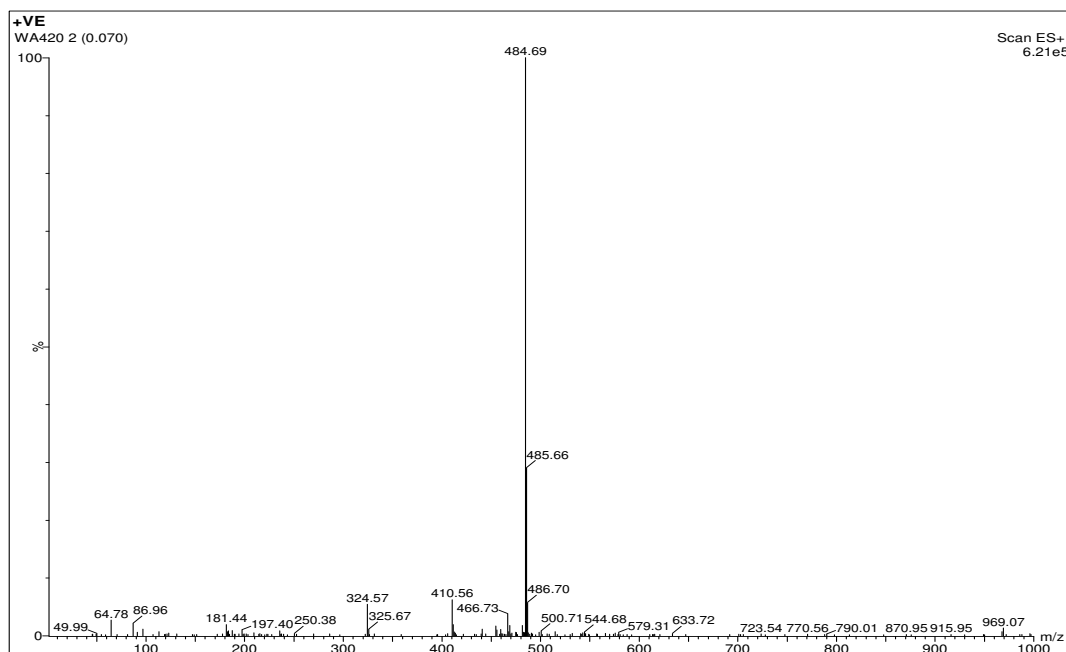
3-(4-bromobutyl)-5-nitro-1-pentyl-1,3-dihydro-2H-benzo[d]imidazol-2-one.
[WA419]

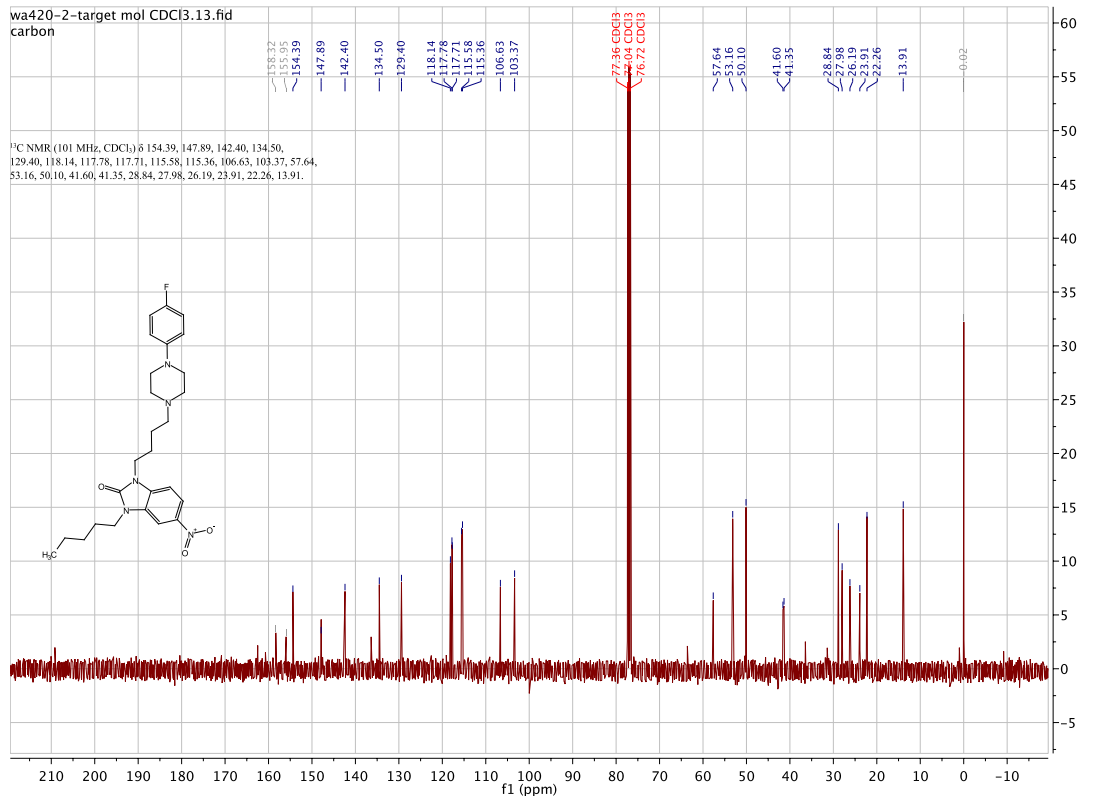
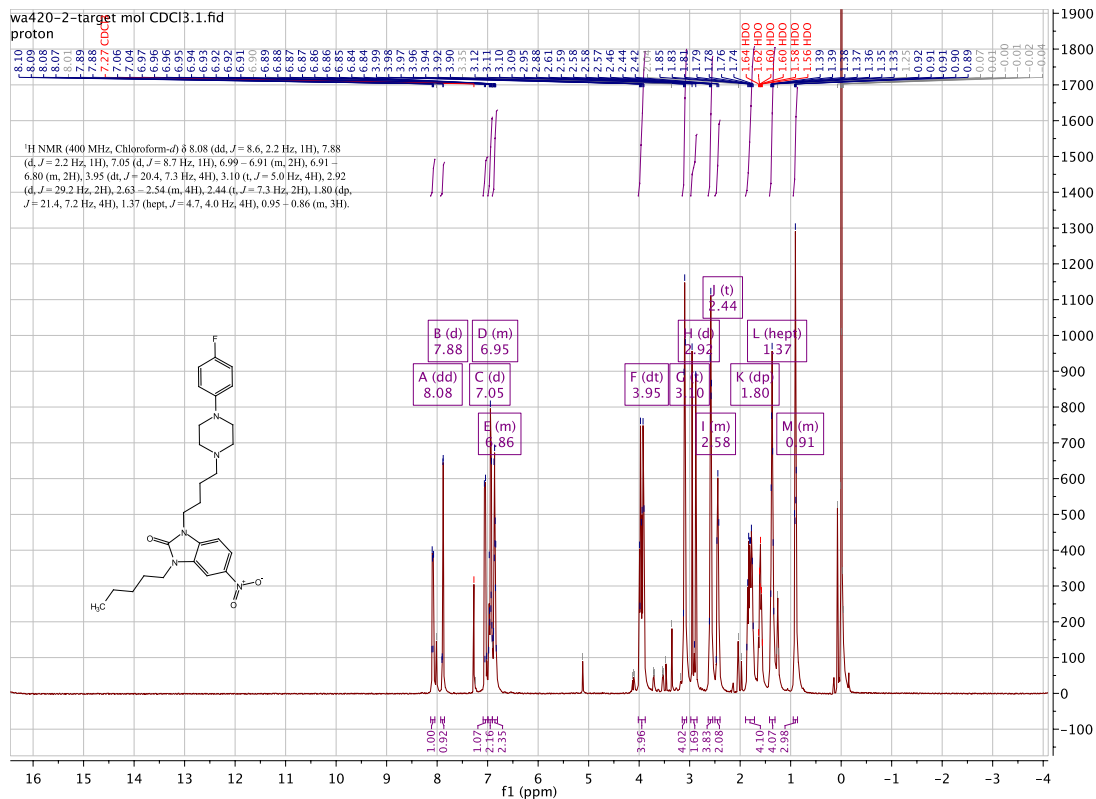


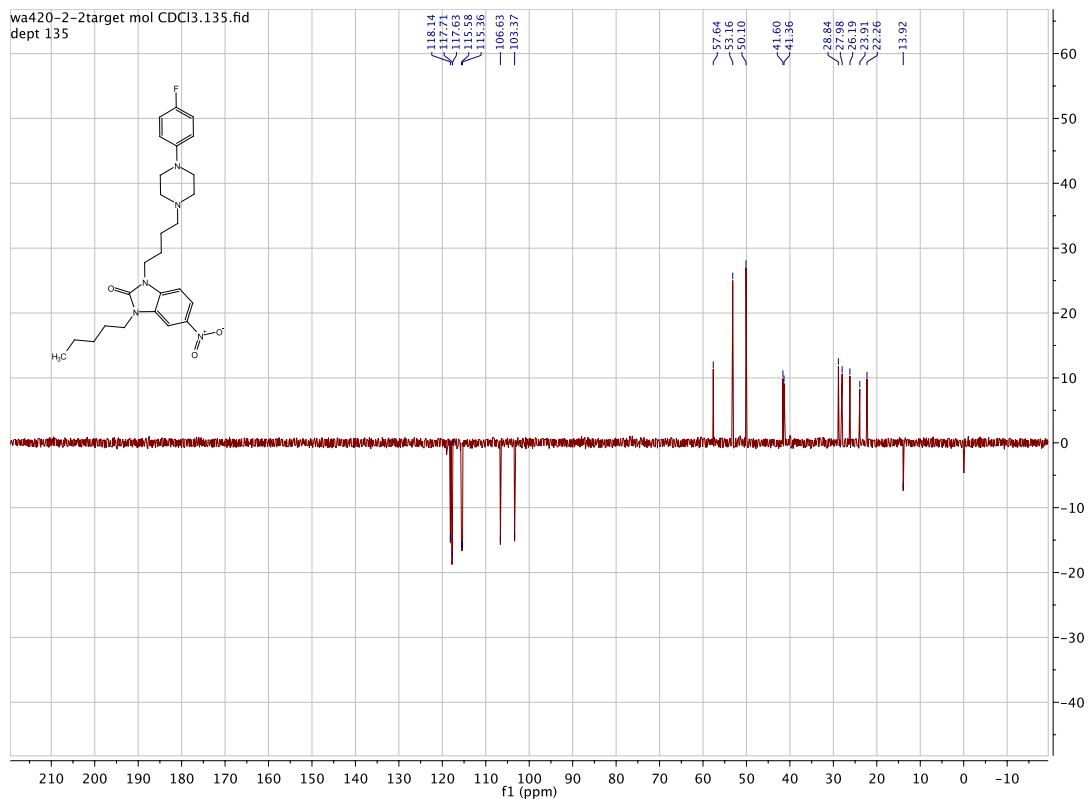




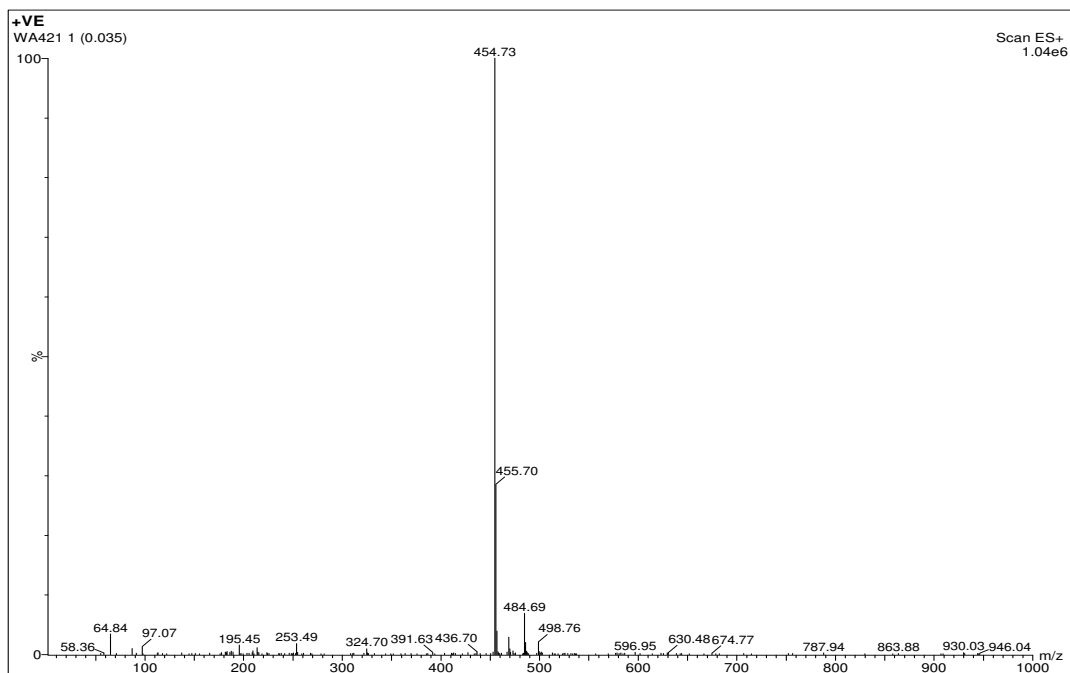
3-(4-(4-(4-fluorophenyl)piperazin-1-yl)butyl)-5-nitro-1-pentyl-1,3-dihydro-2H-benzo[d]imidazol-2-one. [WA420]

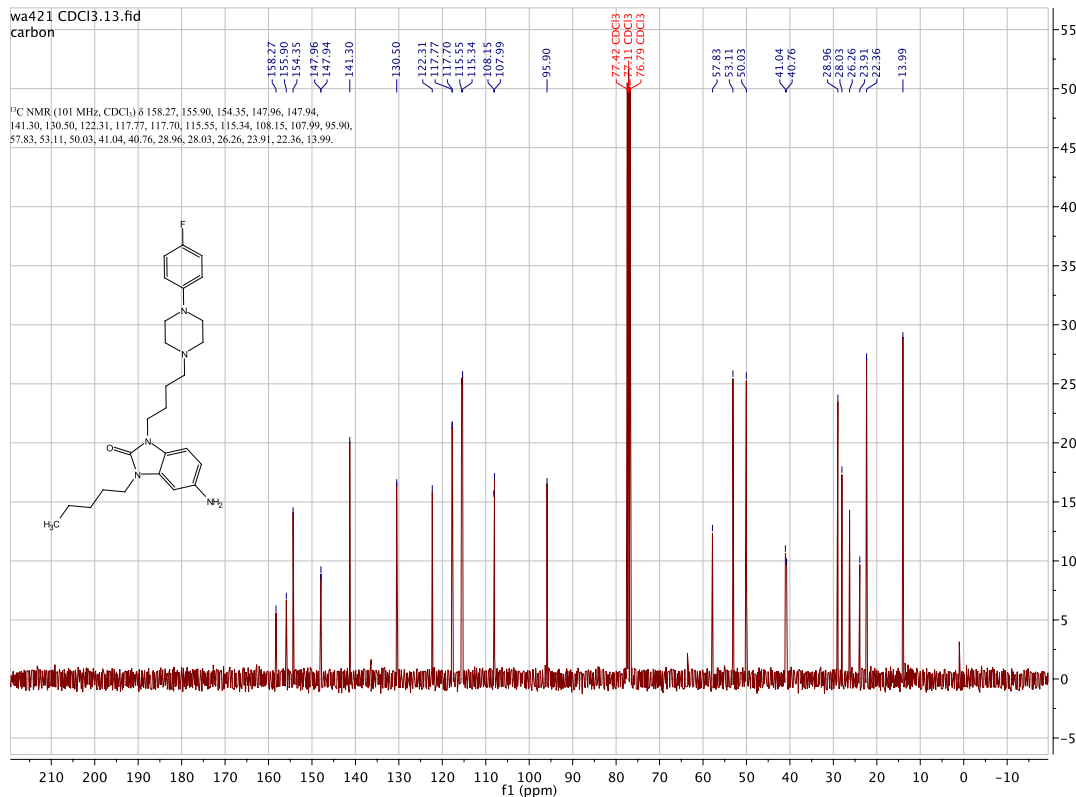
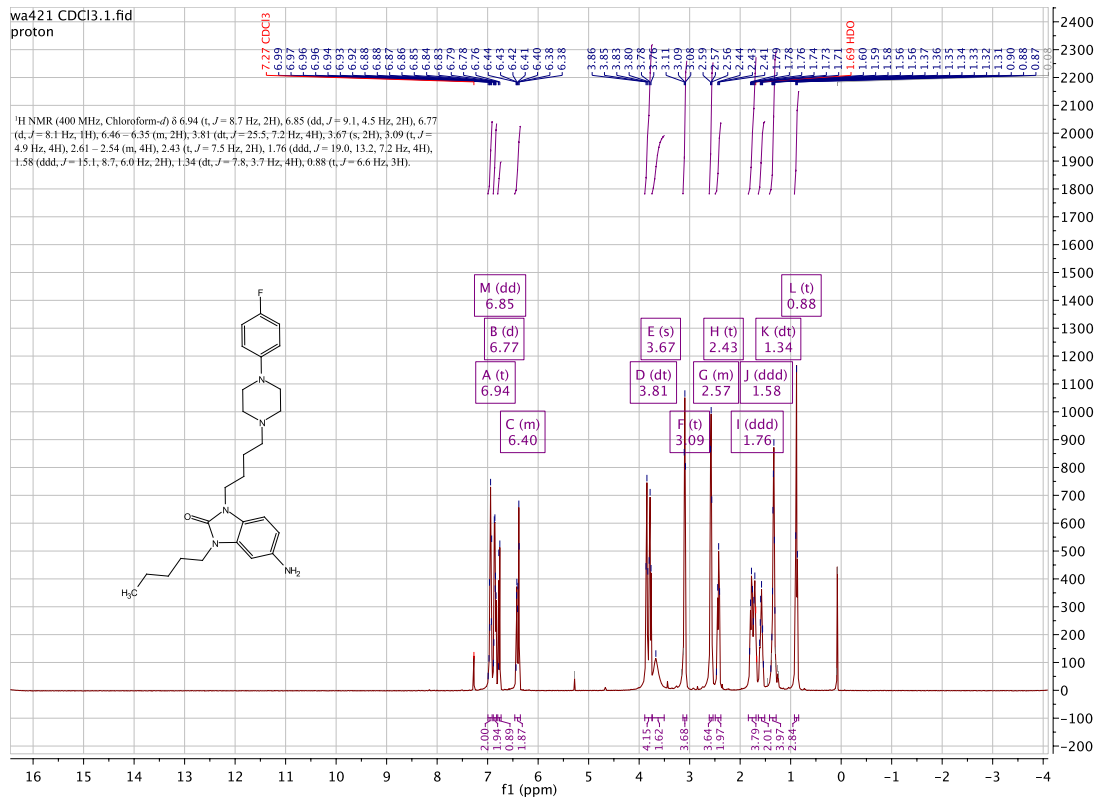


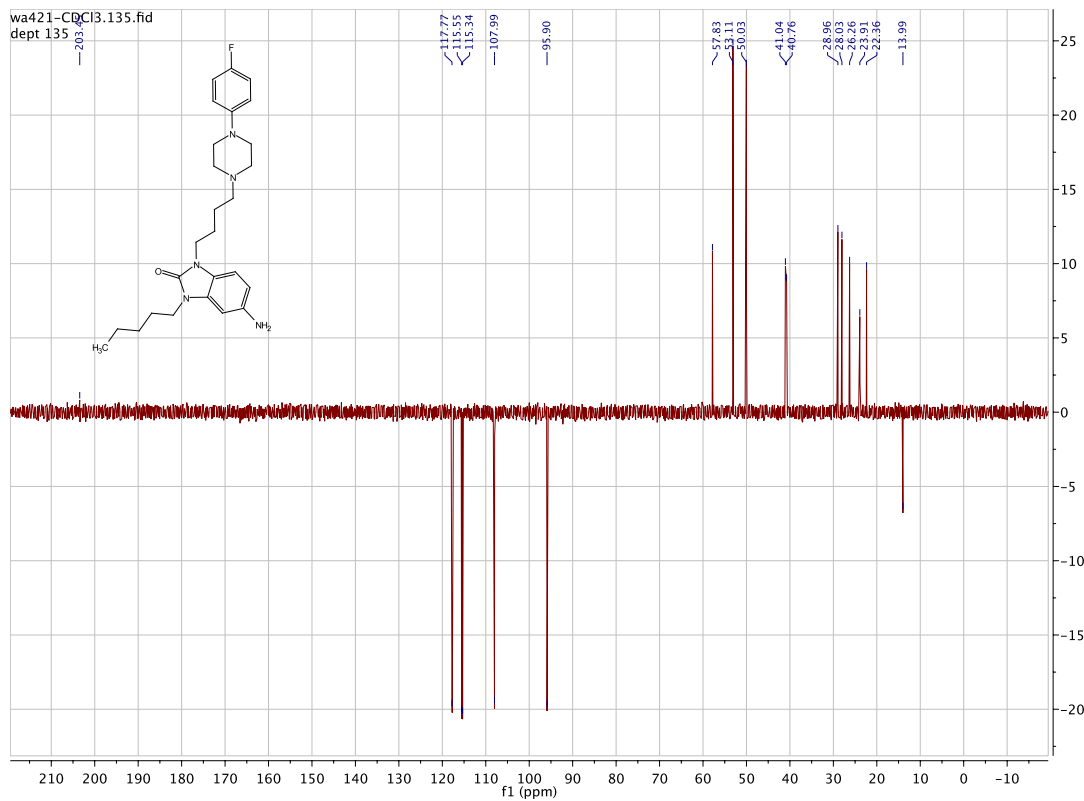




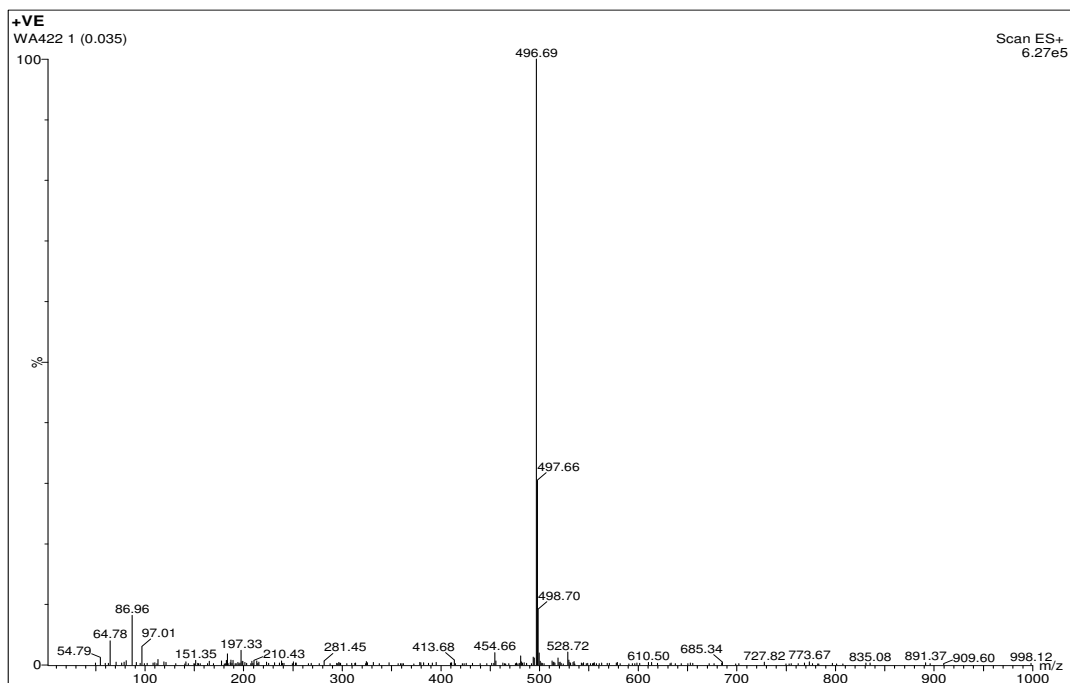
5-amino-3-(4-(4-(4-fluorophenyl)piperazin-1-yl)butyl)-1-pentyl-1,3-dihydro-2H-benzo[d]imidazol-2-one. [WA421]

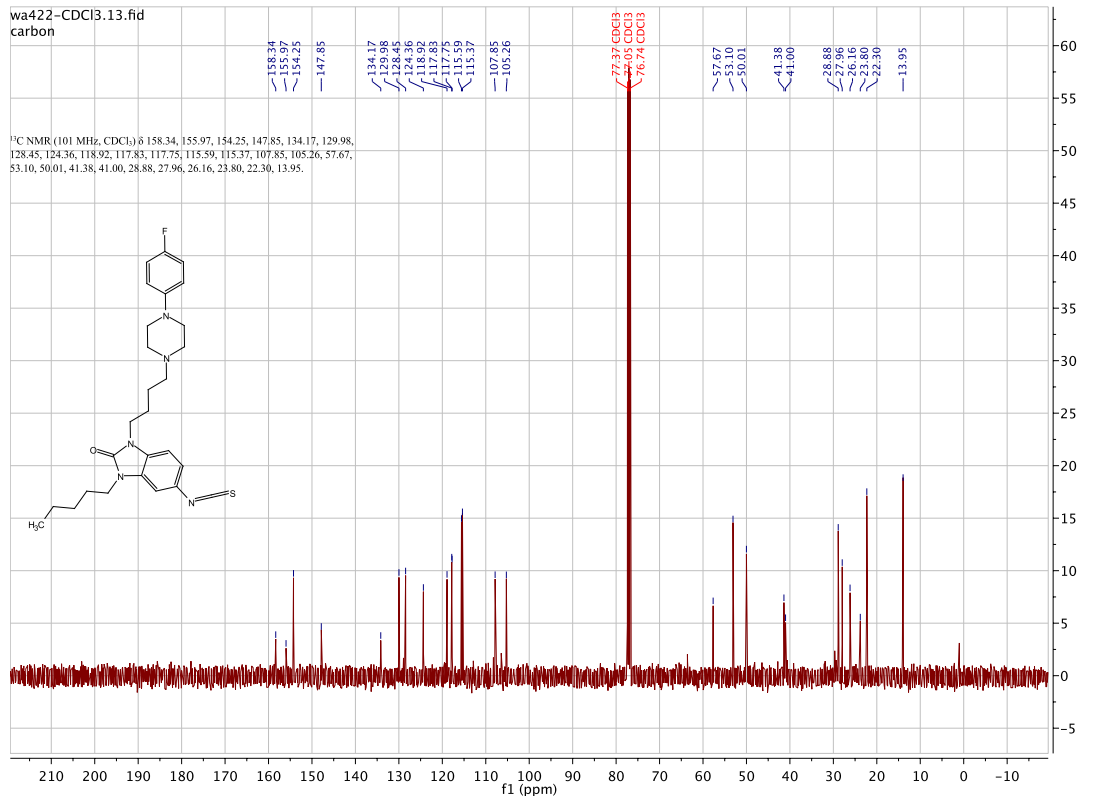
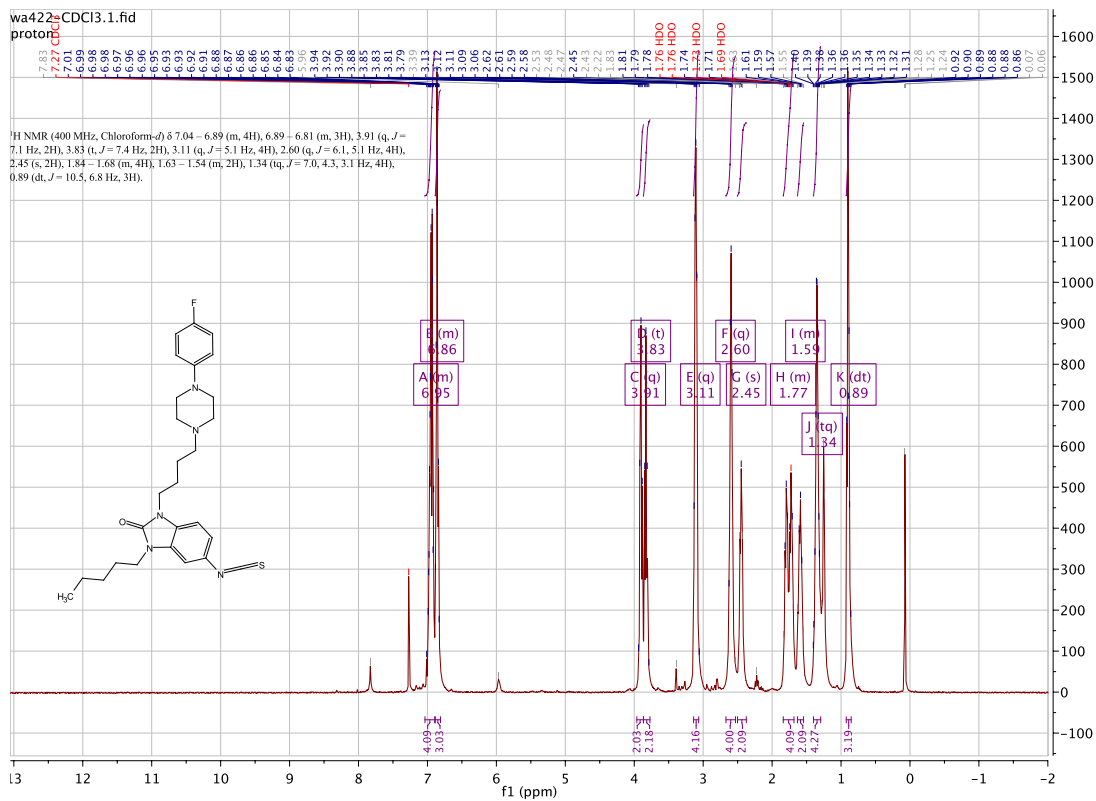


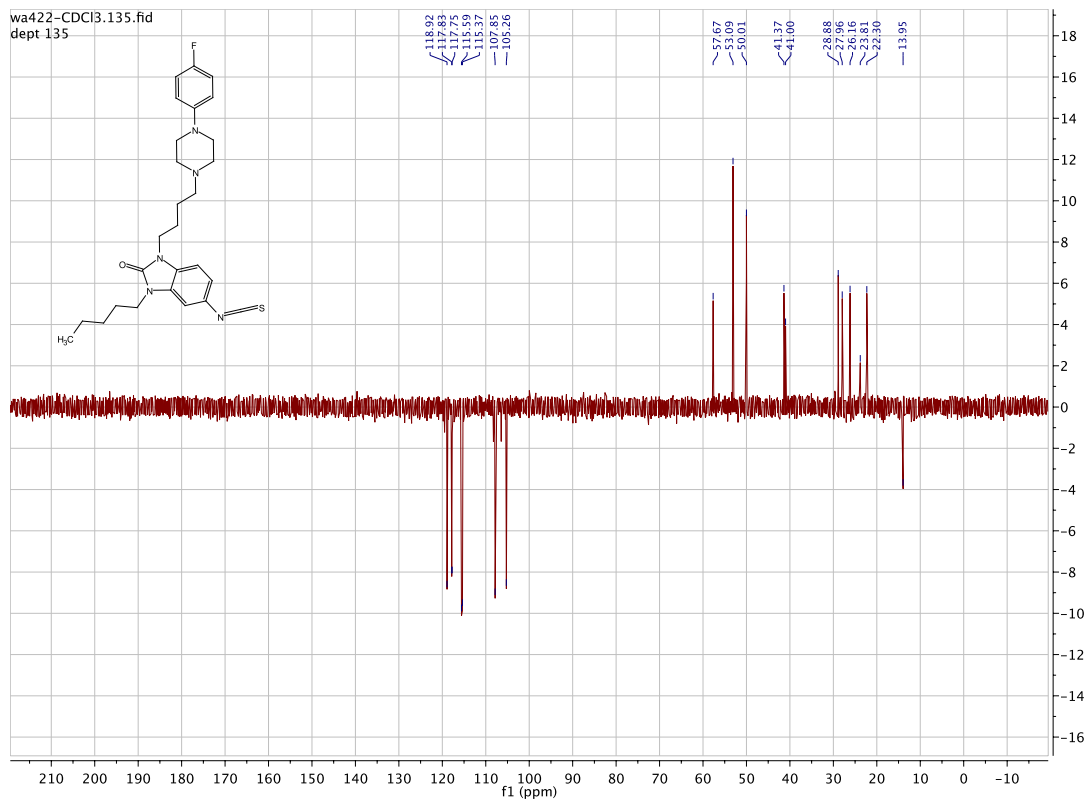




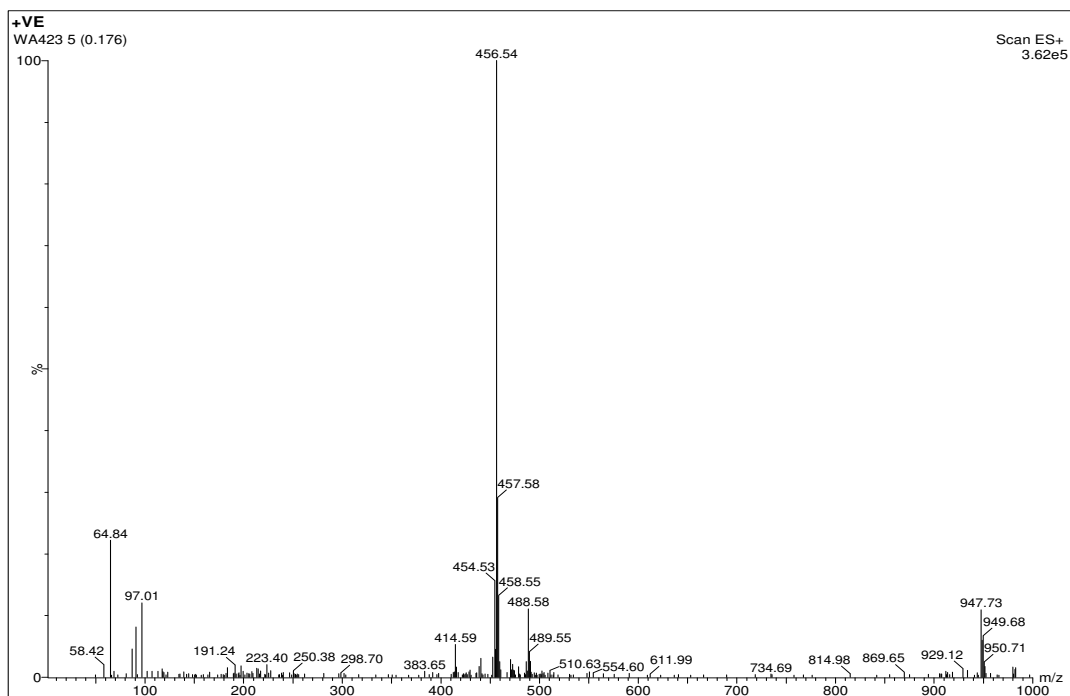
3-(4-(4-(4-fluorophenyl)piperazin-1-yl)butyl)-5-isothiocyanato-1-pentyl-1,3-dihydro-2H-benzo[d]imidazol-2-one. [WA422]

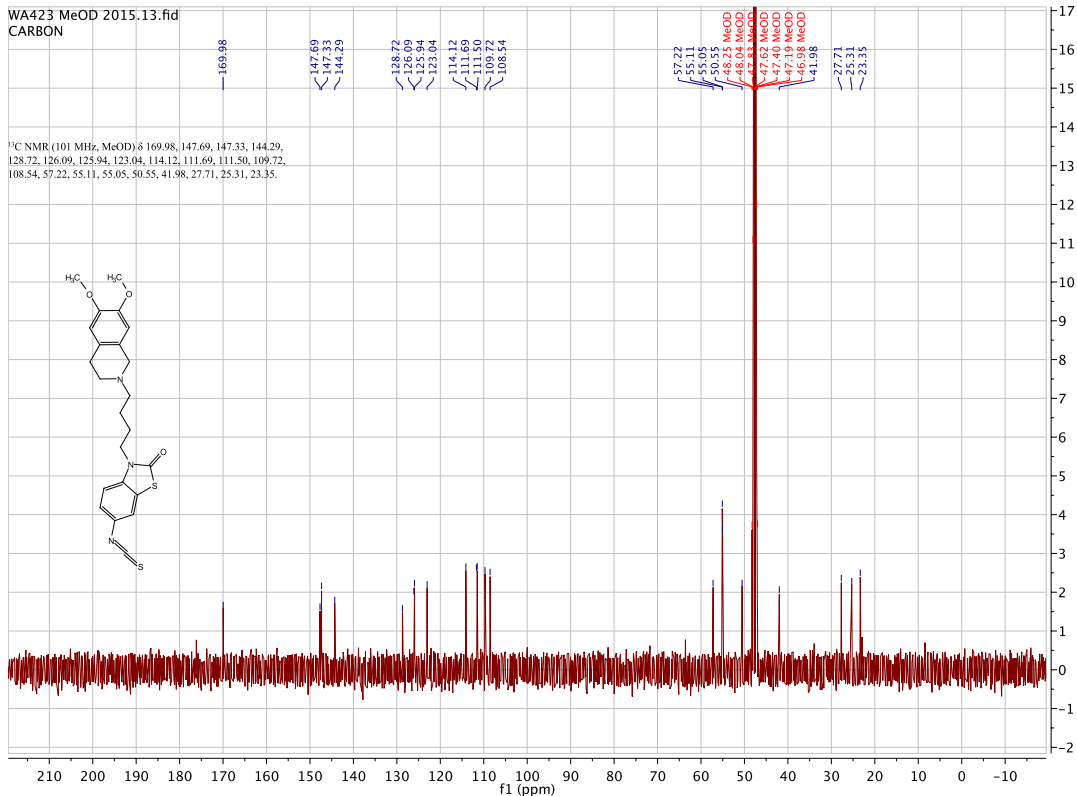
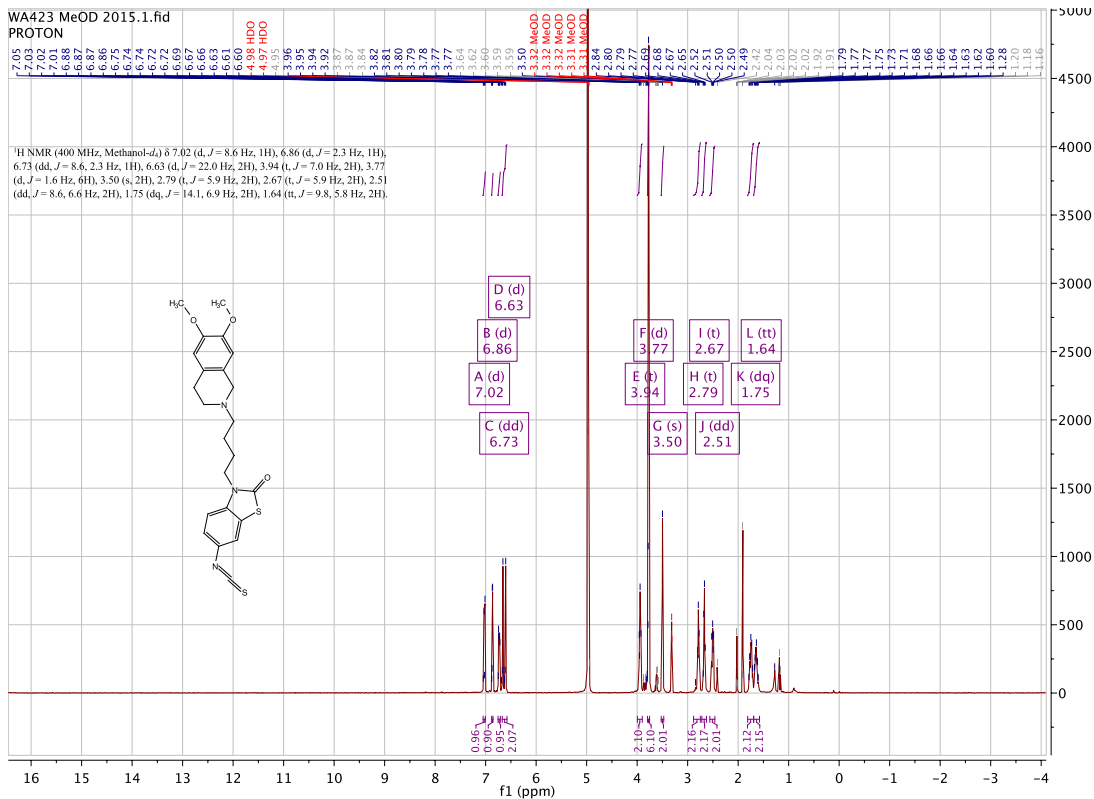


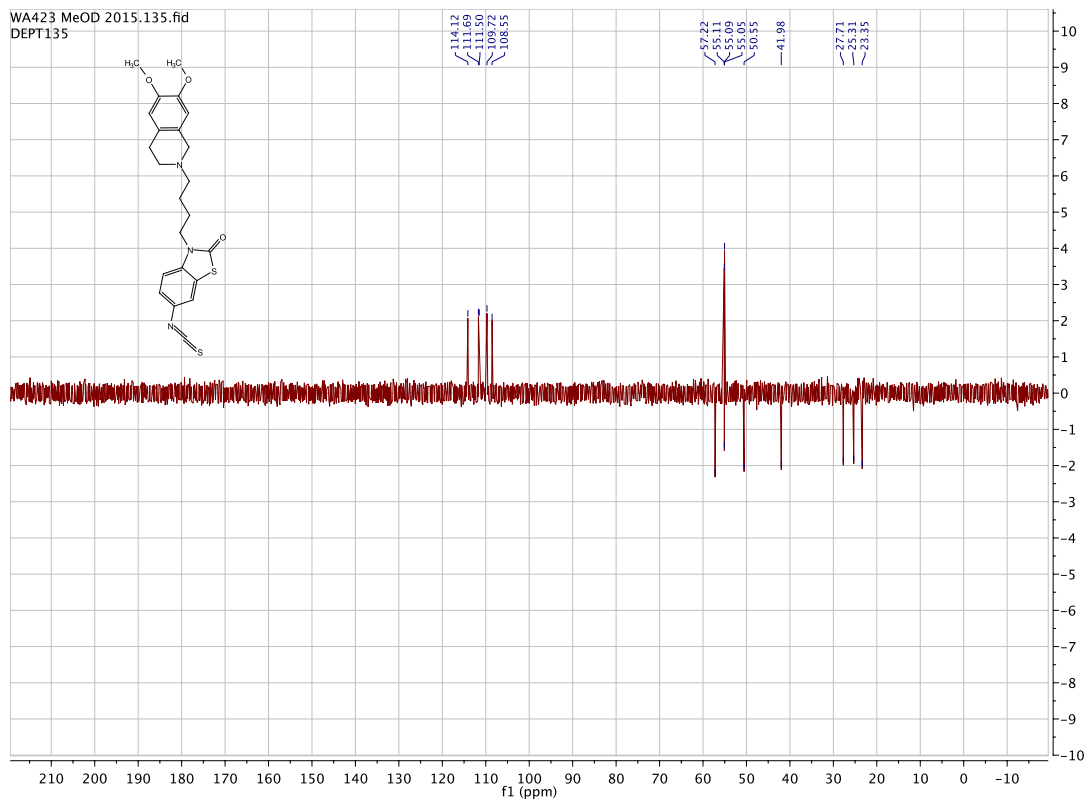




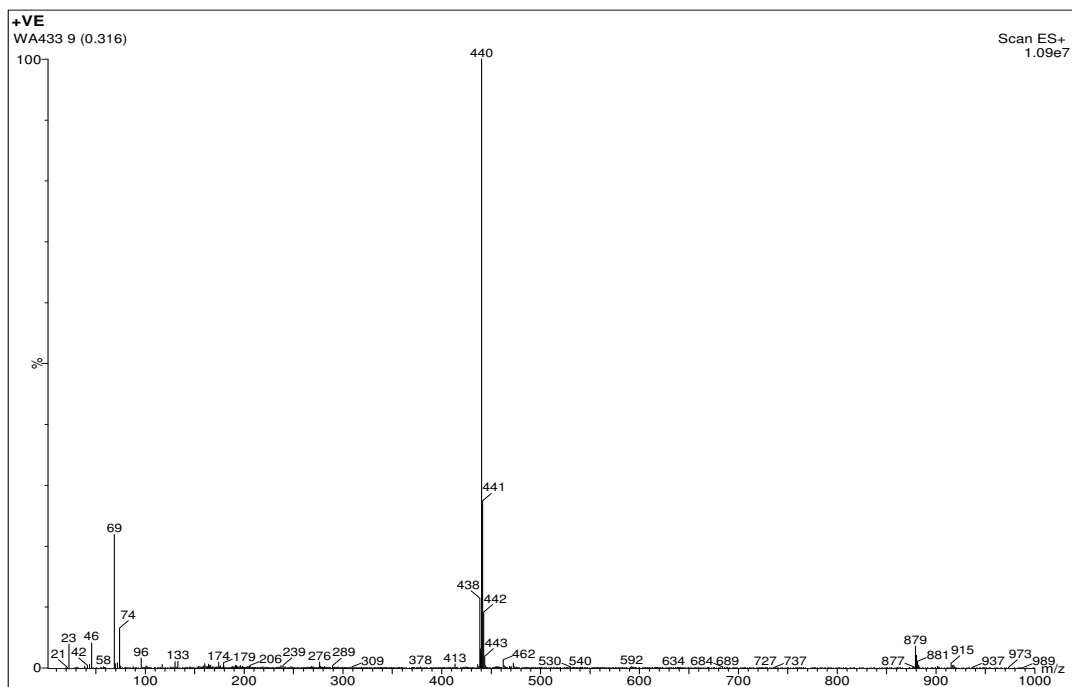
3-(4-(6,7-dimethoxy-3,4-dihydroisoquinolin-2(1H)-yl)butyl)-6-isothiocyanatobenzo[d]thiazol-2(3H)-one. [WA423]

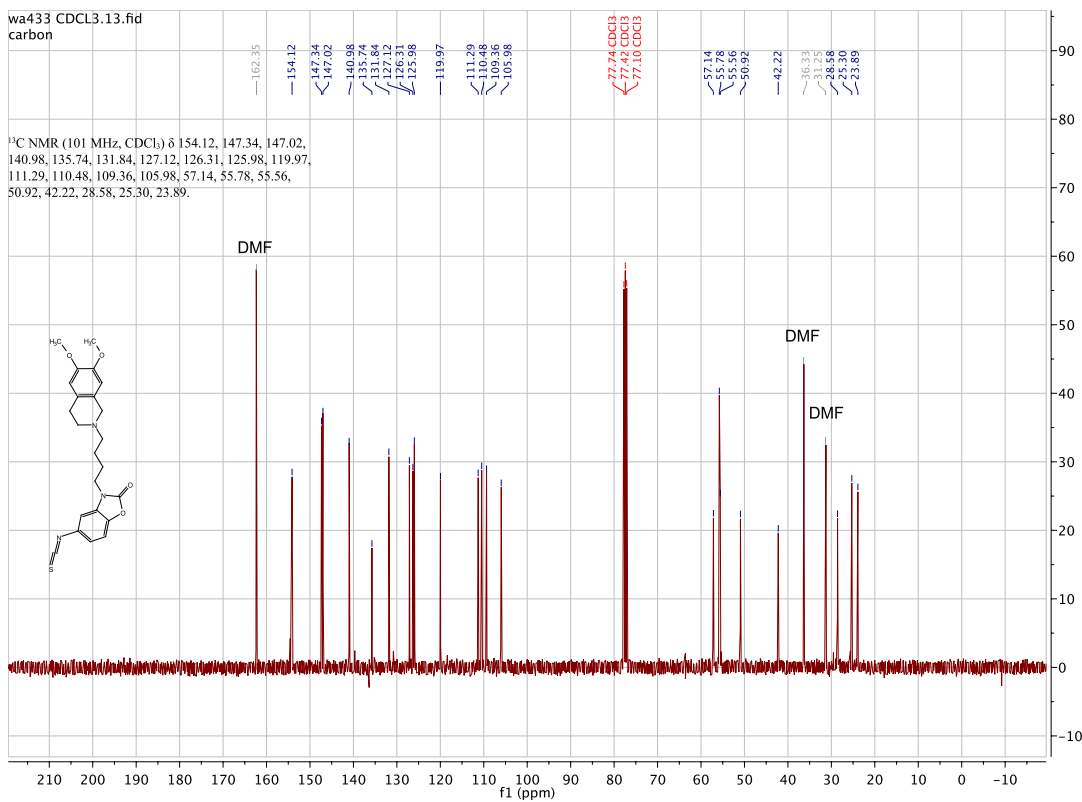
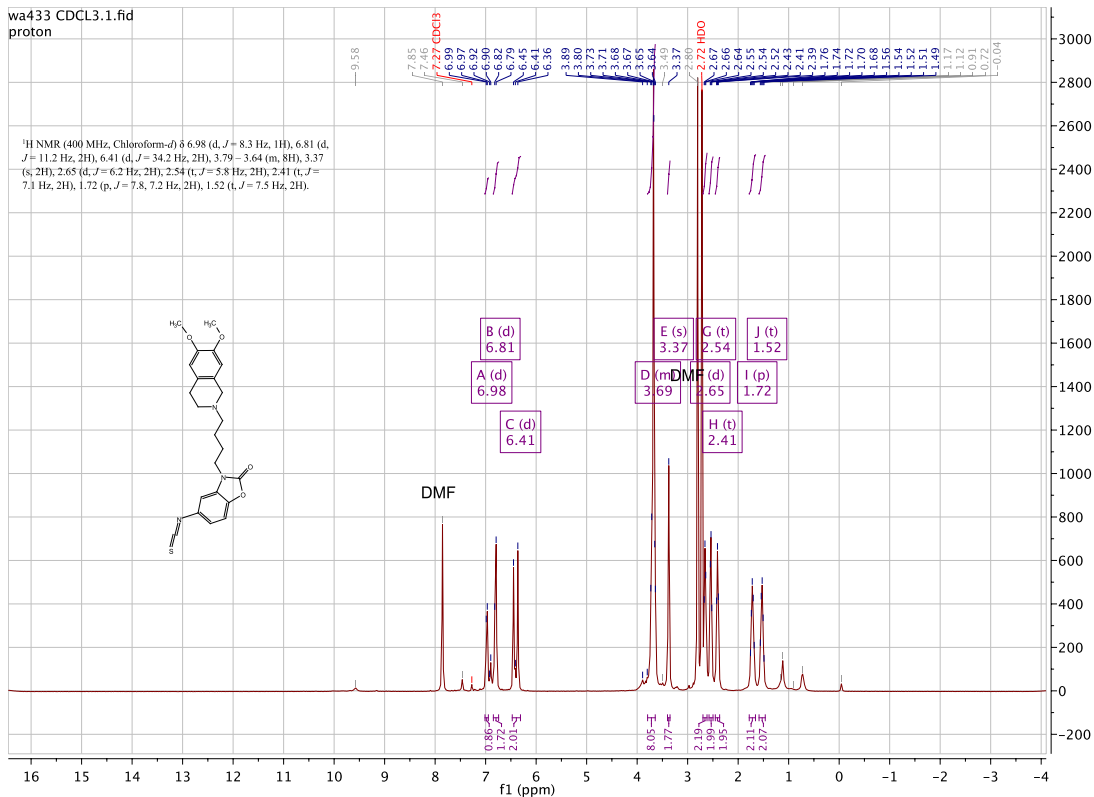


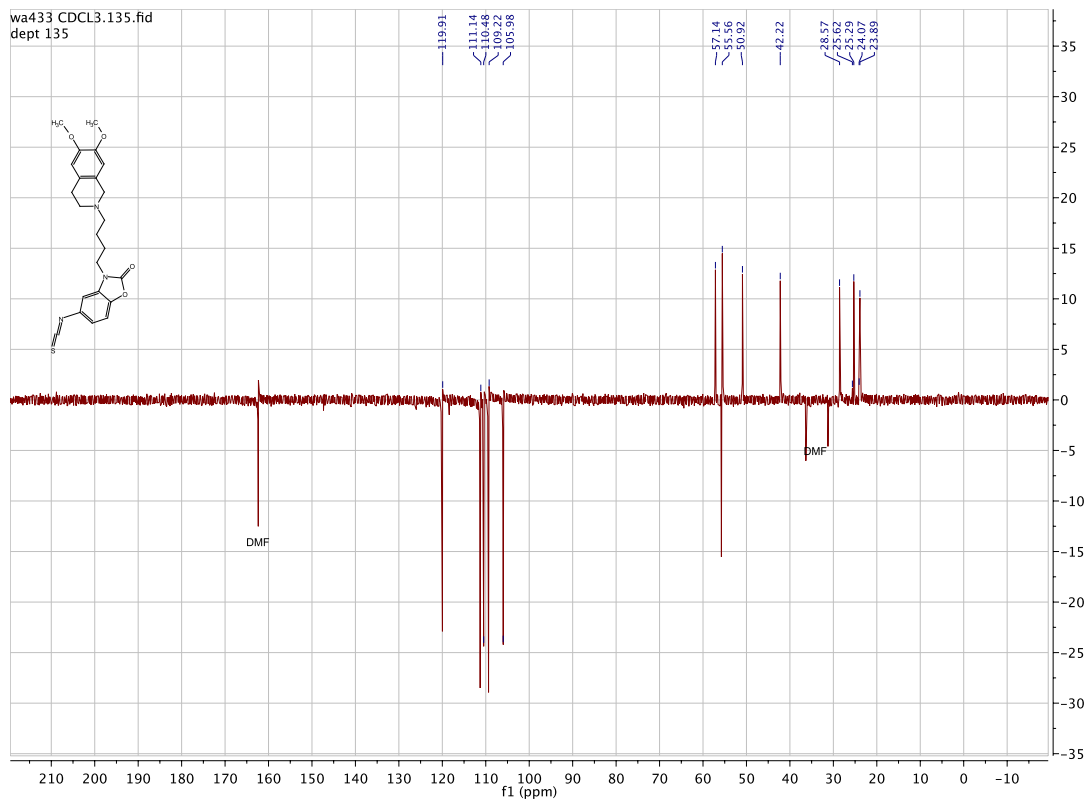




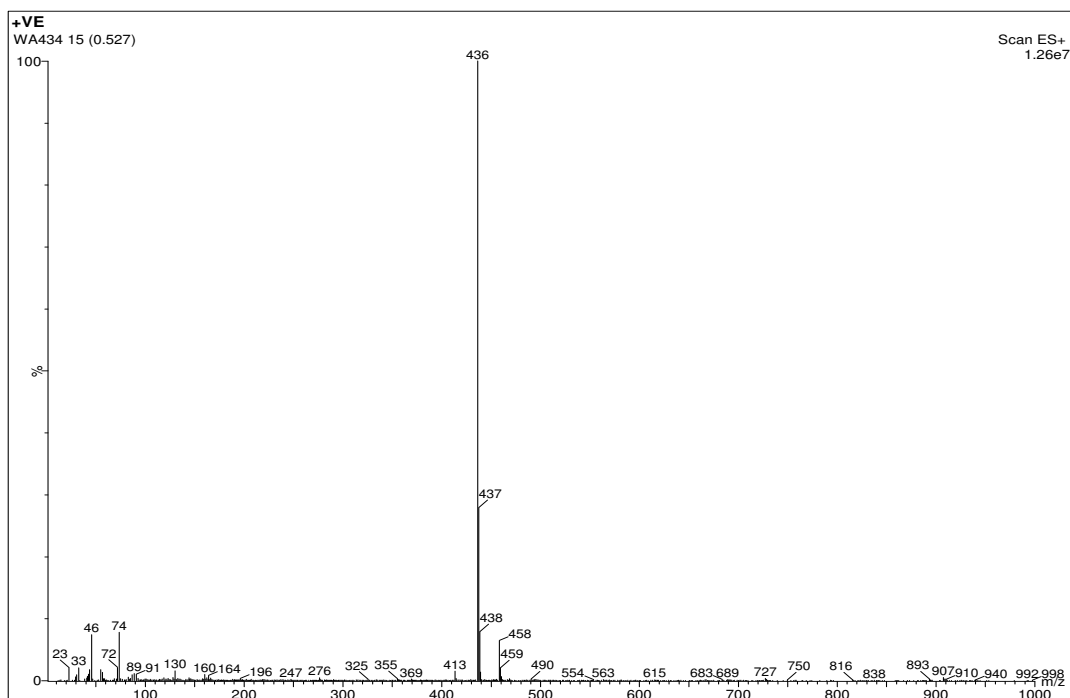
3-(4-(6,7-dimethoxy-3,4-dihydroisoquinolin-2(1H)-yl)butyl)-5-isothiocyanatobenzo[d]oxazol-2(3H)-one. [WA433]

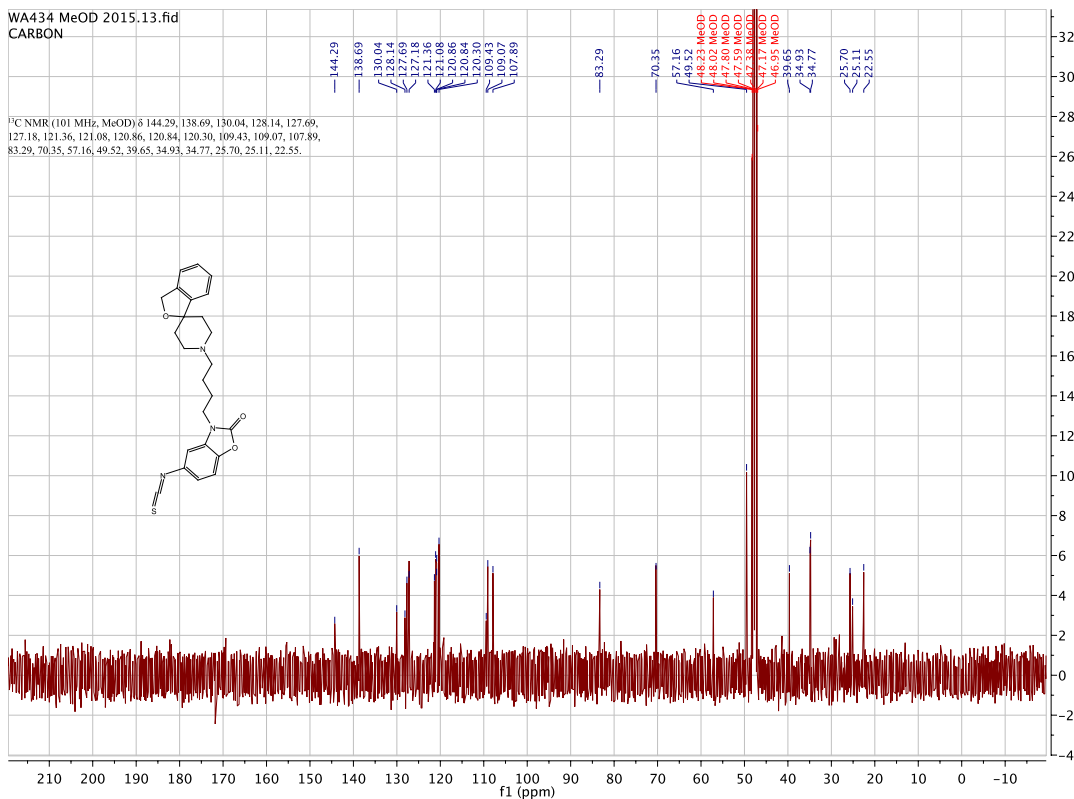
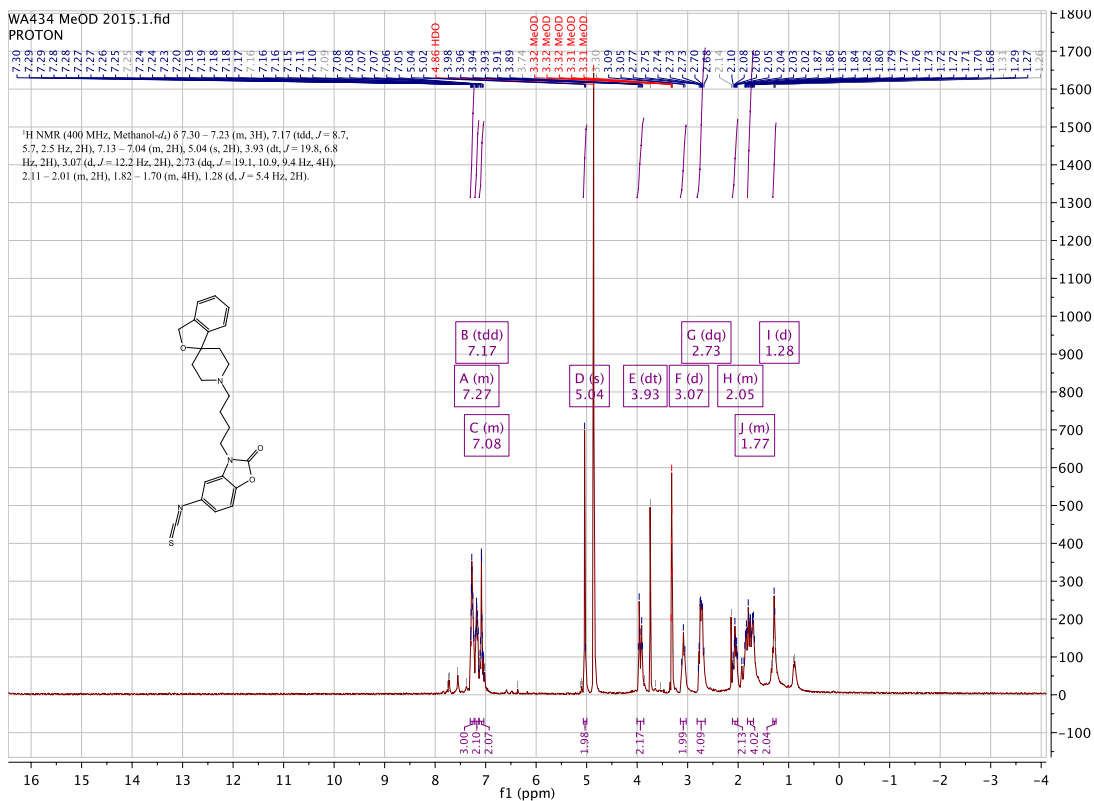


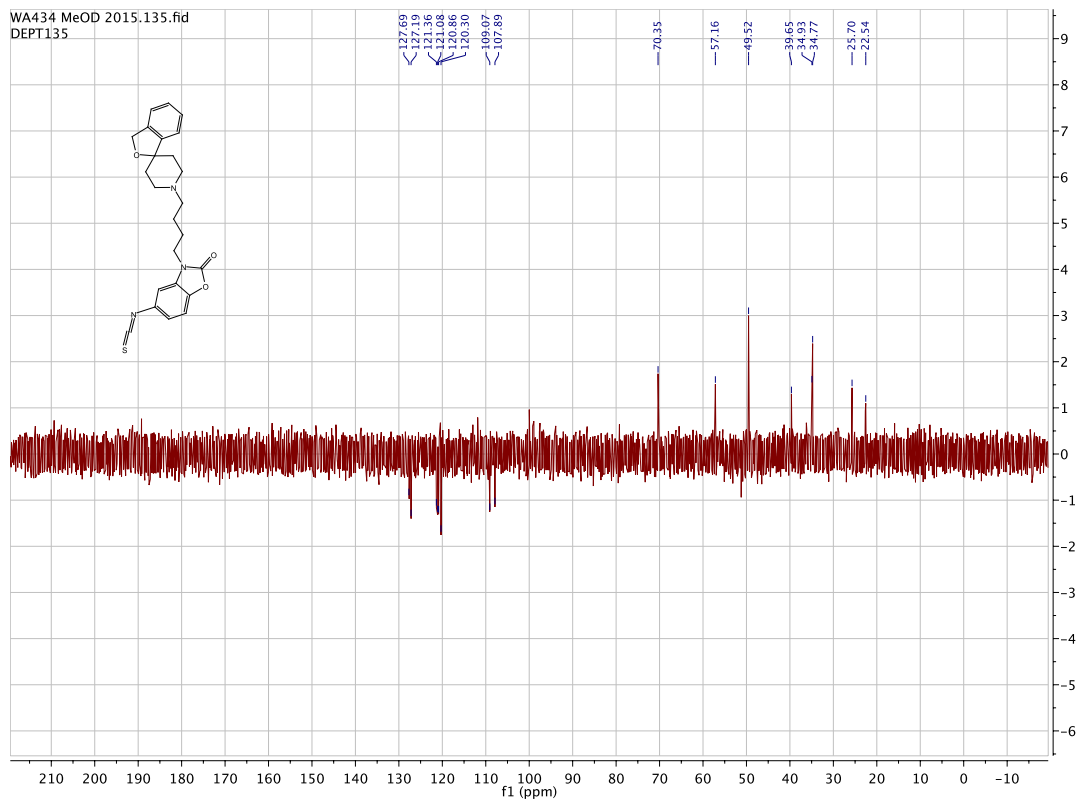




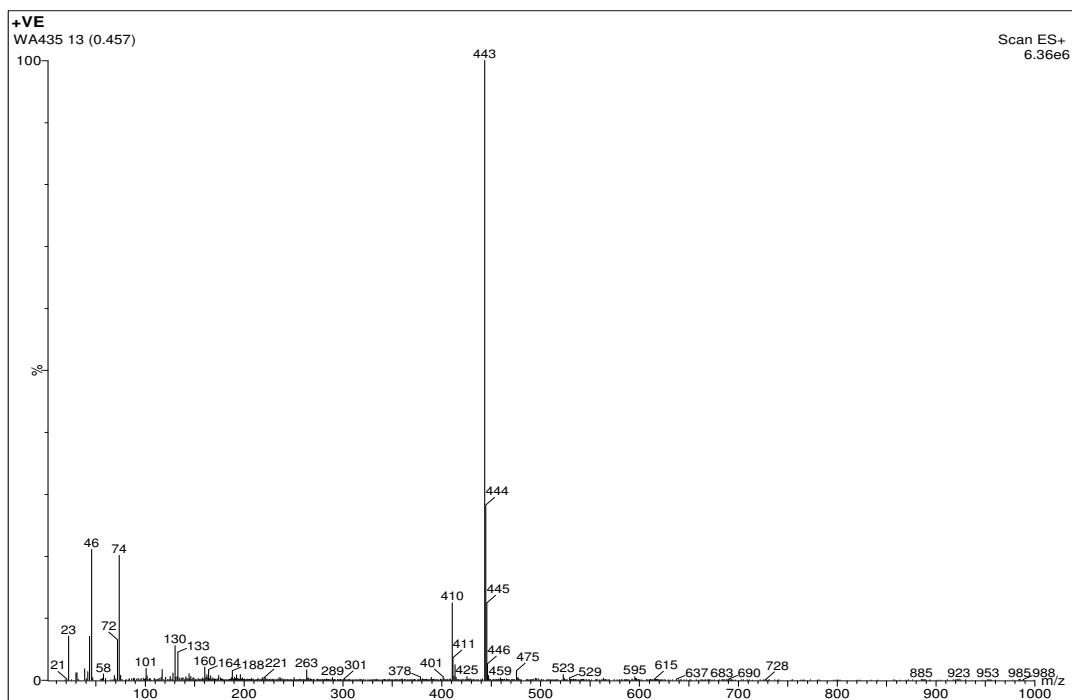
3-(4-(3H-spiro[isobenzofuran-1,4'-piperidin]-1'-yl)butyl)-5-isothiocyanatobenzo[d]oxazol-2(3H)-one. [WA434]





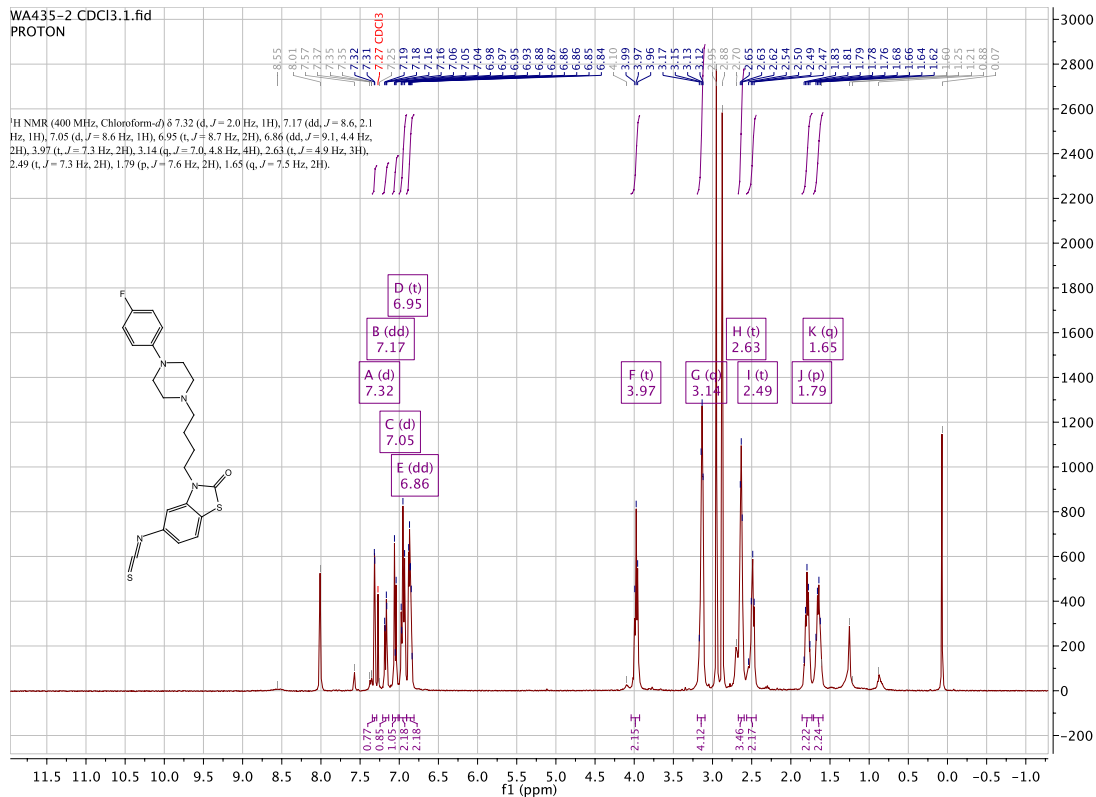


3-(4-(4-(4-fluorophenyl)piperazin-1-yl)butyl)-5-isothiocyanatobenzo[d]thiazol-2(3H)-one. [WA435]



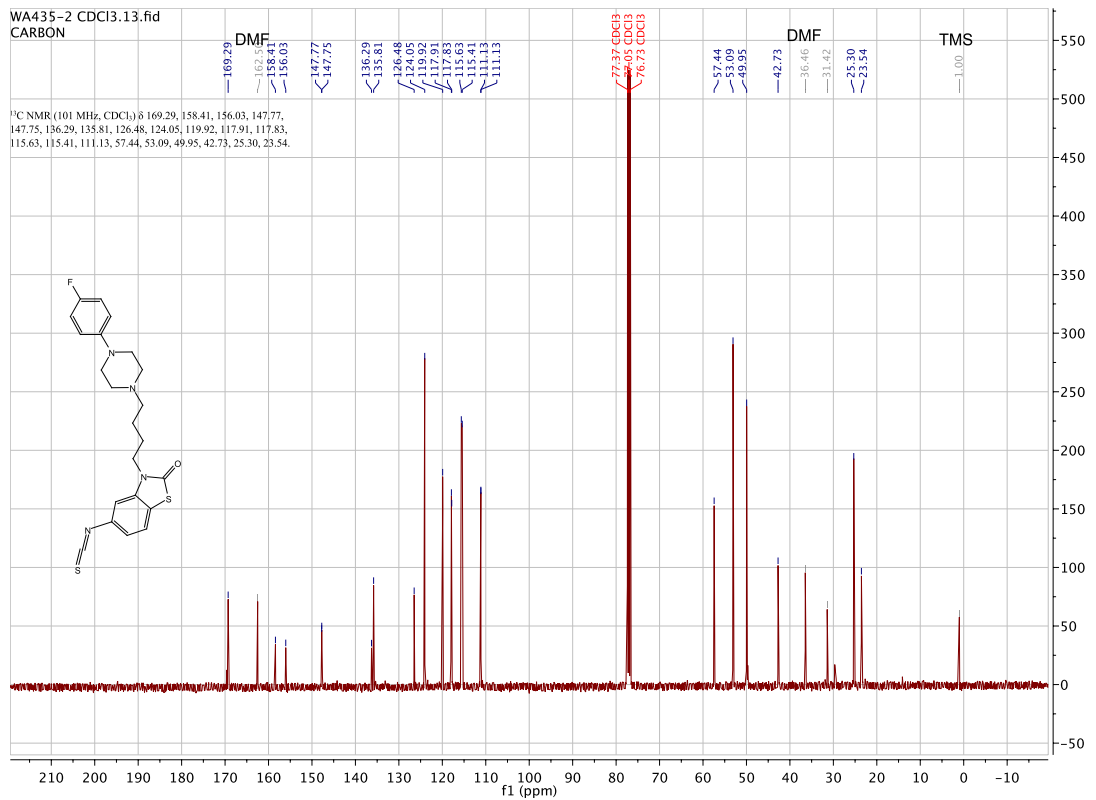
WA435-2 CDCl3.1.fid
 PROTON

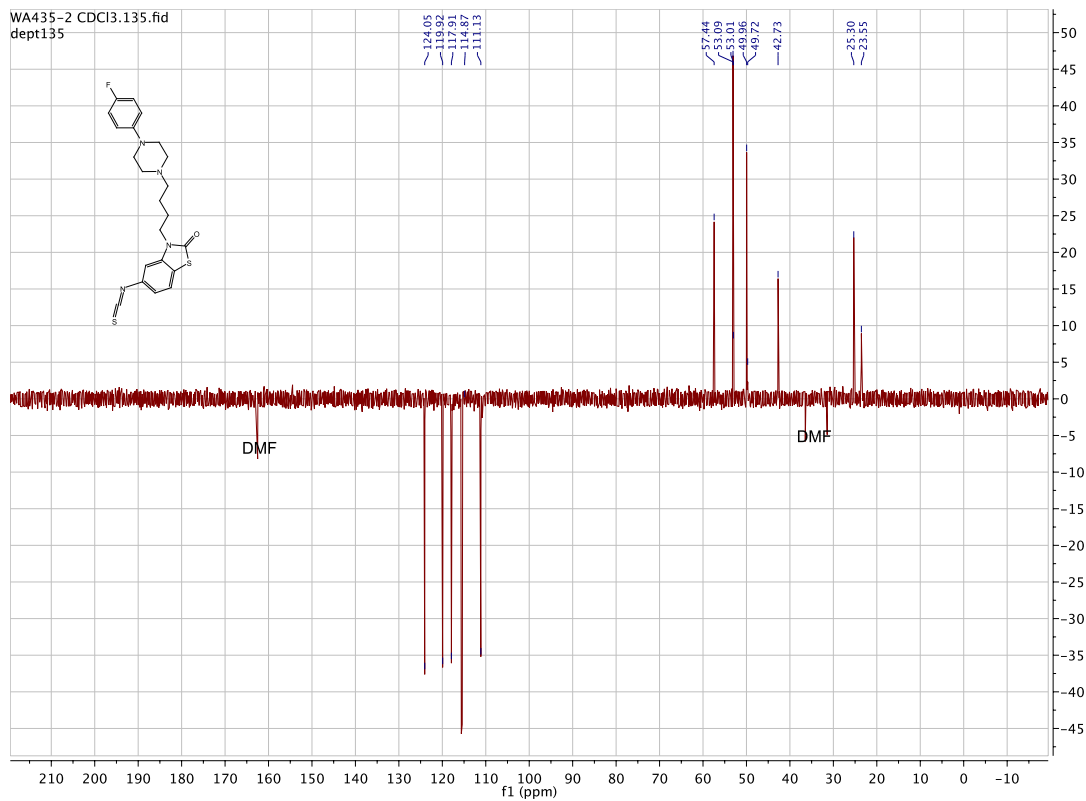
¹H NMR (400 MHz, Chloroform-*d*) δ 7.32 (d, *J* = 2.0 Hz, 1H), 7.17 (dd, *J* = 8.6, 2.1 Hz, 1H), 7.05 (d, *J* = 8.6 Hz, 1H), 6.95 (t, *J* = 8.7 Hz, 2H), 6.86 (dd, *J* = 9.1, 4.4 Hz, 2H), 3.97 (t, *J* = 7.3 Hz, 2H), 3.14 (q, *J* = 7.0, 4.8 Hz, 4H), 2.63 (t, *J* = 4.9 Hz, 3H), 2.49 (t, *J* = 7.3 Hz, 2H), 1.79 (q, *J* = 7.6 Hz, 2H), 1.65 (q, *J* = 7.5 Hz, 2H).



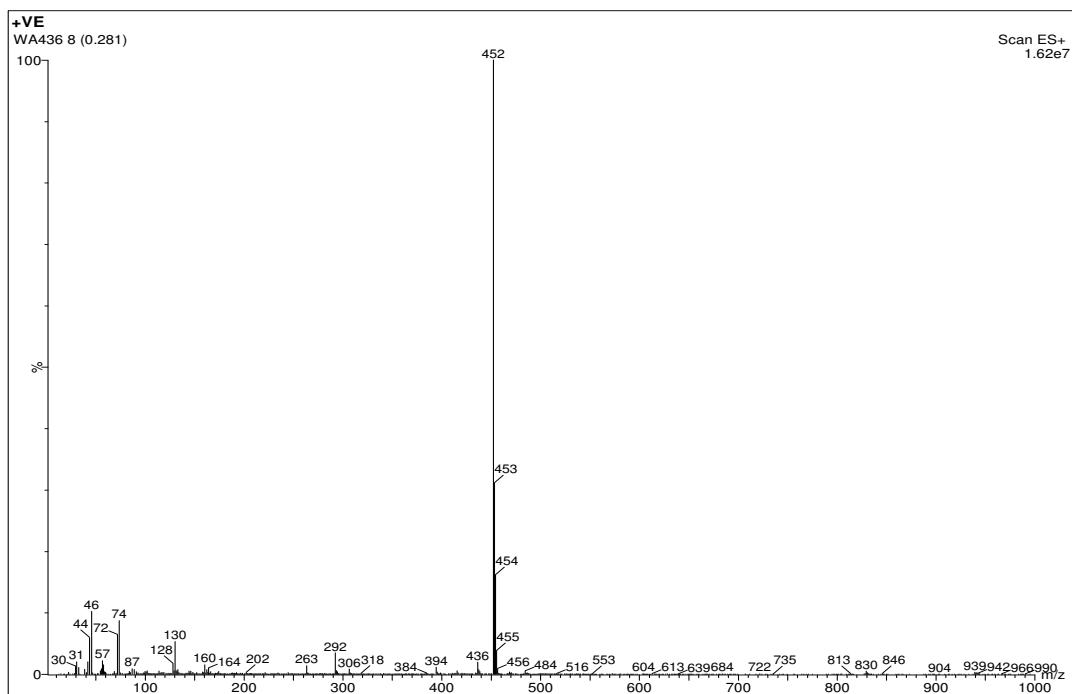
WA435-2 CDCl3.13.fid
 CARBON

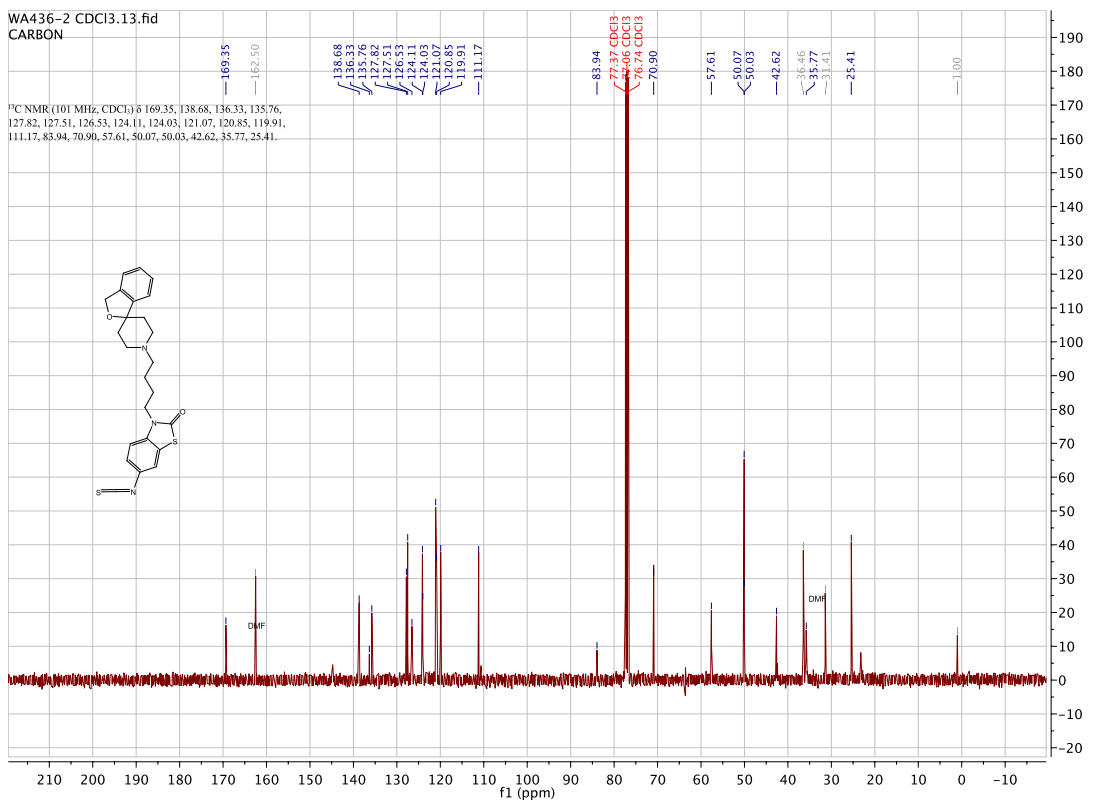
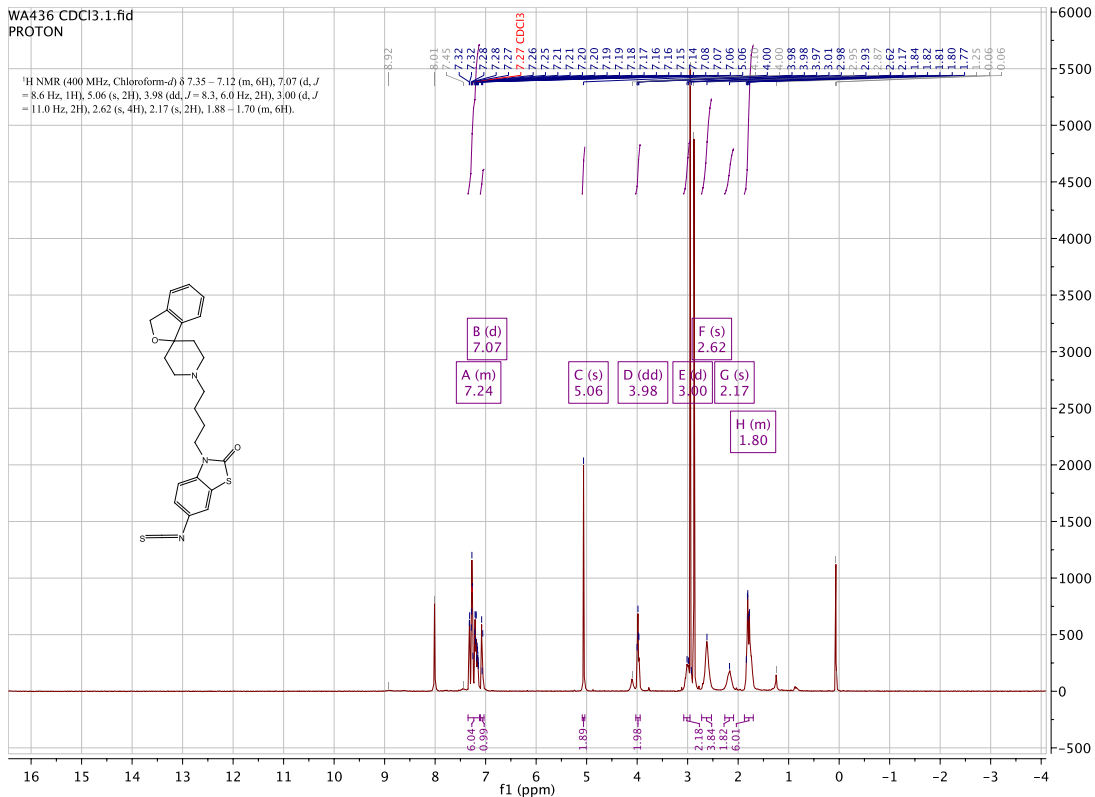
¹³C NMR (101 MHz, CDCl₃) δ 169.29, 158.41, 156.03, 147.77, 147.75, 136.29, 135.81, 126.48, 124.05, 119.92, 117.91, 117.83, 115.63, 115.41, 111.13, 57.44, 53.09, 49.95, 42.73, 25.30, 23.54.



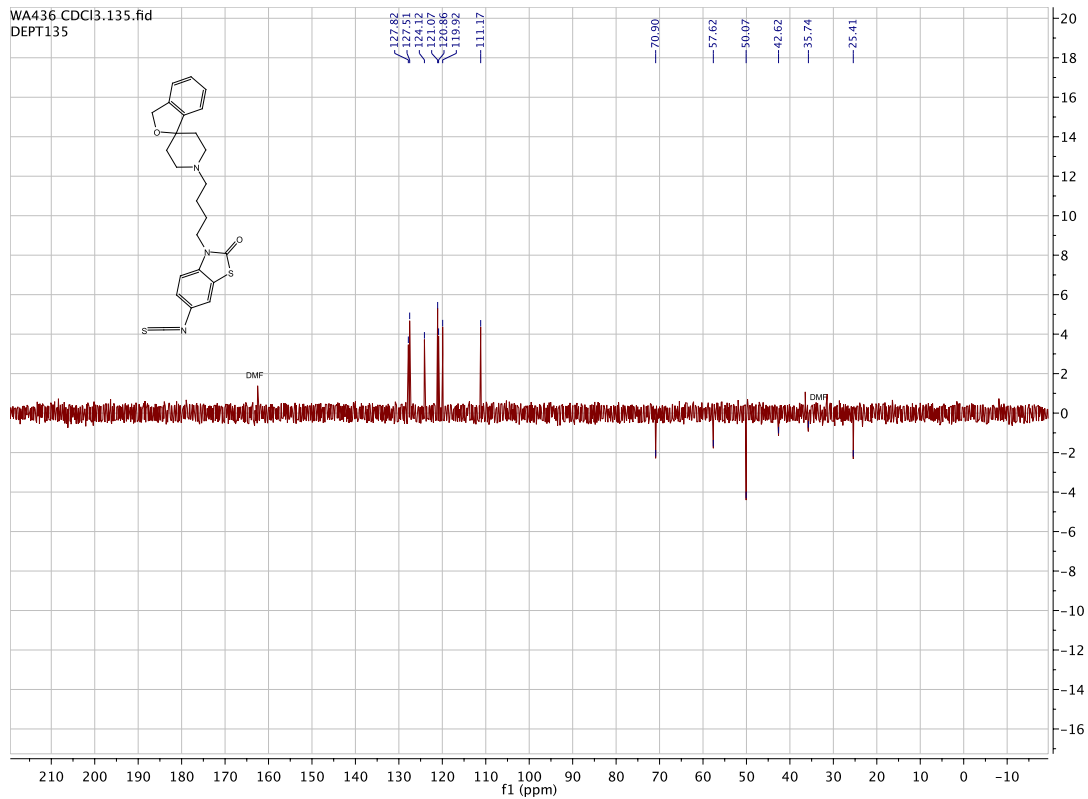


3-(4-(3H-spiro[isobenzofuran-1,4'-piperidin]-1'-yl)butyl)-6-isothiocyanatobenzo[d]thiazol-2(3H)-one. [WA436]

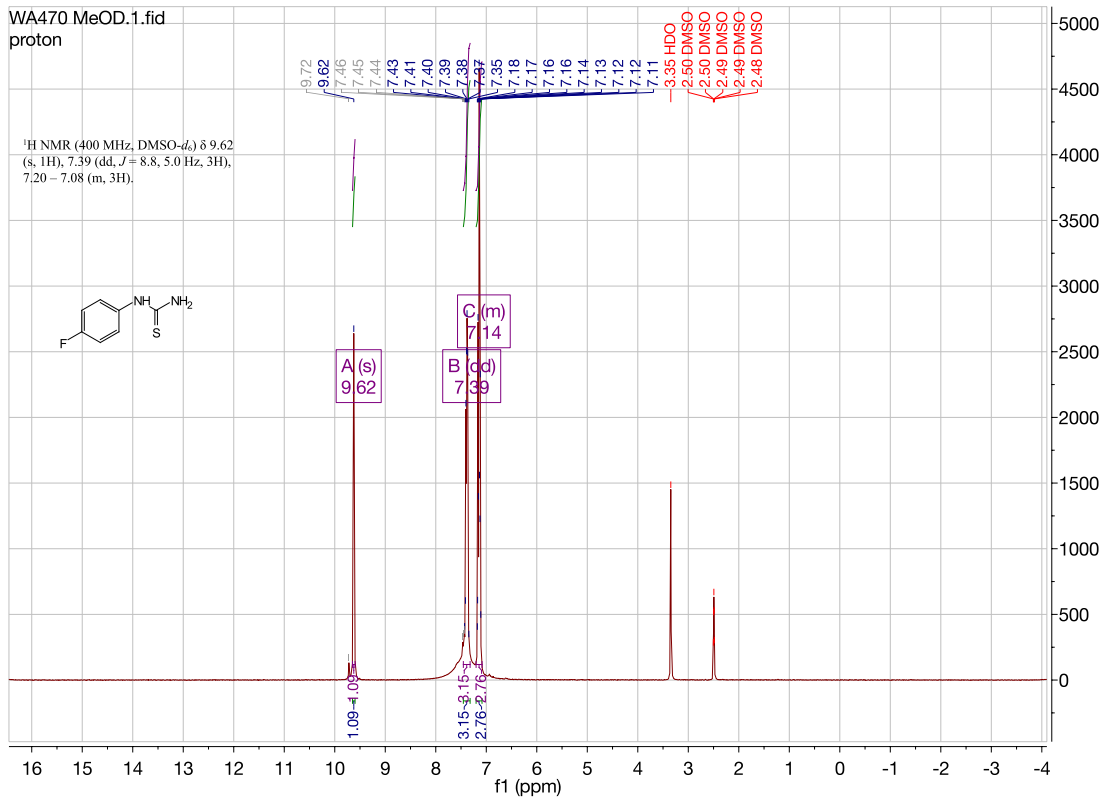
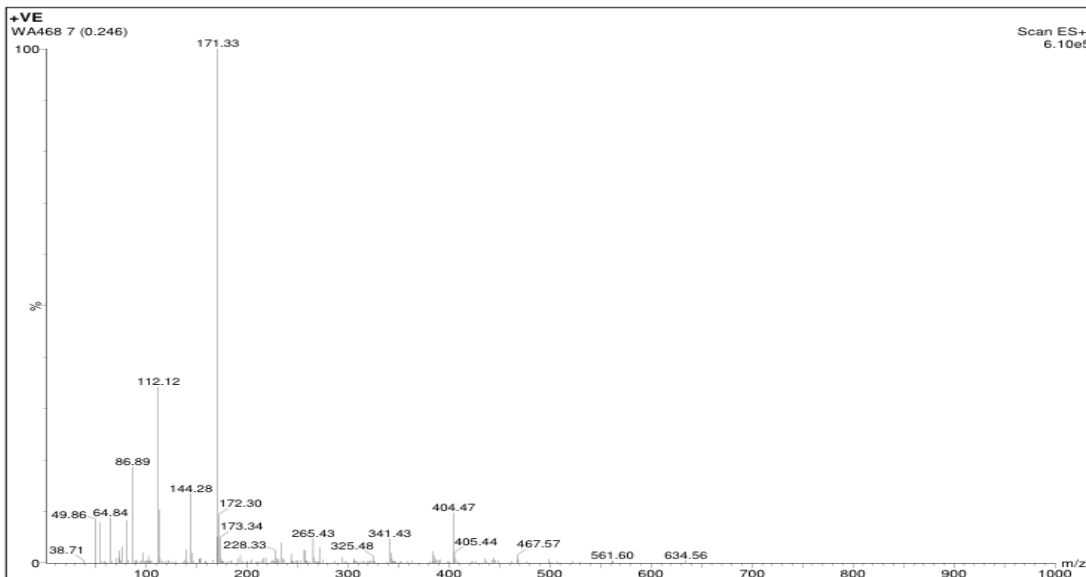


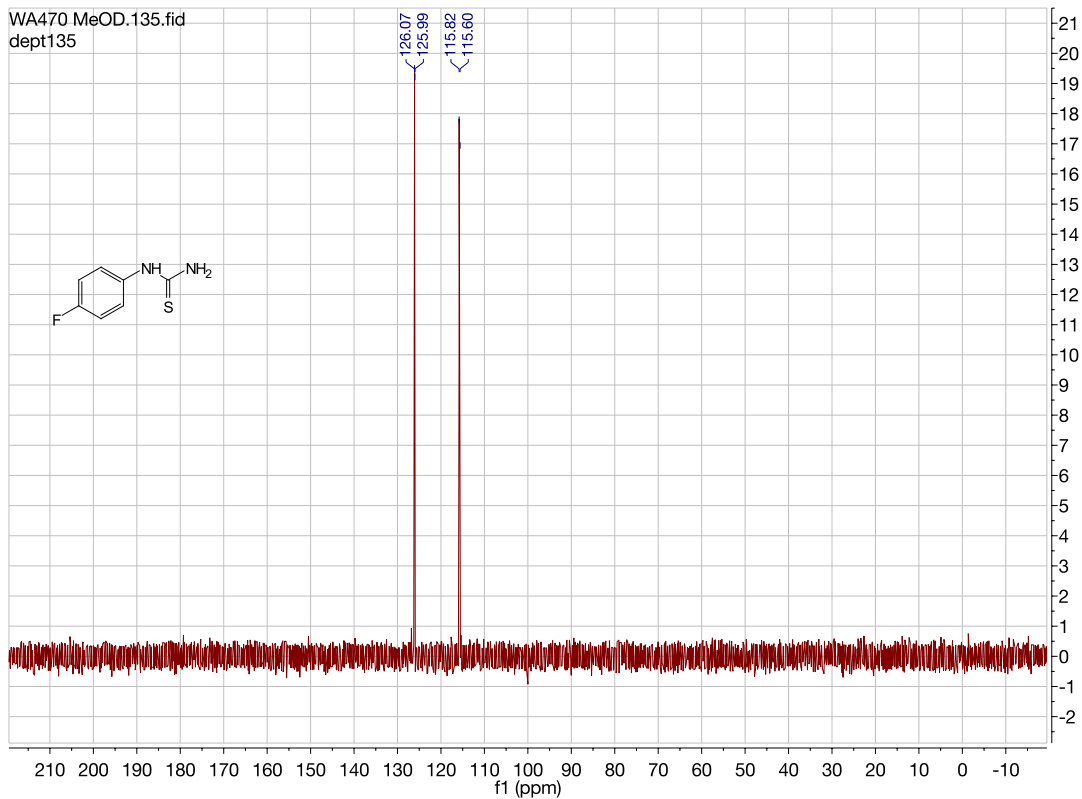
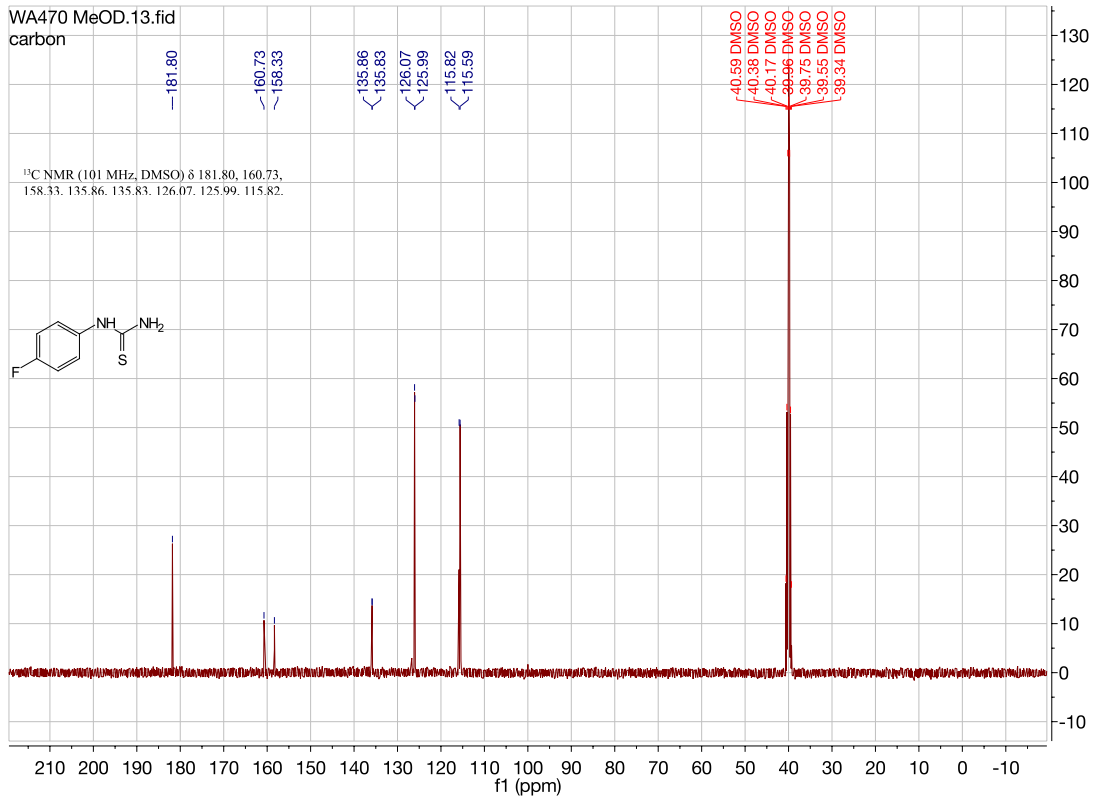


WA436 CDCl3.135.fid
DEPT135

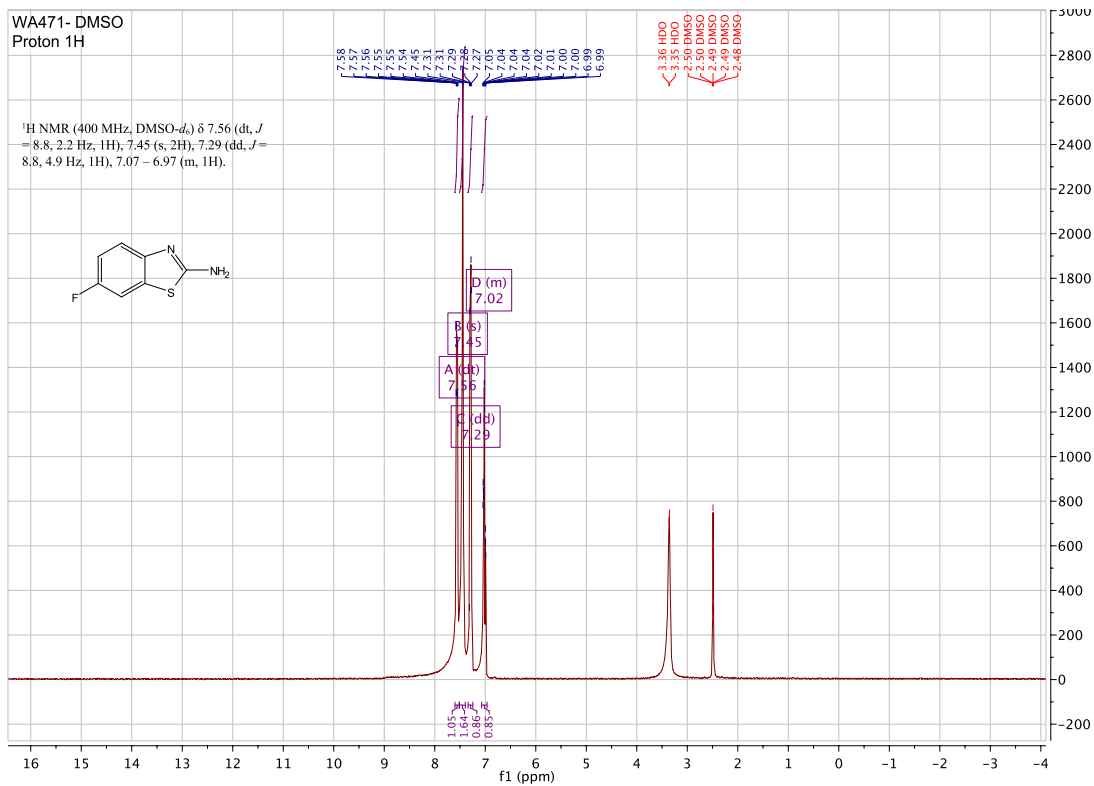
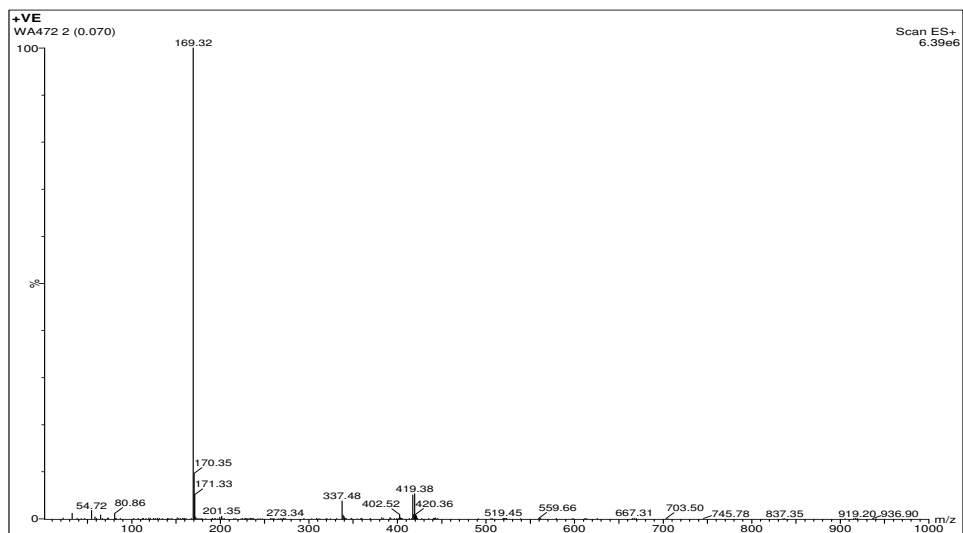


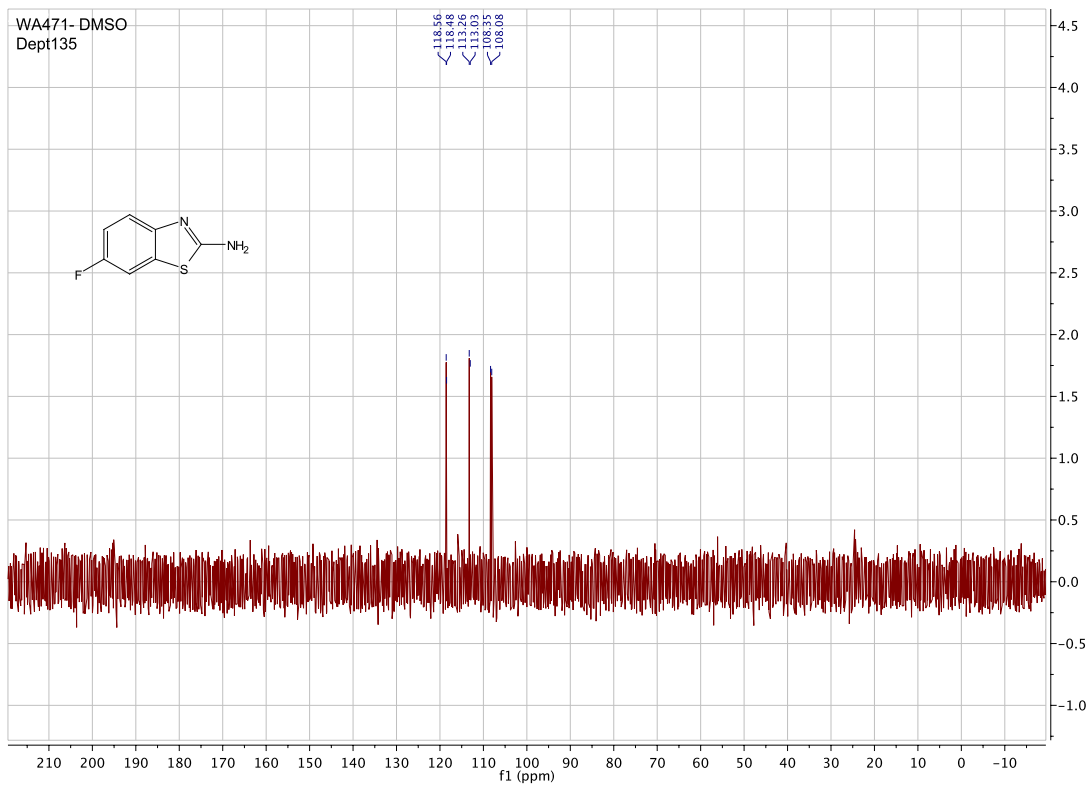
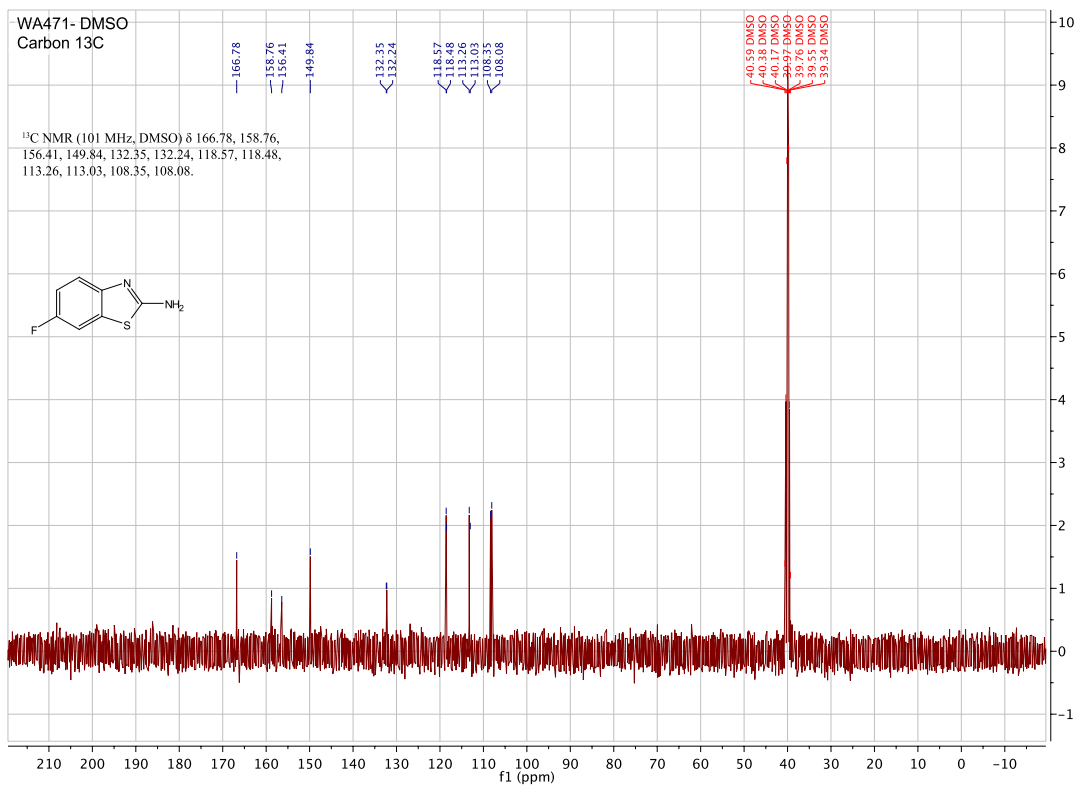
1-(4-fluorophenyl)thiourea. (WA470)



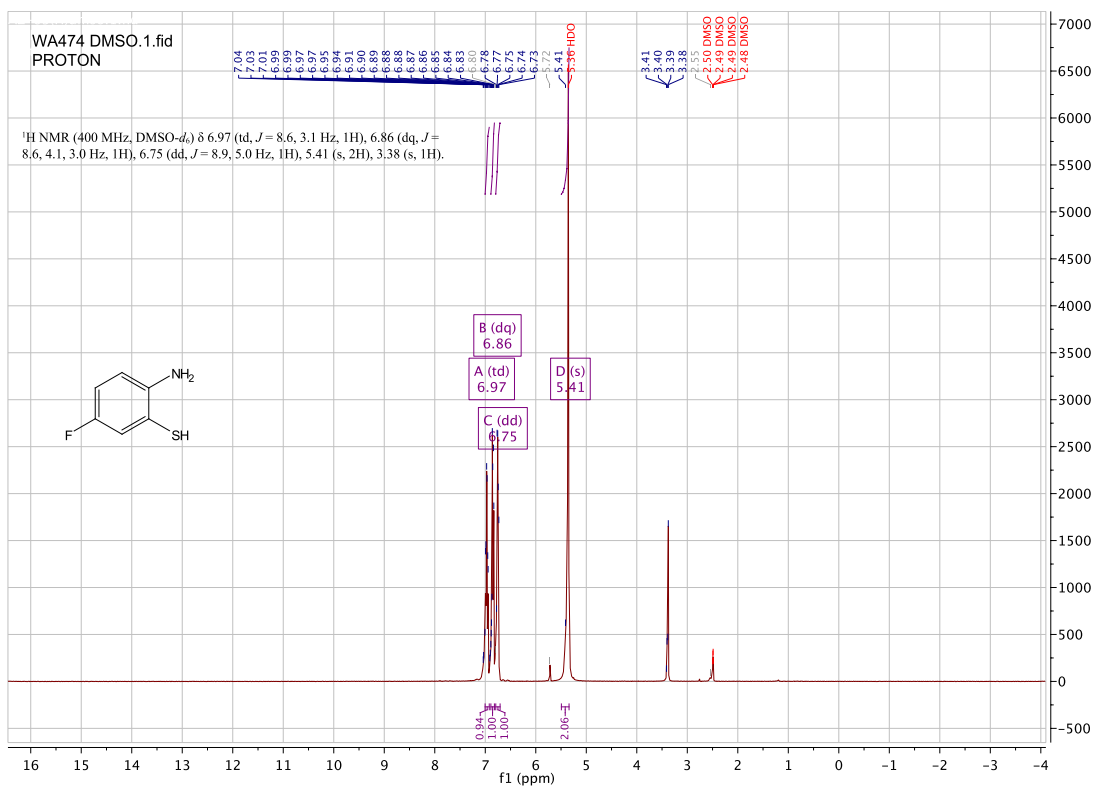
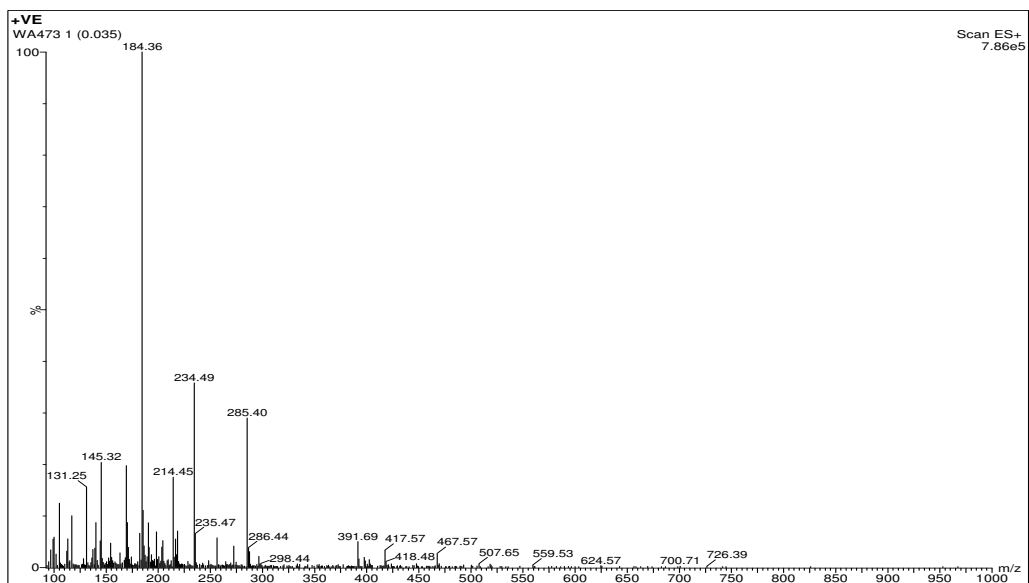


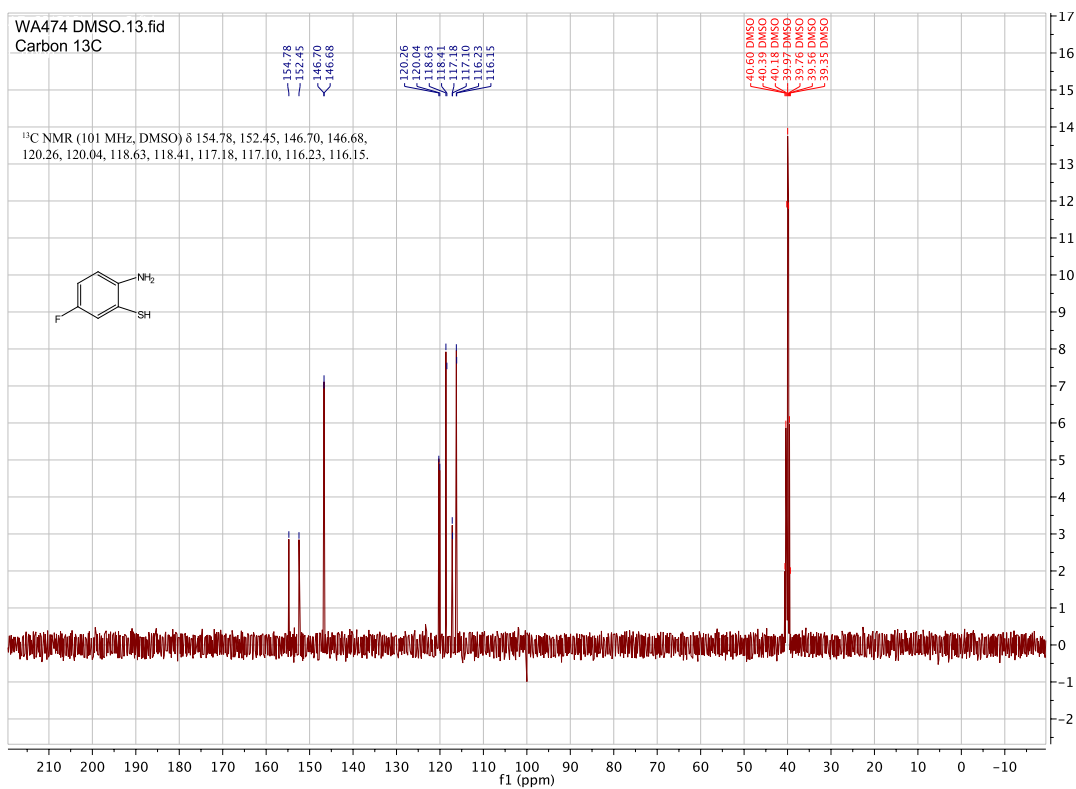
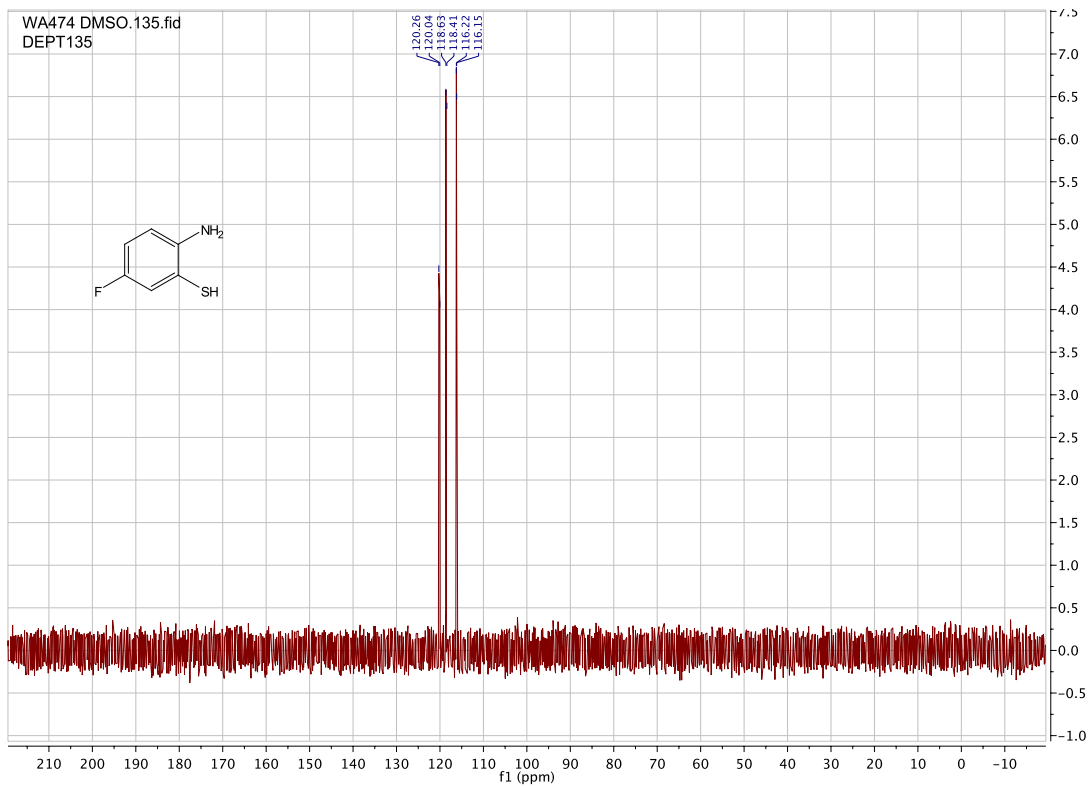
6-fluorobenzo[d]thiazol-2-amine. (WA471)



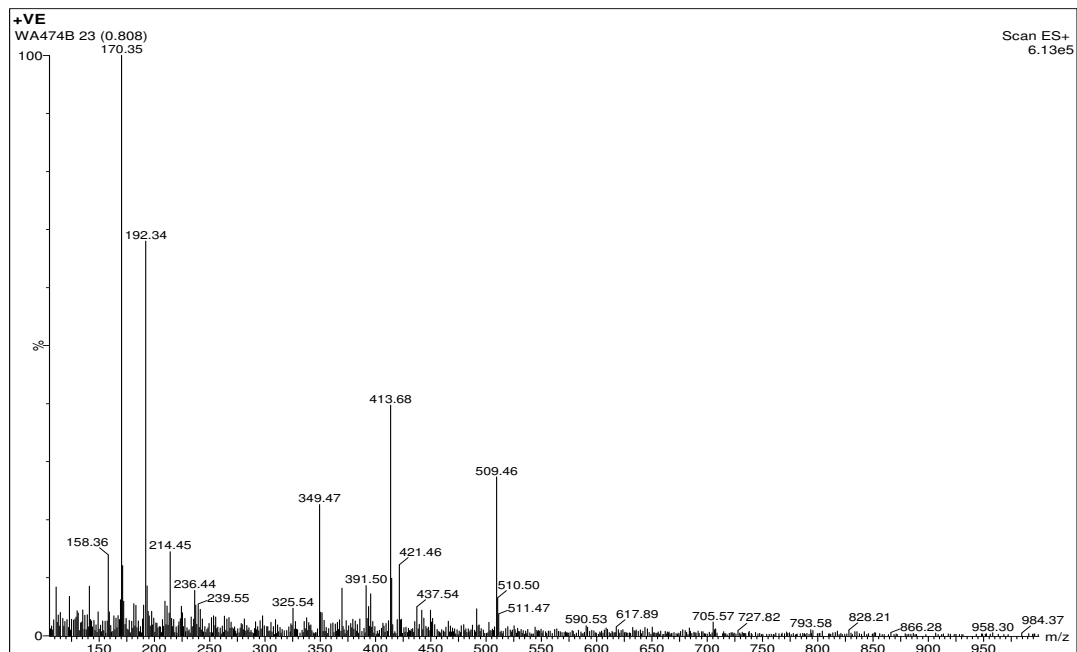
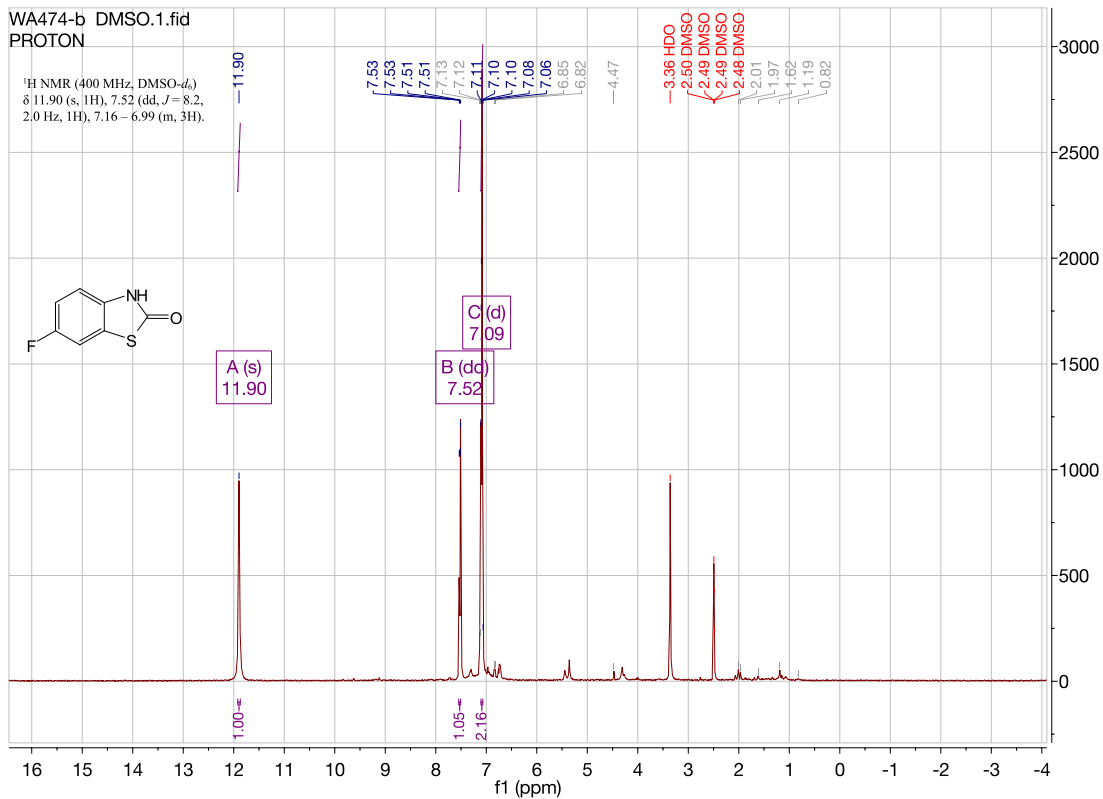


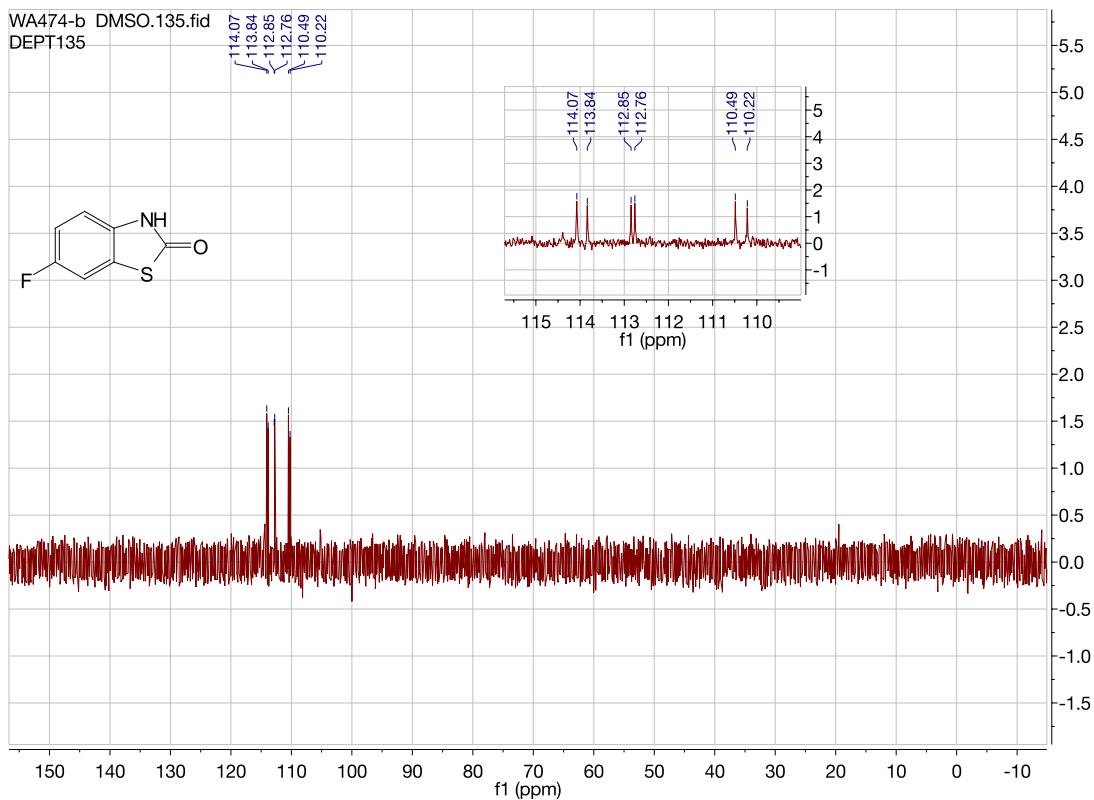
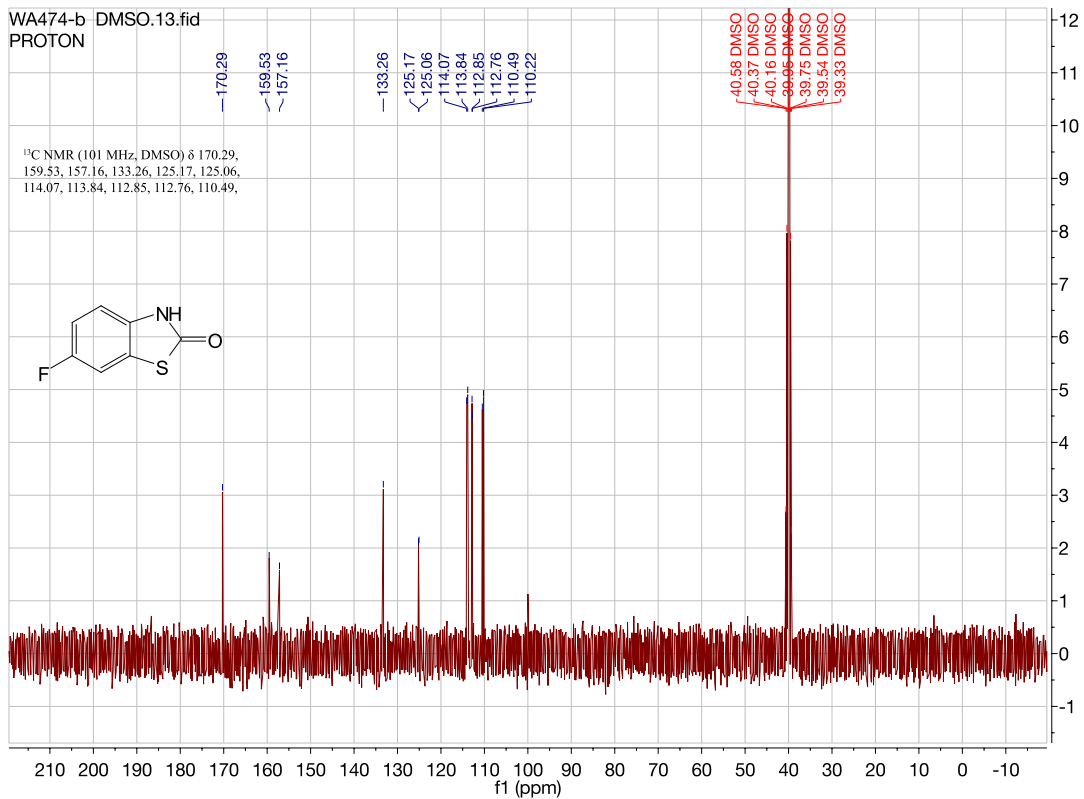
2-amino-5-fluorobenzenethiol. (474)



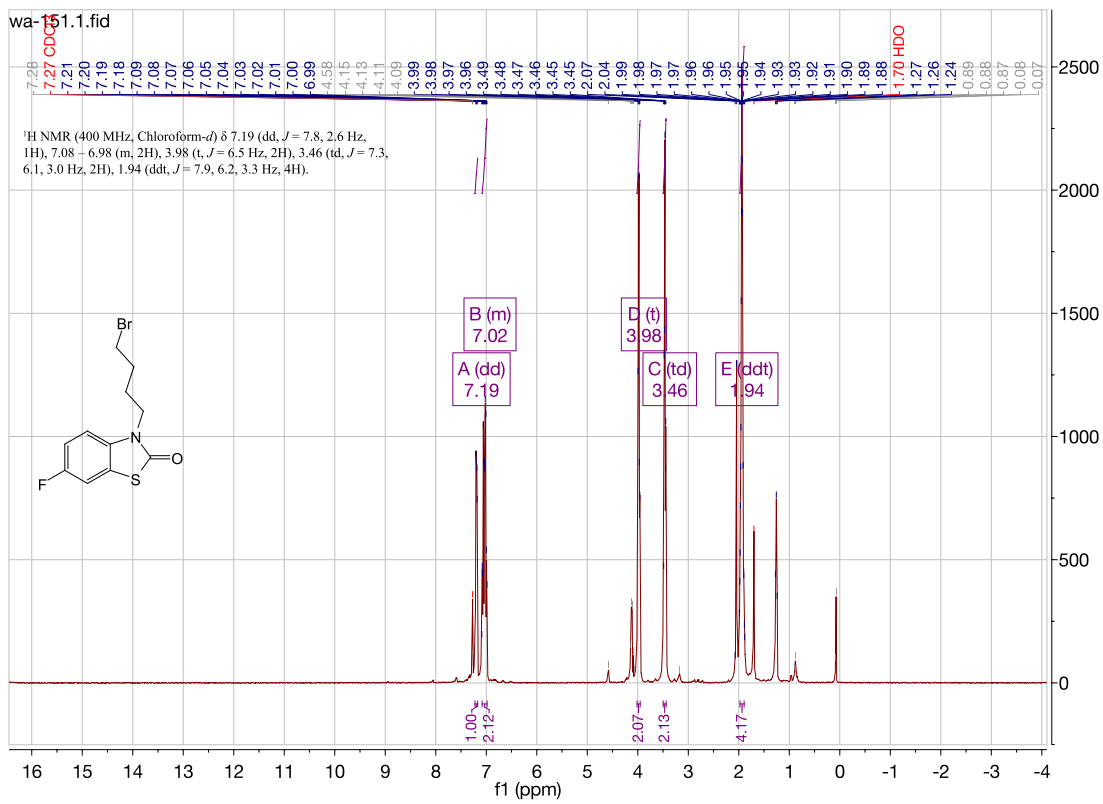
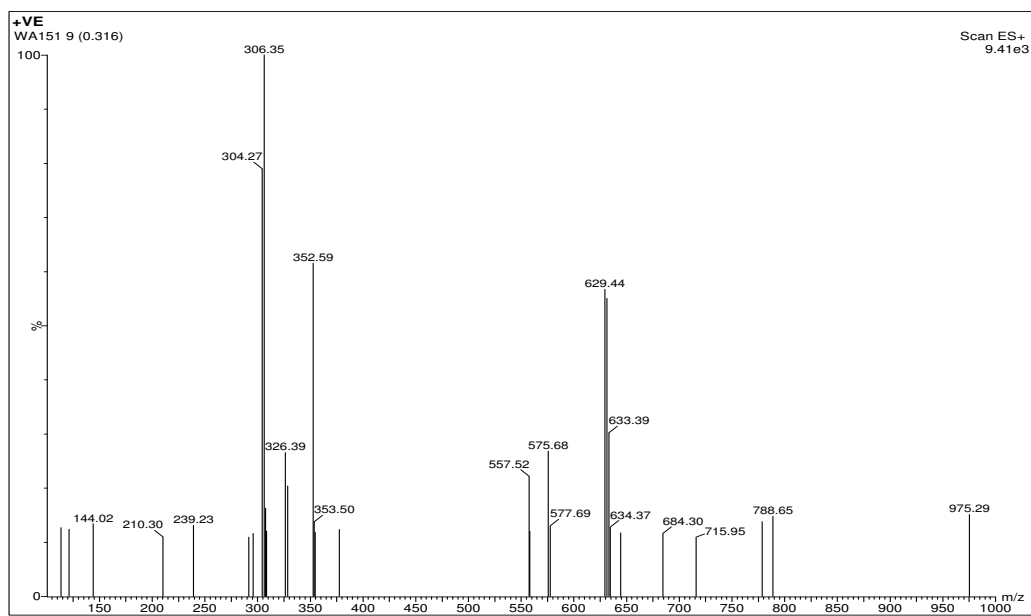


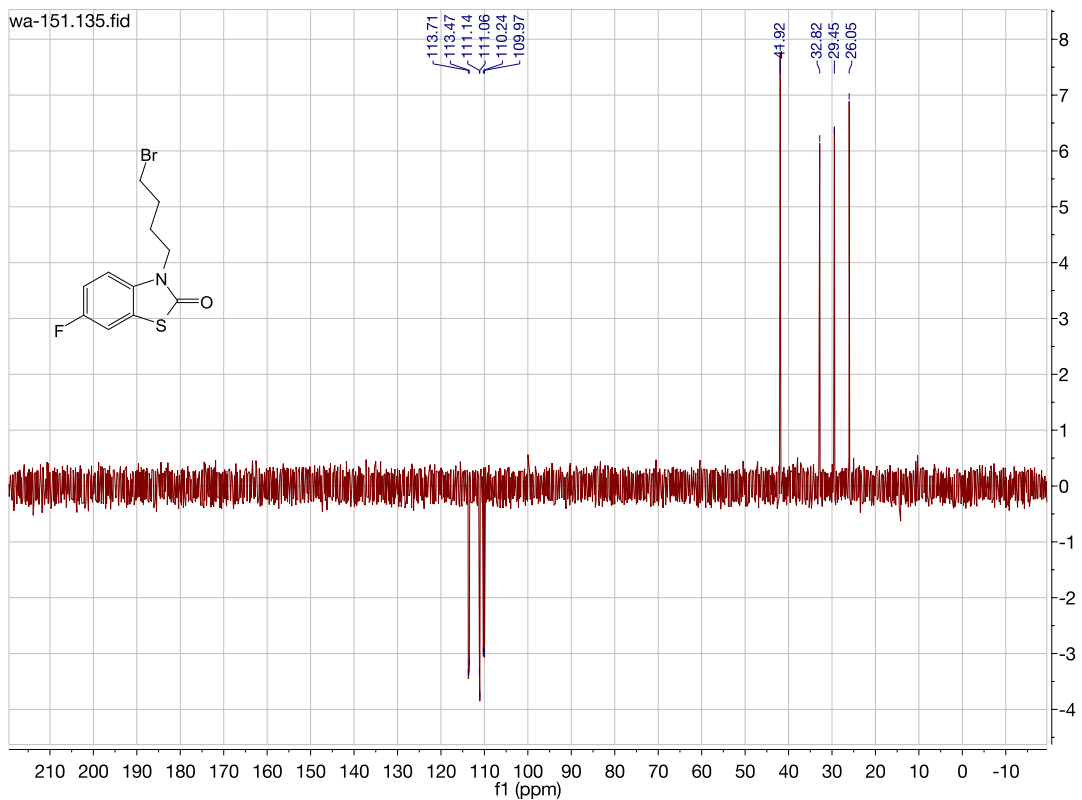
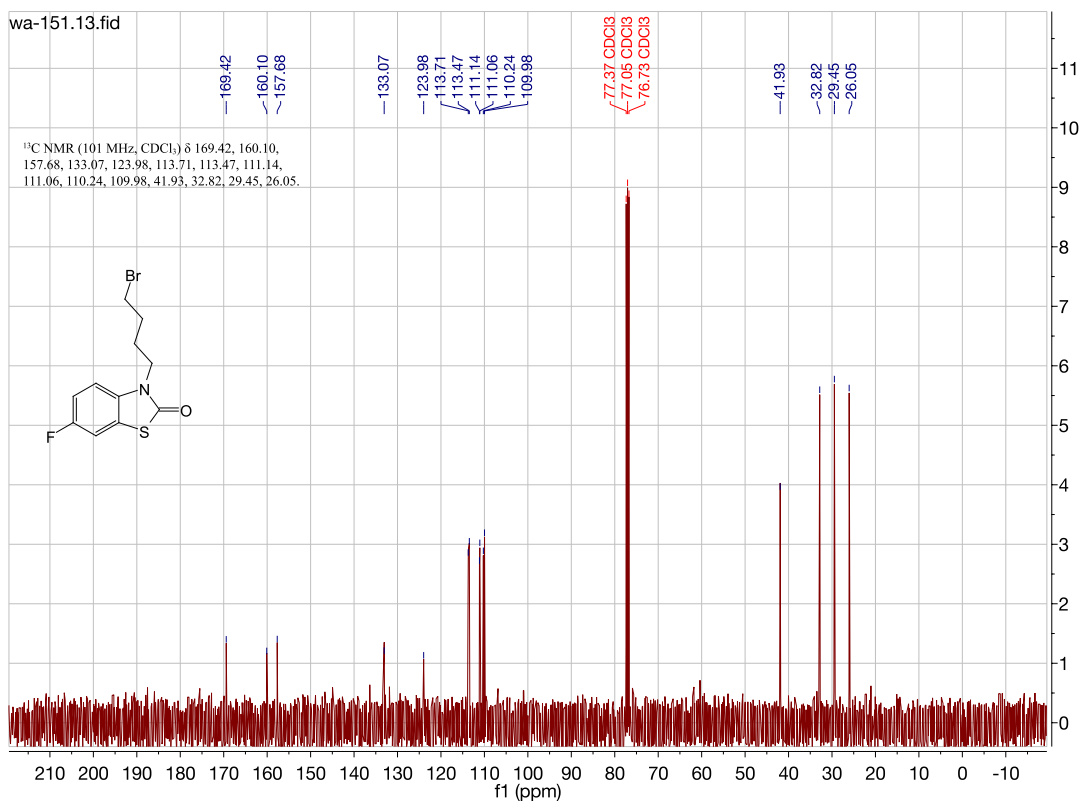
6-fluorobenzo[d]thiazol-2(3H)-one. (WA474B):



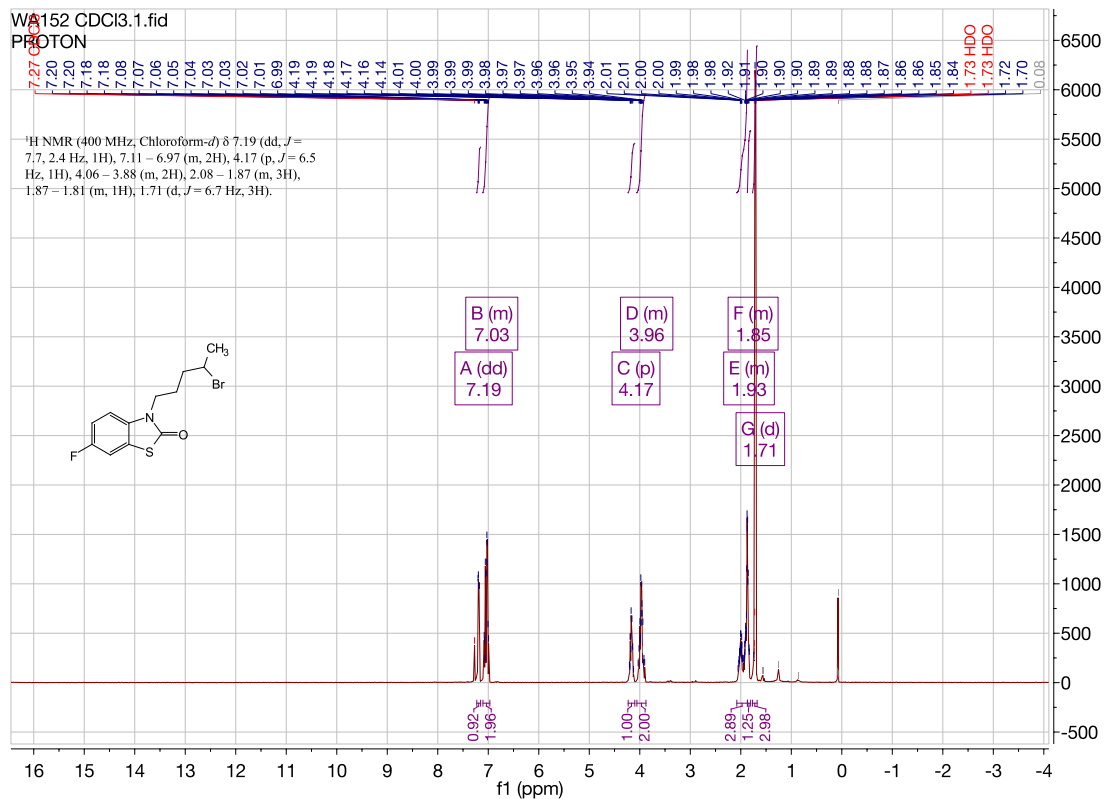
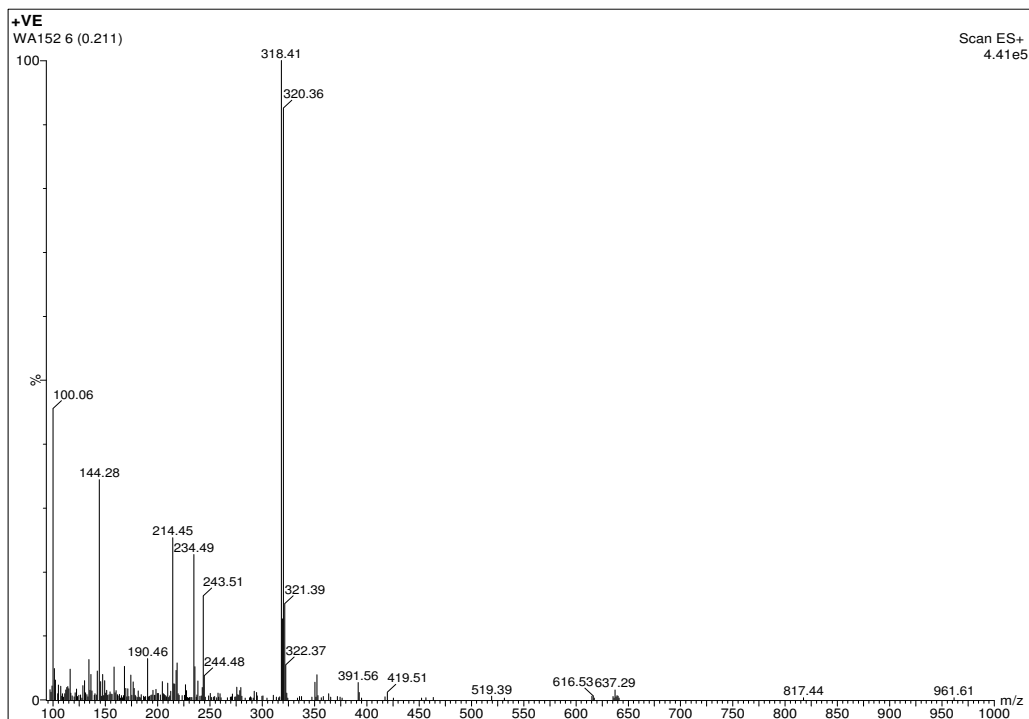


3-(4-bromobutyl)-6-fluorobenzo[d]thiazol-2(3H)-one. (WA151)



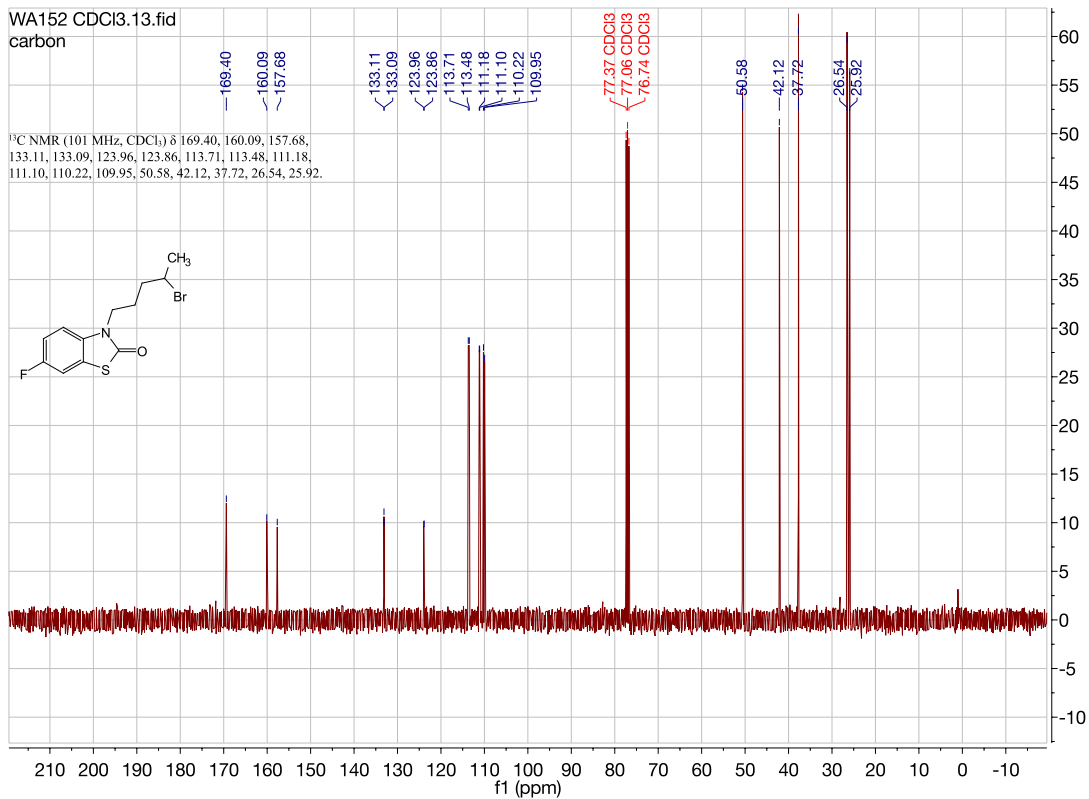
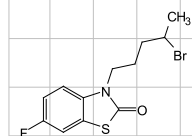


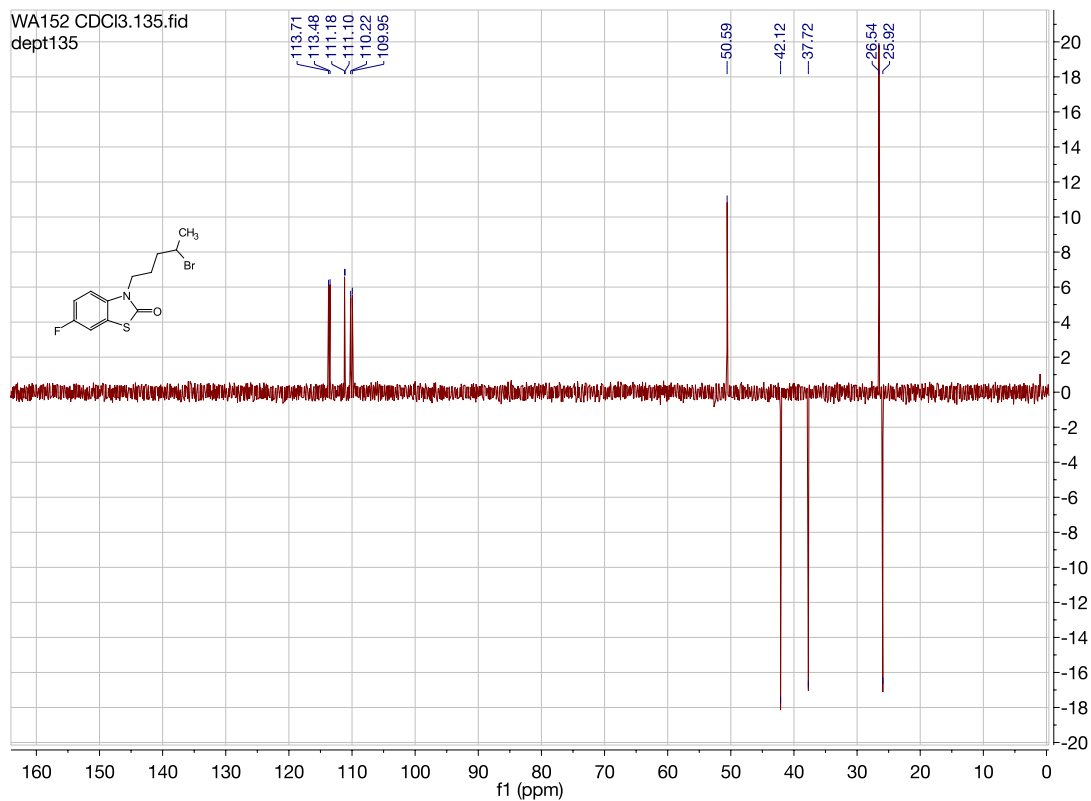
3-(4-bromopentyl)-6-fluorobenzo[d]thiazol-2(3H)-one. (WA152)



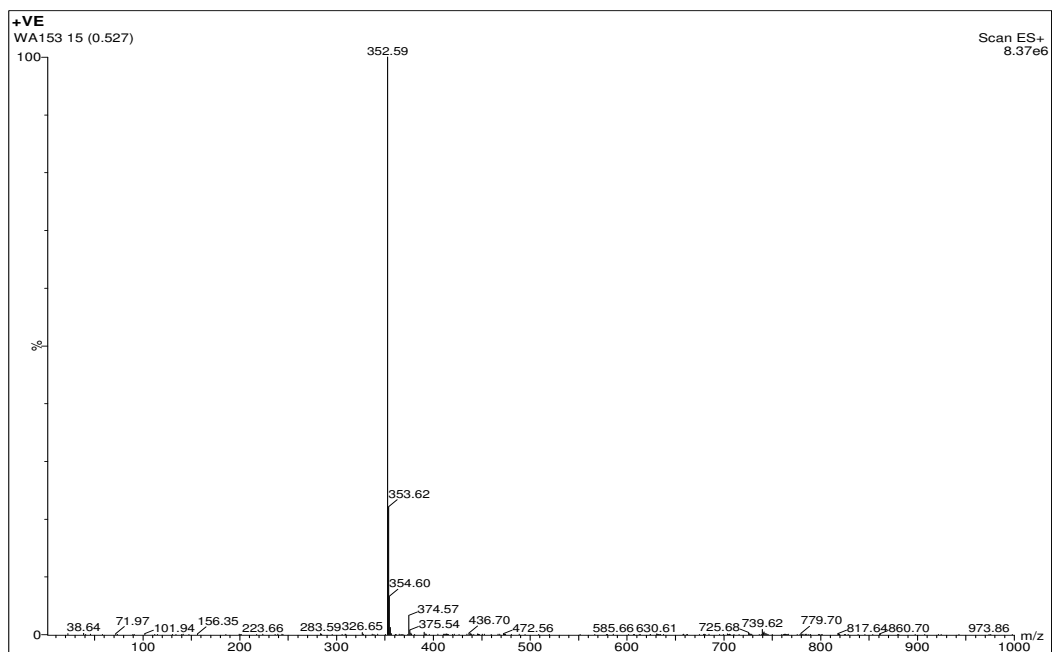
WA152 CDCl3.13.fid
carbon

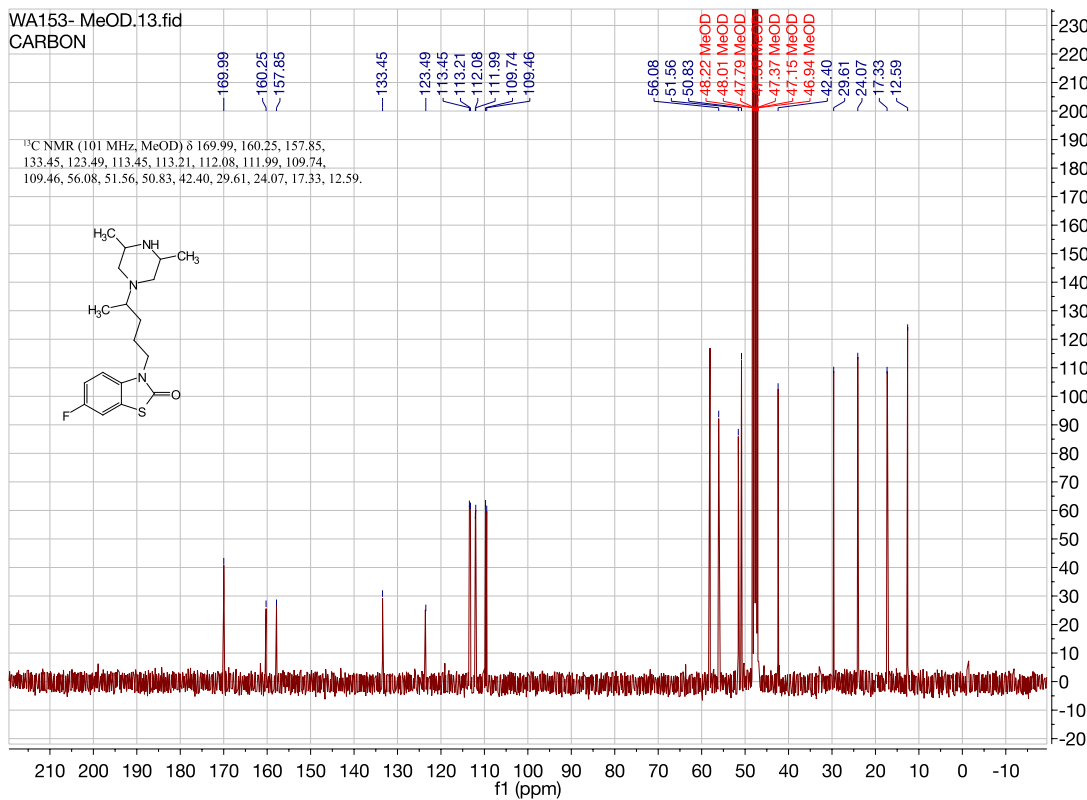
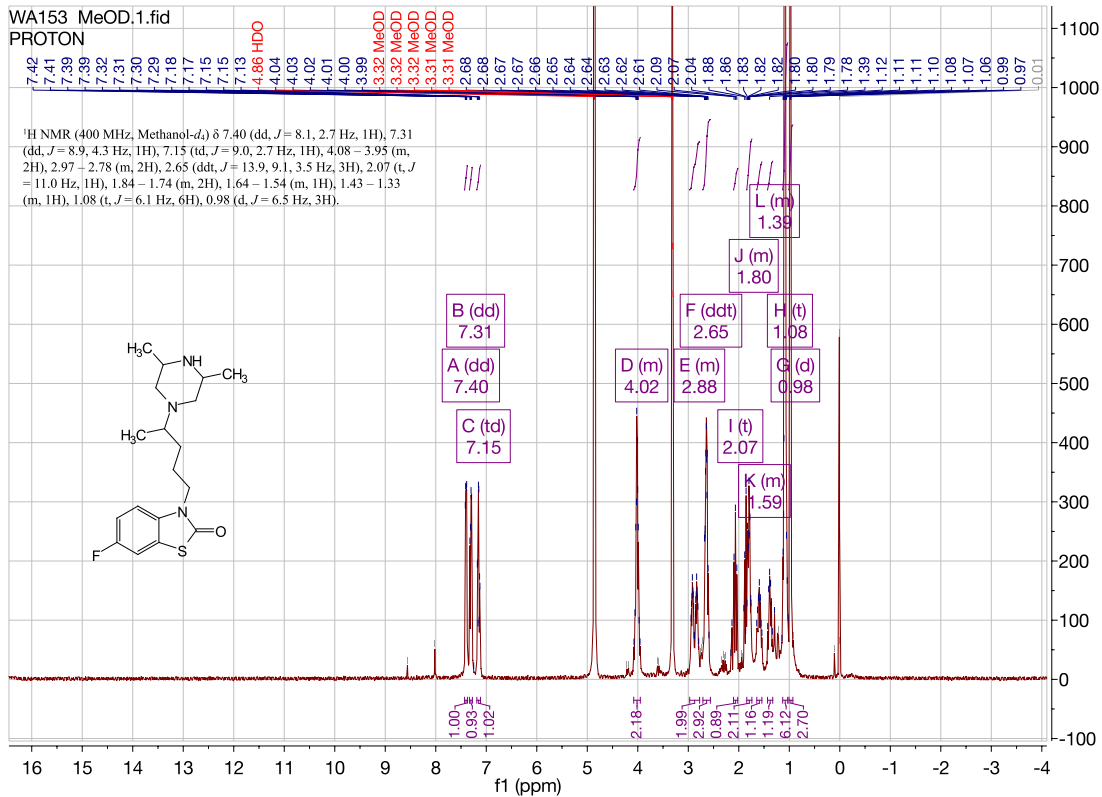
¹³C NMR (101 MHz, CDCl₃) δ 169.40, 160.09, 157.68,
133.11, 133.09, 123.96, 123.86, 113.71, 113.48, 111.18,
111.10, 110.22, 109.95, 50.58, 42.12, 37.72, 26.54, 25.92.



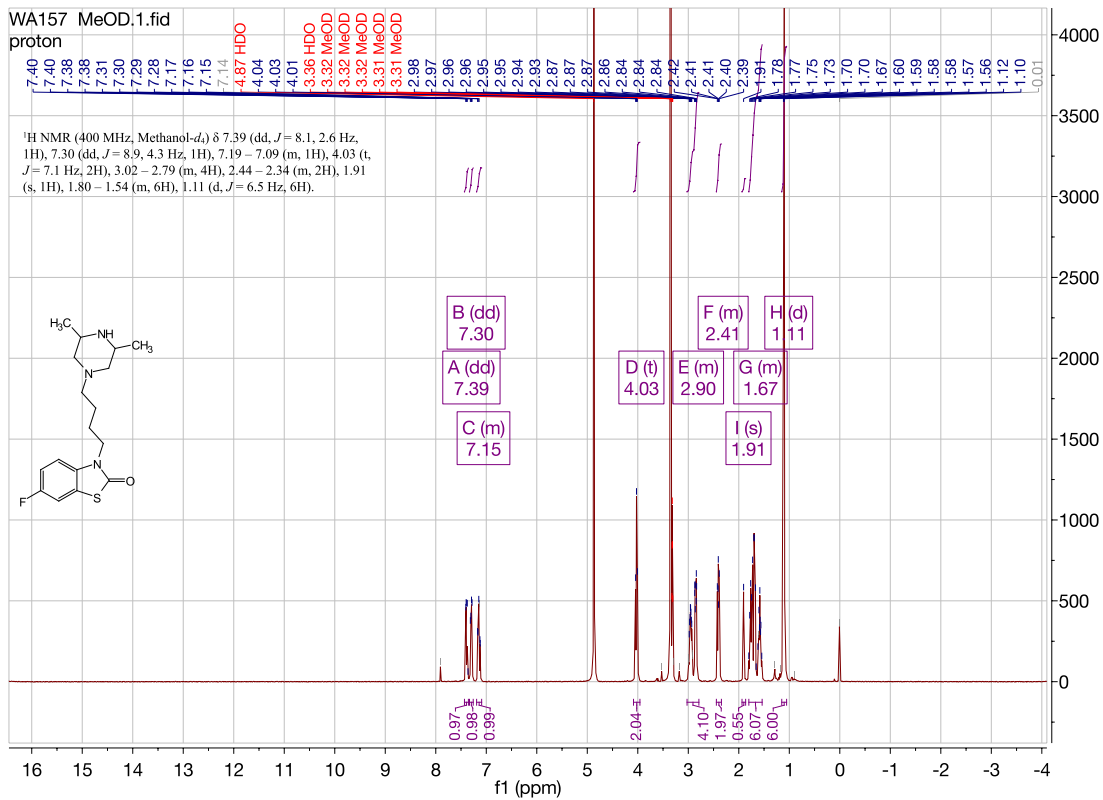
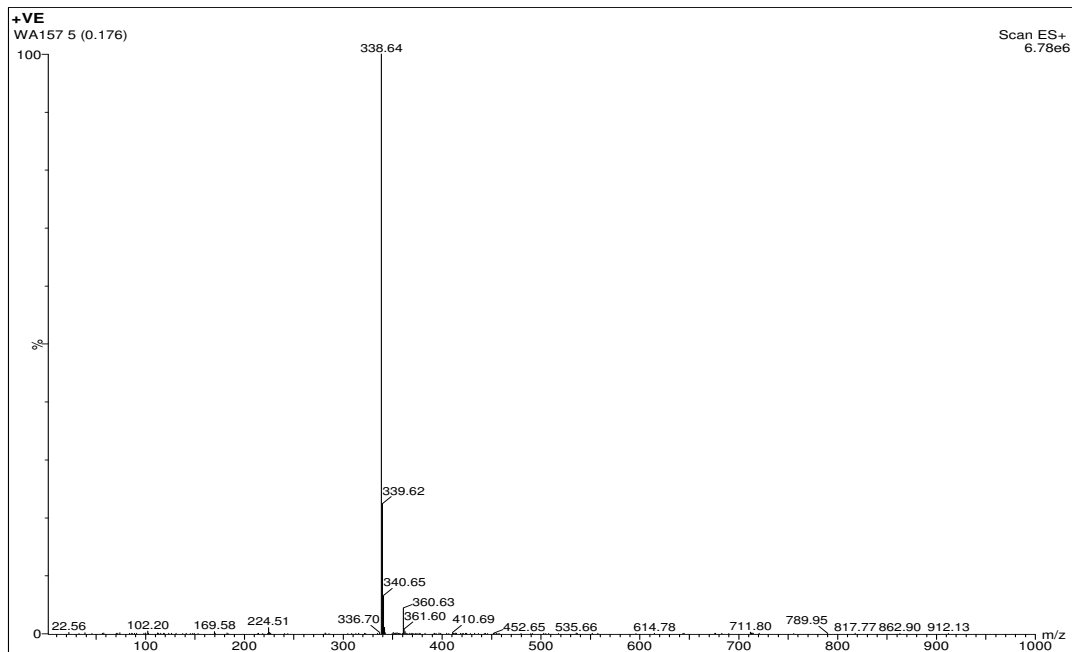


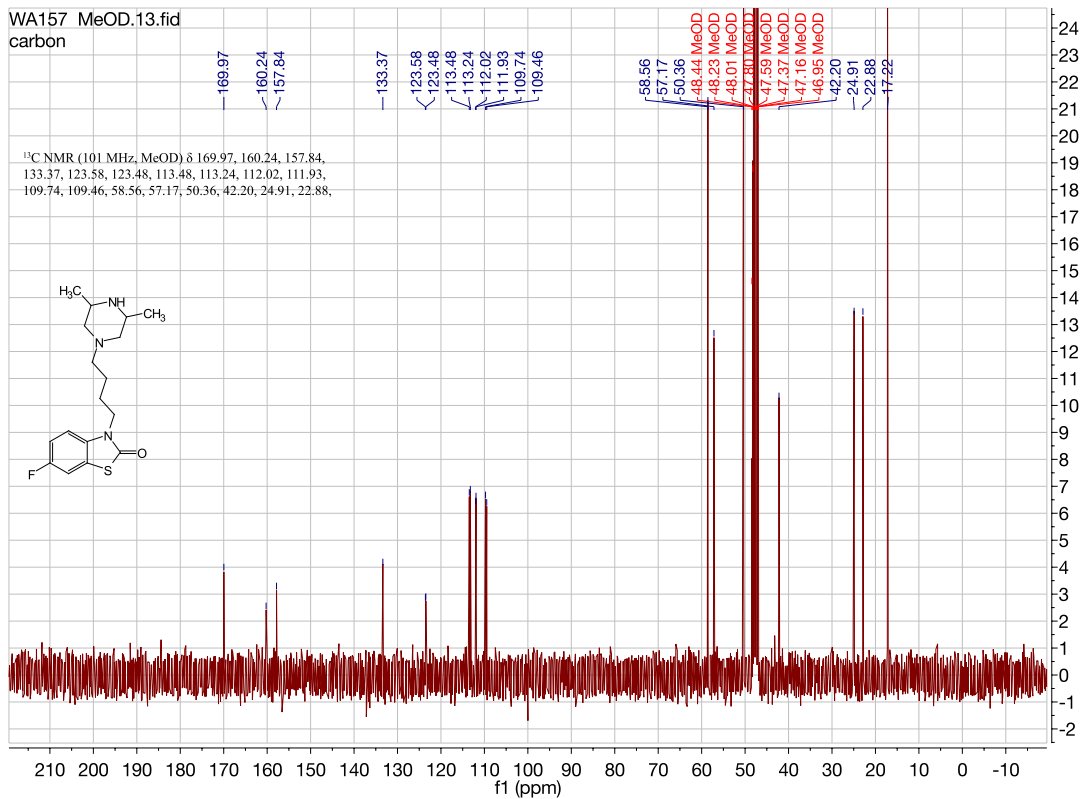
3-(4-(3,5-dimethylpiperazin-1-yl)pentyl)-6-fluorobenzo[d]thiazol-2(3H)-one. (WA153)



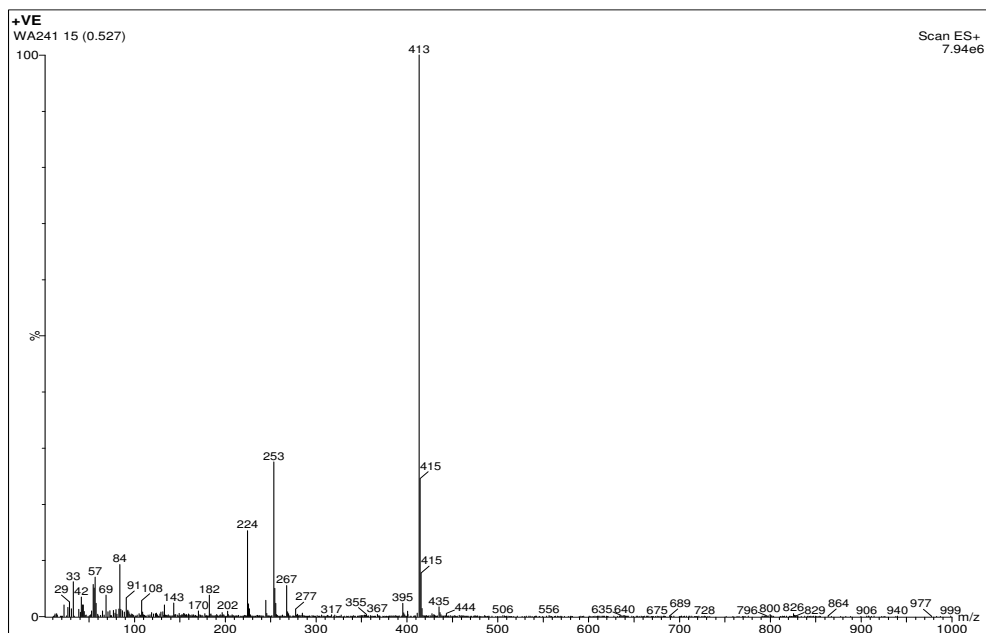


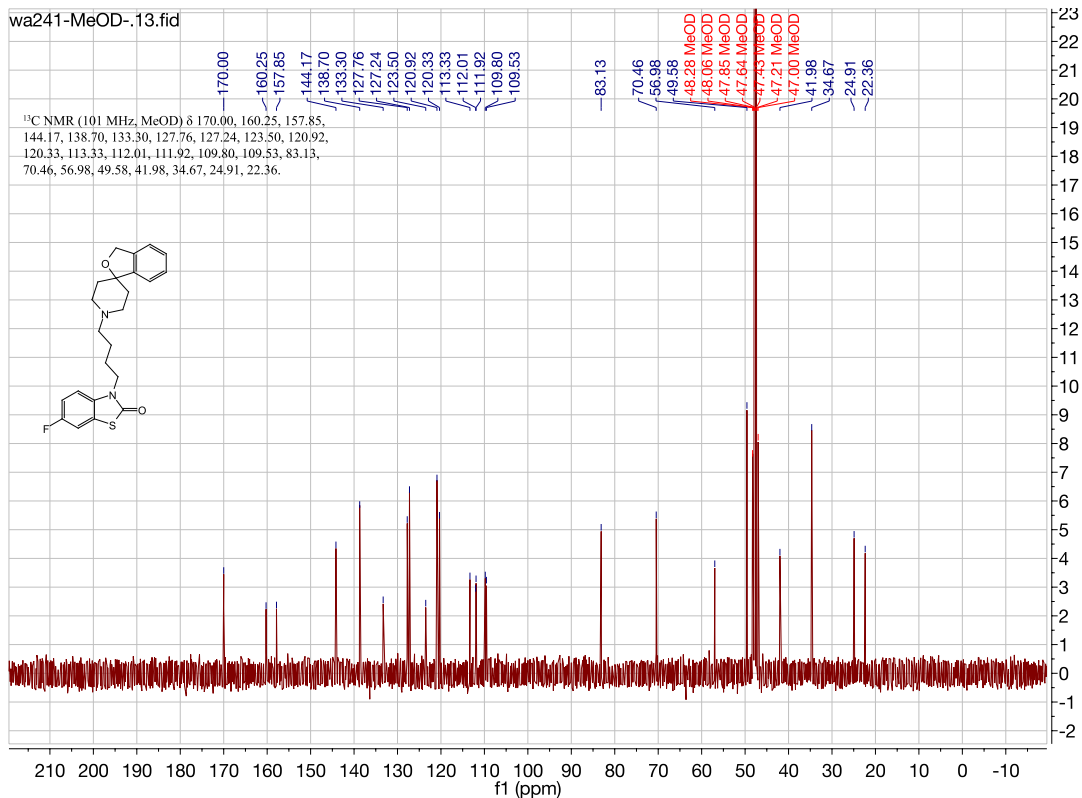
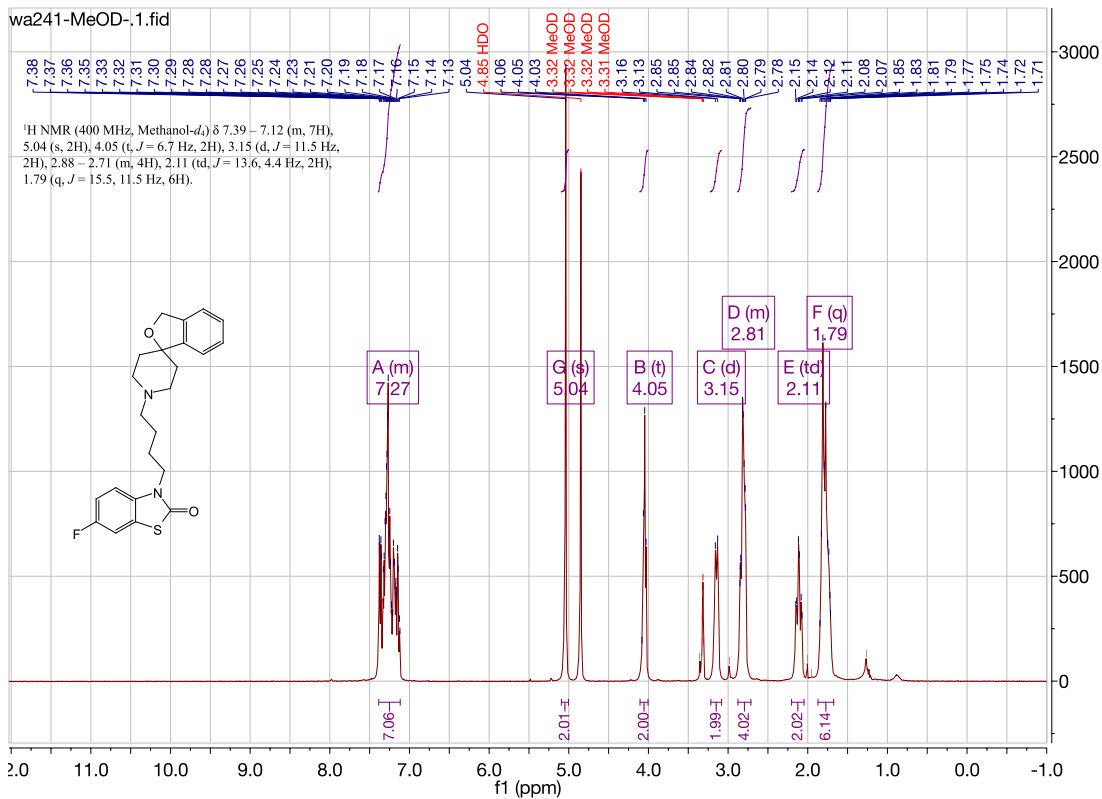
3-(4-(3,5-dimethylpiperazin-1-yl)butyl)-6-fluorobenzo[d]thiazol-2(3H)-one.(WA157)

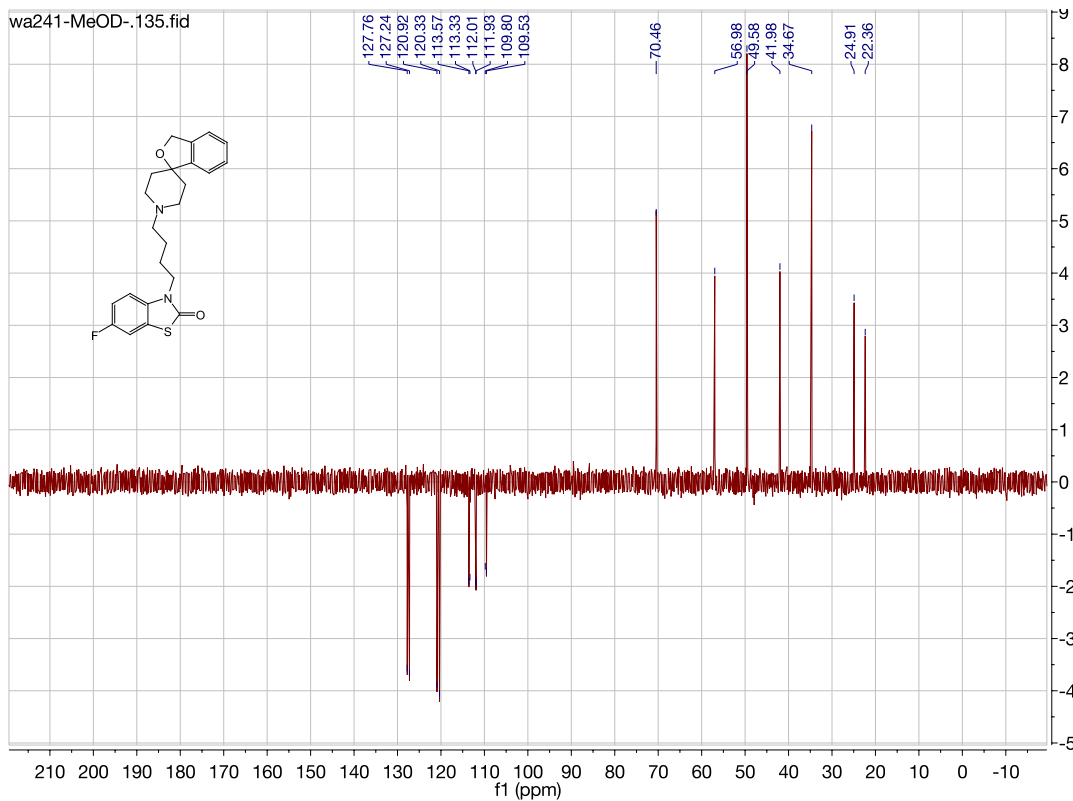




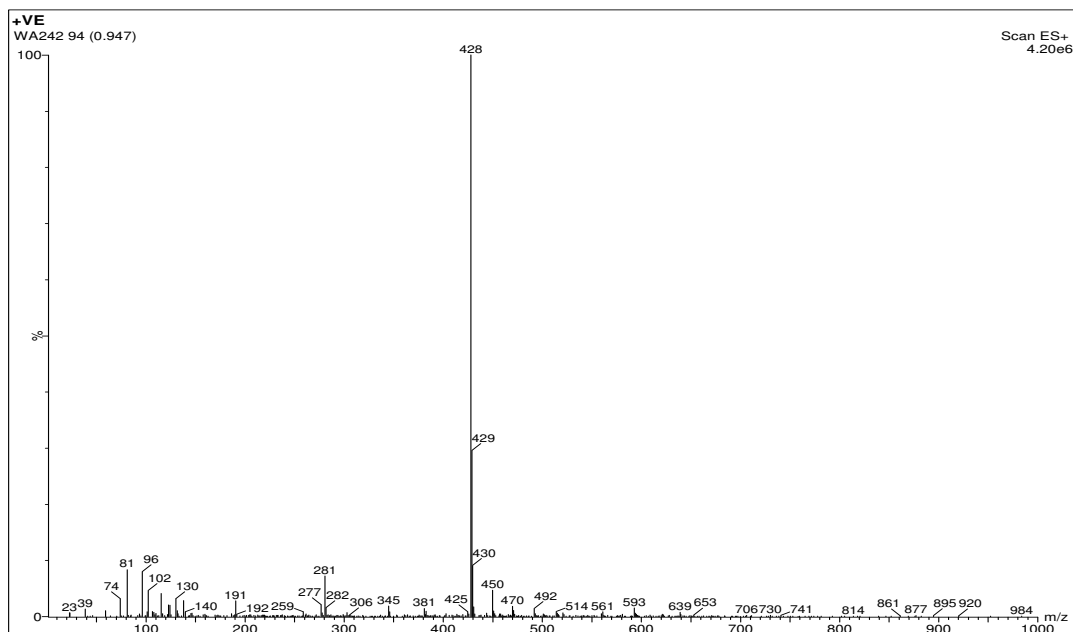
3-(4-(3H-spiro[isobenzofuran-1,4'-piperidin]-1'-yl)butyl)-6-fluorobenzo[d]thiazol-2(3H)-one. (WA241)

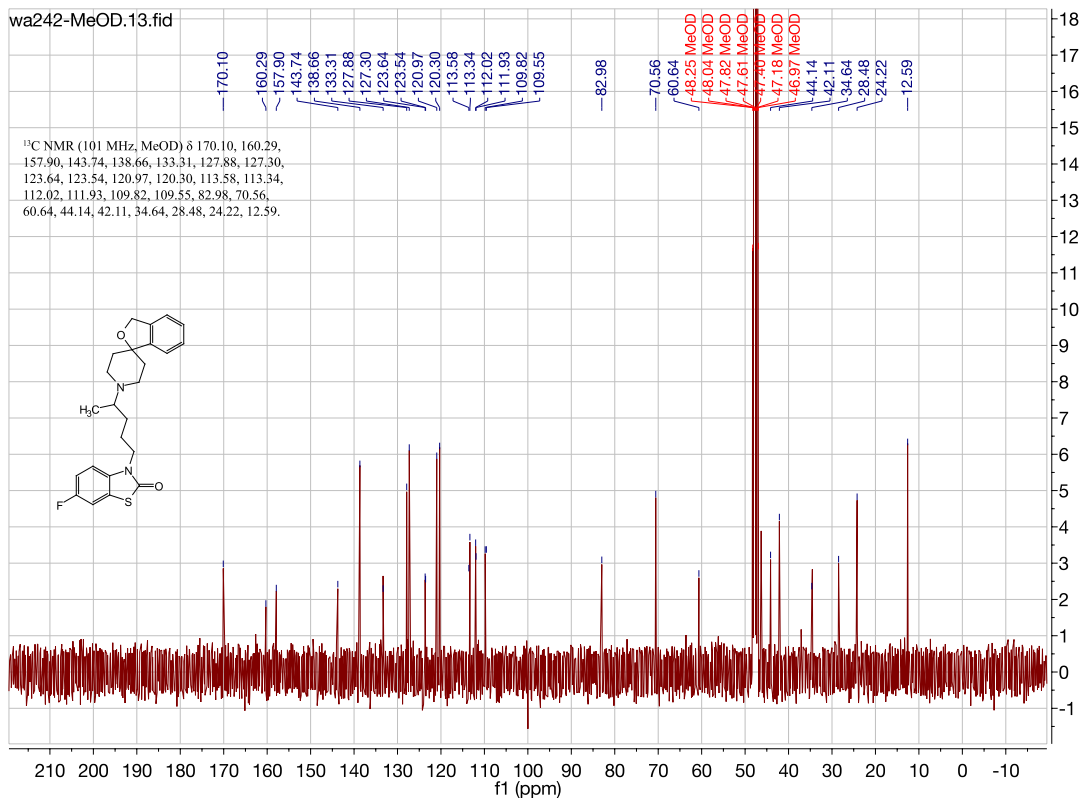
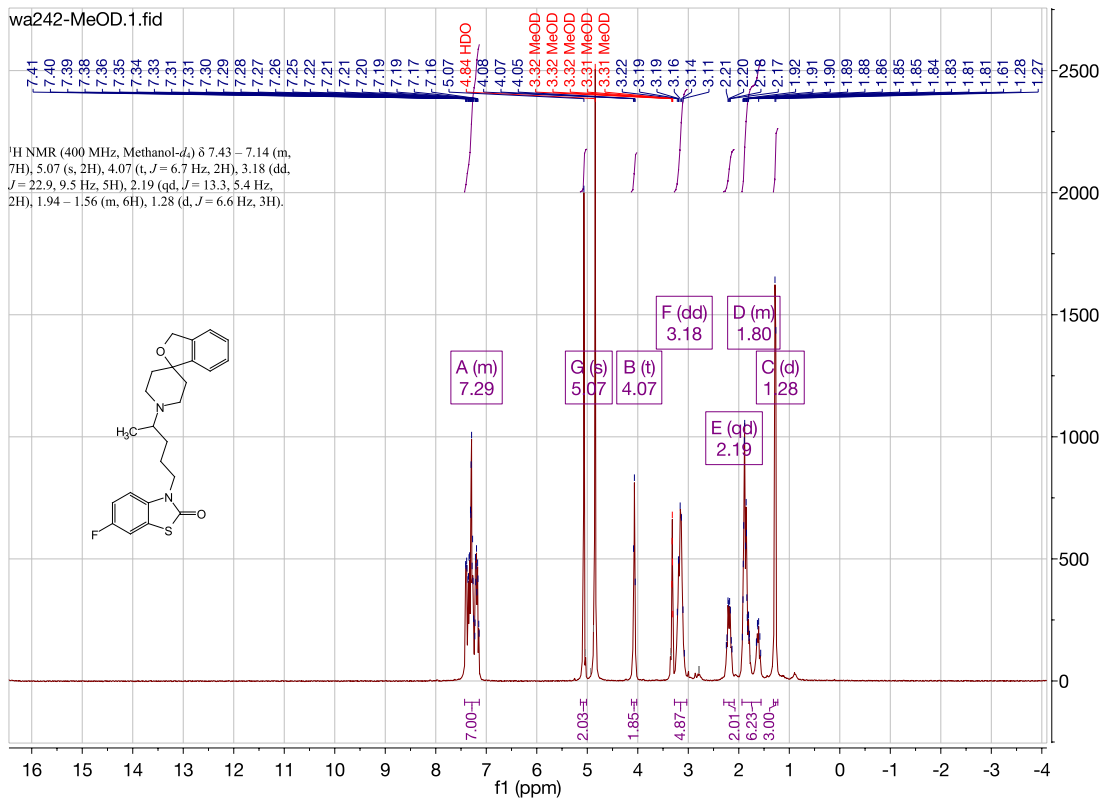


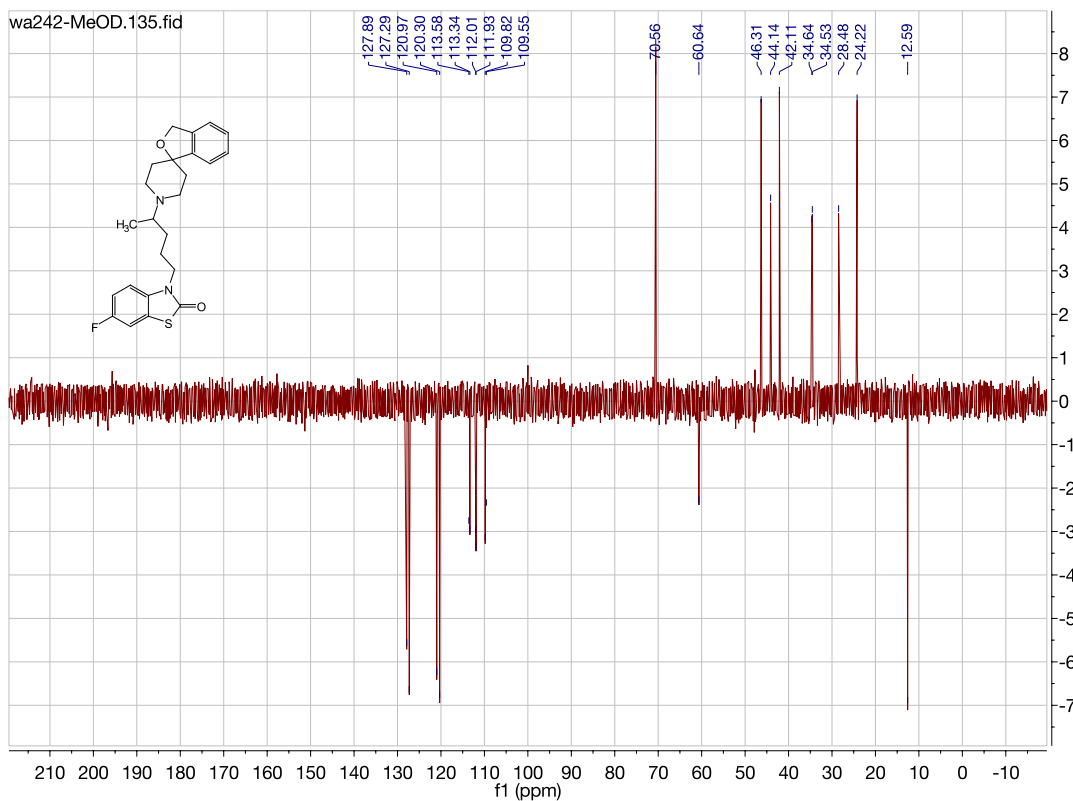




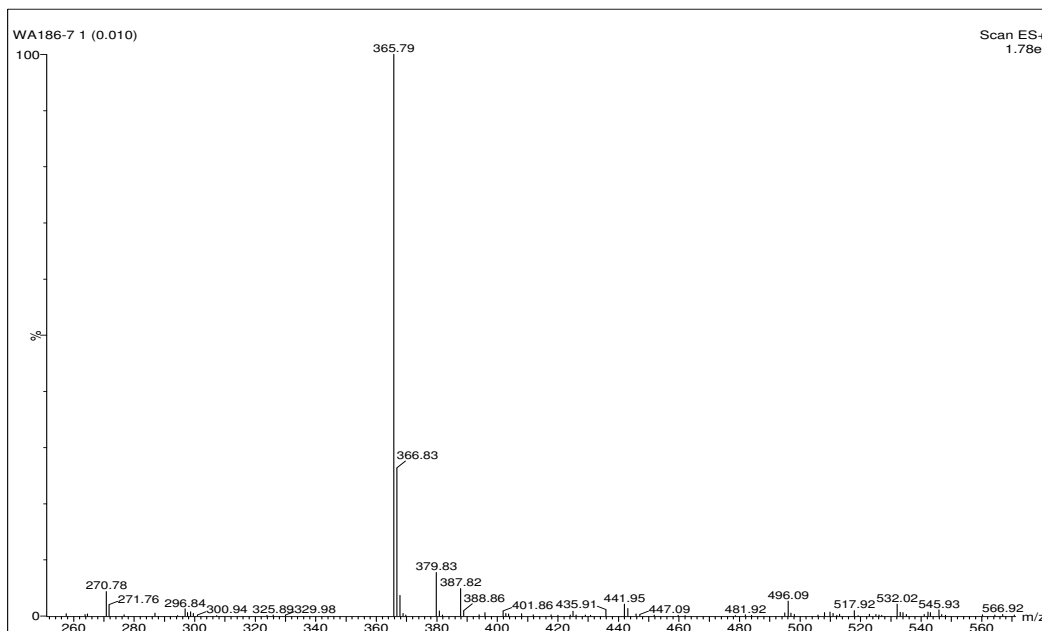
3-(4-(3H-spiro[isobenzofuran-1,4'-piperidin]-1'-yl)pentyl)-6-fluorobenzo[d]thiazol-2(3H)-one.(WA242)



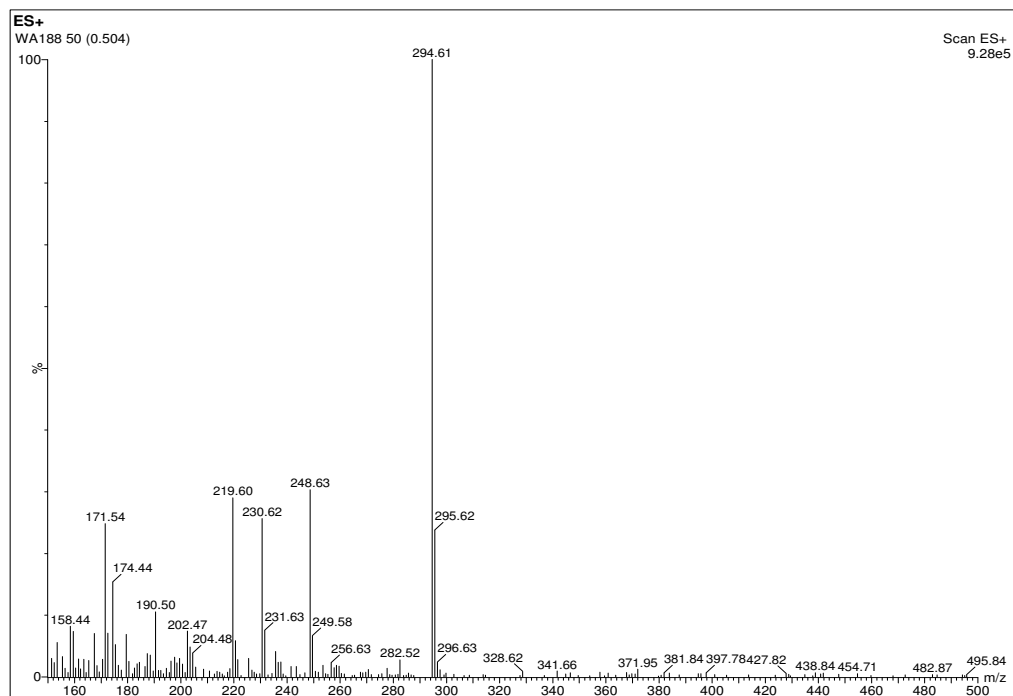




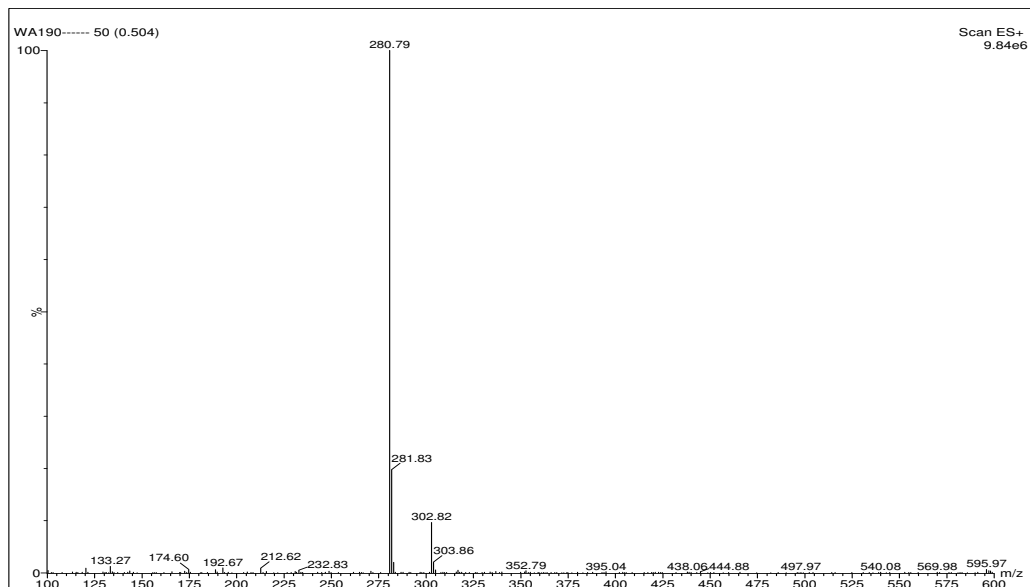
1-benzyl-4-(3-(4,4-dimethyl-4,5-dihydrooxazol-2-yl)phenyl)piperidin-4-ol. (WA186)



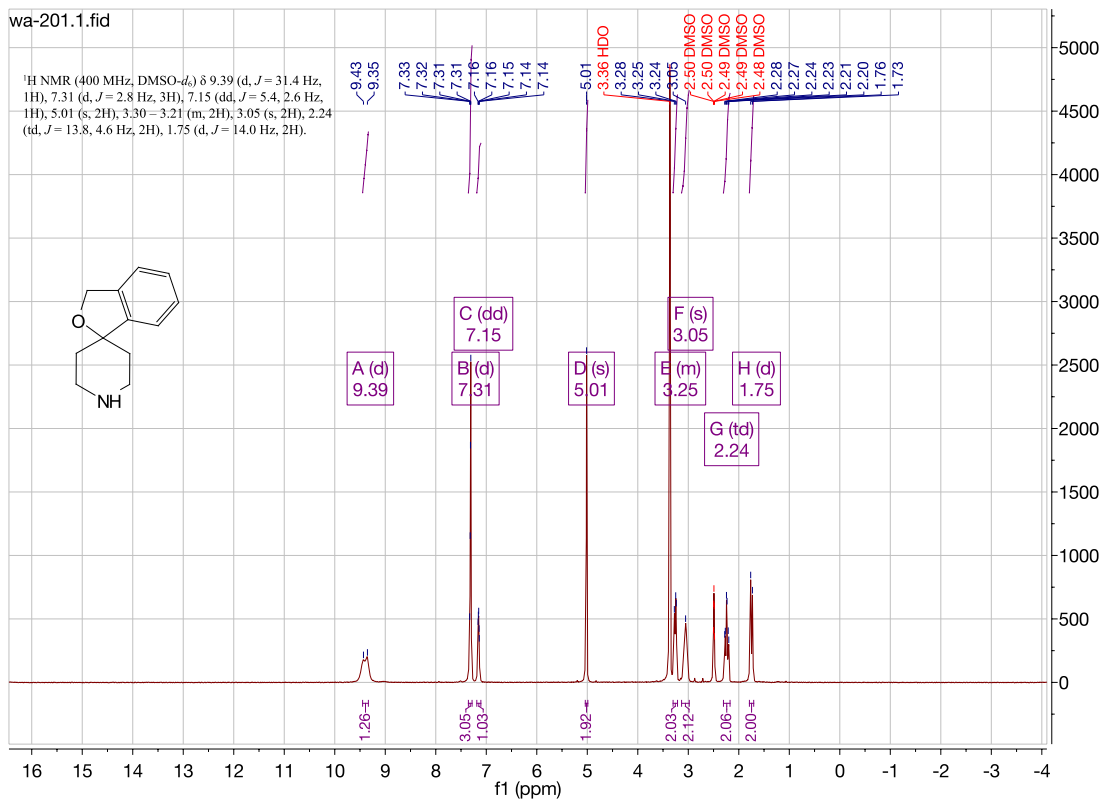
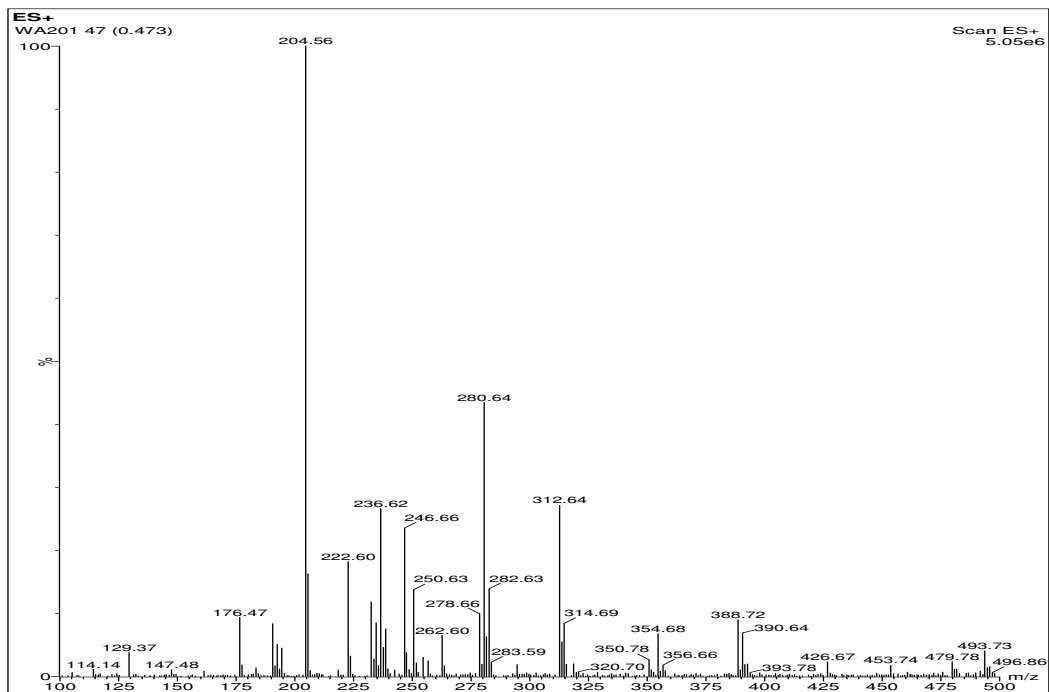
1'-benzyl-3*H*-spiro[isobenzofuran-1,4'-piperidin]-3-one. (WA188)

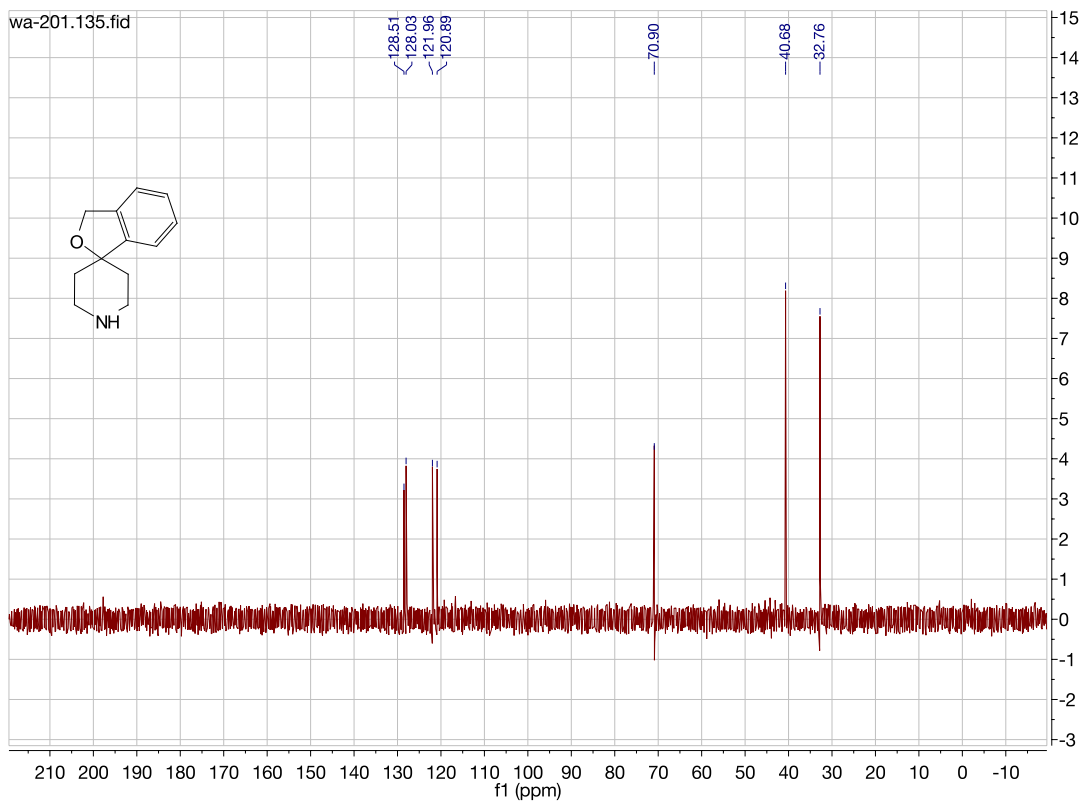
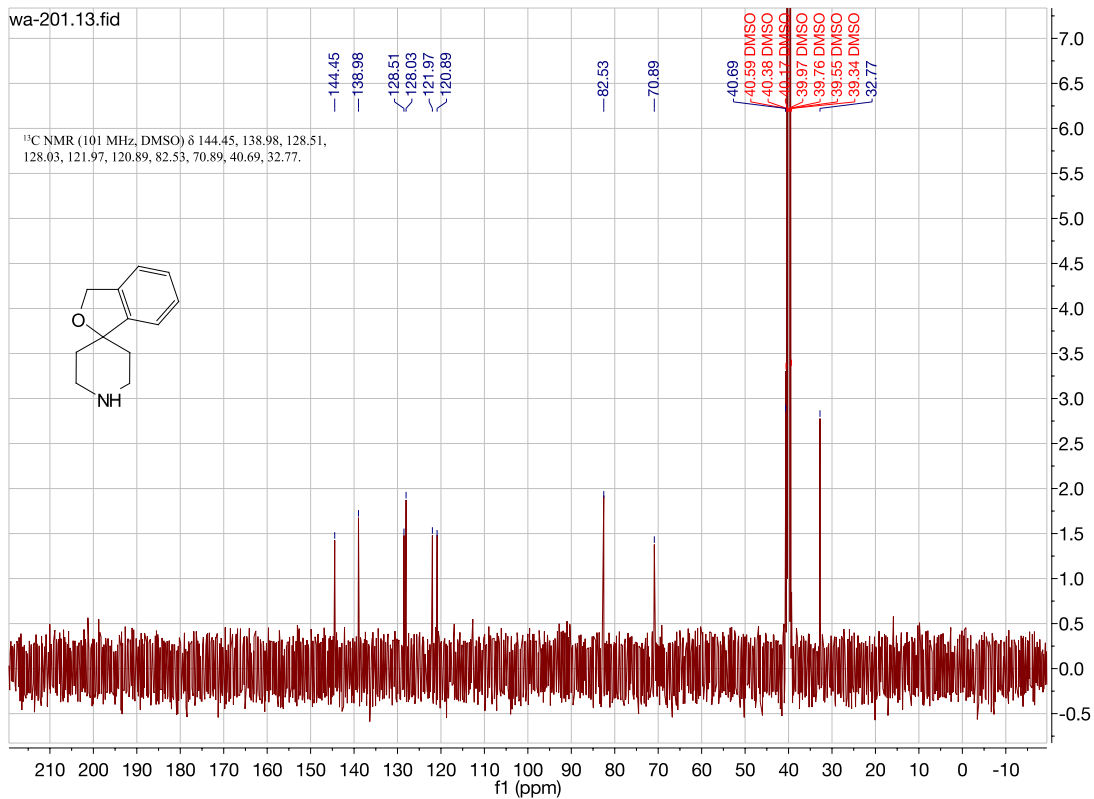


1'-benzyl-3*H*-spiro[isobenzofuran-1,4'-piperidine]. (WA190)

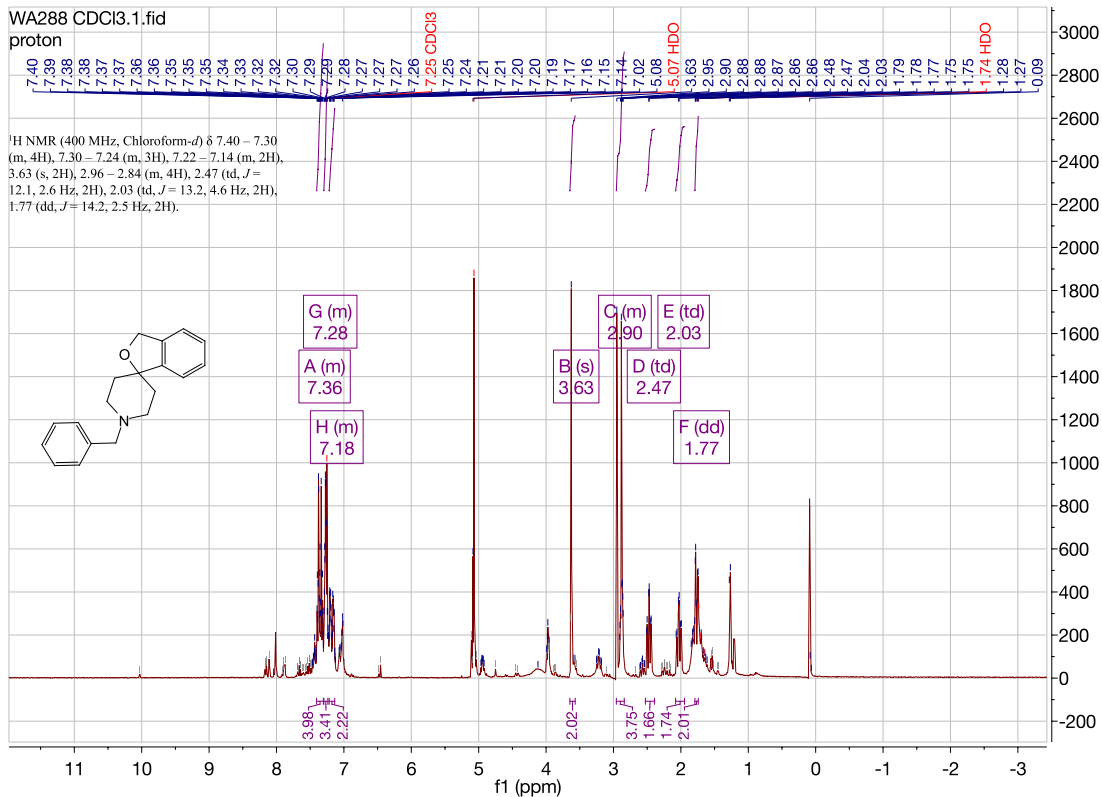
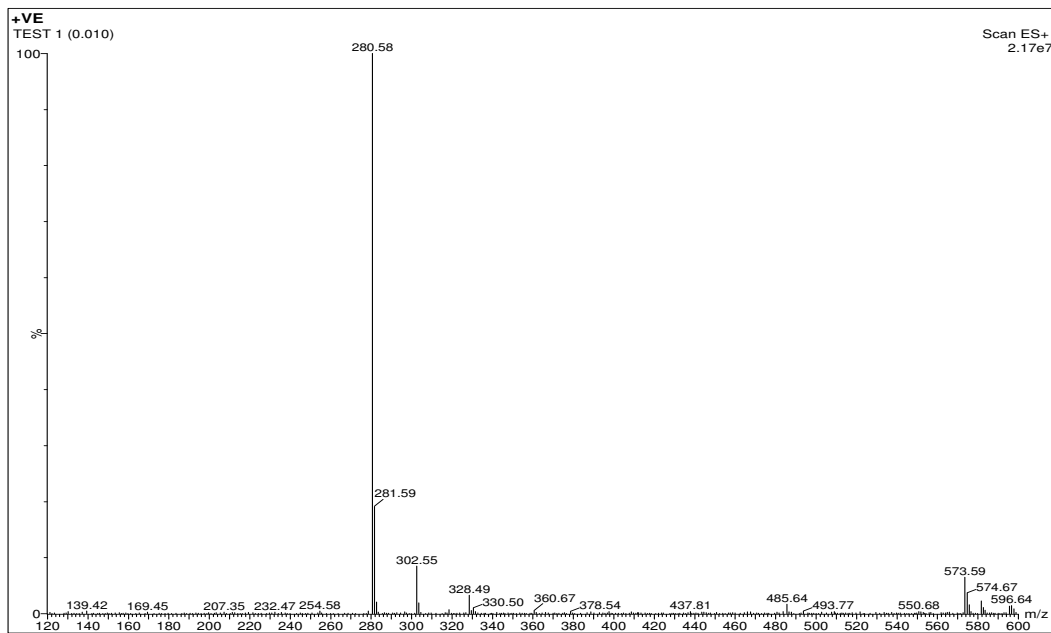


3*H*-spiro[isobenzofuran-1,4'-piperidine]. (WA201)



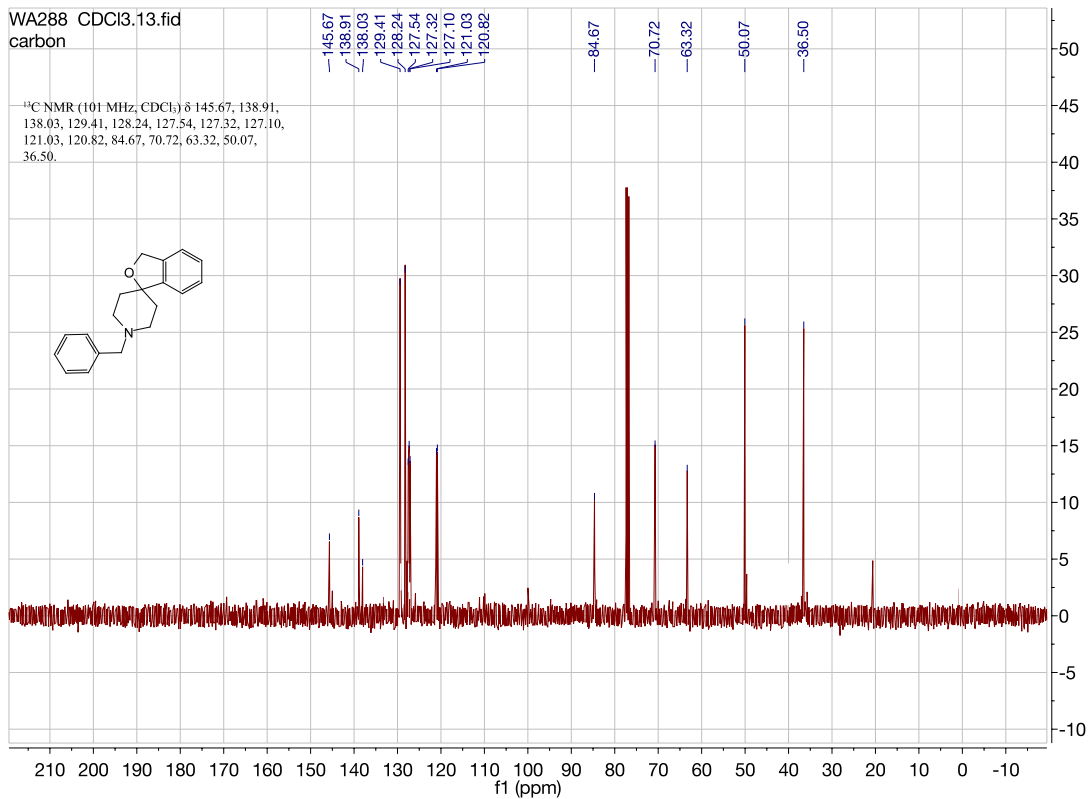


1'-benzyl-3*H*-spiro[isobenzofuran-1,4'-piperidine]. (WA288)

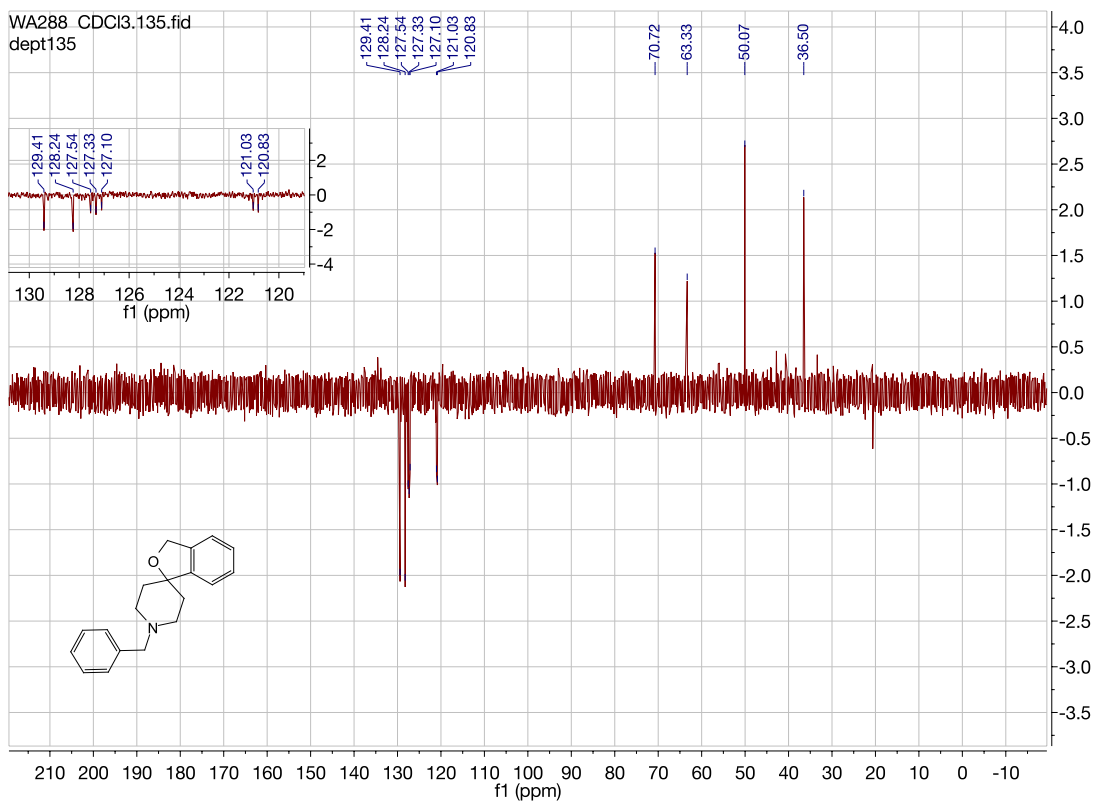


WA288 CDCI3.13.fid
carbon

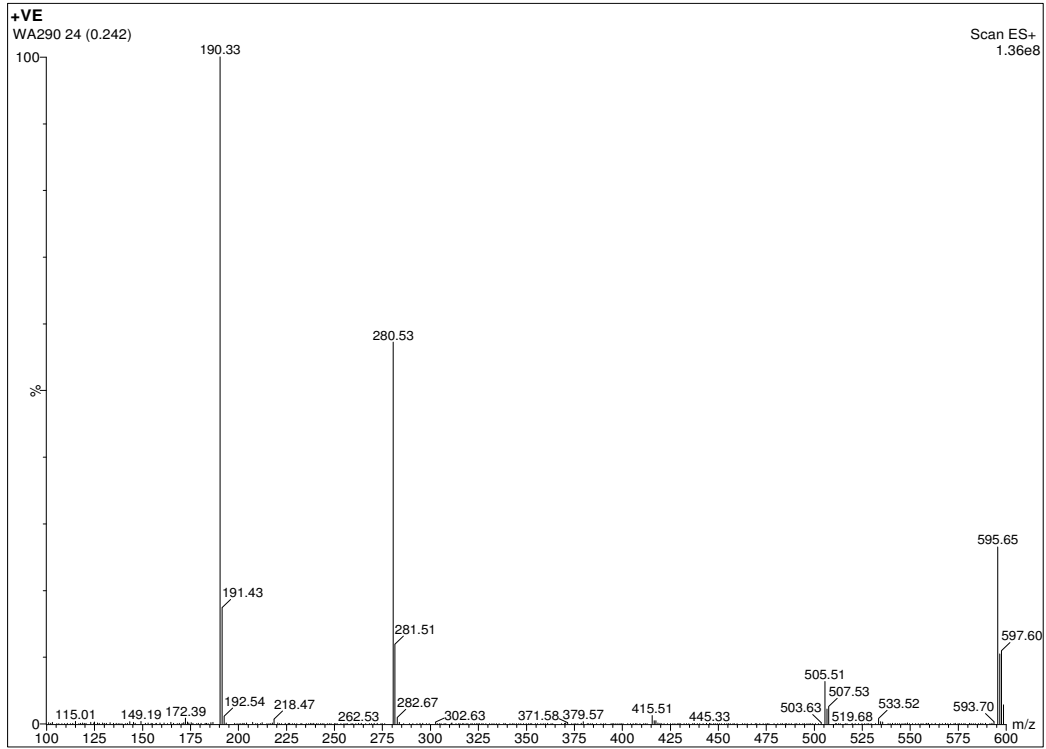
¹³C NMR (101 MHz, CDCl₃) δ 145.67, 138.91, 138.03, 129.41, 128.24, 127.54, 127.32, 127.10, 121.03, 120.82, 84.67, 70.72, 63.32, 50.07, 36.50.



WA288 CDCI3.135.fid
dept135

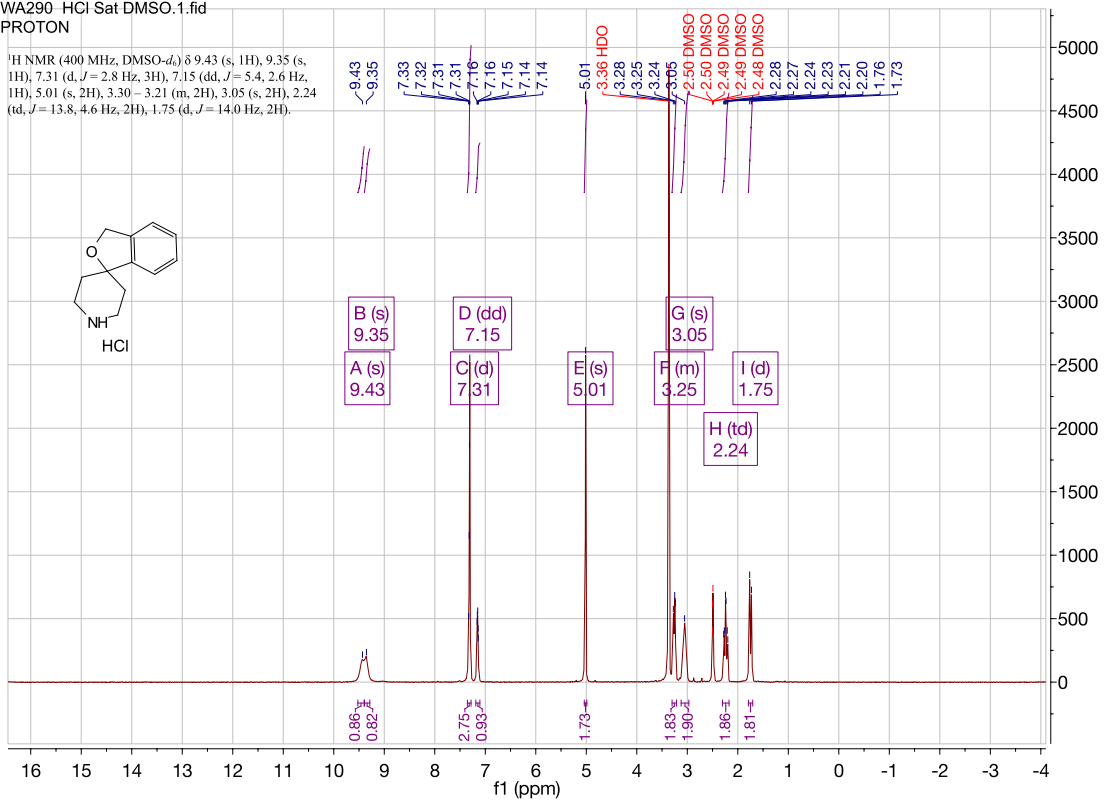


3*H*-spiro[isobenzofuran-1,4'-piperidine]. (WA290)



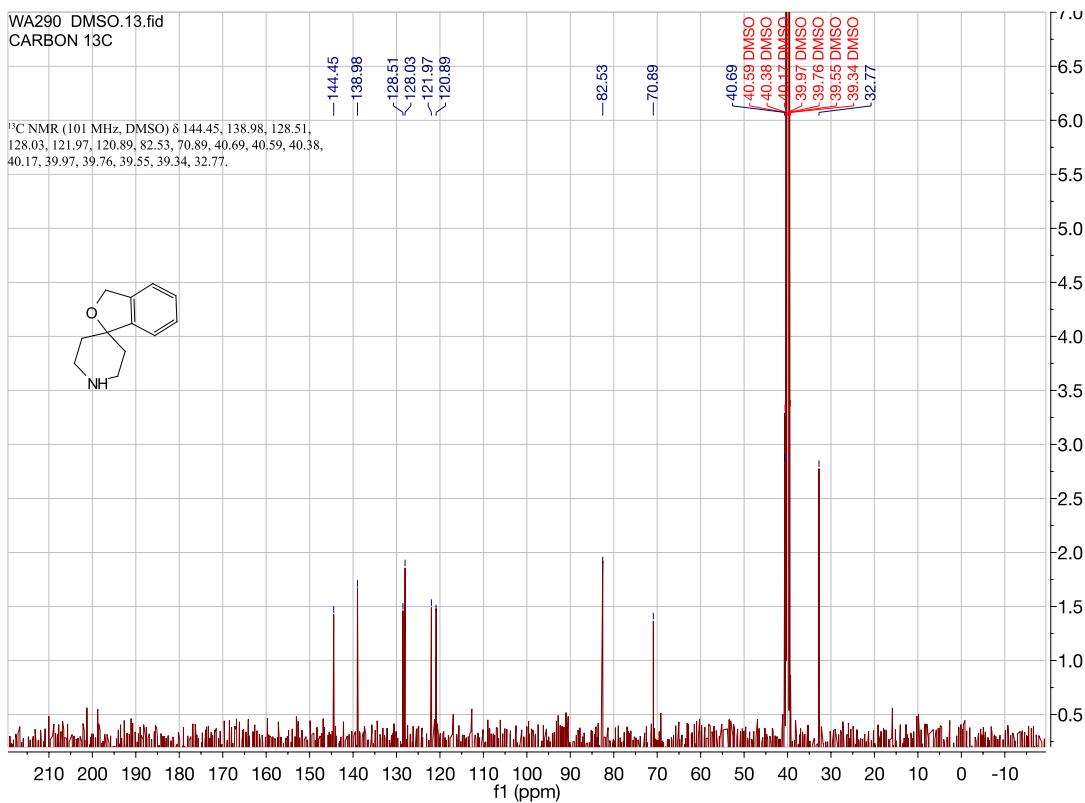
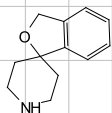
WA290 HCl Sat DMSO-1.fid
PROTON

¹H NMR (400 MHz, DMSO-*d*₆) δ 9.43 (s, 1H), 9.35 (s, 1H), 7.31 (d, *J* = 2.8 Hz, 3H), 7.15 (dd, *J* = 5.4, 2.6 Hz, 1H), 5.01 (s, 2H), 3.30–3.21 (m, 2H), 3.05 (s, 2H), 2.24 (td, *J* = 13.8, 4.6 Hz, 2H), 1.75 (d, *J* = 14.0 Hz, 2H).

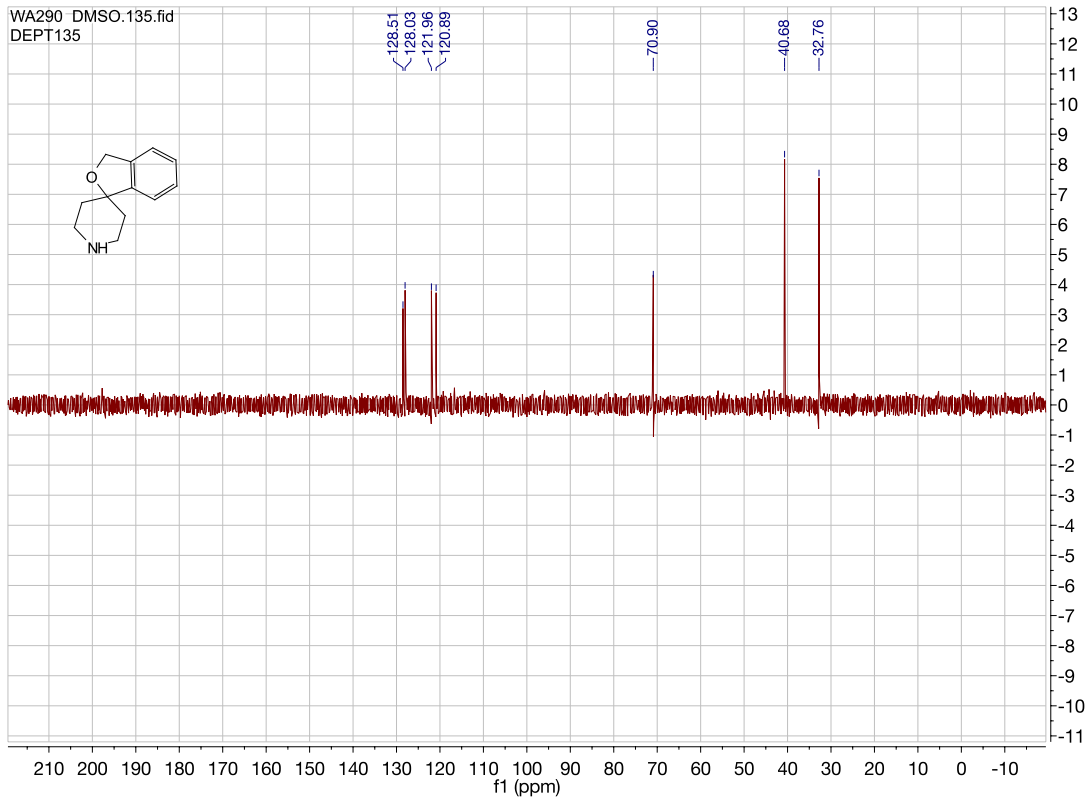


WA290 DMSO.13.fid
CARBON 13C

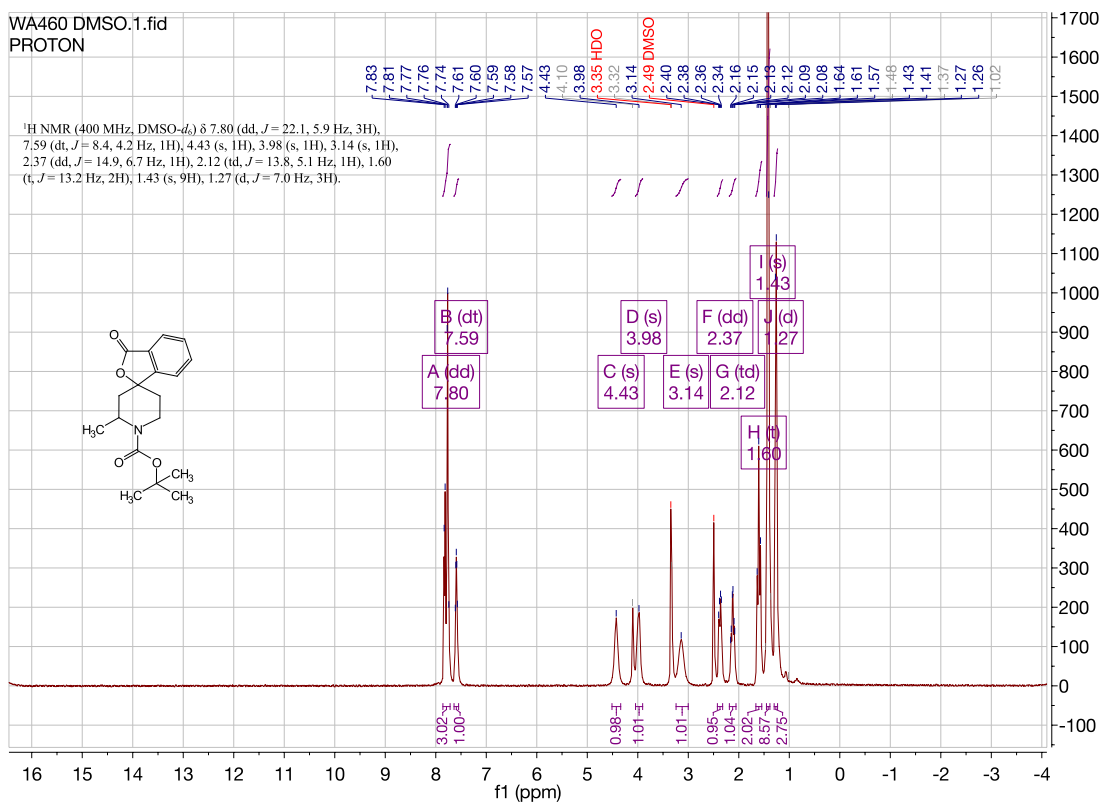
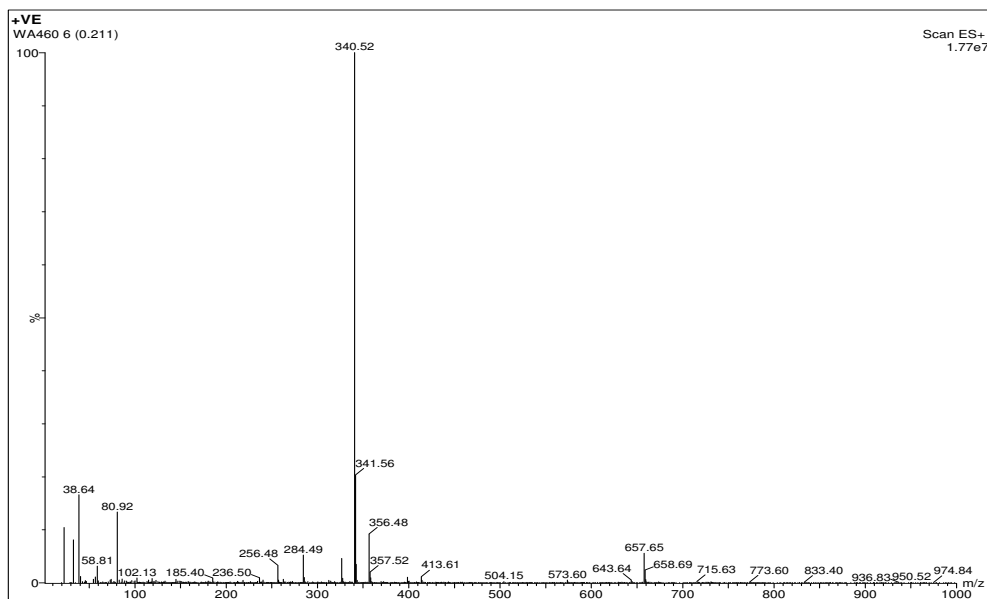
¹³C NMR (101 MHz, DMSO) δ 144.45, 138.98, 128.51, 128.03, 121.97, 120.89, 82.53, 70.89, 40.69, 40.59, 40.38, 40.17, 39.97, 39.76, 39.55, 39.34, 32.77.



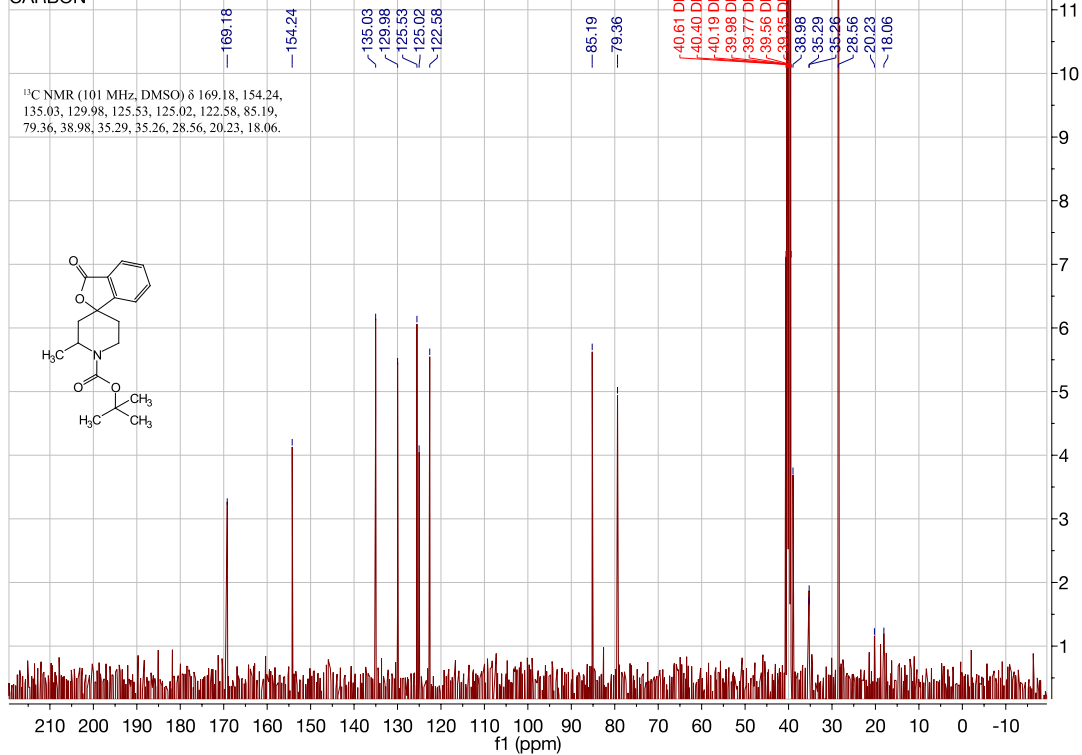
WA290 DMSO.135.fid
DEPT135



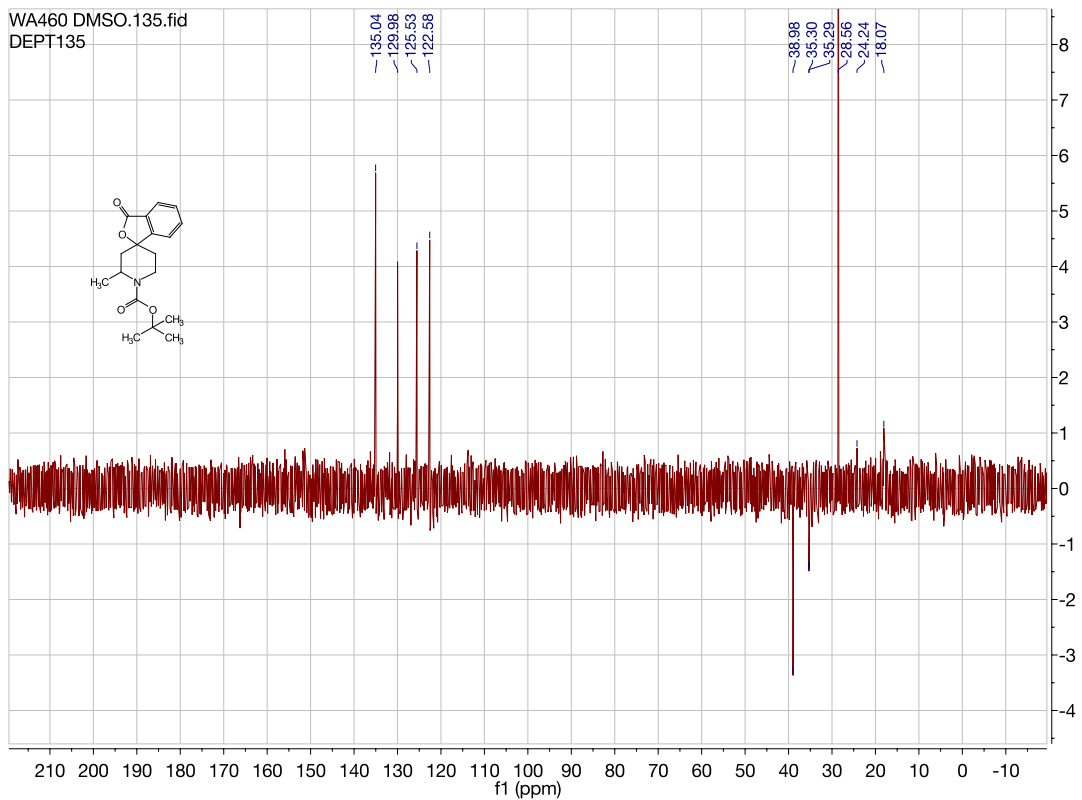
***tert*-butyl-2'-methyl-3-oxo-3*H*-spiro[isobenzofuran-1,4'-piperidine]-1'-carboxylate (WA460)**



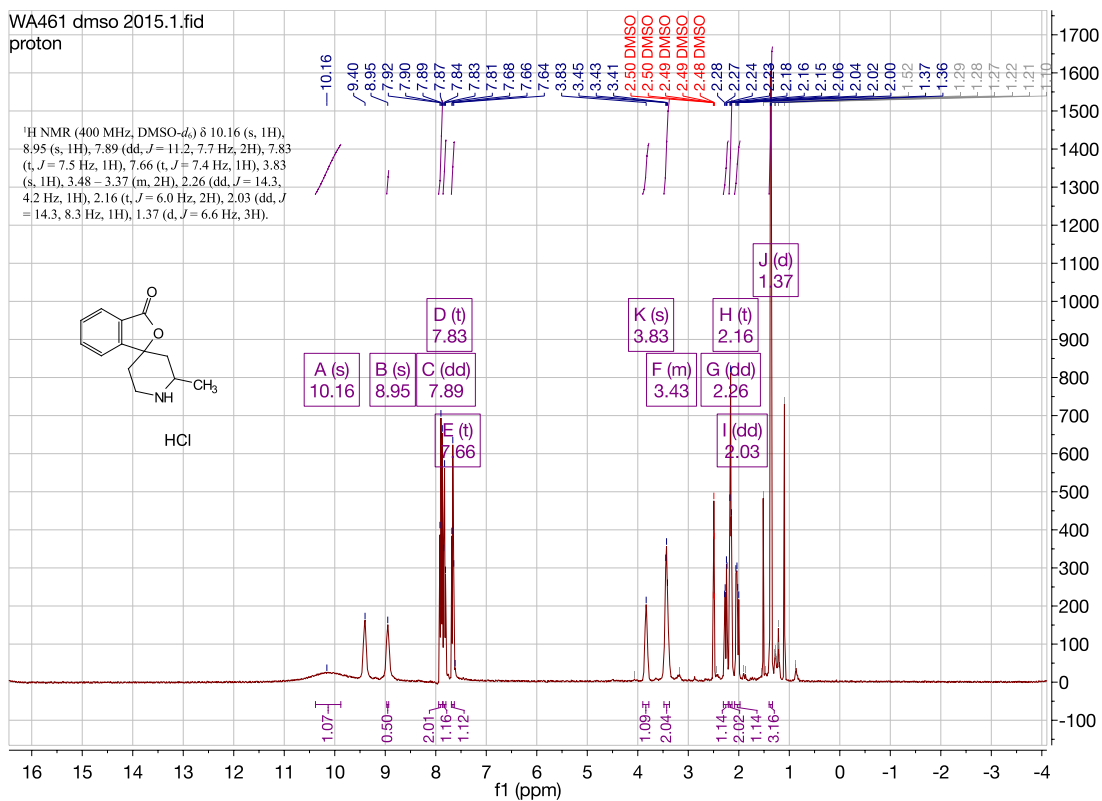
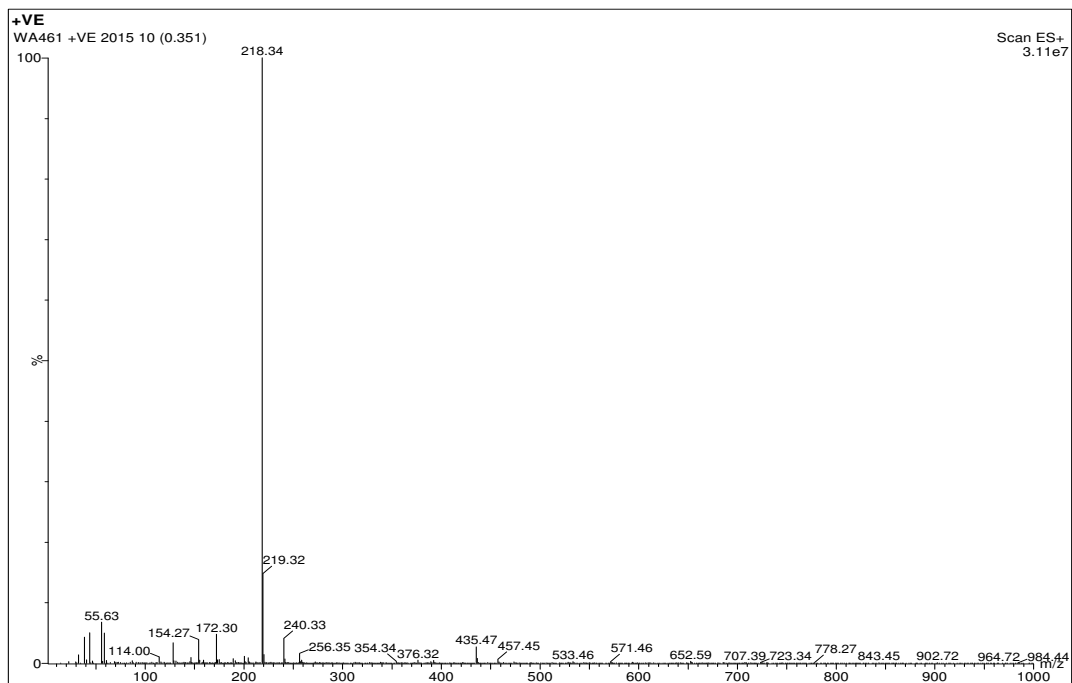
WA460 DMSO.13.fid
CARBON

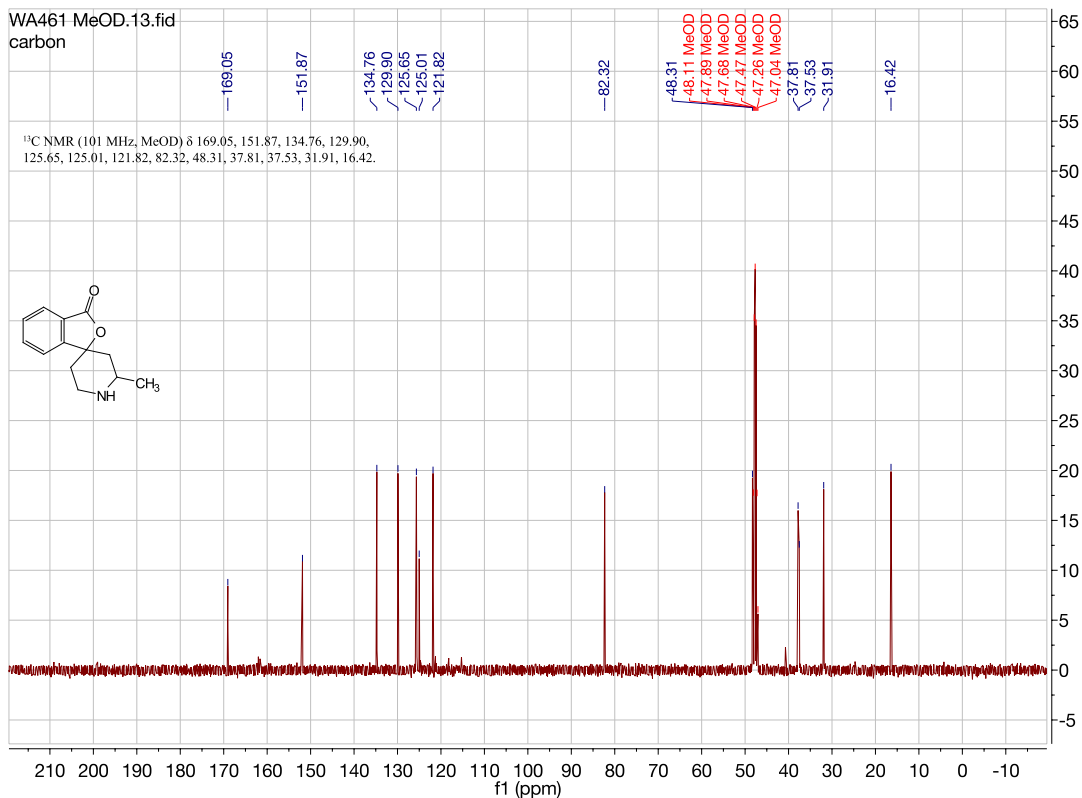
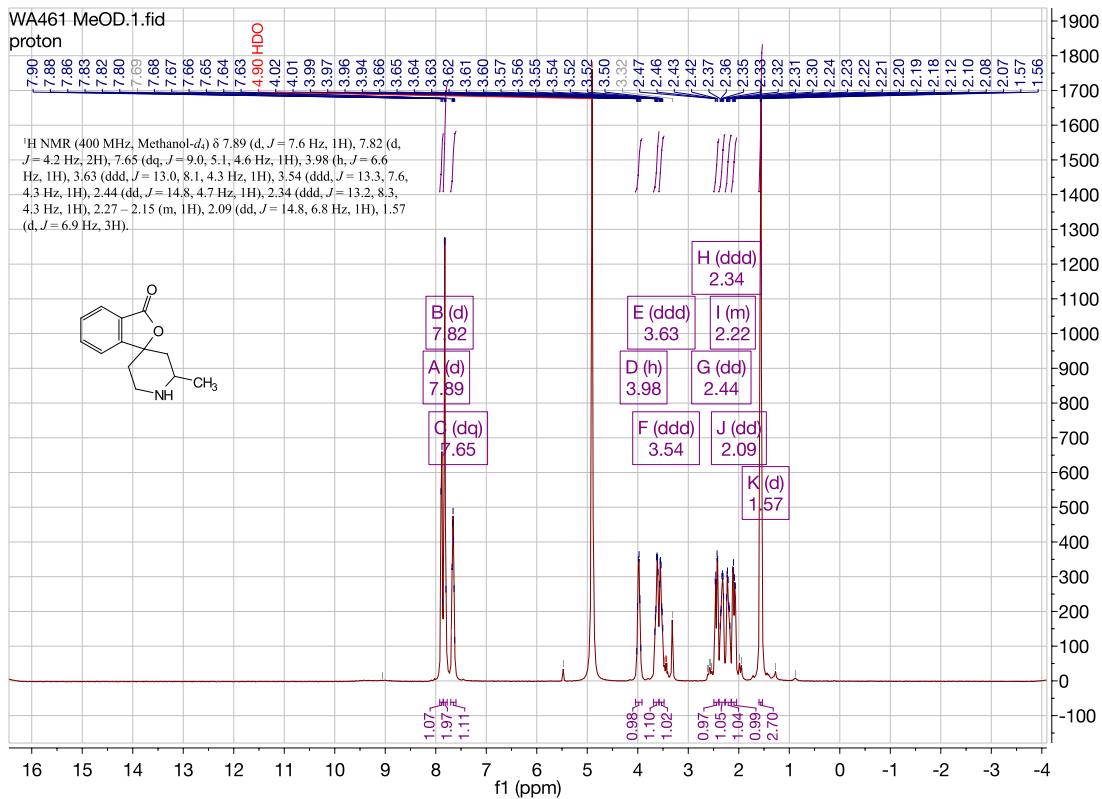


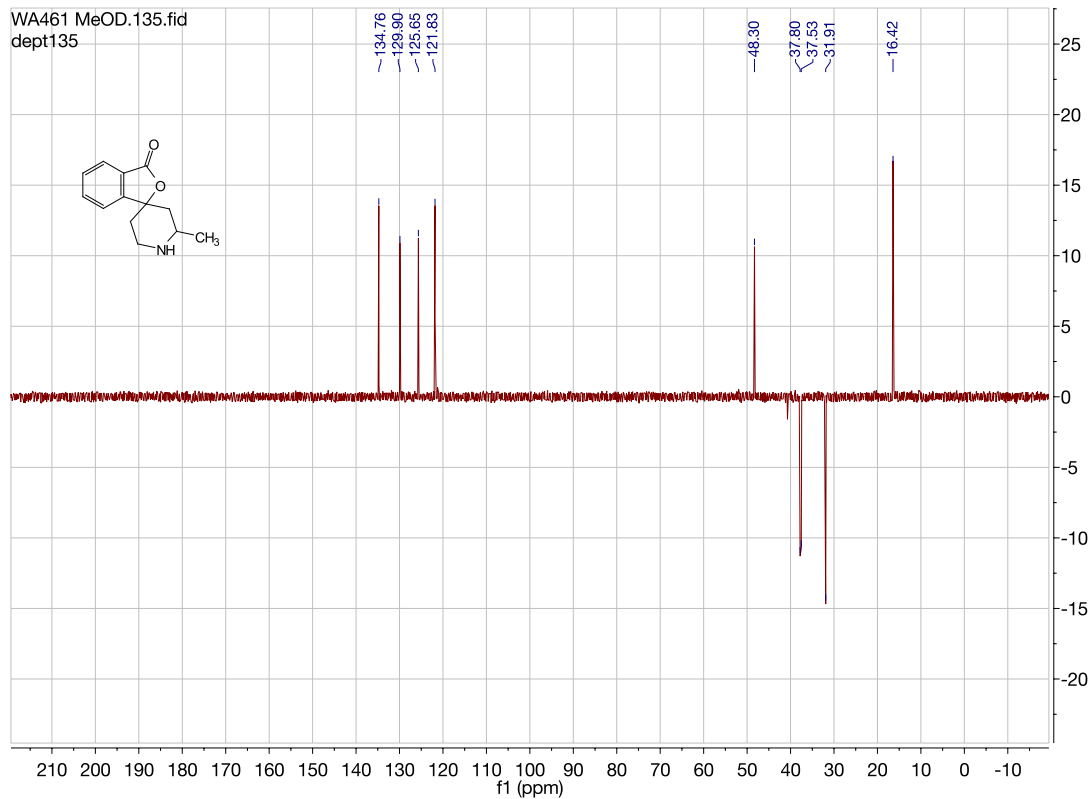
WA460 DMSO.135.fid
DEPT135



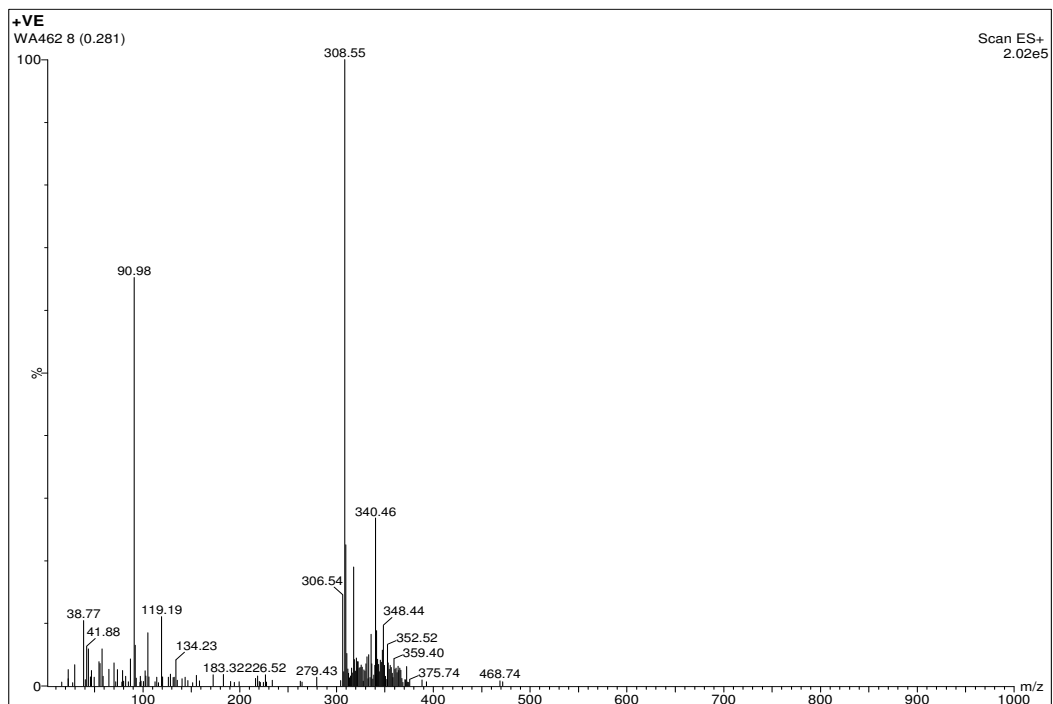
2'-methyl-3H-spiro[isobenzofuran-1,4'-piperidin]-3-one. (WA461)

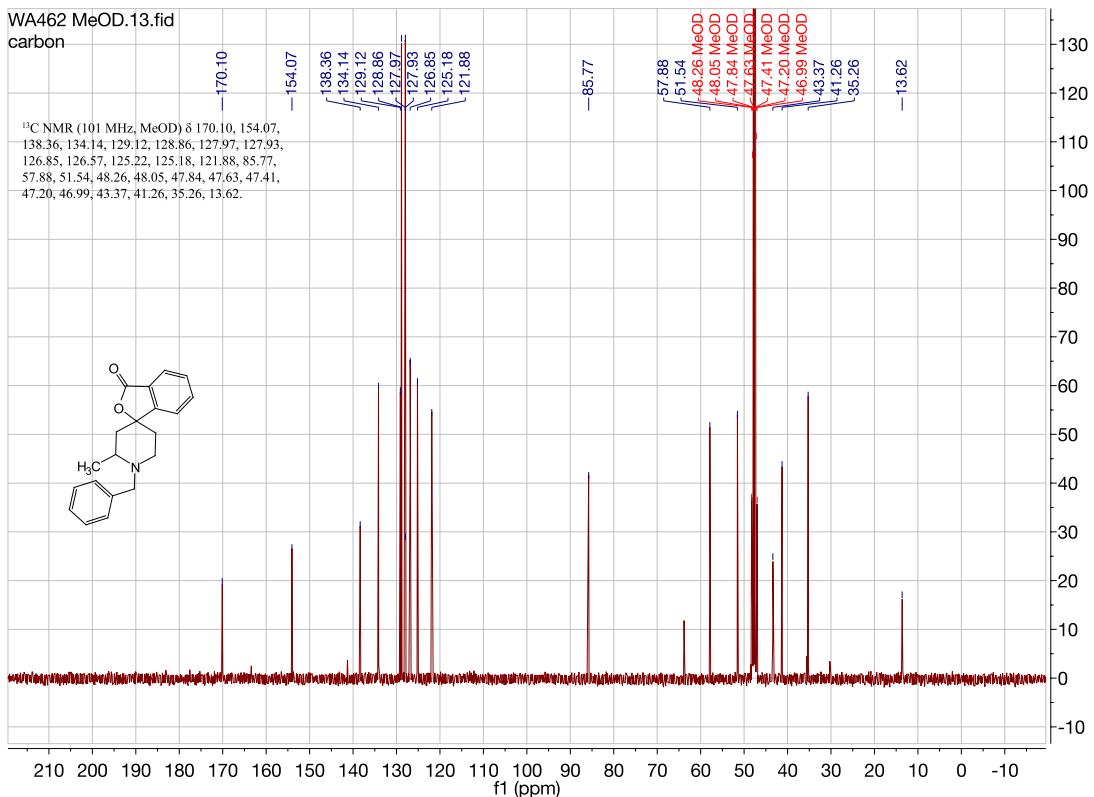
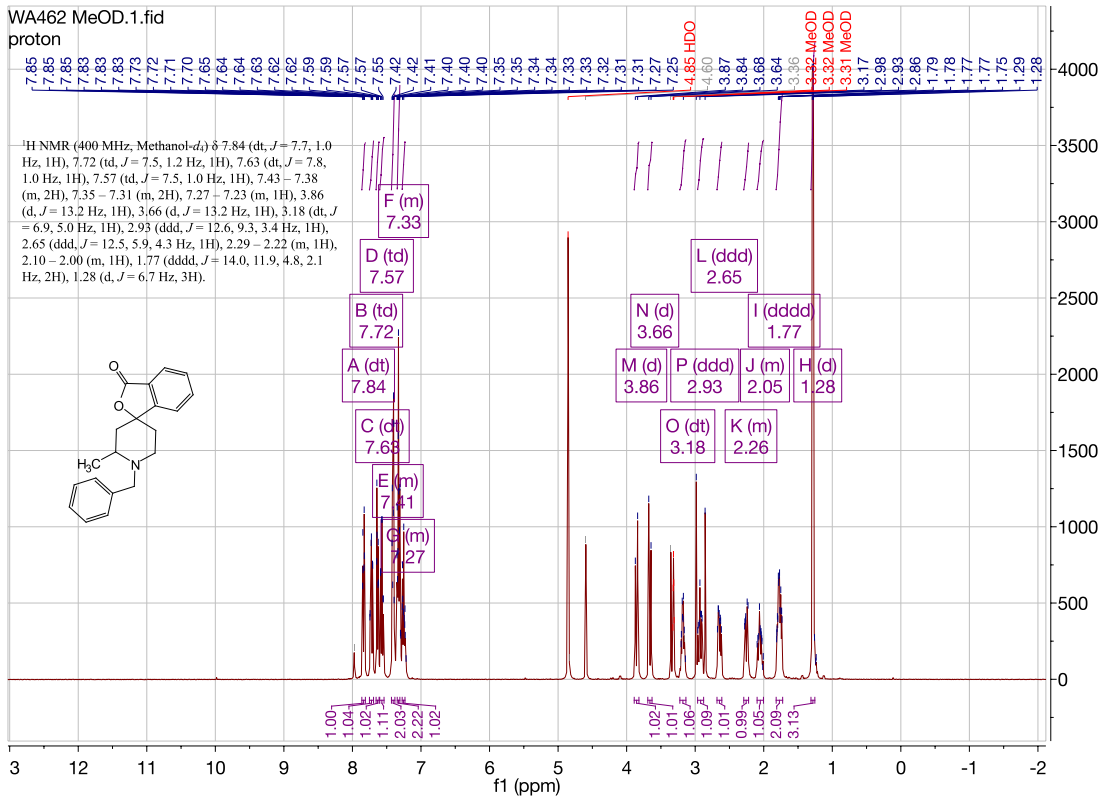


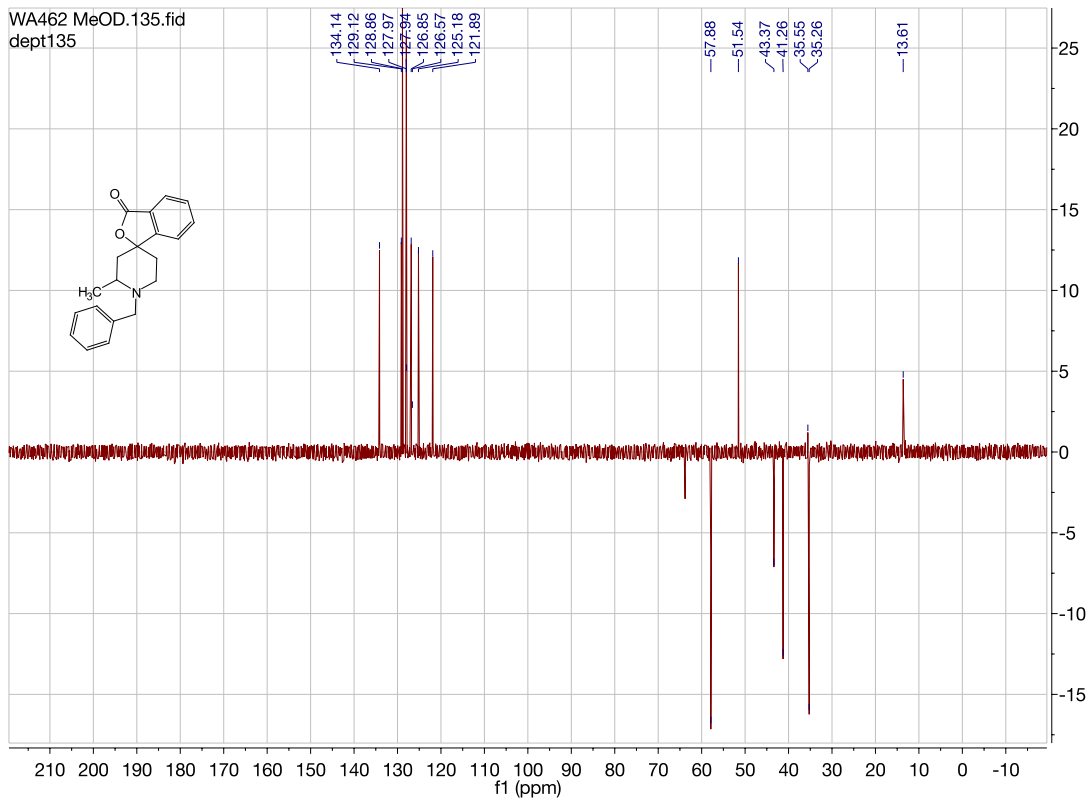




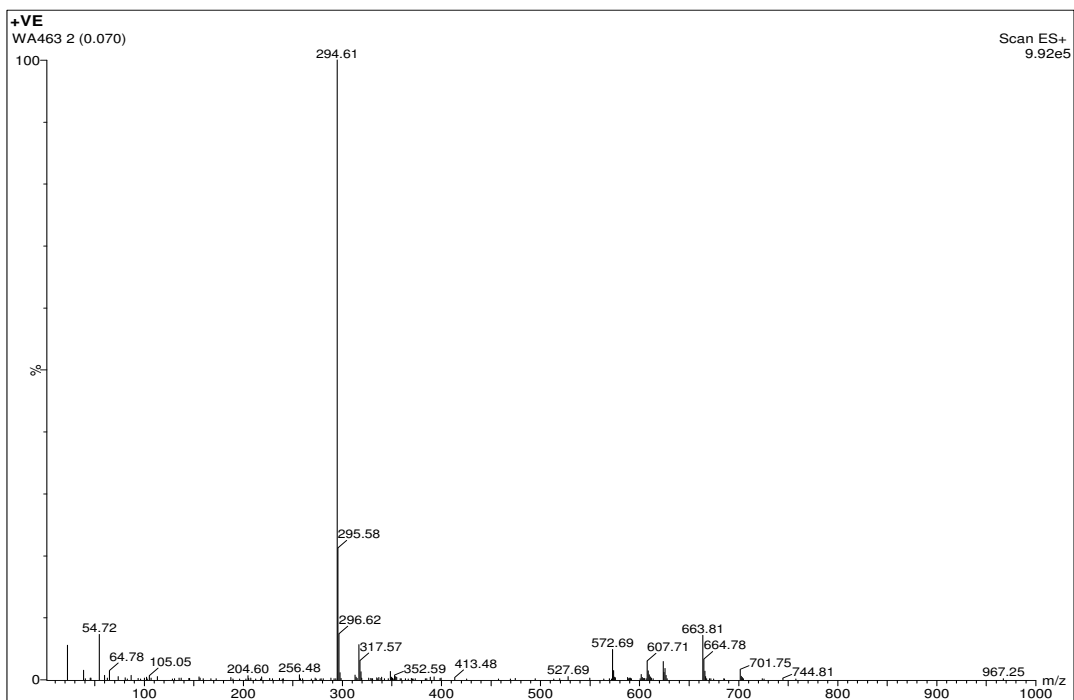
1'-benzyl-2'-methyl-3H-spiro[isobenzofuran-1,4'-piperidin]-3-one. (WA462)

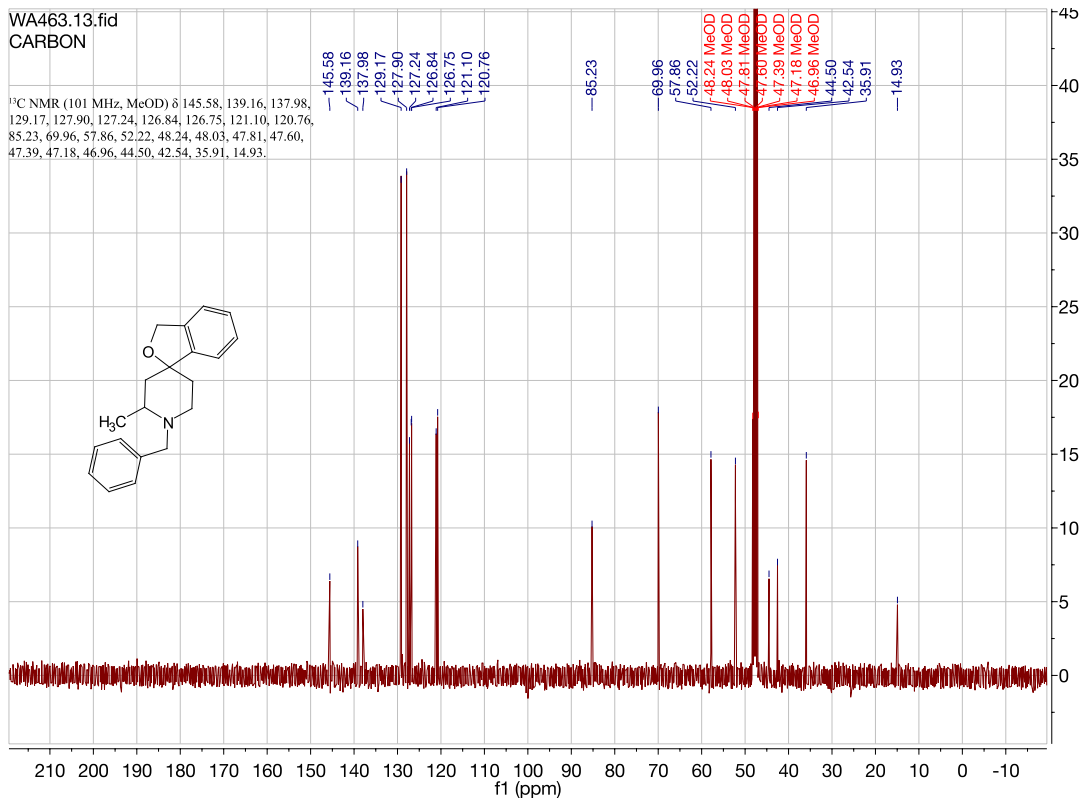
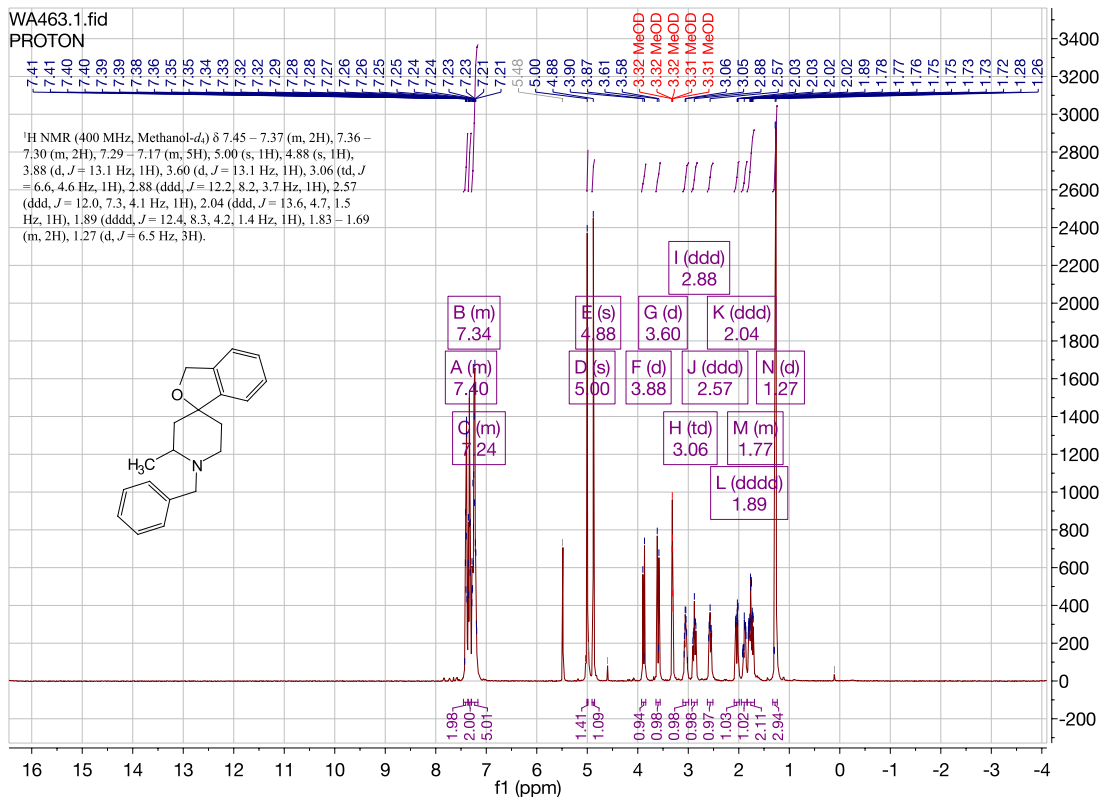


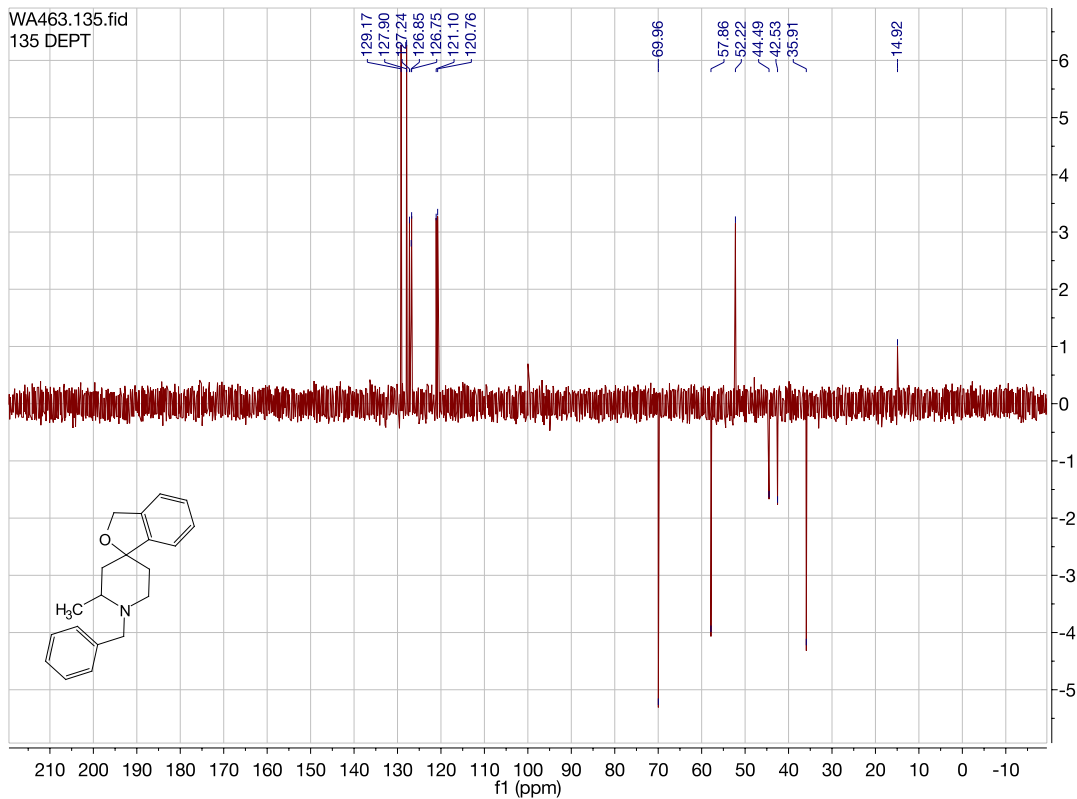




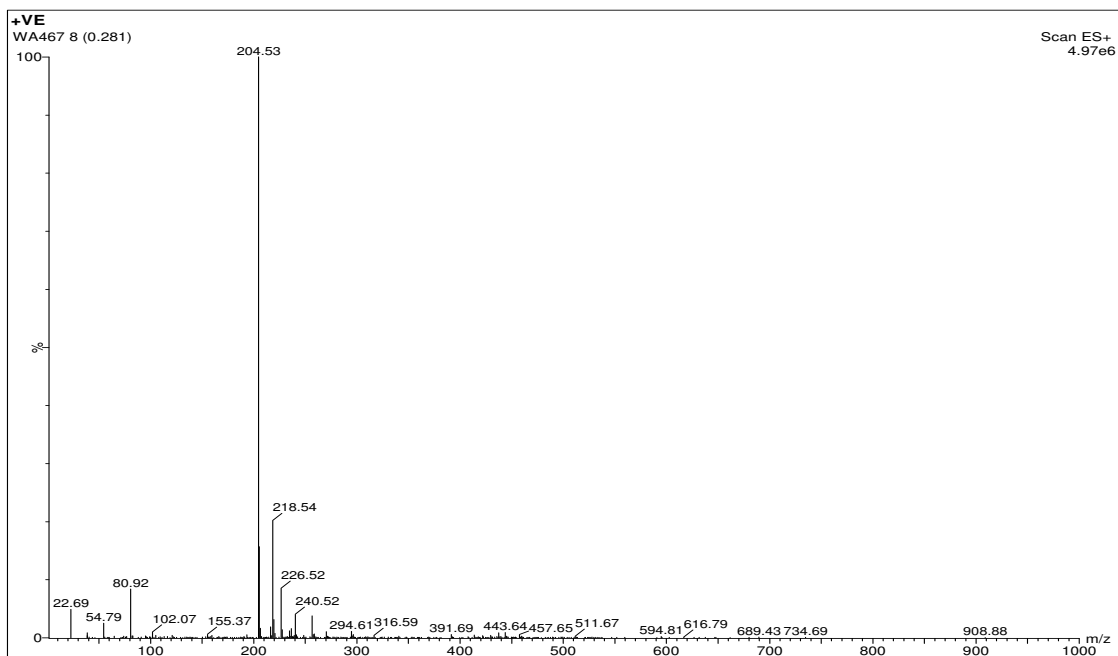
1'-benzyl-2'-methyl-3H-spiro[isobenzofuran-1,4'-piperidine]. (WA463)

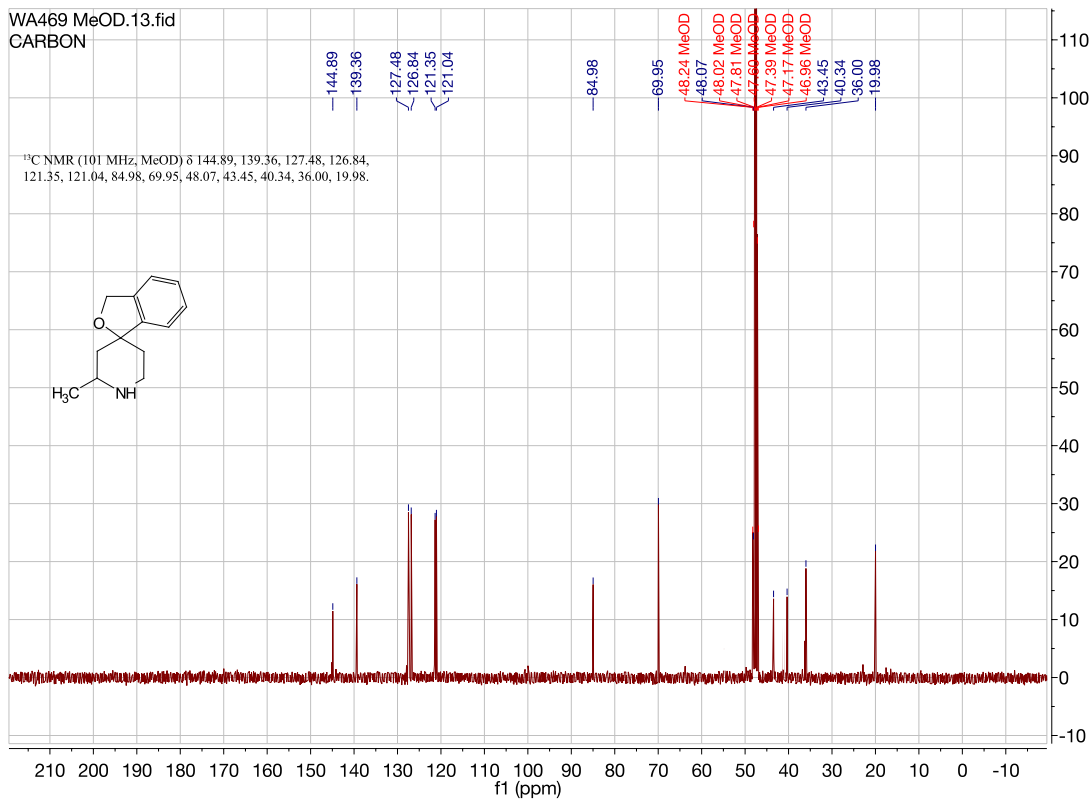
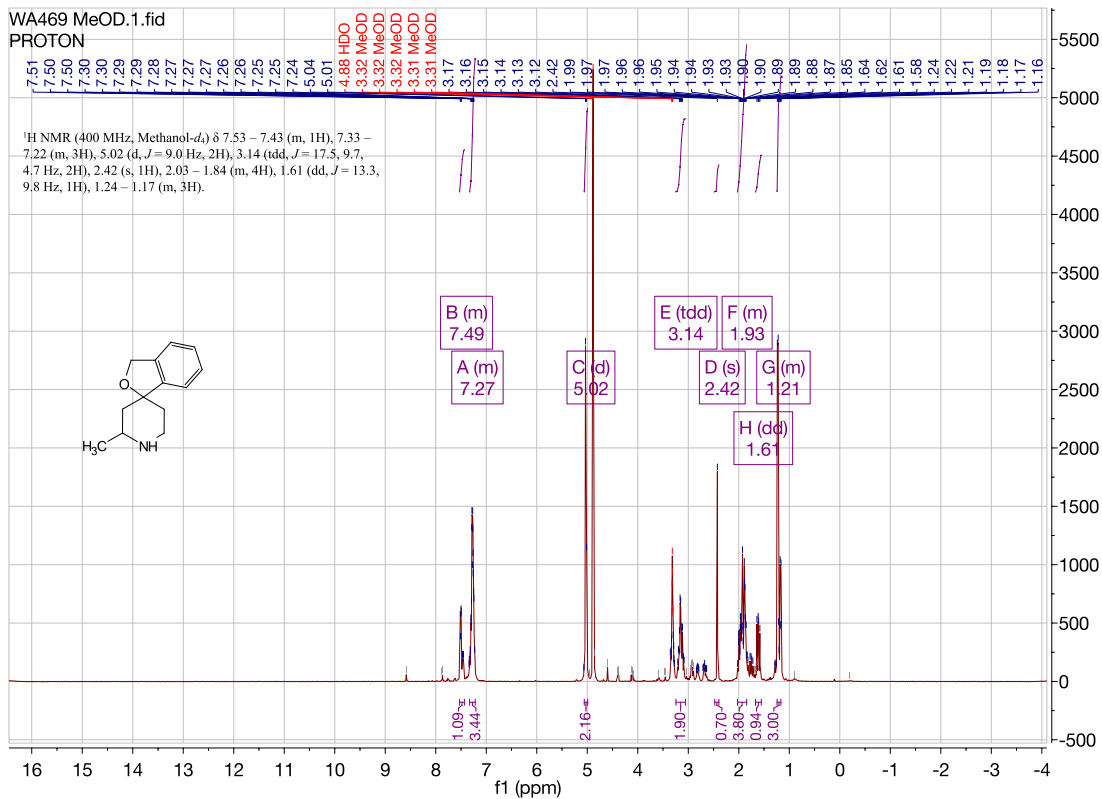


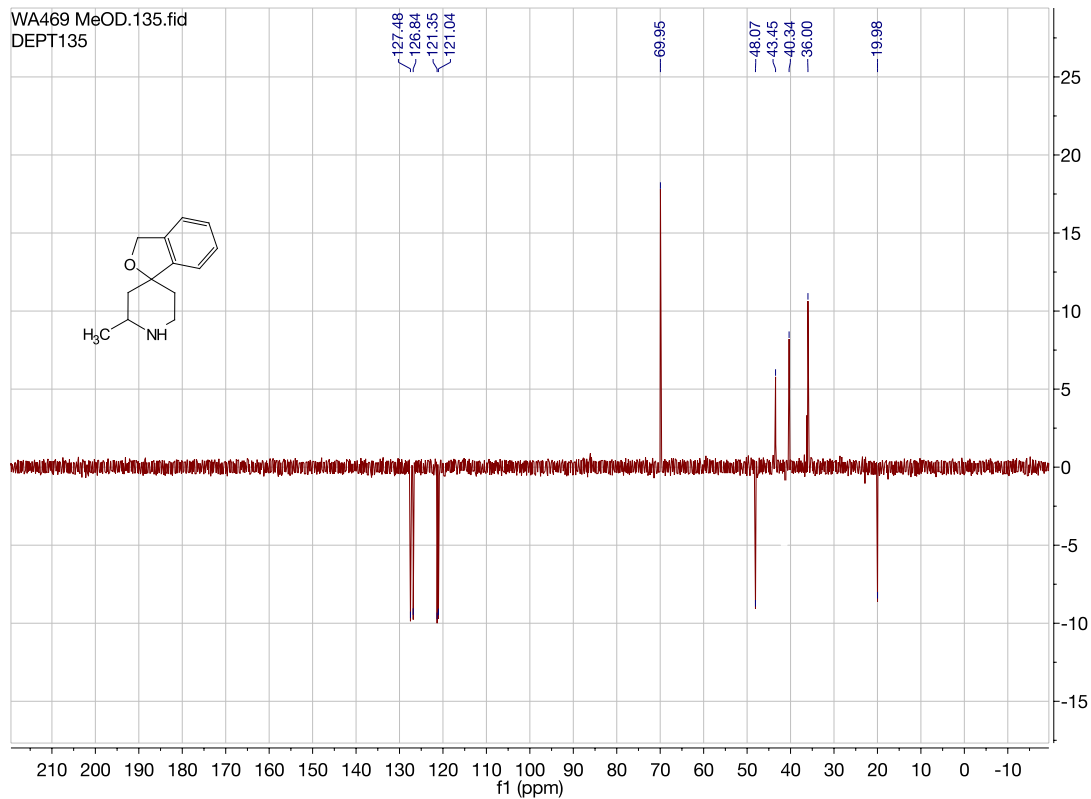




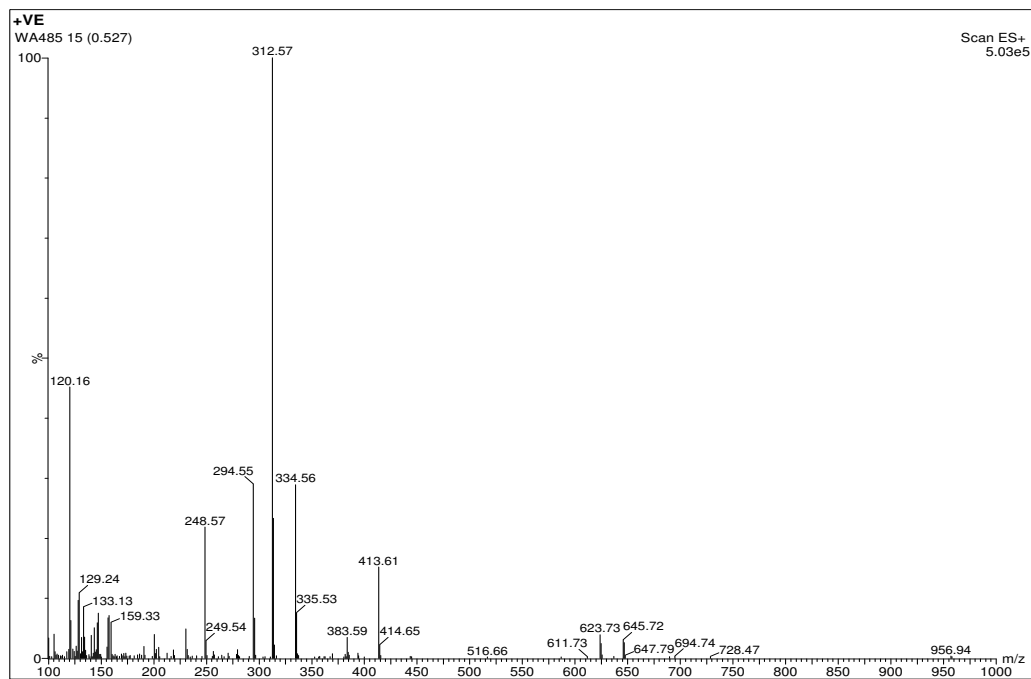
2'-methyl-3H-spiro[isobenzofuran-1,4'-piperidine]. (WA469)

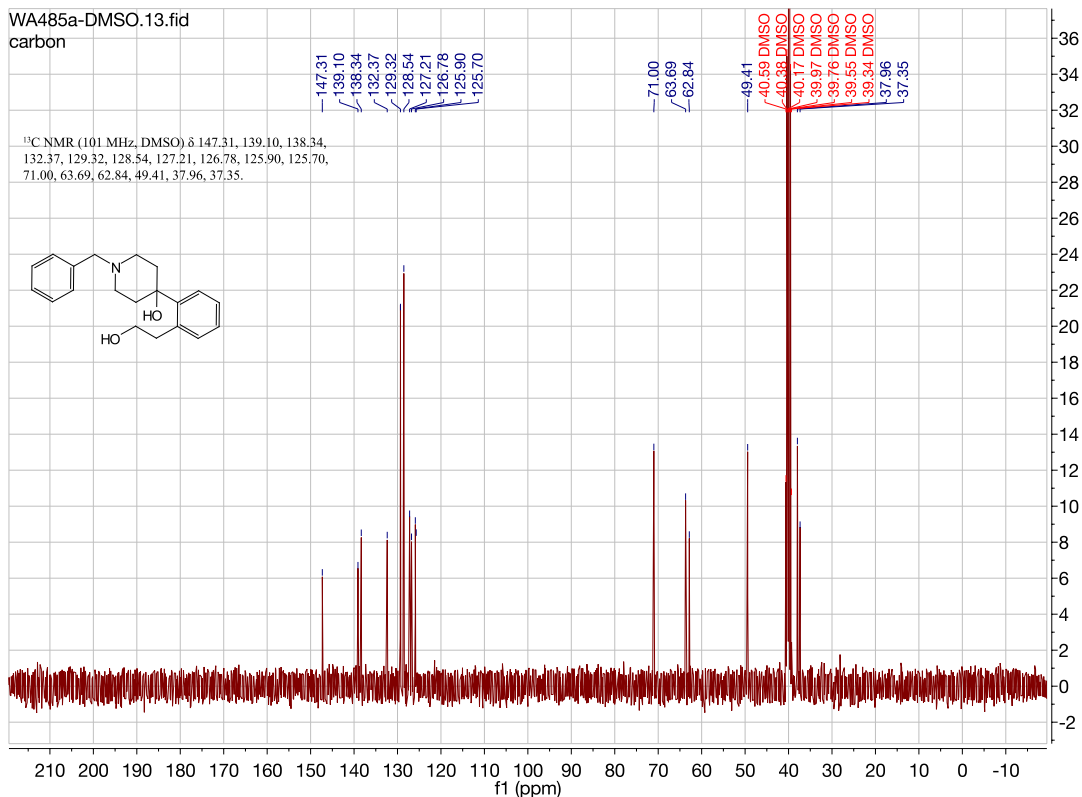
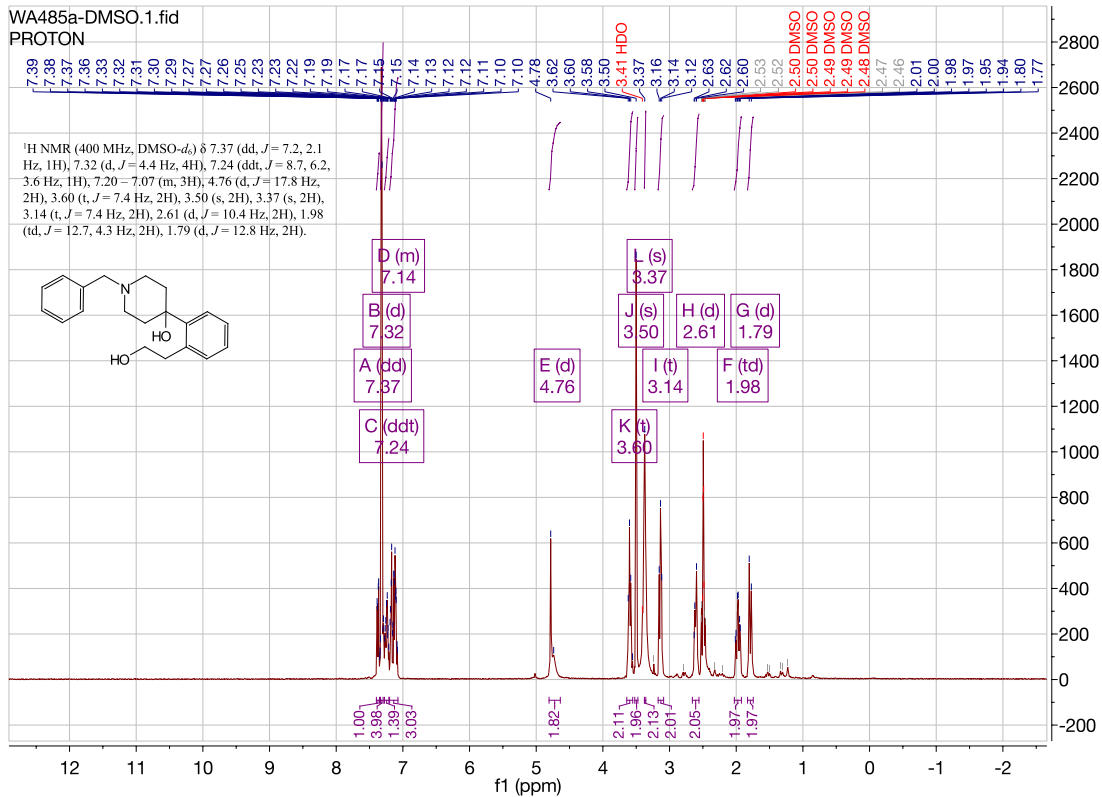


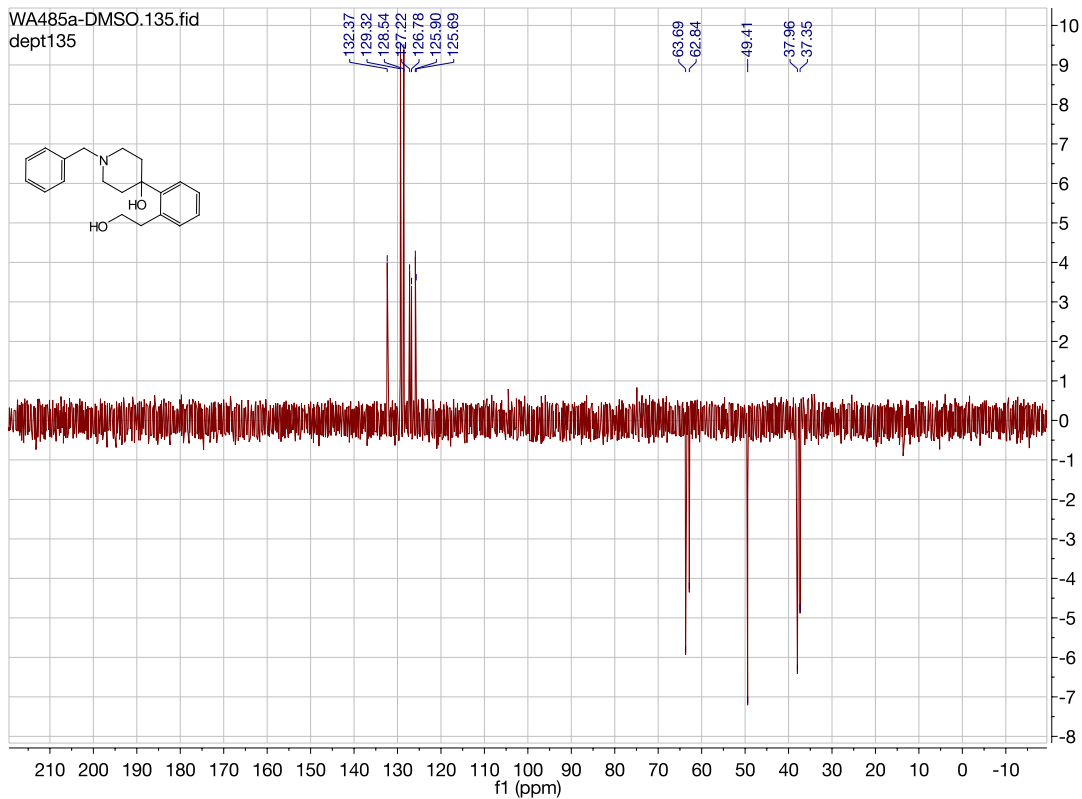




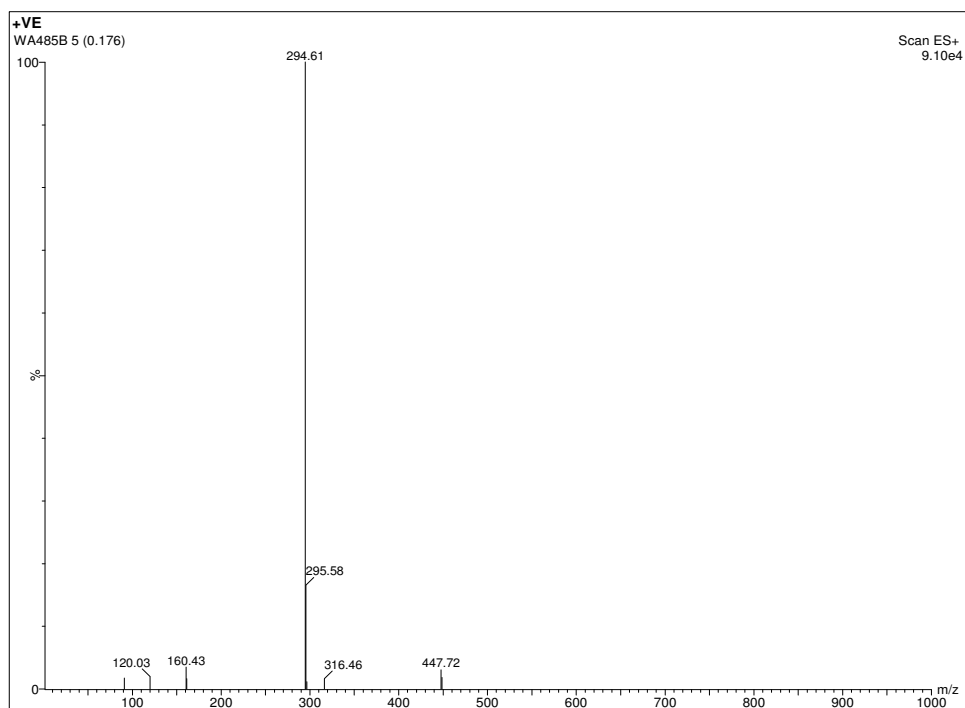
1-benzyl-4-(2-(2-hydroxyethyl)phenyl)piperidin-4-ol. (485a)

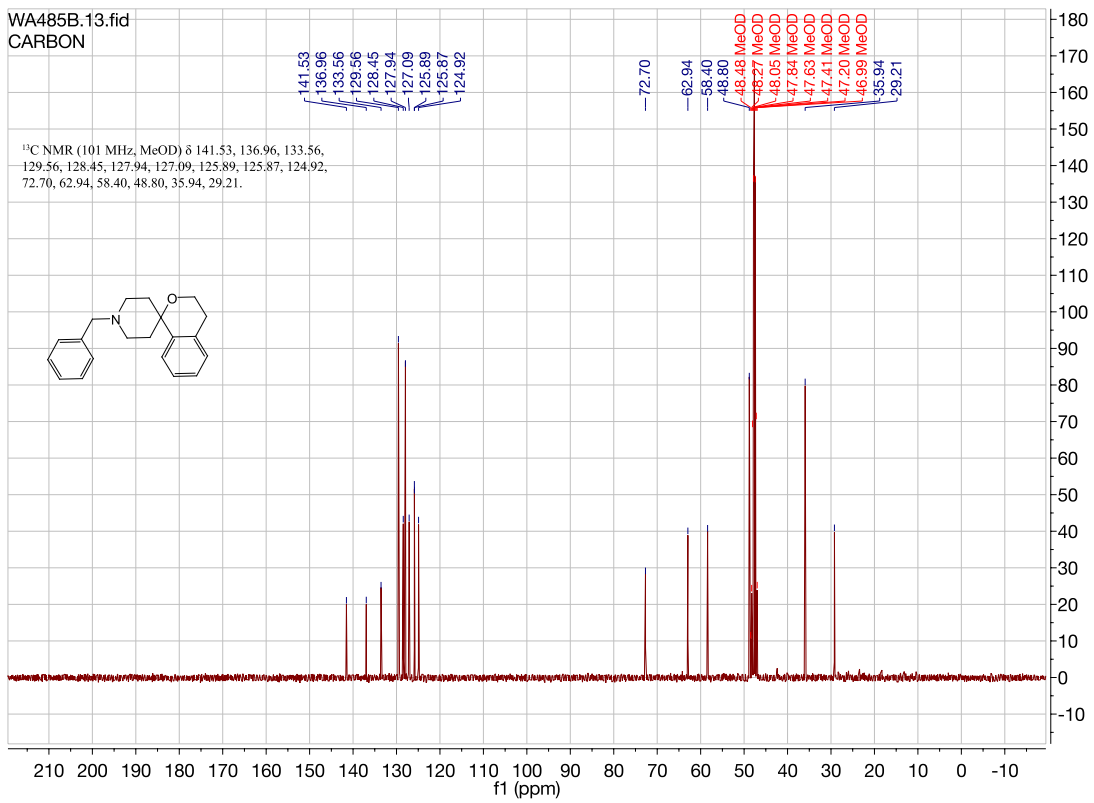
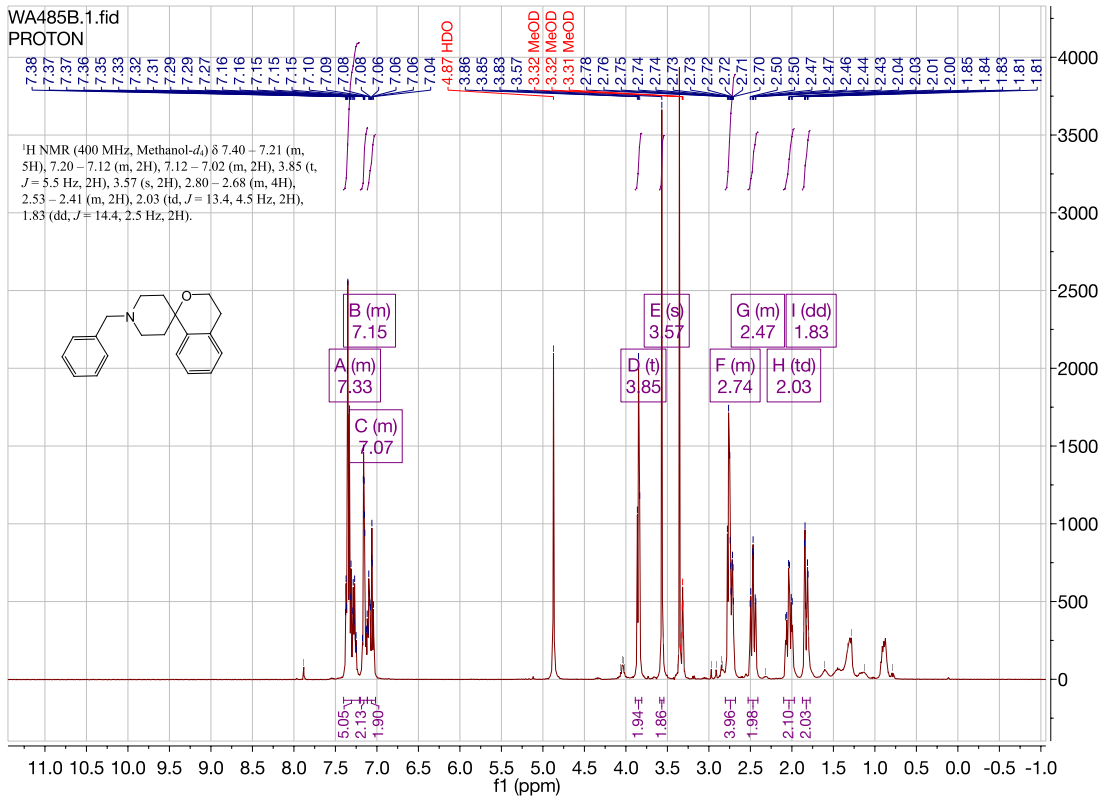


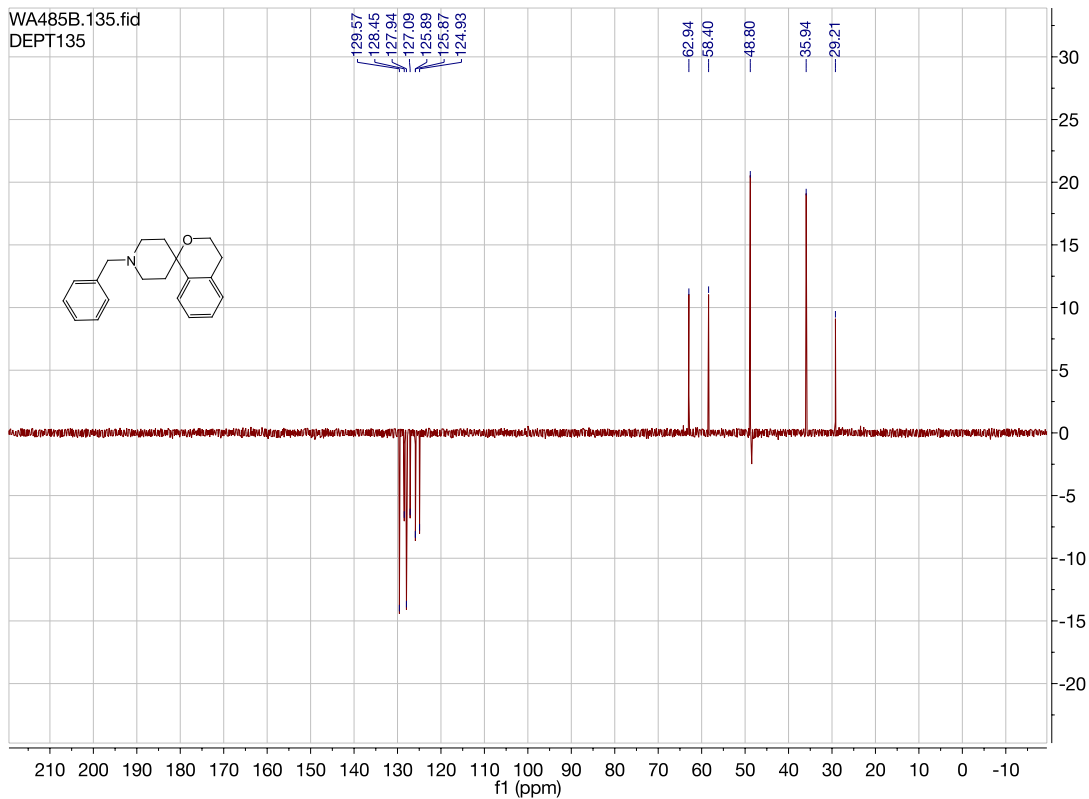




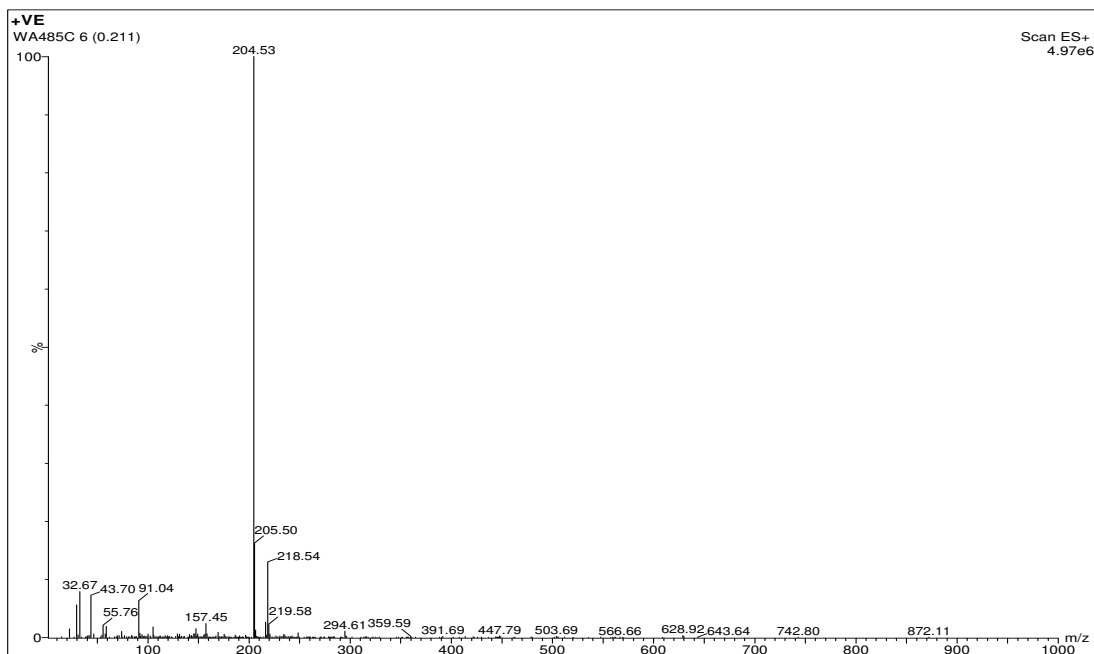
1'-Benzyl-3,4-dihydrospiro[isochromene-1,4'-piperidine]. (WA485b)



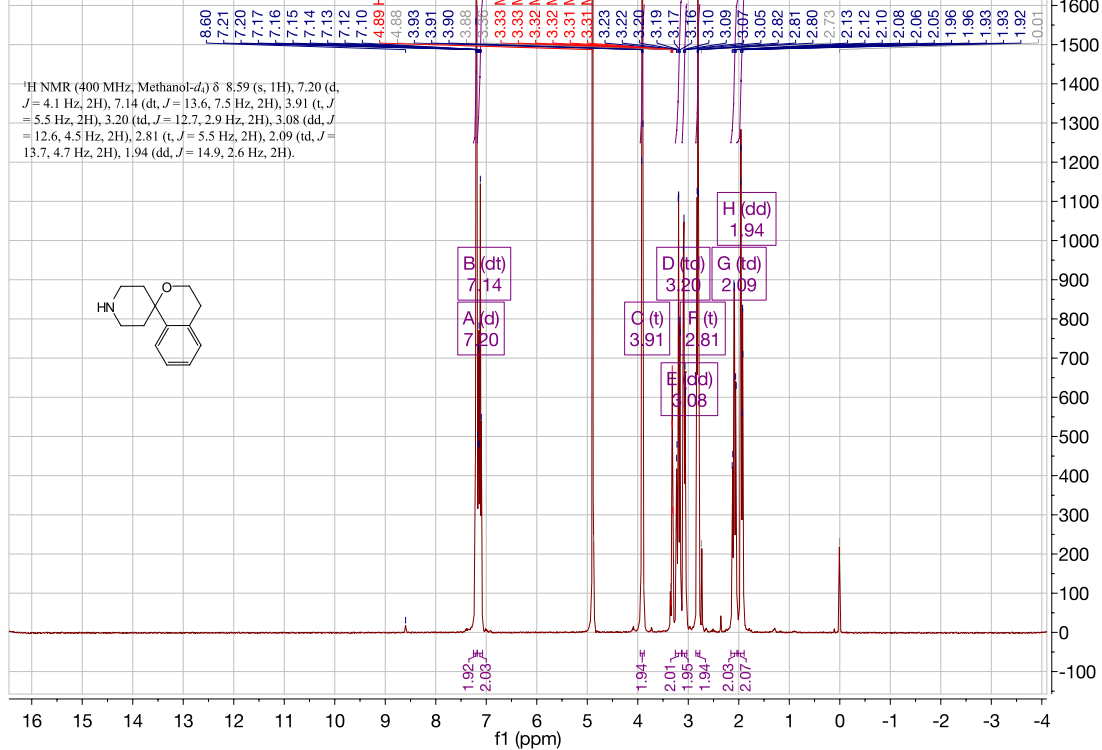




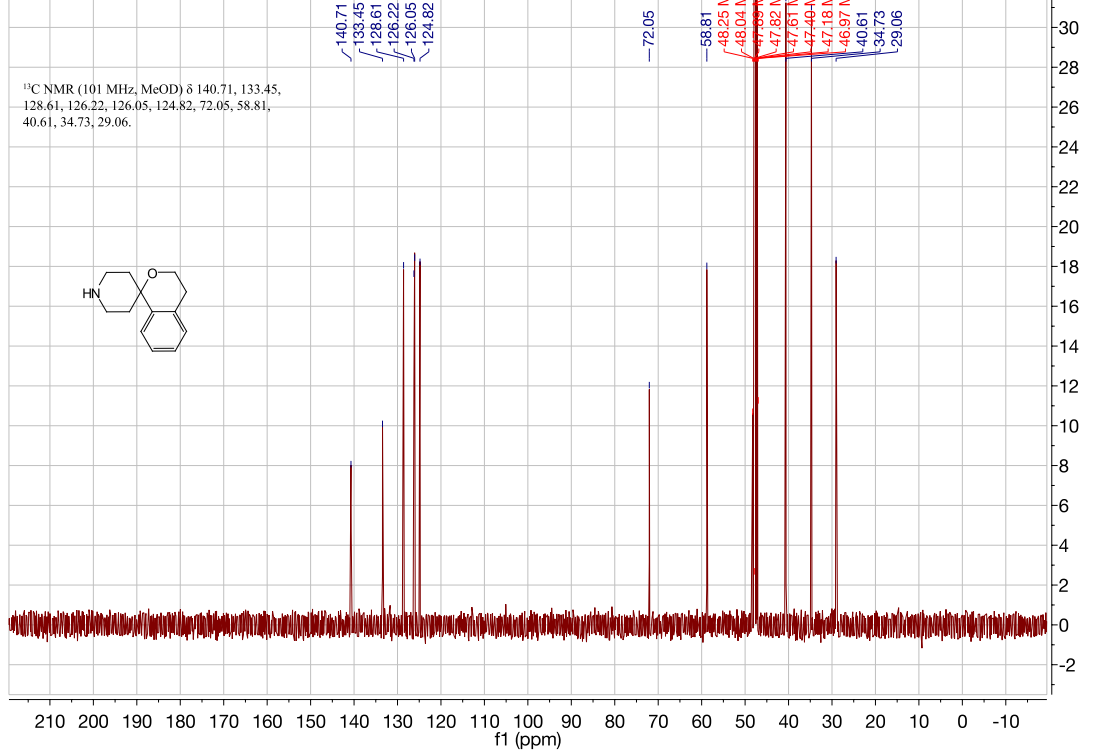
3,4-dihydrospiro[isochromane-1,4'-piperidine]. (485c)

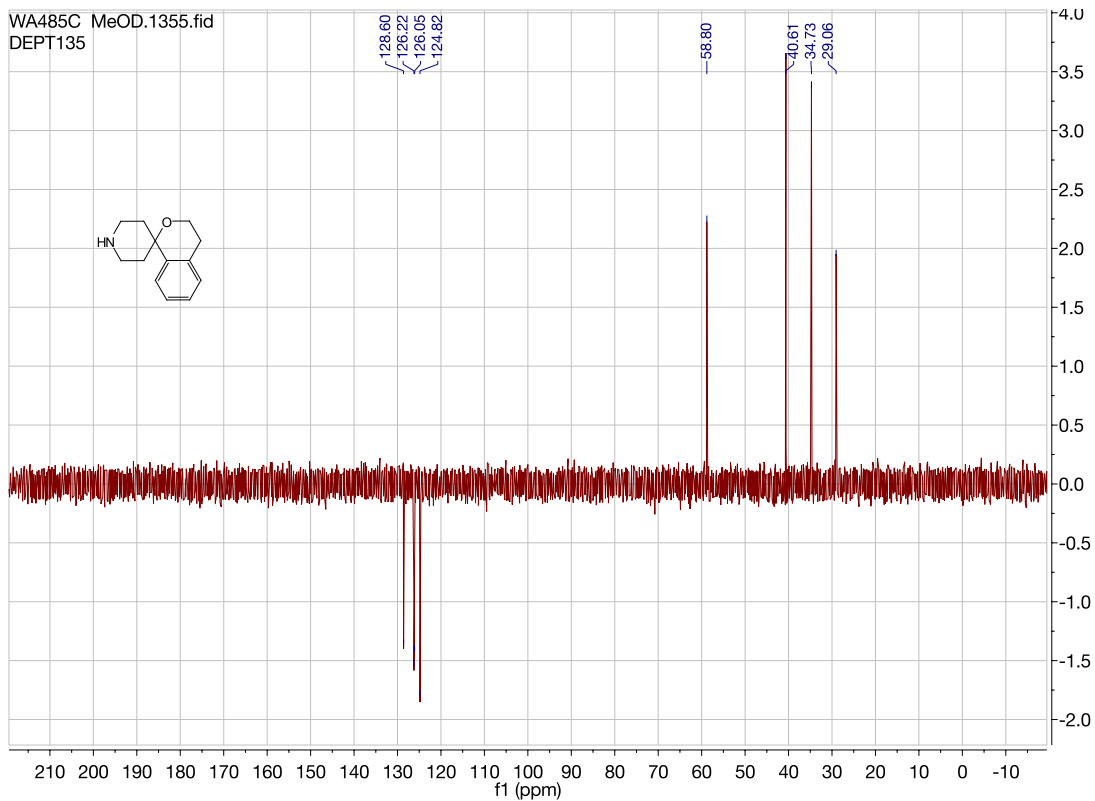


WA485C MeOD.1.fid
PROTON

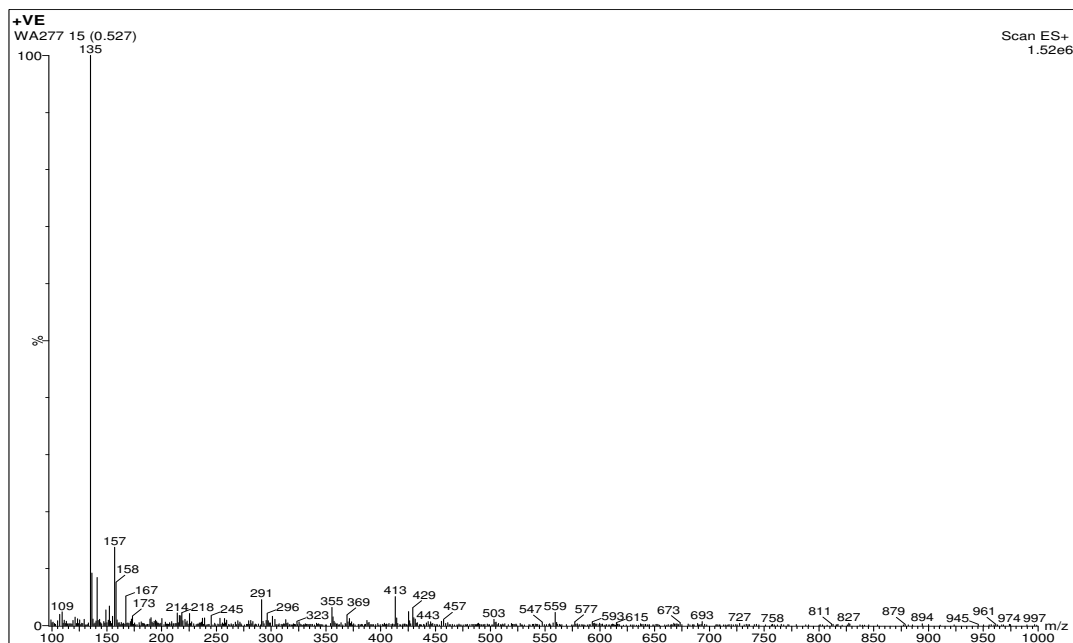


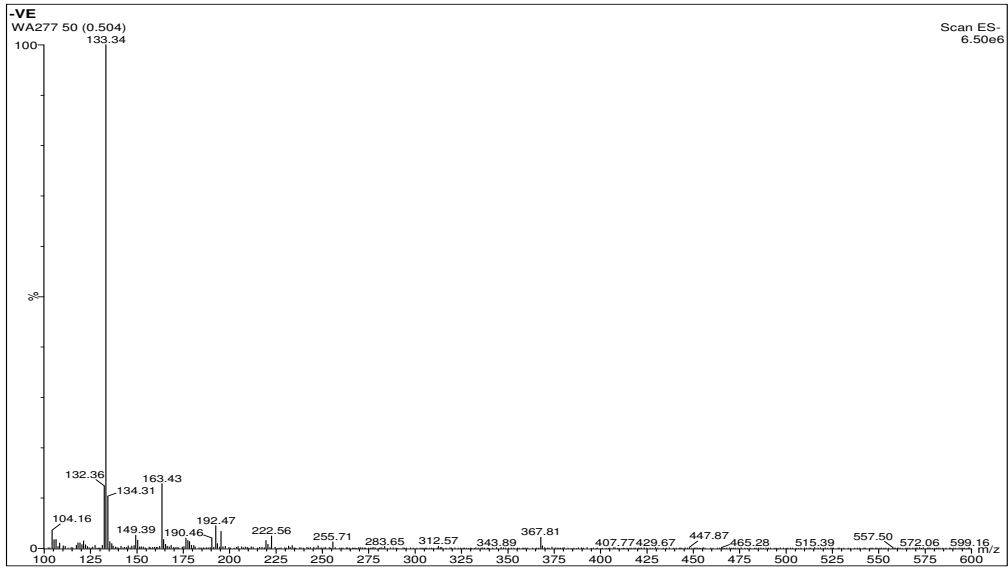
WA485C MeOD.13.fid
CARBON

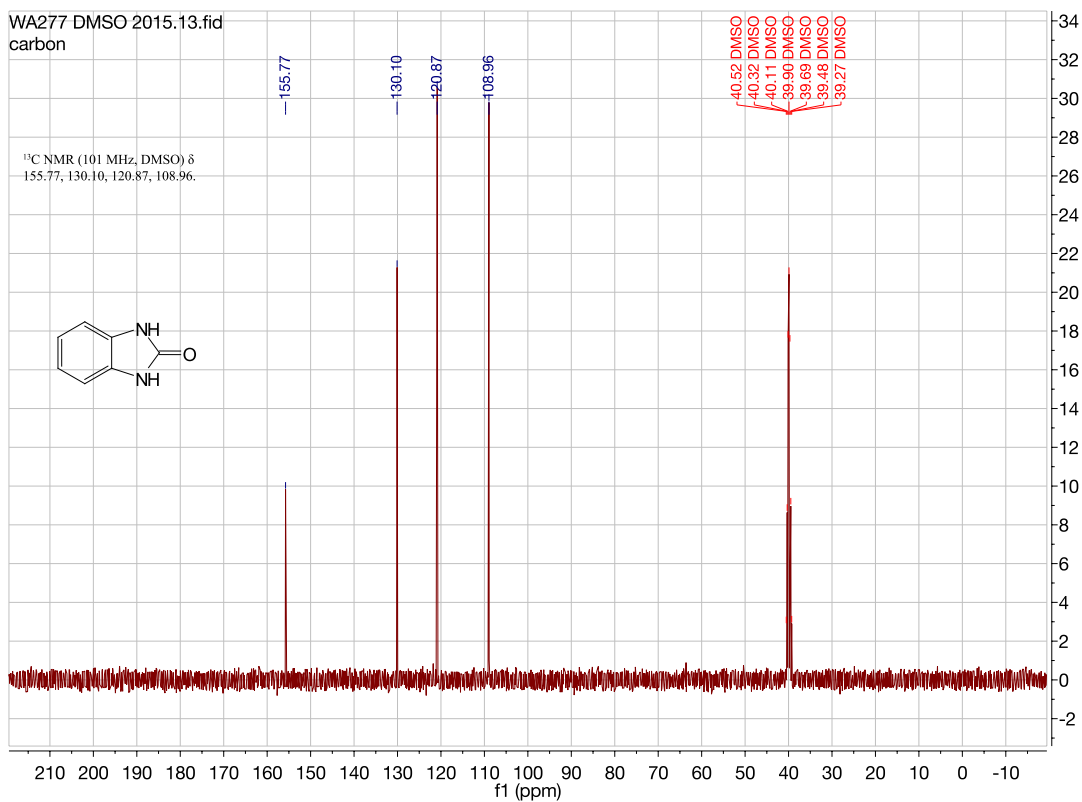
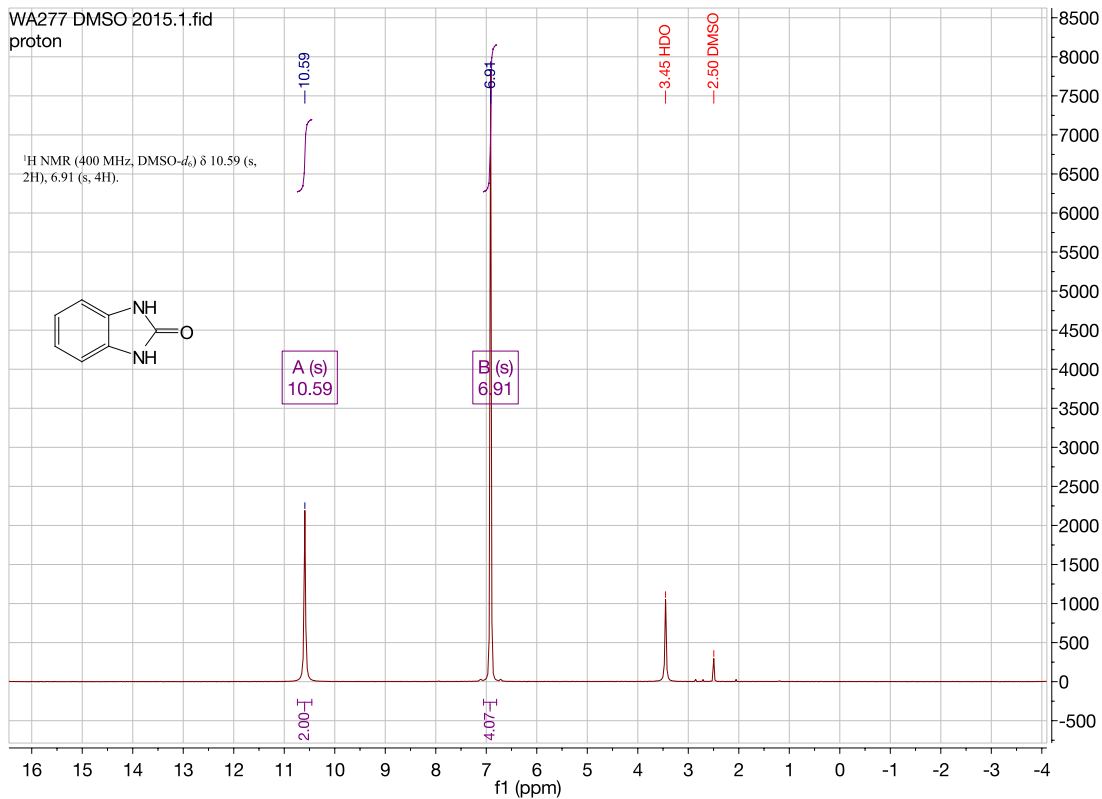


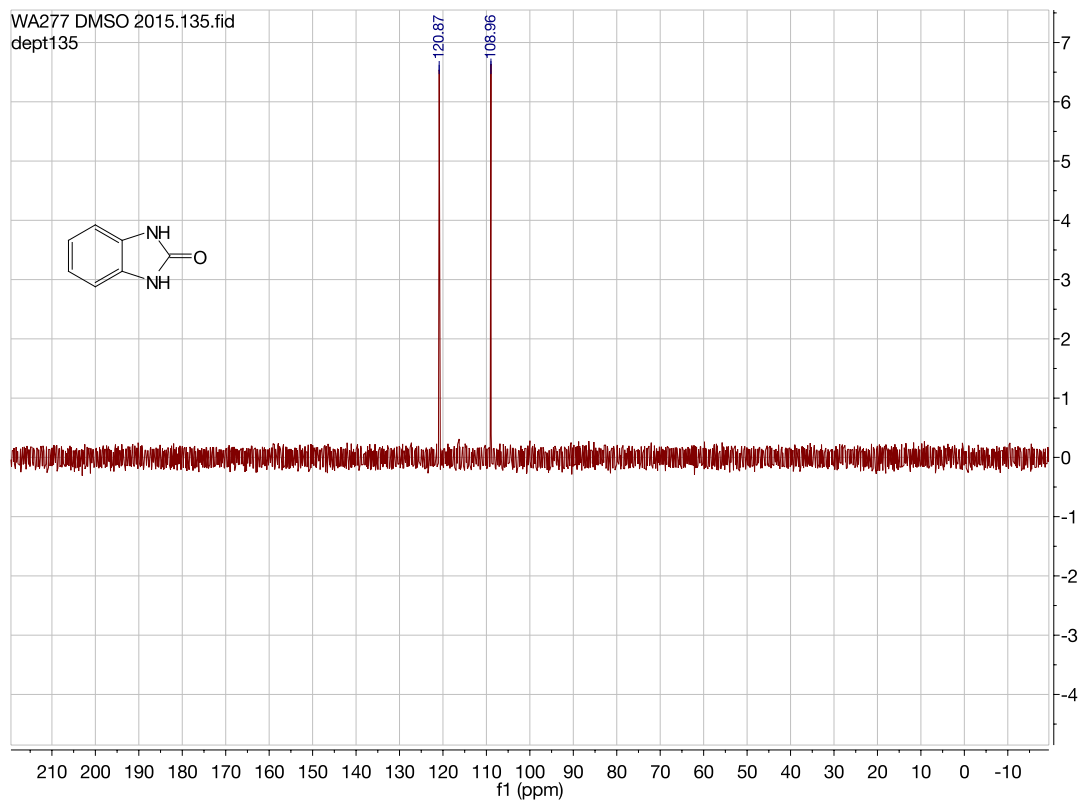


1,3-dihydro-2H-benzo[d]imidazol-2-one. (WA277)

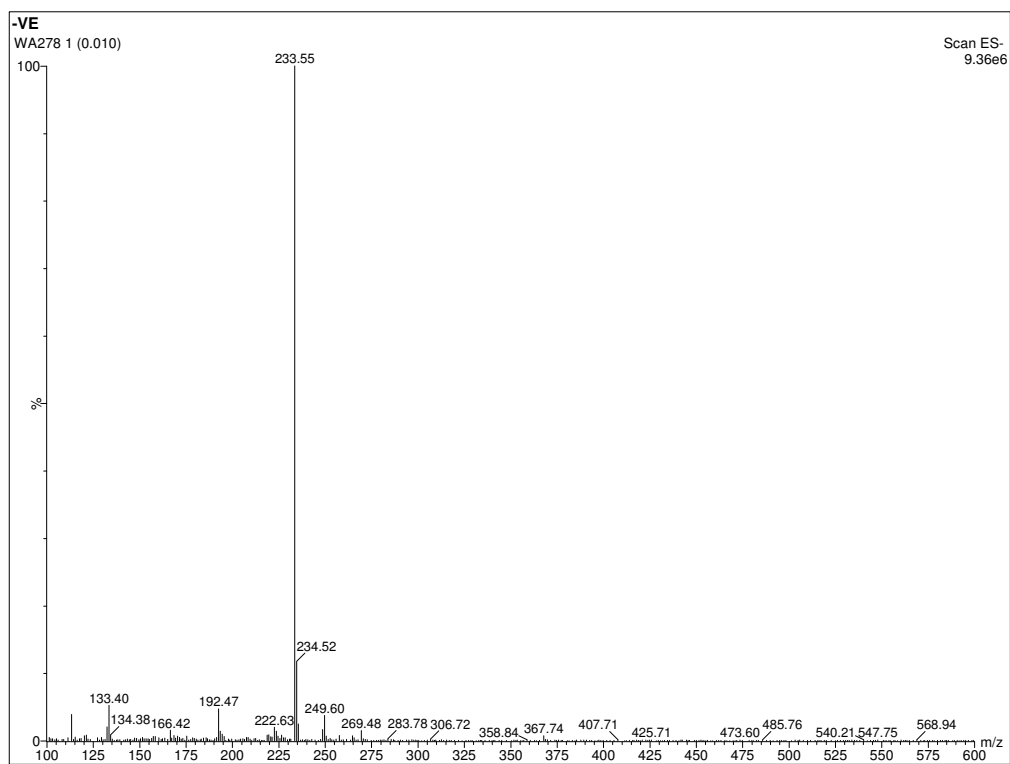


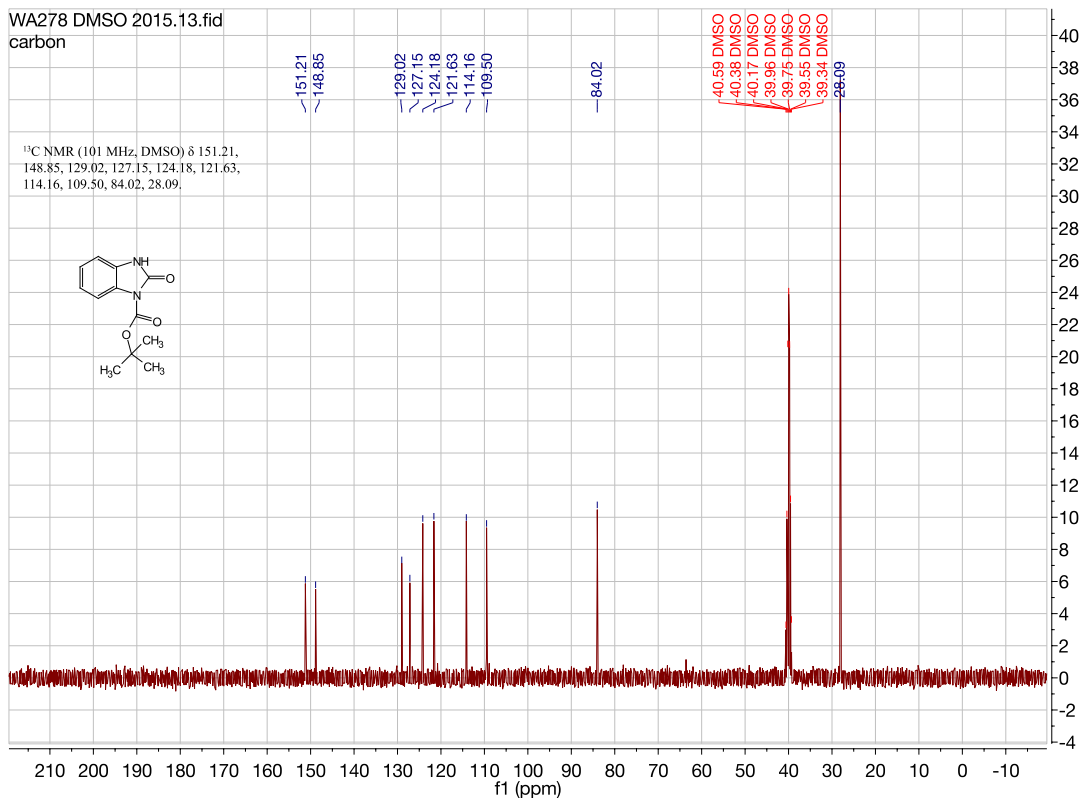
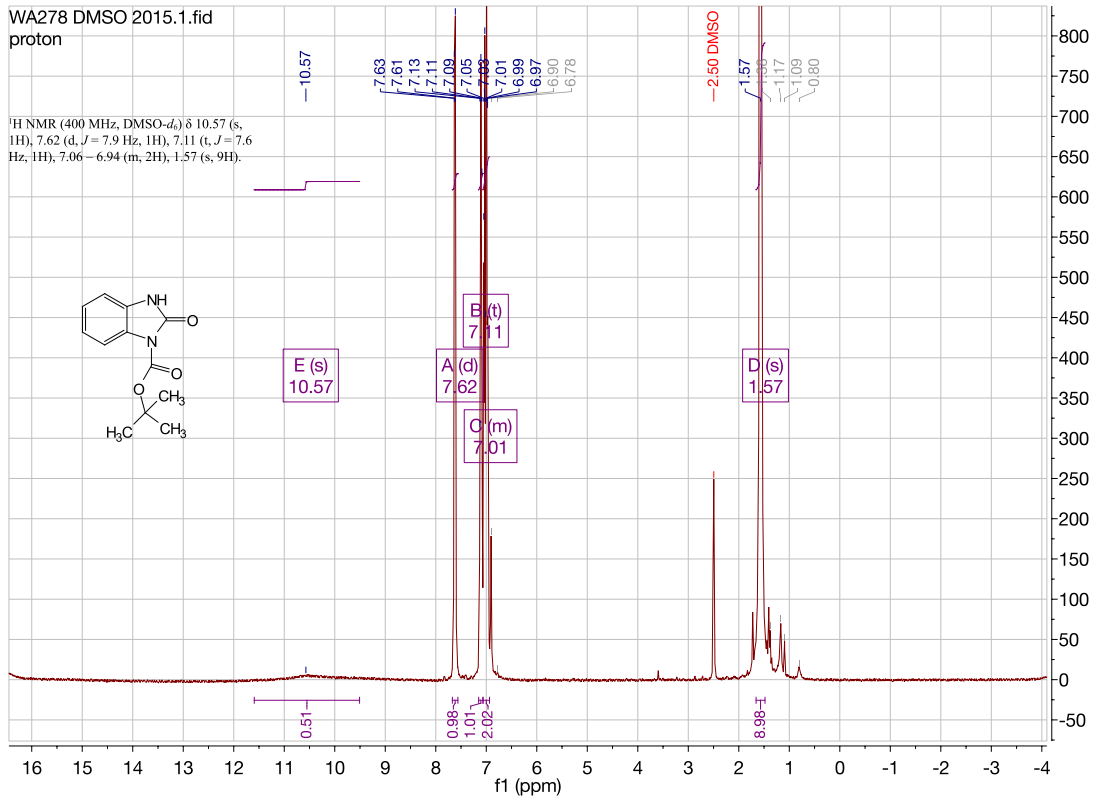


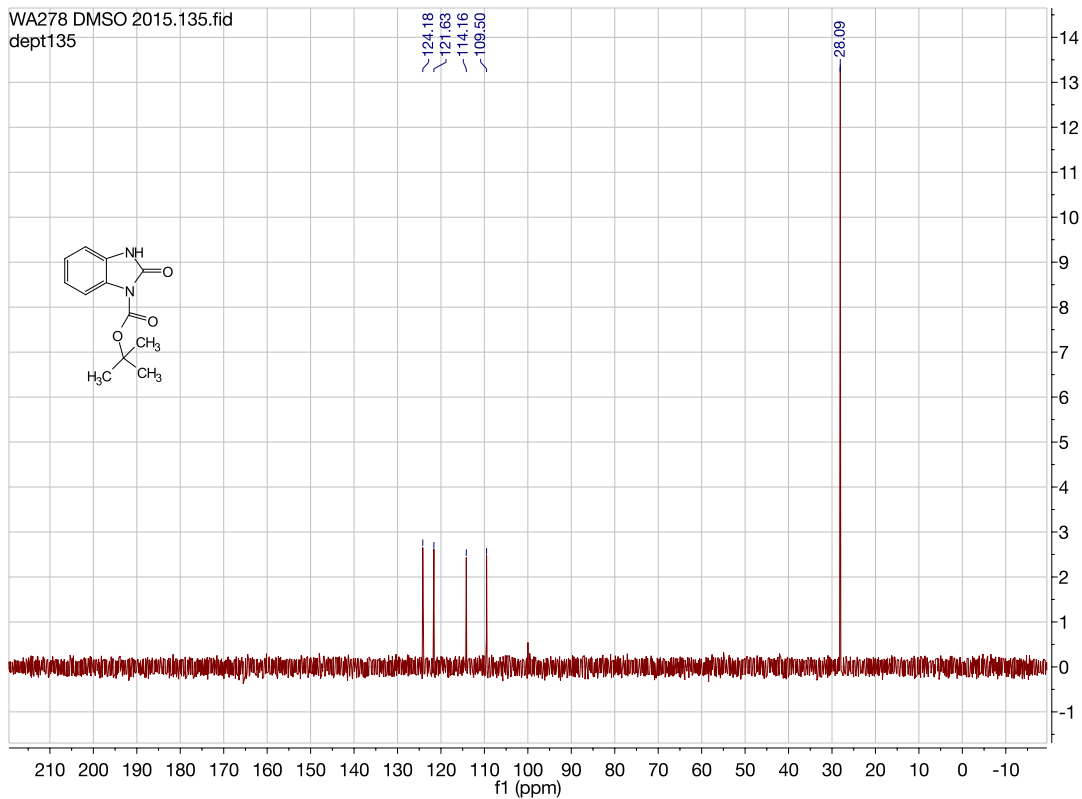




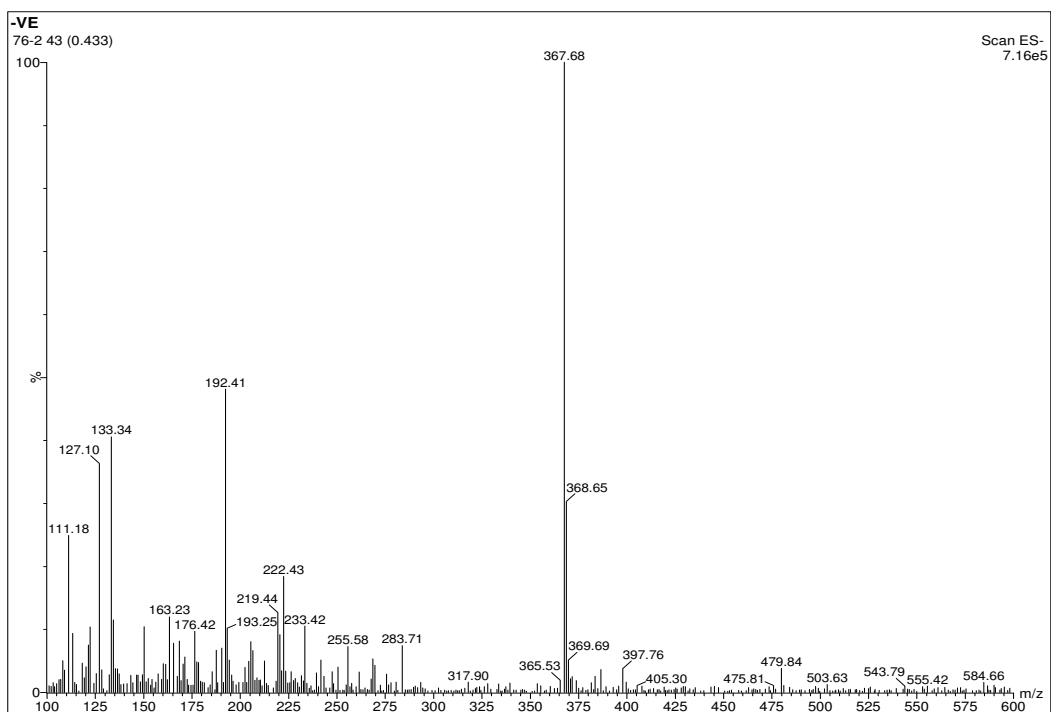
***tert*-butyl 2-oxo-2,3-dihydro-1*H*-benzo[*d*]imidazole-1-carboxylate. (WA278)**

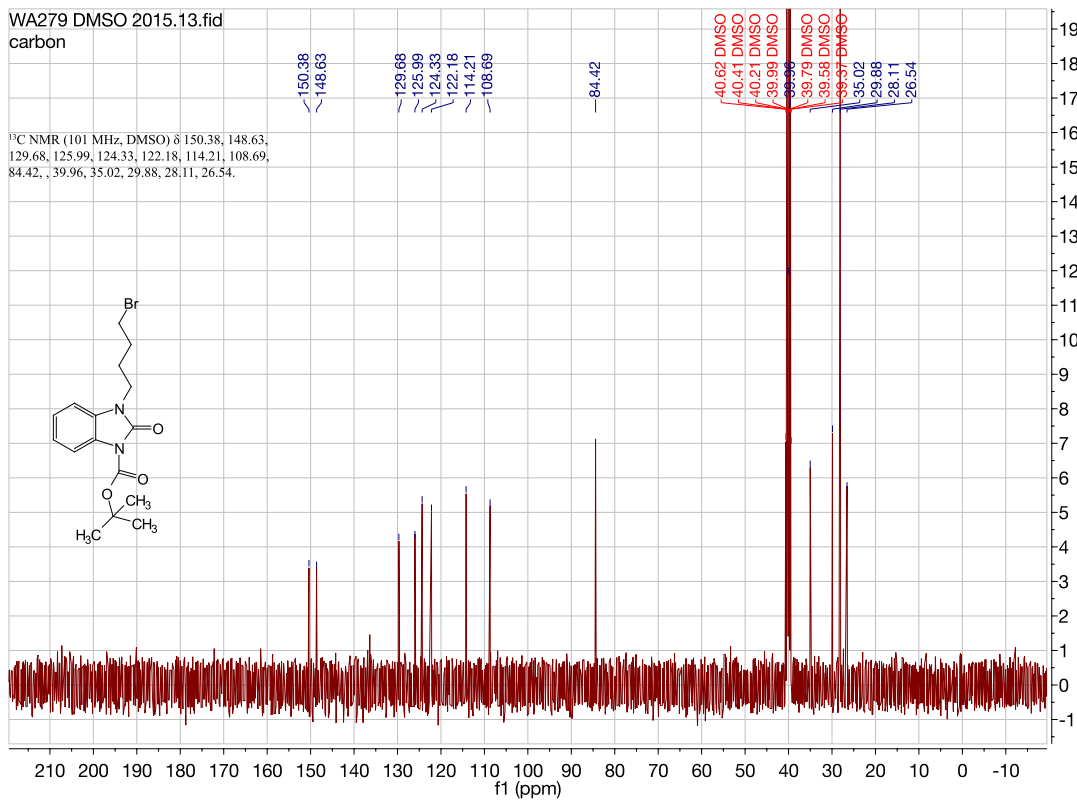
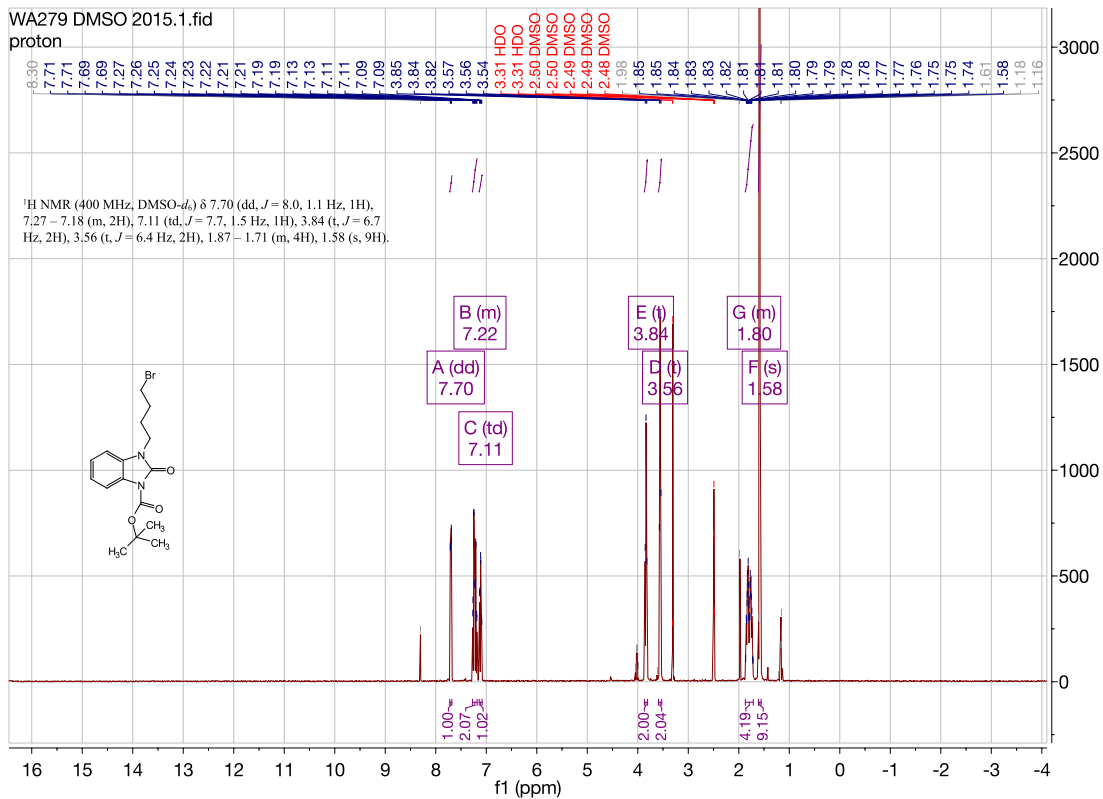


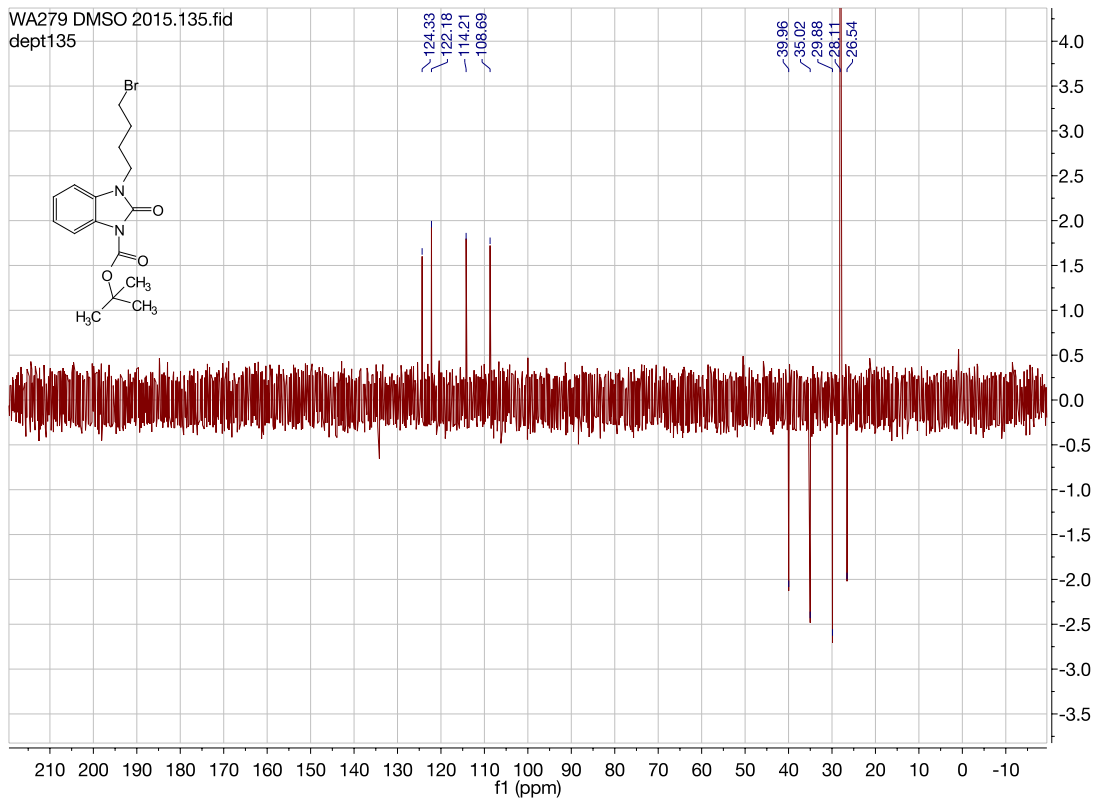




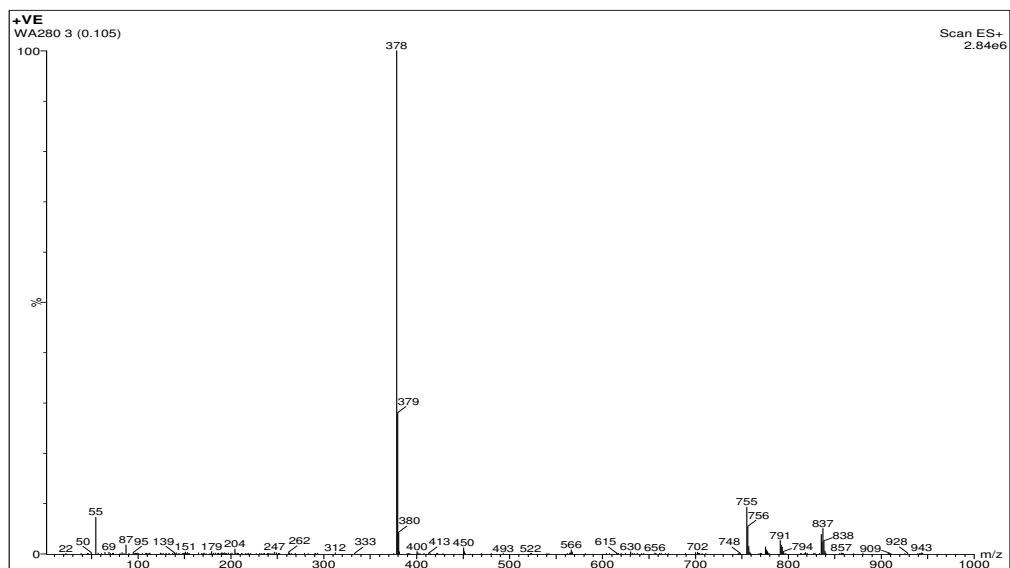
***tert*-butyl 3-(4-bromobutyl)-2-oxo-2,3-dihydro-1*H*-benzo[*d*]imidazole-1-carboxylate.
(WA279)**

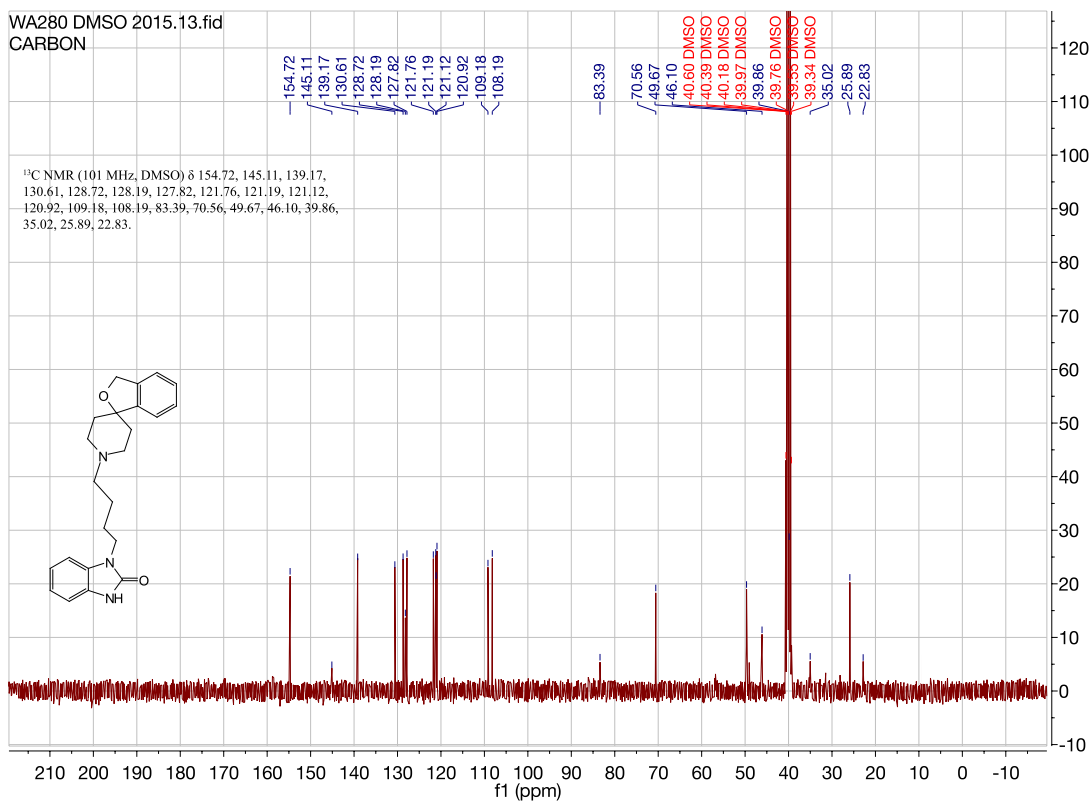
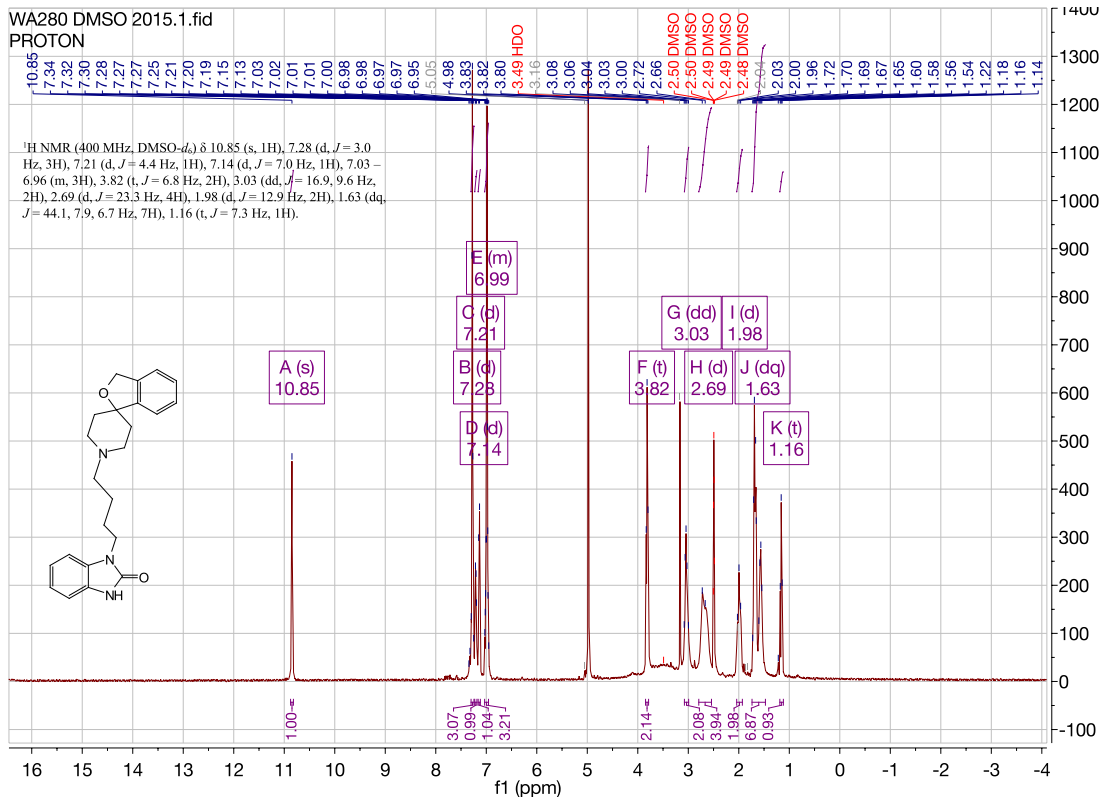




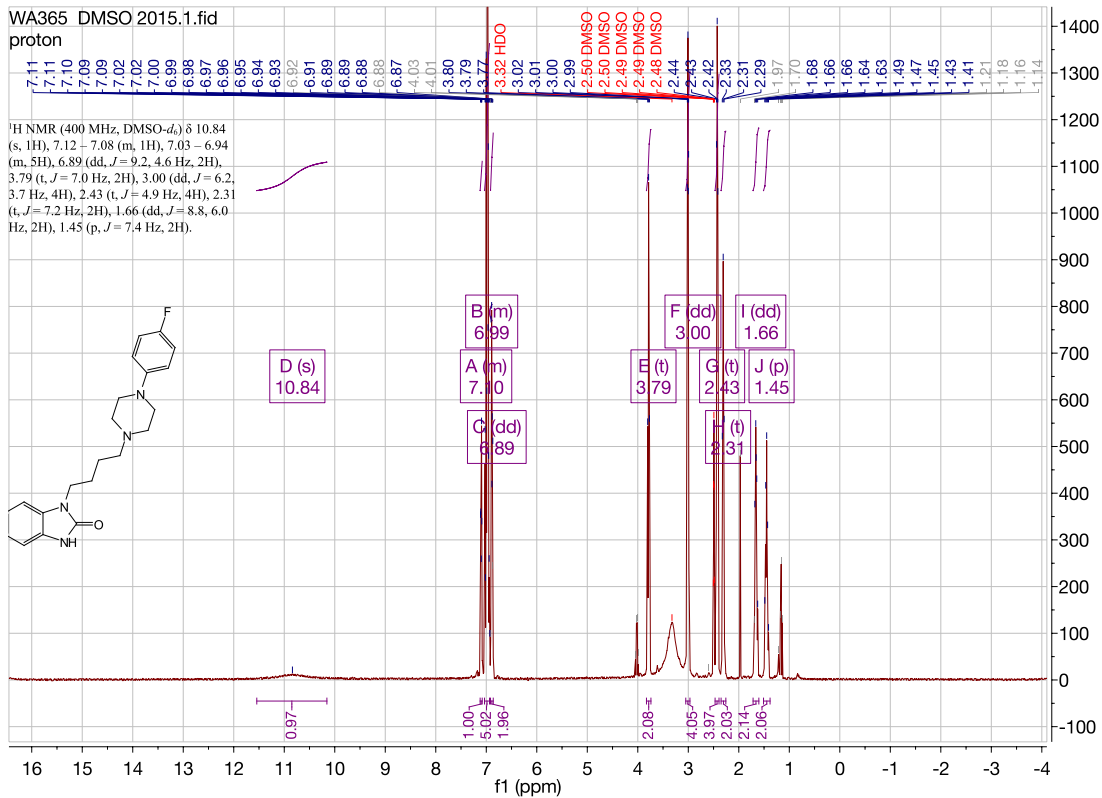
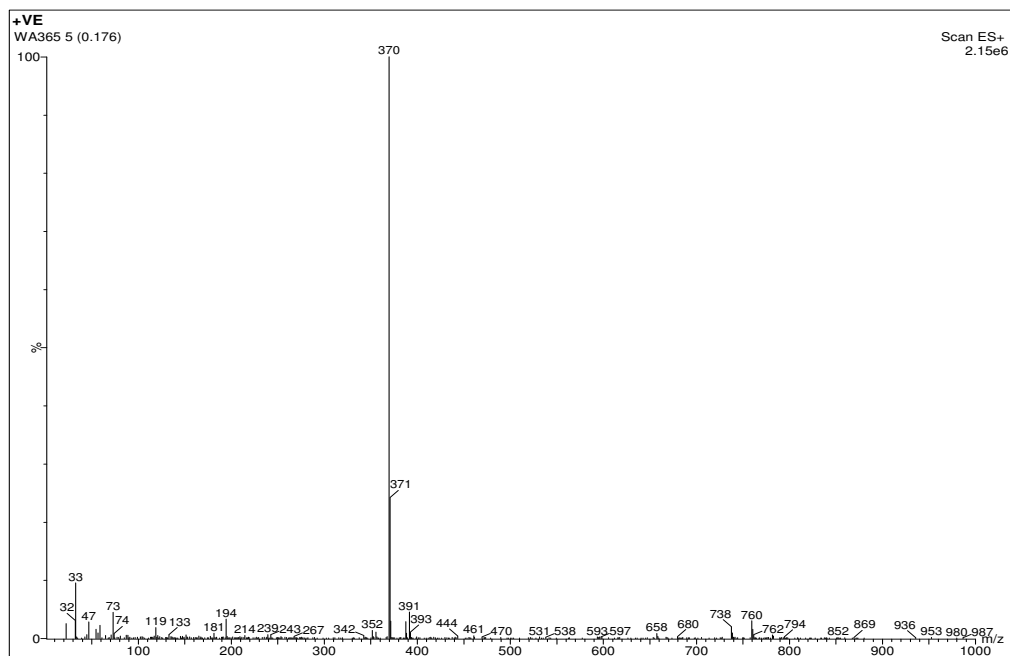


1-(4-(3H-spiro[isobenzofuran-1,4'-piperidin]-1'-yl)butyl)-1,3-dihydro-2H-benzo[d]imidazol-2-one. (WA280)



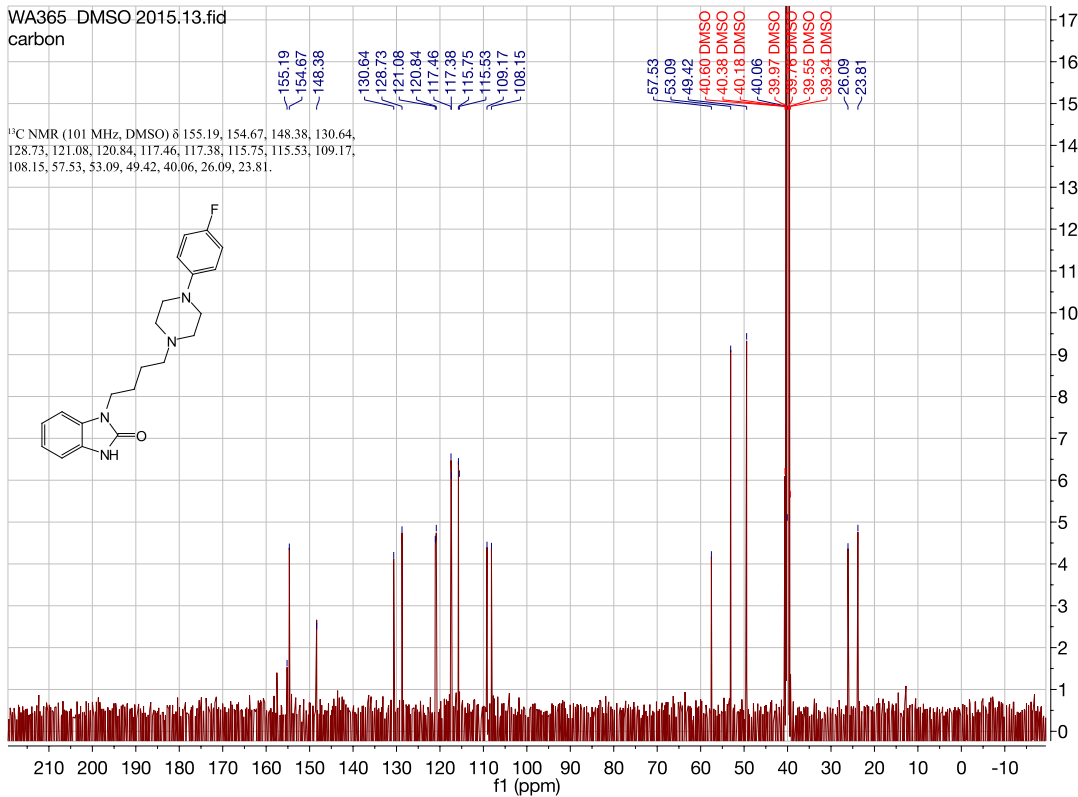
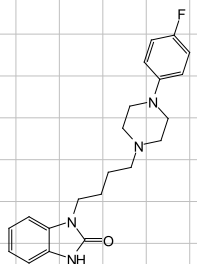


1-(4-(4-(4-fluorophenyl)piperazin-1-yl)butyl)-1,3-dihydro-2H-benzo[d]imidazol-2-one. (WA365)

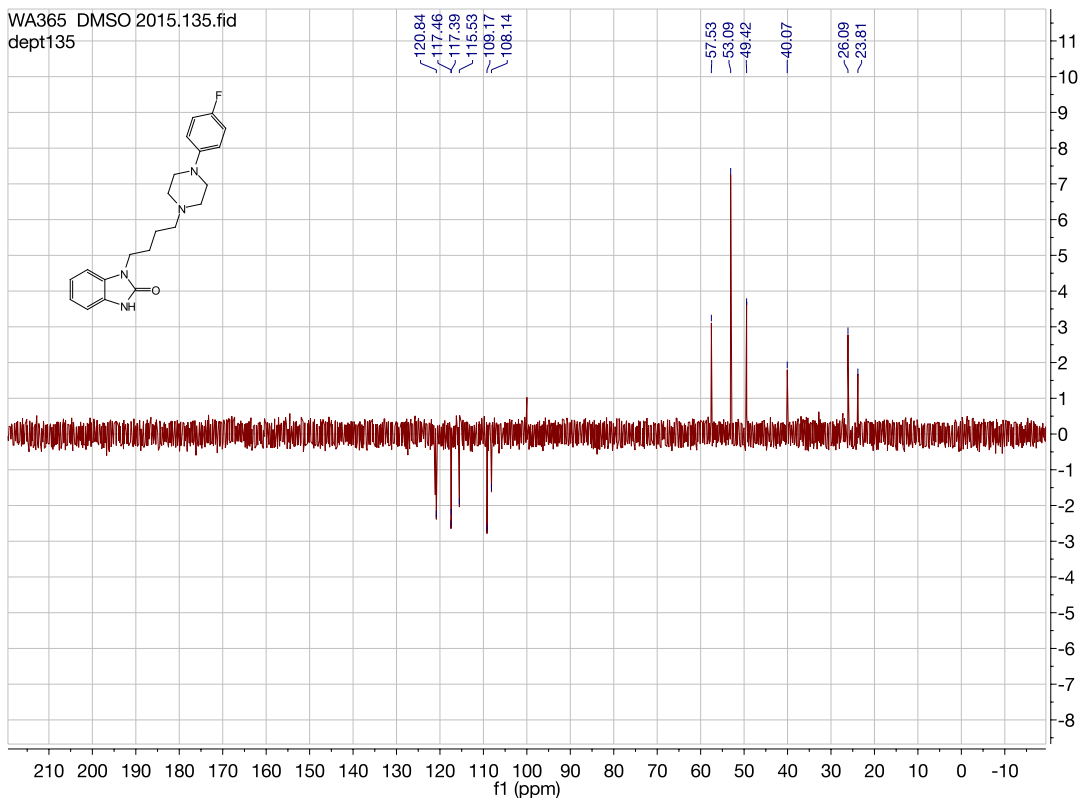


WA365 DMSO 2015.13.fid
carbon

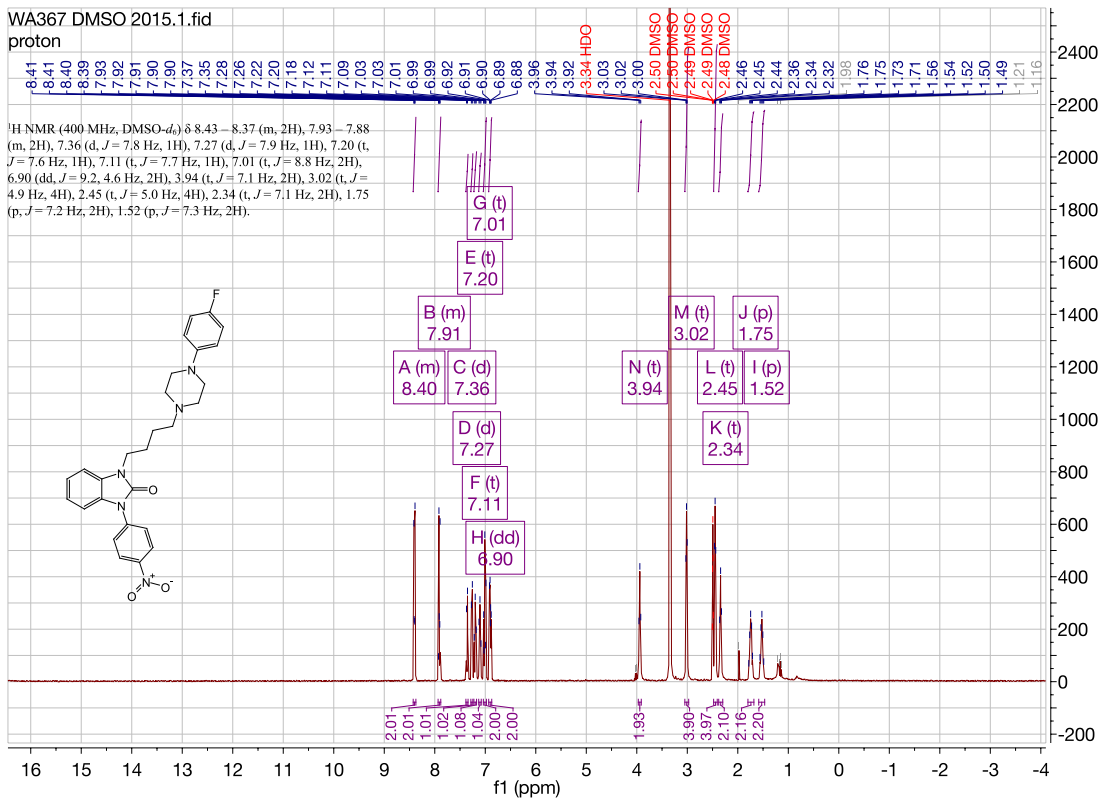
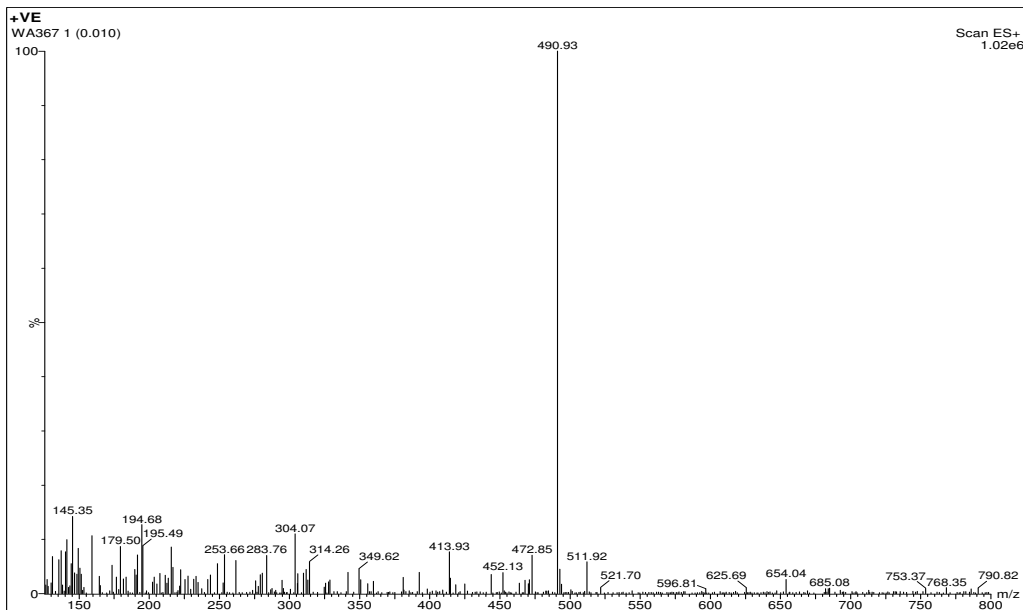
¹³C NMR (101 MHz, DMSO) δ 155.19, 154.67, 148.38, 130.64, 128.73, 121.08, 120.84, 117.46, 117.38, 115.75, 115.53, 109.17, 108.15, 57.53, 53.09, 49.42, 40.60 DMSO, 40.38 DMSO, 40.18 DMSO, 40.06, 39.97 DMSO, 39.76 DMSO, 39.55 DMSO, 39.34 DMSO, 26.09, 23.81



WA365 DMSO 2015.135.fid
dept135

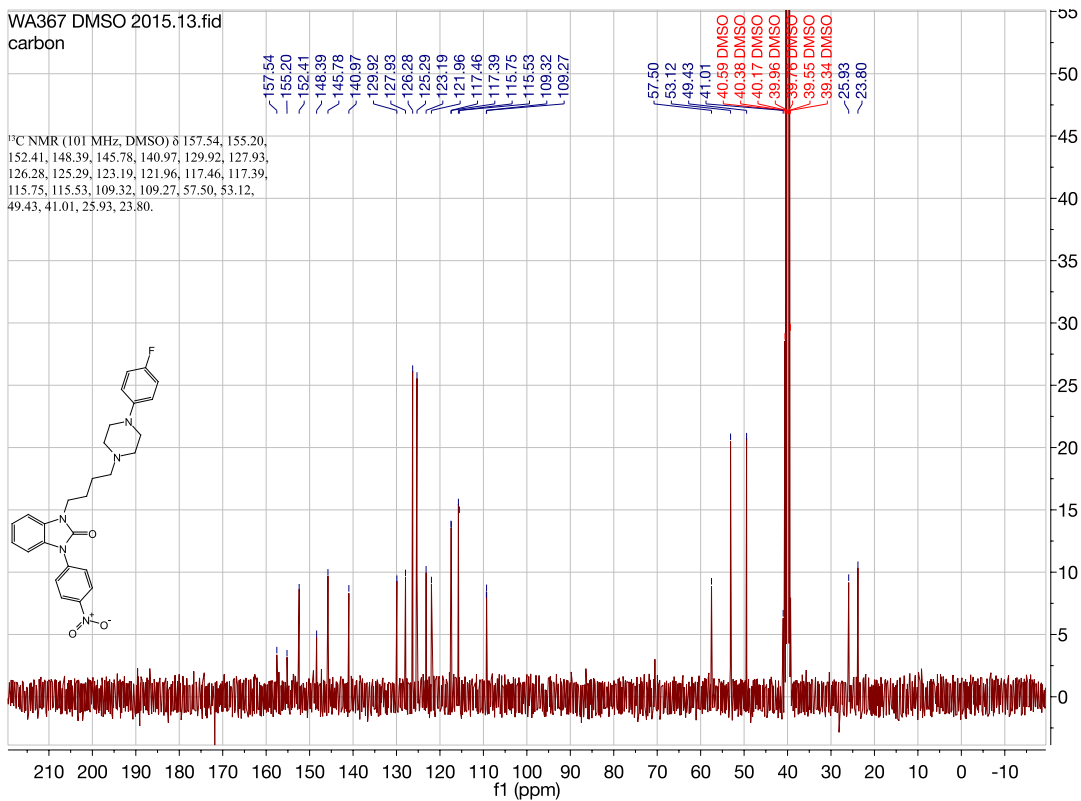
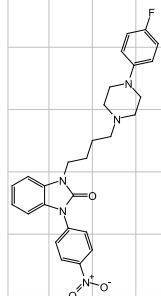


1-(4-(4-(4-fluorophenyl)piperazin-1-yl)butyl)-3-(4-nitrophenyl)-1,3-dihydro-2H-benzo[d]imidazol-2-one. (WA367)

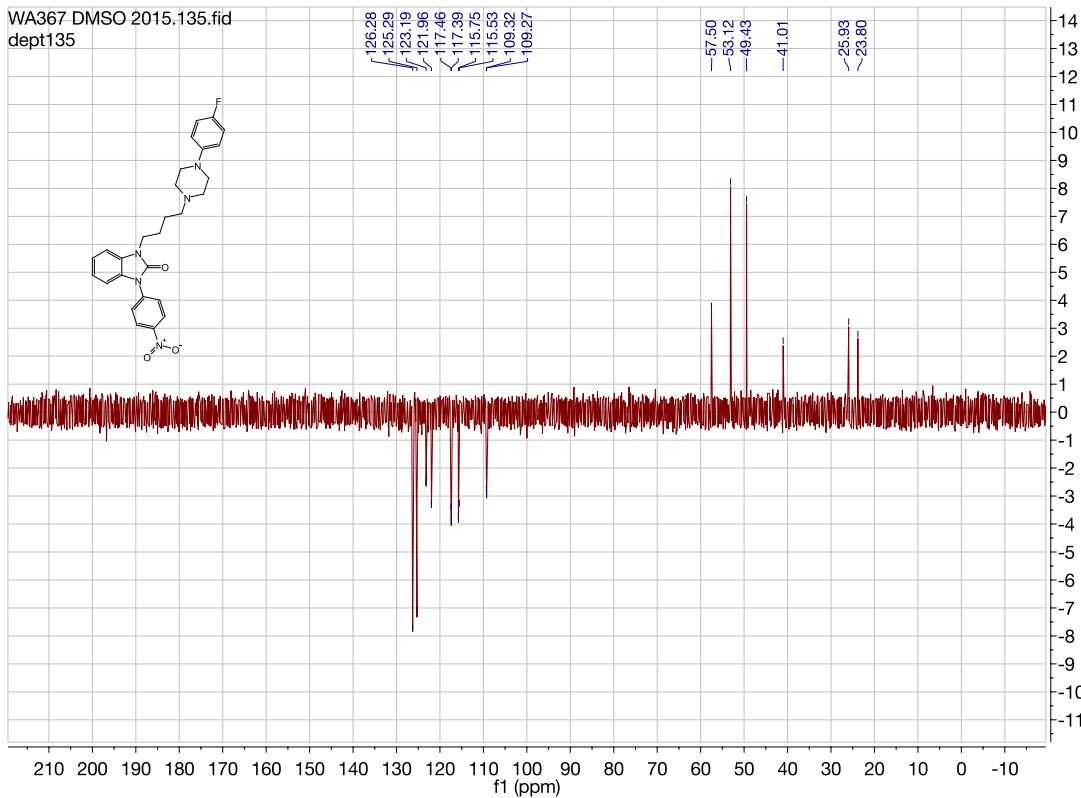


WA367 DMSO 2015.13.fid
carbon

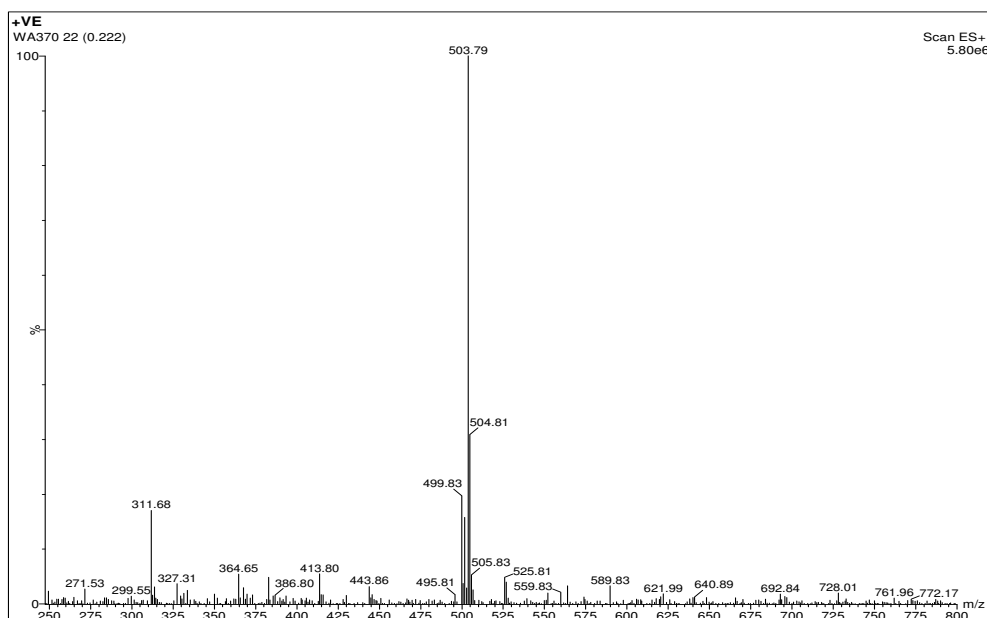
¹³C NMR (101 MHz, DMSO) δ 157.54, 155.20, 152.41, 148.39, 145.78, 140.97, 129.92, 127.93, 126.28, 125.29, 123.19, 121.96, 117.46, 117.39, 115.75, 115.53, 109.32, 109.27, 57.50, 53.12, 49.43, 41.01, 25.93, 23.80.



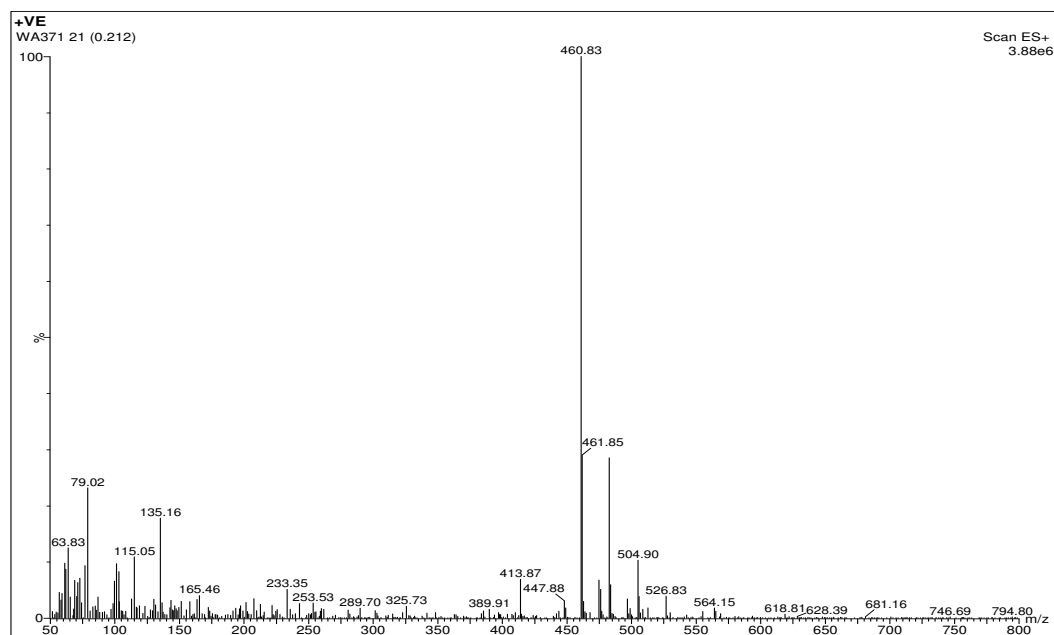
WA367 DMSO 2015.135.fid
dept135

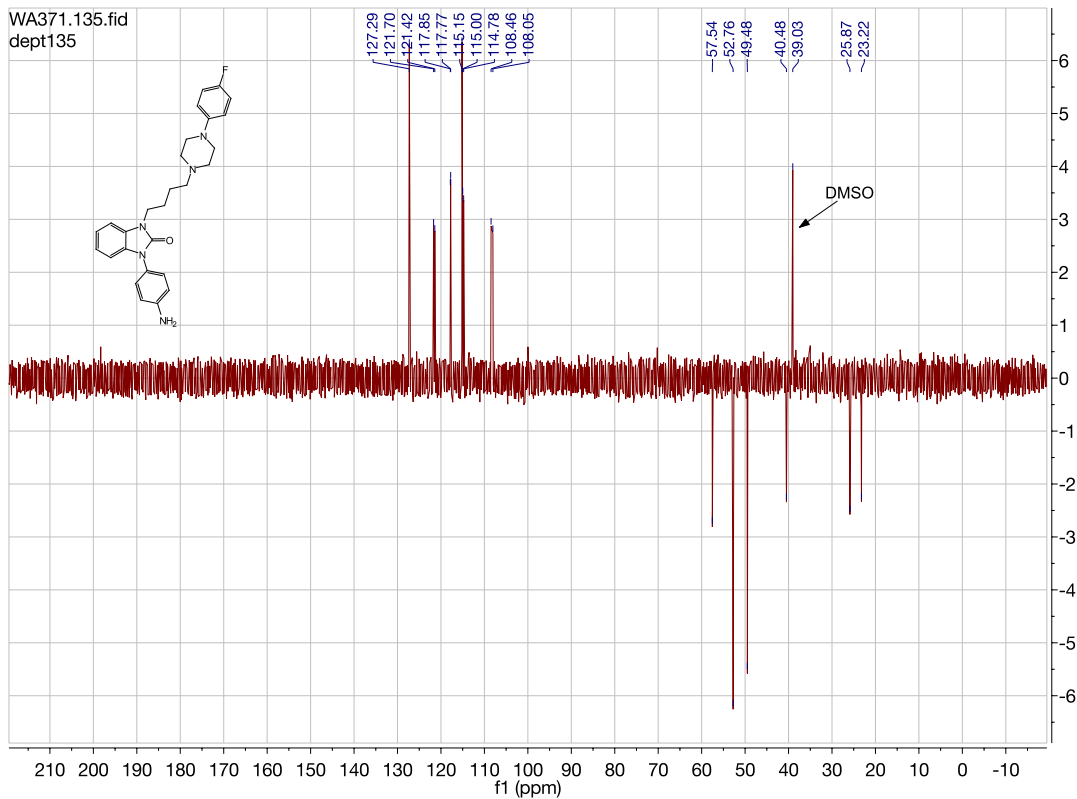


1-(4-(6,7-dimethoxy-3,4-dihydroisoquinolin-2(1*H*)-yl)butyl)-3-(4-nitrophenyl)-1,3-dihydro-2*H*-benzo[*d*]imidazol-2-one. (WA370)

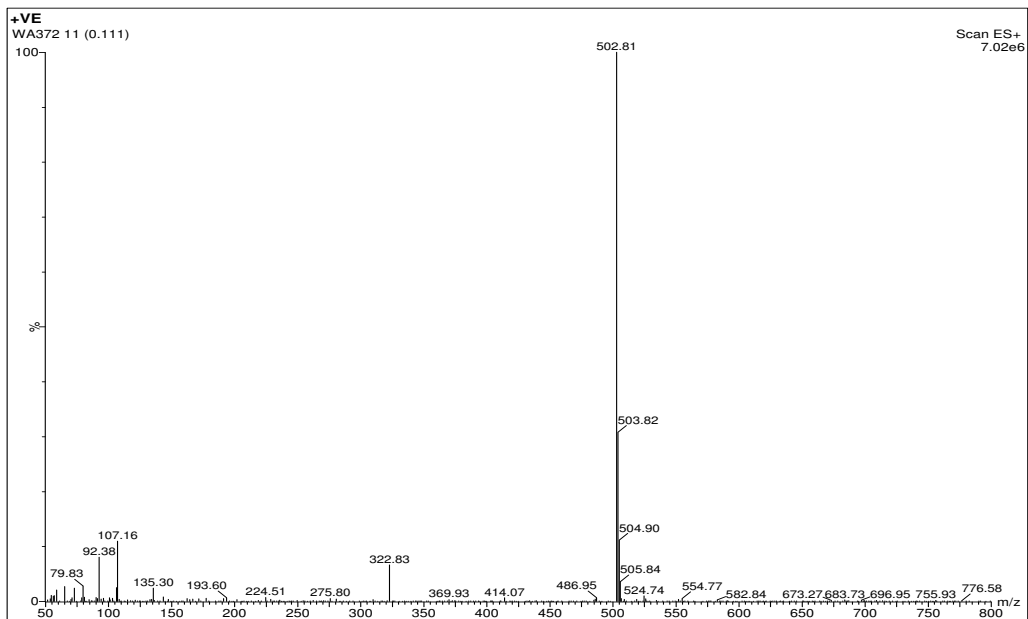


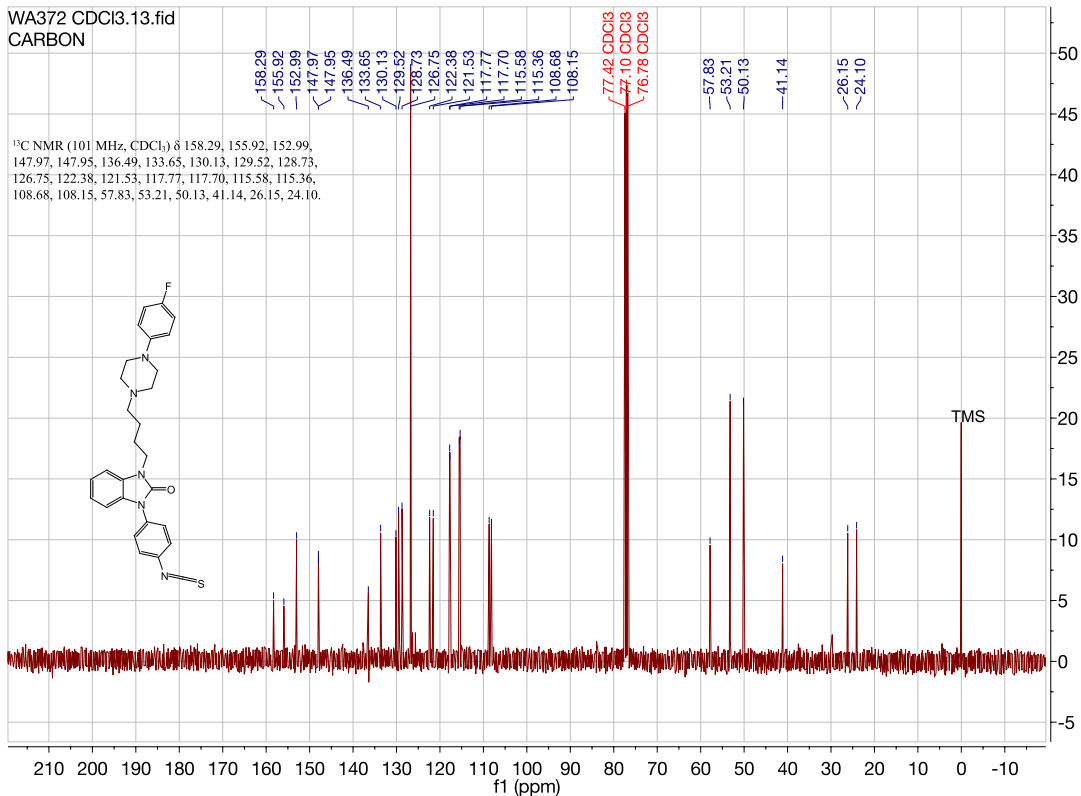
1-(4-aminophenyl)-3-(4-(4-(4-fluorophenyl)piperazin-1-yl)butyl)-1,3-dihydro-2*H*-benzo[*d*]imidazol-2-one. (WA371)

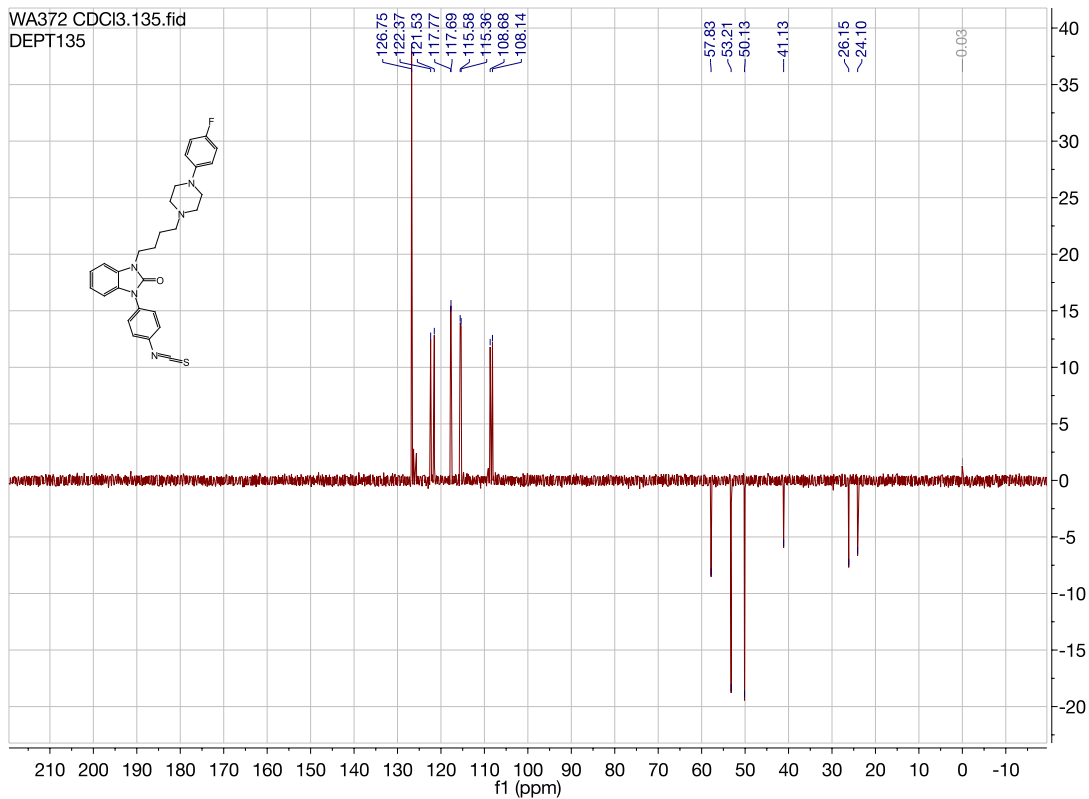




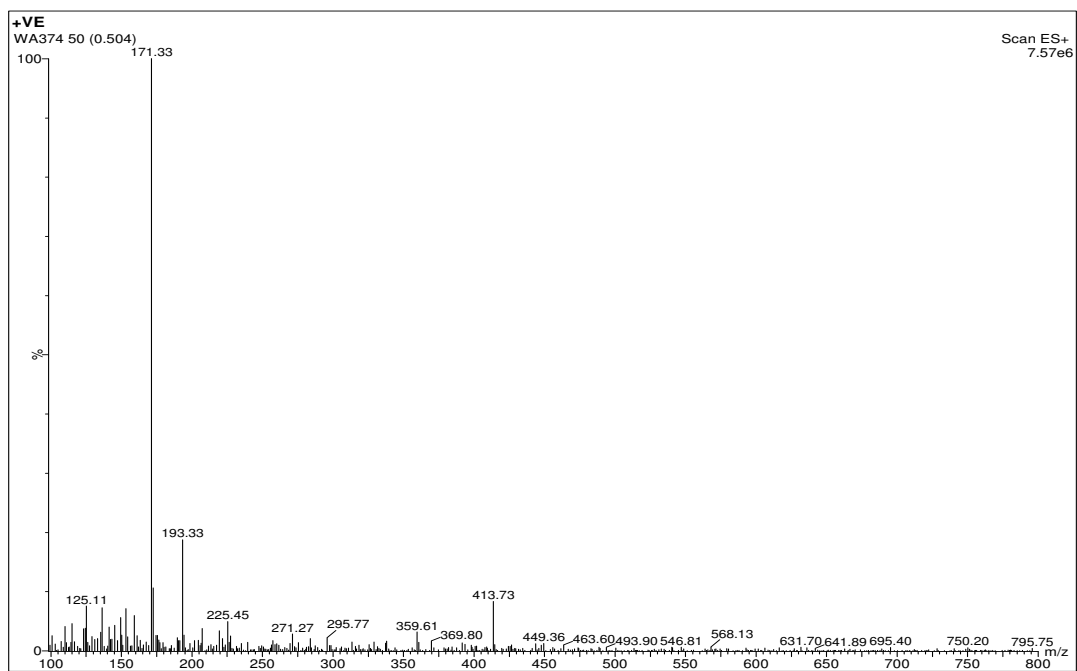
1-(4-(4-(4-fluorophenyl)piperazin-1-yl)butyl)-3-(4-isothiocyantophenyl)-1,3-dihydro-2H-benzo[d]imidazol-2-one. (WA372)

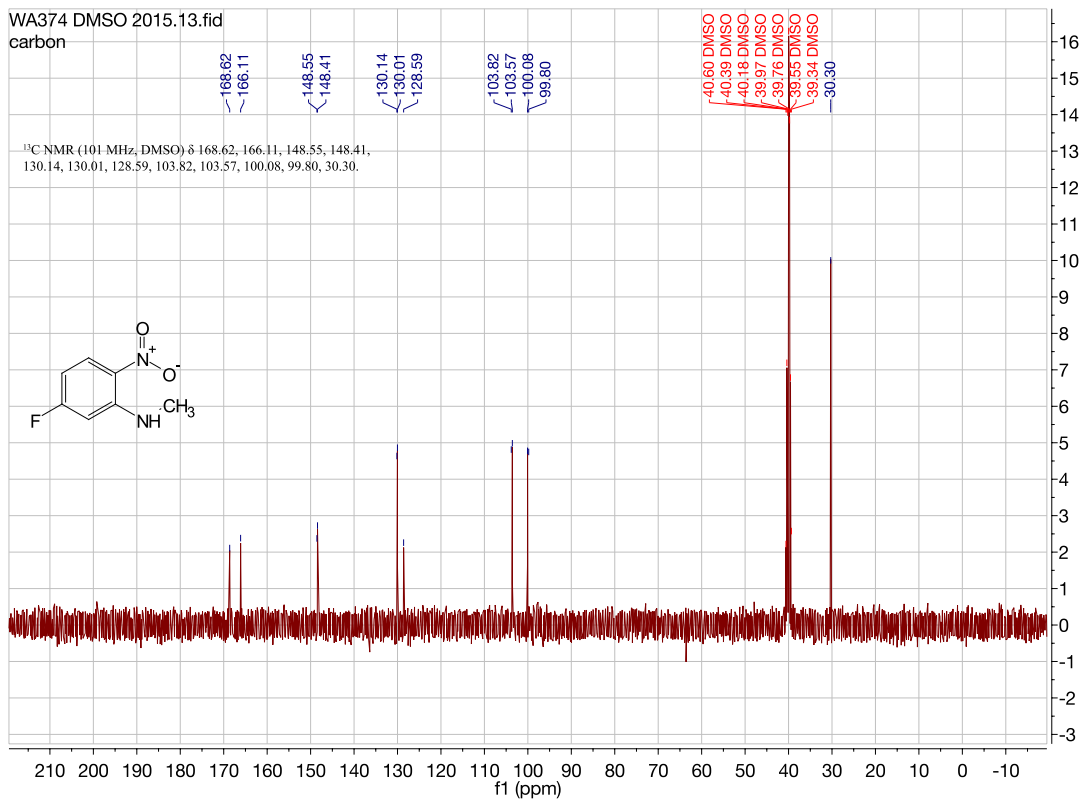
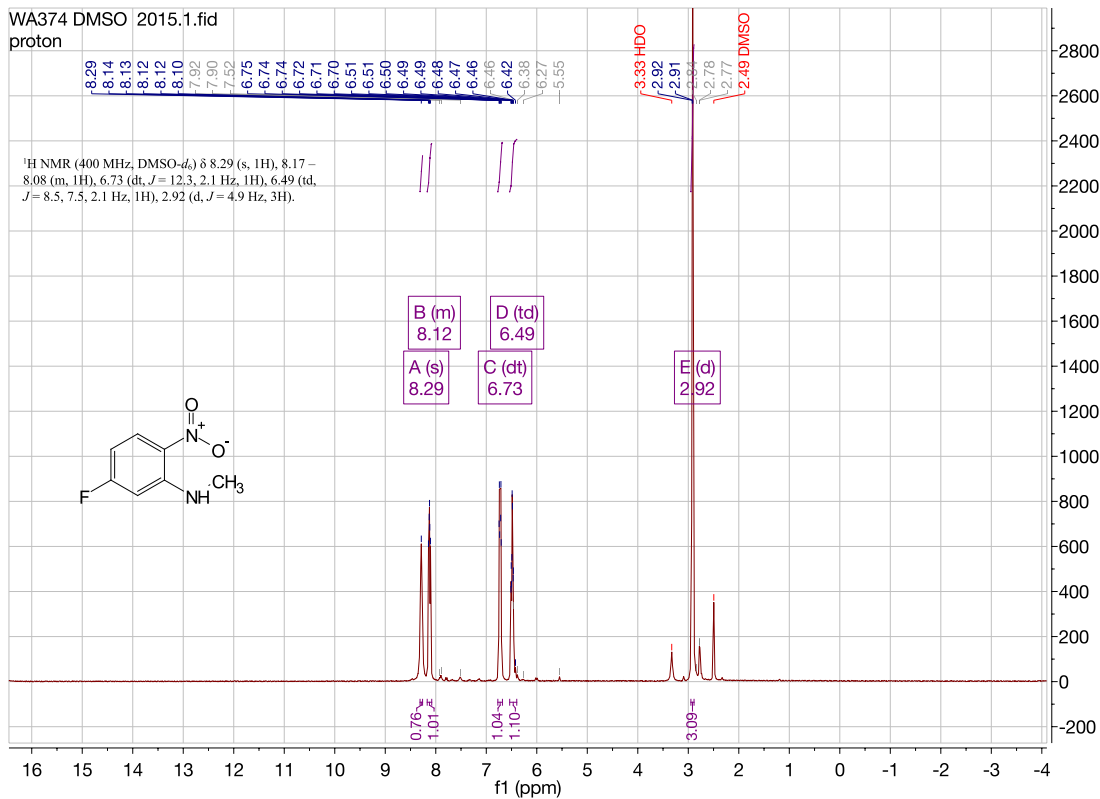


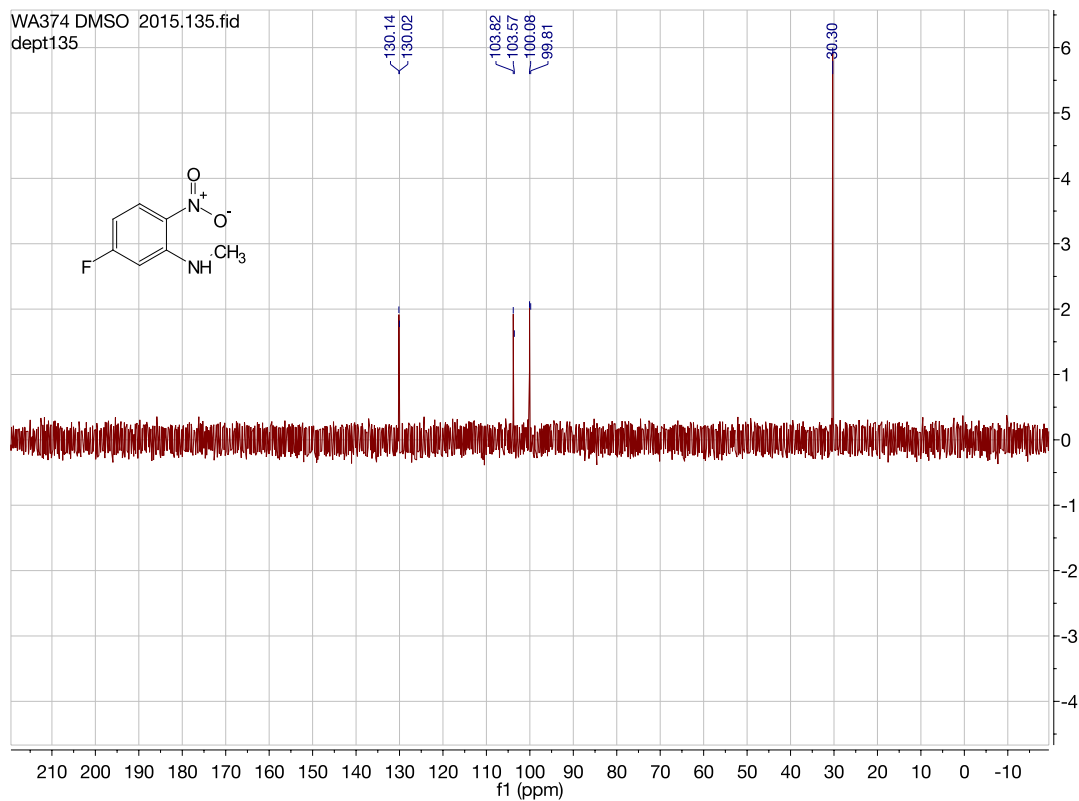




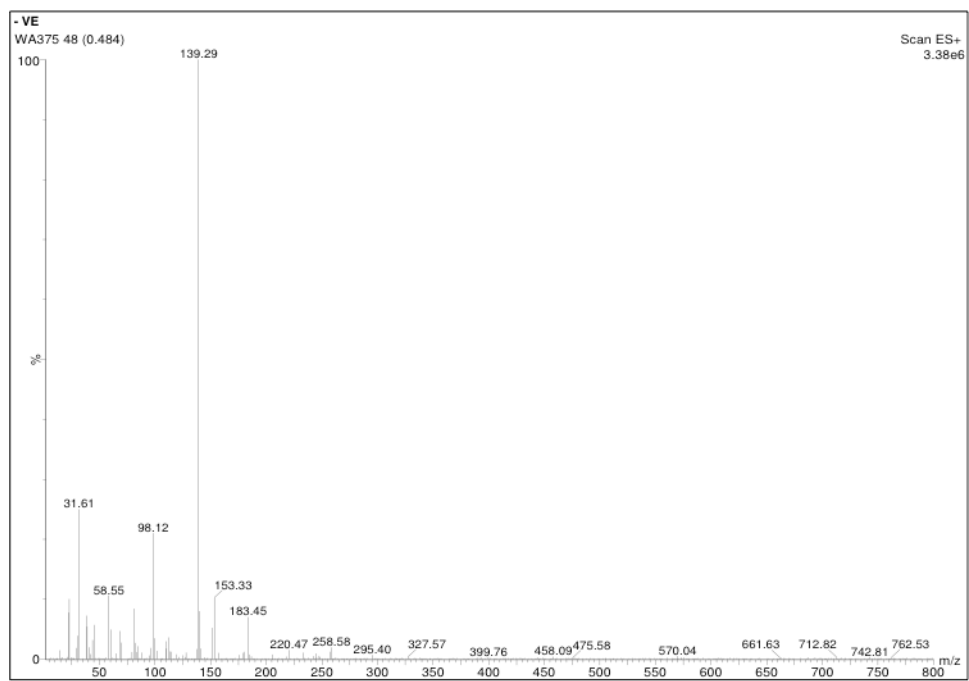
5-fluoro-N-methyl-2-nitroaniline. (WA374)

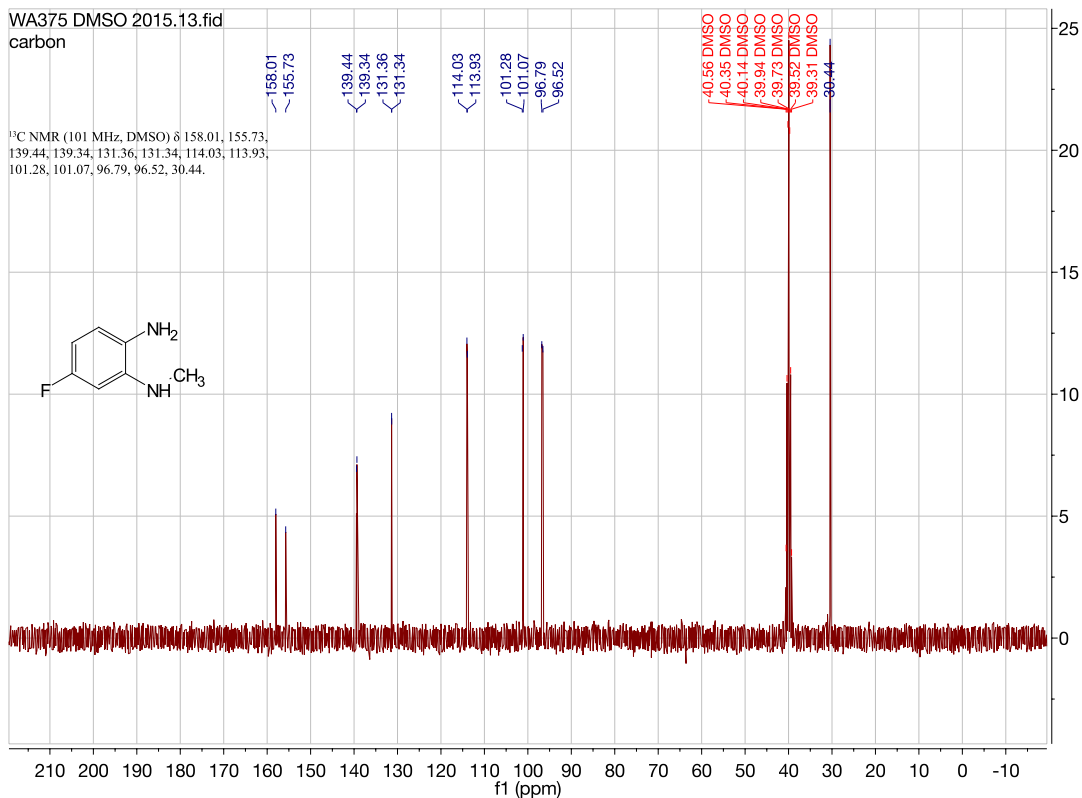
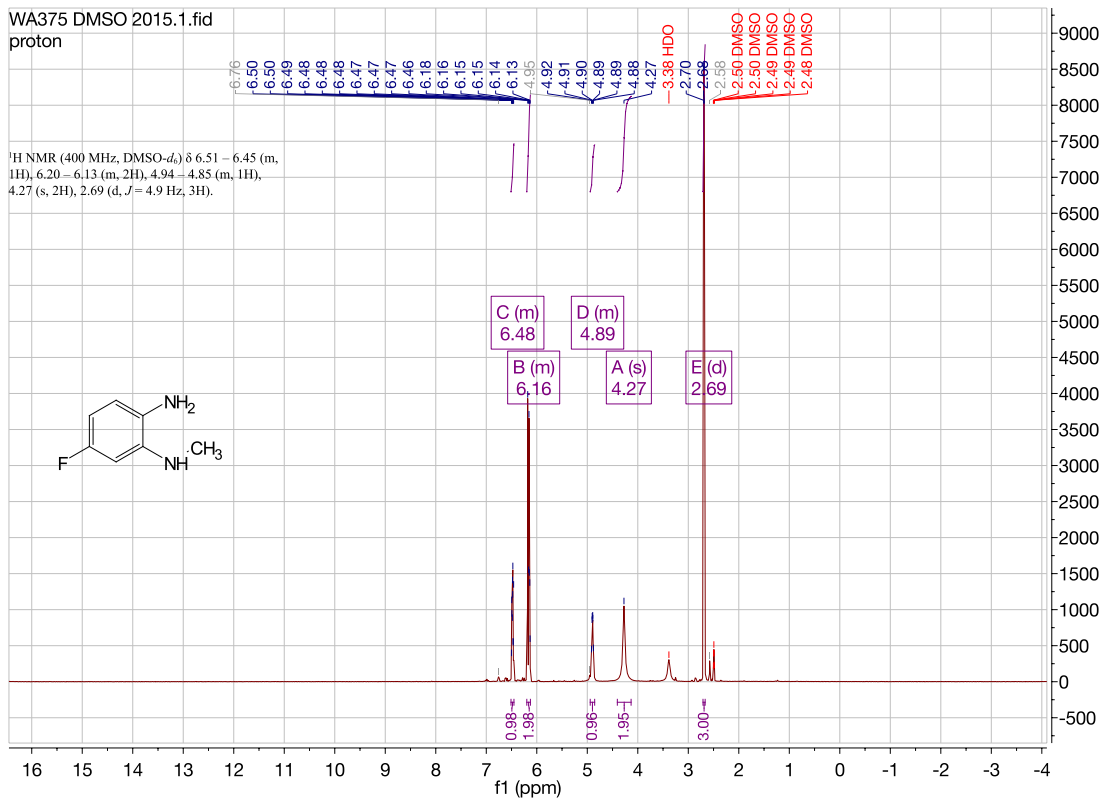




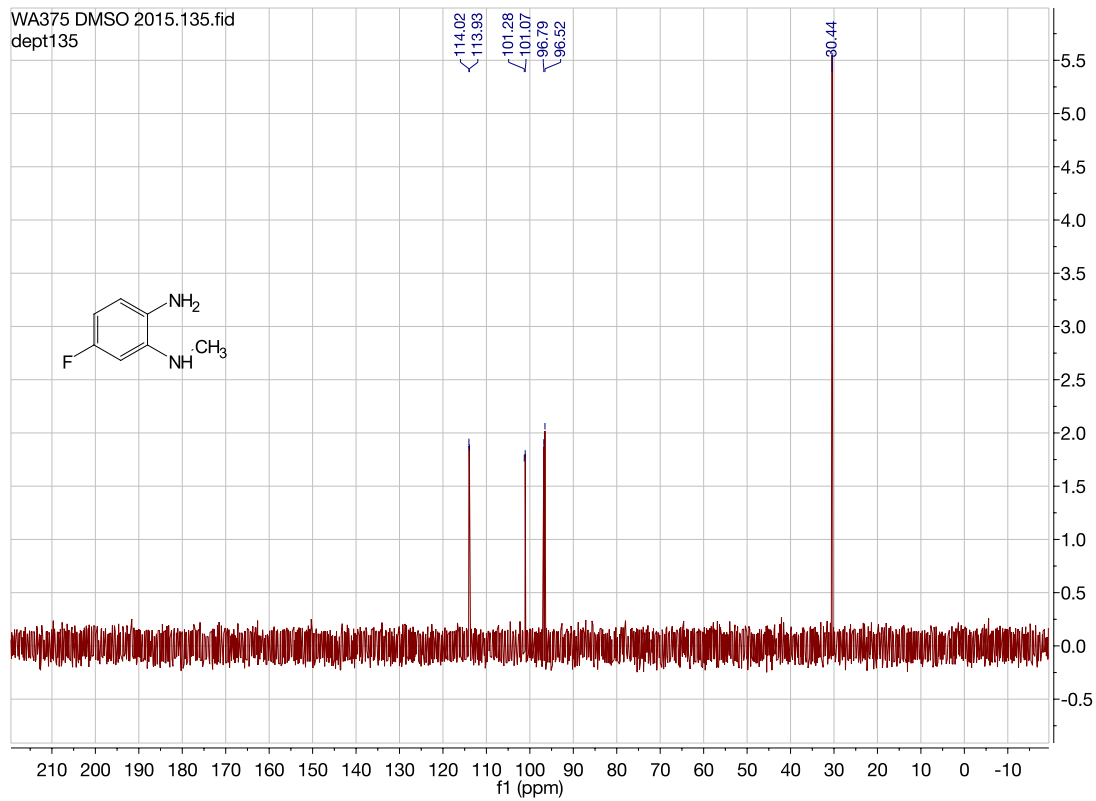


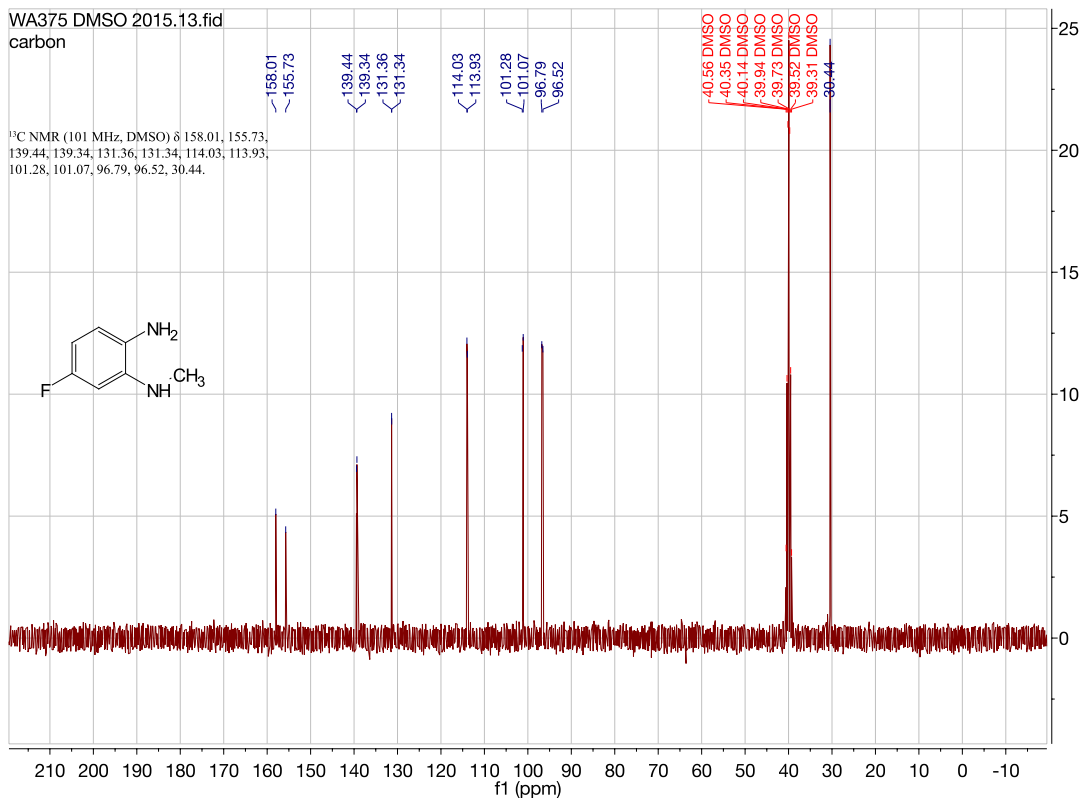
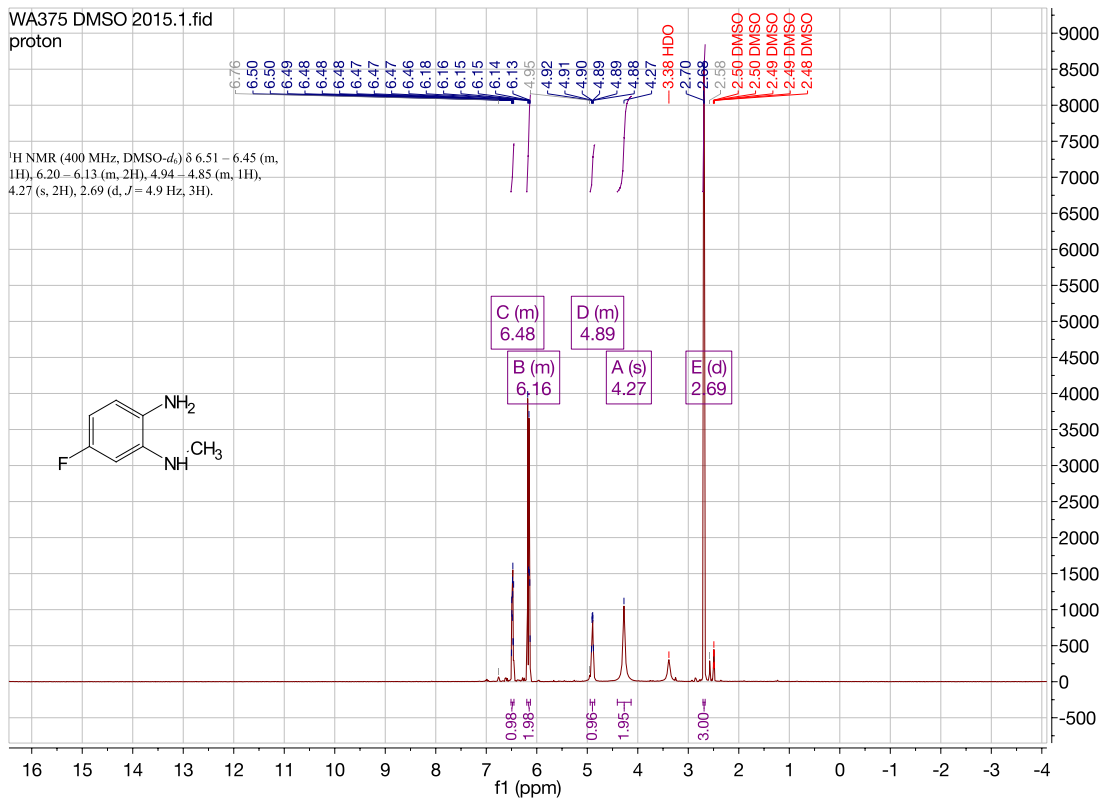
5-fluoro-*N*¹-methylbenzene-1,2-diamine. (WA375)

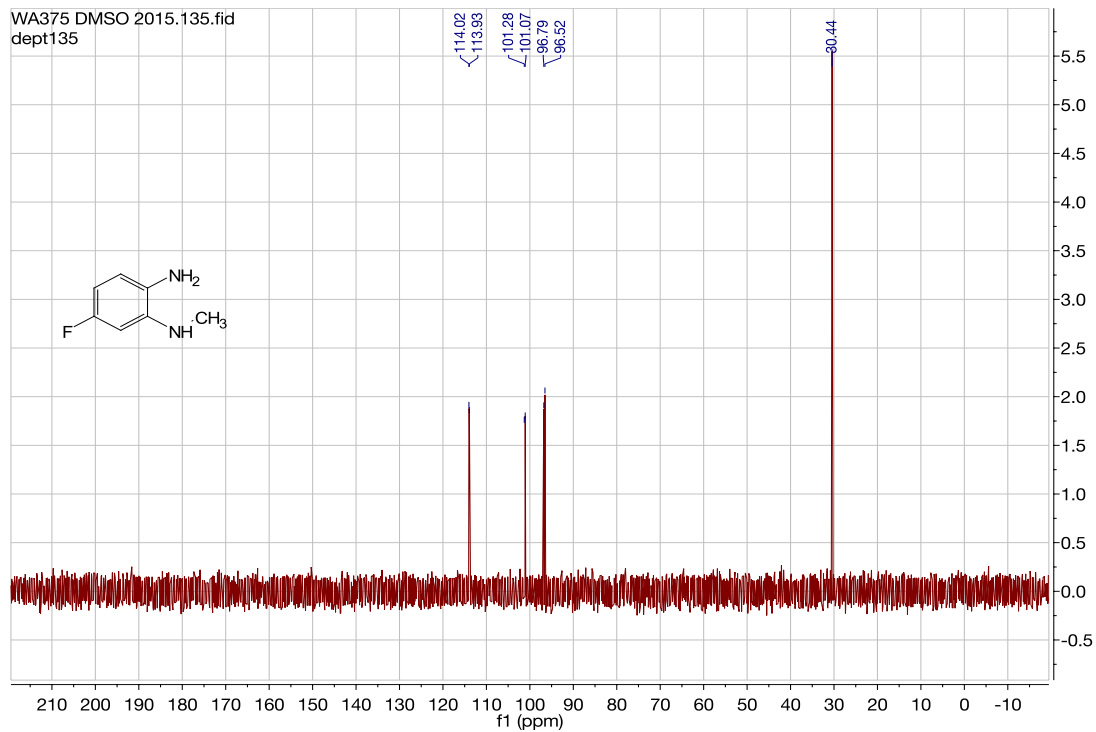




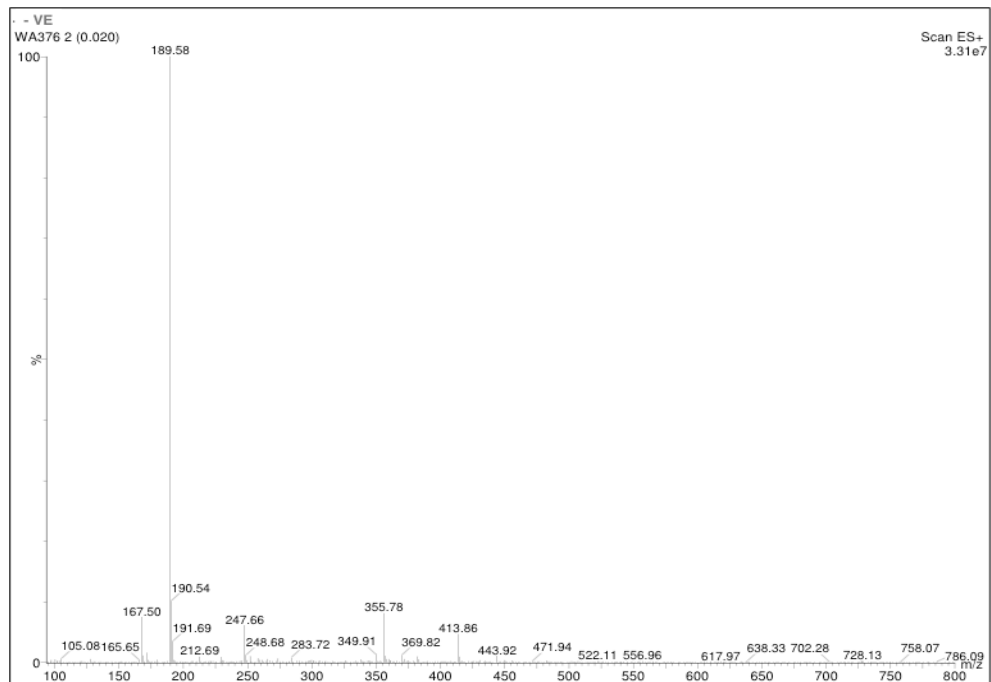
WA375 DMSO 2015.135.fid
dept135

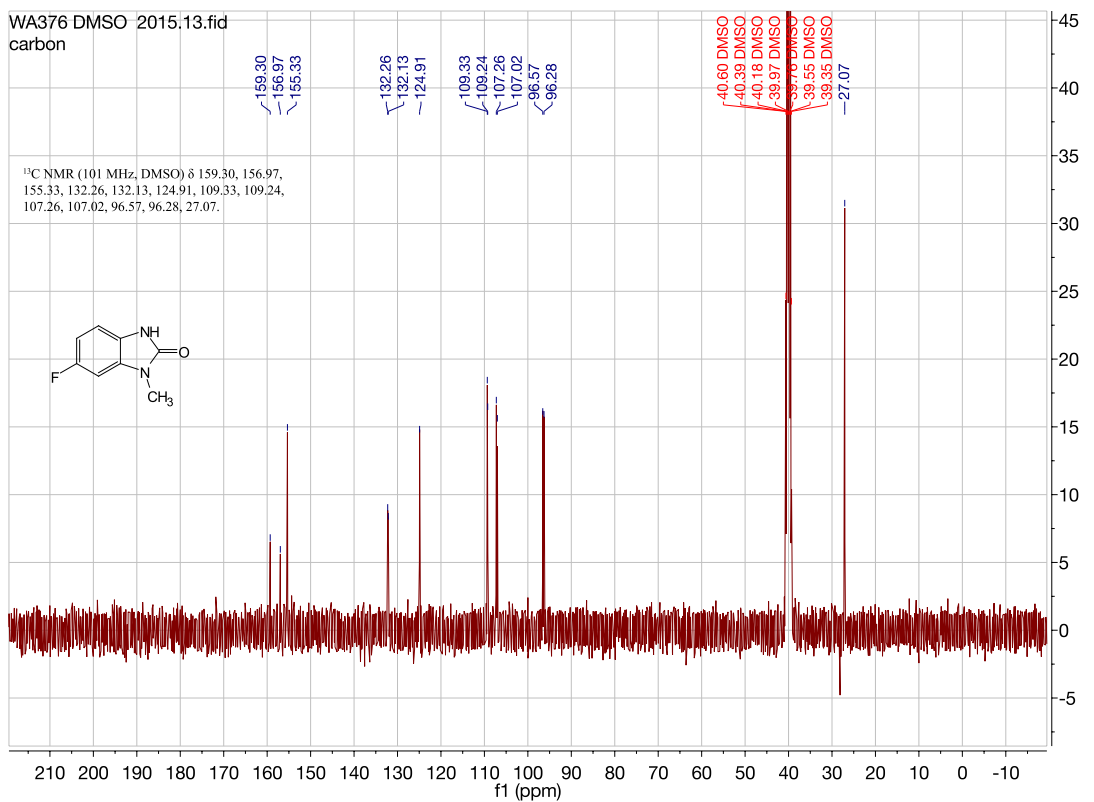
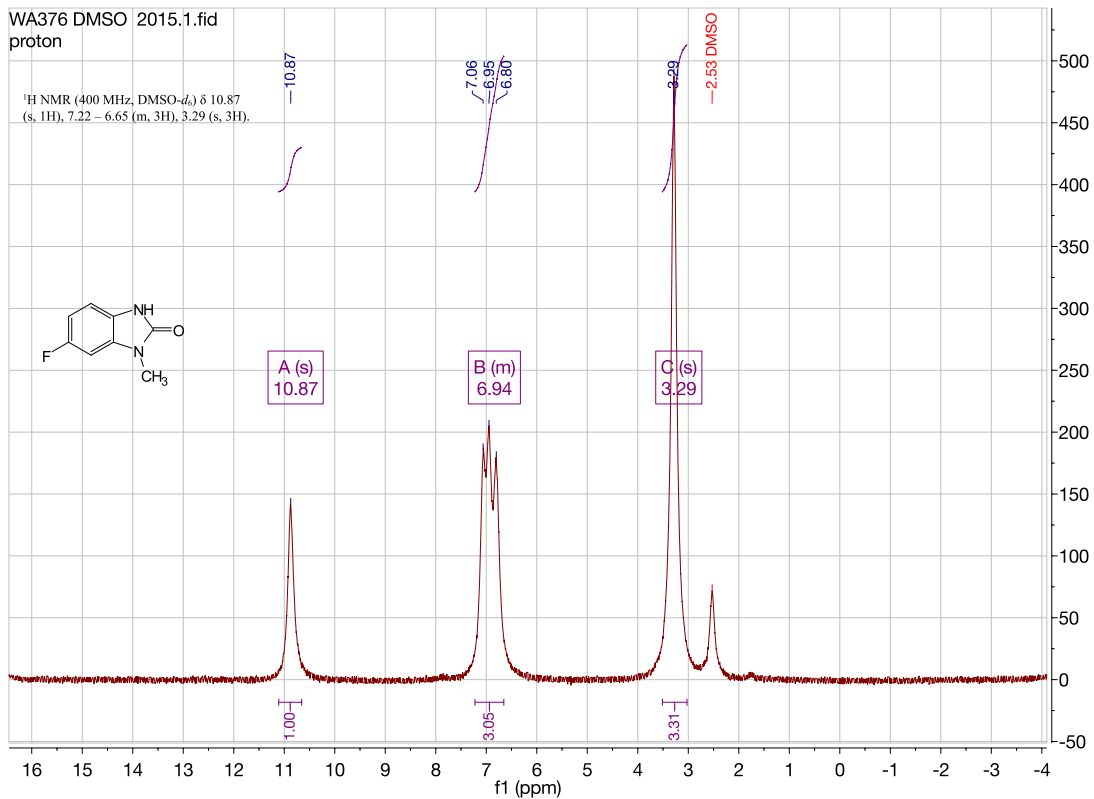


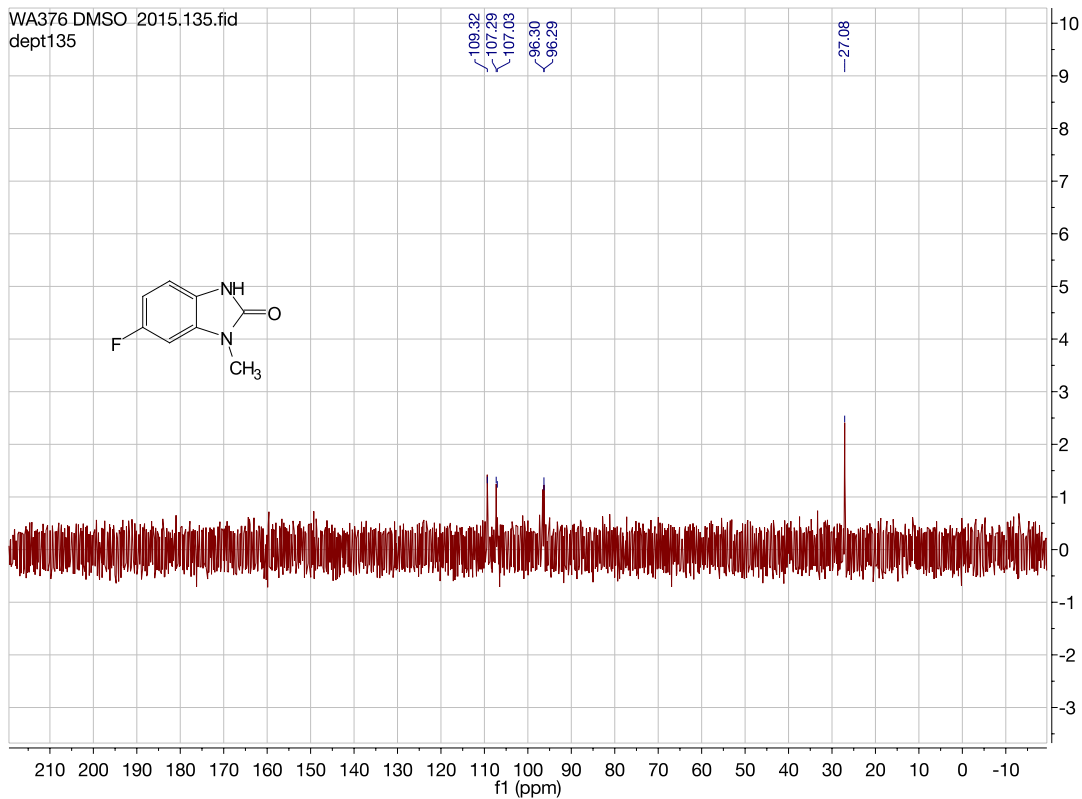




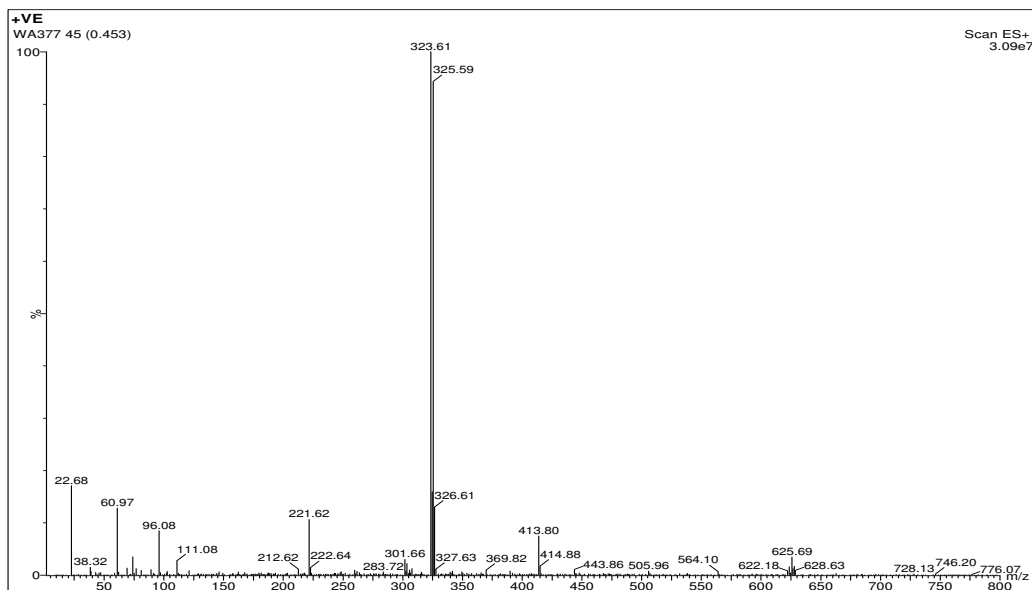
6-fluoro-1-methyl-1,3-dihydro-2H-benzo[d]imidazol-2-one.(WA376)

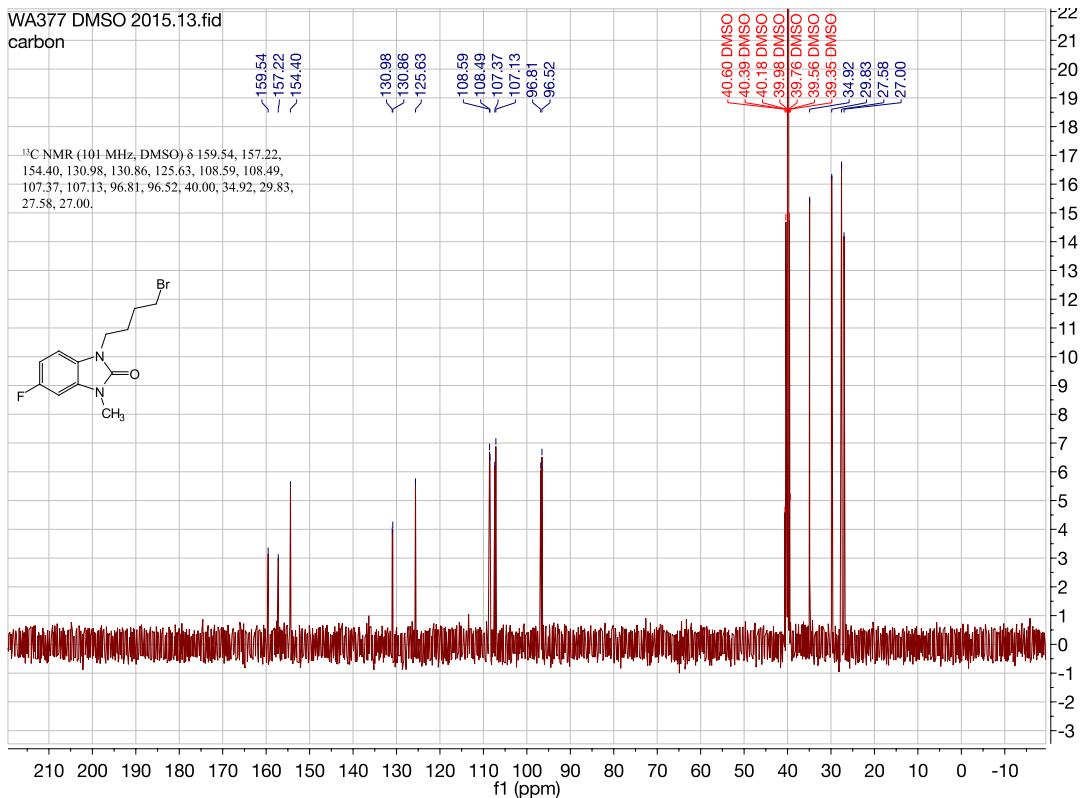
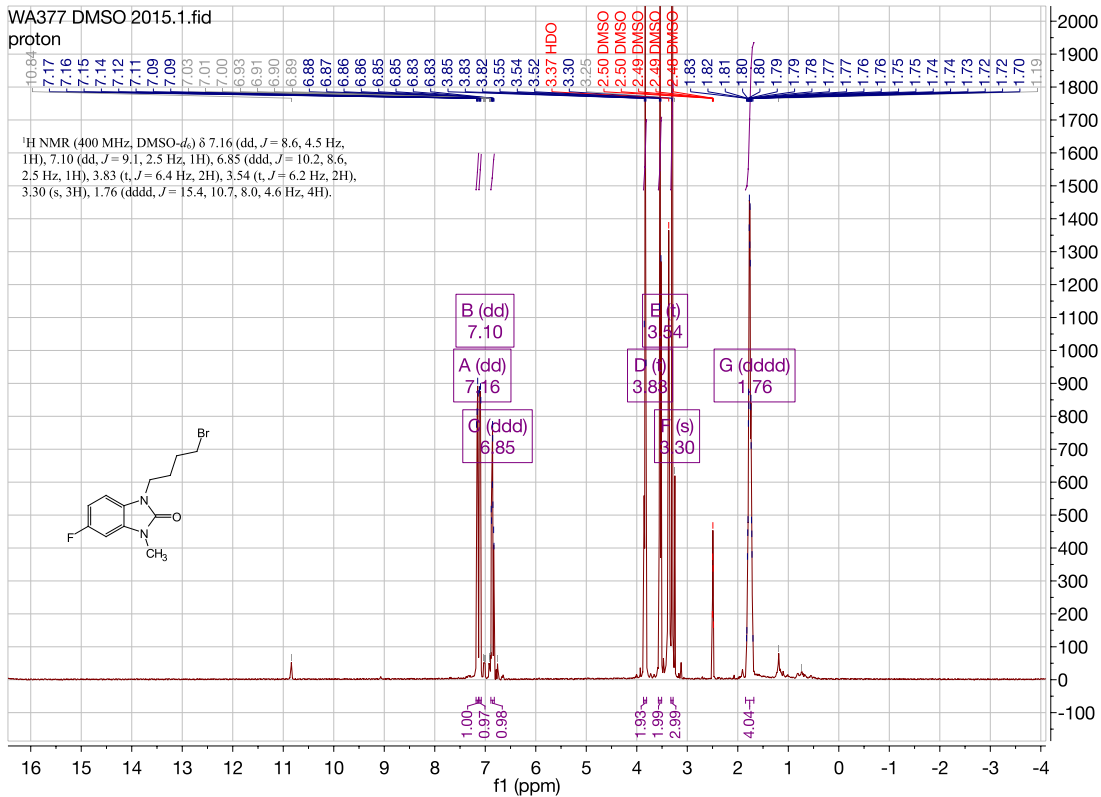


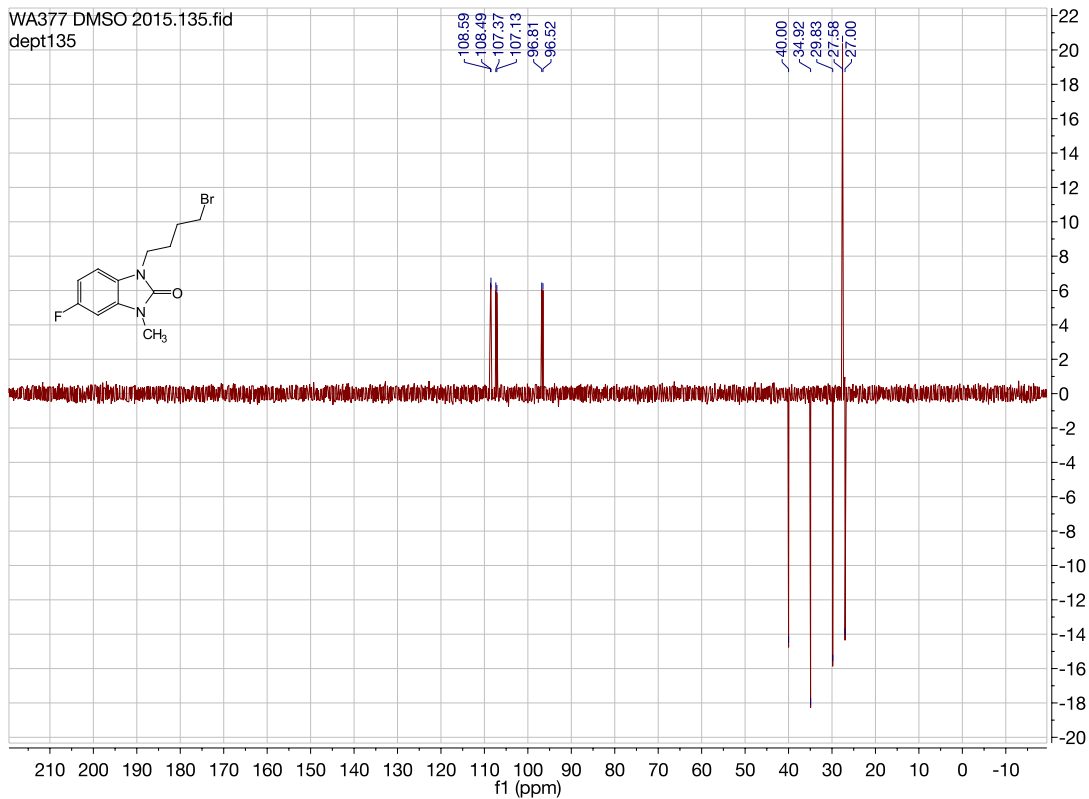




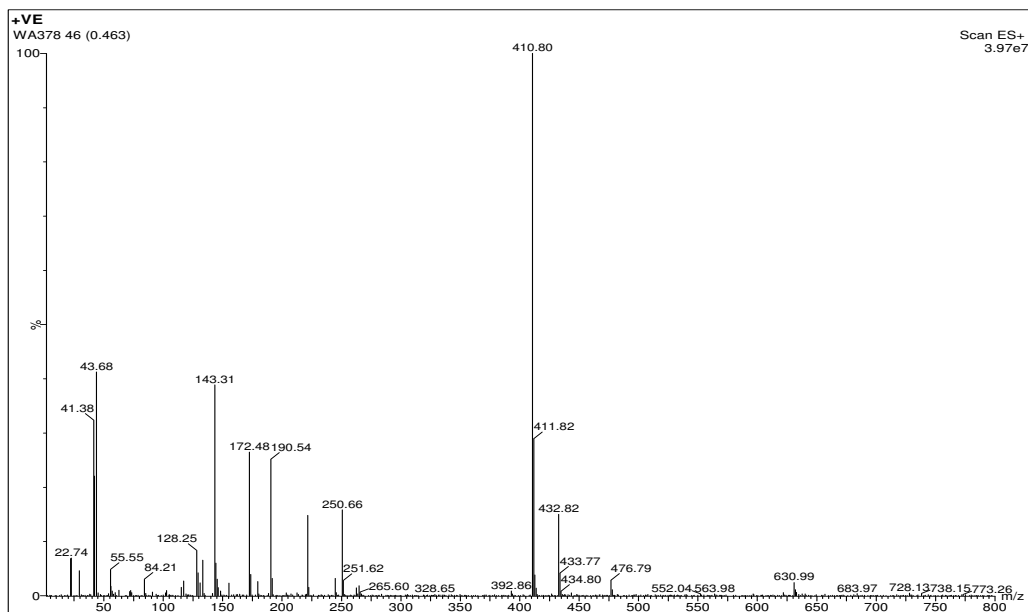
**1-(4-bromobutyl)-5-fluoro-3-methyl-1,3-dihydro-2H-benzo[d]imidazol-2-one.
(WA377)**

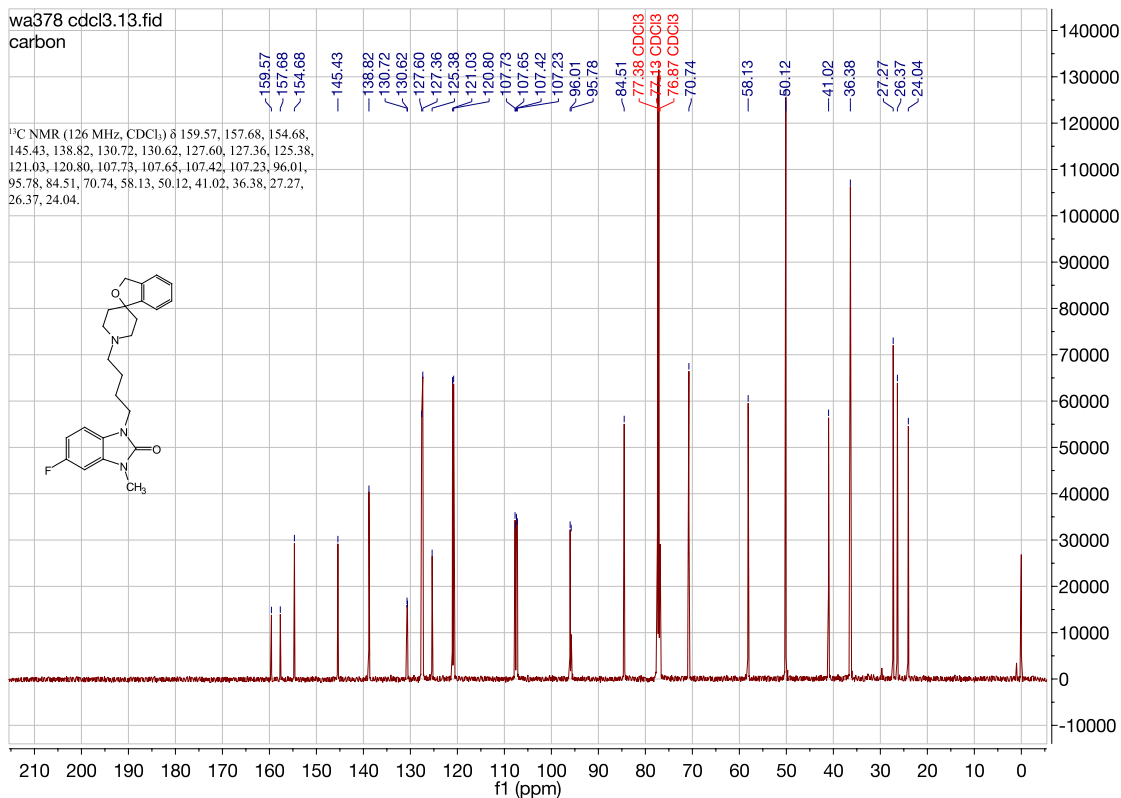
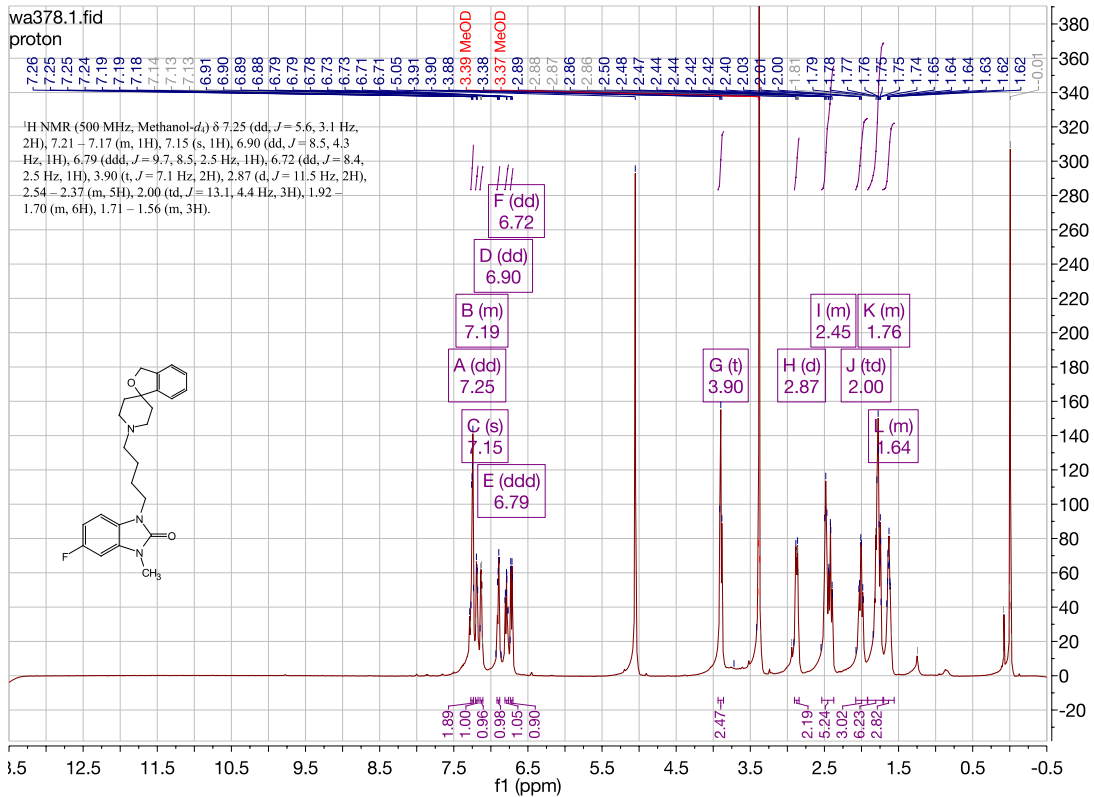


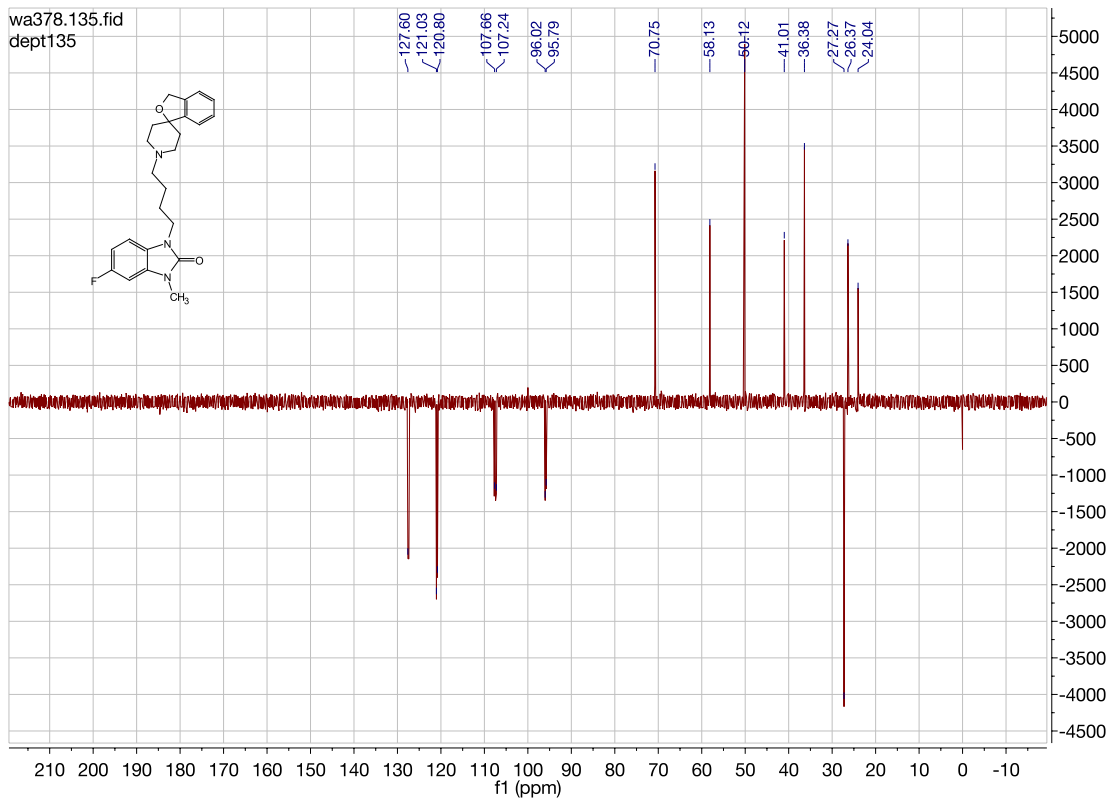




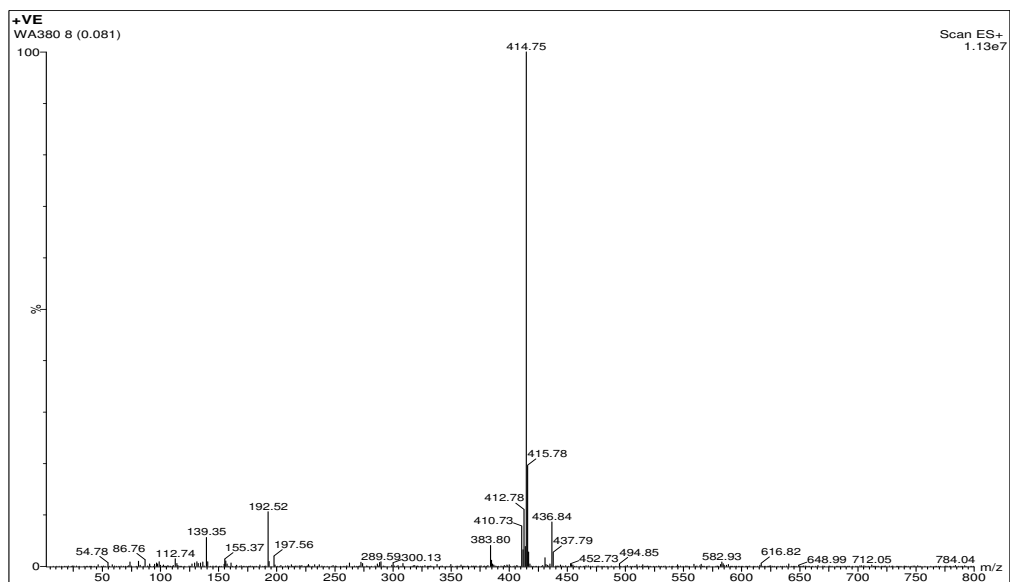
1-(4-(3H-spiro[isobenzofuran-1,4'-piperidin]-1'-yl)butyl)-5-fluoro-3-methyl-1,3-dihydro-2H-benzo[d]imidazol-2-one. (WA378)

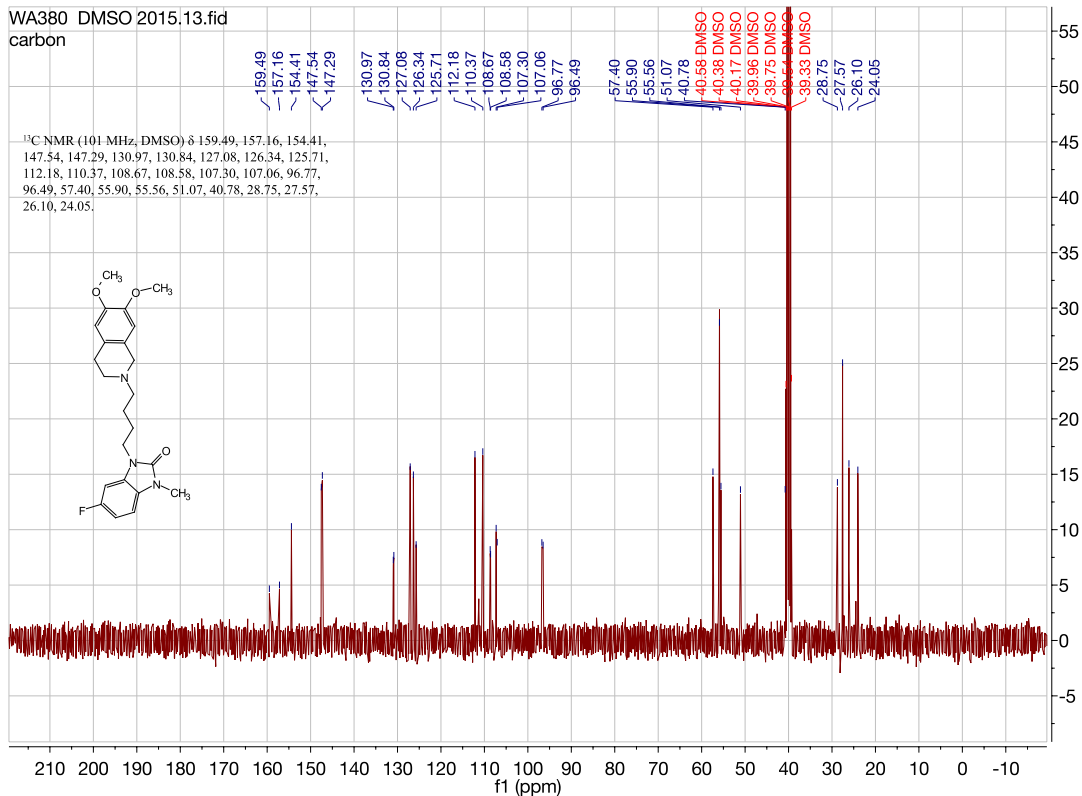
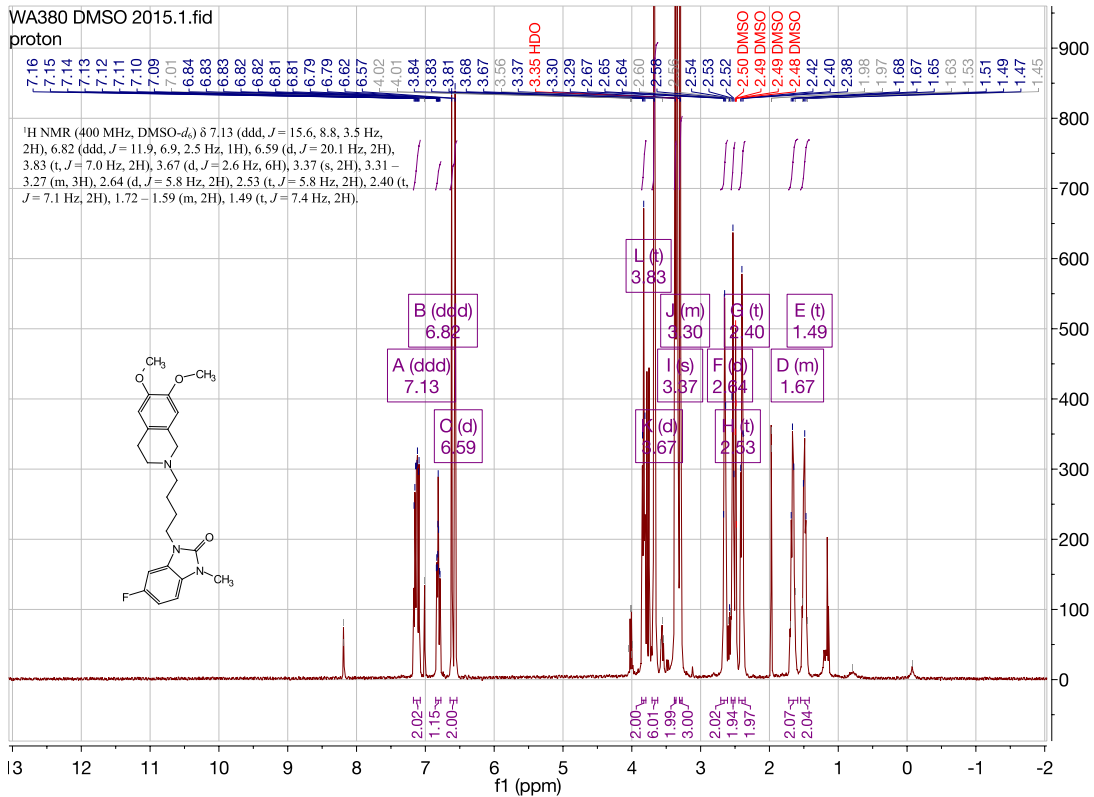


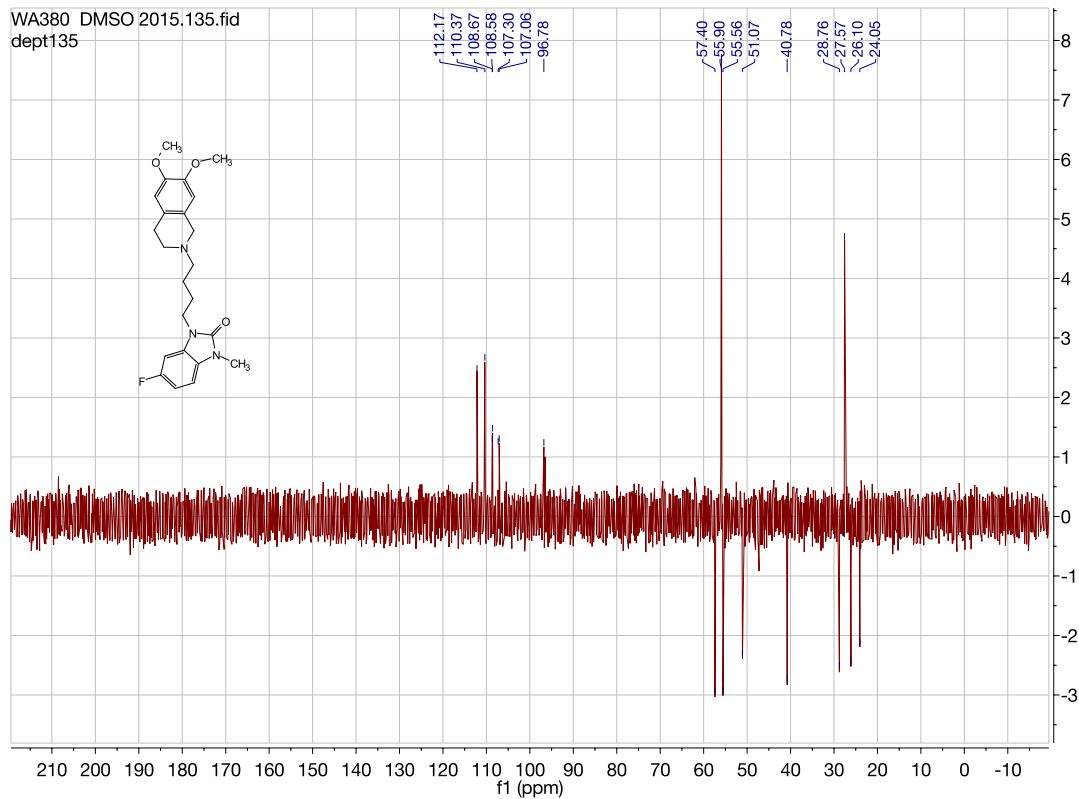




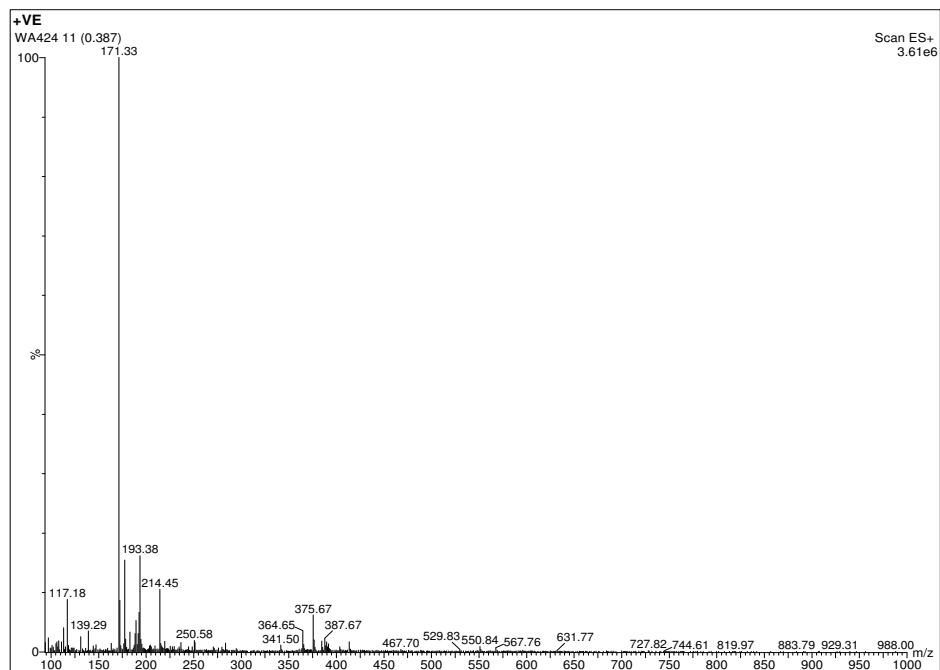
1-(4-(6,7-dimethoxy-3,4-dihydroisoquinolin-2(1H)-yl)butyl)-5-fluoro-3-methyl-1,3-dihydro-2H-benzo[d]imidazol-2-one. (WA380)

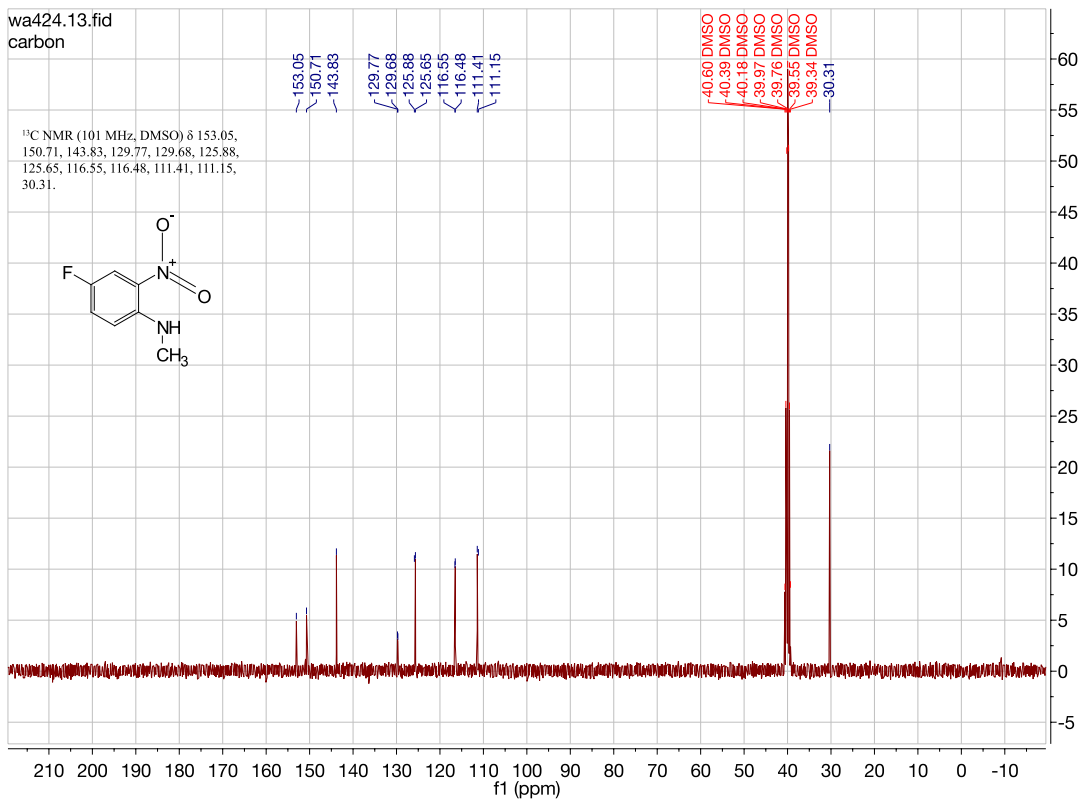
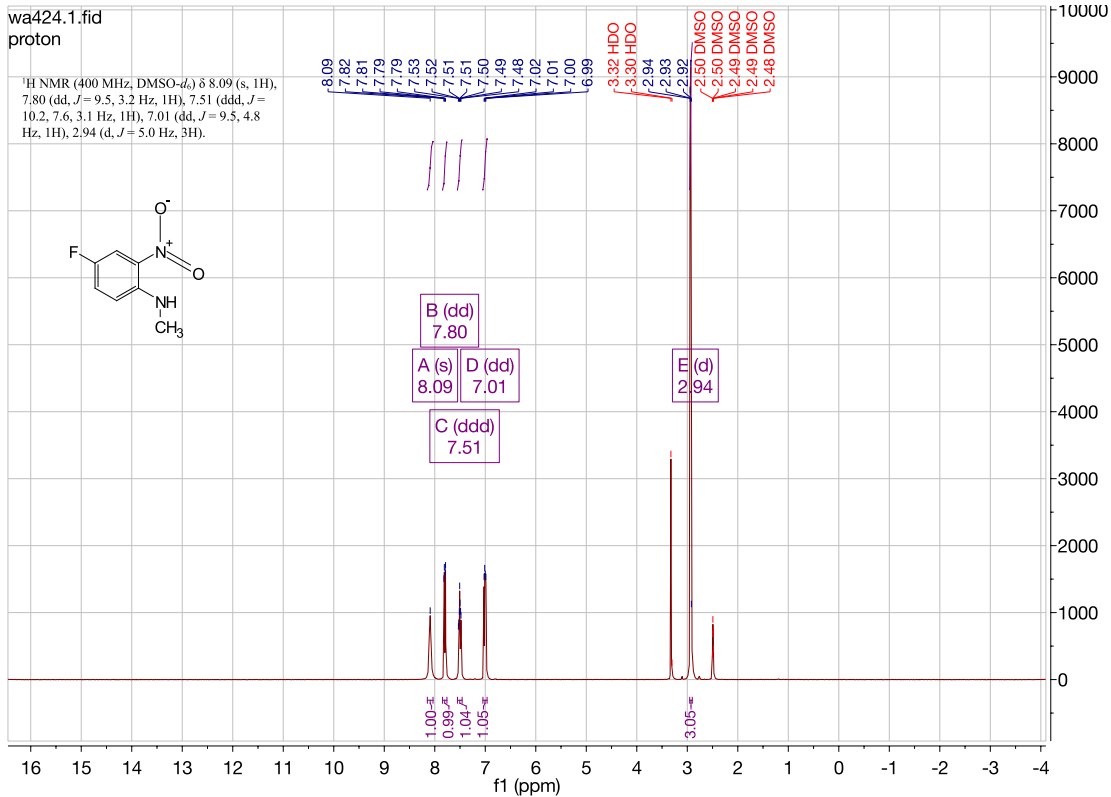


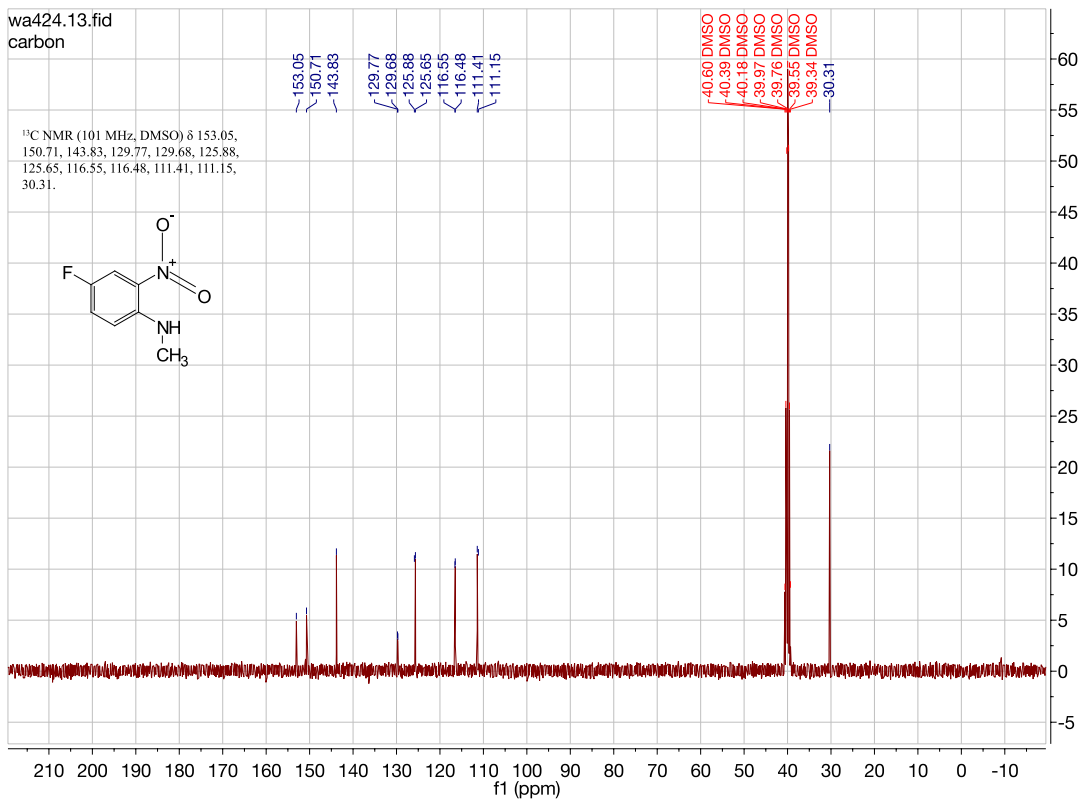
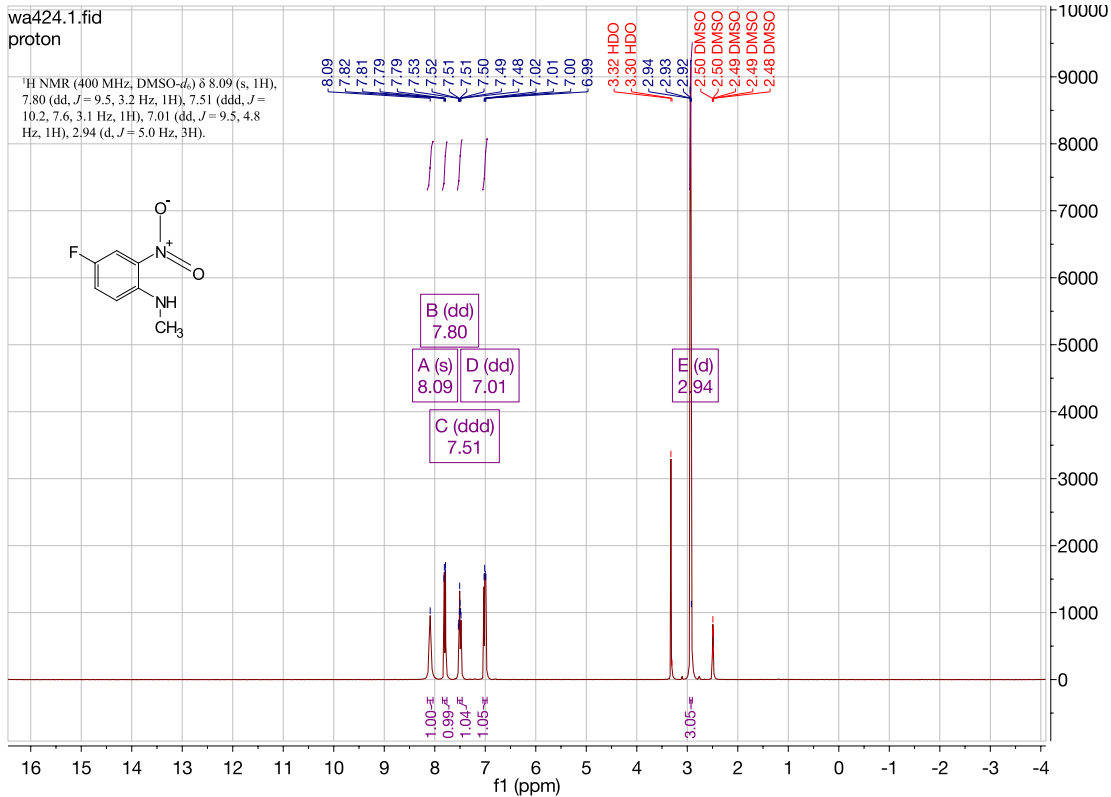


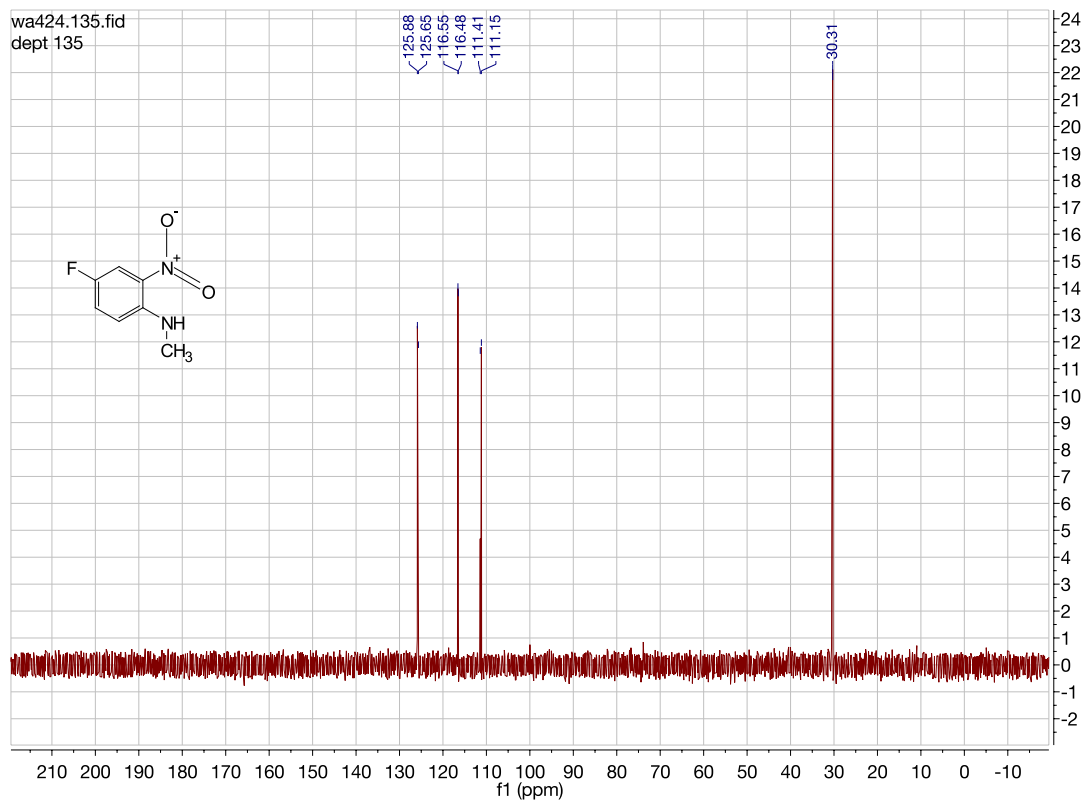


4-fluoro-N-methyl-2-nitroaniline. (WA424)

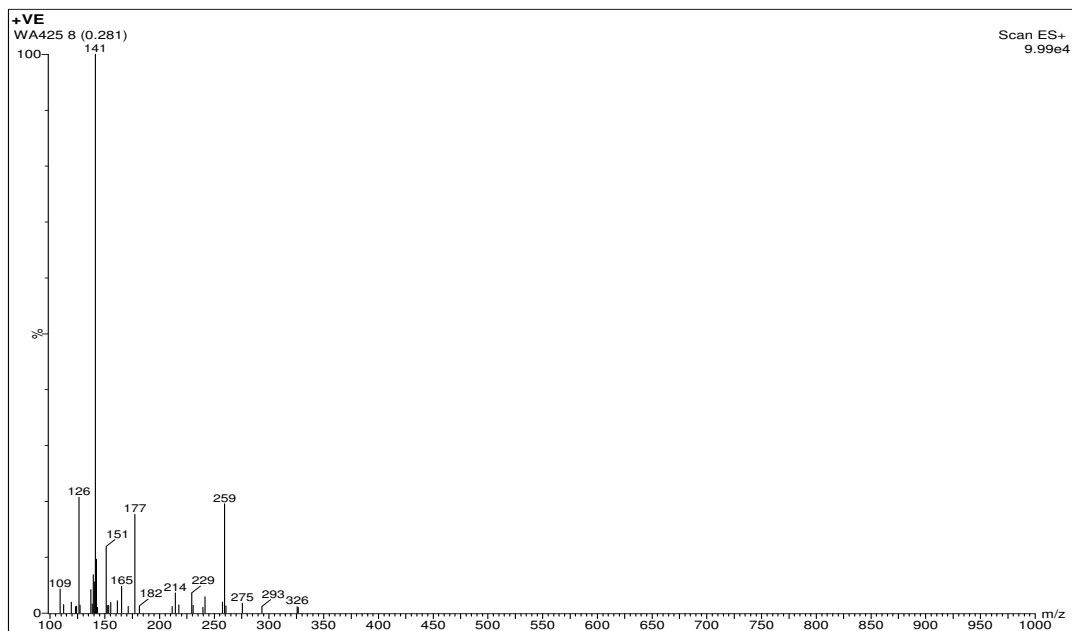


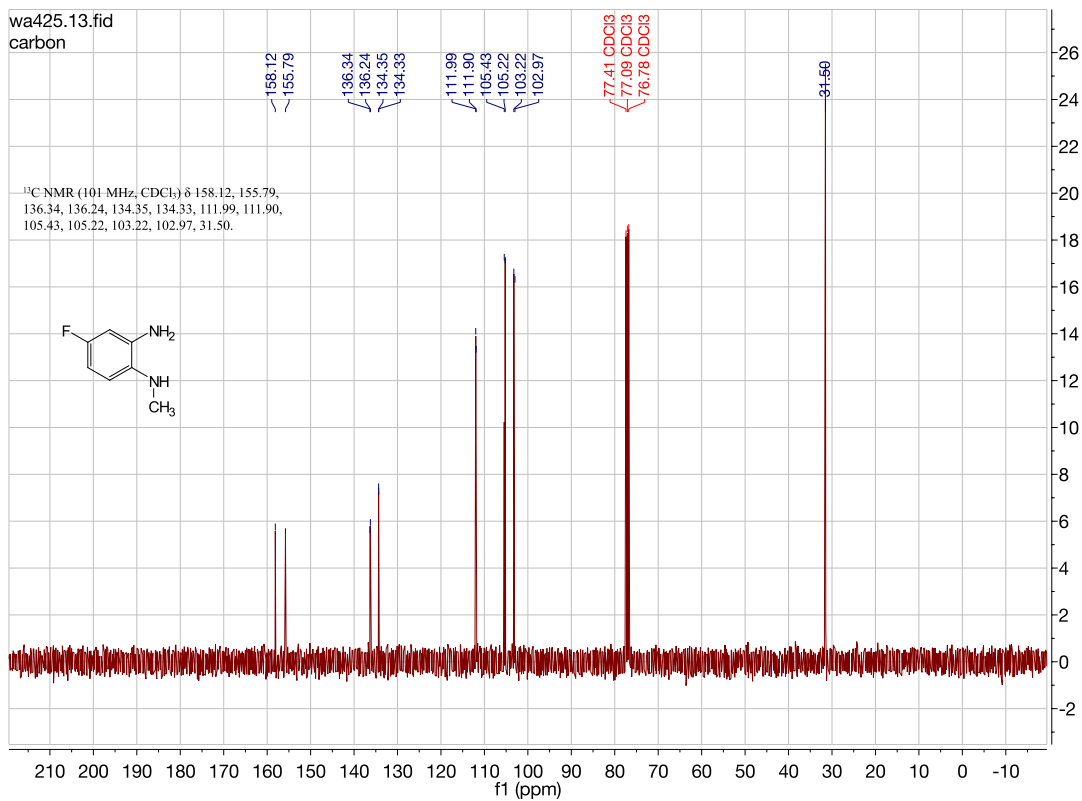
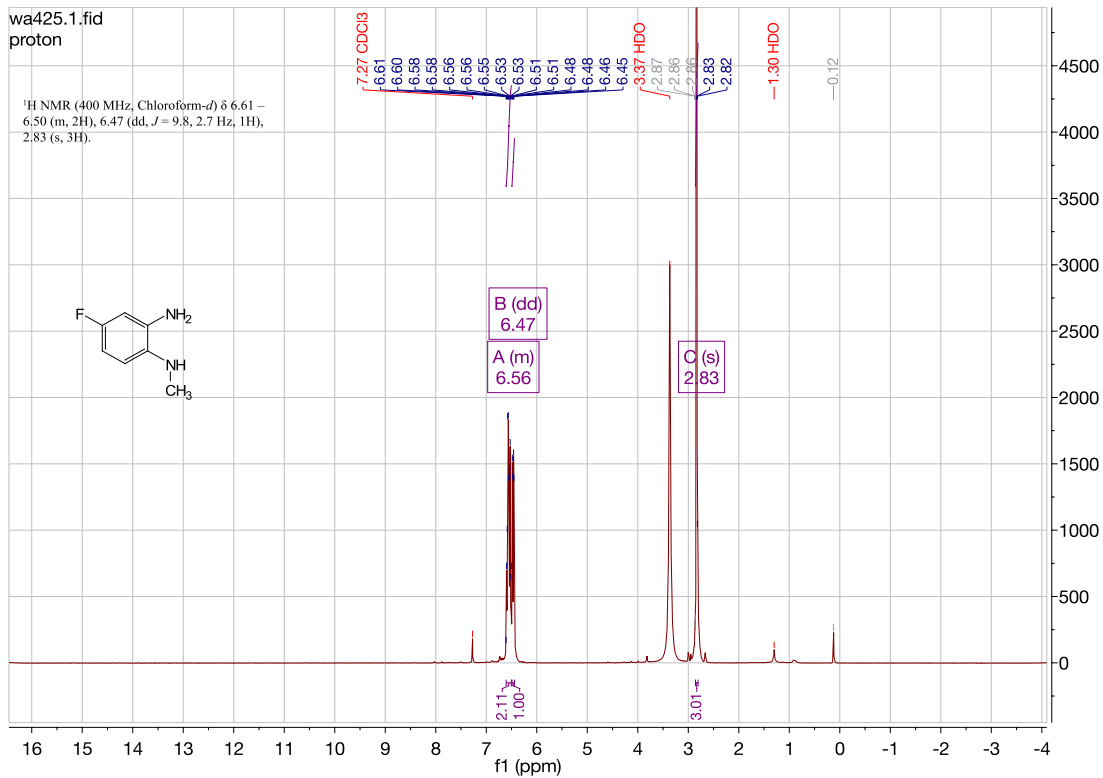


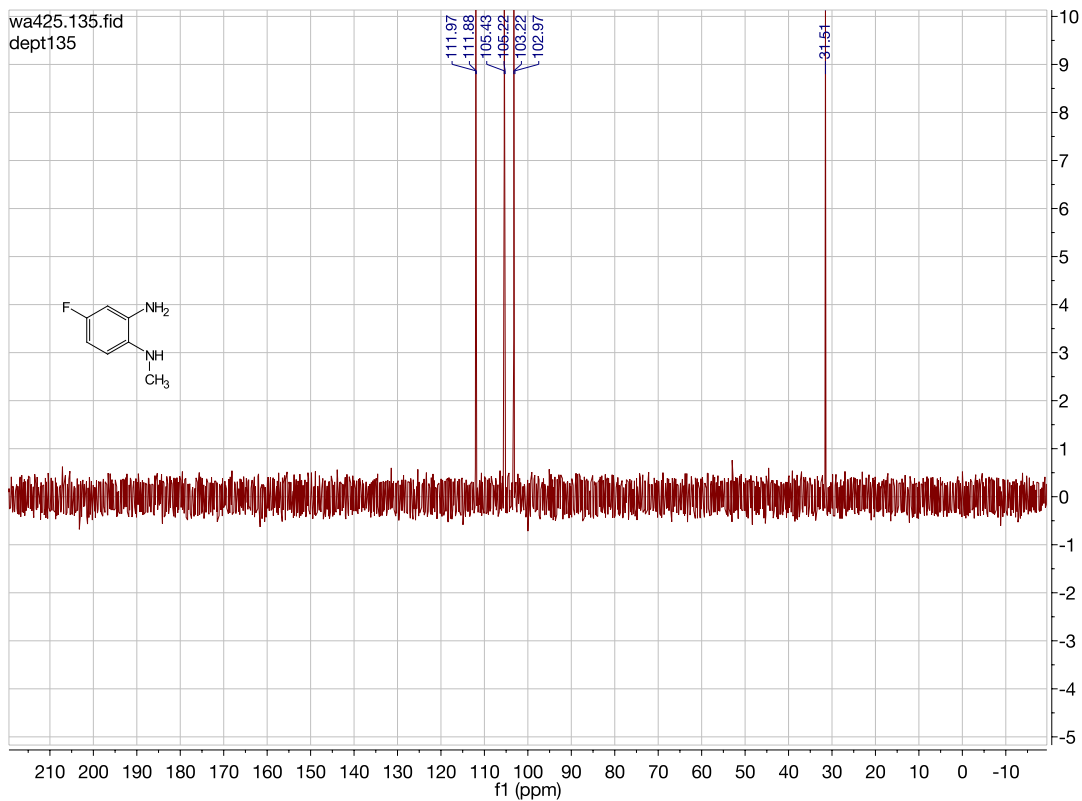




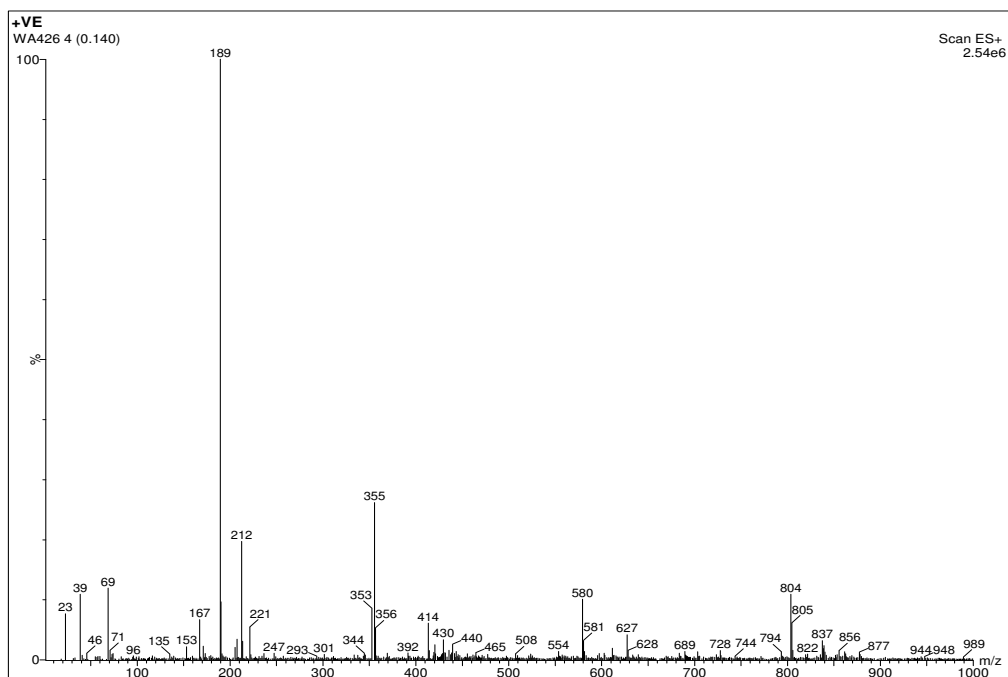
4-fluoro-*N*¹-methylbenzene-1,2-diamine. (WA425)

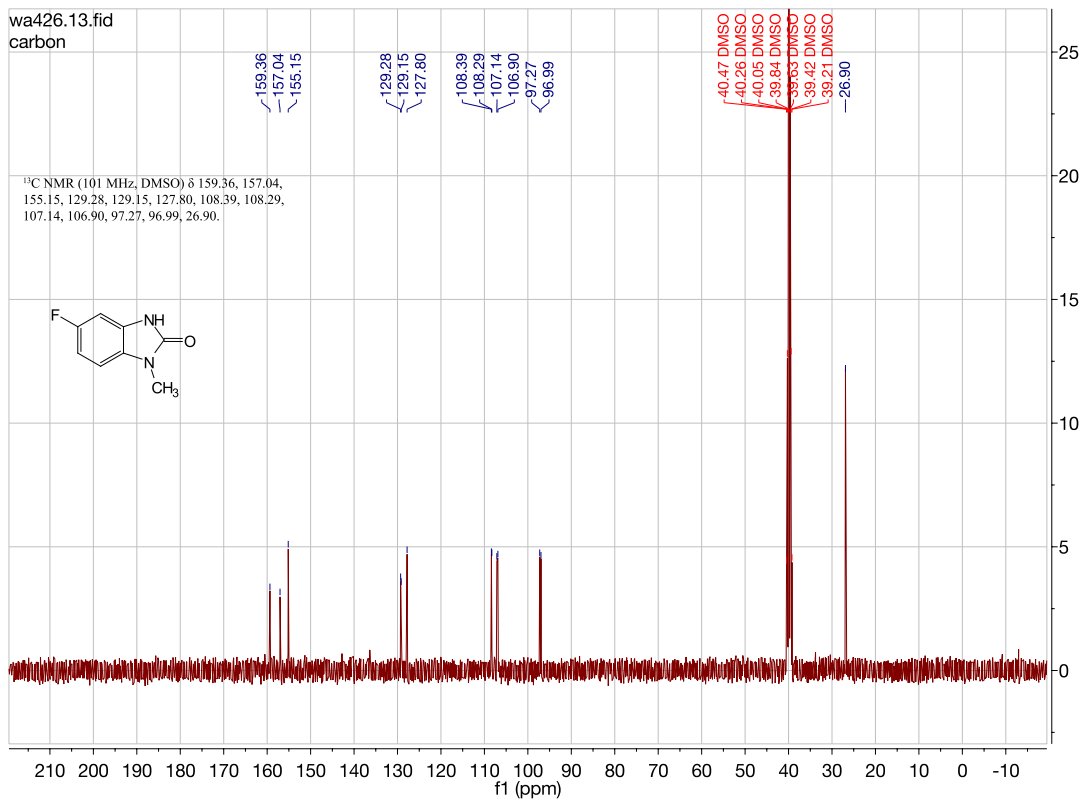
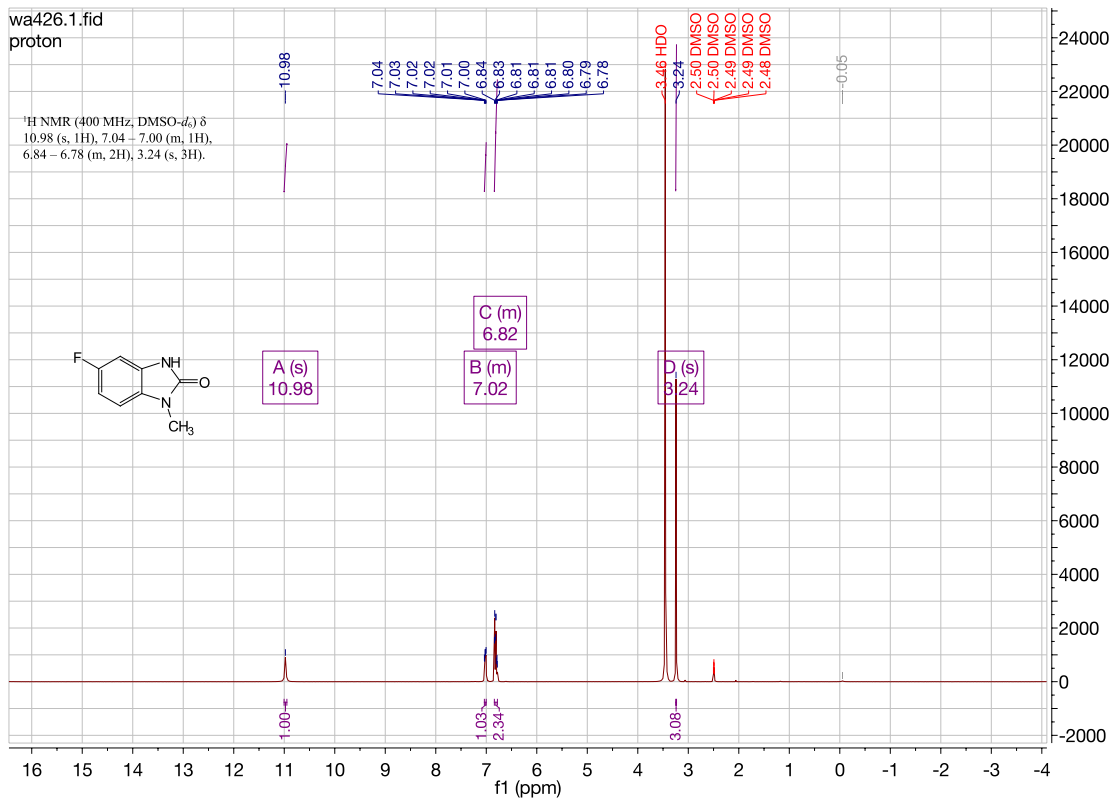


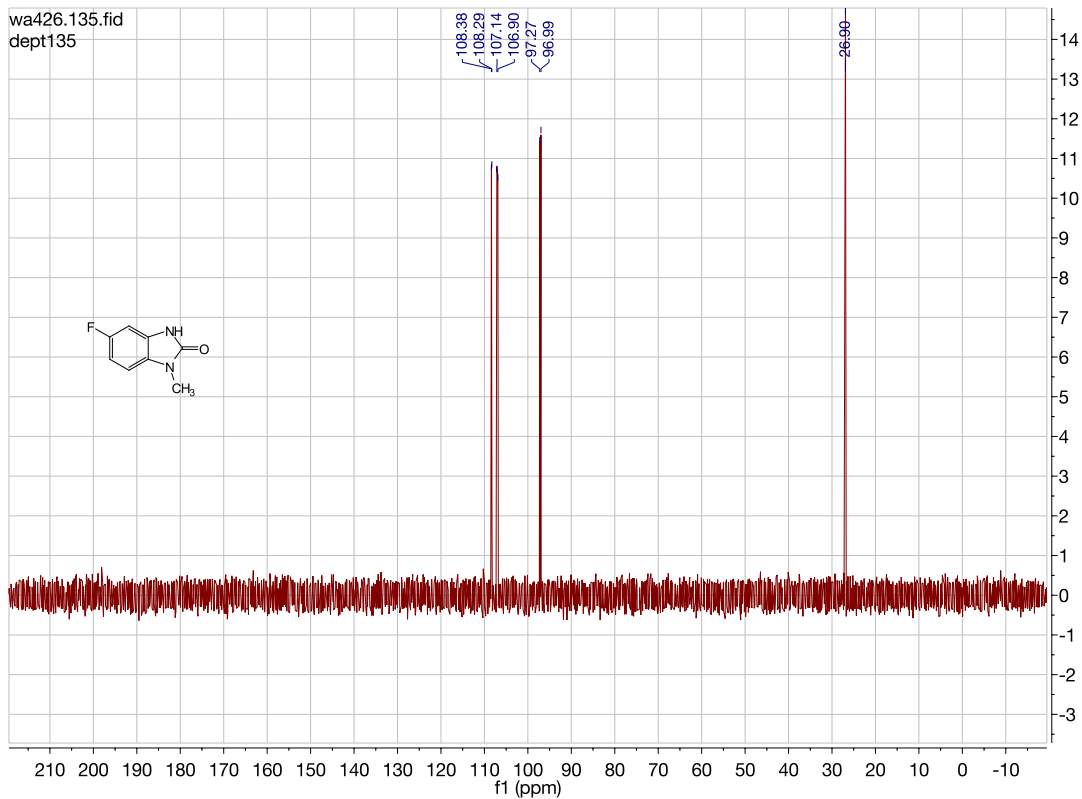




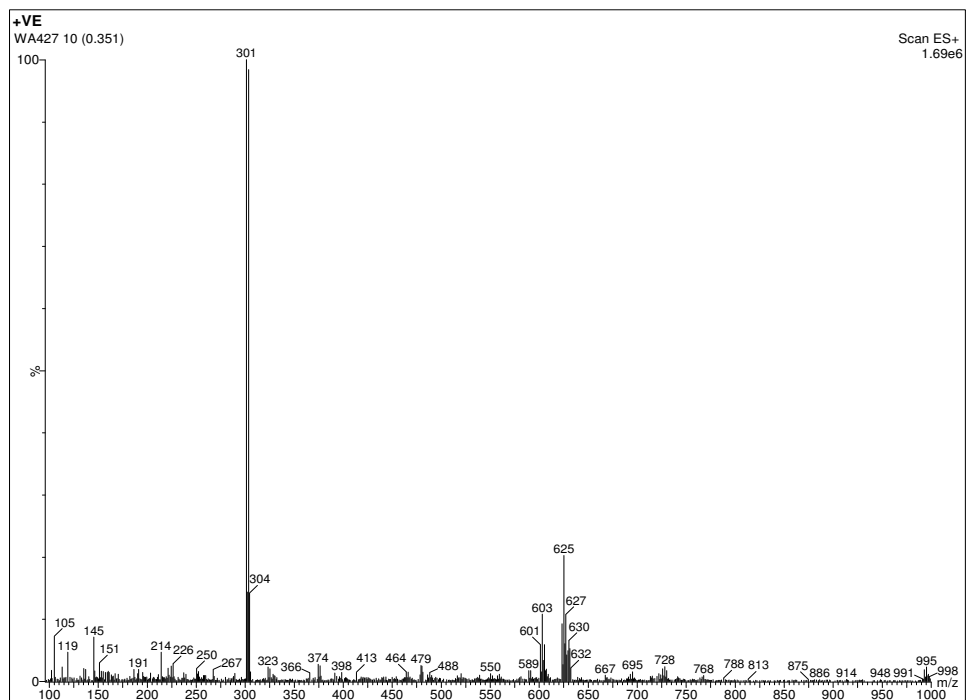
5-fluoro-1-methyl-1,3-dihydro-2H-benzo[d]imidazol-2-one. (WA426)

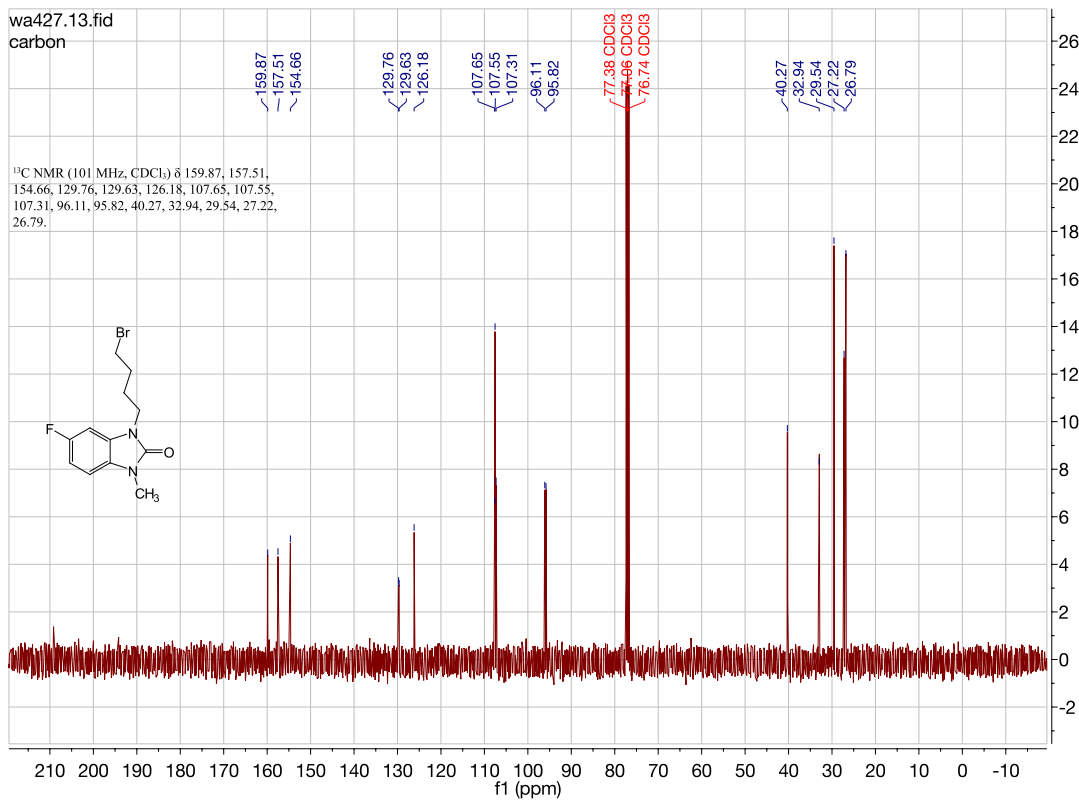
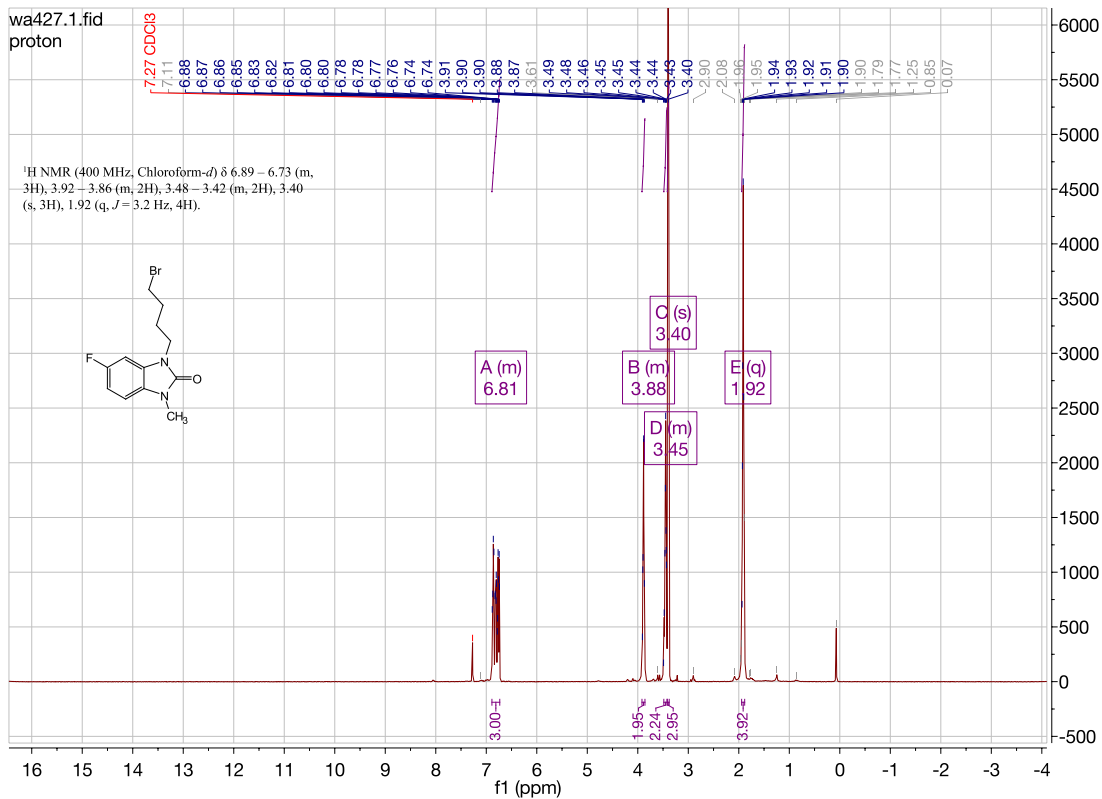


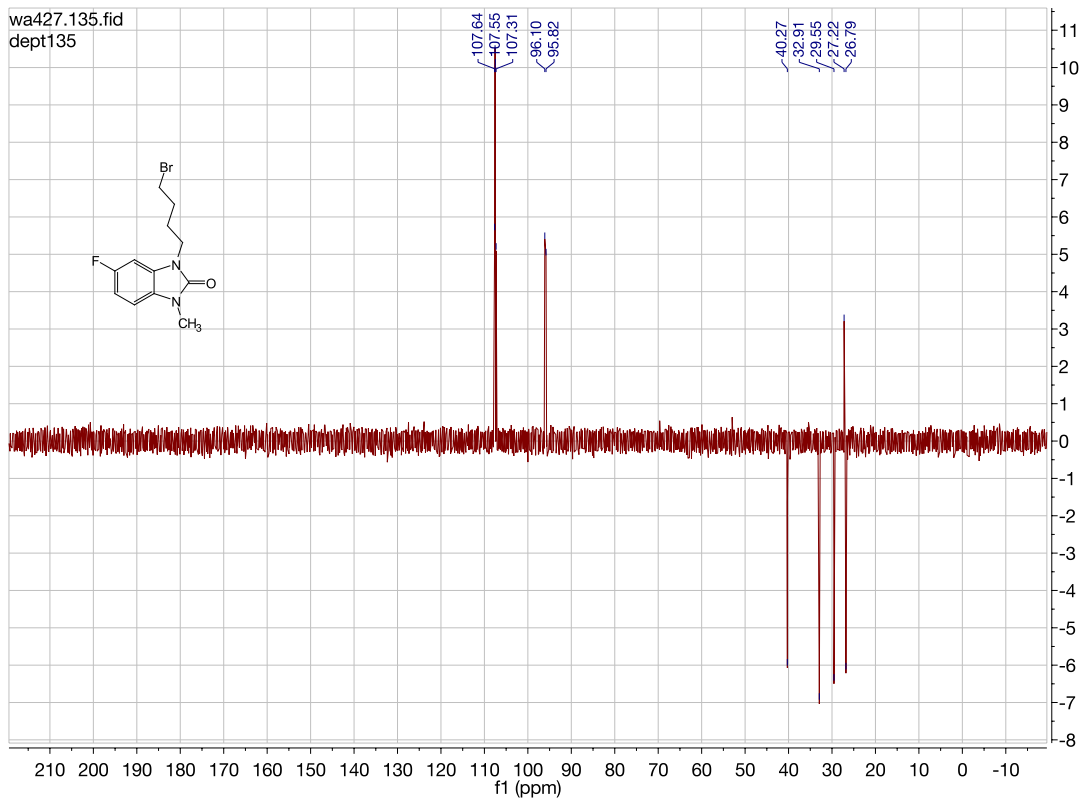




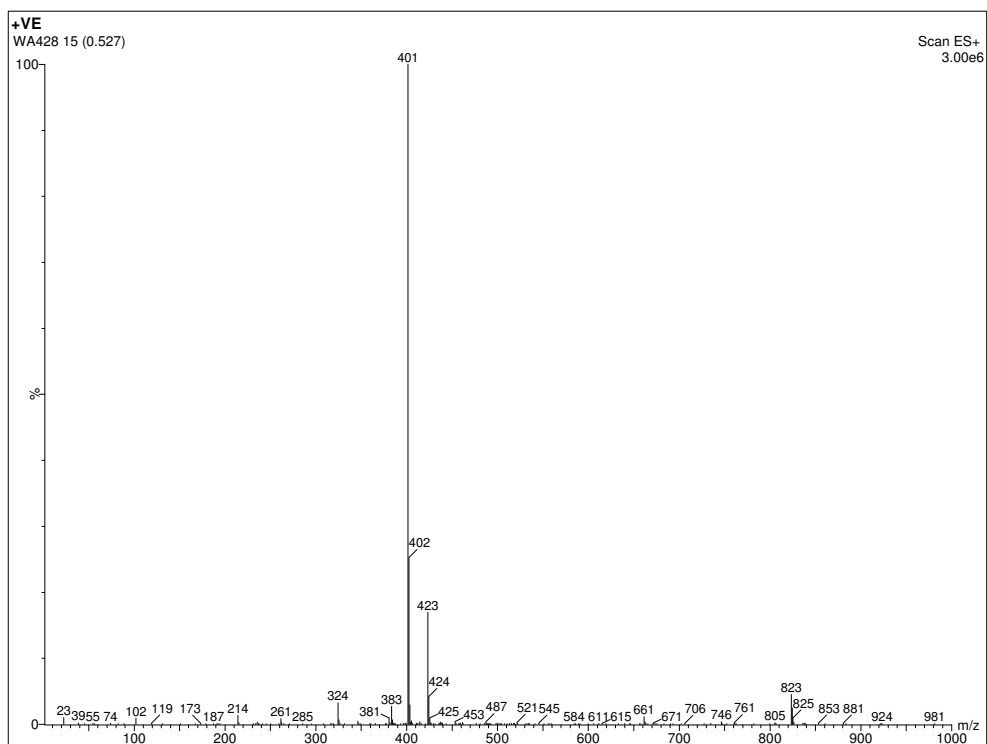
**3-(4-bromobutyl)-5-fluoro-1-methyl-1,3-dihydro-2H-benzo[d]imidazol-2-one.
(WA427)**

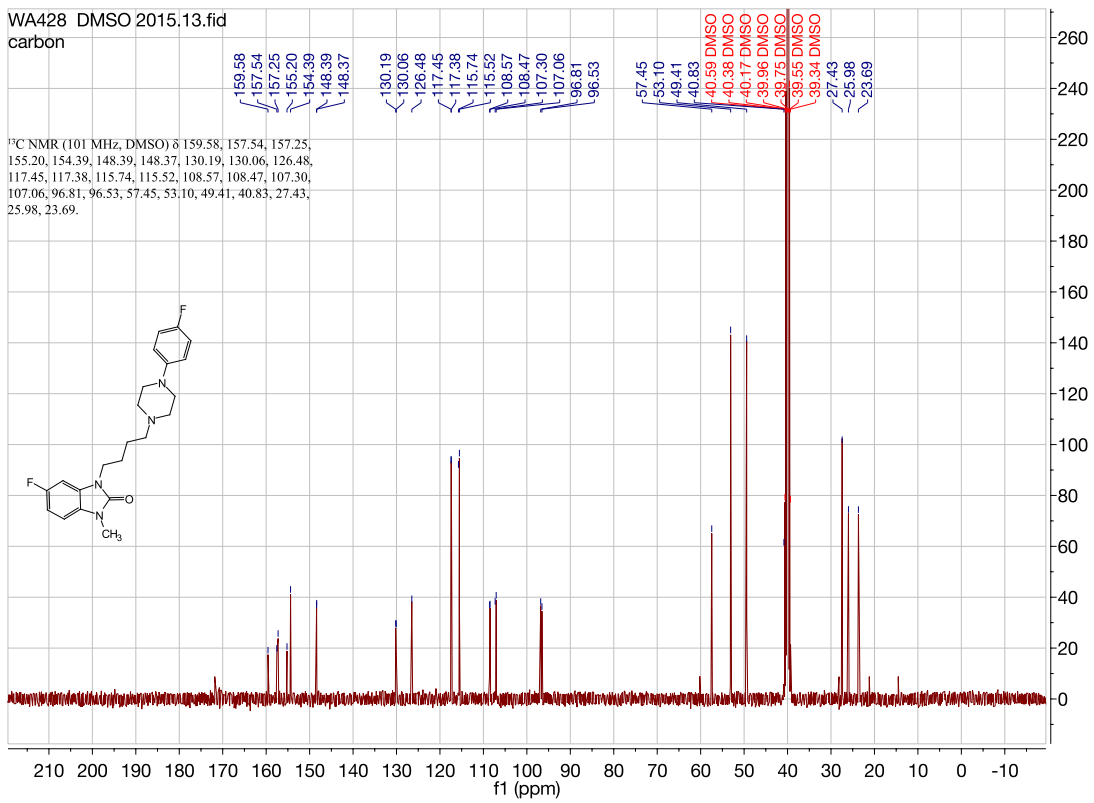
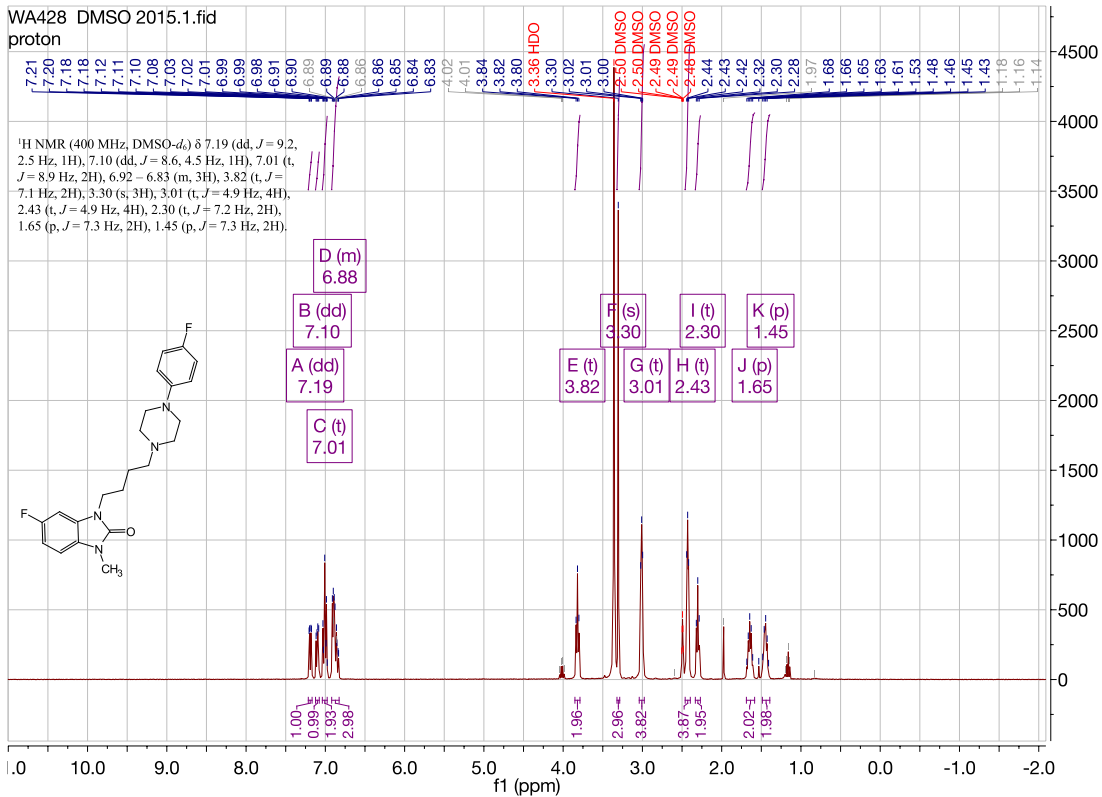


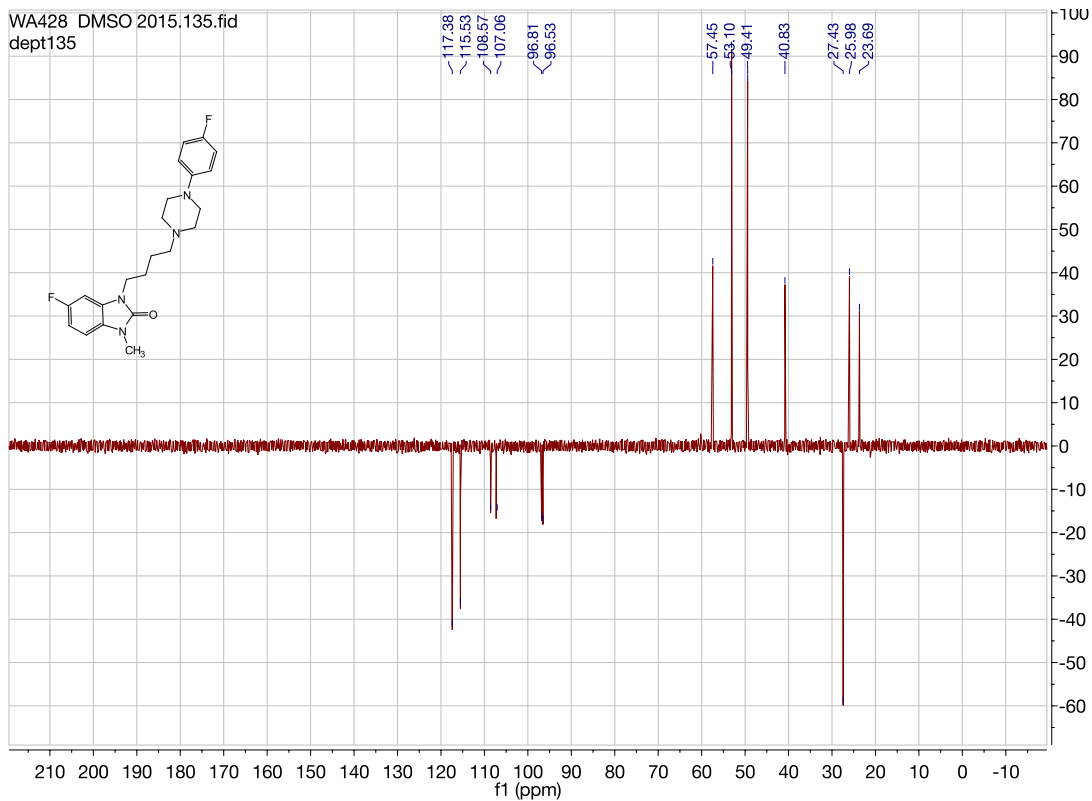




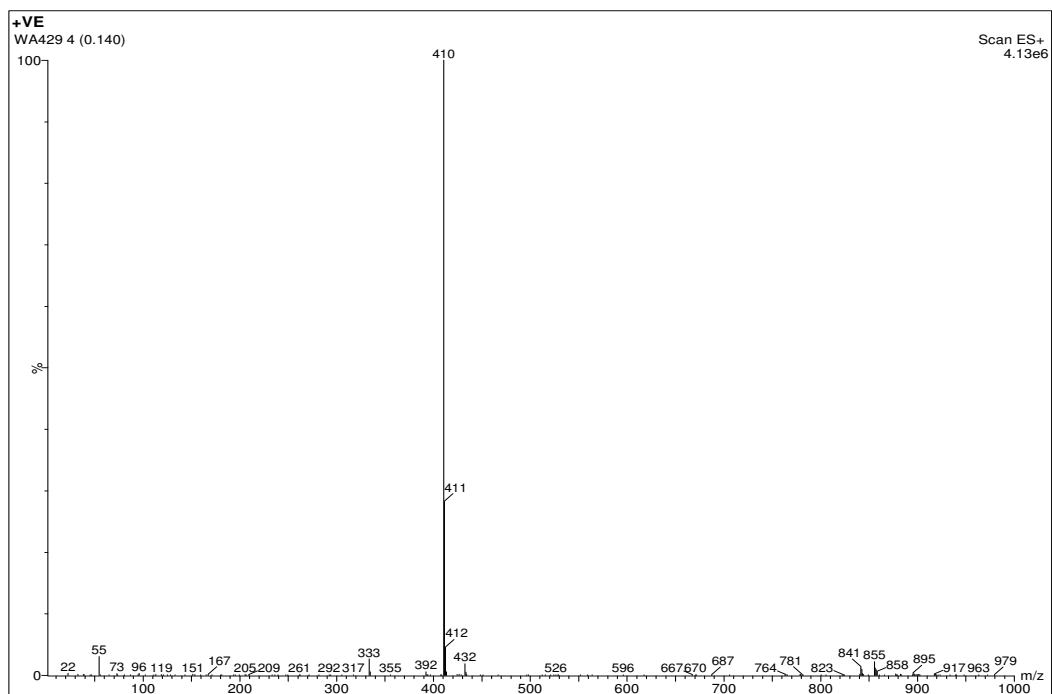
5-fluoro-3-(4-(4-(4-fluorophenyl)piperazin-1-yl)butyl)-1-methyl-1,3-dihydro-2H-benzo[d]imidazol-2-one. (WA428)

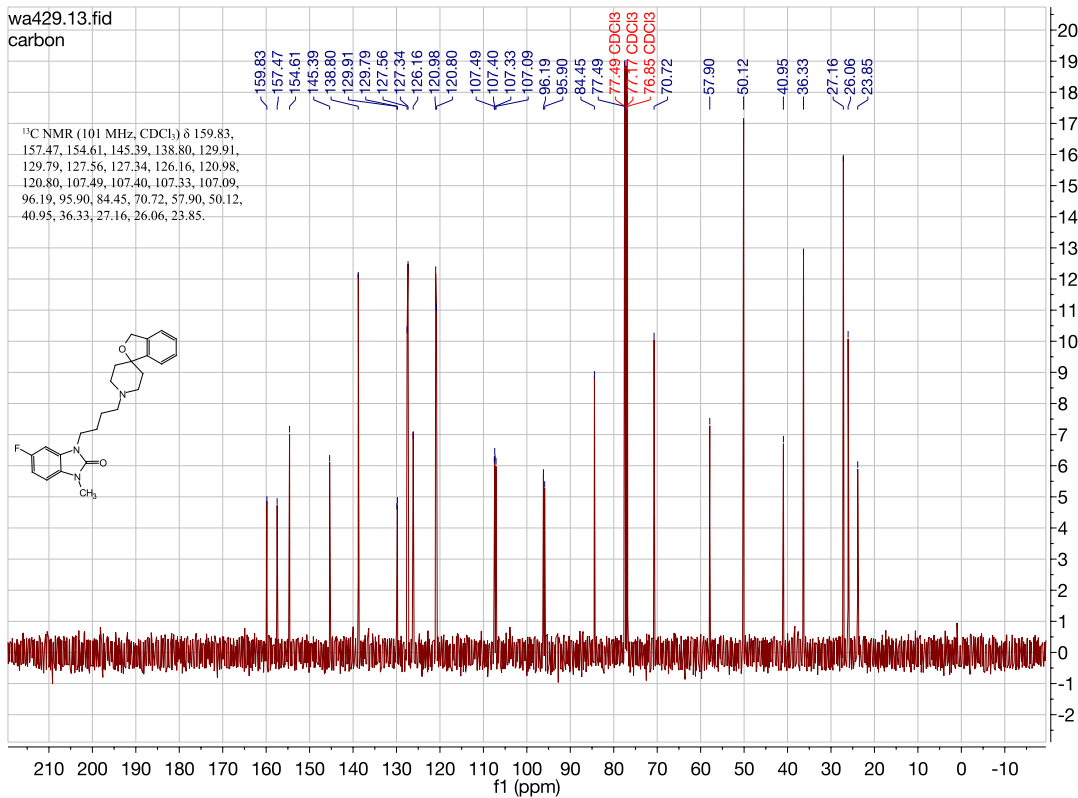
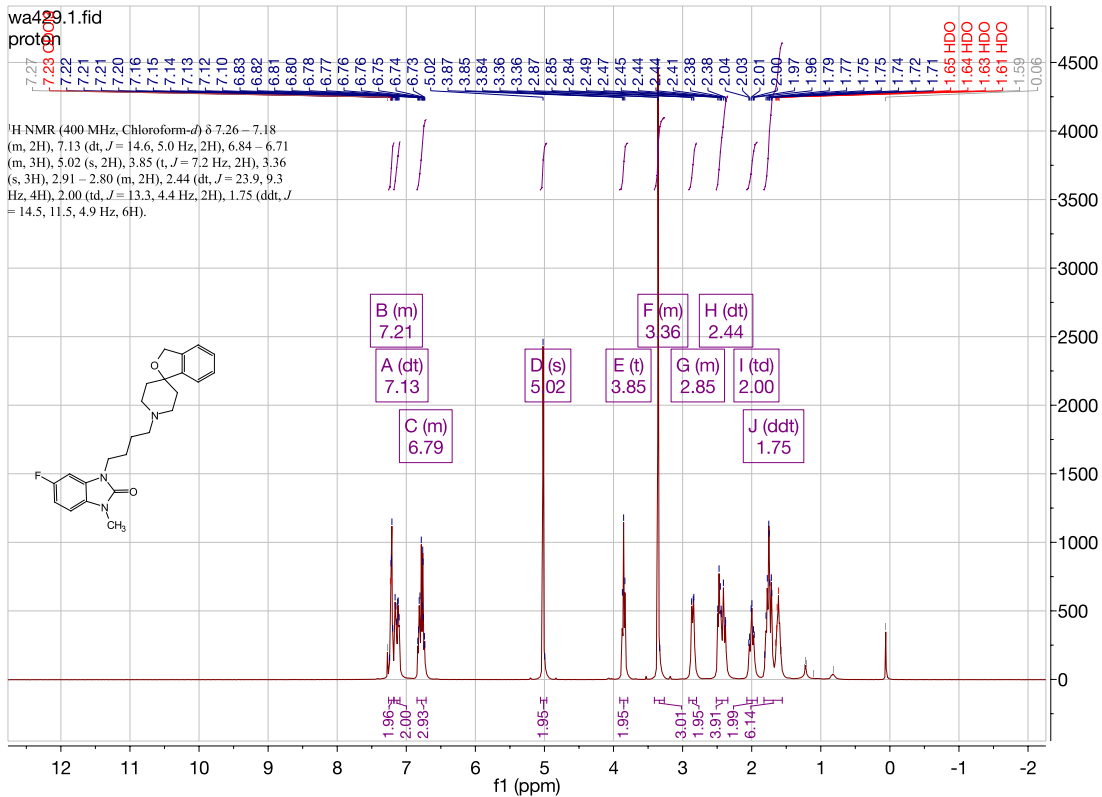


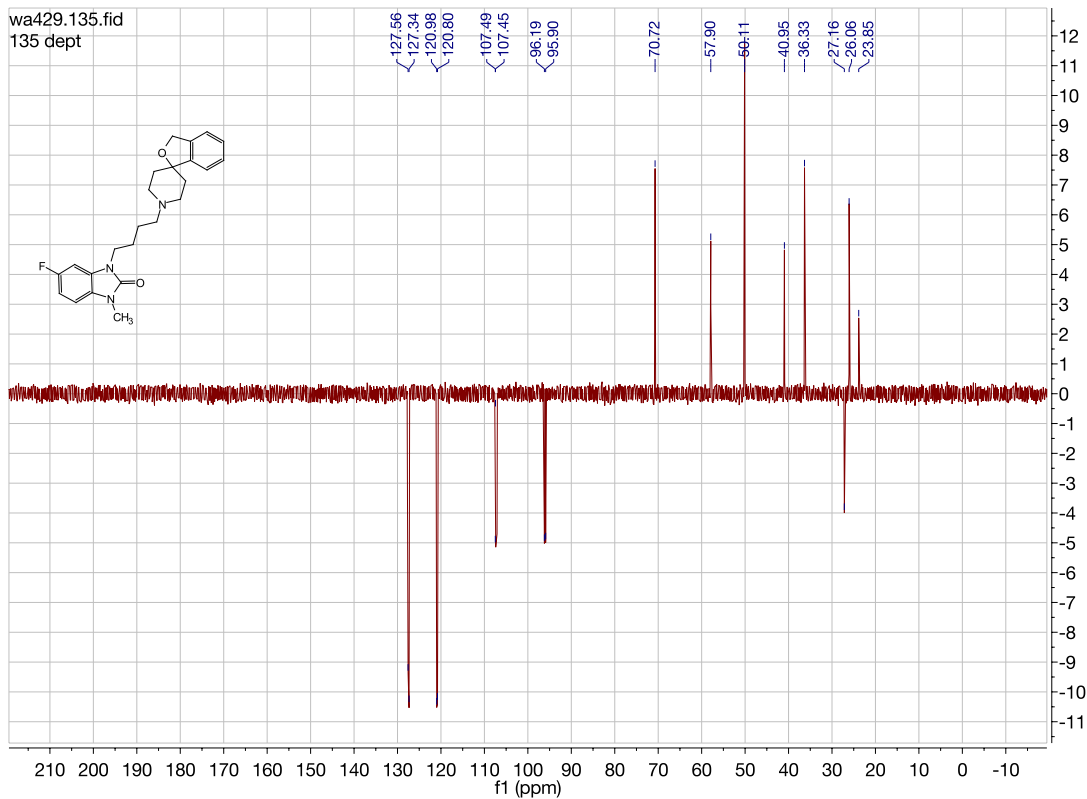




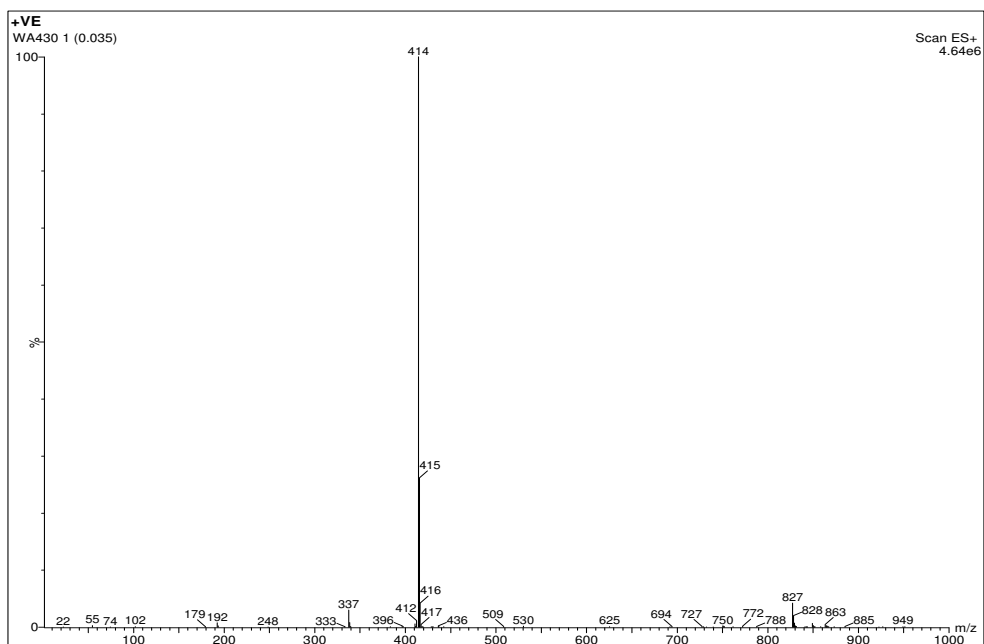
3-(4-(3H-spiro[isobenzofuran-1,4'-piperidin]-1'-yl)butyl)-5-fluoro-1-methyl-1,3-dihydro-2H-benzo[d]imidazol-2-one. (WA429)

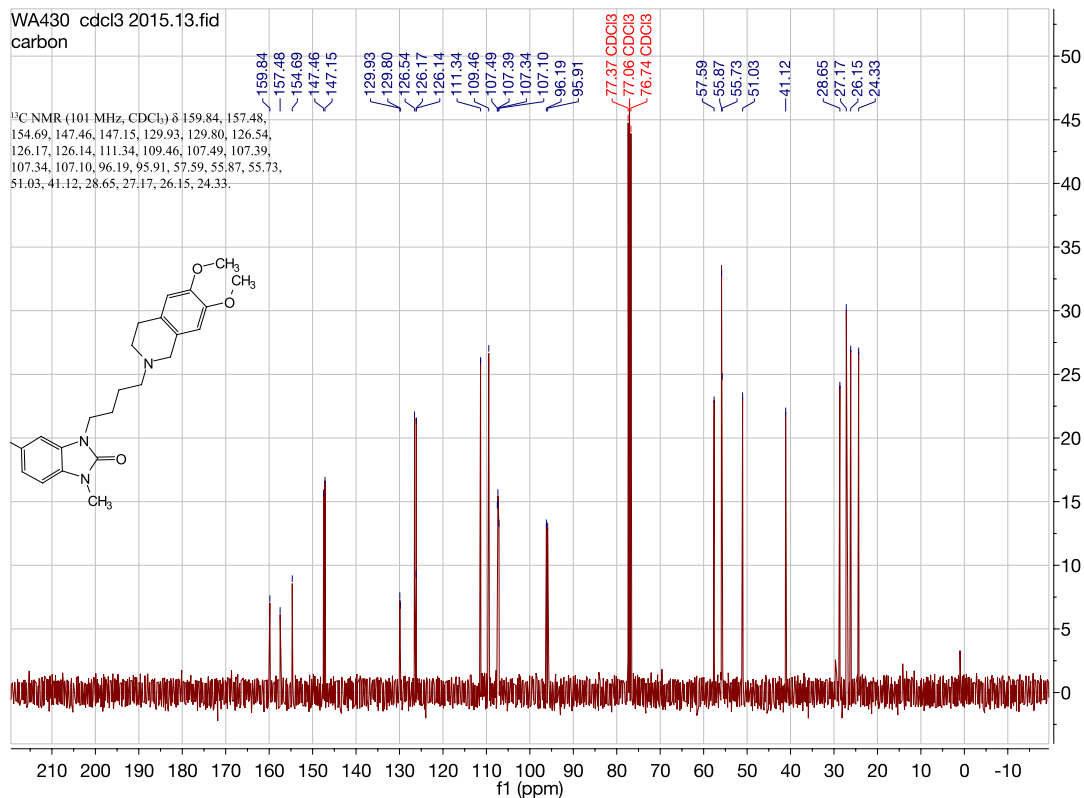
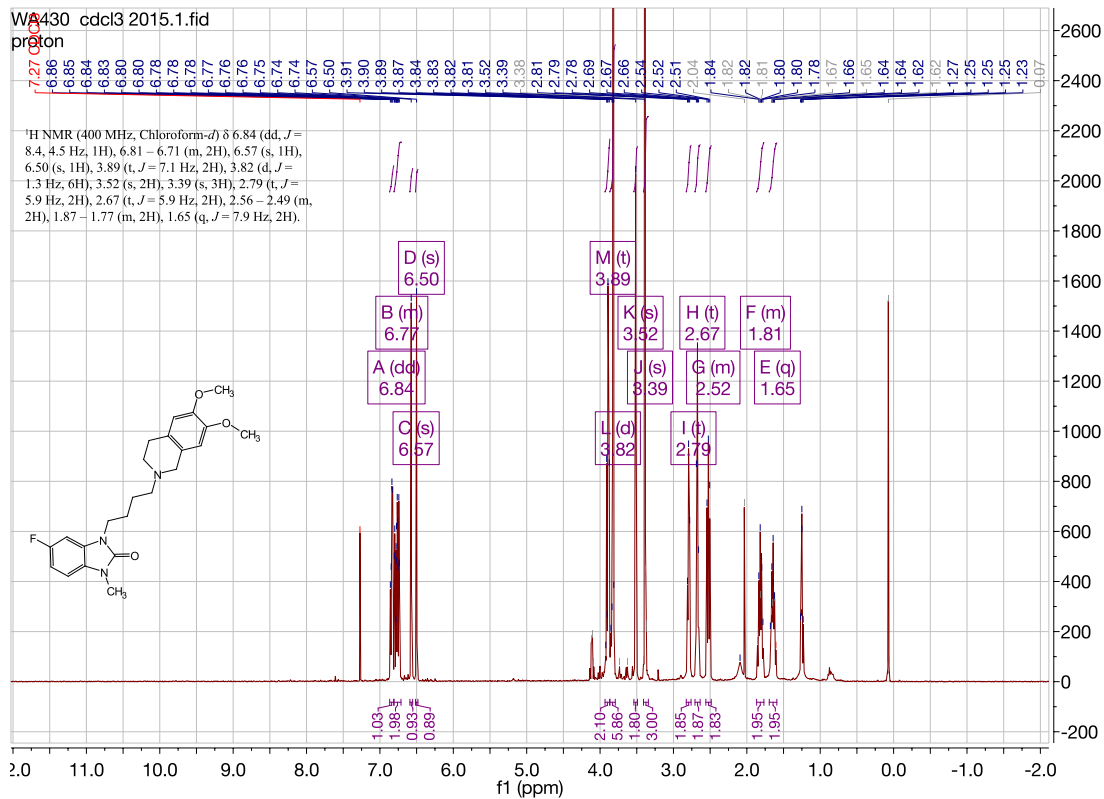


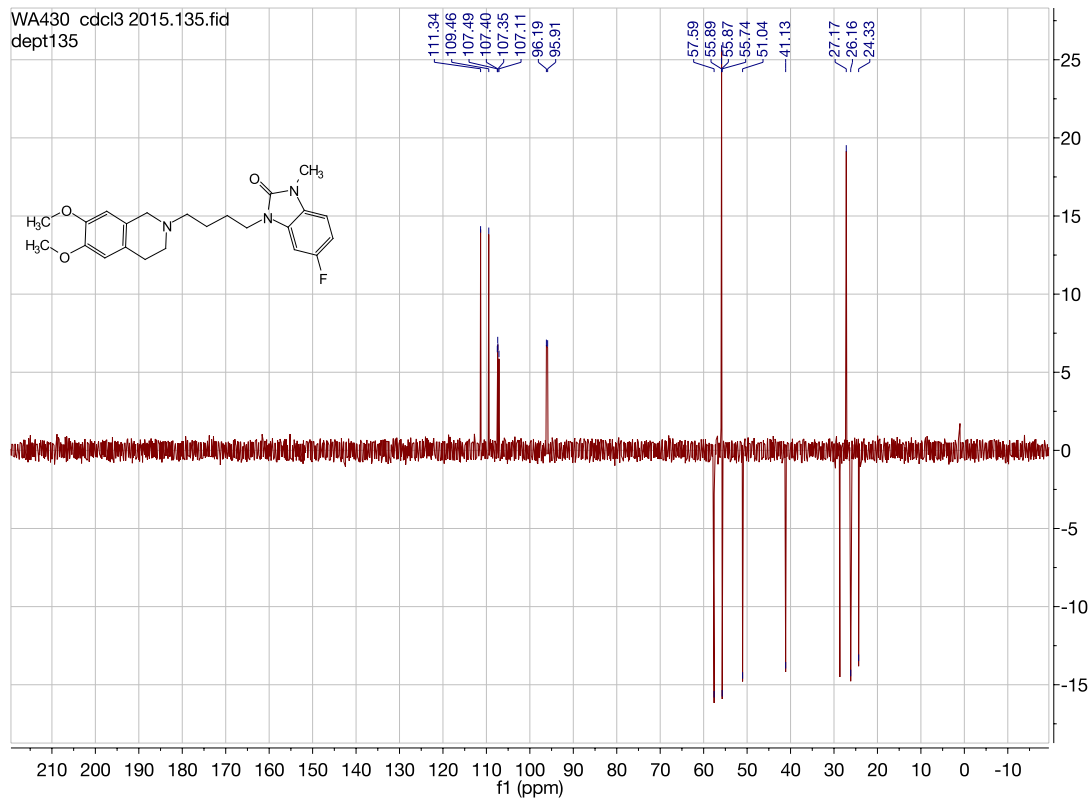




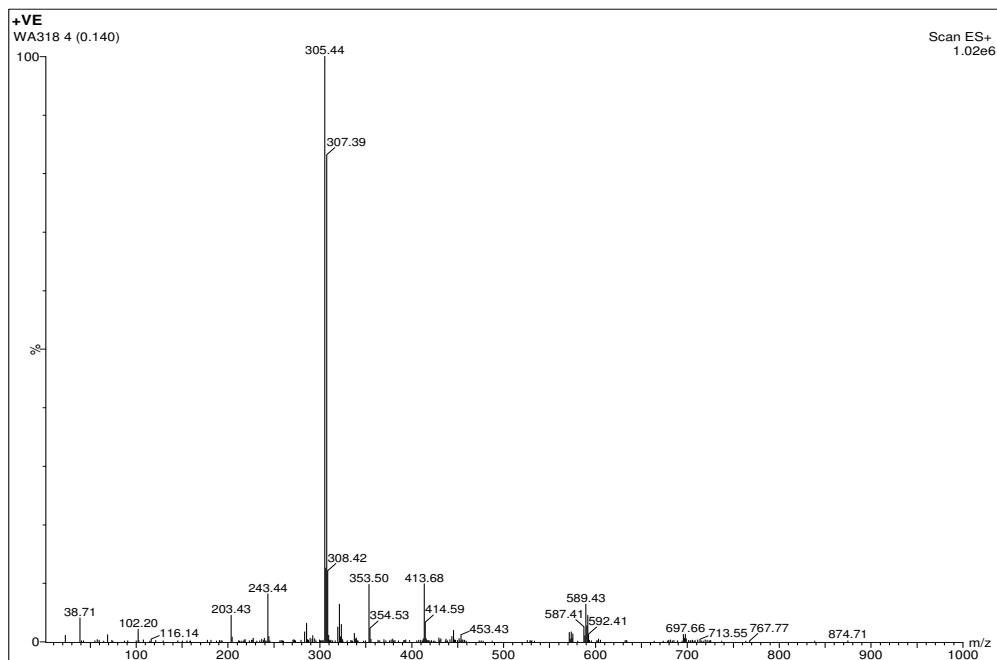
3-(4-(6,7-dimethoxy-3,4-dihydroisoquinolin-2(1H)-yl)butyl)-5-fluoro-1-methyl-1,3-dihydro-2H-benzo[d]imidazol-2-one. (WA430)

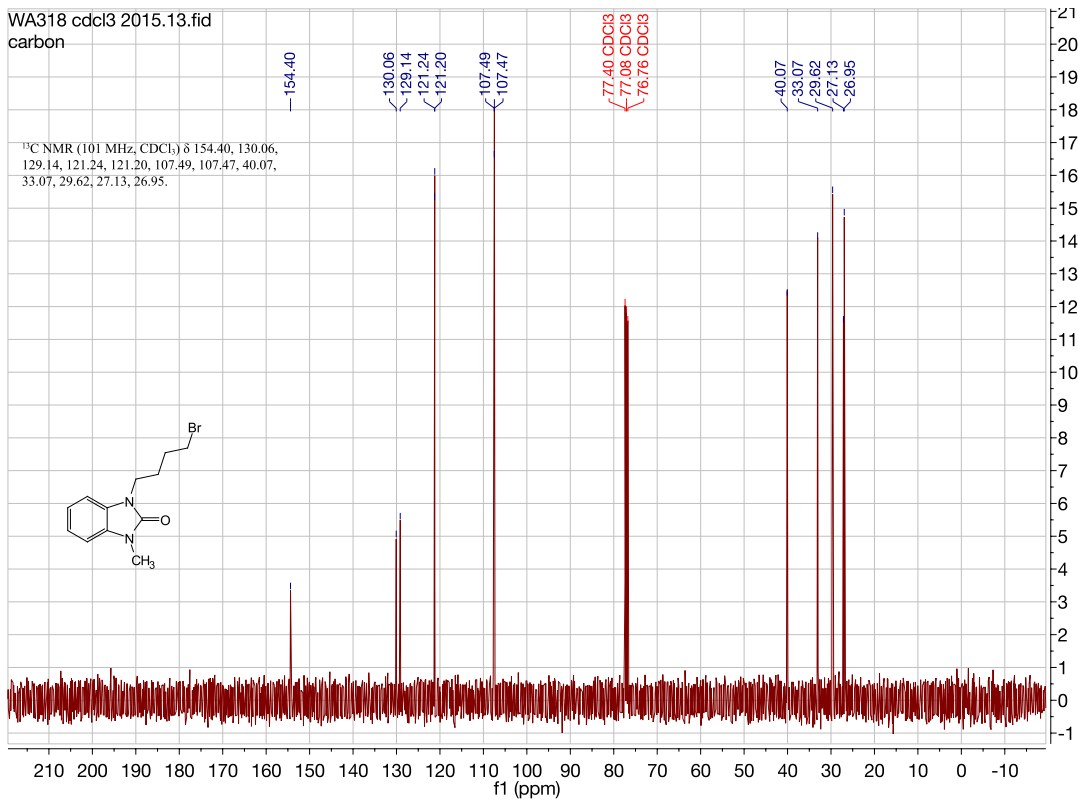
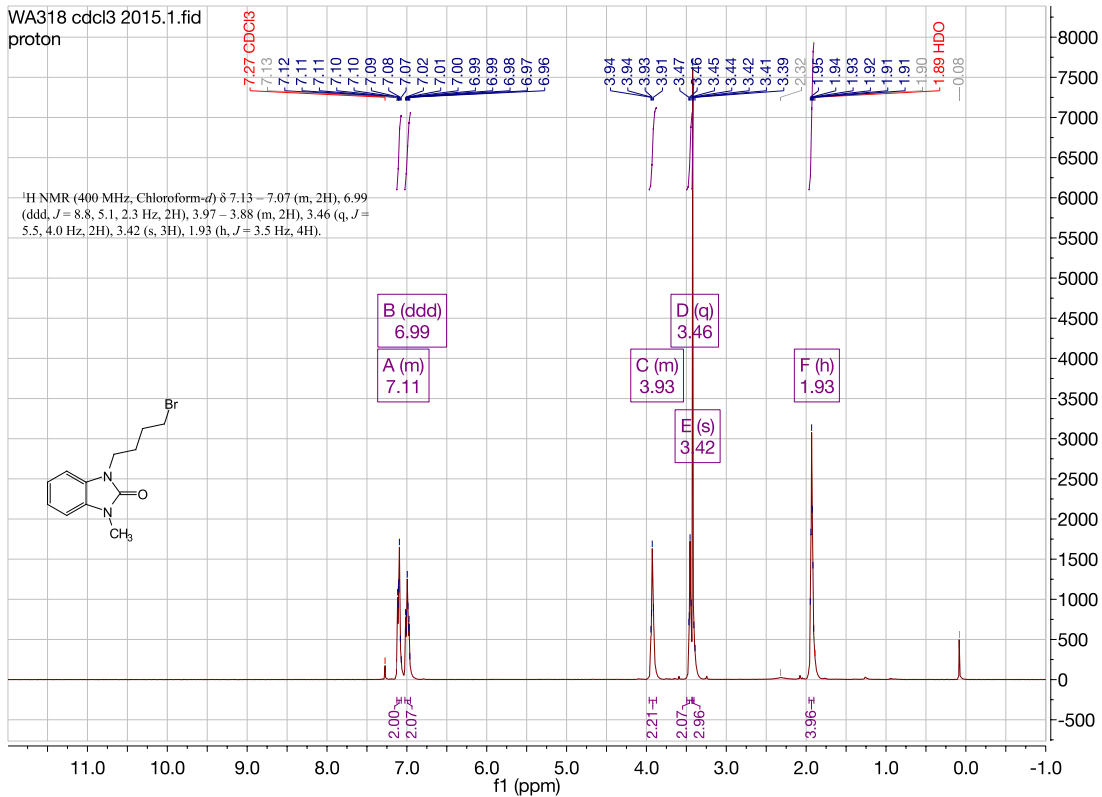


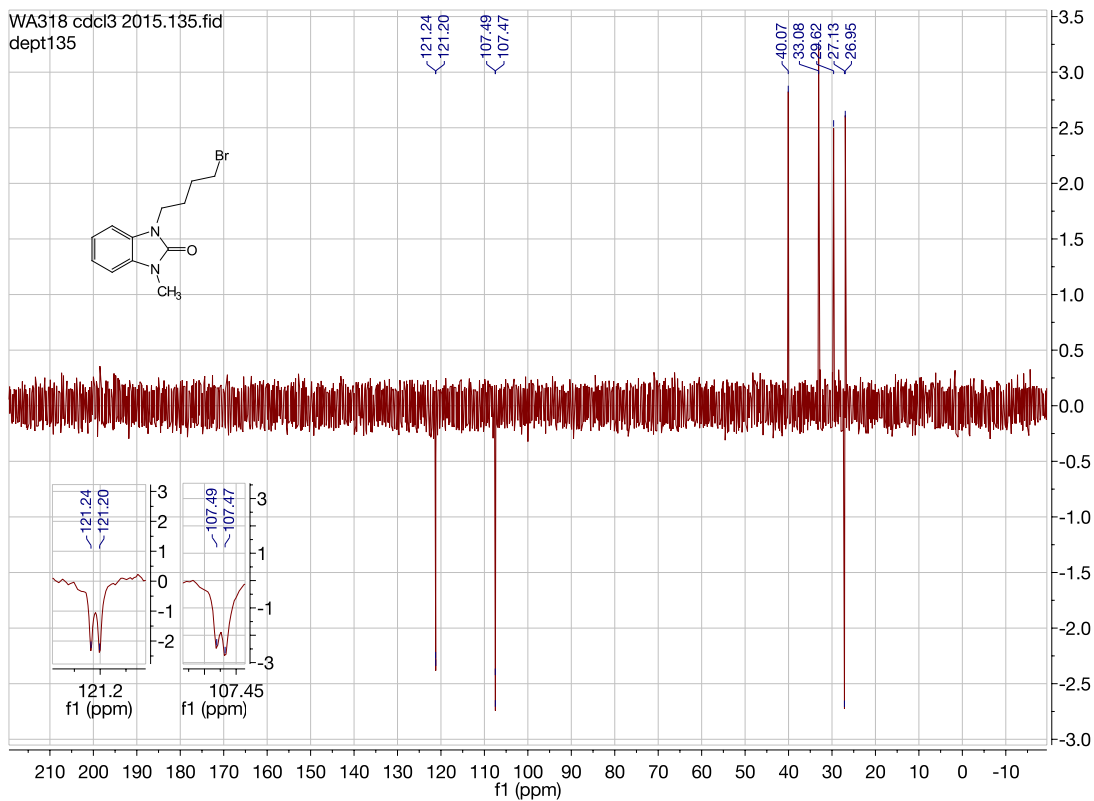




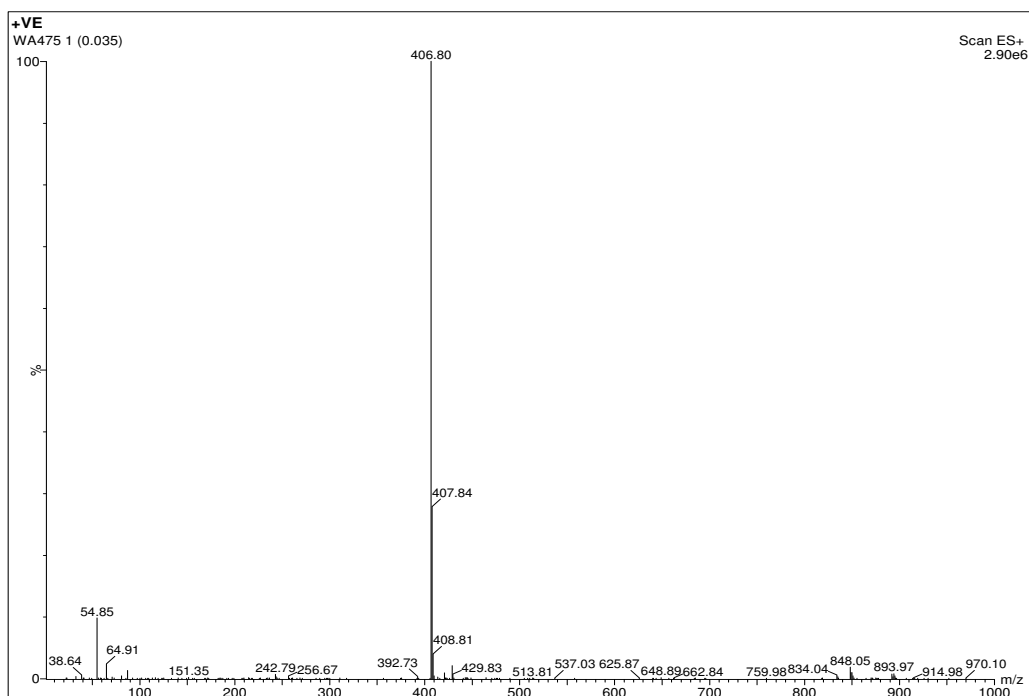
1-(4-bromobutyl)-3-methyl-1,3-dihydro-2H-benzo[d]imidazol-2-one. (WA318)

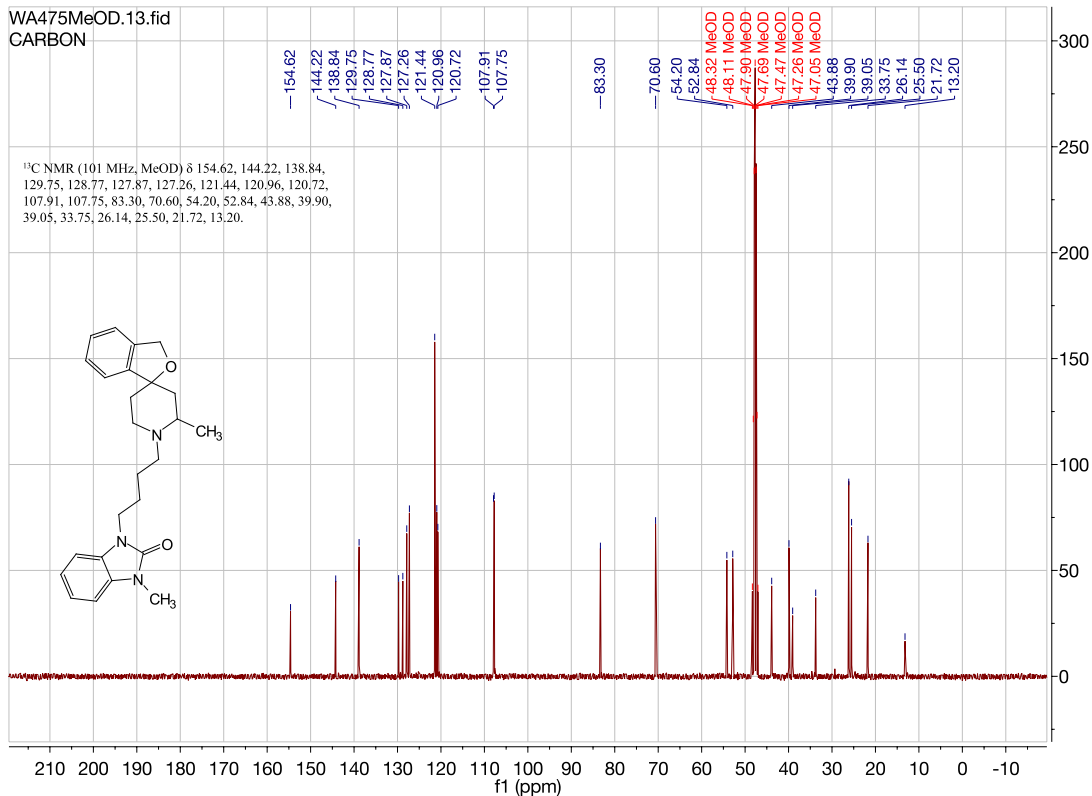
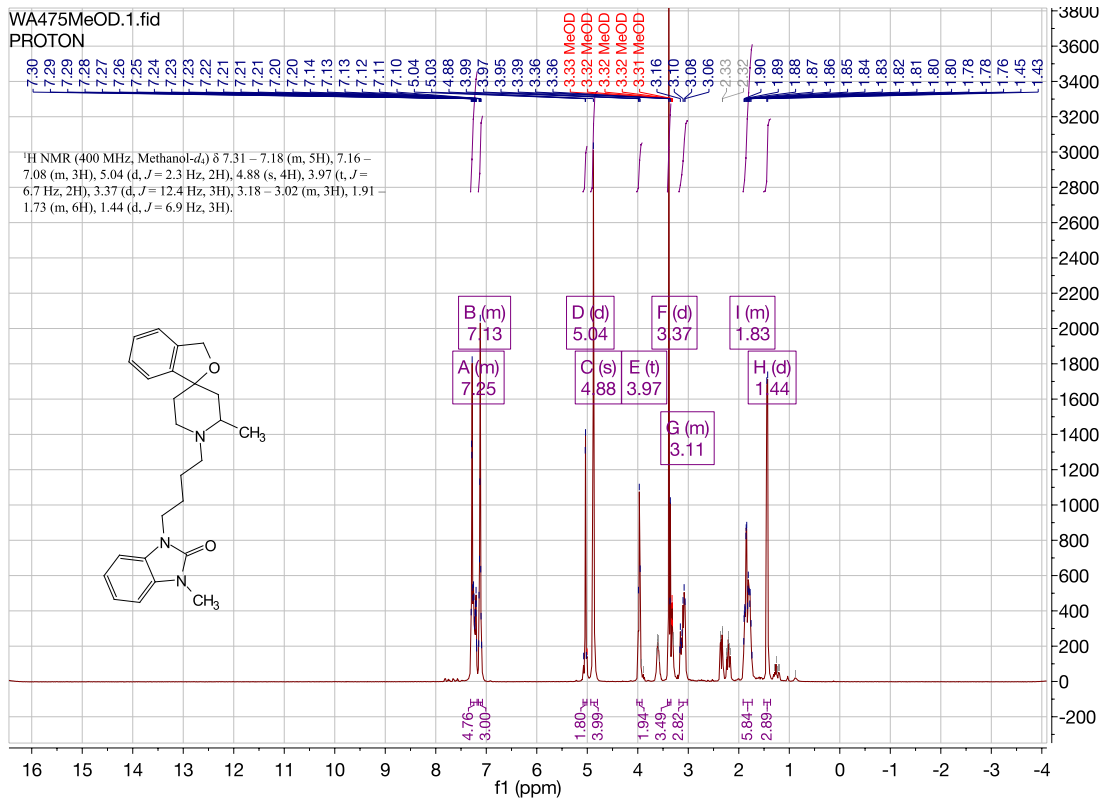


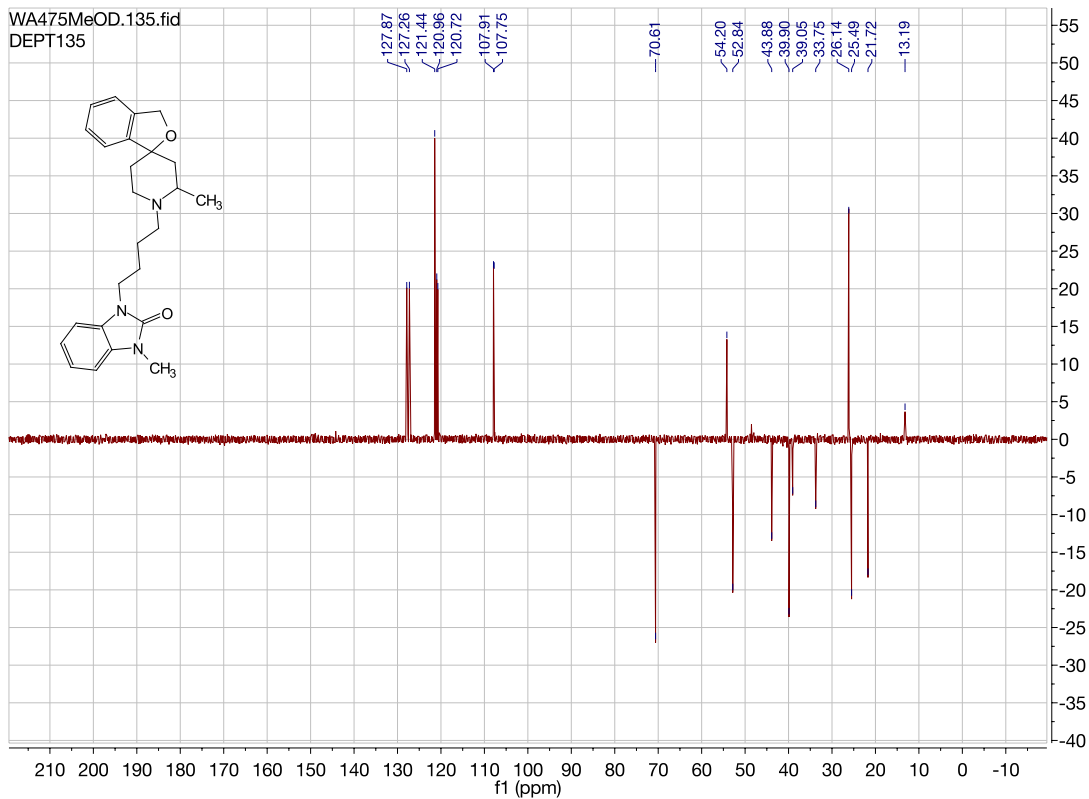




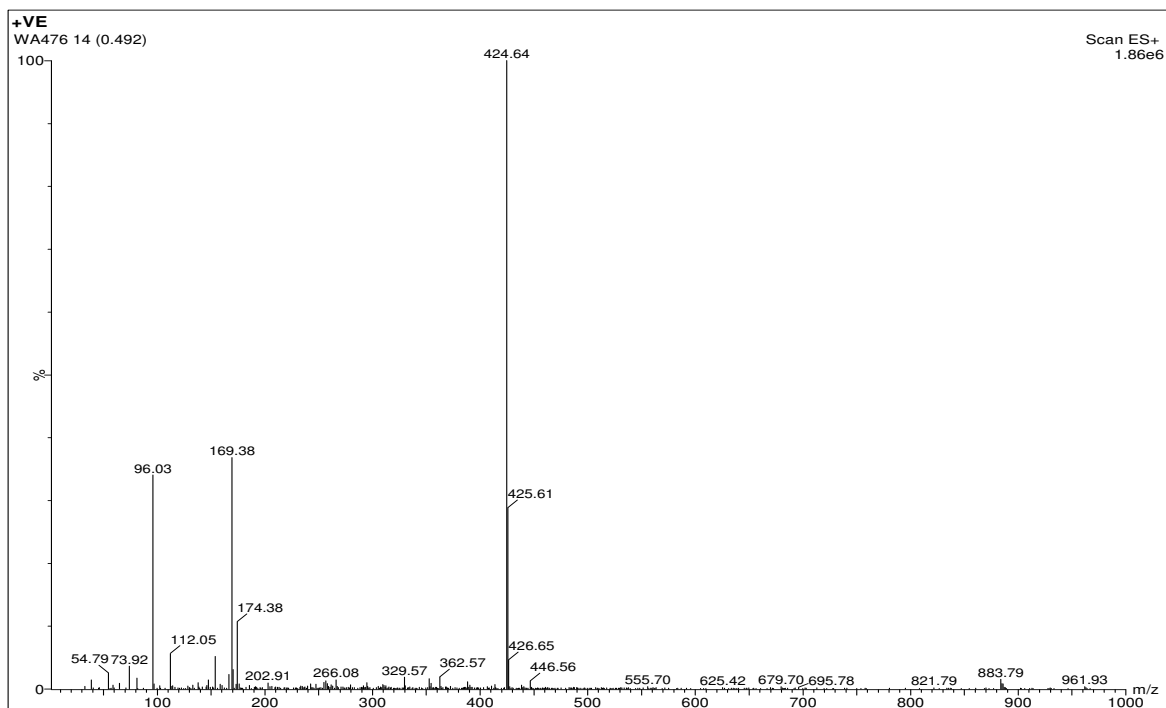
1-methyl-3-(4-(2'-methyl-3H-spiro[isobenzofuran-1,4'-piperidin]-1'-yl)butyl)-1,3-dihydro-2H-benzo[d]imidazol-2-one. (WA475)

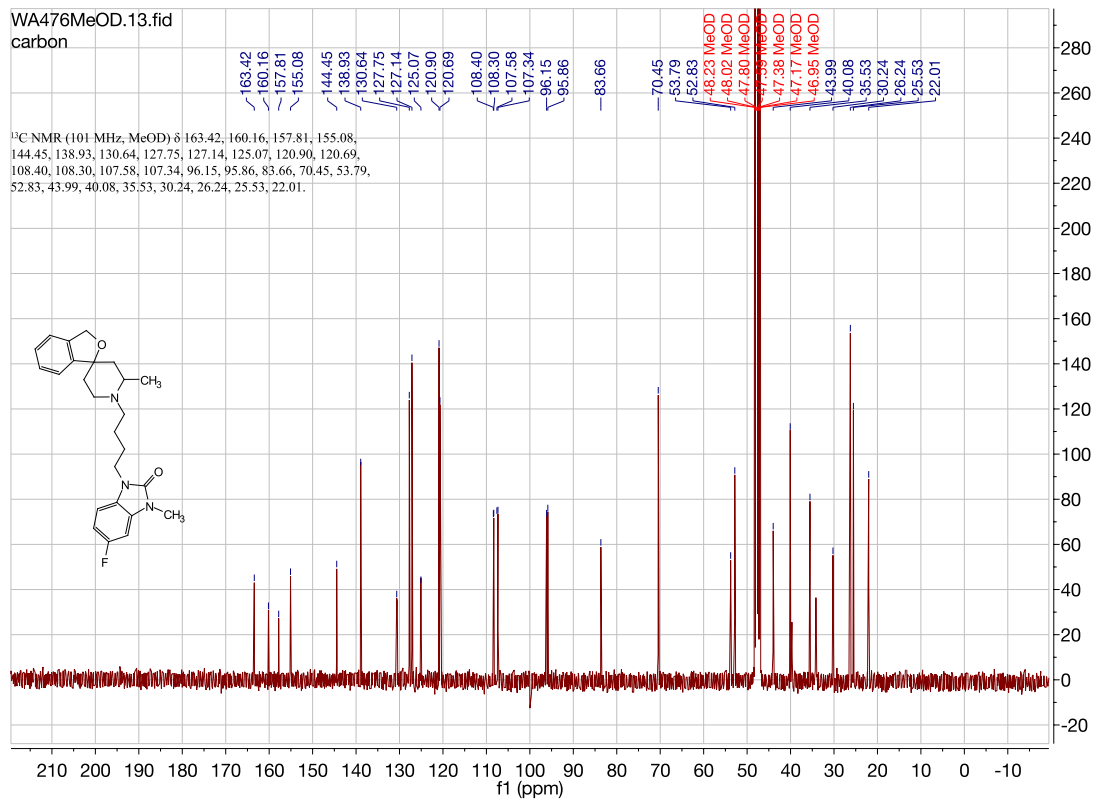
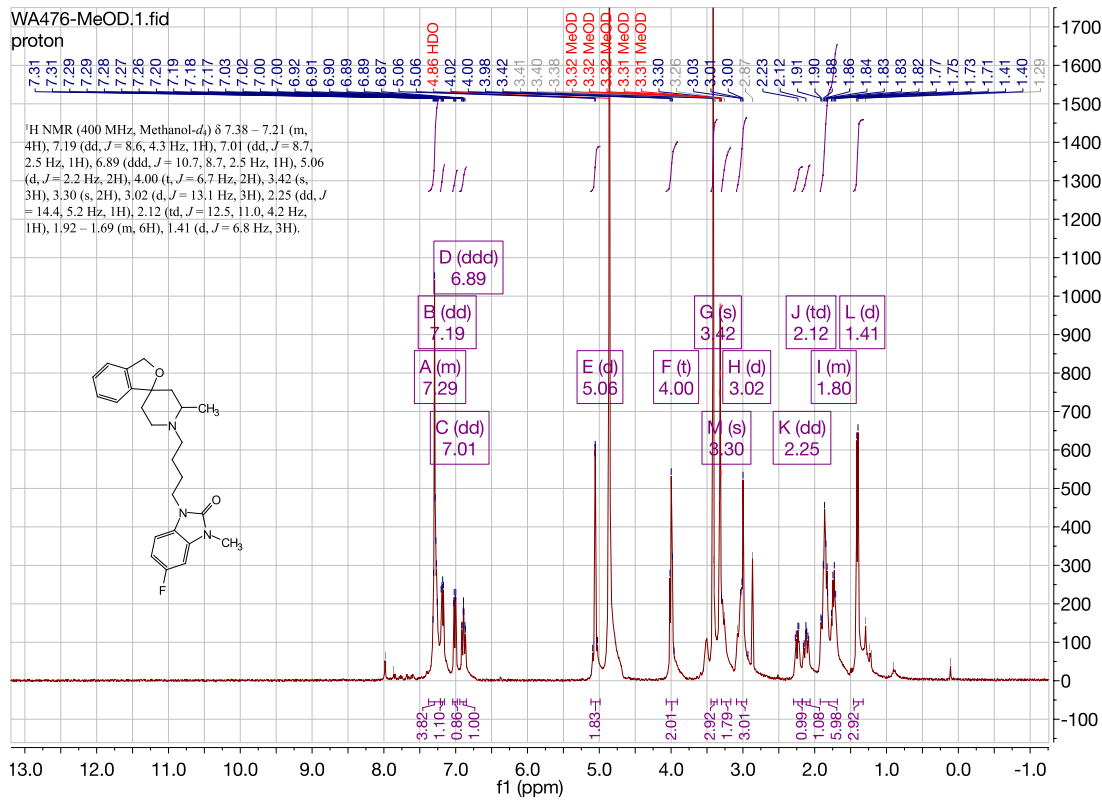




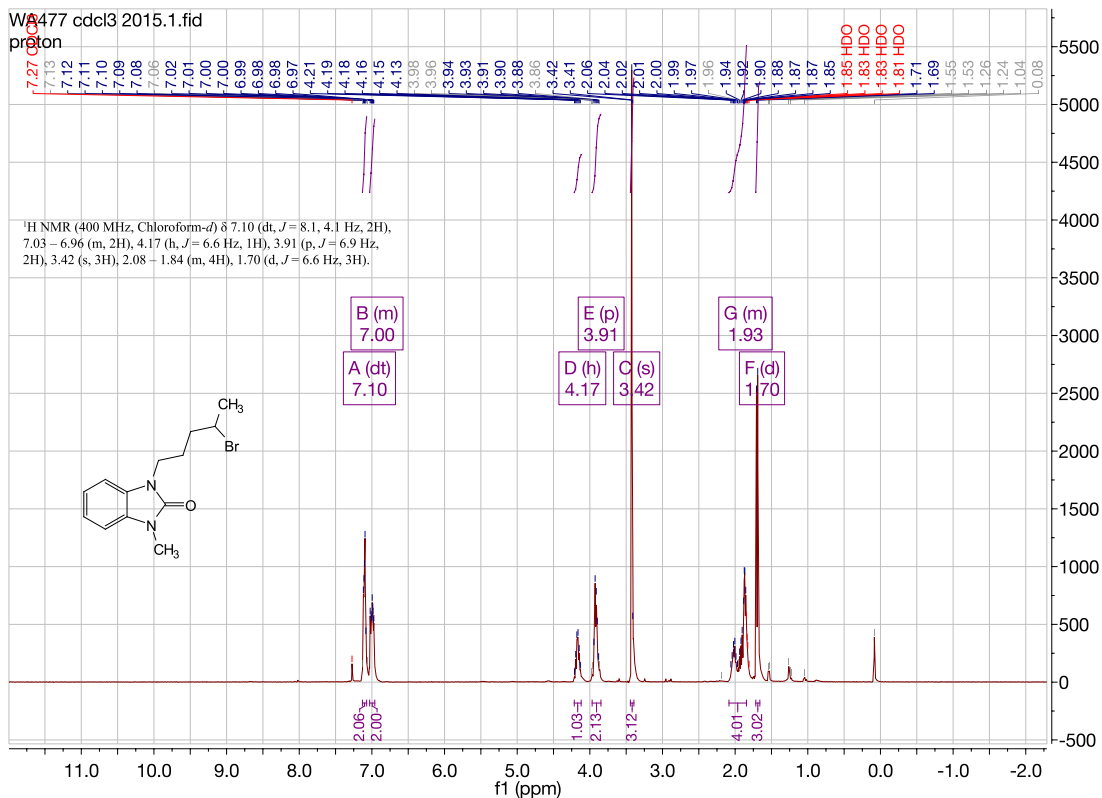
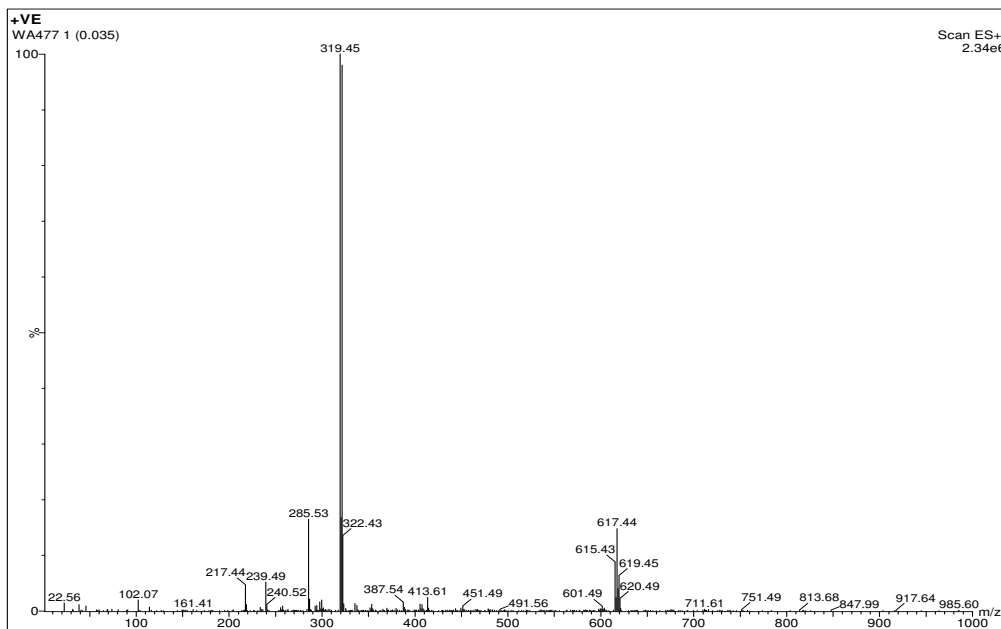


5-fluoro-3-methyl-1-(4-(2'-methyl-3H-spiro[isobenzofuran-1,4'-piperidin]-1'-yl)butyl)-1,3-dihydro-2H-benzo[d]imidazol-2-one. (WA476)

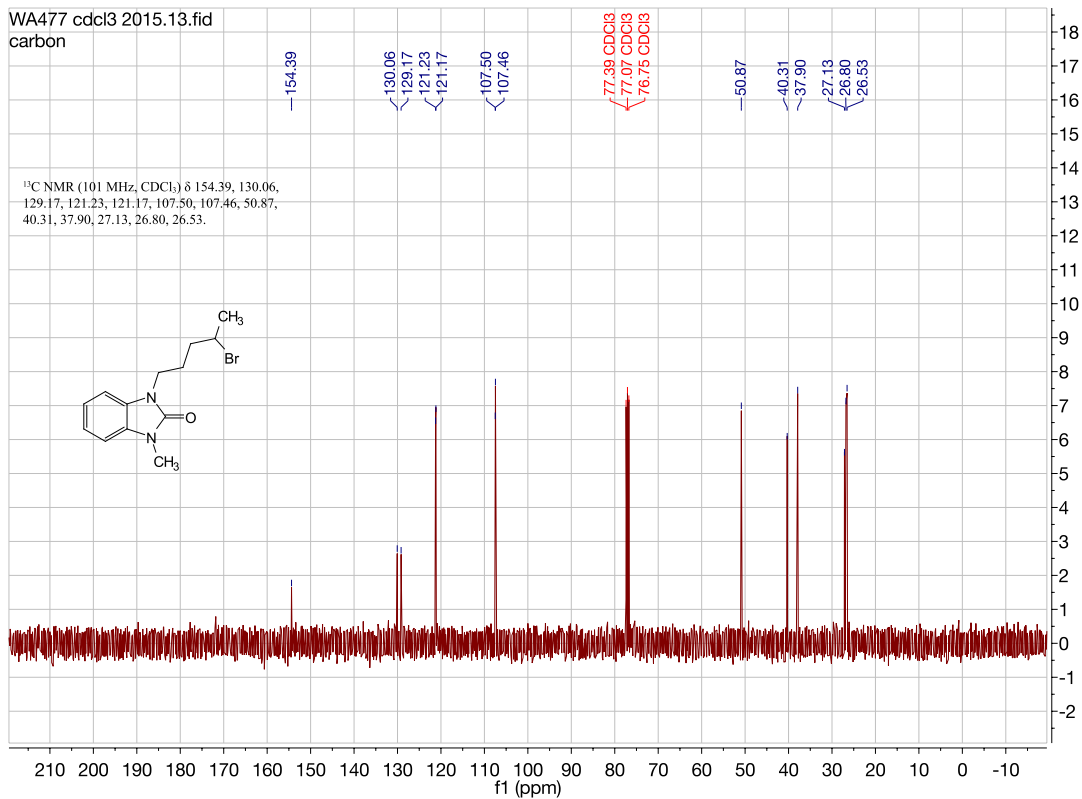




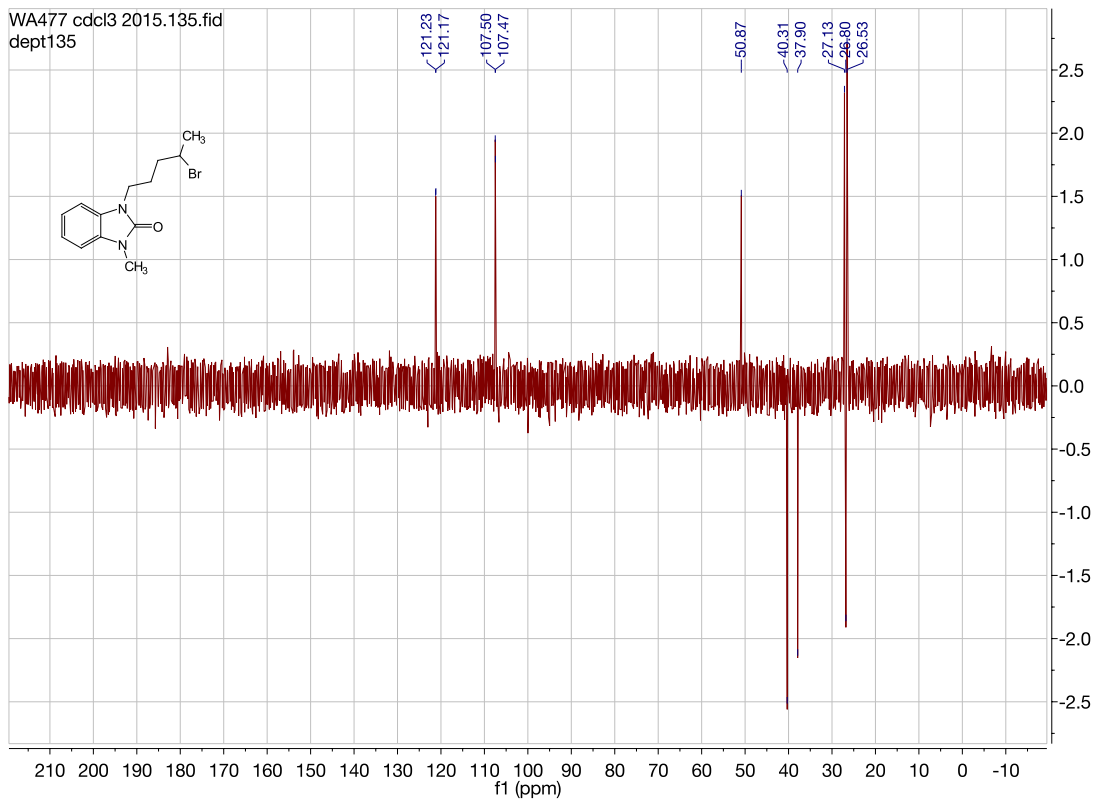
1-(4-bromopentyl)-3-methyl-1,3-dihydro-2H-benzo[d]imidazol-2-one. (WA477)



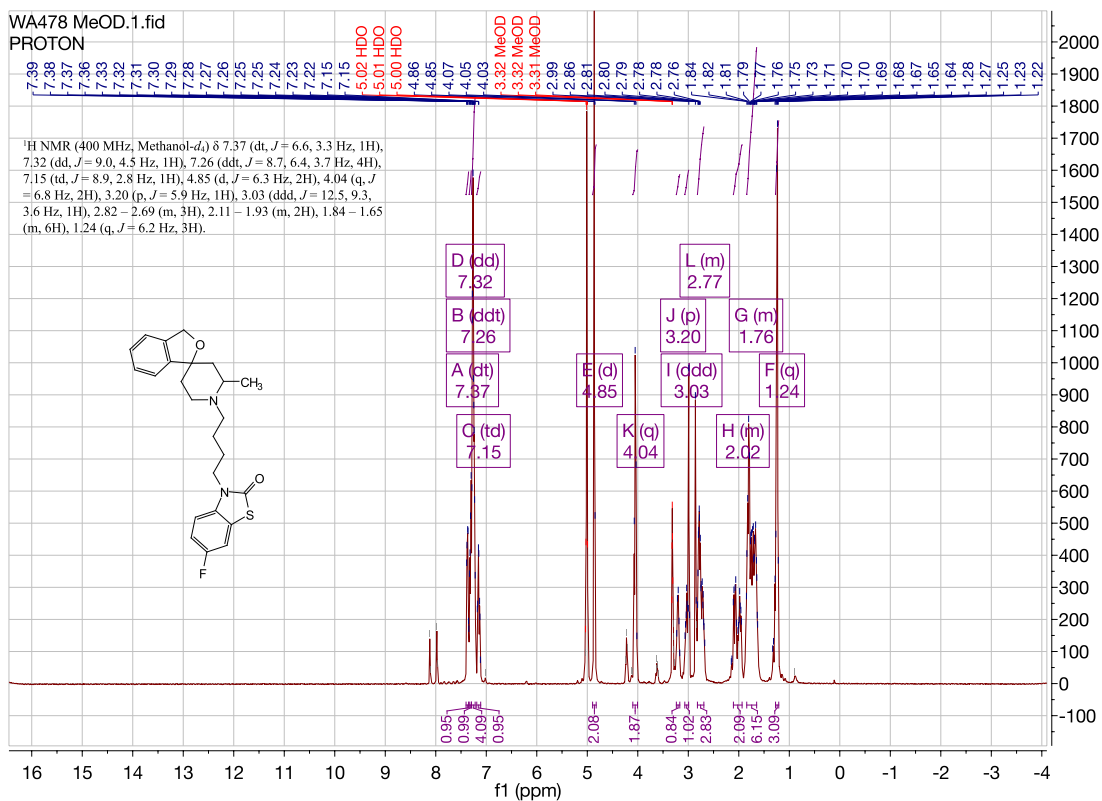
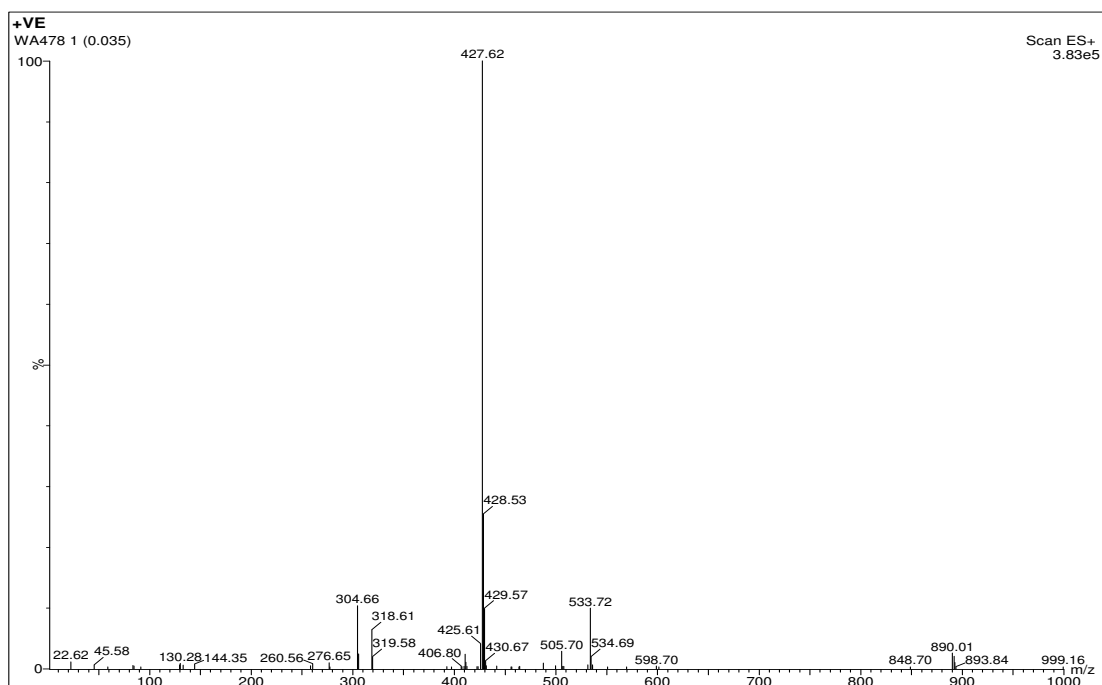
WA477 cdcl3 2015.13.fid
carbon



WA477 cdcl3 2015.135.fid
dept135

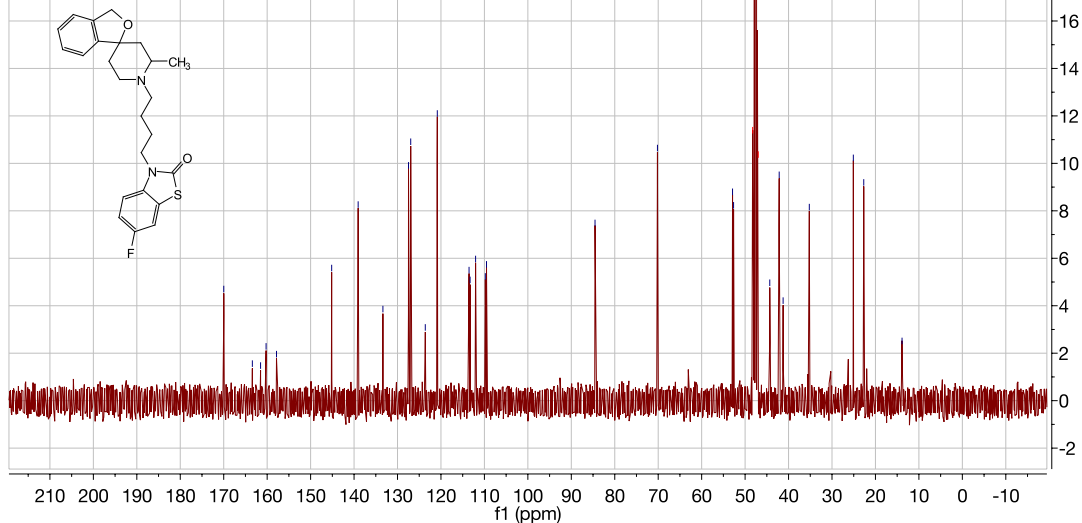


6-fluoro-3-(4-(2'-methyl-3H-spiro[isobenzofuran-1,4'-piperidin]-1'-yl)butyl)benzo[d]thiazol-2(3H)-one. (WA478)

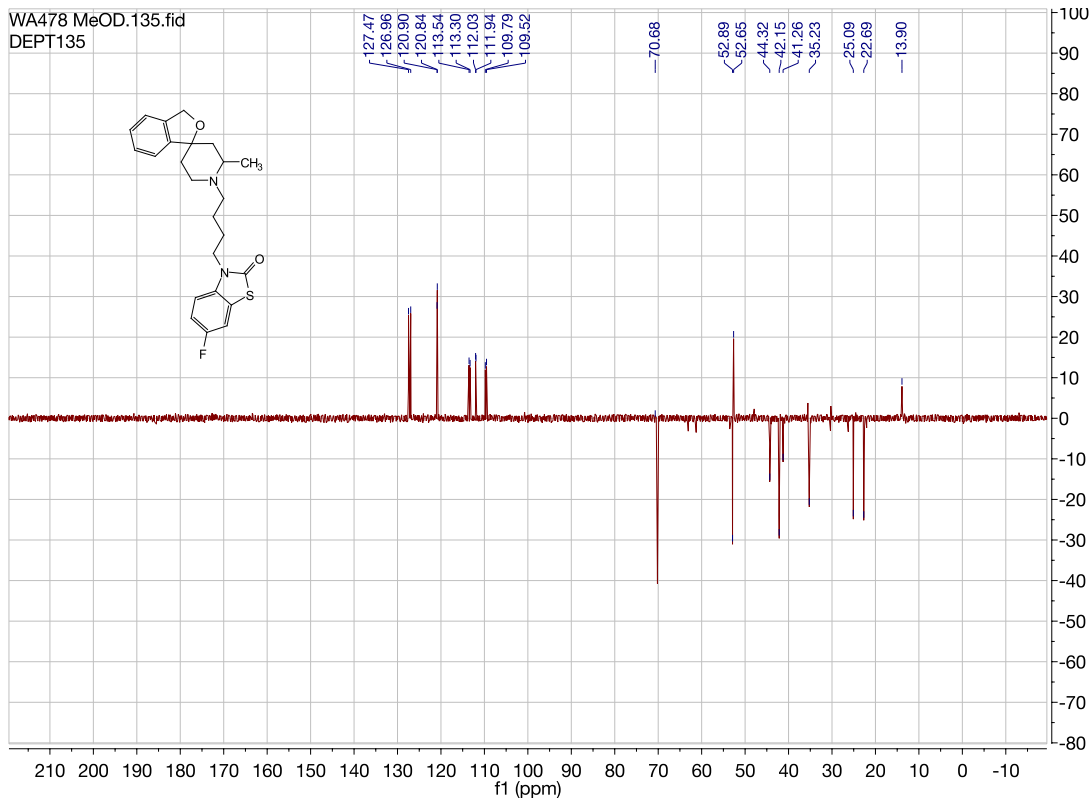


WA478 MeOD.13.fid
CARBON

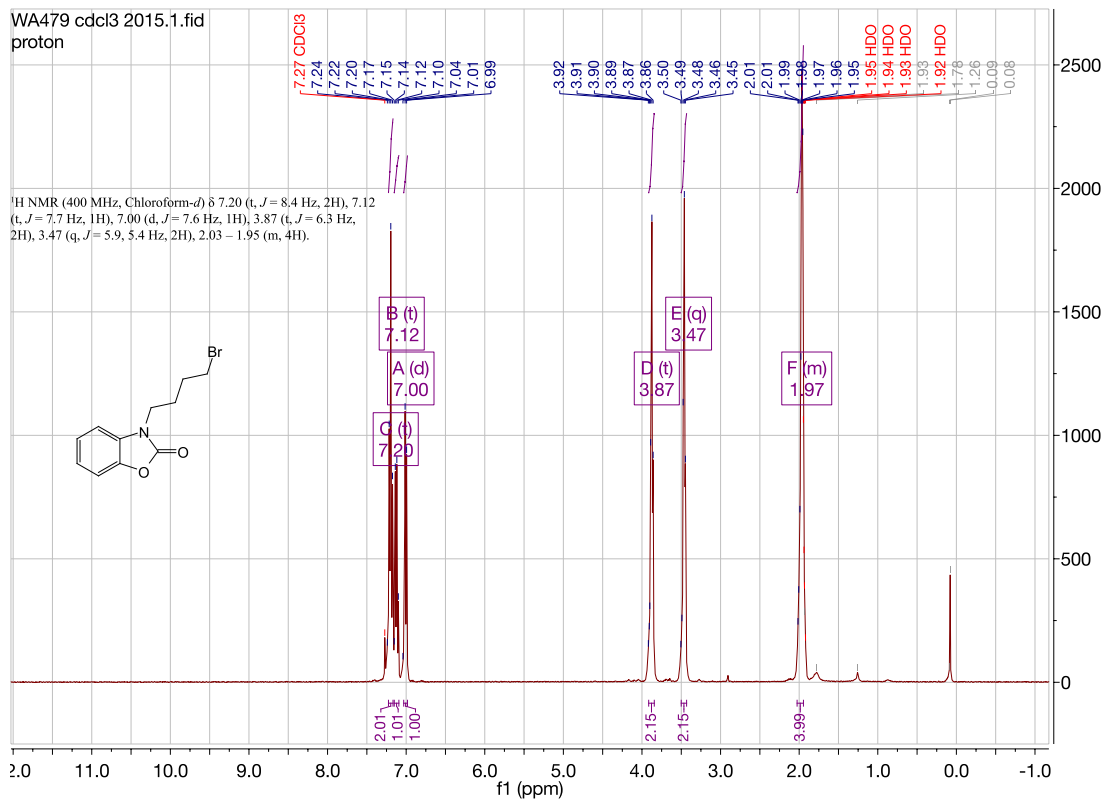
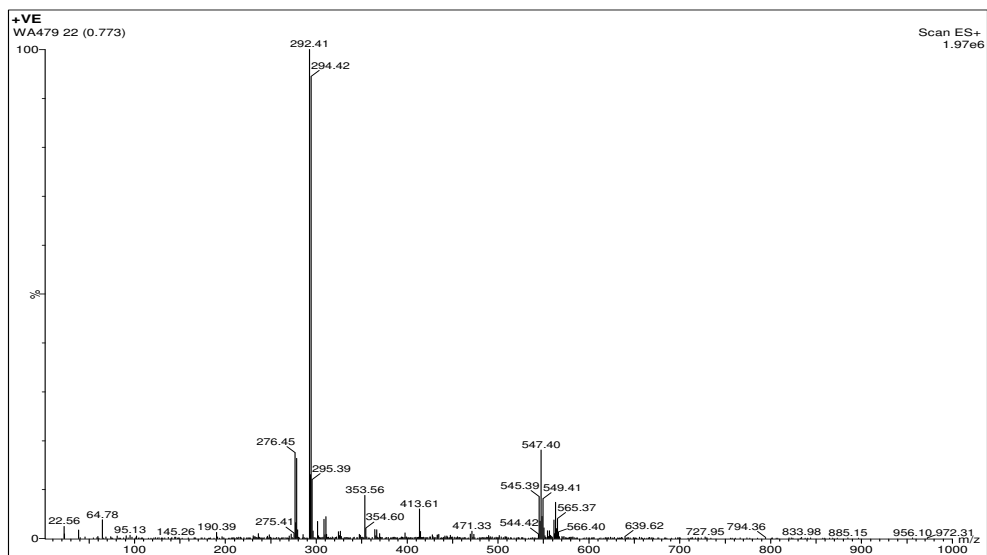
^{13}C NMR (101 MHz, MeOD) δ 169.99, 163.41, 161.52, 160.25,
157.85, 145.15, 139.06, 133.36, 127.47, 126.96, 123.61, 120.84,
113.53, 113.30, 112.03, 109.79, 109.52, 84.54, 70.17, 52.89, 52.65,
44.32, 42.15, 41.25, 35.22, 25.09, 22.69, 13.88.

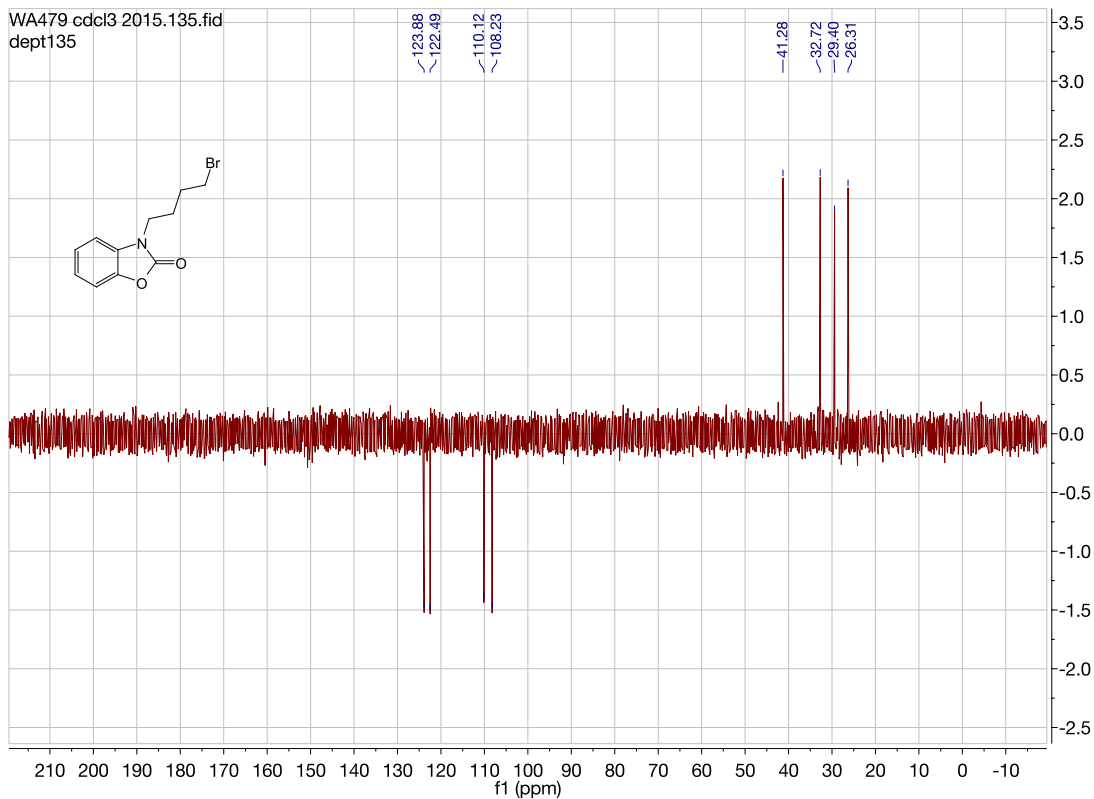
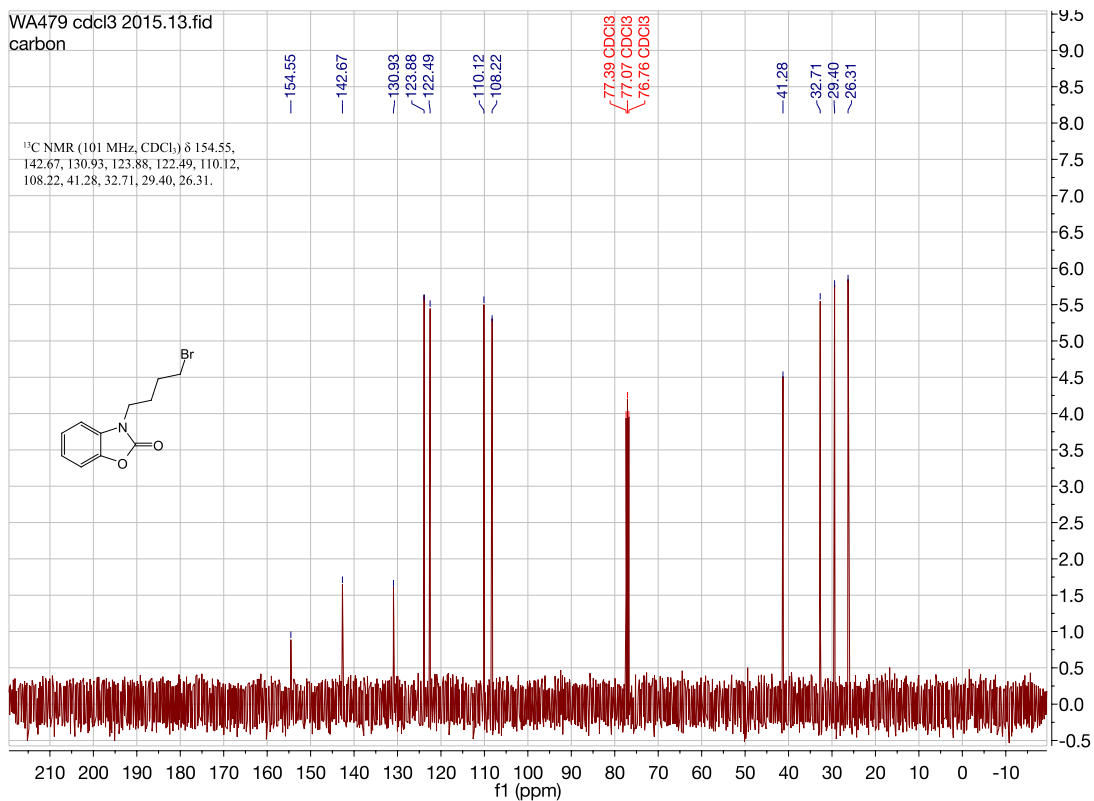


WA478 MeOD.135.fid
DEPT135

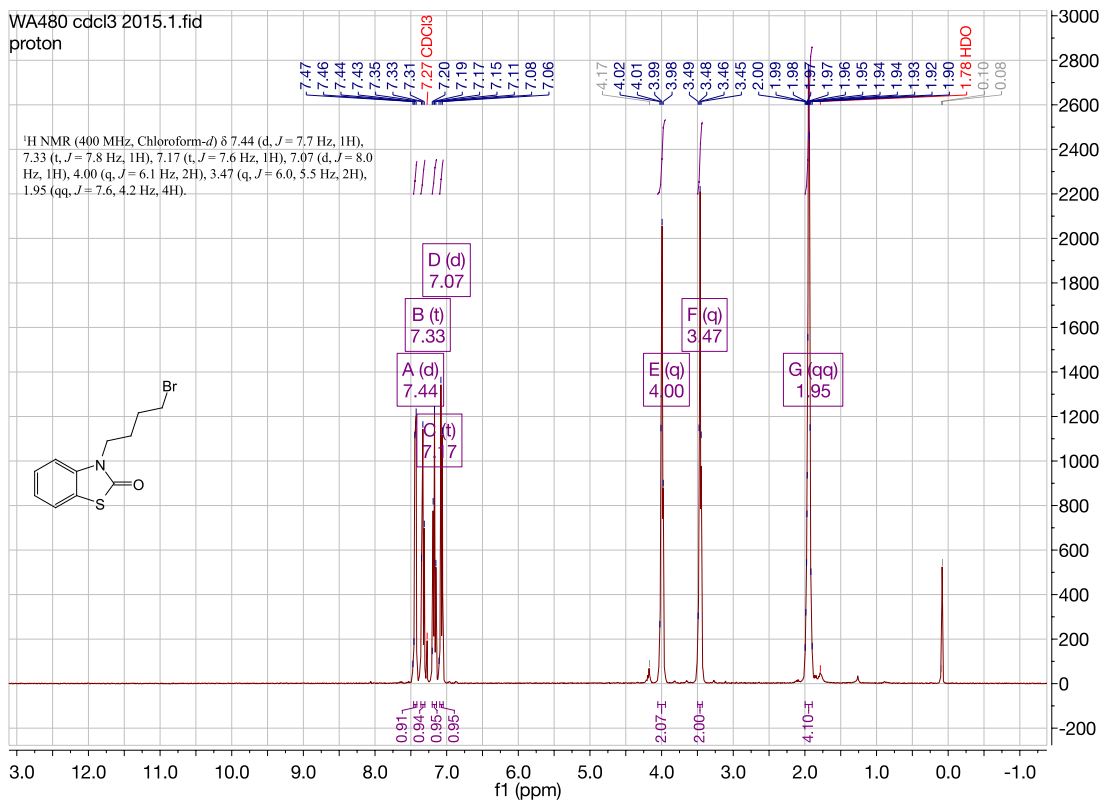
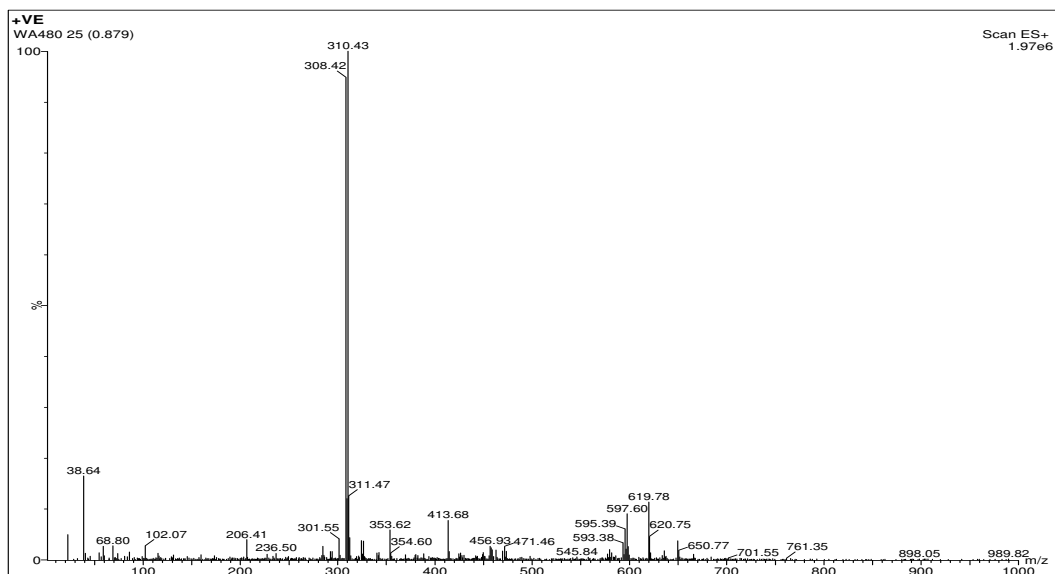


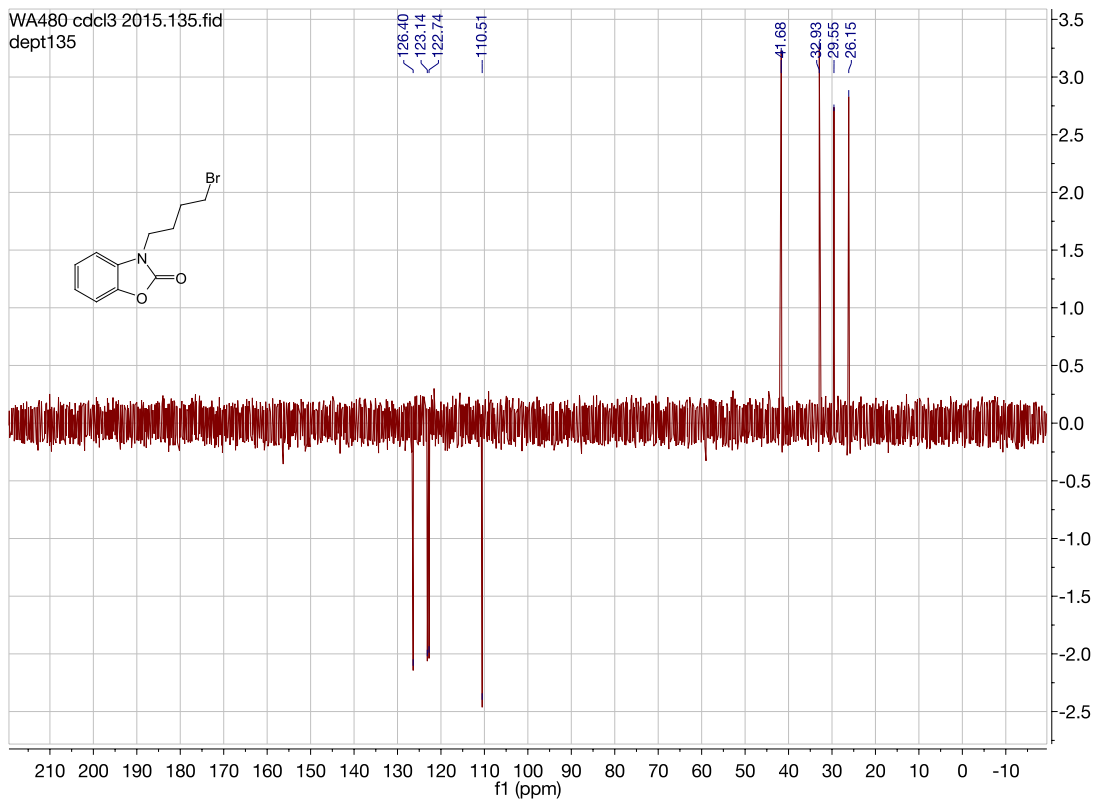
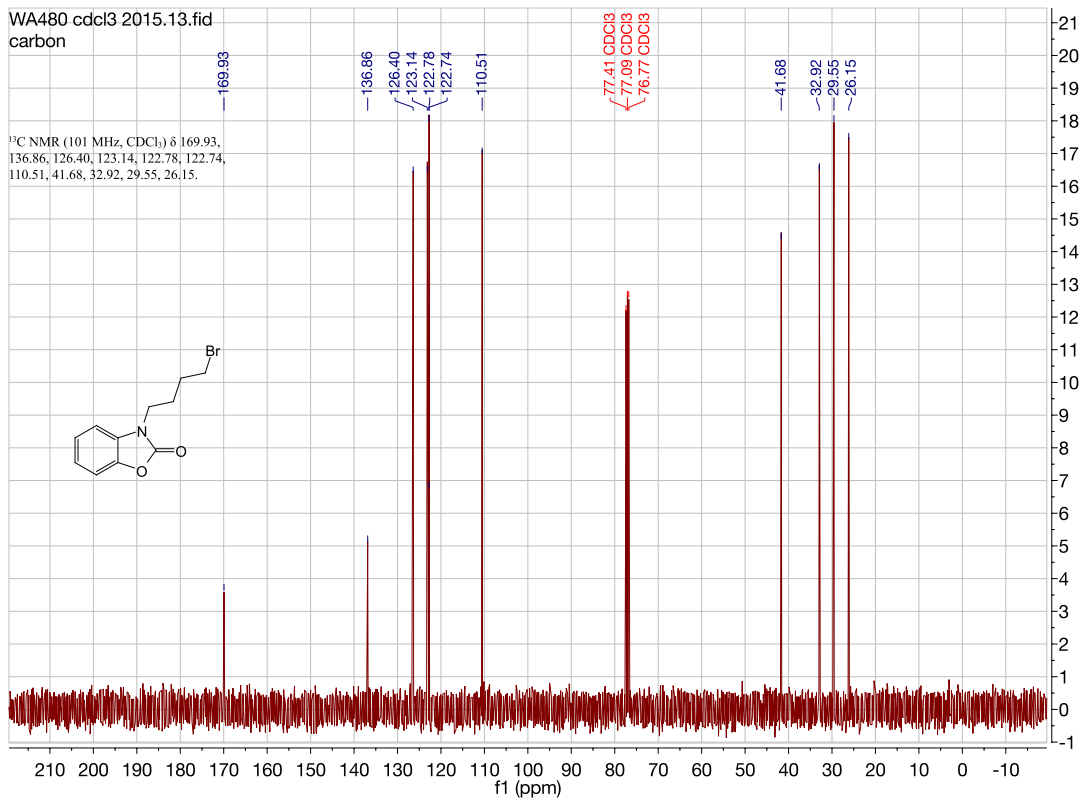
3-(4-bromobutyl)benzo[d]oxazol-2(3H)-one. (WA479)



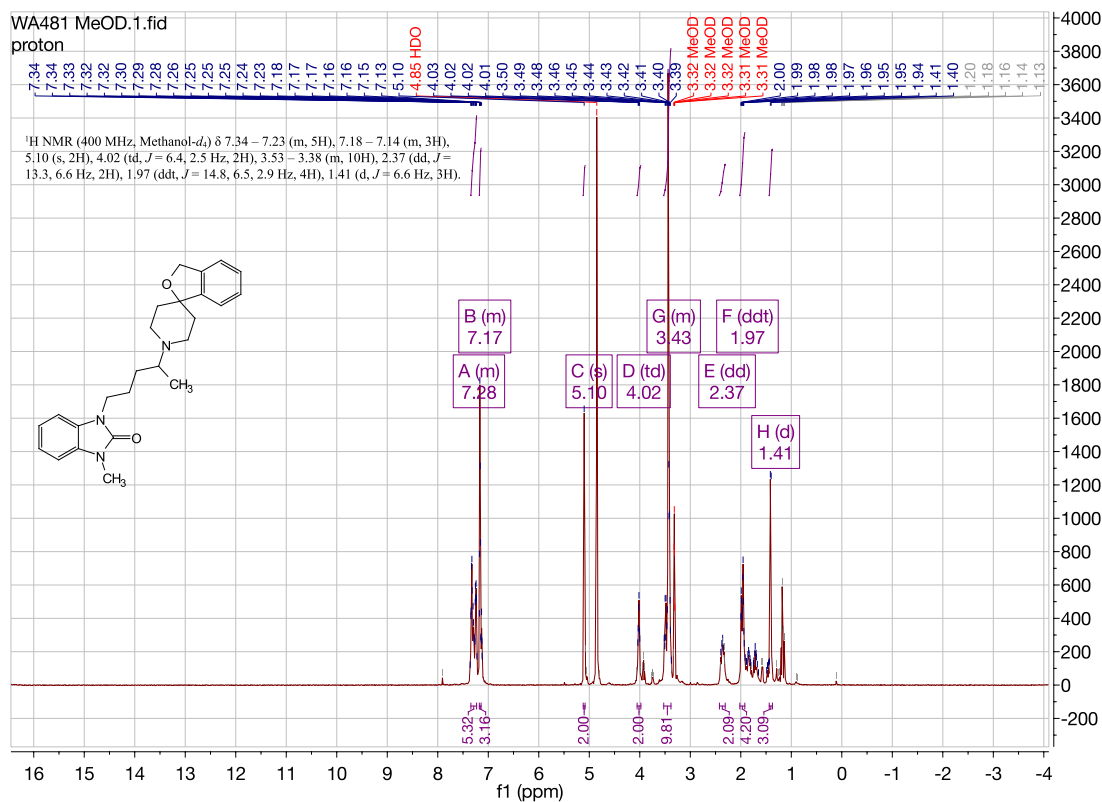
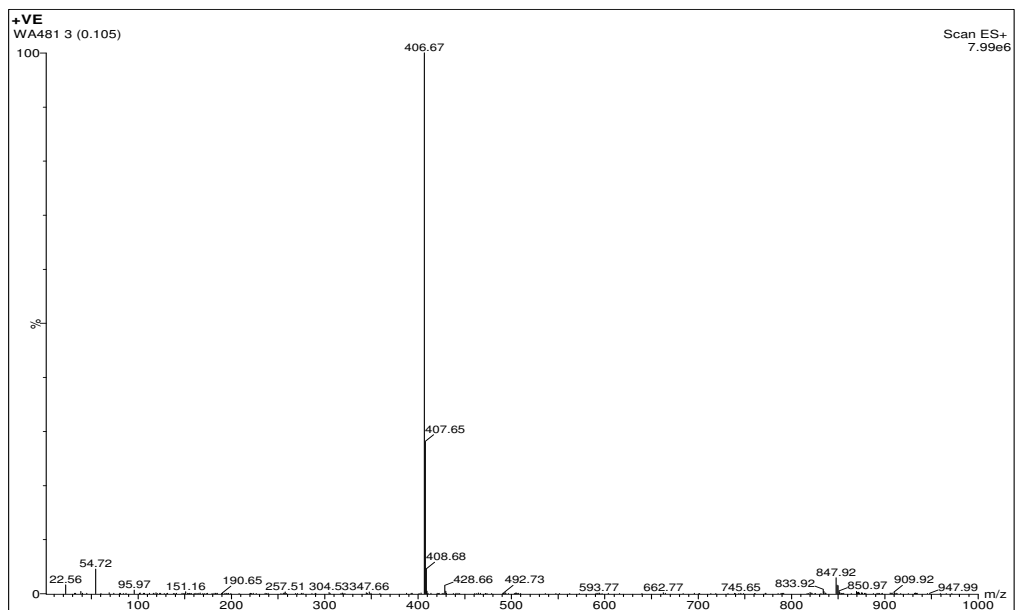


3-(4-bromobutyl)benzo[d]thiazol-2(3H)-one. (WA480)



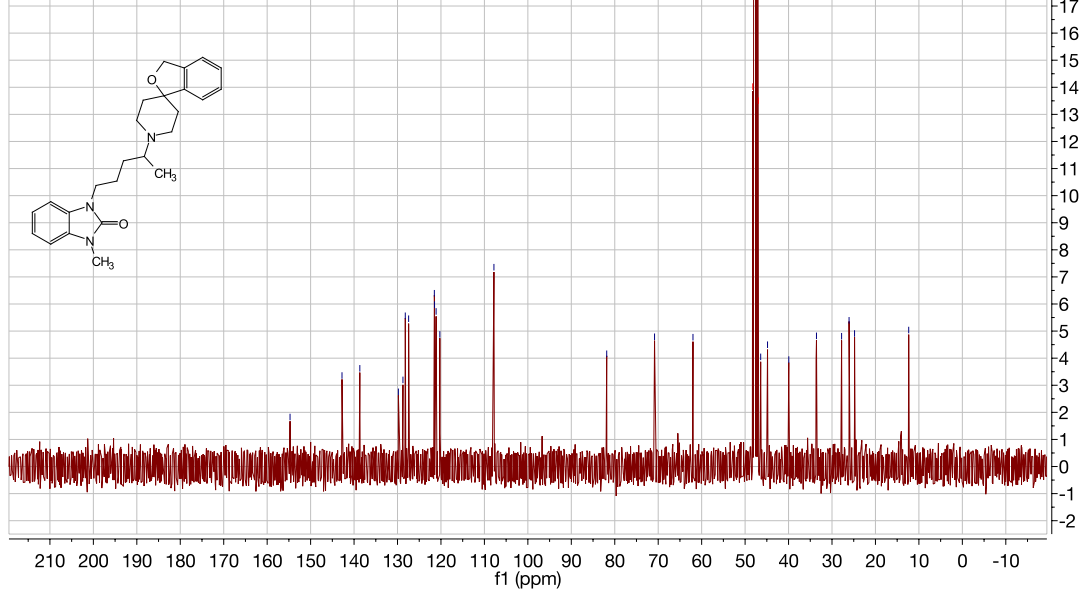


1-(4-(3H-spiro[isobenzofuran-1,4'-piperidin]-1'-yl)pentyl)-3-methyl-1,3-dihydro-2H-benzo[d]imidazol-2-one. (WA481)

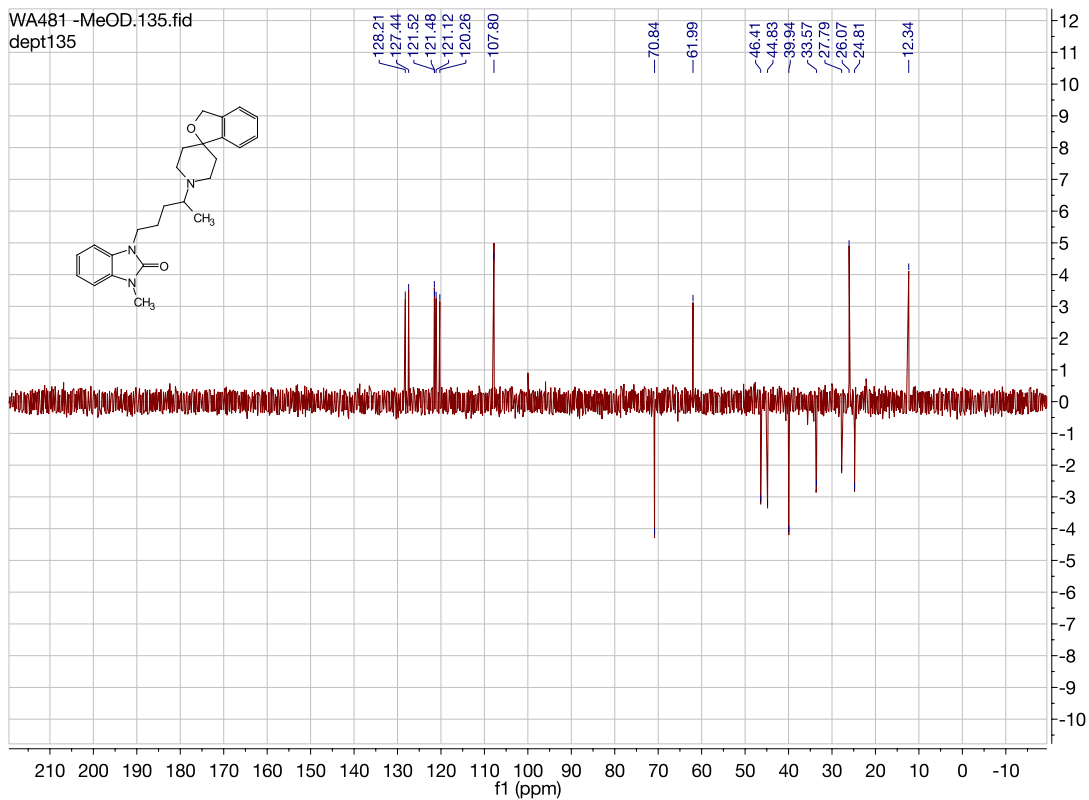


WA481 MeOD.13.fid
carbon

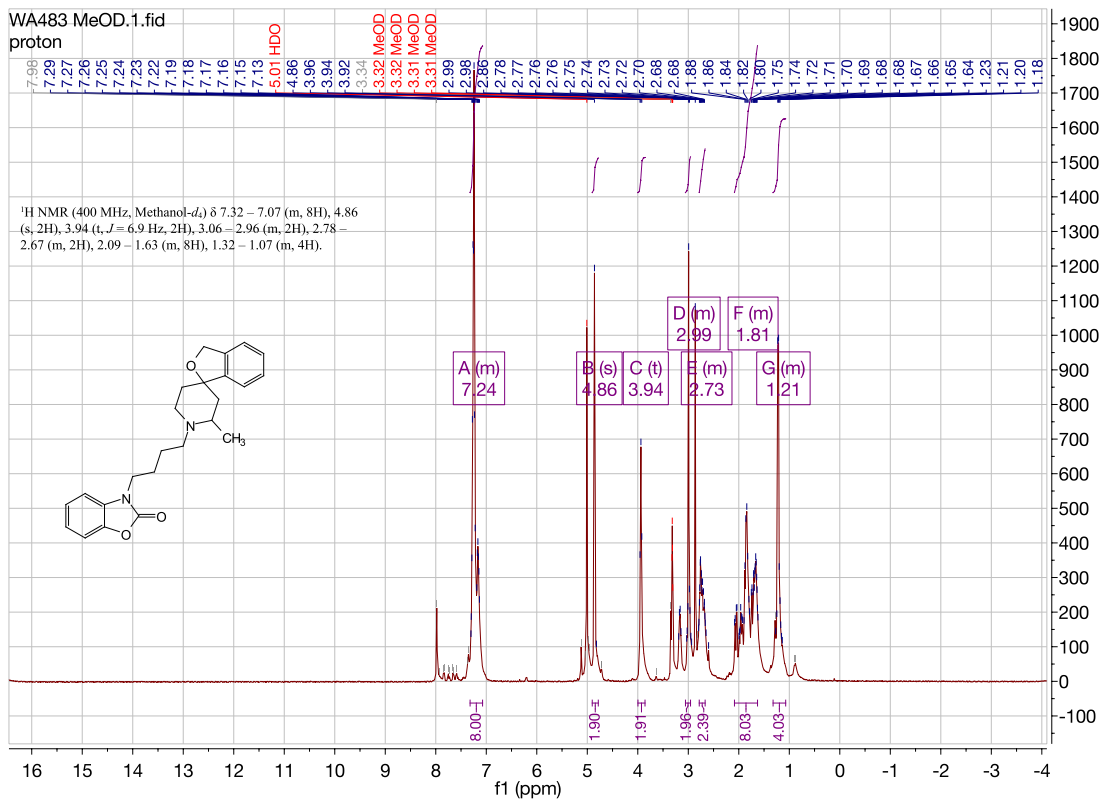
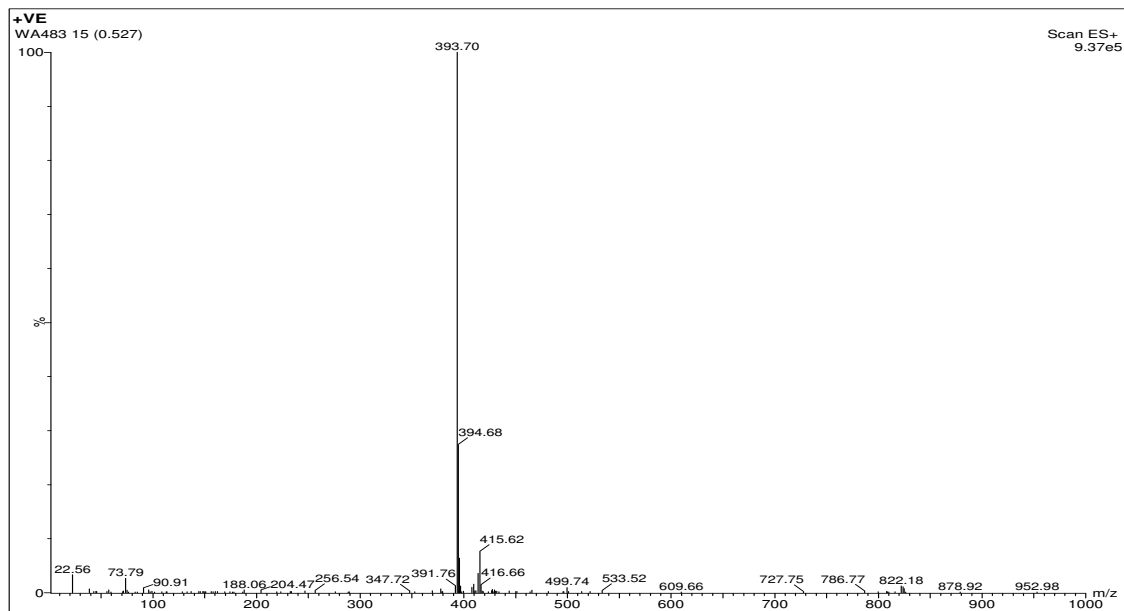
¹³C NMR (101 MHz, MeOD) δ 154.73, 142.78, 138.67, 129.80, 128.75,
128.21, 127.44, 121.52, 121.48, 121.12, 120.26, 107.81, 81.85, 70.84,
62.00, 46.41, 44.84, 39.94, 33.57, 27.79, 26.07, 24.81, 12.35.



WA481 -MeOD.135.fid
dept135

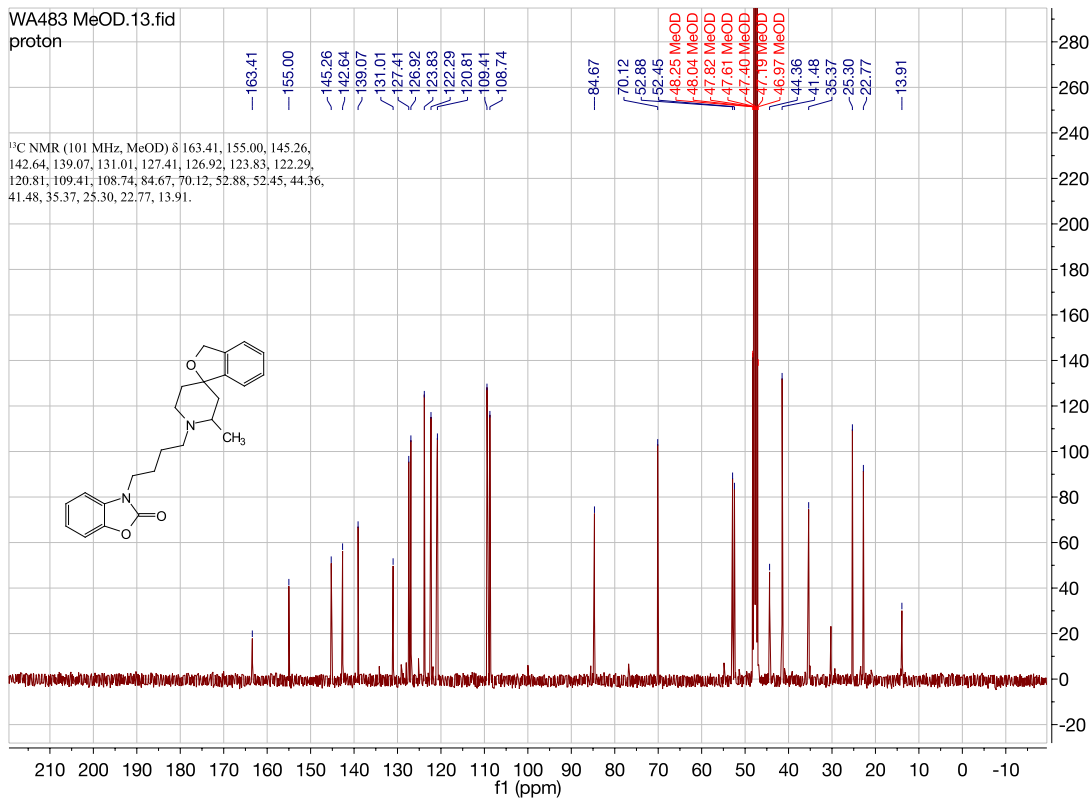


3-(4-(2'-methyl-3*H*-spiro[isobenzofuran-1,4'-piperidin]-1'-yl)butyl)benzo[*d*]oxazol-2(3*H*)-one. (WA483)

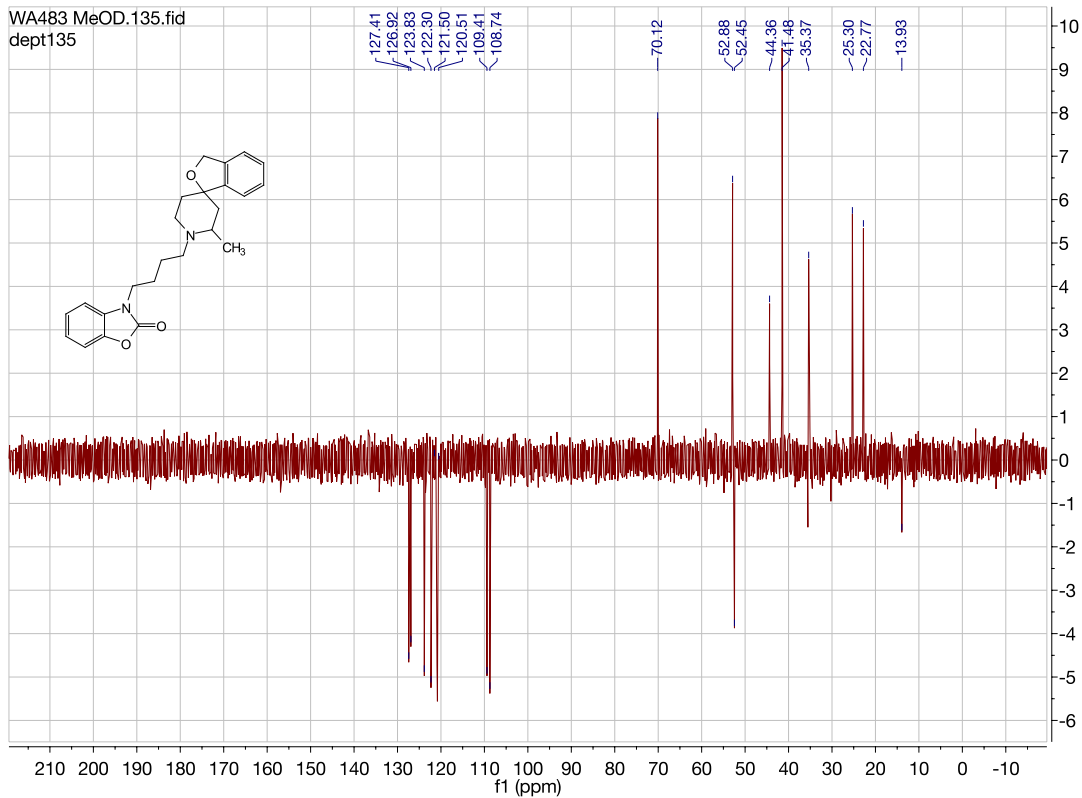


WA483 MeOD.13.fid
proton

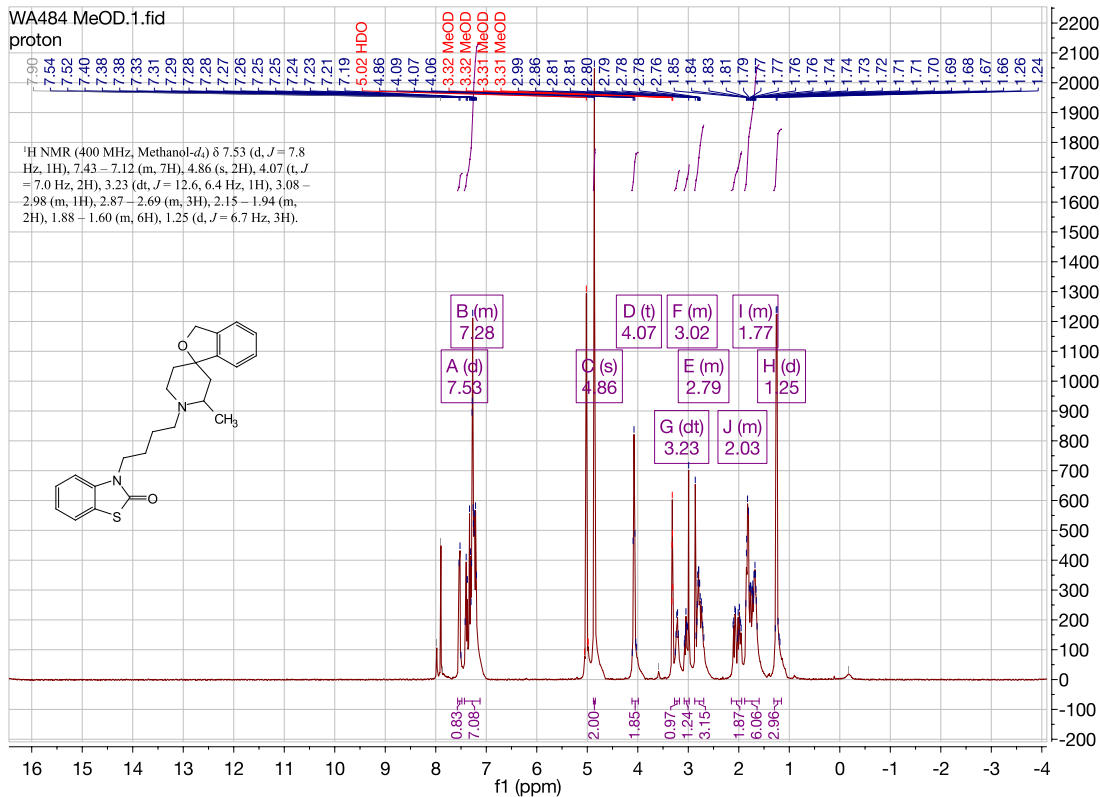
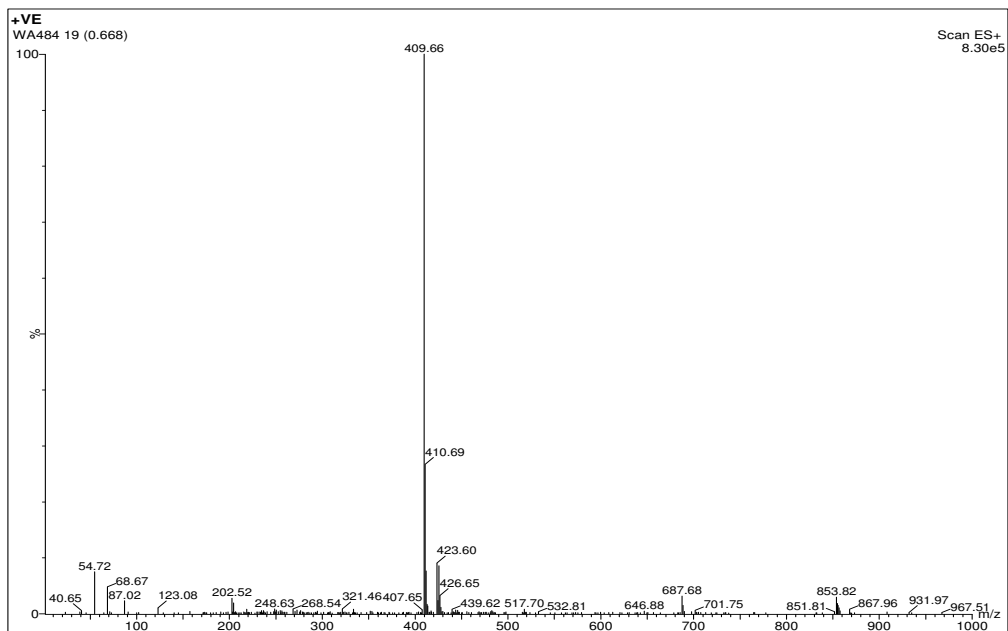
^{13}C NMR (101 MHz, MeOD) δ 163.41, 155.00, 145.26,
142.64, 139.07, 131.01, 127.41, 126.92, 123.83, 122.29,
120.81, 109.41, 108.74, 84.67, 70.12, 52.88, 52.45, 44.36,
41.48, 35.37, 25.30, 22.77, 13.91.

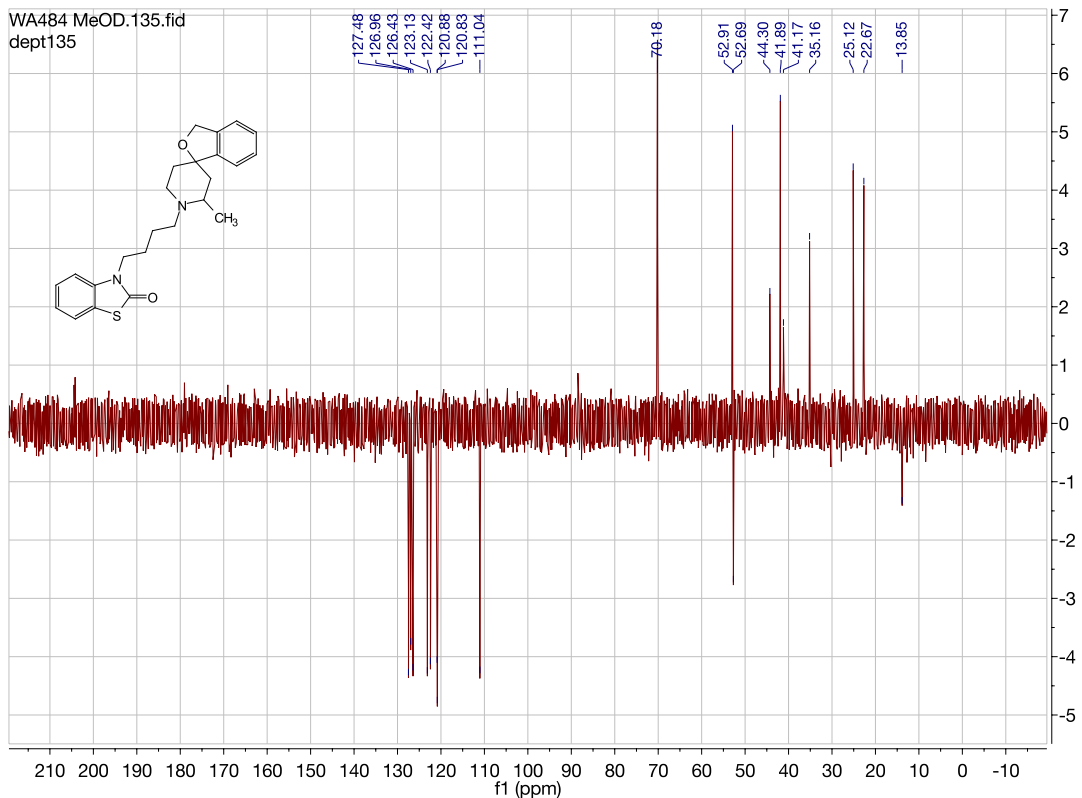
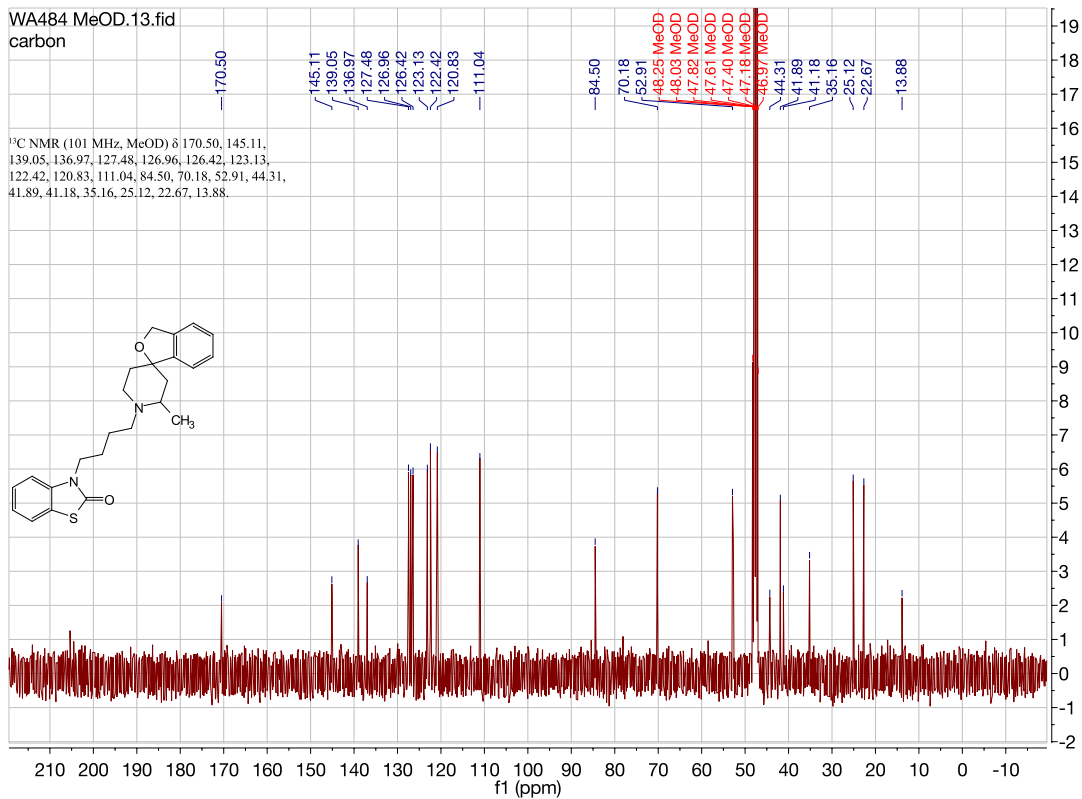


WA483 MeOD.135.fid
dept135

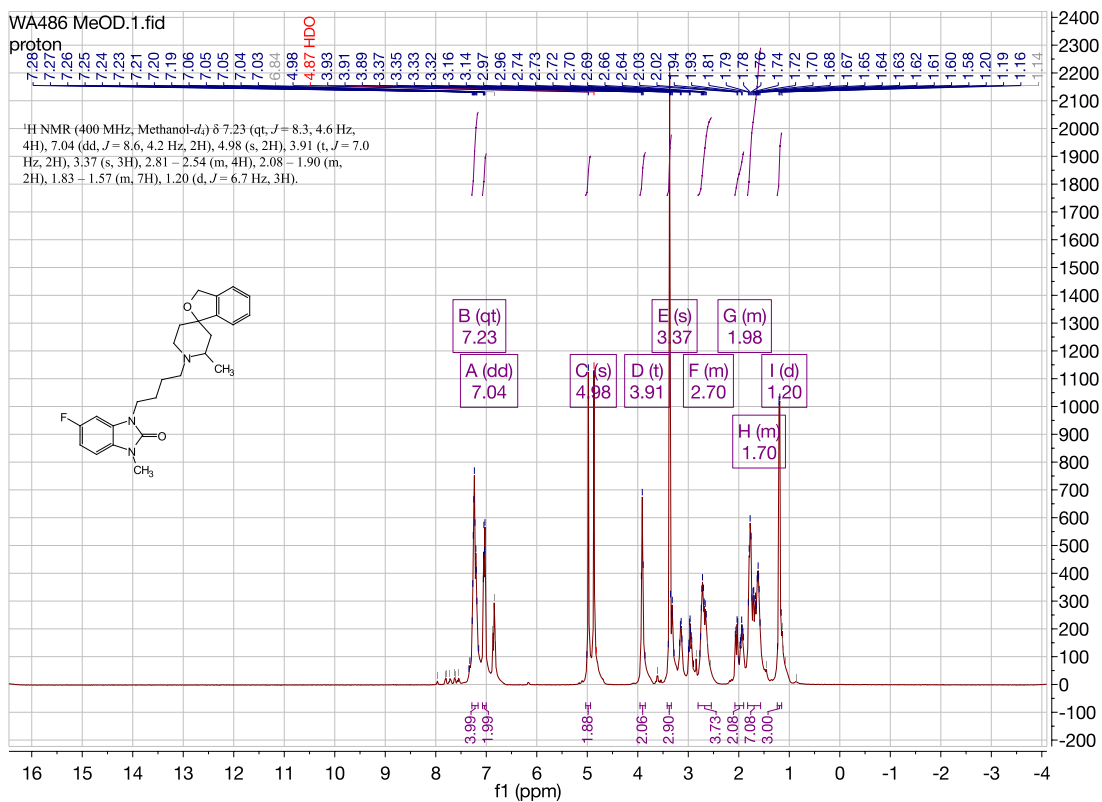
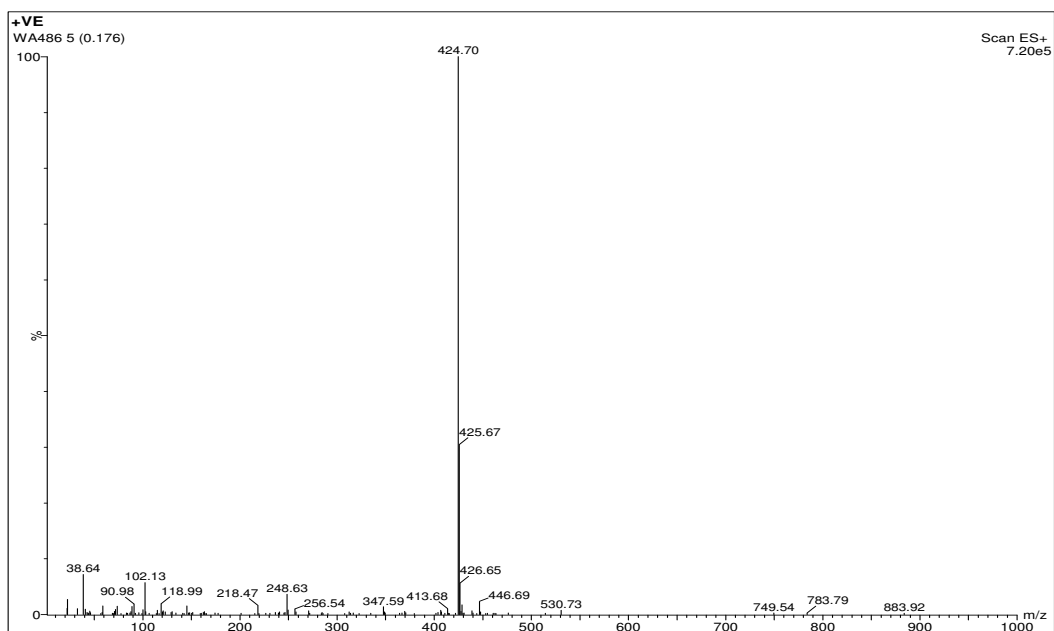


3-(4-(2'-methyl-3*H*-spiro[isobenzofuran-1,4'-piperidin]-1'-yl)butyl)benzo[*d*]thiazol-2(3*H*)-one. (WA484)

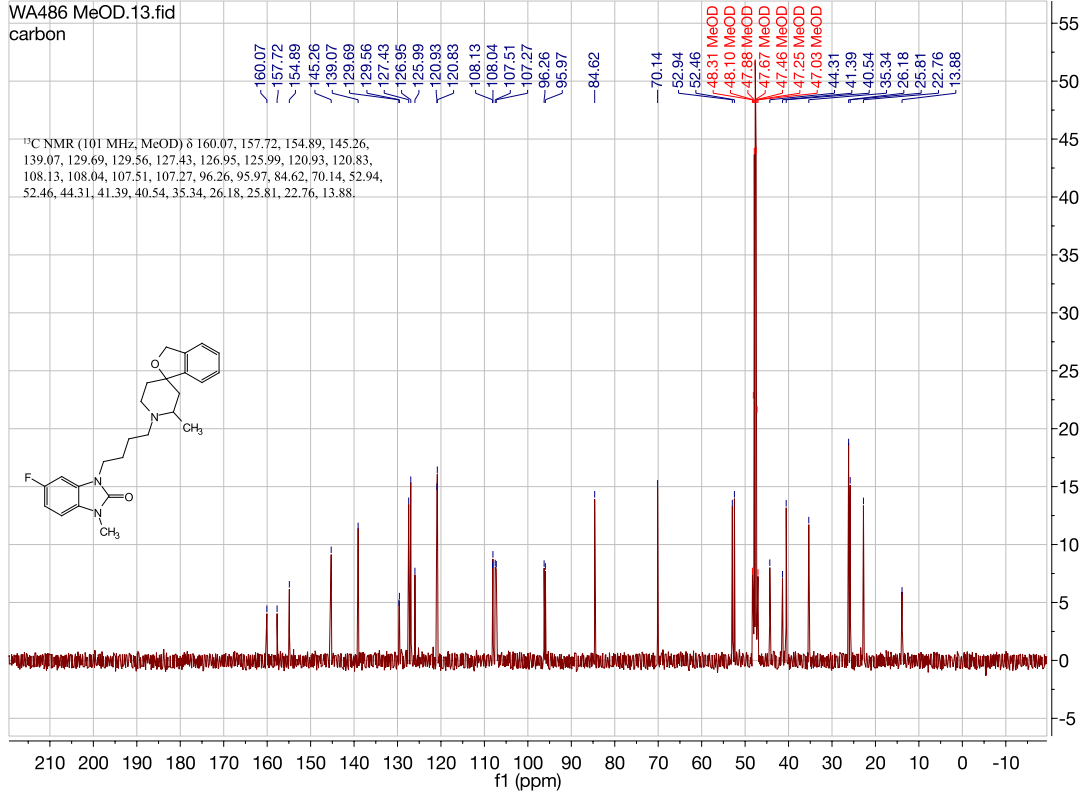




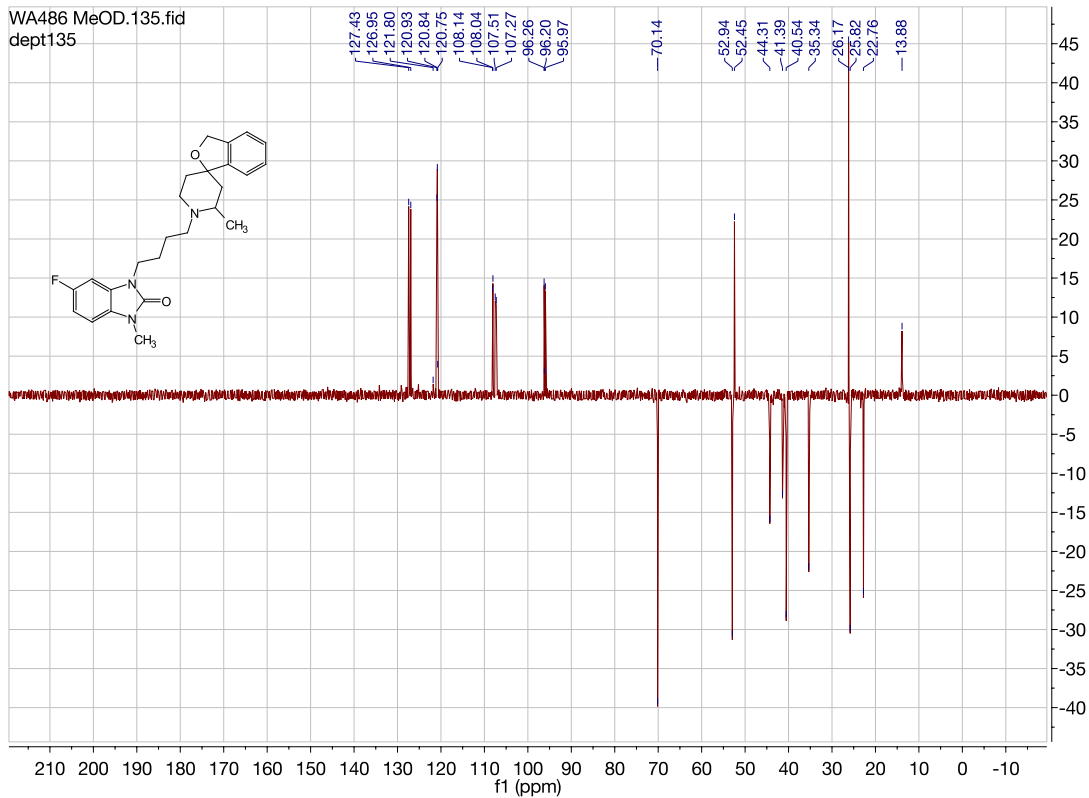
5-fluoro-1-methyl-3-(4-(2'-methyl-3*H*-spiro[isobenzofuran-1,4'-piperidin]-1'-yl)butyl)-1,3-dihydro-2*H*-benzo[*d*]imidazol-2-one. (WA486)



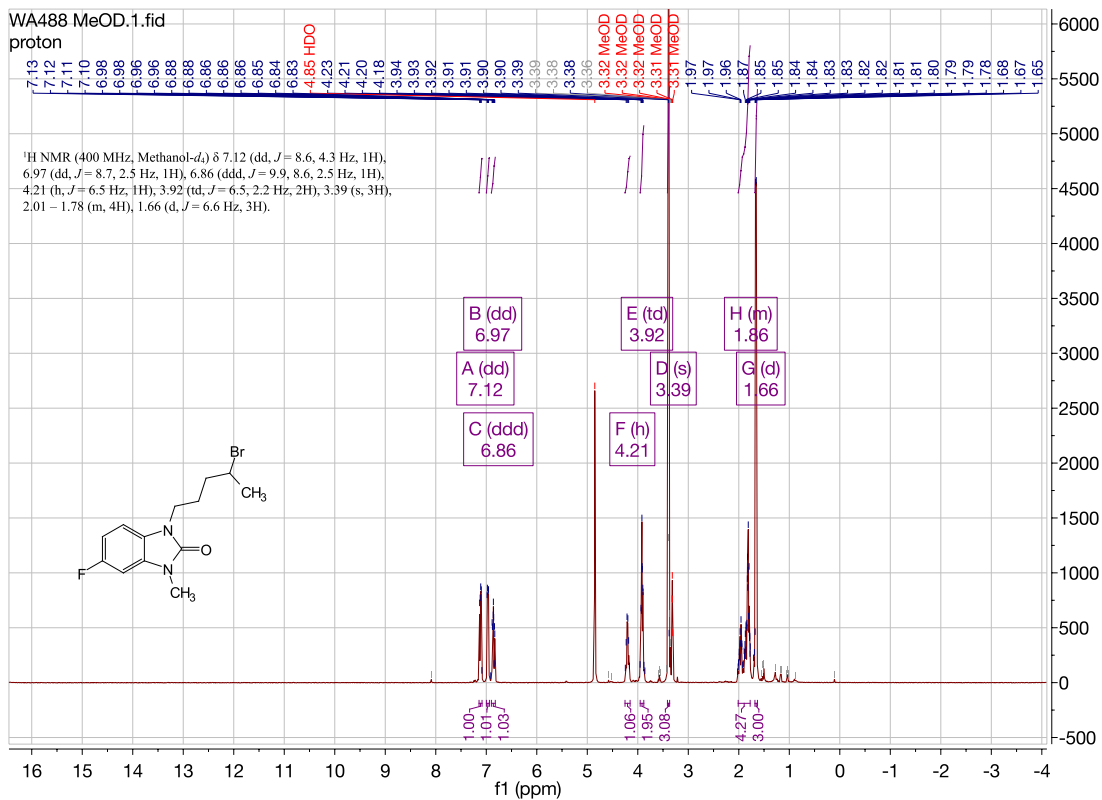
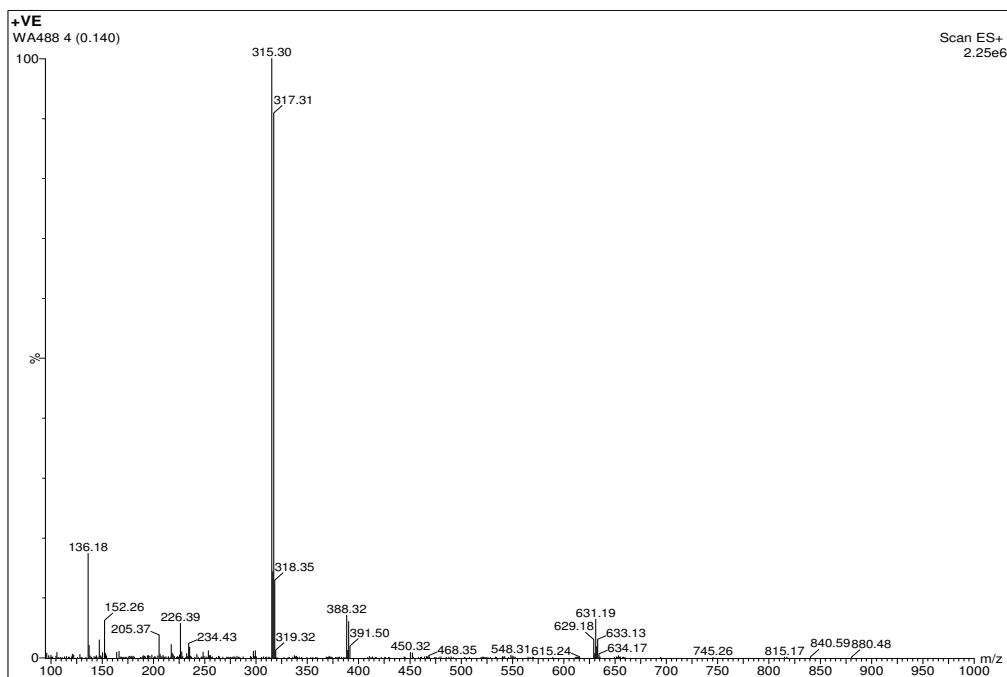
WA486 MeOD.13.fid
carbon



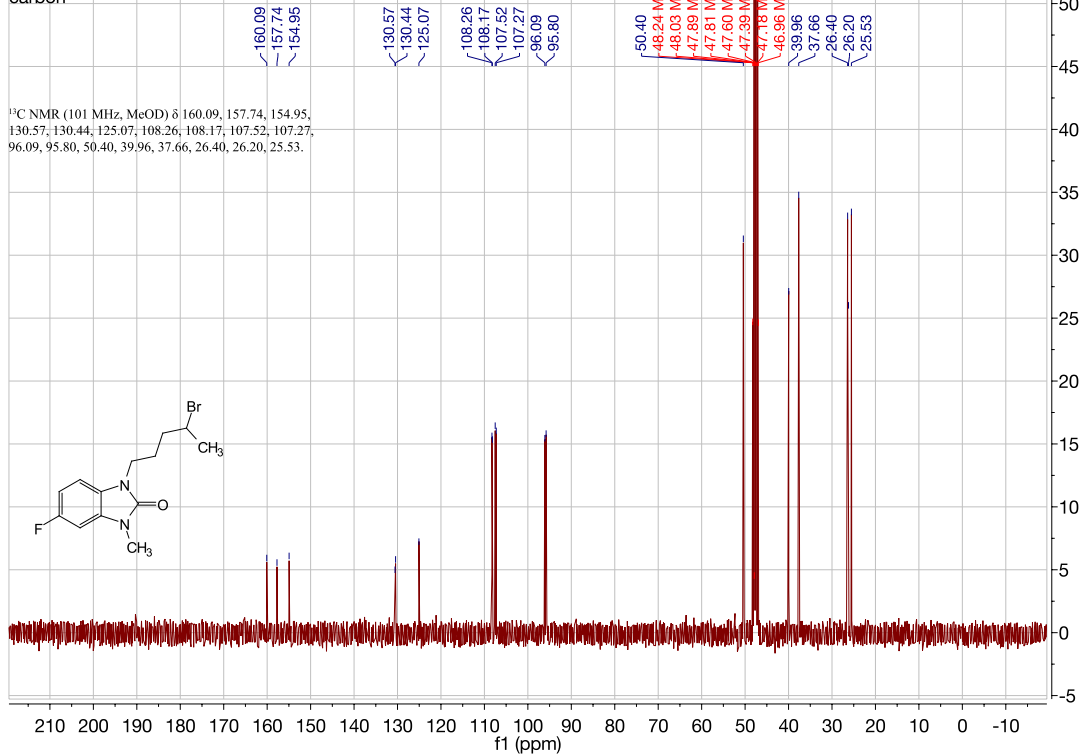
WA486 MeOD.135.fid
dept135



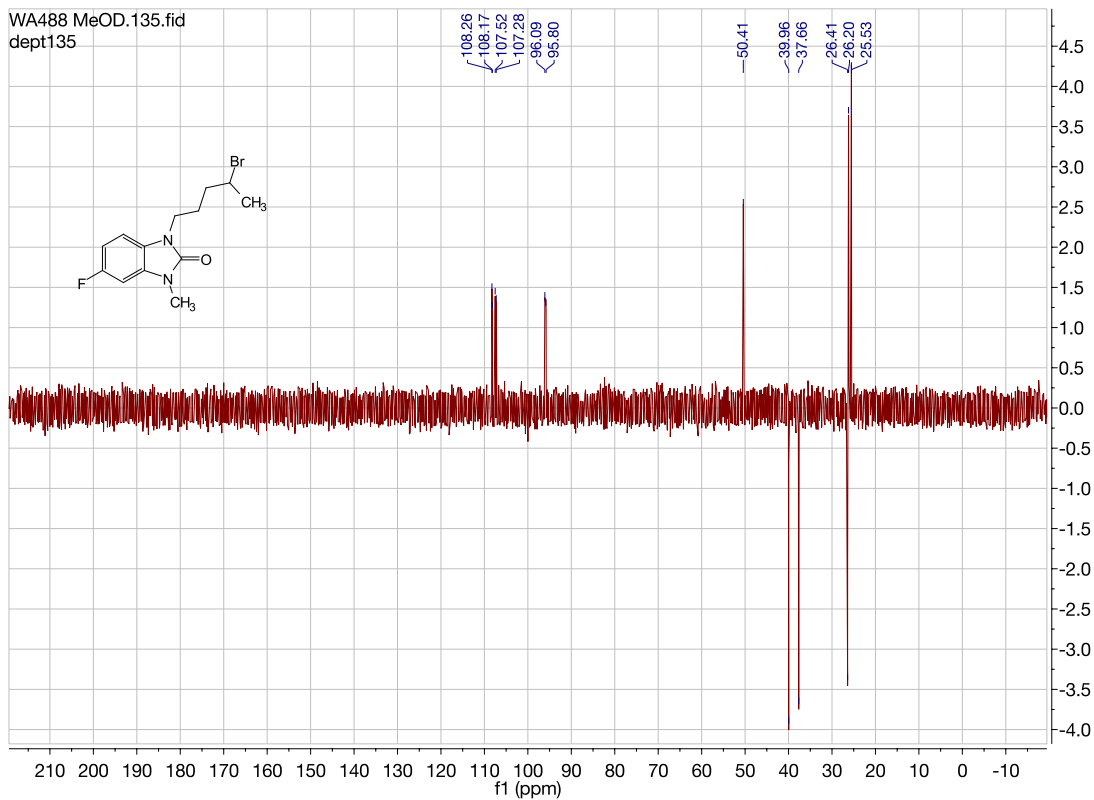
**1-(4-bromopentyl)-5-fluoro-3-methyl-1,3-dihydro-2H-benzo[d]imidazol-2-one
(WA488)**



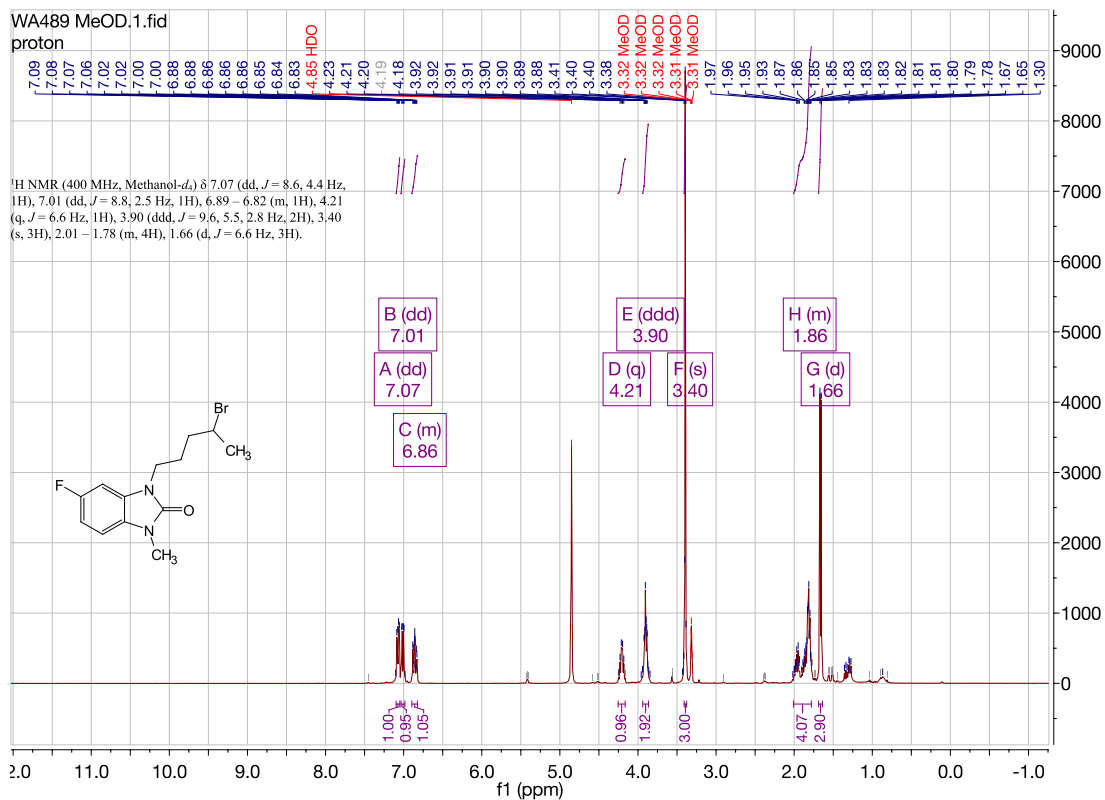
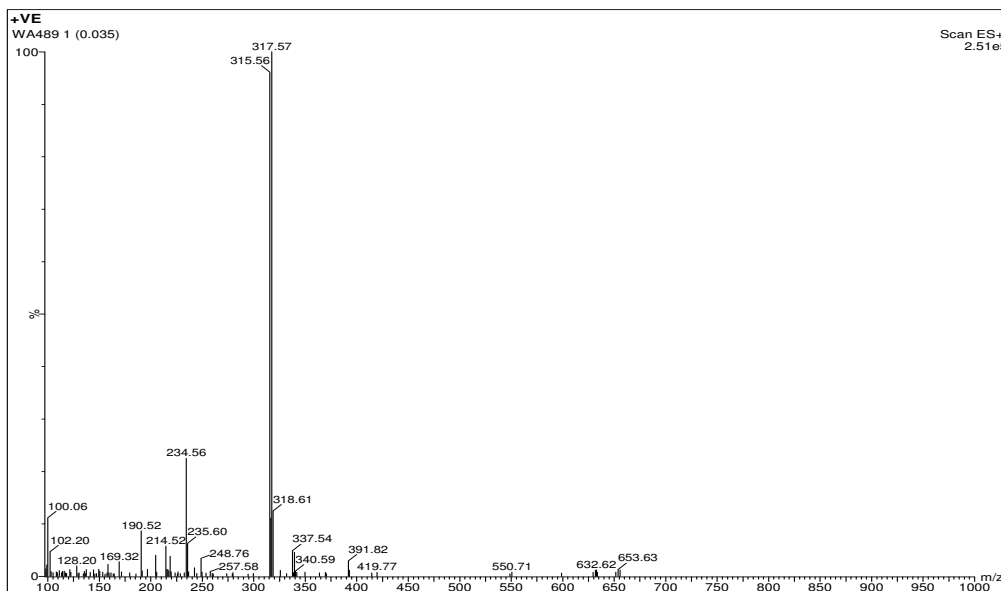
WA488 MeOD.13.fid
carbon



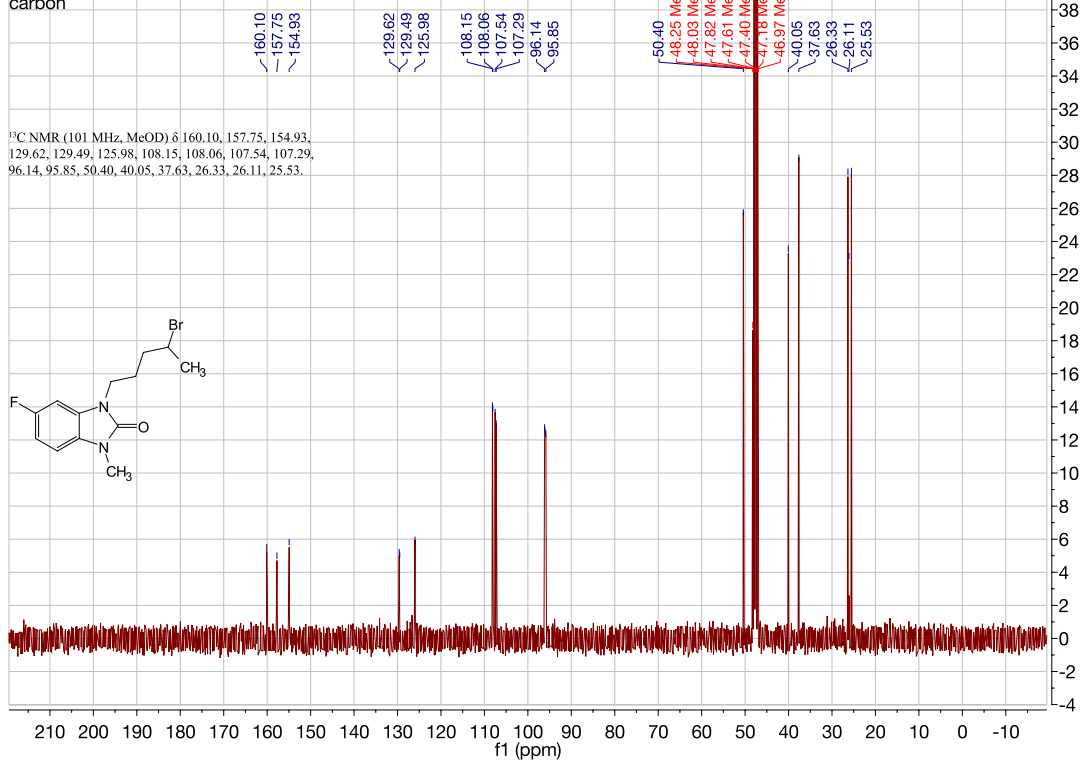
WA488 MeOD.135.fid
dept135



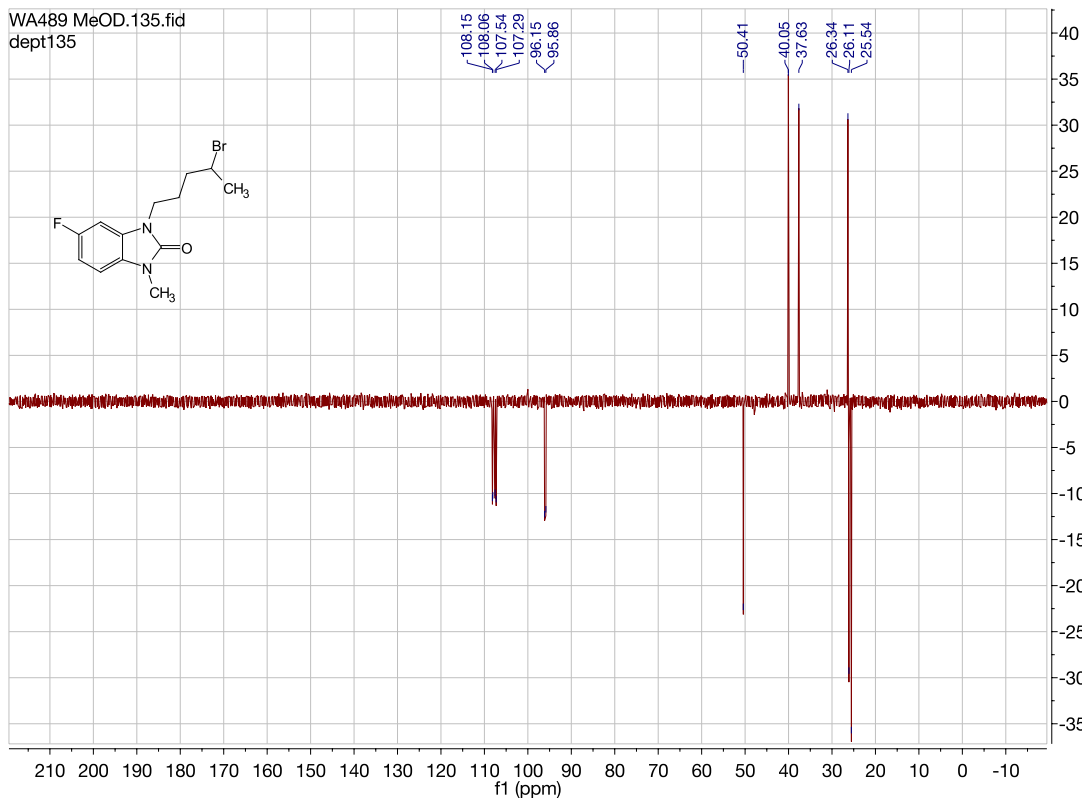
1-(4-bromopentyl)-5-fluoro-3-methyl-1,3-dihydro-2H-benzo[d]imidazol-2-one
(WA488)



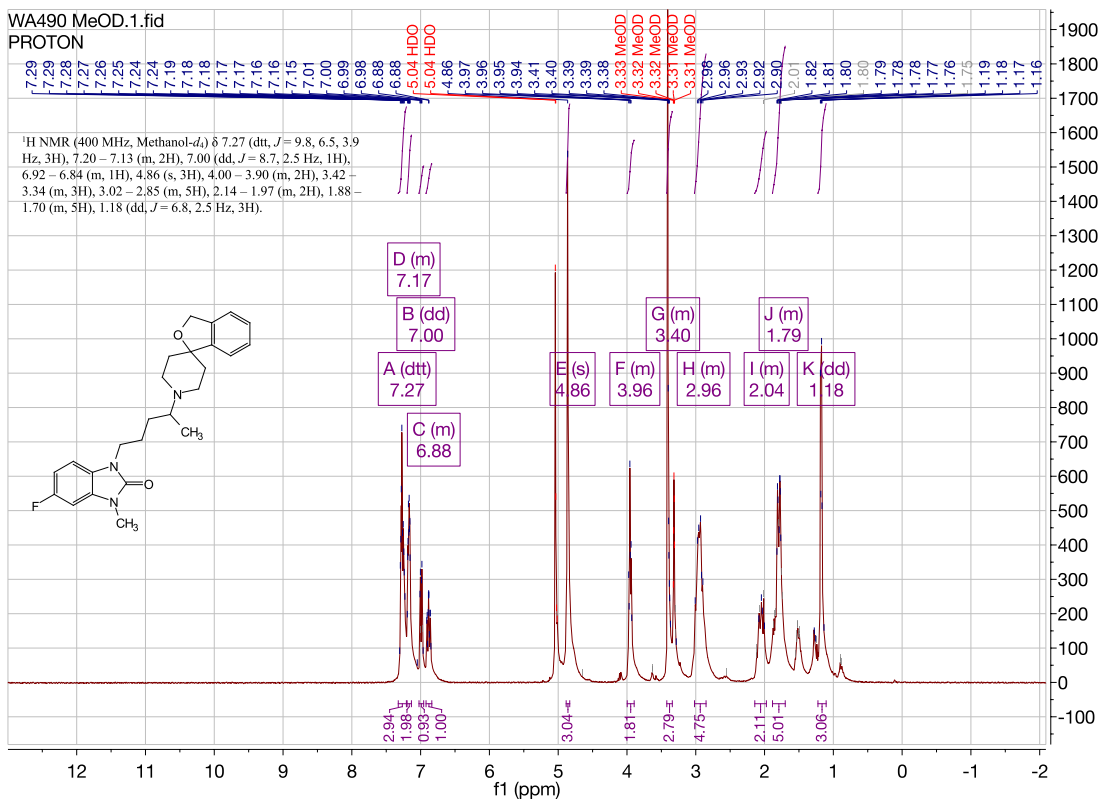
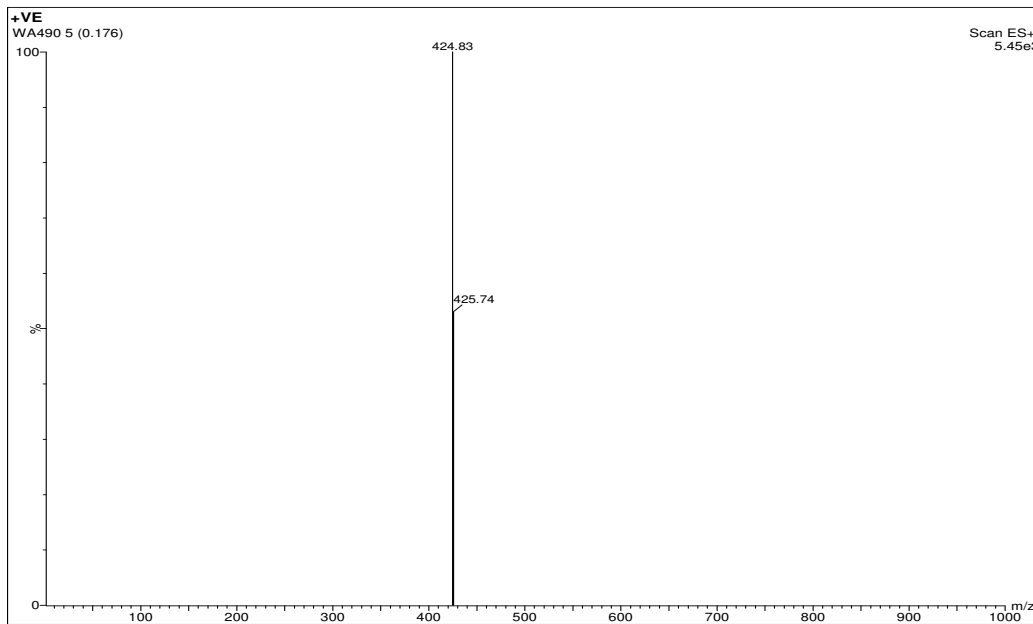
WA489 MeOD.13.fid
carbon



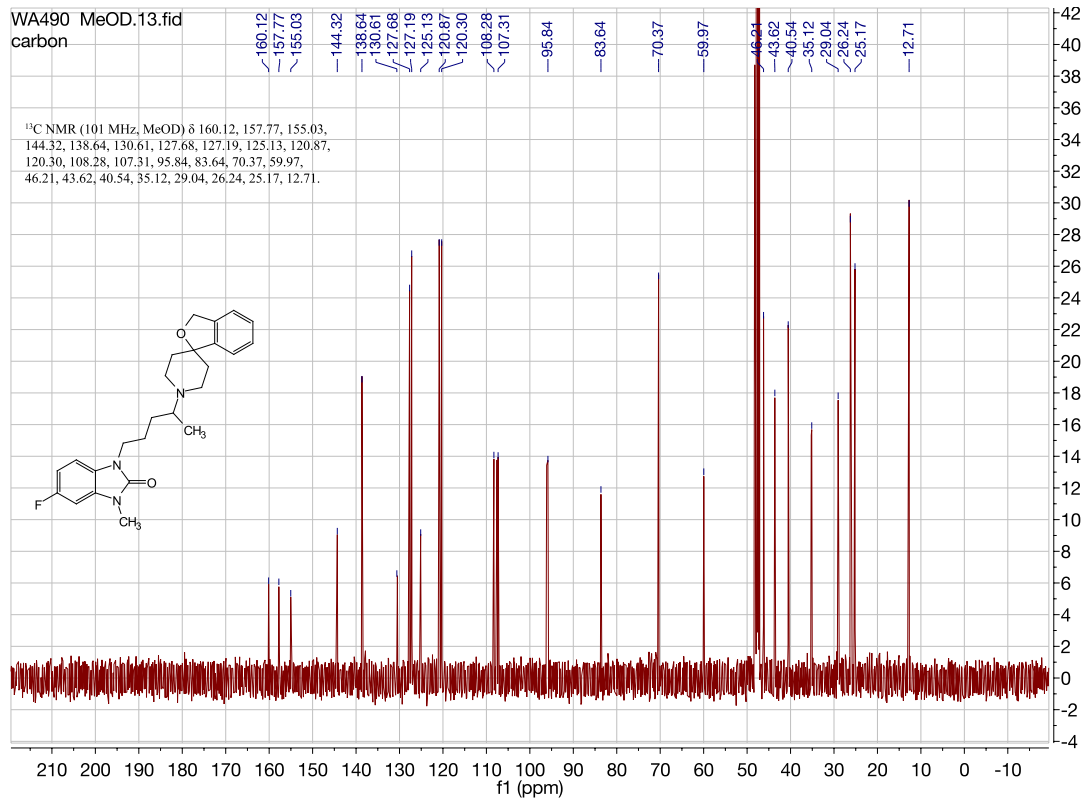
WA489 MeOD.135.fid
dept135

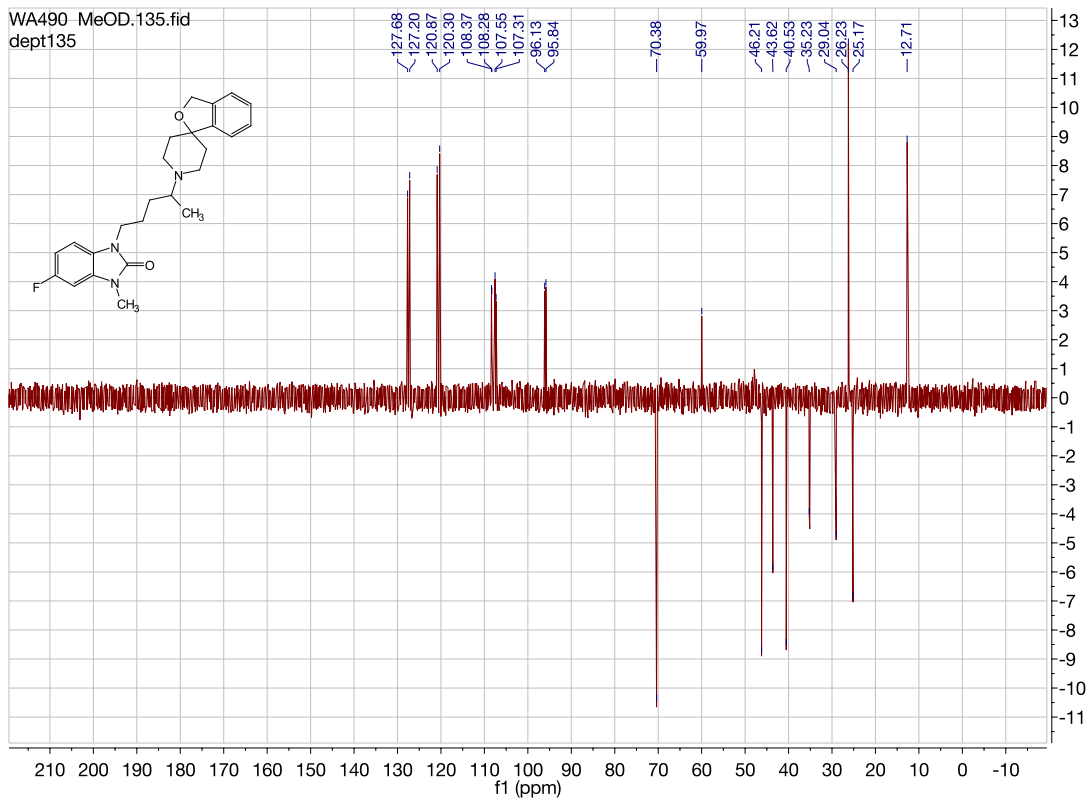


1-(4-(3H-spiro[isobenzofuran-1,4'-piperidin]-1'-yl)pentyl)-5-fluoro-3-methyl-1,3-dihydro-2H-benzo[d]imidazol-2-one. (WA490)

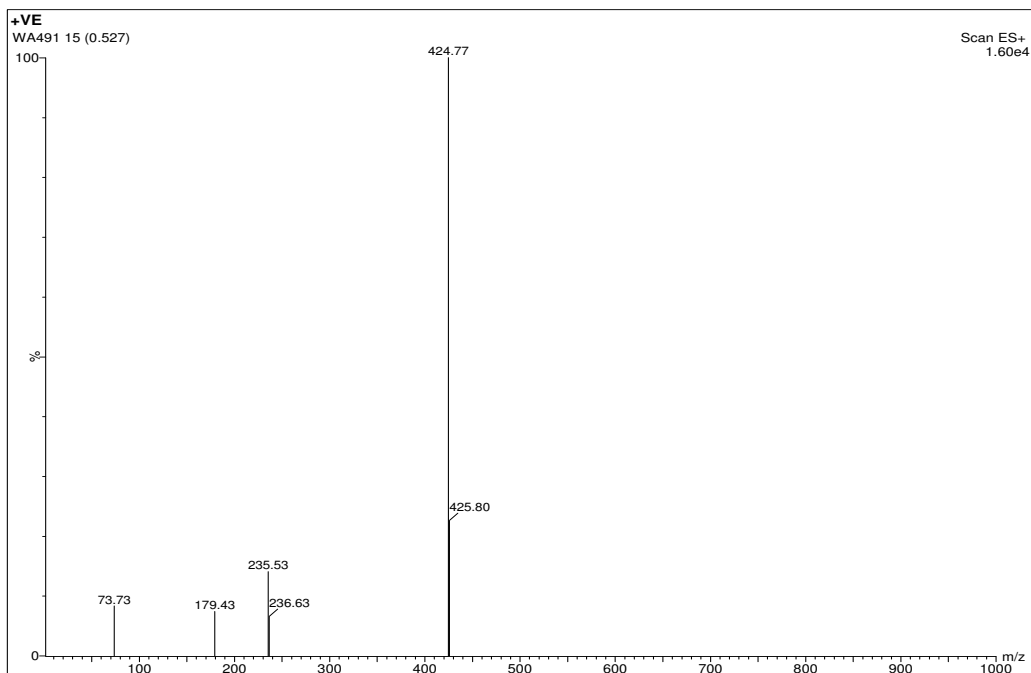


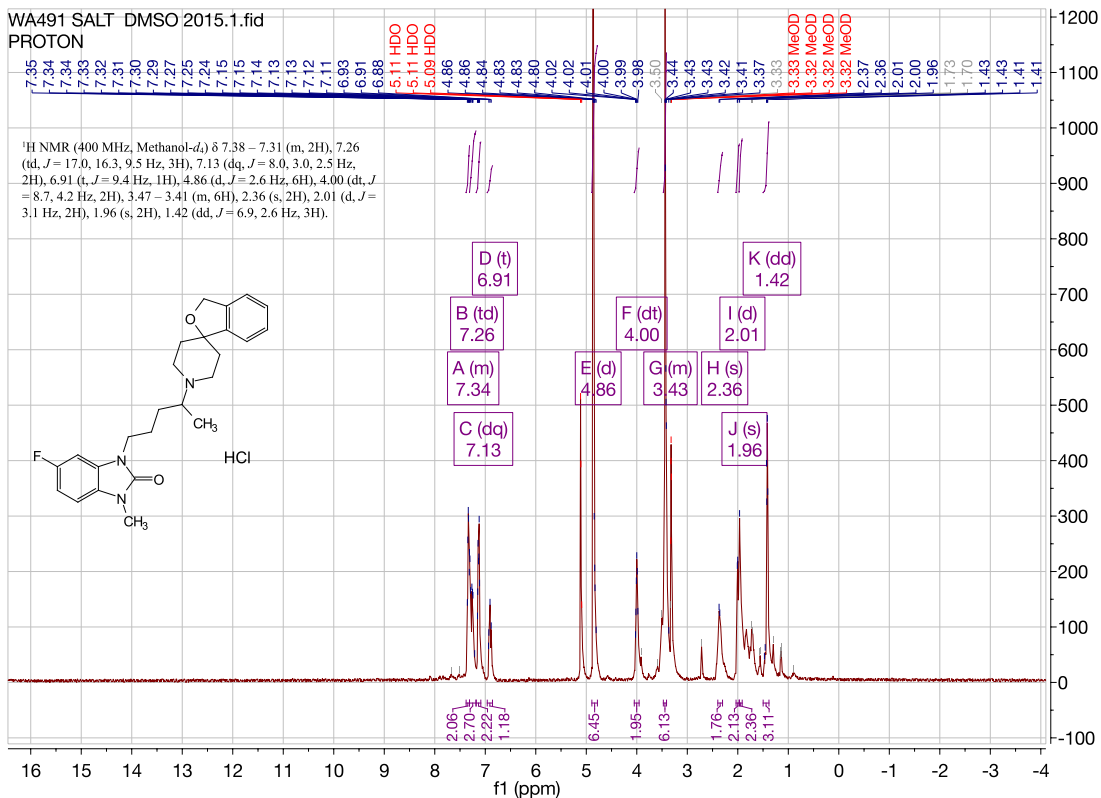
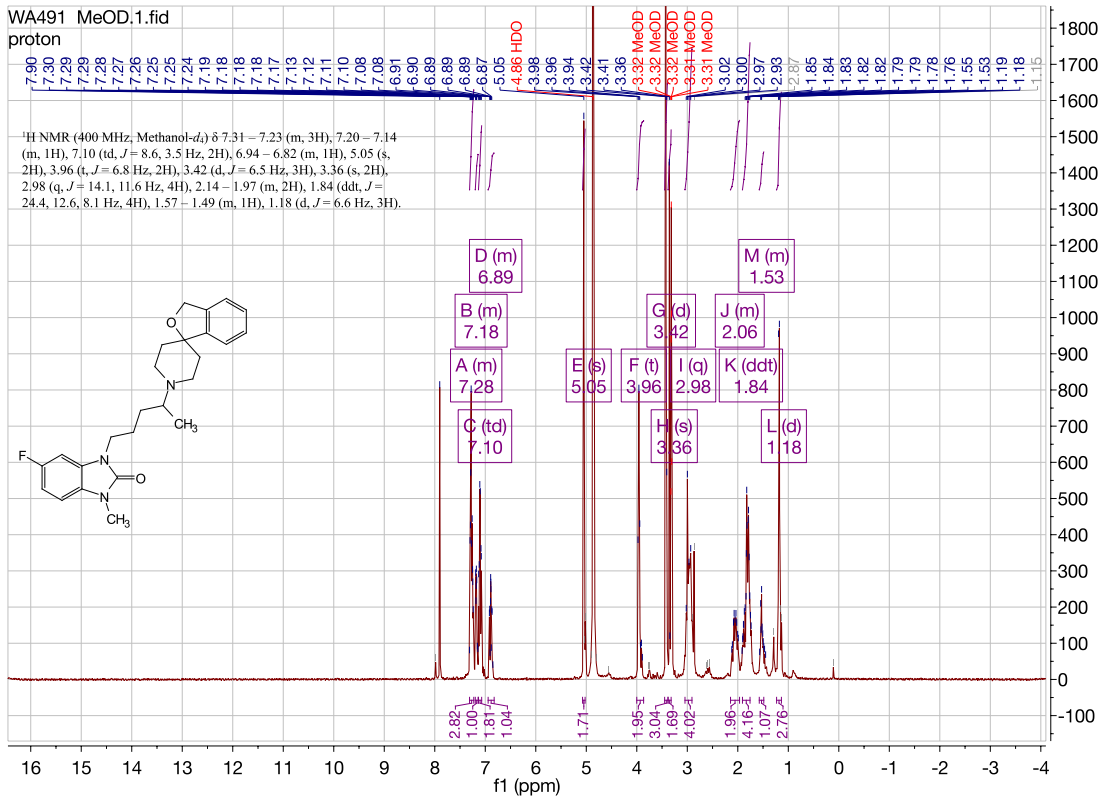
WA490 MeOD.13.fid
carbon



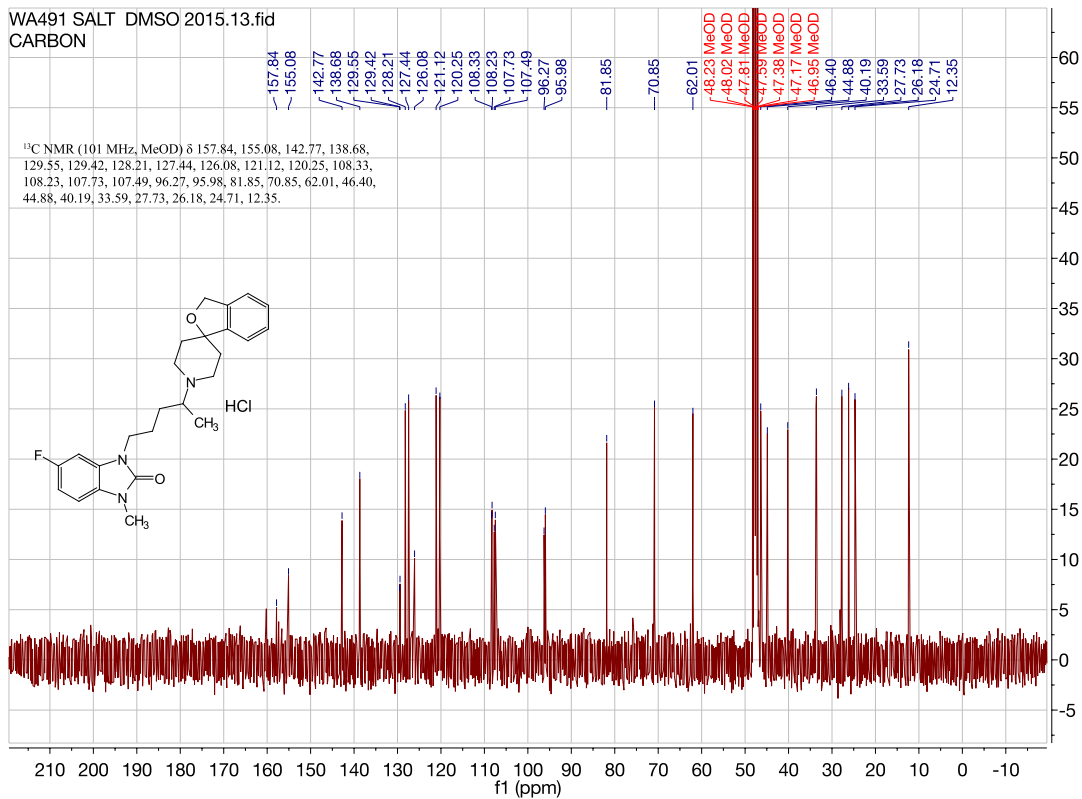


3-(4-(3H-spiro[isobenzofuran-1,4'-piperidin]-1'-yl)pentyl)-5-fluoro-1-methyl-1,3-dihydro-2H-benzo[d]imidazol-2-one. (WA491)

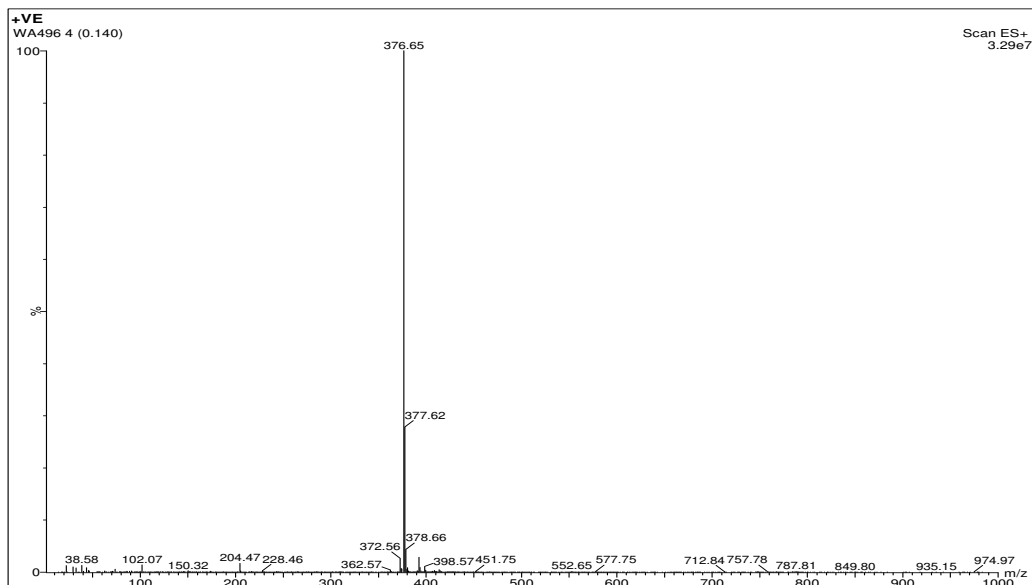


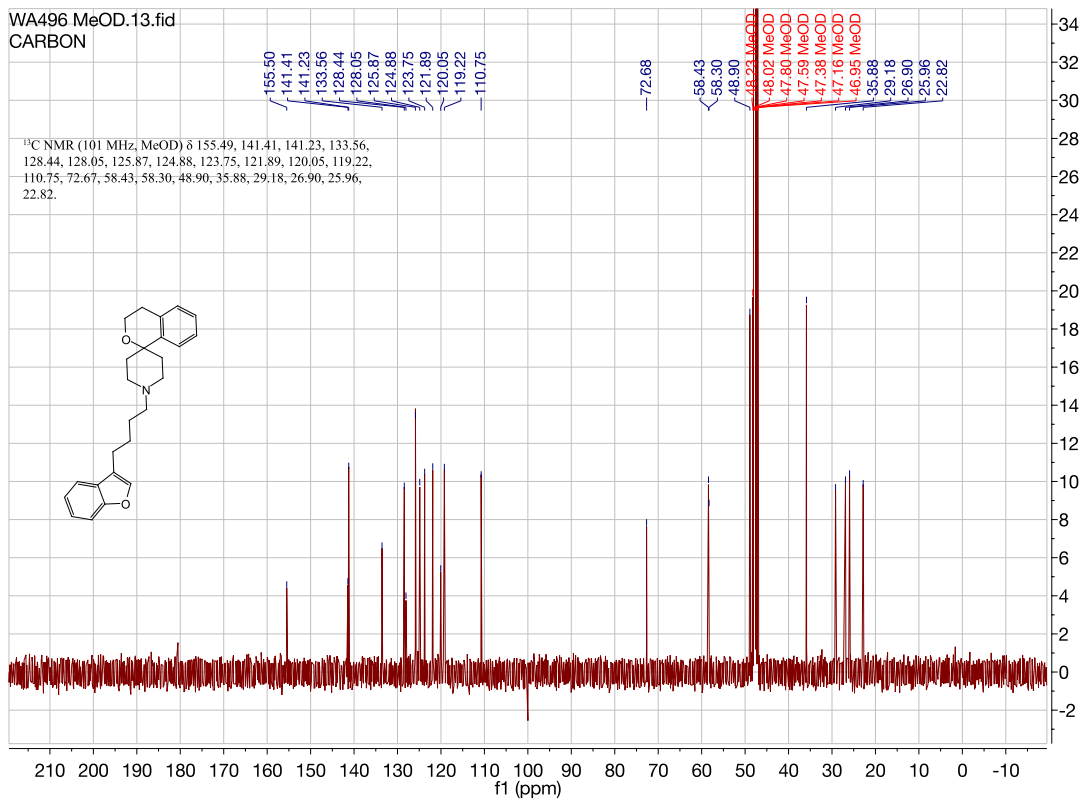
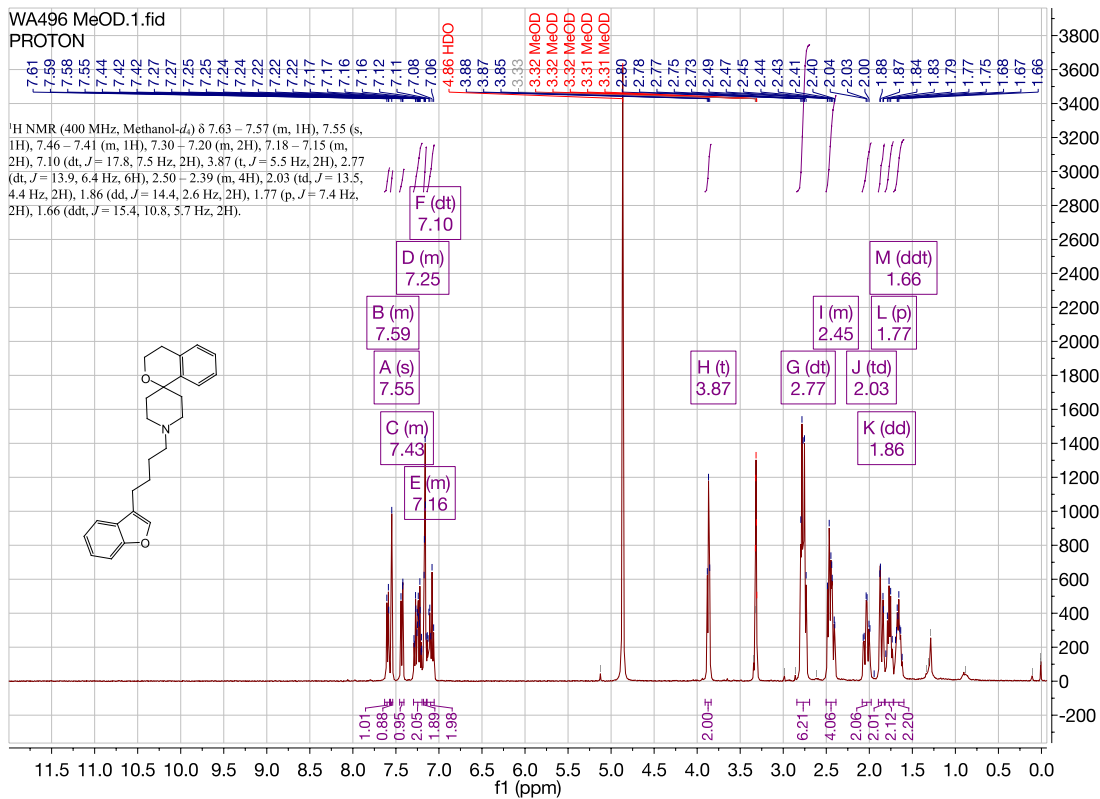


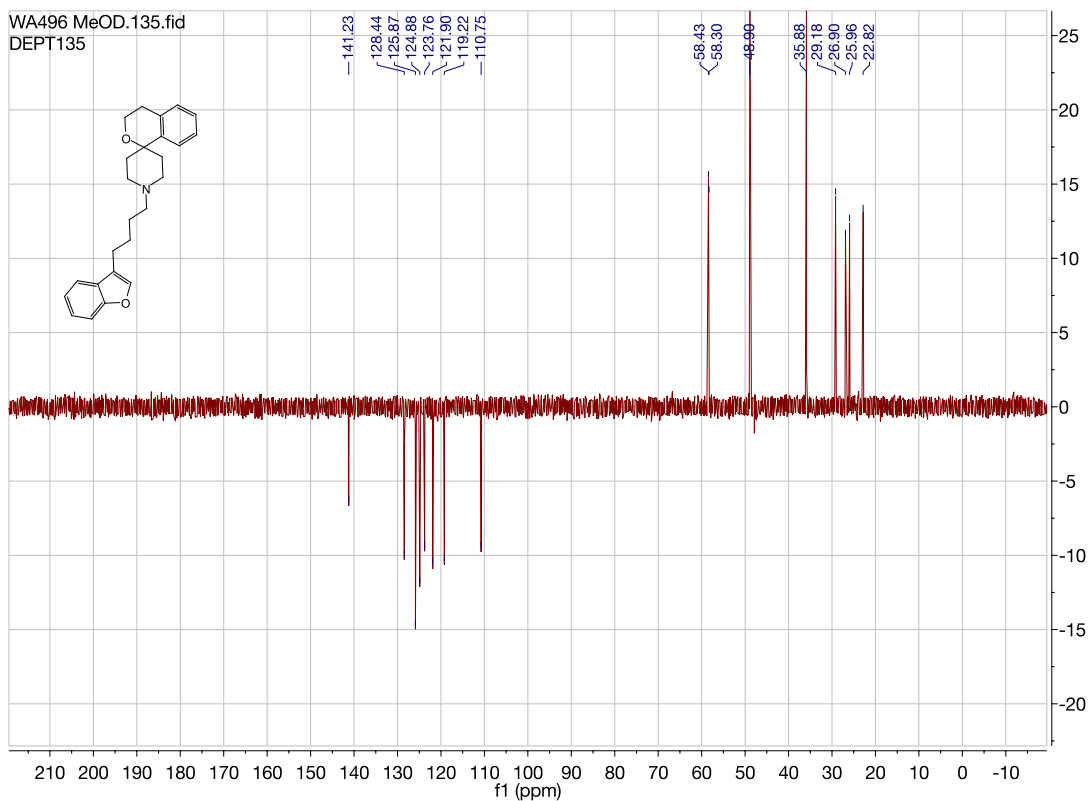
WA491 SALT DMSO 2015.13.fid
CARBON



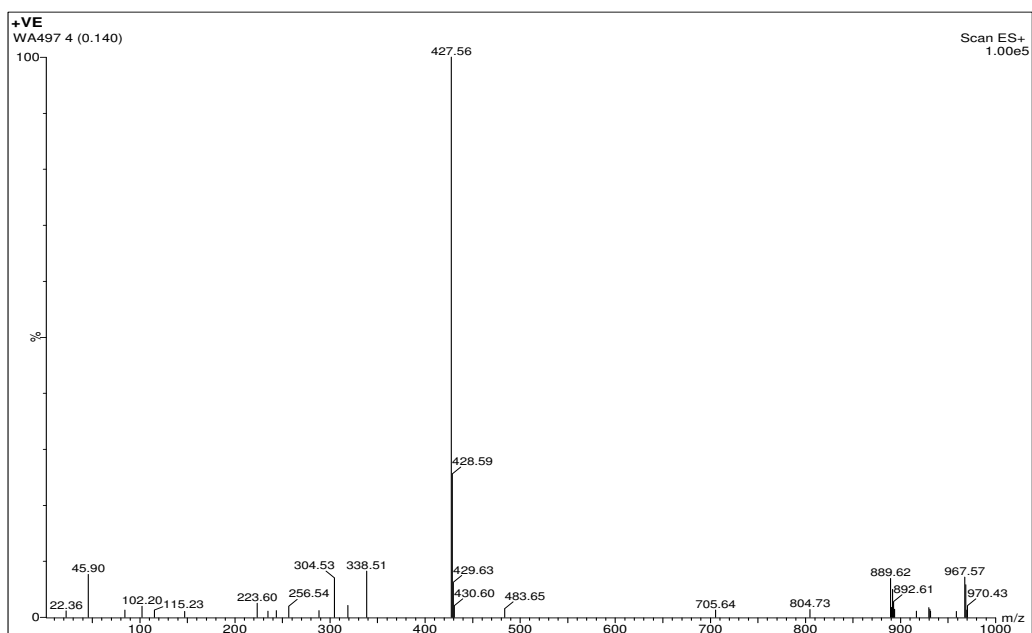
1'-(4-(benzofuran-3-yl)butyl)spiro[isochromane-1,4'-piperidine]. (WA496)

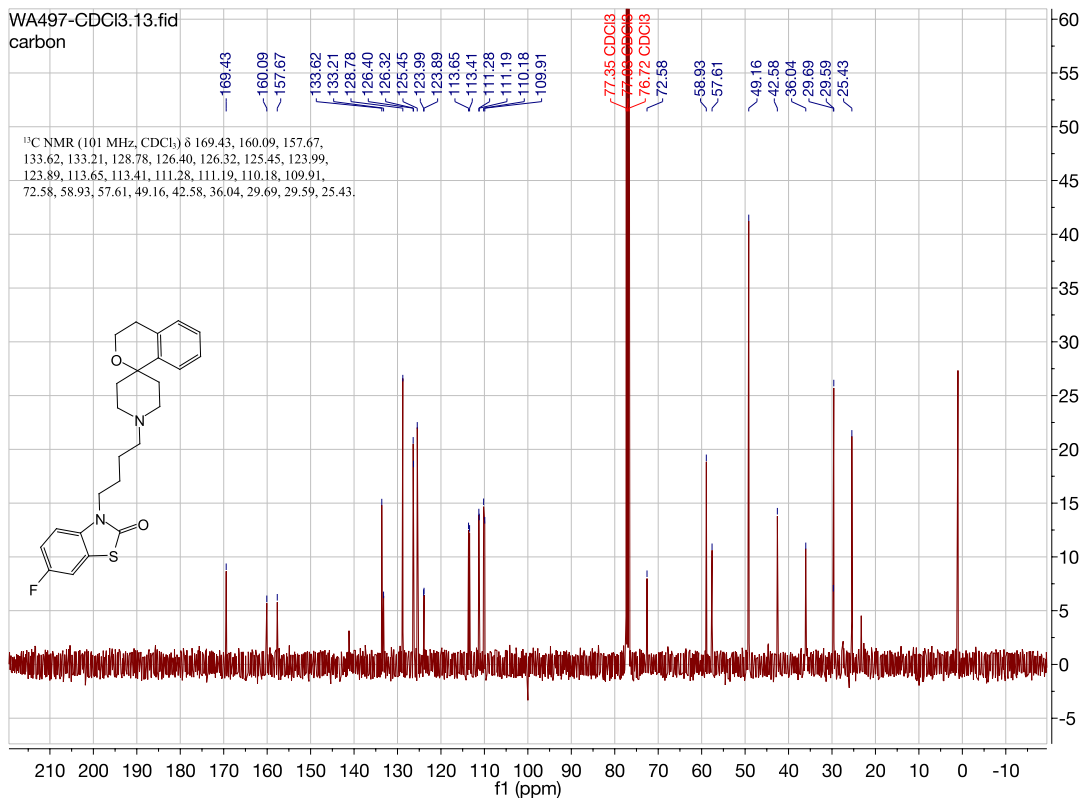
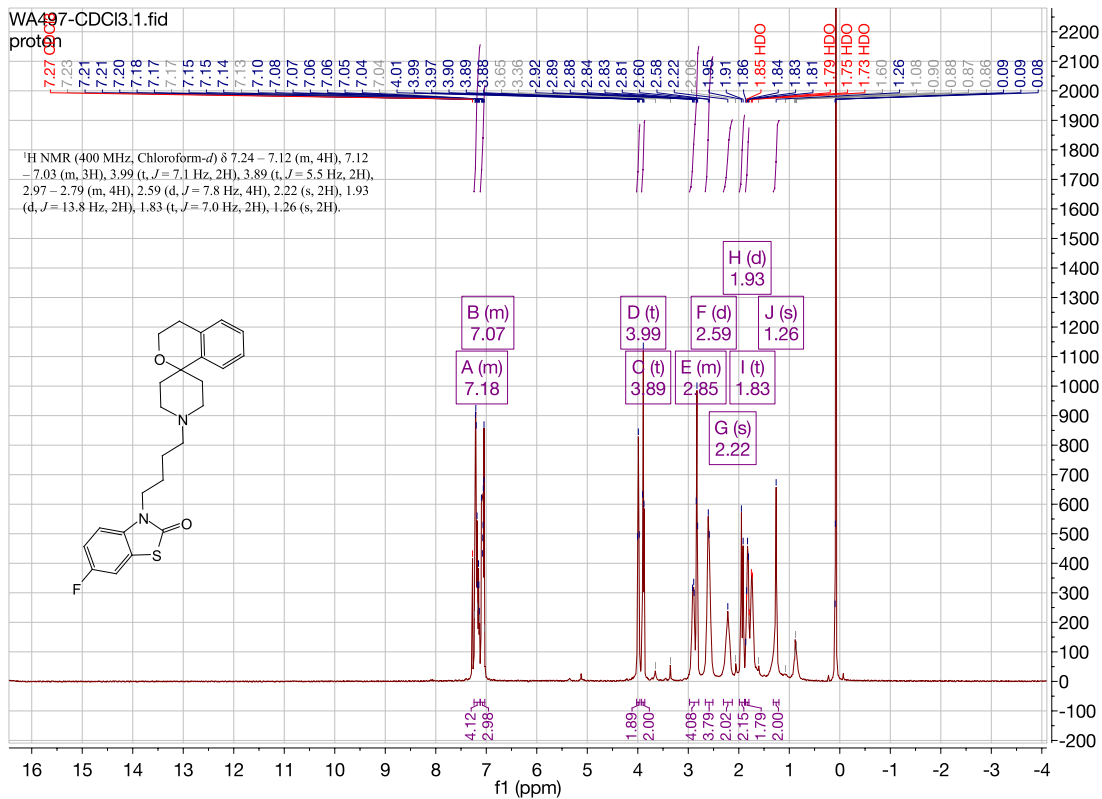


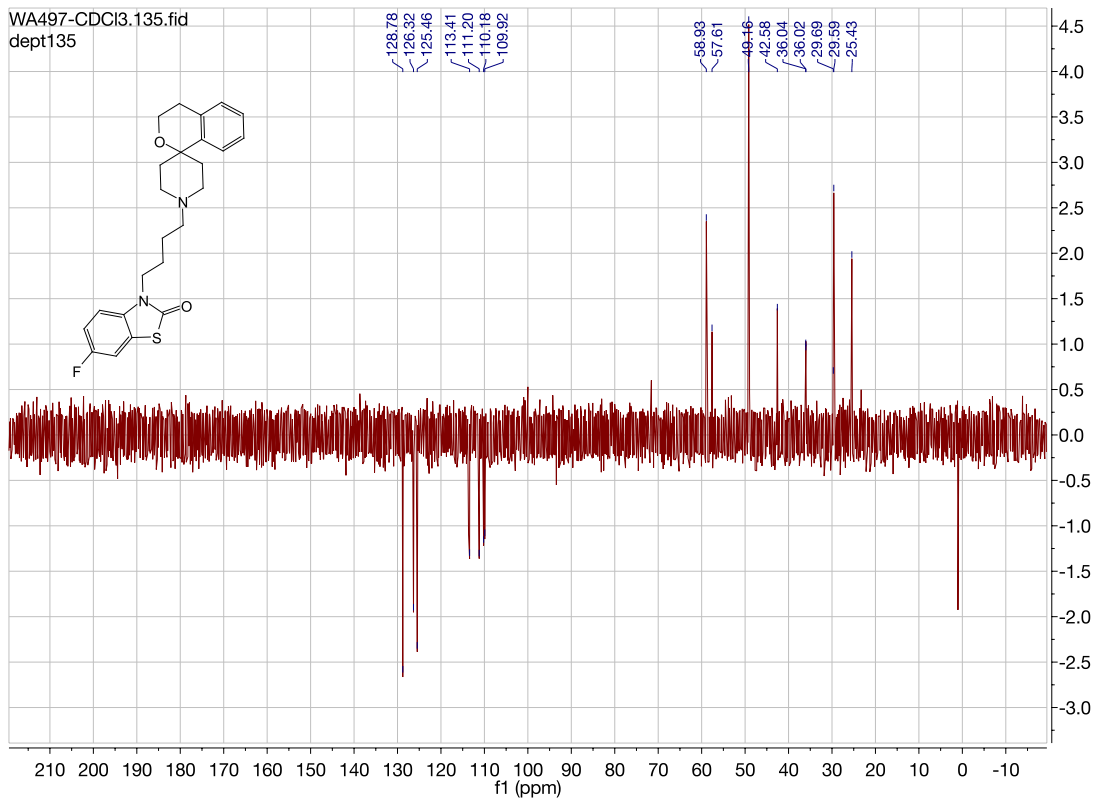




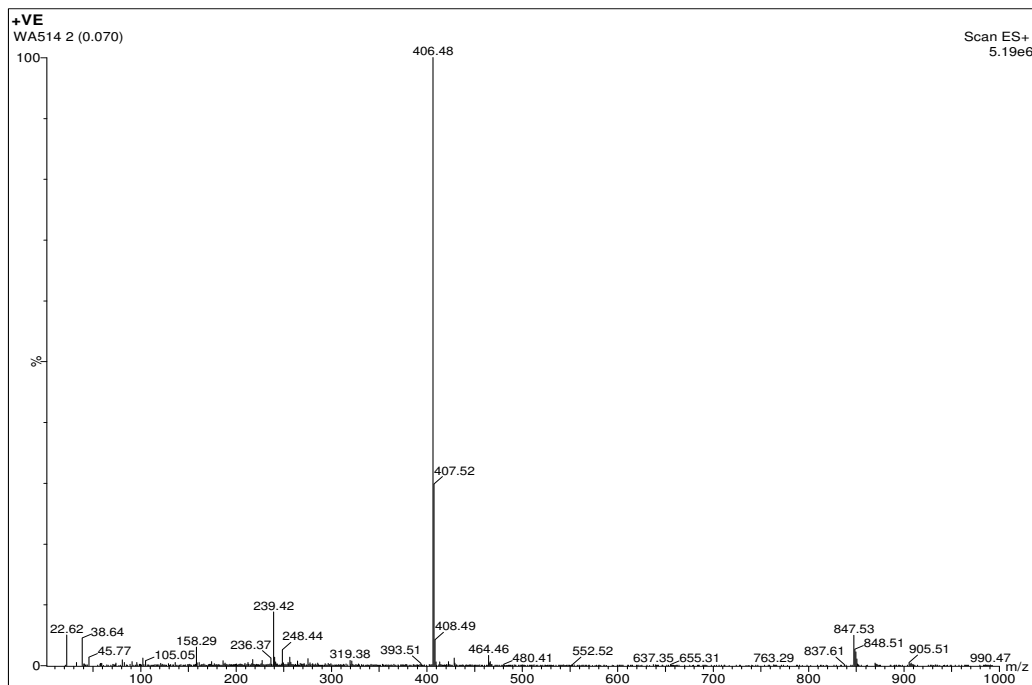
6-fluoro-3-(4-(spiro[isochromane-1,4'-piperidin]-1'-yl)butyl)benzo[d]thiazol-2(3H)-one. (WA497)

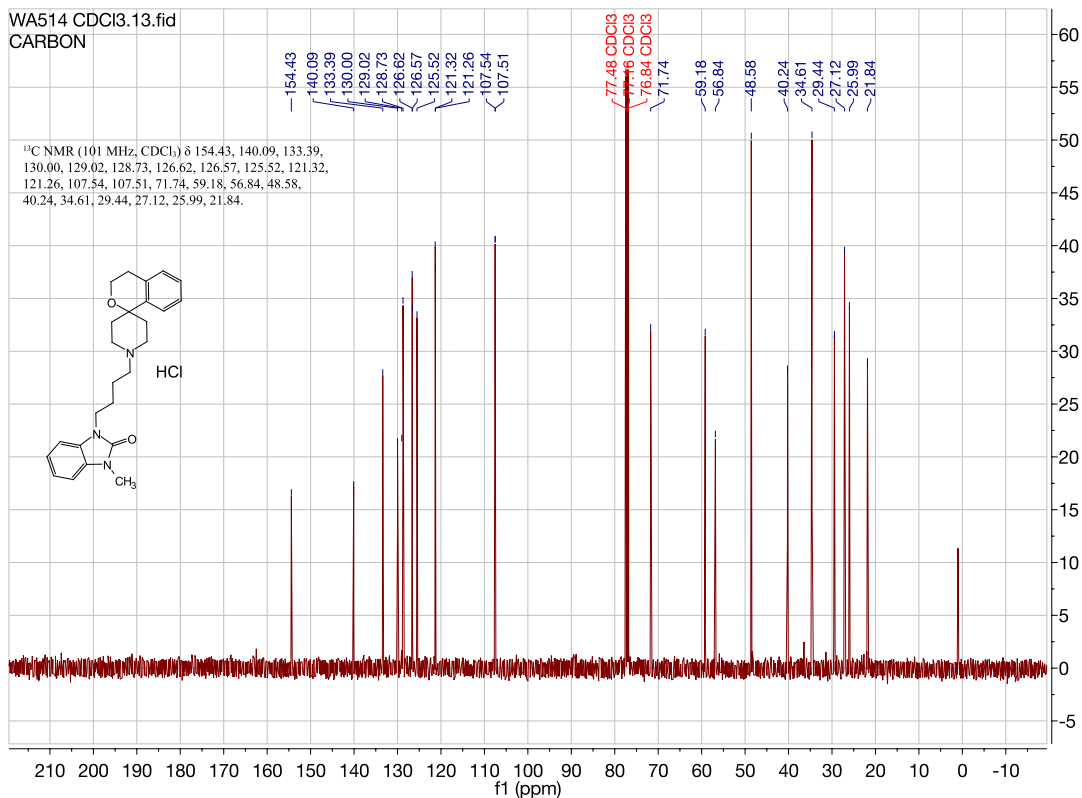
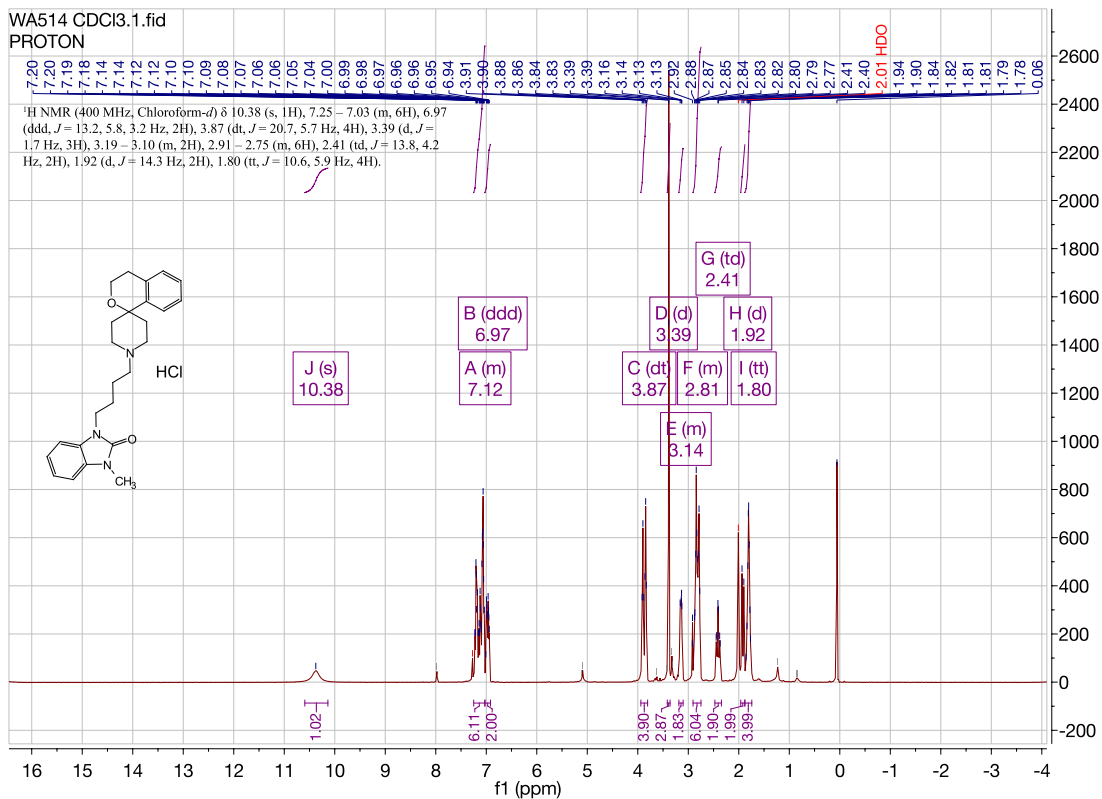


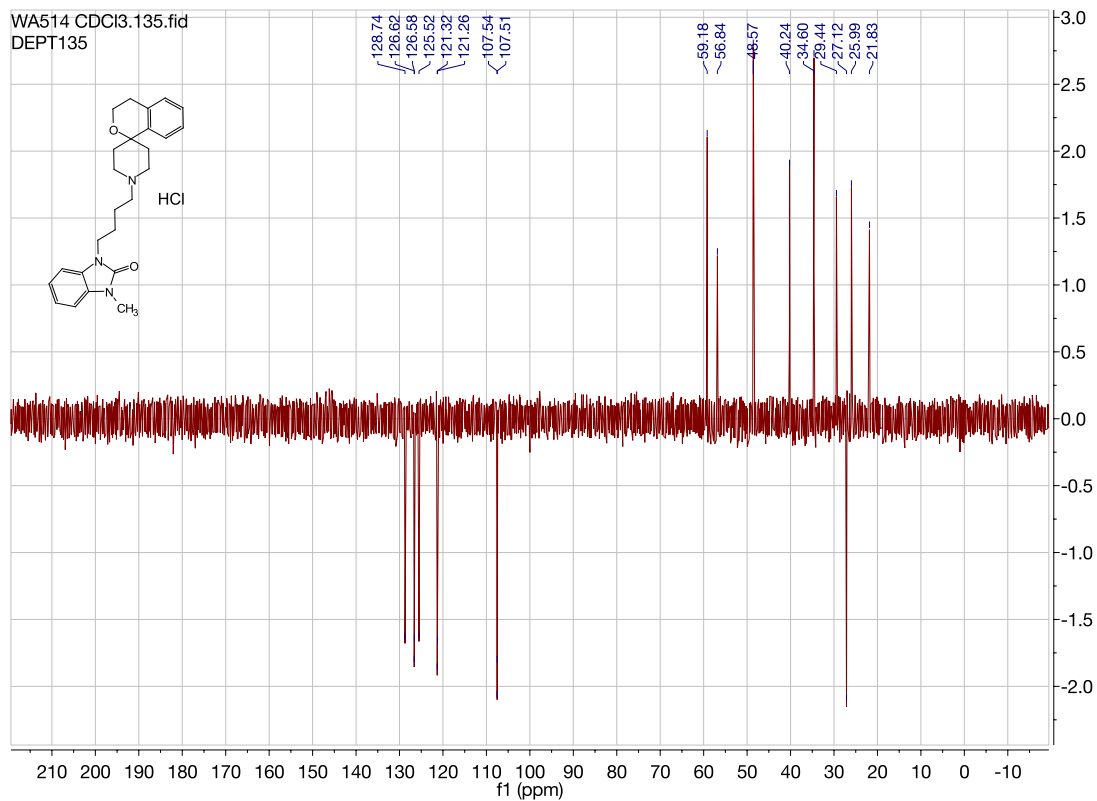




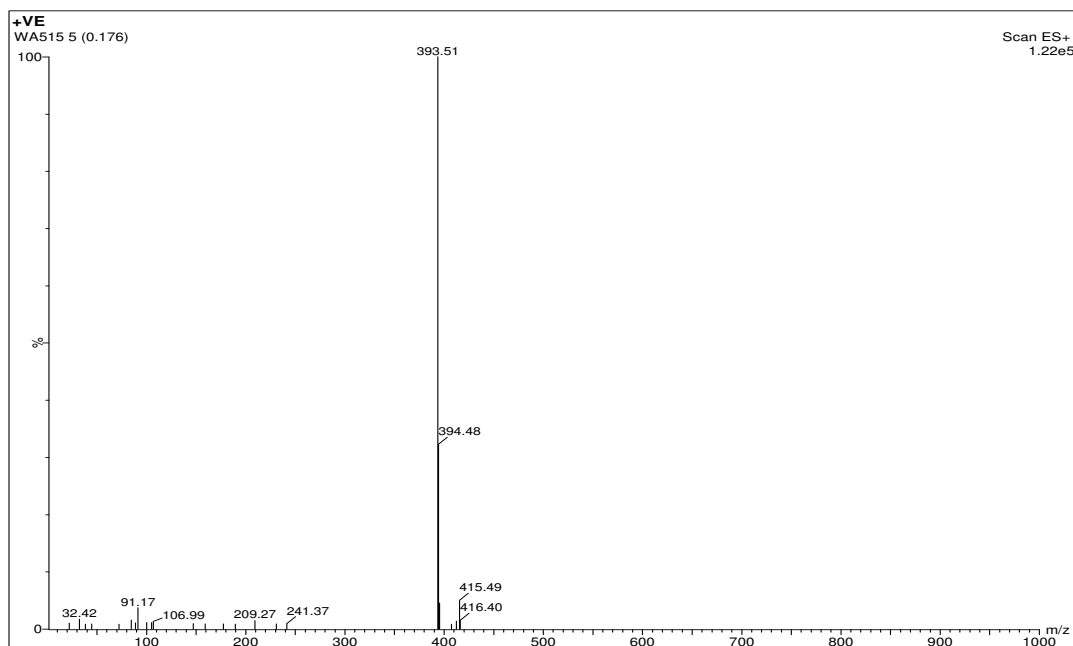
1-methyl-3-(4-(spiro[isochromane-1,4'-piperidin]-1'-yl)butyl)-1,3-dihydro-2H-benzo[d]imidazol-2-one. (WA514)

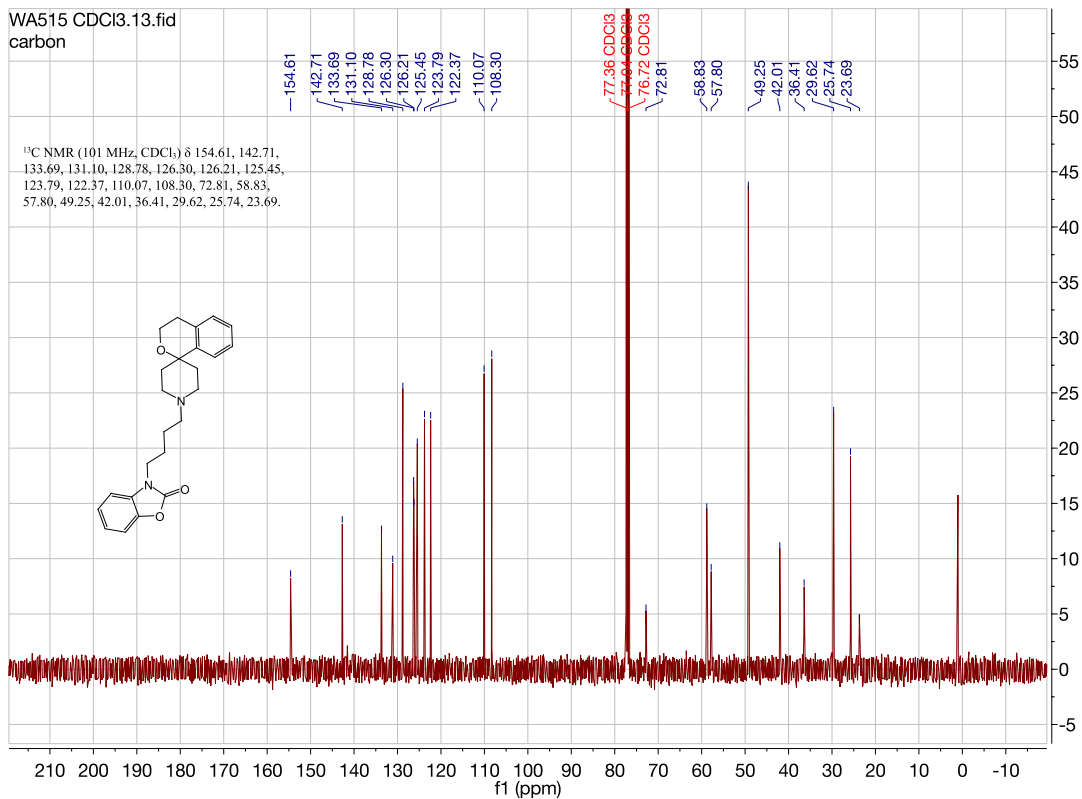
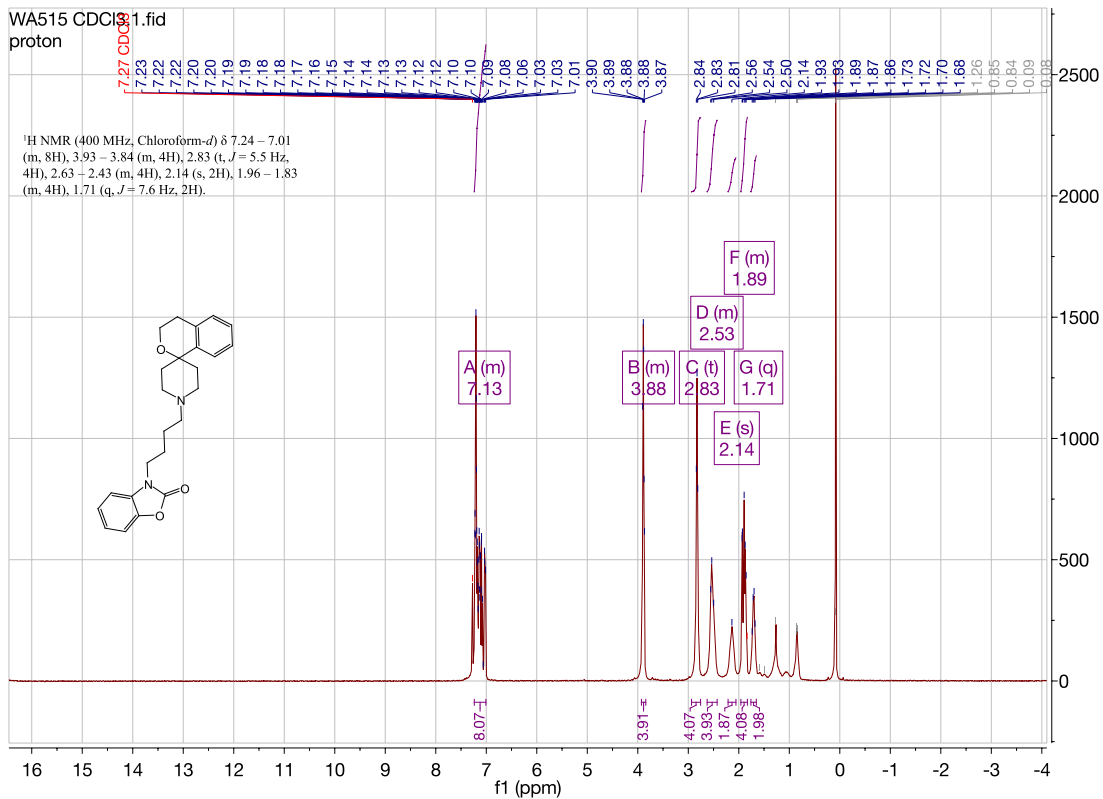


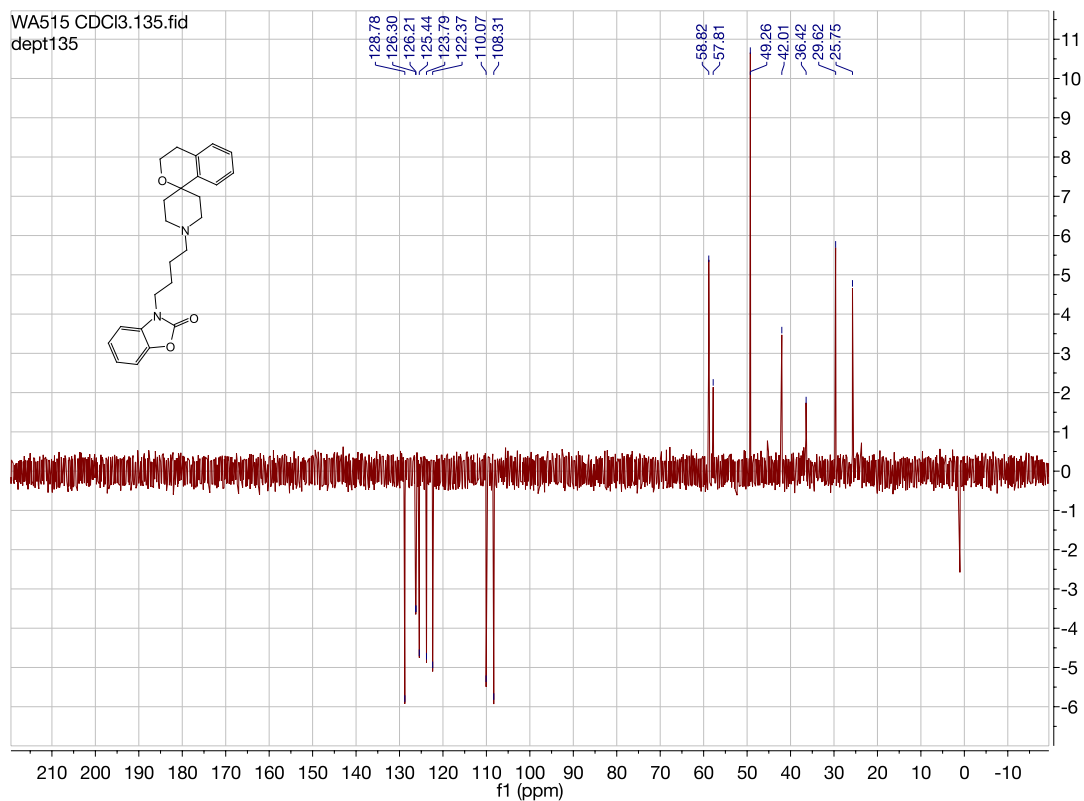




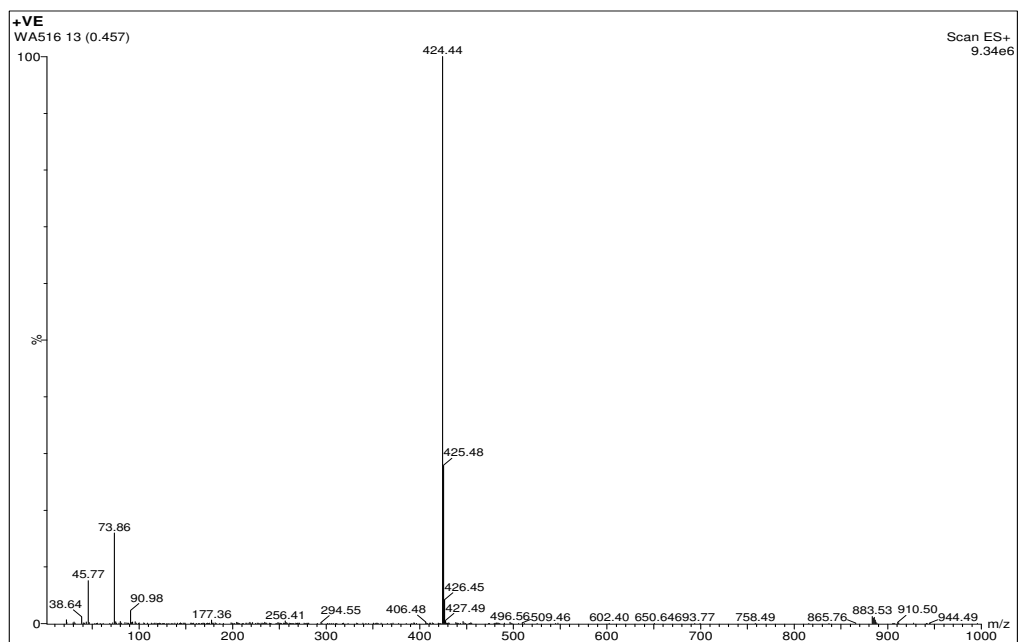
**3-(4-(spiro[isochromane-1,4'-piperidin]-1'-yl)butyl)benzo[d]oxazol-2(3H)-one.
(WA515)**

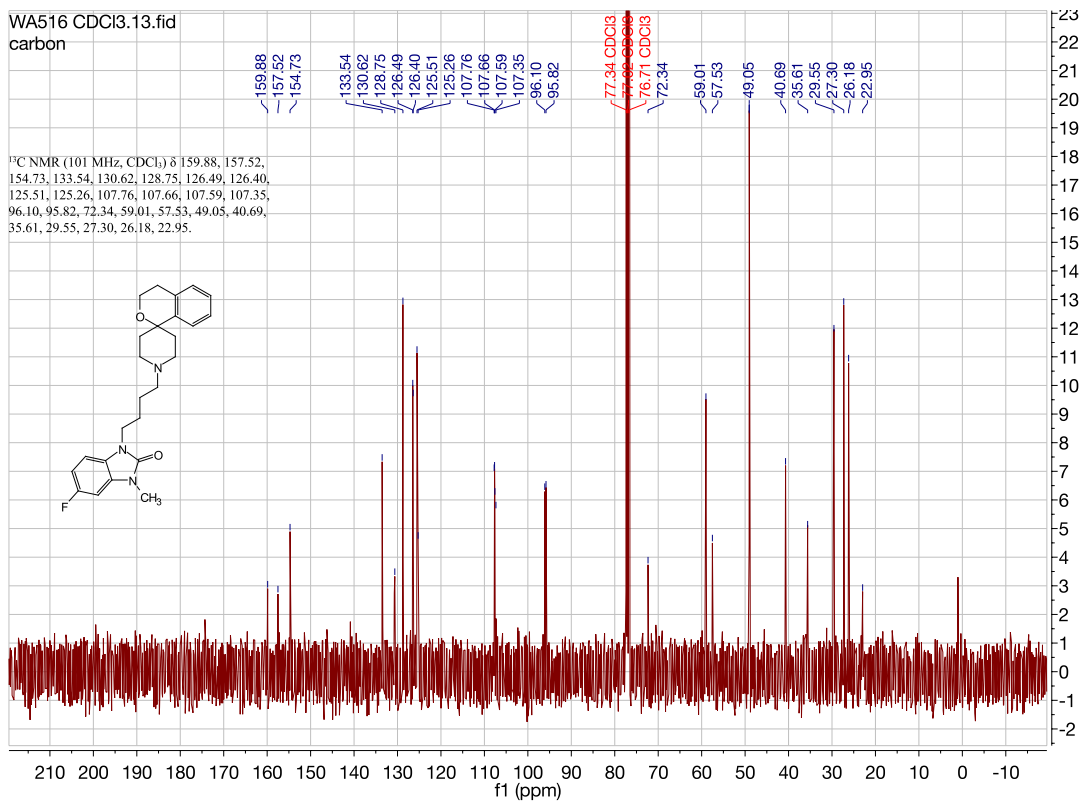
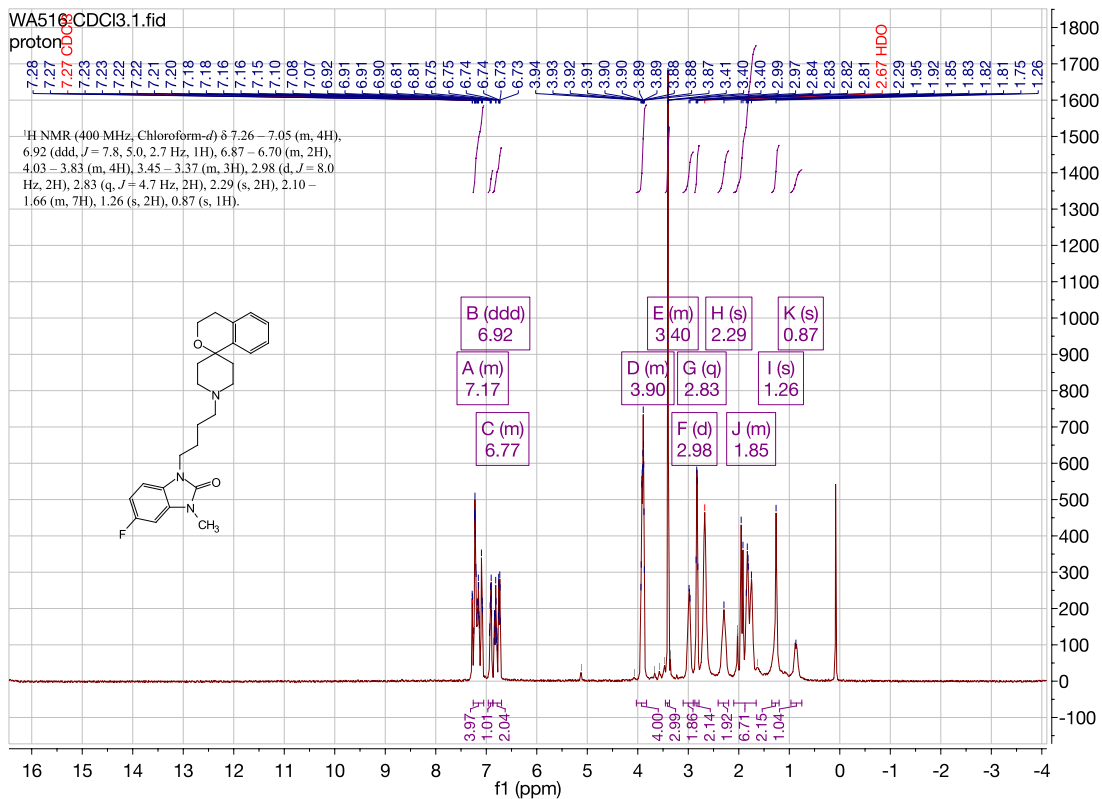


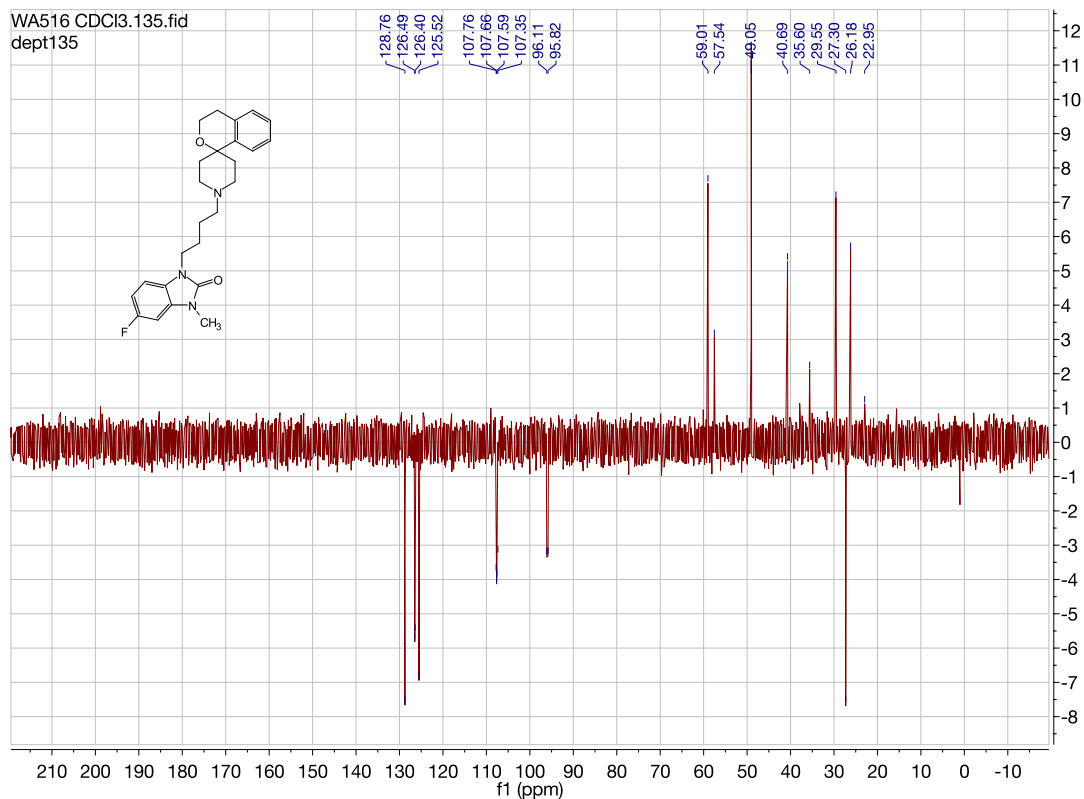




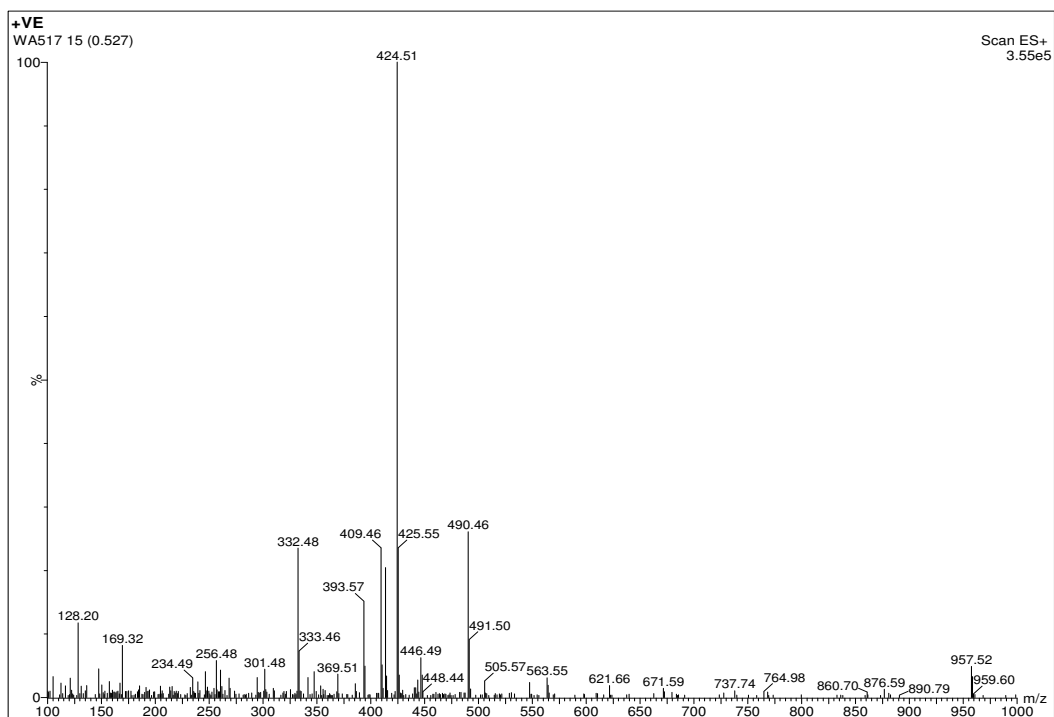
5-fluoro-3-methyl-1-(4-(spiro[isochromane-1,4'-piperidin]-1'-yl)butyl)-1,3-dihydro-2H-benzo[d]imidazol-2-one. (WA516)

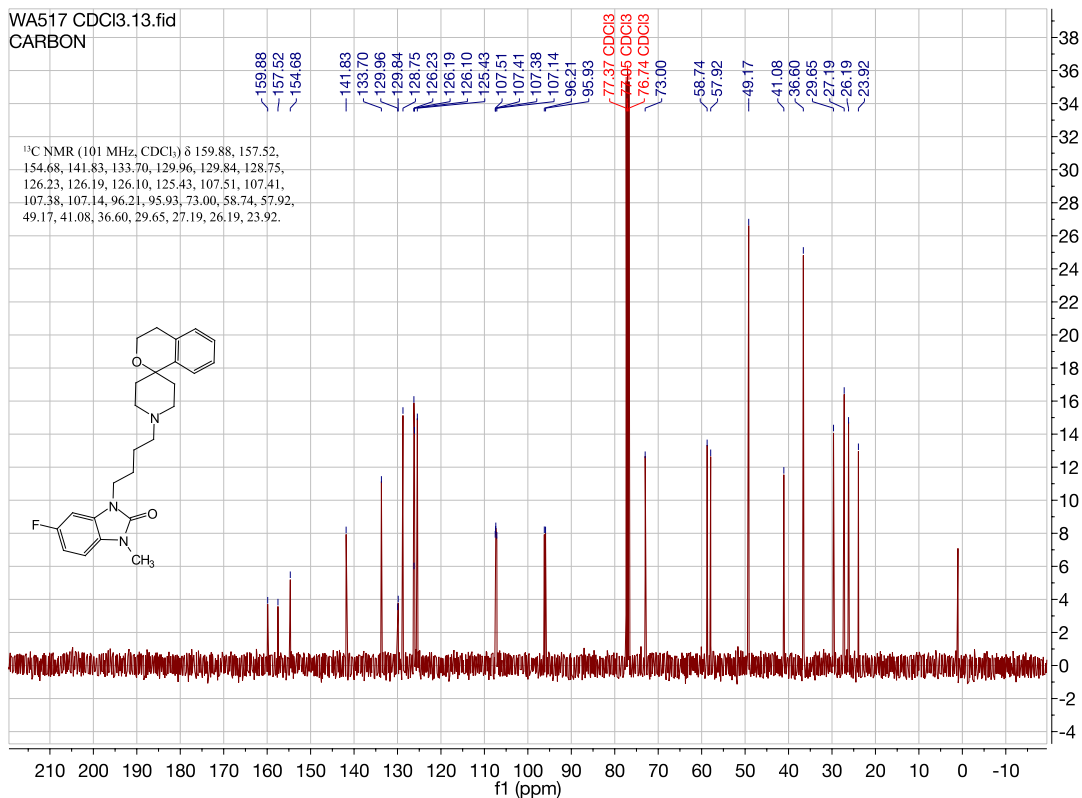
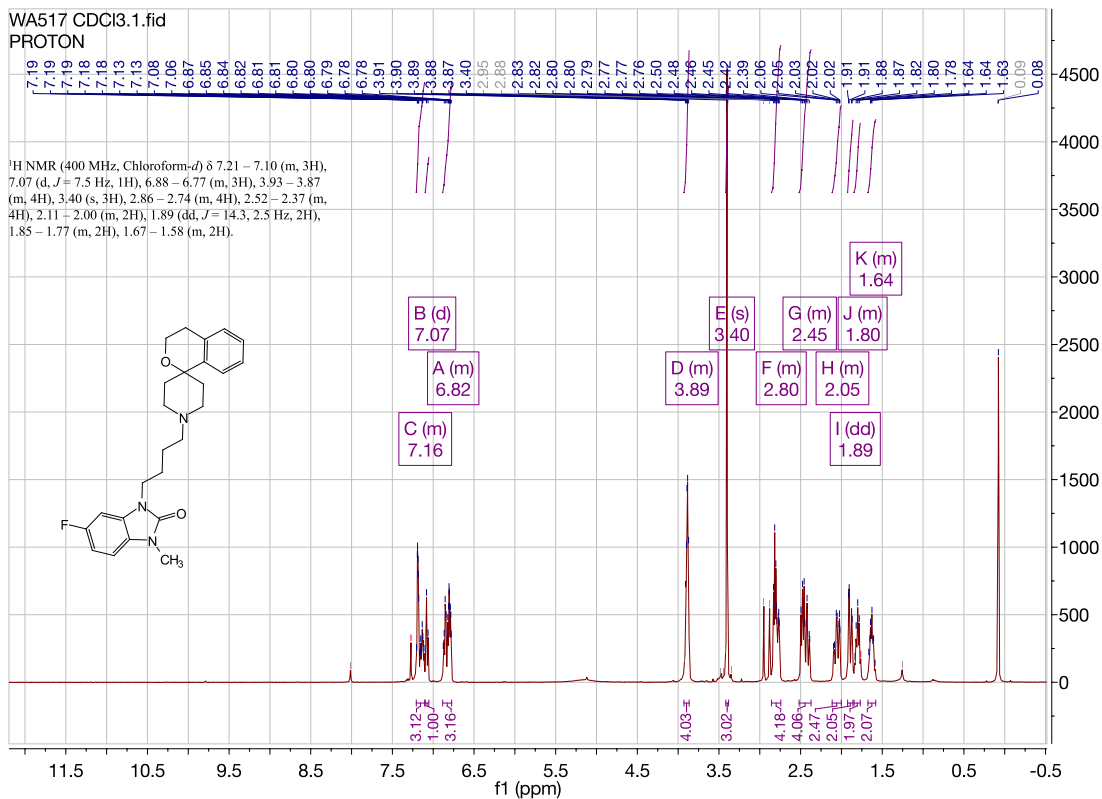


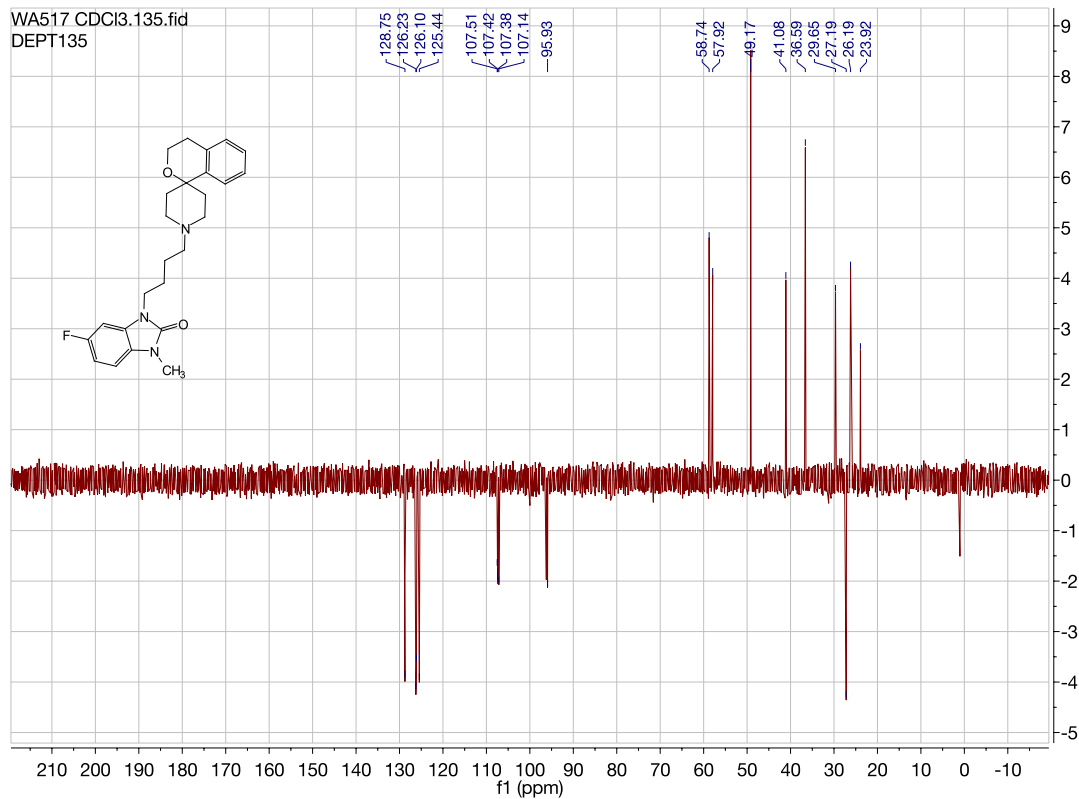




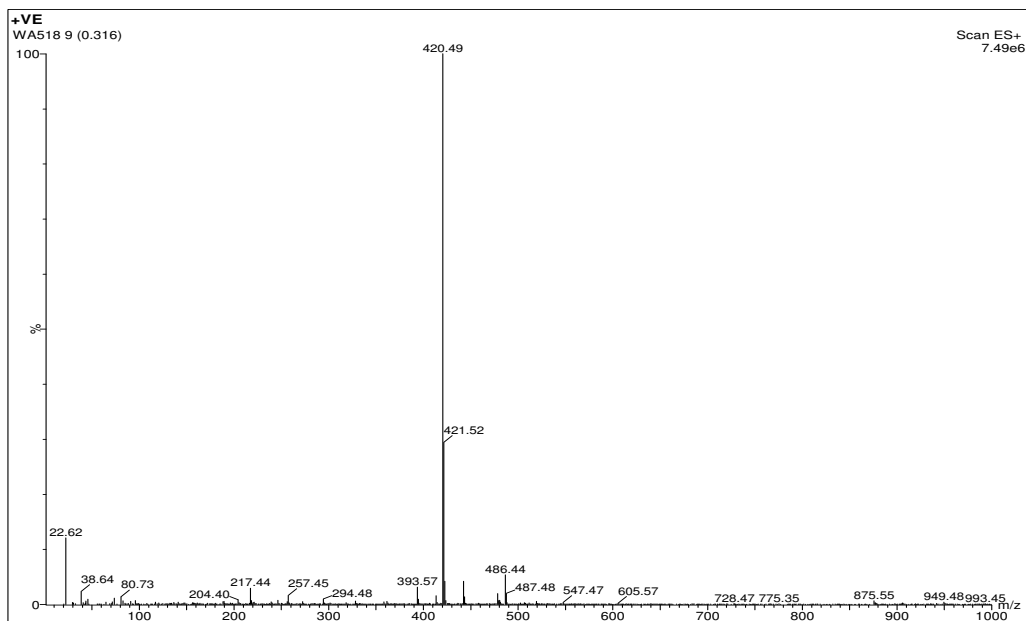
5-fluoro-1-methyl-3-(4-(spiro[isochromane-1,4'-piperidin]-1'-yl)butyl)-1,3-dihydro-2H-benzo[d]imidazol-2-one. (WA517)

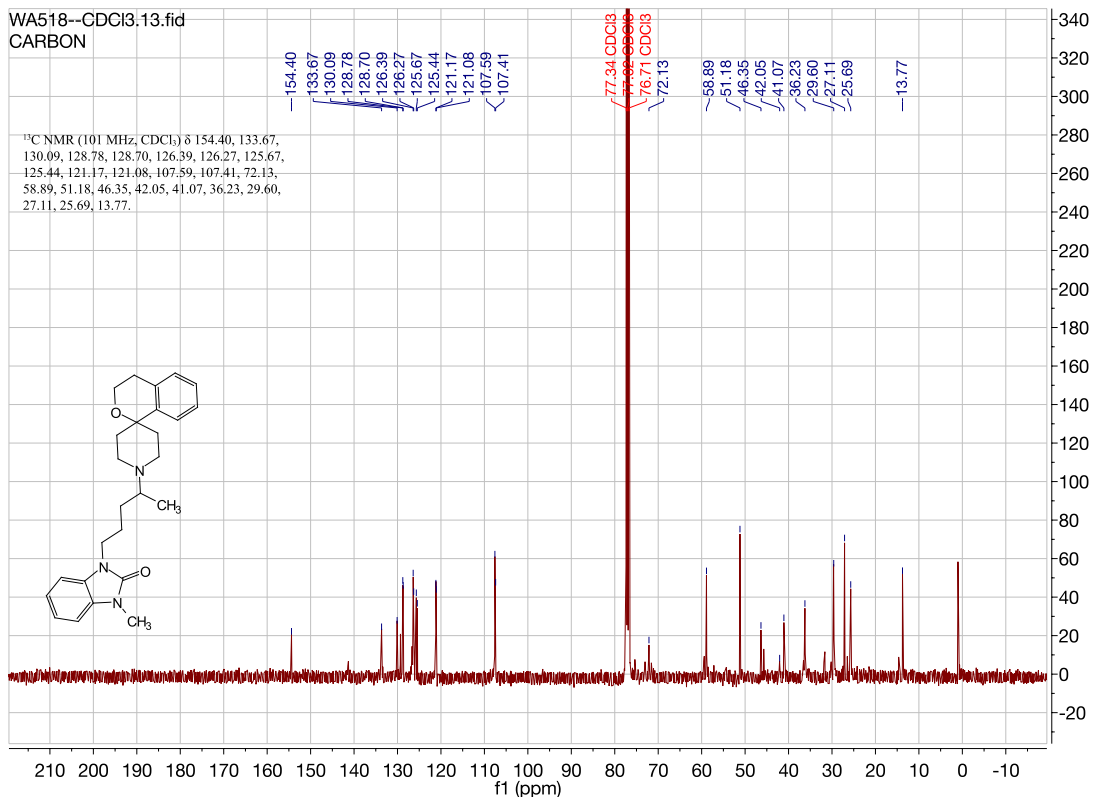
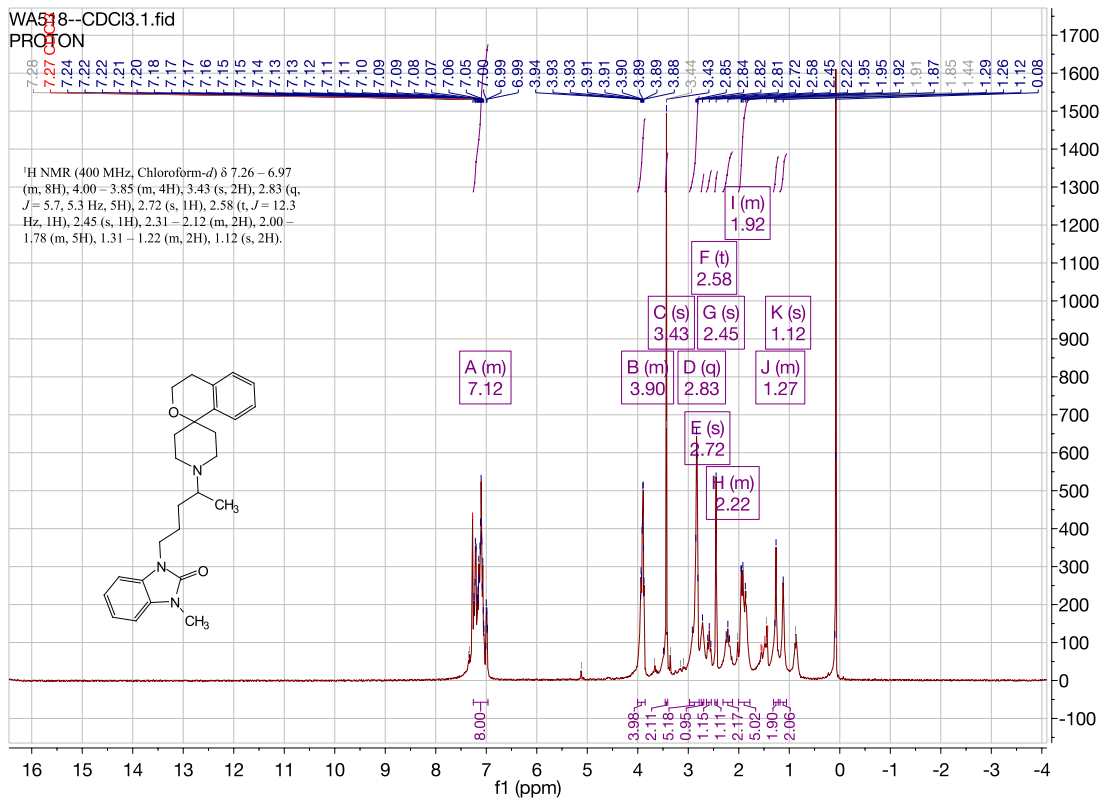


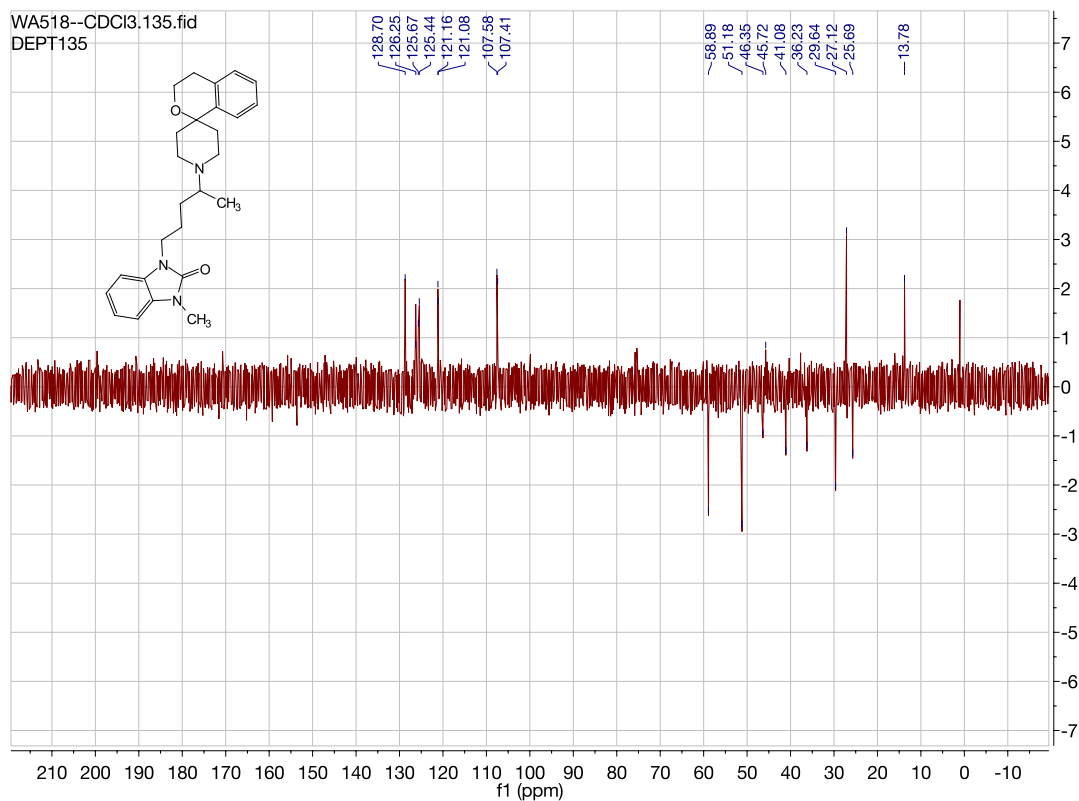




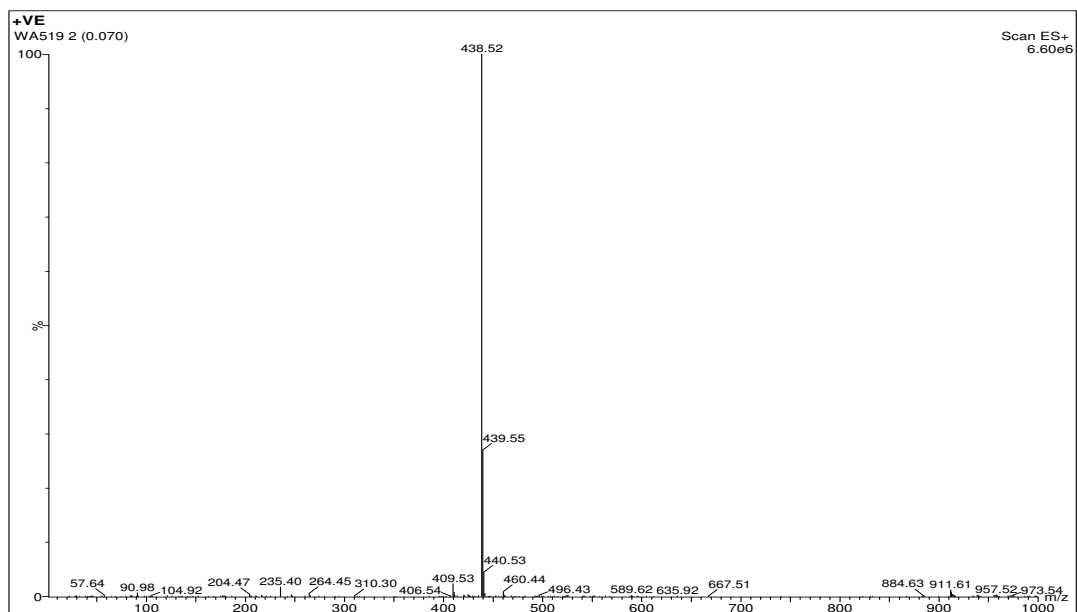
1-methyl-3-(4-(spiro[isochromane-1,4'-piperidin]-1'-yl)pentyl)-1,3-dihydro-2H-benzo[d]imidazol-2-one. (WA518)

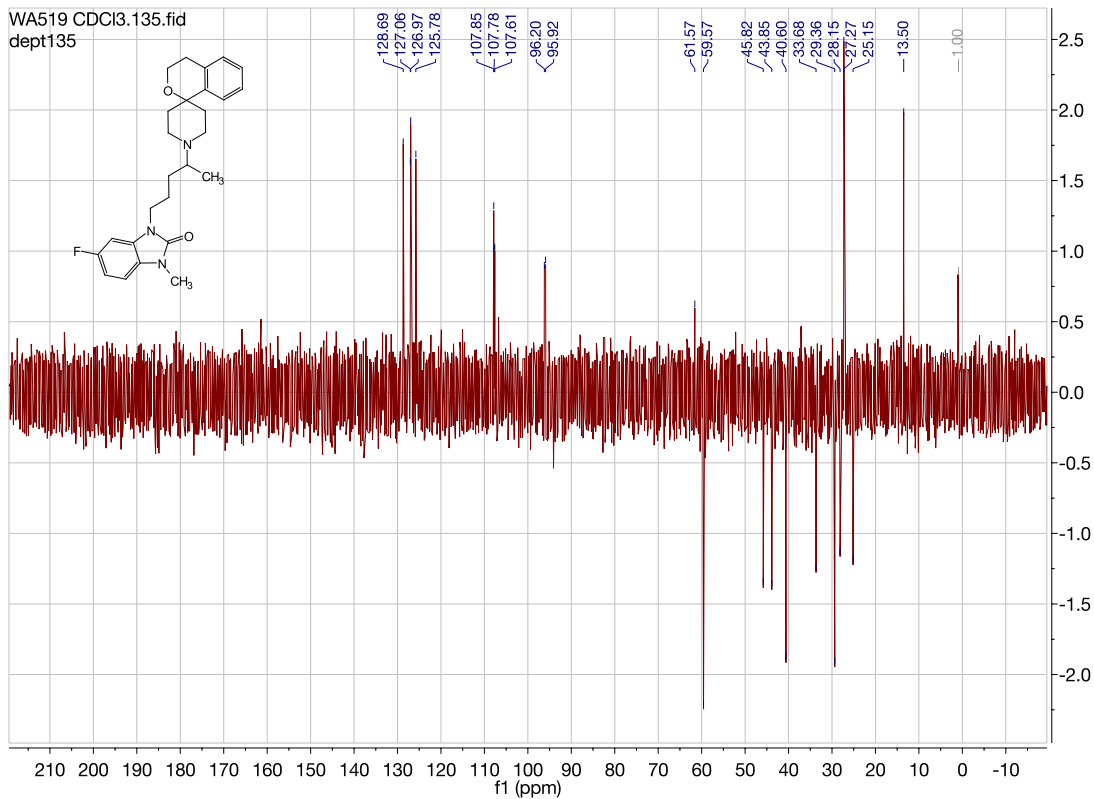




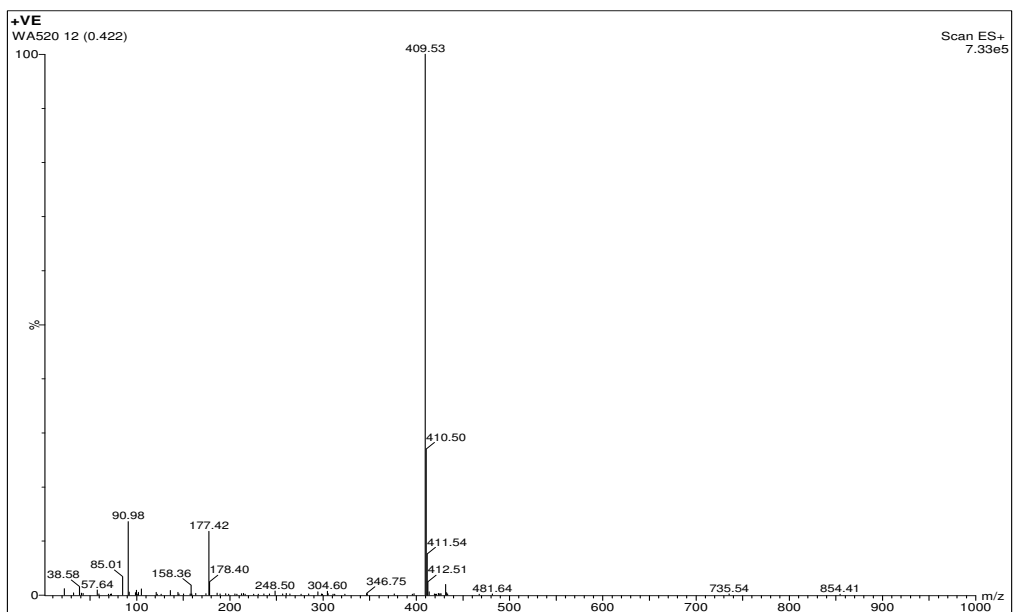


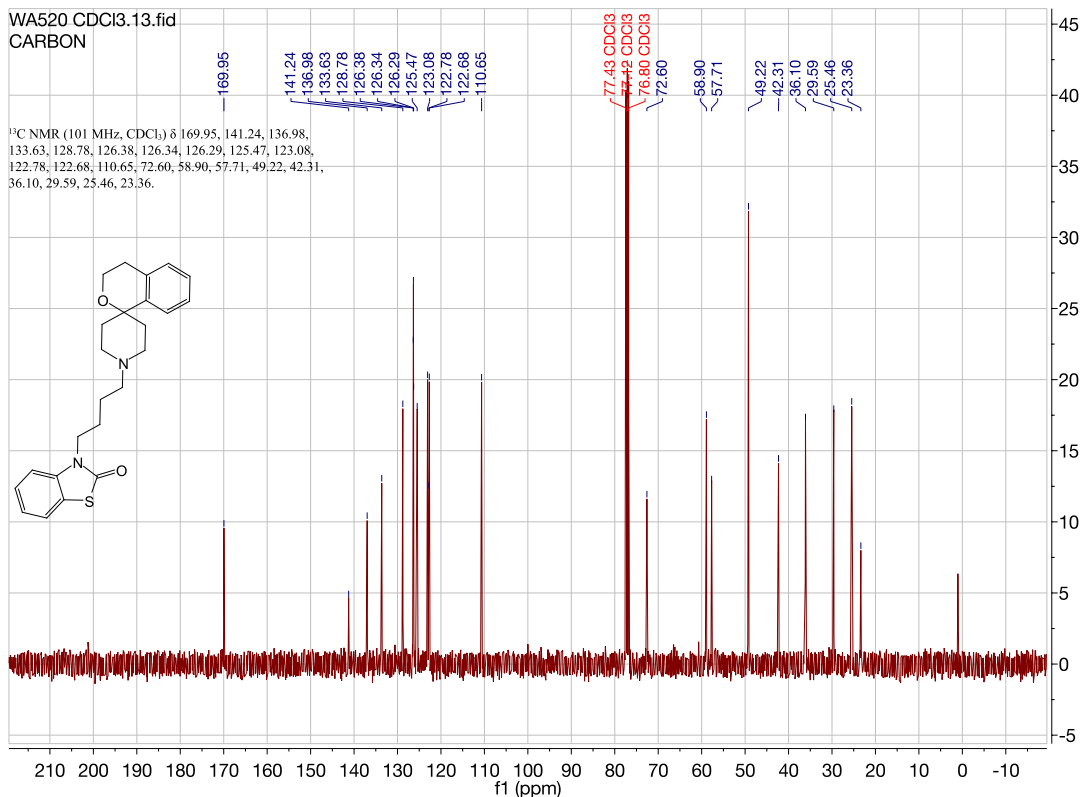
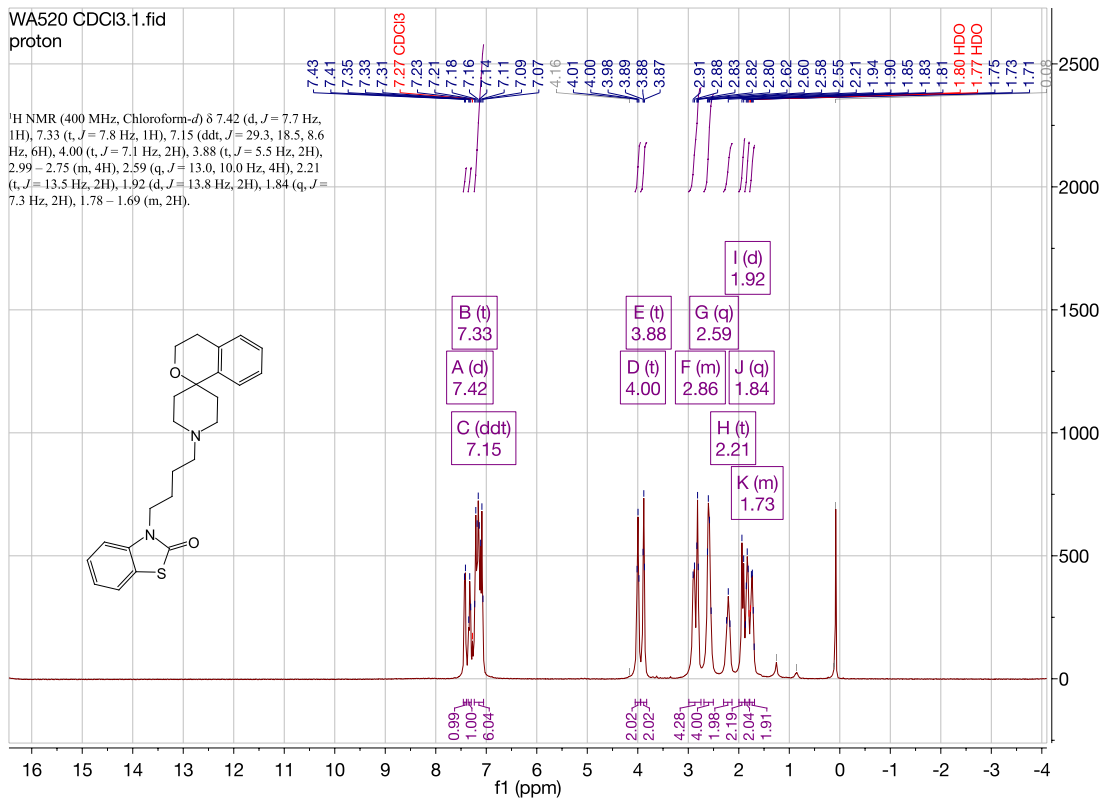
5-fluoro-1-methyl-3-(4-(spiro[isochromane-1,4'-piperidin]-1'-yl)pentyl)-1,3-dihydro-2H-benzo[d]imidazol-2-one. (WA519)

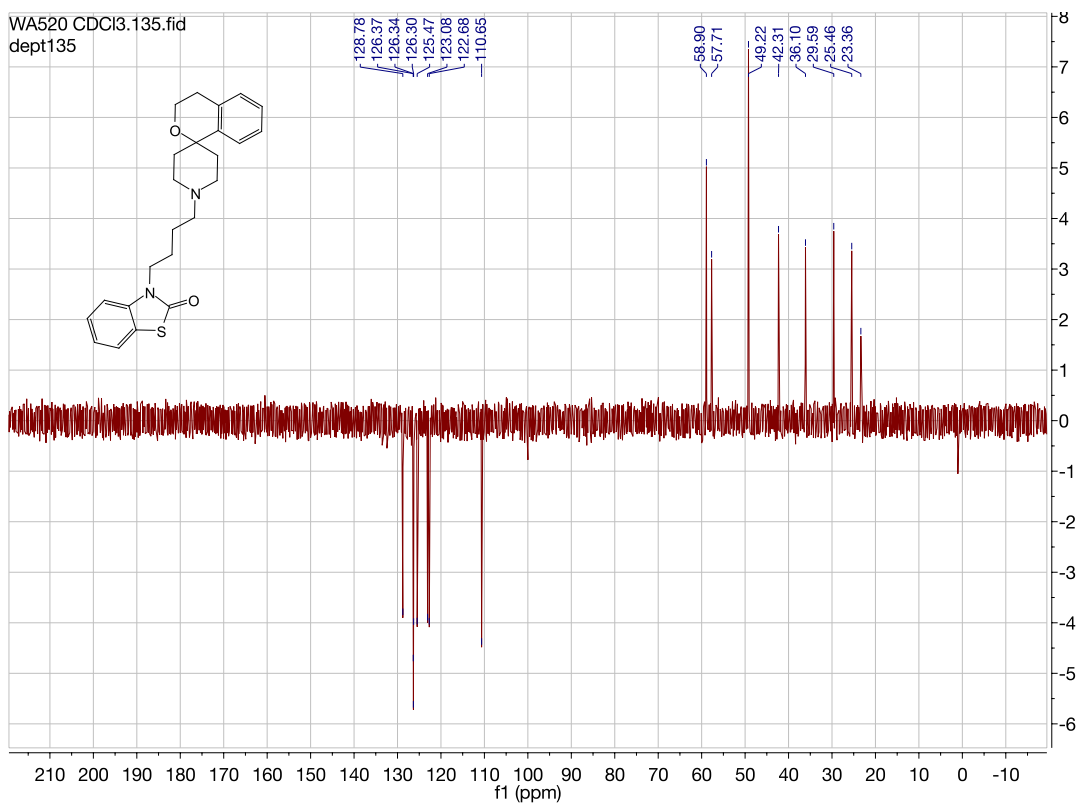




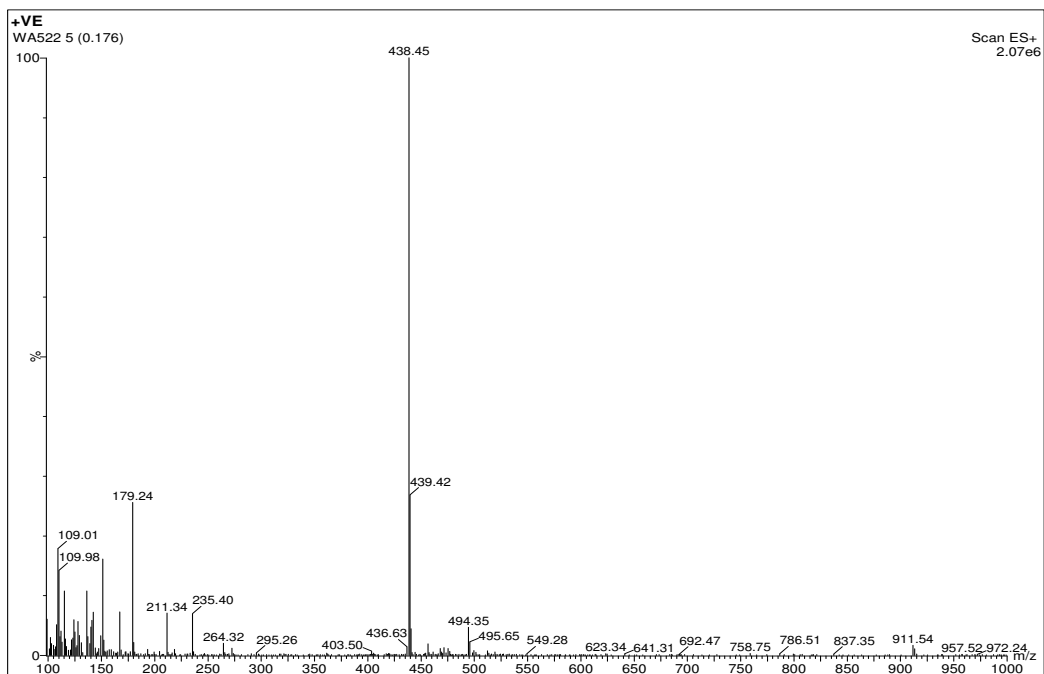
3-(4-(spiro[isochromane-1,4'-piperidin]-1'-yl)butyl)benzo[d]thiazol-2(3H)-one.(WA520)

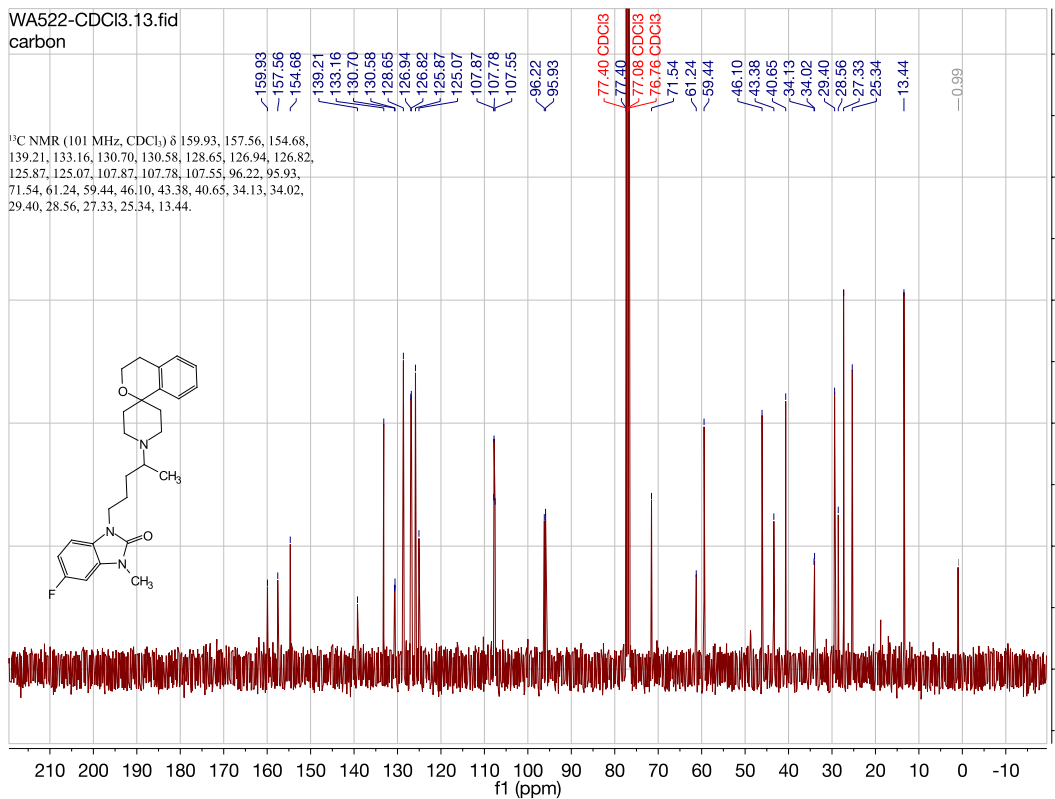
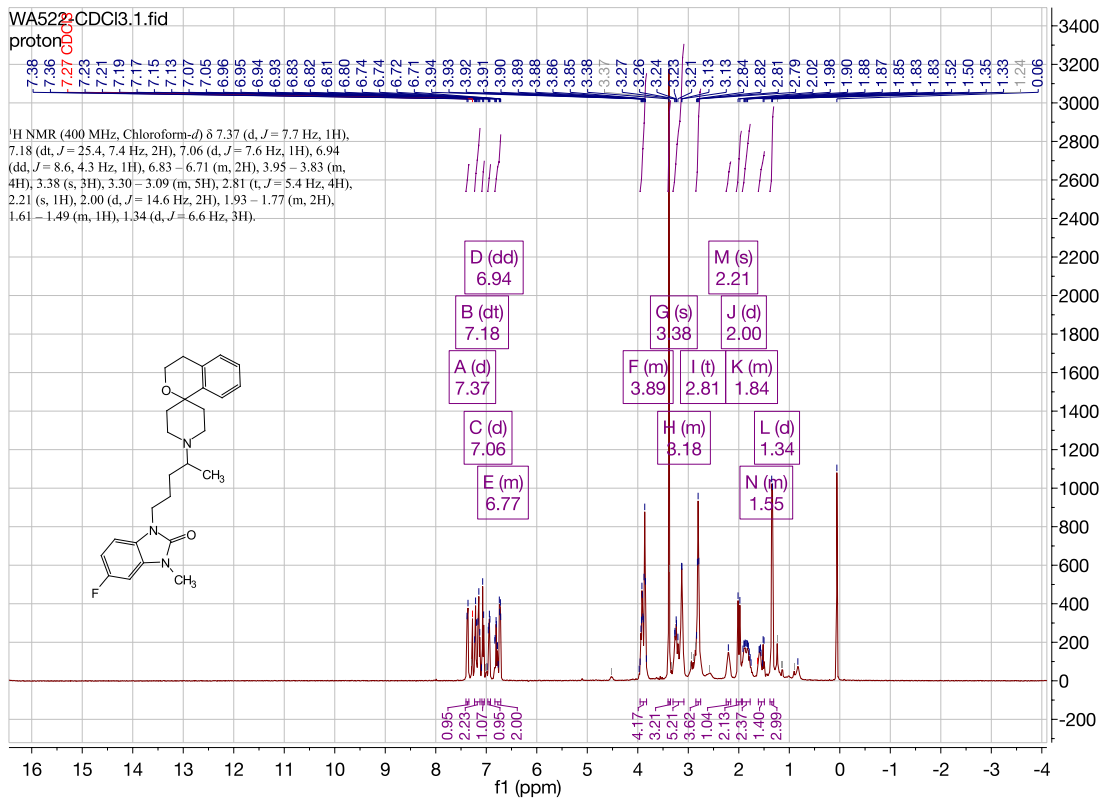




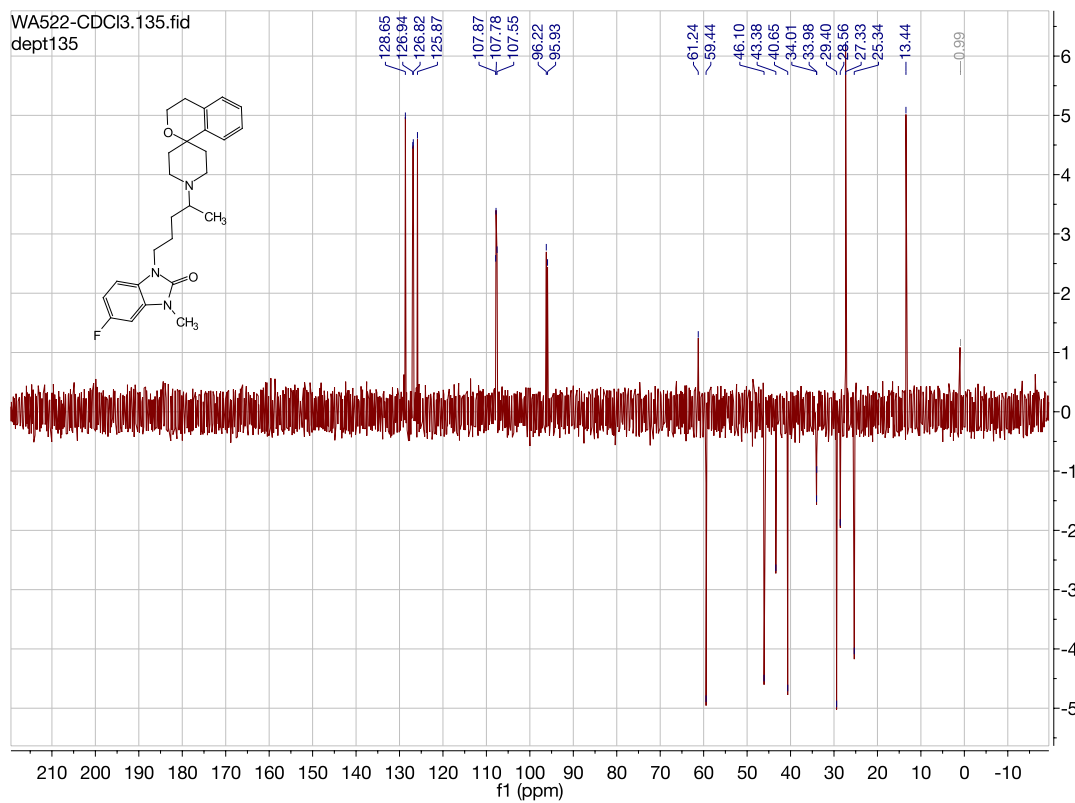


5-fluoro-3-methyl-1-(4-(spiro[isochromane-1,4'-piperidin]-1'-yl)pentyl)-1,3-dihydro-2H-benzo[d]imidazol-2-one. (WA522)

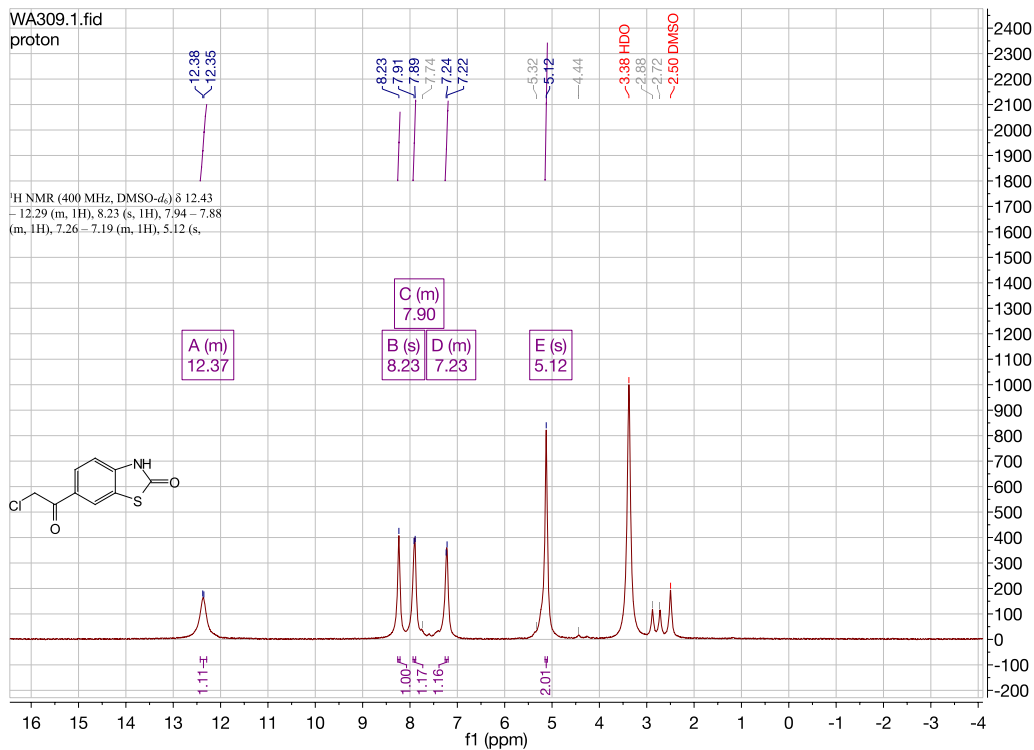
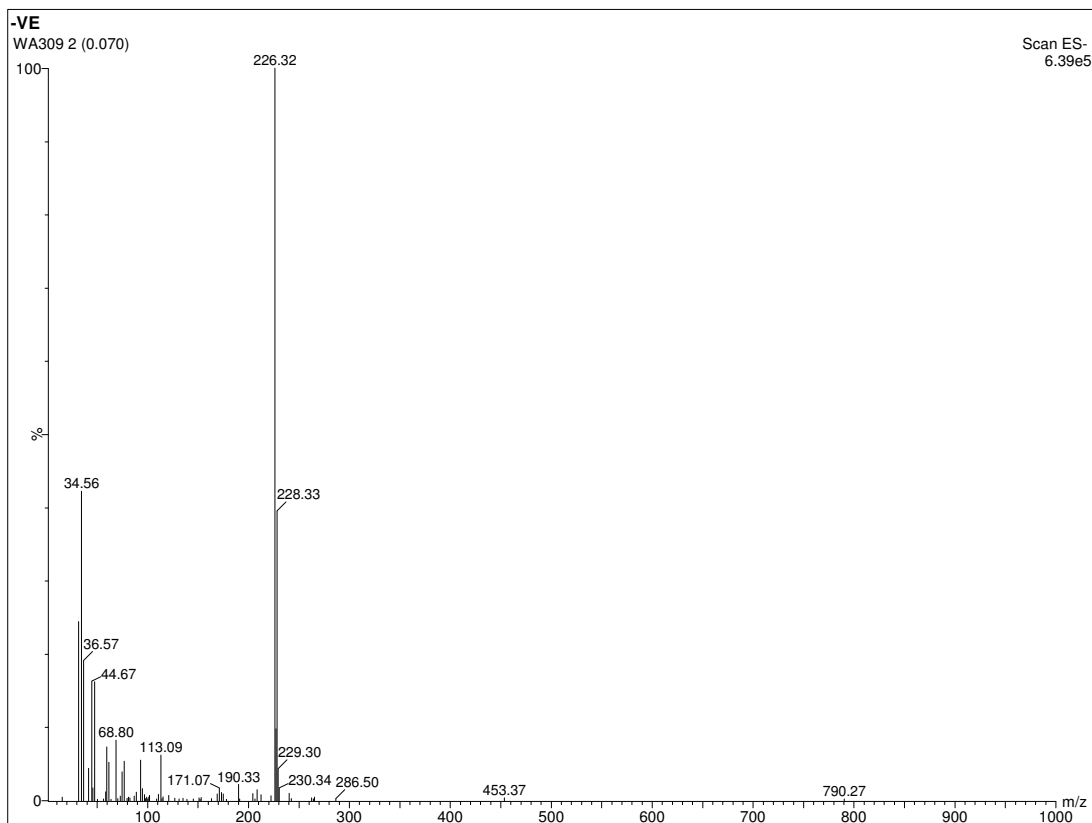


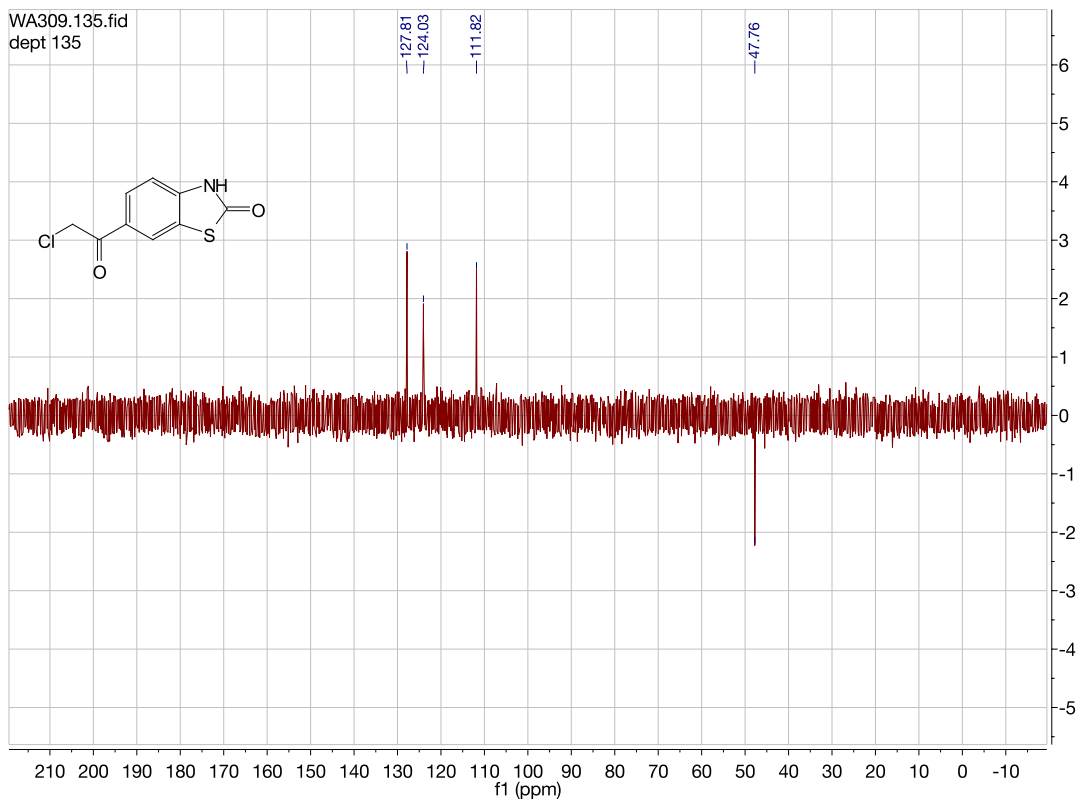
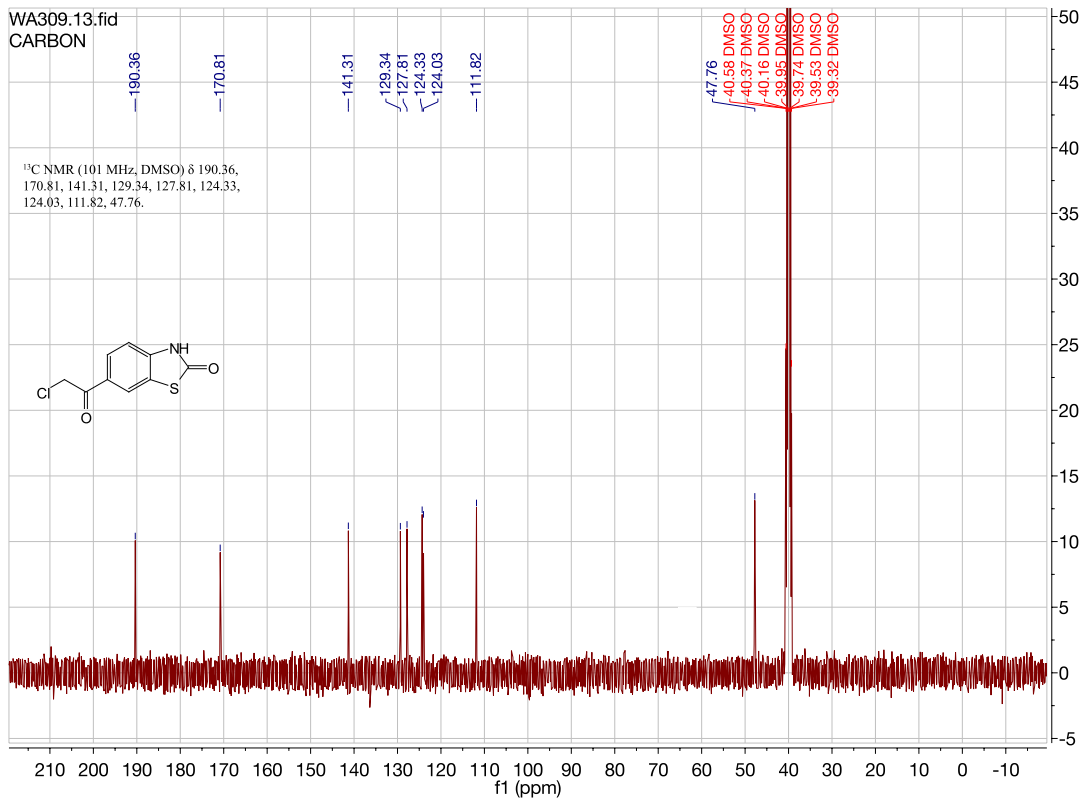


WA522-CDCl3.135.fid
dept135

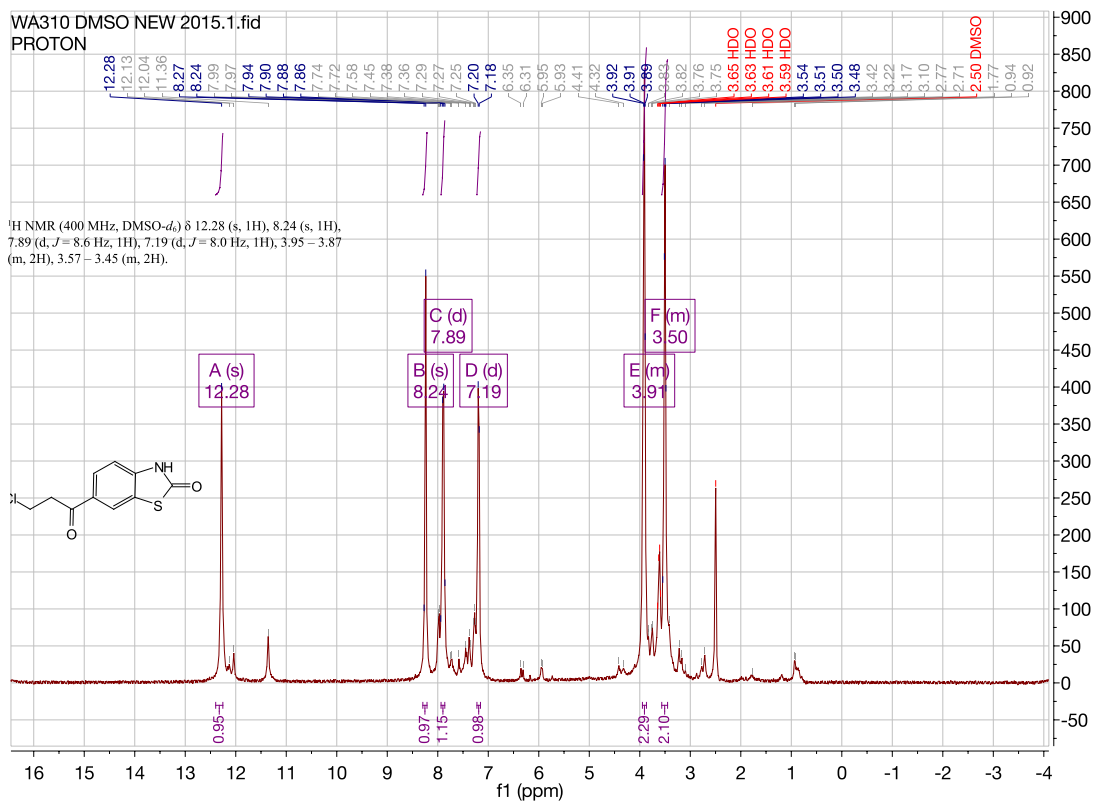
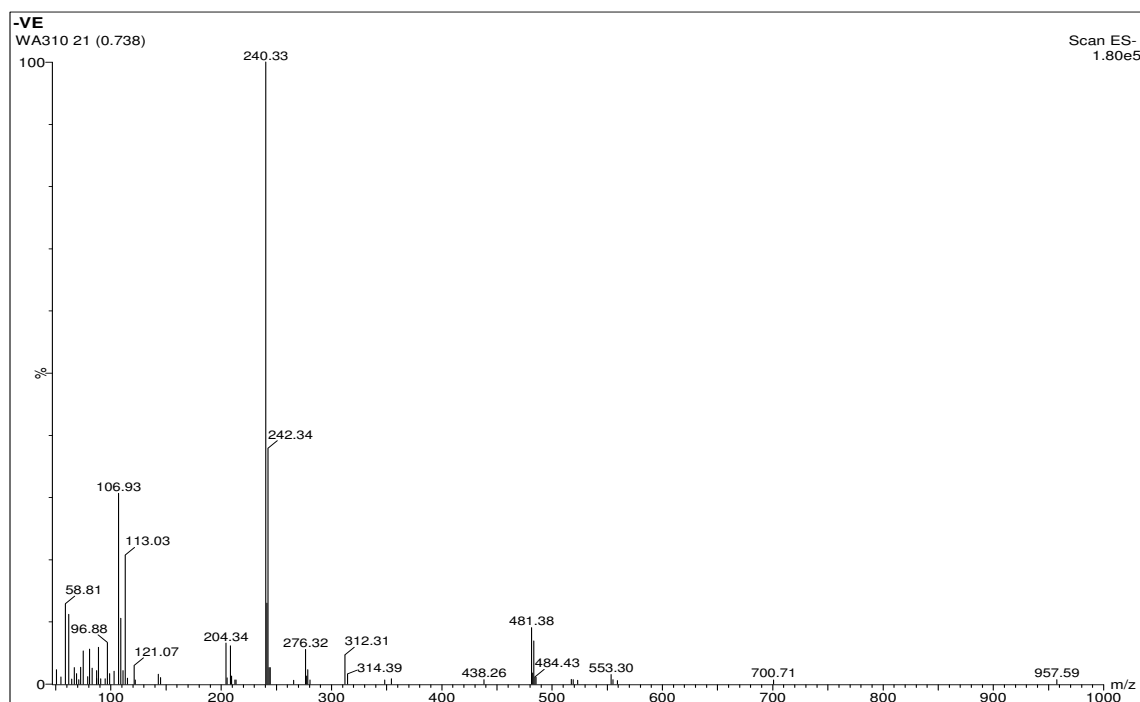


6-(2-chloroacetyl)benzo[d]thiazol-2(3H)-one. [WA309][b1]

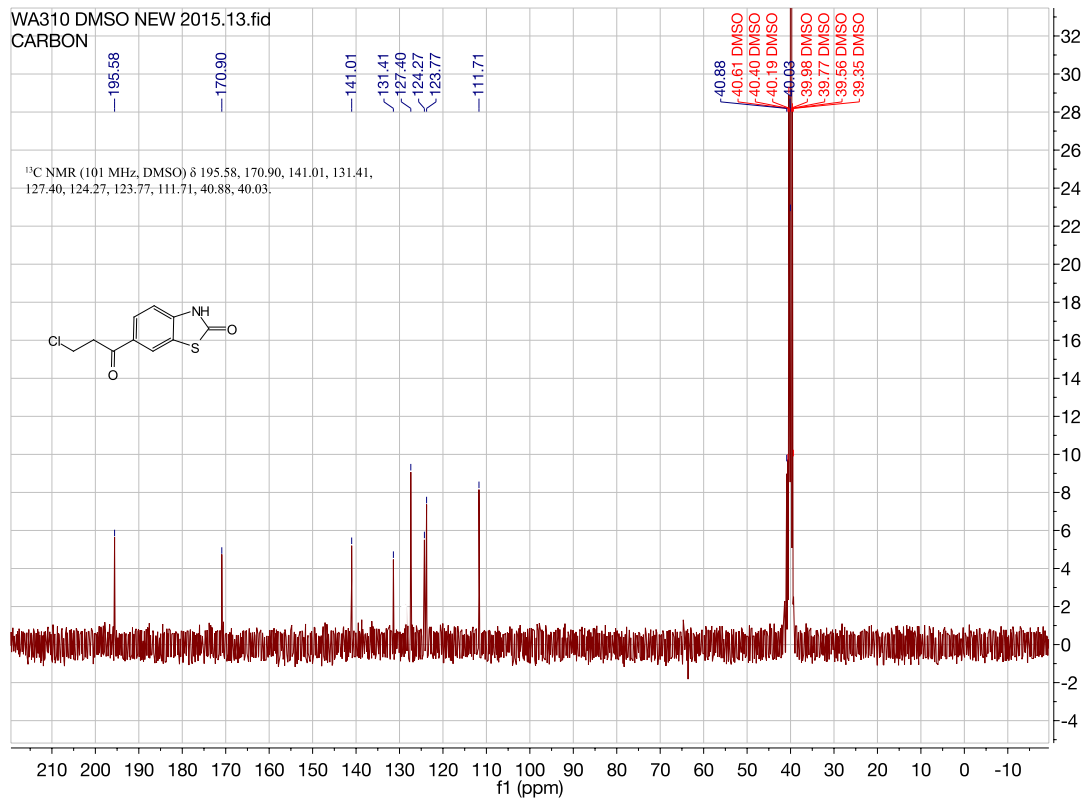




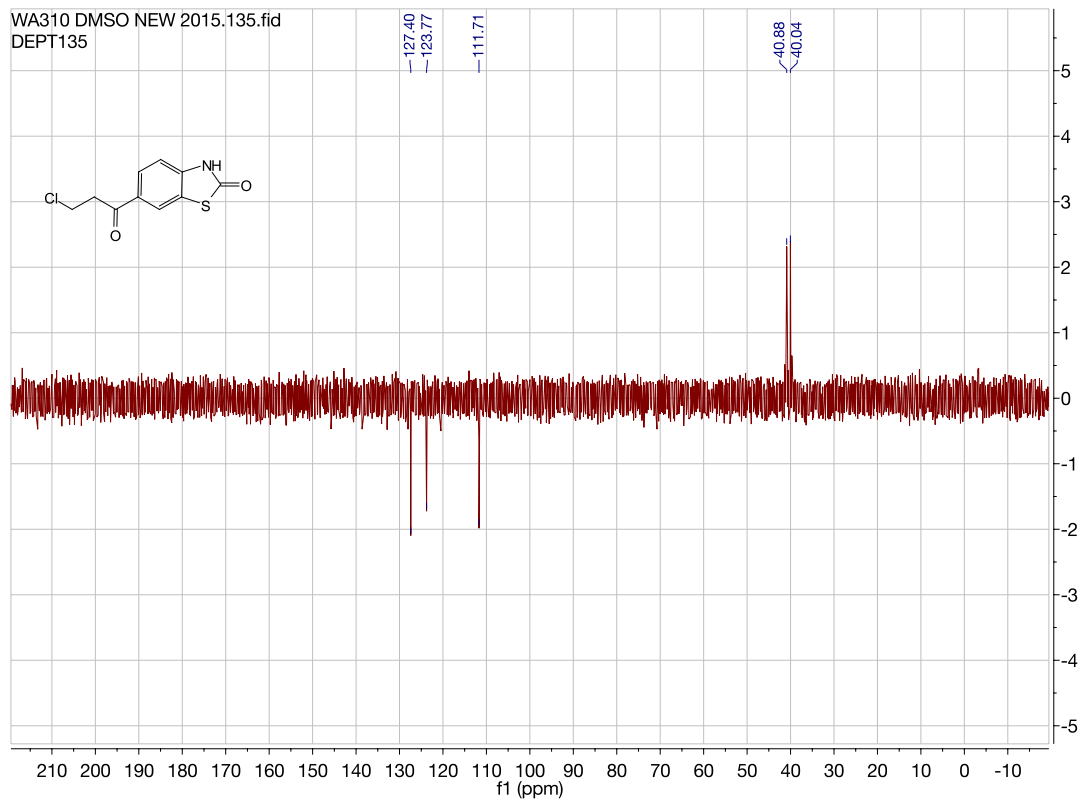
6-(3-chloropropanoyl)benzo[d]thiazol-2(3H)-one. [WA310][b2]



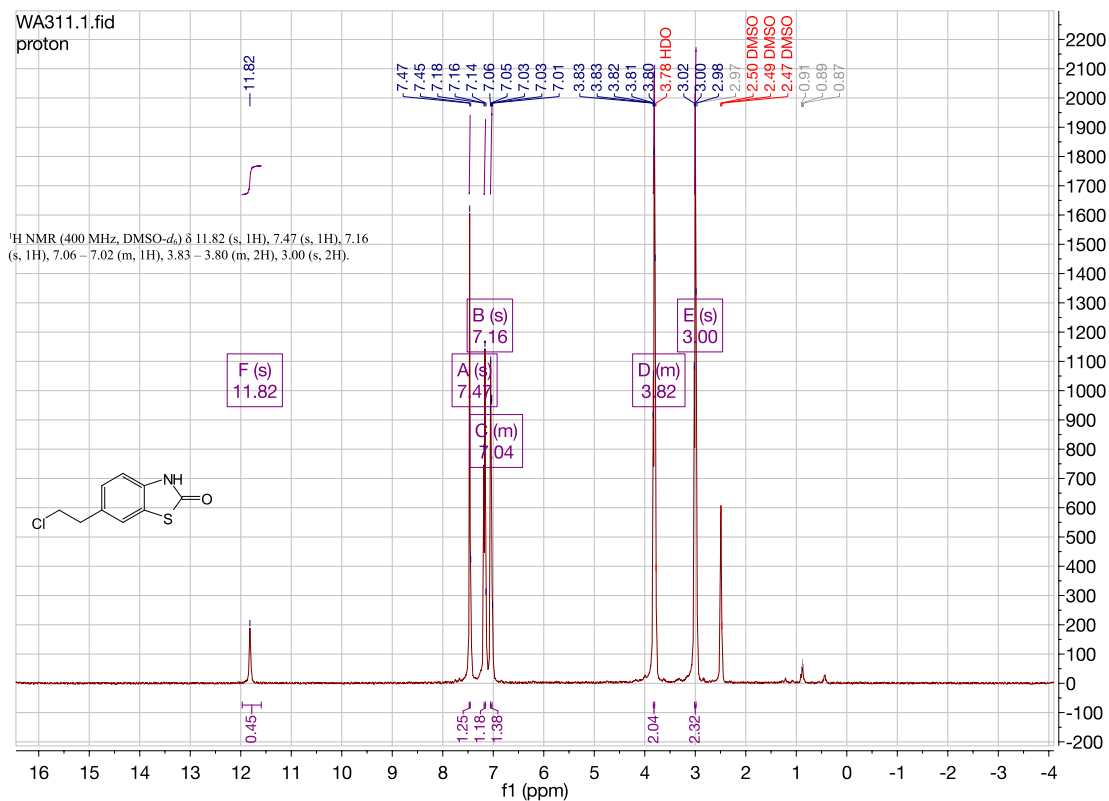
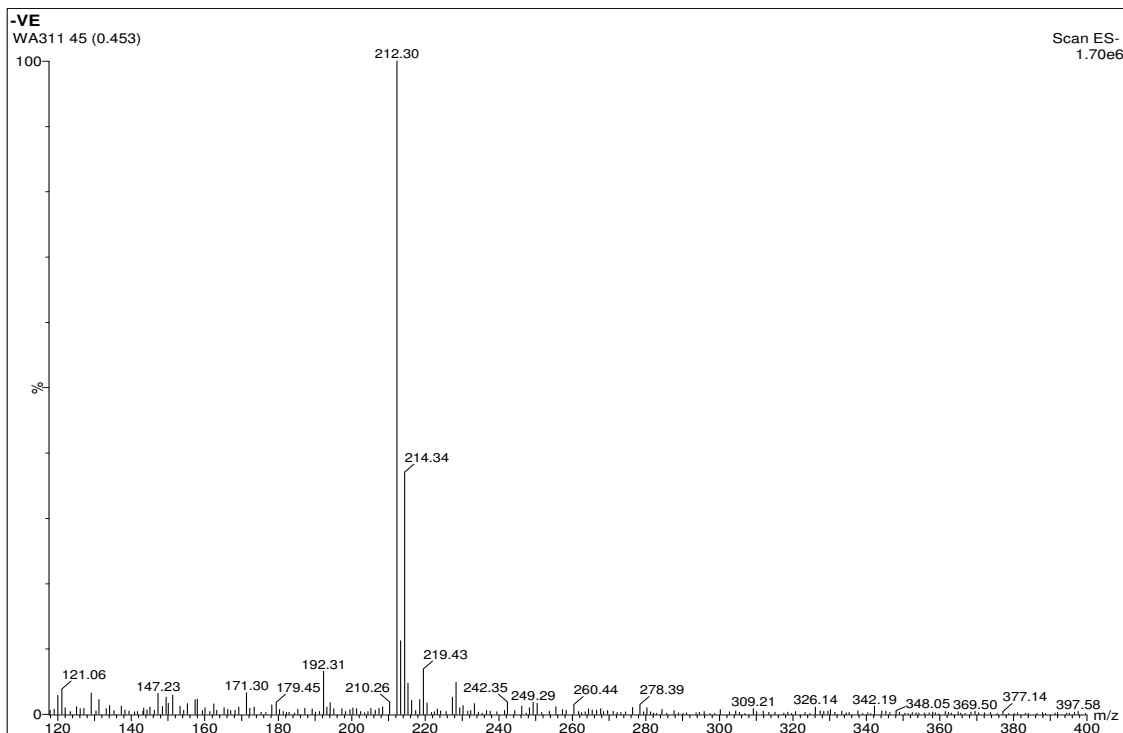
WA310 DMSO NEW 2015.13.fid
CARBON

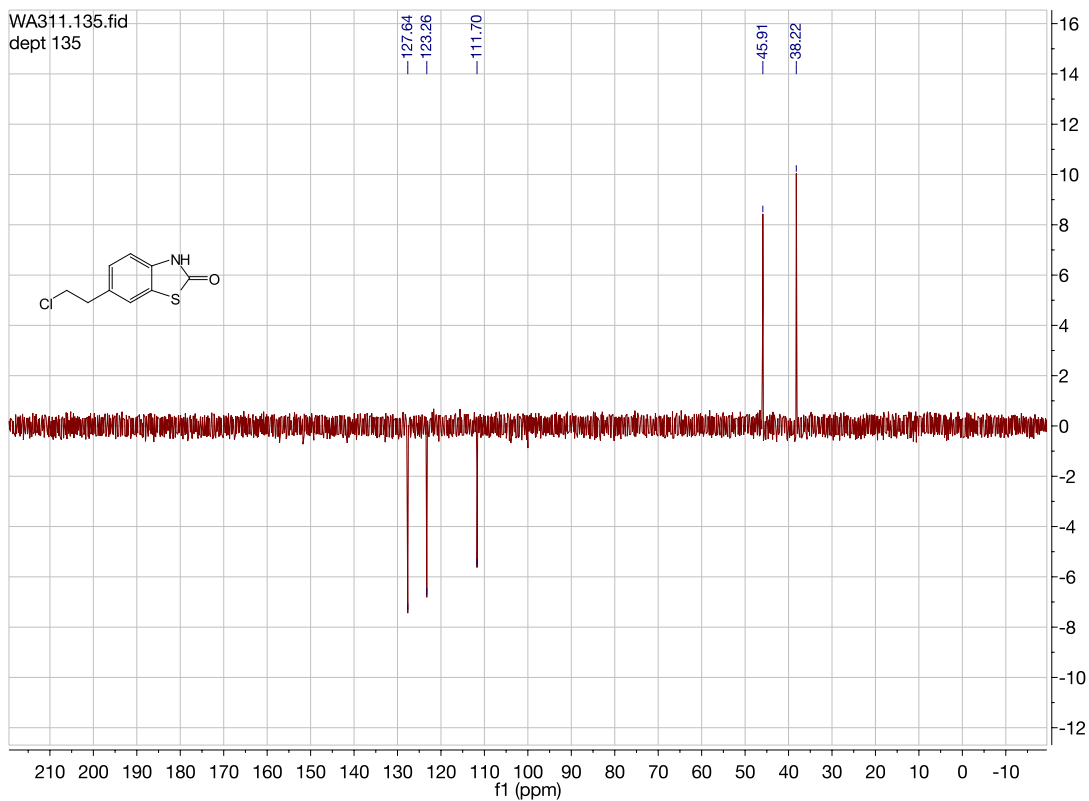
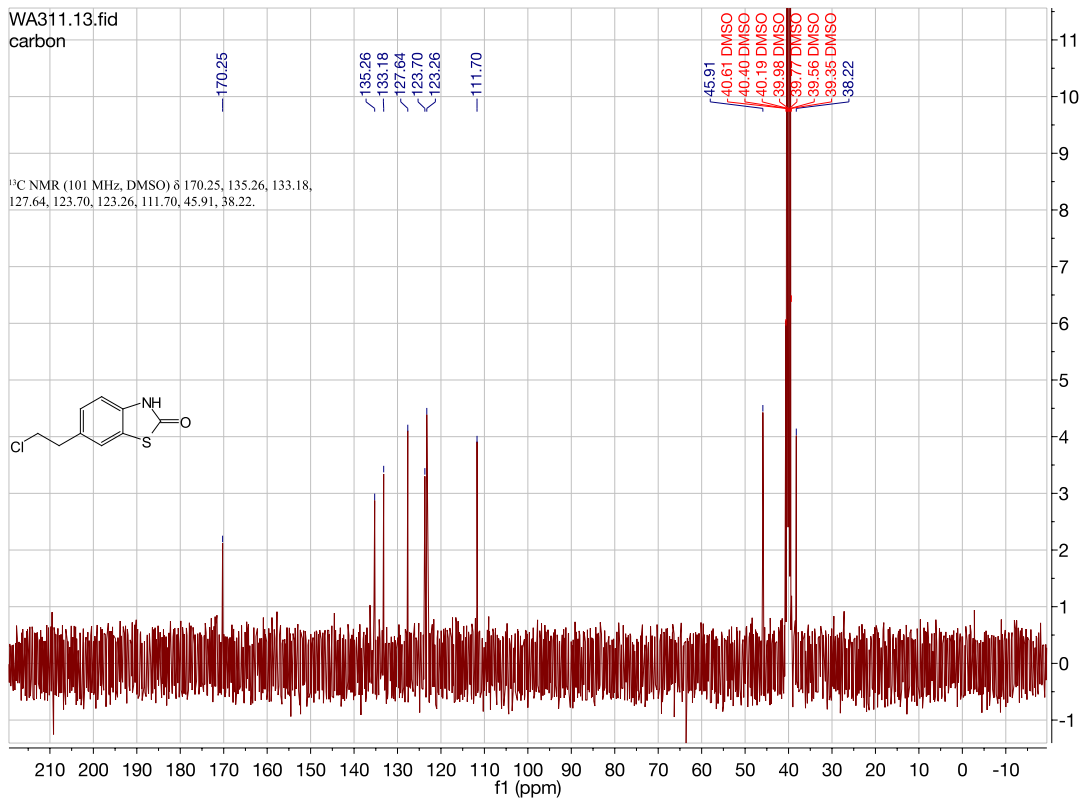


WA310 DMSO NEW 2015.135.fid
DEPT135

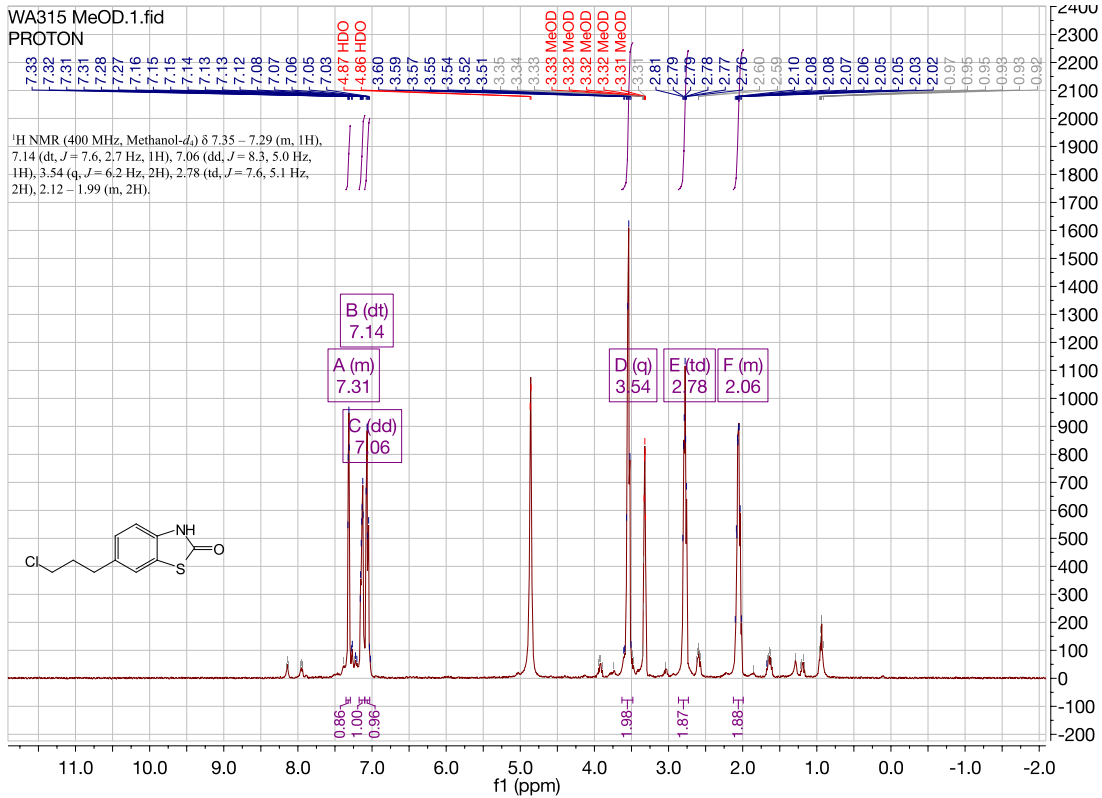
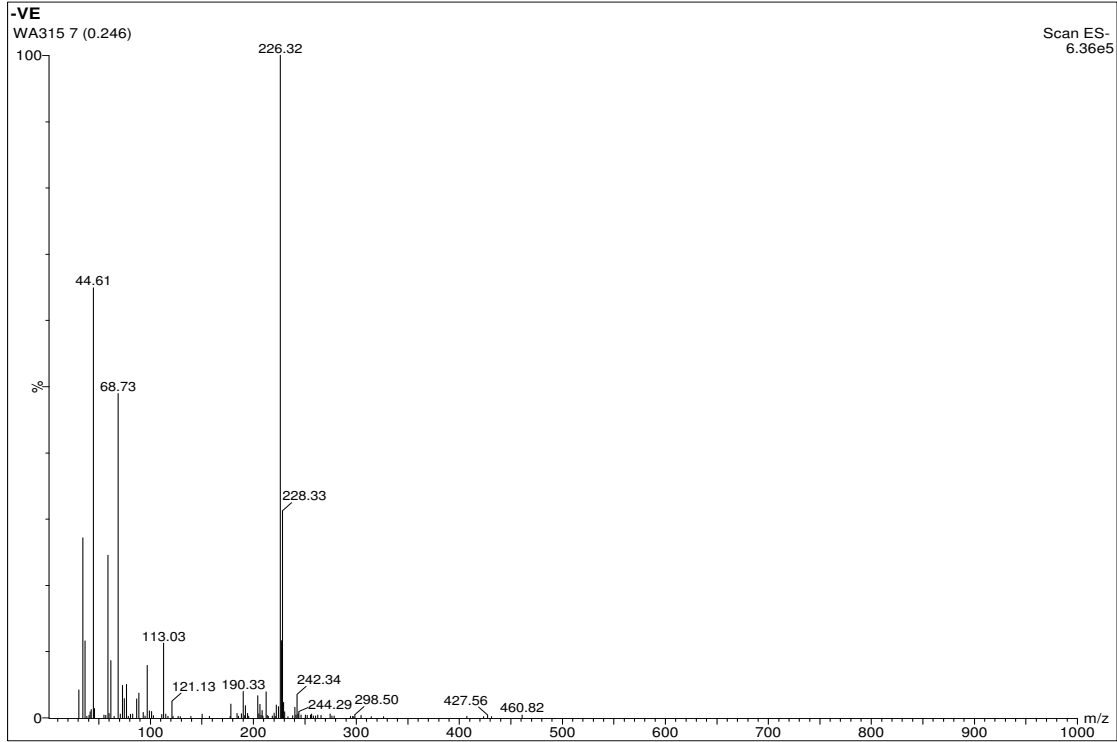


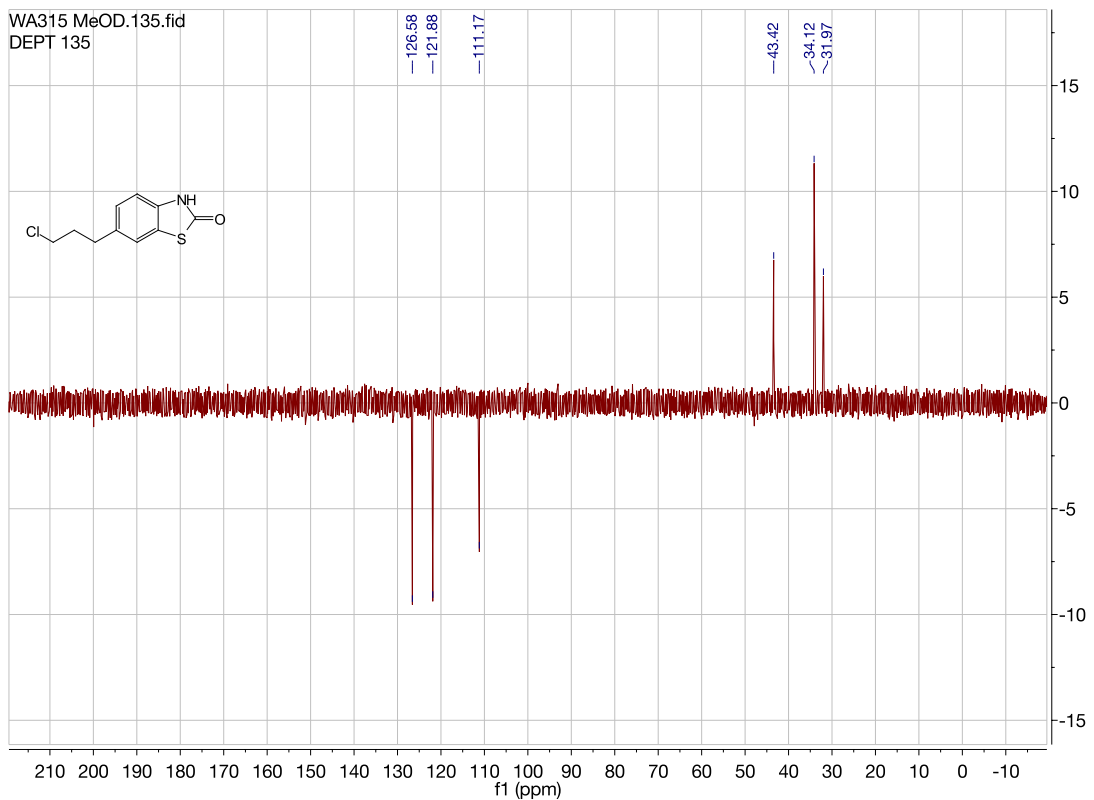
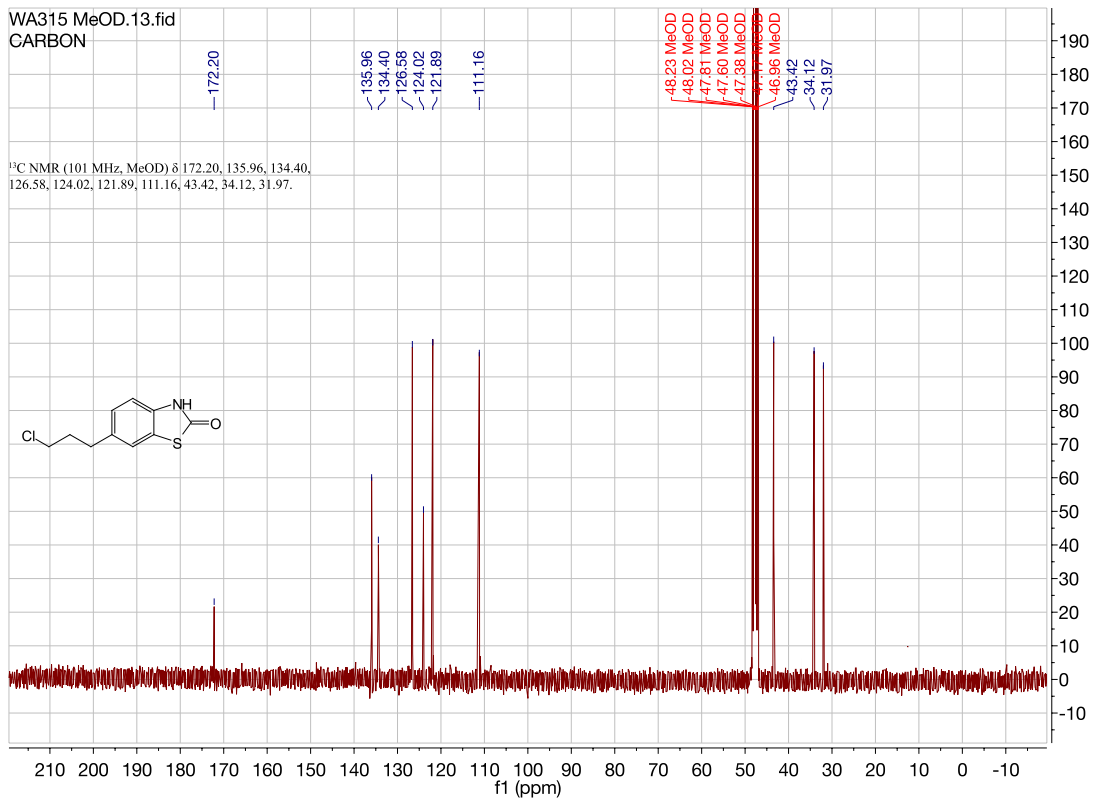
6-(2-chloroethyl)benzo[d]thiazol-2(3H)-one. [WA311][c1]



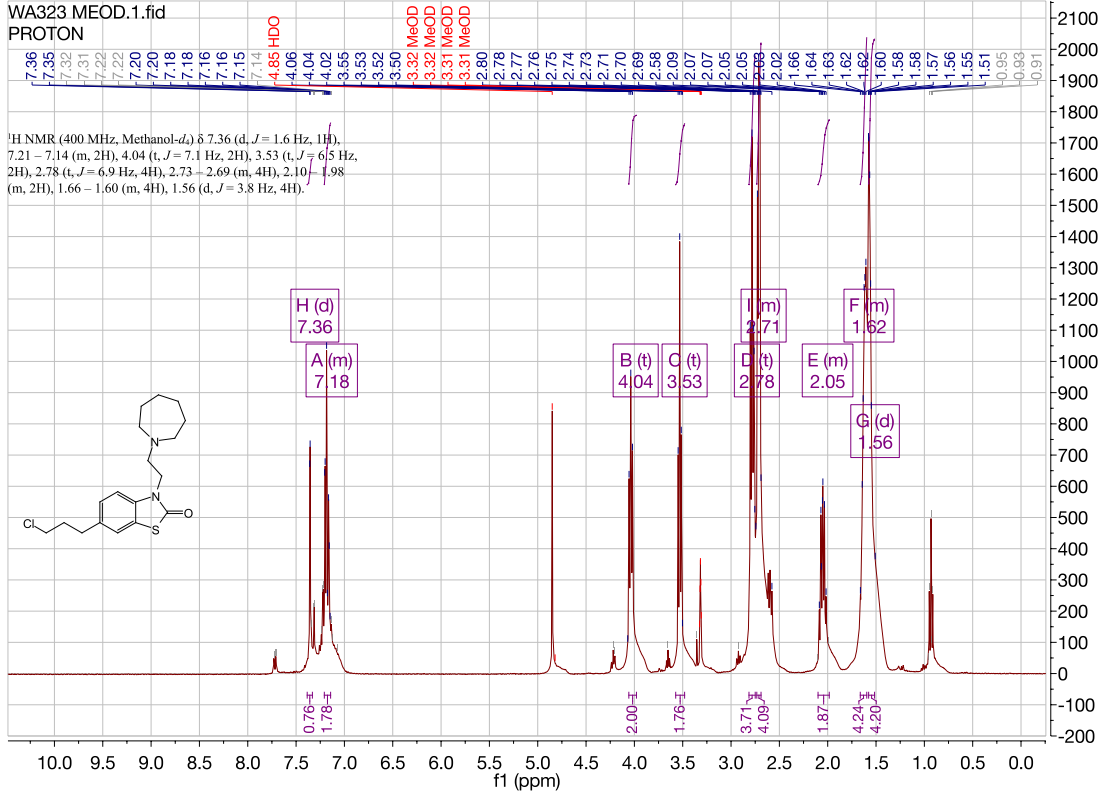
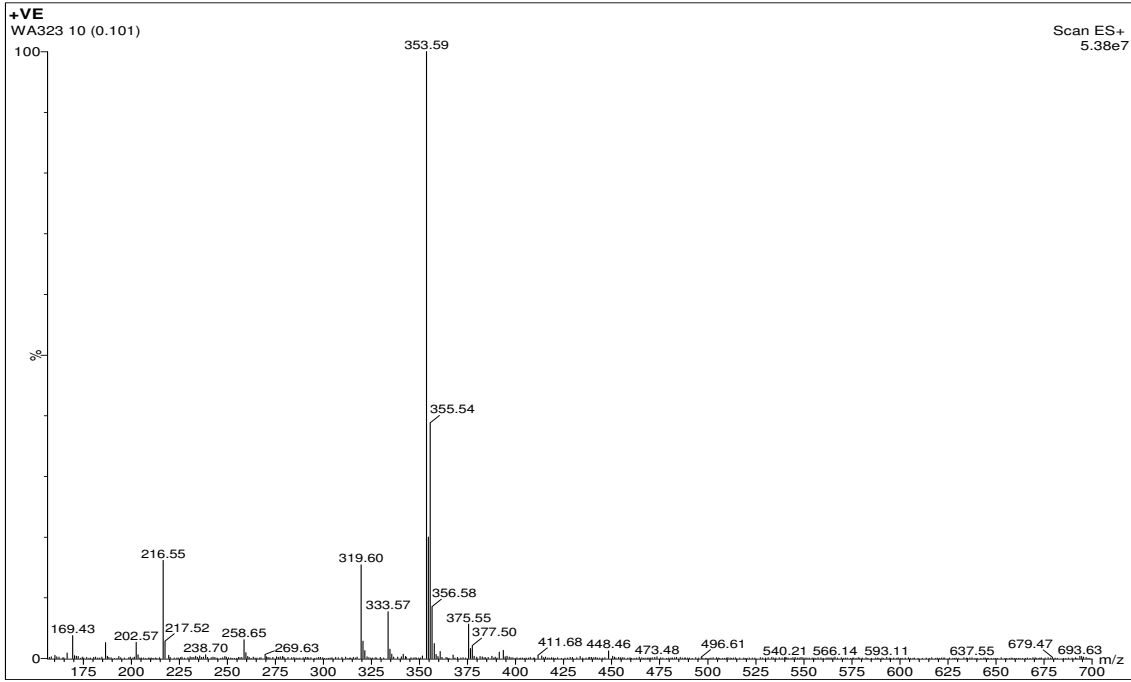


6-(3-chloropropyl)benzo[d]thiazol-2(3H)-one. [WA315][c2]



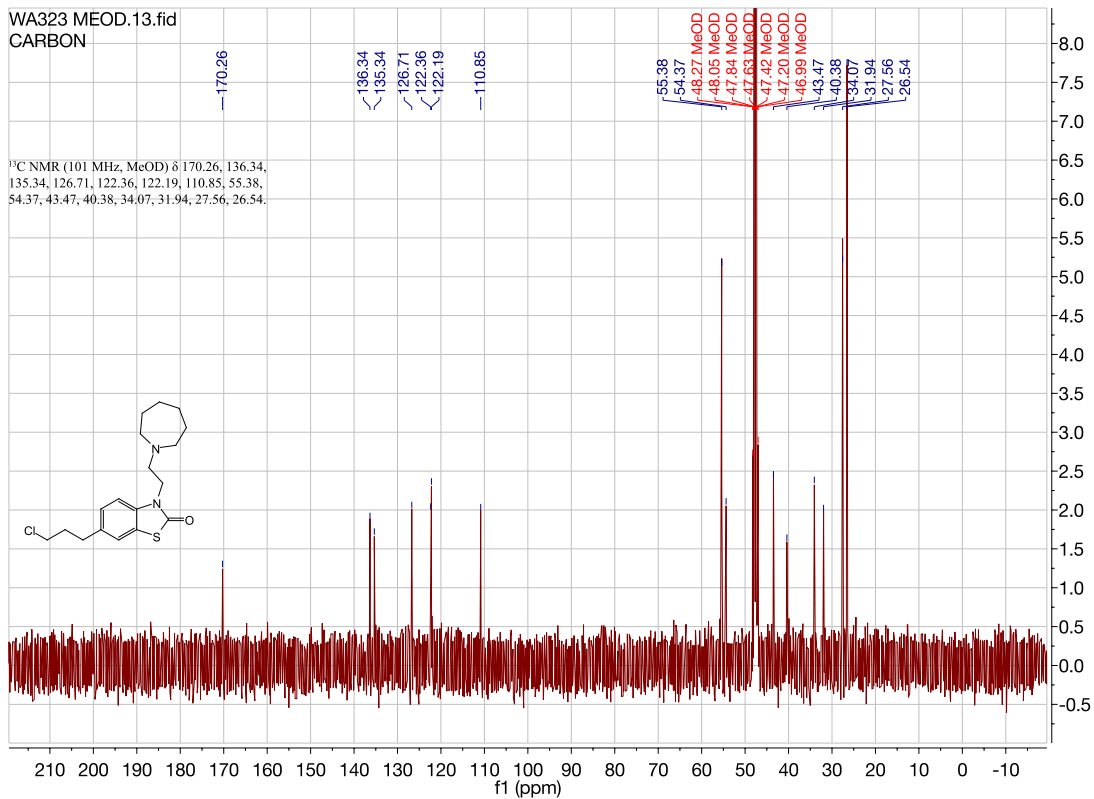


3-(2-(azepan-1-yl)ethyl)-6-(3-chloropropyl)benzo[d]thiazol-2(3H)-one. [WA323][d2]

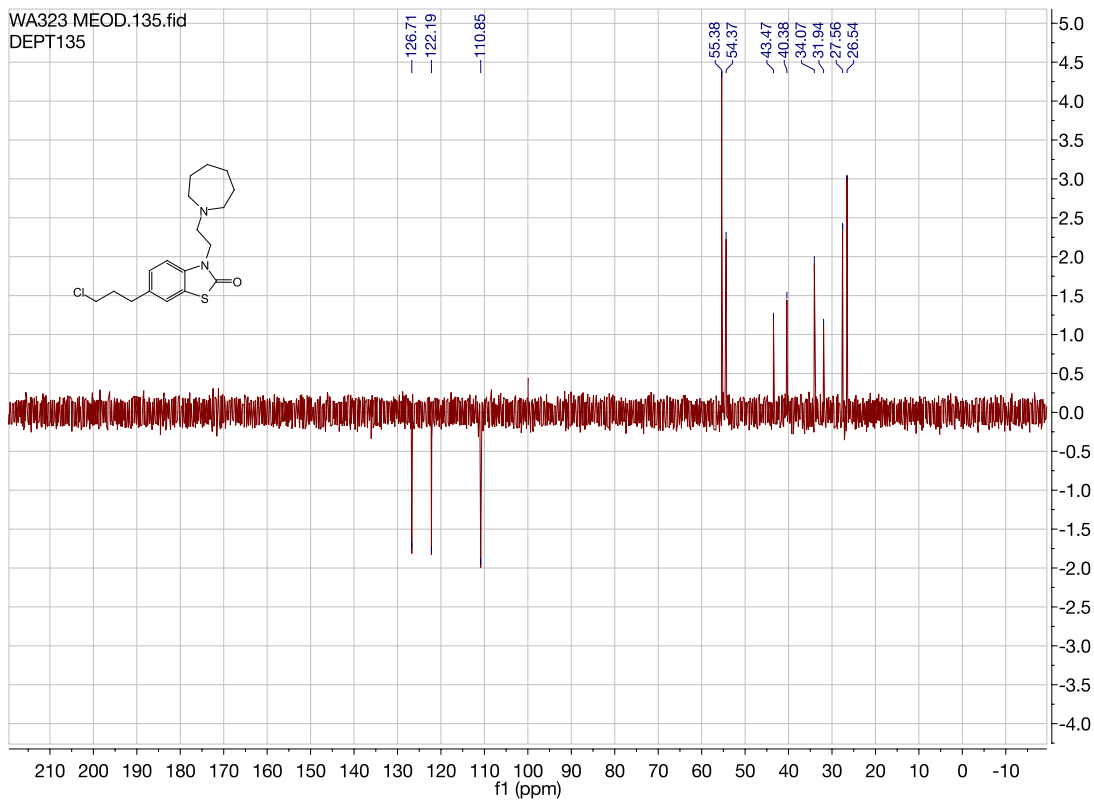


WA323 MEOD.13.fid
CARBON

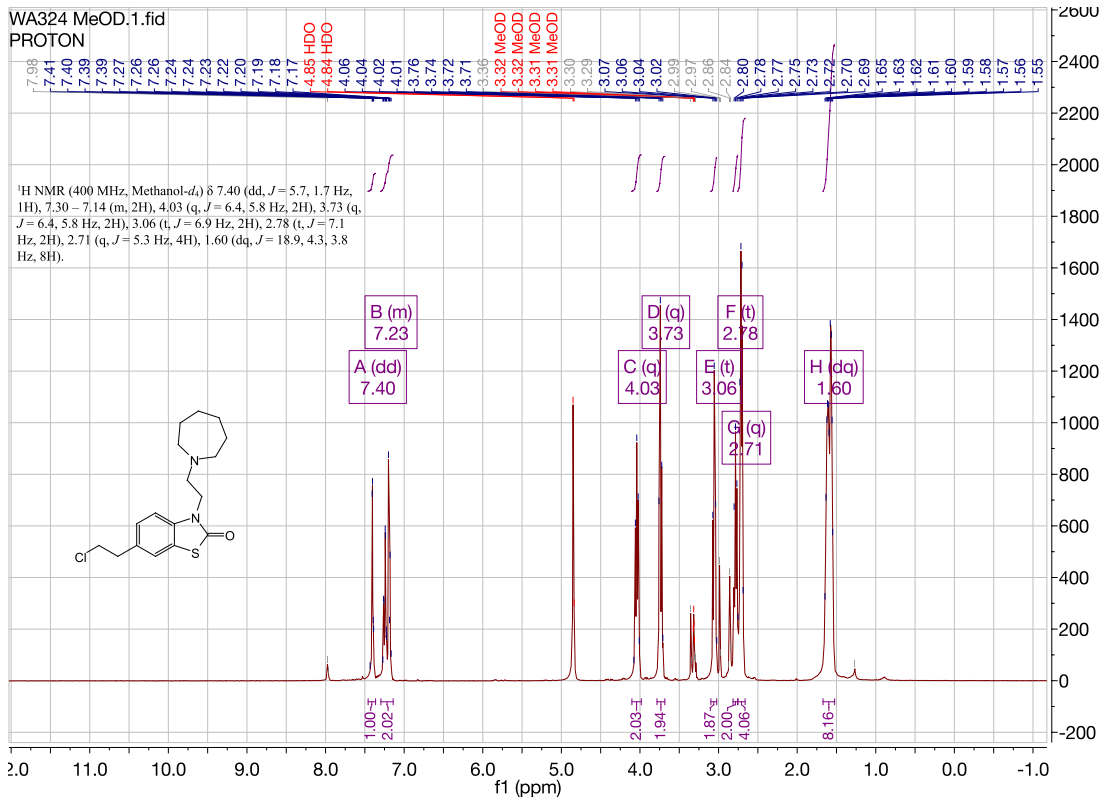
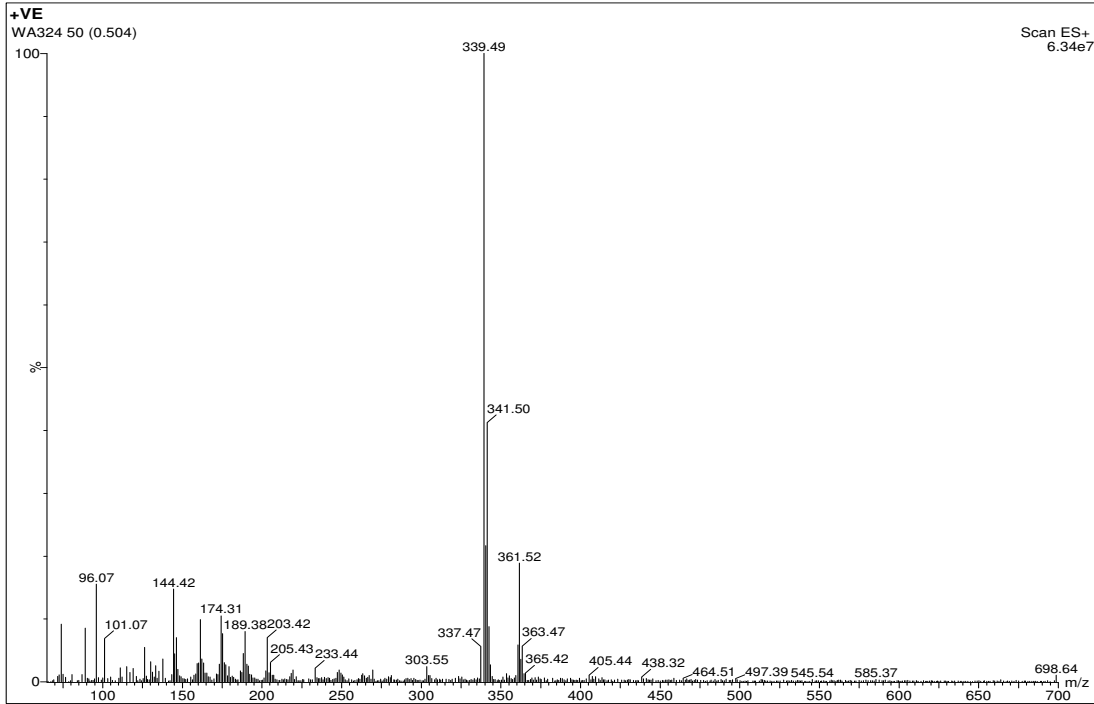
¹³C NMR (101 MHz, MeOD) δ 170.26, 136.34,
135.34, 126.71, 122.36, 122.19, 110.85, 55.38,
54.37, 43.47, 40.38, 34.07, 31.94, 27.56, 26.54.

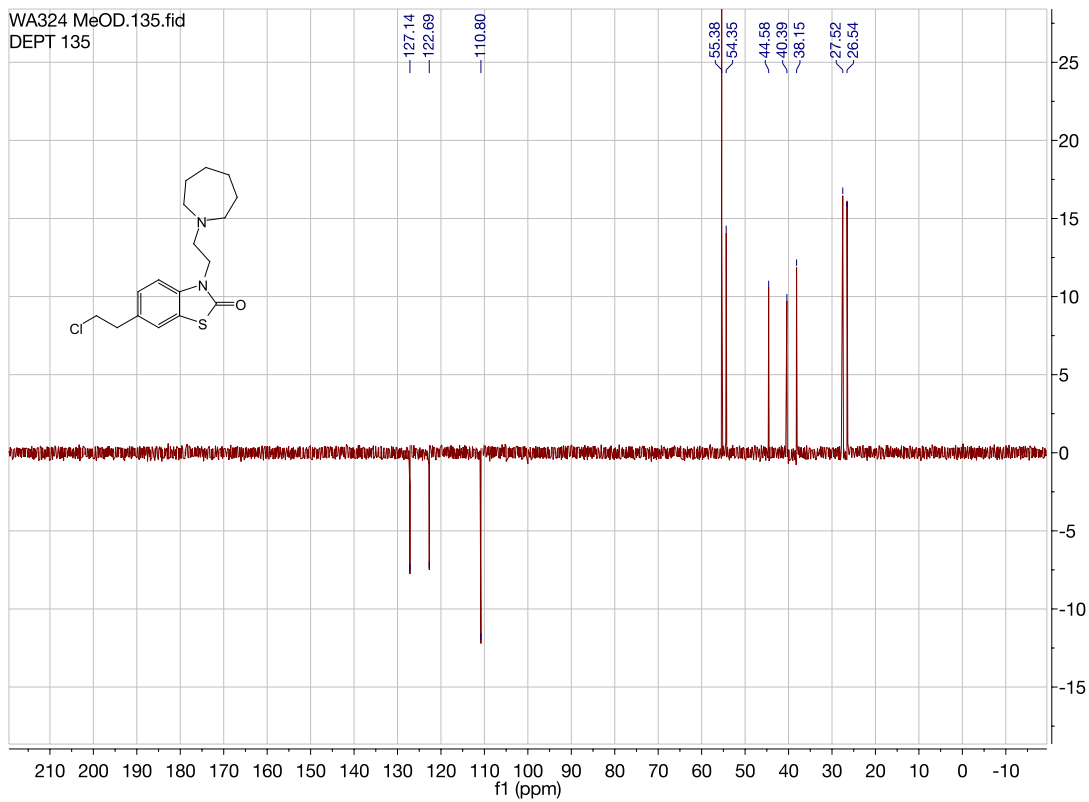
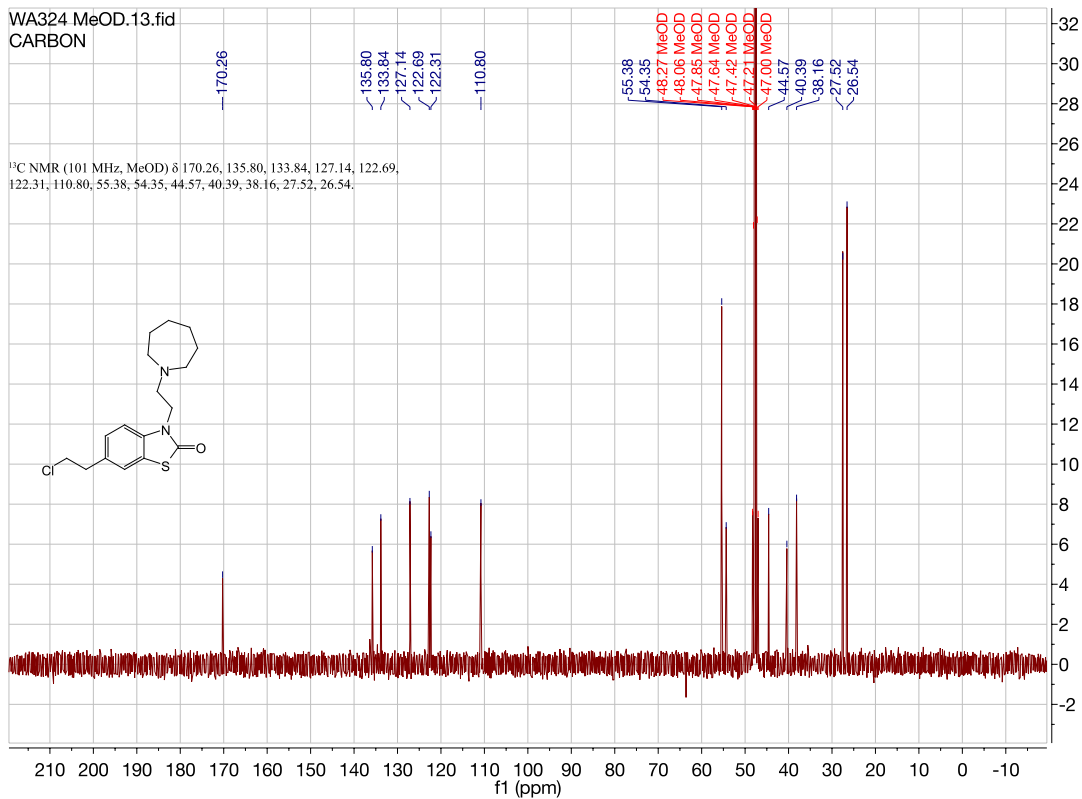


WA323 MEOD.135.fid
DEPT135

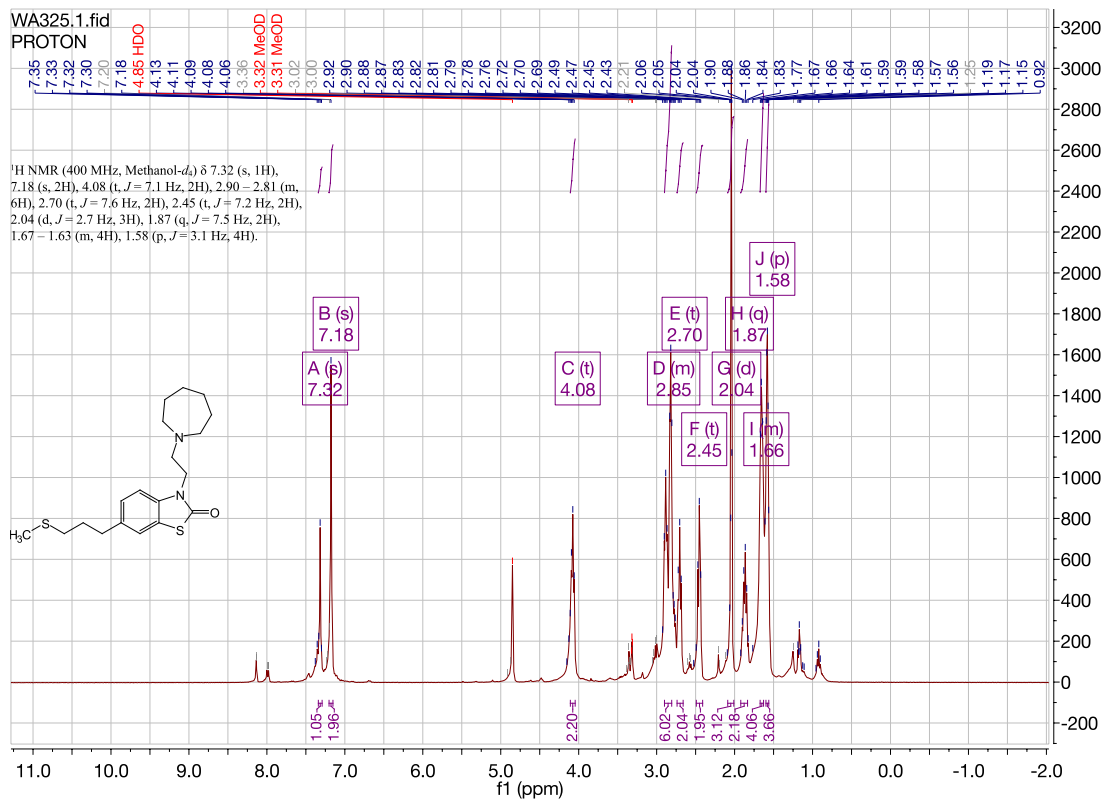
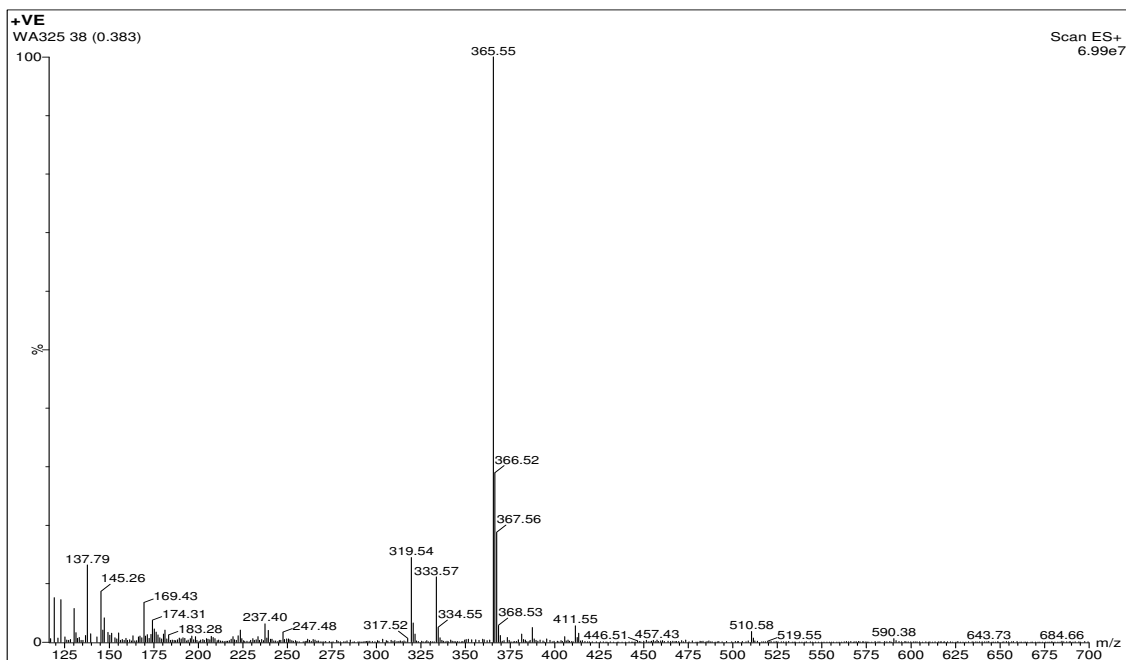


3-(2-(azepan-1-yl)ethyl)-6-(2-chloroethyl)benzo[d]thiazol-2(3H)-one. [WA324][d1]



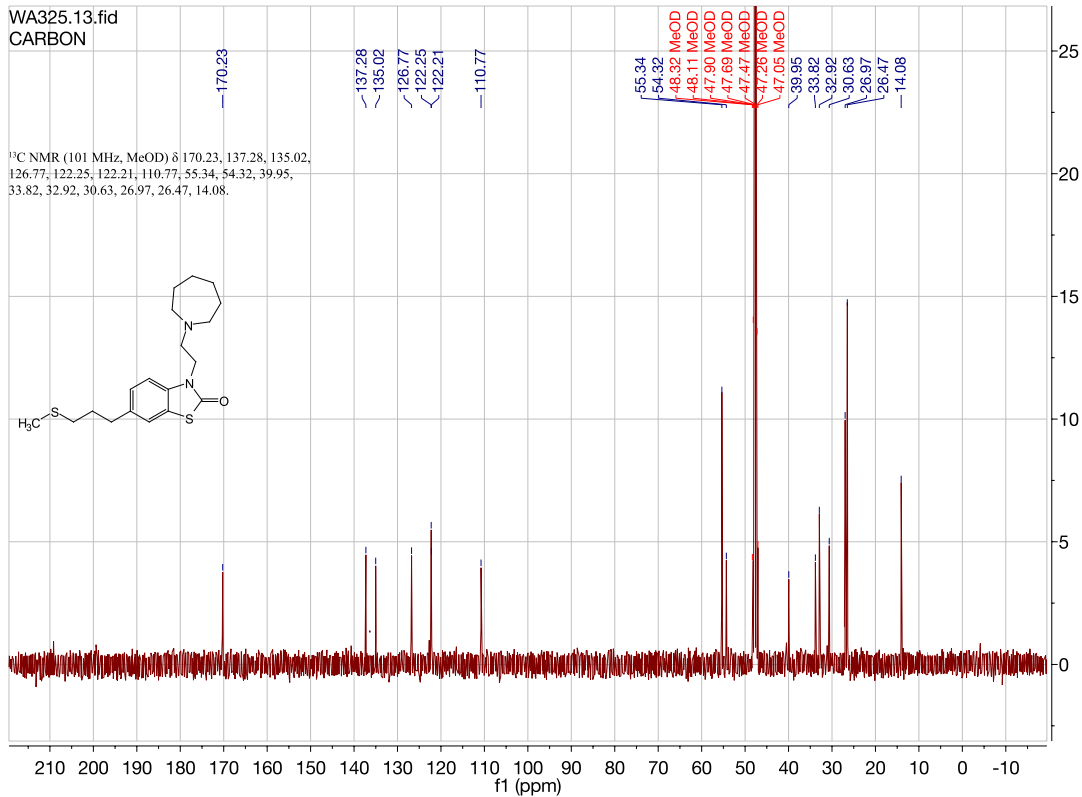
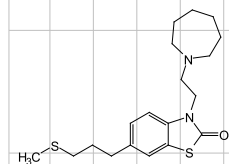


3-(2-(azepan-1-yl)ethyl)-6-(3-(methylthio)propyl)benzo[d]thiazol-2(3H)-one.
[WA325][e2]

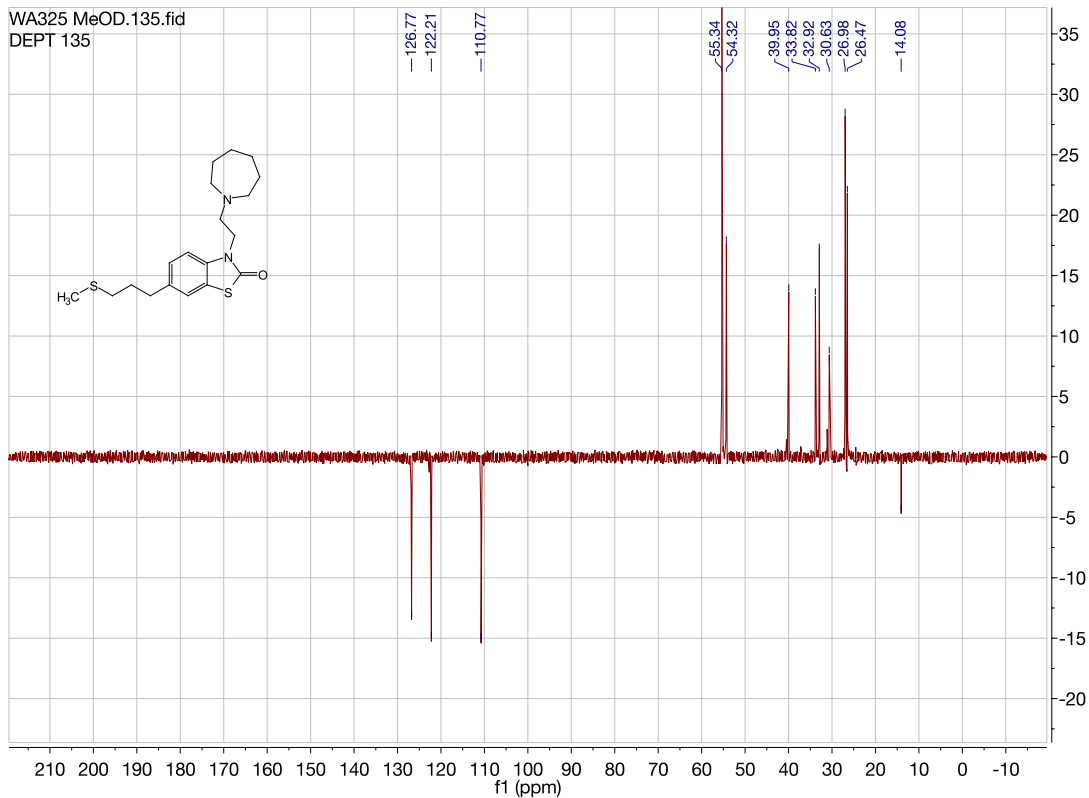
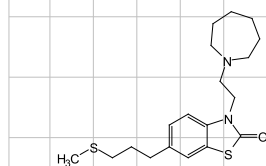


WA325.13.fid
CARBON

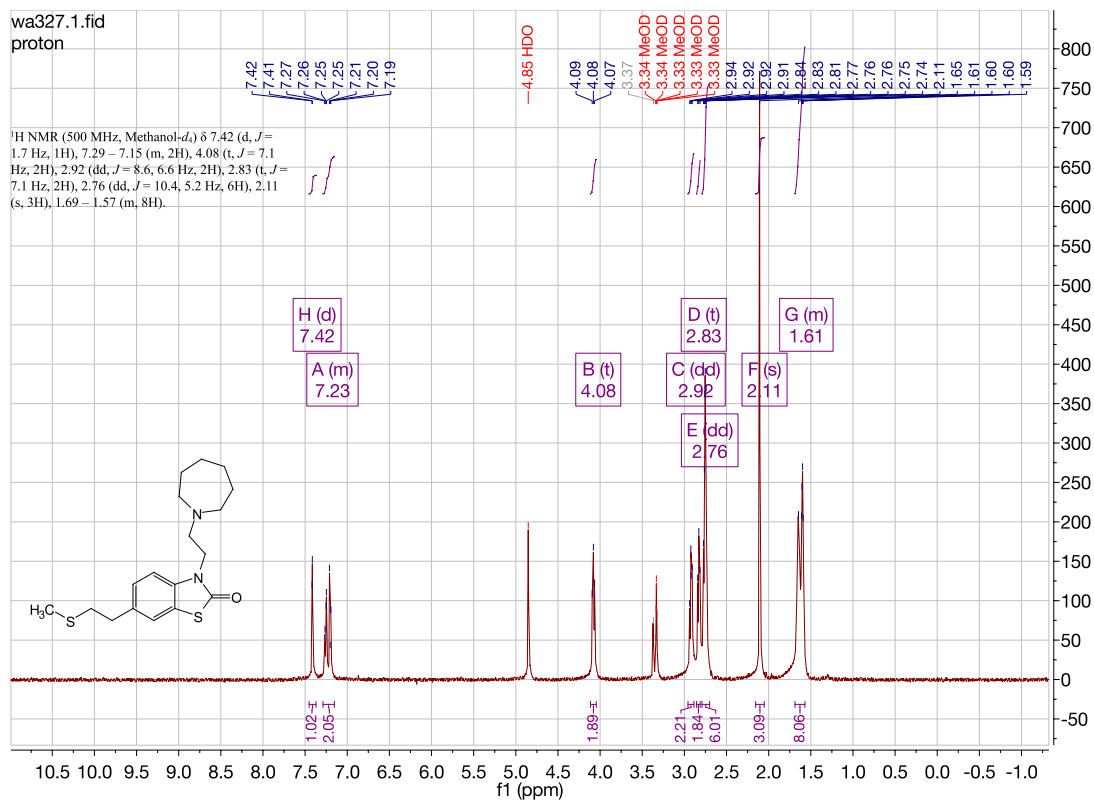
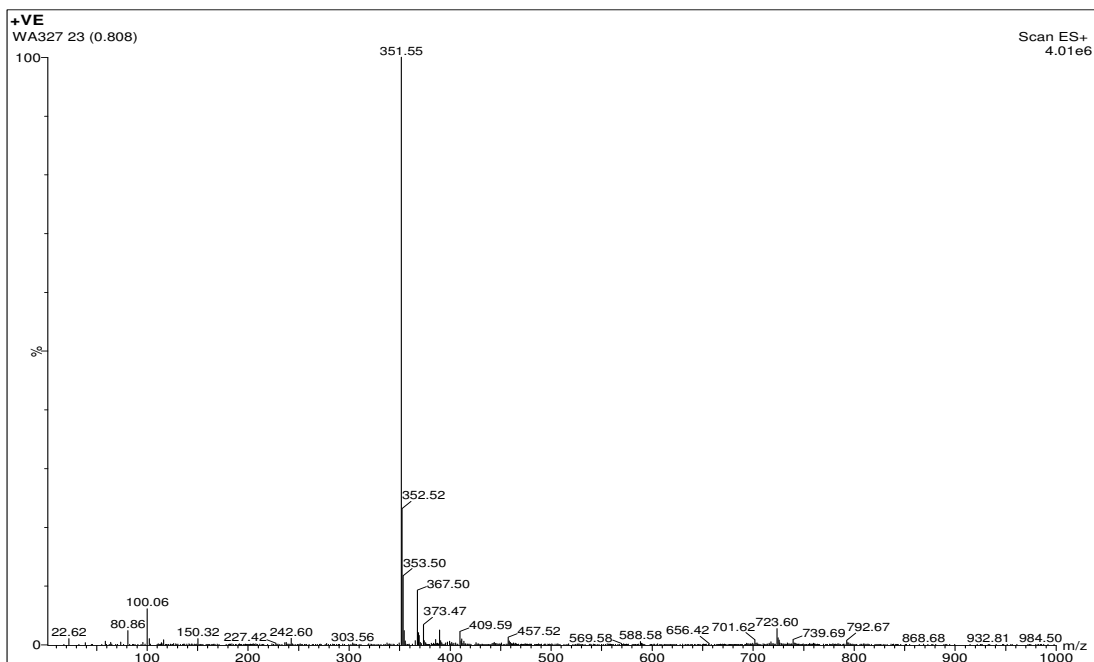
¹³C NMR (101 MHz, MeOD) δ 170.23, 137.28, 135.02, 126.77, 122.25, 122.21, 110.77, 55.34, 54.32, 39.95, 33.82, 32.92, 30.63, 26.97, 26.47, 14.08.

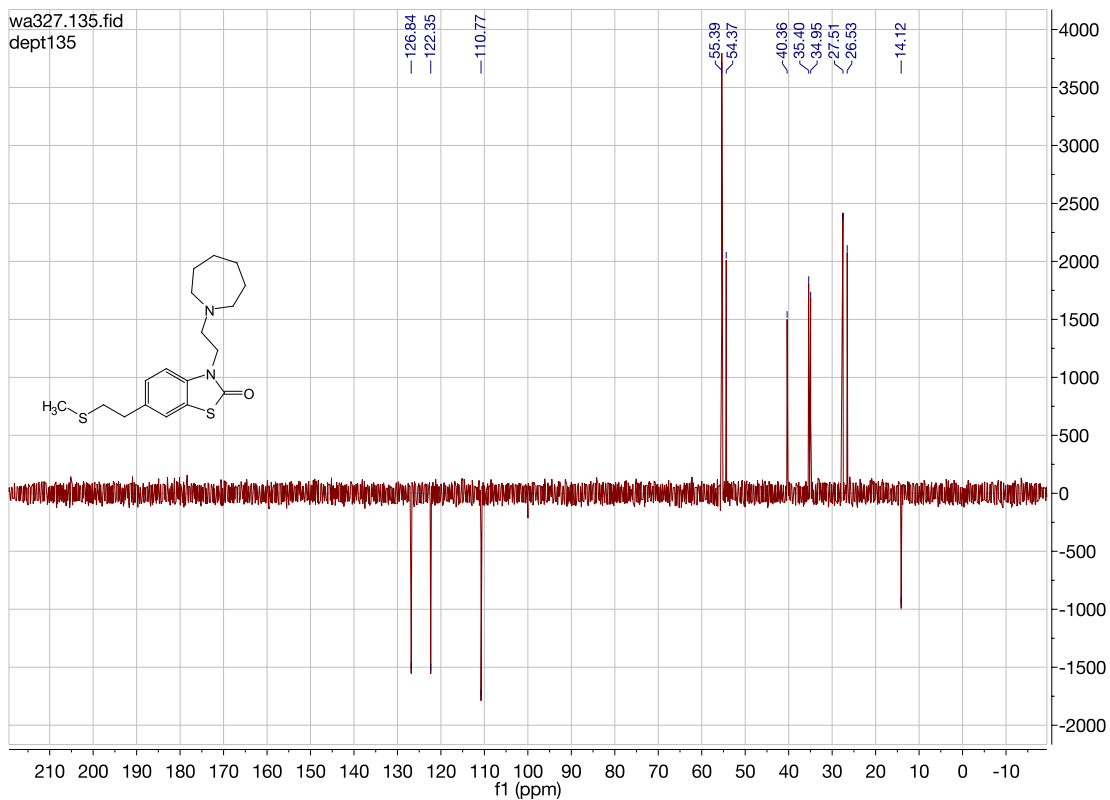
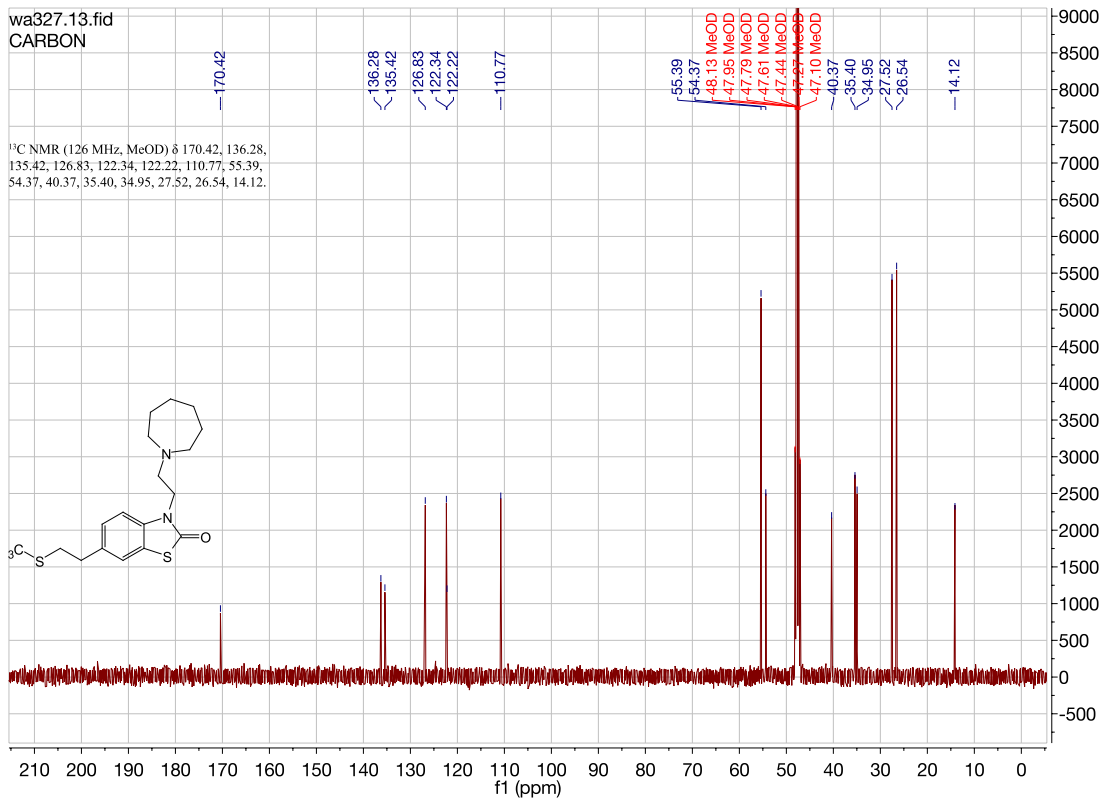


WA325 MeOD.135.fid
DEPT 135

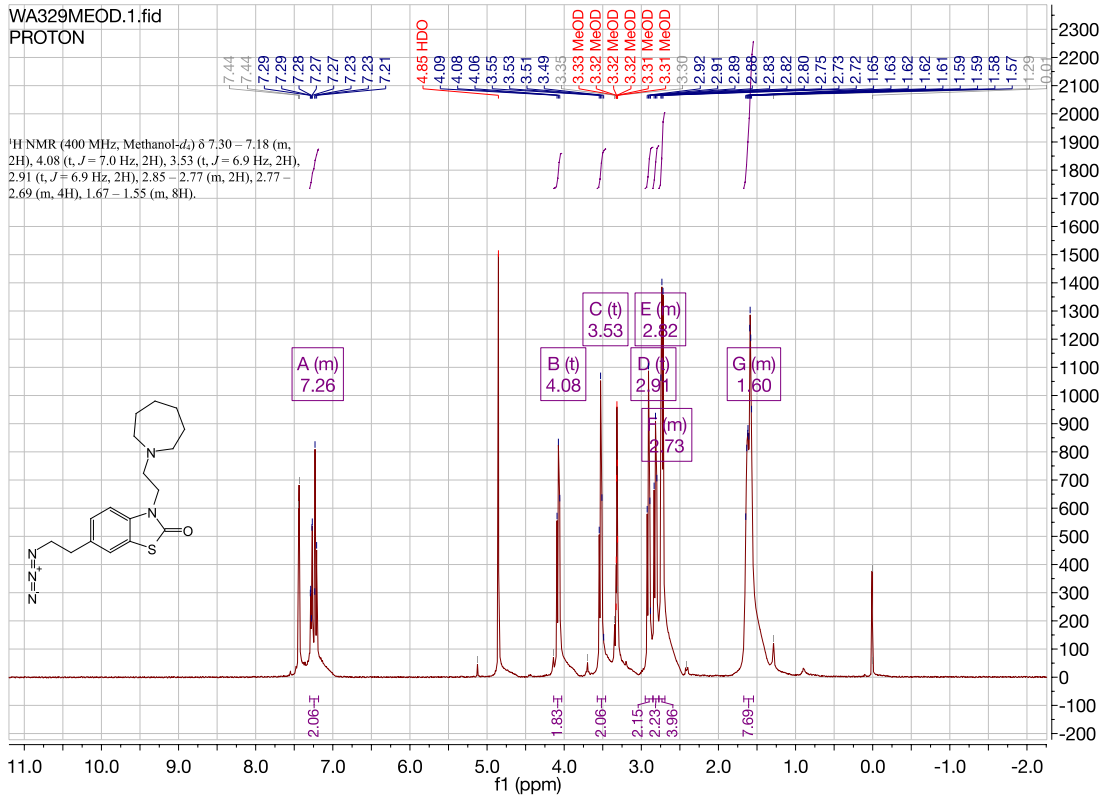
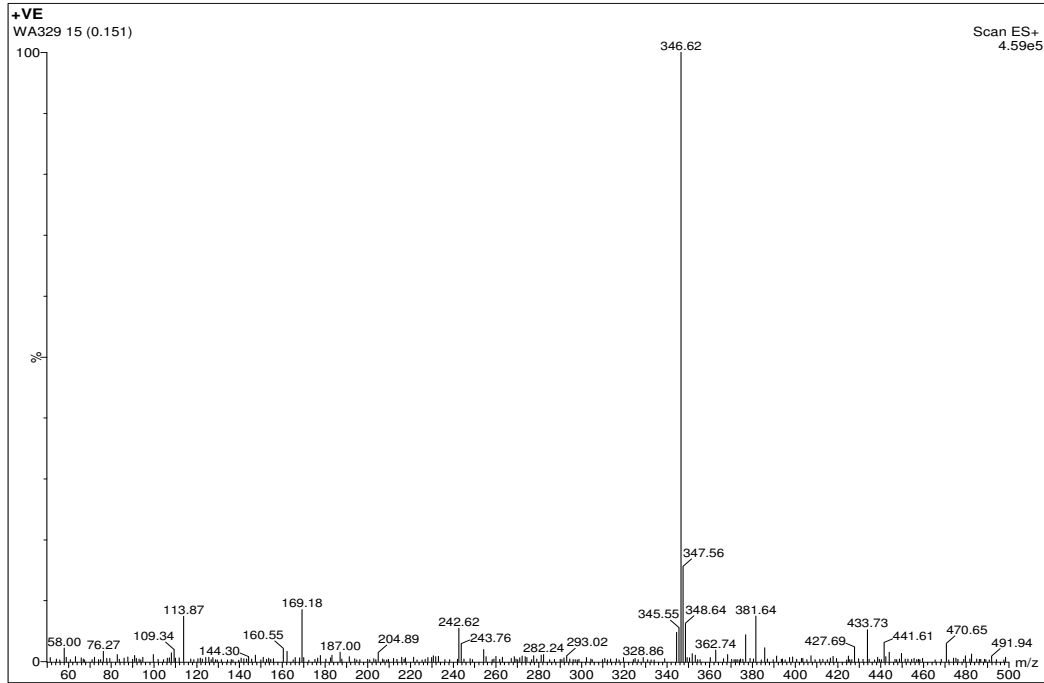


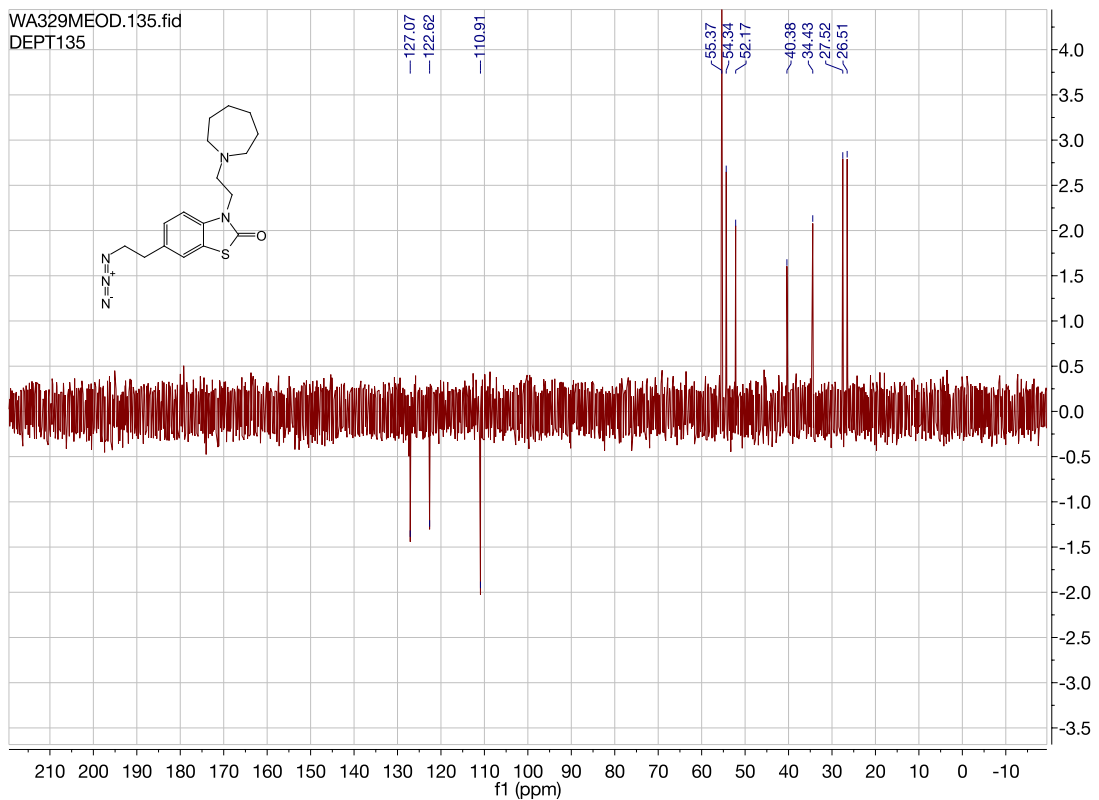
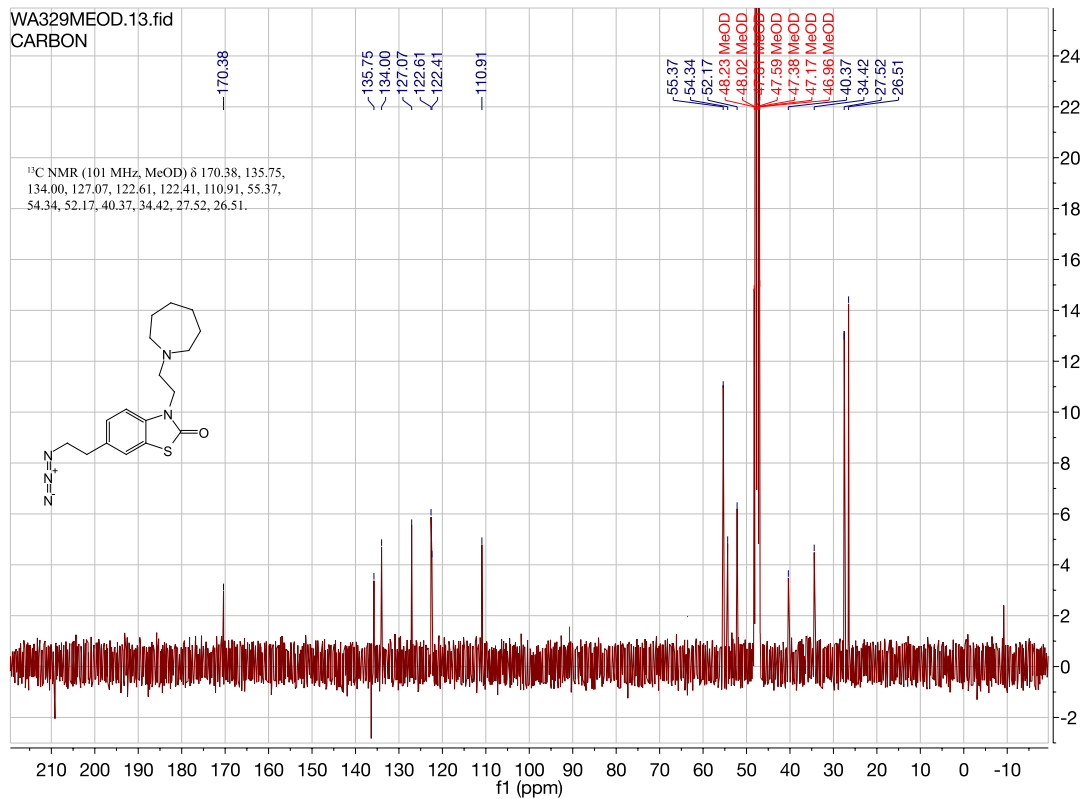
3-(2-(azepan-1-yl)ethyl)-6-(2-(methylthio)ethyl)benzo[d]thiazol-2(3H)-one. [WA327] [e1]



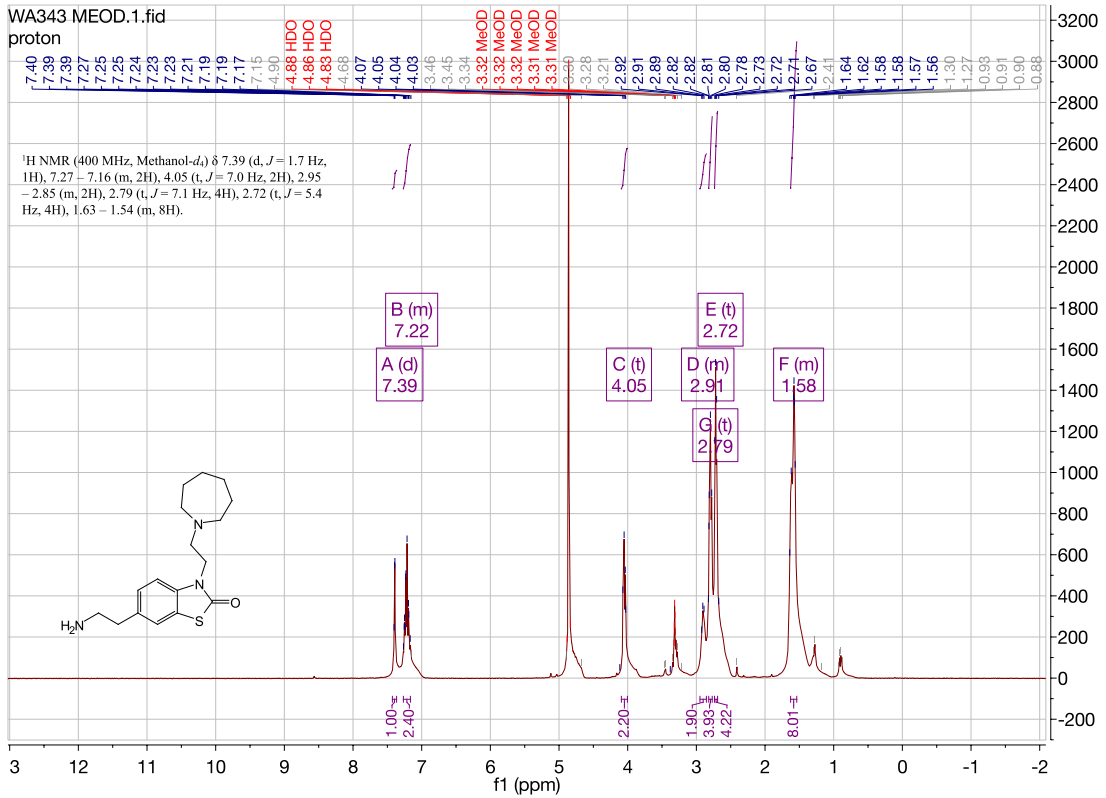
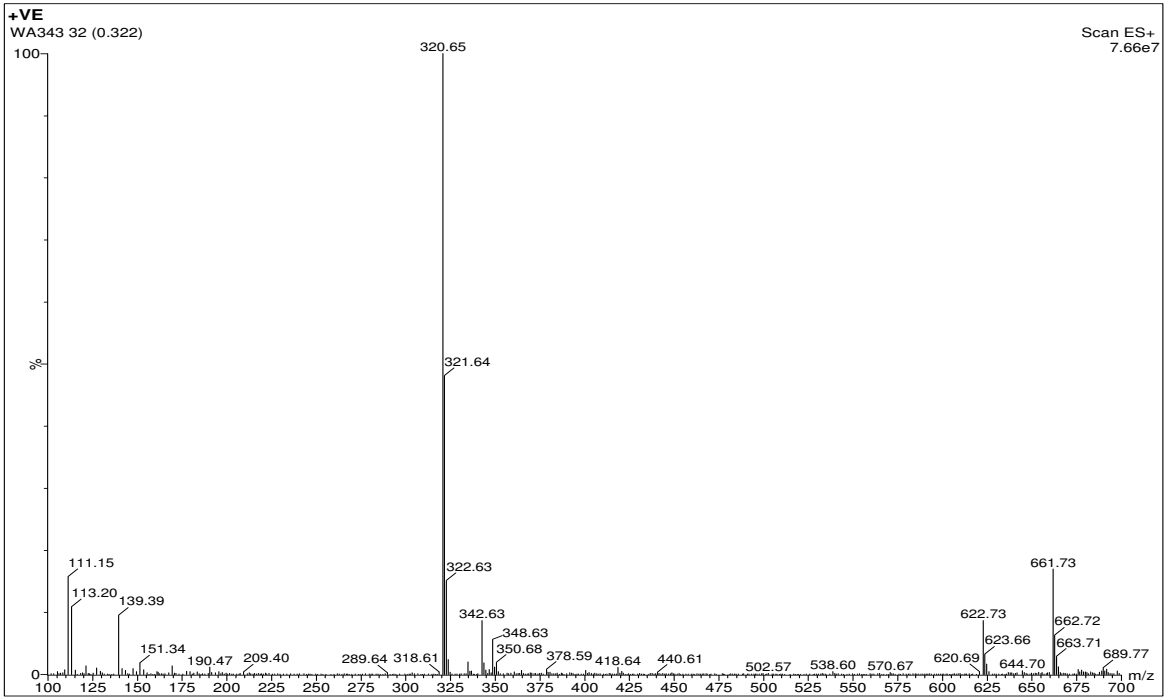


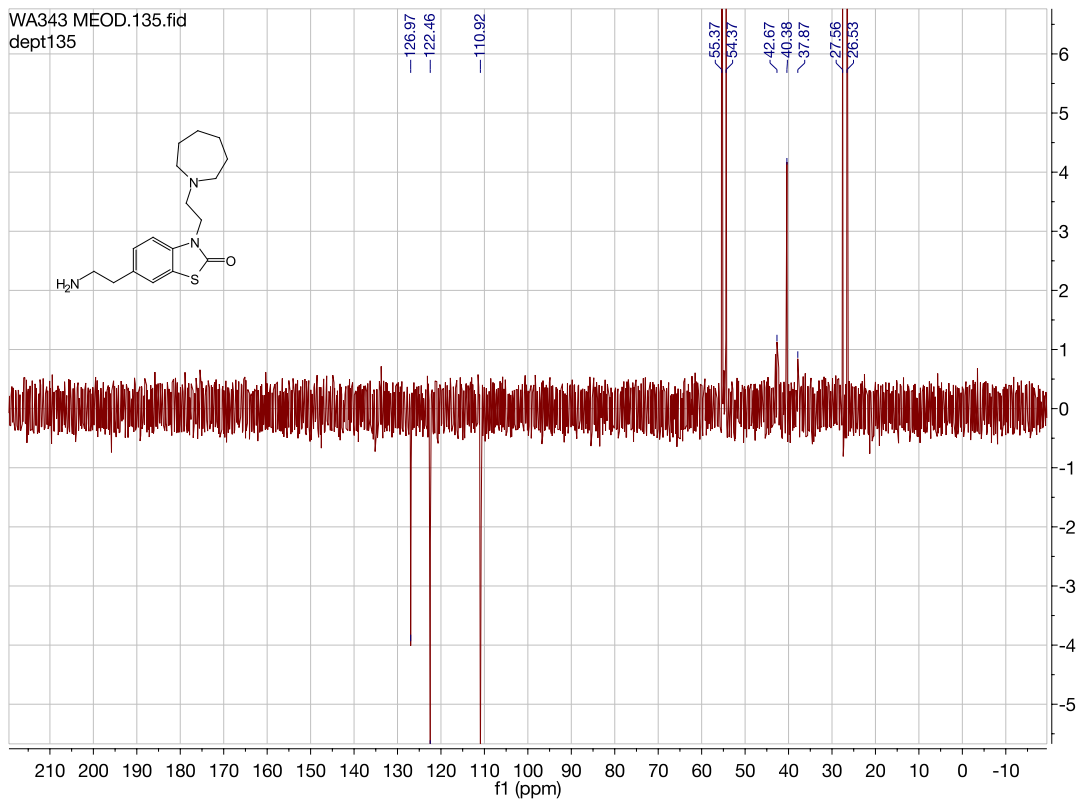
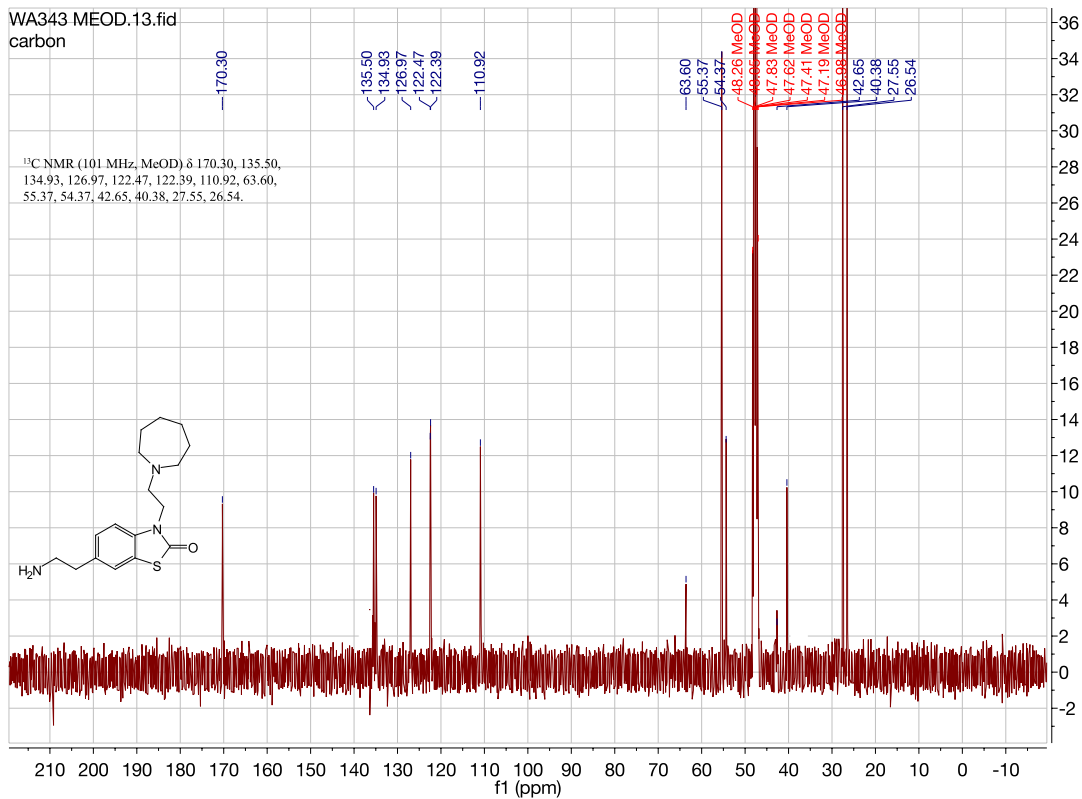
3-(2-(azepan-1-yl)ethyl)-6-(2-azidoethyl)benzo[d]thiazol-2(3H)-one. [WA329][f1]



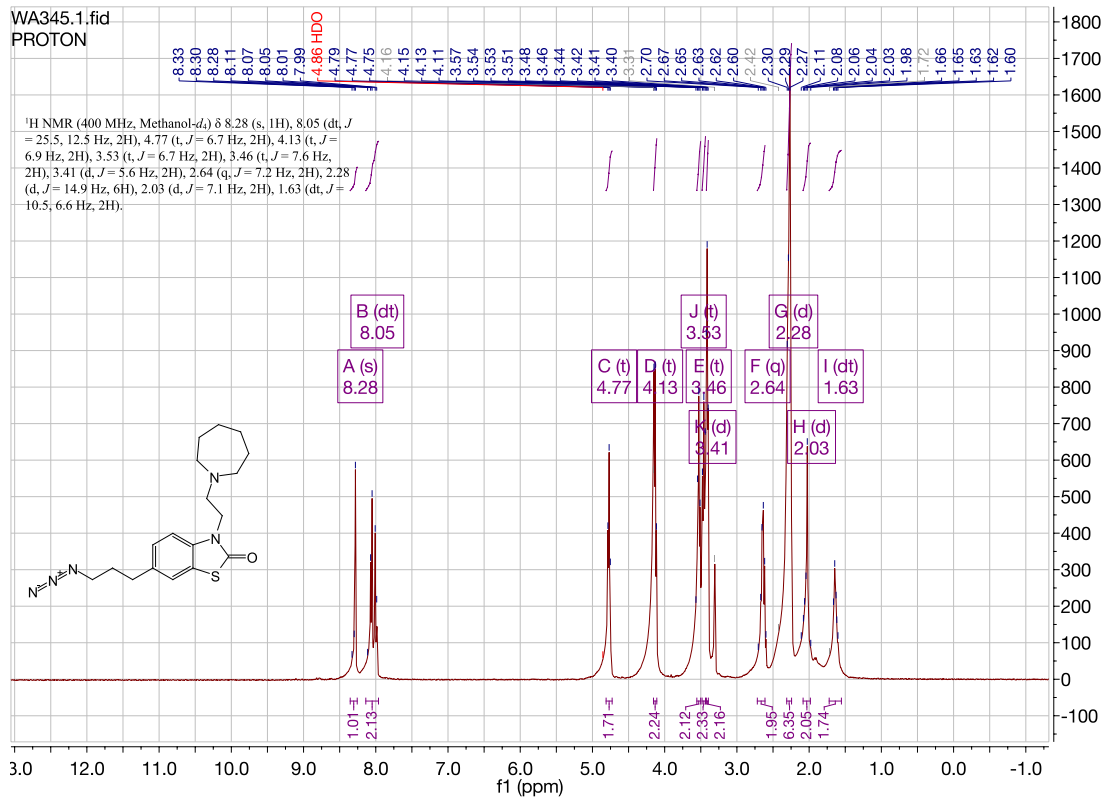
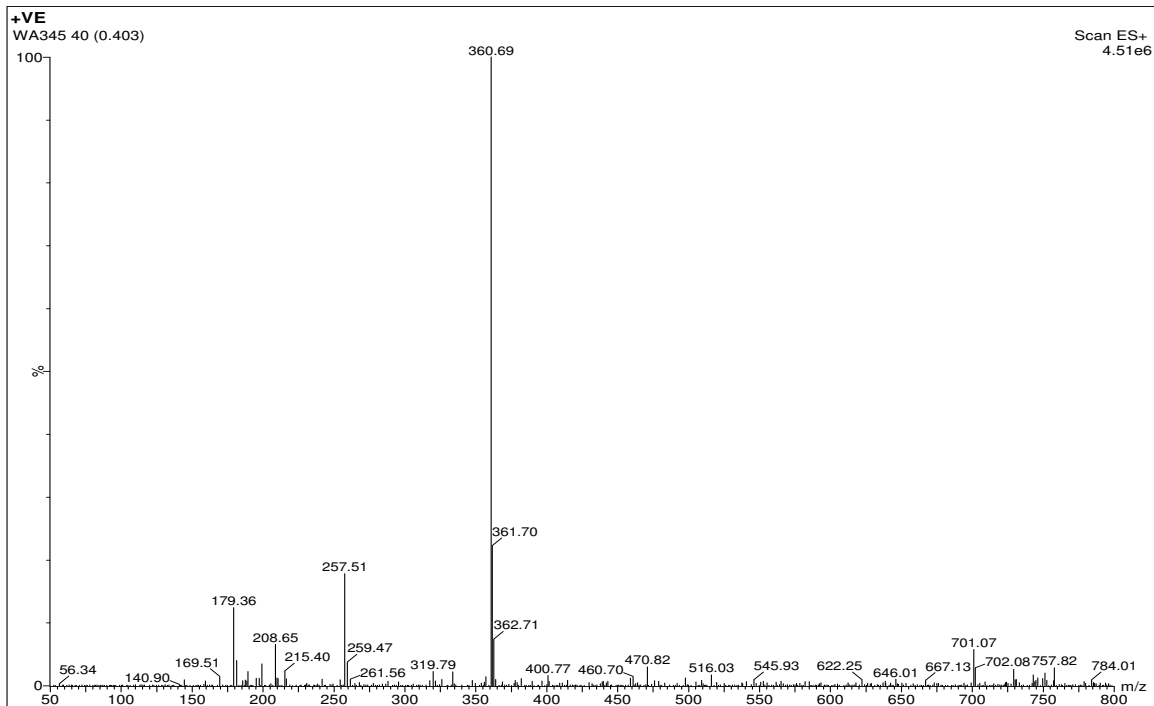


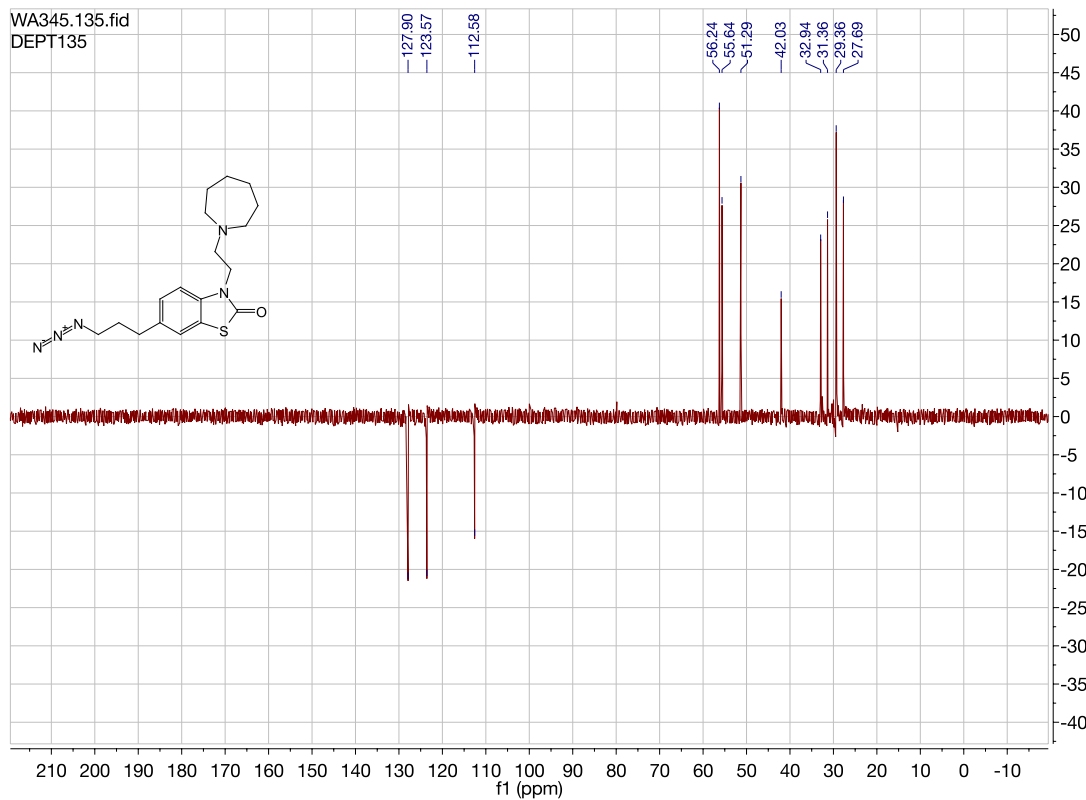
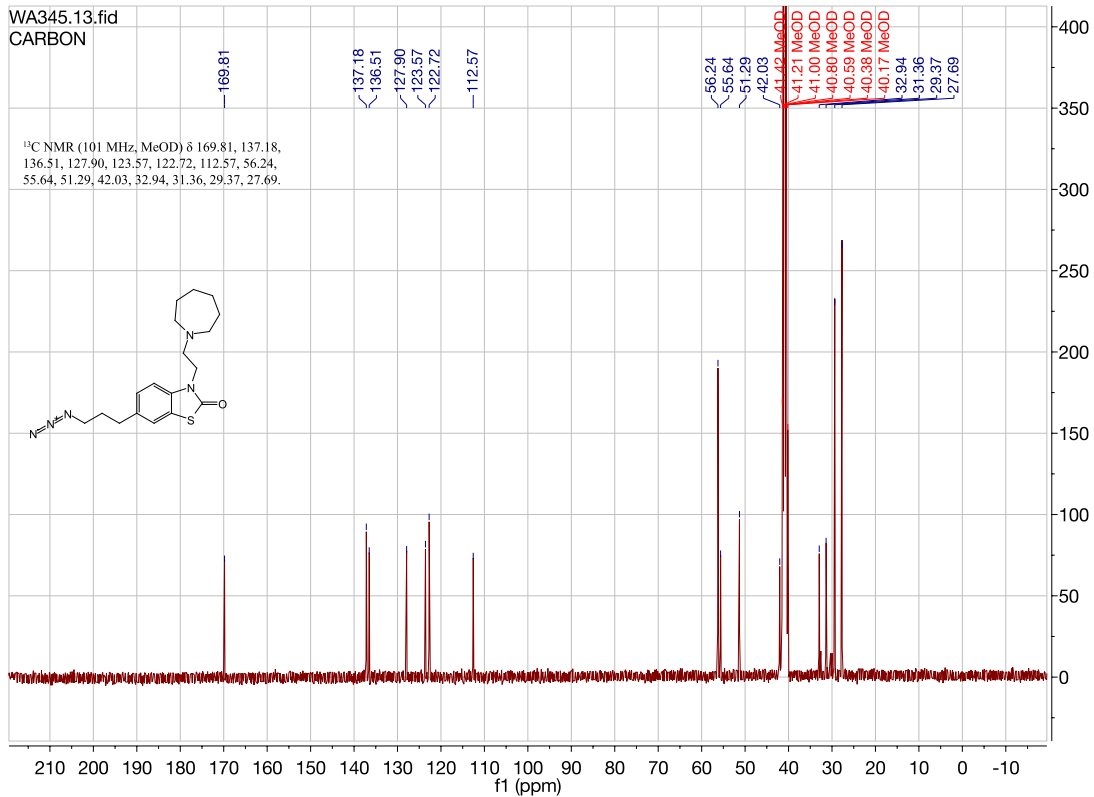
6-(2-aminoethyl)-3-(2-(azepan-1-yl)ethyl)benzo[d]thiazol-2(3H)-one. [WA343][g1]



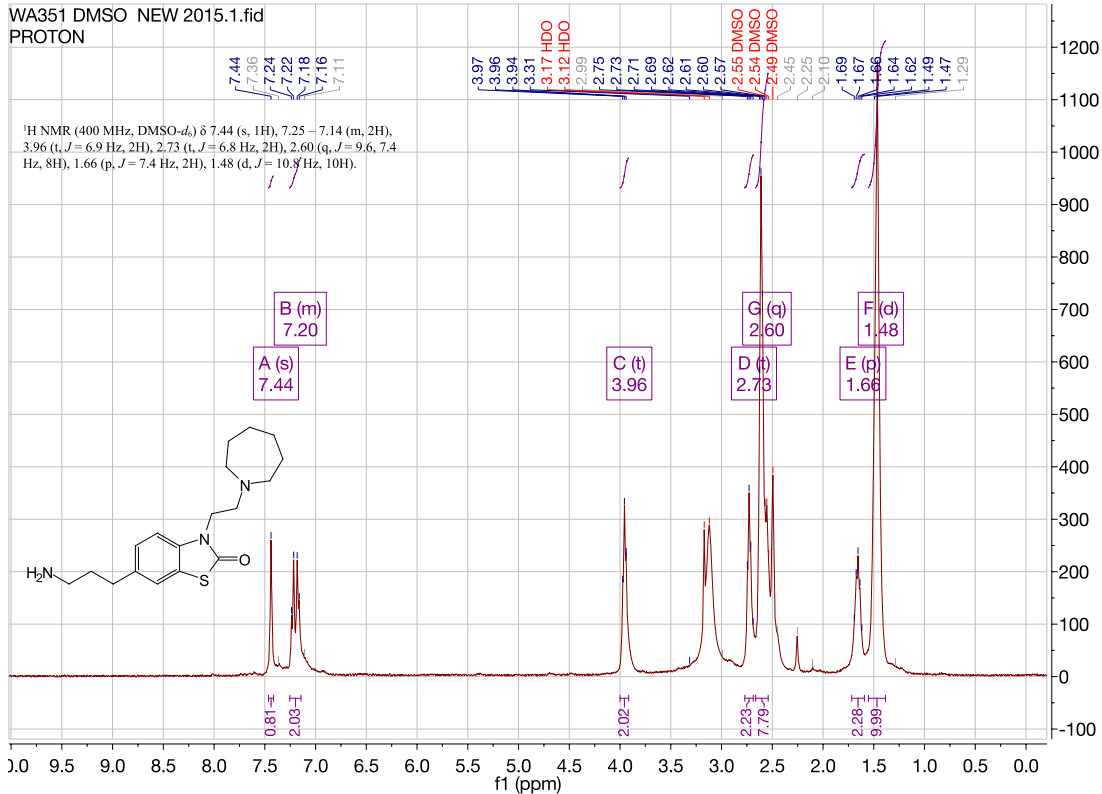
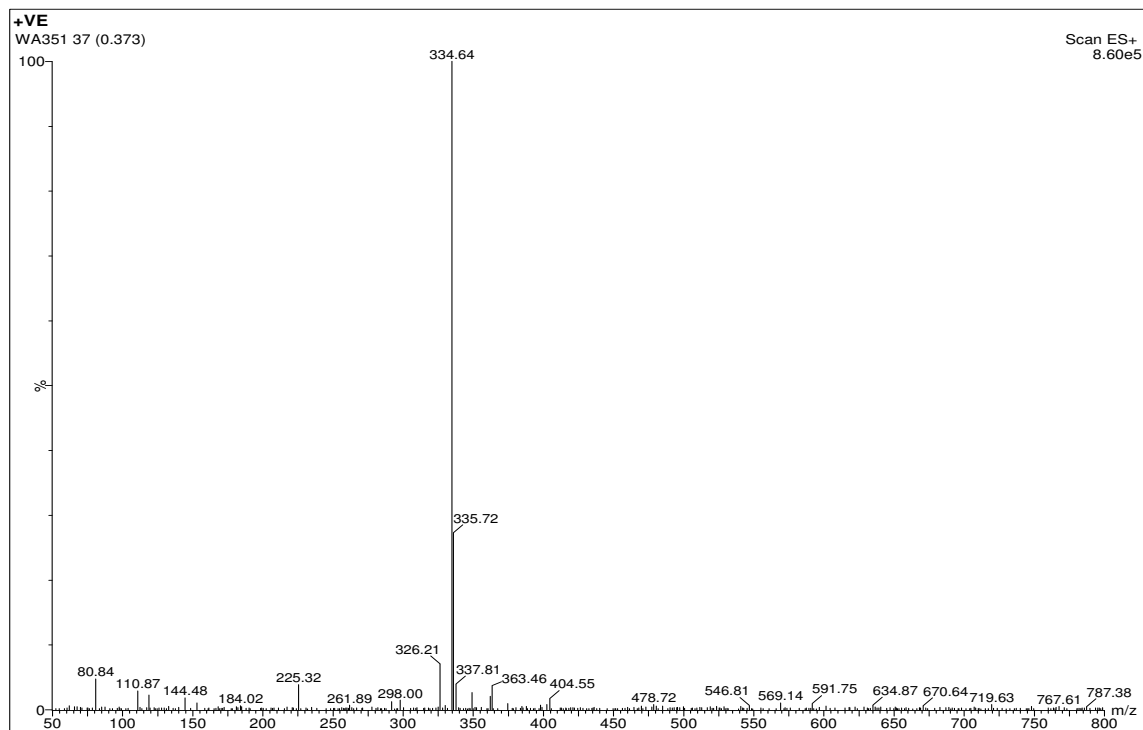


3-(2-(azepan-1-yl)ethyl)-6-(3-azidopropyl)benzo[d]thiazol-2(3H)-one. [WA345][f2]

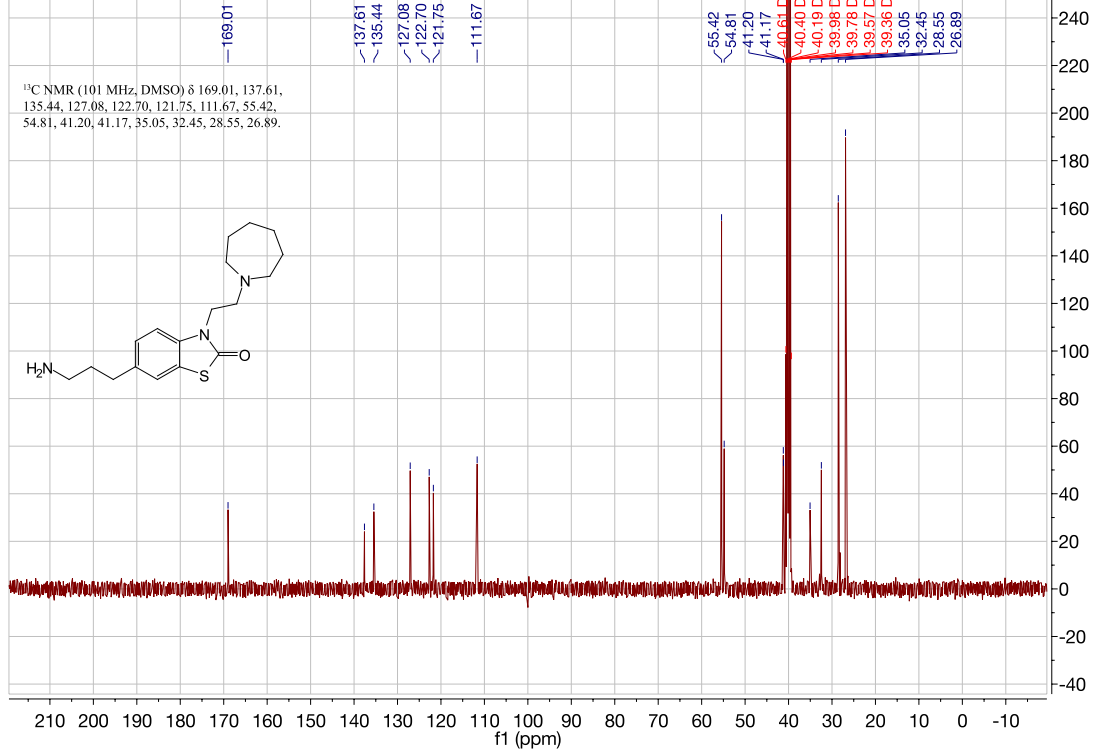




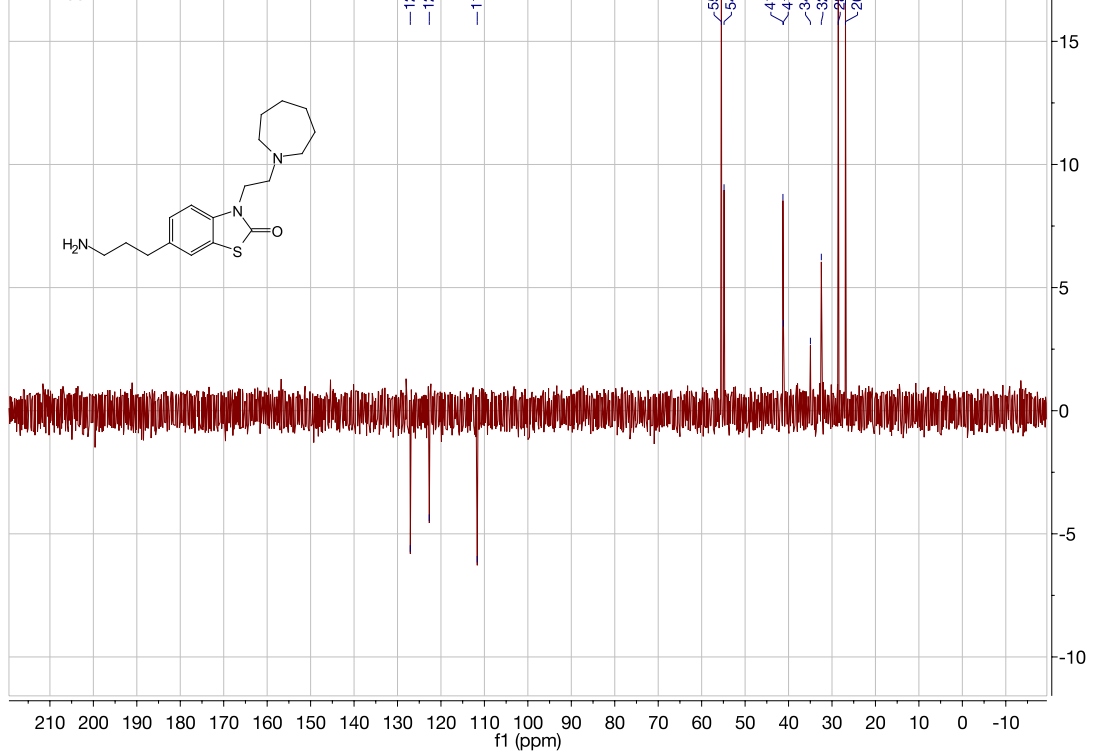
6-(3-aminopropyl)-3-(2-(azepan-1-yl)ethyl)benzo[d]thiazol-2(3H)-one. [WA351][g2]



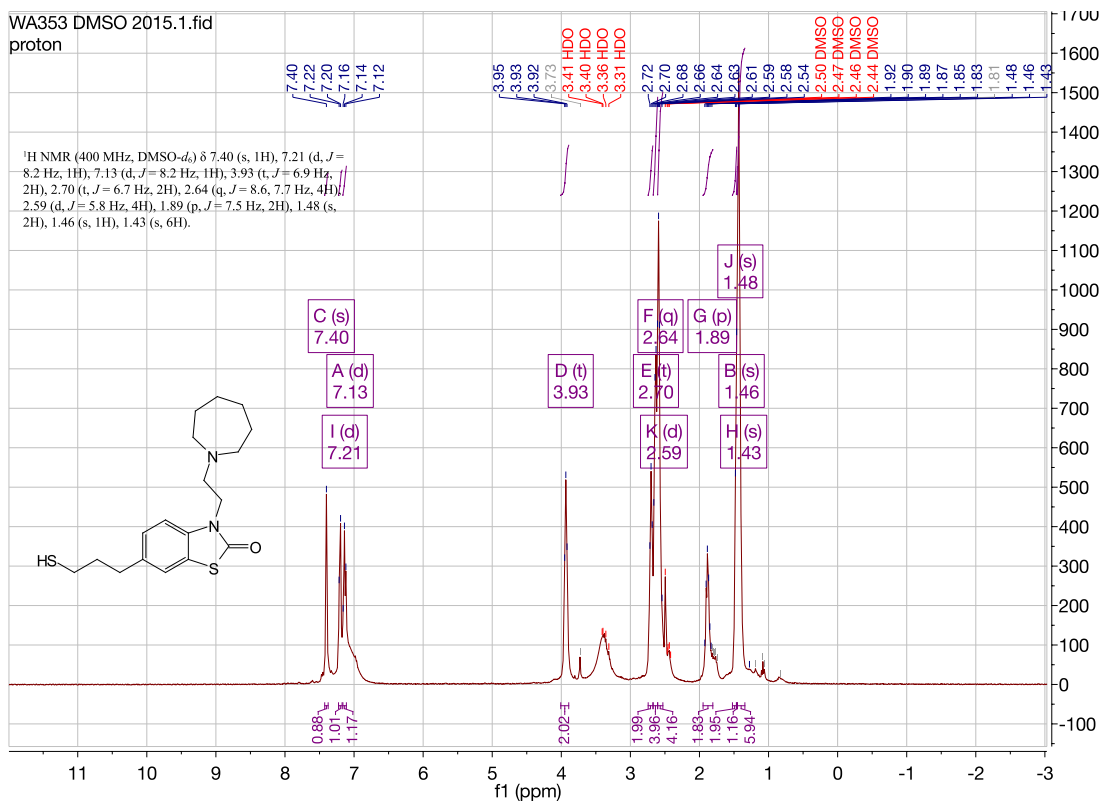
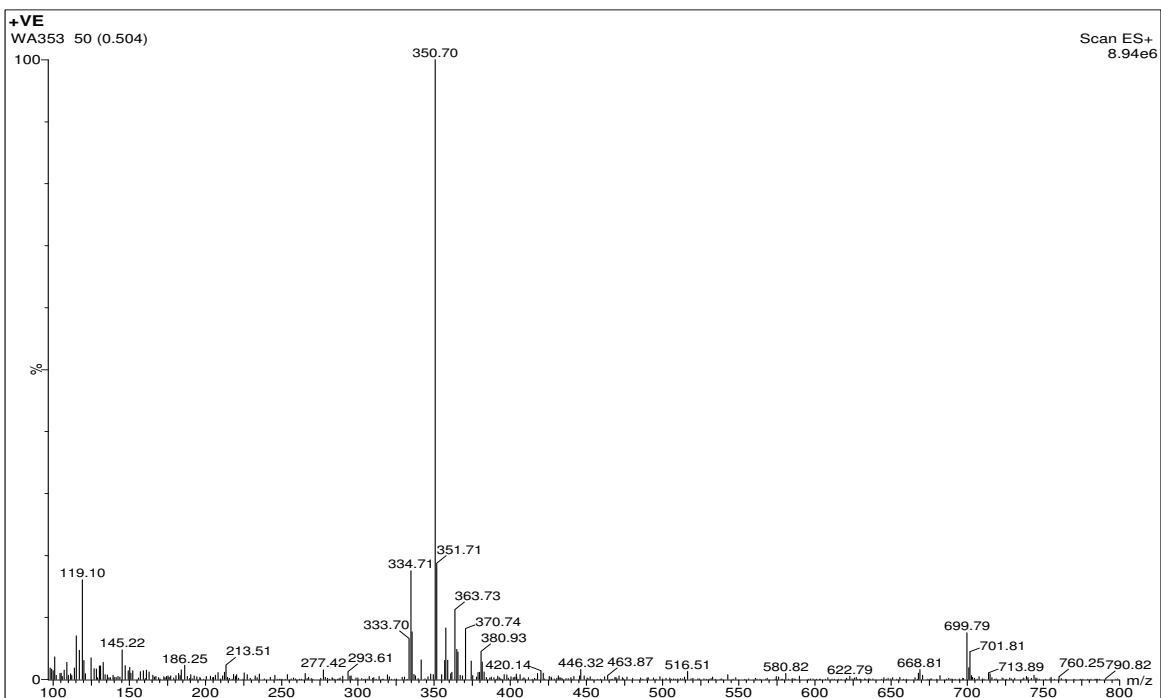
WA351 DMSO NEW 2015.13.fid
CARBON



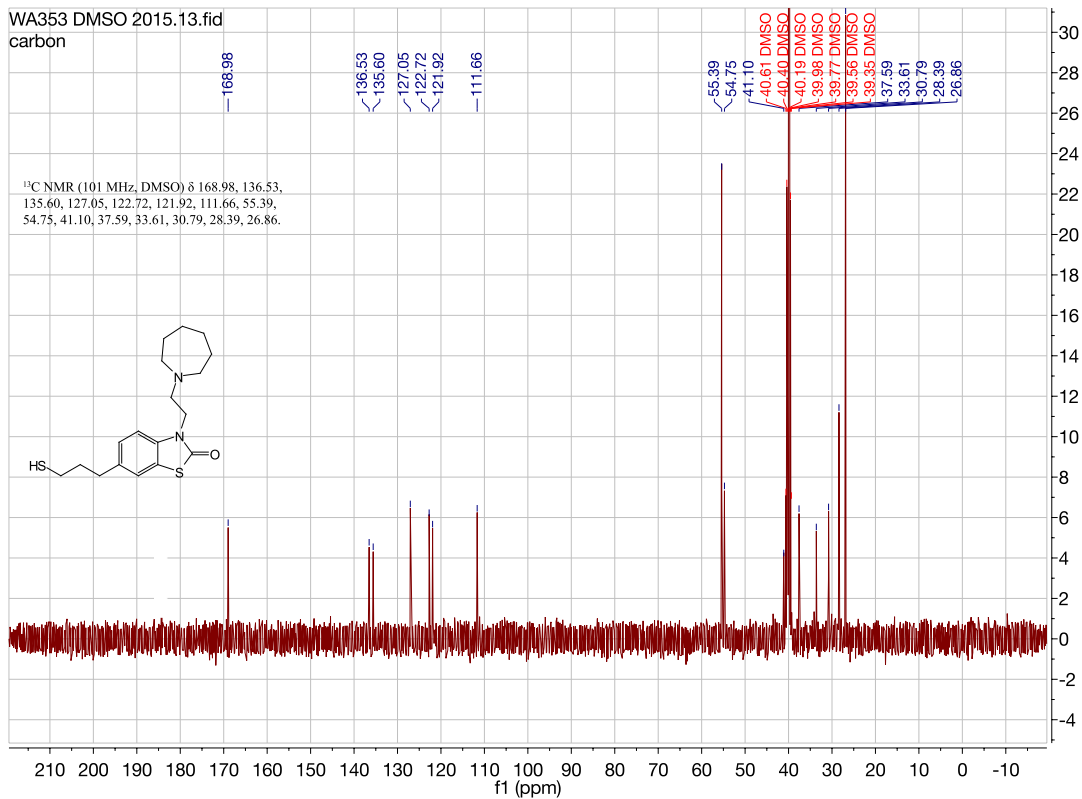
WA351 DMSO NEW 2015.135.fid
DEPT135



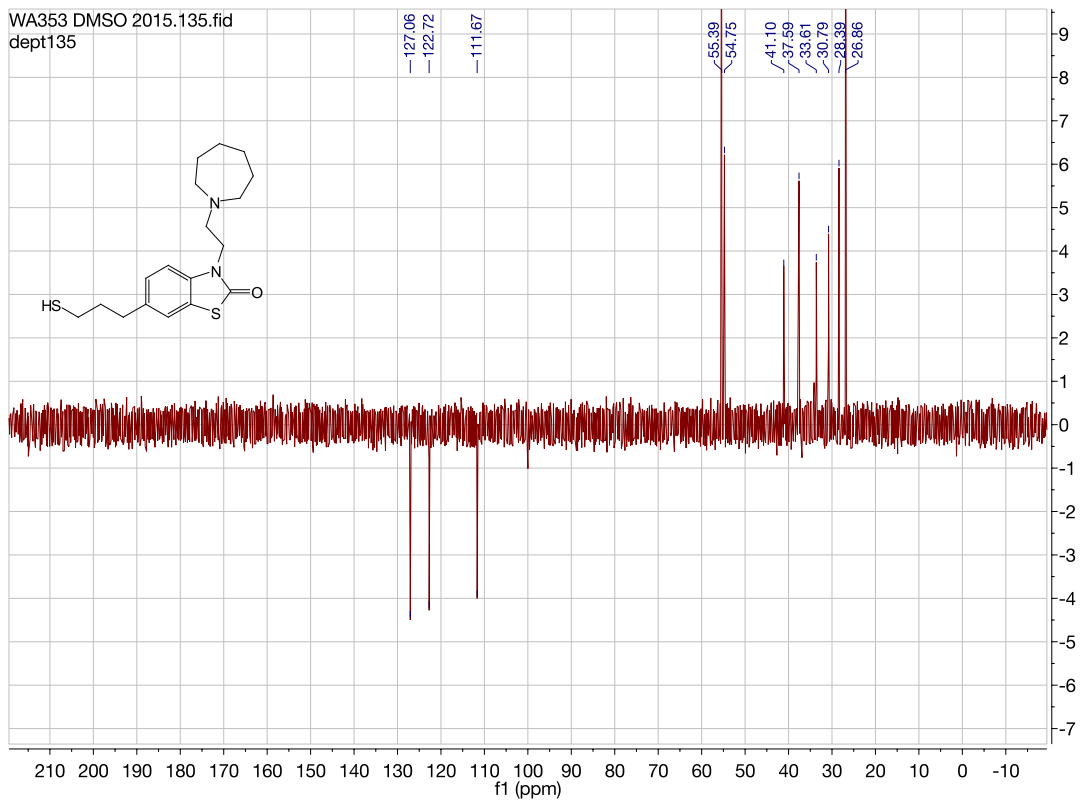
**3-(2-(azepan-1-yl)ethyl)-6-(3-mercaptopropyl)benzo[d]thiazol-2(3H)-one. [WA353]
[h2]**



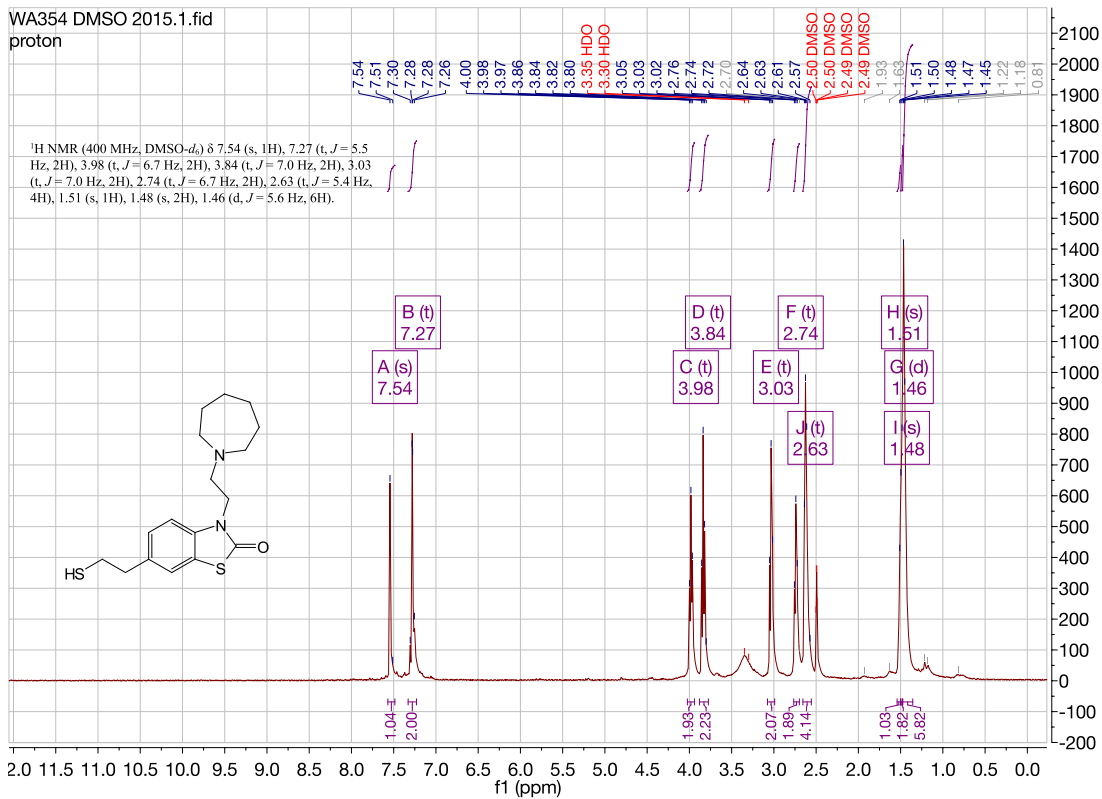
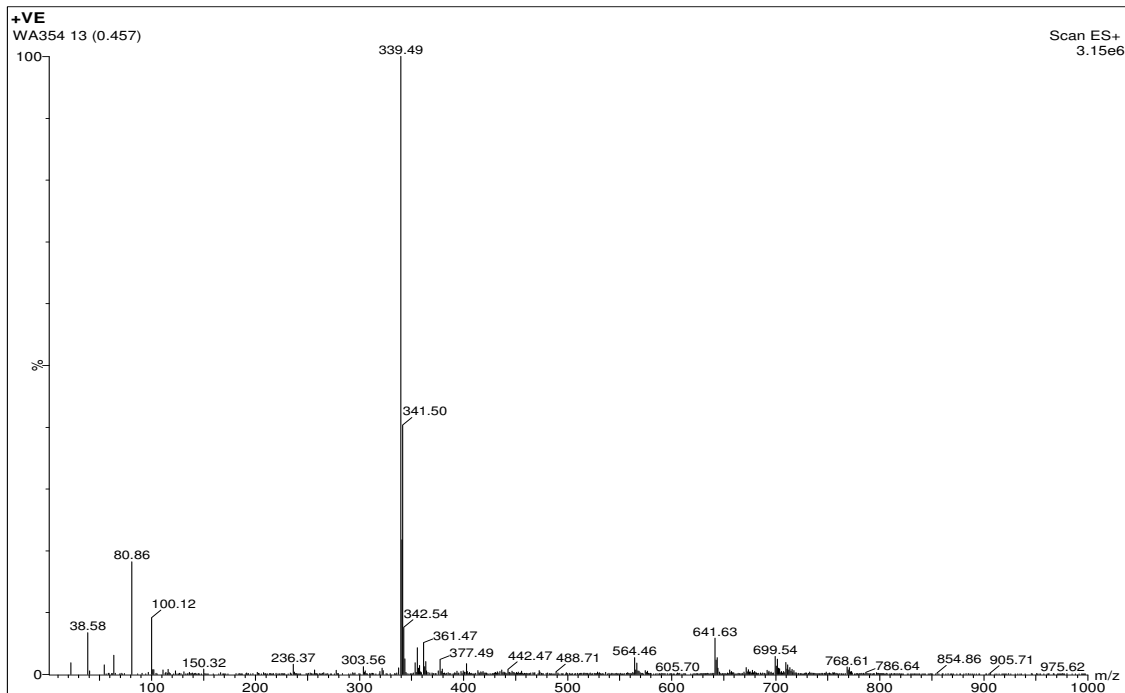
WA353 DMSO 2015.13.fid
carbon

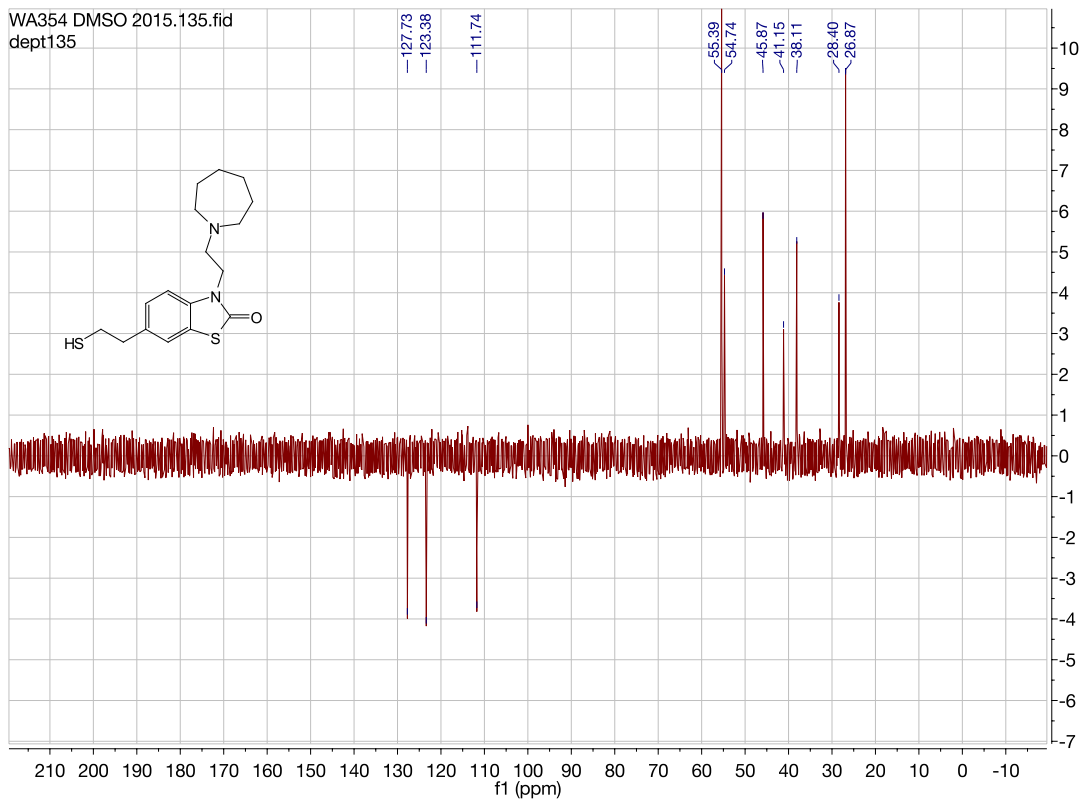
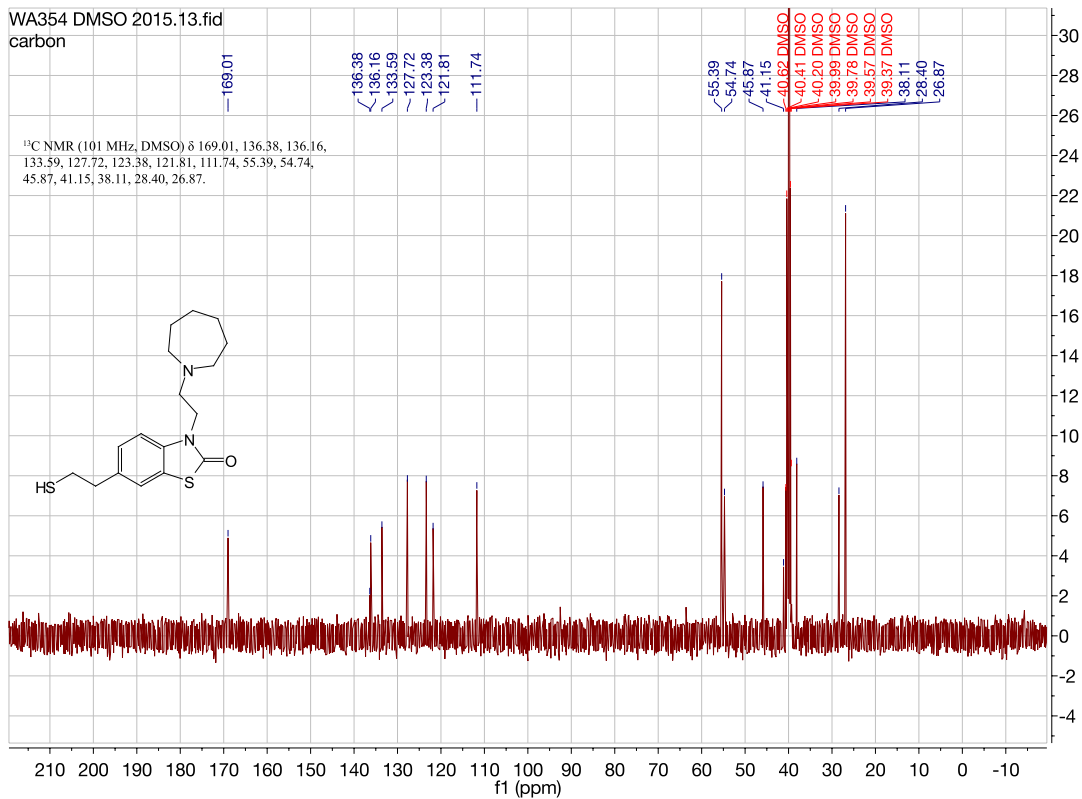


WA353 DMSO 2015.135.fid
dept135

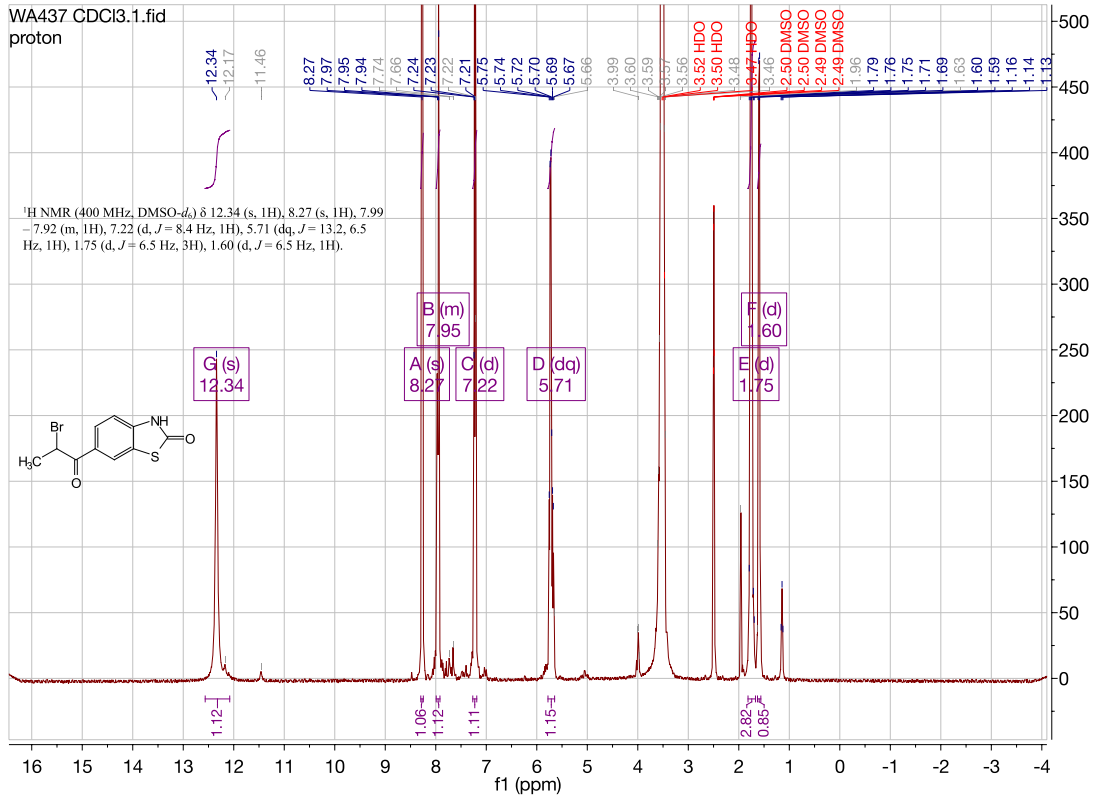
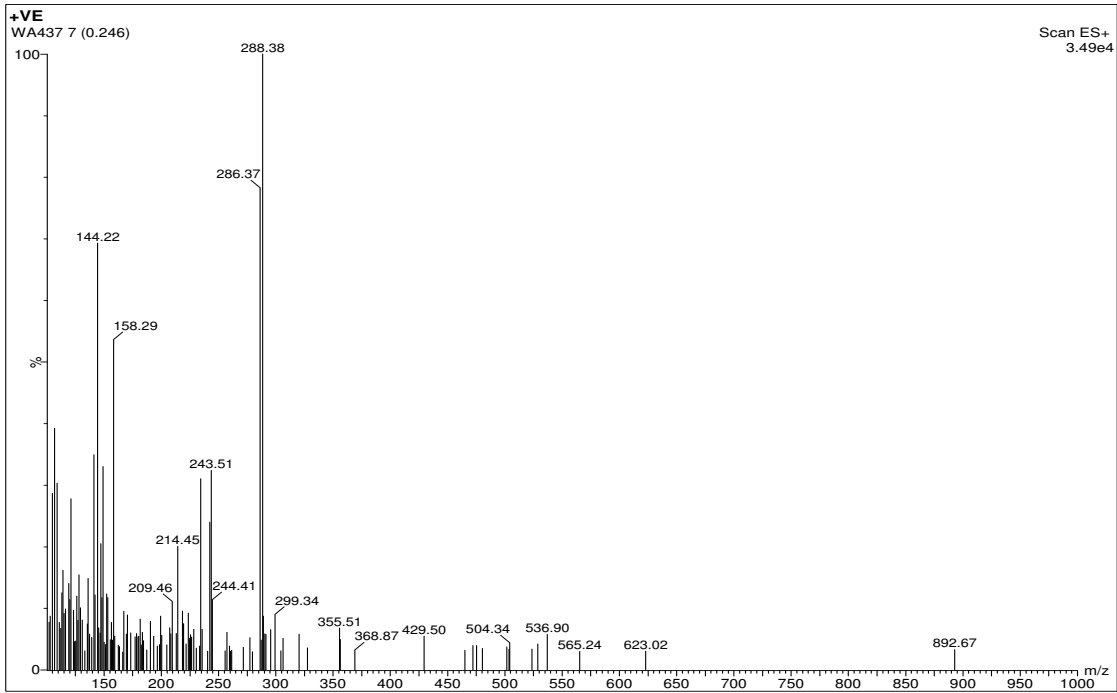


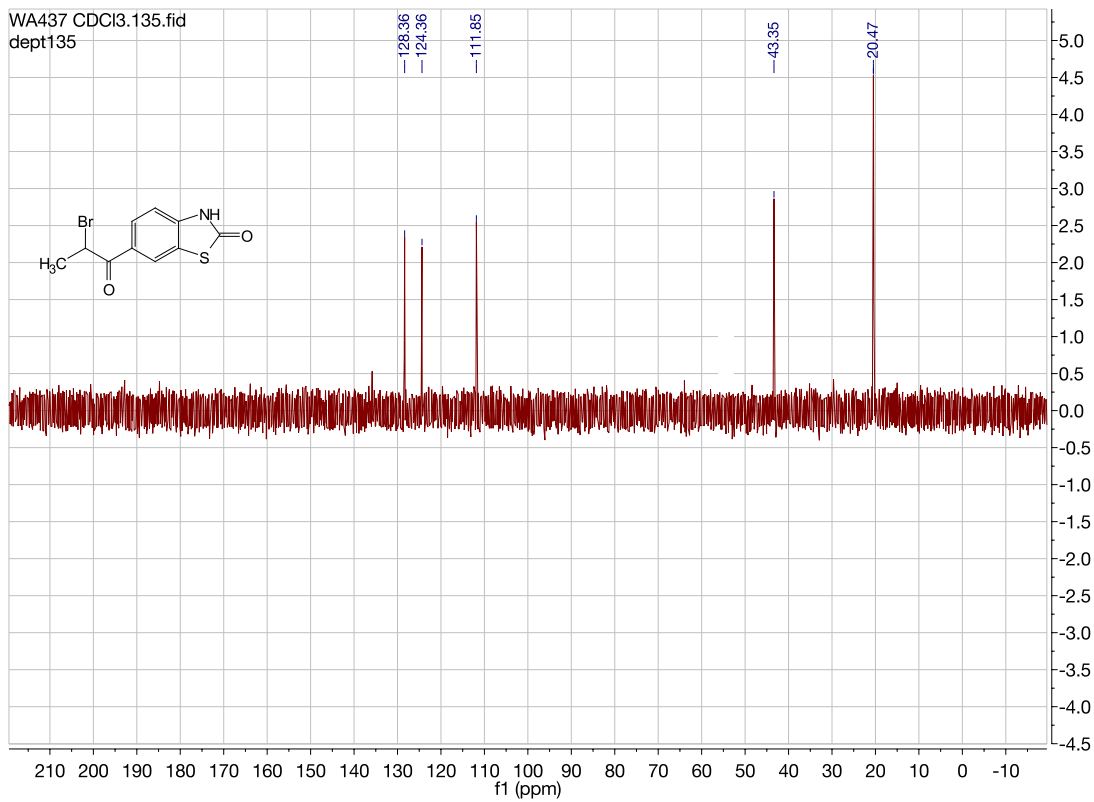
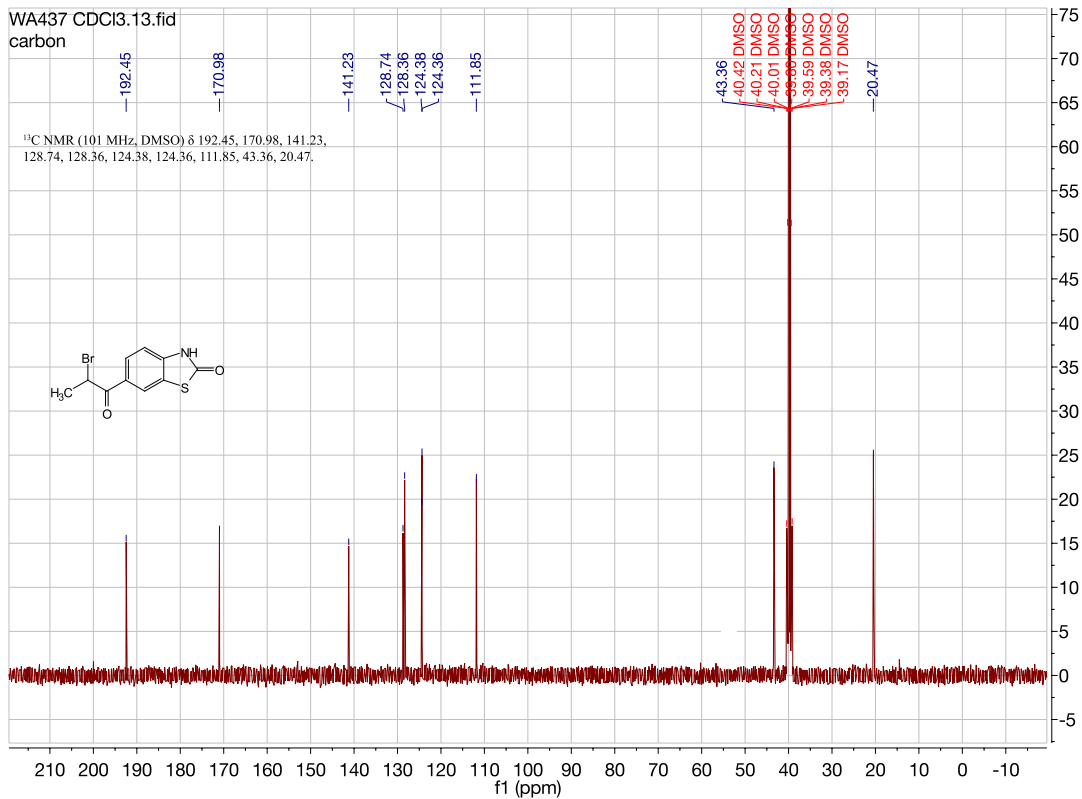
**3-(2-(azepan-1-yl)ethyl)-6-(2-mercaptoethyl)benzo[d]thiazol-2(3H)-one. [WA354]
[h1]**



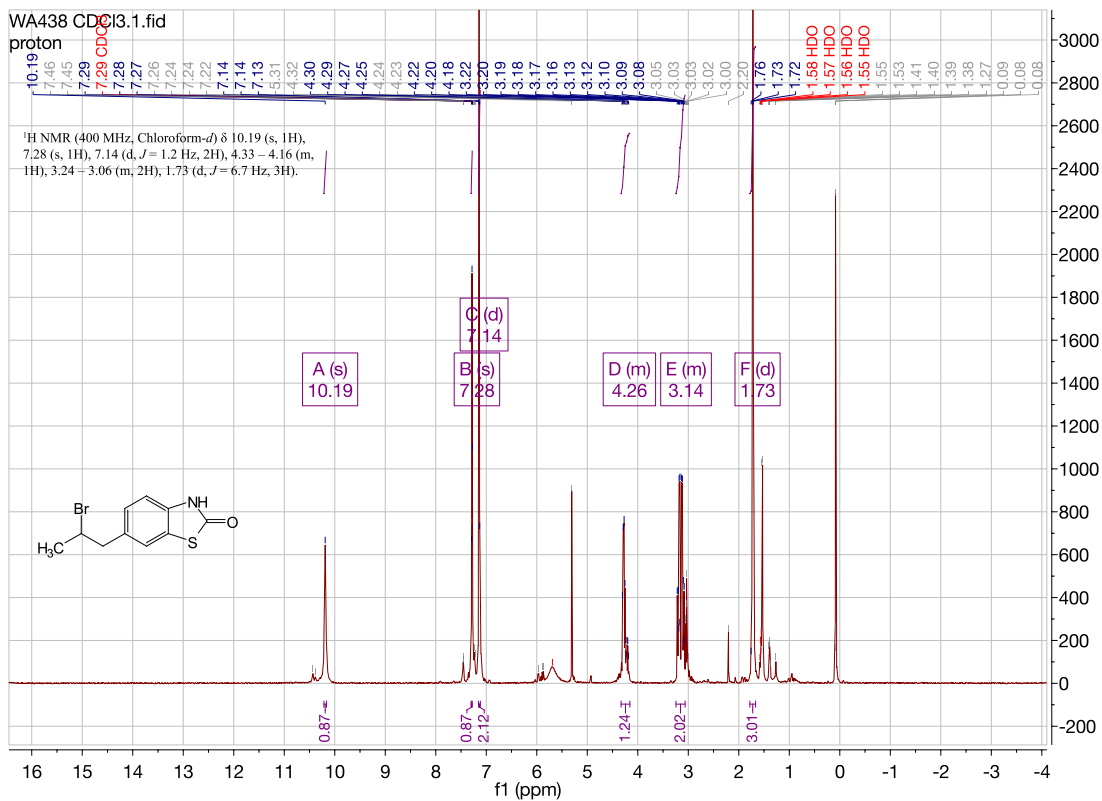
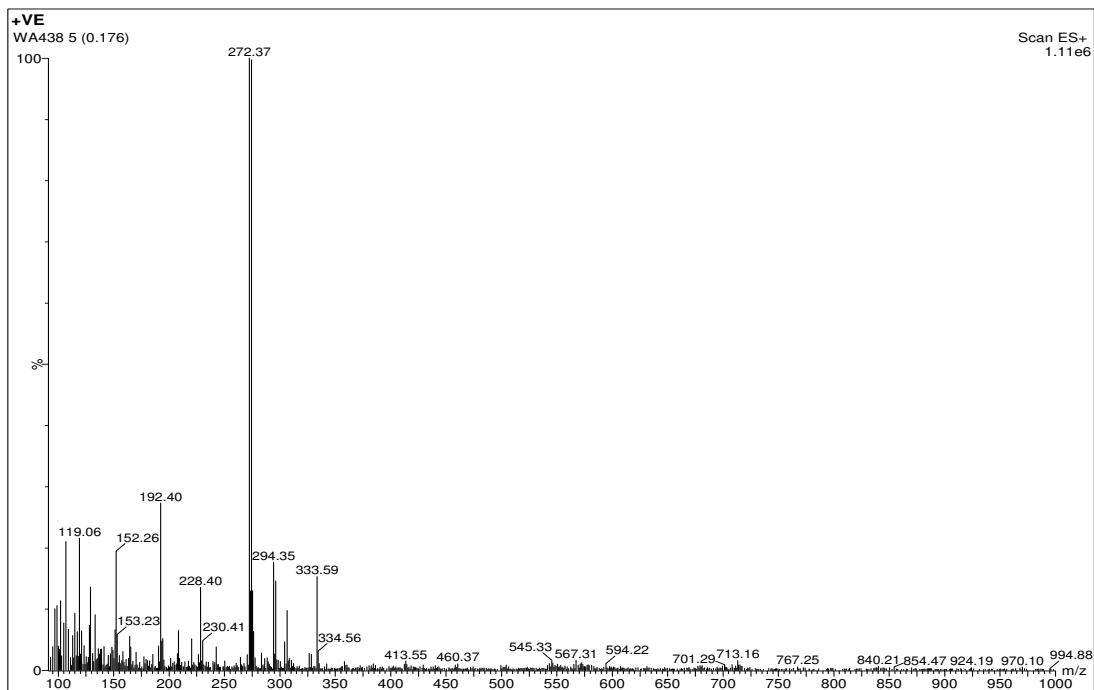


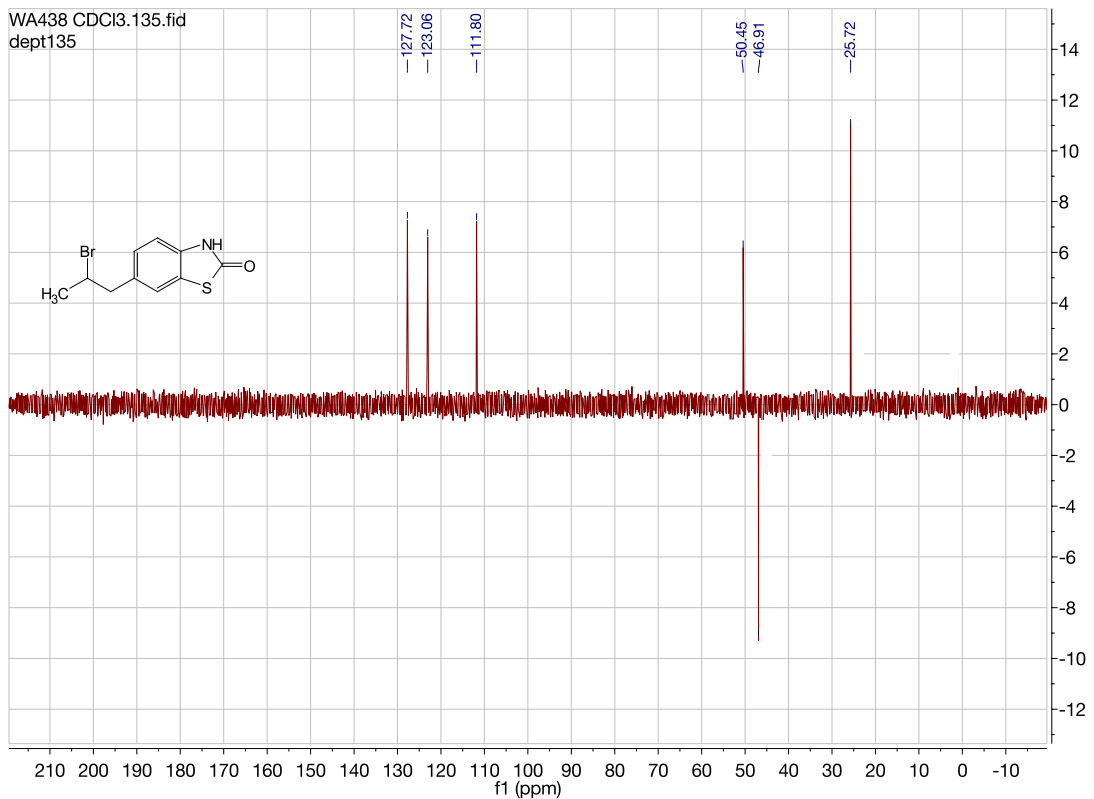
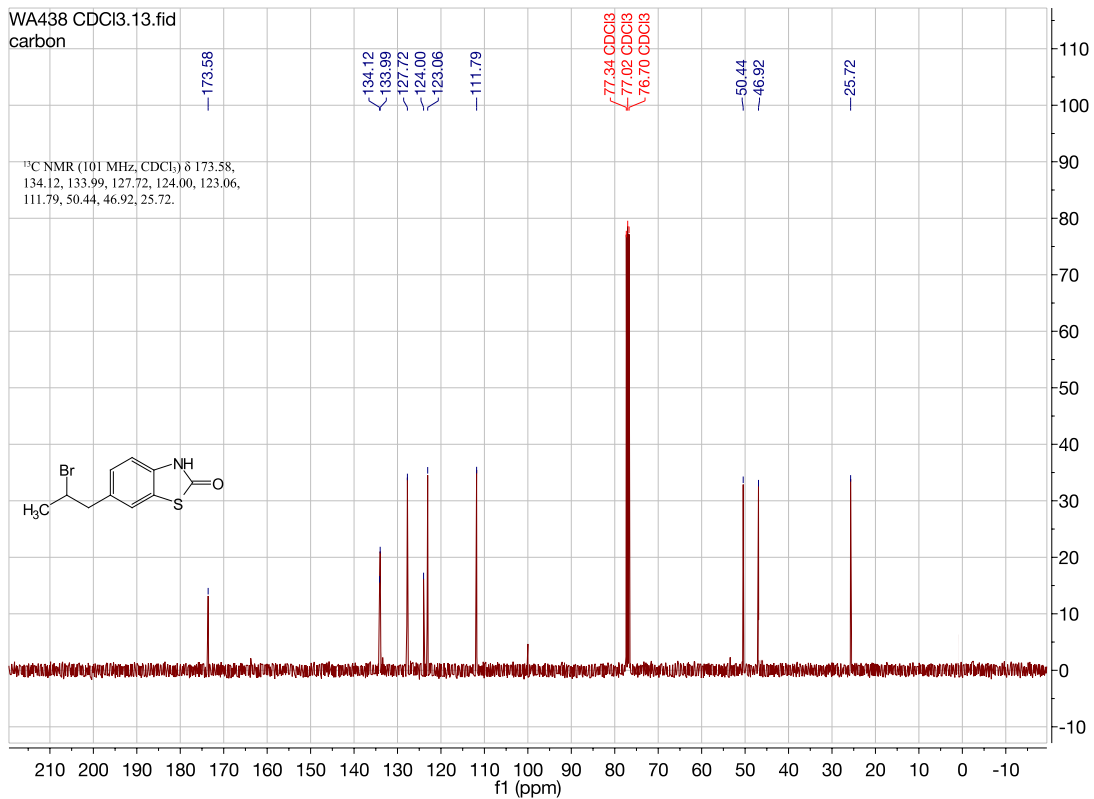
6-(2-bromopropanoyl)benzo[d]thiazol-2(3H)-one. [WA437][b]



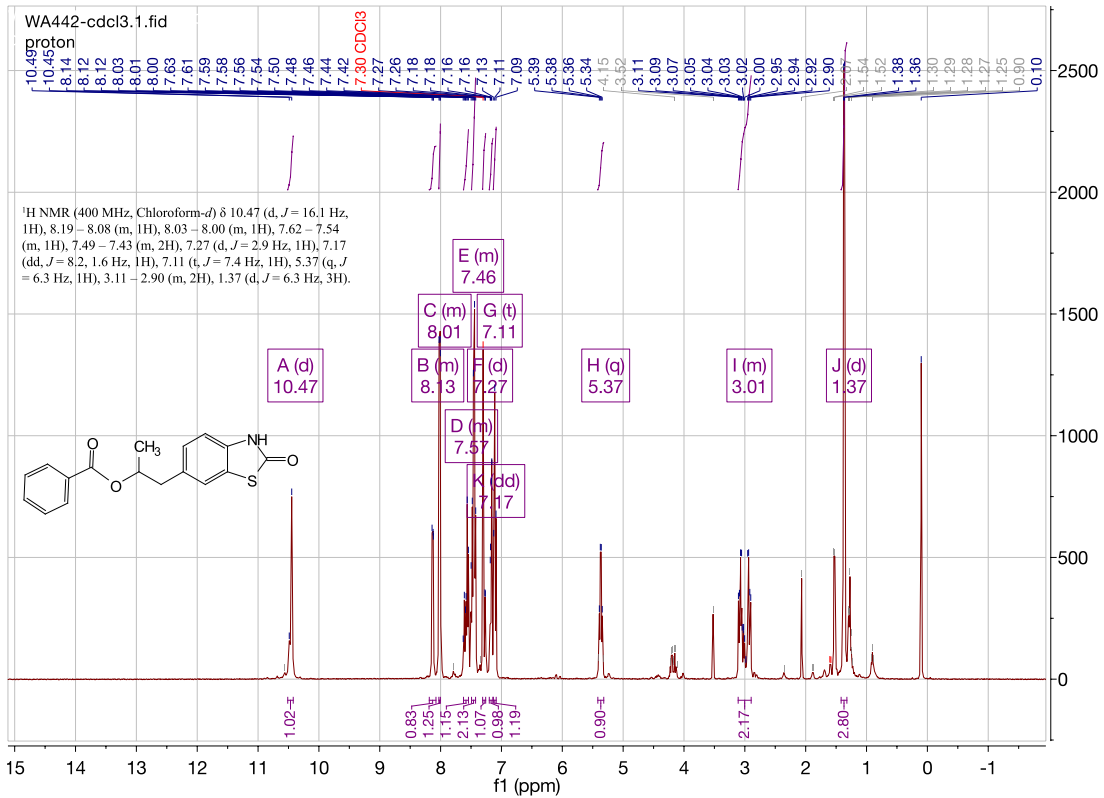
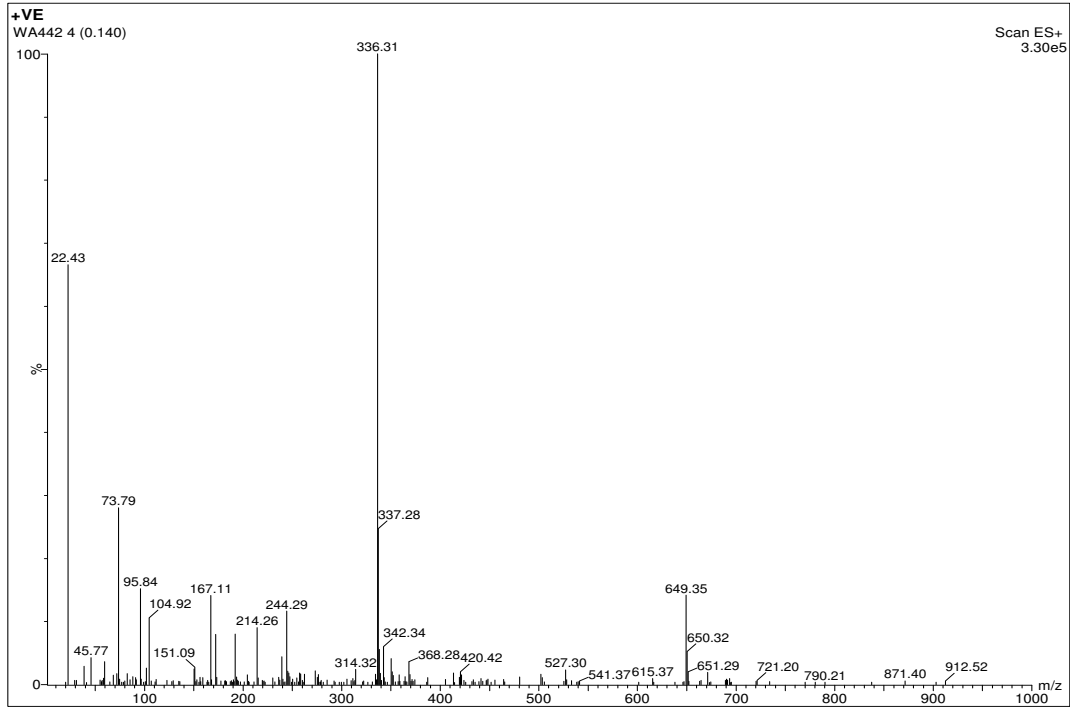


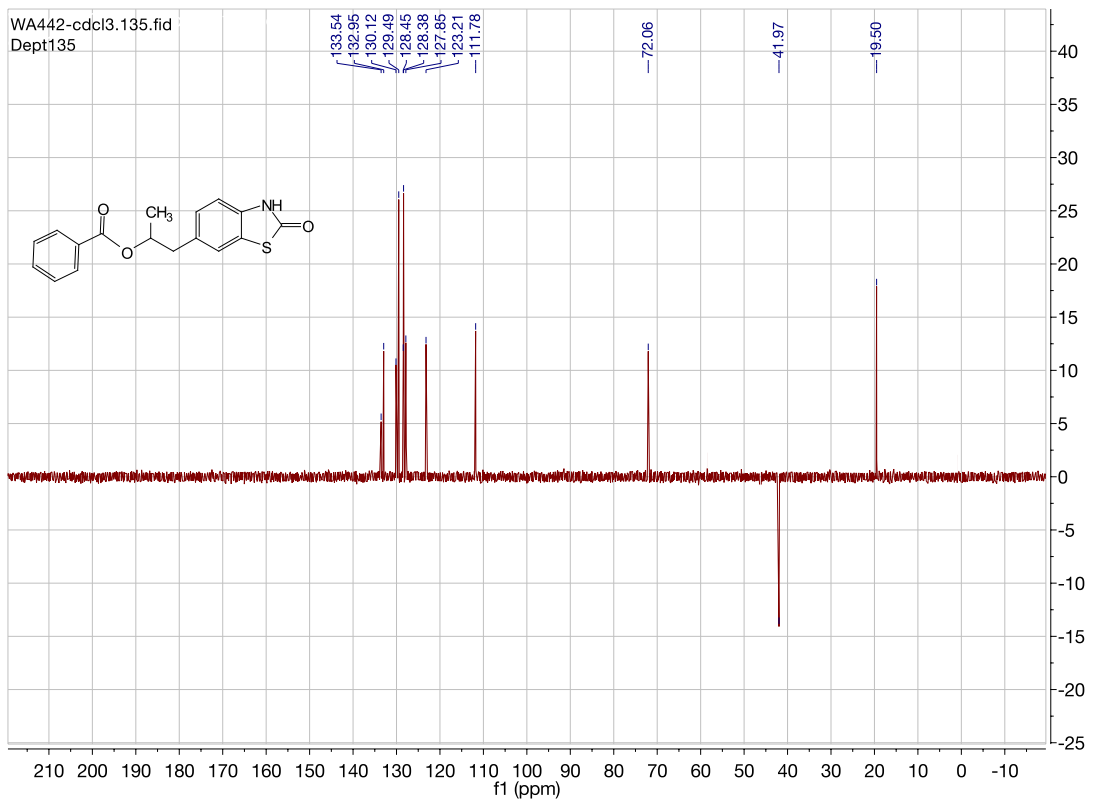
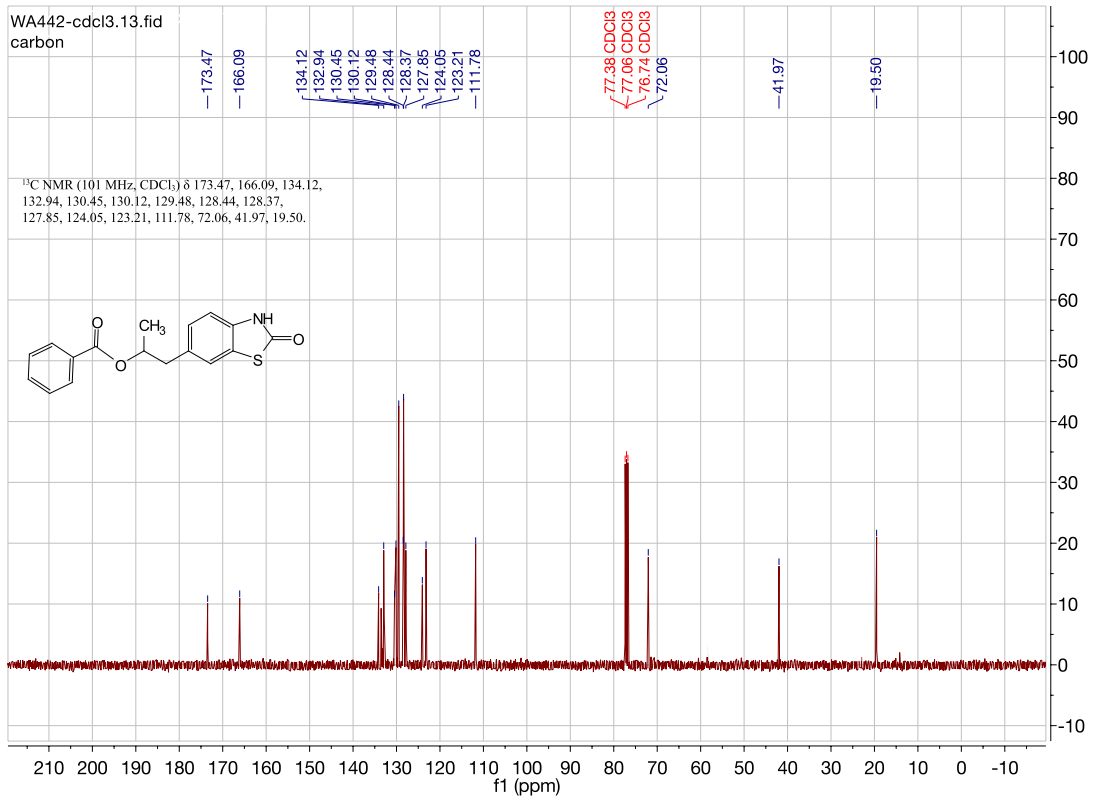
6-(2-bromopropyl)benzo[d]thiazol-2(3H)-one. [WA438][c]



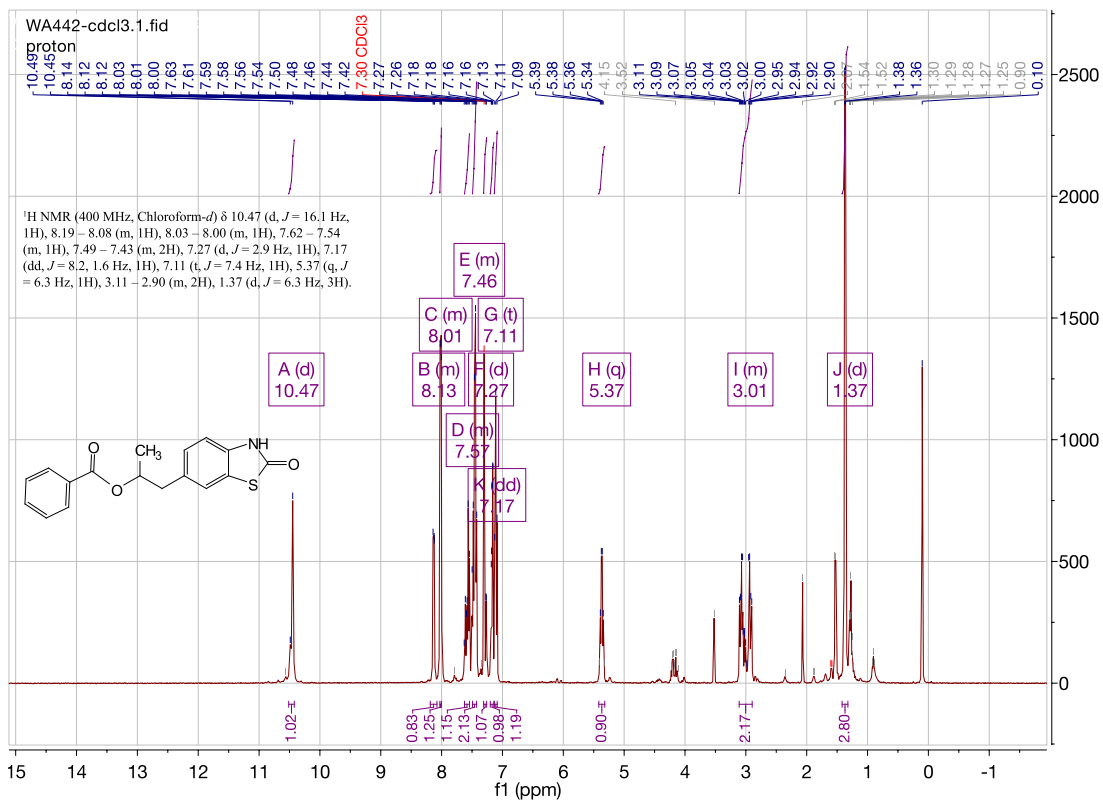
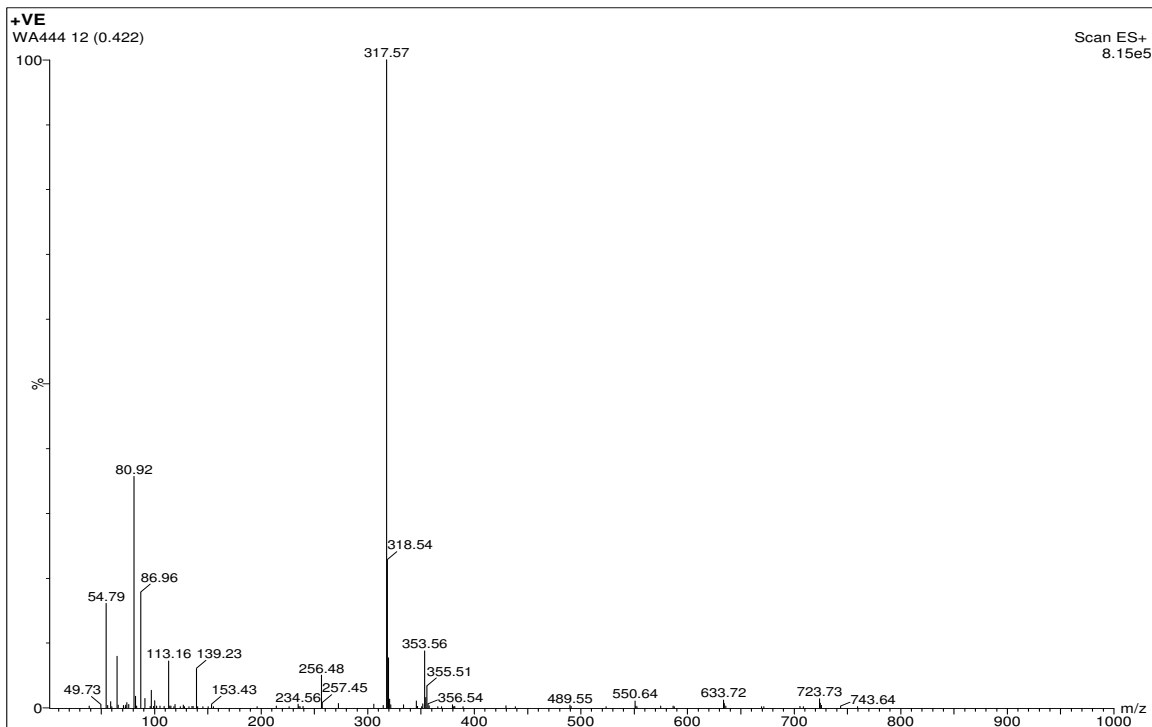


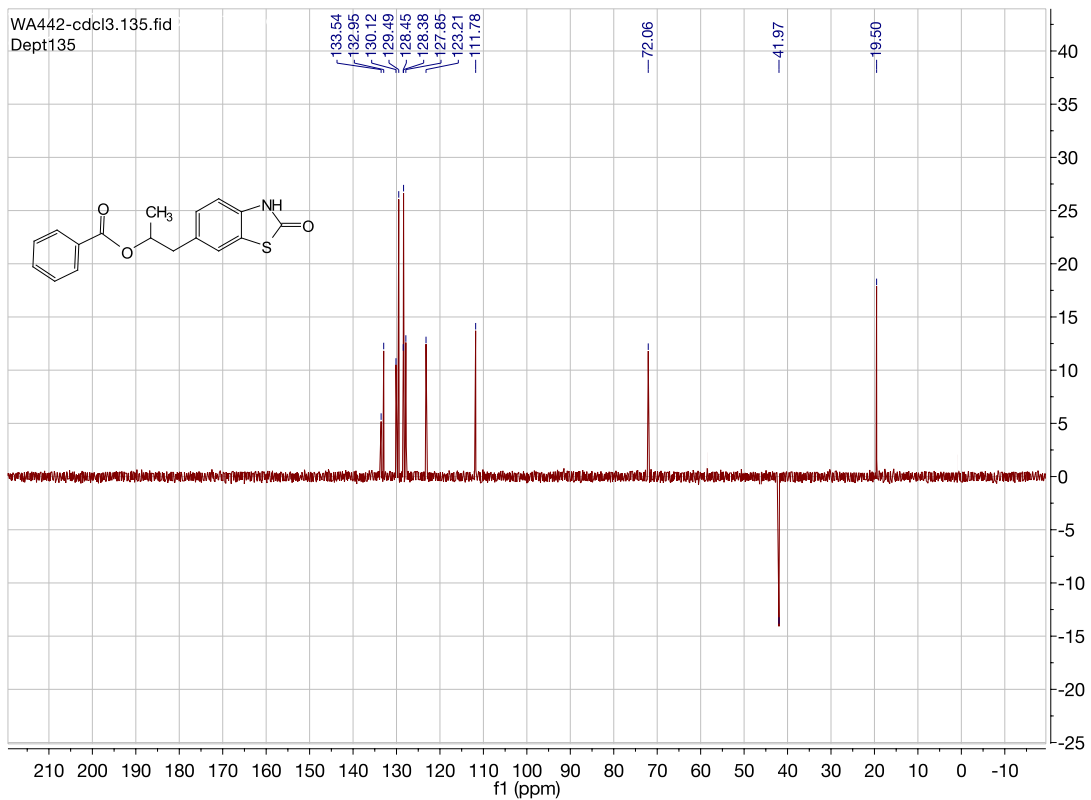
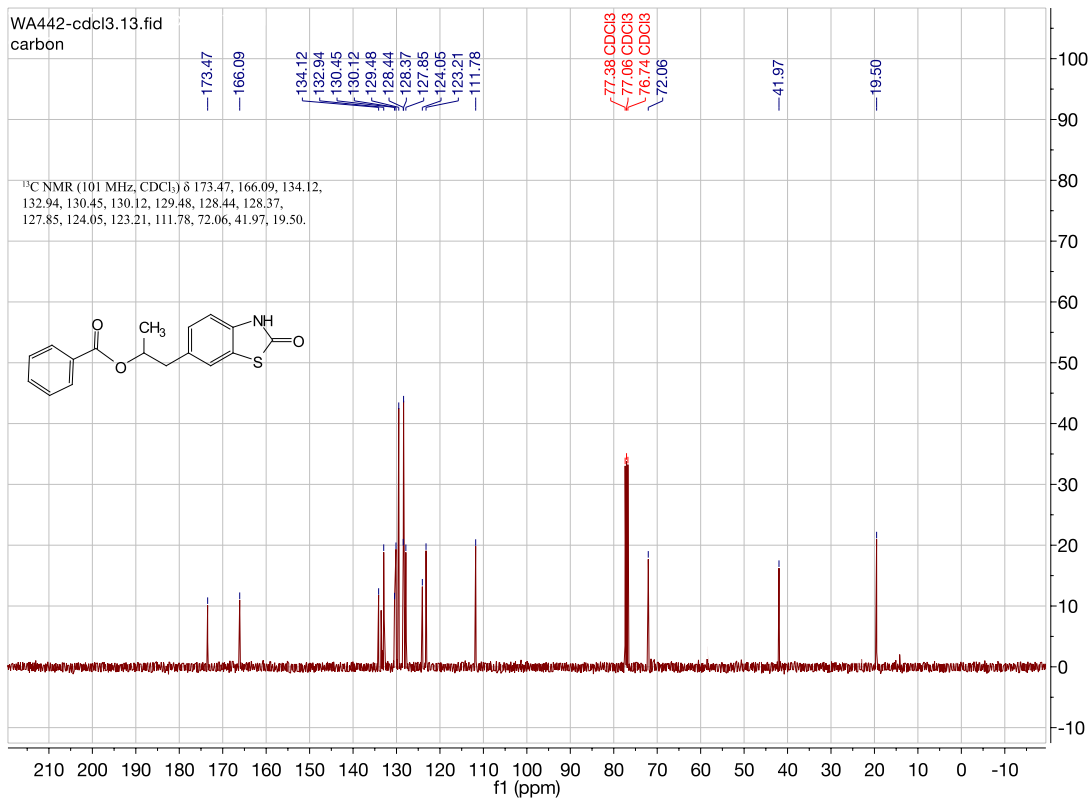
1-(2-oxo-2,3-dihydrobenzo[d]thiazol-6-yl)propan-2-yl benzoate. [WA442][d]



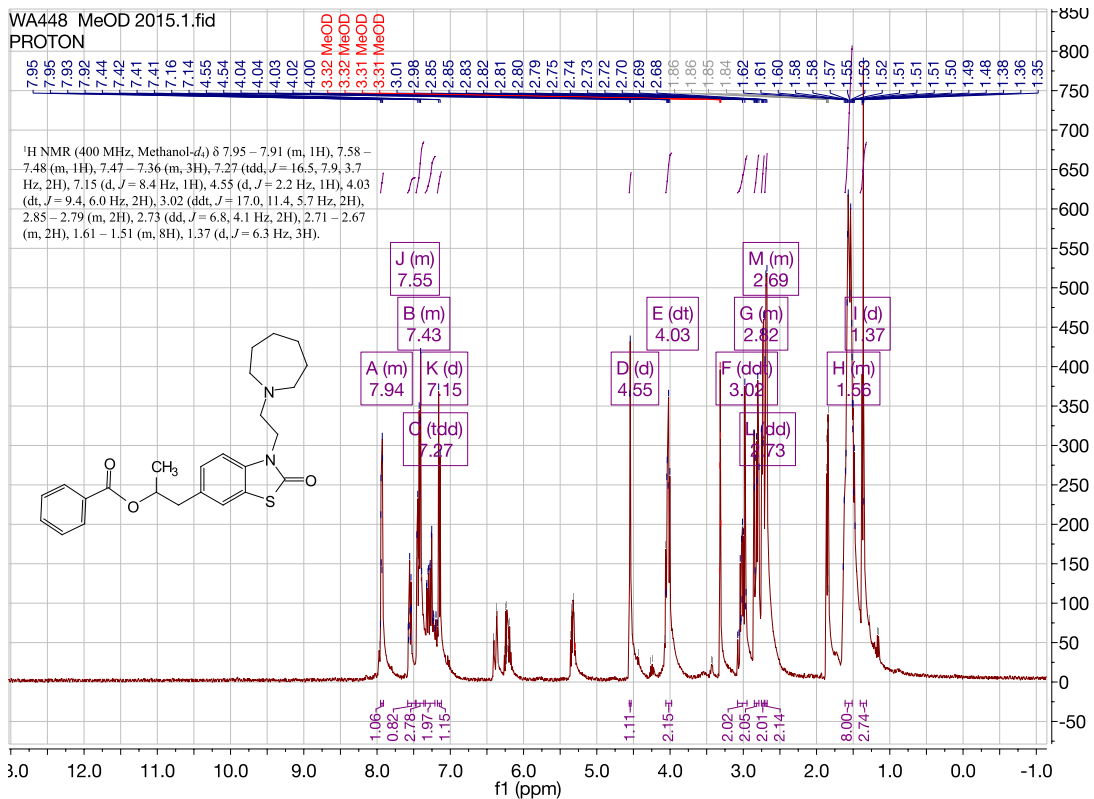
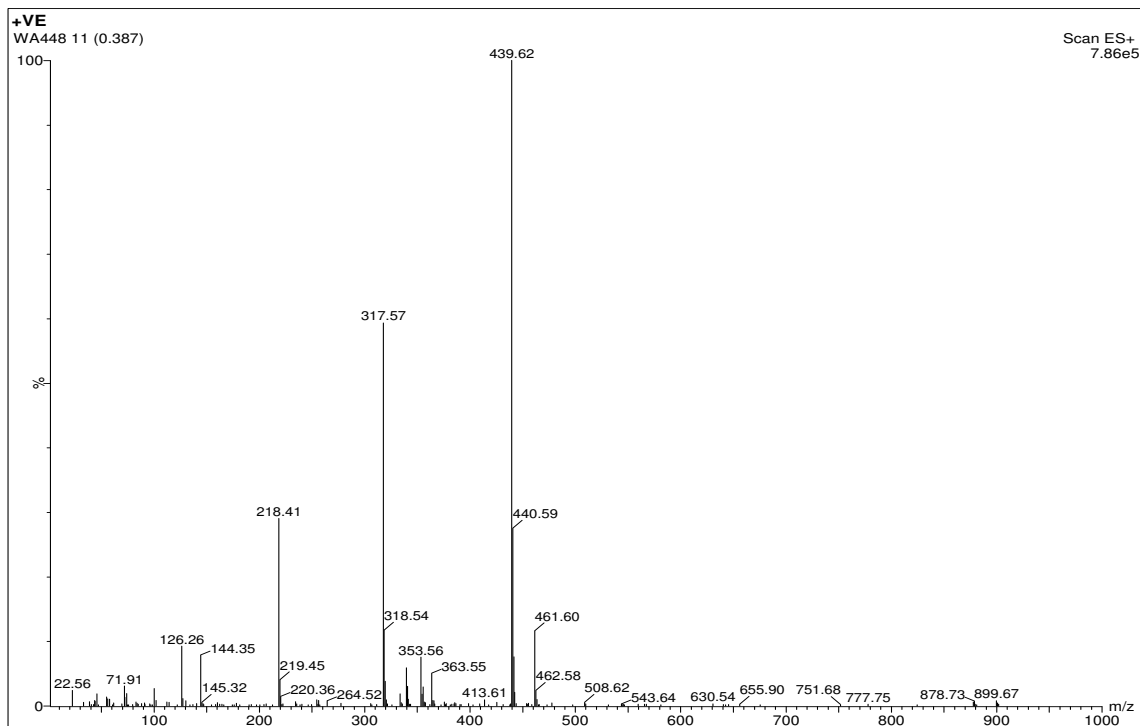


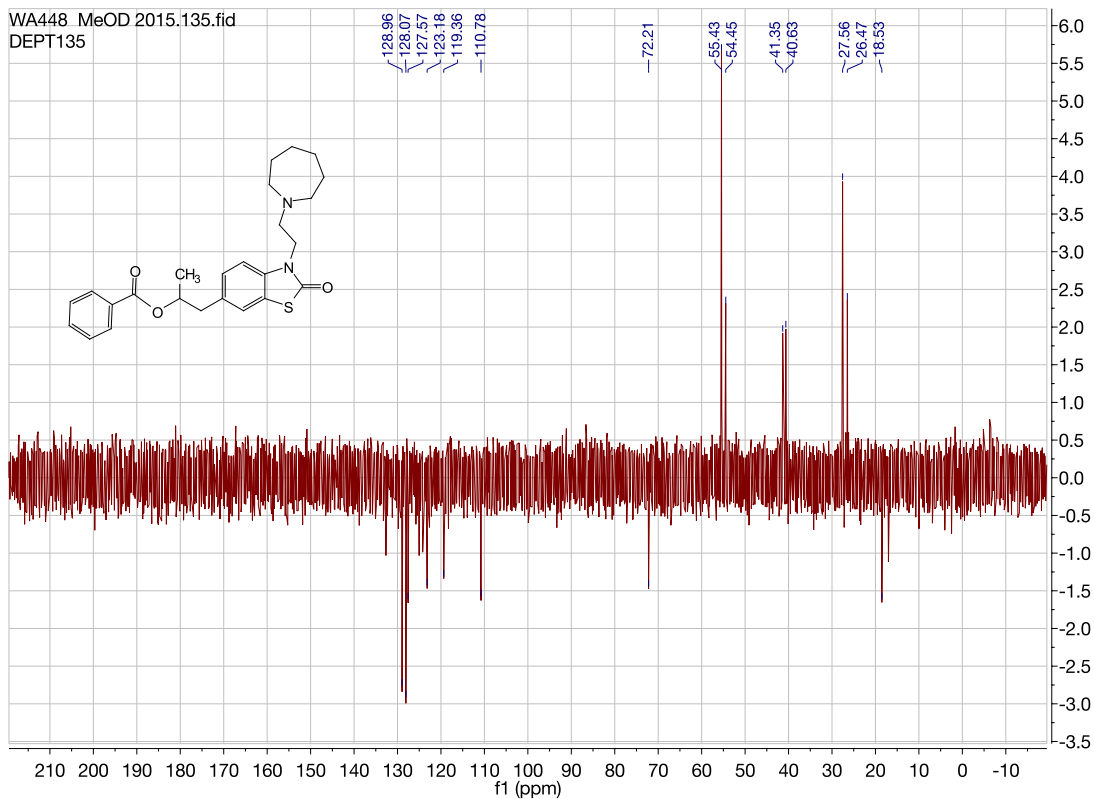
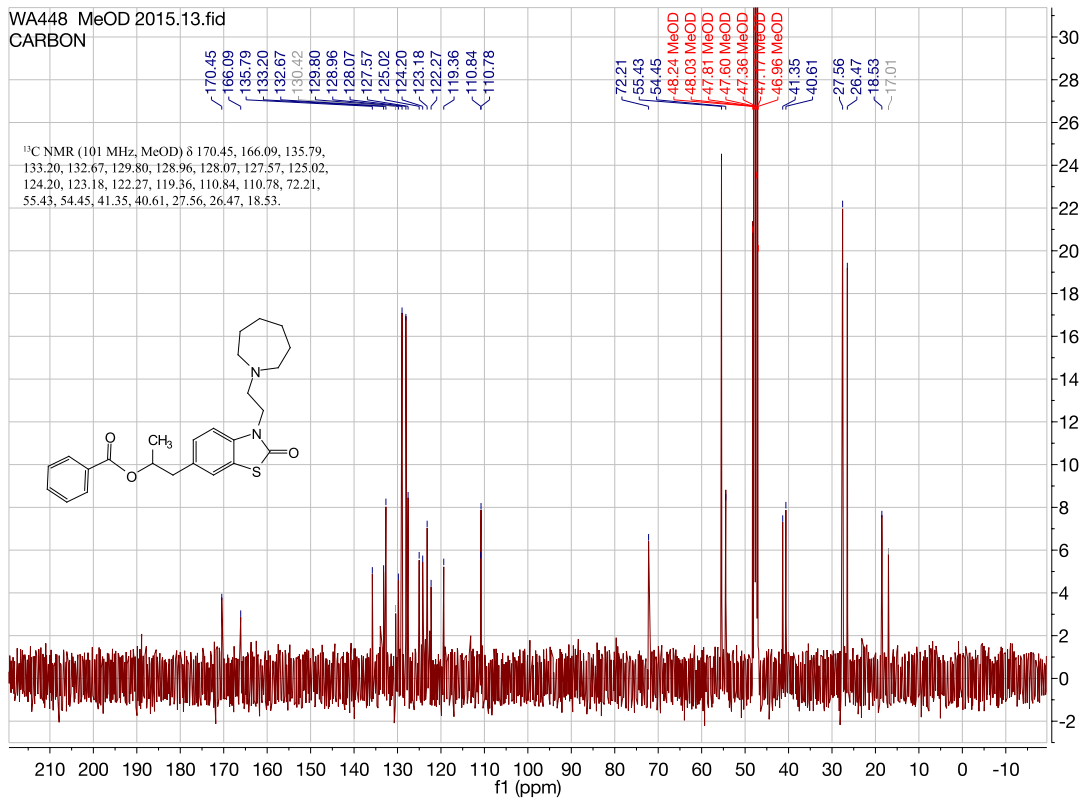
3-(2-(azepan-1-yl)ethyl)-6-(prop-1-en-1-yl)benzo[d]thiazol-2(3H)-one. [WA444b]



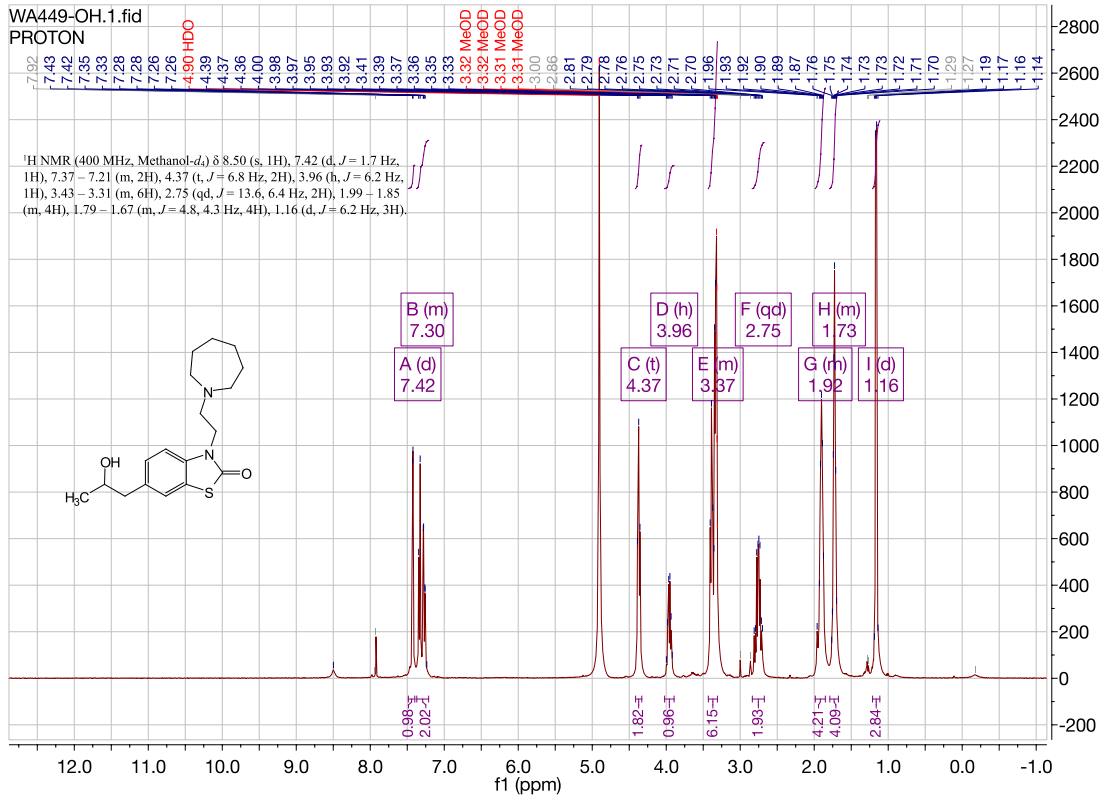
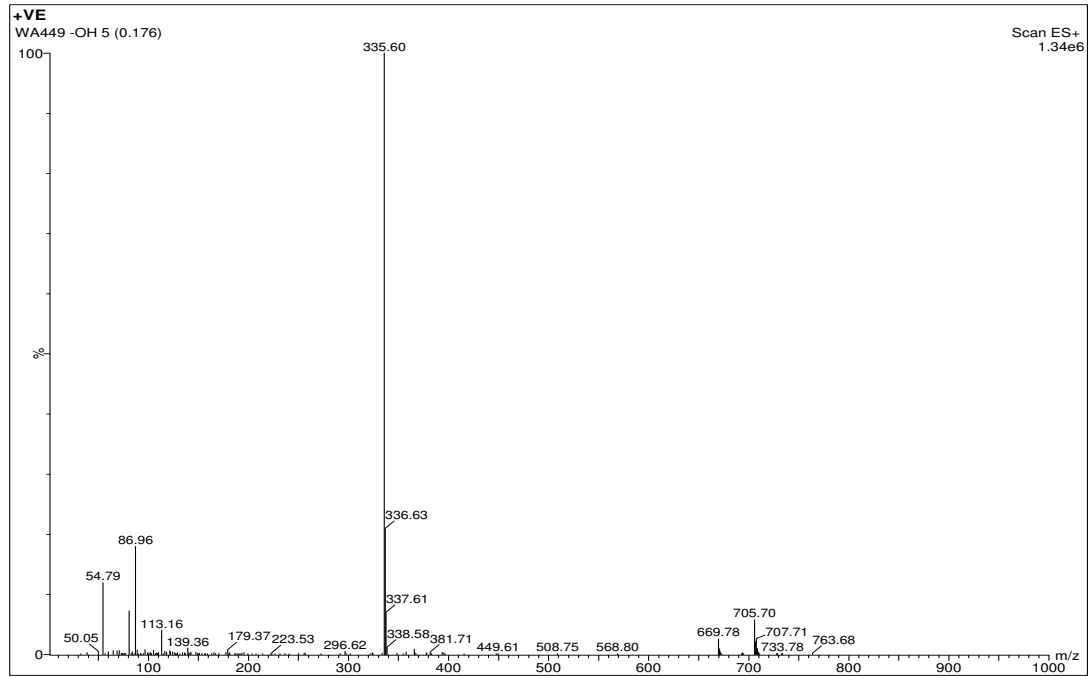


1-(3-(2-(azepan-1-yl)ethyl)-2-oxo-2,3-dihydrobenzo[d]thiazol-6-yl)propan-2-yl benzoate. [WA448][e]



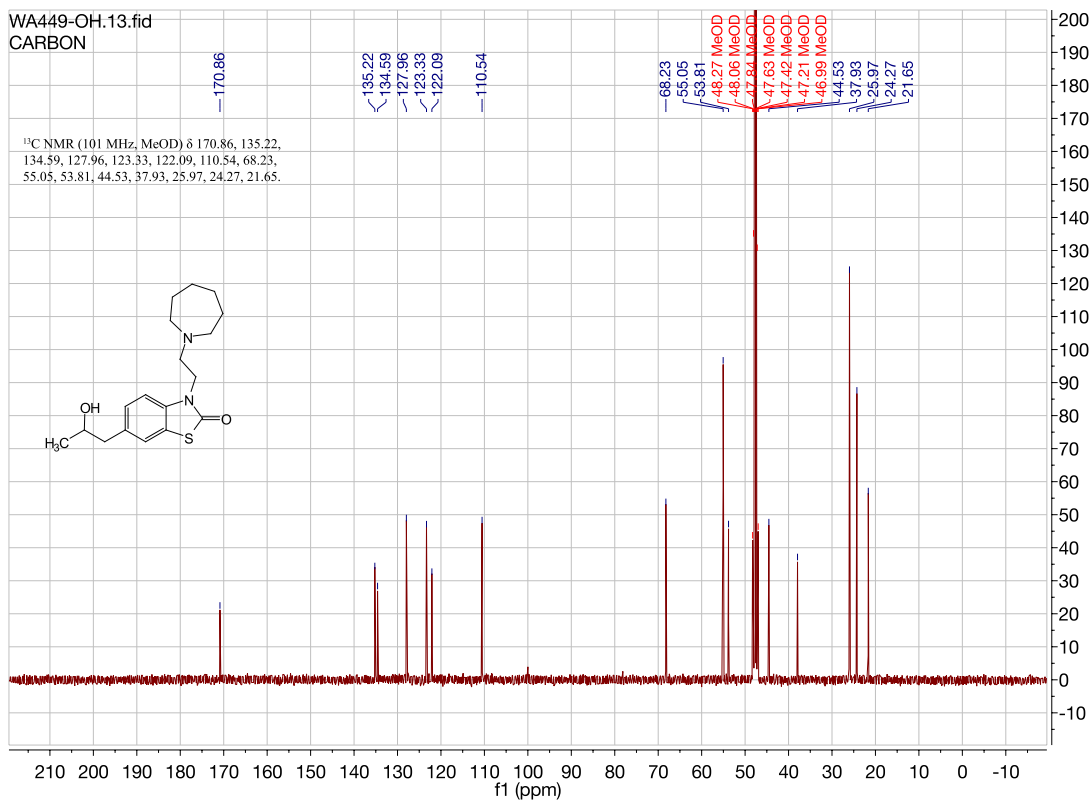


3-(2-(azepan-1-yl)ethyl)-6-(2-hydroxypropyl)benzo[d]thiazol-2(3H)-one. [WA449][g]

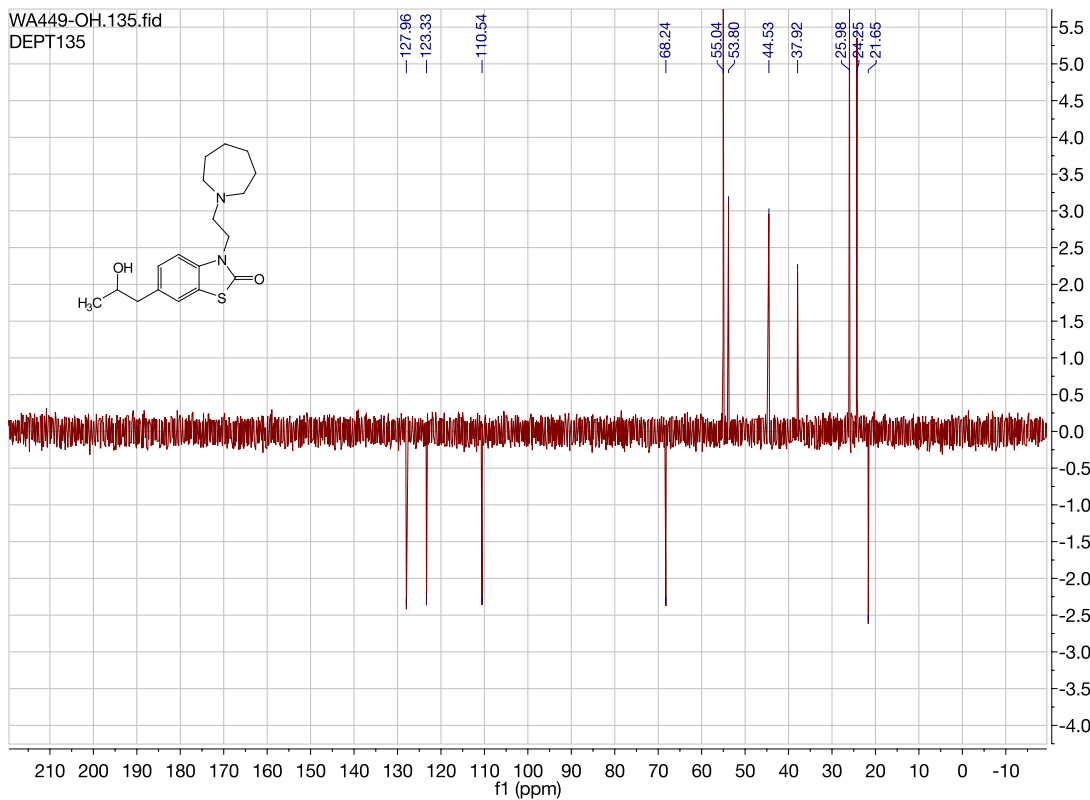


WA449-OH.13.fid
CARBON

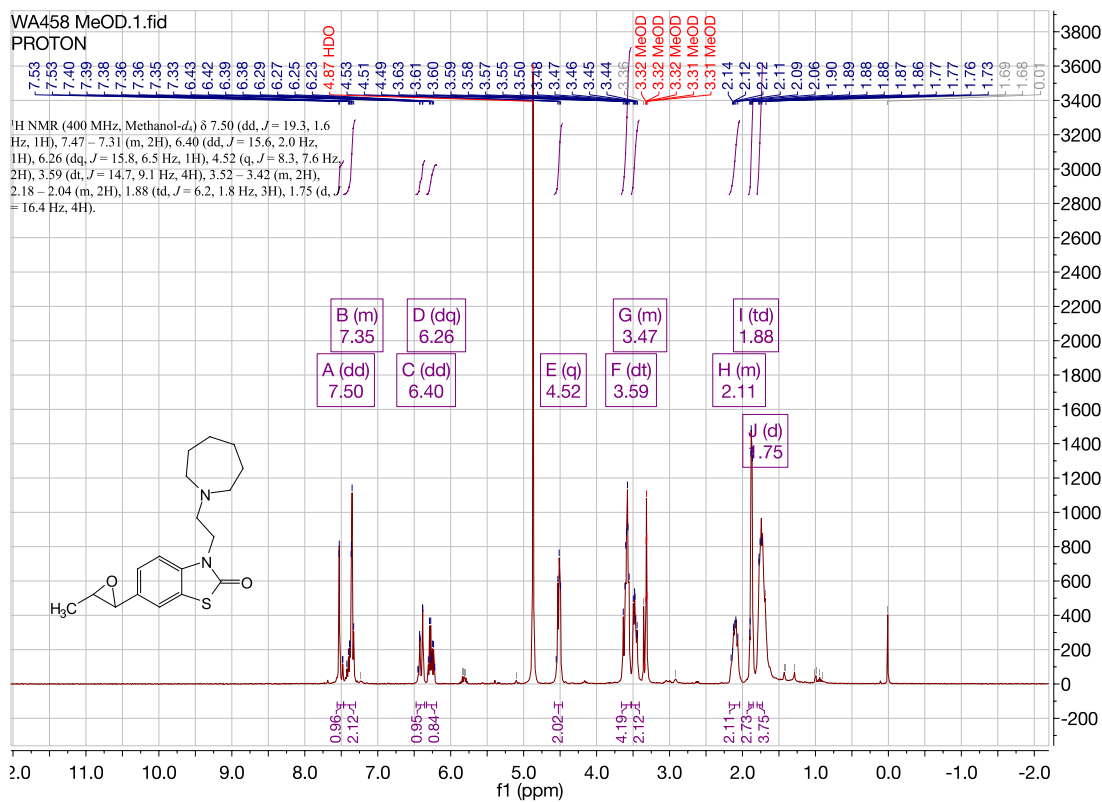
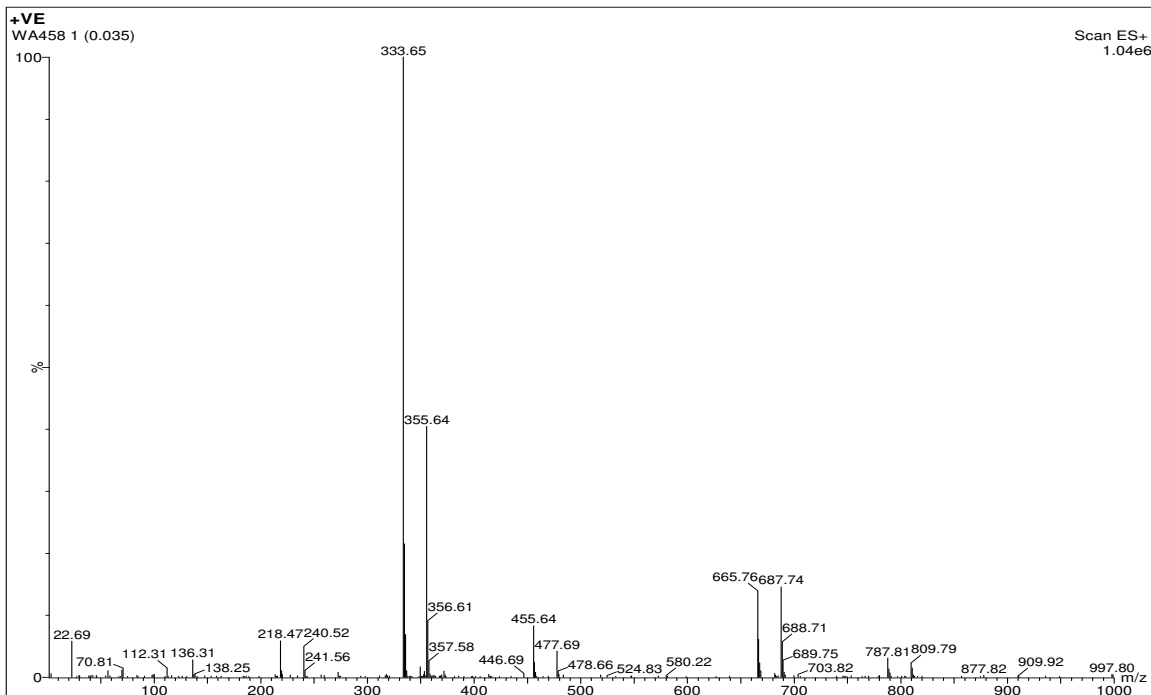
¹³C NMR (101 MHz, MeOD) δ 170.86, 135.22, 134.59, 127.96, 123.33, 122.09, 110.54, 68.23, 55.05, 53.81, 48.27 MeOD, 48.06 MeOD, 47.84 MeOD, 47.63 MeOD, 47.42 MeOD, 47.21 MeOD, 46.99 MeOD, 44.53, 37.93, 25.97, 24.27, 21.65.



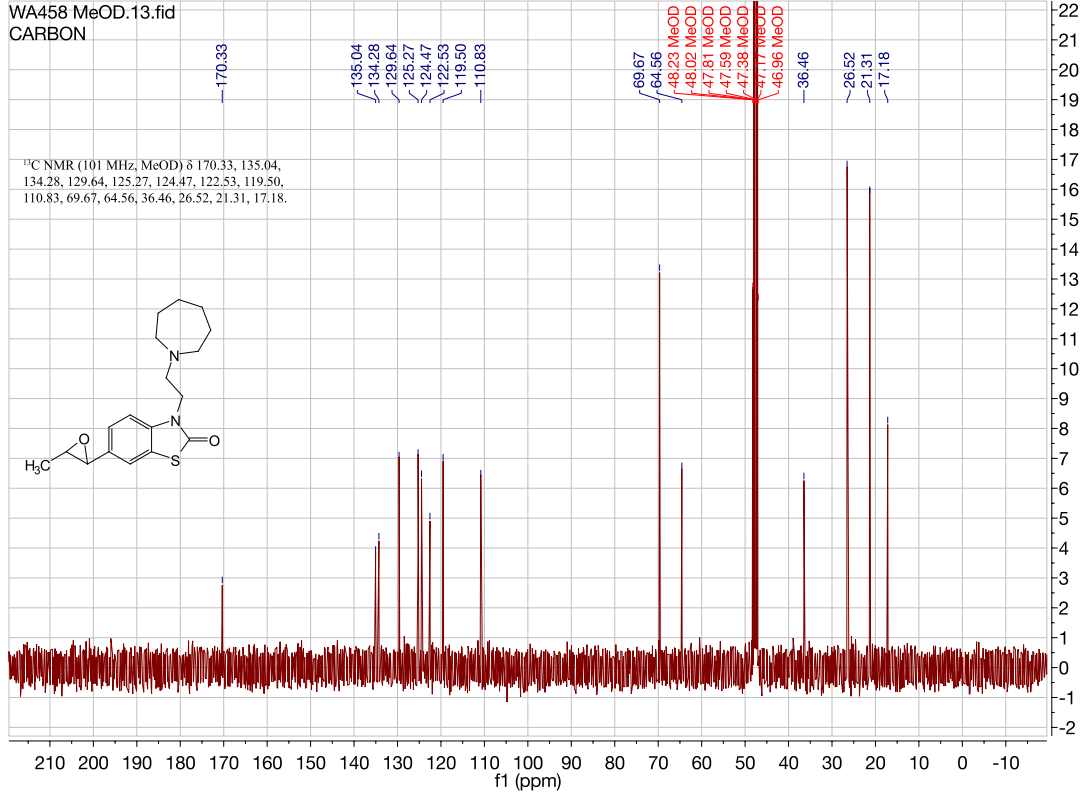
WA449-OH.135.fid
DEPT135



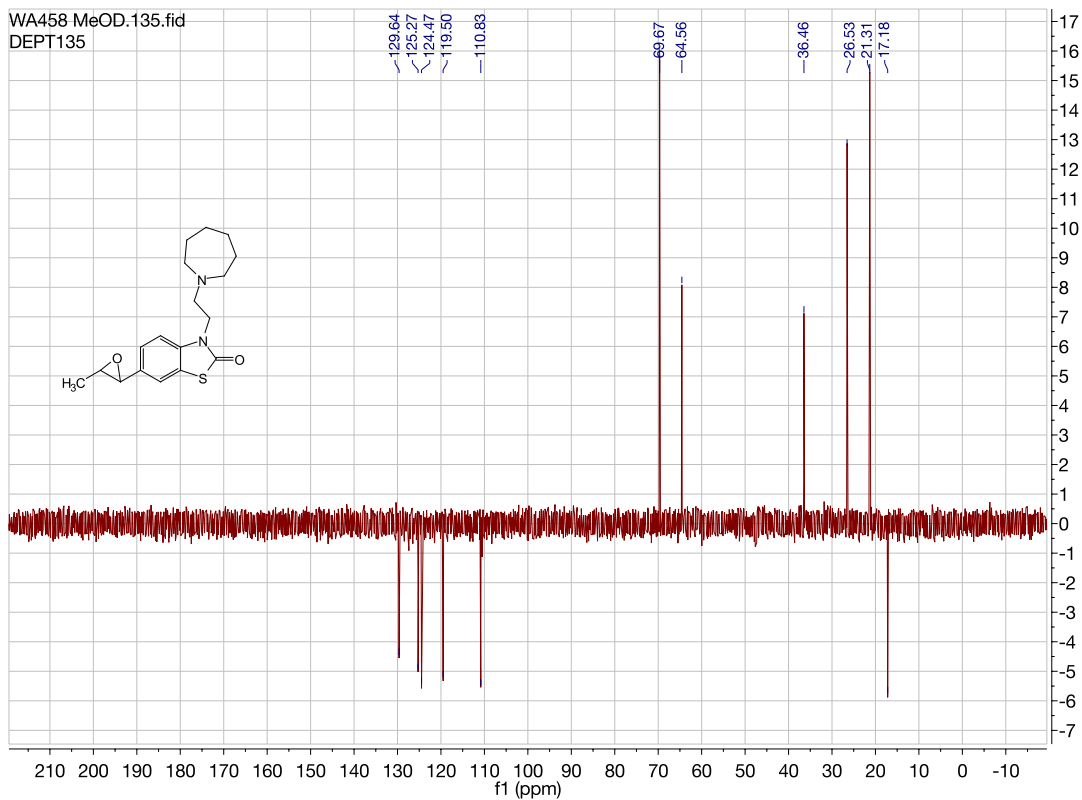
**3-(2-(azepan-1-yl)ethyl)-6-(3-methyloxiran-2-yl)benzo[d]thiazol-2(3H)-one.[WA458]
[f]**



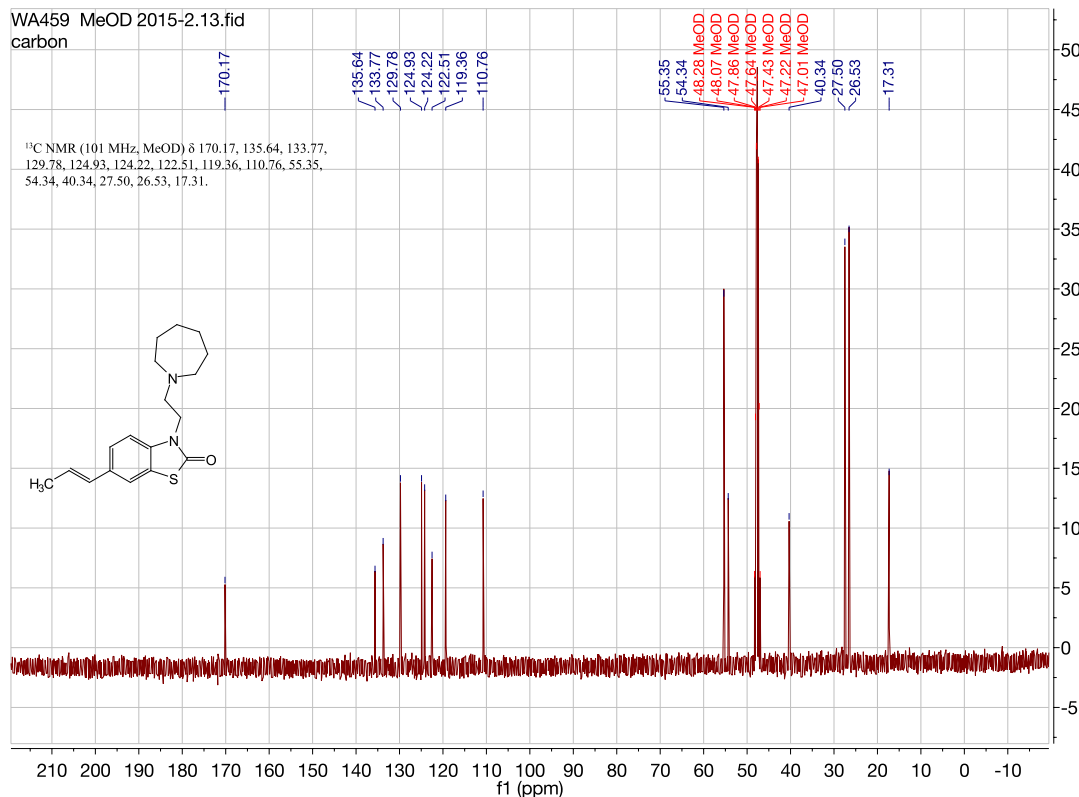
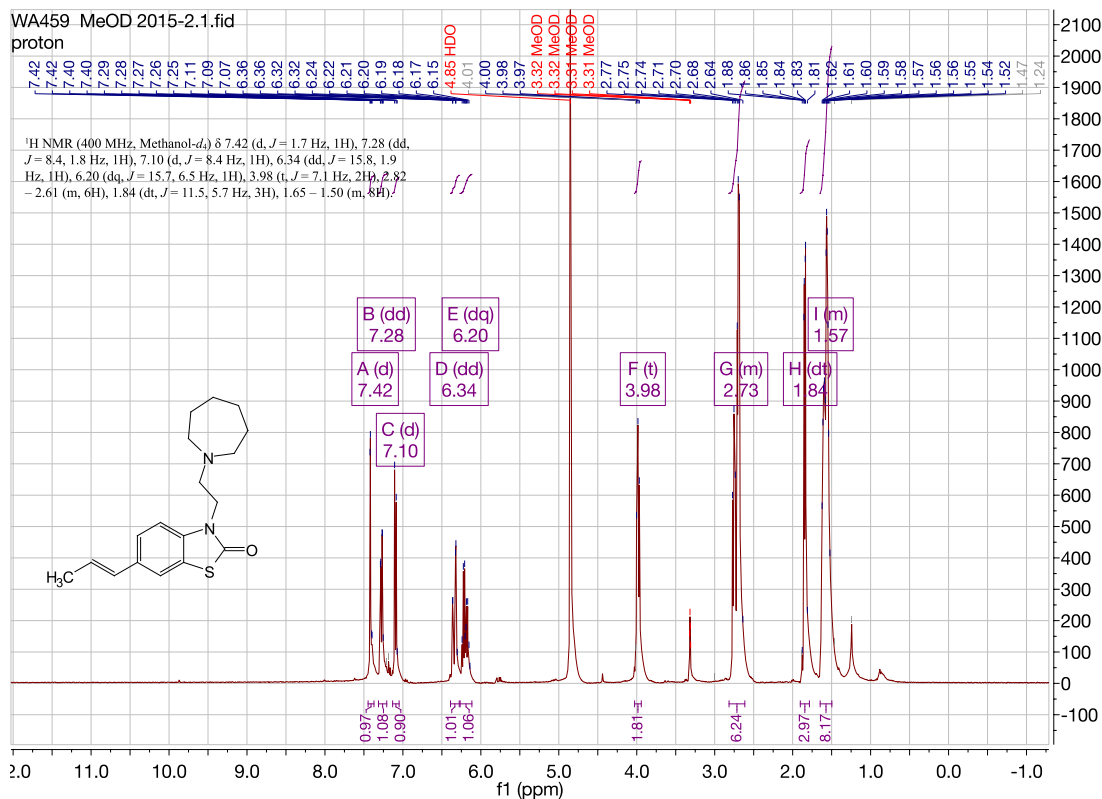
WA458 MeOD.13.fid
CARBON

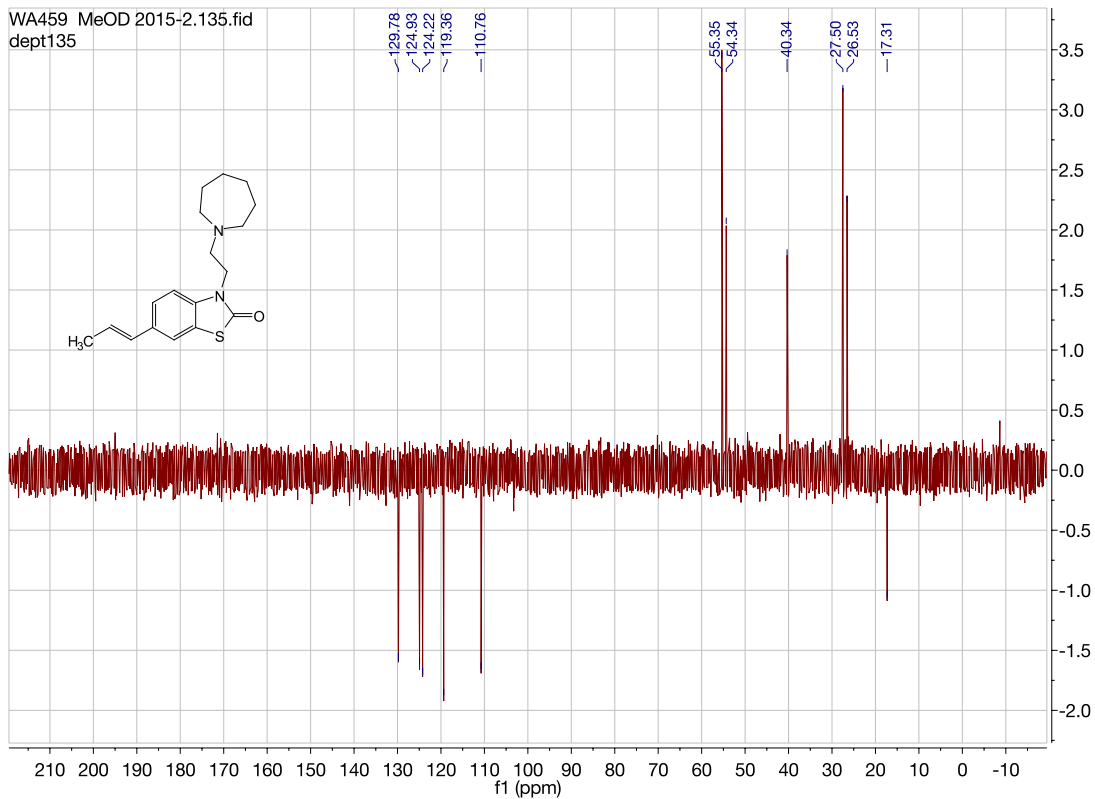


WA458 MeOD.135.fid
DEPT135

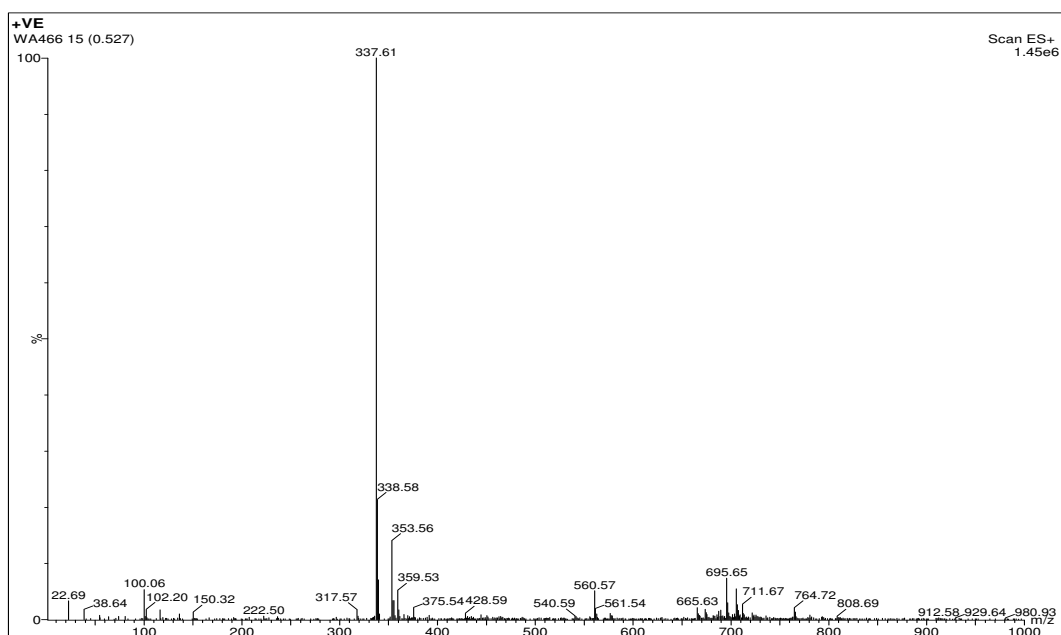


**(E)-3-(2-(azepan-1-yl)ethyl)-6-(prop-1-en-1-yl)benzo[d]thiazol-2(3H)-one. [WA459]
[f]**

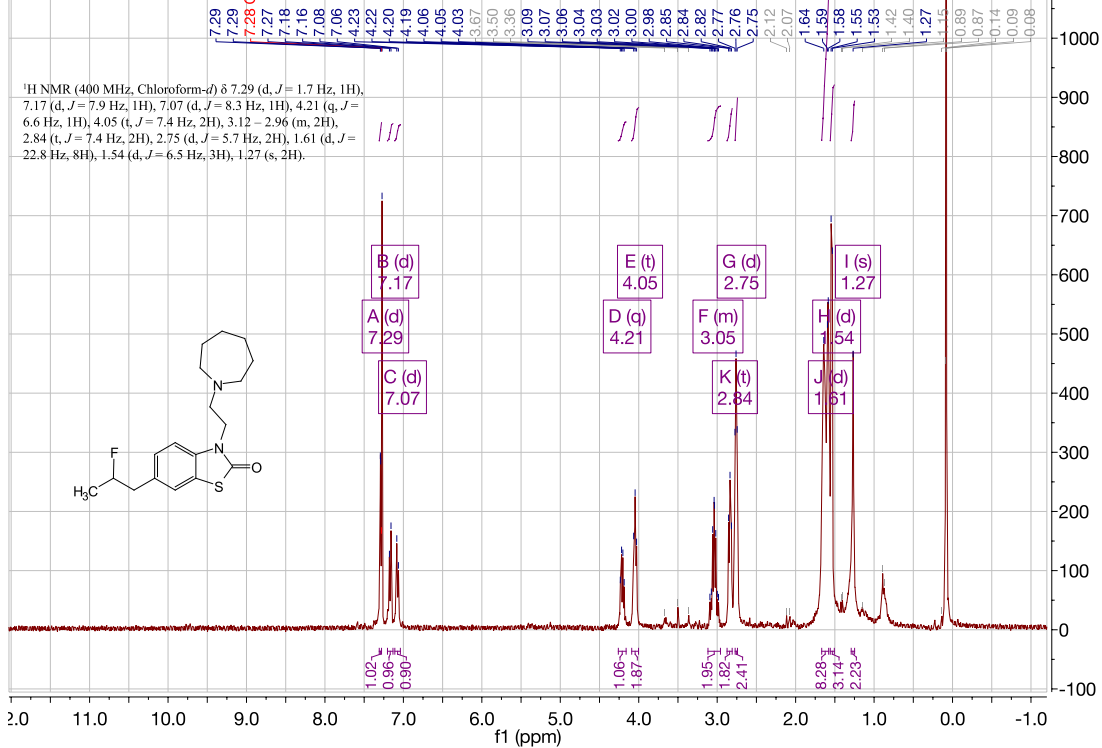




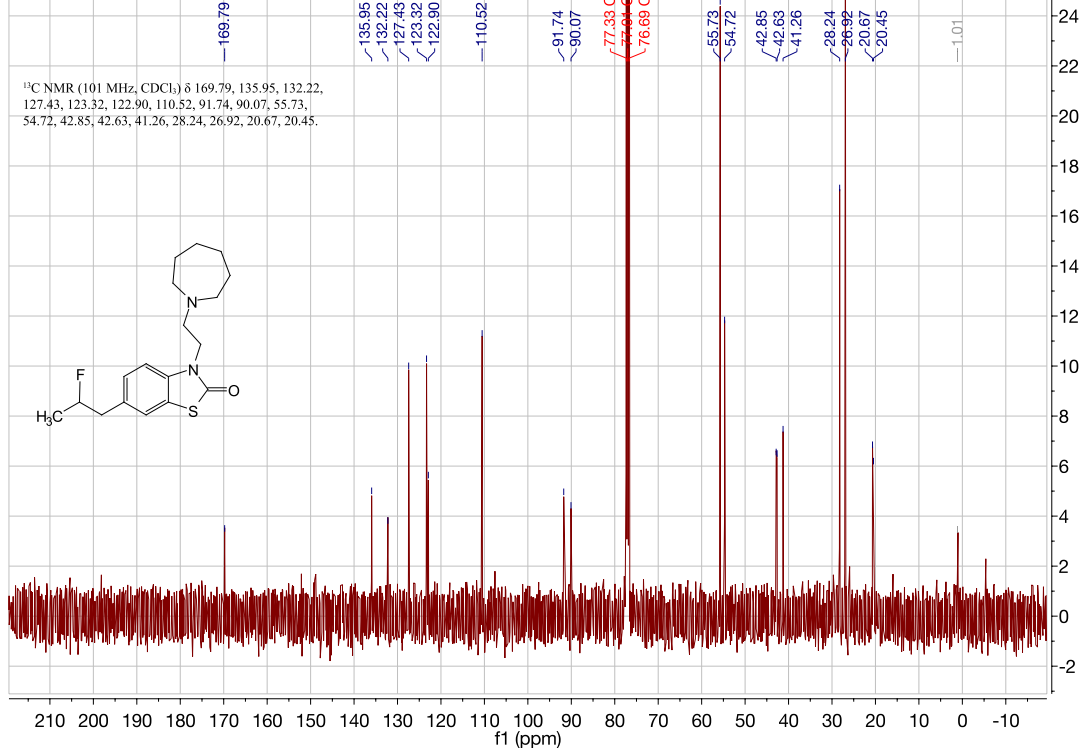
3-(2-(azepan-1-yl)ethyl)-6-(2-fluoropropyl)benzo[d]thiazol-2(3H)-one. [WA466][h]



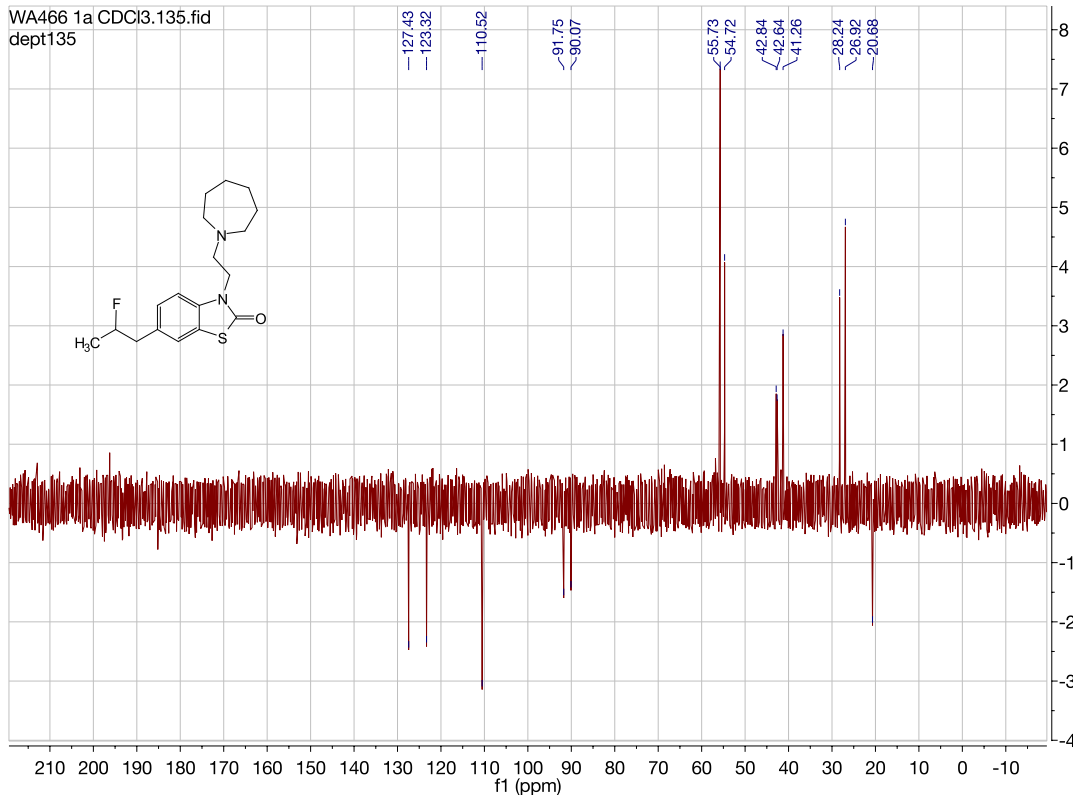
WA466 2b CDCI3.1.fid
proton



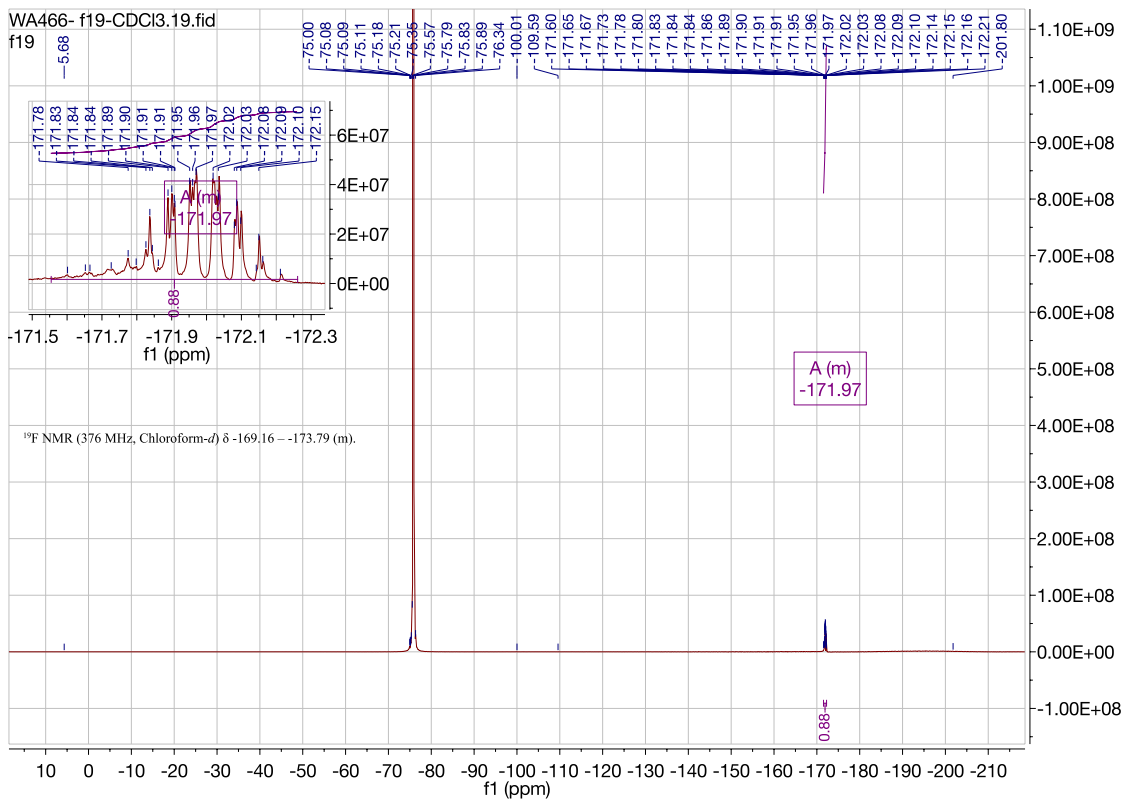
WA466 1a CDCI3.13.fid
carbon



WA466 1a CDCl3.135.fid
dept135



WA466- f19-CDCl3.19.fid
f19



VITA

Walid Alsharif received his bachelor of pharmacy (B.Pharm.) degree from Garyounis University in Libya, and joined Dr. Christopher R. McCurdy's research group at the University of Mississippi (Oxford, MS, USA) in 2010 pursuing his doctorate studies. His doctoral research focused on the design and synthesis of new ligands for sigma receptors with the goals of developing medications that can treat stimulant abuse and addiction from one project, and identifying novel and selective sigma-2 ligands that can be used as pharmacological tools to isolate and identify sigma-2 receptors to gain greater understanding of their roles in cancer.

Walid Alsharif has received several research awards locally and nationally during the last two years. He received consecutive first place award in 2013 and 2014 in the University of Mississippi's local section of the American Chemistry Society (ACS) Poster Competition. He was recognized with the first place poster award at the 2014 Graduate Student Council (GSC) Graduate Research Forum at the University of Mississippi. He also received a GSC Research Grant Award, and has been recommended for funding of a second grant. The Mississippi Academy of Science (MAS) recognized his work with Honorable Mention distinction for his outstanding manuscript at the 2015 MAS Annual meeting. Later in the same year, he was received the first place award in Applied Neuroscience Category in the first Neuroscience Research Showcase Poster Competition, 2015. He also received national recognition from the American Association of Pharmaceutical Scientists when he was awarded the 2014 Graduate Student Research in Drug Discovery and Development Interface Award, in recognition of his excellence in graduate education in the fields of Drug Discovery and Development Interface.